

# Activity Coefficients in Electrolyte Solutions

2nd Edition

Editor

**Kenneth S. Pitzer, Ph.D.**

Professor  
Department of Chemistry  
University of California  
Berkeley, California



CRC Press  
Boca Raton Ann Arbor Boston London

## PREFACE

The progress toward a second edition of "Activity Coefficients in Electrolyte Solutions" was well advanced by Dr. R. M. Pytkowicz, the editor of the first edition, when he resigned in early 1989 for health reasons. After a substantial hiatus, I was asked to take over the editorship. Most of the chapters and authors remain as were planned by Dr. Pytkowicz, but a few changes in authorship or coauthorship were necessary and one new chapter (8) was added. I am responsible for the present organization of the book but am happy to acknowledge the role of Dr. Pytkowicz.

My evaluation concerning the general state of knowledge in this field and the opportunities for advances as well as certain specific comments concerning points of possible misunderstanding are given in the Introduction. At this point, I wish to thank all of the authors for the prompt completion of their chapters and my secretary, Peggy Southard, for assistance on various aspects of this project.

**Kenneth S. Pitzer**

# Activity Coefficients in Electrolyte Solutions

2nd Edition

Editor

**Kenneth S. Pitzer, Ph.D.**

Professor  
Department of Chemistry  
University of California  
Berkeley, California

## INTRODUCTION

It has been eight decades since activity coefficients came into use in the representation of the solute chemical potential in electrolyte solutions, together with the osmotic coefficient for the solvent chemical potential. While ionic solutions in other polar solvents have been and continue to be investigated, aqueous solutions dominate the electrolyte scene with respect to their importance in biological, geological, and industrial systems as well as in the range and intensity of scientific study. Although all of the concepts and theories are equally applicable to nonaqueous electrolytes, almost all of the particular systems that are considered here are aqueous.

In the earlier years, most research concerned pure, single-solute electrolytes at or near room temperature and at low and moderate concentration. Only a few systems were measured over the full molality range available. Subsequently, Robinson and Stokes and others through isopiestic measurements greatly extended the knowledge of a large number of electrolytes at 25°C. In their book Robinson and Stokes<sup>1</sup> summarize this information as well as presenting an excellent account of the principles and the methods of measurement for electrolytes.

While a few measurements of mixed electrolytes were made in very early years, it was Harned<sup>2</sup> and his associates that measured quite a number of mixed systems and stated the rules bearing his name concerning their behavior. Again, this work was confined to temperatures near 25°C and to moderate molalities. Many others made substantial contributions to experimental research on electrolytes prior to the first edition of this book published in 1979. It is impractical to list here all of the important contributors of that period; their names are cited in various chapters.

Even by 1910 it was recognized that the behavior of electrolytes in the dilute range differed from that of nonionic solutions. In 1912, Milner<sup>3</sup> explained theoretically the cause of this difference in terms of the long-range nature of ionic forces, but his mathematical expression was so complex that it received little attention. In 1923, however, Debye and Hückel<sup>4</sup> presented a simple expression that captured the essential consequence of the ionic forces. Subsequently, various theorists investigated the difficult problem of an electrolyte with greater rigor and confirmed the correctness of the limiting law of Debye and Hückel. As is described in certain chapters of this book, several of these later theories also contributed expressions for the behavior of more concentrated electrolytes.

The major advances in this field over the last fifteen years have been, first, in the area of mixed aqueous electrolytes of relatively high concentration extending to the limits of solid solubility, and second, for high temperatures up to 300°C and to pressures of hundreds of bars. Both of these advances are recognized in major additions to Chapter 3, a largely new chapter on natural waters, and new chapters on mineral solubilities and ion association at high temperatures and pressures.

With the ion-interaction (Pitzer) equations, including the theoretical terms for unsymmetrical mixing of ions of the same sign, together with ion-association equilibria where significant, it is now possible to predict activity coefficients and water activities accurately for mixtures of unlimited complexity and to the limits of solid solubility in most cases, provided, of course, that the solid properties are also accurately known. Computer programs are now available for such calculations.<sup>5</sup> Special recognition is due to Harvie and Weare<sup>6</sup> for their pioneering calculations of mineral solubility by these methods including the key case of CaSO<sub>4</sub> solubility in aqueous NaCl where this method gave good results, whereas older ion-association methods gave a qualitatively incorrect trend with NaCl molality. Also important are the numerous treatments extending to solid solubility by Filippov and associates.<sup>7</sup>

In past years, ion-interaction and ion-association methods have been regarded as competitive. The first edition of this book gives a good account of the status and viewpoints of

1979. Clegg and Whitfield discuss both the history and current status of these methods in Section II of Chapter 6. While the title of Chapter 6 is "Activity Coefficients in Natural Waters," this discussion is comprehensive and not limited to "Natural Waters".

For systems with little or no ion association, specific interionic effects are still significant at substantial molality and the ion-interaction method has proven to be excellent. Even where there is unquestioned association to a moderate degree, such as to  $\text{MgSO}_4$  in seawater and similar solutions, the inclusion of a special term in the ion-interaction equations has been found to be a better method at moderate temperatures than the inclusion of a formal association reaction. For  $\text{H}_2\text{SO}_4$ , however, the explicit inclusion of the association reaction to  $\text{HSO}_4^-$  is essential. Thus, when  $\text{HSO}_4^-$  or  $\text{HCO}_3^-$  or similar species are formed by strong association reactions, one requires a combination of ion-interaction and ion-association methods to obtain accurate results. Also, the tendency toward ion association increases at high temperature where the dielectric constant of water becomes small (see Chapter 8).

For pure electrolytes at room temperature, there has been a good database since the 1955 book of Robinson and Stokes,<sup>1</sup> although significant improvements have been made as well as extensions to additional solutes. The appearance of accurate values at high temperatures to 300°C and at high pressures is the second area of major recent advance. Particularly notable are the solvent vapor pressure measurements of Liu and Lindsay<sup>8</sup> for  $\text{NaCl}(\text{aq})$  and the isopiestic measurements of Holmes and Mesmer for several other salt solutions. Heat capacity, heat of dilution, and volumetric measurements have also been made extending to 300°C or above. This has allowed comprehensive thermodynamic treatments; many of these are listed in Chapters 3, 7, and 8.

There have been a number of interesting theoretical advances including those allowing statistical calculations for more realistic physical models; these are reported in Chapter 2. Nevertheless, it remains necessary to use semi-empirical methods to represent data to the full experimental accuracy.

As described in Chapter 1, various measures of composition can be used for electrolytes: mole fraction, molality (moles per kg of solvent), molarity (moles per liter of solution), weight fraction, etc. Most electrolytes have a range of solubility limited to about  $15 \text{ mol} \cdot \text{kg}^{-1}$  or less, and for such solutions molality has been found to be by far the most convenient measurement system. Thus, molality is used very generally in this book, but for exceptional cases of extremely wide solubility range, mole fraction is used. Indeed, for a pure ionic liquid the molality is infinite; hence, the change to mole fraction is necessary.

The words "ideal" or "ideality" are ordinarily associated with behavior that corresponds to unit activity coefficients on the mole fraction basis. The behavior given by unit activity and osmotic coefficients on the molality basis is similar, has the same limiting property at infinite dilution, but is quantitatively different at other compositions. It is very convenient in either system to use expressions for an excess Gibbs energy defined as the difference of the actual Gibbs energy from that of the ideal or another simple reference pattern. In each system, mole fraction or molality, it is most convenient and useful to use, as the reference pattern, that of unit activity coefficients in the same system. Thus, two slightly different "excess Gibbs energies" are now used. No confusion need arise provided each system is used self-consistently and with clear statements and definitions.

That the advances of the last decade are important to geochemistry and chemical oceanography is clear from the results presented in various chapters, especially in Chapters 6 and 7. The application to aerosols which comprise aqueous electrolytes is less obvious but important; at low humidity these aerosol solutions become highly concentrated. This is recognized in Chapter 6.

There are many biologically important aqueous fluids where chemical thermodynamics has been applied and has been essential to an understanding of the complex array of processes taking place. Ions are present in most of these fluids; indeed, it is the activity of a particular

ion that is related to a biological function in many cases.<sup>9-16</sup> The ionic strength is rather low, however, so that a simple approximation for activity coefficients may suffice.

Thus, the numerous reactions involving adenosine mono-, di-, and triphosphates with various ions present and with varying pH constitute a very interesting system subject to treatment by the methods of chemical thermodynamics with equilibrium quotients for various reactions.<sup>9-11</sup> Some of the early treatments were for constant ionic strength. They omitted activity coefficients and used equilibrium quotients assumed to be valid for that fixed ionic strength. Other treatments consider data for different ionic strengths but assume that an activity coefficient depends only on the ion charge and the ionic strength and is independent of the specific ions present.

As the precision of thermodynamic measurements for biologically important systems increases, it will be necessary to recognize the specific effects of other ions on the activity coefficient of a given ion. Since these effects are now accurately known for many ions, this information can be included without introducing unknown parameters. There may be other interactions in a particular case which are not known independently, but it will be a better approximation to include the known ion-interaction terms than to ignore all interionic interactions and use only the ionic strength.

There is one area with a biological connection where highly concentrated electrolytes are involved. This is the use of concentrated solutions of NaCl or other salts to control the moisture content of foods in storage and its relationship to microbiological growth. Kitic et al.<sup>17</sup> have used the ion interaction equations and reported their methods in the literature for food science.

Some biologically oriented investigations are now using the ion-interaction equations (Chapter 7 of the 1st edition, Chapter 3 of this edition) in the treatment of their data. Indeed, Baumgarten<sup>18</sup> has published in a biological journal a simple computer program for this method. It seems probable that the more precise and complete treatments described in this volume will find increasing application in biological systems in the near future.

Finally, I note that in the geological area and in engineering there is great interest in aqueous electrolytes at still higher temperatures, far above 300°C, and this range requires a different theoretical approach from that used in this book. There is the phase separation of water and an appreciable salt solubility in the steam phase. Also, the compressibility of the solvent becomes infinite at its critical point. These aspects require the use of the Helmholtz energy rather than the Gibbs energy as the basic function. While several research contributions have been made, which are related to this higher temperature range, many aspects are still to be investigated. It will be an interesting field both theoretically and in applications in the near future.

## REFERENCES

1. **Robinson, R. A. and Stokes, R. H.**, *Electrolyte Solutions*, revised, Butterworths, London, 1st ed., 1955; 2nd ed., revised 1965.
2. **Harned, H. S. and Owen, B. B.**, *The Physical Chemistry of Electrolyte Solutions*, Reinhold Publishing, New York, 1958.
3. **Milner, S. R.**, The virial of a mixture of ions, *Phil. Mag.*, 23, 551, 1912; 25, 742, 1913.
4. **Debye, P. and Hückel, E.**, Zur theorie der electrolyte, I and II, *Phys. Z.*, 24, 185 and 305, 1923.
5. **Plummer, L. N., Parkhurst, D. L., Fleming, G. W., and Dunkle, S. A.**, A computer program incorporating Pitzer's equations for calculation of geochemical reactions in brines, U.S. Geological Survey, Water-Resources Investigations Report 88-4153, Reston, VA, 1988. Also, see Chapters 3, 6, and 7.
6. **Harvie, C. E. and Weare, J. H.**, The prediction of mineral solubilities in natural waters: the Na-K-Mg-Ca-Cl-SO<sub>4</sub>-H<sub>2</sub>O system from zero to high concentration at 25°C, *Geochim. Cosmochim. Acta*, 44, 981, 1980.
7. **Filippov, V. K., Dmitriev, G. V., and Yakovleva, S. I.**, Use of the Pitzer method for calculating the activity of components in mixed solutions of electrolytes according to data on solubility, *Dokl. Akad. Nauk. SSSR, Fiz. Khim.*, 252, 156, 1980; Engl. transl., 252, 359, 1980; and subsequent papers.
8. **Liu, C. and Lindsay, W. T., Jr.**, Thermodynamics of sodium chloride solutions at high temperatures, *J. Solution Chem.*, 1, 45, 1972.
9. **Alberty, R. A.**, Standard Gibbs free energy, enthalpy, and entropy changes as a function of pH and pMg for several reactions involving adenosine phosphates, *J. Biol. Chem.*, 244, 3290, 1969.
10. **Phillips, R. C., George, P., and Rutman, R. J.**, Thermodynamic data for the hydrolysis of adenosine triphosphate as a function of pH, Mg<sup>2+</sup> ion concentration, and ionic strength, *J. Biol. Chem.*, 244, 3330, 1969.
11. **Goldberg, R. N. and Tewari, Y. B.**, Thermodynamics of the disproportionation of adenosine 5'-diphosphate to adenosine 5'-triphosphate and adenosine 5'-monophosphate, *Biophys. Chem.*, 40, 241, 1991.
12. **Guyrin, R. W., Gelberg, H. J., and Veech, R. L.**, Equilibrium constants of the malate dehydrogenase, citrate synthase, citrate lyase, and acetyl coenzyme A hydrolysis reactions under physiological conditions, *J. Biol. Chem.*, 248, 6957, 1973.
13. **Cohen, C. J., Fozzard, H. A., and Sheu, S.-S.**, Increase in intracellular sodium ion activity during stimulation in mammalian cardiac muscle, *Circ. Res.*, 50, 651, 1982.
14. **Shorofsky, S. R., Field, M., and Fozzard, H. A.**, Mechanism of Cl secretion in canine trachea: changes in intracellular chloride activity with secretion, *J. Membrane Biol.*, 81, 1, 1984.
15. **Biber, T. U. L., Drewnowska, K., Baumgarten, C. M., and Fisher, R. S.**, Intracellular Cl activity changes of frog skin, *Am. J. Physiol.*, 249, F432, 1985.
16. **Gambale, F., Menini, A., and Rauch, G.**, Effects of calcium on the gramicidin A single channel in phosphatidylserine membranes, *Eur. Biophys. J.*, 14, 369, 1987.
17. **Kitic, D., Pollo, M. L., Favetto, G. J., and Chirife, J.**, Mixed saturated salt solutions as standards for water activity measurements in the microbiological growth range, *J. Food Sci.*, 53, 578, 1988, and preceding articles there cited.
18. **Baumgarten, C. M.**, A program for calculation of activity coefficients at selected concentrations and temperatures, *Comput. Biol. Med.*, 11, 189, 1981.

## THE EDITOR

**Kenneth S. Pitzer** was born in Pomona, California in 1914. He received his B.S. degree from the California Institute of Technology in 1935, his Ph.D. from the University of California, Berkeley in 1937, a D.Sc. from Wesleyan University in 1962, and an LL.D. from the University of California in 1963 and from Mills College in 1969. He was a member of the faculty at Berkeley from 1937 to 1960, serving also as Dean of the College of Chemistry from 1951 to 1960. On leave from the University of California, he was Technical Director of the Maryland Research Laboratory, a World War II entity from 1943 to 1944, and was Director of Research for the U.S. Atomic Energy Commission from 1949 to 1951. In 1961, he became President and Professor of Chemistry at Rice University, serving until 1968 when he became President of Stanford University until 1970. In 1971 he returned to the University of California, Berkeley, as Professor until 1984 and thereafter as Professor Emeritus but was recalled for continued service.

His advisory committee and other part-time service included the General Advisory Committee to the AEC, 1958 to 1965 (Chairman 1960 to 1962); President's Science Advisory Committee, 1965 to 1968; Commission on Chemical Thermodynamics of the International Union of Pure and Applied Chemistry, 1953 to 1961; NASA Science and Technology Advisory Committee, 1964 to 1965; Trustee, Harvey Mudd College, 1956 to 1961, Mills College, 1958 to 1961, Pitzer College 1966 to the present, Rand Corporation, 1962 to 1972; Member of the Board of Directors, Owens Illinois, Inc., 1967 to 1986; Federal Reserve Bank of Dallas, 1965 to 1968, the American Council on Education, 1967 to 1971; and Member of the Council of the National Academy of Sciences, 1964 to 1967 and 1973 to 1976.

His research has extended through many areas of physical chemistry and into topics of importance including inorganic and organic chemistry, chemical engineering, and geochemistry. In addition to work on aqueous electrolytes reflected in this volume, his research has included quantum theory and statistical mechanics as applied to chemical problems ranging from the potential restricting rotation about single bonds, to the bonding in polyatomic carbon molecules, and to the effects of relativity on chemical bonds involving very heavy atoms. In addition to many journal articles and several book chapters, his books include *Quantum Chemistry*, 1953; *Selected Values of Physical and Chemical Properties of Hydrocarbons and Related Compounds*, with F. D. Rossini and others, 1947, 2nd edition, 1953; *Thermodynamics*, 2nd edition with L. Brewer, 1961, and a revision of the 1st edition of G. N. Lewis and M. Randall.

His honors and awards include the National Medal of Science, 1975, the Robert A. Welch Award in Chemistry, 1984, the Alumnus of the Year Award, University of California, Berkeley, 1951, and the Alumni Distinguished Service Award, California Institute of Technology, 1966. From the American Chemical Society he received the Award in Pure Chemistry, 1943, in Petroleum Chemistry, 1949, the Gilbert Newton Lewis Medal, 1965, the Priestley Medal, 1969, and the Willard Gibbs Medal, 1976. Other recognitions include many special lectureships, a Guggenheim Fellowship, 1951, and election to the National Academy of Sciences in 1949.



## CONTRIBUTORS

**James N. Butler, Ph.D.**

Professor  
Division of Applied Sciences  
Harvard University  
Cambridge, Massachusetts

**Simon L. Clegg, Ph.D.**

Research Fellow  
School of Environmental Sciences  
University of East Anglia  
Norwich, United Kingdom

**Robert M. Mazo, Ph.D.**

Professor  
Department of Chemistry  
University of Oregon  
Eugene, Oregon

**Robert E. Mesmer, Ph.D.**

Section Head  
Chemistry Division  
Oak Ridge National Laboratory  
Oak Ridge, Tennessee

**Chung Yuan Mou, Ph.D.**

Professor  
Department of Chemistry  
National Taiwan University  
Taipei, Taiwan

**Roberto T. Pabalan, Ph.D.**

Research Scientist  
CNWRA  
Southwest Research Institute  
San Antonio, Texas

**Donald A. Palmer, Ph.D.**

Research Scientist  
Chemistry Division  
Oak Ridge National Laboratory  
Oak Ridge, Tennessee

**Kenneth S. Pitzer, Ph.D.**

Professor  
Department of Chemistry  
University of California  
Berkeley, California

**Robert F. Platford, Ph.D.**

Retired  
Campbellville, Ontario  
Canada

**Joseph A. Rard, Ph.D.**

Chemist  
Earth Sciences Department  
University of California  
Lawrence Livermore National Laboratory  
Livermore, California

**Rabindra N. Roy, Ph.D.**

Chairman and Professor  
Department of Chemistry  
Drury College  
Springfield, Missouri

**J. M. Simonson, Ph.D.**

Research Scientist  
Chemistry Division  
Oak Ridge National Laboratory  
Oak Ridge, Tennessee

**R. H. Stokes**

Professor Emeritus  
Department of Chemistry  
University of New England  
Armidale, Australia

**Michael Whitfield, Ph.D.**

Deputy Director  
Plymouth Marine Laboratory  
Plymouth, United Kingdom

## TABLE OF CONTENTS

Chapter 1	
Thermodynamics of Solutions .....	1
<b>R. H. Stokes</b>	
Chapter 2	
Introduction to the Statistical Mechanics of Solutions .....	29
<b>Robert M. Mazo and Chung Yuan Mou</b>	
Chapter 3	
Ion Interaction Approach: Theory and Data Correlation .....	75
<b>Kenneth S. Pitzer</b>	
Chapter 4	
Experimental Methods: Potentiometric .....	155
<b>James N. Butler and Rabindra N. Roy</b>	
Chapter 5	
Experimental Methods: Isopiestic .....	209
<b>Joseph A. Rard and Robert F. Platford</b>	
Chapter 6	
Activity Coefficients in Natural Waters .....	279
<b>Simon L. Clegg and Michael Whitfield</b>	
Chapter 7	
Mineral Solubilities in Electrolyte Solutions .....	435
<b>Roberto T. Pabalan and Kenneth S. Pitzer</b>	
Chapter 8	
Ion Association at High Temperatures and Pressures .....	491
<b>Robert E. Mesmer, Donald A. Palmer, and J. M. Simonson</b>	
Index .....	531

## Chapter 1

**THERMODYNAMICS OF SOLUTIONS**

R. H. Stokes

**TABLE OF CONTENTS**

I.	Basic Thermodynamic Functions U H V S G A and Their Physical Significance; Differential Relations .....	2
A.	Thermodynamic Functions .....	2
B.	Equations of State .....	3
C.	Conventional and Absolute Values of Thermodynamic Properties.....	3
D.	Physical Meaning of Thermodynamic Quantities .....	3
E.	The Laws of Thermodynamics .....	4
F.	Differential Relations between Thermodynamic Functions.....	5
II.	Solutions: Partial Molar Quantities; Chemical Potentials.....	5
A.	Open Phases: The Chemical Potential .....	5
B.	Partial Molar Quantities .....	6
C.	Additivity of Partial Molar Quantities .....	6
III.	Chemical Potentials and Activity Coefficients; Standard States and Composition Scales for Nonelectrolytes and Electrolytes .....	7
A.	Activities of Components.....	7
B.	Standard States .....	8
C.	Chemical Potentials in Electrolyte Solutions.....	8
D.	Activity, Activity Coefficients, and Standard States .....	9
E.	Mean Activities and Activity Coefficients.....	10
F.	Relations between Activity Coefficients on Different Scales .....	11
G.	The Solvent Chemical Potential, Solvent Activity, and the Osmotic Coefficient .....	12
IV.	The Gibbs-Duhem Relation; Various Forms for Two- and Multicomponent Systems .....	12
A.	The Gibbs-Duhem Equation .....	12
B.	Relation between Mean Activity Coefficient and Osmotic Coefficient .....	13
V.	Ideal Solutions; Entropy of Mixing on Various Statistics; Regular Solutions; Athermal Solutions .....	15
A.	Ideal Solutions .....	15
B.	The Entropy of Mixing.....	15
C.	Regular Solutions .....	17
VI.	Colligative Properties .....	17
A.	Freezing Point Depression.....	17
B.	Boiling Point Elevation.....	19
C.	Osmotic Pressure .....	19

D.	Derivation of Thermodynamic Quantities for Electrolyte Solutions from Electromotive Forces of Cells .....	20
VII.	Enthalpy and Volume Properties; Apparent Molar Quantities .....	21
A.	Temperature and Pressure Dependence of Activity Coefficients .....	21
B.	Pressure Dependence of Activity Coefficients .....	22
C.	Partial Molar Enthalpies and Volumes.....	22
VIII.	Excess Thermodynamic Properties .....	24
IX.	Multicomponent Systems — Thermodynamic Relations; Salting-Out and Salting-In Effects.....	26
A.	Thermodynamic Relations for Multicomponent Solutions .....	26
B.	Salting-Out Effects .....	27
	References.....	28

## I. BASIC THERMODYNAMIC FUNCTIONS U H V S G A AND THEIR PHYSICAL SIGNIFICANCE; DIFFERENTIAL RELATIONS

### A. THERMODYNAMIC FUNCTIONS

The thermodynamic properties of a substance or system at equilibrium may be grouped into (1) intensive properties, of which the most familiar are the temperature and pressure, and (2) extensive quantities, of which the volume and mass are most familiar. The former are independent of the size of the sample taken for measurement and are constant throughout each phase of the system. The temperature, in fact, must be the same in all phases of the system for true equilibrium to exist, though the pressure may be different in different phases, as in osmotic equilibrium. Other intensive properties are the density, refractive index, dielectric constant, percentage composition, and the various molar quantities (see Section II.B).

Extensive quantities are directly proportional to the amount of the sample taken for measurement. The various energy quantities and the entropy are also extensive quantities when they refer to a phase or system as a whole, but their values per mole are intensive quantities.

The most frequently encountered thermodynamic functions in work on solutions are

The total energy or intrinsic energy	U
The enthalpy	$H = U + PV$
The entropy	S
The Gibbs free energy	$G = H - TS$
The Helmholtz free energy	$A = U - TS$
The heat capacities at constant pressure and at constant volume	$C_p = \left(\frac{\partial H}{\partial T}\right)_p$

The isothermal compressibility	$C_v = \left(\frac{\partial U}{\partial T}\right)_v$
The adiabatic compressibility	$\beta_T = -\left(\frac{\partial \ln V}{\partial P}\right)_T$
The thermal expansion coefficient	$\beta_s = -\left(\frac{\partial \ln V}{\partial P}\right)_s$
	$\alpha = \left(\frac{\partial \ln V}{\partial T}\right)_P$

The last three properties above are intensive.

The thermodynamic properties and others defined in terms of them are functions of the state, that is, their values depend only on the existing state of the system and not on the route by which that state has been reached.

### B. EQUATIONS OF STATE

If the nature and amounts of substances are specified, the volume, temperature, and pressure are related by an equation of the form:

$$V = f(T, P)$$

known as the equation of state. Thus only two of V, T, and P can be varied independently.

### C. CONVENTIONAL AND ABSOLUTE VALUES OF THERMODYNAMIC PROPERTIES

The existence of a true zero pressure, that of a perfect vacuum, is obvious, and the absolute zero temperature is equally familiar. The entropy of a pure substance also has a true zero, that of its pure crystalline solid form at zero (Kelvin) temperature, according to the third law of thermodynamics. The energy quantities U, H, G, A, however, do not have a natural zero, and are consequently measured relative to arbitrarily chosen standard states. Thus the total energy U of a compound is usually referred to that of its constituent elements either at absolute zero or at 25°C.

### D. PHYSICAL MEANING OF THERMODYNAMIC QUANTITIES

Temperature, pressure, and volume need no discussion. The total energy U is defined by the first law of thermodynamics

$$dU = q + w \quad (1)$$

where q is the heat absorbed and w the work done on the system in an infinitesimal change. Hence,  $\Delta U$  is measurable as the heat absorbed at constant volume, e.g., in bomb calorimetry. Solution calorimetry, on the other hand, is usually carried out at constant (atmospheric) pressure, and the heat absorbed in this case is identified as  $\Delta H$ . The entropy, and the free energies that involve it, are the least obvious of the thermodynamic functions, and textbooks of general thermodynamics should be consulted for a full explanation.<sup>1,7</sup> The Gibbs free energy G is the most important function in dealing with chemical equilibria, being so defined that it is a minimum for equilibrium at constant temperature and pressure. It may be thought of as the chemical analogue of potential energy in a mechanical system, and, in particular, as closely related to electrical energy through the equation for reversible electrical cells

$$\Delta G = -nEF \quad (2)$$

where  $n$  is the number of electrons transferred and  $E$  is the reversible potential for a cell operating at constant temperature and pressure. The change  $\Delta G$  in a process at constant temperature and pressure is equal in magnitude to the maximum reversible work which can be done by the process.

### E. THE LAWS OF THERMODYNAMICS

The first law of thermodynamics, also known as the law of conservation of energy, says that the quantity  $U$  defined by

$$dU = q + w$$

is a function of the state of a system. Here  $q$  is the heat absorbed by, and  $w$  is the work done on, the system. The second law concerns the behavior of the entropy ( $S$ ), stating that in a natural or spontaneous process taking place at a Kelvin temperature  $T$ , in which the system absorbs heat  $q$  from its surroundings,

$$dS > \frac{q}{T}$$

and that in a reversible change

$$dS = \frac{q}{T}$$

Processes in which  $dS < q/T$  cannot occur according to the second law, and are called unnatural processes.

In measurements of the heat capacity  $C_p$  of a pure substance at constant pressure, heat is added at temperature  $T$  under reversible conditions, so that

$$q = C_p dT$$

where

$$dS = \frac{C_p}{T} dT$$

and

$$\begin{aligned} S(T_2, P) &= S(T_1, P) + \int_{T_1}^{T_2} \frac{C_p}{T} dT \\ \text{or } S(T, P) &= I + \int_0^T \frac{C_p}{T} dT \end{aligned} \quad (3)$$

where  $I$  is an integration constant.

The third law of thermodynamics states that for a pure crystalline solid the integration constant  $I$  is zero, i.e., the entropy itself is zero at the absolute zero. (In some cases allowance has to be made for the existence of different states of nuclear spin, which persist at the absolute zero.) This law arises from the statistical nature of entropy, expressed by Boltzmann's famous equation

$$S = k \ln W \quad (4)$$

where  $W$  is the number of complexions (distinguishable states) of the system.

In a perfect crystal,  $W = 1$ , so  $S = 0$ .

Some authorities refer to a zeroth principle of thermodynamics, which amounts to a statement of the existence of temperature. Guggenheim<sup>1</sup> formulates this as, "If two systems are both in thermal equilibrium with a third system, then they are in thermal equilibrium with each other."

## F. DIFFERENTIAL RELATIONS BETWEEN THERMODYNAMIC FUNCTIONS

For a closed system, i.e., one which no matter enters or leaves, the first and second laws are summed up by the equations

$$\begin{aligned} dU &= TdS - PdV \\ dH &= TdS + VdP \\ dA &= -SdT - PdV \\ dG &= -SdT + VdP \end{aligned} \quad (5)$$

The last of these is the most important in solution thermodynamics, giving the very useful results

$$\left(\frac{\partial G}{\partial T}\right)_P = -S \quad (6)$$

$$\left(\frac{\partial G}{\partial P}\right)_T = V \quad (7)$$

Equation 6 with  $G = H - TS$  yields the very important Gibbs-Helmholz equation:

$$\frac{\partial}{\partial T} \left(\frac{G}{T}\right)_P = -H/T^2 \quad (8)$$

which may also be expressed as

$$\partial(G/T)/\partial(1/T) = H \quad (9)$$

Equations 5 to 9 are used in treating change of equilibrium constants with temperature and pressure.

## II. SOLUTIONS: PARTIAL MOLAR QUANTITIES; CHEMICAL POTENTIALS

### A. OPEN PHASES: THE CHEMICAL POTENTIAL

An open phase is one which matter is able to enter or leave. When a chemical substance is added to or removed from a phase (e.g., when water evaporates from a solution), the thermodynamic properties of the phase are altered. These changes are described by adding to Equation 5 terms representing the energy, enthalpy, or free energy associated with each substance added. Each such term takes the form: chemical potential of substance  $\times$  differential quantity added. Thus

$$\begin{aligned}
 dU &= TdS - PdV + \sum_i \mu_i dn_i \\
 dH &= TdS + VdP + \sum_i \mu_i dn_i \\
 dA &= -SdT - PdV + \sum_i \mu_i dn_i \\
 dG &= -SdT + VdP + \sum_i \mu_i dn_i
 \end{aligned}
 \tag{10}$$

where  $n_i$  denotes the number of moles of species  $i$  present in the phase. The last of these equations gives the clearest physical meaning to the chemical potential, since by considering the addition of  $dn_j$  mol of species  $j$  to a phase at constant temperature and pressure we find

$$\mu_j = \left( \frac{\partial G}{\partial n_j} \right)_{T, P, n_{i \neq j}}
 \tag{11}$$

The subscripts as usual denote which state variables are held constant during the partial differentiation;  $i \neq j$  means that the amounts of all species other than  $j$  are held constant.

### B. PARTIAL MOLAR QUANTITIES

For a phase such as a solution, any of the extensive thermodynamic properties (e.g.,  $V, H, U, S, A, G$ ) can be regarded as a function of the state variables  $P, T$ , and  $n_i$ . Using  $X$  to denote an extensive property in general, we can then define the partial molar value of  $X$  for component  $j$ , denoted  $\bar{X}_j$ , relation:

$$\bar{X}_j = (\partial X / \partial n_j)_{T, P, n_{i \neq j}}
 \tag{12}$$

(The term partial molal is often used instead of partial molar. In this context, either molar or molal means simply per mole, and has nothing to do with the molarity or molality concentration scales.)

The chemical potential of species  $j$  in the solution is thus identical with its partial molar Gibbs free energy:

$$\mu_j \equiv \bar{G}_j
 \tag{13}$$

A physical interpretation of the chemical potential of a substance is therefore that it is the free energy change per mole of substance added to the phase when the amount added becomes vanishingly small; or the Gibbs free energy change when 1 mol of the substance is added to an infinite amount of the phase, the temperature and pressure being held constant in either case.

### C. ADDITIVITY OF PARTIAL MOLAR QUANTITIES

Equation 12 can be integrated at constant temperature and pressure, with respect to the quantity of each component in turn. The components can be added in infinitesimal quantities, each proportional to the final amount of that component in the phase. This process can be described by

$$dn_i = n_i dx$$

where  $dx$  is the same for all components, and  $x$  increases from 0 to 1 during the integration.



$$dX = \sum_i \bar{X}_i dn_i = \sum_i (n_i \bar{X}_i) dx$$

Now the  $n_i$  are constants during the integration (since they describe the final state, and the relative amounts of the components remain unchanged as the additions proceed); hence, the  $\bar{X}_i$  are also constant since they depend on the temperature, pressure, and composition. The integration therefore gives

$$\begin{aligned} X_{\text{final}} - X_{\text{initial}} &= \left( \int_0^1 dx \right) \cdot \sum_i n_i \bar{X}_i \\ &= \sum_i n_i \bar{X}_i \end{aligned}$$

Furthermore,  $X_{\text{initial}}$  refers to the start of the process, when the amount of the phase is zero; so clearly  $X_{\text{initial}}$  is zero. The result is

$$X = \sum_i n_i \bar{X}_i \quad (14)$$

showing that the value of the extensive property  $X$  for a phase is composed additively of the partial molar values of its components, each weighted by the number of moles present. In particular,

$$G = \sum_i n_i \mu_i \quad (15)$$

### III. CHEMICAL POTENTIALS AND ACTIVITY COEFFICIENTS; STANDARD STATES AND COMPOSITION SCALES FOR NONELECTROLYTES AND ELECTROLYTES

#### A. ACTIVITIES OF COMPONENTS

The activity  $a_i$  of a component in a solution is a convenient alternative means of describing its chemical potential:

$$\mu_i = \mu_i^\circ + RT \ln (a_i/a_i^\circ) \quad (16)$$

Here the superscript  $^\circ$  denotes an arbitrarily chosen standard state for the component  $i$ .  $\mu_i^\circ$  is then called the standard chemical potential of  $i$ . It is conventional to choose the corresponding standard activity  $a_i^\circ$  as unity, giving the simpler relation:

$$\mu_i = \mu_i^\circ + RT \ln a_i \quad (17)$$

The reason for the logarithmic form requires some comment. In the simplest case, that of a single-component ideal gas phase containing  $n_1$  mol. Equations 14 and 7 give

$$\begin{aligned} G &= n_1 \mu_1 \\ (\partial G / \partial P)_{T, n_1} &= V = n_1 RT / P_1 \end{aligned}$$

hence

$$dG = n_1 RT d \ln P_1$$

and

$$\mu_i = \text{const} + RT \ln P_i \quad (18)$$

This means that the chemical potential approaches minus infinity as the pressure goes to zero, and the chemical potential is therefore an awkward quantity to discuss or tabulate for low pressures. Similar problems occur with solutions; in this case the logarithmic term involves the concentration instead of the pressure. However, when activities with appropriately chosen standard states are considered, no infinite values occur; they are always positive, tending to zero at infinite dilution.

To avoid problems concerned with units, Equation 18 may be rewritten as

$$\mu_i = \mu_i^\circ + RT \ln (P_i/P^\circ) \quad (19)$$

where  $\mu_i^\circ$  is the chemical potential of the gas at the standard pressure  $P^\circ$ .

## B. STANDARD STATES

It must be emphasized that the choice of standard state is arbitrary; indeed, it is sometimes convenient to use different standard states for the same substance in the same solution. There is nothing arbitrary about the chemical potential itself; for a component of a given solution at a given temperature and pressure, its value is uniquely defined. It follows from Equation 17 that if we change the standard state, we also change the value of the activity.

In some cases it is convenient to use an actual physically realizable state as the standard state. In the thermodynamics of mixed liquid nonelectrolytes, the usual choice is the pure liquid component at the same temperature and pressure as the solution. With this choice, the activity of any component must lie between 0 and 1 at equilibrium. This standard state is also almost invariably adopted for the solvent component of electrolyte solutions. Thus the activity of pure water is defined as unity, and the water activity in any solution is

$$a_w = P_w^*/P_w^{\circ*} \approx P_w/P_w^\circ \quad (20)$$

The starred pressure symbol denotes the fugacity, an idealized partial pressure, which can be evaluated from the actual partial pressure  $P$  by the use of data on the nonideal gas behavior of the vapor.<sup>3,5</sup> The superscript zero refers to pure liquid solvent at the same temperature and hydrostatic pressure as the solution.

## C. CHEMICAL POTENTIALS IN ELECTROLYTE SOLUTIONS

For substances that are solids at the temperature of interest, the use of the pure liquid as the standard state is inconvenient since it represents a metastable or unstable condition. Nevertheless, if the enthalpy and free energy of fusion are known, it is possible to retain this standard state for the solution, as is done, for example, in Hildebrand's<sup>8</sup> treatment of the solubility of solid nonelectrolytes.

For electrolytes, however, a standard state is required which recognizes the ionic character of the solution. This raises a problem peculiar to electrolyte solutions, which must now be discussed. We may define the chemical potential of the ion of species  $i$  by

$$\mu_i = \left( \frac{\partial G}{\partial n_i} \right)_{n_j, n_s, T, P} \quad (21)$$

where  $j$  refers to all ionic species other than  $i$  and  $s$  to the solvent. However, the physical operation represented by Equation 21 cannot be carried out: there is no way in which we

can add to the solution ions of species  $i$  only, because only an electrolyte with equal amounts of positive charge on its cations and negative charge on its anions can be handled. For the electrolyte (formula B) as a whole there is no difficulty; the definition

$$\mu_B = \left( \frac{\partial G}{\partial n_B} \right)_{n_i, T, P} \quad (22)$$

represents a physically realizable process.

Equation 21 is actually incomplete in that it does not recognize that in adding charged ions of one species only, we will build up a charge in the solution. The free energy required to build up this charge from zero is in principle calculable from electrostatic theory, but will depend on the shape of the body of solution involved. Guggenheim<sup>3</sup> proposed the use of the "electrochemical potential" for individual ionic species as a way of avoiding this difficulty. The internal electrical potential  $\psi_{in}$  of any phase, charged or not, may be defined as the work done in bringing a unit of electrical charge from infinity to the interior of the phase. Then the free energy of the phase is the electrochemical potential  $\mu'_i$ .

$$\mu'_i = \mu_i + z_i F \psi_{in}$$

where  $F$  is the faraday and  $z_i$  is the (signed) charge number of the ion. This concept finds its main application in the study of electrodes and other charged interfaces. For the present problem, it suffices to note that provided the internal electrical potential is the same, differences in electrochemical potential are equal to differences in chemical potential defined by Equation 21. This overcomes the conceptual difficulty, but not the physical obstacle that we cannot actually add one kind of ion only. The consequence of this fact of life is that there is no rigorous method of measuring the chemical potential of a single ionic species; all experimental methods lead, if fully analyzed, to values for the chemical potential of an electrically neutral assemblage of ions, or else to differences between the chemical potentials of electrically equivalent amounts of ions of the same sign. Theoretical treatments, on the other hand, frequently lead to calculated values for the chemical potentials of single ionic species. In order to compare these with experiment, they must be combined to give the chemical potential of an electrically neutral assemblage.

#### D. ACTIVITY, ACTIVITY COEFFICIENTS, AND STANDARD STATES

Accepting the conventional use of chemical potentials of individual ionic species, we may write

$$\mu_i = \mu_i^\circ + RT \ln a_i \quad (23)$$

This places no restriction on the choice of standard state. Several different choices are in common use for electrolytes.

First, when the composition of the solution is described in terms of the molality scale, the standard state is the "hypothetical one-molal solution" of the ion. It is so chosen that as the molality approaches zero, the ratio  $a_i/m_i$  tends to unity. This ratio is defined as the molal activity coefficient  $\gamma_i$ :

$$\gamma_i = a_i/m_i; \gamma_i \rightarrow 1 \text{ as } m \rightarrow 0 \quad (24)$$

$$\mu_i = \mu_{i(m)}^\circ + RT \ln (m_i \gamma_i) \quad (25)$$

The additional subscript ( $m$ ) has been added to  $\mu_i^\circ$  to emphasize that the standard state in question applies to the molality scale.

There is an awkward problem of dimensions concealed in Equations 24 and 25. The activity coefficient  $\gamma$  is a dimensionless quantity, tending to 1 at infinite dilution. The molality  $m_i$ , on the other hand, has dimensions  $\text{mol kg}^{-1}$ . Strictly speaking, then, Equations 24 and 25 should be written

$$\begin{aligned}\gamma_i &= a_i m^\circ / m_i \\ \mu_i &= \mu_{i(m)}^\circ + RT \ln (m_i \gamma_i / m^\circ)\end{aligned}$$

where  $m^\circ$  is the unit molality, i.e.,  $1 \text{ mol kg}^{-1}$ . The inconvenience of inserting the  $m^\circ$  factor in all expressions deriving from Equation 25, including equilibrium constants, is, however, sufficient to deter all but the most rigorously minded from doing so, and we shall use the handier form of Equation 25.

The standard state has the same composition as a real 1 molal solution, but its hypothetical character involves the imagined absence of all interactions between ions due to their charge, size, and other relevant properties. In this respect, the analogy between the ideal gas standard state of 1 standard atmosphere pressure and an actual gas at the same pressure is useful. In particular, the standard state must be such that Equations 24 and 25 hold at all temperatures and pressures. It follows from Equations 7 and 9 that the partial molar enthalpy and partial molar volume of the ion have the same values in the standard state as at infinite dilution. Also,  $\gamma_i$  must be unity in the standard state. We see that the standard state is an imaginary one in which the molality of the ion is  $1 \text{ mol kg}^{-1}$ , but all the partial molar functions not involving the entropy have the same value as in the actual infinitely dilute solution.

Second, for the molarity scale ( $c_i =$  moles of ion  $i$  per liter), a different standard state and activity coefficient are used: the hypothetical 1 molar solution and the molar activity coefficient ( $\gamma_i$ ):

$$\mu_i = \mu_{i(c)}^\circ + RT \ln (c_i \gamma_i) \quad (26)$$

Again the standard state is chosen so that  $\gamma_i \rightarrow 1$  as  $c \rightarrow 0$ .

Some care is needed in the use of thermodynamic relations derived from Equation 26 by differentiation with respect to temperature or pressure, e.g., from Equation 6 or 7. It must be remembered that, unlike the molality,  $c$  varies with temperature and pressure.

Third, the mole fraction scale often appears in theoretical treatments, and very recently has come into practical use for very concentrated electrolytes.<sup>9</sup> The standard state is now one that has unit mole fraction of the solute species concerned, but in other respects has the properties of the solute in infinitely dilute solution. This is an even more theological concept than the hypothetical molal and molar solutions.

$$\mu_i = \mu_{i(x)}^\circ + RT \ln x_i f_i \quad (27)$$

where  $f_i$  is the rational or mole-fraction scale activity coefficient.

## E. MEAN ACTIVITIES AND ACTIVITY COEFFICIENTS

Thermodynamic measurements yield chemical properties not of individual ionic species, but of electrolytes as a whole. Taking the general formula to be  $M_{\nu_1} X_{\nu_2}$ , where the cation  $M$  has charge  $= z_1 e$  and the anion  $X$  has charge  $z_2 e$ , we have

$$\nu_1 z_1 = -\nu_2 z_2 \quad (28)$$

for electrical neutrality. The chemical potential of the electrolyte is

$$\begin{aligned}\mu(M_{\nu_1} X_{\nu_2}) &= \nu_1 \mu(M^{z_1e}) + \nu_2 \mu(X^{z_2e}) \\ &= \mu^\circ(M_{\nu_1} X_{\nu_2}) + \nu_1 RT \ln(m_1 \gamma_1) + \nu_2 RT \ln(m_2 \gamma_2)\end{aligned}\quad (29)$$

Here the  $\mu^\circ$  term is a combination of those for the separate ions.

$$\mu^\circ(M_{\nu_1} X_{\nu_2}) = \nu_1 \mu^\circ(M^{z_1e}) + \nu_2 \mu^\circ(X^{z_2e})$$

More briefly, putting B for the formula of the electrolyte and denoting the cation by 1 and the anion by 2:

$$\mu_B = \mu_B^\circ + RT \ln(m_1^{\nu_1} m_2^{\nu_2}) + RT \ln(\gamma_1^{\nu_1} \gamma_2^{\nu_2})\quad (30)$$

The mean molality and mean activity coefficient are now defined as

$$m_{\pm} = (m_1^{\nu_1} m_2^{\nu_2})^{1/\nu}\quad (31)$$

$$\gamma_{\pm} = (\gamma_1^{\nu_1} \gamma_2^{\nu_2})^{1/\nu}\quad (32)$$

where  $\nu = \nu_1 + \nu_2$ , so that Equation 30 becomes

$$\mu_B = \mu_B^\circ + \nu RT \ln(m_{\pm} \cdot \gamma_{\pm})\quad (33)$$

In single electrolytes,  $m_{\pm}$  is easily evaluated from the molality  $m$  and the formula, e.g.,  $m_{\pm} = m$  for 1-1, 2-2, or 3-3 electrolytes, and  $m_{\pm} = 4^{1/3} m$  for 1-2 and 2-1 electrolytes. In mixtures,  $m_{\pm}$  can be evaluated from Equation 31 for any arbitrary choice of the electrolyte B, subject to the condition of electrical neutrality.

The mean activity coefficient is the commonly tabulated quantity, and the subscript ( $\pm$ ) is often omitted from tables and equations where no ambiguity is likely to arise.

## F. RELATIONS BETWEEN ACTIVITY COEFFICIENTS ON DIFFERENT SCALES

Occasionally it is necessary to convert activity coefficients for one concentration scale to those for another, in particular to convert molal activity coefficients  $\gamma$  to molar activity coefficients  $y$ . The relationship can always be established by noting that the chemical potential of a substance in a given solution is unaffected by the choice of composition scale, but the standard states for different scales will differ by a constant amount (which may, however, change with temperature). The amount of this constant difference is fixed by the requirement that as the solution approaches infinite dilution of all components, all the solute activity coefficients must approach unity. (This condition applies to all the concentration scales used for electrolytes, but not to the case of liquid mixtures where the pure liquid component is the standard state.)

The most often needed conversion is between the molality and molarity scales, for which:

$$\gamma_{\pm} = \frac{c}{m d_s} y_{\pm}\quad (34)$$

where  $d_s$  is the density of the pure solvent. Calculation of the ratio  $c/m$  of course requires a knowledge of the density of the solution, or of the apparent or partial molar volumes of the solute components.

**G. THE SOLVENT CHEMICAL POTENTIAL, SOLVENT ACTIVITY, AND THE OSMOTIC COEFFICIENT**

For the solvent s

$$\mu_s = \mu_s^\circ + RT \ln a_s \quad (35)$$

where the standard state is by convention the (real) pure solvent at the same temperature and hydrostatic pressure as the solution. Hence, the activity of the pure solvent is unity. In dilute solutions of electrolytes, the activity, and even the activity coefficient of the solvent are very little different from unity, so that the reporting of solvent properties in these terms requires a large number of significant figures. To overcome this problem and to simplify many calculations the osmotic coefficient  $\phi$  is defined by

$$\phi = -1000 \ln a_s / (M_s \sum_k \nu_k m_k) \quad (36)$$

where  $M_s$  is the molar mass of the solvent, and the electrolyte k is present at molality  $m_k$ ; 1 mol of the electrolyte k gives  $\nu_k$  mol of ions in solution.

The corresponding molar scale osmotic coefficient is seldom used. The osmotic coefficient is so defined that it must tend to unity at infinite dilution of all solutes, i.e., it recognizes the fact that Raoult's law for the solvent component becomes exact at infinite dilution.

**IV. THE GIBBS-DUHEM RELATION; VARIOUS FORMS FOR TWO- AND MULTICOMPONENT SYSTEMS****A. THE GIBBS-DUHEM EQUATION**

A general differentiation of Equation 14 at constant temperature and pressure gives

$$dX = \sum_i n_i d\bar{X}_i + \sum_i \bar{X}_i dn_i \quad (37)$$

However, by Equation 13

$$dX = \sum_i \bar{X}_i dn_i \quad (38)$$

Hence

$$\sum_i n_i d\bar{X}_i = 0 \quad (39)$$

gives a relation between the values of any partial molar extensive property for the components of a solution. This trivial-seeming result is of enormous importance in solution thermodynamics.

When X represents Gibbs free energy, it becomes

$$\sum_i n_i d\mu_i = 0 \quad (40)$$

for any change of composition at constant T and P.

## B. RELATION BETWEEN MEAN ACTIVITY COEFFICIENT AND OSMOTIC COEFFICIENT

Since the chemical potentials in the standard states are independent of composition, Equations 40, 33, and 36 give for a single electrolyte solution

$$\nu m d \ln(m\gamma_{\pm}) = -(1000/M_2) d \ln a_2 = \nu d(\ln \phi) \quad (41)$$

$$d \ln \gamma_{\pm} = d \phi + (\phi - 1) dm/m \quad (42)$$

Integrating from  $m = 0$  (where  $\ln \gamma_{\pm} = 0$ ) we obtain

$$\ln \gamma_{\pm} = \phi - 1 + \int_0^m \frac{\phi - 1}{m} dm \quad (43)$$

Another manipulation of Equation 41 yields

$$\phi = 1 + \frac{1}{m} \int_0^m m d \ln \gamma_{\pm} \quad (44)$$

Equation 43 is used when vapor pressure measurements have been made on a solution, yielding values of  $\phi$  via Equations 36 and 20. It is clear from Equation 43 that the measurements must be made down to as low concentrations as possible, and must be spaced closely enough to permit accurate evaluation of the integral. However, with electrolyte solutes the limiting behavior of the osmotic coefficient at low concentrations makes Equation 43 impractical in the form shown. This is because

$$\phi \rightarrow 1 - Am^{1/2} \text{ as } m \rightarrow 0$$

where  $A$  is the limiting Debye-Hückel slope for the osmotic coefficient. Hence, the integral in Equation 43 becomes

$$-A \int_0^m m^{-1/2} dm$$

in which the integrand approaches  $-\infty$  as  $m \rightarrow 0$ .

This difficulty is overcome by changing the independent variable from  $m$  to  $m^{1/2}$  when Equation 44 becomes

$$\ln \gamma_{\pm} = \phi - 1 + 2 \int_0^{m^{1/2}} \frac{\phi - 1}{m^{1/2}} d m^{1/2} \quad (45)$$

in which the integrand now approaches the finite value  $-A$  as  $m \rightarrow 0$ . The fact that  $A$  is calculable from interionic attraction theory assists in drawing the curve of  $(\phi - 1)/m^{1/2}$  vs.  $m^{1/2}$  in the region where experimental results become inaccurate.

The vast majority of vapor pressure measurements on electrolyte solutions are made by the isopiestic method (see Chapter 5). In this method, a known amount of the solute under study is placed in a small silver or platinum dish, and another dish contains a known amount of a reference solute such as sodium chloride; appropriate amounts of water are added (or already present in the stock solutions if the solutes are used in this form), and the dishes are placed in a desiccator on a copper or silver block to ensure good thermal contact between them. The desiccator is evacuated of air as far as possible and held in a thermostat for a

day or two, with mechanical rocking to keep the solutions uniform. Under these conditions water passes from one solution to the other through the vapor phase until the vapor pressures (and hence the water activities) are equal. The equilibrium molalities  $m$  and  $m_{\text{ref}}$  are then determined by weighing the dishes, and are related to the osmotic coefficients by

$$\begin{aligned} \nu m \phi &= \nu_{\text{ref}} m_{\text{ref}} \phi_{\text{ref}} \\ \phi &= \frac{\nu_{\text{ref}} m_{\text{ref}}}{\nu m} \phi_{\text{ref}} \end{aligned} \quad (46)$$

The ratio  $(m_{\text{ref}}/m)$  is called the isopiestic ratio. In practice it is found that  $\phi$  can be measured with  $\sim 0.1\%$  accuracy by this method at molalities down to about  $0.1 \text{ mol kg}^{-1}$ . With 1-1, 1-2, and 2-1 electrolytes, this is low enough to permit a reasonably accurate estimate of the integrand in Equation 45 between  $0.1 \text{ m}$  and zero concentration (where its value is  $-A$ ), and hence to determine true values of  $\gamma_{\pm}$ . For higher valency-type electrolytes, however, the gap in the integrand between  $0.1 \text{ m}$  and zero concentration is usually too large for this method to be applied. The activity coefficients above  $0.1 \text{ m}$  can then be evaluated only relative to the value at  $0.1$ :

$$\ln \gamma_{\pm}(m) - \ln \gamma_{\pm}(m = 0.1) = \phi(m) - \phi(m = 0.1) + 2 \int_{m=0.1}^m \frac{\phi - 1}{m^{1/2}} dm \quad (47)$$

and recourse must be had to EMF (see Chapter 4) or freezing point studies to determine  $\ln \gamma_{\pm}(m = 0.1)$ .

Equation 44 finds its main application in cases where  $\gamma_{\pm}$  has been found by EMF measurements, and osmotic coefficients are required. The integral may be evaluated graphically or analytically. The results of measurements of activity coefficients are often given in the form of a Debye-Hückel expression plus a power series in  $m$

$$\ln \gamma_{\pm} = -\frac{\alpha m^{1/2}}{1 + \beta m^{1/2}} + \sum_{i=1}^{\dots} B_i m^i \quad (48)$$

for which Equation 47 becomes

$$\phi = 1 - \frac{\alpha m^{1/2}}{3} F(\beta m^{1/2}) + \sum_{i=1}^{\dots} \frac{i}{i+1} B_i m^i \quad (49)$$

where

$$F(x) = 3 [1 + x - 2 \ln(1 + x) - 1/(1 + x)]/x^3 \quad (50)$$

The function  $F(\beta m^{1/2})$  approaches unity as  $m \rightarrow 0$ . The factor  $\alpha/3$  in Equation 49 is the constant  $A$  referred to in the discussion of the integration of Equation 45.

In a solution with several solutes besides the solvent  $S$ , the Gibbs-Duhem relation becomes

$$(1000/M_s) d \ln a_s + \sum_i \nu_i m_i d \ln \gamma_{\pm i} = 0 \quad (51)$$

where the summation is carried over all the solute electrolytes.



## V. IDEAL SOLUTIONS; ENTROPY OF MIXING ON VARIOUS STATISTICS; REGULAR SOLUTIONS; ATHERMAL SOLUTIONS

### A. IDEAL SOLUTIONS

The ideal solution is defined by the condition that the chemical potential of component  $i$  at all compositions is given by

$$\mu_i = \mu_i^\circ(x) + RT \ln x_i \quad (52)$$

Hence the activity coefficients  $f_i$  are unity at all concentrations. If there are only two components, it is sufficient to specify that one of them obeys Equation 52; it can then be proved by the Gibbs-Duhem equation that Equation 52 must hold for the other component, also. It should be noted that though the mole fraction scale activity coefficient  $f_i$  is unity, this does not hold for the molal activity coefficient  $\gamma$  or the molar activity coefficient  $y$  in an ideal solution.\* Consider a nonelectrolyte A, which forms an ideal solution in the solvent S, at molality  $m$ , and let  $n_s^\circ$  denote the number of moles of S in 1 kg of pure solvent. Then

$$\mu_A = \mu_A^\circ(x) + RT \ln \frac{m}{m + n_s^\circ} \quad (53)$$

$$\mu_A = \mu_A^\circ(m) + RT \ln m\gamma_A \quad (54)$$

Hence,  $\ln \gamma = B/(m + n_s^\circ)$  where  $B$  is a constant to be fixed by the condition  $\gamma_A \rightarrow 1$  as  $m \rightarrow 0$ . Thus,  $B = n_s^\circ$ , and  $\gamma_A = 1/(1 + m/n_s^\circ)$  for an ideal solution of a nonelectrolyte. For an ideal solution of an electrolyte in water (an unrealizable case) we should obtain

$$\gamma_\pm = 1/(1 + 0.018 \nu m) \quad (55)$$

where  $\nu$  is the ion number defined in Section III.E. This expression is found as a term in some versions of the Debye-Hückel equation, when it is argued that the solution would be ideal but for the ion-ion interactions.

Ideal solutions have (as a necessary consequence of Equation 52) the property of mixing without enthalpy or volume changes, i.e., the partial molar enthalpies and volumes of the components in solution are the same as those of the pure liquids. One can probably say with safety that no actual solution is known that conforms exactly to the ideal solution model, but mixtures of substances differing only in isotopic composition come very close to it, and Equation 52 can also be shown to hold for the solvent as a limiting case in very dilute solutions.

### B. THE ENTROPY OF MIXING

When  $n_1$  mol of substance 1 are mixed with  $n_2$  mol of 2 at constant temperature to form a single phase, the entropy of mixing  $\Delta S_{\text{mix}}$  is defined by:

$$\Delta S_{\text{mix}} = S(\text{solution}) - n_1 \bar{S}_1^\circ - n_2 \bar{S}_2^\circ \quad (56)$$

where the superscript zero refers to the pure substances.

If the solution is ideal, it follows from Equation 52 that

\* One may define  $\phi = 1$ ,  $\gamma_\pm = 1$  as an alternate reference pattern of solution behaviour in the molality system; see Chapter 3, Equations 25 through 33.

$$\Delta S_{\text{mix}} (\text{ideal}) = -R(n_1 \ln x_1 + n_2 \ln x_2) \quad (57)$$

where the mole fraction  $x_1 = 1 - x_2 = n_1/(n_1 + n_2)$ . Also, the partial molar entropies are

$$\bar{S}_1 = S_1^\circ - R \ln x_1; \bar{S}_2 = S_2^\circ - R \ln x_2 \quad (58)$$

These equations clearly generalize for any number of ideal components.

The statistical mechanics of the entropy of mixing of molecules of differing shape and size have been intensively studied.<sup>10</sup> Flory and Huggins, dealing with the problem of long, flexible, polymer molecules dissolved in normal small-molecular solvents such as benzene, concluded that the entropy of mixing should be given more accurately by

$$\Delta S_{\text{mix}} = -R(n_1 \ln \Phi_1 + n_2 \ln \Phi_2) \quad (59)$$

where  $\Phi$ , the volume fraction of the component, has replaced the mole fraction of Equation 57.

Since  $\Phi_1 = n_1 \bar{V}_1 / (n_1 \bar{V}_1 + n_2 \bar{V}_2)$ , the Flory-Huggins equation reduces to the ideal mixing Equation 57 only when  $\bar{V}_1 = \bar{V}_2$ .

Solutions which obey Equation 59 as regards  $\Delta S_{\text{mix}}$ , but which also have the ideal properties of no volume change or enthalpy change on isothermal mixing, are called athermal solutions.

The expression Equation 59 is frequently and appropriately used in discussing polyelectrolyte solutions in regard to that part of the entropy of mixing that does not arise from coulombic interactions. It has also been used with some success in the case of simple electrolytes,<sup>11,12</sup> where it was first proposed by Glueckauf<sup>11</sup> for dealing with the entropy of mixing of solvated ions with the solvent. Its theoretical foundation in this case is a good deal more shaky, for the solute is now far different from the flexible chain model used for polymers.

A question with obvious relevance to the simple electrolyte problem is what is the observed behavior of the entropy of mixing of globular molecules of widely different sizes? This has been studied particularly by Marsh<sup>13,14</sup> and collaborators, who have measured free energies and enthalpies of mixing of cyclo-paraffin solutions of other cyclo-paraffins and of siloxanes such as octamethyl cyclo-tetrasiloxane. From these measurements, entropies of mixing are derived by the relation

$$\Delta G_m = \Delta H_m - T \Delta S_m \quad (60)$$

The general conclusion is that the entropy of mixing of these real molecules usually lies between the ideal value (Equation 57) and the value given by the Flory-Huggins or "volume-fraction statistics" (Equation 59) and somewhat nearer to the latter. To this extent, it supports the use of Equation 59 in calculations on electrolyte solutions.

In this case, however, it must be understood that it refers only to a part of the entropy of mixing, that part due to neither the coulombic forces between ions nor to the entropy changes that occur as the result of solvation of the ions or their effects on the structure of water, but due essentially to the differences of size between water molecules and (solvated) ions.

In many models of electrolyte solutions, starting with that of Debye and Hückel, the ions are treated as charged hard spheres, and the solvent as a structureless continuum separating them, characterized only by its dielectric constant; this is known as the primitive model. With this model the above discussion of the entropy of mixing is scarcely relevant. A more appropriate model would treat the water molecules as another collection of hard spheres. The entropy of mixing of hard spheres of different sizes has been calculated by

Lebowitz and Rowlinson,<sup>15</sup> and differs from the ideal value by amounts depending on both the ratio of diameters and the packing density. The complexity of the expressions is, however, such that they are unlikely to find general use in electrolyte theory except for molten salts.

### C. REGULAR SOLUTIONS

A "regular solution" is defined as one for which the entropy of mixing is given by the ideal expression Equation 52, but the enthalpy of mixing is nonzero, being given by

$$\Delta H_m = Wx_1x_2 \quad (61)$$

where  $W$  is a constant characterizing the interaction of the two species, and  $\Delta H_m$  is the enthalpy increase when 1 mol of solution is made at constant temperature by mixing  $x_1$  and  $x_2$  mol of the components. From this definition, it follows that the mole-fraction activity coefficients are

$$\begin{aligned} \ln f_1 &= (W/RT) x_2^2 \\ \ln f_2 &= (W/RT) x_1^2 \end{aligned} \quad (62)$$

Further, it can be shown that when  $W > 2RT$  there will be a range of compositions for which the solution will separate into two phases: the upper critical solution temperature is given by  $T_c = W/2R$ .

This model is mainly used for mixtures of nonelectrolytes, sometimes in combination with Equation 59 instead of Equation 56 for the entropy of mixing. The regular solution is the next simplest approximation to the ideal solution. It is relevant to electrolyte solutions in suggesting an appropriate form for the "nonelectrolyte" interaction terms to be added to theoretical expressions for the coulombic contributions to the activity coefficient. The  $f_1$  and  $f_2$  in the above equations are referred to unity in the standard state of the pure liquid component. This is the standard state used for the solvent component in electrolytes, so Equation 52 suggests that the nonelectrolyte interactions will contribute to  $\ln a_+$ , a term of the form

$$\Delta \ln a_+ = (W/RT) x_1^2 \approx a m^2$$

The corresponding contribution to the osmotic coefficient  $\phi$  will be

$$\Delta \phi = a' m \quad (63)$$

where  $a$  and  $a'$  are constants.

By Equations 48 and 49, a similar term in the first power of  $m$  will appear in the expression for  $\ln \gamma$ . This argument gives a qualitative justification for the inclusion of first-order terms in  $m$  in the expressions for osmotic and activity coefficients. Higher integral powers are sometimes necessary as well.

## VI. COLLIGATIVE PROPERTIES

### A. FREEZING POINT DEPRESSION

Freezing point depression measurements provide a useful means of studying activities in electrolyte solutions and fill an important gap in the region below 0.1 m where the isopiestic method is insufficiently accurate. The only other feasible method in this region is the measurement of EMF of cells, and this is frequently impossible because no suitable reversible electrodes are known.

At the freezing point  $T_f$  of a solution, the chemical potential of the solvent in the solution is equal to the chemical potential of the pure solid solvent at  $T_f$ . The latter quantity can be calculated from the freezing point of the solvent by the Gibbs-Helmholtz equation, provided that the latent heat of fusion of the pure solvent and its temperature dependence are known. For the solvent S in the solution we use unprimed symbols, and for the pure solid, primed symbols. Then for equilibrium at temperature T

$$\mu_s^\circ(T) + RT \ln a_s(T) = \mu'_s(T) \quad (64)$$

$$\ln a_s(T) = [\mu'_s(T) - \mu_s^\circ(T)]/RT \quad (65)$$

For an infinitesimal change of composition, while equilibrium between solid and solution is maintained by a corresponding infinitesimal change in T:

$$\begin{aligned} \frac{d \ln a_s(T)}{dT} &= \frac{\partial}{\partial T} \left( \frac{\mu'_s}{RT} \right) - \frac{\partial}{\partial T} \left( \frac{\mu_s^\circ}{RT} \right) \\ &= \frac{\bar{H}'_s}{RT^2} - \frac{\bar{H}_s^\circ}{RT^2} \\ &= \frac{\Delta \bar{H}_f}{RT^2} \end{aligned} \quad (66)$$

where  $\Delta \bar{H}_f$  is the molar enthalpy of fusion of the pure solvent. In general,  $\Delta \bar{H}_f$  is not quite constant but is a function of T

$$\Delta \bar{H}_f = \Delta \bar{H}_f^\circ + \Delta \bar{C}_p (T - T^\circ) \quad (67)$$

where  $T^\circ$  is the freezing point of the pure solvent.

Integrating Equation 66, subject to Equation 67 with  $\Delta C_p$  assumed independent of T, gives

$$\ln a_s = \frac{-\Delta H_f^\circ}{RT} + \frac{\Delta C_p}{R} \left( \ln T + \frac{T^\circ}{T} \right) + D \quad (68)$$

where D is an integration constant.

To evaluate the integration constant, take the case of the pure solvent, where  $a_s = 1$  and  $T = T^\circ$ , finding

$$D = \frac{\Delta H_f^\circ}{RT^\circ} - \frac{\Delta C_p}{R} \ln T^\circ - \frac{\Delta C_p}{R}$$

so that

$$\ln a_s(T) = \frac{\Delta H_f^\circ}{R} \left( \frac{1}{T^\circ} - \frac{1}{T} \right) + \frac{\Delta C_p}{R} \left[ \ln \left( \frac{T}{T^\circ} \right) + \frac{T_f}{T} - 1 \right] \quad (69)$$

This equation may be simplified by expansion in powers for  $\Delta T/T^\circ$ , where  $\Delta T$  is the freezing point depression  $\Delta T = T^\circ - T$ , but there is little point in this in the age of personal electronic calculators. The left-hand side of Equation 69 reminds us that freezing point data give the solvent activity at the temperature of the freezing point of the solution concerned.

For dilute solutions, where T is no more than a degree or so below  $T^\circ$ , the difference

between  $\ln a_1$  for the same solution at  $T$  and at  $T^\circ$  is usually negligible. However, the freezing point method can be used at higher concentrations; in that case the conversion from  $T$  to  $T^\circ$  requires the use of data on enthalpies of dilution, as discussed in Section VII. These data are also needed in conversion from  $T^\circ$  to higher temperatures.

Activity coefficients may be obtained from freezing point data via Equations 69, 36, and 45. Alternative methods of calculating are available to give them more directly, but as both osmotic and activity coefficients are of interest there is no particular advantage in doing this.

## B. BOILING POINT ELEVATION

Boiling point elevation measurements may also be used to determine solvent activities, though they are not popular since the same information may be obtained more conveniently by high-temperature isopiestic measurements. The freezing point method assumes that only the pure solvent freezes out from a solution. With electrolyte solutes, this is generally true, but a long-standing discrepancy in the activity coefficients of ammonium chloride was resolved by the discovery that the solid phase in this case is a dilute solid solution. Similarly, the boiling point method assumes that the solute is involatile.

Direct measurement of the vapor pressure is important chiefly as having provided some of the standard osmotic coefficient data<sup>2</sup> for the reference electrolytes used in isopiestic measurements — e.g., NaCl, CaCl<sub>2</sub>, and H<sub>2</sub>SO<sub>4</sub>.

## C. OSMOTIC PRESSURE

The osmotic pressure of electrolyte solutions is of great biological importance, but its measurement is seldom used as a direct source of thermodynamic data on simple electrolytes owing to the difficulty of making genuinely semipermeable membranes for small ions. Because of the industrial importance of "reverse osmosis" in water purification, the basic thermodynamic relation is shown below.

In osmotic equilibrium across a truly semipermeable membrane, the solution under a pressure  $P = P^\circ + \Pi$  is in equilibrium with pure solvent at pressure  $P^\circ$  and at the same temperature. Hence, for the solvent component:

$$\mu_1(P) = \mu_1^\circ(P^\circ) \quad (70)$$

Now the pressure dependence of  $\mu_1$  is given by Equation 7:

$$\frac{\partial \mu_1}{\partial P} = \bar{V}_1 \quad (71)$$

where  $\bar{V}_1$  is the partial molar volume of the solvent. Making the approximation of treating this as independent of the pressure (i.e., depending on temperature and composition only), we have for a given temperature and composition by integrating Equation 71

$$\begin{aligned} \mu_1(P) &= \mu_1(P^\circ) + \bar{V}_1(P^\circ - P) \\ &= \mu_1^\circ(P^\circ) + RT \ln a_1(P^\circ) + \bar{V}_1(P^\circ - P) \end{aligned}$$

Hence, by Equation 70

$$\ln a_1(P^\circ) = \bar{V}_1(P^\circ - P)/RT = -\Pi\bar{V}_1/RT \quad (72)$$

from which follow various approximate forms, including the familiar equation for dilute nonelectrolyte solutions

$$\Pi \approx RTc \quad (73)$$

Equation 71 with 36 shows that the osmotic pressure is related to the osmotic coefficient  $\phi$  and the molality

$$\Pi = RT \nu m \phi M_s / 1000 \bar{V}_s \quad (74)$$

This is a case where a careful look at the units involved is required. If Equation 36 were written with proper attention to units, it would read

$$\phi = - \frac{1 \text{ kg m}^\circ}{M_s \nu m} \ln a_s \quad (75)$$

where  $m^\circ$  is unit molality ( $1 \text{ mol} \cdot \text{kg}^{-1}$ ) and the 1000 in Equation 36 is recognized as really meaning 1000 g.

Hence, Equation 74 should strictly be

$$\Pi = (RT M_s / \bar{V}_s) (1 \text{ mol kg}^{-1}) (\nu m \phi / m^\circ) \quad (76)$$

e.g., for 0.1 m aqueous NaCl at 25°C, taking  $\phi = 0.932$ ,  $\bar{V}_s = 18.0 \text{ cm}^3 \cdot \text{mol}^{-1}$ ,  $M_s = 18.016 \text{ g} \cdot \text{mol}^{-1}$ , and  $\nu = 2$ , we obtain

$$\begin{aligned} \Pi &= 8.314 \times 298.15 \times 18.016 \times 0.2 \times 0.932 / 1000 \times 18.0 \text{ J} \cdot \text{cm}^{-3} \\ &= 0.462 \text{ J} \cdot \text{cm}^{-3} \\ &= 4.62 \times 10^5 \text{ Pa} = 4.62 \text{ bar} \end{aligned}$$

It should be noted that the basic osmotic pressure Equation 72 holds for any mixed electrolyte or nonelectrolyte solution, since it involves directly only solvent properties  $a_s$ ,  $\bar{V}_s$ , and  $M_s$ . The first two of these are, of course, functions of the composition, though for dilute solutions  $\bar{V}_s$  is close to the pure solvent value. In a solution of a single solute at concentration  $c$ ,  $\bar{V}_s$  is conveniently calculated from

$$\bar{V}_s = M_s / \left( \rho - c \frac{\partial \rho}{\partial c} \right) \quad (77)$$

where  $\rho$  is the density of the solution.

#### D. DERIVATION OF THERMODYNAMIC QUANTITIES FOR ELECTROLYTE SOLUTIONS FROM ELECTROMOTIVE FORCES OF CELLS

The applications of electromotive force measurements are the subject of another chapter in this volume. Here we give only some basic thermodynamic relations. If an electrical cell with perfectly reversible electrodes is held at constant temperature and pressure, and its EMF  $E$  is measured under conditions of zero current drain, the Gibbs free energy change for the cell reaction is given by

$$\Delta G = -nEF \quad (78)$$

where  $n$  is the number of electrons transferred in the equation for the cell reaction, and  $F$  is the faraday. Equation 78 implies that  $E$  is counted as positive for the spontaneous cell reaction, so that the spontaneous free energy change is negative. In other words,  $E$  is given the sign of the electrode from which electrons are abstracted in the spontaneous cell reaction.

For a particular cell,  $E$  depends on the chemical potentials of all the substances involved in the cell reaction. If these are all taken to be in their standard states, the EMF is the standard cell potential  $E^\circ$ , and Equation 78 then gives the standard free energy change for the spontaneous reaction,  $\Delta G^\circ$ . Since the electrode constituents themselves are usually pure substances (or are at least in states that do not alter with the solution composition), the quantity  $E - E^\circ$  can be expressed in terms of the activities of the components of the cell solution. It should be noted that these may include the solvent as well as the electrolyte and nonelectrolyte solutes, and it is essential to start the thermodynamic analysis of EMF data by writing out the chemical equations for the electrode and cell reactions, to be sure that no relevant component is overlooked.

From Equation 78, other thermodynamic quantities such as activity coefficients and equilibrium constants can be derived. Also, by measuring the temperature dependence of  $E$ , the entropy change and hence the enthalpy change can be obtained:

$$\Delta S = nF \left( \frac{\partial E}{\partial T} \right)_{P, \text{comp}}$$

$$\Delta H = \Delta G + T\Delta S \quad (79)$$

Some care must be taken in assessing the reliability of entropy and enthalpy data obtained in this way.

For a cell reaction involving a one-electron transfer ( $n = 1$ ), Equation 78 shows that an error of 0.1 mV in  $E$  corresponds to approximately 10 J/mol uncertainty in  $\Delta G$  for the cell reaction. The same error in  $\Delta E$  over a  $10^\circ$  temperature range, i.e., an error of  $10^{-5}$   $\text{VK}^{-1}$  in  $\partial E/\partial T$ , corresponds to  $1 \text{ JK}^{-1} \text{ mol}^{-1}$  in  $\Delta S$ , and therefore to  $\sim 300 \text{ J mol}^{-1}$  in  $\Delta H$ . These are realistic limits for the best EMF data, and it follows that enthalpy changes can often be obtained more reliably from direct calorimetric studies.

## VII. ENTHALPY AND VOLUME PROPERTIES; APPARENT MOLAR QUANTITIES

### A. TEMPERATURE AND PRESSURE DEPENDENCE OF ACTIVITY COEFFICIENTS

The chemical potential of component  $i$  of a solution may be written:

$$\frac{\mu_i}{T} = \frac{\mu_i^\circ}{T} + R \ln m_i \gamma_i \quad (80)$$

Applying the Gibbs-Helmholtz relation Equation 9 to Equation 80 gives, since  $m_i$  is independent of  $T$ :

$$\left( \frac{\partial \ln \gamma_i}{\partial T} \right)_{P, \text{comp}} = \frac{H_i^\circ - H_i}{RT^2} \quad (81)$$

Because the standard state is so chosen that at all temperatures  $\ln \gamma_i \rightarrow 1$  as  $m \rightarrow 0$ , it follows that

$$\lim_{m \rightarrow 0} H_i = H_i^\circ$$

confirming an earlier remark that the partial molar enthalpy in the standard state is the same as at infinite dilution. The term on the right of Equation 81 may therefore be written  $(\bar{H}_i^\circ$

–  $\bar{H}_i$ )/ $RT^2$  for any solute component. For the solvent, the corresponding result is

$$\left(\frac{\partial \ln a_s}{\partial T}\right)_{P,\text{comp}} = \frac{\bar{H}_s^\circ - \bar{H}_s}{RT^2} \quad (82)$$

where  $\bar{H}_s^\circ$  is the enthalpy of the pure solvent.

For an electrolyte B, applying Equation 81 to each ion, we find

$$\left(\frac{\partial \ln \gamma_{\pm}}{\partial T}\right)_{P,\text{comp}} = \frac{\bar{L}_B}{\nu RT^2} \quad (83)$$

where  $\bar{L}_B = \bar{H}_B - \bar{H}_B^\infty$  is the relative partial molar enthalpy of the electrolyte (i.e., relative to infinite dilution).

## B. PRESSURE DEPENDENCE OF ACTIVITY COEFFICIENTS

By a similar argument based on Equation 7, we find for the variation of activity coefficients with pressure at constant temperature and composition

$$\left(\frac{\partial \ln \gamma_{\pm}}{\partial P}\right)_{T,\text{comp}} = \frac{\bar{V}_B - \bar{V}_B^\circ}{\nu RT} \quad (84)$$

where  $\bar{V}_B$  is the partial molar volume of the solute, and also

$$\left(\frac{\partial \ln a_s}{\partial P}\right)_{T,\text{comp}} = \frac{\bar{V}_s - \bar{V}_s^\circ}{RT} \quad (85)$$

## C. PARTIAL MOLAR ENTHALPIES AND VOLUMES

Equations 82 to 85 involve the partial molar quantities corresponding to the extensives H and V.

$$\bar{H}_i = \left(\frac{\partial H}{\partial n_i}\right)_{T,P,n_j}; \quad \bar{V}_i = \left(\frac{\partial V}{\partial n_i}\right)_{T,P,n_j} \quad (86)$$

For electrolytes, both these partials vary with composition, the variation of  $\bar{H}$  being more pronounced than that of  $\bar{V}$ . It is possible in principle to approximate physically to the operations implied by Equation 86, e.g., when  $i$  is the solvent, a small amount of it can be added to the solution and  $\Delta H$  or  $\Delta V$  can be observed directly. This method is quite practical with nonelectrolytes, using, respectively, the isothermal dilution calorimeter<sup>16</sup> or the isothermal dilution dilatometer.<sup>17</sup> For electrolytes, however, the  $\sqrt{c}$ -dependence makes it difficult to use such methods at low enough concentrations. Most experimental methods therefore depend on measurement of apparent molar quantities and the analytical conversion of these to partials.

The apparent molar value  ${}^\phi X_B$  of the extensive X for the solute component B of a solution is defined by

$${}^\phi X_B = \frac{X - n_s \bar{X}_s^\circ}{n_B} \quad (87)$$

where  $n_s$  and  $n_B$  are the numbers of moles of the components present, X is the value of the extensive for the total quantity of solution ( $n_s + n_B$  mol), and  $\bar{X}_s^\circ$  is the molar extensive



for the pure solvent at the same temperature and pressure. Thus in the case of volume,  ${}^{\phi}V_B = (\text{volume of solution} - \text{volume of solvent before mixing})/\text{moles of solute}$ , or

$$V = n_B {}^{\phi}V_B + n_S \bar{V}_S \quad (88)$$

This is to be compared with

$$V = n_B \bar{V}_B + n_S \bar{V}_S \quad (89)$$

where  $\bar{V}_B$  and  $\bar{V}_S$  are the partial molar volumes.

By differentiating Equation 88 partially with respect to  $n_B$  we find

$$\bar{V}_B = {}^{\phi}V_B + n_B (d{}^{\phi}V_B/dn_B)_{n_S, T, P}$$

and since the molality  $m$  is defined for constant  $n_S$ , this becomes

$$\bar{V}_B = {}^{\phi}V_B + m(d{}^{\phi}V_B/dm) \quad (90)$$

$\bar{V}_S$  then follows from Equation 89.

The advantage of this method is that  ${}^{\phi}V_B$  can be determined directly from the composition of the solution and the densities of the solution and the pure solvent by Equation 87; the differentiation is carried out graphically or analytically using Equation 90.

For electrolytes, theory shows that the limiting behavior of  ${}^{\phi}V$  in dilute solutions is given by

$${}^{\phi}V = {}^{\phi}V^{\circ} + A m^{1/2} \quad (91)$$

where the limiting slope  $A$  is known from theory. Hence Equation 90 is transformed to

$$\bar{V}_B = {}^{\phi}V_B + 1/2 m^{1/2} (d{}^{\phi}V_B/d m^{1/2}) \quad (92)$$

before calculating the differential.

The limiting value  ${}^{\phi}V$  may be obtained by plotting  ${}^{\phi}V$  against  $m^{1/2}$  according to Equation 91, the extrapolation being guided by the requirement that the theoretical slope should be approached as  $m^{1/2} \rightarrow 0$ .

The accuracy with which  ${}^{\phi}V$  can be determined in this way depends essentially on the uncertainty in the quantity  $(\rho - \rho^{\circ})/m$ . Pycnometrically determined densities have errors of (at least) a few parts in a million, and the error in  ${}^{\phi}V$  is therefore inversely proportional to  $m$ . With higher valency types than 1-1 electrolytes, it is necessary to go to quite low concentrations ( $<0.01 m$ ) in order to reach the region of validity of Equation 91, and the errors become unacceptably large. They may be reduced by using a dilatometric method<sup>17</sup> for the dilute solutions. A stock solution is prepared of such concentration that  ${}^{\phi}V$  for it may be obtained, within say  $0.01 \text{ cm}^3 \text{ mol}^{-1}$  by density measurement. A known amount of the stock solution, containing  $n_B$  mol of solute, is then mixed isothermally with a much larger volume of solvent in a dilatometer, in which the volume change  $\Delta V$  on mixing can be directly observed in a calibrated capillary. The apparent molar volume of the solute in the solution after mixing is then given by

$${}^{\phi}V = {}^{\phi}V(\text{stock}) + \Delta V/n_B \quad (93)$$

For example, if  $0.5 \text{ cm}^3$  of  $2.0 M$  solution is mixed with water in a dilatometer of  $1 \text{ l}$  volume,

$n_B \approx 0.001$  mol, and  $\Delta V$  may be measured within  $\sim 2 \times 10^{-4}$  cm<sup>3</sup>, so that  ${}^{\phi}V$  for the final (0.001 *M*) solution is known within  $\pm 0.2$  cm<sup>3</sup> mol<sup>-1</sup>. The uncertainty in  $\Delta V$  arises mainly from variations in temperature before and after mixing; the figure quoted corresponds to a change of  $\sim 0.001$  K on the 1-l volume, which is well within the capacity of a good thermostat. To obtain the same accuracy in  ${}^{\phi}V$  by direct density measurements at 0.001 *M* would require an accuracy of  $1 \times 10^{-7}$  g cm<sup>-3</sup> in both  $\rho$  and  $\rho^{\circ}$ .

Enthalpy changes for electrolytes are measured in two main ways. First, the enthalpy of solution of the solid electrolyte is measured in a calorimeter<sup>18</sup> in which usually a known quantity of the solute is contained in a thin-walled bulb that is broken under a known mass of solvent, and the heat change is measured against an electrical heating standard. Second, the enthalpy of dilution of various solutions is measured.<sup>19,20</sup> This is frequently done<sup>19</sup> in a twin calorimeter. In one vessel, pure solvent is mixed with pure solvent; in the other, a similar amount of a solution is mixed with the pure solvent. Stirring is necessary, and in this method its heating effects are largely cancelled. The temperature difference between the two vessels is followed and kept close to zero by heating one or the other liquid electrically. Another technique uses an isothermal dilution calorimeter<sup>16</sup> in which solution is progressively added to the pure solvent, electrical heating (and cooling, if necessary) being used to hold the temperature constant. Both these methods measure changes in the apparent molar enthalpy,  ${}^{\phi}H$ , and after extrapolation to infinite dilution one obtains values of the relative apparent molar enthalpy  ${}^{\phi}L$ . From these values the partial molar enthalpies  $L_B$  and  $L_S$  (Equation 83) relative to infinite dilution may be calculated by methods similar to that discussed above for the volume.

### VIII. EXCESS THERMODYNAMIC PROPERTIES

An ideal solution has the following thermodynamic functions of mixing at constant temperature and pressure:

$$\begin{aligned}\Delta H_{\text{mix}} &= \Delta U_{\text{mix}} = 0 \\ \Delta V_{\text{mix}} &= 0 \\ \Delta S_{\text{mix}} &= -R \sum x_i \ln x_i \\ \Delta G_{\text{mix}} &= RT \sum x_i \ln x_i\end{aligned}\quad (94)$$

Molar excess functions,  $X^E$ , are defined by the general equation (where *X* denotes any extensive)

$$X^E = X(\text{actual}) - X(\text{ideal}) \quad (95)$$

and conveniently refer to 1 mol of the mixture. Hence, for example,

$$G^E = RT \sum x_i \ln f_i \quad (96)$$

If we consider an electrolyte solution containing 1 kg of solvent (= *s* mol of solvent) and *m<sub>i</sub>* mol of various ionic species *i*, its total free energy *G* is given by

$$\begin{aligned}G &= s \mu_s + \sum m_i \mu_i \\ &= s (\mu_s^{\circ} + RT \ln a_s) + \sum m_i [\mu_i^{\circ} + RT \ln (m_i \gamma_i)]\end{aligned}\quad (97)$$

For the corresponding ideal solution, where the activity coefficients  $f_i$  and  $f_i^{\circ}$  are unity:

$$G(\text{ideal}) = s \left( \mu_s^\circ + RT \ln \frac{s}{s + \sum m_i} \right) + \sum m_i \left( \mu_i^{\circ'} + RT \ln \frac{m_i}{s + \sum m_i} \right) \quad (98)$$

For the solvent, the standard states in Equations 97 and 98 are the same (the pure solvent); but for the solute species  $\mu_i^{\circ'}$  is not identical with  $\mu_i^\circ$ . To establish the relation between them, we note that  $\mu_i$  is independent of the composition scale

$$\begin{aligned} \mu_i &= \mu_i^\circ + RT \ln m_i + RT \ln \gamma_i \\ &= \mu_i^{\circ'} + RT \ln \frac{m_i}{s + \sum m_i} + RT \ln f_i \end{aligned} \quad (99)$$

Considering the special case when all  $m_i \rightarrow 0$ , and  $f_i$  and  $\gamma_i \rightarrow 1$ , Equation 99 gives

$$\mu_i^\circ = \mu_i^{\circ'} - RT \ln s \quad (100)$$

From Equations 97, 98, and 100 we find

$$(G - G_{\text{ideal}})/RT = \sum m_i \ln \gamma_i + s \ln a_s + (s + \sum m_i) \ln \frac{s + \sum m_i}{s} \quad (101)$$

Applying this to the case of a single electrolyte at molality  $m$ , and using

$$\begin{aligned} \sum m_i \ln \gamma_i &= \nu m \ln \gamma_\pm \\ \phi &= -\frac{s}{\nu m} \ln a_s \end{aligned}$$

we obtain for the excess free energy of the solution per mole of electrolyte present

$$\begin{aligned} \bar{G}^E &= (G - G_{\text{ideal}})/m \\ &= \nu RT \left( \ln \gamma_\pm - \phi + \frac{s + \nu m}{\nu m} \ln \frac{s + \nu m}{s} \right) \end{aligned} \quad (102)$$

Since  $s$  (in aqueous solutions at least, where  $s = 55.51$ ) is typically large compared to  $\nu m$ , we may expand the logarithm in the last term of Equation 102 to give

$$(s/\nu m) \ln(1 + \nu m/s) = 1 - \frac{1}{2}(\nu m/s) + \quad (103)$$

where

$$\bar{G}^E \approx \nu RT(\ln \gamma_\pm + 1 - \phi) \quad (104)$$

The approximate expression Equation 104 is treated in many papers as giving  $G^E$  exactly.\* Certainly the error is usually small, and being a function of  $m$  only, it cancels when comparing  $G^E$  values for different electrolytes of the same valency type; also, it disappears on taking derivatives of  $G^E$  at constant composition, as, for example,

\* With the alternate definition  $\gamma_\pm = 1$ ,  $\phi = 1$  as a reference pattern in the molality system, Equation 104 becomes the exact expression for the excess quantity in that system; see Chapter 3, Equations 25 through 33.

$$\begin{aligned}
 -S^E &= (\partial G^E/\partial T)_{p,m} \\
 V^E &= (\partial G^E/\partial P)_{T,m} \\
 H^E &= -RT^2(\partial G^E/\partial T)_{p,m}
 \end{aligned}
 \tag{105}$$

From Equation 101, however, the exact expression for  $G^E$  is

$$\bar{G}^E = RT[\nu \ln \gamma_{\pm} + (s/m) \ln f_{\pm}] \tag{106}$$

Here  $f_{\pm}$  is the mole-fraction scale activity coefficient of the solvent:  $f_{\pm} = a_{\pm}/x_{\pm}$ , where  $x_{\pm}$  is calculated counting each water molecule and ion as a separate particle.

## IX. MULTICOMPONENT SYSTEMS — THERMODYNAMIC RELATIONS; SALTING-OUT AND SALTING-IN EFFECTS

### A. THERMODYNAMIC RELATIONS FOR MULTICOMPONENT SOLUTIONS

The total Gibbs free energy  $G$  of a solution containing  $n_1, n_2, n_3$  mol of components 1, 2, 3, . . . , respectively, can be written in terms of the chemical potentials of the components

$$G = n_1 \mu_1 + n_2 \mu_2 + n_3 \mu_3 + \dots \tag{107}$$

One relation between the chemical potentials is the Gibbs-Duhem Equation 40. Another may be obtained by using the cross-differentiation relation of partial differential calculus. If  $W = f(x, y, \dots)$ , then

$$\frac{\partial}{\partial y} \cdot \frac{\partial W}{\partial x} = \frac{\partial}{\partial x} \cdot \frac{\partial W}{\partial y} = \frac{\partial^2 W}{\partial x \partial y} \tag{108}$$

This relation states that the order of two successive partial differentiations with respect to different variables is immaterial. From Equation 107

$$\mu_1 = \frac{\partial G}{\partial n_1} \quad \mu_2 = \frac{\partial G}{\partial n_2} \tag{109}$$

Applying Equation 108 to these results

$$\begin{aligned}
 \frac{\partial \mu_1}{\partial n_2} &= \frac{\partial}{\partial n_2} \left( \frac{\partial G}{\partial n_1} \right) = \frac{\partial}{\partial n_1} \left( \frac{\partial G}{\partial n_2} \right) \\
 &= \frac{\partial \mu_2}{\partial n_1}
 \end{aligned}
 \tag{110}$$

It is understood here that temperature, pressure, and all the  $n$ 's except the one that appears in the denominator of the partial are kept constant.

When using Equation 110 in solution thermodynamics, it is usual to express the composition in terms of the molality of each electrolyte present. In the case of a solvent  $S$  with two solutes 1 and 2, this amounts to putting

$$n_{\pm} = 1000 \text{ g}/M_{\pm}$$

$$n_1 = m_1$$

$$n_2 = m_2$$

so that Equation 110 becomes

$$\left(\frac{\partial \mu_1}{\partial m_2}\right)_{m_1} = \left(\frac{\partial \mu_2}{\partial m_1}\right)_{m_2} \quad (111)$$

Equations 40 and 110 make it possible in principle to determine the changes in chemical potentials of all the components of a solution from measurements of the chemical potential of any one component over the entire range of solution compositions. Thus isopiestic vapor pressure measurements on mixtures of two electrolytes can be used to find the activity coefficients of both electrolytes. For most electrolytes, however, solute solubility limits the range of composition for the solution, and this restricts the possibility of calculation of other activities from measurements of the activity of one solute (see Chapter 3, Section IV.C).

Equation 111 can be expressed in terms of the mean activity coefficients. If there is no common ion,

$$\mu_1 = \mu_1^\circ + \nu_1 RT \ln (Qm_1 \gamma_1) \quad (112)$$

where Q is a numerical factor calculable from the formula of the electrolyte. Hence

$$\left(\frac{\partial \mu_1}{\partial m_2}\right)_{m_1} = \nu_1 RT \left(\frac{\partial \ln \gamma_1}{\partial m_2}\right)_{m_1} \quad (113)$$

and Equation 108 becomes

$$\nu_1 \left(\frac{\partial \ln \gamma_1}{\partial m_2}\right)_{m_1} = \nu_2 \left(\frac{\partial \ln \gamma_2}{\partial m_1}\right)_{m_2} \quad (114)$$

For a nonelectrolyte solute,  $\nu$  is replaced by 1 and  $\gamma$  is simply the molal activity coefficient rather than the mean activity coefficient.

## B. SALTING-OUT EFFECTS

Salting-out (or salting-in) is the phenomenon by which the solubility of one solute in a solvent is altered by the presence of another solute. In a solution saturated with respect to a solute 1, the chemical potential of 1 is constant at constant temperature and pressure, because:  $\mu_1(\text{sat}) = \mu_1(\text{solid}) = \hat{f}(T,P)$  only.

Hence

$$\left(\frac{\partial \mu_1(\text{sat})}{\partial m_2}\right)_{T,P} = 0 \quad (115)$$

and from Equation 112

$$\left(\frac{\partial \ln m_1(\text{sat})}{\partial m_2}\right)_{T,P} = -\left(\frac{\partial \ln \gamma_1}{\partial m_2}\right)_{T,P} \quad (116)$$

Thus, if the addition of solute 2 to the solution increases the activity coefficient of solute 1, the solubility of solute 1 is reduced, i.e., 1 is "salted-out" by 2. In dilute solutions of

electrolytes,  $\gamma_1$  decreases as the ionic strength increases, and the right-hand side of Equation 116 is therefore positive. The solubility of a sparingly soluble salt is therefore increased by the presence of low concentrations of another salt. This argument implicitly assumes that the added salt has no ion in common with the first salt.

When there is a common ion, Equations 111 and 40 still hold, but  $\mu_1$  does not take the simple form of Equation 112. Considering the case of two electrolytes, say NaCl and KCl at molalities  $m_1$  and  $m_2$ :

$$\begin{aligned}\mu_1 &= \mu_1^\circ + RT\{\ln[(m_{K^+})(\gamma_{K^+})] + \ln[(m_{Cl^-})(\gamma_{Cl^-})]\} \\ &= \mu_1^\circ + RT\{\ln(m_1\gamma_{K^+}) + \ln[(m_1 + m_2)\gamma_{Cl^-}]\} \quad (117)\end{aligned}$$

and the calculation of  $(\partial m_1(\text{sat})/\partial m_2)_{T,P}$  follows.

The uses of solubility measurements in solution thermodynamics are discussed elsewhere in this volume.

## REFERENCES

1. **Harned, H. S. and Owen, B. B.**, *The Physical Chemistry of Electrolytic Solutions*, 3rd ed., Reinhold, New York, 1963.
2. **Robinson, R. A. and Stokes, R. H.**, *Electrolyte Solutions*, 2nd ed., Butterworths, London, 1968.
3. **Guggenheim, E. A.**, *Thermodynamics*, 4th ed., North-Holland, Amsterdam, 1959.
4. **Kortum, G.**, *Treatise on Electrochemistry*, 2nd ed., Elsevier, New York, 1965.
5. **Pitzer, K. S. and Brewer, L.**, *Thermodynamics*, (revision of Lewis and Randall's), McGraw-Hill, New York, 1961.
6. **Ives, D. J. G.**, *Chemical Thermodynamics*, Macdonald, London, 1971.
7. **Hepler, L. G. and Angrist, S. W.**, *Order and Chaos*, Basic Books, New York, 1967.
8. **Hildebrand, J. H. and Scott, R. L.**, *The Solubility of Non-Electrolytes*, 3rd ed., Dover Publishers, New York, 1964.
9. **Simonson, J. M. and Pitzer, K. S.**, Thermodynamics of multicomponent, miscible, ionic systems: the system  $\text{LiNO}_3 - \text{KNO}_3 - \text{H}_2\text{O}$ , *J. Phys. Chem.*, 90, 3009, 1986.
10. **Guggenheim, E. A.**, *Mixtures*, Clarendon Press, Oxford, 1952, chap. 10.
11. **Glueckauf, E. A.**, The influence of ionic hydration on activity coefficients in concentrated electrolyte solutions, *Trans. Faraday Soc.*, 51, 1235, 1955.
12. **Robinson, R. A. and Stokes, R. H.**, Ionic hydration and activity in electrolyte solutions, *J. Am. Chem. Soc.*, 70, 1870, 1948.
13. **Marsh, K. N. and Ewing, M. B.**, Thermodynamics of cycloalkane and cycloalkane mixtures, *J. Chem. Thermodyn.*, 9, 863, 1977.
14. **Ewing, M. B. and Marsh, K. N.**, Thermodynamics of mixtures of 2,3 dimethyl butane and cycloalkanes, *J. Chem. Thermodyn.*, 9, 357, 1977.
15. **Lebowitz, J. L. and Rowlinson, J. S.**, Thermodynamic properties of mixtures of hard spheres, *J. Chem. Phys.*, 41, 133, 1964.
16. **Hamilton, D. and Stokes, R. H.**, Enthalpies of dilution of urea solutions in six polar solvents at several temperatures, *J. Solution Chem.*, 1, 223, 1972.
17. **Stokes, R. H., Levien, B. J., and Marsh, K. N.**, A continuous dilution dilatometer, *J. Chem. Thermodyn.*, 2, 43, 1970.
18. **O'Hare, P. A. G. and Hockstra, H. R.**, Thermochemistry of uranium compounds. II. Standard enthalpy of formation of  $\alpha$ -sodium uranate, *J. Chem. Thermodyn.*, 5, 769, 1973.
19. **Lange, E. and Robinson, A. L.**, The heats of dilution of strong electrolytes, *Chem. Rev.*, 9, 89, 1931.
20. **Messikomer, E. E. and Wood, R. H.**, The enthalpy of dilution of aqueous sodium chloride at 298.15 to 373.15 K measured with a flow calorimeter, *J. Chem. Thermodyn.*, 7, 119, 1975.

## Chapter 2

# INTRODUCTION TO THE STATISTICAL MECHANICS OF SOLUTIONS

Robert M. Mazo and Chung Yuan Mou

## TABLE OF CONTENTS

I.	Introduction .....	30
II.	Some Formalism .....	31
	A. Partition Functions .....	31
	B. Ideal Solutions .....	33
	C. Molecular Distribution Functions .....	34
	D. Potentials of Mean Force .....	35
	E. Composition Fluctuations .....	36
III.	Exact Theories .....	37
	A. Kirkwood-Buff Theory .....	37
	B. McMillan-Mayer Theory .....	38
IV.	Molecular Interactions in Solutions .....	41
	A. Solute-Solute Interactions .....	41
	B. Solute-Solvent Interactions .....	41
	C. Solvent-Solvent Interactions .....	42
	D. Additivity of Intermolecular Potentials .....	42
	E. The Potential of Mean Force .....	42
V.	Lattice and Cell Models .....	44
	A. Lattice Models .....	45
	B. Cell Models .....	46
VI.	Perturbation Theory and Variational Methods .....	48
	A. Perturbation Theory .....	48
	B. Variational Methods .....	50
VII.	Monte Carlo and Molecular Dynamics .....	50
	A. Monte Carlo Methods .....	50
	B. Molecular Dynamics Method .....	52
VIII.	Statistical Mechanical Theories for Electrolyte Solutions .....	53
	A. Potential Energy Approach (Debye-Hückel Theory and Its Descendants) .....	54
	B. Cluster Expansion Theory .....	57
	C. Integral Equation Approaches .....	59
	D. Ion Pairing .....	62
	E. Kirkwood-Buff Approach .....	64
	F. Survey of Some Numerical Results .....	65

IX. Summary and Conclusions .....	69
Acknowledgments .....	70
General References .....	70
References .....	71

## I. INTRODUCTION

Statistical mechanics is the science of drawing macroscopic conclusions from microscopic hypotheses about systems composed of a large number of particles, atoms, molecules, ions, etc. In this chapter, we shall outline how statistical mechanics has been applied to electrolyte solutions. Our object will be to provide an overview and an introduction to the more detailed considerations of several of the later chapters. We shall try to concentrate on the physical ideas necessary for understanding liquid solutions, particularly ionic solutions, and how these ideas are reflected in the mathematical formalism. We shall not be sparing of equations, though we shall, more often than not, omit detailed derivations. Our treatment is not intended for the complete novice. We hope it will appeal to the partially knowledgeable scientist who may not be conversant with development in solution theory and wishes an entrée to the subject.

It is customary to distinguish between the theory of *liquids* and the theory of *solutions*, even though one may be primarily interested in liquid solutions. The difference is that any theory of liquids, pure or mixed, is essentially a description of a dense, disordered phase of matter. A theory of solutions, which by its very nature refers only to mixtures, is concerned primarily with the differences between the mixture properties at differing concentrations and those of its pure components. In solution theory, many of the vexing questions of liquid theory (such as, why does a liquid state exist at all?) are merely not asked; the properties of the pure components are regarded as given. Of course, one is not compelled to adopt this distinction, but it is commonly done. In this chapter we shall concentrate on solution theory.

We shall treat only classical systems and not discuss quantal mixtures at all. Furthermore, we restrict ourselves to equilibrium theory and do not even mention transport phenomena from here on.

Statistical mechanics begins with given data; the microscopic nature of the system must be known. We must know the nature of the particles that constitute the system, and we must know their interactions, that is, the intermolecular forces. Given these data, there is a well-defined, unambiguous algorithm for computing the macroscopic thermodynamic properties. Although the problem is solved in principle, in practice rigorous computations are often beyond our capabilities. We must be content with approximations.

Statistical mechanics has had much of its success in cases where the interactions between particles are small. Either the interactions can be transformed away (phonons in solids), are intrinsically weak (a case beloved by theoreticians, but not common in practice), or the system is dilute (so that the interactions, while possibly strong, are rare). Unfortunately, none of these circumstances holds for liquids, in general, and solutions, in particular. Solution theory is therefore replete with models and approximations.



## II. SOME FORMALISM

### A. PARTITION FUNCTIONS

In the description of systems containing many particles of different species, the notation specifying the state of the system becomes a problem. We shall adopt the following concise notation. Our system consists of  $N_1$  particles of 1,  $N_2$  of type 2, . . . .  $N_\sigma$  of type  $\sigma$ . We shall denote the set  $N_1, \dots, N_\sigma$  by  $\mathbf{N}$ . The coordinates of the  $j$ th particle of species  $s$  will be denoted by  $(j, s)$ . The coordinates of  $n_s$  molecules of species  $s$  will be denoted by  $\{n_s\}$  rather than  $x_{1s}, y_{1s}, z_{1s}, \dots, x_{n_s s}, y_{n_s s}, z_{n_s s}$ . In general, a boldface symbol will refer to a set of variables, one for each species. Thus we will write  $\mathbf{N} = N_1, \dots, N_\sigma$ ,  $\{\mathbf{N}\} = \{N_1\}, \{N_2\}, \dots, \{N_\sigma\}$ . The chemical potentials of the species in the system are  $\mu_1, \mu_2, \dots, \mu_\sigma$ , which we write collectively as  $\boldsymbol{\mu}$ . The sum  $\sum_{k=1}^{\sigma} N_k \mu_k$  often arises; we shall abbreviate this by  $\mathbf{N} \cdot \boldsymbol{\mu}$ . Similarly, we shall write  $\mathbf{N}!$  for  $N_1! N_2! \dots N_\sigma!$  and  $\mathbf{a}^{\mathbf{b}}$  for  $a_1^{b_1} a_2^{b_2} \dots a_\sigma^{b_\sigma}$ .

We shall have occasion to integrate over very many variables so we need a shorthand for such integrals, also. For particle  $j$  of species  $s$ , we shall write,

$$d(j, s) = dx_{j,s}, dy_{j,s}, dz_{j,s} \quad (1a)$$

$$d\{n_s\} = d(1, s) d(2, s) \dots d(n_s, s) \quad (1b)$$

$$d\{\mathbf{N}\} = d\{N_1\} \dots d\{N_\sigma\} \quad (1c)$$

It takes a bit of practice to get used to this notation, but it proves to be extremely convenient. It is due to McMillan and Mayer.<sup>1</sup>

The quantity that one must calculate in classical equilibrium statistical mechanics is the partition function, defined by

$$Q(\mathbf{N}, T, V) = (\lambda^{-3N} / \mathbf{N}!) \int \exp[-\beta U(\mathbf{N})] d\{\mathbf{N}\} \quad (2)$$

Here  $U(\{\mathbf{N}\})$  is the potential energy of interaction of the  $\mathbf{N}$  particles in the system, as a function of their mutual configuration.  $V$  is the volume of the system.  $\beta$  is defined by  $\beta = (kT)^{-1}$ , and  $\lambda_s$  is defined by  $\lambda_s = (2\pi m_s kT/h^2)^{-1/2}$ .  $m_s$  is the mass of a particle of species  $s$ ,  $k$  is Boltzmann's constant,  $h$  is Planck's constant, and  $T$ , the absolute temperature. The integral is over all possible configurations of the molecules.

Our notation has tacitly assumed that the molecules that make up the system under consideration have only translational degrees of freedom. Of course, in reality, molecules also have orientational and vibrational degrees of freedom. In the interests of keeping the notation and the ideas as simple as possible, we shall, in this chapter, consistently neglect such internal degrees of freedom. This is not to say that internal degrees of freedom are unimportant, but only that we can present the ideas we want to emphasize without their explicit introduction.

Let us return to the partition function, Equation 2, and inquire into the meaning of the various factors. The  $\lambda^{-3N}$  factors come from integrating  $\exp(-\beta K)$  over momentum space, where  $K$  is the kinetic energy of the entire system. These factors are essentially uninteresting in the sense that when one calculates the changes of thermodynamic properties on mixing, they cancel out. The  $\mathbf{N}!$  factors correct for an overcounting of configurations in the integral of Equation 2. For any given configuration of labeled particles, any permutation of like particles gives a physically indistinguishable configuration, differing only in the labels assigned to the particles at the given positions. The labels are mathematical artifices for the integration variables; the particles of a given species are indistinguishable. Hence, we must divide by the number of possible permutations of  $\mathbf{N}$  particles, namely,  $\mathbf{N}!$

The integral can be looked on as follows: one can write

$$\begin{aligned} Z &= \int \exp(-\beta U(\{\mathbf{N}\})) d\{\mathbf{N}\} \\ &= \int \exp(-(\beta E)\delta(U(\{\mathbf{N}\}) - E) dE d\{\mathbf{N}\} \\ &= \int g(E)\exp(-\beta E) dE \end{aligned} \quad (3)$$

where  $g(E) = \int \delta(U - E) d\{\mathbf{N}\}$ , and  $\delta$  is the Dirac delta function.  $g(E)$  is the volume of configuration space corresponding to energy  $E$ . By Boltzmann's formula

$$g(E) = \exp(S(E)/k) \quad (4)$$

where  $S(E)$  is the entropy of a system with energy  $E$ . Since the Helmholtz function is given by  $\beta A = \beta(E - TS)$ , we can finally write Equation 3 as

$$Z = \int \exp(-\beta A_c(E)) dE \quad (5)$$

That is, the configuration integral,  $Z$ , can be interpreted as a sort of average of the exponential of a local configurational free energy,  $A_c$ , over energy. Note that  $A_c$  is not a macroscopical thermodynamic quantity. It is a function of the system's configuration energy,  $E$ . It is the Boltzmann factor containing the local free energy, and not the energy alone, which weighs the various energy regions.

The relation between  $Q$  and the Helmholtz free energy,  $A$ , is

$$A = -kT \ln Q \quad (6)$$

We shall not derive this fundamental formula here, though the preceding paragraph may serve to motivate it. Once the Helmholtz free energy is determined through Equation 6, all other thermodynamic functions can be obtained by standard thermodynamic derivatives, e.g.,

$$E = [\partial(A/T)/\partial(1/T)]_v \quad (7a)$$

$$p = -(\partial A/\partial V)_T \quad (7b)$$

$$S = -(\partial A/\partial T)_v \quad (7c)$$

$Q(N, T, V)$  is called the canonical partition function. It is the appropriate quantity to compute to describe a system with a given temperature,  $T$ , volume,  $V$ , and number of particles,  $N$ . The problems of statistical thermodynamics are solved, in principle, by Equations 2 and 6. However, in practice, the rigorous evaluation of  $Q$  is usually impossibly difficult.

In the theory of solutions, it is often more convenient to work with a different quantity, the grand canonical partition function,  $\Xi$ , defined by

$$\Xi(\boldsymbol{\mu}, V, T) = \sum_n \exp(\beta N \cdot \boldsymbol{\mu}) Q(N, V, T) \quad (8)$$

In the summation over  $N_1 \dots N_\sigma$ , we arbitrarily define  $Q(0, V, T) = 1$  and the sum is over  $0 \leq N_i < \infty$ .

$\Xi$  is the appropriate quantity for the treatment of an open system in contact with reservoirs of given chemical potentials,  $\mu$ . In practice, whether to use  $Q$  or  $\Xi$  is a matter of computational convenience. They are thermodynamically equivalent.  $\Xi$  is related to thermodynamics by the formula

$$pV/kT = \ln \Xi \quad (9)$$

and various thermodynamic relations, e.g.,

$$(\partial(pV/kT)/\partial T)_{V, \mu, kT} = E/kT^2 \quad (10a)$$

$$(\partial(pV/kT)/\partial V)_{\mu, T} = p/kT \quad (10b)$$

$$(\partial(pV/kT)/\partial(\mu_i/kT))_{V, T} = N_i, \quad i = 1, \dots, \sigma \quad (10c)$$

In deciding whether to compute  $Q$  or  $\Xi$  in a given setting, one has to balance two sets of considerations.  $\Xi$  is usually easier to compute mathematically; the elimination of the constraint of fixed  $N$  is often a considerable simplification. On the other hand,  $N$  is a more common thermodynamic independent variable than is  $\mu$ . Answers in terms of  $\mu$  usually need appreciable manipulation to get them in terms of  $N$ . Which of these considerations wins out depends on the case at hand. In solution theory,  $\Xi$  is often the function of choice.

One might think that the most direct evaluation technique for the partition function would be direct numerical evaluation of the multiple integral, say Equation 2. This is not feasible because numerical integration methods require evaluation of the integrand at a grid of points in the integration region. The number of grid points needed increases exponentially with the dimension of the integration region; each additional particle cubes the needed number of points. A ten-particle system with each axis broken into ten intervals would need  $10^{10}$  points. Obviously this is impractical.

However, there is a powerful numerical method which is much less demanding. This is the Monte Carlo method, which was first applied to statistical mechanics by Metropolis et al.<sup>3</sup> It has proved to be a very useful tool in the statistical mechanics of liquids, and is discussed in Section VII.

## B. IDEAL SOLUTIONS

The microscopic property giving rise to ideal gas behavior is the absence of intermolecular forces. The microscopic property giving rise to ideal solution behavior is the independence of the intermolecular forces of the species of the interacting molecules. The interactions may be as strong as one wishes. In other words,  $U(\{N\})$  is independent of the precise values of  $N_1 \dots N_\sigma$ , as long as  $\sum_i N_i = N$ . Let us see how this gives rise to thermodynamically ideal behavior.

For simplicity, we consider a two-component system, with components a and b,  $N = (N_a, N_b)$ . We wish to compute the difference of Helmholtz free energy,  $\Delta A_n = A(N_a + N_b) - A(N_a) - A(N_b)$ . Using Equation 2,

$$\Delta A_n = -kT \ln \frac{Q(N_a + N_b)}{Q(N_a) Q(N_b)} \quad (11)$$

Now  $A$  is an extensive quantity for a pure system. Therefore,  $Q(N, V, T)$  must be of the form  $[q(\rho, T)]^N$  where  $\rho$  is the number density,  $N/V$ . However, because of our hypothesis

about  $U(\{\mathbf{N}\})$  above.  $Q(N_a + N_b)$  for the mixture can be written as

$$Q(N_a + N_b) = \frac{N!}{N_a! N_b!} Q(N) = \frac{N!}{N_a! N_b!} q^{N_a + N_b} \quad (12)$$

where  $Q(N)$  is the partition function for a hypothetical pure material.  $Q(N_a)$  and  $Q(N_b)$  are  $q^{N_a}$  and  $q^{N_b}$ , respectively. Hence, Equation 11 becomes

$$\Delta A_M = -kT \ln \frac{(N_a + N_b)!}{N_a! N_b!} \quad (13)$$

Using Stirling's approximation for the factorials, this can be written

$$\begin{aligned} \Delta A_M &= (N_a + N_b)kT(x_a \ln x_a + x_b \ln x_b) \\ x_a &= N_a/(N_a + N_b); x_b = 1 - x_a \end{aligned} \quad (14)$$

which is well-known ideal mixing law. The function  $q$ , which is, in general, difficult to compute, cancels out completely and does not have to be computed! In other words, the free energies of the pure components,  $a$  and  $b$ , may be quite complicated functions of temperature and density. However, they do not enter into the mixing property  $\Delta A_M$  because of the hypothesis that the intermolecular forces are species independent. The  $\lambda$  factors all cancel, also. It is quite simple to extend this calculation to a  $\sigma$ -component system.

Thus we have shown that a sufficient condition for ideality of a mixture is that, for a given configuration of the molecules, the interaction energy is independent of which species are there. In nature there are no ideal solutions, strictly speaking. Isotope mixtures come closest. The deviations of isotope mixtures from ideality are due to quantum effects and are quite small, except for He and  $H_2$  at low temperatures. There do exist pairs of species whose interactions are so similar that the mixtures can be described as ideal to a good approximation; chlorobenzene-bromobenzene is one such pair. However, the condition for forming an ideal mixture is rather severe; the class of ideal solutions is rather small. We therefore pass on to more general cases.

### C. MOLECULAR DISTRIBUTION FUNCTIONS

In this section we shall describe some functions useful for solution theory and for liquid theory in general. They can be defined either from the canonical (definite  $\mathbf{N}$ ) or grand canonical (definite  $\boldsymbol{\mu}$ ) point of view. We shall only deal with the grand canonical case. The functions to be defined describe the probability density for finding  $\mathbf{N}$  particles in a specific configuration,  $\{\mathbf{N}\}$ , in a grand ensemble, that is averaged over the positions of all of the other particles that may be in the system. We can get a proper definition by the following considerations.

According to the fundamental hypothesis of the grand ensemble, the probability that the system contains  $\mathbf{N} + \mathbf{n}$  particles in the configuration  $\{\mathbf{N} + \mathbf{n}\}$  is

$$P_{\mathbf{N}+\mathbf{n}}(\{\mathbf{N} + \mathbf{n}\}) = \Xi^{-1} \lambda^{-3(N+n)} \exp[\beta\boldsymbol{\mu} \cdot (\mathbf{N} + \mathbf{n}) - \beta U(\{\mathbf{N} + \mathbf{n}\})] \quad (15)$$

Integrating  $P_{\mathbf{N}+\mathbf{n}}$  with respect to  $d\{\mathbf{n}\}$ , and dividing by  $\mathbf{n}!$  averages over configurations of the  $\mathbf{n}$  particles that are present in addition to the  $\mathbf{N}$  we wish to consider. To complete the story, we must sum over all possible values of  $\mathbf{n}$ , the number of "extra" particles. The result is a function which has the physical meaning we described, the probability density for finding  $\mathbf{N}$  particles in configuration  $\{\mathbf{N}\}$ .

We shall call this function  $\rho^N F_N(\{N\})$ . Here  $\rho_j = \langle N_j \rangle / V$ , where  $\langle N_j \rangle$  is determined by Equation 10c.  $\rho_j$  is the mean number density of species  $j$ .  $\rho_j$  is the concentration variable that we shall use throughout this chapter.

As a result of the manipulations described above, we can write

$$\rho^N F_N(\{N\}) = \Xi^{-1} z^N \sum_{\mathbf{n}} \int \frac{z^{\mathbf{n}}}{\mathbf{n}!} \exp\{-\beta U(\{N + \mathbf{n}\})\} d\{\mathbf{n}\} \quad (16)$$

where we have introduced the notation

$$z_i = \lambda_i^{-3} e^{\beta \mu_i} \quad (17)$$

$z_i$  is called the *absolute activity* of species  $i$ . Do not be misled by the name. While  $z_i$  is related to the conventional thermodynamic activity, it is not the same thing.

The functions  $F_N$  are called molecular distribution functions for  $N$  particles. Of course, they depend on  $T$  and  $\mu$  as well as  $\{N\}$ ; we have omitted specific mention of  $T$ ,  $\mu$  on the left-hand side of Equation 16, in order not to make the notation too heavy.

The factor of  $\rho^N$  is factored out as a matter of convention in order to give  $F_N$  the property that  $F_N(\{N\}) \rightarrow 1$  as all of the coordinates, symbolized by  $\{N\}$ , get far from each other. This occurs because when the specified  $N$  particles are far apart, they are statistically independent, and the probability density of  $N$  statistically independent particles is  $\rho^N$ . Note that, as  $\mu$  gets large and negative ( $\mu \rightarrow -\infty$ ),  $\rho$  goes to zero in such a manner that  $\rho^N \rightarrow \exp(+\beta N \cdot \mu) / \lambda^N$ , and  $\rho V / kT \rightarrow \sum_i N_i$ . This follows from the statistical mechanics of ideal gases, which we assume known. Hence in this limit

$$\lim_{\rho \rightarrow 0} F_N(\{N\}) = \exp\{-\beta U(\{N\})\} \quad (18)$$

which is further corroboration of the probabilistic meaning of  $F_N$ , since the probabilistic interpretation of the Boltzmann factor in Equation 18 is well known. It is important to remember that Equation 18 is valid only in the limit of dilute gases.

The most important  $F_N$  functions in practice are those for which  $\sum_i N_i = 2$ . These functions are often given the special symbols  $g_{ij}$ , where  $i$  and  $j$  refer to the species of the two particles being considered. They are called pair correlation functions, or radial distribution functions. This latter name arises because, for spherically symmetric interactions,  $U$ , and for homogeneous systems,  $g_{ij}(\mathbf{r}_1, \mathbf{r}_2) = g_{ij}(|\mathbf{r}_1 - \mathbf{r}_2|)$ , a function of the radial distance between the two particles only.

#### D. POTENTIALS OF MEAN FORCE

We can give a further physical meaning to the functions  $F_N$ . In a given configuration of a system of  $N$  particles,  $\{N\}$ , the force on a particular particle, say particle 1 for definiteness, is

$$f_1(\{N\}) = -\nabla_{\mathbf{r}_1} U(\{N\}) \quad (19)$$

We have assumed that the system is conservative; the force is derivable from a potential,  $U$ .

Now let us consider a slightly different problem. We have  $N$  particles in configuration  $\{N\}$  in an open system, so that there are more than  $N$  particles in the volume considered. If particle 1 is one of the  $N$  fixed particles, what is the average force on particle 1? From

Equation 15, the average force is

$$\langle f_i(\{\mathbf{N}\}) \rangle = \sum_{\mathbf{n}} \int f_i(\{\mathbf{N} + \mathbf{n}\}) P_{\mathbf{N}, \mathbf{n}}(\{\mathbf{N} + \mathbf{n}\}) d\{\mathbf{n}\} \quad (20)$$

where we have used carets,  $\langle \dots \rangle$ , to denote average values. Some manipulation then yields

$$\langle f_i(\{\mathbf{N}\}) \rangle = -\nabla_{\mathbf{r}_i} W_{\mathbf{N}}(\{\mathbf{N}\}) \quad (21)$$

where  $W_{\mathbf{N}}$  is defined by

$$F_{\mathbf{N}}(\{\mathbf{N}\}) = e^{-\beta W_{\mathbf{N}}(\{\mathbf{N}\})} \quad (22)$$

In other words, the average, or mean force on a particle, when  $\mathbf{N}$  particles are held fixed, is also derivable from a potential,  $W_{\mathbf{N}}$ . This potential is not  $U$ ; it is simply related to  $F_{\mathbf{N}}$ , by Equation 22, or, alternatively, by

$$W_{\mathbf{N}}(\{\mathbf{N}\}) = -kT \ln F_{\mathbf{N}}(\{\mathbf{N}\}) \quad (23)$$

$F_{\mathbf{N}}$  bears the same relationship to the mean force that the Boltzmann factor,  $\exp(-\beta U(\{\mathbf{N}\}))$ , bears to the unaveraged force.  $W_{\mathbf{N}}$  is often called the potential of mean force.

### E. COMPOSITION FLUCTUATIONS

In any open system, the composition is not fixed. In an open system describable by a grand canonical partition function, the mean composition is determined by Equation 10c. Fluctuations about the mean can occur, because the system is open. The magnitudes of these fluctuations are very small (except near critical points, which are not discussed in this chapter). Nevertheless, fluctuations can, on the one hand, be related to observable thermodynamic properties, and on the other hand, they can be expressed in terms of molecular distribution functions. These observations form the basis of the Kirkwood-Buff theory<sup>1</sup> of solutions which we discuss shortly. For the present, we want to show the relations between composition fluctuations and molecular distribution functions, which are as follows:

$$\rho_i \int F_1(\{1_i\}) d\{1\} = \langle N_i \rangle \quad (24a)$$

$$\rho_i \rho_j \int F_2(\{1_i, 1_j\}) d\{2\} = \langle N_i N_j \rangle - \langle N_i \rangle \delta_{ij} \quad (24b)$$

or

$$\rho_i \rho_j \int [g_{ij} - 1] d\{2\} = \langle N_i N_j \rangle - \langle N_i \rangle \langle N_j \rangle - \langle N_i \rangle \delta_{ij} \quad (24c)$$

In a uniform system,  $F_1$  is just 1, so that Equation 24a is a rather trivial statement. Equations 24b and 24c express the fluctuations; they say the same thing in different notation. The right-hand side of Equation 24a is just the mean value of  $N_i$ , whereas Equations 24b and 24c are the second-order moments. Of course, fluctuations are irregular and complex phenomena and are not characterized completely by their second-order moments. Nevertheless, the mean square values do suffice for applications to solution theory.

We cannot give an intuitive argument for these formulas. In fact, they are rather remarkable. They state that the local distribution of type  $i$  molecules in the neighborhood of

a type  $j$  molecule determines the overall fluctuation in composition of the entire system. The left-hand members are local quantities, even though integrals over the entire system, because the  $F_2$  functions are short ranged. The right-hand members are clearly overall descriptors of the magnitude of the fluctuations. The reader wishing to see a derivation of Equation 24 may consult References 3 or 4.

### III. EXACT THEORIES

There are a number of exact theories of solutions. Among them, those due to Kirkwood and Buff<sup>3</sup> and to McMillan and Mayer<sup>1</sup> are particularly worthy of note. Both theories are based on the grand partition function, and both are exact. They are therefore completely equivalent. However, they look quite different on the surface. We will discuss both of them.

#### A. KIRKWOOD-BUFF THEORY<sup>3</sup>

We have previously asserted that composition fluctuations are related to thermodynamic quantities. If we differentiate Equation 8 with respect to  $\beta\mu_i$ , we get  $\langle N_i \rangle$ ; that is Equation 10c. If we differentiate again, we get

$$\left( \frac{\partial^2 \ln \Xi}{\partial \beta \mu_i \partial \beta \mu_j} \right)_{T, V, \mu'} = \langle N_i N_j \rangle - \langle N_i \rangle \langle N_j \rangle \quad (25)$$

where the prime on  $\mu$  means that all of the  $\mu$ 's, except those displayed, are kept constant in the differentiation. However, the left-hand side is  $kT(\partial \langle N_i \rangle / \partial \mu_i)_{T, V, \mu'}$ . It is a standard result of many-variable calculus that the inverse matrix to  $(\partial \langle N_i \rangle / \partial \mu_i)_{T, V, \mu'}$  is  $(\partial \mu_i / \partial \langle N_i \rangle)_{T, V, \langle N \rangle}$ . Hence, we can move from chemical potentials to particle numbers as independent variables. Finally, we can use Equation 24c to write

$$\frac{1}{kT} \left( \frac{\partial \mu_i}{\partial \langle N_i \rangle} \right)_{T, V, \langle N \rangle} = \frac{|R|_{ij}}{|R|} \quad (26)$$

where  $|R|$  denotes the determinant of the matrix  $\mathbf{R}$ , and  $|R|_{ij}$  denotes the cofactor of  $R_{ij}$  in  $\mathbf{R}$ .  $\mathbf{R}$  is the matrix whose elements are

$$R_{ij} = \rho_i \delta_{ij} + \rho_i \rho_j G_{ij} \quad (27a)$$

$$G_{ij} = (1/V) \int [g_{ij} - 1] d\{2\} \quad (27b)$$

Equations 26 and 27 express chemical potential derivatives in terms of composition fluctuations.

This does not finish the story, since we are still using volume as an independent variable, and not pressure. The pressure,  $p$ , is a more convenient experimental variable. One can go from  $V$  to  $p$  by standard thermodynamic derivative manipulation and one finds

$$\left( \frac{\partial \mu_i}{\partial \langle N_i \rangle} \right)_{T, V, \langle N \rangle} = \left( \frac{\partial \mu_i}{\partial \langle N_i \rangle} \right)_{T, p, \langle N \rangle} + \frac{\bar{V}_i \bar{V}_j}{\kappa V} \quad (28)$$

where  $\bar{V}_i$ ,  $\bar{V}_j$  are the partial molecular volumes of species  $i$  and  $j$ , and  $\kappa$  is the isothermal compressibility. The partial molecular volumes and the compressibility can also be expressed in terms of the composition fluctuations, i.e., in terms of the matrix  $\mathbf{R}$ , and the final result

is

$$\frac{V}{kT} \left( \frac{\partial \mu_1}{\partial \langle N_j \rangle} \right)_{T, \rho_1, N_j} = \frac{1}{|R|} \sum_{k,l} \frac{[\rho_k \rho_l (|R|_{lj} |R|_{kl} - |R|_{lk} |R|_{il})]}{\sum_{k,l} \rho_k \rho_l |R|_{kl}} \quad (29)$$

To see what this plethora of summation signs and indices means, let us look at two component systems. Equation 25 becomes

$$\frac{1}{kT} \left( \frac{\partial \mu_2}{\partial \rho_2} \right)_{T, p} = \frac{1}{\rho_2} + \frac{G_{12} - G_{22}}{1 + \rho_2 (G_{22} - G_{12})} \quad (30)$$

and

$$\bar{V}_1 = \frac{1 + \rho_2 (G_{22} - G_{12})}{\rho_1 + \rho_2 + \rho_1 \rho_2 (G_{11} + G_{22} - 2G_{12})} \quad (31)$$

$(\partial \mu_i / \partial \rho_i)_{T, p}$  and  $\bar{V}_2$  can be obtained by just switching indices, and  $(\partial \mu_i / \partial p_i)_{T, p}$  is computable from the Gibbs-Duhem equation.

Another quantity of interest for solutions is the osmotic pressure  $\pi$ . This can also be expressed in terms of our density fluctuation integrals.

$$\left( \frac{\partial \pi}{\partial \rho_1} \right)_{T, \mu_1, p'} = kT \sum_{k=2}^{\sigma} \rho_k \frac{|R'|_{ik}}{|R'|} \quad (32)$$

where  $R'$  is the  $(\sigma - 1) \times (\sigma - 1)$  dimensional matrix formed by omitting the first row and first column from  $R$ . For a two-component system, this becomes

$$\left( \frac{\partial \pi}{\partial \rho_2} \right)_{T, \mu_1} = \frac{kT}{1 + G_{22} \rho_2} \quad (33)$$

Here we have called the solvent component 1, and  $\mu_1$  is a useful independent variable, since, in osmotic pressure experiments, one works at constant chemical potential of the solvent.

The reader interested in pursuing the details of the derivation of these formulas may consult the treatise by Rice and Nagasawa,<sup>4</sup> Section 1.2, based on unpublished lecture notes of one of the present authors, gives many of the intermediate algebraic steps.

## B. MCMILLAN-MAYER THEORY<sup>1</sup>

The McMillan-Mayer theory is logically equivalent to the Kirkwood-Buff theory, but looks quite different on the surface. In point of time, it was the earlier of the two. In the McMillan-Mayer development,<sup>1</sup> solution theory is cast into a form which has strong superficial resemblances to the theory of gases, the intermolecular potentials being replaced by the potentials of mean force between solute molecules. The solvent does not appear explicitly in the theory. However, it is not gone, just hidden, for it is the solvent which largely determines the potential of mean force. The technical details of the derivation are rather intricate; we intend to give only an outline and some motivation here.

The first observation is that Equation 16 expresses  $F_N(\{N\})$  in terms of the set of functions,  $\exp[-\beta U(\{N + \mathbf{n}\})]$ , i.e., the Boltzmann factors. As we have seen in Equation 18, these latter functions can be thought of as the  $F_N$  in the limit  $\rho \rightarrow 0$ , i.e.,  $\mathbf{z} \rightarrow 0$ . In other words, Equation 16 expressed  $F_N(\mathbf{z}; \{N\})$  as a Taylor's expansion in  $\mathbf{z}$ , with coefficients determined



by the set of functions  $F_{N,n}(0; N + n)$ . For the sake of clarity, we have here reintroduced the  $\mathbf{z}$  dependence of the  $F$ 's into the notation.

Now the set of Equation 16, one for each  $\mathbf{N}$ , can be inverted, i.e., solved, for  $F_N(0; \mathbf{N})$  in terms of the entire set of  $F_{N,n}(\mathbf{z}; \{\mathbf{N} + \mathbf{n}\})$ . This is the difficult part of the derivation and we content ourselves here with the mere assertion that it can be done. There is, of course, nothing privileged about the fugacity  $\mathbf{z}$  we started with, so that  $F_N(0; \{\mathbf{N}\})$  can be expressed in terms of  $F_{N,n}(\boldsymbol{\zeta}; \{\mathbf{N} + \mathbf{n}\})$  for any fugacity set,  $\boldsymbol{\zeta}$ . Once this is realized, we can return to Equation 16 and insert in it our new expressions for  $\exp\{-\beta U(\{\mathbf{N} + \mathbf{n}\})\}$  in terms of the distribution functions at fugacity  $\boldsymbol{\zeta}$ . We shall only write down the end result

$$\frac{\Xi(\mathbf{z})}{\mathbf{z}^N} \rho^N F_N(\mathbf{z}; \{\mathbf{N}\}) = \Xi(\boldsymbol{\zeta}) \sum_{\mathbf{n}} \frac{(\mathbf{z} - \boldsymbol{\zeta})^{\mathbf{n}}}{\mathbf{n}! \boldsymbol{\zeta}^{N+\mathbf{n}}} \rho(\boldsymbol{\zeta})^{N+\mathbf{n}} \int F_{N,n}(\boldsymbol{\zeta}; \{\mathbf{N} + \mathbf{n}\}) d\{\mathbf{n}\} \quad (34)$$

This remarkably symmetrical result is the product of a great deal of complicated analysis.

The obvious next question is, why is this interesting or useful? We partially answer this question by considering the special case  $\mathbf{N} = 0$ . By definition  $F_0 = 1$  for all  $\mathbf{z}$ . Therefore, we have an expression for  $\Xi(\mathbf{z})$ , the grand partition function at fugacity  $\mathbf{z}$ , in terms of  $\Xi(\boldsymbol{\zeta})$  and molecular distributions at fugacity  $\boldsymbol{\zeta}$ . The fugacity set,  $\boldsymbol{\zeta}$ , may be regarded as a reference state.

Now, specialize still further. We single out one component as the solvent: call this component 1. Take  $\mathbf{z}$  to be the set  $\{z_1, z_2, z_3, \dots, z_\sigma\}$ . Take  $\boldsymbol{\zeta}$  to be the set  $\{z_1, 0, \dots, 0\}$ . These are so-called osmotic conditions. One can think of two phases, one pure, one a solution, for which component 1 has the same chemical potential in both phases. Then, since  $\Xi = \exp(\beta p V)$ , we have immediately

$$\exp(\pi V/kT) = \Xi(\mathbf{z})/\Xi(\boldsymbol{\zeta}) \quad (35)$$

for the particular  $\mathbf{z}$  and  $\boldsymbol{\zeta}$  being considered, where  $\pi$  is the osmotic pressure. Recall that the osmotic pressure is the pressure difference between pure solvent and a solution in equilibrium with it.

Equation 30 now reads

$$\exp(\pi V/kT) = \sum' \frac{\mathbf{z}^{\mathbf{n}}}{\mathbf{n}! \boldsymbol{\gamma}^{\mathbf{n}}} \int F_{N,n}(\boldsymbol{\zeta}; \{\mathbf{N} + \mathbf{n}\}) d\{\mathbf{n}\} \quad (36)$$

The prime on the summation sign in Equation 32 means that only solute molecule numbers,  $n_2, \dots, n_\sigma$ , are to be summed over. All terms with  $n_1 = 0$  vanish, since they all contain  $z_1 - \zeta_1$ , which is zero by construction.  $\boldsymbol{\gamma}$  is the set of numbers

$$\gamma_i = \lim_{c_i \rightarrow 0} \zeta_i/\rho_i, \quad i = 2, \dots, \sigma \quad (37)$$

$\gamma_i$  denotes the activity coefficient of component  $i$  in a solution infinitely dilute with respect to the solutes but not the solvent.  $\gamma_i$  is *not* the usual thermodynamic activity coefficient, which is unity at infinite dilution in the solvent, for we have defined  $\gamma_i$  to be unity in the ideal gas limit, when all components, including the solvent, are dilute.

Thus we have the osmotic pressure as a power series in the fugacity, in a form extremely analogous to the fugacity expansion of the pressure of a nonideal gas. Indeed, the nonideal gas is a special case of Equation 36, with the solvent taken as vacuum. There are two further steps to be taken, both of which also have close formal analogies with gas theory. The first

is to take the logarithm of Equation 36, to bring the osmotic pressure "downstairs", so to speak. Since the logarithm of a power series (with nonzero constant term) is itself a power series, this operation will yield a power series in  $\mathbf{z}$  for the osmotic pressure,  $\pi$ . The determination of the coefficients in this new series in terms of those in the old series can be carried out by standard techniques. In the present context, the coefficients are called cluster integrals. They are integrals of sums of products of the  $F_N$  functions; we omit formulas.

The fugacity,  $\mathbf{z}$ , is not a very convenient experimental variable; the concentration  $\boldsymbol{\rho}$  is preferable. So the second step is to eliminate the  $\mathbf{z}$  variables in terms of the concentrations  $\rho_i = \langle N_i \rangle / V$ . This is another technically difficult part of the theory. The general idea is as follows: from Equation 10c and 35, one has

$$\rho_i = \frac{z_i}{\gamma_i} \left( \frac{\partial \pi / kT}{\partial (z_i / \gamma_i)} \right)_{z, T} \quad (38)$$

The power series for  $\pi$  as a function of  $\mathbf{z}$  thus gives rise to a power series for  $\boldsymbol{\rho}$  as a function of  $\mathbf{z}/\boldsymbol{\gamma}$ . This series can be inverted to give  $\mathbf{z}/\boldsymbol{\gamma}$  as a power series in  $\boldsymbol{\rho}$ . One then inserts these series for  $\mathbf{z}/\boldsymbol{\gamma}$  in the original power series for  $\pi$ , and collects terms with given powers of the  $\rho_i$ .

The net result is an expansion of  $\pi$  in powers of the concentrations,  $\boldsymbol{\rho}$ . This is conventionally written in the form

$$\pi / kT = \sum_{i=1}^a \rho_i - \sum_n \left( \sum_s n_s - 1 \right) B_{0,n} \boldsymbol{\rho}^n \quad (39)$$

Again, the sum is only over solute species. The  $B_{0,n}$  are called irreducible cluster integrals. The zero subscript means that they are evaluated at infinite dilution in the solvent. For a two-component system (one solute-one solvent), the first several B's are

$$\begin{aligned} B_{02} &= \frac{1}{2!V} \iint d\{2\} (F_2(z_i, 0; \{2\}) - 1) \\ B_{03} &= \frac{1}{3!V} \iint d\{3\} [F_3(\{3\}) - F_2(1,2)F_2(1,3) \\ &\quad - F_2(2,3)F_2(1,2) - F_2(1,3)F_2(2,3) \\ &\quad + F_2(1,2) + F_2(1,3) + F_2(2,3) - 1] \end{aligned} \quad (41)$$

In Equation 41, we have omitted the fugacity arguments of the F's; they are all  $(z_i, 0)$ .  $F_2(1,2)$  means  $F_2(R_1, R_2)$  etc. The higher B's get notationally complicated rather rapidly.

If we recall Equation 22, it is clear that the B's are rather like the virial coefficients in a gas, in a formal sense. The physical difference is that, in the solution case, the potentials of average force at infinite dilution in the solvent replace the bare intermolecular potentials which occur in gas theory.

Both of the solution theories described above are exact formal theories although the computation procedures are quite different. Our ability to use them is limited by our ability to compute the molecular correlation functions that appear in the formulas. This ability is meager at present. Nevertheless, the theories are useful. They provided a framework upon which one can attempt to hang physically motivated approximations.

Different kinds of solutions involve quite different kinds of interactions between molecules constituting the solution. The kind of force will dictate the kind of approximation or

model one uses to describe the solution being considered. For ionic solutions, the subject of this book, this will be particularly apparent. Before we discuss various approaches of approximation, we will turn our attention briefly to the variety of intermolecular forces.

#### IV. MOLECULAR INTERACTIONS IN SOLUTIONS

From the previous sections, one sees that a complete calculation of the thermodynamic properties of a solution requires knowledge of all interactions,<sup>5</sup> solute-solute, solute-solvent, and solvent-solvent. We will discuss them separately at first, with special reference to ionic solutions.

##### A. SOLUTE-SOLUTE INTERACTIONS

**Coulomb interactions** — Obviously these are the dominant interactions between isolated ions.

$$u_{ij} = \frac{e_i e_j}{r_{ij}}, \quad r_{ij} = |\mathbf{r}_i - \mathbf{r}_j| \quad (42)$$

Since  $u_{ij}$  varies as  $r^{-1}$ , this potential is very long ranged. It is this long range that causes most of the special problems associated with electrolytes.

**Charge-induced dipole** — The ions induce dipole moments in other ions, which are polarizable, resulting in a polarization interaction potential proportional to  $r^{-4}$  and to the ion polarizabilities,  $\alpha_1$  and  $\alpha_2$ .

$$u_{12} = -(z_1^2 \alpha_2 + z_2^2 \alpha_1)/r_{12}^4 \quad (43)$$

$z_1$  and  $z_2$  are the charges. In contrast to coulomb interactions, these interactions are not pairwise additive, although in dilute solution they can often be approximated as additive. See Section IV.D.

**Dispersion interaction** — When two molecules approach each other, the mutual influence of the fluctuating electronic clouds of the two molecules produces an attractive potential proportional to  $r^{-6}$ . In London's quantum mechanical approximation, the dispersion energy for a pair of atoms is

$$u_{ij} = -(\frac{3}{2}) \alpha_1 \alpha_2 I_1 I_2 / (I_1 + I_2) r_{ij}^6 \quad (44)$$

where the  $I$ 's are the ionization potentials of the atoms. These attractive potentials also operate for ions, with the interpretation of  $I$  as the energy required to remove an electron from the ion.

**Core repulsion** — The finite size of the ions results from the high energy of overlapping of the electronic clouds when two ions approach each other very closely. Usually, this repulsion can be approximated by an exponential function  $Ae^{-br}$ , but, for mathematical convenience, an even simpler approximation, a hard-core model, is often used.

##### B. SOLUTE-SOLVENT INTERACTIONS

Except for coulomb interactions, the other three types of interactions also operate between solute and solvent molecules. In addition, solvent molecules often have permanent dipole moments, quadrupole moments, and so on. The interaction of ions with water is of special interest because important chemical and biophysical phenomena are related to ion-water interaction. Recent experimental and theoretical investigations have given detailed information about ion hydration. Among the experimental techniques, X-ray and neutron scat-

tering yield much insight about ion-solvent interactions. With the advent of efficient *ab initio* computation methods, quantum chemical calculation can give us fairly good ion-solvent potentials for simple ions. For a review see Reference 6. Ion-solvent interaction potentials are often used directly in computer simulations of ion-solvent liquid structures, or indirectly in interpretation of the above-mentioned experimental results concerning ion-solvent structure. For investigating activity coefficients of concentrated ionic solutions, ion-solvent interactions will strongly influence the short-range structure of ion-ion correlations. This happens when hydration shells of ions overlap substantially as two hydrated ions approach each other. We will discuss this more in detail in Section IV.E.

### C. SOLVENT-SOLVENT INTERACTIONS

All of the above interactions, with the exception of charge-charge or charge-dipole interactions, are operative between the neutral solvent molecules. In addition, multipole moments induced by the ionic solutes in the solvent molecules will interact.

### D. ADDITIVITY OF INTERMOLECULAR POTENTIALS

It is very commonly assumed that the total potential energy of interaction,  $U(\{\mathbf{N}\})$ , is a sum of contributions from pairs of particles,  $u_{\alpha\beta}(r_{ij})$ .

$$U(\{\mathbf{N}\}) = (1/2) \sum_{\alpha, \beta=1}^n \sum_{i \neq j} u_{\alpha, \beta}(r_{ij})$$

where, in this formula, Greek letters label species and Latin letters label particles. This means that the presence of a third, fourth, etc. body does not influence the interaction of a given pair of particles. For certain kinds of forces, this assumption is a good approximation to reality; for others, it is a poor one.

For example, coulomb forces are pairwise additive. Dispersion forces are largely pairwise additive, but there are nonnegligible many-body contributions at liquid densities. Any interactions involving induced moments are not pairwise additive. To see this imagine that a body labeled 2 is interacting with a body labeled 1. A third body, capable of inducing a moment in 2, is brought up. The moment of 2 depends on where 3 happens to be. So the interaction of 1 and 2 depends not only on where 1 and 2 are, but also on the position of 3. Thus the interaction energy would not be pairwise additive in this case.

Many-body potentials are difficult to handle analytically. For the most part, what is done is to assume pairwise additive potentials, determined semiempirically. One hopes that this takes some of the many-body contributions into account in an average way. For example, in Equation 44, one would retain the  $r^{-6}$  dependence, but determine the coefficient from experiment. The effects of many-body forces on the properties of matter are not well understood as well as we should like. References 5 and 6 give descriptions of the current state of our knowledge.

### E. THE POTENTIAL OF MEAN FORCE

With all of these contributions to the interactions of molecules, an *a priori* statistical mechanical calculation will be, indeed, very complicated. Further simplification of the problem is necessary. From the point of view of the Kirkwood-Buff theory, one needs to calculate all the  $g_{ij}$ 's; simplification can be obtained only through approximation of individual  $u_{ij}$ 's. One has to know both the solvent-solute and solvent-solvent interactions, at least approximately. On the other hand, the McMillan-Mayer theory offers one conceptual advantage for electrolyte solutions. The theory is formulated so that pure solvent is the reference state and the effect of solvent-solvent and solute-solvent interactions can be completely included in an effective solute-solute interaction, the potentials of mean force  $W_{ij}(r)$ . From

the discussion in Section II.D, one would not expect that the potential of mean force  $W_N(\{N\})$  will be pairwise additive. Using Equation 23 without making the pairwise additivity assumption will make the MacMillan-Mayer level theory formally correct. However, it will make it also computationally unfeasible. It seems likely that the MacMillan-Mayer approach will be useful mainly when applied to models in which  $W_N$  is pairwise additive. At present, it is often done in some semiempirical way. The potential of mean force  $W_{ij}(r)$  is split into a short- and long-range part.

In the case of simple electrolytes, the long-range behavior of  $W_{ij}$  can be represented by using a single dielectric constant,  $\epsilon$ , for the solvent, to account for the indirect influence of solvent on solute.

$$W_{ij}(r) = W_{ij}^*(r) + \frac{z_i z_j e^2}{\epsilon r} \quad (45)$$

where  $W_{ij}^*(r)$  is the short-range part of  $W_{ij}(r)$ .

The long-range term, with the dielectric constant in the denominator, seems intuitively reasonable for large  $r$ , based on the macroscopic interactions of charges in a dielectric medium. Nevertheless, a real justification of Equation 45, based on a model involving hard core plus dipole for the solvent, and hard core plus charge for the solute, is relatively recent. In physical terms, what happens is that one ion polarizes the surrounding solvent. The induced moments in the solvent molecules then interact with the other charge. The net effect is a reduction of the direct coulomb forces by the factor  $1/\epsilon$ . The reader interested in seeing how this works out in detail for charged impurities in a nonconducting crystal may consult an article by Mahan and Mazo.<sup>7</sup> Bellemans and Stecki<sup>8</sup> have also considered the general case for fluids.

The short-range part  $W_{ij}^*(r)$  is nonadditive because it includes (1) the direct short-range interaction between ions, and (2) the effect of solvent, including ion-solvent structuring. The simplest assumption about  $W_{ij}^*(r)$  is that it is zero. However, this is insufficient; there would be nothing to prevent the positive and negative charges from piling up on top of each other, and the system would be unstable toward collapse. The next simplest assumption, which is certainly idealized, is that  $W_{ij}^*(r)$  is a hard core potential, i.e.,

$$W_{ij}^*(r) = \begin{cases} \infty & r < a_i + a_j \\ 0 & r > a_i + a_j \end{cases} \quad (46)$$

where  $a_i, a_j$  are the radii of ions  $i$  and  $j$ . This is called the primitive model; the case  $a_i = a_j$  for all  $i, j$ , is called the restricted primitive model. The importance of this model is that it does full justice to the coulomb part of the interaction, and it can be solved by many different approximate approaches, which we will discuss in later sections. Monte Carlo calculations<sup>9,12</sup> for the model can be used for comparison with the approximations, and thus the usefulness of different theoretical approaches assessed. Since the primitive model contains the two extreme elements of the function  $W_{ij}$  (short range and long range), it does provide a severe test case for any approximate statistical mechanical theory. However, model calculations based on the primitive model are found to be in poor agreement with experimental data for real systems except for very dilute systems. Evidently a better model for the short-range forces is needed. To get a better model for the solvent-averaged potential of mean force at short range and in the same time making it effectively pairwise additive, one usually uses an adjustable potential consisting of two terms to treat  $W_{ij}^*(r)$ .<sup>11</sup>

$$W_{ij}^*(r) = \text{COR}_{ij}(r) + \text{GUR}_{ij}(r) \quad (47)$$

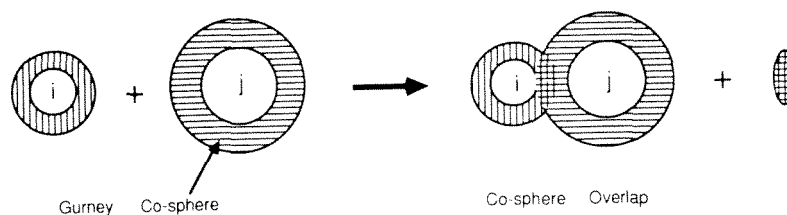


FIGURE 1. Cosphere overlap in the Gurney model of ion hydration. The shaded area is hydration cosphere with higher free energy density. When two ions  $i$  and  $j$  are close enough that cosphere overlaps, the net free energy becomes lower. The energy of attraction is thus proportional to the overlap volume.

The first term is the core repulsion term representing ionic size. It is often taken in the form

$$\text{COR}_{ij}(r) = c (s_{ij}/r)^9 \quad (48)$$

with  $s_{ij}$  taken to be the sum of ionic radii of ion “ $i$ ” and “ $j$ ”.

The second term is called the Gurney term and is due to the overlap of ion-cospheres; a cosphere is a region of polarized, abnormal water structure caused by the strong electric field near an ion.<sup>13</sup> Let  $w$  be the thickness of abnormal water near an ion. When the interionic distance is greater than  $s_{ab} + 2w$ , the Gurney term is small and can be neglected. However, an effective, attractive potential exists when cospheres overlap because a region of high free energy would be reduced in size (see Figure 1). In the first approximation,  $\text{GUR}_{ij}(r)$  is assumed to be proportional to the overlapping volume  $V_{ij}(r)$ ,

$$\text{GUR}_{ij}(r) = A_{ij} V_{ij}(r) \quad (49)$$

where  $A_{ij}$  is an adjustable parameter.

Other forms for the Gurney term have been tried, a square-well potential, for example. In applying Equation 47 to calculate the free energy of mixing and osmotic coefficients, the results can be brought into good agreement with experimental data up to 1  $M$  concentration for typical strong electrolytes by reasonable choice of parameters.<sup>14</sup>

In the last decade, due to rapid advances in computer simulation techniques, one has been able to obtain fairly realistic approximations to the pair contributions to potentials of mean force. The Monte Carlo or molecular dynamics method can be used to evaluate the distribution functions in Equation 23 and  $W_{ij}^*(r)$  calculated. For example, Dang and Pettitt<sup>15</sup> calculated the potential of mean force for the ion pairs  $\text{Cl}^- \text{Cl}^-$  and  $\text{Na}^+ \text{Na}^+$  in water (with a realistic potential for water) using Monte Carlo and molecular dynamics methods. They show more structure than would be given by Equation 49, due to the hydrogen bonding of the water molecules. The integral equation method has also been used to calculate the potential of mean force in aqueous electrolytes.<sup>16</sup> It is likely that more work will be needed to obtain an accurate picture of the molecular details of ion-ion potential of mean force, especially the nonadditive contribution.

## V. LATTICE AND CELL MODELS

If we return, for a moment, to Equation 2, we see that the fundamental technical problem of equilibrium statistical mechanics is to evaluate the integral of a rather complicated function over a very high dimensional space: the partition function. Lattice and cell models are devices for simplifying this difficult problem, through replacing the physical system of actual

interest by a simpler system. The criteria of simplicity are that the calculations should be easier, but that no important qualitative physical effects discarded.

### A. LATTICE MODELS

In the integral of Equation 2, the possible configurations of the particles of the system are distributed continuously in space. Let us permit the particles to occupy a set of discrete points only and replace the integral by a sum over these discrete points. For the sake of symmetry and computational convenience, the discrete points are usually taken to be the points of some crystallographic lattice. This procedure gives rise to a class of theories called lattice theories.<sup>17</sup>

Newcomers often remark that lattice theories cannot possibly treat kinetic energy contributions to the partition function correctly. This is true, but irrelevant. By the time one has reached Equation 2, the kinetic energy has already been accounted for, completely and exactly. Lattice models are only designed to treat the configurational aspect of the problem.

As an illustration of lattice theories, let us suppose we have a binary mixture of particles of type A and of type B. Restrict the location of the particles to the lattice points of a simple cubic lattice (for simplicity of visualization), and suppose the intermolecular forces are short ranged, so that a particle will only interact with its nearest neighbors on the lattice. The number of A molecules is denoted by  $N_A$ , the number of B molecules by  $N_B$ ,  $N_A + N_B = N$ , the total number of available lattice sites. Let us call the total number of A-A nearest-neighbor pairs of particles on the lattice  $N_{AA}$ , the number of B-B nearest-neighbor pairs,  $N_{BB}$ , and of A-B pairs,  $N_{AB}$ . Let  $E_{AA}$  be the interaction energy of a nearest-neighbor A-A pair and similarly for  $E_{BB}$ ,  $E_{AB}$ .

The numbers  $N_{AA}$ ,  $N_{BB}$ , and  $N_{AB}$  are not independent. For example, the total number of pairs must be  $zN/2$ , where  $z$  is the coordination number of the lattice ( $z = 6$  for the simple case we are considering); and there are other restrictions. When these are taken into account, one sees that the energy of a given configuration depends only on one of the  $N_{ij}$ 's, say  $N_{AA}$ , and on the single parameter  $w = E_{AA} + E_{BB} - 2E_{AB}$ . The canonical partition function for the lattice model can be written

$$Q_L = \frac{1}{N_A!N_B!} \sum_{N_{AA}} g(N_{AA}) e^{-\beta w N_{AA} + C} \quad (50)$$

Here  $g(N_{AA})$  is the number of configurations of particles on the lattice consistent with a given number of A-A pairs,  $N_{AA}$ , and  $C$  is a number which may depend on  $N_A$ ,  $N_B$ , and the  $E$ 's, but is independent of configuration.  $g$ , as used in this section, should not be confused with the two-body distribution function.

Thus, at the expense of restricting the particles to lattice sites the problem has been reduced from a very complicated integral to what is essentially a counting problem, i.e., the determination of  $g$ . If  $g(N_{AA})$  is known, carrying out the sum in Equation 50 is no real problem. Of course,  $g$  and, therefore  $Q_L$  also depend on  $N_A$  and  $N_B$ . These are the variables which fix the composition of the system.

The calculation of  $g(N_{AA})$  is no easy task. In three-dimensional cases, we only have approximations to guide us. However, suppose we were to solve the three-dimensional case exactly. How much could we trust the answer? After all, in going from the continuum liquid to the lattice, we have changed the very problem. At best, we have a theory of solid solutions. The answer is that lattice models for liquids can only be expected to give indications of trends, of qualitative features, and of phenomena taking place on a scale large compared to the lattice spacing.

In the case of electrolyte solutions, the long range of the forces makes Equation 50, or any close analog, even qualitatively inappropriate, since Equation 50 was written down

using the hypothesis of nearest-neighbor force. In principle, it is possible to incorporate long-range forces into a lattice theory. The very successful theory of ionic crystals is a case in point. For dense systems, such as fused salts, modifications taking the long-range forces into account have also proved useful.<sup>18</sup> For dilute systems, an assumed lattice appears to be too unlike the actual physical distribution of ions for lattice theories of this type to be sensible. An example of some historical interest is a theory of dilute solutions of electrolytes due to Ghosh,<sup>19</sup> based on lattice ideas. This theory predicted deviations from ideal solution laws varying as  $c^{1/3}$ ,  $c$  being number density. This excited a great deal of interest, because, as Planck<sup>20</sup> wrote in 1921, it was "in agreement with the measurement to date". We now know that the theory was wrong and the measurements not sufficiently accurate.

One thing seems to be intuitively very clear: lattice models of fluids overly restrict the available configurations. This, then, underestimates the entropy of the system. It is possible to correct this, in part only, by allowing the particles some limited freedom of motion about their lattice sites. The resulting models are called cell models.

## B. CELL MODELS<sup>21</sup>

In order to introduce the idea of cell models, let us first consider a pure fluid. Equation 2 gives us the partition function,  $Q$ , which we cannot evaluate rigorously. So, let us suppose that the volume,  $V$ , is divided into  $N$  cells, each of a volume  $V/N$ . Each cell will contain one particle, and the integration over the  $j$ th particle's coordinates will only be carried out over the interior of cell  $j$ ,  $\Delta_j$ . In this approximation

$$Q = \lambda^{3N}/N! \int_{\Delta_1} \dots \int_{\Delta_N} d\{\mathbf{I}\}_1 \dots d\{\mathbf{N}\} e^{-\beta U(\{\mathbf{N}\})} \quad (51)$$

However, this does not help very much, since the intermolecular correlations in  $U(\{\mathbf{N}\})$  make the integration almost as difficult as in Equation 2. The next step is to assume that the potential that a given particle, say the one in cell  $j$ , sees is an average potential, averaged over the positions of all of the particles in neighboring cells. It only depends on the coordinates of particle  $j$  in the  $j$ th cell, since all other coordinate dependence is averaged out. If we call this average potential  $u(j)$ , then Equation 51 becomes

$$Q = [\lambda^3 \int_{\Delta} e^{-\beta u(j)}]^N / N! \quad (52)$$

So, once the potential,  $u$ , is determined, the problem is reduced to a single particle (three-dimensional) integration, which is relatively easy to carry out, numerically if necessary.

But what is the mean potential,  $u$ ? It cannot be arbitrarily chosen, but must bear some relationship to  $U$ .  $u$  must be determined by a self-consistency argument. The function  $\exp(-\beta u)$  determines the distribution of a given particle in its cell. This distribution determines the average potential experienced by another particle, and this average potential is, itself,  $u$ . The self-consistent potential,  $u$ , can be obtained by solving a certain integral equation expressing the self-consistency requirement. We need not go into the details of this.

For mixtures, or solutions, there is an additional complication. How do we distribute the particles of various species over the cells? Clearly, the mean potential experienced by a particle depends on the nature of its neighbors. In principle, one has the order-disorder problem of atomic arrangements to solve simultaneously with the determination of  $u$ .

In practice, one adopts still a further approximation, that of random mixing. If we have a mixture of species A and B, and  $u_A$  is the self-consistent potential of an A particle in pure



A,  $u_B$ , that for a B particle in pure B, then one might guess

$$u = x_A u_A + x_B u_B \quad (53)$$

where  $x_A$  and  $x_B$  are the mole fractions of A and B, respectively. A basic condition for Equation 53 to be reasonable is that the molecules have roughly the same size, since Equation 53 scales the strengths of the interactions, not the ranges. The approximation can be generalized to molecules of different size.

The advantage of this procedure is that the partition function is just like that of a pure fluid (aside from the  $N!$  factors that give rise to the ideal mixing terms). The fictitious "pure" fluid has a certain effective potential (Equation 53 in the equal size case) and the composition dependence of the thermodynamic functions arises from the composition dependence of this effective potential. Higher order effects, due to deviations from random mixing, are calculable in principle, but are very difficult to obtain.

The idea of using some sort of average potential can be divorced from the cell model, and the theory thus developed, the *average potential model*, is not subject to the artificial geometrical constraints of the cell theory. In its crudest form, the average potential model is an application of the law of corresponding states. Let us suppose that  $U$  is a sum of pair potentials

$$U(\{N\}) = \frac{1}{2} \sum_{\alpha, \beta} \sum_{i, j} u_{\alpha\beta}(r_{ij}) \quad (54)$$

where  $u_{\alpha\beta}(r_{ij})$  is the potential between particles  $i$  of species  $\alpha$  and particle  $j$  of species  $\beta$ . Furthermore, suppose that the  $u$ 's are conformal, in the sense that

$$u_{\alpha\beta}(r) = \epsilon_{\alpha\beta} f(r/\sigma_{\alpha\beta}) \quad (55)$$

The function  $f$  is supposed the same for all pairs,  $i, j$ . Only the energy parameters,  $\epsilon_{\alpha\beta}$ , and size parameters,  $\sigma_{\alpha\beta}$ , differ from pair to pair.

As an approximation, we replace  $U$  in Equation 54 by

$$\begin{aligned} U'(\{N\}) &= \sum_{i, j} u(r_{ij}) \\ u(r) &= \epsilon f(r/\sigma) \end{aligned} \quad (56)$$

$\epsilon$  and  $\sigma$  are some composition-dependent averages of the  $\epsilon_{\alpha\beta}$  and  $\sigma_{\alpha\beta}$ . The partition function derived from Equation 56 is that of a pure fluid, plus, of course, the ideal mixing terms. This pure fluid is hypothetical; it is characterized by potential parameters which do not, in general, correspond to any fluid found in nature. Note, however, that the  $\epsilon$  enters into  $Q$  only in the combination  $\epsilon/kT$  (refer to Equation 2) and  $\sigma$  enters only in the combination  $V/\sigma^3$ . Therefore, the hypothetical fluid, at temperature  $T$  and number density  $N/V$ , will have exactly the same thermodynamic properties as a real fluid,  $\alpha$ , at temperature  $\epsilon_{\alpha\alpha} T/\epsilon$ , density  $(N/V)(\sigma/\sigma_{\alpha\alpha})^3$ . This is the law of corresponding states for the present situation. Thus the properties of the hypothetical fluid and, hence, the approximate properties of the mixture may be obtained from experimental information on pure fluids.

Clearly, this approximation can only be expected to be reasonable if the intermolecular forces among the several components of the solution are similar. For example, it is clear that Equation 55 cannot hold for all pairs, if some of the components are polar, some nonpolar, or some charged. Nevertheless, when the hypotheses are fulfilled, the results are very reasonable. Furthermore — and this is a great advantage — the theory is very easy to apply.

## VI. PERTURBATION THEORY AND VARIATIONAL METHODS

### A. PERTURBATION THEORY<sup>22</sup>

In quantitative physical theories, it is a well-known fact of experience that there are very few problems that have been solved exactly. The problems are not intrinsically insoluble. It is just that we are not good enough mathematicians to solve them. One can, however, often make progress by a series of successive approximations. We want to describe several ways of doing this in context of solution theory. Suppose one has a potential  $U_0(\{\mathbf{N}\})$ , for which one can evaluate the partition function and the molecular distribution functions exactly. Unfortunately, one is interested, not in  $U_0$ , but in a different function,  $U$ . Let us suppose that  $U = U - U_0$  is, in some sense, small, and let us expand in powers of this "small" quantity. We write

$$\begin{aligned} Q &= \frac{\lambda^{-3N}}{N!} \int e^{-\beta U} d\{\mathbf{N}\} = \frac{\lambda^{-3N}}{N!} \int e^{-\beta(U_0 + \Delta U)} d\{\mathbf{N}\} \\ &= \frac{\lambda^{-3N}}{N!} \int e^{-\beta U_0} \sum_{n=0}^{\infty} \frac{(-\beta)^n}{n!} (\Delta U)^n d\{\mathbf{N}\} \end{aligned} \quad (57)$$

This can be expressed in the form

$$Q = Q_0 \sum_{n=1}^{\infty} \frac{(-\beta)^n}{n!} \langle (\Delta U)^n \rangle_0 \quad (58)$$

where

$$\begin{aligned} Q_0 &= (\lambda^{-3N}/N!) \int e^{-\beta U_0} d\{\mathbf{N}\} \\ \langle (\Delta U)^n \rangle_0 &= \int e^{-\beta U_0} (\Delta U)^n d\{\mathbf{N}\} / \int e^{-\beta U_0} d\{\mathbf{N}\} \end{aligned} \quad (59)$$

The quantity of interest, of course, is  $\ln Q = -A/kT$ . So, taking logarithms, we have

$$-\beta A = -\beta A_0 - \beta \langle \Delta U \rangle_0 + \beta^2/2 \{ \langle (\Delta U)^2 \rangle_0 - \langle \Delta U \rangle_0^2 \} + \dots \quad (60)$$

In going from Equation 59 to Equation 60, we have used the expansion of the logarithm  $\ln(1+x) = x - x^2/2 + \dots$ , and have only written the terms of first and second order in  $\Delta U$ .

There is another way to formulate the perturbation theory which may sometimes be useful. Suppose that  $U$  depends on some parameters,  $\gamma$  (force constants, molecular radii, etc.). We write  $U(\gamma)$  to emphasize this dependence and drop, for typographical reason only, the explicit dependence on  $\{\mathbf{N}\}$ , the coordinates. Choose  $\gamma_0$  as some reference set of parameters. Then

$$A(\gamma) = A(\gamma_0) + \sum_i (\gamma_i - \gamma_{i0}) (\partial A / \partial \gamma_{i0}) + \dots \quad (61)$$

This is just the Taylor expansion of  $A(\gamma)$  about  $\gamma_0$ . The coefficients  $(\partial A / \partial \gamma_i)_0$  are  $\langle \partial U / \partial \gamma_i | \gamma_0 \rangle$ , and the higher terms are similar, but more complicated, averages. The usefulness of this expansion, again, depends on our ability to evaluate the individual terms.

Note that, at any given finite order, Equations 60 and 61 are not necessarily equivalent, for these two equations represent  $A$  expanded with respect to different expansion parameters. Which should one choose? The one that converges more rapidly. How can one tell? Only by trial and error, or well-developed intuition.

This is the entire formal structure of the classical statistical mechanical perturbation theory. Those familiar with the perturbation theory in other fields, e.g., quantum theory, will appreciate how much simpler the statistical perturbation theory is. Of course, the real problems are hidden in the simple formalism, namely, how to evaluate  $A_0$ ,  $\langle \Delta U \rangle_0$ , etc.

The art of applying the perturbation theory consists of choosing a  $U_0$  with two primary properties: (1) it is simple enough to handle and (2) it contains as much as possible of the physically important part of the interactions. If the important physics is in  $U_0$ , then the higher order terms, which are usually difficult to compute, will not be too important. Unfortunately, desiderata (1) and (2) are generally incompatible. Simplicity and realism are not comfortable partners. Compromises must be made.

Let us look at the significance of the various terms in Equation 60. The first term,  $\beta A_0$ , is just the free energy of the unperturbed system. The second term (first-order perturbation) is the mean value of the perturbation energy. The higher order terms, not exhibited in Equation 60, are higher order fluctuations. It is interesting that powers of  $\Delta U$  occur in  $Q$ , but that fluctuations of  $\Delta U$  occur in  $A$ . This transition from powers to fluctuations is typical of the many-body perturbation theory. Technically, it corresponds to passing from moments to cumulants. We shall not pause to explain the meaning of these terms. It seems reasonable to conjecture that the series for  $A$  would converge better than that for  $Q$ , but we are not aware of a general proof of this.

Let us consider an interesting special case. Suppose  $U(\{N\})$  is of the form given by Equations 54 and 55. Take  $U_0$  to be

$$U_0 = \sum_{i,j} u_0(r_{ij}) \quad (62)$$

with

$$u_0(r) = \sum_{i,j} x_i x_j u_{ij}(r) \quad (63)$$

with  $x_i$  the mole fraction of species  $i$ . Then  $\langle \Delta U \rangle_0 = 0$ . The leading corrections to the unperturbed free energy,  $A_0$ , are thus second order in the perturbation. If one decides to ignore terms of second order, one has  $A \cong A_0$ , and  $A_0$  is the free energy of a pure fluid with pair potential  $u_0$ . Unfortunately,  $u_0$  is not necessarily conformal with the  $u$ , as in Equations 55 and 56, so that  $A_0$  cannot, in general, be determined by corresponding states arguments.

What information is needed to compute the correction terms  $\langle \Delta U \rangle$ ,  $\langle (\Delta U)^2 \rangle - \langle \Delta U \rangle^2$ , etc.? The answer for  $\langle \Delta U \rangle$  is simple if  $U$  is a sum of pair potentials. In fact, from Equation 54 and 62

$$\langle \Delta U \rangle = \sum_{i,j} \int \rho_i \rho_j [u_{ij}(r_{12}) - u_0(r_{12})] g(r_{12}) d(\mathbf{2}) \quad (64)$$

(see Section II.C for the definition of  $g$ ).

If  $U_0$  is not of the form of Equation 62, but is species dependent, then Equation 64 becomes more complicated, but still only depends on pair correlation functions for the reference fluid, i.e., the fluid interacting according to the potential  $U_0$ . These pair correlation functions are sometimes available, for example, from corresponding states arguments or Monte Carlo calculations.

The second-order terms are more complicated. Each second-order term contains two  $u$ 's. These can be of three types: (1)  $u^2(r_{ij})$ ; (2)  $u(r_{ij})u(r_{jk})$ ; and (3)  $u(r_{ij})u(r_{kl})$ . The terms of type 1 involve only two body correlations and can be expressed in terms of the pair correlation functions,  $g$  or  $F_2$ , of the reference fluid. This is the same information needed to evaluate the first-order term, Equation 64. The terms of type (2), however, involve three particles,  $i$ ,  $j$ , and  $k$ , and one needs  $F_3(\{\mathbf{3}\})$  to evaluate them. Similarly, terms of type (3) require knowledge of  $F_4(\{\mathbf{4}\})$  for carrying out the average. Unfortunately, one rarely knows  $F_3$  or  $F_4$ .

Higher order perturbation terms involve higher order  $F_n$ 's for the reference system; these  $F_n$ 's have never been studied in any detail. As a rule of thumb, one can say that if second or higher order terms are necessary for the desired accuracy, one has probably chosen an inconvenient reference system.

Perturbation theories are of little direct use in treating coulombic interactions in electrolyte theory. This is because the electrical contribution to the free energy is a collective effect, depending on the simultaneous interaction of all of the ions present. This is a consequence of the long range of coulomb forces. Collective effects are not handled properly in any finite order of perturbation theory. The same is true for problems such as electrons in metals, and plasmas, as well as electrolyte solutions. On the other hand, if one constructs a theory for a reference system that treats the electrical, coulombic effects as accurately as possible, then effects due to short-range forces can be taken into account by perturbation theory.

## B. VARIATIONAL METHODS

Nowadays, students learn about variational methods in quantum mechanics courses. However, there are variational principles in statistical mechanics, too, and these have been applied to solution theory. They have been reviewed at some length by Girardeau and Mazo.<sup>23</sup>

The basic formula is simple. Let  $U(\{\mathbf{N}\})$  be the intermolecular potential for a system of interest, and  $A$  its free energy. Let  $U_0(\{\mathbf{N}\})$  be some reference potential and  $A_0$  the free energy of the corresponding system. Then

$$A \leq A_0 + \langle U - U_0 \rangle_0 \quad (65)$$

where the caret,  $\langle \dots \rangle$ , is defined as in Equation 59, i.e.,  $\langle X \rangle_0$  is the average of  $X$ , over the distribution function of the reference system.

Equation 65 is the Gibbs-Bogoliubov variational principle. It was published by Gibbs for classical statistical mechanics in 1901.<sup>24</sup> It is a variational principle, since  $U_0$  is at our disposal, and we may vary  $U_0$  to minimize the right-hand side of Equation 65.

Let us note that Equation 65 can be interpreted as saying that, once having picked  $U_0$ , the first-order perturbation theory (refer to Equation 60) gives an upper bound for  $A$ . On the other hand, as we have mentioned in Section V.A, it is possible to formulate the perturbation theory in other ways, which have no obvious relation to variational methods.

## VII. MONTE CARLO AND MOLECULAR DYNAMICS

In Section II.A we mentioned the Monte Carlo method for the direct evaluation of thermodynamic and structural properties. There is also another method based on the use of high speed computers, the molecular dynamics method. In this section we present the basic ideas of these techniques.

### A. MONTE CARLO METHODS

The fundamental idea of the Monte Carlo method is to invent a game whose mean or average score is the quantity which one wants. The game need have nothing to do with the

original problem. It is only required that one be able to prove that the average score is the same as the answer to the original problem. Instead of solving the original problem directly, one then plays the game a number of times (usually on a computer) and averages the outcomes of the trials. This provides an estimate of the true, but unknown, mean score, and hence of the quantity one wants.

To give an example of how this might work, suppose one wants to evaluate  $\int_0^1 f(x) dx$ , where  $0 \leq f(x) \leq 1$  and  $f$  is a given function. A Monte Carlo method for evaluating the integral would be to draw a graph of  $f(x)$  on paper of a convenient size, attach the paper to a wall, blindfold oneself, and throw darts at the paper. The ratio of the number of darts which hit the paper below the graph of  $f$  to the total number which hit the paper is an estimate of the area below the graph of  $f$ , and hence of the integral.

Of course, this is a terribly inefficient way to evaluate a one-dimensional integral, but it illustrates the general idea of Monte Carlo. Better Monte Carlo methods are available. However, one would not ordinarily use them on one-dimensional integrals either. Monte Carlo methods become more efficient relative to ordinary grid sampling methods as the dimensionality of the integration region increases. In practice, of course, one would not throw darts, but instead generate pairs of random numbers on a computer to simulate the coordinates of the dart's impact point in the illustration just given. In most problems, a very large number of trials is needed for acceptable accuracy. However, the needed number of trials does not increase exponentially with the dimensionality of the integral as does the number of points necessary for grid sampling methods.

The number one gets from a set of trials is only an estimate of the integral. A different set of trials would give a different numerical estimate. In other words, the result of a Monte Carlo experiment is a random variable whose mean value is the quantity one wants. It is obviously also desirable to have an estimate of the probable error, the deviation of the trial value from the true but unknown mean. Such an estimate can often be obtained in the same way as one estimates the precision of replicated laboratory experiments.

One can compute the sample standard deviation from the same set of trials used to calculate the sample mean. Standard statistical methods then yield the probable error of the mean. The probable error, roughly speaking the precision of the estimated value, decreases as the inverse square root of the number of trials. To get one more decimal place in evaluating an integral, one needs 100 times as many points. It is therefore important to try to minimize the fluctuations about the mean.

Techniques which enable one to do this are called variance reduction techniques. One such technique is importance sampling. In the evaluation of an integral, the regions where the integrand is large contribute more to the integral than do the regions where the integrand is small. Importance sampling means devising a technique to sample preferentially from the former regions, and to weight these contributions properly. If the weighting is done correctly, the true mean value will be unaffected, but random deviations about the mean may be appreciably reduced.

This is very important for evaluating configurational averages in statistical mechanics, in particular the configurational integral,  $Z$ , Equation 3. If one considers a system of several hundred particles in a volume at typical liquid densities and places the centers of the particles in the region at random (uniform distribution), the vast majority of the configurations so generated will have overlapping molecules. Thus they make negligible contributions to  $Z$ . The probable error of such a uniform sampling technique for the integrand of  $Z$  is so large, when only a finite number of configurations is sampled, as to make the method useless. The original paper of Metropolis et al.<sup>3</sup> devised a method to avoid this problem for liquid state simulations.

One wants to sample from the Boltzmann distribution  $\exp(-U/kT)/Z$  in order to evaluate configuration averages. As just discussed, this is inefficient, and, in fact,  $Z$  is unknown.

The Metropolis et al. idea was to sample from the Boltzmann distribution by first constructing the transition matrix of a Markov chain of configurations in the configuration space of the molecules. This chain is constructed so that the limiting form of the probability distribution, as the number of states in the chain becomes very large, is the Boltzmann distribution. Thus, if one takes enough samples, one is eventually sampling from the Boltzmann distribution, although one does not have to construct the distribution directly. This avoids the evaluation of  $Z$ . Other Markov chain algorithms have subsequently been proposed and used, also.<sup>25</sup>

To construct the Markov chain, one starts with an arbitrary configuration and chooses a particle at random. The chosen particle is moved randomly to a new location, and  $U$  for the move is computed. If  $\Delta U$  is negative, the move is accepted. If  $\Delta U$  is positive, the move is accepted with probability  $\exp(-\Delta U/kT)$ . This can be done by comparing  $\exp(-\Delta U/kT)$  with a random number between 0 and 1.

This set of operations is repeated, giving a sequence of configurations which, after many repetitions, are Boltzmann distributed. This asymptotic property is not obvious and must be proved. We shall not give the proof here. Note that the transition probabilities are independent of the (unknown) configuration integral,  $Z$ . The first group of configurations generated from the arbitrary initial configuration is discarded, since the Boltzmann distribution has not been reached for it. Averages are then calculated using the set of configurations retained. One might, in a practical case, take  $10^5$  configurations to equilibrate to the limiting Boltzmann distribution and another  $10^5$  or more for the averaging.

There is another problem in the implementation of the Monte Carlo method for fluids. This concerns the size of the system. Real physical systems of experimental interest have of the order of Avogadro's number of particles; they are effectively infinite. The systems which one can handle on presently available computers have only several hundred particles. This finite size means that surface effects can become important. Although surface effects can never be completely avoided, they can be minimized by using periodic boundary conditions. The volume in question is supposed to be part of an infinite periodic lattice of identical volumes. Thus the surroundings of particles near the boundary of the chosen volume are fluid-like, and not wall-like. Although the imposed periodicity generates strong correlations between distant particles, for particles with short-range interactions experience has shown that these residual correlations are not important.

On the other hand, for ionic systems the forces are of long range, as we have often emphasized. Therefore the distant periodic images of the chosen volume will exert forces on the particles in the chosen volume which fall off only slowly with distance. Valleau and Whittington<sup>26</sup> have suggested that the effects of these artificially imposed long-range correlations may be appreciable. However, subsequent authors<sup>27</sup> have shown that the effects are rather small compared to other errors introduced by the finite size of the system, and periodic boundary conditions are commonly used.

The review articles by Valleau and Whittington<sup>26</sup> and Valleau and Torrie<sup>28</sup> give more details on the technique than we can give here. More recent reviews by Levesque et al.<sup>29a,29b</sup> are a good source for further references on the technique and on specific applications.

## **B. MOLECULAR DYNAMICS METHOD**

A second numerical technique which has been used with profit on electrolyte solutions is the molecular dynamics method. Like the Monte Carlo method, it computes quantities of interest by averaging over configurations generated on a computer. In the Monte Carlo method, the configurations are generated by some artificial probability scheme. On the contrary, in molecular dynamics the configurations are those which fall on the natural trajectories of the system. By natural trajectories are meant the orbits on which the particles would actually move if they existed in fact, and not just in the memory of a computer. These orbits are determined by the numerical integration of Newton's equations of motion

for the particles. The integration is carried out for some period of time, and then quantities of interest are computed by time averaging along the trajectories.

In a simple case,<sup>30</sup> the time step for the numerical integration might be  $10^{-15}$  s and a trajectory might be calculated for  $10^{-12}$  s in a system of 256 particles of dense fluid density.

Current Monte Carlo calculations are restricted to yielding structural and thermodynamic information about the equilibrium states of the system. Molecular dynamics calculations yield these quantities, also. Because they utilize the true (within the numerical precision of the integration of the equations of motion) orbits of the system, they also give dynamical information, time correlation functions, and transport properties, for example. Such time-dependent properties are outside the scope of this review.

Molecular dynamics has the same small system difficulties which we have discussed above. Generally speaking, Monte Carlo calculations are less demanding of machine capabilities and time than are molecular dynamics. Therefore, unless time-dependent properties are desired, Monte Carlo is usually the method of choice. A recent review of molecular dynamics calculations has been given by Heinzinger.<sup>31</sup>

Numerical simulations are extremely demanding of computer time and storage. However, the calculations are feasible, in contrast to direct numerical integration, which is completely impractical. Because of the large amount of computer time necessary, simulations are usually carried out only on certain key problems rather than on a variety of potentials, although with improvement in computing facilities and technique this situation is changing. The simulation results may be looked upon as experimental results for these model systems, and serve as bench marks for assessing the quality of various approximate analytical methods that might be used to evaluate thermodynamic properties.

In comparing theory with experiment for real systems, there are always two questions which must be asked in interpreting results. First, how well does the theoretical model approximate the real system? For example, is the potential energy function realistic? Second, how good is the theoretical method? For Monte Carlo and molecular dynamics calculations, the first question is irrelevant. The simulation and any subsequent analytical theories are performed on the same model. Thus we have a pure case of testing theoretical methods.

## VIII. STATISTICAL MECHANICAL THEORIES FOR ELECTROLYTE SOLUTIONS

We have seen that the McMillan-Mayer theory<sup>1</sup> provides a clear framework for developing approximate calculations of the thermodynamic properties of solutions, and of electrolyte solutions in particular. One naive way to proceed might be through the simple virial expansion of Equation 39. However, when one attempts to apply Equation 39 to electrolyte solutions, a serious difficulty arises. Since the potential of mean force falls off as  $r^{-1}$ , the cluster integrals in Equations 40 and 41 do not converge, and the expansion appears meaningless. For a long time, this difficulty was a stumbling block for the statistical mechanics of ionic systems.

The reason the integrals do not converge is because of the long range of the coulomb potential, and this suggests the cure for the disease. If the interionic potential is of long range, the particles cannot be considered as acting as independent pairs in first approximation, independent pairs and triples in second approximation, etc. Rather, many, many particles must interact all at once. This is often expressed by saying that the system acts collectively. In ionized gases, plasmas, where there is no solvent present, such collective effects can be clearly seen in charge density oscillations of the gas, the plasma oscillations. In electrolyte solutions, such oscillations are strongly damped by solvent friction, but the collective modes are still present.

The presence of collective effects means that any power series representation of the

thermodynamics of a solution is bound to fail if the coefficients purport to represent the effects of small interacting clusters of solute ions. A technical way to introduce the collective effects within the present formalism would be to replace the potential of mean force by one of finite range, and sum the density series to infinite order. Then, let the potential of mean force become coulombic, i.e., let the range become infinite, after the sum has been carried out.

It is the infinite sum of the divergent terms (divergent in the coulombic limit) which expresses, mathematically, the physical collective behavior that is occurring. The collective effects give rise to a screening of the long-range ionic forces.

At present, there are many different approaches to the statistical mechanical theory of electrolyte solution. Various starting points focusing on the mean electrostatic potential, the free energy, or pair correlation functions characterize the different approaches. For each approach, various approximations at different levels further enrich the development. It is one of the purposes of this introductory chapter to present the fundamental ideal of several popular approaches. Detailed developments and comparison with experiment can be found in several of the general references.

#### A. POTENTIAL ENERGY APPROACH (DEBYE-HÜCKEL THEORY AND ITS DESCENDANTS)

The basic assumption in this approach is that the nonideal behavior of an electrolyte solution can be separated into an electrostatic part and a short-range nonelectrostatic contribution. Thus if  $A$  is the Helmholtz free energy of the solution, and  $A_0$  the free energy when all the ions are discharged, one has

$$A - A_0 = -kT \ln \int e^{-\beta U(\mathbf{N})} d\{\mathbf{N}\} / \int e^{-\beta U(e_1=e_2=\dots=0)} d\{\mathbf{N}\} \quad (66)$$

Debye and Hückel further assume that  $A_0$ , the uncharged free energy, is to be taken as the free energy of an *ideal* solution. Thus the activity coefficient,  $\gamma_i$ , is

$$kT \ln \gamma_i = \partial \Delta A / \partial \rho_i \quad (67)$$

In this section, as earlier, we shall use the theoretically convenient concentration unit,  $\rho_i$ , as the number density of species  $i$ . The practical concentration unit, molar concentration,  $c_i$ , is related to  $\rho_i$  by  $c_i = 1000 \rho_i / N_A$ , where  $N_A$  is Avogadro's number.

Now, if one assumes that the ionic charges,  $e_i$ , can be varied independently and considers a variation of the charges  $de_i$ , the change of the free energy,  $A$ , can be written as

$$dA = \sum_i (\partial A / \partial e_i)_{T, V, de_i} = \sum_i \psi_i^* de_i \quad (68)$$

Writing  $(\partial A / \partial e_i) = \psi_i^*$  is, of course, mere notation. The physical significance of  $\psi_i^*$  is that it is the mean electrostatic potential at the position of particle  $i$ , due to all of the other ions. The justification for this interpretation is that  $(\partial A / \partial \lambda)_{T, V} \delta \lambda$  is the work done in making a small change,  $\delta \lambda$ , in some parameter,  $\lambda$ , determining the system. If the parameter,  $\lambda$ , is taken as a species charge,  $e_i$ , then the work done is the potential times the variation in charge. This gives the identification of  $\psi_i^*$  with the electrostatic potential.

Of course, we cannot physically change the ionic charges by infinitesimal amounts. However, we can certainly do it mathematically, in our equations, and that is all that is necessary.



Integrating Equation 68, one obtains

$$\Delta A/V = \sum_s e_s \rho_s \int_0^1 \psi_s^*(\lambda) d\lambda \quad (69)$$

The summation is over all species of ions,  $\rho_s$  is the concentration of ionic species  $s$ , and  $\lambda$  is the charging parameter, i.e., the fraction of the total charge at any stage of the charging process.

Equation 69 is called the Debye charging process. Since  $A$  is a state function, other charging processes (paths) could also be used. Guntelberg<sup>33</sup> showed that

$$kT \ln \gamma_s = e_s \int_0^1 \psi_s^*(\lambda) d\lambda \quad (70)$$

by considering the charging of one test ion only, while the remaining  $N-1$  ions have their full charge. Equations 69 and 70 should give the same result if one has the correct  $\psi_s^*$ . For an approximate  $\psi_s^*$ , these two equations need not give the same answer. The extent to which the answers agree constitutes a consistency test for the approximation.

Therefore, a statistical mechanical calculation of the mean potential  $\psi_s^*$  is equivalent to a calculation of  $A$ , so we compute  $\psi_s^*$ . The easiest way to compute this quantity is actually to consider a more general problem. We ask what is the potential,  $\psi_i(r)$  at a distance  $r$  from ion  $i$ ? Then

$$\psi_i^* = \lim_{r \rightarrow \infty} (\psi_i(r) - e_i/\epsilon r) \quad (71)$$

where the potential due to ion  $i$  itself has been subtracted off.

The potential  $\psi_i(r)$ , at a distance  $r$  from an ion  $i$ , is the coulomb potential, due to all ions, averaged. However, the averaging process is conditional. That is, the other ions are not randomly distributed, but their distribution in space is condition by the fact that ion  $i$  is fixed. The conditional distribution is just exactly what is described by the pair correlation function,  $g_{is}$ , and the formal expression of these facts is

$$\begin{aligned} \psi_i(r) &= \sum_s e_s \rho_s \int \frac{g_{is}(\mathbf{R})}{\epsilon |\mathbf{r} - \mathbf{R}|} d^3\mathbf{R} \\ g_{is}(\mathbf{R}) &= \exp(-\beta W_{is}(\mathbf{R})) \end{aligned} \quad (72)$$

where  $W_{is}(\mathbf{R})$  is the potential of mean force between ions  $i$  and  $s$ . Equation 72 excludes the contribution of ion  $i$ . Using the Laplacian to eliminate the integration, Equation 72 can be rewritten as

$$\nabla^2 \psi_i(r) = -(4\pi/\epsilon) \sum_s e_s \rho_s \exp(-\beta W_{is}(r)) \quad (73)$$

Of course, Equation 73 is just an exact relation rephrasing the definition, Equation 72, of  $\psi_i$  in terms of the potentials of mean force  $W_{is}(\mathbf{R})$ . In general, in the presence of thermal fluctuations, the mean potential energy,  $e_s \psi_s$ , is different from the potential of mean force.  $\psi_i(r)$  represents the mean potential at a distance  $r$  from ion  $i$  regardless of what, if anything, is present at  $r$ . On the other hand,  $W_{is}(r)$  gives the potential at  $r$ , if it is known that an ion of type  $s$  is present at  $r$ . The presence of an  $s$  ion at  $r$  will change the average ionic distribution about the  $i$ - $s$  pair, and there is, thus, no reason for  $e_s \psi_s(r)$  and  $W_{is}$  to be simply related.

Debye and Hückel made the closure assumption (central approximation) that

$$W_{is} = e_s \psi_i \quad (74)$$

With this approximation, Equation 73 becomes closed; it yields an equation called the Poisson-Boltzmann equation

$$\begin{aligned} \nabla^2 \psi_i(r) &= -(4\pi/\epsilon) \sum_s e_s \rho_s \exp(-\beta e_s \psi_i(r)); r > a \\ \nabla^2 \psi_i(r) &= 0; r < a \end{aligned} \quad (75)$$

where  $a$  is the hard-sphere diameter. The reason for the name is that Equation 75 can be regarded as a form of Poisson's equation of electrostatics, with Boltzmann's law being used to relate the charge density to the potential.

Assuming  $\beta e_s \psi_i \ll 1$ , Debye and Hückel then linearized Equation 75 to get

$$\nabla^2 \psi_i = (4\pi\beta/\epsilon) \left( \sum_s e_s^2 \rho_s \right) \psi_i = \kappa^2 \psi_i; r > a \quad (76)$$

which has the solution obeying proper boundary conditions

$$\psi_i(r) = (e_i/\epsilon r) \exp(-\kappa|r - a|)/(1 + \kappa a); r > a \quad (77)$$

By using either the Debye or Guntelberg charging process, one obtains

$$kT \ln \gamma_i = -\kappa e_i^2 / 2\epsilon(1 + \kappa a) \quad (78)$$

$$\propto \rho^{1/2} \text{ as } \rho \rightarrow 0 \quad (79)$$

The resulting limiting law behavior, Equation 79, has been confirmed by extensive experiments and also by later, more rigorous statistical mechanical derivations.

In dealing with experimental data, the Debye-Hückel limiting law, Equation 78, is of use as an extrapolation formula. One needs to know higher order terms in  $\kappa$  in order to treat the finite concentration region. If one looks at Equation 78, it does provide an extrapolation formula that can be used at higher concentration, but usually one has to choose  $a$  empirically to fit experimental data. Such a procedure is not satisfactory for two reasons. Theoretically, Equation 78 has been only derived at the price of several severe approximations, e.g., the central approximation, linearization, and the oversimplification of the primitive model itself. Practically, even if one tries to use Equation 78, the empirical value one has to use for  $a$  usually is concentration dependent and no physical interpretation of  $a$  can be really meaningful.

Within the framework of the potential approach, many attempts have been directed at improving the original approximations in the Debye-Hückel theory. The most obvious one is the linearization approximation, which has been the subject of much concern. This approximation was avoided by direct integration of the *nonlinear* Poisson-Boltzmann equation as done in Guggenheim's book.<sup>34</sup> However, when nonlinear terms are considered in the Poisson-Boltzmann equation, the approach becomes thermodynamically inconsistent; the two charging processes, Equations 69 and 70, give different results. This is due to the central approximation (Equation 72), which neglects the mutual fluctuation effect of the central ion with respect to other neighboring ions.<sup>35</sup> More recently,<sup>36</sup> the Poisson-Boltzmann equation has been reinvestigated using a variational principle in an attempt to provide the "best" estimate of  $\psi_i$ .

Going back to the exact equation, Equation 73, Kirkwood<sup>37</sup> was able to show that

$$\nabla^2 \psi_i(r) = -(4\pi/\epsilon) \sum_s \rho_s \xi_{is} e^{-\beta(\epsilon_s \psi_i(r) + \phi_{is}(r))} \quad (80)$$

$\xi$  is a short-range function; it approaches unity rapidly, as  $r \rightarrow \infty$ , and is sometimes called the "volume term".  $\phi_{is}$  has the form of a third-order fluctuation, representing mainly the departure of the potential of mean force from the mean potential; it is given by

$$\phi_{is}(r) = \int_0^{\epsilon_1} \int_0^{\epsilon_2} \int_0^{\epsilon_3} \frac{\partial^2 \psi_i}{\partial \epsilon_1^2} \Big|_{\epsilon_1 = r - \epsilon_1} d\epsilon_1 d\epsilon_2 d\epsilon_3 \quad (81)$$

for an s ion at r.

In the limit of infinite dilution,  $\psi_i$  becomes a linear function of charge; Equation 81 thus gives a vanishing value for  $\phi_{is}$  in this limit. Therefore, the Poisson-Boltzmann equation is exact in the limit of zero concentration. However, in general, the mean potential  $\psi_i$  is a nonlinear function of charge, and  $\phi_{is}$  is not zero. Kirkwood and Poirier have given approximate solutions of Equations 80 and 81. Further attempts to treat the fluctuation terms more exactly have been carried out by Falkenhagen and Kelbg,<sup>39</sup> Kelbg,<sup>40</sup> Bell and Levine,<sup>41</sup> and more recently, Outwaite and Bhuiyan.<sup>42</sup>

Because of the technical difficulties in going beyond the Debye-Hückel approximation in the potential approach, other approaches have been investigated. We now turn to some of these.

## B. CLUSTER EXPANSION THEORY<sup>43</sup>

We recall from Section II that the McMillan-Mayer theory enables us to apply the formal procedures, originally developed for gases, to solutes in solution. Equation 39 has the same form as a density expansion of the pressure for an n-component gaseous mixture. For simplicity, let us write Equation 39 for the case of a two-component system. We have

$$\pi/kT = \rho_1 + \rho_2 - \sum_{n_1, n_2} (n_1 + n_2 - 1) B_{n_1, n_2} \rho_1^{n_1} \rho_2^{n_2} \quad (82)$$

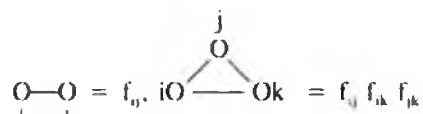
where  $B_{n_1, n_2}$  is an integral of the form

$$B_{n_1, n_2} = (1/n_1! n_2! V) \int \dots \int S_{1,2} d(n_1 + n_2) \quad (83)$$

and the integrand, S, is a sum of products of Mayer's  $f_{ij}$  functions, where

$$f_{ij} = e^{-\beta w_{ij}} - 1$$

One can represent the individual terms in any S by a diagram notation<sup>44</sup>



etc. This is an extremely useful notation, so much so that the integrals themselves are often referred to, by a mild abuse of language, as diagrams.

Equation 82 involves a triple summation, considering the integral as a sum (in the case

of simple pure fluid, it would be a double summation). For a normal dilute solution (or dilute gas), one usually does the summation for  $B_{n_1, n_2}$  first (i.e., the integral) and obtains a straightforward density expansion; truncations to low powers of the density can be expected to be good approximations. However, for dense or strongly interacting systems, such a procedure converges very slowly, or the series does not converge at all. For long-range interactions, like coulomb systems, even the individual terms, the  $B_{n_1, n_2}$ , diverge. Such divergences are artifacts of the summation procedure. An alternative procedure can be developed by summing the series in Equation 82 over all values of  $n_1, n_2$  first, for some specified types of term or cluster diagrams in  $B_{n_1, n_2}$ , and then summing all types of diagram. By doing this in a particular way, a convergent result can be obtained.

For electrolytes, Mayer classified the cluster integrals in the following way:<sup>45</sup> from Equation 45, the effect of short-range and long-range interactions can be separated in  $f_{ij}$ ; by defining two kinds of function

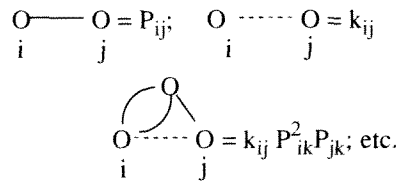
$$k_{ij}(r) = |e^{-w_{ij}^*(r)/kT} - 1| \quad (84)$$

$$P_{ij}(r) = \frac{z_i z_j e^2}{\epsilon r k T} \quad (85)$$

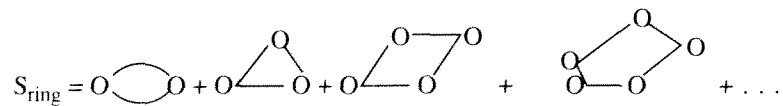
then

$$\begin{aligned} f_{ij} &= k_{ij} + (k_{ij} + 1)(e^{-P_{ij}} - 1) \\ &= k_{ij} + (k_{ij} + 1) \sum_{l=1}^{\infty} \frac{(-1)^l}{l!} P_{ij}^l \end{aligned} \quad (86)$$

These may be represented diagrammatically by drawing a dotted line for a  $k$ -bond between two particles and a solid line for each  $P$ -bond. Some examples are



Then the various terms in  $S_{n_1, n_2}$  can be classified according to their topological nature. The simplest kinds of diagram are the so-called ring diagrams, e.g., all points in the diagram are connected by  $P$ -bonds, forming a ring. They are



The contribution of all these ring diagrams to the free energy can be summed in closed form by a technical trick which we shall forego describing. The result is,<sup>45</sup> for the free energy per unit volume,

$$\beta \Delta A_{(ring)} = - \kappa^3 / 12 \quad (87)$$

where  $\kappa$  is given by Equation 76. This is just the Debye-Hückel result for point charges!

However, note that to obtain this result we had to retain diagrams containing arbitrarily many particles. This is a manifestation of the collective effects discussed earlier.

Higher order diagrams involve the short-range interaction terms  $k_{ij}$  in addition to the coulomb bond  $P_{ij}$ ; they are complicated, and the resummation procedure involves classification of each  $S$  into various types of contribution according to the topological structure of the diagrams.

Within each topological type of diagram the summations over  $n_1, n_2$  are performed first to obtain a new convergent cluster integral  $B_{s,t}(\kappa)$ . The formal result of these resummations of the series for the free energy is<sup>45</sup>

$$\beta\Delta A = -\kappa^3/12 - \sum_{s,t} \sum_{n \geq 2} \rho_s^n \rho_t^n B_{s,t}^{2n}(\kappa) \quad (88)$$

The classification of diagrams is, of course, not unique. Each classification corresponds to a different ordering of the higher terms in the expansion, Equation 88.<sup>46</sup> The interested reader should consult Reference 43 for details of the cluster summation method.

It is difficult to develop a feel for the intuitive meaning of these expansions without working directly with the expansions themselves. Even in the short-range case, the cluster symbolized by the diagrams are mathematical clusters, not physical clusters. In the case of long-range forces, the conceptual problems are compounded by the extra resummation necessary to account for the collective effects. Equation 88 is no longer a density expansion, since each  $B_{s,t}^n(\kappa)$  depends on density through the Debye parameter  $\kappa$ , because of the series summation which defines the  $B$ 's (refer to Equation 87).

If one only keeps the first term in the series of Equation 83, one has the so-called DHLL +  $B_2$  approximation<sup>43</sup> (DHLL stands for Debye-Hückel limiting law).

$$\beta\Delta A = -\kappa^3/12 - \sum_{s,t} \rho_s \rho_t B_{s,t}(\kappa) \quad (89)$$

where

$$B_{st}(\kappa) = 2\pi \int_0^\infty \{\exp(-\beta W_{st}^* + q_{st}) - 1 - q_{st}^2/2\} r^2 dr \quad (90)$$

with

$$q_{st} = -e_s e_t \exp(-\kappa r) / \epsilon k T r \quad (91)$$

The DHLL +  $B_2$  approximation is useful, since the first correction to the Debye-Hückel limiting law due to short-range interactions can be investigated carefully.  $W_{st}^*$  need not be limited to a hard core interaction, as in the previous potential approach.

Higher order terms than those included in Equation 89, comparison with experiment, and the consideration of more realistic potentials,  $W_{st}^*$  are beyond the scope of this chapter.

### C. INTEGRAL EQUATION APPROACHES<sup>47</sup>

As we have seen, knowledge of the radial distribution functions,  $g_{ij}(r)$ , also yields the thermodynamic properties of the solution. The structural information contained in  $g_{ij}(r)$  is more complete than that contained in the mean electrostatic potential. Hence, recent approaches to electrolyte solution theory have tended to shift to the determination of  $g_{ij}(r)$  rather than  $\psi_i(r)$ . This is also, no doubt, due to the rapid advances in the theory of simple fluids, made in the past three decades.<sup>48,49</sup>

There are three known routes for determining the thermodynamic properties from the

functions  $g_{ij}(r)$ . Let us consider the internal energy  $E$ . Using the definition of the partition function  $Q$ , Equation 2, we can write

$$E = \frac{3}{2} NkT - \frac{\partial \ln Z}{\partial \beta} = \frac{3}{2} NkT + \langle U \rangle \quad (92)$$

$$\langle U \rangle = \int U e^{-\beta U} d\{\mathbf{N}\} / \int e^{-\beta U} d\{\mathbf{N}\} \quad (93)$$

The first term in Equation 92 is the mean kinetic energy, and the second term is the mean potential energy. Let us assume that the total potential energy of the system is the sum of pair interaction energies.

$$U = \left(\frac{1}{2}\right) \sum_{i \neq j} u_{ij}(r_{ij}) \quad (94)$$

$U$  is the sum of  $N_i N_j / 2$  terms for a pair of species  $i$  and  $j$ , all of which give the same contribution upon carrying out the integration for  $\langle U \rangle$ . We then have

$$\begin{aligned} \langle U \rangle &= \sum_{i,j} \frac{N_i N_j}{2 Z} \int e^{-\beta U(\mathbf{N})} u_{ij} d\{\mathbf{N}\} \\ &= \sum_{i,j} \frac{N_i N_j}{2} \int u_{ij} d(i) d(j) \int e^{-\beta U(\mathbf{N})} d\{\mathbf{N} - 2\} / Z \\ &= \sum_{i,j} \frac{N_i N_j}{2 V} \int u_{ij}(r) g_{ij}(r) d^3 r \end{aligned} \quad (95)$$

therefore

$$\beta E/V = \left(\frac{3}{2}\right) \sum_i \rho_i + \sum_{i,j} (\beta \rho_i \rho_j / 2) \int_0^\infty u_{ij} g_{ij} 4\pi r^2 dr \quad (96)$$

Next we shall consider the pressure, which is  $p = kT (\partial \ln Q / \partial V)_{N,T}$ . Upon carrying out the differentiation, under the pair additivity assumption of Equation 94 one obtains

$$\beta p = \sum_i \rho_i - \sum_{i,j} \frac{\rho_i \rho_j \beta}{6} \int_0^\infty r \frac{\partial u_{ij}}{\partial r} g_{ij} 4\pi r^2 dr \quad (97)$$

Another relation relating  $g_{ij}$  to thermodynamic functions is the compressibility equation. This can appear in several equivalent forms for multicomponent systems; they have been derived in Section III.A on the Kirkwood-Buff theory. One example is Equation 32. For a simple 1-1 electrolyte system of number densities  $\rho_+ = \rho_- = \rho$ , Equation 32 becomes

$$\beta \frac{\partial \pi}{\partial \rho} = \frac{2 + \rho (G_{++} + G_{--} - 2G_{+-})}{1 + \rho (G_{++} + G_{--}) + \rho^2 (G_{++} G_{--} - G_{+-}^2)} \quad (98)$$

The summation is over the charged species only, and we have replaced literal subscripts with the sign of the ionic charge for the species concerned. In Equation 98, the properties of the solvent do not enter explicitly on the right-hand side, but lay implicitly in the potential of mean force that determines  $g_{ij}$ . Recently, a completely general development was given for the fluctuation thermodynamic properties of multi-salt solution that includes ionic association.<sup>50</sup>

Equations 96 to 98 are three routes to thermodynamic equations from pair correlation functions. For any given approximate  $g_{ij}(r)$ , the results of the three routes may not be thermodynamically consistent. The extent to which they are consistent constitutes a check of the accuracy of  $g_{ij}$ . Other thermodynamic properties, such as chemical potential derivatives, can also be obtained from the  $g$ 's, as shown in Section III.A.

In the McMillan-Mayer formalism,<sup>1</sup> the solutes can be treated as particles interacting through a potential of mean force  $W(r)$  in a vacuum. The excess thermodynamic quantities can be calculated directly. Equations 96 and 97 can be rewritten as

$$\beta E^{\text{ex}} = (1/2) \beta \sum_{ij} \rho_i \rho_j \int_0^\infty \partial \beta W_{ij} / \partial \beta g_{ij} 4\pi r^2 dr \quad (99)$$

$$\beta p^{\text{ex}} = \beta \pi = \sum (\rho_i \rho_j / 6) \int_0^\infty r (\partial W_{ij} / \partial r) g_{ij} 4\pi r^2 dr \quad (100)$$

Here, the summation is over solute components only. One should note that Equations 99 and 100 involve one more assumption — the pair additivity of  $W_{ij}(r)$ . This assumption is not exactly correct even if the  $u_{ij}$  are pairwise additive; however, for the long-range part of  $W(r)$ , it is usually a good approximation.

Now, the next step is to derive approximate pair correlation functions  $g_{ij}$ , from the knowledge of pair interactions,  $u_{ij}$ , or the potentials of mean force (in the infinite dilution limit)  $W_{ij}$ . In Section III, we sketched the derivation of a density expansion, pressure as a power series in the activity, and then we were able to convert that to a power series in the density. We can use the same kind of procedure to calculate a density expansion of the pair correlation function.<sup>48,49</sup> Again, we should not be surprised to find that the straightforward density expansion is not useful for electrolyte solutions; one has to perform complicated cluster diagram analysis for  $g_{ij}$  just as for  $A$ . The techniques are quite similar to those mentioned previously and will not be further discussed here. Rather, in the following, we will present some of the currently interesting approximations to  $g_{ij}$  in an alternative way, through the introduction of another useful function — the direct correlation function. It is defined by the Ornstein-Zernike equation.<sup>48,49</sup>

$$g_{ij} - 1 = c_{ij} + \sum_s \rho_s \int (g_{is} - 1) c_{sj} d(s) \quad (101)$$

The direct correlation function is usually a simpler looking function than the pair correlation; its long-range behavior reflects the long-range part of the direct interaction  $u_{ij}$  very simply. It has been shown rigorously that the asymptotic behavior of  $c_{ij}$  is

$$c_{ij}(r) \xrightarrow{r \rightarrow \infty} -\beta u_{ij}(r) \quad (102)$$

Note that Equation 101, by itself, is just a definition of  $c_{ij}$ . Without other information, it does not help us to derive an approximate solution for the pair correlation functions in any systematic way. However, if we had an additional relation between  $c_{ij}$  and  $g_{ij}$ , and known pair interactions, we would have a set of equations whose solution we could investigate, rather than merely a definition. In the following, we will present several currently useful approximate integral equations, using Equation 101 as a starting point. We will not discuss their solutions, however. Returning to Equation 101, if one chooses

$$c_{ij} = g_{ij} - 1 - \ln g_{ij} - \beta u_{ij} \quad (103)$$

one has the hypernetted-chain approximation (HNC). The picturesque name comes from the diagram analysis of the cluster expansion of the pair correlation function, in which only diagrams having a certain chain-like structure are retained.<sup>49</sup> Another closure is to let

$$c_{ij} = g_{ij} (1 - \exp(\beta u_{ij})) \quad (104)$$

One then has the Percus-Yevick approximation (PY).<sup>52</sup>

For the primitive model, both the HNC and PY approximations have been solved numerically by Carley<sup>53</sup> and Rasaiah and Friedman,<sup>54</sup> and compared with Monte Carlo simulations.<sup>55,56</sup> It is found that HNC provides very good results for the primitive model in the case of 1-1 electrolytes up to 1 M concentration compared to MC simulations.<sup>55,56</sup> With adjustable short-range interaction potentials, the HNC gives a fairly good description of common salt solution mixtures.<sup>57</sup> As an example of further developments of the HNC approach, Kusalik and Patey<sup>58</sup> have developed the so-called RHNC approximation<sup>59</sup> (reference hypernetted-chain); the closure is based on the separation of the pair potential and correlation functions into reference and perturbation parts. In this work the reference system is taken to be a mixture of spherical particles. A mixture of spherical ions immersed in a solvent of multipolar polarizable particles can be treated. This is a combination of the integral equation approach with the perturbation theory.

There are some other closure approximations for the Ornstein-Zernike equation. Another integral equation, especially designed for the primitive model of electrolyte solutions, is the mean spherical approximation (MSA).<sup>60</sup> Here, one has an exact condition on the pair correlation function

$$g_{ij} = 0 \text{ for } r_{ij} < a_{ij} \quad (105)$$

due to the hard sphere potential. On the other hand, one knows the asymptotic behavior of  $c_{ij}$ , from Equation 102. We agree to approximate  $c_{ij}$  for all  $r_{ij} > a_{ij}$  by its asymptotic behavior.

$$c_{ij} = -\beta \frac{z_i z_j e^2}{\epsilon r_{ij}}; r_{ij} > a_{ij} \quad (106)$$

which strictly holds only for  $r_{ij} \rightarrow \infty$ .

Equation 106 with the exact relation, Equation 105 (the Ornstein-Zernike equation), can be solved exactly. Waisman and Lebowitz<sup>60</sup> first did this for the case of the restricted primitive model. Recent Monte Carlo calculations<sup>61</sup> of ionic chemical potentials find good agreement with MSA at low to moderate concentration.

There have been proposals to improve the MSA scheme, among them the generalized mean spherical approximation (GMSA).<sup>62</sup> In the GMSA, one tries to improve the direct correlation function by adding an extra short-range term of the Yukawa potential form with its parameters chosen by thermodynamic self-consistency requirements.<sup>63</sup> With this chosen form of the direct correlation function, the GMSA can be solved analytically; this is a distinct advantage. The GMSA represents a significant improvement over the MSA when compared with Monte Carlo simulations.<sup>63</sup>

MSA has the advantage that it can often be solved analytically for more realistic treatment of solute and solvent molecules. So one can investigate the effect of solvent dipole on potentials of mean force analytically. In a recent example,<sup>64</sup> one can solve MSA for arbitrary mixture of ions and dipolar solvent.

#### D. ION PAIRING<sup>65-67</sup>

The Debye-Hückel theory is essentially a theory of weak interactions, although the long-range force causes complications, as we have seen. Physical interactions are weak at large



distances, but may become quite strong for short distances. This suggests that one might try to treat the long-range and short-range parts of the interaction separately. An intuitively appealing way to make the separation is due to Bjerrum,<sup>68</sup> and is called the ion pair theory.

An important length in the electrolyte theory is

$$d = \left| \frac{z_+ z_- e^2}{\epsilon kT} \right| \quad (107)$$

If  $r > d$ , the potential energy of a pair of ions is less than their (average) kinetic energy, while if  $r < d$ , the potential energy is greater than the kinetic. The length,  $d$ , would, thus, seem to be a reasonable dividing line between the regions of weak interactions ( $r > d$ ) and strong interactions ( $r < d$ ).

Bjerrum proposed that two ions whose mutual distance was less than a length  $q$ , of order of magnitude  $d$ , be regarded as a separate neutral species, an ion pair. These *ion pairs* are assumed to be in equilibrium with free ions



with association constant  $K$

$$K = \frac{[(AB)^{z_+ - z_-}]}{[A^{z_+}] [B^{z_-}]} \quad (109)$$

If the association process is completely described by the coulomb attraction, then the association constant  $K$  is given by

$$K = 4\pi N \int_a^q \exp(-z_+ z_- e^2 / \epsilon kTr) r^2 dr \quad (110)$$

Unfortunately, we do not know exactly how close a pair of ions needs to be before they can be regarded as "associated ions". Bjerrum took the choice that the potential energy is equal to  $2kT$  at  $q$ ; e.g.,

$$q = \left| \frac{z_+ z_- e^2}{2\epsilon kT} \right| \quad (111)$$

Equations 109 to 111 enable one to compute the concentration of ion pairs for any given electrolyte concentration. For the case of a simple one-component electrolyte (symmetric), one further assumes that the ion pair is a *neutral* species, not interacting with other charges through coulomb forces. The ion pairs contribute nothing to the electrical part of excess thermodynamic quantities (or to electric conductivity). The rest of the "free" ions can be treated by the Debye-Hückel theory, and the equilibrium properties of the ionic system can be calculated by methods already discussed. For complex unsymmetric ionic systems, a simple pairing procedure, such as Equation 108, will not lead to neutral ion pairs; one may need to consider more complicated equilibria than that suggested by Equation 108.<sup>66</sup> The ion pairing idea has been mostly used for interpreting emf, conductance, Raman, and NMR data on ionic solutions, since it gives us an easy interpretation of the physical process involved.<sup>66</sup>

In highly concentrated electrolyte solution, higher aggregates of ions also need to be considered. Experimental evidence is mostly indirect, such as the minimum in conductivity;<sup>66</sup> and in some ionic systems one finds coexisting phases which are taken to be differing in ionic association.<sup>69</sup> In Monte Carlo simulations<sup>70</sup> of 2-2 electrolytes, it has been found that

the like pair correlation  $g_{++}$  shows remarkably large enhancement at nearly twice the ionic diameter. This was interpreted at the formation of triplet and higher clusters.

From the point of view of rigorous statistical mechanics, the ion pair theory is unsatisfactory, not only because of the oversimplified energy calculation of the ionic association constant, but also because of the ambiguous nature of the very definition of pairs. Different choices of  $q$  have been made by other investigators, but these are really mostly dependent on how well the data can be fitted. Furthermore, the meaning of independent species can be quite different for different kinds of experiments, for example, in conductance, thermodynamic, and spectroscopic studies. On a practical level, the choice of  $q$  has to be carefully balanced against two factors. The larger  $q$ , the worse will be the approximation of treating all pairs as ideal neutral species. If  $q$  becomes too small, the Debye-Hückel equation itself will be an increasing invalid description, since the ionic interaction at small distance can be much larger than  $kT$ . Friedman and Larson<sup>69,71</sup> have made extensive studies of the Bjerrum ion pair theory in relation to integral equation and simulation results.

In a hybrid approach mixing the idea of integral equations and ion pairing, one can modify Bjerrum's theory in two steps: (1) an ion pair is defined in an abstract way by associating it with a mass action constant and (2) the unpaired ions are approximated by the primitive model or with added short-range interactions, treated by some integral equation such as the MSA or HNC. The separation of overall ionic particles into free and paired ions can be done by minimizing the total free energy.

The work by Ebeling and Grigo, termed the MSA-MAL,<sup>72</sup> using the MSA with the primitive model, exemplifies this approach. These authors calculated osmotic coefficients and the coexistence curve for a 2-2 electrolyte and obtained very good results.

Tani and Henderson<sup>73</sup> generalized this approach by considering all dimer and trimer clusters, and the choice of cluster diameter  $q$  to be such that the thermodynamic functions are independent of  $q$ . This seems to be more satisfactory than the choice of constant  $q$  by Bjerrum. In this improvement, the theory incorporates the possibility of ionic clustering when it is necessary to account for large short-range interionic interactions, i.e., in excess of those included in the MSA. The total partition function of the system has two contributions, an intracuster contribution which can be calculated by evaluating coulombic partition function, and an intercluster contribution which may be calculated using the MSA. For this distinction of clustering to be possible, strong long-range attractive forces should play a leading role in the energetics of the system. The notion of cluster has physical meaning only if typical cluster sizes are smaller than the mean interparticle distance which is proportional to  $c^{-1/3}$ . Later, Gillan<sup>74</sup> and Pitzer and Schreiber<sup>75</sup> suggested that clusters having 3-6 ions are important in describing ionic systems affected by strong interionic coupling. They, therefore, refined this approach further by including clusters up to hexamers. With this refinement, it is possible to have significant improvement over MSA.<sup>76</sup>

### E. KIRKWOOD-BUFF APPROACH

Most of the theories of electrolyte based on correlation functions belong to the McMillan-Mayer approach. Applications of the Kirkwood-Buff approach to electrolytes face some intrinsic difficulties and hence lag far behind.

For solutions of uncharged species, each component can be independently varied and the thermodynamic expressions (Equations 26 to 33) in terms of correlation functions can be directly applied. However, for electrolytes one has correlation functions between dependent constituents; the chemical potentials of the ions are dependent due to the charge-neutrality condition; and the computational application of the Kirkwood-Buff theory then is not immediately obvious. Friedman and Ramanathan<sup>77</sup> indicated that the applications of Equations 26 to 33 become indeterminate.

Nonetheless, the Kirkwood-Buff theory of solution can be useful for electrolytes in two

respects. First, it is particularly useful for extracting thermodynamic quantities from distribution functions generated by other methods<sup>78</sup> (integral equation approach or potential theories). For example, recently Newman,<sup>79</sup> starting from the nonlinear Poisson-Boltzmann distribution function, has used the Kirkwood-Buff equations to forge the connections with the chemical potential. Thus, one avoids the thermodynamic inconsistency incurred in a charging process. Indeed, Newman found that he can model the activity coefficients of KCl solution up to 4 *M* by just using two parameters.<sup>79</sup> The approach holds considerable advantage for the analysis of the thermodynamic properties of electrolytes.<sup>80</sup> It should be developed further in the future.

Another advantage of the Kirkwood-Buff approach is it gives explicit treatment of solvent structural function together with ion-solvent ones. This is desirable when one wants to include the solvent as a discrete molecular species. At present, this approach is mostly limited to simple (spherical) solvent particles.<sup>81,82</sup>

## F. SURVEY OF SOME NUMERICAL RESULTS

We have described many theoretical methods for the description of electrolyte solutions. To finish off the story, we should indicate how useful these theories are. First, it is necessary to be more precise on the usefulness of a theory. One can list three possible uses: the accurate prediction of the results of the experiment, the provision of a conceptual framework for the understanding of experimental results, and the furnishing of functional forms for the empirical fitting of experimental data. In this chapter, the second of these is the most emphasized. The accuracy of a theory is usually ascertained by comparisons with simulation results. In these comparisons, we have to distinguish between thermodynamic properties and structural properties (correlation functions). At present, there are several theories which give a concentration dependence for thermodynamic properties that is at least qualitatively reasonable. When viewed as structural theories, on the other hand, most of the approximations must be regarded as disappointing. In this section, we will limit ourselves only to thermodynamic properties. For the third use of theories, many semiempirical constructs for thermodynamic properties of electrolyte solution are based on the theories discussed in this chapter; the Debye-Hückel theory and its descendants are particularly useful in this respect. We do not discuss these developments. Readers should consult Chapter 3 for details.

With respect to the accurate prediction of the results of the experiment, at the present time one cannot expect much success for ionic solutions at high concentrations. The reason is that one must have both an accurate approximate theory and an accurate intermolecular force law in order to make an accurate prediction. To paraphrase an analogy by Andersen,<sup>83</sup> if a patient has a diseased appendix and a brain tumor, and the appendix is successfully removed, the patient still is very ill. At the present state of our knowledge of intermolecular force, accurate predictions cannot be expected for solutions at high concentrations, where deviations at short range from Coulomb's law for the potential of mean force are to be expected.

As an example of this, consider the primitive model of electrolyte solutions. The HNC theory for this model has been compared to Monte Carlo calculations for the same model.<sup>86</sup> The two computations agree quite well, indicating that the HNC approximation is a good approximation for coulomb interactions in solutions up to 2 *M*. On the other hand, the comparison of these results with experiment is quite poor above 0.5 *M*. This indicates that the hypothesis of pure pairwise coulomb interactions (aside from the hard core) for the potentials of mean force is the culprit spoiling agreement with experiment. Reviews of these calculations have been given by Friedman<sup>47</sup> and Andersen.<sup>83</sup>

In order to see how a different intermolecular force might change this agreement, let us look at the calculation of Kusalik and Patey.<sup>56</sup> These authors solved the RHNC equation numerically for a model consisting of spherical ions with a hard core in a solvent made up

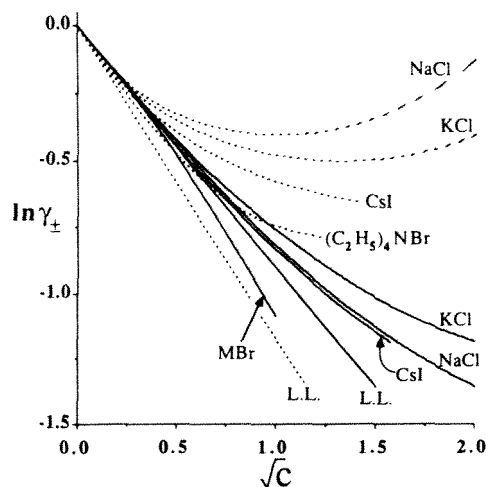


FIGURE 2. The concentration dependence of mean ionic activity coefficients ( $\ln \gamma_{\pm}$ ). The solid and dashed lines represent theoretical (RHNC) and experimental results, respectively. The limiting law lines are labeled (L.L.). (From Kusalik, P. G. and Patey, G. N., *J. Chem. Phys.*, 88, 7715, 1988. With permission.)

of polarizable particles with permanent multiple moments. Specifically, the solvent molecules had a dipole moment and a quadrupole moment appropriate to tetrahedral symmetry; the values for the moments and the polarizability were chosen to be those of water. The dielectric constant for the model is 93.5, which should be compared to the experimental value of 78.5 for water. Note that hydrogen bonding has not been specifically introduced.

We shall only discuss the results for the activity coefficients, although other thermodynamic functions were also considered by the authors.<sup>58</sup> Since the dielectric constant is different from the experimental one, the limiting slope of the activity coefficient will necessarily be different from the experimental slope because of the explicit occurrence of this quantity in the DHLL (cf. Equation 78). However, even aside from this discrepancy in the limiting slope, whose origin is easy to understand, the agreement between theory and experiment is poor. The relation between experiment and theory is shown in Figure 2.

How should one understand this? The thermodynamic properties of ionic solutions are sensitive to the potential of mean force between the ions, except at the lowest concentrations. Hence what might seem to be minor changes in the potential model used can give marked effects on the thermodynamics. In particular, the integral  $G_{+s}$  (cf. Kirkwood-Buff theory, Section III.A), the correlation integral between solvent and the positive ion, has a large effect on the activity coefficient, so that the deviation from pure coulomb forces is emphasized.

Kusalik and Patey<sup>84</sup> have made another calculation which exemplifies this same sensitivity. From the computations previously discussed, they have calculated the portion of the potential of mean force which is expressible as a sum of pair potentials. They then used this potential in the HNC equation and solved it. According to the McMillan-Mayer theory, if the potential of mean force is exact and the integral equations are exact, this should be equivalent to the previous calculation. In fact, for some ions the results differ by as much as 20%. For NaCl, the iterative solution of the equations does not even converge for concentrations above 0.25 *M*. Clearly, the nonpairwise additive part of the potential of mean force cannot be ignored. It is also possible that a part of the discrepancy is due to the approximate nature of the RHNC and HNC equations.

This calculation by Kusalik and Patey does not use the primitive model. A solvent made up of molecules with specific intermolecular force is used. Pettitt and Rossky<sup>45</sup> had previously done a similar calculation using a different integral equation for a solvent treated as multicentered, the RISM equation (which we have not previously discussed). From this model the potential of mean force was calculated, then was used in the HNC equation to compute thermodynamic functions. Agreement with experiment is reasonably good up to about 0.7  $M$  and satisfactory up to 1  $M$ .

These calculations exemplify the point made at the beginning of this section; one needs both a good set of intermolecular potentials and an accurate theory to reproduce the results of experiment.

There does not appear to be any Monte Carlo calculation for ionic solutions beyond the primitive model, i.e., in which the molecular nature of the solvent is given full weight. (For a single ion in waterlike solvents such calculations have been carried out to study solvation.) Monte Carlo results on the restricted primitive model have been reviewed by Friedman.<sup>47</sup> More recently, results for the primitive model with ions of unequal size have been reported. Abramo et al.<sup>12</sup> have studied 1-1 electrolytes for several ratios of anion-to-cation radius, from 0.1 to 2  $M$ , and compared their results to the MSA and to the HNC approximation. Their results are reported in terms of the osmotic coefficient instead of the activity coefficient; there are not enough data points to make an accurate transformation to the activity coefficient of the salt, so we present their results in Figure 3.

It was found that the HNC equation agreed well with the Monte Carlo results in the few cases where HNC results were available. MSA results were available over a somewhat wider range of radius ratio and concentration. Both of these approximate integral equations seem to be competitive in accuracy in the parameter range where the available data overlap.

Valleau and Cohen<sup>10</sup> have studied the restricted primitive model for electrolytes of higher valence type than 1-1, also by Monte Carlo. Their Monte Carlo technique used a Metropolis sampling technique in a grand canonical ensemble where the chemical potentials are fixed, but particles can be randomly inserted and removed, in addition to just being displaced. The advantage of this method is that it avoids a certain extrapolation needed in conventional canonical ensemble Monte Carlo to obtain activity coefficients from the computer output. The extrapolation leads to numerical uncertainties which it would be desirable to avoid. Grand canonical Monte Carlo is not efficient at liquid densities, according to the authors, but is sufficiently efficient at the ionic densities met in electrolyte solutions.

We show in Figure 4 the results for the activity coefficient for 1-1, 2-1, 3-1, and 2-2 electrolytes. It will be seen that the results from grand canonical Monte Carlo and canonical Monte Carlo are in very good agreement for 1-1 salts. For higher valence-type electrolytes the agreement is less good, as is to be expected because of the inherent extrapolation problem mentioned above. The grand canonical results are more reliable. There is some scatter in the 2-2 results at concentrations greater than 2  $M$  due to excessively large dependence on particle number (compared to the other cases) in the numerical experiments. They further compared Monte Carlo results with various theories of a dilute coulombic system for 2:2 primitive model electrolytes.<sup>11</sup> It is found that HNC, DHLL + B<sub>2</sub>, and MPB (modified Poisson-Boltzmann) are comparably successful; they are accurate in the dilute regime ( $C < 0.04 M$ ).

Qualitatively, the Monte Carlo numerical results for activity coefficients are just those which one would expect from experimental experience. One must remember, however, that a detailed comparison with experiment is not warranted because these are restricted primitive model results.

Another demonstration of the use of theory in providing a conceptual framework for the understanding of experimental results is the liquid-liquid coexistence region at low temperature and density. Graham and Valleau<sup>46</sup> reported a Monte Carlo study of the restricted

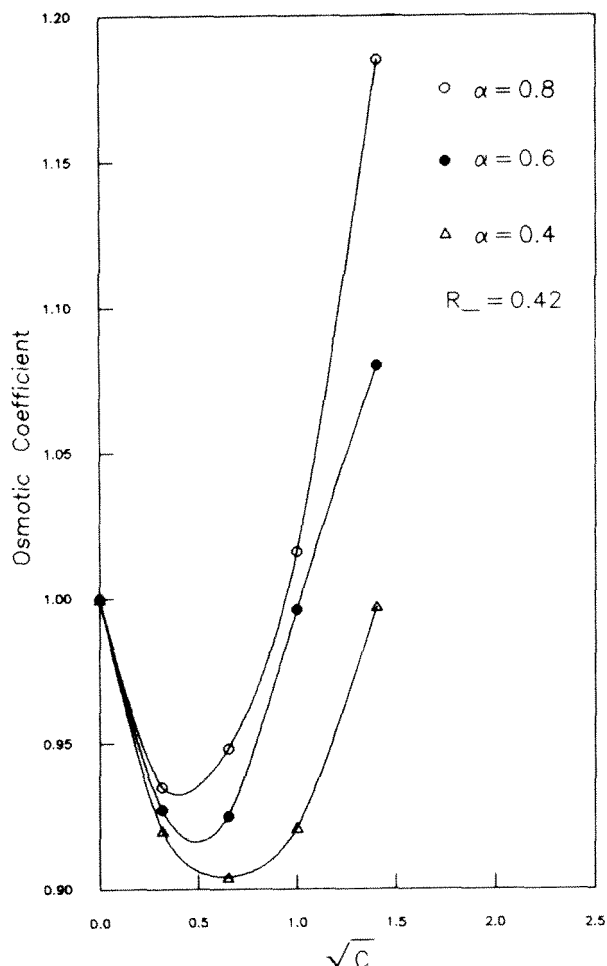


FIGURE 3. Osmotic coefficients ( $PV/NkT$ ) at various radius ratios. Primitive model for 1-1 electrolytes.  $\alpha = R_+/R_-$ , and  $R_- = 0.42$  nm. (From Abramo et al., *J. Chem. Phys.*, 89, 4396, 1984. With permission.)

primitive model around the critical point of this region. Their results allow one to obtain some bounds on the location of the critical point; and their data allows one to evaluate various theoretical predictions about the location of the transition.

We cannot leave the subject of the numerical results of theories without mentioning a very careful study of very low concentration ionic solutions by Sorensen.<sup>87</sup> This paper studied the primitive model with moderate Bjerrum parameter,  $d/a$  (c.f. Equation 111) and low concentration with  $\kappa a = 0.015$  to  $0.45$  by Monte Carlo. This corresponds to concentrations of  $1.3 \times 10^{-4}$  to  $0.12$  M for water at room temperature, assuming  $a = 0.4$  nm. The number of particles used varied from  $N = 32$  to  $1000$ . At these low concentrations there is appreciable  $N$  dependence of the results of the computation, and Sorensen finds that a very careful extrapolation to infinite  $N$  is necessary for reliable results. In fact, he reports that  $\ln \gamma_{\pm}$  must be extrapolated against  $N^{-1/3}$  for reliable results, while the internal energy must be extrapolated against  $N^{-2/3}$ . This is in contrast to previous work which extrapolated with respect to particle number according to  $1/N$ . The conclusion of this work is that the true limiting law for low concentrations is the Debye-Hückel law with  $\kappa a$  corrections (Equation 77 in this paper) and not the DHLL, which is only a "secondary consequence", according to Sorensen.

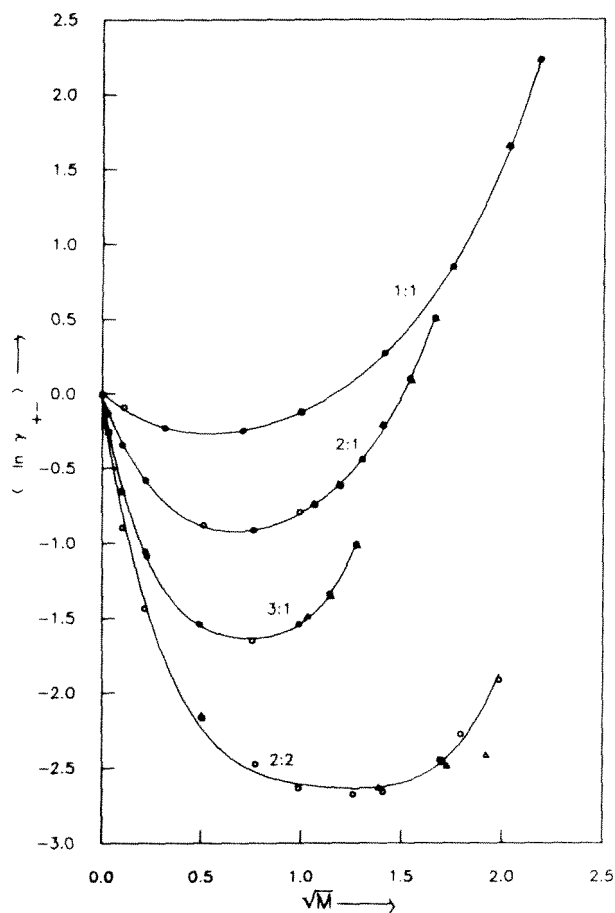


FIGURE 4. Mean ionic activity coefficients ( $\ln \gamma_{\pm}$ ) as a function of concentration calculated by Monte Carlo simulations for primitive model. (From Valleau, J. P. and Cohen, L. K., *J. Chem. Phys.*, 72, 5935, 1980. With permission.)

In all of the computations described in this section, the determination of activity coefficients was only a part of the effort. Pair correlation functions, internal energies, and other thermodynamic functions were also calculated. Different methods of extracting these functions from the raw numerical data were also considered, since methods which are equivalent when applied to exact results need not be when applied to approximate data. There is still much to be done in this field, however. In particular, Monte Carlo calculations which take the molecular nature of the solvent into account, though difficult and expensive, would be quite valuable.

## IX. SUMMARY AND CONCLUSIONS

In this chapter we have tried to present some basic concepts in the statistical mechanical theory of solutions, with special reference to solutions of electrolytes. Our purpose has been to introduce the reader to some of the theoretical ideas which underlie the notion of activity coefficient. We have purposely tried to avoid emphasis on technical details. On the other hand, we have tried to emphasize the physical and mathematical ideas that have been found to be important in this area. We can only hope that we have sailed successfully between

the Scylla of superficial discussion and the Charybdis of overly technical exposition. Each reader must judge this for himself.

Over the past 20 years, a great deal of progress has been made in the theory of fluids, particularly through the distribution function approach. The ionic solution theory has shared in this progress. Numerical simulations, Monte Carlo and molecular dynamics, have developed to a high degree of sophistication and have been of the utmost importance in the development of the theory. For simple electrolyte models, direct Monte Carlo simulations have become routine, providing us with a kind of ideal experimental test of the statistical mechanical methods applied. At present, theories such as the cluster expansion, HNC, or MSA can be trusted to give reliable predictions for the primitive model with soft short-range potentials from infinitely dilute to moderately concentrated solutions. For highly concentrated solutions and fused salts the theory is still underdeveloped. Here, numerical simulations will perhaps show us the directions in which our analytical theories must go.

Still, the development of more realistic models of ionic solutions is very important. Recently, more attention has been paid to treating the solvent as a molecular system, not as a continuum, and attempts have been made to take the dipolar nature to most common solvents (of electrolytes) into account. However, explicit treatment of solvents, like water, with complex hydrogen-bonding interactions is still a problem for the future.

It seems to us that the direction in which theoretical research must go to improve our understanding of electrolyte solutions beyond the limiting law regime is in the direction of shorter distance interactions. A better treatment of the long-range collective effects is always desirable, of course. However, we believe that the bottleneck is in our understanding of short-range effects and their subtle interplay with long-range phenomena. We hope we have given enough background so that the reader can, at least, appreciate these problems.

## ACKNOWLEDGMENTS

This work was supported by a NSF grant CH 8609377 (R. Mazo) and a NSC of ROC grant NSC78-0208-M002-09 (C. Y. Mou).

## GENERAL REFERENCES

The list below contains books and review articles which may be useful for further study. Some of them are cited in the text, but most are not.

- Allen, M. P. and Tildesley, D. J.**, *Computer Simulation of Liquids*, Oxford University Press, New York, 1987.  
**Barker, J. A. and Henderson, D.**, What is a liquid? Understanding the states of matter, *Rev. Mod. Phys.*, 48, 587, 1976.  
**Bellissent-Funel, M.-C. and Neilson, G. W.**, *The Physics and Chemistry of Aqueous Ionic Solutions*, NATO ASI Series Vol. 205, Reidel, Holland, 1987.  
**Carnie, S. L. and Torrie, G. M.**, The statistical mechanics of the electrical doublelayer, *Adv. Chem. Phys.*, 56, 141, 1984.  
**Conway, B. E. and Barradas, R. G.**, *Chemical Physics of Ionic Solution*, John Wiley & Sons, New York, 1966.  
**Ebeling, W. and Krienke, H.**, *The Chemical Physics of Solvation*, Part C, Dognadze, R. E. et al., Eds., Elsevier, Amsterdam, 1988.  
**Eyring, H., Henderson, D., and Jost, W.**, *Physical Chemistry, an Advanced Treatise, Vol. 8*, Academic Press, New York, 1971.  
**Falkenhagen, H.**, *Theorie der Electrolyte*, Hirzel, Leipzig, 1971.  
**Friedman, H. L.**, *Annu. Rev. Phys. Chem.*, 32, 179, 1981.  
**Friedman, H. L.**, *Ionic Solution Theory*, Interscience, New York, 1962.  
**Friedman, H. L.**, *A Course in Statistical Mechanics*, Prentice-Hall, Englewood Cliffs, NJ, 1985.



- Guggenheim, E. A., *Applications of Statistical Mechanics*, Oxford University Press, Oxford, 1966.
- Hill, T. L., *Statistical Mechanics*, McGraw-Hill, New York, 1956.
- Maitland, G. C., Rigby, M., Smith, E. B., and Wakeham, W. A., *Intermolecular Forces: Their Origin and Determination*, Clarendon Press, Oxford, 1981.
- March, N. H. and Tosi, M. P., *Coulomb Liquids*, Academic Press, London, 1984.
- Mayer, J. E. and Mayer, M. G., *Statistical Mechanics*, 2nd ed., John Wiley & Sons, New York, 1977.
- McQuarrie, D. A., *Statistical Mechanics*, Harper & Row, New York, 1976.
- Rasaiah, J. C., A view of electrolyte solution. *J. Solution Chem.*, 2, 301, 1973.
- Resibois, P. M. V., *Electrolytic Theory*, Harper & Row, New York, 1968.
- Rowlinson, J. S. and Swinton, F. I., *Liquids and Liquid Mixtures*, 3rd ed., Butterworths, London, 1982.
- Valleau, J. P. and Whittington, S. G., A guide to Monte Carlo for statistical mechanics: 1. Highways, in *Statistical Mechanics, Part A: Equilibrium Techniques*, Berne, B., Ed., Plenum Press, New York, 1977.
- Valleau, J. P. and Torrie, G. M., A guide to Monte Carlo for statistical mechanics: 2. Byways, in *Statistical Mechanics, Part A: Equilibrium Techniques*, Berne, B., Ed., Plenum Press, New York, 1977.
- Outhwaite, C. W., Equilibrium theory of electrolyte solutions, in *Specialist Periodical Reports, Statistical Mechanics*, Vol. 2, The Chemical Society, London, 1975.

## REFERENCES

1. McMillan, W. G. and Mayer, J. E., The statistical thermodynamics of multicomponent systems, *J. Chem. Phys.*, 13, 276, 1945.
2. Metropolis, N., Rosenbluth, A. W., Rosenbluth, M. N., Teller, A. H., and Teller, E., Equation of state calculations by fast computing machines, *J. Chem. Phys.*, 21, 1087, 1953.
3. Kirkwood, J. G. and Buff, F. P., The statistical mechanical theory of solutions. I, *J. Chem. Phys.*, 19, 774, 1951.
4. Rice, S. A. and Nagasawa, M., *Polyelectrolyte Solutions*, Academic Press, New York, 1961, chap. 1.
5. Maitland, G. C., Rigby, M., Smith, E. B., and Wakeham, W. A., *Intermolecular Forces: Their Origin and Determination*, Clarendon Press, Oxford, 1981.
- 6a. Kihara, T., *Intermolecular Forces*, John Wiley & Sons, New York, 1978.
- 6b. Kaplan, I. G., *Theory of Molecular Interactions*, Elsevier Amsterdam, 1986.
7. Mahan, G. D. and Mazo, R. M., Coulomb interactions in an atomic dielectric, *Phys. Rev.*, 175, 1191, 1968.
8. Bellemans, A. and Steckl, J., Molecular theory of electrostatic interactions between ions in a solvent. II and III, *Bull. Acad. Pol. Sci.*, 9, 343, 1961.
9. Turq, P., Computer simulation of electrolyte solution, in *Physical Chemistry of Aqueous Ionic Solutions*, NATO ASI Ser. C, 1987, 205.
10. Valleau, J. P. and Cohen, I. K., Primitive model electrolytes. I. Grand canonical Monte Carlo computations, *J. Chem. Phys.*, 72, 5935, 1980.
11. Valleau, J. P., Cohen, I. K., and Card, D. N., Primitive model electrolytes. II. The symmetrical electrolyte, *J. Chem. Phys.*, 72, 5942, 1980.
12. Abramo, M. C., Caccamo, C., Malescio, G., Pizzimenti, G., and Rogde, S. A., Equilibrium properties of charged hard spheres of different diameters in the electrolyte solution regime: Monte Carlo and integral equation results, *J. Chem. Phys.*, 80, 4396, 1984.
13. Ramanathan, P. S. and Friedman, H. L., Study of a refined model for aqueous 1-1 electrolytes, *J. Chem. Phys.*, 54, 1086, 1971.
14. Friedman, H. L. and Krishnan, C. V., *Water, Comprehensive Treatise Vol. 3*, Francks, F., Ed., Plenum Press, New York, 1973.
15. Dang, L. X. and Pettitt, B. M., A theoretical study of like ion pairs in solution, *J. Phys. Chem.*, 94, 4303, 1990.
16. Pettitt, B. M. and Rosky, P. J., Alkali halides in water: ion-solvent correlations and ion-ion potential of mean force at infinite dilution, *J. Chem. Phys.*, 84, 5837, 1986.
17. Guggenheim, E. A., *Mixtures*, Oxford University Press, London, 1952.
18. Stillinger, F. H., Equilibrium theory of pure fused salts, in *Molten Salt Chemistry*, Blander, M., Ed., Interscience, New York, 1964.
19. Ghosh, J. C., The abnormality of strong electrolytes. I and III, *J. Chem. Soc.*, 113, 449 and 707, 1918.
20. Planck, M., *Treatise on Thermodynamics*, (transl. from 7th German ed.), Longman, Green, London, 1921.
21. Prigogine, I., *Molecular Theory of Solutions*, North-Holland, Amsterdam, 1958.
22. Henderson, D. and Barker, J. A., Perturbation theories, in *Physical Chemistry, an Advanced Treatise*, Vol. 8A, Eyring, H., Henderson, D., and Jost, W., Eds., Academic Press, New York, 1971.

23. Girardeau, M. D. and Mazo, R. M., Variational methods in statistical mechanics, in *Advances in Chemical Physics*, Vol. 24, Prigogine, I. and Rice, S. A., Eds., Interscience, New York, 1973.
24. Gibbs, J. W., Elementary principles in statistical mechanics, in *The Collected Works of J. Willard Gibbs*, Vol. 2, Yale University Press, New Haven, 1948.
25. Barker, A., Monte Carlo calculations of the radial distribution function for a proton-electron plasma, *Aust. J. Phys.*, 18, 119, 1965.
26. Valleau, J. P. and Whittington, S. G., A guide to Monte Carlo for statistical mechanics: 1. Highways, in *Statistical Mechanics, Part A: Equilibrium Techniques*, Berne, B., Ed., Plenum Press, New York, 1977.
27. Adams, D., Computer simulation of ionic solutions: the distorting effects of the boundary conditions, *Chem. Phys. Lett.*, 62, 329, 1979.
28. Valleau, J. P. and Torrie, G. M., A guide to Monte Carlo for statistical mechanics: 2. Byways, in *Statistical Mechanics, Part A: Equilibrium Techniques*, Berne, B., Ed., Plenum Press, New York, 1977.
- 29a. Levesque, D., Weis, J.-J., and Hansen, J.-P., Simulation of classical fluids, in *Applications of the Monte Carlo Method in Statistical Physics*, Binder, K., Ed., Springer-Verlag, New York, 1984.
- 29b. Levesque, D., Weis, J.-J., and Hansen, J.-P., Recent developments in the simulation of classical fluids, in *Monte Carlo Methods in Statistical Physics*, Binder, K., Ed., Springer-Verlag, New York, 1986.
30. Caillol, J. M., Levesque, D., and Weis, J.-J., Theoretical calculation of ionic solution properties, *J. Chem. Phys.*, 85, 6645, 1986.
31. Heinzinger, K., Computer simulation of aqueous electrolyte solutions, *Physica*, 131B, 196, 1985.
32. Debye, P. and Hückel, E., Zur Theorie der Elektrolyte. I and II, *Phys. Z. (Leipzig)*, 24, 185 and 305, 1923.
33. Guntelberg, E., Untersuchungen über Ioneninteraktion, *Z. Phys. Chem.*, 123, 199, 1926.
34. Guggenheim, E. A., *Applications of Statistical Mechanics*, Oxford University Press, Oxford, 1966.
35. McQuarrie, D. A., *Statistical Mechanics*, Harper & Row, New York, 1976.
36. Sharp, K. A. and Honig, B., Calculating total electrostatic energies with the nonlinear Poisson-Boltzmann equation, *J. Phys. Chem.*, 94, 7684, 1990.
37. Kirkwood, J. G., On the theory of strong electrolyte solution, *J. Chem. Phys.*, 2, 767, 1934.
38. Kirkwood, J. G. and Poirier, J. C., The statistical mechanical basis of the Debye-Hückel theory of strong electrolytes, *J. Phys. Chem.*, 58, 591, 1954.
39. Falkenhagen, H. and Kelbg, G., Klassische Statistik unter Berücksichtigung des Raumbedarfs der Teilchen, *Ann. Phys. (Leipzig)*, 6(2), 60, 1952.
40. Kelbg, G., Untersuchungen zur Statistisch-mechanischer Theorie starker Elektrolyte. I, II, III, and IV, *Z. Phys. Chem. (Leipzig)*, 214, 8, 26, 141, and 153, 1960.
41. Bell, G. M. and Levine, S., *Discuss. Faraday Soc.*, 24, 69, 1957.
42. Outhwaite, C. W. and Bhuiyan, L. B., An improved modified Poisson-Boltzmann equation in electrical-double-layer theory, *J. Chem. Soc. Faraday Trans. 2*, 78, 775, 1983.
43. Friedman, H. L., *Ionic Solution Theory*, Interscience, New York, 1962.
44. Mayer, J. E. and Mayer, M. G., *Statistical Mechanics*, John Wiley & Sons, New York, 1940.
45. Mayer, J. E., The theory of ionic solutions, *J. Chem. Phys.*, 18, 1426, 1950.
46. Andersen, H. C. and Chandler, D., Mode expansion in equilibrium statistical mechanics. I, II, and III, *J. Chem. Phys.*, 53, 547, 1970; 54, 26, 1971; 55, 1497, 1971.
47. Friedman, H. L., Computed thermodynamic properties and distribution functions for simple models of ionic solutions, in *Modern Aspects of Electrochemistry*, Bockris, J. O. and Conway, B. E., Eds., Plenum Press, New York, 1971.
48. Montroll, E. W. and Lebowitz, J. L., *The Liquid State of Matter: Fluids, Simple and Complex*, North-Holland, Amsterdam, 1982.
49. Hansen, J. P. and McDonald, I. R., *Theory of Simple Liquids*, 2nd ed., Academic Press, London, 1986.
50. Perry, R. L., Cabezas, H., Jr., and O'Connell, J. P., Fluctuation thermodynamic properties of strong electrolyte solutions, *Mol. Phys.*, 63, 189, 1988.
51. Stell, G., Fluids with long-range forces; towards a simple analytic theory, in *Modern Theoretical Chemistry*, Vol. 5B, B. Berne, Ed., Plenum Press, New York, 1976.
52. Percus, J. K. and Yevick, G. J., Analysis of classical mechanics by means of collective coordinates, *Phys. Rev.*, 110, 1, 1958.
53. Carley, D. D., Radial distributions of ions for a primitive model of an electrolyte solution, *J. Chem. Phys.*, 46, 3783, 1967.
54. Rasaiah, J. C. and Friedman, H. L., Integral equation computations for aqueous 1-1 electrolytes; accuracy of the methods, *J. Chem. Phys.*, 50, 3965, 1969.
55. Vorontsov-Vel'yaminov, P. N. and El'yashevich, A. M., A theoretical study of the thermodynamic properties of solutions of strong electrolytes by the Monte Carlo method, *Elektrokhimiya*, 4, 1430, 1968 (English transl., *Sov. Electrochem.*).

56. Vorontsov-Vel'yaminov, P. N., El'yashevich, A. M., Rasaiah, J. C., and Friedman, H. L., Comparison of hypermetted chain equation and Monte Carlo results for a system of charged hard cores, *J. Chem. Phys.*, 52, 1013, 1970.
57. Lim, T. K., Zhong, E. C., and Friedman, H. L., Contribution to the theory of electrolyte mixtures at equilibrium, *J. Phys. Chem.*, 90, 144, 1986.
58. Kusalik, P. G. and Patey, G. N., On the molecular theory of aqueous electrolyte solutions. I. The solution of the RHNC approximation for models at finite concentration, *J. Chem. Phys.*, 88, 7715, 1988.
59. Lado, F., Perturbation correction to radial distribution function, *Phys. Rev. A*, 135, 1013, 1964.
60. Waisman, E. and Lebowitz, J. L., Mean spherical model integral equations for charged hard spheres. I and II, *J. Chem. Phys.*, 56, 3086 and 3094, 1972.
61. Sloth, P. and Sorensen, T. S., Monte Carlo simulations of single ion chemical potentials. Results for the unrestricted primitive model, *Chem. Phys. Lett.*, 146, 452, 1988.
62. Hoye, J. S., Lebowitz, J., and Stell, G., Generalized mean spherical approximation for polar and ionic fluids, *J. Chem. Phys.*, 61, 3253, 1974.
63. Stell, G. and Sun, S. F., Generalized mean spherical approximation for charged hard spheres: the electrolyte regime, *J. Chem. Phys.*, 63, 5333, 1975.
64. Blum, L. and Wei, D. Q., Analytical solution of the mean spherical approximation for arbitrary mixture of ions in a dipolar solvent, *J. Chem. Phys.*, 87, 556, 1987.
65. Fowler, R. H. and Guggenheim, E. A., *Statistical Thermodynamics*, Cambridge University Press, London, 1956.
66. Nancollas, G. H., *Interactions in Electrolyte Solutions*, Elsevier, New York, 1966.
67. Davies, C. W., *Ion Association*, Butterworths, London, 1962.
68. Bjerrum, N., Untersuchungen uber Ionenassoziation. I, *K. Dan. Vidensk. Selsk. Mat. Fys. Medd.*, 7, 1, 1926.
69. Friedman, H. L. and Larson, B., A Monte Carlo study of the coexistence region of the restricted primitive model, *J. Chem. Phys.*, 70, 92, 1979.
70. Rosky, P. J., Dudowicz, J. B., Tembe, B. L., and Friedman, H. L., Ionic association in model 2-2 electrolyte solution, *J. Chem. Phys.*, 73, 3372, 1980.
71. Friedman, H. L. and Larson, B., Ion pairing and related topics, *Pure Appl. Chem.*, 51, 2147, 1979.
72. Ebeling, W. and Grigo, M., An analytical characterization of the equation of states and the critical point in a dense classical fluid of charged hard spheres, *Ann. Phys.*, 37, 21, 1980.
73. Tani, A. and Henderson, D., A cluster theory for electrolytes, *J. Chem. Phys.*, 79, 2390, 1983.
74. Gillan, M. J., Liquid-vapor equilibrium in the restricted primitive model for ionic liquid, *Mol. Phys.*, 49, 421, 1983.
75. Pitzer, K. S. and Shreiber, D. R., The restricted primitive model for ionic fluids: properties of the vapor and critical region, *Mol. Phys.*, 60, 1067, 1987.
76. Laria, D., Corti, H. R., and Fernandez-Prini, R., The cluster theory for electrolyte solution, *J. Chem. Soc. Faraday Trans.*, 86, 1051, 1990.
77. Friedman, H. L. and Ramanathan, P. S., Theory of mixed electrolyte solutions and application to a model for aqueous lithium chloride-cesium chloride, *J. Phys. Chem.*, 74, 3756, 1970.
78. Kusalik, P. G. and Patey, G. N., The thermodynamic properties of electrolyte solutions: some formal results, *J. Chem. Phys.*, 86, 5110, 1987.
79. Newman, K. E., A Kirkwood-Buff theoretical approach to Debye-Hückel theory, *J. Chem. Soc. Faraday Trans. 1*, 85, 485, 1989.
80. Zaitsev, A. L., Petrenko, V. E., and Kessler, Yu. M., Solution structure and Kirkwood-Buff theory: informativity and sensitivity to specific interactions, *J. Solution Chem.*, 18, 115, 1989.
81. Kusalik, P. G. and Patey, G. N., Theoretical results for dielectric and structural properties of aqueous electrolytes. The influence of ion size and charge, *J. Chem. Phys.*, 79, 4468, 1983.
82. Patey, G. N. and Carnie, S. L., Theoretical results for aqueous electrolytes. Ion-ion potentials of mean force and the solute-dependent dielectric constant, *J. Chem. Phys.*, 78, 5183, 1983.
83. Andersen, H. C., Improvements in the Debye-Hückel theory of ionic solutions, in *Modern Aspects of Electrochemistry*, Vol. 11, Conway, B. E. and Bockris, J. O., Eds., Plenum Press, New York, 1975.
84. Kusalik, P. G. and Patey, G. N., On the molecular theory of aqueous electrolyte solutions. III. A comparison between Born-Oppenheimer and McMillan-Mayer levels of description, *J. Chem. Phys.*, 89, 7478, 1988.
85. Pettitt, B. M. and Rosky, P. J., Alkali halides in water: ion-solvent correlations and ion-ion potentials of mean force at infinite dilution, *J. Chem. Phys.*, 84, 5836, 1986.
86. Graham, R. and Valleau, J. P., Corresponding states for ionic fluids, *J. Phys. Chem.*, 94, 7894, 1990.
87. Sorensen, T. S., How wrong is the Debye-Hückel approximation for dilute primitive model electrolytes with moderate Bjerrum parameter?, *Chem. Soc. Faraday Trans.*, 6, 1815, 1990.



## Chapter 3

**ION INTERACTION APPROACH: THEORY AND DATA  
CORRELATION**

Kenneth S. Pitzer

**TABLE OF CONTENTS**

I.	Introduction .....	76
II.	Similarity of Nonideal Solutions to Imperfect Gases .....	77
	A. Theoretical Basis .....	77
	B. For imperfect Gases: Virial Coefficients or Association Equilibria .....	77
	C. For Electrolyte Solutions: Similarities to Imperfect Gases and Additional Features for Electrolytes .....	80
III.	Historical Aspects .....	81
	A. Bronsted's Postulate .....	81
	B. Guggenheim's Equations .....	81
	C. Variable Coefficients for Concentrated Solutions .....	82
IV.	Theoretical Basis and Working Equations .....	82
	A. Theoretical Background and General Equations .....	82
	B. Pure Electrolytes .....	86
	C. Mixed Electrolytes .....	88
	D. Single-Ion Activity Coefficients; pH .....	91
	E. Mixing Terms .....	92
	F. Neutral Solutes .....	92
	G. Association Equilibria .....	93
	H. Temperature and Pressure Effects; Enthalpies, Heat Capacities, and Molal Volumes .....	95
V.	Evaluation of Parameters from Experimental Data .....	98
	A. Debye-Hückel Parameters .....	98
	B. Parameters for Pure Electrolytes at 25°C .....	98
	C. Pure Electrolyte Parameters for High Temperatures .....	104
	D. Parameters for Mixtures at 25°C .....	113
	Acknowledgment .....	120
	Appendix A: Additional Theory Related to the General Equation .....	120
	Appendix B: Theory for Unsymmetrical Mixing of Ions of the Same Sign and the Calculation of $\beta^0$ and $\beta^{\prime}$ .....	122
	Appendix C: Theory and Alternate Parameters for Symmetrical Mixing of Ions of the Same Sign .....	126
	Appendix D: Ionic Strength Effect on Ion-Neutral Interactions .....	129

Appendix E:	Dielectric Constant of Water and the Debye-Hückel Parameters.....	129
Appendix F:	Higher Order Terms Involving Neutral Species .....	131
Appendix G:	Computer Codes.....	132
Appendix H:	Equations with Additional Terms.....	133
Appendix I:	Equations Based on Composition in Mole Fraction.....	136
	A. Definitions: Ideal Mixing Terms .....	136
	B. Excess Gibbs Energy from Short-Range Forces .....	139
	C. Debye-Hückel Effect .....	143
References.....		147

## I. INTRODUCTION

The first objective of this chapter is the accurate, compact, and convenient representation of the experimentally determined properties of electrolyte solutions. The equations must be consistent with the basic principles of thermodynamics and statistical mechanics. A second and equally important objective is the prediction of properties of systems not directly measured but related to those measured. This predictive capacity must be based on the underlying statistical mechanical theory. In particular, we shall show that the properties of mixed electrolytes can be predicted with considerable accuracy if the properties of each pure component are known and that the accuracy is further improved if there is some minimum knowledge of simple mixtures of these or similar solutes. The accuracy of these equations is now established for a wide temperature range extending to 300°C or a little higher. Much of this chapter is based on a series of papers by Mayorga, Kim, Silvester, Roy, Bradley, Rogers, Peiper, Busey, Phutela, Simonson, Pabalan, or Yang, and the writer.<sup>1-26</sup> In many cases, these papers give details or references in addition to those included below. Also, a recent review (Pitzer<sup>27</sup>) summarized this work with emphasis on aspects of geochemical interest. These equations are now commonly called the “Pitzer equations”.

While there are alternate approaches to these objectives, the merit of the ion interaction method is strongly supported by the successful applications to complex mixed electrolytes by Harvie and Weare,<sup>28</sup> Harvie et al.,<sup>29,31</sup> Filippov and associates,<sup>32-41</sup> and others.<sup>42-47</sup> The primary advantages of the specific interaction approach are its simplicity in calculation, a major factor for a complex mixture, and its adaptability for the inclusion of repulsive interactions and of higher order interactions without disturbing the basic pattern. In its simplest form, a limitation arises when there is a strong association of ions; then an association equilibrium should be recognized. There is no difficulty in combining an association equilibrium for particular ions with an ion interaction treatment for all other species, as was illustrated for phosphoric<sup>6</sup> and sulfuric<sup>7</sup> acids and for carbonates.<sup>13,18,19</sup> Neutral species may be included in the same equations.

The current status of basic statistical theories for electrolytes is reviewed in Chapter 2, but it seems desirable to summarize briefly my own views. Although theories for liquid

water are rapidly improving, they remain very cumbersome. Thus, any useful theory for aqueous electrolytes must start with assumptions about the interionic potential of mean force in the solvent and make use of the McMillan-Mayer theory<sup>48</sup> to derive solution properties from these potentials. Thus, current theories do not start from first principles or from the properties of ions and molecules determined in microscopic experiments, but rather from plausible models. However, the electric charges on the ions and the dielectric properties of water are well known, as is the repulsion of ions at short distances, and these yield the essential features of the model potentials. We do now have an exact theory which can be applied numerically to any desired accuracy relating the thermodynamic properties to these interionic potentials of mean force<sup>49,50</sup> (also see Chapter 2). This theory yields also the radial distribution functions (or pair correlation functions) for the various species.

Thus, there is no longer any need to speculate about the inaccuracies of the Debye-Hückel theory or other approximate treatments of a particular model. These questions can be answered by comparison with calculations based on the use of exact equations for the same model.<sup>51</sup>

For practical purposes where the representation and generalization of experimental data are the first objective, some mixture of theory with empirical parameters is indicated. Theory should be used for the effect of the electrical charges in the dielectric of the solvent, while effects of short-range forces are described empirically. The empiricism can be introduced either at the level of a model for interionic forces or at a later stage. Both methods should be explored. For practical purposes, however, it is more convenient and more precise to obtain the proper form of thermodynamic equation from basic statistical theory and then to evaluate empirically those parameters whose numerical values cannot be obtained from theory. That is the approach described here.

In most of the literature on ionic solutions, the composition is given in terms of molality, moles of solute per kilogram of solvent, and the primary presentation of this chapter is on that basis. Molality becomes inappropriate for extremely concentrated solutions, however, and some recent research on ionic systems has been reported in terms of mole fractions. Equations based on the same general concepts but using mole fraction as the composition measure are given in Appendix I. Chapters 6 and 7 contain applications using these equations.

## II. SIMILARITY OF NONIDEAL SOLUTIONS TO IMPERFECT GASES

### A. THEORETICAL BASIS

In 1945 McMillan and Mayer<sup>48</sup> showed that the relationship of the osmotic pressure of a solution to potentials of mean force of solute species in the solvent was the same as the relationship of the pressure of a gas to interparticle potentials. Other solution properties can be calculated from the osmotic pressure. Corrections are needed to obtain solution properties at constant pressure — the condition under which most measurements are made, however. But, these corrections are small and do not affect the general similarity of nonideal solutions to imperfect gases in relation to the appropriate interparticle potentials. Thus, a comparison of solutions with gases is useful in selecting an optimum general formulation of an equation for solution properties.

### B. FOR IMPERFECT GASES: VIRIAL COEFFICIENTS OR ASSOCIATION EQUILIBRIA

In the case of imperfect gases one has, as an ideal state for comparison, the ideal or perfect gas defined by the equations

$$PV = nRT \quad (1)$$

$$(\partial U/\partial V)_T = 0 \quad (2)$$

Here  $n$  is the number of moles,  $R$  the gas constant, and  $U$  the energy content, while  $P$ ,  $V$ , and  $T$  have their usual meanings. Real gases generally approach ideal behavior as the pressure is lowered at constant temperature.

A common type of equation for the volumetric behavior of a real (imperfect) gas is an expansion in series in either  $P$  or  $1/V$ . The perfect gas expression appears as the first term and the coefficients of the terms in  $P$  or  $1/V$  are known as virial coefficients. Thus for 1 mol

$$\frac{PV}{RT} = 1 + \frac{B}{V} + \frac{C}{V^2} + \frac{D}{V^3} + \dots \quad (3)$$

or

$$PV = RT + BP + C'P^2 + D'P^3 + \dots \quad (4)$$

The perfect gas term is the first virial coefficient. The second virial coefficient  $B$  is the same in either Equation 3 or 4; the higher coefficients are different but interrelated. It is readily shown by statistical mechanics that the second virial coefficient arises from the intermolecular forces between pairs of molecules; the third virial coefficient from the interaction of three molecules with each other; etc. If the intermolecular force between a pair of molecules depends only on the distance  $r$  and is given by the potential  $u(r)$ , the equation for the second virial coefficient is

$$B = 2\pi N_0 \int_0^\infty [1 - \exp(-u/kT)] r^2 dr \quad (5)$$

where  $N_0$  is Avogadro's number if  $B$  is for 1 mol and  $k$  is the Boltzmann constant. While the intermolecular force for diatomic or polyatomic molecules depends on other coordinates in addition to  $r$ , this dependence can often be ignored. Thus, Equation 5 applies strictly for Ar, Kr, etc., and approximately for  $N_2$ ,  $CH_4$ , etc. For neutral molecules in a gas,  $u$  falls off rapidly with  $r$  and the integral converges. Parenthetically, we note that for electrostatic forces between charged particles,  $u$  falls off only as  $r^{-1}$  and the integral diverges; this is the special problem of electrolytes which must be handled by the Debye-Hückel method or some equivalent procedure.

Typically,  $u(r)$  is large and positive at small  $r$  and then negative for a region before approaching zero (usually as  $r^{-6}$ ) at large  $r$ . One speaks of repulsive forces in the inner region and attractive forces in the intermediate region. Such a function yields a positive contribution to  $B$  in the inner region of positive  $u$  and a negative contribution in the region where  $u$  is negative. Thus,  $B$  may have either sign. This is shown in Figure 1 where the compressibility factor ( $PV/RT$ ) at finite pressure is greater than 1 at high temperature and less than 1 at low temperature. From the curvature in various parts of the diagram, one can see that  $C$ ,  $D$ , etc. become significant and that at least some of them may have either sign.

We are interested primarily in the region of relatively low pressure where the curves are nearly straight lines; here the initial slope is  $B$  and the effect of  $C$  is small. It is evident that a virial equation will represent the observed behavior as accurately as desired with only a few terms. Also, there are thermodynamic relationships between the temperature derivatives of the virial coefficients and the difference in enthalpy, entropy, heat capacity, etc. of the real gas from that of the ideal gas. Thus, the virial coefficient method is convenient for these various functions; also, from Equation 5 there is the relationship to the intermolecular potential, i.e., to the properties of the system at the molecular level.



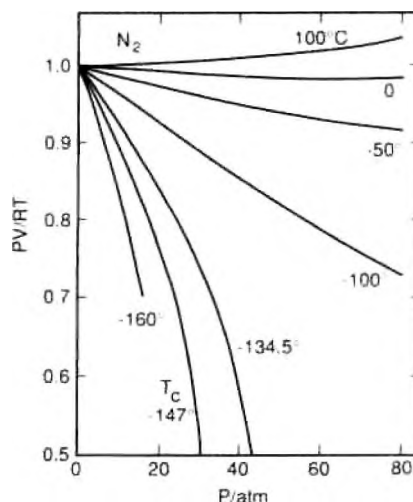


FIGURE 1. The compressibility factor ( $PV/RT$ ) for nitrogen.

While the pattern shown in Figure 1 is typical of all normal gases or fluids, there are exceptional cases showing different behavior. An example is  $\text{NO}_2$  which associates to the dimer  $\text{N}_2\text{O}_4$ .



This equilibrium can be described by the familiar equilibrium constant expression

$$K_a = \frac{f_2}{f_1^2} \quad (6)$$

where  $f_2$  and  $f_1$ , the fugacities of the dimer and monomer, respectively, are given approximately by the partial pressures  $P_2$  and  $P_1$  if the gas is nearly ideal (except for the association). Also, in this approximation and if  $\alpha$  is the fraction of  $\text{NO}_2$  associated,  $P_1 = (1 - \alpha) P_0$  and  $P_2 = \alpha P_0/2$ , where  $P_0$  is the pressure which would arise for complete dissociation. Then

$$K_a = \frac{\alpha}{2(1 - \alpha)^2 P_0} \quad (7)$$

The actual pressure is

$$P = P_1 + P_2 = (1 - \alpha/2) P_0 \quad (8)$$

and we see that the observed value of  $PV/RT$  will decrease from 1 to  $1/2$  as the  $\text{NO}_2$  associates to  $\text{N}_2\text{O}_4$ .

For any gas which associates in this manner under pressures where it would otherwise be nearly an ideal gas, this association treatment is clearly the proper method to use. However, we also note from Figure 1 that  $PV/RT$  for  $\text{N}_2$  decreases to  $1/2$  at about 30 atm at  $-147^\circ\text{C}$ . Thus, in a formal sense we might assert that the  $\text{N}_2$  has, on the average, associated into double molecules ( $\text{N}_1$ ). Actually,  $PV/RT$  for  $\text{N}_2$  at  $-147^\circ\text{C}$  continues to decrease below  $1/2$  as the pressure increases; also, there is a negative curvature ( $C$  is negative). Hence, we must assume further association to larger clusters of molecules.

Let us return to the region of low pressure and of low association of  $\text{NO}_2$ . In this region of small  $\alpha$ , Equations 7 and 8 may be approximated by

$$\alpha \cong 2PK_a \quad (9)$$

and for 1 mol of  $\text{NO}_2$

$$PV \cong RT - (RTK_a)P \quad (10)$$

Thus,  $-RTK_a$  is an effective second virial coefficient for the associating  $\text{NO}_2$ , assumed otherwise to be an ideal gas. At very low temperatures and pressures, this is a good approximation even for normal gases such as  $\text{N}_2$ .

In a limited region of temperature and pressure, the association and virial treatments are both satisfactory for either normal gases or the special examples of associating gases. Frequently, one wishes also to represent the properties of the gas over a wider range, and one then chooses the method which is valid over that larger domain. If one wishes to consider high temperatures, it is apparent from Equation 5 or Figure 1 that  $B$  becomes positive. This would correspond to a negative association constant which is impossible. Also, in the higher pressure domain for a normal gas the higher virial coefficients provide a convenient expression, whereas Equations 7 and 8 do not fit the data. Thus, for normal gases the virial equation method is preferred.

### C. FOR ELECTROLYTE SOLUTIONS: SIMILARITIES TO IMPERFECT GASES AND ADDITIONAL FEATURES FOR ELECTROLYTES

Although the complete theoretical analysis for electrolytes is considerably more complex than for imperfect gases, the same comparative features of interaction coefficients and association equilibrium methods are still valid. Since neutral molecule solutions are very similar to imperfect gases, when treated in the McMillan-Mayer theory, the principal addition for electrolytes is that introduced by long-range electrostatic forces; it adds a special term in the square root of the ionic strength for the logarithm of the activity coefficient or for similar properties. This is the term given in its simplest form by the Debye-Hückel limiting law. There are various slightly more complex forms for this "Debye-Hückel" (or D-H) term which reduce to the limiting law at low concentration but yield better agreement at higher concentration. However, in any case one must add terms for short-range interionic forces which are specific to each solute. These terms can be presented as interaction or virial coefficients for each solute. Alternatively, unusually strong attractive interactions can be represented by association equilibrium constants for individual solutes. The problem of apparent negative association constants where repulsive forces predominate arises for solutions as it did for gases, however.

As in the case of imperfect gases, there are examples where association reactions are so strong that the association equilibrium must be recognized and this can be done with other effects handled in either system. There are many cases where either method is satisfactory. However, for mixed electrolytes the required calculations are much simpler for the interaction coefficient approach, and therein lies a major advantage. The simultaneous solution of several association equilibria with their effects on the ionic strength and the secondary effects on various activity coefficients becomes very burdensome. Also, it is relatively simple to add third virial coefficients for triple interactions when required at high concentration; this is much simpler than the solution of the equations for the array of association equilibria when triple ions, quadruple ions, etc. are included. The second major advantage is the straightforward treatment of cases where repulsive interactions predominate.

### III. HISTORICAL ASPECTS

In this section the historical development of the ion interaction method is reviewed very briefly. The peculiarities of strong electrolyte solutions were a major puzzle to physical chemists in the first two decades of this century. The significance of the long-range character of electrostatic forces was pointed out by several scientists, and Milner<sup>52</sup> constructed an appropriate theory in 1912, but its mathematical form was complex and he obtained only approximate results. In 1923 Debye and Hückel<sup>53,54</sup> effected a great simplification by approximations in the formulation of the theory, and obtained the simple limiting law which resolved the primary puzzle. However, before Debye and Hückel, Lewis and Linhart<sup>55</sup> had obtained essentially the same limiting law on an empirical basis, Bronsted<sup>56</sup> had proposed an interaction coefficient extension of the limiting law, and Lewis and Randall<sup>57</sup> had proposed the ionic strength as the appropriate electrical concentration. The ionic strength is

$$I = \frac{1}{2} \sum m_i z_i^2 \quad (11)$$

where  $m$  is the molality of the  $i$ th species of charge  $z_i$ , protonic units.

#### A. BRONSTED'S POSTULATE

From both empirical and theoretical arguments, Bronsted<sup>56</sup> proposed in 1922 (before the Debye and Hückel paper) the following form of equations for 1-1 electrolytes:

$$1 - \phi = (\alpha/3)m^{1/2} + \beta m \quad (12)$$

$$\ln \gamma = -\alpha m^{1/2} - 2\beta m \quad (13)$$

where  $\phi$  and  $\gamma$  are the osmotic and activity coefficients, respectively. Of the two parameters, Bronsted recognized that  $\alpha$  is a general nonspecific property of the charges on the ions and the solvent (it is, of course, the Debye-Hückel parameter), while  $\beta$  is a specific parameter for each solute.

Bronsted<sup>58</sup> also postulated that there would be specific interaction only between ions of the opposite sign and that the interaction between ions of the same sign would depend purely on the electrical charges. We shall find this Bronsted principle of specific interaction to be a good approximation but not fully in agreement with the best data now available. The theoretical basis is straightforward; ions of the same sign tend to stay away from one another, and thus differences in short-range forces between them should have little consequence. In contrast, ions of opposite charge tend to come as close together as possible and are affected strongly by the short-range forces, and these short-range forces are specific to each particular pair of ions.

#### B. GUGGENHEIM'S EQUATIONS

Guggenheim<sup>59</sup> adopted the general principles advanced by Bronsted as well as those of Debye and Hückel and suggested the following modification in the form of equations for improved agreement with experiment. Guggenheim and Turgeon<sup>60</sup> later used these equations to treat an extensive array of data. Also, the equations were generalized to mixed electrolytes and to any valence type. For a single electrolyte they obtained

$$1 - \phi = \frac{1}{2} \alpha |z_+ z_-| I^{1/2} - \left( \frac{2\nu_+ \nu_-}{\nu_+ + \nu_-} \right) \beta m \quad (14)$$

where  $\nu_+$  and  $\nu_-$  are the numbers of positive and negative ions in the formula and

$$\sigma(y) = (3/y^3)[1 + y - (1 + y)^{-1} - 2 \ln(1 + y)] \quad (15)$$

$$\ln \gamma_{\pm} = -\alpha|z_+z_-| \frac{I^{1/2}}{1 + I^{1/2}} + \left( \frac{2\nu_+ \nu_-}{\nu_+ + \nu_-} \right) (2\beta)m \quad (16)$$

The first term now corresponds to the Debye-Hückel expression for a value near 3 Å for the hard-core ion diameter, but this is still a general function. The only term depending on the specific solute is  $\beta$ .

For mixed electrolytes, the equation for the activity coefficient of the MX solute becomes

$$\ln \gamma_{MX} = -\alpha|z_M z_X| \frac{I^{1/2}}{1 + I^{1/2}} + \frac{2\nu_+}{\nu_+ + \nu_-} \sum_a \beta_{Ma} m_a + \frac{2\nu_-}{\nu_+ + \nu_-} \sum_c \beta_{cX} m_c \quad (17)$$

where the sums in a and c are over all anions and cations, respectively.

Since the  $\beta_{ca}$  quantities can be obtained from measurements on pure electrolytes, Equation 17 allows the prediction of the activity coefficients in mixed electrolytes from data on pure electrolytes which is a major objective.

Guggenheim and Turgeon<sup>60</sup> state that these equations "represent the facts with a useful degree of accuracy, at least for uni-univalent, bi-univalent, and uni-bivalent electrolytes, up to an ionic strength of about 0.1". The present author agrees with the evaluation, and it was only to greatly extend the range of concentration over which good agreement could be obtained that he suggested further elaboration of this general system.

### C. VARIABLE COEFFICIENTS FOR CONCENTRATED SOLUTIONS

For the treatment of data at higher concentration, one may solve Equations 14 and 15 for  $\beta$ , which is now not necessarily a constant.

$$\beta = m^{-1}[\phi - 1 + (1/3) \alpha|z_+z_-|I^{1/2} \sigma(I^{1/2})](\nu_+ + \nu_-)/2\nu_+\nu_- \quad (18)$$

$$\beta = (2m)^{-1} [\ln \gamma_{\pm} + \alpha|z_+z_-|I^{1/2}/(1 + I^{1/2})](\nu_+ + \nu_-)/2\nu_+\nu_- \quad (19)$$

This procedure was suggested by Scatchard<sup>61</sup> and was used by Brewer and the writer<sup>62</sup> to provide a compact summary of the extensive data on aqueous electrolytes at room temperature. Actually, the quantity tabulated was  $B = 2\beta/2.303$ , which corresponds to Equation 19 rewritten for base 10 logarithms, and was shown as  $B'$  to indicate the variability of  $B$  with  $m$ . Since  $B'$  varies only slowly with  $m$ , it is convenient for compact tabulation. However, once the  $B$ 's (or  $\beta$ 's) are dependent on concentration, many of the advantages of these equations are lost since rigorous thermodynamic transformations now become complex.

Figure 2 shows the variation of  $B'$  with molality for a few simple solutes. The remarkable aspect is that  $B'$  shows a consistent large variation at low molality, yet becomes nearly constant at high molality. It seemed important to understand the cause of this peculiar behavior before attempting to improve these general methods.

## IV. THEORETICAL BASIS AND WORKING EQUATIONS

### A. THEORETICAL BACKGROUND AND GENERAL EQUATIONS

The most important advance of recent statistical mechanics for electrolyte theory is a rigorous relationship which yields thermodynamic functions from knowledge of the interionic potentials of mean force and the radial distribution functions (also called binary correlation functions). The charging process used by Debye and Hückel<sup>53,54</sup> and others prior to about 1945 to obtain thermodynamic properties is an approximation which is valid for the coulombic

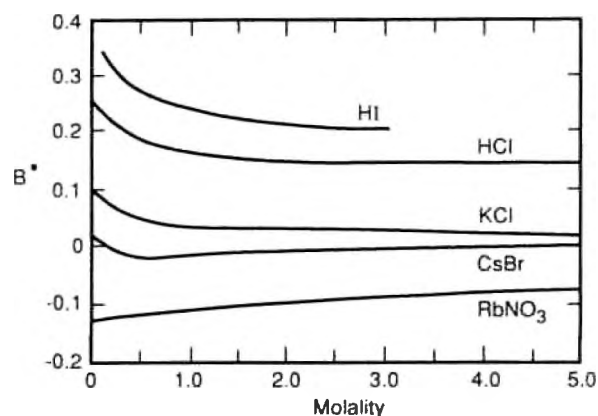


FIGURE 2. The apparent ion interaction coefficient  $B^*$  for a few 1-1 electrolytes. (From *Thermodynamics*, by Pitzer, K. S. and Brewer, L., revised from 1st ed. by Lewis, G. N. and Randall, M. Copyright 1961 by McGraw-Hill Book Company. Used with permission of McGraw-Hill Book Company.)

forces but which omits all of the direct effects of short-range forces. Thus, the older calculations obtained the correct limiting law but only a crude approximation at best for the properties at higher concentrations. Terms to represent these latter effects were added on an ad hoc basis by Bronsted,<sup>56,58</sup> Guggenheim,<sup>59</sup> and others.

There are alternate formulations of rigorous statistical mechanics for multicomponent fluid systems; see Chapter 2. The McMillan-Mayer<sup>60</sup> system is appropriate where a solvent, in our case water, is always the most abundant component. In this system the interactions between solute species are given by potentials of mean force in the solvent, and the detailed interaction of individual solvent molecules can largely be ignored. The excess Helmholtz energy can be expressed in a power series in concentrations  $c_1, c_2, \dots$  of solute species

$$A^{ex}/VKT = \sum_i \sum_j c_i c_j B_{ij}^0 + \sum_i \sum_j \sum_k c_i c_j c_k C_{ijk}^0 + \dots \quad (20)$$

The quantities  $B_{ij}^0, C_{ijk}^0$ , etc. arise from the binary, tertiary, etc. solute-solute interactions in the presence of the solvent and in the limit of low solute concentration; they depend on the solvent and the temperature but not on the solute concentrations. They can be calculated from the potentials of mean force and can be called the second, third, etc. virial coefficients.

When ions are present, with long-range ( $R^{-1}$ ) interparticle potentials, the integrals for  $B_{ij}^0, C_{ijk}^0$ , etc. for interionic interactions diverge. Mayer<sup>61</sup> showed how the calculation could be rearranged to avoid this divergence, and Friedman<sup>62</sup> further developed this method. Friedman's Equations 6.10 and 13.44, with minor changes in symbols, give for the excess Helmholtz energy

$$A^{ex}/VKT = -\kappa^3/12\pi + \sum_i \sum_j c_i c_j B_{ij}(\kappa) + \sum_i \sum_j \sum_k c_i c_j c_k C_{ijk}(\kappa) + \dots \quad (21)$$

The first term on the right is just the Debye-Hückel limiting law with the reciprocal length  $\kappa$  defined by

$$\kappa^2 = (4\pi e^2/\epsilon kT) \sum_i c_i z_i^2 \quad (22)$$

Here  $\epsilon$  is the dielectric constant or relative permittivity of the solvent,  $e$  the electronic charge, and  $z_i$  the number of charges on particle  $i$ . In SI units there is the additional factor  $4\pi\epsilon_0$  in the denominator, with  $\epsilon_0$  the permittivity of free space. The sum in Equation 22 is clearly related to the ionic strength.

In Equation 21 the virial coefficients  $B_{ij}$ ,  $C_{ijk}$ , etc. differ from the corresponding  $B_{ij}^\circ$ ,  $C_{ijk}^\circ$ , etc. in Equation 20 by the omission of the terms which, when rearranged, become the Debye-Hückel term. This transformation gives  $B_{ij}$ ,  $C_{ijk}$ , etc. a dependence on  $\kappa$  in addition to their dependence on solvent properties etc.

While the virial coefficients  $B_{ij}(\kappa)$ ,  $C_{ijk}(\kappa)$ , . . . are, in principle, related to the interionic potentials of mean force in the solvent, at present they can be calculated only for simple models. We prefer to regard them as empirical quantities to be evaluated from experimental data. Theoretical guidance concerning the ionic strength dependence of  $B$  will be discussed below in Appendix A. We proceed now to the adoption of a general equation.

For this general equation, we prefer to use the variable molality instead of concentration, since the latter is dependent on pressure and temperature. One could use mole fraction; indeed, it must be used for very concentrated electrolytes approaching fused salts (see Appendix I), but molality is most generally used in the electrolyte literature. Also, we prefer pressure as an independent variable instead of volume. This last choice does introduce a limitation to conditions of limited compressibility, which implies that the equation cannot be used close to the critical point of the solvent or solution. Thus, we base the general equation on the excess Gibbs energy expressed as a series of terms in increasing powers of molality of the same form as Equation 21. The Debye-Hückel term can be transformed exactly, and it can be shown that other changes arising from the new basis are absorbed into the virial coefficients which are to be obtained empirically (see Appendix A). One then has the following equation for the excess Gibbs energy:

$$G^{ex}/w_w RT = f(I) + \sum_i \sum_j m_i m_j \lambda_{ij}(I) + \sum_i \sum_j \sum_k m_i m_j m_k \mu_{ijk} + \dots \quad (23)$$

here  $w_w$  is the number of kilograms of water and  $m_i$ ,  $m_j$ , . . . are the molalities of all solute species. The ionic strength is given by

$$I = 1/2 \sum_i m_i z_i^2 \quad (24)$$

where  $z_i$  is the number of charges on the  $i$ th solute. The first term on the right in Equation 23 includes the Debye-Hückel limiting law, but is an extended form chosen for empirical effectiveness. Note that  $f(I)$  depends only on the ionic strength and not on individual ionic molalities or other solute properties. The matrices of  $\lambda_{ij}$  and  $\mu_{ijk}$  are symmetric, i.e.,  $\lambda_{ij} = \lambda_{ji}$  etc.

The quantity  $\lambda_{ij}(I)$  represents the short-range interaction in the presence of the solvent between solute particles  $i$  and  $j$ . This binary interaction parameter or second virial coefficient does not itself have any composition dependence for neutral species, but for ions it is dependent on the ionic strength; it does depend, of course, on the particular solute species  $i$  and  $j$  and the temperature and pressure. The similar quantity for triple interaction is  $\mu_{ijk}$ ; in principle it is ionic strength dependent, but with a single possible exception<sup>20</sup> there is no experimental indication of such dependence. Hence, we shall write our equations without considering any  $I$ -dependence for  $\mu$ . Fourth or higher order interactions could be added; they are not included in our primary presentation but are considered in Appendix H. They are needed only for extremely concentrated solutions,<sup>64</sup> and then alternate methods may be preferable (see Appendix I and Filippov et al.,<sup>41</sup> Pitzer,<sup>65</sup> Simonson and Pitzer,<sup>66</sup> Pabalan and Pitzer<sup>67</sup>).

Before proceeding further, we recall certain basic relationships for solution thermodynamics in the molality system.\* For solute species the chemical potentials  $\mu_i$ , the activities  $a_i$ , and the activity coefficients  $\gamma_i$  are related by

$$\mu_i = \mu_i^\circ + RT \ln a_i \quad (25)$$

$$a_i = m_i \gamma_i \quad (26)$$

where  $\mu_i^\circ$  is the chemical potential in the solute (molality) standard state. For the solvent, here taken to be water, the chemical potential is

$$\mu_w = \mu_w^\circ + RT \ln a_w \quad (27)$$

with  $\mu_w^\circ$  the chemical potential of pure liquid water; also, the activity  $a_w$  is commonly expressed by the osmotic coefficient  $\phi$ ,

$$\phi = -(\Omega/\Sigma n_i) \ln a_w \quad (28)$$

Here  $\Omega$  is the number of moles of solvent in a kilogram (55.51 for water), and the sum covers all solute species.

The total Gibbs energy of mixing from the standard states is

$$\begin{aligned} \Delta_{\text{mix}}G &= n_w(\mu_w - \mu_w^\circ) + \Sigma n_i(\mu_i - \mu_i^\circ) \\ &= RT(n_w \ln a_w + \Sigma n_i \ln a_i) \end{aligned} \quad (29)$$

If one then substitutes Equations 26 and 28 for the activities and notes that  $m_i = n_i\Omega/n_w$ , one obtains

$$\Delta_{\text{mix}}G = RT \Sigma n_i[-\phi + \ln(m_i\gamma_i)] \quad (30)$$

It is useful to separate this expression into two parts: one part independent of  $\gamma_i$  or  $\phi$ , which gives the primary dependence of Gibbs energy on solution composition, and a second part for the "corrective" terms in  $(1 - \phi)$  and  $\gamma_i$ . The latter can be called an "excess" quantity; on that basis, one defines

$$G^{\text{ex}} = \Delta_{\text{mix}}G + RT \Sigma n_i(1 - \ln m_i) \quad (31)$$

Then Equation 30 yields

$$G^{\text{ex}} = RT \Sigma n_i(1 - \phi + \ln \gamma_i) \quad (32)$$

Often, one prefers to use expressions based upon 1 kg of solvent; these are obtained by division by  $w_w = n_w/\Omega$ .

$$G^{\text{ex}}/w_w = \Delta_{\text{mix}}G/w_w + RT \Sigma m_i(1 - \ln m_i) \quad (33a)$$

$$= RT \Sigma m_i(1 - \phi + \ln \gamma_i) \quad (33b)$$

Alternate definitions are also used (see Chapter 1). Also note that mole fraction-based definitions are used in Appendix I, while the molality basis is used throughout the remainder of this chapter.

One may now proceed to obtain  $\gamma_i$  and  $\phi$  by differentiation of  $(G^{ex}/w_w RT)$ .

$$\begin{aligned} \ln \gamma_i &= [\partial(G^{ex}/w_w RT)/\partial m_i]_{n_w} \\ &= (z_i^2/2)f' + 2 \sum_j \lambda_{ij} m_j + (z_i^2/2) \sum_j \sum_k \lambda'_{jk} m_j m_k \\ &\quad + 3 \sum_j \sum_k \mu_{ijk} m_j m_k + \dots \end{aligned} \quad (34)$$

$$\begin{aligned} \phi - 1 &= - (\partial G^{ex}/\partial w_w)_{n_i} / RT \sum_i m_i \\ &= (\sum_i m_i)^{-1} [If' - f] + \sum_i \sum_j (\lambda_{ij} + I\lambda'_{ij}) m_i m_j \\ &\quad + 2 \sum_i \sum_j \sum_k \mu_{ijk} m_i m_j m_k + \dots \end{aligned} \quad (35)$$

Here  $f'$  and  $\lambda'$  are the ionic strength derivatives of  $f$  and  $\lambda$ . The multiple sums in Equations 34 and 35 are unrestricted, i.e., each sum covers all solute species. For solutions containing ions, the requirement of electrical neutrality makes it impossible to evaluate certain individual ionic quantities. This becomes more explicit as one derives the working equation for an electrolyte with a single solute.

## B. PURE ELECTROLYTES

If the electrolyte  $MX$  has  $\nu_M$  positive ions of charge  $z_M$  in its formula and  $\nu_X$  negative ions of charge  $z_X$ , neutrality requires  $z_M \nu_M = |z_X| \nu_X$ ; also, we take  $\nu = \nu_M + \nu_X$ . For a salt molality  $m$ , the ion molalities are  $m_M = \nu_M m$  and  $m_X = \nu_X m$ . The osmotic coefficient becomes

$$\begin{aligned} \phi - 1 &= (\nu m)^{-1} \{ (If' - f) + m^2 [2\nu_M \nu_X (\lambda_{MX} + I\lambda'_{MX}) + \nu_M^2 (\lambda_{MM} + I\lambda'_{MM}) \\ &\quad + \nu_X^2 (\lambda_{XX} + I\lambda'_{XX})] + m^3 (6\nu_M^2 \nu_X \mu_{MMX} + 6\nu_M \nu_X^2 \mu_{MXX} + 2\nu_M^3 \mu_{MMM} \\ &\quad + 2\nu_X^3 \mu_{XXX}) + \dots \} \end{aligned} \quad (36)$$

From the experimentally measured properties of the pure electrolyte, together with the Debye-Hückel term  $(If' - f)$ , one can evaluate only the bracketed term in  $\lambda'$ 's, a function of ionic strength, and the final term in parentheses involving  $\mu$ 's. Thus, we define  $f^\phi$ ,  $B^\phi(I)$ , and  $C^\phi$  as follows:

$$f^\phi = (f' - f/I)/2 \quad (37)$$

$$B_{MX}^\phi = \lambda_{MX} + I\lambda'_{MX} + (\nu_M/2\nu_X)(\lambda_{MM} + I\lambda'_{MM}) + (\nu_X/2\nu_M)(\lambda_{XX} + I\lambda'_{XX}) \quad (38)$$

$$C_{MX}^\phi = [3/(\nu_M \nu_X)^{1/2}] (\nu_M \mu_{MMX} + \nu_X \mu_{MXX}) \quad (39)$$

At this point, we could have included the terms in  $\mu_{MMM}$  and  $\mu_{XXX}$  in the definition of  $C^\phi$ , but we shall neglect them later so omit them now. These terms relate to short-range interactions of three ions, all of the same sign. Since electrical repulsions make it unlikely that three ions of the same sign are often close together, these terms are expected to be very small, and no indication has arisen that they need to be included. Equation 36 now reduces to the simple form:



$$\phi - 1 = |z_M z_X| f^\phi + m(2\nu_M \nu_X / \nu) B_{MX}^\phi + m^2 [2(\nu_M \nu_X)^{3/2} / \nu] C_{MX}^\phi \quad (40)$$

For a 1-1 electrolyte all of the coefficients become unity.

In the original development of this model,<sup>1</sup> two choices were made at this point: the extended form of the Debye-Hückel term  $f^\phi$  and the form for the ionic strength dependence of  $B_{MX}^\phi$ . All combinations of the most likely forms were tested with an array of accurately measured experimental osmotic coefficients for several 1-1-, 2-1-, and 1-2-type salts at 25°C, and the best results were obtained for the forms:

$$f^\phi = -A_\phi I^{1/2} / (1 + bI^{1/2}) \quad (41)$$

$$B_{MX}^\phi = \beta_{MX}^{(0)} + \beta_{MX}^{(1)} \exp(-\alpha I^{1/2}) \quad (42)$$

The general pattern of ionic strength dependence was indicated theoretically for each function (see Appendix A), but alternate forms were equally plausible, and the choice was made for empirical effectiveness. Here  $b$  is a universal parameter with the value  $1.2 \text{ kg}^{1/2} \cdot \text{mol}^{-1/2}$  and  $\alpha$  has the value  $2.0 \text{ kg}^{1/2} \cdot \text{mol}^{-1/2}$  for all of the salts in the test set. It will be possible to use a different value of  $\alpha$  for other salts or salts of other charge types; this will be discussed below. The parameters  $\beta_{MX}^{(0)}$  and  $\beta_{MX}^{(1)}$  are specific to the salt MX. It was expected that these parameters representing short-range interactions would be specific to the interacting ions.

As salts of other valence types were studied, it was found that Equation 42 with  $\alpha = 2.0$  served well for 3-1 and even 4-1 salts, but not for 2-2 salts such as  $\text{MgSO}_4$ .<sup>2,3</sup> The 2-2-type salts show an electrostatic ion pairing effect which has usually been represented by considering the ion pair as a separate solute species. Introduction of such a species in equilibrium with other species complicates the calculations considerably, however. We found that good agreement with observed properties was obtained for the 2-2 salts if one simply added another term to  $B_{MX}^\phi$  as follows:

$$B_{MX}^\phi = \beta_{MX}^{(0)} + \beta_{MX}^{(1)} \exp(-\alpha_1 I^{1/2}) + \beta_{MX}^{(2)} \exp(-\alpha_2 I^{1/2}) \quad (43)$$

The values  $\alpha_1 = 1.4 \text{ kg}^{1/2} \cdot \text{mol}^{-1/2}$  and  $\alpha_2 = 12 \text{ kg}^{1/2} \cdot \text{mol}^{-1/2}$  were satisfactory for all 2-2 electrolytes at 25°C. The parameter  $\beta_{MX}^{(2)}$  is negative and is related to the association equilibrium constant.

In a very extensive investigation of aqueous HCl, where some association is expected at high molality, Holmes et al.<sup>68</sup> found that the  $\beta^{(2)}$  term was unnecessary below 250°C. From 250 to 375°C they obtained a good fit with a  $\beta^{(2)}$  term and with  $\alpha_1 = 1.4$  and  $\alpha_2 = 6.7 A_\phi$ . There is theoretical support for the proportionality of  $\alpha_2$  to the Debye-Hückel parameter  $A_\phi$ ; this is considered by Phutela and Pitzer<sup>21</sup> in relation to  $\text{MgSO}_4(\text{aq})$  at high temperature.

Finally, we note the theoretical expression for the Debye-Hückel parameter

$$A_\phi = (1/3) (2\pi N_0 d_w / 1000)^{1/2} (e^2 / \epsilon kT)^{3/2} \quad (44)$$

*the must be given in g/m<sup>3</sup>!*

with  $N_0$  Avogadro's number,  $d_w$  the density of water,  $e$  the electronic charge,  $k$  Boltzmann's constant, and  $\epsilon$  the dielectric constant or the relative permittivity of water. For SI units  $\epsilon$  is multiplied by  $4\pi\epsilon_0$ , with  $\epsilon_0$  the permittivity of free space. In many papers the symbol  $D$  is used instead of  $\epsilon$  for the dielectric constant.

Next we transform  $B_{MX}^\phi$  and  $C_{MX}^\phi$  as defined by Equations 38 and 39 to the corresponding forms for the excess Gibbs energy as follows:

$$B_{MX} = \lambda_{MX} + (\nu_M / 2\nu_X) \lambda_{MM} + (\nu_X / 2\nu_M) \lambda_{XX} \quad (45)$$

$$C_{MX} = (3/2)(\mu_{MMX}/z_M + \mu_{MXX}/|z_X|) \quad (46)$$

The excess Gibbs energy for a pure electrolyte now becomes

$$G^{ex}/(n_w RT) = f(I) + m^2(2\nu_M\nu_X)[B_{MX} + m(\nu_M z_M)C_{MX}] \quad (47)$$

Introduction of the selected forms from Equations 41 and 43 yields

$$f = -(4IA_\phi/b)\ln(1 + bI^{1/2}) \quad (48)$$

$$B_{MX} = \beta_{MX}^{(0)} + \beta_{MX}^{(1)} g(\alpha_1 I^{1/2}) + \beta_{MX}^{(2)} g(\alpha_2 I^{1/2}) \quad (49)$$

$$g(x) = 2[1 - (1 + x) \exp(-x)]/x^2 \quad (50)$$

Further manipulations yield the useful relationships

$$B'_{MX} = [\beta_{MX}^{(1)} g'(\alpha_1 I^{1/2}) + \beta_{MX}^{(2)} g'(\alpha_2 I^{1/2})]/I \quad (51)$$

$$g'(x) = -2[1 - (1 + x + x^2/2)\exp(-x)]/x^2 \quad (52)$$

$$C_{MX} = C^\phi/2|z_M z_X|^{1/2} \quad (53)$$

For the activity coefficient equation, it is useful to define the following:

$$f^\gamma = -A_\phi[I^{1/2}/(1 + bI^{1/2}) + (2/b)\ln(1 + bI^{1/2})] \quad (54)$$

$$B_{MX}^\gamma = B_{MX} + B_{MX}^\phi \quad (55)$$

$$C_{MX}^\gamma = 3C_{MX}^\phi/2 \quad (56)$$

The mean activity coefficient for a salt is defined as

$$\ln \gamma_\pm = (\nu_M \ln \gamma_M + \nu_X \ln \gamma_X)/\nu \quad (57)$$

and for the present model with a single salt this becomes

$$\ln \gamma_\pm = |z_M z_X| f^\gamma + m(2\nu_M \nu_X / \nu) B_{MX}^\gamma + m^2 [2(\nu_M \nu_X)^{3/2} / \nu] C_{MX}^\gamma \quad (58)$$

Equations 40 and 58 were applied to the very extensive array of data for 25°C with excellent agreement to about 6 mol · kg<sup>-1</sup> for various types of electrolytes.<sup>2,3</sup> The resulting parameters are discussed in a subsequent section.

### C. MIXED ELECTROLYTES

In order to treat mixed electrolytes, it is desirable to rewrite Equation 23 in terms of the experimentally determinable quantities  $B$  and  $C$  instead of the individual ion quantities  $\lambda$  and  $\mu$ . Appropriate transformations yield for the excess Gibbs energy

$$\begin{aligned} G^{ex}/(w_w RT) = & f(I) + 2 \sum_c \sum_a m_c m_a [B_{ca} + (\sum_c m_c z_c) C_{ca}] \\ & + \sum_{c' > c} m_c m_{c'} [2\Phi_{cc'} + \sum_a m_a \psi_{cc'a}] + \sum_{a' > a} m_a m_{a'} [2\Phi_{aa'} + \sum_c m_c \psi_{caa'}] \\ & + 2 \sum_n \sum_c m_n m_c \lambda_{nc} + 2 \sum_n \sum_a m_n m_a \lambda_{na} + 2 \sum_{n' > n} m_{n'} m_n \lambda_{n'n} + \sum_n m_n^2 \lambda_{nn} + \dots \quad (59) \end{aligned}$$

where the sums are over the various cations  $c, c'$  and over the anions  $a, a'$ . If neutral solute species  $n, n'$  are present, the terms from Equation 23 in  $\lambda_{ij}$  and  $\mu_{ijk}$  are retained; only those in  $\lambda_{ij}$  are shown in the last four sums. Appendix F gives the additional terms arising from triple interactions including one or more neutral species for various equations; these terms are usually negligible. Difference combinations of  $\lambda$ 's and  $\mu$ 's arise which are defined as follows:

$$\Phi_{cc'} = \lambda_{cc'} - (z_{c'}/2z_c)\lambda_{cc} - (z_c/2z_{c'})\lambda_{c'c'} \quad (60)$$

$$\psi_{cc'a} = 6\mu_{cc'a} - (3z_{c'}/z_c)\mu_{cca} - (3z_c/z_{c'})\mu_{c'c'a} \quad (61)$$

Analogous expressions for  $\Phi_{aa'}$  and  $\psi_{caa'}$  arise from permutation of the indices. Terms involving three ions of the same sign are expected to be negligible and are omitted. These quantities account for interactions between ions of like sign, which arise only for mixed solutions, and can best be determined from simple common-ion mixtures.

In terms of various quantities defined above, the following equations give the osmotic coefficient of the mixed electrolyte and the activity coefficients of cation M and anion X, respectively.

$$\begin{aligned} (\phi - 1) = & (2/\sum_i m_i) [-A_\phi I^{3/2}/(1 + bI^{1/2}) + \sum_c \sum_a m_c m_a (B_{ca}^\phi + Z C_{ca}) \\ & + \sum_{c < c'} \sum m_c m_{c'} (\Phi_{cc'}^\phi + \sum_a m_a \psi_{cc'a}) + \sum_{a < a'} \sum m_a m_{a'} (\Phi_{aa'}^\phi + \sum_c m_c \psi_{caa'}) \\ & + \sum_n \sum_c m_n m_c \lambda_{nc} + \sum_n \sum_a m_n m_a \lambda_{na} + \sum_{n < n'} \sum m_n m_{n'} \lambda_{nn'} + (1/2) \sum_n m_n^2 \lambda_{nn} \dots] \quad (62) \end{aligned}$$

$$\begin{aligned} \ln \gamma_M = & z_M^2 F + \sum_a m_a (2B_{Ma} + Z C_{Ma}) + \sum_c m_c (2\Phi_{Mc} + \sum_a m_a \psi_{Mca}) \\ & + \sum_{a < a'} \sum m_a m_{a'} \psi_{Maa'} + z_M \sum_c \sum_a m_c m_a C_{ca} + 2 \sum_n m_n \lambda_{nM} + \dots \quad (63) \end{aligned}$$

$$\begin{aligned} \ln \gamma_X = & z_X^2 F + \sum_c m_c (2B_{cX} + Z C_{cX}) + \sum_a m_a (2\Phi_{Xa} + \sum_c m_c \psi_{cXa}) \\ & + \sum_{c < c'} \sum m_c m_{c'} \psi_{cc'X} + |z_X| \sum_c \sum_a m_c m_a C_{ca} + 2 \sum_n m_n \lambda_{nX} + \dots \quad (64) \end{aligned}$$

The third virial terms for neutrals are omitted in Equations 62 to 64.

The quantity F includes the Debye-Hückel term and other terms as follows:

$$F = f' + \sum_c \sum_a m_c m_a B'_{ca} + \sum_{c < c'} \sum m_c m_{c'} \Phi'_{cc'} + \sum_{a < a'} \sum m_a m_{a'} \Phi'_{aa'} \quad (65)$$

Also,  $\Phi'$  is the ionic strength derivative of  $\Phi$ , and

$$Z = \sum_i m_i |z_i| \quad (66)$$

$$\Phi_{cc'}^\phi = \Phi_{cc'} + I \Phi'_{cc'} \quad (67)$$

The mean activity coefficient for the electrolyte  $M_\nu X_\nu$  in a mixture is readily obtained from Equations 63 and 64.

$$\begin{aligned} \ln \gamma_{MX} = & |z_M z_X| F + (\nu_M/\nu) \sum_a m_a [2B_{Ma} + Z C_{Ma} \\ & + 2(\nu_X/\nu_M) \Phi_{Xa}] + (\nu_X/\nu) \sum_c m_c [2B_{cX} + Z C_{cX} \\ & + 2(\nu_M/\nu_X) \Phi_{Mc}] + \sum_c \sum_a m_c m_a \nu^{-1} [2\nu_M z_M C_{ca} \\ & + \nu_M \psi_{Mca} + \nu_X \psi_{caX}] + \sum_{c \neq c'} \sum m_c m_{c'} (\nu_X/\nu) \psi_{cc'X} \\ & + \sum_{a \neq a'} \sum m_a m_{a'} (\nu_M/\nu) \psi_{Maa'} + 2 \sum_n m_n (\nu_M \lambda_{nM} + \nu_X \lambda_{nX})/\nu \end{aligned} \quad (68)$$

There are many somewhat simplified forms of Equation 68 for cases where all solutes are of the same valence type and further where this is a simple type or where there is a common cation or a common anion or where there are only two solutes. Since these transformations are quite straightforward and in many cases do not shorten the expression very much, we will not burden this paper with them. For a mixture of just two symmetrical electrolytes of charge  $z$  and with a common anion, the expression is considerably simplified. We write  $y$  for the solute fraction of the component  $NX$ . The activity coefficient of  $MX$  is

$$\begin{aligned} \ln \gamma_{MX} = & z^2 \gamma + m \{ B_{MX} + (1 - y) B_{MX}^\phi + y B_{NX}^\phi + m[(3/2 - y) C_{MX}^\phi + y C_{NX}^\phi] \\ & + y[\Phi_{MN} + (1 - y/2)m\psi_{MNX} + (1 - y)|\Phi_{MN}'] \} \end{aligned} \quad (69)$$

In this case the ionic strength is, of course,  $I = mz^2$ ; also, we have substituted  $B^\phi = B + IB'$  and  $C^\phi = 2zC$ .

Another observable combination of activity coefficients is that for the exchange of an amount of one ion by an equal electrical charge of a different ion of the same sign. This occurs, for example, with exchange between two liquid phases when positive ions are complexed to form neutral molecular species in the nonaqueous phase and in certain electrical cells. The pertinent combination of activity coefficients may be written, for  $M'^{\nu_M}$  and  $N'^{\nu_N}$ ,

$$\begin{aligned} z_N \ln \gamma_M - z_M \ln \gamma_N = & z_N z_M (z_M - z_N) F + \sum_a m_a [2z_N B_{Ma} \\ & - 2z_M B_{Na} + Z(z_N C_{Ma} - z_M C_{Na})] + 2 \sum_c m_c (z_N \Phi_{Mc} - z_M \Phi_{Nc}) \\ & + \sum_c \sum_a m_c m_a (z_N \psi_{Mca} - z_M \psi_{Nca}) + \sum_{a \neq a'} \sum m_a m_{a'} (z_N \psi_{Maa'} - z_M \psi_{Naa'}) \end{aligned} \quad (70)$$

The corresponding equation for the difference in activity coefficients of anions is readily obtained by transposing symbols in Equation 70.

It is an interesting question to ask whether it is possible to determine the chemical potentials of all other components of a solution from measurements of the chemical potential of one component over the entire range of solution compositions. If the measurements are of the solvent, one obtains the osmotic coefficient, and one notes from Equation 62 that all parameters are included. Thus with sufficient precision of measurement and range of composition, all parameters can be determined, and by Equation 68, the chemical potential of any solute component can be calculated.

If the measurements are of a solute component MX, however, an examination of Equation 68 shows that terms in  $\beta_{ca}^{(0)}$  do not appear unless either c is M or a is X. Thus, it is not possible to evaluate  $\beta_{ca}^{(0)}$ , a very important parameter, for any component ca not involving either M or X, and consequently the chemical potential of that component.

In the case where there is a common ion and  $\nu_M = \nu_X$ , one finds that the quantities  $\beta_{Ma}^{(0)}$  and  $\Phi_{Xa}$  (and  $\beta_{cX}^{(0)}$  and  $\Phi_{Xc}$ ) appear with exactly the same composition dependence. Thus, only the sum can be determined from measurements of  $\gamma_{MX}$ . Again, the activity coefficient or chemical potential of another solute component Ma (or cX) cannot be determined without some additional measurement.

Further analysis shows that the general proposition is valid provided the solution exists in the same phase over the entire composition range including each pure component. This is seldom the case for an electrolyte where the pure salt is usually a solid of limited solubility. Also, the molality cannot be used to describe solution compositions to pure solutes because m becomes infinite. Where only a limited composition range is available, it is important whether this range extends to the pure component whose activity was measured. Where it does, as for the solvent, then other component activities can be calculated. However, if it does not, as for solutes of limited solubility, then such calculations of other activities are not ordinarily possible.

In practical work, this limitation on calculations based on solute activities is not serious since some information on the osmotic coefficient is almost always obtainable. That additional information will allow the evaluation of the remaining parameter. The more serious limitations are those related to the uncertainties in the experimental data and the near redundancy of parameters with only slightly different composition dependencies for a given set of measurements.

In a mixture with many components there are a large number of terms in Equations 62 to 66 and 68 and accurate parameter values may not be available for every term. It is apparent, however, that terms involving very small molalities, and especially those involving a product of two very small molalities, will have little or no effect on the osmotic coefficient or activity coefficient. Thus, many successful applications have been made without values for the parameters for some of these very small terms. In calculations for solutes of very small solubility, the parameters for that solute may be unimportant; an example would be the solubility of  $BaSO_4$  in a solution dominated by  $BaCl_2$  or  $Na_2SO_4$  where the important parameters are  $B_{BaCl}$ ,  $B'_{BaCl}$ ,  $C_{BaCl}$ , and  $\Phi_{ClSO_4}$ , or  $B_{NaSO_4}$ ,  $B'_{NaSO_4}$ ,  $C_{NaSO_4}$ , and  $\Phi_{NaBa}$ , respectively, but the parameters  $B_{BaSO_4}$ ,  $B'_{BaSO_4}$ , and  $C_{BaSO_4}$  can be set to zero or estimated to be the same as those for  $CaSO_4$ .

#### D. SINGLE-ION ACTIVITY COEFFICIENTS; pH

It should be remembered that single-ion activity coefficients are not measurable by ordinary thermodynamic methods because of space charge limitations. Also, in the transformation from Equation 34 to 63 and 64, certain terms in  $\lambda$ 's and  $\mu$ 's remain which cancel for any neutral combination of ions. The complete expression from this transformation for Equation 63 is

$$\begin{aligned}
 \ln \gamma_M = & z_M^2 F + \sum_a m_a (2B_{Ma} + Z C_{Ma}) + \sum_c m_c (2\Phi_{Mc} + \sum_a m_a \psi_{Mca}) \\
 & + \sum_{a < a'} \sum m_a m_{a'} \psi_{Maa'} + z_M \sum_c \sum_a m_c m_a C_{ca} + 2 \sum_n m_n \lambda_{nM} \\
 & + z_M \left\{ \sum_c m_c \lambda_{cc} / z_c - \sum_a m_a \lambda_{aa} / |z_a| \right. \\
 & \left. + (3/2) \sum_c \sum_a m_c m_a (\mu_{cca} / z_c - \mu_{caa} / |z_a|) \right\} \quad (71)
 \end{aligned}$$

Terms for triple interactions with all ions of the same sign are omitted. The corresponding expression for a negative ion X is obtained by interchanging X for M, a for c, and c for a throughout. It is important to note that the final set of terms (given by  $z_M$  times the quantity in braces) cancels when the mean activity coefficient for a neutral electrolyte is calculated. Since these terms are not measurable (at least at present), they are omitted in calculations of single-ion activity coefficients, and as noted above this omission has no effect on the measurable quantities.

For complex mixed electrolytes, the use of the single-ion activity coefficients is much more convenient than the use of mean activity coefficients and electrically neutral differences of activity coefficients, although the final results are identical.

While an exact measurement of the activity of hydrogen ions is not possible, an approximation can be made which, with certain definitions, is unambiguous and useful. This quantity is usually presented as  $\text{pH} = -\log a(\text{H}^+)$ . The conventional definitions are appropriate for dilute solutions where specific ion interactions are small. At higher molalities, ion interactions should be included, and Equations 63 and 64 provide unambiguous expressions for single-ion activity coefficients which could be incorporated in a defined pH. Indeed, Knauss et al.<sup>69</sup> have proposed a system of this type, and have found it to be successful in tests for a variety of concentrated electrolytes.

### E. MIXING TERMS

Since like charged ions repel one another, we expect their short-range interactions to be small and that  $\lambda_{cc}$  and  $\lambda_{c'c'}$ , etc. are all small. We further note that  $\Phi_{cc'}$  and  $\Psi_{cc'a}$  are differences between these small quantities; hence, they should certainly be small. Indeed, both Bronsted<sup>56,58</sup> and Guggenheim<sup>59</sup> neglected these terms completely. We do not neglect these quantities, but we do find them to be small in most cases. There is an exception where the long-range electrical forces yield a term that appears in  $\Phi_{cc'}$  in this formulation. It appears only for unsymmetrical mixing, i.e., where the charges on c and c' (or a and a') differ. This term is given by theory.<sup>5,15,49</sup> The complete expressions for  $\Phi_{ij}$  are

$$\Phi_{ij} = \theta_{ij} + {}^E\theta_{ij}(I) \quad (72)$$

$$\Phi'_{ij} = {}^E\theta'_{ij}(I) \quad (73)$$

$$\Phi_{ij}^\phi = \theta_{ij} + {}^E\theta_{ij}(I) + I{}^E\theta'_{ij}(I) \quad (74)$$

where  ${}^E\theta(I)$  and  ${}^E\theta'(I)$  account for these electrostatic unsymmetrical mixing effects and depend only on the charges of the ions i and j, the total ionic strength, and on the solvent properties  $\epsilon$  and  $d_w$  (hence, on the temperature and pressure). The theory and equations for calculating these terms are given in Appendix B, which also describes a method of numerical calculation by Chebyshev approximations devised by Harvie.<sup>20</sup> The remaining term  $\theta_{ij}$  arising from short-range forces is taken as a constant for any particular c,c' or a,a' at a given T and P. Its ionic strength dependence is very small and is neglected.

For symmetrical mixing the  ${}^E\theta_{ij}(I)$  term disappears, and it is found that  $\Phi_{ij}$  may be taken as independent of ionic strength in good approximation. From Equation 60, however, one notes that  $\Phi_{ij}$  may have an ionic strength dependence, and this has been detected for the heat of mixing in a few cases<sup>20</sup> (see Appendix C which also considers the pertinent theory).

### F. NEUTRAL SOLUTES

The situation is much simpler for uncharged solute species, and there is no need to rearrange the terms in  $\lambda_{ij}$  in the basic Equations 23, 34, and 35. The terms for neutral species were included in Equations 63 and 64 for the activity coefficients of ions. The corresponding

equation for the activity coefficient of a neutral species is

$$\ln \gamma_N = 2 \left( \sum_c m_c \lambda_{Nc} + \sum_a m_a \lambda_{Na} + \sum_n m_n \lambda_{Nn} \right) \quad (75)$$

Third virial terms from Equation 25 can be added to Equation 75, if needed (Appendix F). Even for neutral molecules interacting with ions, the forces are short ranged, and there is no need to modify the  $\lambda$ 's. Electrical neutrality limits the evaluation of  $\lambda$ 's to electrically neutral sums and differences, but it does not seem worthwhile to define new quantities. Often it is convenient to set to zero all ion-neutral parameters involving one particular ion, e.g.,  $H^+$ , whereupon the other ion-neutral parameters are determined. Since Setchenow in 1892, the departure of neutral-species activity coefficients from unity has traditionally been described in terms equivalent to the  $\lambda$ 's of these equations. An extensive review of neutral solutes in aqueous salt solutions was presented by Long and McDevit.<sup>70</sup>

Empirically, there is no evidence for an ionic-strength dependence for the  $\lambda$ 's for neutral species. Thus all  $\lambda_{ij}$  terms in Equations 34 and 35 can be omitted for both neutral-neutral and neutral-ion interactions. There is some theoretical basis for a small ionic strength effect for interactions of ions with neutrals having large dipole moments (or higher order electric moments); this is described in Appendix D. However, this effect is so small that there is no reason to complicate the equations at present.

Also, the question may be asked whether the dielectric constant should be that of a mixed solvent, including neutral solute species, instead of the value for water. It is possible to set up equations for mixed solvents, and this is necessary if the solvent composition varies over a wide range, e.g., from pure water to pure methanol. However, the present equations assume a pure solvent, and its dielectric constant must be used. The effect of neutral-molecule solutes on interionic effects via changes in dielectric constant is included along with other effects in the second and third virial coefficients, including a possible ionic-strength dependence of the ion-neutral second virial coefficient. Such an ionic-strength dependence has not been detected up to the present, but the possibility should be kept in mind.

An example for the activity coefficient of a neutral species  $Si(OH)_4$  in various electrolytes is discussed in terms of the present equations in a recent review.<sup>27</sup> A somewhat more complex case is that of the system  $NaCl-CO_2-H_2O$ <sup>71</sup> where third virial terms were needed for the  $CO_2$ - $NaCl$  interaction. See Appendix F for additional comments on systems with neutral species.

## G. ASSOCIATION EQUILIBRIA

Up to this point, we have assumed that the selection of solute species was unambiguous and that electrical neutrality was the only supplementary relationship between solute molalities. However, there may be association equilibria as  $H^+ + HCO_3^- = CO_2(aq) + H_2O$  which relate one solute molality to other molalities. The chemical thermodynamics of each such equilibrium is straightforward, with an equilibrium constant relationship involving molalities and activity coefficients. For the carbonic acid this is

$$K_{assoc.} = a_{H_2O} m_{CO_2} \gamma_{CO_2} / m_H \cdot m_{HCO_3^-} \gamma_H \cdot \gamma_{HCO_3^-} \quad (76)$$

Each such equilibrium adds one or more relationships between the molalities and an equilibrium-constant equation, all of which must be satisfied simultaneously in the complete solution of the problem.

For carbonates and many other cases, the association constants are large (i.e., the dissociation constants are very small) and there is no question about the need to recognize the associated species. Examples treated using the present model include  $Na^+$ -

$\text{HCO}_3^-$ ,  $\text{CO}_3^{2-}$ -Cl<sup>-</sup>-CO<sub>2</sub>-H<sub>2</sub>O,<sup>13</sup>  $\text{H}^+$ -HSO<sub>4</sub><sup>-</sup>-SO<sub>4</sub><sup>2-</sup>-H<sub>2</sub>O,<sup>7</sup> and  $\text{H}^+$ -K<sup>+</sup>-H<sub>2</sub>PO<sub>4</sub><sup>-</sup>-H<sub>3</sub>PO<sub>4</sub>-H<sub>2</sub>O.<sup>6</sup> The last example is interesting in that it models the phosphoric acid to such high molality that a third virial coefficient for triple interaction of the neutral species is required.

In some cases the association, although significant, is not strong, and the fraction in the associated form is never large. In the dilute range the degree of association increases with concentration. However, at higher concentration, the activity coefficients of the ions decrease, and the degree of association levels off and may even decrease. This last effect is particularly strong for multiple charged ions such as the divalent metal sulfates. In the case of the  $\text{M}^{2+}$ -SO<sub>4</sub><sup>2-</sup> solutions, it was found<sup>3</sup> that the associated species could be omitted provided an additional ionic-strength-dependent term with a large exponent  $\alpha_2$  was added to the second virial coefficient (see Equation 43). The coefficient in this term  $\beta_{\text{MX}}^{(2)}$  is negative and, in the limit of low molality, is related to the association constant  $K$  by  $\beta^{(2)} = -K/2$ . Also, the exponent  $\alpha_2$  is related to the Debye-Hückel parameter  $A_\phi$ . Indeed, the equation without the MSO<sub>4</sub> neutral species and with the  $\beta^{(2)}$  term represented the properties to high molality without difficulty. In contrast, association treatments with the simple inclusion of the ion-pair association equilibrium constant are not successful at high molality; further terms are required — either virial coefficients involving the MSO<sub>4</sub> species or association equilibria to triple or quadruple ions. Thus, the treatment with the  $\beta^{(2)}$  term and without the association equilibrium has many advantages.

With increase in temperature in the dielectric constant of water decreases rapidly and one expects ion pairing to become stronger. Archer and Wood<sup>72</sup> found this to be the case in a general treatment of MgSO<sub>4</sub>(aq). They included not only the neutral ion pair, but also the triplets ( $\text{M}_2\text{X}^+ + \text{MX}_2^-$ ) and a sextuplet  $\text{M}_3\text{X}_3$  with association constants at 25°C of 126.4 for the pair, 557.3 for the sum of the triplets, and  $3.813 \times 10^6$  for the sextuplet, and enthalpies of association of approximately 6, 6, and 27 kJ · mol<sup>-1</sup>, respectively. They also adjusted heat capacities of association for each reaction as well as a simple pattern of temperature-dependent second and third virial coefficients to account for repulsive interactions and obtained good agreement with the available data up to 3 mol · kg<sup>-1</sup> and 150°C. Soon thereafter, Phutela and Pitzer<sup>21</sup> presented high-temperature heat capacity measurements for MgSO<sub>4</sub>(aq) and a comprehensive treatment of that system without association equilibria, but with temperature-dependent  $\beta^{(0)}$ ,  $\beta^{(1)}$ ,  $\beta^{(2)}$ , and  $C^\phi$ . They found that  $-\beta^{(2)}$  increased with temperature, as expected. They also investigated the effect of change of the exponent  $\alpha_2$  with temperature proportionally to  $A_\phi$ . The temperature-dependent  $\alpha_2$  gave better agreement below 0.1 mol · kg<sup>-1</sup>, but there was no difference above 0.1 mol · kg<sup>-1</sup>. Thus, for mixed electrolytes at ionic strength above 0.4 mol · kg<sup>-1</sup> the simple treatment with constant  $\alpha_2$  is usually satisfactory. The general agreement for various properties for the two treatments was comparable; the treatment without association equilibria gave agreement for the osmotic coefficient at 110°C to higher molality (5 mol · kg<sup>-1</sup>) and better agreement at 140°C. The association treatment gives a better fit to the heats of dilution at high temperatures in the dilute range below 0.03 mol · kg<sup>-1</sup>. The more recent heat capacity measurements were not available at the time of Archer and Wood's treatment; as expected, the Phutela and Pitzer treatment fits these data much more accurately.

In estimating the need to introduce associated species, these results for MgSO<sub>4</sub> give the best guide for 2-2 electrolytes. For less highly charged ions, the ion pairs must be recognized for somewhat smaller values of the association constant because the activity coefficient for the ions decreases less rapidly with increase of molality. The case of aqueous HCl was investigated very thoroughly by Holmes et al.<sup>68</sup> They found no need to include a  $\beta^{(2)}$  term below 250°C. For higher temperatures up to 375°C, they obtained good agreement with an equation including a  $\beta^{(2)}$  term. In the range of their data,  $-\beta^{(2)}$  is as large as 32, corresponding to an association constant of 64.

At room temperature most 1-1 electrolytes are either unambiguously associated, such



as acetic acid or ammonia, or are clearly strong electrolytes where the present equations are adequate without the  $\beta^{(2)}$  term. The situation for 2-1 or 1-2 electrolytes at 25°C was studied carefully by Harvie et al.;<sup>31</sup> they concluded that association should be recognized for cases with association constants greater than 20 (or dissociation constants less than 0.05).

#### H. TEMPERATURE AND PRESSURE EFFECTS; ENTHALPIES, HEAT CAPACITIES, AND MOLAL VOLUMES

In addition to the excess Gibbs energy and the activity and osmotic coefficients, there is interest in the enthalpy, heat capacity, and volume of electrolyte solutions. These quantities will be derived from appropriate derivatives of the Gibbs energy. This process could be extended to the compressibility or other properties, but such extensions are straightforward and need not be given in detail. Since these equations involve temperature and pressure derivatives of the parameters for the osmotic and activity coefficients, they yield the information needed to calculate these quantities at other temperatures and pressures.

The pertinent thermodynamic equations for the relative enthalpy, the heat capacity, and the volume are

$$L = H - H^\circ = -T^2[\partial(G^{ex}/T)/\partial T]_{P,m} \quad (77)$$

$$\begin{aligned} C_p &= (\partial H/\partial T)_{P,m} \\ &= C_p^\circ + (\partial L/\partial T)_{P,m} \end{aligned} \quad (78)$$

$$V = V^\circ + (\partial G^{ex}/\partial P)_{T,m} \quad (79)$$

where the subscript m indicates constancy of composition (as well as pressure or temperature) for the partial derivatives. It is useful to recall that the excess Gibbs energy for a pure electrolyte is given by Equation 47, while the operational expression for a mixed electrolyte was given in Equation 59. We shall write out the explicit equations for enthalpy etc. only for a pure electrolyte, but the more general equations for mixtures are obtained by application of the same methods to Equation 59.

Experimental measurements of the enthalpy usually yield the apparent relative molal enthalpy,  ${}^\phi L$ , defined as

$${}^\phi L = L/n_2 \quad (80)$$

where  $n_2$  is the number of moles of solute. If one takes the derivatives as indicated in Equation 77, one obtains

$$\begin{aligned} {}^\phi L &= \nu|z_M z_X|(A_L/2b)\ln(1 + bI^{1/2}) \\ &\quad - 2\nu_M \nu_X RT^2[mB_{MX}^L + m^2(\nu_M z_M)C_{MX}^L] \end{aligned} \quad (81)$$

where

$$\begin{aligned} B_{MX}^L &= (\partial B_{MX}/\partial T)_{P,I} \\ &= \beta^{(0)L} + \beta^{(1)L} g(\alpha_1 I^{1/2}) + \beta^{(2)L} g(\alpha_2 I^{1/2}) \end{aligned} \quad (82a)$$

$$\beta^{(i)L} = (\partial \beta^{(i)}/\partial T)_P, \quad i = 0, 1, 2 \quad (82b)$$

and

$$C_{MX}^I = (\partial C_{MX}/\partial T)_p = (\partial C_{MX}^\phi/\partial T)_p/2|z_M z_X|^{1/2} \quad (83)$$

Also, the Debye-Hückel parameter for enthalpy is

$$\begin{aligned} A_L/RT &= 4T(\partial A_\phi/\partial T)_p \\ &= -6A_\phi[1 + T(\partial \ln \epsilon/\partial T)_p + T\alpha_w/3] \end{aligned} \quad (84)$$

where  $\alpha_w = (\partial \ln V/\partial T)_p$  is the coefficient of thermal expansion of water.

A common type of enthalpy measurement is the heat of dilution. If this is reported for the dilution of solution containing 1 mol of solute from  $m_1$  to  $m_2$ , it is related as follows to the apparent molal enthalpy:

$$\Delta \bar{H}_D(m_1 \rightarrow m_2) = {}^\phi L_2 - {}^\phi L_1 \quad (85)$$

The integral heat of solution of a solid salt MX is taken as the heat effect for the reaction



The enthalpy change for this reaction is given as

$$\Delta H_\zeta = n_1 \bar{H}_1 + n_2 \bar{H}_2 - n_1 H_1^\circ - n_2 H_2^\circ(\text{s}) \quad (86)$$

which may be rewritten as

$$\Delta H_\zeta = L + n_2[\bar{H}_2^\circ - H_2^\circ(\text{s})]$$

As the concentration  $m$  approaches zero, we have

$$\lim_{m \rightarrow 0} (\Delta H_\zeta/n_2) = \Delta \bar{H}_2^\circ - H_2^\circ(\text{s}) \quad (87)$$

where  $\Delta \bar{H}_2^\circ$  is the heat of solution per mole of salt at infinite dilution. At finite concentrations we therefore have

$$\Delta H_\zeta = \Delta \bar{H}_2^\circ + {}^\phi L \quad (88)$$

The value of  $\Delta \bar{H}_2^\circ$  at a given temperature may be found by fitting the experimental values of  $\Delta \bar{H}_\zeta$  to Equations 81 and 88, treating  $\Delta \bar{H}_2^\circ$  as an adjustable parameter.

The apparent molal heat capacity,  ${}^\phi C_p$ , is defined to be

$${}^\phi C_p = (C_p - n_1 C_{p1}^\circ)/n_2 \quad (89)$$

From Equations 78 and 80, we find that

$${}^\phi C_p - \bar{C}_{p,2}^\circ = (\partial {}^\phi L/\partial T)_{p,m} \quad (90)$$

From Equations 78 and 81 one then obtains

$$\begin{aligned} {}^\phi C_p &= \bar{C}_{p,2}^\circ + \nu|z_M z_X|(A_j/2b) \ln(1 + bI^{1/2}) \\ &\quad - 2\nu_M \nu_X RT^2 [mB_{MX}^I + m^2 (\nu_M z_M) C_{MX}^I] \end{aligned} \quad (91)$$

where

$$B_{MX}^J = \left( \frac{\partial^2 B_{MX}}{\partial T^2} \right)_{P,I} + \frac{2}{T} \left( \frac{\partial B_{MX}}{\partial T} \right)_{P,I} \quad (92)$$

$$C_{MX}^J = \left( \frac{\partial^2 C_{MX}}{\partial T^2} \right)_P + \frac{2}{T} \left( \frac{\partial C_{MX}}{\partial T} \right)_P \quad (93)$$

$$A_J = (\partial A_L / \partial T)_P \quad (94)$$

The superscript J is used in view of its definition as the relative heat capacity,  $J = (\partial L / \partial T)_P$ , and to minimize confusion between the use of the letter C with different subscripts for the third virial coefficient and for the heat capacity.

Heat capacity data on electrolytes are obtained by direct measurements on the solution using a calorimeter. The resulting total heat capacities, converted to  ${}^\phi C_p$ , may then be fitted to Equation 91, treating  $\bar{C}_{P_2}^\circ$  as an adjustable parameter. Values of  ${}^\phi C_p$  may also be obtained from heat of solution data according to

$$(\partial \Delta H_s / \partial T)_P = {}^\phi C_p - C_{P_2}^\circ(s) \quad (95)$$

provided  $\bar{C}_{P_2}^\circ(cr)$ , the heat capacity of the pure salt in the crystalline solid phase, is known.

For the volumetric properties, the derivations are similar and only the results will be stated. The definition of the apparent molal volume parallels that for the apparent molal heat capacity. The result is

$$\begin{aligned} \phi V = & \bar{V}_2^\circ + \nu |z_M z_X| (A_v / 2b) \ln(1 + bI^{1/2}) \\ & + 2\nu_M \nu_X RT [m B_{MX}^V + m^2 (\nu_M z_M) C_{MX}^V] \end{aligned} \quad (96)$$

where

$$B_{MX}^V = \beta^{(0)V} + \beta^{(1)V} g(\alpha_1 I^{1/2}) + \beta^{(2)V} g(\alpha_2 I^{1/2}) \quad (97a)$$

$$\beta^{(i)V} = (\partial \beta^{(i)} / \partial P)_T, \quad i = 0, 1, 2 \quad (97b)$$

$$C_{MX}^V = (\partial C_{MX} / \partial P)_T = (\partial C_{MX}^\phi / \partial P)_T / 2 |z_M z_X|^{1/2} \quad (98)$$

$$A_v = 2A_\phi RT [3(\partial \ln \epsilon / \partial P)_T + (\partial \ln V_w / \partial P)_T] \quad (99)$$

Equations for the partial molal enthalpies, heat capacities, and volumes are readily derived from the appropriate derivatives of equations given above, while entropies are readily obtained from enthalpies and Gibbs energies. Some of these expressions are given in Reference 17.

The most important use of the partial molal enthalpies and volumes is in calculating the effects of temperature and pressure on activity and osmotic coefficients. That task is best accomplished by the use of the temperature derivatives of the virial coefficients, which are more directly determined from the apparent molal quantities as described above. Consequently, equations for partial molal enthalpies and volumes will be omitted here.

## V. EVALUATION OF PARAMETERS FROM EXPERIMENTAL DATA

### A. DEBYE-HÜCKEL PARAMETERS

Before proceeding to the evaluation of data for particular substances, one needs the Debye-Hückel parameters. Equations 44, 84, 94, and 99, which depend on the dielectric constant and density of water. At room temperature these quantities are well known and yield  $A_\phi = 0.391_5 \pm 0.001$ . We are also interested, however, in solutions at high temperatures and pressures and in the volume, the enthalpy, and the heat capacity. This last function involves the first and second temperature derivatives of the dielectric constant which are much less accurately known. There is also a need for consistency between parameter values at high temperatures and those involving derivatives, which is best attained from a general equation for the dielectric constant as a function of density and temperature. Such an equation was developed by Bradley and Pitzer<sup>11</sup> and is given in Appendix E together with discussion.

Table 1 gives the resulting values for the Debye-Hückel parameters over a range of temperatures extending to 350°C. Below 100°C the parameters apply to the standard pressure of 1 bar, while above 100°C they apply to water under its own vapor pressure. Values for higher pressures are given elsewhere.<sup>11,73</sup> The uncertainties increase considerably near 350°C.

All of the tabulated entries have dimensions  $\text{kg}^{1/2} \cdot \text{mol}^{-1/2}$  except  $A_\psi$ , which has  $\text{cm}^3 \cdot \text{kg}^{1/2} \cdot \text{mol}^{-3/2}$ ; also,  $R = 8.3144 \text{ J} \cdot \text{mol}^{-1} \cdot \text{K}^{-1} = 1.9872 \text{ cal} \cdot \text{mol}^{-1} \cdot \text{K}^{-1}$ .

### B. PARAMETERS FOR PURE ELECTROLYTES AT 25°C

There is an extensive array of carefully evaluated data for the osmotic and activity coefficients of pure aqueous electrolytes at room temperature. The most extensive group is given by Robinson and Stokes.<sup>74</sup> Their data, together with other measurements available in 1973 for particular systems, were fitted<sup>2,3</sup> by least squares to the appropriate equations of preceding sections to evaluate the parameters  $\beta^{(0)}$ ,  $\beta^{(1)}$ , and  $C^\phi$ . Ordinarily the data were weighted equally up to ionic strength of  $4 \text{ mol} \cdot \text{kg}^{-1}$  and then as  $(4/I)^2$ . The third virial coefficient  $C^\phi$  was omitted in cases where the data extend only to moderate concentration, usually  $2 \text{ M}$ . In most cases the fit was satisfactory over the full range of experimental data available, frequently to  $6 \text{ M}$ , but in some cases there was significant deviation and the range of fit was reduced. The maximum allowable deviation in osmotic coefficient was 0.01, except for valence types higher than 1-1, 2-1, or 1-2 and for some organic salts where the data seemed less accurate; in those cases the limit was usually 0.02. In all cases a good fit was required for the dilute range and the weighting system was changed, as necessary, in a few cases to obtain this.

For electrolytes with one or both ions singly charged, the detailed references to sources other than Robinson and Stokes<sup>74</sup> are given elsewhere,<sup>2</sup> together with comments on various particular situations. The present tables also include results from fitting<sup>2</sup> these equations to an extensive array of excellent data for the rare earth chlorides, nitrates, and perchlorates from the laboratory of F. H. Spedding. Also given in these tables are the maximum molality for which the fit was satisfactory (or to which the data extended) and the standard deviation of fit  $\sigma$ . Where data of several types were simultaneously fitted the letter a indicates very high precision, while b and c indicate lower precisions.<sup>2</sup> Tables 2 to 10 give the results for solutes with one or both ions univalent.

For salts of  $\text{Th}^{4+}$  there is considerable hydrolysis; hence, the parameters<sup>2</sup> based on experiments where this was not considered are subject to large correction and have not been included in Table 10. For certain special purposes, they may still be useful and they can be found in Reference 2 or the 1979 edition of this book. This problem may affect other entries with highly charged ions, but will be less serious where the charge is widely distributed as in  $\text{Mo}(\text{CN})_6^{4-}$ .

**TABLE 1**  
**Debye-Hückel Parameters for the Osmotic Coefficient, Volume,**  
**Enthalpy, and Heat Capacity**

t (°C)	$A_\phi$ [(kg/mol) <sup>1/2</sup> ]	$A_v$ (cm <sup>3</sup> kg <sup>1/2</sup> /mol <sup>3/2</sup> )	$A_L/RT$ [(kg/mol) <sup>1/2</sup> ]	$A_p/R$ [(kg/mol) <sup>1/2</sup> ]
0.0	0.3767	1.504	0.556	2.95
10.0	0.3821	1.643	0.649	3.39
20.0	0.3882	1.793	0.749	3.76
25.0	0.3915	1.875	0.801	3.94
30.0	0.3949	1.962	0.854	4.13
40.0	0.4023	2.153	0.965	4.51
50.0	0.4103	2.372	1.081	4.92
60.0	0.4190	2.622	1.203	5.37
70.0	0.4283	2.909	1.331	5.86
80.0	0.4384	3.238	1.467	6.40
90.0	0.4491	3.615	1.611	7.00
100.0	0.4606	4.050	1.764	7.66
110.0	0.4727	4.550	1.927	8.40
120.0	0.4857	5.127	2.102	9.24
130.0	0.4994	5.795	2.290	10.17
140.0	0.5140	6.572	2.492	11.23
150.0	0.5295	7.477	2.712	12.45
160.0	0.5460	8.536	2.951	13.84
170.0	0.5634	9.779	3.213	15.47
180.0	0.5820	11.25	3.500	17.38
190.0	0.6017	12.99	3.819	19.65
200.0	0.6228	15.07	4.175	22.38
210.0	0.6453	17.6	4.576	25.72
220.0	0.6694	20.6	5.032	29.85
230.0	0.6953	24.3	5.556	35.05
240.0	0.7232	28.8	6.165	41.73
250.0	0.7535	34.4	6.885	50.46
260.0	0.7865	41.5	7.749	62.15
270.0	0.823	50.5	8.806	78.18
280.0	0.863	62.3	10.13	100.8
290.0	0.908	77.8	11.82	133.7
300.0	0.960	98.7	14.05	183.4
310.0	1.02	127.	17.1	261.
320.0	1.09	169.	21.4	391.
330.0	1.18	231.	28.0	622.
340.0	1.29	330.	38.6	1060.
350.0	1.44	493.	57.3	1920.

Alternate values for the rare-earth salts were given recently by Kodytek and Dolejs,<sup>75</sup> who included terms in  $\beta^{(2)}$ . Since their values of  $\beta^{(2)}$  are positive, there is no indication of ion pairing. However, the extra flexibility does give a better fit for the low molalities. Their treatment is considered further in Appendix H, which includes examples of their parameters.

Recent values for certain carbonates and bicarbonates<sup>13,18,19,76</sup> are included. Also, Kim and Frederick<sup>77,78</sup> have published extensive tables of values. Many of their entries are essentially the same as the older values<sup>2</sup> but vary a little because of a different pattern for weighting the data. In a few cases where Kim and Frederick have treated new solutes or have clearly superior parameters, their values are included and so identified. For several highly soluble solutes, parameters are given for fits to very high molality, but the precision of fit is much lower. One should be cautious in using these parameters, but they may be useful for some purposes. In several other cases, recent values for individual solutes<sup>79,96</sup> are included and so identified by the reference number in parentheses; where no reference is given, the values are from Reference 2 or 8.

**TABLE 2**  
**Inorganic Acids, Bases, and Salts of 1-1 Type**

	$\beta^{(0)}$	$\beta^{(1)}$	$C^\phi = 2C$	Max m	$\sigma$
HCl	0.1775	0.2945	0.00080	6	a
HBr (79)	0.2085	0.3477	0.00152	6.2	0.003
HI (80)	0.2211	0.4907	0.00482	6	b
HClO <sub>2</sub>	0.1747	0.2931	0.00819	5.5	0.002
HNO <sub>3</sub> (80)	0.1168	0.3546	-0.00539	6	a
H(HSO <sub>3</sub> ) (7)	0.2103	0.4711			
H(HSO <sub>3</sub> ) (31)	0.2065	0.5556			
LiCl	0.1494	0.3074	0.00359	6	0.001
LiBr	0.1748	0.2547	0.0053	2.5	0.002
LiI	0.2104	0.373		1.4	0.006
LiOH	0.015	0.14		4	c
LiClO <sub>3</sub> (77)	0.1705	0.2294	-0.00524	4.2	0.002
LiClO <sub>4</sub>	0.1973	0.3996	0.0008	3.5	0.002
LiBrO <sub>3</sub> (77)	0.0893	0.2157	0.0000	5	0.001
LiNO <sub>2</sub>	0.336	0.325	-0.0053	6	0.003
LiNO <sub>3</sub>	0.1420	0.2780	-0.00551	6	0.001
NaF	0.0215	0.2107		1	0.001
NaCl	0.0765	0.2664	0.00127	6	0.001
NaBr	0.0973	0.2791	0.00116	4	0.001
NaI	0.1195	0.3439	0.0018	3.5	0.001
NaOH	0.0864	0.253	0.0044	6	b
NaClO <sub>3</sub>	0.0249	0.2455	0.004	3.5	0.001
NaClO <sub>4</sub>	0.0554	0.2755	-0.00118	6	0.001
NaBrO <sub>3</sub>	-0.0205	0.1910	0.0059	2.5	0.001
NaCNS	0.1005	0.3582	-0.00303	4	0.001
NaNO <sub>2</sub>	0.0641	0.1015	-0.0049	5	0.005
NaNO <sub>3</sub>	0.0068	0.1783	-0.00072	6	0.001
NaHSe (81)	0.040	(0.253)		2	c
NaHCO <sub>3</sub> (13)	0.028	0.044			
NaHSO <sub>3</sub> (31)	0.0454	0.398			
NaH <sub>2</sub> PO <sub>4</sub>	-0.0533	0.0396	0.00795	6	0.003
NaH <sub>2</sub> AsO <sub>4</sub>	-0.0442	0.2895		1.2	0.001
NaB(OH) <sub>3</sub>	-0.0526	0.1104	0.0154	4.5	0.004
NaBF <sub>4</sub>	-0.0252	0.1824	0.0021	6	0.006
KF	0.08089	0.2021	0.00093	2	0.001
KCl	0.04835	0.2122	-0.00084	4.8	0.0005
KBr	0.0569	0.2212	-0.00180	5.5	0.001
KI	0.0746	0.2517	-0.00414	4.5	0.001
KOH	0.1298	0.320	0.0041	5.5	b
KClO <sub>3</sub>	-0.0960	0.2481		0.7	0.001
KBrO <sub>3</sub>	-0.1290	0.2565		0.5	0.001
KCNS	0.0416	0.2302	-0.00252	5	0.001
KNO <sub>2</sub>	0.0151	0.015	0.0007	5	0.003
KNO <sub>3</sub>	-0.0816	0.0494	0.00660	3.8	0.001
KHCO <sub>3</sub> (18)	-0.0107	0.0478			
KHSO <sub>3</sub> (31)	0.0003	0.1735			
KH <sub>2</sub> PO <sub>4</sub>	-0.0678	-0.1042		1.8	0.003
KH <sub>2</sub> AsO <sub>4</sub>	-0.0584	0.0626		1.2	0.003
KSCN (77)	0.0389	0.2536	-0.00192	5	0.001
KPF <sub>6</sub>	-0.163	-0.282		0.5	0.001
RbF	0.1141	0.2842	-0.0105	3.5	0.002
RbCl (82)	0.0431	0.1539	-0.00109	7.8	0.003
RbBr	0.0396	0.1530	-0.00144	5	0.001
RbI	0.0397	0.1330	-0.00108	5	0.001
RbNO <sub>3</sub>	0.0269	-0.1553	-0.00366	5	0.002

TABLE 2 (continued)  
Inorganic Acids, Bases, and Salts of 1-1 Type

	$\beta^{(0)}$	$\beta^{(1)}$	$C^\phi = 2C$	Max m	$\sigma$
RbNO <sub>3</sub>	-0.0789	-0.0172	0.00529	4.5	0.001
CsF	0.1306	0.2570	-0.0043	3.2	0.002
CsCl (83)	0.0347 <sub>8</sub>	0.0397 <sub>4</sub>	-0.00049 <sub>6</sub>	7.4	0.002
CsBr	0.0279	0.0139	0.00004	5	0.002
CsI	0.0244	0.0262	-0.00365	3	0.001
CsOH	0.150	0.30			b
CsNO <sub>2</sub>	0.0427	0.060	-0.0051	6	0.004
CsNO <sub>3</sub>	-0.0758	-0.0669		1.4	0.002
AgNO <sub>3</sub>	-0.0856	0.0025	0.00591	6	0.001
TiClO <sub>4</sub>	-0.087	-0.023		0.5	0.001
TiNO <sub>3</sub>	-0.105	-0.378		0.4	0.001
NH <sub>4</sub> Cl	0.0522	0.1918	-0.00301	6	0.001
NH <sub>4</sub> Br	0.0624	0.1947	-0.00436	2.5	0.001
NH <sub>4</sub> I (77)	0.0570	0.3157	-0.00308	7.5	0.002
NH <sub>4</sub> HCO <sub>3</sub> (76)	-0.038	0.070		0.7	—
NH <sub>4</sub> H <sub>2</sub> PO <sub>4</sub> (37)	-0.0704	-0.4156	0.00669	3.5	0.003
NH <sub>4</sub> ClO <sub>4</sub>	-0.0103	-0.0194		2	0.004
NH <sub>4</sub> NO <sub>3</sub>	-0.0154	0.1120	-0.00003	6	0.001
(MgOH)Cl (31)	-0.10	1.658	—	—	—

Note: The numbers in parentheses are references; all other entries are either from Reference 2 or 8.

In selection of expressions for the second virial coefficient, it was noted that there should be some relationship between the two parameters  $\beta^{(0)}$  and  $\beta^{(1)}$  for various electrolytes. This is shown in Figure 3 for the simpler 1-1 solutes. It is seen that there is, indeed, a general relationship between these two parameters for most solutes but that it does not appear to be an exact dependence. The corresponding figures for other valence types are given elsewhere.<sup>2</sup> The relationships displayed in these figures should be used to estimate  $\beta^{(1)}$  when there are no accurate measurements at low molality.

In a few cases [MgCl<sub>2</sub>, CaCl<sub>2</sub>, SrCl<sub>2</sub>, Cu(NO<sub>3</sub>)<sub>2</sub>, Na<sub>2</sub>SO<sub>4</sub>, Cs<sub>2</sub>SO<sub>4</sub>, and (NH<sub>4</sub>)<sub>2</sub>SO<sub>4</sub> in Table 7 and MgSO<sub>4</sub> in Table 11], two sets of parameters are given. In each case one, without reference number in Table 7 or with Reference 3 in Table 11, is the original set from References 2 and 3; these sets of values have been widely used in various calculations for mixed electrolytes including those of Harvie and associates.<sup>28-31</sup> It is best to retain these values for use in connection with the mixing parameters of Tables 16, 18, and 20, most of which were derived on this basis. This will avoid possible inconsistencies. The differences are very small, however, as is apparent from the values listed.

Various chloride complex ions of copper and silver, CuCl<sub>2</sub><sup>-</sup>, CuCl<sub>3</sub><sup>2-</sup>, . . . , AgCl<sub>2</sub><sup>-</sup>, AgCl<sub>3</sub><sup>2-</sup>, . . . , with H<sup>+</sup>, Na<sup>+</sup>, K<sup>+</sup>, and NH<sub>4</sub><sup>+</sup> as cations were considered by Fritz<sup>97-100</sup> and by Sharma and Millero.<sup>101</sup> In the work of Fritz, the composition measure is molar concentration instead of molality; also, in many cases  $\beta^{(1)}$  was determined from the general correlation with  $\beta^{(0)}$  (Figure 3 and discussion above). Fritz also gives the association equilibrium constants and, in some cases, temperature coefficients of some parameters. Parameters for chloride complexes of Pb<sup>2+</sup> were evaluated by Millero and Byrne.<sup>102</sup>

In a number of cases where there is a tendency toward complex ion formation at high molality (e.g., ZnCl<sub>2</sub>), the standard equation fits in the dilute range with large negative  $C^\phi$ . Various methods, which are considered in Appendix H, have been used to obtain a good fit at higher molality.

Also of note are very recent values for several borates from Simonson et al.,<sup>103,104</sup> from

**TABLE 3**  
Salts of Carboxylic Acids (1-1 Type)

	$\beta^{00}$	$\beta^{11}$	$C^{\phi} = 2C$	Max m	$\sigma$
Li acetate	0.1124	0.2483	-0.00525	4	0.001
Na formate	0.0820	0.2872	-0.00523	3.5	0.001
Na acetate	0.1426	0.3237	-0.00629	3.5	0.001
Na propionate	0.1875	0.2789	-0.01277	3	0.001
NaH malonate	0.0229	0.1600	-0.00106	5	0.002
NaH succinate	0.0354	0.1606	0.00040	5	0.001
NaH adipate	0.0472	0.3168		0.7	0.001
K acetate	0.1587	0.3251	-0.00660	3.5	0.001
KH malonate	-0.0095	0.1423	0.00167	5	0.004
KH succinate	0.0111	0.1564	0.00274	4.5	0.002
KH adipate	0.0419	0.2523		1	0.001
Rb acetate	0.1622	0.3353	-0.00551	3.5	0.001
Cs acetate	0.1628	0.3605	-0.00555	3.5	0.001
Tl acetate	0.0082	0.0131	-0.00127	6	0.001

**TABLE 4**  
Tetraalkylammonium Halides

	$\beta^{00}$	$\beta^{11}$	$C^{\phi} = 2C$	Max m	$\sigma$
Me <sub>4</sub> NF	0.2677	0.2265	0.0013	3	0.002
Et <sub>4</sub> NF	0.3113	0.6155	0.0349	2	0.002
Pr <sub>4</sub> NF	0.4463	0.4090	0.0537	2	0.002
Bu <sub>4</sub> NF	0.6092	0.402	-0.0281	1.7	0.005
Me <sub>4</sub> NCl	0.0430	-0.029	0.0078	3.4	0.005
Et <sub>4</sub> NCl	0.0617	-0.099	0.0105	3	0.002
Pr <sub>4</sub> NCl	0.1346	-0.300	0.0119	2.5	0.002
Bu <sub>4</sub> NCl	0.2339	-0.410	0.0567	2.5	0.001
Me <sub>4</sub> NBr	0.0082	-0.147	0.0105	3.5	0.004
Et <sub>4</sub> NBr	0.0176	-0.394	0.0156	4	0.001
Pr <sub>4</sub> NBr	0.0390	-0.772	0.0099	3.5	0.003
Bu <sub>4</sub> NBr	-0.0277	-0.525	0.0011	4.5	0.007
Me <sub>4</sub> NI	0.0345	-0.585		0.3	0.003
Et <sub>4</sub> NI	0.179	-0.571	0.0412	2	0.007
Pr <sub>4</sub> NI	-0.2839	-0.863		0.5	0.005

Felmy and Weare,<sup>105</sup> and from Hershey et al.<sup>106</sup> Hershey and Millero<sup>107</sup> give parameters for Na [Si(OH)<sub>2</sub>O] and Na<sub>2</sub>[Si(OH)<sub>2</sub>O<sub>2</sub>], while Thurmond and Millero<sup>108,109</sup> give further consideration of carbonates. Clegg and Brimblecombe<sup>110</sup> give values for BeCl<sub>2</sub> obtained indirectly from ternary solutions, but these results are probably affected by hydrolysis. Values for NaCl below 0°C are given by Thurmond and Brass.<sup>111</sup> Many of these and other values are given in Chapter 6.

As was indicated above, there are special problems related to 2-2 or higher valence types of electrolytes in water. For the 2-2 type, at least, these can be handled by adding a third term to the second virial coefficient, Equations 36 and 42.

The full array of data for the sulfates of Mg, Ni, Cu, Zn, and Cd were fitted<sup>3</sup> by least-squares regression of the four parameters  $\beta^{00}$ ,  $\beta^{11}$ ,  $\beta^{22}$ , and  $C^{\phi}$  for each substance. A series of values of  $\alpha_1$  and  $\alpha_2$  were used. While the optimum values of  $\alpha_1$  and  $\alpha_2$  varied a little from case to case, the values  $\alpha_1 = 1.4$  and  $\alpha_2 = 12.0$  fitted all cases very well and were adopted for all 2-2 electrolytes. This value of  $\alpha_1$  is somewhat smaller than the value 2.0



**TABLE 5**  
**Sulfonic Acids and Salts (1-1 Type) (SA = Sulfonic Acid;**  
**S = Sulfonate)**

	$\beta^{(0)}$	$\beta^{(1)}$	$C^\phi = 2C$	Max $m$	$\sigma$
Methane SA (84)	0.1544	0.4775	-0.0041	6	
Li methane S	0.1320	0.271	-0.0030	4	0.010
Na methane S	0.0787	0.274	-0.0024	4	0.002
K methane S	0.0581	0.165	-0.0046	4	0.001
NH <sub>4</sub> methane S	0.0661	0.191	-0.0041	4	0.001
Me <sub>2</sub> N methane S	0.1458	0.168	-0.0043	4	0.004
Et <sub>3</sub> N methane	0.1548	0.090	-0.0034	4	0.005
Bu <sub>4</sub> N methane S	0.2145	0.235	-0.0392	4	0.015
Ethane SA	0.1536	0.341	-0.0056	4	0.003
Li ethane S	0.1799	0.319	-0.0118	4	0.007
Na ethane S	0.1316	0.374	-0.0082	4	0.003
K ethane S	0.0965	0.250	-0.0074	4	0.001
NH <sub>4</sub> ethane S	0.1142	0.179	-0.0114	4	0.003
Me <sub>2</sub> N ethane S	0.1796	0.083	-0.0116	4	0.004
Et <sub>3</sub> N ethane S	0.1805	0.075	-0.0040	4	0.014
Bu <sub>4</sub> N ethane S	0.1827	0.445	-0.0374	4	0.013
Benzene SA	0.0526	0.445	0.0036	5	0.002
Li benzene S	0.1134	0.466	-0.0075	4.5	0.002
Na benzene S	0.0842	0.351	-0.0181	2.5	0.001
<i>p</i> -Toluene SA	-0.0366	0.281	0.0137	5	0.002
Li <i>p</i> -toluene S	0.0189	0.399	0.0046	4.5	0.004
Na <i>p</i> -toluene S	-0.0344	0.396	0.0043	4	0.003
K <i>p</i> -toluene S	-0.0985	0.453	0.0122	3.5	0.002
2,5 Me <sub>2</sub> benzene SA	-0.0965	0.141	0.0210	4.5	0.01
Li 2,5 Me <sub>2</sub> benzene S	-0.0098	0.361	0.0039	3.5	0.002
Na 2,5 Me <sub>2</sub> benzene S	-0.0277	0.228		1	0.005
<i>p</i> -Et benzene SA	-0.1736	0.435	0.0383	2	0.007
Li <i>p</i> -Et benzene S	-0.1438	0.804	0.0317	5	0.01
Na <i>p</i> -Et benzene S	-0.2240	0.895	0.0355	2.5	0.01
Mesitylene SA	-0.2209	0.248	0.0432	2	0.01
Li mesitylene S	-0.1998	0.871	0.0456	2	0.004
Na mesitylene S	-0.2018	0.767		1	0.003

used for most electrolytes. There is some theoretical justification<sup>3</sup> for a value near 12 for  $\alpha_2$ . The resulting values, the concentration range of data used, the accuracy of fit, and references are given in Table 11. It is apparent that agreement is obtained substantially within experimental error.

For most of the solutes in Table 11, the data extend over a wide concentration range, and the resulting parameters should be reliable. Since data for CaSO<sub>4</sub> are solubility limited to dilute solutions, the third virial coefficient was omitted and  $\beta^{(0)}$  was set at 0.20 on the basis of the results for other solutes. The data sufficed to evaluate the two remaining parameters.

There are no data below 0.1 *M* for the last two solutes, BeSO<sub>4</sub>, and UO<sub>2</sub>SO<sub>4</sub>; hence, no meaningful value can be given for  $\beta^{(2)}$ . If an estimate is desired, the rounded value -40 might be chosen as typical of this type of solute.

For the osmotic coefficient, the large value of  $\alpha_2$  makes the term in  $\beta^{(2)}$  negligible above 0.1 *M*. We see from Equations 49, 50, 55, and 58, however, that the corresponding term in the logarithm of the activity coefficient approaches the constant value  $(2m\beta^{(2)}/\alpha_2 I) = \beta^{(2)}/288$  at high concentration. Since this term is constant, it does not affect the relative values of the activity coefficient (or other functions) at various concentrations above 0.1 *M*,

TABLE 6  
Additional 1-1 Type Organic Salts

	$\beta^{(0)}$	$\beta^{(1)}$	$C^+ = 2C$	Max $m$	$\sigma$
Choline Cl	0.0457	-0.196	0.0008	6	0.004
Choline Br	-0.0066	-0.227	0.0036	6	0.004
MeNH <sub>2</sub> ClO <sub>4</sub> (77)	-0.0337	0.0057	0.00345	4	0.002
Me <sub>2</sub> NH <sub>2</sub> ClO <sub>4</sub> (77)	-0.0440	-0.1719	0.0024	7.5	0.001
Me <sub>3</sub> NHClO <sub>4</sub> (77)	-0.1145	-0.1713	0.01348	1.8	0.002
Me <sub>3</sub> BzNCl	-0.0821	-0.178	0.0162	3.5	0.01
Me <sub>3</sub> BzNBr	-0.1517	-0.545	0.0187	3	0.01
Me <sub>2</sub> OEtBzNCl	-0.0879	-0.343	0.0134	4	0.01
Me <sub>2</sub> OEtBzNBr	-0.1518	-0.778	0.0177	3	0.01
(HOC <sub>2</sub> H <sub>4</sub> ) <sub>2</sub> NF	0.0938	0.128	-0.0030	4	0.001
(HOC <sub>2</sub> H <sub>4</sub> ) <sub>2</sub> NBr	-0.0474	-0.259	0.0106	3	0.002
Me <sub>3</sub> SCl	0.0314	-0.184	0.0023	6	0.005
Me <sub>3</sub> SBr	-0.0228	-0.245	0.0044	6	0.004
Me <sub>3</sub> SI	-0.0601	-0.604	-0.0006	6	0.01
Bu <sub>3</sub> SCl	0.0726	-0.245	-0.0099	6	0.01
Bu <sub>3</sub> SBr	-0.0803	-0.616	0.0053	6	0.01

but it does affect the relationship to the solute standard state and the absolute values of the activity coefficients. This indicates the category of calculations which are valid even though  $\beta^{(2)}$  is not known and the different category where  $\beta^{(2)}$  is required.

For salts of even higher charge types, there are few data. Recently, Reardon<sup>114</sup> has considered Al<sub>2</sub>SO<sub>4</sub> and recommends the parameters:  $\beta^{(0)} = 0.854$ ,  $\beta^{(1)} = 18.53$ ,  $\beta^{(2)} = -500$ ,  $C^+ = -0.0911$  with  $\alpha_1 = 2$  and  $\alpha_2 = 50$ . Rard<sup>115</sup> gives alternate sets of values for Lu<sub>2</sub>(SO<sub>4</sub>)<sub>3</sub>.

The data on heat of dilution or heat of solution have been fitted<sup>9,10</sup> to Equations 81 to 88 which yield the temperature derivatives of the ion interaction parameters  $\beta^{(0)}$  etc. See Appendix E concerning a small shift in the Debye-Hückel parameter from the value used in References 9 and 10. Where heat of solution data were included, a value of  $\Delta H^{\circ}$ , the heat of solution of the solid to the infinitely dilute standard state, was also obtained; these values are given in Reference 9. Detailed references and discussions of special problems for individual substances or evaluation methods are given elsewhere.<sup>9,10</sup> The results are listed in Table 12 for 1-1 electrolytes and in Table 13 for other valence types. These values may be used to convert the parameters for activity coefficients from 25°C to other temperatures not too different.

Volumetric data can be fitted to Equations 96 to 99 which yield the pressure derivatives of the ion interaction parameters  $\beta^{(0)}$  etc. This treatment also yields the partial molar volume  $V_2^{\circ}$  in the infinitely dilute standard state. As an example of such calculations, the values of  $V_2^{\circ}$ ,  $\beta^{(0)v}$ , etc. are given in Table 14 for the major sea salts involving Na<sup>+</sup>, Mg<sup>2+</sup>, Cl<sup>-</sup>, and SO<sub>4</sub><sup>2-</sup>. Two sets of values are given for NaCl; for the other salts the values are those of Connaughton et al.<sup>117</sup> in both sources.<sup>14,117</sup> Equations or tables are given for these parameters at other temperatures, while Simonson and Ryther<sup>118</sup> present values for NaOH. Monnin<sup>119a,119b</sup> presents parameters for several additional solutes at 25°C and as a function of temperature. Kumar<sup>120</sup> and Pogue and Atkinson<sup>121</sup> have given equations and tables for a large number of cases. Chapter 6 includes many additional values for the volume parameters; the parameters for compressibility are also considered there.

### C. PURE ELECTROLYTE PARAMETERS FOR HIGH TEMPERATURES

Various measurements can be used to obtain the pure electrolyte parameters for high temperatures. The isopiestic method, which is so useful at 25°C, has provided valuable data

TABLE 7  
Inorganic Compounds of 2-1 Type

	$\frac{4}{3} \beta^{(0)}$	$\frac{4}{3} \beta^{(1)}$	$\frac{2}{3} 2^{5/2} C^{\phi} = \frac{16}{3} C$	Max <i>m</i>	$\sigma$
MgCl <sub>2</sub>	0.4698	2.242	0.00979	4.5	0.003
MgCl <sub>2</sub> (85)	0.4679 <sub>1</sub>	2.201	0.01227	4	0.003
MgBr <sub>2</sub>	0.5769	2.337	0.00589	5	0.004
MgI <sub>2</sub>	0.6536	2.4055	0.01496	5	0.003
Mg(ClO <sub>4</sub> ) <sub>2</sub>	0.6615	2.678	0.01806	2	0.002
Mg(NO <sub>3</sub> ) <sub>2</sub>	0.4895	2.113	-0.03889	2	0.003
Mg(HCO <sub>3</sub> ) <sub>2</sub> (19)	0.044	1.133			
Mg(HSO <sub>4</sub> ) <sub>2</sub> (31)	0.6328	2.305			
CaCl <sub>2</sub>	0.4212	2.152	-0.00064	2.5	0.003
CaCl <sub>2</sub> (86)	0.4071	2.278	0.00406	4.3	0.003
CaBr <sub>2</sub>	0.5088	2.151	-0.00485	2	0.002
CaI <sub>2</sub>	0.5839	2.409	-0.00158	2	0.001
Ca(ClO <sub>4</sub> ) <sub>2</sub>	0.6015	2.342	-0.00943	2	0.005
Ca(NO <sub>3</sub> ) <sub>2</sub>	0.2811	1.879	-0.03798	2	0.002
Ca(HCO <sub>3</sub> ) <sub>2</sub> (31)	0.533	3.97			
Ca(HSO <sub>4</sub> ) <sub>2</sub> (31)	0.286	3.37			
SrCl <sub>2</sub>	0.3810	2.223	-0.00246	4	0.003
SrCl <sub>2</sub> (83)	0.3779 <sub>2</sub>	2.167 <sub>5</sub>	-0.00168	3.8	0.002
SrBr <sub>2</sub>	0.4415	2.282	0.00231	2	0.001
SrI <sub>2</sub>	0.5350	2.480	0.00501	2	0.001
Sr(ClO <sub>4</sub> ) <sub>2</sub>	0.5692	2.089	-0.02472	2.5	0.003
Sr(NO <sub>3</sub> ) <sub>2</sub>	0.1795	1.840	-0.03757	2	0.002
BaCl <sub>2</sub>	0.3504	1.995	-0.03654	1.8	0.001
BaBr <sub>2</sub>	0.4194	2.093	-0.03009	2	0.001
BaI <sub>2</sub>	0.5625	2.249	-0.03286	1.8	0.003
Ba(OH) <sub>2</sub>	0.229	1.60		0.1	
Ba(ClO <sub>4</sub> ) <sub>2</sub>	0.4819	2.101	-0.05894	2	0.003
Ba(NO <sub>3</sub> ) <sub>2</sub>	-0.043	1.07		0.4	0.001
MnCl <sub>2</sub> (82)	0.4429 <sub>7</sub>	2.019 <sub>5</sub>	-0.04278	4	0.003
FeCl <sub>2</sub>	0.4479	2.043	-0.01623	2	0.002
Fe(HSO <sub>4</sub> ) <sub>2</sub> (87)	0.5697	4.64			
CoCl <sub>2</sub>	0.4857	1.967	-0.02869	3	0.004
CoBr <sub>2</sub>	0.5693	2.213	-0.00127	2	0.002
CoI <sub>2</sub>	0.695	2.23	-0.0088	2	0.01
Co(NO <sub>3</sub> ) <sub>2</sub>	0.4159	2.254	-0.01436	5.5	0.003
NiCl <sub>2</sub> (88)	0.4665 <sub>5</sub>	2.040	-0.00888 <sub>1</sub>	2.5	0.002
CuCl <sub>2</sub>	0.3955	1.855	-0.06792	2	0.002
Cu(NO <sub>3</sub> ) <sub>2</sub> (35)	0.3743	2.310	-0.01580	8	0.003
Cu(NO <sub>3</sub> ) <sub>2</sub>	0.4224	1.907	-0.04136	2	0.002
ZnCl <sub>2</sub> (89)	0.3043 <sub>3</sub>	2.308 <sub>5</sub>	-0.1235 <sub>6</sub>	1.5	0.007
ZnBr <sub>2</sub>	0.6213	2.179	-0.2035	1.6	0.007
ZnI <sub>2</sub>	0.6428	2.594	-0.0269	0.8	0.002
Zn(ClO <sub>4</sub> ) <sub>2</sub>	0.6747	2.396	0.02134	2	0.003
Zn(NO <sub>3</sub> ) <sub>2</sub>	0.4641	2.255	-0.02955	2	0.001
Cd(NO <sub>3</sub> ) <sub>2</sub>	0.3820	2.224	-0.04836	2.5	0.002
Pb(ClO <sub>4</sub> ) <sub>2</sub>	0.4443	2.296	-0.01667	6	0.004
Pb(NO <sub>3</sub> ) <sub>2</sub>	-0.0482	0.380	0.01005	2	0.002
UO <sub>2</sub> Cl <sub>2</sub>	0.5698	2.192	-0.06951	2	0.001
UO <sub>2</sub> (ClO <sub>4</sub> ) <sub>2</sub>	0.8151	2.859	0.04089	2.5	0.003
UO <sub>2</sub> (NO <sub>3</sub> ) <sub>2</sub>	0.6143	2.151	-0.05948	2	0.002
Li <sub>2</sub> SO <sub>4</sub>	0.1817	1.694	-0.00753	3	0.002
Na <sub>2</sub> SO <sub>4</sub>	0.0261	1.484	0.00938	4	0.003
Na <sub>2</sub> SO <sub>4</sub> (90)	0.0249 <sub>2</sub>	1.466	0.010463	4	0.003
Na <sub>2</sub> S <sub>2</sub> O <sub>3</sub>	0.0882	1.701	0.00705	3.5	0.002

TABLE 7 (continued)  
Inorganic Compounds of 2-1 Type

	$\frac{4}{3} \beta^{(0)}$	$\frac{4}{3} \beta^{(1)}$	$\frac{2}{3} 2^{s,2} C^{\phi} = \frac{16}{3} C$	Max <i>m</i>	$\sigma$
Na <sub>2</sub> CrO <sub>4</sub>	0.1250	1.826	- 0.00407	2	0.002
Na <sub>2</sub> CO <sub>3</sub> (13)	0.0483	2.013	0.0098		
Na <sub>2</sub> HPO <sub>4</sub>	- 0.0777	1.954	0.0554	1	0.002
Na <sub>2</sub> HA <sub>2</sub> O <sub>4</sub>	0.0407	2.173	0.0034	1	0.001
K <sub>2</sub> SO <sub>4</sub>	0.0666	1.039		0.7	0.002
K <sub>2</sub> CrO <sub>4</sub>	0.1011	1.652	- 0.00147	3.5	0.003
K <sub>2</sub> CO <sub>3</sub> (18)	0.1717	1.911	0.00094		
K <sub>2</sub> Pt(CN) <sub>4</sub>	0.0881	3.164	0.0247	1	0.005
K <sub>2</sub> HPO <sub>3</sub>	0.0330	1.699	0.0309	1	0.002
K <sub>2</sub> HA <sub>2</sub> O <sub>2</sub>	0.1728	2.198	- 0.0336	1	0.001
Rb <sub>2</sub> SO <sub>4</sub>	0.0772	1.481	- 0.00019	1.8	0.001
Cs <sub>2</sub> SO <sub>4</sub> (40)	0.0952	1.601	0.00549	5	
Cs <sub>2</sub> SO <sub>4</sub>	0.1184	1.481	- 0.01131	1.8	0.001
(NH <sub>4</sub> ) <sub>2</sub> SO <sub>4</sub> (37)	0.0521	0.8851	- 0.00156	5.8	0.002
(NH <sub>4</sub> ) <sub>2</sub> SO <sub>4</sub>	0.0545	0.878	- 0.00219	5.5	0.004
<i>cis</i> [Co(en) <sub>2</sub> NH <sub>2</sub> NO <sub>2</sub> ](NO <sub>3</sub> ) <sub>2</sub>	- 0.0928	0.271		0.6	0.002
<i>trans</i> [Co(en) <sub>2</sub> NH <sub>2</sub> NO <sub>2</sub> ](NO <sub>3</sub> ) <sub>2</sub>	- 0.0901	0.249		0.8	0.002
<i>cis</i> [Co(en) <sub>2</sub> NH <sub>2</sub> NO <sub>2</sub> ](Cl) <sub>2</sub>	- 0.0327	0.684	0.0121	2.8	0.005
<i>trans</i> [Co(en) <sub>2</sub> NH <sub>2</sub> NO <sub>2</sub> ](Cl) <sub>2</sub>	0.0050	0.695	0.0066	2.4	0.005
<i>cis</i> [Co(en) <sub>2</sub> NH <sub>2</sub> NO <sub>2</sub> ](Br) <sub>2</sub>	- 0.1152	0.128	0.0158	1	0.004
<i>trans</i> [Co(en) <sub>2</sub> NH <sub>2</sub> NO <sub>2</sub> ](Br) <sub>2</sub>	- 0.0912	0.424	0.0223	2.4	0.005
<i>cis</i> [Co(en) <sub>2</sub> NO <sub>2</sub> NO <sub>2</sub> ](I) <sub>2</sub>	- 0.1820	0.594		0.6	0.004
<i>trans</i> [Co(en) <sub>2</sub> NO <sub>2</sub> NO <sub>2</sub> ](I) <sub>2</sub>	- 0.1970	1.003		0.3	0.003

TABLE 8  
Organic Electrolytes of 2-1 Type  
(SA = Sulfonic Acid; S = Sulfonate)

	$\frac{4}{3} \beta^{(0)}$	$\frac{4}{3} \beta^{(1)}$	$\frac{2}{3} 2^{s,2} C^{\phi} = \frac{16}{3} C$	Max <i>m</i>	$\sigma$
<i>m</i> -Benzenedi SA	0.5611	2.637	- 0.0463	1.6	0.004
Li, <i>m</i> -Benzenedi S	0.5464	2.564	0.0622	2.5	0.004
Na <sub>2</sub> <i>m</i> -Benzenedi S	0.3411	2.698	- 0.0419	3	0.004
4,4'-Bibenzylidi SA	0.1136	2.432	0.0705	2	0.01
Li, 4,4'-bibenzylidi S	0.1810	1.755	0.0462	1.2	0.007
Na, 4,4'-bibenzylidi S	0.0251	1.969	—	0.4	0.01
Na <sub>2</sub> fumarate	0.3082	1.203	0.0378	2	0.003
Na <sub>2</sub> maleate	0.1860	0.575	- 0.0170	3	0.004
Na succinate (91)	0.4175	2.3915	- 0.0924	1.4	0.004
K succinate (92)	0.1673	2.1851	—	1.5	0.003

up to about 250°C. The reference solution is usually NaCl which has been thoroughly studied by other methods including the vapor pressure relative to that of pure water. Heats of dilution can be measured quite accurately at high temperature. Provided the heat of dilution as well as the excess Gibbs energy is known at 25°C, measurements of the heat capacity at higher temperatures provide the required information for both the solution parameters and the standard state entropy and chemical potential. In practice, two or more methods are usually used, and the parameters determined from a least squares optimization of the parameters to fit all of the accurate measurements.

There is now an extensive array of data for the most geochemically or industrially

TABLE 9  
3-1 Electrolytes

	$\frac{3}{2}\beta^{(0)}$	$\frac{3}{2}\beta^{(1)}$	$\frac{3^{3/2}}{2} C^* = 9C$	Max $m$	$\sigma$
AlCl <sub>3</sub>	1.0490	8.767	0.0071	1.6	0.005
ScCl <sub>3</sub>	1.0500	7.978	-0.0840	1.8	0.005
YCl <sub>3</sub> (93)	0.939 <sub>6</sub>	8.40	-0.040 <sub>6</sub>	4.1	0.006
LaCl <sub>3</sub>	0.883 <sub>4</sub>	8.40	-0.061 <sub>9</sub>	3.9	0.006
CeCl <sub>3</sub>	0.907 <sub>2</sub>	8.40	-0.074 <sub>6</sub>	1.8	0.007
PrCl <sub>3</sub>	0.883 <sub>8</sub>	8.40	-0.054 <sub>9</sub>	3.9	0.006
NdCl <sub>3</sub>	0.878 <sub>4</sub>	8.40	-0.049 <sub>3</sub>	3.9	0.006
SmCl <sub>3</sub>	0.900 <sub>0</sub>	8.40	-0.053 <sub>5</sub>	3.6	0.007
EuCl <sub>3</sub>	0.911 <sub>5</sub>	8.40	-0.054 <sub>7</sub>	3.6	0.006
GdCl <sub>3</sub>	0.913 <sub>9</sub>	8.40	-0.049 <sub>4</sub>	3.6	0.006
TbCl <sub>3</sub>	0.922 <sub>9</sub>	8.40	-0.046 <sub>8</sub>	3.6	0.004
DyCl <sub>3</sub>	0.929 <sub>0</sub>	8.40	-0.045 <sub>6</sub>	3.6	0.005
HoCl <sub>3</sub>	0.937 <sub>6</sub>	8.40	-0.045 <sub>0</sub>	3.7	0.006
ErCl <sub>3</sub>	0.928 <sub>5</sub>	8.40	-0.038 <sub>9</sub>	3.7	0.006
TmCl <sub>3</sub>	0.926 <sub>2</sub>	8.40	-0.036 <sub>2</sub>	3.7	0.005
YbCl <sub>3</sub>	0.923 <sub>5</sub>	8.40	-0.033 <sub>5</sub>	3.7	0.005
LuCl <sub>3</sub>	0.922 <sub>8</sub>	8.40	-0.033 <sub>2</sub>	4.1	0.005
CrCl <sub>3</sub>	1.1046	7.883	-0.1172	1.2	0.005
Cr(NO <sub>3</sub> ) <sub>3</sub>	1.0560	7.777	-0.1533	1.4	0.004
Ga(ClO <sub>4</sub> ) <sub>3</sub>	1.2381	9.794	0.0904	2	0.008
InCl <sub>3</sub>	-1.68	-3.85		0.01	
Y(NO <sub>3</sub> ) <sub>3</sub> (93)	0.915 <sub>8</sub>	7.70	-0.189 <sub>8</sub>	2.0	0.008
La(NO <sub>3</sub> ) <sub>3</sub> (94)	0.737 <sub>4</sub>	7.70	-0.198 <sub>9</sub>	1.5	0.007
Pr(NO <sub>3</sub> ) <sub>3</sub> (88)	0.724 <sub>5</sub>	7.70	-0.173 <sub>4</sub>	1.5	0.005
Nd(NO <sub>3</sub> ) <sub>3</sub> (95)	0.702 <sub>3</sub>	7.70	-0.142 <sub>7</sub>	2.0	0.008
Sm(NO <sub>3</sub> ) <sub>3</sub>	0.701	7.70	-0.131	1.5	0.007
Eu(NO <sub>3</sub> ) <sub>3</sub> (93)	0.713 <sub>3</sub>	7.70	-0.125 <sub>7</sub>	2.0	0.007
Gd(NO <sub>3</sub> ) <sub>3</sub>	0.776	7.70	-0.170	1.4	0.005
Tb(NO <sub>3</sub> ) <sub>3</sub>	0.838	7.70	-0.202	1.4	0.005
Dy(NO <sub>3</sub> ) <sub>3</sub> (96)	0.848 <sub>4</sub>	7.70	-0.1809	2.0	0.008
Ho(NO <sub>3</sub> ) <sub>3</sub> (96)	0.876 <sub>9</sub>	7.70	-0.1852	2.0	0.009
Er(NO <sub>3</sub> ) <sub>3</sub>	0.938	7.70	-0.226	1.5	0.006
Tm(NO <sub>3</sub> ) <sub>3</sub>	0.952	7.70	-0.222	1.5	0.006
Yb(NO <sub>3</sub> ) <sub>3</sub>	0.948	7.70	-0.208	1.5	0.006
Lu(NO <sub>3</sub> ) <sub>3</sub> (88)	0.926 <sub>4</sub>	7.70	-0.174 <sub>9</sub>	2.0	0.008
La(ClO <sub>4</sub> ) <sub>3</sub>	1.15 <sub>8</sub>	9.80	0.001 <sub>6</sub>	2.0	0.009
Pr(ClO <sub>4</sub> ) <sub>3</sub>	1.13 <sub>2</sub>	9.80	0.016 <sub>3</sub>	2.0	0.006
Nd(ClO <sub>4</sub> ) <sub>3</sub>	1.13 <sub>1</sub>	9.80	0.019 <sub>4</sub>	2.0	0.007
Sm(ClO <sub>4</sub> ) <sub>3</sub>	1.14 <sub>6</sub>	9.80	0.014 <sub>0</sub>	2.0	0.005
Gd(ClO <sub>4</sub> ) <sub>3</sub>	1.17 <sub>3</sub>	9.80	0.014 <sub>0</sub>	2.0	0.007
Tb(ClO <sub>4</sub> ) <sub>3</sub>	1.19 <sub>3</sub>	9.80	0.012 <sub>3</sub>	2.0	0.006
Dy(ClO <sub>4</sub> ) <sub>3</sub>	1.20 <sub>1</sub>	9.80	0.014 <sub>2</sub>	2.0	0.006
Ho(ClO <sub>4</sub> ) <sub>3</sub>	1.19 <sub>8</sub>	9.80	0.013 <sub>2</sub>	2.0	0.004
Er(ClO <sub>4</sub> ) <sub>3</sub>	1.20 <sub>2</sub>	9.80	0.014 <sub>4</sub>	1.8	0.004
Tm(ClO <sub>4</sub> ) <sub>3</sub>	1.19 <sub>3</sub>	9.80	0.024 <sub>5</sub>	2.0	0.005
Yb(ClO <sub>4</sub> ) <sub>3</sub>	1.20 <sub>6</sub>	9.80	0.013 <sub>7</sub>	1.8	0.004
Lu(ClO <sub>4</sub> ) <sub>3</sub>	1.18 <sub>6</sub>	9.80	0.029 <sub>0</sub>	2.0	0.006
Na <sub>3</sub> PO <sub>4</sub>	0.2672	5.777	-0.1339	0.7	0.003
Na <sub>3</sub> AsO <sub>4</sub>	0.3582	5.895	-0.1240	0.7	0.001
K <sub>3</sub> PO <sub>4</sub>	0.5594	5.958	-0.2255	0.7	0.001
K <sub>3</sub> P <sub>2</sub> O <sub>7</sub>	0.4867	8.349	-0.0886	0.8	0.004
K <sub>3</sub> AsO <sub>4</sub>	0.7491	6.511	-0.3376	0.7	0.001
K <sub>3</sub> Fe(CN) <sub>6</sub>	0.5035	7.121	-0.1176	1.4	0.003
K <sub>3</sub> Co(CN) <sub>6</sub>	0.5603	5.815	-0.1603	1.4	0.008
Co(en) <sub>3</sub> Cl <sub>3</sub>	0.2603	3.563	-0.0916	1	0.003
Co(en) <sub>3</sub> (NO <sub>3</sub> ) <sub>3</sub>	0.1882	3.935		0.3	0.01
Co(en) <sub>3</sub> (ClO <sub>4</sub> ) <sub>3</sub>	0.1619	5.395		0.6	0.007
Co(pn) <sub>3</sub> (ClO <sub>4</sub> ) <sub>3</sub>	0.2022	3.976		0.3	0.003

TABLE 10  
4-1 and 5-1 Electrolytes

4-1 solute	$\frac{8}{5} \beta^{(0)}$	$\frac{8}{5} \beta^{(1)}$	$\frac{16}{5} C^\phi = \frac{64}{5} C$	Max m	$\sigma$
$\text{Na}_3\text{P}_2\text{O}_7$	0.699	17.16		0.2	0.01
$\text{K}_4\text{P}_2\text{O}_7$	0.977	17.88	-0.2418	0.5	0.01
$\text{K}_4\text{Fe}(\text{CN})_6$	1.021	16.23	-0.5579	0.9	0.008
$\text{K}_4\text{Mo}(\text{CN})_8$	0.854	18.53	-0.3499	0.8	0.01
$\text{K}_4\text{W}(\text{CN})_8$	1.032	18.49	-0.4937	1	0.005
$(\text{Me}_3\text{N})_2\text{Mo}(\text{CN})_8$	0.938	15.91	-0.3330	1.4	0.01
5-1 solute	$\frac{5}{3} \beta^{(0)}$	$\frac{5}{3} \beta^{(1)}$	$\frac{5^{3/2}}{3} C^\phi = \frac{50}{3} C$		
$\text{Na}_3\text{P}_3\text{O}_{10}$	1.869	36.10	-1.630	0.4	0.01
$\text{K}_3\text{P}_3\text{O}_{10}$	1.939	39.64	-1.055	0.5	0.015

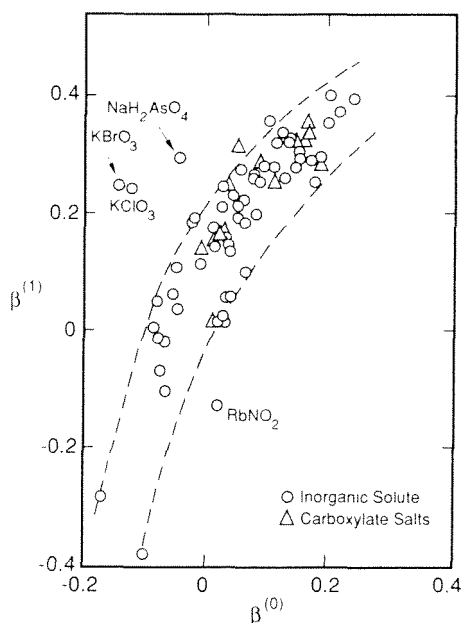


FIGURE 3. The relationship of  $\beta^{(1)}$  to  $\beta^{(0)}$  for 1-1 electrolytes. Inorganic solutes appear as circles and carboxylate salts as triangles. (Reprinted with permission from Pitzer, K. S. and Mayorga, G., *J. Phys. Chem.*, 77, 2300, 1973. Copyright by the American Chemical Society.)

important aqueous solutes extending upward in temperature, as indicated in Table 15. However, in many cases, additional work would be welcome to extend the temperature range further, to better account for the effect of pressure, and to increase accuracy.

Convenient equations and tables of parameters are given by Møller<sup>17</sup> and by Greenberg and Møller<sup>122</sup> for several solutes. Their equations are valid for temperatures up to 250°C in most cases but are limited to a single pressure (1 bar below 100°C and saturation pressure above). A review by Pitzer<sup>27</sup> assembles literature equations which include the pressure

**TABLE 11**  
**2-2 Electrolytes ( $\alpha_1 = 1.4 \text{ kg}^{1/2} \cdot \text{mol}^{-1/2}$ ,  $\alpha_2 = 12.0 \text{ kg}^{1/2} \cdot \text{mol}^{-1/2}$  throughout)**

Electrolyte	$\beta^{(0)}$	$\beta^{(1)}$	$\beta^{(2)}$	$C^\phi = 4C$	Range	$\sigma$	Ref.
MgSO <sub>4</sub>	0.2210	3.343	-37.23	0.0250	0.006—3.0	0.004	3
	0.2150	3.365	-32.74	0.0280	0.006—3.6	0.004	90
NiSO <sub>4</sub>	0.1702	2.907	-40.06	0.0366	0.005—2.5	0.005	3
MnSO <sub>4</sub>	0.213	2.938	-41.91	0.0155 <sub>1</sub>	0.1—5.0	0.005	82
FeSO <sub>4</sub>	0.2568	3.063	(-42)	0.0209	0.1—2.0	—	87
CoSO <sub>4</sub>	0.1631	3.346	-30.7	0.03704	0.2—2.4	0.001	32
CuSO <sub>4</sub>	0.2340	2.527	-48.33	0.0044	0.005—1.4	0.003	112
ZnSO <sub>4</sub>	0.1949	2.883	-32.81	0.0290	0.005—3.5	0.004	3
CdSO <sub>4</sub>	0.2053	2.617	-48.07	0.0114	0.005—3.5	0.002	3
CaSO <sub>4</sub>	0.20	3.197 <sub>3</sub>	-54.24	—	0.004—0.011	0.003	31
SrSO <sub>4</sub>	0.220	2.88	-41.8	0.019	—	—	113
BeSO <sub>4</sub>	0.317	2.914	?	0.0062	0.1—4.0	0.004	3
UO <sub>2</sub> SO <sub>4</sub>	0.322	1.827	?	-0.0176	0.1—5.0	0.003	3

**TABLE 12**  
**Temperature Derivatives of Parameters for 1-1 Electrolytes**  
**Evaluated from Calorimetric Data**

	$10^4 \beta^{(0)L}$	$10^4 \beta^{(1)L}$	$10^5 C^{\phi L} = 2 \times 10^5 C^L$	Max $m$
HCl	-3.08 <sub>1</sub>	1.41 <sub>9</sub>	-6.21 <sub>3</sub>	4.5
HBr	-2.04 <sub>9</sub>	4.46 <sub>7</sub>	-5.68 <sub>5</sub>	6.
HI	-0.23 <sub>0</sub>	8.86	-7.32	6.
HClO <sub>4</sub>	4.90 <sub>5</sub>	19.3 <sub>1</sub>	-11.7 <sub>7</sub>	6.
LiCl	-1.68 <sub>5</sub>	5.36 <sub>6</sub>	-4.52 <sub>0</sub>	6.4
LiBr	-1.81 <sub>0</sub>	6.63 <sub>6</sub>	-2.81 <sub>1</sub>	6.
LiClO <sub>4</sub>	0.38 <sub>6</sub>	7.00 <sub>9</sub>	-7.71 <sub>2</sub>	4.
NaF	5.36 <sub>1</sub>	8.70	—	0.7
NaCl	7.15 <sub>0</sub>	7.00 <sub>5</sub>	-10.5 <sub>4</sub>	6.
NaBr	7.69 <sub>2</sub>	10.7 <sub>9</sub>	-9.30	9.
NaI	8.35 <sub>5</sub>	8.28	-8.35	6.
NaOH	7.00	1.34	-18.9 <sub>4</sub>	4.2
NaClO <sub>3</sub>	10.35	19.0 <sub>7</sub>	-9.29	6.4
NaClO <sub>4</sub>	12.96	22.9 <sub>7</sub>	-16.2 <sub>3</sub>	6.
NaBrO <sub>3</sub>	5.59	34.3 <sub>7</sub>	—	0.1
NaIO <sub>3</sub>	20.6 <sub>6</sub>	60.5 <sub>7</sub>	—	0.1
NaCNS	7.80	20.0	—	0.1
NaNO <sub>3</sub>	12.66	20.6 <sub>0</sub>	-23.1 <sub>6</sub>	2.2
KF	2.14	5.44	-5.9 <sub>5</sub>	5.9
KCl	5.79 <sub>4</sub>	10.71	-5.09 <sub>5</sub>	4.5
KBr	7.39	17.4 <sub>0</sub>	-7.00 <sub>4</sub>	5.2
KI	9.91 <sub>4</sub>	11.86	-9.44	7.
KClO <sub>3</sub>	19.8 <sub>7</sub>	31.8	—	0.1
KClO <sub>4</sub>	0.6 <sub>0</sub>	100.7	—	0.1
KCNS	6.87	37.0	0.43	3.1
KNO <sub>3</sub>	2.06	64.5	39.7	2.4
KH <sub>2</sub> PO <sub>4</sub>	6.04 <sub>5</sub>	28. <sub>6</sub>	-10.1 <sub>1</sub>	1.8
RbF	-0.76	14.7	—	1.0
RbCl	5.52 <sub>2</sub>	15.0 <sub>6</sub>	—	0.8
RbBr	6.78 <sub>0</sub>	20.3 <sub>5</sub>	—	1.0
RbI	8.57 <sub>8</sub>	23.8 <sub>3</sub>	—	0.7
CsF	0.95	5.9 <sub>7</sub>	—	1.1
CsCl	8.28	15.0	-12.2 <sub>5</sub>	3.0
CsBr	7.80	28.4 <sub>4</sub>	—	1.0

TABLE 12 (continued)  
 Temperature Derivatives of Parameters for 1-1 Electrolytes  
 Evaluated from Calorimetric Data

	$10^4\beta^{(0)}$	$10^4\beta^{(1)}$	$10^5C^{(1)} = 2 \times 10^5C^1$	Max $m$
CsI	9.75	34.7 <sub>1</sub>	—	0.7
NH <sub>2</sub> Cl	0.77 <sub>4</sub>	12.5 <sub>8</sub>	2.1 <sub>0</sub>	4.
NH <sub>4</sub> H <sub>2</sub> PO <sub>4</sub>	1.51	22.8	-2.8 <sub>2</sub>	3.4
Me <sub>2</sub> NF	-0.82	16.0	-9.2 <sub>1</sub>	3.
Et <sub>2</sub> NF	-16.4	43.4	—	0.5
Pr <sub>2</sub> NF	-39.1	41.6	—	0.8
Bu <sub>2</sub> NF	-117 <sub>8</sub>	105 <sub>1</sub>	43.5	1.9
MeH <sub>3</sub> NCl	1.1 <sub>1</sub>	10.8	—	0.5
Me <sub>2</sub> H <sub>2</sub> NCl	0.2 <sub>1</sub>	18 <sub>2</sub>	—	0.5
Me <sub>3</sub> HNCI	0.2 <sub>1</sub>	35.3	—	0.5
Me <sub>2</sub> NCl	5.93	49.0	-7.66	8.1
Et <sub>2</sub> NCl	2.0 <sub>0</sub>	61.4	-13.1	5.3
Pr <sub>2</sub> NCl	-32.2	85.1	11.3	4.4
Bu <sub>2</sub> NCl	-122 <sub>8</sub>	163 <sub>6</sub>	258 <sub>5</sub>	2.5
Me <sub>2</sub> NBr	6.9 <sub>1</sub>	60.2	-6.69	5.5
Et <sub>2</sub> NBr	3.8 <sub>1</sub>	73.4	-11.3 <sub>1</sub>	4.6
Pr <sub>2</sub> NBr	-31.0	109.0	26.5	3.0
Bu <sub>2</sub> NBr	-116 <sub>2</sub>	167 <sub>2</sub>	284 <sub>1</sub>	3.0
Me <sub>3</sub> NI	-7.0 <sub>6</sub>	100 <sub>6</sub>	—	0.3
Et <sub>2</sub> NI	-1.9 <sub>1</sub>	92 <sub>0</sub>	-36 <sub>1</sub>	2.
Pr <sub>2</sub> NI	-23.4	107 <sub>0</sub>	—	0.5

dependency and are valid in some cases to 300°C. Parameters for temperatures below 25°C and as low as -60°C are given by Spencer et al.<sup>123</sup> for several common salts.

For NaCl(aq), there is an extensive array of thermodynamic data as reported by Pitzer et al.<sup>17</sup> Their evaluation of these data yields a complete set of parameters valid in the region 0 to 300°C and saturation pressure to 1 kbar. A more convenient expression based on the same data base is given by Pabalan and Pitzer<sup>23</sup> and is also included in Reference 27. Solubility data were not used in the general regression; hence a comparison of calculated solubilities with experimentally measured values is a check on a prediction. As shown in Figure 4, there is excellent agreement between calculated and experimentally determined values with a maximum deviation of 1.5% at 275°C. This general equation is also consistent with the very recent heat capacity measurements of Gates et al.;<sup>124</sup> most values agree within the uncertainty stated for the equation.

For KCl(aq), Pabalan and Pitzer<sup>24</sup> combined their heat capacity measurements with other literature data to yield a thermodynamically consistent set of parameters for KCl solutions extending to 300°C and to 500 bars.

In the case of MgCl<sub>2</sub>, there is no fully satisfactory general treatment. The ion interaction parameters of de Lima and Pitzer<sup>125</sup> were based on isopiestic measurements of Holmes et al.<sup>126</sup> at high temperature and Rard and Miller<sup>85</sup> at 25°C. Pabalan and Pitzer<sup>23</sup> (see also their chapter in this book) adjusted the trend of  $C^\phi$  at the higher temperatures to better fit the solubility of the various hydrates of MgCl<sub>2</sub> which rises to 14 mol · kg<sup>-1</sup> at 200°C. This adjustment affects the agreement with the osmotic coefficients of Holmes et al., which extend only to 3.5 mol · kg<sup>-1</sup>, but the agreement is still good with standard deviations less than 0.003. The standard-state heat capacity is taken from Phutela et al.<sup>127</sup> This investigation also reported ion interaction parameters, but their validity is limited to about 2 mol · kg<sup>-1</sup>; hence, they are not useful at higher molality or for solubility calculations. A comparison of calculated and observed solubilities is shown on Figure 5.



**TABLE 13**  
**Temperature Derivatives of Parameters Evaluated from**  
**Calorimetric Data. Results for Higher Valence Types**

Part I: 2-1 and 1-2 Electrolytes<sup>a</sup>

	$10^3\beta^{(0)L}$	$10^3\beta^{(1)L}$	$10^3C^L$	Max <i>m</i>
MgCl <sub>2</sub>	-0.19 <sub>4</sub>	2.78	-0.58	2.0
MgBr <sub>2</sub>	-0.05 <sub>6</sub>	3.8 <sub>6</sub>	—	0.1
Mg(ClO <sub>4</sub> ) <sub>2</sub>	0.52 <sub>3</sub>	4.5 <sub>0</sub>	-1.25	3.2
Mg(NO <sub>3</sub> ) <sub>2</sub>	0.51 <sub>5</sub>	4.4 <sub>9</sub>	—	0.1
CaCl <sub>2</sub> (116)	-0.56 <sub>1</sub>	2.6 <sub>6</sub>	-0.72 <sub>3</sub>	6.
CaBr <sub>2</sub>	-0.52 <sub>3</sub>	6.0 <sub>4</sub>	—	0.6
Ca(NO <sub>3</sub> ) <sub>2</sub>	0.53 <sub>0</sub>	9.1 <sub>0</sub>	—	0.1
Ca(ClO <sub>4</sub> ) <sub>2</sub>	0.83 <sub>0</sub>	5.0 <sub>8</sub>	-1.09	4.
SrCl <sub>2</sub>	0.71 <sub>7</sub>	2.8 <sub>4</sub>	—	0.1
SrBr <sub>2</sub>	-0.32 <sub>8</sub>	6.5 <sub>3</sub>	—	0.1
Sr(NO <sub>3</sub> ) <sub>2</sub>	0.17 <sub>7</sub>	12.4 <sub>7</sub>	—	0.2
Sr(ClO <sub>4</sub> ) <sub>2</sub>	1.14 <sub>3</sub>	5.3 <sub>9</sub>	-1.10	3.
BaCl <sub>2</sub>	0.64 <sub>0</sub>	3.2 <sub>3</sub>	-0.5 <sub>4</sub>	1.8
BaBr <sub>2</sub>	-0.33 <sub>8</sub>	6.7 <sub>8</sub>	—	0.1
Ba(NO <sub>3</sub> ) <sub>2</sub>	-2.91	29.1	—	0.1
Mn(ClO <sub>4</sub> ) <sub>2</sub>	0.39 <sub>7</sub>	5.0 <sub>3</sub>	-1.18	4.
Co(ClO <sub>4</sub> ) <sub>2</sub>	0.54 <sub>3</sub>	5.3 <sub>6</sub>	-1.27	4.
Ni(ClO <sub>4</sub> ) <sub>2</sub>	0.66 <sub>6</sub>	4.7 <sub>6</sub>	-1.35	4.
CuCl <sub>2</sub>	-2.7 <sub>1</sub>	8.5	—	0.6
Zn(ClO <sub>4</sub> ) <sub>2</sub>	0.59 <sub>6</sub>	5.0 <sub>9</sub>	-1.36	4.
Li <sub>2</sub> SO <sub>4</sub>	0.50 <sub>6</sub>	1.41	-0.82 <sub>5</sub>	3.0
Na <sub>2</sub> SO <sub>4</sub>	2.36 <sub>7</sub>	5.63	-1.72 <sub>5</sub>	3.0
K <sub>2</sub> SO <sub>4</sub>	1.44	6.7 <sub>0</sub>	—	0.1
Rb <sub>2</sub> SO <sub>4</sub>	0.94	8.6 <sub>4</sub>	—	0.1
Cs <sub>2</sub> SO <sub>4</sub>	-0.89 <sub>3</sub>	14.4 <sub>8</sub>	—	0.1

<sup>a</sup>  $C^{(0)L} = 2^{3/2} C^L$ .

Part II: 3-1 and 2-2 Electrolytes<sup>a</sup>

	$10^3\beta^{(0)L}$	$10^2\beta^{(1)L}$	$10\beta^{(2)L}$	$10^3C^L$	Max <i>m</i>
LaCl <sub>3</sub> <sup>b</sup>	0.25 <sub>3</sub>	0.79 <sub>8</sub>	—	-0.10 <sub>7</sub>	3.6
La(ClO <sub>4</sub> ) <sub>3</sub> <sup>b</sup>	0.15 <sub>2</sub>	1.50 <sub>3</sub>	—	-0.19 <sub>4</sub>	2.1
La(NO <sub>3</sub> ) <sub>3</sub> <sup>b</sup>	0.17 <sub>3</sub>	1.09 <sub>5</sub>	—	-0.13 <sub>0</sub>	2.2
Na <sub>3</sub> Fe(CN) <sub>5</sub>	3.05	1.52	—	—	0.1
K <sub>3</sub> Fe(CN) <sub>6</sub>	-0.87	3.15	—	—	0.1
K <sub>4</sub> Fe(CN) <sub>6</sub>	4.74	3.92	—	—	0.2
MgSO <sub>4</sub>	-0.69	1.53 <sup>c</sup>	-2.53	0.13 <sub>1</sub>	2.0
CaSO <sub>4</sub>	—	5.46 <sup>c</sup>	-5.16	—	0.02
CuSO <sub>4</sub>	-4.4	2.3 <sub>8</sub> <sup>c</sup>	-4.7 <sub>3</sub>	1.2 <sub>0</sub>	1.0
ZnSO <sub>4</sub>	-3.6 <sub>6</sub>	2.3 <sub>3</sub> <sup>c</sup>	-3.3 <sub>3</sub>	0.9 <sub>9</sub>	1.0
CdSO <sub>4</sub>	-2.7 <sub>9</sub>	1.7 <sub>1</sub> <sup>c</sup>	-5.2 <sub>2</sub>	0.6 <sub>5</sub>	1.0

<sup>a</sup> For 3-1 electrolytes  $C^{(0)L} = 2\sqrt{3}C^L$ ; for 2-2 electrolytes  $C^{(0)L} = 4C^L$ .

<sup>b</sup> Parameters for other rare earths are given in Reference 8.

<sup>c</sup> The parameter  $\alpha_1$  is 1.4 for these cases; it is 2.0 in all other cases;  $\alpha_2 = 12.0$ .

**TABLE 13 (continued)**  
**Temperature Derivatives of Parameters Evaluated from**  
**Calorimetric Data. Results for Higher Valence Types**

Part III: 3:2 and 4:2 Electrolytes<sup>a</sup>

	$\beta^{0L}$	$\beta^{1L}$	$\beta^{2L}$	Max <i>m</i>
$\text{Ca}_3(\text{Fe}(\text{CN})_6)_2$	-0.0052	0.087	-2.13 <sub>c</sub>	0.04
$\text{Ba}_3(\text{Fe}(\text{CN})_6)_2$	0.0008	0.065 <sub>b</sub>	-3.54 <sub>c</sub>	0.04
$\text{La}_3(\text{SO}_4)_3$	0.082 <sub>b</sub>	-0.202	-51.3	0.024
$\text{Mg}_3\text{Fe}(\text{CN})_6$	0.016 <sub>c</sub>	0.041 <sub>c</sub>	-23.9	0.04
$\text{Ca}_3\text{Fe}(\text{CN})_6$	0.0016	0.158 <sub>c</sub>	-7.47	0.04
$\text{Sr}_3\text{Fe}(\text{CN})_6$	0.0052	0.118 <sub>c</sub>	-19.5	0.04

<sup>a</sup>  $\alpha_1 = 2.0$ ;  $\alpha_2 = 50$  throughout.

**TABLE 14**  
**Volumetric Properties and the Pressure Derivatives of Parameters for the**  
**Major Sea Salts at 25°C**

Salt	NaCl <sup>a</sup>	NaCl <sup>b</sup>	Na <sub>2</sub> SO <sub>4</sub> <sup>b</sup>	MgCl <sub>2</sub> <sup>b</sup>	MgSO <sub>4</sub> <sup>b</sup>
$\bar{V}_m^0/\text{cm}^3\text{mol}^{-1}$	16.68	16.68	11.48	14.40	-7.48
$10^5 \beta^{0N}/\text{kg}\cdot\text{mol}^{-1}\cdot\text{bar}^{-1}$	1.234	1.255	4.466	1.843	5.137
$10^4 \beta^{1N}/\text{kg}\cdot\text{mol}^{-1}\cdot\text{bar}^{-1}$	—	—	1.802	-0.846	1.319
$10^3 \beta^{2N}/\text{kg}\cdot\text{mol}^{-1}\cdot\text{bar}^{-1}$	—	—	—	—	1.49 <sub>c</sub>
$10^2 C^{0N}/\text{kg}^2\cdot\text{mol}^{-2}\cdot\text{bar}^{-1}$	-1.29	-1.376	-3.71 <sub>d</sub>	-1.948	—

<sup>a</sup> Reference 14.<sup>b</sup> Reference 117.<sup>c</sup>  $C^{0N} = 2C^{1N}$ .

Pabalan and Pitzer<sup>25</sup> extended to 300°C the heat capacity measurements on Na<sub>2</sub>SO<sub>4</sub>(aq) and combined these with other heat capacities<sup>12</sup> and various other data<sup>128</sup> to develop a comprehensive treatment for the range to 300°C and to 200 bars. Holmes and Mesmer<sup>128</sup> made isopiestic measurements to 225°C and treated these and other available data for several alkali metal sulfates.

In the case of MgSO<sub>4</sub>(aq) solutions, a comprehensive regression of heat capacity, enthalpy, and osmotic coefficient data by Phutela and Pitzer<sup>21</sup> yielded parameters that are valid from 25 to 200°C. Figure 6 shows that calculated solubilities are in very good agreement with experimental data to 200°C.

Holmes et al.<sup>68</sup> presented a comprehensive treatment for HCl(aq). They gave three sets of parameters for the present model. The first set, valid to 523 K and 7 mol · kg<sup>-1</sup>, involves only the usual terms for a 1-1 electrolyte. A second treatment adds a fourth virial coefficient and is valid to 16 mol · kg<sup>-1</sup>. For temperatures from 523 to 648 K and from 0 to 7 mol · kg<sup>-1</sup>, they include a  $\beta^{(2)}$  term.

For NaOH(aq), an early treatment of Pabalan and Pitzer<sup>22</sup> extending to 350°C has been superseded for the range below 250°C by a study by Simonson et al.<sup>129</sup> which incorporates very recent measurements of heat capacities and heats of dilution.

For LiCl and CsCl, equations are given by Holmes and Mesmer,<sup>130</sup> for NH<sub>4</sub>Cl by Thiessen and Simonson,<sup>131</sup> while data for CsCl and several other 1-1 electrolytes are given by Saluja

**TABLE 15**  
**Pure Electrolyte Solutions with**  
**Available High Temperature Data**

	Range of T and P		Ref.
	T/°C	P/kbar	
<b>1:1 Electrolytes</b>			
HCl	0—375	0—0.4	68
LiCl	0—250	<sup>a</sup>	130
NaCl	0—300	0—1.0	17
NaI	25—100	0—0.1	132
NaOH	0—350	0—0.4	22, 129
KCl	0—325	0—0.5	24
CsF	25—100	0—0.1	132
CsCl	0—250	0—0.1	130, 132
CsI	25—100	0—0.1	132
NH <sub>4</sub> Cl	25—250	0—0.35	131
<b>1:2 or 2:1 Electrolytes</b>			
Li <sub>2</sub> SO <sub>4</sub>	0—225	<sup>a</sup>	128
Na <sub>2</sub> SO <sub>4</sub>	0—300	0—0.2	25
K <sub>2</sub> SO <sub>4</sub>	0—225	<sup>a</sup>	128
Cs <sub>2</sub> SO <sub>4</sub>	0—225	<sup>a</sup>	128
MgCl <sub>2</sub>	25—200	0—0.1	<sup>b</sup>
CaCl <sub>2</sub>	25—250	0—0.1	47, 64
SrCl <sub>2</sub>	25—200	0—0.1	127
<b>2:2 Electrolytes</b>			
MgSO <sub>4</sub>	25—200	0—0.1	21
CaSO <sub>4</sub>	25—250	<sup>a</sup>	47

<sup>a</sup> 1 bar below 100°C and P<sub>sat</sub> above.

<sup>b</sup> See text.

et al.<sup>132</sup> Values for SrCl<sub>2</sub> are given by Phutela et al.<sup>127</sup> Very recently, Møller<sup>47</sup> treated CaCl<sub>2</sub>(aq) and CaSO<sub>4</sub>(aq) and gave equations for the range 25 to 250°C along the nonisobaric path 1 atm to 100°C and saturated water pressure from 100 to 250°C. The nonisobaric aspect is not serious for activity coefficients but should be considered if temperature derivatives are taken. The situation for CaSO<sub>4</sub> is complex, and her equations are based almost entirely on solubility data; hence, Møller's paper<sup>47</sup> should be consulted for the full account. For CaCl<sub>2</sub>(aq), Møller's equation is valid to about 4.5 mol · kg<sup>-1</sup>. Ananthaswamy and Atkinson<sup>64</sup> also treated CaCl<sub>2</sub>(aq) to 100°C but to higher molality, and their equation, which involves six virial coefficients, should be used where appropriate.

#### D. PARAMETERS FOR MIXTURES AT 25°C

In the analysis of experimental data for mixed electrolytes with the use of the equations presented above, we seek two principal results. First, we want to learn how accurate our prediction would be on the basis of parameters from pure electrolytes only. Second, we wish to obtain values for the difference parameters  $\Phi$  (or  $\theta$ ) and  $\psi$ , if they are of significant magnitude, or to determine that they are negligible and can be taken to be zero. It should be remembered that the principal effects on mixing electrolytes arise from differences in the pure electrolyte parameters  $\beta^{(0)}$ ,  $\beta^{(1)}$ , and  $C^\phi$  and that the parameters  $\Phi$  and  $\psi$  have only a small effect, if any.

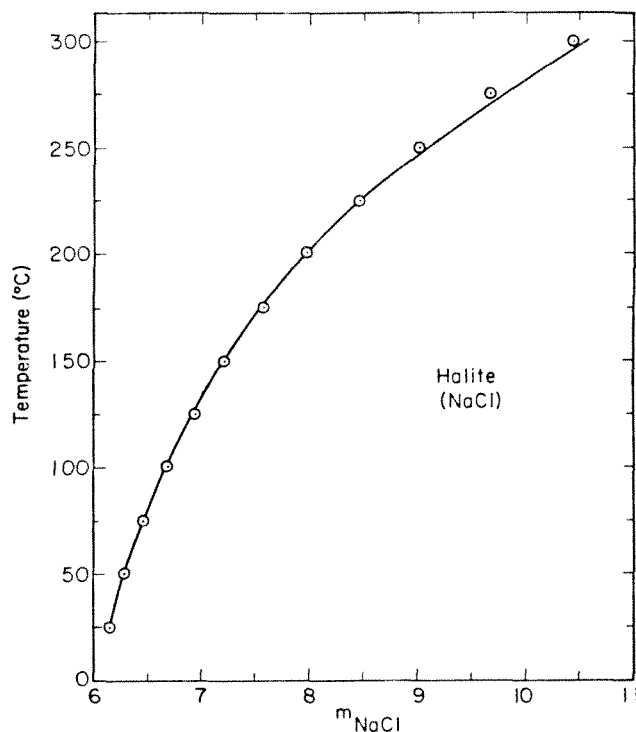


FIGURE 4. Calculated NaCl (halite) solubilities compared to experimental values; details are given by Pabalan and Pitzer.<sup>21</sup> (Reprinted with permission from Pabalan, R. T. and Pitzer, K. S., *Geochim. Cosmochim. Acta*, 51, 2429, 1987, Pergamon Press plc.)

In principle, the  $\Phi_{ij}$  depend on the ionic strength since they constitute differences between  $\lambda_{ij}$ 's which are functions of  $I$  (Equation 60). Also, Friedman<sup>49</sup> has derived, from cluster theory, separate limiting laws for symmetrical and for unsymmetrical mixing. Each is valid in the limit  $m \rightarrow 0$ , and its parameter is related to the Debye-Hückel parameter. For the unsymmetrical case, this ionic-strength dependence can be substantial, especially for 3-1 or 4-1 mixing. Usually, it should be included by methods described below and in Appendix B. For symmetrical mixing, the effect is much smaller and can be ignored in practical calculations at the present level of precision. Thus, the main treatment for symmetrical mixing is given below on the basis that each  $\Phi_{ij}$  at a given  $T$  is a constant which will be written as  $\theta_{ij}$  following Equation 72. Also,  $\Phi'_{ij}$  is zero in this case. It is possible, however, to treat symmetrical mixing in a manner fully consistent with Friedman's limiting law, and this is described in Appendix C.

The results are summarized in Table 16 for symmetrical binary mixtures with a common ion. The sources are cited in References 4, 78, and 133. The values of  $\theta$  and  $\psi$  were obtained by calculating the difference between the experimental value of  $\phi$  or  $\ln \gamma$  and the value calculated with the appropriate values for all pure-electrolyte terms, but with zero values for  $\theta$  and  $\psi$  in Equation 62 or 68. This difference, when multiplied by a function of composition, is found to be equal to  $\theta$  plus  $\psi$  times another function of composition. For the osmotic coefficient of a MX-NX mixture, one obtains

$$\Delta\phi[\sum m_i/2m_M m_N] = \theta_{MN} + m_X \psi_{MNX} \quad (100)$$

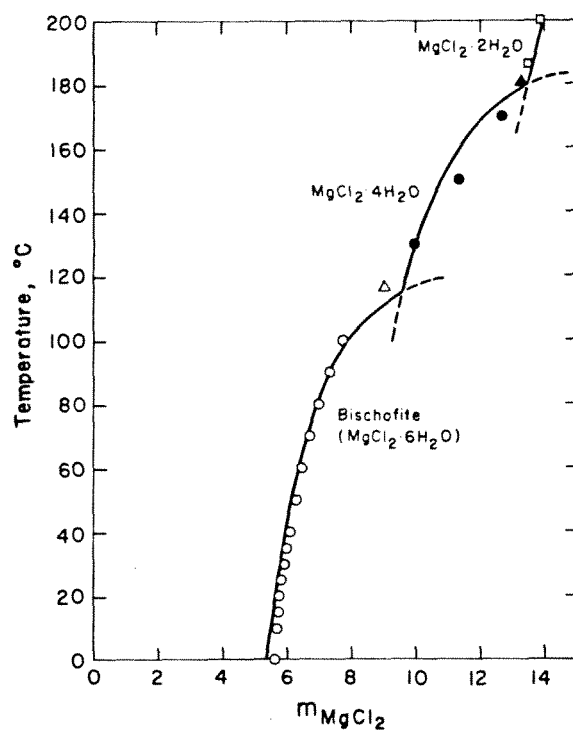


FIGURE 5. Calculated solubilities of  $\text{MgCl}_2$  compared to experiment; details are given by Pabalan and Pitzer.<sup>23</sup> (Reprinted with permission from Pabalan, R. T. and Pitzer, K. S., *Geochim. Cosmochim. Acta*, 51, 2429, 1987, Pergamon Press plc.)

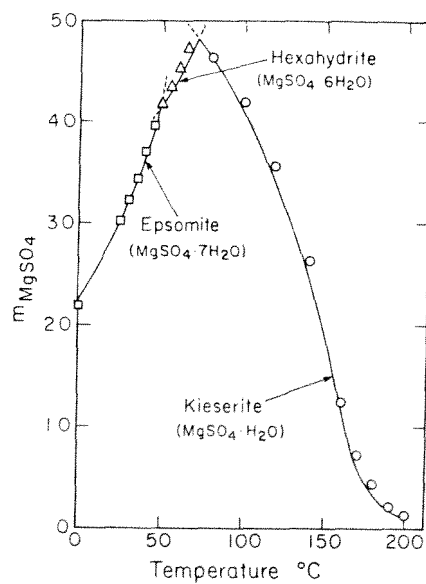


FIGURE 6. Calculated solubilities in the system  $\text{MgSO}_4\text{-H}_2\text{O}$  compared to experiment; details are given by Pabalan and Pitzer.<sup>23</sup> (Reprinted with permission from Pabalan, R. T. and Pitzer, K. S., *Geochim. Cosmochim. Acta*, 51, 2429, 1987, Pergamon Press plc.)

**TABLE 16**  
**Binary Symmetrical Mixtures with a Common Ion at 25°C**

System	Experimental	Max I	$\theta = \frac{\sigma}{z} = 0$	$\theta$	$\psi$	$\sigma$ with $\theta$ and $\psi$
HCl-LiCl	$\ln \gamma$	5	0.023	0.015	0.000	0.007
HBr-LiBr	$\ln \gamma$	2.5	0.027	0.015	0.000	0.011
HClO <sub>4</sub> -LiClO <sub>4</sub>	$\phi$	4.5	0.006	0.015	-0.001 <sub>2</sub>	0.001
HCl-NaCl	$\ln \gamma$	3	0.040	0.036	-0.004	0.002
HBr-NaBr	$\ln \gamma$	3	0.028	0.036	-0.012	0.002
HClO <sub>4</sub> -NaClO <sub>4</sub>	$\phi$	5	0.025	0.036	-0.016	0.002
HCl-KCl	$\ln \gamma$	3.5	0.014	0.005	-0.007	0.010
HBr-KBr	$\ln \gamma$	3	0.030	0.005	-0.021	0.008
HCl-CsCl	$\ln \gamma$	3	0.082	-0.044	-0.019	0.005
HCl-NH <sub>4</sub> Cl	$\ln \gamma$	2		-0.019	0.000	
HBr-NH <sub>4</sub> Br	$\ln \gamma$	3.0		-0.019	0.000	
HCl-Me <sub>4</sub> NCl	$\ln \gamma$	0.1	0.003	-0.0		0.003
HCl-Et <sub>4</sub> NCl	$\ln \gamma$	0.1	0.003	-0.0		0.003
HBr-Pr <sub>4</sub> NBr	$\ln \gamma$	2.0		-0.17	-0.15	
HBr-Bu <sub>4</sub> NBr	$\ln \gamma$	1.0		-0.22		
LiCl-NaCl	$\phi$	6	0.002	0.012	-0.003	0.001
LiNO <sub>3</sub> -NaNO <sub>3</sub>	$\phi$	6	0.014	0.012	-0.007 <sub>2</sub>	0.002
LiClO <sub>4</sub> -NaClO <sub>4</sub>	$\phi$	2.6	0.003	0.012	-0.008 <sub>3</sub>	0.001
LiOAc-NaOAc	$\phi$	3.5	0.004	0.012	-0.004 <sub>3</sub>	0.002
LiCl-KCl	$\phi$	4.8	0.045	-0.022	-0.010	0.003
LiCl-CsCl	$\phi$	5	0.100	-0.095	0.009 <sub>3</sub>	0.004
NaCl-KCl	$\phi$	4.8	0.014	-0.012	-0.001 <sub>8</sub>	0.001
NaBr-KBr	$\phi$	4	0.009	-0.012	-0.002 <sub>2</sub>	0.003
NaNO <sub>3</sub> -KNO <sub>3</sub>	$\phi$	3.3	0.008	-0.012	-0.001 <sub>2</sub>	0.001
Na <sub>2</sub> SO <sub>4</sub> -K <sub>2</sub> SO <sub>4</sub>	$\phi$	3.6	0.011	-0.012	-0.010	0.004
NaCl-CsCl	$\phi$	7	0.03	-0.0388 <sub>6</sub>	-0.0013 <sub>5</sub>	0.001
KCl-CsCl	$\phi$	5	0.003	0.000	-0.001 <sub>3</sub>	0.001
NaCl-NaF	$\ln \gamma$	1	0.00			
NaCl-NaBr	$\phi$	4.4	0.001	0.000	0.000	0.001
KCl-KBr	$\phi$	4.4	0.002	0.000	0.000	0.002
NaCl-NaOH	$\ln(\gamma/\gamma')$	3	0.155	-0.050	-0.006	0.002
KCl-KOH	$\ln(\gamma/\gamma')$	3.5	0.196	-0.050	-0.008	0.008
NaBr-NaOH	$\ln(\gamma/\gamma')$	3	0.225	-0.065	-0.018	0.009
KBr-KOH	$\ln(\gamma/\gamma')$	3	0.212	-0.065	-0.014	0.012
LiCl-LiNO <sub>3</sub>	$\phi$	6	0.008	0.016	-0.003	0.004
NaCl-NaNO <sub>3</sub>	$\phi$	5	0.007	0.016	-0.006	0.001
KCl-KNO <sub>3</sub>	$\phi$	4	0.003	0.016	-0.006	0.001
MgCl <sub>2</sub> -Mg(NO <sub>3</sub> ) <sub>2</sub>	$\phi$	4	0.008	0.016	0.000	0.002
CaCl <sub>2</sub> -Ca(NO <sub>3</sub> ) <sub>2</sub>	$\phi$	6	0.014	0.016	-0.017	0.003
NaCl-NaH <sub>2</sub> PO <sub>4</sub>	$\phi$	1		0.10	0.00	
KCl-KH <sub>2</sub> PO <sub>4</sub>	$\phi$	1		0.10	-0.1	

or the equivalent for mixing anions. For the activity coefficient of MX in this mixture one has

$$(\Delta \ln \gamma_{MX}) [\nu/2\nu_M m_N] = \theta_{MN} + \frac{1}{2}(m_X + m_M |z_M/z_X|) \psi_{MNX} \quad (101)$$

with equivalent expressions for other cases.

The quantity on the left was plotted against the coefficient of  $\psi$  on the right. One should obtain a linear plot with intercept  $\theta$  and slope  $\psi$ . This presentation of the results, to which estimated errors could be attached, allowed one to judge whether values of  $\theta$  or  $\psi$  were significantly different from zero and whether the data were consistent with these equations within reasonable limits of error.

Table 16 gives, in the fourth column, the root mean square average of  $\Delta\phi$  or  $\Delta \ln \gamma$  when  $\theta$  and  $\psi$  are taken as zero. Then the selected values of  $\theta$  and  $\psi$  are given for the mixing indicated and finally the standard deviation when these values of  $\theta$  and  $\psi$  are included. Thus

**TABLE 17**  
**Binary Mixtures without Common Ion at 25°C**

System	Experimental	Max I	$\sigma$	$\sigma$ with $\theta$ and $\psi$
			$\theta = \psi = 0$	$\psi$
NaCl-KBr	$\phi$	4	0.012	0.002
KCl-NaBr	$\phi$	4	0.012	0.001
NaCl-KNO <sub>3</sub>	$\phi$	4	0.007	0.001
NaNO <sub>3</sub> -KCl	$\phi$	4	0.007	0.002

for the first entry, the system HCl-LiCl relates to  $\theta_{H,Li}$  and  $\psi_{H,Li,Cl}$ ; the quantity measured is  $\ln \gamma_{HCl}$ ; the data range is up to  $I = 5$ ; and the root mean square  $\Delta \ln \gamma$  is 0.023 with  $\theta = \psi = 0$ . The value  $\theta_{H,Li} = 0.015$  is selected from consideration of the first three systems, all of which involve mixing of  $H^+$  with  $Li^+$ . For the chloride,  $\psi$  was found to be zero and with these  $\theta$  and  $\psi$  values the standard deviation is reduced to 0.007.

The values of  $\sigma$  with  $\theta = \psi = 0$  give an estimate of the accuracy to be obtained without difference parameters. However, these deviations are usually proportional to molality. Hence, a better estimate is obtained by noting the effect of  $\theta_{cc}$  or  $\theta_{aa}$  in Equation 62 or 68. Thus, in the former one finds the result  $(m_c m_c / \sum m_i) \cdot \theta_{cc}$ ; and, if one has an equimolar mixture of  $HClO_4$  and  $LiClO_4$ , for example,  $(m_c m_c / \sum m_i)$  is  $m/8$  where  $m$  is the total molality of  $ClO_4^-$ . With  $\theta_{H,Li} = 0.015$  one calculates the effect on the osmotic coefficient to be 0.0019  $m$ . This is negligible for most purposes unless  $m$  is large (considerably above 1  $M$ ). The example chosen has a typical  $\theta$ ; in some cases the effect of  $\theta$  and  $\psi$  is even smaller, while in a few cases it is somewhat larger.

In a few cases data are available only for rather dilute solutions, and these results can be fitted quite well without the difference terms involving  $\theta$  and  $\psi$ . In these cases we report 0.0 for  $\theta$  in Table 16 to indicate that the correct value of  $\theta$  must be small but is not determined accurately.

Table 17 contains some results for binary mixtures of the 1-1 type without a common ion. In this case we show only the standard deviation without the difference terms  $\theta$  and  $\psi$  and that with these terms. It is apparent that in most of these examples, quite good results are obtained with only the pure electrolyte terms and in all cases there is good agreement when the  $\theta$  and  $\psi$  values are included. The values of  $\theta$  and  $\psi$  were determined from the mixtures with common ion; hence, there were no adjustable parameters in this treatment of the mixtures without common ion.

In Tables 16 and 17, the maximum  $I$  is usually that of the most concentrated mixed electrolyte measured, but in a few cases the limit of validity of the equations for pure electrolytes determined the maximum  $I$  for valid comparison. In cases involving  $K_2SO_4$ , where solubility limits pure electrolyte data to  $I = 2.1 M$ , good fits were obtained for mixtures to considerably higher concentration, as shown in the tables. This suggests that the equation for pure  $K_2SO_4$  is valid somewhat above  $I = 2.1 M$ .

For unsymmetrical mixtures, one has to consider the additional electrostatic terms  ${}^E\theta_{ij}$  and  ${}^E\theta'_{ij}$ , which are derived from theory (see Equations 72 to 74). It was originally thought<sup>5,133</sup> that these terms were important only for 3-1 mixing and that they could be neglected for 2-1 mixing provided the  $\theta$  values were calculated without the  ${}^E\theta$  terms. It was shown by Harvie and Weare,<sup>28</sup> however, that these terms are important for the activity coefficient of  $CaSO_4$  in mixtures with NaCl. For best results with accurate data, the  ${}^E\theta_{ij}$  and  ${}^E\theta'_{ij}$  terms should be included. All parameters reported in Table 18 are calculated with  ${}^E\theta_{ij}$ ,  ${}^E\theta'_{ij}$  included where applicable. Now one must add additional terms to Equations 100 and 101, but this is straightforward with modern computers. Appendix B describes the derivation of  ${}^E\theta$  and  ${}^E\theta'$  as well as methods of numerical calculation of their values.

In addition to single-phase data on mixed electrolytes, solubility-equilibrium data on

**TABLE 18**  
**Mixing Parameters for 25°C (with  $\theta$  and  $\theta'$  Included for Unsymmetrical Mixing)**

c	c'	$\theta_{cc'}$	$\psi_{cc'Cl}$	$\psi_{cc'SO_4}$	$\psi_{cc'HSO_4}$	$\psi_{cc'SO_3}$	$\psi_{cc'HCO_3}$	$\psi_{cc'CO_3}$
Li	Na	0.0029	—	-0.0039	—	—	—	—
	K	-0.0563	—	-0.0086	—	—	—	—
	Rb	-0.0908	—	0.0024	—	—	—	—
	Cs	-0.1242	—	0.0088	—	—	—	—
Na	K	-0.012	-0.0018	-0.010	—	—	-0.003	0.003
	Rb	-0.0319	—	0.0048	—	—	—	—
	Cs	-0.0153	—	-0.0035	—	—	—	—
	NH <sub>4</sub>	0	-0.0003	-0.0013	—	—	—	—
	Ca	0.07	-0.007	-0.055	—	—	—	—
	Mg	0.07	-0.012	-0.015	—	—	—	—
	MgOH	0	—	—	—	—	—	—
	H	0.036	-0.004	—	-0.0129	—	—	—
	K	Cs	-0.0049	—	-0.0016	—	—	—
K	Ca	0.032	-0.025	—	—	—	—	—
	Mg	0.0	-0.022	-0.048	—	—	—	—
	MgOH	0	—	—	—	—	—	—
	H	0.005	-0.011	—	-0.0265	—	—	—
	Mg	MgOH	0.0	0.028	—	—	—	—
Mg	Cu	0.0085	—	—	—	-0.0031	—	—
	H	0.10	-0.011	—	-0.0178	—	—	—
	Ca	Mg	0.007	-0.012	0.024	—	—	—
Ca	MgOH	0	—	—	—	—	—	—
	Cu	-0.0558	—	—	—	0.0026	—	—
	H	0.092	-0.015	—	—	—	—	—
	Sr	H	0.0642	0.0033	—	—	—	—
Ba	H	0.0708	0.0018	—	—	—	—	
Ni	Cu	0.0131	—	—	—	-0.0031	—	—
	H	0.0690	0.0056	—	—	—	—	—
a	a'	$\theta_{aa'}$	$\psi_{aa'Na}$	$\psi_{aa'K}$	$\psi_{aa'Ca}$	$\psi_{aa'Mg}$	$\psi_{aa'MgOH}$	$\psi_{aa'H}$
Cl	SO <sub>4</sub>	0.030	0.000	-0.005	-0.002	-0.008	—	—
	HSO <sub>4</sub>	-0.006	-0.006	—	—	—	—	0.013
	OH	-0.050	-0.006	-0.006	-0.025	—	—	—
	HCO <sub>3</sub>	0.03	-0.015	—	—	-0.096	—	—
	CO <sub>3</sub>	-0.02	0.0085	0.004	—	—	—	—
SO <sub>4</sub>	HSO <sub>4</sub>	—	-0.0094	-0.0677	—	-0.0425	—	—
	OH	-0.013	-0.009	-0.050	—	—	—	—
	HCO <sub>3</sub>	0.01	-0.005	—	—	-0.161	—	—
	CO <sub>3</sub>	0.02	-0.005	-0.009	—	—	—	—
OH	CO <sub>3</sub>	0.10	-0.017	-0.01	—	—	—	—
HCO <sub>3</sub>	CO <sub>3</sub>	-0.04	0.002	0.012	—	—	—	—

mixtures are particularly sensitive to the values of  $\psi_{ijk}$ . Harvie and Weare<sup>28</sup> and Harvie et al.<sup>31</sup> have considered many such cases, as have Filippov and associates;<sup>32,40,134,139</sup> their values are shown in Table 18 along with values from single-phase data. Values from Roy et al.<sup>140,143</sup> from electrochemical cell measurements are also included in Table 18. In a few cases, values in Table 18 differ from those in Table 16. The differences are not large, but values of both  $\theta$  and  $\psi$  should be taken from the same table.

Kim and Frederick<sup>78</sup> give  $\theta$  and  $\psi$  values for additional interactions. Other values are given in References 5, 27, and 144 to 147. Several values of ion-neutral mixing parameters for CO<sub>2</sub>(aq) are given in Table 19; parameters for NH<sub>3</sub>(aq) are given by Clegg and Brimblecombe,<sup>148</sup> while Reference 27 gives information involving silica. Some of these and other parameters are given in Chapters 6 and 7.



**TABLE 19**  
**Ion-Neutral Parameter**  
**Values for 25°C**

i	$\lambda_{\text{CO}_2, i}$
H	0.0
Na	0.100
K	0.051
Ca	0.183
Mg	0.183
MgOH	—
Cl	0.005
SO <sub>4</sub>	0.097
HSO <sub>4</sub>	-0.003

**TABLE 20**  
**Mixing Parameters for 25°C for Use without  ${}^{\text{H}}\theta$  and  ${}^{\text{H}}\theta'$**

c	c'	$\theta_{cc}$	$\psi_{cc\text{Cl}}$	$\psi_{cc\text{SO}_4}$	c	c'	$\theta_{cc}$	$\psi_{cc\text{Cl}}$	$\psi_{cc\text{SO}_4}$
H	Sr	-0.037 <sub>n</sub>	0.020 <sub>n</sub>	—	Na	Mn	0.0432	-0.0136	-0.0216
	Ba	-0.036	0.024	—	Na	Co	-0.0194	-0.0085	-0.0174
	Mn	0	0	—	Na	Ni	0.0591 <sub>n</sub>	0.0115 <sub>n</sub>	—
Li	Mg	0	—	0	Na	Cu	0.000	-0.014	-0.011
	Mn	0	—	0	Na	Zn	0.0507	—	-0.0389
	Co	0	—	0	Na	Cd	-0.0003	—	-0.0152
	Ni	0	—	0	K	Mg	-0.0828	-0.0139	-0.0235
	Cu	0	—	0	K	Ca	-0.040	-0.015	—
	Zn	0	—	0	K	Ba	-0.072	0.000	—
	Ba	-0.070	0.019	—	Cs	Ba	-0.150	0.000	—
Na	Mg	0	0	0	NH <sub>4</sub>	Mg	-0.0275	—	0.0334
	Ba	-0.003	0	—					
	a	a'	$\theta_{aa}$	$\psi_{aa\text{SO}_4}$	$\psi_{\text{NaCl}}$	$\psi_{\text{NaSO}_4}$	$\psi_{\text{ClSO}_4}$		
	Cl	SO <sub>4</sub>	-0.020	0.004	-0.007	-0.007	0.043		

In many cases of 2-1 mixing, where there are data only for rather concentrated solutions, the inclusion of the  ${}^{\text{H}}\theta$  and  ${}^{\text{H}}\theta'$  terms has little effect and no advantage. Indeed, it is often impractical to evaluate both  $\theta$  and  $\psi$ , and one assumes one or the other to be zero. Filippov and associates<sup>12, 19, 149, 153</sup> report several situations of this type. In some cases, solid solubilities are the only data available for the mixed systems, and one obtains satisfactory results on the basis  $\theta = 0$  and  $\psi$  zero or nonzero, as indicated. In these cases, the insertion of an  ${}^{\text{H}}\theta$  term serves no useful purpose and it has been omitted. Table 20 presents mixing parameters for use without the  ${}^{\text{H}}\theta$  and  ${}^{\text{H}}\theta'$  terms.

Sulfuric acid is both interesting and important. The species HSO<sub>4</sub><sup>-</sup> must be recognized whereupon the solution becomes a mixed electrolyte with anions HSO<sub>4</sub><sup>-</sup> and SO<sub>4</sub><sup>2-</sup>. A comprehensive treatment was first given<sup>7</sup> without  ${}^{\text{H}}\theta$  and  ${}^{\text{H}}\theta'$ . The problem of redundancy of parameters was carefully considered; only  $\beta_{\text{H}, \text{SO}_4}^{\text{H}} = 0.0027$  and  $C_{\text{H}, \text{SO}_4}^{\text{H}} = 0.0416$  were needed in addition to the H, HSO<sub>4</sub> parameters in Table 2. Subsequently, slightly different parameters were obtained when  ${}^{\text{H}}\theta$  and  ${}^{\text{H}}\theta'$  were included by Harvie et al.<sup>31</sup> for 25°C and by Reardon and Beckie<sup>87</sup> for the range 0 to 70°C. It is important that the ion interaction parameters be consistent with the dissociation constant for HSO<sub>4</sub><sup>-</sup>. Thus, it is probably best to use the full set of parameters from either Reference 7, 31 or 87. Interesting applications

to multicomponent electrolyte systems including  $\text{H}_2\text{SO}_4$  were made by Reardon and Beckie<sup>87</sup> for  $\text{FeSO}_4\text{-H}_2\text{SO}_4\text{-H}_2\text{O}$  and by Reardon<sup>154</sup> for  $\text{NiSO}_4\text{-H}_2\text{SO}_4\text{-H}_2\text{O}$ .

Volume changes on mixing are related to the pressure derivatives of  $\theta_{ij}$  and  $\psi_{ijk}$  ( $\theta^v = \partial\theta/\partial P$ ). For mixing of the major sea salts ( $\text{NaCl}$ ,  $\text{MgCl}_2$ ,  $\text{Na}_2\text{SO}_4$ ,  $\text{MgSO}_4$ ), measurements were made and equations fitted by Millero et al.<sup>155</sup> and Connaughton et al.<sup>156,157</sup> Oakes et al.<sup>158</sup> report data for the system  $\text{NaCl-CaCl}_2\text{-H}_2\text{O}$  at 25 and 35°C. Monnin<sup>119a,119b</sup> considered many mixed systems and concluded that the effects of  $\theta^v$  and  $\psi^v$  were within the range of experimental uncertainty in most cases. Consequently, he omitted these terms in his calculations for various brines.

Both  $\theta_{ij}$  and  $\psi_{ijk}$  undoubtedly vary with temperature, and there are heat of mixing data which give their temperature derivatives at 25°C.<sup>15,20</sup> Until heat of mixing measurements become generally available at higher temperature, however, we must depend on isopiestic and solubility data for the values of  $\theta_{ij}$  and  $\psi_{ijk}$  at high temperatures. Chapter 7 of this book concerns solubility calculations with these equations, and mixing parameters at high temperatures will be considered there.

In the sections on evaluation of parameters, an extensive array of results are presented of various types, but many other results have been published (see Chapter 6 of this book). It is beyond the scope of this chapter to present a complete bibliography. An extensive bibliography has been presented by Plummer et al.<sup>159</sup> in a report on the computer program PHRQPITZ.

Finally, we note that for very concentrated solutions, molality is no longer an appropriate measure of composition and that it is best to use mole fraction instead. Appendix I presents equations on the mole fraction basis and examples of their use are given in Chapters 6 and 7.

## ACKNOWLEDGMENT

A considerable amount of the research that forms the basis of this chapter received support from the Atomic Energy Commission or the Energy Research and Development Administration or the Department of Energy. Many of these tables and figures were first published in the *Journal of Physical Chemistry*, the *Journal of the American Chemical Society*, the *Journal of Solution Chemistry*, or *Geochimica et Cosmochimica Acta*, and I thank their publishers for permission to use this material here.

## APPENDIX A: ADDITIONAL THEORY RELATED TO THE GENERAL EQUATION

Included here is material related to the shift in the Debye-Hückel term from the limiting law to an extended form and to the ionic strength dependence of the second virial coefficients  $\lambda_{ij}$  and  $B_{ij}$ . After the shift from the Helmholtz energy to the Gibbs energy and to molality instead of concentration, one has

$$G^\circ/n_w RT = -\alpha I^{1/2} + \sum_i \sum_j m_i m_j \beta_{ij}(I) + \dots \quad (\text{A-1})$$

where  $n_w$  is the number of kilograms of water and  $\alpha$  is the Debye-Hückel parameter. One now finds that the ionic strength dependency of  $\beta_{ij}$  is very great, but that it can be reduced by replacing the Debye-Hückel limiting law by an extended term. This was first suggested on an empirical basis by Guggenheim.<sup>160</sup> A test<sup>1</sup> of several extended forms for the Debye-Hückel term led to the choice  $(\alpha/b)\ln(1 + bI^{1/2})$  with  $b$  an empirical constant. This can be expanded and rearranged

$$\begin{aligned}
\alpha \ln(1 + bI^{1/2})/b &= \alpha(I^{3/2} - bI^2/2 + b^2I^{5/2}/3 \dots) \\
&= \alpha I^{3/2} - I^2 \alpha q(I) \\
&= \alpha I^{3/2} - \sum_i \sum_j m_i m_j z_i^2 z_j^2 q(I) (\alpha/4)
\end{aligned} \tag{A-2}$$

where  $q(I)$  is a function of ionic strength but not of individual molalities. Thus, in addition to the limiting law term  $\alpha I^{3/2}$ , the remaining contribution of the extended D-H term has exactly the same molality dependence as the second virial coefficient term of Equation A-1, and these can be combined. The particular form for the extended D-H term was chosen to minimize the ionic strength dependence of the resulting second virial coefficient term

$$\lambda_{ij}(I) = \beta_{ij}(I) + z_i^2 z_j^2 q(I) (\alpha/4) \tag{A-3}$$

In order to obtain more physical insight into this ionic strength dependence, it is useful to consider another basic formulation which involves the radial distribution function. The basic equation is

$$\begin{aligned}
\phi - 1 &= (\Pi/c_k T) - 1 \\
&= -(6ckT)^{-1} \sum_i \sum_j c_i c_j \int_0^\infty (\partial u_{ij}/\partial r) g_{ij} 4\pi r^3 dr
\end{aligned} \tag{A-4}$$

where  $u_{ij}$  is the potential of mean force,  $g_{ij}$  is the radial distribution function,  $c_i$  is the concentration of the  $i$ -th solute species, and  $c$  is the total concentration of all solute species.

Given the osmotic coefficient, one can derive the activity coefficient and other functions by thermodynamic methods.

If one adopts the hard-core or primitive model, the potential of mean force is

$$u_{ij} = \infty, r < a \tag{A-5a}$$

$$= z_i z_j e^2 / \epsilon r, r \geq a \tag{A-5b}$$

where  $\epsilon$  is the dielectric constant of the solvent. Now there is a mathematical anomaly at  $r = a$  where  $\partial u/\partial r$  is infinite but  $g(r)$  is zero. This can be resolved and one obtains, for a single symmetrical electrolyte,

$$\begin{aligned}
\phi - 1 &= (e^2/24\epsilon kT)(cz^2) \int_a^\infty [g_{++}(r) - g_{+-}(r)] 4\pi r dr \\
&\quad + c(\pi a^3/6)[g_{++}(a) + g_{+-}(a)]
\end{aligned} \tag{A-6}$$

Here  $g_{++} = g_{--}$  is the radial distribution function for like-charged ions; also  $g_{ij}(a)$  is the value for  $r = a + \delta$ , i.e., the limiting value of  $g_{ij}(r)$  as  $r-a$  approaches zero from the positive side.

The radial distribution functions can be calculated by any one of several methods. A method which is exact in principle, though numerically approximate in execution, is the Monte Carlo method as applied by Card and Valleau.<sup>50</sup> Other results are compared with those from the Monte Carlo method by Rasaiah et al.<sup>51</sup>

The first term on the right in Equation A-6 includes the coulombic forces and yields results for the osmotic coefficient similar to those of Debye and Hückel or to the first term in Equation 36. The second term is very sensitive to short-range forces, since it is proportional to  $a^3$ , and it would be strictly proportional to the concentration if the final factor in brackets

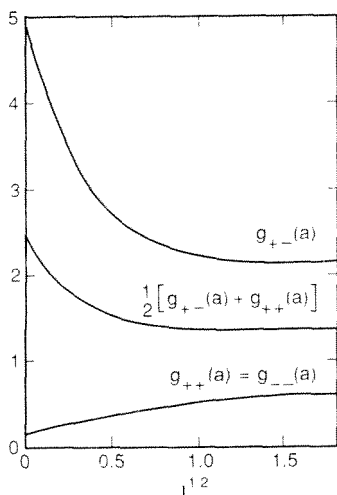


FIGURE A-1. Radial distribution functions at hard-core contact for the primitive model for a 1-1 electrolyte. Also shown is the sum  $g_{+-}(a) + g_{++}(a)$ , which appears in the expression for the ion interaction coefficient.

were constant. Thus the second term Equation in A-6 is analogous to the second term in Equation 36. It is found, however, that the sum  $g_{+-}(a) + g_{++}(a)$  is not constant but depends on ionic strength, as shown in Figure A-1. One notes at once the similarity between the curve for  $g_{+-}(a) + g_{++}(a)$  in Figure A-1 to those for  $B'$  in Figure 2 for such solutes as HCl and KCl. Here we have the explanation of the ionic-strength dependence of  $B$  or  $\beta$  in the Guggenheim equations. The relative probability of ions being close together (when corrected for the normal effects of concentration) is greater at low ionic strength than at high ionic strength. Also, this function  $g_{+-}(a) + g_{++}(a)$  changes rapidly in very dilute solutions and then approaches a nearly constant value at high concentration.

**APPENDIX B: THEORY FOR UNSYMMETRICAL MIXING OF IONS OF THE SAME SIGN AND THE CALCULATION OF  $\epsilon\theta$  AND  $\epsilon\theta'$**

Here we give the theory and a practical method of calculation for the higher-order electrostatic term for unsymmetrical mixing.<sup>5,15</sup> The second virial coefficient  $B_{ij}(\kappa)$  of Equation 21 is shown by Friedman<sup>49</sup> to be given by

$$B_{ij}(\kappa) = (2\pi z_i z_j / \kappa^2) J_{ij}(\kappa, z_i, z_j, \dots) \tag{B-1}$$

with the electrostatic length

$$l = e^2 / \epsilon kT \tag{B-2}$$

We note that the interionic potential of mean force can be written as

$$v_{ij} = u_{ij} + kT z_i z_j / r \tag{B-3}$$

where the second term is the electrostatic interaction and  $u_{ij}$ , a function of the interionic distance  $r$ , is the short-range potential. Then the function  $J_{ij}$  of Equation B-1 is

$$J_{ij} = -(\kappa^2 / z_i z_j l) \int_0^\infty [\exp(q_{ij} - u_{ij}/kT) - 1 - q_{ij} - q_{ij}^2/2] r^2 dr \tag{B-4}$$

with

$$q_{ij} = -(z_i z_j / r) \exp(-\kappa r) \quad (\text{B-5})$$

The integral in Equation B-4 cannot be evaluated, in general, without knowledge of the short-range potential  $u_{ij}$ . Since the quantity is not known accurately, the entire second virial coefficient is treated as an empirical quantity. However, for the particular case of ions of the same sign, an approximation yields useful results.

Ions of the same sign repel one another strongly enough that they seldom approach one another closely; hence, the short-range potential should have little or no effect. This can be seen mathematically in Equation B-4. If  $q_{ij}$  is large and negative for the range of  $r$  for which  $u_{ij}$  differs from zero, then the value of  $\exp(q_{ij})$  is extremely small throughout this range. Thus, provided  $u_{ij}$  is positive (or if negative, is small), the effect of  $u_{ij}$  will be negligible.

In view of this situation, one can evaluate the effect of electrostatic forces on the difference terms  $\Phi_{ij}$  without making any detailed assumption about short-range forces. We write

$$\Phi_{ij} = \theta_{ij} + {}^E\theta_{ij}(I) \quad (\text{B-6})$$

where the first term on the right arises from the combined effects of short-range forces acting directly or through the solvent, of the use of molalities instead of concentration, and of the difference in the Debye-Hückel term in Equation 21 from that in 23 and 41. The second term  ${}^E\theta_{MN}$  will be calculated from the corresponding terms of the cluster-integral theory with the omission of short-range forces. From the definition of  $\Phi_{MN}$  we have

$${}^E\theta_{MN} = {}^E\lambda_{MN} - (z_N/2z_M){}^E\lambda_{MM} - (z_M/2z_N){}^E\lambda_{NN} \quad (\text{B-7})$$

$${}^E\lambda_{ij} = (z_i z_j / 4I) J_{ij} \text{ with } u_{ij} = 0 \quad (\text{B-8})$$

$$J_{ij} = \frac{\kappa^2}{z_i z_j I} \int_0^\infty (1 + q_{ij} + \frac{1}{2} q_{ij}^2 - e^{q_{ij}}) r^2 dr \quad (\text{B-9})$$

With the substitutions

$$y = \kappa r \quad (\text{B-10})$$

$$x = z_i z_j I \kappa \quad (\text{B-11})$$

$$q = -(x/y) e^{-y} \quad (\text{B-12})$$

$$J(x) = x^{-1} \int_0^\infty (1 + q + \frac{1}{2} q^2 - e^q) y^2 dy \quad (\text{B-13})$$

In our working units

$$x_{ij} = 6z_i z_j A_\pm I^{1/2} \quad (\text{B-14})$$

where for ions of the same sign  $x_{ij}$  is always positive. Also,

$${}^E\theta_{MN} = (z_M z_N / 4I) [J(x_{MN}) - \frac{1}{2} J(x_{MM}) - \frac{1}{2} J(x_{NN})] \quad (\text{B-15})$$

We also need the ionic strength derivative of  ${}^E\theta$  and therefore of  $J$ . If  $J' = \partial J / \partial x$ , we find for  ${}^E\theta'$  the expression

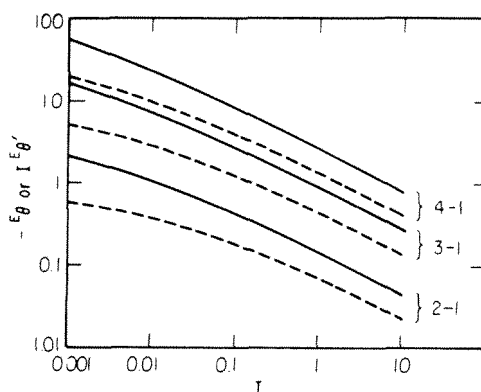


FIGURE B-1. The functions  ${}^{\epsilon}\theta$  (solid curves) and  $I{}^{\epsilon}\theta'$  (dashed curves) for mixing ions of charge types 2-1, 3-1, and 4-1. (Reprinted with permission from Pitzer, K. S., *J. Solution Chem.*, 4, 249, 1975.)

$${}^{\epsilon}\theta'_{MN} = -{}^{\epsilon}\theta_{MN}/I + (Z_M Z_N / 8I^2) [x_{MN} J'(x_{MN}) - \frac{1}{2} x_{MM} J'(x_{MM}) - \frac{1}{2} x_{NN} J'(x_{NN})] \quad (\text{B-16})$$

For  $J$  the integrals of the second and third terms in the parentheses in Equation B-13 are straightforward, with the results

$$J = \frac{1}{4} x^{-1} + J_2 \quad (\text{B-17})$$

$$J' = \frac{1}{4} - (J_2/x) + J_3 \quad (\text{B-18})$$

$$J_2 = x^{-1} \int_0^{\infty} (1 - e^{-y}) y^2 dy \quad (\text{B-19})$$

$$J_3 = x^{-1} \int_0^{\infty} \exp(q - y) y dy \quad (\text{B-20})$$

There are no simple integrals for  $J_2$  and  $J_3$  but they are readily evaluated numerically with modern computers. The resulting functions  ${}^{\epsilon}\theta$  and  ${}^{\epsilon}\theta'$  for 2-1, 3-1, and 4-1 mixing are shown in Figure B-1.

For more efficient computation of these functions than numerical integration, several methods have been proposed.<sup>5,16,29</sup> Harvie's method uses two Chebyshev polynomial approximations, one for  $x \leq 1$  and the other for  $x \geq 1$ . The appropriate equations for these regions follow:

Region I.  $x \leq 1$

$$z = 4 - x^{1.5} - 2 \quad (\text{B-21})$$

$$\frac{dz}{dx} = \frac{3}{5} x^{-0.5} \quad (\text{B-22})$$

$$b_k = z b_{k-1} - b_{k-2} + a_k^1 \quad (\text{B-23})$$

$$k = 0, 20$$

**TABLE B-1**  
**Numerical Arrays for Calculating  $J(x)$  and  $J'(x)$**

$k$	$a_k^I$	$a_k^{II}$
0	1.925154014814667	0.628023320520852
1	-0.060076477753119	0.462762985338493
2	-0.029779077456514	0.150044637187895
3	-0.007299499690937	-0.028796057604906
4	0.000388260636404	-0.036552745910311
5	0.000636874599598	-0.001668087945272
6	0.000036583601823	0.006519840398744
7	-0.000045036975204	0.001130378079086
8	-0.000004537895710	-0.000887171310131
9	0.000002937706971	-0.000242107641309
10	0.000000396566462	0.000087294451594
11	-0.000000202099617	0.000034682122751
12	-0.000000025267769	-0.000004583768938
13	0.000000013522610	-0.000003548684306
14	0.000000001229405	-0.000000250453880
15	-0.000000000821969	0.000000216991779
16	-0.00000000050847	0.000000080779570
17	0.000000000046333	0.000000004558555
18	0.000000000001943	-0.0000000006944757
19	-0.000000000002563	-0.0000000002849257
20	-0.000000000010991	0.000000000237816

$$d_k = b_{k+1} + z d_{k+1} - d_{k+2} \quad (\text{B-24})$$

Region II.  $x \geq 1$

$$z = {}^{40/9}x^{-1/10} - {}^{22/9} \quad (\text{B-25})$$

$$\frac{dz}{dx} = -\frac{40}{90} x^{-11/10} \quad (\text{B-26})$$

$$b_k = z b_{k+1} - b_{k+2} + a_k^{II} \quad (\text{B-27})$$

$$k = 0, 20$$

$$d_k = b_{k+1} + z d_{k+1} - d_{k+2} \quad (\text{B-28})$$

Using the calculated values for the  $b_k$  and the  $d_k$ ,  $J(x)$  and  $J'(x)$  can be calculated from the following formulas:

$$J(x) = {}^{1/2}x^{-1} + {}^{1/2}(b_0 - b_2) \quad (\text{B-29})$$

$$J'(x) = {}^{1/2} + {}^{1/2} \frac{dz}{dx} (d_0 - d_2) \quad (\text{B-30})$$

Some discussion with regard to the calculation of the arrays  $b_k$  and  $d_k$  is appropriate. The coefficients  $a_k^I$  and  $a_k^{II}$  are given in Table B-1. By definition  $b_{21} = b_{22} = d_{21} = d_{22} = 0$ . Therefore, by using Equation B-23 or B-27, the numbers  $b$  can be generated in decreasing sequence. Similar arguments apply to the array  $d$ . The values  $J(1) = 0.116437$  and  $J'(1) = 0.160527$  can be used to check a program for this calculation.

### APPENDIX C: THEORY AND ALTERNATE PARAMETERS FOR SYMMETRICAL MIXING OF IONS OF THE SAME SIGN

While the relatively large ionic-strength dependence of  $\Phi_{MN}$  for unsymmetrical mixing of ions, described in Appendix B, disappears for the symmetrical case, there is a much smaller effect which can be understood in terms of the radial distribution function at contact, Figure A-1. The magnitude of  $g_{+-}(a)$  is much smaller than  $g_{++}(a)$  and the change of  $g_{+-}(a)$  with ionic strength is likewise much smaller, but it is not zero. Also, the mixing term  $\Phi_{MN}$  involves the difference between  $\lambda_{MN}$  and the average of  $\lambda_{MM}$  and  $\lambda_{NN}$ . Thus, the expected magnitude of the ionic-strength dependence of  $\Phi_{MN}$  is expected to be very much smaller than that of  $B_{MX}$ .

Friedman<sup>49</sup> derived the limiting law for this effect from cluster expansion theory. In terms of the Debye-Hückel parameter  $A_\phi$  and our general equation, it is

$$\partial \ln g_0 / \partial I^{1/2} = 6z^2 A_\phi \quad (C-1)$$

where  $z$  is the number of charges on the ions mixed and  $g_0$  is the basic parameter in a widely used expression for the mixing process at constant ionic strength,

$$\Delta_m G / (n_w RT^2) = y(1 - y)[g_0 + (1 - 2y)g_1 + \dots] \quad (C-2)$$

Here  $y$  is the fraction of one of the solutions mixed and  $(1 - y)$  the fraction of the other solution.

After appropriate substitution of the molalities of various species into Equation C-2, one finds, for the simple case of the 1-1 type, common-ion mixing of MX with NX

$$g_0 = 2\Phi_{MN} + I\psi_{MNX} \quad (C-3)$$

Similar expressions with different numerical coefficients are found for other cases. Thus, for the 2-1 type  $MX_2-NX_2$  (mixing the doubly charged ions), one obtains

$$g_0 = 2\Phi_{MN}/9 + 2I\psi_{MNX}/27 \quad (C-4)$$

while for mixing the singly charged ions  $M_2X-N_2X$  the result is

$$g_0 = 8\Phi_{MN}/9 + 4I\psi_{MNX}/27 \quad (C-5)$$

In the case of 2-2-type mixing the result becomes

$$g_0 = \Phi_{MN}/8 + I\psi_{MNX}/64 \quad (C-6)$$

For  $\Phi_{MN}$  we use the same form of  $I$  dependency as was adopted for the  $B_{MX}$  expressions

$$\Phi_{MN} = \theta_{MN}^{(0)} + (2\theta_{MN}^{(1)}/\alpha^2 D)[1 - (1 + \alpha I^{1/2})\exp(-\alpha I^{1/2})] \quad (C-7)$$

and give  $\alpha$  the usual value of  $2.0 \text{ kg}^{1/2} \cdot \text{mol}^{-1/2}$ .

Differentiation of Equation C-7 with respect to  $I^{1/2}$  yields an expression which, in the limit  $I \rightarrow 0$ , becomes

$$\partial \Phi / \partial I^{1/2} = -2\alpha \theta^{(1)}/3 \quad (C-8)$$

Also, in the limit  $I \rightarrow 0$ , one has



$$g_0 = K\Phi = K[\theta^{(0)} + \theta^{(1)}] \quad (\text{C-9})$$

where K is a numerical constant depending on the charge type, as illustrated in Equations C-3 to C-6. If one combines Equations C-7 to C-9, one obtains

$$\theta^{(1)} = -\theta^{(0)}/(1 + \alpha/9z^2A_\phi) \quad (\text{C-10})$$

Thus, the limiting law serves to determine  $\theta^{(1)}$  in terms of  $\theta^{(0)}$  and the Debye-Hückel parameter, together with other known factors. If Equation C-7 is a good approximation, one now has an expression for the dependence of  $\theta$  on ionic strength which is valid, not only in the limit of small ionic strength, but at all values of the ionic strength.

The available experimental measurements are those of the osmotic coefficient of the solution or of the activity coefficient of one component. Yang and Pitzer<sup>26</sup> developed working equations and treated most of the available cases of symmetrical, common-ion mixing with the results shown in Table C-1.

The limiting law for symmetrical mixing can also be applied to heat of mixing. Now the general equation is

$$\Delta_m H/(n_w RTI^2) = y(1 - y)[h_0 + (1 - 2y)h_1 \dots] \quad (\text{C-11})$$

and  $h_0$  is related to  $g_0$  by

$$h_0 = -T(\partial g_0/\partial T)_P \quad (\text{C-12})$$

Substitution of Equation C-1 and rearrangement yields

$$\partial h_0/\partial I^{1/2} = 6z^2(A_\phi h_0 - A_H g_0/4RT) \quad (\text{C-13})$$

One now assumes for  $\Phi^L = \partial\Phi/\partial T$  the same form as Equation C-7:

$$\Phi_{MN}^L = \theta_{MN}^{(0)L} + (2\theta_{MN}^{(1)L}/\alpha^2 I)[1 - (1 + \alpha I^{1/2})\exp(-\alpha I^{1/2})] \quad (\text{C-14})$$

Also for 1-1 mixing of MX with NX,

$$h_0 = -T(2\Phi_{MN}^L + I\psi_{MNX}^L) \quad (\text{C-15})$$

with other numerical coefficients for other charge types. Eventually, one obtains

$$\theta^{(1)L} = -[\theta^{(0)L} + (\theta^{(0)} + \theta^{(1)})A_H/4RT^2A_\phi]/(1 + \alpha/9z^2A_\phi) \quad (\text{C-16})$$

Note that the parameters  $\theta^{(0)}$  and  $\theta^{(1)}$  for the Gibbs energy enter Equation C-16 as well as  $\theta^{(0)L}$  for the enthalpy.

The experimental data for heats of mixing were treated by this method by Phutela and Pitzer.<sup>20</sup> Good agreement was obtained with the experimental values and the resulting parameters are listed in Table C-2 for several cases. The enthalpy calculations were actually made before the Gibbs energy treatment had been made on the I-dependent basis; hence, the I-dependent values of  $\theta$  were used instead of the sum  $(\theta^{(0)} + \theta^{(1)})$  in Equation C-16. The effect of this difference is small and usually of no significance.

**TABLE C-1**  
**Mixing Parameters<sup>a</sup> for 298.15 K Consistent with the Limiting Law for**  
**Symmetrical Mixing**

System	Type	Max I	$10^2\theta^{(0)}$	$10^2\theta^{(1)}$	$10^3\psi$	$10^3\sigma$
HCl-LiCl	ln $\gamma$	5.0	2.2	-1.4	-0.3 <sub>6</sub>	6.2
HBr-LiBr	ln $\gamma$	2.5	2.2	-1.4	-0.1 <sub>5</sub>	6.2
HClO <sub>4</sub> -LiClO <sub>4</sub>	$\phi$	4.5	2.2	-1.4	-0.3 <sub>7</sub>	6.2
HCl-NaCl	ln $\gamma$	3.0	5.0	-3.2	-0.80	7.1
HBr-NaBr	ln $\gamma$	3.0	5.0	-3.2	-1.33	7.1
HClO <sub>4</sub> -NaClO <sub>4</sub>	$\phi$	5.0	5.0	-3.2	-1.92	7.1
HCl-KCl	ln $\gamma$	3.5	0.30	-0.2	-0.6 <sub>6</sub>	10
HBr-KBr	ln $\gamma$	3.0	0.3	-0.2	-5.2	10
HCl-CsCl	ln $\gamma$	3.0	-5.9	+3.7	-1.2 <sub>4</sub>	4.4
HCl-NH <sub>4</sub> Cl	ln $\gamma$	3.0	-1.5 <sub>6</sub>	1.0	-0.7 <sub>8</sub>	4.4
LiCl-NaCl	$\phi$	6.0	1.2 <sub>7</sub>	-0.8 <sub>1</sub>	0.3 <sub>5</sub>	3.4
LiNO <sub>3</sub> -NaNO <sub>3</sub>	$\phi$	6.0	1.2 <sub>7</sub>	-0.8 <sub>1</sub>	0.7 <sub>1</sub>	3.4
LiClO <sub>4</sub> -NaClO <sub>4</sub>	$\phi$	3.5	1.27	-0.8 <sub>1</sub>	0.9 <sub>0</sub>	3.4
LiOAc-NaOAc	$\phi$	3.5	1.2 <sub>7</sub>	-0.8 <sub>1</sub>	-0.4 <sub>4</sub>	3.4
LiCl-KCl	$\phi$	4.8	-2.5 <sub>3</sub>	1.6 <sub>1</sub>	-0.8 <sub>9</sub>	3.5
LiCl-CsCl	$\phi$	5.0	-10.0	6.3 <sub>5</sub>	-0.91	6.1
NaCl-KCl	$\phi$	4.8	-2.1 <sub>3</sub>	1.3 <sub>6</sub>	0.05	3.2
NaBr-KBr	$\phi$	4.0	-2.1 <sub>3</sub>	1.3 <sub>6</sub>	-0.07	3.2
NaNO <sub>3</sub> -KNO <sub>3</sub>	$\phi$	3.5	-2.1 <sub>3</sub>	1.3 <sub>6</sub>	0.09	3.2
Na <sub>2</sub> SO <sub>4</sub> -K <sub>2</sub> SO <sub>4</sub>	$\phi$	3.0	-2.1 <sub>3</sub>	1.3 <sub>6</sub>	0.3	3.2
NaCl-RbCl	$\phi$	4.7	-3.5 <sub>0</sub>	2.2 <sub>2</sub>	0.0 <sub>1</sub>	4.4
NaNO <sub>3</sub> -RbCl	$\phi$	4.8	3.5 <sub>0</sub>	2.2 <sub>2</sub>	0.1 <sub>3</sub>	4.4
NaNO <sub>3</sub> -NH <sub>4</sub> NO <sub>3</sub>	$\phi$	6.0	-1.6 <sub>9</sub>	1.0 <sub>8</sub>	0.2 <sub>6</sub>	0.5
KCl-CsCl	$\phi$	5.0	-0.3 <sub>7</sub>	0.2 <sub>4</sub>	-0.06	1.8
NaCl-NaBr	$\phi$	4.4	0.2 <sub>8</sub>	-0.1 <sub>9</sub>	-0.0 <sub>8</sub>	1.4
KCl-KBr	$\phi$	4.4	0.2 <sub>8</sub>	-0.1 <sub>9</sub>	-0.1 <sub>5</sub>	1.4
NaCl-NaOH	ln( $\gamma/\gamma'$ )	3.0	-7.0	4.4 <sub>3</sub>	-0.3 <sub>2</sub>	2.4
KCl-KOH	ln( $\gamma/\gamma'$ )	3.5	-7.0	4.4 <sub>3</sub>	0.1 <sub>6</sub>	2.4
NaBr-NaOH	ln( $\gamma/\gamma'$ )	3.0	-8.5	5.4	-0.9 <sub>0</sub>	5.8
KBr-KOH	ln( $\gamma/\gamma'$ )	3.0	-8.5	5.4	-0.6 <sub>6</sub>	5.8
LiCl-LiNO <sub>3</sub>	$\phi$	6.0	2.2 <sub>6</sub>	-1.4 <sub>3</sub>	-0.4 <sub>2</sub>	3.6
NaCl-NaNO <sub>3</sub>	$\phi$	5.0	2.2 <sub>6</sub>	-1.4 <sub>3</sub>	-0.7 <sub>2</sub>	3.6
KCl-KNO <sub>3</sub>	$\phi$	4.0	2.2 <sub>6</sub>	-1.4 <sub>3</sub>	-0.9 <sub>3</sub>	3.6
MgCl <sub>2</sub> -Mg(NO <sub>3</sub> ) <sub>2</sub>	$\phi$	4.0	2.2 <sub>6</sub>	-1.4 <sub>3</sub>	-0.7 <sub>7</sub>	3.6
CaCl <sub>2</sub> -Ca(NO <sub>3</sub> ) <sub>2</sub>	$\phi$	6.0	2.2 <sub>6</sub>	-1.4 <sub>3</sub>	-2.2 <sub>1</sub>	3.6
HCl-HClO <sub>4</sub>	ln $\gamma$	3.0	3.7 <sub>1</sub>	-2.3 <sub>8</sub>	-0.7 <sub>4</sub>	5.9
NaCl-NaOAc	$\phi$	3.0	-1.9 <sub>3</sub>	1.2 <sub>4</sub>	0.2 <sub>7</sub>	1.5
KCl-KOAc	$\phi$	3.0	-1.9 <sub>3</sub>	1.2 <sub>4</sub>	0.3 <sub>9</sub>	1.5

<sup>a</sup> Units are kg · mol<sup>-1</sup> for  $\theta^{(0)}$  and  $\theta^{(1)}$  and kg<sup>2</sup> · mol<sup>-2</sup> for  $\psi$ .

The values of  $\theta^{(0)}$ ,  $\theta^{(1)}$ ,  $\psi$  in Table C-2 give the temperature derivatives at 298 K of the parent quantities  $\theta^{(0)}$ ,  $\theta^{(1)}$ ,  $\psi$  in Table C-1. Thus, the values of the parent parameters are available for reasonable ranges of temperature near 298 K.

At the present level of experimental measurement, the refinement of this Appendix is not significant for osmotic or activity coefficients. For enthalpies of mixing, however, it is very important for a few cases, LiCl-CsCl and KCl-Bu<sub>4</sub>NCl, and significant for several other cases with substantial values of  $\theta^{(0)}$ . Details are given in Reference 20. Also, as precision improves in the future, these theoretically based equations should become valuable in practical calculations of activity coefficients.

**TABLE C-2**  
**Heat of Mixing Parameters at 298.15 K<sup>a</sup>**

System	I Range	10 <sup>4</sup> θ <sup>(0)L</sup>	10 <sup>4</sup> θ <sup>(1)L</sup>	10 <sup>4</sup> ψ <sup>L</sup>
<b>1:1 Electrolytes</b>				
HCl-NaCl	1.0—3.0	-5.53	3.13	1.81
HCl-KCl	1.0—3.0	0.00	-0.05	1.05
LiCl-NaCl	0.1—6.0	-3.25	1.94	0.76
LiCl-KCl	0.1—3.0	1.72	-0.86	0.71
LiCl-CsCl	0.03—3.0	5.99	-3.55	0.78
NaF-KF	0.2—0.9	1.44	-0.79	-0.49
NaCl-KCl	0.1—4.8	1.44	-0.79	-0.22
NaBr-KBr	0.1—1.2	1.44	-0.79	-0.13
NaI-KI	0.2—1.0	1.44	-0.79	0.02
NaOAc-KOAc	0.2—1.0	1.44	-0.79	-0.34
KCl-CsCl	1.0—3.0	-0.42	0.27	0.29
KCl-Bu <sub>4</sub> NCl	0.02—1.0	84.9	-57.0	-21.0 <sub>6</sub>
NaCl-NaBr	0.5—6.0	-0.13	0.08	0.00
<b>1:2 or 2:1 Electrolytes</b>				
Li <sub>2</sub> SO <sub>4</sub> -Na <sub>2</sub> SO <sub>4</sub>	1.0—9.0	-3.25	1.94	1.59
Na <sub>2</sub> CO <sub>3</sub> -K <sub>2</sub> CO <sub>3</sub>	0.15—1.05	1.44	-0.79	-2.69
MgCl <sub>2</sub> -SrCl <sub>2</sub>	0.6—3.0	-1.12	0.98	0.00
MgCl <sub>2</sub> -BaCl <sub>2</sub>	0.3—3.0	-2.42	2.12	0.00
MgCl <sub>2</sub> -MgBr <sub>2</sub>	1.0—6.0	-0.13	0.08	0.00

<sup>a</sup> Units: θ<sup>(0)L</sup> and θ<sup>(1)L</sup>, kg · mol<sup>-1</sup> · K<sup>-1</sup>; ψ<sup>L</sup>, kg<sup>2</sup> · mol<sup>-2</sup> · K<sup>-1</sup>.

## APPENDIX D: IONIC STRENGTH EFFECT ON ION-NEUTRAL INTERACTIONS

Another theoretical topic concerns the possible ionic-strength dependence of second virial coefficients for interactions of ions with neutral molecules containing dipole or higher electrical moments. The work of Kirkwood<sup>160</sup> pertains to this question, but it considers only electrical effects subject to a distance of closest approach and ignores all other effects of short-range forces which are normally the dominant terms. For charge-dipole effects on the activity coefficient of the dipolar molecule *i*, Kirkwood's Equation (21) yields

$$\delta \ln \gamma_i = - \frac{3\pi e^2 \mu_i^2 \sum_j c_j z_j^2}{2a\epsilon^2 k^2 T^2 (1 + \kappa a + \kappa^2 a^2 / 3)} \quad (\text{D-1})$$

with  $\mu_i$  the dipole moment of *i* and  $c_j$  and  $z_j$  the concentration and charge on ion *j*. Also, *a* is the distance of closest approach of an ion to the molecule and  $\kappa$  is the Debye reciprocal length, which is related to the ionic strength. For each term in the sum, Equation D-1 yields the electrical contribution to a second virial coefficient  $\lambda_{ij}$ . The appearance of  $\kappa$  in the denominator indicates an ionic-strength dependence. However, for typical values of the dipole moment and other quantities, this term is very small compared to that for short-range forces. For quadrupole or higher moments, the corresponding term is even smaller. Hence, there is no present indication that an ionic-strength dependence need be considered for the second virial coefficients for neutral-ion interactions.

## APPENDIX E: DIELECTRIC CONSTANT OF WATER AND THE DEBYE-HÜCKEL PARAMETERS

Most calculations based on the methods described here have used the equation of Bradley and Pitzer<sup>11</sup> for the dielectric constant or relative permittivity of water and the equation of

**TABLE E-1**  
**Values of the Constants in**  
**Equations E-1 to E-4 for the**  
**Dielectric Constant of Water**

$U_1 = 3.4279E2$	$U_6 = -1.8289E2$
$U_2 = -5.0866E-3$	$U_7 = -8.0325E3$
$U_3 = 9.4690E-7$	$U_8 = 4.2142E6$
$U_4 = -2.0525$	$U_9 = 2.1417$
$U_5 = 3.1159E3$	

Haar et al.<sup>161</sup> for the density. The density is so accurately known that further comment is unnecessary. The equation for the dielectric constant is

$$\epsilon = \epsilon_{1000} + C \ln [(B + P)/(B + 1000)] \quad (\text{E-1})$$

where the pressure  $P$  and the parameter  $B$  are in bars. The temperature dependencies are given by

$$\epsilon_{1000} = U_1 \exp(U_2 T + U_3 T^2) \quad (\text{E-2})$$

$$C = U_4 + U_5/(U_6 + T) \quad (\text{E-3})$$

$$B = U_7 + U_8/T + U_9 T \quad (\text{E-4})$$

with the temperature in K and the various  $U$ 's in the appropriate powers of K. The numerical values are given in Table E-1. The range of validity for Equations E-1 to E-4 is 0 to 350°C and to 1 kbar pressure.

Although the uncertainty in  $\epsilon$  is small, it is desirable to avoid error by retaining the same value of  $\epsilon$  as was used in determining other parameters. This is more important for derivative quantities such as volumes or enthalpies and especially important for heat capacities which involve the second temperature derivative of the dielectric constant. In attempting to fit closely the measurements of  $\epsilon$  over a very wide range of temperature and pressure, one is tempted to use a many-term equation which can "overfit" the data and give spurious derivatives. The Bradley-Pitzer (B-P) equation was designed to avoid this overfitting difficulty.

In the research prior to the development of the B-P equation in 1979, a different equation was used<sup>162</sup> that gives exactly the same value of  $\epsilon$  at 25°C but a slightly different value of  $\partial\epsilon/\partial T$ . Thus, no correction is needed for the older results for  $\beta^{(0)}$ ,  $\beta^{(1)}$ ,  $\beta^{(2)}$ ,  $C^{\phi}$ , but there is a small problem for values of the temperature derivatives in Tables 12 and 13. For most purposes, any correction would not be significant and is not needed. For optimum accuracy in reproducing the enthalpy values, it is best to use the original Debye-Hückel parameter. This was  $A_H/RT = 1.1773$  on the basis used in Reference 9. Subsequently, the definition was changed (see Reference 11), and on the basis of Equations 81 to 84  $A_H/RT = 1.1773 (2/3) = 0.7849$ . If one's interest is in temperature derivatives of  $\beta^{(0)}$ ,  $\beta^{(1)}$ , etc., for use with other quantities on the basis of the Debye-Hückel parameters of Table 1, one can make corrections to the values in Tables 12 and 13. For 1-1 electrolytes, the corrections are  $-1.8E-5$ ,  $+1.2E-4$ , and  $+5.0E-6$  for  $\beta^{(0)l}$ ,  $\beta^{(1)l}$ , and  $C^{bl}$ , respectively. Corresponding values can be derived for other charge types (Table 13).

Several other equations have been used for the dielectric constant of water. There is good agreement for  $\epsilon$  itself, and therefore for  $A_{\phi}$ , but there are significant differences for the derivatives of  $\epsilon$  and especially for  $\partial^2\epsilon/\partial T^2$ , which is needed for the heat capacity parameter  $A_J$ . Recently, Archer and Wang<sup>163</sup> have presented an improved equation and have discussed fully the differences among the earlier equations. Their equation has a very wide range of validity extending from the supercooled liquid at 238 to 823 K in the supercritical range

and for pressures to 5 kbar. In comparison with the new equation, the B-P equation is in good agreement over its more restricted temperature range, although the second derivative does show some difference below 280 K, i.e., from 273 to 280 K. Archer<sup>164</sup> has also presented a convenient method of making a very small adjustment in the parameters  $\beta^{(0)}$ ,  $\beta^{(1)}$ ,  $C^\phi$  for the slight shift in  $A_\phi$  from the B-P equation for  $\epsilon$  to the new Archer-Wang (A-W) equation. This method can be used, of course, for the adjustment in the opposite direction from the A-W or any other new  $A_\phi$  to the B-P  $A_\phi$ ; indeed, this will be the more useful procedure in the near future. For a multicomponent system, it will be easier to convert a small number of entries that may have been evaluated on a new basis to the B-P basis rather than to convert the remaining large number of values that have already been entered into a comprehensive computer program.

## APPENDIX F: HIGHER ORDER TERMS INVOLVING NEUTRAL SPECIES

In Equations 59 to 64 and 75 the binary terms for neutral-neutral and neutral-ion interactions are included but the triple interaction terms are omitted. Some binary ion-neutral parameters are given in Table 19. This appendix gives the additional terms representing three-particle interactions with at least one neutral particle. Also included are two examples where these terms are needed.

The terms under consideration here are all included in the final sum in Equation 23,

$$G^{ex}/w_wRT = \dots + \sum_i \sum_j \sum_k m_i m_j m_k \mu_{ijk} \quad (F-1)$$

We introduce the symbols c for cation, a for anion, and n for neutral, whereupon the terms including at least one neutral can be rearranged and collected to yield

$$\begin{aligned} G^{ex}/w_wRT = & \dots + \sum_n m_n^3 \mu_{nnn} + 3 \sum_{n' > n} m_n m_{n'}^2 \mu_{nnn'} \\ & + 6 \sum_{n' > n} \sum_{n'' > n'} m_{n''} m_{n'} m_n \mu_{nn'n''} + 3 \sum_n \sum_c m_n m_c (m_n \mu_{nnc} + m_c \mu_{ncc} \\ & + 2 \sum_{c' > c} m_{c'} \mu_{ncc'}) + 3 \sum_n \sum_a m_n m_a (m_n \mu_{nna} + m_a \mu_{naa} + 2 \sum_{a' > a} m_{a'} \mu_{naa'}) \\ & + 6 \sum_{n' > n} \sum_n m_n m_{n'} (\sum_c m_c \mu_{nn'c} + \sum_a m_a \mu_{nn'a}) + 6 \sum_n \sum_c \sum_a m_n m_c m_a \mu_{nca} \end{aligned} \quad (F-2)$$

It is convenient to define two new quantities

$$\zeta_{nca} = 6\mu_{nca} + 3 \left| \frac{Z_a}{Z_c} \right| \mu_{ncc} + 3 \left| \frac{Z_c}{Z_a} \right| \mu_{naa} \quad (F-3)$$

$$\eta_{ncc'} = 6\mu_{ncc'} - 3 \left( \frac{Z_c'}{Z_c} \right) \mu_{ncc} - 3 \left( \frac{Z_c}{Z_c'} \right) \mu_{nc'c'} \quad (F-4)$$

The analogous quantity  $\eta_{naa'}$  is obtained by substitution of a and a' for c and c'. The other terms in Equation F-2 can be retained as written. Then the terms for Equation 59 become

$$\begin{aligned} G^{ex}/w_wRT = & \dots + \sum_n m_n^3 \mu_{nnn} + 3 \sum_{n' > n} m_n m_{n'}^2 \mu_{nnn'} \\ & + 6 \sum_{n' > n} \sum_{n'' > n'} m_{n''} m_{n'} m_n \mu_{nn'n''} + 3 \sum_n \sum_c m_n^2 m_c \mu_{nnc} \end{aligned}$$

$$\begin{aligned}
& + 3 \sum_n \sum_a m_n^2 m_a \mu_{na} + 6 \sum_{n' \cdot n} m_{n'} m_n \left( \sum_c m_c \mu_{nn'c} + \sum_a m_a \mu_{nn'a} \right) \\
& + \sum_n \sum_c \sum_a m_n m_c m_a \zeta_{nca} + \sum_n \sum_{c' \cdot c} m_n m_c m_{c'} \eta_{ncc'} + \sum_{n' \cdot a' \cdot a} m_{n'} m_{a'} m_a \eta_{naa'} \quad (\text{F-5})
\end{aligned}$$

After appropriate differentiation one obtains the additional terms for Equations 62 to 64 and 75.

$$\begin{aligned}
\phi - 1 = & (2/\Sigma m_i) \left[ \dots + \sum_n m_n^3 \mu_{nnn} + 3 \sum_{n' \cdot n} m_{n'} m_n^2 \mu_{nnn'} \right. \\
& + 6 \sum_{n' \cdot n' \cdot n} m_{n'} m_{n'} m_n \mu_{nn'n'} + 3 \sum_n \sum_c m_n^2 m_c \mu_{nnc} \\
& + 3 \sum_n \sum_a m_n^2 m_a \mu_{naa} + 6 \sum_{n' \cdot n} m_{n'} m_n \left( \sum_c m_c \mu_{nn'c} + \sum_a m_a \mu_{nn'a} \right) \\
& \left. + \sum_n \sum_c \sum_a m_n m_c m_a \zeta_{nca} + \sum_n \sum_{c' \cdot c} m_n m_c m_{c'} \eta_{ncc'} + \sum_{n' \cdot a' \cdot a} m_{n'} m_{a'} m_a \eta_{naa'} \right] \quad (\text{F-6})
\end{aligned}$$

$$\ln \gamma_M = \dots + \sum_n [3m_n^2 \mu_{nnM} + m_n (6 \sum_{n' \cdot n} m_{n'} \mu_{nn'M} + \sum_a m_a \zeta_{nMa} + \sum_c m_c \eta_{nMc})] \quad (\text{F-7})$$

$$\ln \gamma_X = \dots + \sum_n [3m_n^2 \mu_{nnX} + m_n (6 \sum_{n' \cdot n} m_{n'} \mu_{nn'X} + \sum_c m_c \zeta_{nXc} + \sum_a m_a \eta_{nXa})] \quad (\text{F-8})$$

$$\begin{aligned}
\ln \gamma_N = & \dots + 3 \sum_n m_n^2 \mu_{Nnn} + 6 \sum_{n' \cdot n} \sum_{n''} m_{n'} m_n \mu_{Nnn''} + 6 \sum_{n''} m_n m_{Nn} \mu_{Nnn''} \\
& + 6 m_N \left( \sum_c m_c \mu_{Nnc} + \sum_a m_a \mu_{NNa} \right) + 6 \sum_{n''} \left( \sum_c m_c \mu_{Nnc} + \sum_a m_a \mu_{Nna} \right) \\
& + \sum_c \sum_a m_c m_a \zeta_{Nca} + \sum_{c' \cdot c} m_c m_{c'} \eta_{Ncc'} + \sum_{a' \cdot a} m_a m_{a'} \eta_{Naa'} \quad (\text{F-9})
\end{aligned}$$

In the last equation the prime mark on certain sums indicates that  $N = n$  or  $N = n'$  is excluded, while in the first sum without a prime  $N = n$  is included.

While the triple interaction terms involving neutral species are not required for many systems, they can be significant. For phosphoric acid<sup>6</sup> the value 0.0109<sub>5</sub> was found for  $\mu_{\text{HA}, \text{HA}, \text{HA}}$ . In their treatment of borate systems, Felmy and Weare<sup>105</sup> obtained values for  $\zeta_{nca}$  for  $\text{B}(\text{OH})_3$  with  $\text{H}^+$ ,  $\text{Cl}^-$  and with  $\text{Na}^+$ ,  $\text{SO}_4^{2-}$ ; indeed, they first used the symbol  $\zeta_{nca}$  for this interaction. It seems likely, however, that only a few of these terms, at most, will be needed for any particular system. Corti et al.<sup>71</sup> treated the system  $\text{NaCl}-\text{CO}_2-\text{H}_2\text{O}$  and found that  $\zeta_{\text{CO}_2, \text{Na}, \text{Cl}}$  was needed but that  $(\mu_{\text{CO}_2, \text{CO}_2, \text{Na}} + \mu_{\text{CO}_2, \text{CO}_2, \text{Cl}})$  could be neglected. Their investigation extended in temperature to 250°C and in pressure to 600 bars.

## APPENDIX G: COMPUTER CODES

A general code based on the equations of this chapter for multicomponent electrolytes (PHRQPITZ) was developed by Plummer et al.<sup>159</sup> Copies of that report (U.S.G.S. Water-Resources Investigations Report 88-4153) are available from U.S.G.S., Books and Open File Reports Section, Federal Center, Bldg. 810, P.O. Box 25425, Denver, CO 80225, while the software is available from WATSTORE PROGRAM OFFICE, U.S.G.S., 437 National Center, Reston, VA 22092.

Additional information on computer codes is given in Chapters 6 and 7 and the Introduction of this volume and in Chapters 8 to 10 of Reference 165.

## APPENDIX H: EQUATIONS WITH ADDITIONAL TERMS

Although the basic Equation 23 constitutes a power series with the possibility of many terms with increasing powers of molality, the standard working Equations 40 through 70 include only terms for binary and ternary solute particle interactions. This basis has proven adequate to represent the properties of most aqueous salt solutions at 25°C to saturation with the solid. For a few solutes such as HNO<sub>3</sub> at 25°C or for any low-melting salt at its melting point, one may be interested in the entire range of composition to the pure liquid electrolyte. In that case, one cannot use molality as a measure of composition since it becomes infinite for pure solute; equations using mole fraction must then be used, and they are discussed in Appendix I. There are also intermediate cases such as CaCl<sub>2</sub>(aq) or ZnCl<sub>2</sub>(aq) where the molality basis may be used to saturation composition but where additional terms are required to represent the observed properties. Certain cases of this type are discussed below.

Also, there are systems where a modification of the standard pattern of Equation 49 for the binary interaction term  $B_{MX}(I)$  yields an improved fit at low and moderate molality. Often this improvement extends also to higher molality. The simplest example of this type is the series of alkali metal sulfates where Holmes and Mesmer<sup>128</sup> obtain better agreement with  $\alpha = 1.4$  instead of the standard value of  $2.0 \text{ kg}^{1/2} \cdot \text{mol}^{-1/2}$ . In that case no additional terms are needed.

For the lanthanide chlorides, nitrates, and perchlorates, Kodytek and Dolejs<sup>75</sup> used the full three-term expression for  $B_{MX}(I)$  but with very different values of  $\beta^{(2)}$  and  $\alpha_2$  than are appropriate for the divalent metal sulfates. For the sulfates,  $\beta^{(2)}$  is large and negative and the term models a partial ion association. In contrast, for the lanthanide salts with singly charged negative ions,  $\beta^{(2)}$  is positive. Hence, there is no indication of ion pairing; rather the extra term is just a small adjustment of the normal pattern of ionic-strength dependence of  $B_{MX}(I)$ . Table H-1 gives the parameters for the lanthanum and lutecium salts as examples. The values for the other lanthanides are similar and usually intermediate. The standard deviations of fit are reduced to about half by inclusion of the additional term.

Filippov and associates used the third term for  $B_{MX}(I)$  for several cases including MnCl<sub>2</sub>,<sup>166</sup> NiCl<sub>2</sub>,<sup>39</sup> CoCl<sub>2</sub>,<sup>149</sup> Ca(NO<sub>3</sub>)<sub>2</sub>,<sup>134</sup> Mg(NO<sub>3</sub>)<sub>2</sub>,<sup>134</sup> Ni(NO<sub>3</sub>)<sub>2</sub>,<sup>35</sup> NaH<sub>2</sub>PO<sub>4</sub>,<sup>136</sup> and HCl.<sup>166</sup> The extended equations for various salts were successfully used for treatments of salt solubility in multicomponent systems. The case of HCl is especially interesting since the inclusion of the extra term made it possible to fit the properties up to  $16 \text{ mol} \cdot \text{kg}^{-1}$ , whereas the standard expression was fitted only to  $6m$ . The parameters are compared in Table H-2. Over the extended range the  $\sigma$  is 0.005, considerably larger as compared to about 0.001 for the original fit to  $6m$ .

Holmes et al.<sup>68</sup> report a very comprehensive treatment of various thermodynamic properties of HCl(aq) over a wide range of temperatures. They present three equations: (1) a standard equation valid to 523 K and  $7 \text{ mol} \cdot \text{kg}^{-1}$ , (2) an equation valid to 523 K and  $16 \text{ mol} \cdot \text{kg}^{-1}$  with a standard  $B(I)$  but with a fourth virial coefficient  $D^\phi$ , and (3) an equation valid above 523 K including a term with negative  $\beta^{(2)}$  modeling ion association. The parameters for the second equation valid to  $16m$  are given in Table H-2; those for the first equation are essentially the same as the original values of Reference 2 shown in Table 2. It is interesting that the addition of the fourth virial coefficient leaves  $\beta^{(0)}$  and  $\beta^{(1)}$  essentially unchanged but does affect  $C^\phi$ .

The standard equation fits the data for CaCl<sub>2</sub>(aq) only to about  $4m$ ,<sup>86</sup> while the solubility is about  $9m$  at 25°C and increases with temperature. Ananthaswamy and Atkinson<sup>64</sup> added fourth, fifth, and sixth virial coefficients to the standard expressions and reported parameters, including their temperature dependency, for CaCl<sub>2</sub> to  $11 \text{ mol} \cdot \text{kg}^{-1}$  and for 0 to 100°C. They considered enthalpy and heat capacity data as well as osmotic and activity coefficients. Note that a term in  $\beta^{(2)}$  was not used for CaCl<sub>2</sub>.

**TABLE H-1**  
Parameters for Lanthanide Salts When an Additional Term in  $\beta^{(2)}$  Is Included<sup>75</sup>

Salt	$\frac{3}{2}\beta^{(0)}$	$\alpha_1$	$\frac{3}{2}\beta^{(1)}$	$\alpha_2$	$\frac{3}{2}\beta^{(2)}$	$\frac{3^{3/2}}{2}C^\phi$	$\sigma$
LaCl <sub>3</sub>	0.7951	1.6	5.52	6.0	8.0	-0.0224	0.0010
LuCl <sub>3</sub>	0.8254	1.6	5.79	6.0	8.0	0.0100	0.0015
La(NO <sub>3</sub> ) <sub>3</sub>	0.4960	1.4	4.88	6.0	6.0	-0.0621	0.0023
Lu(NO <sub>3</sub> ) <sub>3</sub>	0.7034	1.4	4.93	6.0	6.0	-0.0659	0.0040
La(ClO <sub>4</sub> ) <sub>3</sub>	1.0253	1.6	6.55	6.0	8.0	0.0656	0.0024
Lu(ClO <sub>4</sub> ) <sub>3</sub>	1.0663	1.6	6.61	6.0	8.0	0.0856	0.0020

**TABLE H-2**  
Alternate Parameters for HCl(aq) at 25°C

$\beta^{(0)}$	$\alpha_1$	$\beta^{(1)}$	$\alpha_2$	$\beta^{(2)}$	10 <sup>3</sup> C <sup>φ</sup>	10 <sup>4</sup> D <sup>φ</sup>	Max <i>m</i>	Ref.
0.1775	2	0.2945	—	—	0.80	—	6	2
0.17571	2	0.2940	—	—	2.085	-2.6657	16	68
0.23159	2	0.61349	1	-0.25785	-5.254	—	16	166

In the initial treatment<sup>3</sup> for various salts, the standard equation did not yield a satisfactory fit for CdCl<sub>2</sub>, CdBr<sub>2</sub>, or CdI<sub>2</sub> where there is known to be strong ion association and complex ion formation of CdX<sub>3</sub><sup>-</sup> and CdX<sub>4</sub><sup>2-</sup>. Filippov et al.<sup>41</sup> however, obtained a good representation of the osmotic and activity coefficients of CdCl<sub>2</sub> with an extended equation. They included a  $\beta^{(2)}$  term in B(I) and added fourth and fifth order terms to represent the association to CdCl<sub>3</sub><sup>-</sup> and CdCl<sub>4</sub><sup>2-</sup>. The expression was also used successfully for the treatment of the ternary systems of CdCl<sub>2</sub> with CdSO<sub>4</sub> or with NaCl and H<sub>2</sub>O. Even the five-component system CdCl<sub>2</sub>-CdSO<sub>4</sub>-NaCl-Na<sub>2</sub>SO<sub>4</sub>-H<sub>2</sub>O was successfully described using this treatment for CdCl<sub>2</sub>. The terms to be added to the equations of Section IV are

$$\Delta G^{\circ}/w_w RT = \omega(\text{Cd},3\text{Cl})m_{\text{Cd}} m_{\text{Cl}}^3 + \omega(\text{Cd},4\text{Cl})m_{\text{Cd}} m_{\text{Cl}}^4 \quad (\text{H-1})$$

$$\Delta \phi = (\sum m_i)^{-1} [3\omega(\text{Cd},3\text{Cl})m_{\text{Cd}} m_{\text{Cl}}^3 + 4\omega(\text{Cd},4\text{Cl})m_{\text{Cd}} m_{\text{Cl}}^4] \quad (\text{H-2})$$

$$\Delta \ln \gamma_{\text{Cd}} = \omega(\text{Cd},3\text{Cl})m_{\text{Cl}}^3 + \omega(\text{Cd},4\text{Cl}) m_{\text{Cl}}^4 \quad (\text{H-3})$$

$$\Delta \ln \gamma_{\text{Cl}} = 3\omega(\text{Cd},3\text{Cl})m_{\text{Cd}} m_{\text{Cl}}^2 + 4\omega(\text{Cd},4\text{Cl})m_{\text{Cd}} m_{\text{Cl}}^3 \quad (\text{H-4})$$

The parameters for this equation for CdCl<sub>2</sub> are given in Table H-3. The fit for the osmotic coefficient is excellent with  $\sigma = 0.001$ . The negative values of several parameters indicate ion association.

For the multicomponent systems, the usual  $\theta_{ij}$  and  $\psi_{ijk}$  parameters were evaluated and, in addition,  $\omega(\text{Na},\text{Cd},2\text{Cl})$ ,  $\omega(\text{Na},\text{Cd},3\text{Cl})$ , and  $\omega(\text{Na},\text{Cd},4\text{Cl})$ . Reference 41 should be consulted for the remarkably successful treatment of the five-component system.

Very recently, Anstiss and the writer<sup>167</sup> considered the extremely soluble and complex-forming salt ZnCl<sub>2</sub> by applying the extended equation of Filippov with the terms in  $\omega(\text{M},3\text{Cl})$  and  $\omega(\text{M},4\text{Cl})$ . Although concentrated solutions of ZnCl<sub>2</sub> and CdCl<sub>2</sub> are similarly strongly complexed, dilute solutions are different. CdCl<sub>2</sub> shows association to CdCl<sup>-</sup> at low concentration, as is indicated by the large negative  $\beta^{(2)}$  in Table H-3. In contrast, dilute ZnCl<sub>2</sub> is a strong electrolyte and was well represented by the standard equation up to 1.4 mol · kg<sup>-1</sup>



**TABLE H-3**  
**Parameters for CdCl<sub>2</sub>(aq) and**  
**ZnCl<sub>2</sub>(aq)**

	CdCl <sub>2</sub>	ZnCl <sub>2</sub>
$\beta^{(0)}$	-0.0169	0.041312
$\alpha_1$	1	1.5347
$\beta^{(1)}$	-0.3468	1.8016
$\alpha_2$	4	—
$\beta^{(2)}$	-5.829	—
$C^b$	0.00747	0.010082
$\omega(M,3Cl)$	-0.000249	-0.0001773
$\omega(M,4Cl)$	$5.8 \times 10^{-6}$	$1.3068 \times 10^{-6}$

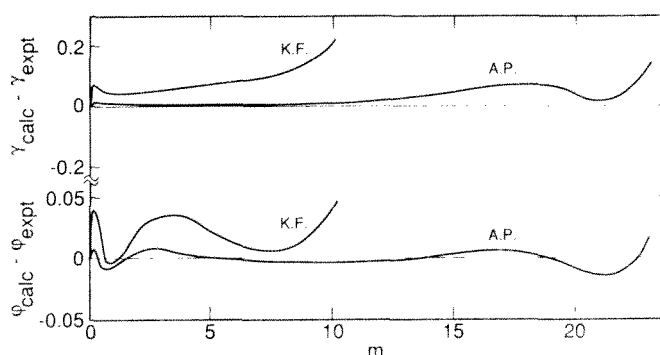


FIGURE H-1. The deviations of the osmotic coefficient and the activity coefficient of ZnCl<sub>2</sub> for the Anstiss-Pitzer (AP) equation and the Kim-Frederick (KF) equation from the evaluated experimental function of Goldberg.

with normal values of  $\beta^{(0)}$  and  $\beta^{(1)}$  (see Table 7). However, above 1 *m*, ZnCl<sub>2</sub> shows association to ZnCl<sub>2</sub> and at higher concentrations to ZnCl<sub>3</sub><sup>-</sup> and ZnCl<sub>4</sub><sup>2-</sup>.

Goldberg<sup>168</sup> evaluated various data for ZnCl<sub>2</sub> and presented an empirical equation and table of recommended values of the osmotic and activity coefficients extending to 23 mol · kg<sup>-1</sup>. Rard and Miller<sup>89</sup> subsequently made further isopiestic measurements and present recommended values, but their treatment extends only to 13 mol · kg<sup>-1</sup>. Since we were especially interested in the high molality range, the Goldberg treatment was chosen. Regression of the full set of parameters of the CdCl<sub>2</sub> equation for the osmotic-coefficient data for ZnCl<sub>2</sub> indicated no need for the  $\beta^{(2)}$  term, provided  $\alpha_1$  was optimized, as shown in Figures H-1 and H-2, with the parameters shown in Table H-3.

Figure H-1 shows the differences of the calculated values from the selected experimental curves for both the osmotic coefficient, which was fitted directly, and for the derived activity-coefficient equation. The former is fitted essentially within experimental uncertainty of 0.005 at moderate *m* and 0.01 or 0.02 at high *m*. However, the slope is large above 22 mol · kg<sup>-1</sup>, which indicates that this type of equation would be unreliable for extrapolation to higher molality. Also shown on Figure H-1 are the curves for the expression of Kim and Frederick<sup>77</sup> (KF), who fitted the standard equation to the same osmotic data to 10 mol · kg<sup>-1</sup>. The deviations for the KF treatment far exceed experimental uncertainty, but their expression may be useful for some purposes. Figure H-2 shows, for the dilute region, the experimental osmotic coefficient, together with the curve for the standard expression fitted to data below 1.5 mol · kg<sup>-1</sup>,<sup>89</sup> as well as the curves for the KF treatment and for the extended equation

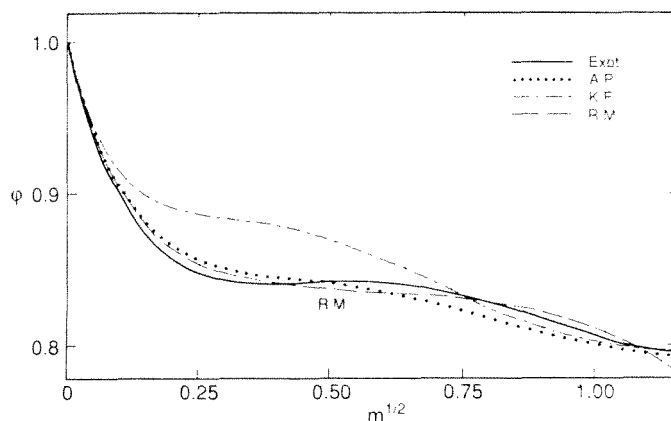


FIGURE H-2. The osmotic coefficient of  $\text{ZnCl}_2$  in the dilute range for the evaluated experimental curve and three equations. See text for details.

(AP). The substantial deviation of the KF treatment is apparent, while the other expressions yield agreement within experimental uncertainty.

These examples indicate that simple extensions of the standard form of the ion interaction equations give useful expressions without adding great complexity.

## APPENDIX I: EQUATIONS BASED ON COMPOSITION IN MOLE FRACTION

While the equations presented above have been very successful for systems of molality up to  $6 \text{ mol} \cdot \text{kg}^{-1}$  and somewhat higher with additional terms, they become unsatisfactory at still higher concentration and for a pure fused salt the molality is infinite. Thus an alternate framework is required for systems miscible to the fused salt and such an approach has been found to be advantageous for other systems of very high but limited solubility.

In this appendix we present equations appropriate for miscible, ionic systems with an unlimited number of components of ions or neutral species. This system is essentially that of Pitzer and Simonson,<sup>169</sup> which was based in part on earlier treatments of several aqueous systems with low melting metal nitrates<sup>65,170</sup> and of the  $\text{NaCl-H}_2\text{O}$  system<sup>171</sup> in the range 373 to 823 K.

### A. DEFINITIONS: IDEAL MIXING TERMS

For a miscible system the appropriate measure of composition is a mole fraction, but for an ionic system one may either recognize or ignore the ionization of the salt. While much of the literature uses nonionized mole fractions for salts, it is both theoretically and empirically preferable to recognize the ionization.\* Indeed, this is necessary for mixtures without common ions. Thus, the mole fraction of the  $j$ -th species (ion or neutral) is

$$x_i = \frac{n_i}{\sum_j n_j} \quad (\text{I-1})$$

where  $n_i$  is the number of moles of the  $i$ th species with cations and anions included as separate species. Electrical neutrality must also be maintained, of course.

\* At very high temperatures for aqueous systems and for many nonaqueous systems, the degree of ionization remains very small except at extreme dilution; then the use of nonionized mole fraction is appropriate.

The ideal entropy and Gibbs energy of mixing are

$$\Delta_m S^I/R = -\sum_i n_i \ln(x_i/x_i^0) \quad (\text{I-2})$$

$$\Delta_m G^I/RT = \sum_i n_i \ln(x_i/x_i^0) \quad (\text{I-3})$$

where  $x_i^0$  is the mole fraction of the  $i$ th species before mixing; i.e.,  $x^0 = 1/2$  for each ion in a pure salt MX and  $x^0 = 1$  for a neutral species. This simple result is readily derived for the case that all particles mix randomly without respect to charge but that charge neutrality must be maintained for each pure component and for the mixture. Such completely random mixing is, of course, a poor structural model for fused salts where there is a strong pattern of alternation of charge. However, for the mixing of salts where the ions have the same magnitude of charge, the assumption that there is no cation-anion mixing when cations mix randomly and anions mix randomly (Temkin model) yields the same entropy of mixing as is given by Equation I-2. This was demonstrated by Laity<sup>172</sup> and by Blander.<sup>173</sup> Various models have been proposed for mixing of unsymmetrical fused salts but none have been sufficiently justified to justify more complicated definitions for our purposes. Thus we take Equations I-2 and I-3 as definitions of ideal mixing and limit the present treatment to singly charged ions in a pure-fused-salt reference state. When the infinitely dilute reference state is used, the limitation to single charges is no longer necessary. Then  $x_i^0$  takes the value for the standard state as defined below.

The excess Gibbs energy for any amount of material is  $G^E$  and, per mole of particles, is  $g^E$ . Thus

$$\Delta_m G = \Delta_m G^I + G^E \quad (\text{I-4})$$

$$g^E = G^E/\sum_i n_i \quad (\text{I-5})$$

Since the symbol  $\gamma_i$  is commonly used<sup>174</sup> for activity coefficients on a mole fraction basis, we follow that practice.<sup>169</sup> Superscripts  $x$  and  $m$  can be used to distinguish the mole fraction and molality bases whenever there is ambiguity. Since all activity coefficients in this appendix, with one exception, are on a mole fraction basis, we omit the  $x$ . The exception is Equation I-12b where  $\gamma^m$  is shown for the molality-based quantity.

The activities  $a_j$  and activity coefficients  $\gamma_j$  are related by

$$\ln a_j = \ln(x_j \gamma_j/x_j^0) \quad (\text{I-6a})$$

and for a salt MX

$$\ln a_{MX} = \ln(a_M a_X) \quad (\text{I-6b})$$

Differentiation of  $G^E$  with respect to  $n_j$  at constant  $T$ ,  $P$ , and other  $n_i$  yields the excess chemical potential  $\mu_j^E$ ; also

$$\mu_j^E = RT \ln \gamma_j \quad (\text{I-7})$$

$$g^E = \sum_i x_i \mu_i^E = RT \sum_i x_i \ln \gamma_i \quad (\text{I-8})$$

For electrolytes the activities and activity coefficients can ordinarily be measured only

for neutral combinations of ions. Thus for a salt mixture containing  $M^+$ ,  $N^+$ ,  $X^-$ ,  $Y^-$  one can determine  $(a_X a_Y)$ ,  $(a_M a_N)$ ,  $(a_N a_X)$ , and  $(a_M a_Y)$  but not any of the individual  $a$ 's.

For systems with all pure components liquid at the conditions of interest, the normal standard states are the pure liquid components. This yields  $\gamma_j = 1$  and  $a_j = 1$  for the pure liquid in Equation I-6. Even if a component melts at a somewhat higher temperature, it may be useful to take the supercooled liquid as the reference state; this procedure was successful for the system NaCl-H<sub>2</sub>O at temperatures well below the melting point of NaCl.

Where there are more than one species of both cation and anion, the reference basis of pure fused salts becomes ambiguous. Thus an equimolar system of Na<sup>+</sup>, K<sup>+</sup>, Cl<sup>-</sup>, NO<sub>3</sub><sup>-</sup> can be referenced to NaCl and KNO<sub>3</sub> or to KCl and NaNO<sub>3</sub>. In some cases there is a preference. Thus in a system dominated by NaCl the reference should be to pure NaCl and to the Na<sup>+</sup> salts of other anions and the Cl<sup>-</sup> salts of other cations. However, in other cases an arbitrary choice may be required.

There are various reasons for wishing to define an infinitely dilute reference state on a mole fraction basis and for relating it to the standard state on a molality basis. While we first define an infinitely dilute solute state for either a pure or a mixed solvent, we will consider thereafter only the case with a pure solvent which will be taken as component 1. We follow Prausnitz<sup>174</sup> and others in using the symbol  $\gamma_j^*$  for an activity coefficient based on the infinitely dilute reference state; thus on a mole fraction basis

$$\begin{aligned} \gamma_j &\rightarrow 1 \text{ as } x_j \rightarrow x_j^0 \\ \gamma_j^* &\rightarrow 1 \text{ as } x_j \rightarrow 0, \gamma_j \rightarrow 1.0 \\ (\gamma_j^*/\gamma_j) &= \lim_{x_j \rightarrow 0} \gamma_j^{-1} \end{aligned} \quad (I-9)$$

where  $x_j^0$  is the value for the pure fused salt.

In the limit of very small fraction of species  $j$  in a single molecular solvent, the mole fraction becomes a mole ratio.

$$x_j \rightarrow n_j/n_1 \text{ as } x_j \rightarrow 0$$

Under these conditions the molality is

$$m_j = (n_j/n_1)(1000/M_1) \quad (I-10)$$

where  $M_1$  is the molecular weight of the solvent. If one has a mixed solvent,  $n_1$  is replaced by the total number of moles of solvent and  $M_1$  by the mean molecular weight. The ratio of  $m_j$  to  $x_j$  is

$$m_j/x_j = 1000/M_1 \quad (I-11)$$

with  $M_1$  replaced by a mean solvent molecular weight when required.

The chemical potential must be the same for a given composition on either basis. Thus, in the very dilute range and with  $\gamma_j^0$  the activity coefficient on a molality basis

$$\mu_j(\text{mole fraction}) = \mu_j^0(\text{mole fraction}^*) + RT \ln(x_j \gamma_j^*) \quad (I-12a)$$

$$\mu_j(\text{molality}) = \mu_j^0(\text{molality}) + RT \ln(m_j \gamma_j^0) \quad (I-12b)$$

$$\mu_j^0(\text{mole fraction}^*) = \mu_j^0(\text{molality}) + RT \ln(1000/M_1) \quad (I-12c)$$

where the last equation gives the conversion from the conventional standard Gibbs energy on a molality basis to that for the mole fraction basis retaining the infinitely dilute reference state. Again these  $\mu$ 's are ordinarily measurable only for neutral combinations of ions.

The chemical potential for the pure liquid standard state may also be related to that for the infinitely dilute reference state. Take a salt MX as an example:

$$\mu_{MX} = \mu^0(MX, \text{liq}) + RT \ln(x_M x_X \gamma_M \gamma_X / x_M^0 x_X^0) \quad (\text{I-13a})$$

$$= \mu_{MX}^0(\text{mole fraction}^*) + RT \ln(x_M x_X \gamma_M^* \gamma_X^*) \quad (\text{I-13b})$$

$$\mu_{MX}^0(\text{mole fraction}^*) = \mu^0(MX, \text{liq}) - RT \ln(x_M^0 x_X^0 \gamma_M^{*0} \gamma_X^{*0}) \quad (\text{I-13c})$$

where  $\gamma_j^{*0}$  is the value of  $\gamma_j^*$  in the pure liquid MX. For a neutral molecular liquid these equations simplify for a single particle and  $x_j^0$  is then unity.

We turn now to the excess Gibbs energy which arises from inequalities in interparticle forces. If there is a substantial ionic concentration, interionic forces are effectively screened from the  $R^{-2}$  long range to short range. Then interionic forces can be combined with all other interparticle forces on the same basis and one expects the same type of expression for excess Gibbs energy as was found for nonelectrolytes. At very low ionic concentration, however, the alternating charge pattern and its accompanying screening effect is lost and the long-range nature of ionic forces must be considered. This is the effect described by the Debye-Hückel treatment. For the full range of composition one expects the excess Gibbs energy to comprise two terms: a short-range force term  $G^S$  and a Debye-Hückel term  $G^{DH}$ ; thus

$$G^E = G^S + G^{DH} \quad (\text{I-14a})$$

$$g^E = g^S + g^{DH} \quad (\text{I-14b})$$

where the last equation refers to 1 mol of particles. The logarithms of the activity coefficients are similarly sums of terms for short-range forces and for the Debye-Hückel effect.

## B. EXCESS GIBBS ENERGY FROM SHORT-RANGE FORCES

There is an extensive literature concerning semiempirical or purely empirical expressions for the excess Gibbs energy of nonelectrolytes. Prausnitz<sup>174</sup> discusses the merits of many of these equations. Among the simplest and most generally effective are the van Laar equation, which involves two parameters for a binary system, and the various extensions of the Margules equation, which comprise series expansions. A "three-suffix" Margules equation also involves two parameters for a binary system. Either equation can be generalized to multiple-component systems, but the Margules system, as generalized by Wohl,<sup>175,176</sup> is more flexible and has been found to be more successful in various tests on nonelectrolytes.<sup>177</sup>

A general Margules expansion can be written

$$g^S/RT = \sum_i \sum_j a_{ij} x_i x_j + \sum_i \sum_j \sum_k a_{ijk} x_i x_j x_k + \dots \quad (\text{I-15})$$

where  $a$ 's with all suffixes equal are zero. If there are only two components, one has

$$\begin{aligned} g^S/RT &= x_1 x_2 (2a_{12} + 3x_1 a_{112} + 3x_2 a_{122}) \\ &= x_1 x_2 [w_{12} + u_{12}(x_1 - x_2)] \end{aligned} \quad (\text{I-16})$$

with

$$w_{12} = 2a_{12} + (3/2)(a_{112} + a_{122}) \quad (\text{I-17a})$$

$$u_{12} = (3/2)(a_{112} - a_{122}) \quad (\text{I-17b})$$

where the second line for Equation I-16 shows that only two of the three parameters in the first line are independent.

If one generalizes the definitions of Equation I-17 and defines a third quantity related to  $a_{123}$ , one can write for the general case

$$g^S/RT = \sum_j \sum_{i \neq j} x_i x_j [w_{ij} + u_{ij}(x_i - x_j)] + \sum_k \sum_{j \neq i} x_i x_j x_k C_{ijk} - g^{SO}/RT \quad (\text{I-18a})$$

$$w_{ij} = 2a_{ij} + (3/2)(a_{iij} + a_{ijj}) \quad (\text{I-18b})$$

$$u_{ij} = (3/2)(a_{iij} - a_{ijj}) \quad (\text{I-18c})$$

$$C_{ijk} = 6a_{ijk} - (3/2)(a_{iij} + a_{ijj} + a_{iik} + a_{ikk} + a_{jik} + a_{jkk}) \quad (\text{I-18d})$$

Note that interchange of subscripts leaves  $w_{ij}$  or  $C_{ijk}$  unchanged but changes the sign of  $u_{ij}$ . Also,  $g^{SO}$  is the value for the same material in the reference states of the various components. The values are zero for neutral species but not for electrolytes if the pure-fused-salt reference state is used. In that case a term involving  $w_{M,X}$  remains for a pure fused salt MX.

A notation used by Wohl<sup>176</sup> and others<sup>174,177</sup> is related by  $A'_{ji} = w_{ij} - u_{ij}$  and  $A'_{ij} = w_{ij} + u_{ij}$ . We prefer a form in which one parameter ( $u_{ij}$ ) will become zero in a symmetrical case rather than two parameters becoming equal. Our third parameter,  $C_{ijk}$ , is equivalent, except for sign, to the  $C^*$  or  $Q'$  used by others. Here we prefer a positive sign for  $a_{ijk}$  in Equation I-18a.

The expression for the short-range-force contribution to an activity coefficient is obtained by differentiation of Equation I-18a.

$$\begin{aligned} \ln \gamma_i^S &= \sum_j' x_j [(1 - x_i)w_{ij} + (2x_i - 2x_i^2 + 2x_i x_j - x_j)u_{ij}] \\ &\quad - \sum_k \sum_{j \neq i} x_j x_k [w_{jk} + 2(x_j - x_k)u_{jk} - (1 - 2x_j)C_{ijk}] \\ &\quad - \sum_{l \neq k \neq j} \sum_{i \neq l} 2x_i x_k x_l C_{ikl} - \gamma_i^{SO} \end{aligned} \quad (\text{I-19a})$$

The prime on the summations is a reminder that terms with any two indices equal are omitted and that neither  $j$  nor  $k$  nor  $l$  may equal  $i$  in the multiple sums. The last term is a reference-state correction which is zero for the solvent. For salts on the pure liquid reference basis, it is best considered for the complete salts. For ions or neutral solutes on an infinitely dilute reference basis, it has the value

$$\ln \gamma_i^{*SO} = w_{li} + u_{li} \quad (\text{I-19b})$$

Before concluding this section it is interesting to consider a few examples which illustrate the extent to which the parameters measurable from simple systems are able to determine the properties of more complex systems. Consider first the common ion mixture of two salts MX and NX with a cation fraction  $F$  of ion M. Then the mole fractions are  $x_M = F/2$ ,  $x_N = (1 - F)/2$ ,  $x_X = 1/2$ , and

$$\ln(\gamma_M\gamma_X)^S = (1/4)\{2w_{M,X} + (1 - F)^2[2w_{M,N} + C_{M,N,X} - u_{M,X} - u_{N,X} - (1 - 4F)u_{M,N}]\} - \ln(\gamma_M\gamma_X)^{SC} \quad (I-20)$$

For pure liquid MX,  $F = 1$ ,  $\gamma_M^S = \gamma_X^S = 1$ , and  $\ln(\gamma_M\gamma_X)^{SC} = w_{M,X}/2$ . It is convenient to define

$$W_{MX,NX} = (2w_{M,N} + C_{M,N,X} - u_{M,X} - u_{N,X})/4 \quad (I-21a)$$

$$U_{M,N} = u_{M,N}/4 \quad (I-21b)$$

whereupon

$$g^S/RT = F(1 - F)[W_{MX,NX} - (1 - 2F)U_{M,N}]/2 \quad (I-22a)$$

$$\ln(\gamma_M\gamma_X)^S = (1 - F)^2[W_{MX,NX} - (1 - 4F)U_{M,N}] \quad (I-22b)$$

$$\ln(\gamma_N\gamma_X)^S = F^2[W_{MX,NX} + (4F - 3)U_{M,N}] \quad (I-22c)$$

In the transformation from Equation I-22b to I-22c, wherein M and N are interchanged as are F and (1 - F),  $W_{MX,NX}$  remains unchanged, but the term in  $U_{M,N}$  changes sign because  $U_{N,M} = -U_{M,N}$ . Measurements at a variety of values of F allow the two parameters  $W_{MX,NX}$  and  $U_{M,N}$  to be determined.

Consider next the binary mixture of a neutral species, 1, with a single symmetrical ionic component MX. Now  $x_M = x_X = (1 - X_1)/2$  and

$$g^S/RT = (1/4)x_1(1 - x_1)[2w_{1,M} + 2w_{1,X} - w_{M,X} + (3x_1 - 1)(u_{1,M} + u_{1,X}) + (1 - x_1)C_{1,M,X}] \quad (I-23a)$$

$$\ln \gamma_1^S = (1/4)(1 - x_1)^2[2w_{1,M} + 2w_{1,X} - w_{M,X} + (6x_1 - 1)(u_{1,M} + u_{1,X}) + (1 - 2x_1)C_{1,M,X}] \quad (I-23b)$$

$$\ln(\gamma_M\gamma_X)^S = x_1^2[w_{1,M} + w_{1,X} - w_{M,X}/2 + (3x_1 - 2)(u_{1,M} + u_{1,X}) + (1 - x_1)C_{1,M,X}] \quad (I-23c)$$

Now define

$$W_{1,MX} = (2w_{1,M} + 2w_{1,X} - w_{M,X} + 2u_{1,M} + 2u_{1,X})/4 \quad (I-24a)$$

$$U_{1,MX} = -(3/4)(u_{1,M} + u_{1,X}) + C_{1,M,X}/4 \quad (I-24b)$$

whereupon

$$g^S/RT = x_1(1 - x_1)[W_{1,MX} + (1 - x_1)U_{1,MX}] \quad (I-25a)$$

$$\ln \gamma_1^S = (1 - x_1)^2[W_{1,MX} + (1 - 2x_1)U_{1,MX}] \quad (I-25b)$$

$$\ln(\gamma_M\gamma_X)^S = x_1^2[2W_{1,MX} + 4(1 - x_1)U_{1,MX}] \quad (I-25c)$$

Again we note in Equations I-24a and I-24b the combinations of the original parameters that can be measured with this system.

From Equation I-9 one finds for the infinitely dilute reference basis

$$\ln(\gamma_{x_1}^* \gamma_{x_2}^*)^S = 2(x_1^2 - 1)W_{1,MX} + 4x_1^2(1 - x_1)U_{1,MX} \quad (I-25d)$$

Next, consider the three-component system with a neutral species (1) and two symmetrical salts with a common ion MX, NX and with cation fraction  $F$  of M. Also define a total mole fraction of ions  $x_1 = (1 - x_1)$  whereupon  $x_M = Fx_1/2, x_N = (1 - F)x_1/2$ , and  $x_X = x_1/2$  and use the definitions of Equations I-23a, I-23b, I-24a, and I-24b.

$$g^S/RT = x_1 x_1 \{FW_{1,MX} + (1 - F)W_{1,NX} + x_1 [FU_{1,MX} + (1 - F)U_{1,NX} + F(1 - F)Q_{1,MX,NX}]\} + x_1^2 F(1 - F)[W_{MX,NX} + x_1(2F - 1)U_{M,N}]/2 \quad (I-26a)$$

$$\begin{aligned} \ln \gamma_1^S &= x_1^2 \{FW_{1,MX} + (1 - F)W_{1,NX} - F(1 - F)W_{MX,NX}/2 \\ &+ (x_1 - x_1)[FU_{1,MX} + (1 - F)U_{1,NX} + F(1 - F)Q_{1,MX,NX}] \\ &+ x_1 F(1 - F)(1 - 2F)U_{M,N}\} \end{aligned} \quad (I-26b)$$

$$\begin{aligned} \ln(\gamma_M \gamma_N)^S &= 2x_1 \{(1 - x_1 F)W_{1,MX} + x_1(1 - F + 2Fx_1)U_{1,MX} \\ &- x_1(1 - F)[W_{1,NX} + (x_1 - x_1)U_{1,NX} - (1 - 2x_1 F)Q_{1,MX,NX}]\} \\ &+ x_1(1 - F)\{(1 - x_1 F)W_{MX,NX} + x_1[3F - 1 + 2x_1 F(1 - 2F)]U_{M,N}\} \end{aligned} \quad (I-26c)$$

$$\begin{aligned} \ln(\gamma_M^* \gamma_N^*)^S &= 2[x_1(1 - x_1 F) - 1]W_{1,MX} + 2x_1 x_1 \{(1 - F + 2Fx_1)U_{1,MX} \\ &- (1 - F)[W_{1,NX} + (x_1 - x_1)U_{1,NX} - (1 - 2x_1 F)Q_{1,MX,NX}]\} \\ &+ x_1(1 - F)\{(1 - x_1 F)W_{MX,NX} + x_1[3F - 1 + 2x_1 F(1 - 2F)]U_{M,N}\} \end{aligned} \quad (I-26d)$$

$$Q_{1,MX,NX} = (u_{1,M} + u_{1,N} + C_{1,M,N})/4 + (u_{M,X} + u_{N,X} - C_{M,N,X})/8 \quad (I-26e)$$

Thus we note that, for this ternary system, all but one of the parameters of Equation I-26 can be determined from the binary systems. The additional parameter  $Q_{1,MX,NX}$  enters only with rather small coefficients and its effect may be rather small, but that remains to be determined from measurements on real systems.

A two-component system with an unsymmetrical electrolyte  $MX_2$  with a solvent can be treated without ambiguity with the infinitely dilute reference state. We illustrate this case with only the binary interaction terms. Now  $x_M = (1 - x_1)/3$  and  $x_X = 2(1 - x_1)/3$ .

$$g^S/RT = x_1(1 - x_1)(3w_{1M} + 6w_{1X} - 2w_{MX})/9 \quad (I-27a)$$

$$\ln \gamma_1^S = (1 - x_1)^2(3w_{1M} + 6w_{1X} - 2w_{MX})/9 \quad (I-27b)$$

$$\ln \gamma_M^{*S} = \left(\frac{x_1^2}{3} + \frac{2x_1}{3} - 1\right)w_{1M} - \frac{2x_1(1 - x_1)}{3}w_{1X} + \frac{2(1 - x_1)(2 + x_1)}{9}w_{MX} \quad (I-27c)$$

$$\ln \gamma_X^{*S} = \left(\frac{2x_1^2}{3} + \frac{x_1}{3} - 1\right)w_{1X} - \frac{x_1(1 - x_1)}{3}w_{1M} + \frac{(1 - x_1)(1 + 2x_1)}{9}w_{MX} \quad (I-27d)$$

$$\ln(\gamma_M^* \gamma_X^*)^S = (x_1^2 - 1)(3w_{1M} + 6w_{1X} - 2w_{MX})/3 \quad (I-27e)$$

Note that the same combination of  $w_{1M}, w_{1X}, w_{MX}$  appears in three of these equations but not in the other two.



Another important type of three-component systems involves two neutral species numbered 1 and 2, and one ionic species MX. Now  $x_1 = 1 - x_1 - x_2 = 2x_M = 2x_X$ . We give only the excess Gibbs energy in this case, but the activity coefficients can be derived by differentiation.

$$\begin{aligned} g^S/RT = & x_1x_2[w_{1,2} + (x_1 - x_2)u_{1,2} + x_1Z_{1,2,MX}] \\ & + x_1x_1[W_{1,MX} + (2/3)(1 - x_1 + x_1/2)U_{1,MX}] + x_2x_1[W_{2,MX} \\ & + (2/3)(1 - x_2 + x_1/2)U_{2,MX}] \end{aligned} \quad (I-28a)$$

$$Z_{1,2,MX} = (C_{1,2,M} + C_{1,2,X})/2 - (C_{1,M,X} + C_{2,M,X})/6 \quad (I-28b)$$

Again, only one new ternary parameter appears in addition to those for the binaries in Equations I-16 and I-25.

While it would be desirable to present an equation for an indefinitely complex system, this becomes very involved when the ternary terms are included. Thus we give only the general equation for binary terms. Now the mole fractions of neutral species are  $x_n, x_n, \dots$  and the total mole fraction of ions  $x_1 = 1 - \sum x_n$ . For the ions the cation fractions are  $F_c, F_c, \dots$  and the anion fractions are  $F_a, F_a, \dots$ . Then

$$\begin{aligned} g^S/RT = & \sum_{n' > n} x_n x_n w_{n'n} + \sum_n \sum_c \sum_a x_n x_1 F_c F_a W_{n,ca} \\ & + (x_1^2/2) \left[ \sum_{c' > c} \sum_a F_{c'} F_c F_a W_{c'a,ca} + \sum_{a' > a} \sum_c F_a F_a F_c W_{ca',ca} \right] \end{aligned} \quad (I-29)$$

It is evident that all of the parameters in Equation I-29 can be determined from two-component systems. Presumably, all ternary parameters for the general system could be determined from the full array of three-component systems.

For practical work with specific systems of four (or possibly a few more) components, the expression for the excess Gibbs energy with ternary terms can be derived more easily than the completely general expression. The types of terms will be those appearing in Equations I-26 and I-28, together with a few others if there are more than two neutral species or more than two salts.

The equations of this section are limited to second- and third-order Margules terms. This has been found to be adequate for most systems, but fourth- or higher order terms can be added when needed. It seems unlikely that the full array of all possible fourth-order terms will be required; hence it seems best to add just the particular term or terms required to fit the experimental data for a particular system. This was done by Clegg and Brimblecombe<sup>178</sup> for nitric acid.

### C. DEBYE-HÜCKEL EFFECT

In dilute ionic solutions the distribution changes from a random pattern at extremely low concentration to one of alternating positive and negative charges at moderately higher concentration. Debye and Hückel gave a simple treatment which describes this effect. The limiting term at low concentration is given rigorously; the effect at higher concentration is given approximately. There are various alternate forms with respect to the higher concentration range. We choose a form which has its origin in the pressure equation of statistical mechanics and has been most satisfactory in empirical tests.<sup>1,170</sup>

The basic variable is the ionic concentration weighted by the square of the charge. Concentration is replaced by molality for most work at moderate dilution, but is replaced by mole fraction for our present problem of systems continuously miscible to the fused salt. Thus, ionic strength on a mole fraction basis is defined as

$$I_{\kappa} = (1/2) \sum_i x_i z_i^2 \quad (\text{I-30})$$

where  $z_i$  is the charge on the  $i$ th species of ions; and for singly charged ions  $I_{\kappa} = x_i/2$ . Then the activity coefficient of a single uncharged solvent is<sup>65,170</sup>

$$(\ln \gamma_1)^{\text{DH}} = 2A_{\kappa} I_{\kappa}^2 / (1 + \rho I_{\kappa}^2) \quad (\text{I-31})$$

The excess Gibbs energy is

$$g^{\text{DH}}/RT = -(4A_{\kappa} I_{\kappa} / \rho) \ln[(1 + \rho I_{\kappa}^2) / (1 + \rho(I_{\kappa}^0)^2)] \quad (\text{I-32})$$

where  $I_{\kappa}^0$  represents  $I_{\kappa}$  for pure fused salt which is  $1/2$  for singly charged ions. The Debye-Hückel parameter  $A_{\kappa}$  is

$$A_{\kappa} = (1/3)(2\pi N_A d_1 / M_1)^{1/2} (e^2 / 4\pi \epsilon_0 \epsilon kT)^{3/2} \quad (\text{I-33})$$

where  $d_1$ ,  $M_1$ , and  $\epsilon$  are the density, molecular weight, and dielectric constant (relative permittivity) of the solvent while  $N_A$  is Avogadro's number,  $e$  is the electronic charge,  $k$  is Boltzmann's constant, and  $\epsilon_0$  is the permittivity of free space. Most of the literature on electrolytes is now written for esu's; in that case  $\epsilon_0 = (4\pi)^{-1}$ .

A Gibbs-Duhem transformation of Equation I-31 or differentiation of Equation I-32 yields the mean activity coefficient of an ionic component of charge  $z_i$  for the infinitely dilute reference state

$$\begin{aligned} (\ln \gamma_i^*)^{\text{DH}} = & -z_i^2 A_{\kappa} \{ (2/\rho) \ln(1 + \rho I_{\kappa}^2) \\ & + I_{\kappa}^2 (1 - 2I_{\kappa} / z_i^2) / (1 + \rho I_{\kappa}^2) \} \end{aligned} \quad (\text{I-34})$$

or for the pure fused salt reference state

$$\begin{aligned} (\ln \gamma_i)^{\text{DH}} = & -z_i^2 A_{\kappa} \{ (2/\rho) \ln[(1 + \rho I_{\kappa}^2) / (1 + \rho(I_{\kappa}^0)^2)] \\ & + I_{\kappa}^2 (1 - 2I_{\kappa} / z_i^2) / (1 + \rho I_{\kappa}^2) \} \end{aligned} \quad (\text{I-35})$$

Here  $I_{\kappa}^0$  is the ionic strength of the pure fused salt which is  $z_i^2/2$  for the MX type. One may note that when  $z_i^2$  reduces to zero, Equations I-34 and I-35 reduce to Equation I-31.

Many ionic systems are miscible to high mole fraction or to the fused salt only at high temperatures, and in most of these cases the measurements are of limited precision. Equations I-31 through I-35 are adequate in these cases. Indeed, a precise optimization of the parameter  $\rho$  is not required. It is important, however, to maintain consistency between  $\rho$  and the parameters for the short-range terms since there is considerable correlation between some of them. Thus, it was possible<sup>66</sup> to treat the mixed electrolyte  $\text{LiNO}_3\text{-KNO}_3\text{-H}_2\text{O}$  over the range 373 to 436 K with the constant value  $\rho = 14.9$ . For work of the highest precision, however, the adjustment of  $\rho$  is more sensitive. Then, if the values of  $\rho$  for two or more pure electrolytes differ, one cannot use Equations I-31 to I-35 for a multicomponent system comprising these electrolytes.

The problem just described concerns the behavior of equations at low to moderate concentrations and was recognized in research using the molality system. The most successful solution was that described in this chapter in which an additional, ionic strength-dependent term was introduced. The analogous treatment for the mole fraction system is described immediately below. An alternate approach using different values of  $\rho$  is presented subsequently.

Equation 62 for the osmotic coefficient, when converted to the activity coefficient of the solvent and rearranged, yields

$$\ln \gamma_1 = 2\Omega^{1/2}A_\phi I^{3/2}/(1 + bI^{1/2}) + \sum_c \sum_a m_c m_a \beta_{ca}^{(1)} \exp(-\alpha I^{1/2}) + \sum_c \sum_a m_c m_a \beta_{ca}^{(0)} + \dots \quad (I-36)$$

Here the terms in  $\beta_{ca}^{(0)}$  and all subsequent terms correspond to the short-range-force terms given in an earlier section of this appendix and need not concern us further. The first term becomes Equation I-31 when  $I$  is converted to  $I_x$ , whereupon  $b$  becomes  $\rho$  and  $\Omega^{1/2}A_\phi$  becomes  $A_x$ . It is the terms in the second sum,  $\beta_{ca}^{(1)} \exp(-\alpha I^{1/2})$ , that need to be converted to the mole fraction system and added to Equation I-31. Then the D-H contribution to the activity coefficient of the solvent becomes

$$\ln \gamma_1^{DH} = \frac{2A_x I_x^{3/2}}{1 + \rho I_x^{1/2}} + \sum_c \sum_a x_c x_a B_{ca} \exp(-\alpha I_x^{1/2}) \quad (I-37)$$

The parameter  $\alpha$  can be written  $\alpha_x$  if desired to avoid ambiguity; its magnitude is expected to be larger than the  $\alpha$  in the molality equations by the factor  $\Omega^{1/2} = 7.45$ ; thus values in the range 10 to 15 are expected. Each parameter  $B_{ca}$  is clearly specific to the electrolyte  $ca$ . From the experience in the molality system, it seems likely that a constant value of  $\alpha$  will suffice for a variety of electrolytes, but different values can be used without significant complications.

Standard transformations then yield for the excess Gibbs energy and the activity coefficient of an ion the following:

$$\frac{g^{DH}}{RT} = -\frac{4A_x I_x}{\rho} \ln \left[ \frac{1 + \rho I_x^{1/2}}{1 + \rho (I_x^0)^{1/2}} \right] + \sum_c \sum_a x_c x_a B_{ca} g(\alpha I_x^{1/2}) \quad (I-38)$$

$$g(x) = 2[1 - (1 + x)\exp(-x)]/x^2 \quad (50)$$

$$\begin{aligned} (\ln \gamma_M^*)^{DH} = & -z_M^2 A_x \left[ \frac{2}{\rho} \ln(1 + \rho I_x^{1/2}) + \frac{I_x^{1/2}(1 - 2I_x/z_M^2)}{1 + \rho I_x^{1/2}} \right] \\ & + \sum_a x_a B_{Ma} g(\alpha I_x^{1/2}) - \sum_c \sum_a x_c x_a B_{ca} \left[ \frac{z_M^2 g(\alpha I_x^{1/2})}{2I_x} \right. \\ & \left. + \left( 1 - \frac{z_M^2}{2I_x} \right) \exp(-\alpha I_x) \right] \quad (I-39) \end{aligned}$$

Here the function  $g(x)$  is the same as that obtained in the molality system. For an anion  $x$ , one changes  $M$  to  $X$ ,  $c$  to  $a$ , and  $a$  to  $c$  in Equation I-39. The change of the activity coefficient for an ion to that based on the pure-fused-salt standard state is readily obtained if desired.

When the need arises, this system can be implemented by fitting the array of accurate data for several pure electrolytes using a common value of  $\rho$  but individual values of  $B_{ca}$  and the various short-range-force parameters. Tests should be made using either a common value of  $\alpha$  or individual values for each solute; then a choice can be made. After these parameters are all established, the equations can be applied to multicomponent systems.

It is possible, as an alternative, to devise a system using different values of  $\rho_{ca}$  for different electrolytes. For equations in molality, this was done by Scatchard et al.<sup>179</sup> It is assumed that  $\rho$  is related to the distance of closest approach of ions of opposite sign, i.e.,

$\rho$  is associated with interactions c-a, c-a', c'-a, etc., and not c-c' or a-a' in mixed electrolytes. Thus, we need to transform the expression of Equation I-30 for  $I_\kappa$  into a sum over the various cations c and anions a; the result is

$$I_\kappa = \sum_c \sum_a x_c z_c x_a |z_a| (z_c + |z_a|) / \sum_i x_i |z_i| \quad (\text{I-40})$$

where the sum over  $i$  in the denominator includes all ions. Then, one can use this expression for  $I_\kappa$  to weight different terms in ca in Equation I-32 for the excess Gibbs energy. We define a function of  $\rho_{ca}$  and  $I_\kappa$  as follows:

$$Y_{ca} = \frac{1}{\rho_{ca}} \ln \left[ \frac{1 + \rho_{ca} I_\kappa^{1/2}}{1 + \rho_{ca} (I_{\kappa,ca}^0)^{1/2}} \right] \quad (\text{I-41})$$

where  $I_{\kappa,ca}^0$  is the ionic strength of pure liquid electrolyte ca. Then

$$\frac{g^{DH}}{RT} = -4A_\kappa \sum_c \sum_a x_c z_c x_a |z_a| (z_c + |z_a|) Y_{ca} / \sum_i x_i |z_i| \quad (\text{I-42})$$

One notes that if all values of  $\rho_{ca}$  are the same, this reduces to Equation I-32.

Activity coefficients can now be obtained by appropriate differentiation. For a neutral solvent, one obtains

$$\ln \gamma_i = \frac{2A_\kappa}{\sum_i x_i |z_i|} \sum_c \sum_a \frac{x_c z_c x_a |z_a| (z_c + |z_a|) I_\kappa^{1/2}}{1 + \rho_{ca} I_\kappa^{1/2}} \quad (\text{I-43})$$

or for a cation M

$$\begin{aligned} \ln \gamma_M = & -\frac{A_\kappa}{\sum_i x_i |z_i|} \sum_a x_a |z_a| \left\{ z_M (z_M + |z_a|) Y_{Ma} \right. \\ & \left. + \sum_c x_c z_c (z_c + |z_a|) \left[ \frac{z_M^2 - 2I_\kappa}{4I_\kappa^{1/2} (1 + \rho_{ca} I_\kappa^{1/2})} - \frac{z_M Y_{ca}}{\sum_i x_i |z_i|} \right] \right\} \quad (\text{I-44}) \end{aligned}$$

For the infinitely dilute standard state, one omits the denominator in  $Y_{ca}$ , i.e.,

$$Y_{ca}^* = \rho_{ca}^{-1} \ln(1 + \rho_{ca} I_\kappa^{1/2}) \quad (\text{I-45})$$

whereupon the same expression in Equation I-44 applies. For an anion X one changes M to X,  $z_M$  to  $|z_X|$ , c to a, and a to c in Equation I-44. The mean activity coefficient  $\gamma_\pm$  of an electrolyte MX is readily obtained from the expressions for  $\gamma_M$  and  $\gamma_X$ .

Eventually, as highly accurate data are obtained for various electrolytes over a wide range of mole fraction, I expect that Equations I-37 to I-39 with the terms in  $B_{ca}$  will prove to be most effective. This is based on experience with the equations in the molality system. In this system even more terms can be added as required in special situations. The results for multicomponent systems are now extensive and very satisfactory. In the meantime, the equations with different  $\rho_{ca}$  values will be useful since they do not require reevaluation of parameters for an extensive array of data.

In addition to the systems  $\text{HNO}_3\text{-H}_2\text{O}$ <sup>178</sup> and  $\text{LiNO}_3\text{-KNO}_3\text{-H}_2\text{O}$ <sup>66</sup> already mentioned, these mole fraction-based equations have been successfully applied to a number of other systems;<sup>180</sup> several are discussed in Chapters 6 and 7.

## REFERENCES

1. **Pitzer, K. S.**, Thermodynamics of electrolytes. I. Theoretical basis and general equations, *J. Phys. Chem.*, 77, 268, 1973.
2. **Pitzer, K. S. and Mayorga, G.**, Thermodynamics of electrolytes. II. Activity and osmotic coefficients for strong electrolytes with one or both ions univalent, *J. Phys. Chem.*, 77, 2300, 1973; 78, 2698, 1974.
3. **Pitzer, K. S. and Mayorga, G.**, Thermodynamics of electrolytes. III. Activity and osmotic coefficients for 2-2 electrolytes, *J. Solution Chem.*, 3, 539, 1974.
4. **Pitzer, K. S. and Kim, J. J.**, Thermodynamics of electrolytes. IV. Activity and osmotic coefficients for mixed electrolytes, *J. Am. Chem. Soc.*, 96, 5701, 1974.
5. **Pitzer, K. S.**, Thermodynamics of electrolytes. V. Effects of higher-order electrostatic terms, *J. Solution Chem.*, 4, 249, 1975.
6. **Pitzer, K. S. and Silvester, L. F.**, Thermodynamics of electrolytes. VI. Weak electrolytes including  $H_2PO_4$ , *J. Solution Chem.*, 5, 269, 1976.
7. **Pitzer, K. S., Roy, R. N., and Silvester, L. F.**, Thermodynamics of electrolytes. VII. Sulfuric acid, *J. Am. Chem. Soc.*, 99, 4930, 1977.
8. **Pitzer, K. S., Peterson, J. R., and Silvester, L. F.**, Thermodynamics of electrolytes. IX. Rare earth chlorides, nitrates, and perchlorates, *J. Solution Chem.*, 7, 45, 1978.
9. **Silvester, L. F. and Pitzer, K. S.**, Thermodynamics of electrolytes. X. Enthalpy and the effects of temperature on the activity coefficients, *J. Solution Chem.*, 7, 327, 1978.
10. **Pitzer, K. S. and Silvester, L. F.**, Thermodynamics of electrolytes. XI. Properties of 3:2, 4:2, and other high-valence types, *J. Phys. Chem.*, 82, 1239, 1978.
11. **Bradley, D. J. and Pitzer, K. S.**, Thermodynamics of electrolytes. XII. Dielectric properties of water and Debye-Huckel parameters to 350°C and 1 kbar, *J. Phys. Chem.*, 83, 1599, 1979; 87, 3798, 1983.
12. **Rogers, P. S. Z. and Pitzer, K. S.**, High-temperature thermodynamic properties of aqueous sodium sulfate solutions, *J. Phys. Chem.*, 85, 2886, 1981; 86, 2110, 1982.
13. **Peiper, J. C. and Pitzer, K. S.**, Thermodynamics of aqueous carbonate solutions including mixtures of mixed carbonate, bicarbonate, and chloride, *J. Chem. Thermodyn.*, 14, 613, 1982.
14. **Rogers, P. S. Z. and Pitzer, K. S.**, Volumetric properties of aqueous sodium chloride solutions, *J. Phys. Chem. Ref. Data*, 11, 15, 1982.
15. **Pitzer, K. S.**, Thermodynamics of unsymmetrical electrolyte mixtures: enthalpy and heat capacity, *J. Phys. Chem.*, 87, 2360, 1983.
16. **Roy, R. N., Gibbons, J. J., Peiper, J. C., and Pitzer, K. S.**, Thermodynamics of the unsymmetrical mixed electrolyte  $HCl-LaCl_3$ , *J. Phys. Chem.*, 87, 2365, 1983; 90, 3452, 1986.
17. **Pitzer, K. S., Peiper, J. C., and Busey, R. H.**, Thermodynamic properties of aqueous sodium chloride solutions, *J. Phys. Chem. Ref. Data*, 13, 1, 1984.
18. **Roy, R. N., Gibbons, J. J., Williams, R., Godwin, L. G., Baker, G., Simonson, J. M., and Pitzer, K. S.**, Thermodynamics of aqueous carbonate solutions. II. Mixtures of potassium carbonate, bicarbonate, and chloride, *J. Chem. Thermodyn.*, 16, 303, 1984.
19. **Pitzer, K. S., Olsen, J., Simonson, J. M., Roy, R. N., Gibbons, J. J., and Rowe, L. A.**, Thermodynamics of aqueous magnesium and calcium bicarbonates and mixtures with chloride, *J. Chem. Eng. Data*, 30, 14, 1985.
20. **Phutela, R. C. and Pitzer, K. S.**, Thermodynamics of electrolyte mixtures. Enthalpy and the effect of temperature on the activity coefficient, *J. Solution Chem.*, 15, 649, 1986.
21. **Phutela, R. C. and Pitzer, K. S.**, Heat capacity and other thermodynamic properties of aqueous magnesium sulfate to 473 K, *J. Phys. Chem.*, 90, 895, 1986.
22. **Pabalan, R. T. and Pitzer, K. S.**, Thermodynamics of  $NaOH(aq)$  in hydrothermal solutions, *Geochim. Cosmochim. Acta*, 51, 829, 1987.
23. **Pabalan, R. T. and Pitzer, K. S.**, Thermodynamics of concentrated electrolyte mixtures and the prediction of mineral solubilities to high temperatures for mixtures in the system  $Na-K-Mg-Cl-SO_4-OH-H_2O$ , *Geochim. Cosmochim. Acta*, 51, 2429, 1987.
24. **Pabalan, R. T. and Pitzer, K. S.**, Apparent molar heat capacity and other thermodynamic properties of aqueous  $KCl$  solutions to high temperatures and pressures, *J. Chem. Eng. Data*, 33, 354, 1988.
25. **Pabalan, R. T. and Pitzer, K. S.**, Heat capacity and other thermodynamic properties of  $Na_2SO_4(aq)$  in hydrothermal solutions and the solubilities of sodium sulfate minerals in the system  $Na-Cl-SO_4-OH-H_2O$  to 300°C, *Geochim. Cosmochim. Acta*, 52, 2393, 1988. (In Table 4, the rows of entries for  $t_1(T_r, 1 \text{ bar})$  and  $t_1(T_r, 1 \text{ bar})$  should be interchanged.)
26. **Yang, J.-Z. and Pitzer, K. S.**, Thermodynamics of electrolyte mixtures. Activity and osmotic coefficients consistent with the higher-order limiting law for symmetrical mixing, *J. Solution Chem.*, 17, 909, 1988.
27. **Pitzer, K. S.**, A thermodynamic model for aqueous solutions of liquid-like density, *Rev. Mineral.*, 17, 97, 1987.

28. **Harvie, C. E. and Weare, J. H.**, The prediction of mineral solubilities in natural waters: the Na-K-Mg-Ca-Cl-SO<sub>4</sub>-H<sub>2</sub>O system from zero to high concentration at 25°C. *Geochim. Cosmochim. Acta*, 44, 981, 1980.
29. **Harvie, C. E.**, Theoretical Investigations in Geochemistry and Atom Surface Scattering, Ph.D. dissertation, U. C. San Diego. #AAD82-03026, University Microfilm International, Ann Arbor, MI, 1981.
30. **Harvie, C. E., Eugster, H. P., and Weare, J. H.**, Mineral equilibria in the six-component seawater system, Na-K-Mg-Ca-SO<sub>4</sub>-Cl-H<sub>2</sub>O at 25°C. II. Compositions of the saturated solutions, *Geochim. Cosmochim. Acta*, 46, 1603, 1982.
31. **Harvie, C. E., Møller, N., and Weare, J. H.**, The prediction of mineral solubilities in natural waters: the Na-K-Mg-Ca-H-Cl-SO<sub>4</sub>-OH-HCO<sub>3</sub>-CO<sub>2</sub>-H<sub>2</sub>O system to high ionic strengths at 25°C. *Geochim. Cosmochim. Acta*, 48, 723, 1984.
32. **Filippov, V. K., Dmitriev, G. V., and Yakovleva, S. I.**, Use of the Pitzer method for calculating the activity of components in mixed solutions of electrolytes according to data on solubility, *Dokl. Akad. Nauk SSSR Fiz. Khim.*, 252, 156, 1980; English transl., 252, 359, 1980.
33. **Filippov, V. K. and Nokhrin, V. I.**, The Li<sub>2</sub>SO<sub>4</sub>-MSO<sub>4</sub>-H<sub>2</sub>O systems (M = Mg, Ni, Zn) at 25°C. *Russ. J. Inorg. Chem.*, 30, 282, 1985.
34. **Filippov, V. K. and Nokhrin, V. I.**, Li<sub>2</sub>SO<sub>4</sub>-MSO<sub>4</sub>-H<sub>2</sub>O (M = Mn, Co, and Cu) systems at 25°C. *Russ. J. Inorg. Chem.*, 30, 513, 1985.
35. **Filippov, V. K., Barkov, D. S., and Federov, Ju. A.**, Die anwendung der Pitzer-gleichungen für die berechnung der löslichkeit im system Cu(NO<sub>3</sub>)<sub>2</sub>-Ni(NO<sub>3</sub>)<sub>2</sub>-H<sub>2</sub>O bei 25°C. *Z. Phys. Chem. Leipzig*, 266, 129, 1985.
36. **Filippov, V. K., Nokhrin, V. I., and Muzalevskaya, A. P.**, A thermodynamic study of the Na<sub>2</sub>SO<sub>4</sub>-ZnSO<sub>4</sub>-H<sub>2</sub>O and Na<sub>2</sub>SO<sub>4</sub>-CdSO<sub>4</sub>-H<sub>2</sub>O systems at 25°C. *Russ. J. Inorg. Chem.*, 30, 2407, 1985.
37. **Filippov, V. K., Charykova, M. V., and Trofimov, Yu. M.**, Thermodynamics of the system NH<sub>4</sub>H<sub>2</sub>PO<sub>4</sub>-(NH<sub>4</sub>)<sub>2</sub>SO<sub>4</sub>-H<sub>2</sub>O at 25°C. *J. Appl. Chem. U.S.S.R.*, 58, 1807, 1985.
38. **Filippov, V. K. and Nokhrin, V. I.**, Solubility in the Na<sub>2</sub>SO<sub>4</sub>-CuSO<sub>4</sub>-H<sub>2</sub>O system at 25°C. *Russ. J. Inorg. Chem.*, 30, 1688, 1985.
39. **Filippov, V. K., Charykov, N. A., and Fedorov, Yu. A.**, The NaCl-NiCl<sub>2</sub>-H<sub>2</sub>O and NaCl-CuCl<sub>2</sub>-H<sub>2</sub>O systems at 25°C. *Russ. J. Inorg. Chem.*, 31, 1071, 1986.
40. **Filippov, V. K., Kalinkin, A. M., and Vasin, S. K.**, Thermodynamics of phase equilibria of aqueous (Li<sub>2</sub>SO<sub>4</sub> + Cs<sub>2</sub>SO<sub>4</sub>), (Na<sub>2</sub>SO<sub>4</sub> + Cs<sub>2</sub>SO<sub>4</sub>), and (K<sub>2</sub>SO<sub>4</sub> + Cs<sub>2</sub>SO<sub>4</sub>) at 298.15 K using Pitzer's model. *J. Chem. Thermodyn.*, 19, 185, 1987.
41. **Filippov, V. K., Charykov, N. A., and Rumyantsev, A. V.**, Application of Pitzer's method to water-salt systems with complex formation, *Dokl. Akad. Nauk SSSR Fiz. Khim.*, 296, 665, 1987; English transl., 296, 936, 1987.
42. **Clegg, S. L. and Brimblecombe, P.**, Equilibrium partial pressures of strong acids over concentrated saline solutions. I. HNO<sub>3</sub>. II. HCl. *Atmos. Environ.*, 22, 91, 1988; 22, 117, 1988.
43. **Brimblecombe, P. and Clegg, S. L.**, The solubility and behavior of acid gases in the marine aerosol. *J. Atmos. Chem.*, 7, 1, 1988.
44. **Krumgalz, B. S. and Millero, F. J.**, Physico-chemical study of Dead Sea waters. I. Activity coefficients of major ions in Dead Sea water. *Mar. Chem.*, 11, 209, 1982.
45. **Krumgalz, B. S. and Millero, F. J.**, Physico-chemical study of Dead Sea waters. III. On gypsum saturation in Dead Sea waters and their mixtures with Mediterranean Sea water. *Mar. Chem.*, 13, 127, 1983.
46. **Millero, F. J. and Byrne, R. H.**, Use of Pitzer's equations to determine the media effect in the formation of lead chloro complexes, *Geochim. Cosmochim. Acta*, 48, 1145, 1984.
47. **Møller, N.**, The prediction of mineral solubilities in natural waters: a chemical equilibrium model for the CaSO<sub>4</sub>-NaCl-CaCl<sub>2</sub>-H<sub>2</sub>O system to high temperature and concentration, *Geochim. Cosmochim. Acta*, 52, 821, 1988.
48. **McMillan, W. G. and Mayer, J. E.**, The statistical thermodynamics of multicomponent systems. *J. Chem. Phys.*, 13, 276, 1945.
49. **Friedman, H. L.**, *Ionic Solution Theory*. Wiley-Interscience, New York, 1962.
50. **Card, D. N. and Valleau, J. P.**, Monte Carlo study of the thermodynamics of electrolyte solutions. *J. Chem. Phys.*, 52, 6232, 1970.
51. **Rasaiah, J. C., Card, D. N., and Valleau, J. P.**, Calculations on the "restricted primitive model" for 1-1 electrolyte solutions. *J. Chem. Phys.*, 56, 248, 1972; **Sørensen, T. S.**, How wrong is the Debye-Hückel approximation for dilute primitive model electrolytes with moderate Bjerrum parameter. *J. Chem. Soc. Faraday Trans.*, 86, 1815, 1990.
52. **Milner, S. R.**, The virial of a mixture of ions, *Philos. Mag.*, 23, 551, 1912; The effect of interionic forces on the osmotic pressure of electrolytes, *Philos. Mag.*, 25, 742, 1913.
53. **Debye, P. and Hückel, E.**, Zur theorie der electrolyte. I. *Phys. Z.*, 24, 185, 1923.
54. **Debye, P.**, Osmotische zustandsgleichung und activitat verdünnter starker elektrolyte, *Phys. Z.*, 25, 97, 1924.

55. Lewis, G. N. and Linhart, G. A., The degree of ionization of very dilute electrolytes, *J. Am. Chem. Soc.*, 41, 1951, 1919
56. Bronsted, J. N., Calculation of the osmotic and activity functions in solutions of uni-univalent salts, *J. Am. Chem. Soc.*, 44, 938, 1922
57. Lewis, G. N. and Randall, M., The activity of strong electrolytes, *J. Am. Chem. Soc.*, 43, 1112, 1921
58. Bronsted, J. N., Studies on solubility. IV. The principle of specific interactions of ions, *J. Am. Chem. Soc.*, 44, 877, 1922
59. Guggenheim, E. A., The specific thermodynamic properties of aqueous solutions of strong electrolytes, *Philos. Mag.*, 19, 588, 1935
60. Guggenheim, E. A. and Turgeon, J. C., Specific interaction of ions, *Trans. Faraday Soc.*, 51, 747, 1955
61. Scatchard, G., Concentrated solutions of strong electrolytes, *Chem. Rev.*, 19, 309, 1936
62. Pitzer, K. S. and Brewer, L., Revision of Lewis and Randall's *Thermodynamics*, McGraw-Hill, New York, 1961
63. Mayer, J. E., The theory of ionic solutions, *J. Chem. Phys.*, 18, 1426, 1950
64. Ananthaswamy, J. and Atkinson, G., Thermodynamics of concentrated electrolyte mixtures. V. A review of the thermodynamic properties of aqueous calcium chloride in the temperature range 273.15 — 373.15 K, *J. Chem. Eng. Data*, 30, 120, 1985
65. Pitzer, K. S., The treatment of ionic solutions over the entire miscibility range, *Ber. Bunsenges. Phys. Chem.*, 85, 952, 1981
66. Simonson, J. M. and Pitzer, K. S., Thermodynamics of multicomponent, miscible, ionic systems: the system LiNO<sub>3</sub>-KNO<sub>3</sub>-H<sub>2</sub>O, *J. Phys. Chem.*, 90, 3009, 1986
67. Pabalan, R. T. and Pitzer, K. S., Models for aqueous electrolyte mixtures for systems extending from dilute solutions to fused salts, in *Chemical Modeling of Aqueous Systems II*, Melchior, D. C. and Bassett, R. L., Eds., A.C.S. Symp. Ser. 416, American Chemical Society, Washington, D.C., 1990, chap. 4
68. Holmes, H. F., Busey, R. H., Simonson, J. M., Mesmer, R. E., Archer, D. G., and Wood, R. H., The enthalpy of dilution of HCl(aq) to 648 K and 40 MPa; thermodynamic properties, *J. Chem. Thermodyn.*, 19, 863, 1987
69. Knauss, K. G., Wolery, T. J., and Jackson, K. J., A new approach to measuring pH in brines and other concentrated electrolytes, *Geochim. Cosmochim. Acta*, 54, 1519, 1990
70. Long, F. A. and McDevit, W. F., Activity coefficients of nonelectrolyte solutes in aqueous salt solutions, *Chem. Rev.*, 51, 119, 1952
71. Corti, H. R., de Pablo, J. J., and Prausnitz, J. M., Phase equilibria for aqueous systems containing salts and carbon dioxide. Application of Pitzer theory for electrolyte solutions, *J. Phys. Chem.*, 94, 7876, 1990
72. Archer, D. G. and Wood, R. H., Chemical equilibrium model applied to aqueous magnesium sulfate solutions, *J. Solution Chem.*, 14, 757, 1985
73. Ananthaswamy, J. and Atkinson, G., Thermodynamics of concentrated electrolyte mixtures. IV. Pitzer-Debye-Huckel limiting slopes for water from 0 to 100°C and from 1 atm to 1 kbar, *J. Chem. Eng. Data*, 29, 81, 1984
74. Robinson, R. A. and Stokes, R. H., *Electrolyte Solutions*, 2nd ed., revised, Butterworths, London, 1965
75. Kodytek, V. and Dolejs, V., On the Pitzer equation for the osmotic coefficient of aqueous solutions of 3:1 rare earth electrolytes, *Z. Phys. Chem. Leipzig*, 267, 743, 1986
76. Roy, R. N., Hufford, K., Lord, P. J., Mrad, D. R., Roy, L. N., and Johnson, D. A., The first acidity constant of carbon dioxide in solutions of ammonium chloride from e.m.f. measurements at 278.15 to 318.15 K, *J. Chem. Thermodyn.*, 20, 63, 1988
77. Kim, H.-T. and Frederick, W. J., Jr., Evaluation of Pitzer ion interaction parameters of aqueous electrolytes at 25°C. I. Single salt parameters, *J. Chem. Eng. Data*, 33, 177, 1988
78. Kim, H.-T. and Frederick, W. J., Jr., Evaluation of Pitzer ion interaction parameters of aqueous mixed electrolyte solutions at 25°C. II. Ternary mixing parameters, *J. Chem. Eng. Data*, 33, 278, 1988
79. Macaskill, J. B. and Bates, R. G., Osmotic coefficients and activity coefficients of aqueous hydrobromic acid solutions at 25°C, *J. Solution Chem.*, 12, 607, 1983
80. Clegg, S. L., (Calculated from data of Hamer, W. J. and Wu, Y. C.) Osmotic and activity coefficients of uni-univalent electrolytes in water, *J. Phys. Chem. Ref. Data*, 1, 1047, 1972
81. Levy, D. E. and Myers, R. J., Spectroscopic determination of the second dissociation constant of H<sub>2</sub>Se and the activity coefficients and spectral shifts of its ions, *J. Phys. Chem.*, 94, 7842, 1980
82. Rard, J. A., Isopiestic determination of the osmotic and activity coefficients of aqueous MnCl<sub>2</sub>, MnSO<sub>4</sub>, and RbCl at 25°C, *J. Chem. Eng. Data*, 29, 443, 1984
83. Rard, J. A. and Miller, D. G., Isopiestic determination of the osmotic and activity coefficients of aqueous CsCl, SrCl<sub>2</sub>, and mixtures of NaCl and CsCl at 25°C, *J. Chem. Eng. Data*, 27, 169, 1982
84. Clegg, S. L., (Calculated from the data of Covington, A. K., Robinson, R. A., and Thompson, R.) Osmotic and activity coefficients for aqueous methane sulfonic acid solutions at 25°C, *J. Chem. Eng. Data*, 18, 422, 1973

85. **Rard, J. A. and Miller, D. G.**, Isopiestic determination of the osmotic and activity coefficients of aqueous  $\text{MgCl}_2$  solutions at 25°C. *J. Chem. Eng. Data*, 26, 38, 1981.
86. **Phutela, R. C. and Pitzer, K. S.**, Thermodynamics of aqueous calcium chloride, *J. Solution Chem.*, 12, 201, 1983.
87. **Reardon, E. J. and Beckie, R. D.**, Modelling chemical equilibria of acid mine-drainage: the  $\text{FeSO}_4\text{-H}_2\text{SO}_4\text{-H}_2\text{O}$  system, *Geochim. Cosmochim. Acta*, 51, 2355, 1987.
88. **Rard, J. A.**, Isopiestic determination of the osmotic and activity coefficients of aqueous  $\text{NiCl}_2$ ,  $\text{Pr}(\text{NO}_3)_3$ , and  $\text{Lu}(\text{NO}_3)_3$  and solubility of  $\text{NiCl}_2$  at 25°C. *J. Chem. Eng. Data*, 32, 334, 1987.
89. **Rard, J. A. and Miller, D. G.**, Isopiestic determination of the osmotic and activity coefficients of aqueous  $\text{ZnCl}_2$  at 298.15 K. *J. Chem. Thermodyn.*, 21, 463, 1989.
90. **Rard, J. A. and Miller, D. G.**, Isopiestic determination of the osmotic coefficients of aqueous  $\text{Na}_2\text{SO}_4$ ,  $\text{MgSO}_4$ , and  $\text{Na}_2\text{SO}_4\text{-MgSO}_4$  at 25°C. *J. Chem. Eng. Data*, 26, 33, 1981.
91. **Esteso, M. A., Fernandez-Merida, L., and Hernandez-Luis, F. F.**, Activity coefficients for  $\text{Na}_2$  succ. solutions from EMF measurements. *J. Electroanal. Chem.*, 230, 69, 1987.
92. **Esteso, M. A., Fernandez-Merida, L., Gonzalez-Diaz, D., and Hernandez-Luis, F. F.**, Activity coefficients for aqueous solutions of potassium succinate at 25°C. *J. Chem. Soc. Faraday Trans.*, 1, 85, 2575, 1989.
93. **Rard, J. A. and Spedding, F. H.**, Isopiestic determination of the activity coefficients of some aqueous rare-earth electrolyte solutions at 25°C. VI.  $\text{Eu}(\text{NO}_3)_3$ ,  $\text{Y}(\text{NO}_3)_3$ , and  $\text{YCl}_3$ . *J. Chem. Eng. Data*, 27, 454, 1982.
94. **Rard, J. A.**, Osmotic and activity coefficients of aqueous  $\text{La}(\text{NO}_3)_3$  and densities and apparent molal volumes of aqueous  $\text{Eu}(\text{NO}_3)_3$  at 25°C. *J. Chem. Eng. Data*, 32, 92, 1987.
95. **Rard, J. A., Miller, D. G., and Spedding, F. H.**, Isopiestic determination of the activity coefficients of some aqueous rare earth electrolyte solutions at 25°C. IV.  $\text{La}(\text{NO}_3)_3$ ,  $\text{Pr}(\text{NO}_3)_3$ , and  $\text{Nd}(\text{NO}_3)_3$ . *J. Chem. Eng. Data*, 24, 348, 1979.
96. **Rard, J. A. and Spedding, F. H.**, Isopiestic determination of the activity coefficients of some aqueous rare-earth electrolyte solutions at 25°C. V.  $\text{Dy}(\text{NO}_3)_3$ ,  $\text{Ho}(\text{NO}_3)_3$ , and  $\text{Lu}(\text{NO}_3)_3$ . *J. Chem. Eng. Data*, 26, 391, 1981.
97. **Fritz, J. J.**, Chloride complexes of  $\text{CuCl}$  in aqueous solution. *J. Phys. Chem.*, 84, 2241, 1980.
98. **Fritz, J. J.**, Representation of the solubility of  $\text{CuCl}$  in solutions of various aqueous chlorides. *J. Phys. Chem.*, 85, 890, 1981.
99. **Fritz, J. J.**, Heats of solution of cuprous chloride in aqueous  $\text{HCl-HClO}_4$  mixtures. *J. Solution Chem.*, 13, 369, 1984.
100. **Fritz, J. J.**, Thermodynamic properties of chloro-complexes of silver chloride in aqueous solution. *J. Solution Chem.*, 14, 865, 1985.
101. **Sharma, V. K. and Millero, F. J.**, Equilibrium constants for the formation of  $\text{Cu}(\text{I})$  halide complexes. *J. Solution Chem.*, 19, 375, 1990.
102. **Millero, F. J. and Byrne, R. H.**, Use of Pitzer's equations to determine the media effect on the formation of lead chloro complexes. *Geochim. Cosmochim. Acta*, 48, 1145, 1984.
103. **Simonson, J. M., Roy, R. N., Connole, J., Roy, L. N., and Johnson, D. A.**, The thermodynamics of aqueous borate solutions. I. Mixtures of boric acid with sodium or potassium borate and chloride. *J. Solution Chem.*, 17, 791, 1988.
104. **Simonson, J. M., Roy, R. N., Mrad, D., Lord, P., Roy, L. N., and Johnson, D. A.**, The thermodynamics of aqueous borate solutions. II. Mixtures of boric acid with calcium or magnesium borate and chloride. *J. Solution Chem.*, 17, 435, 1988.
105. **Felmy, A. R. and Weare, J. H.**, The prediction of borate mineral equilibria in natural waters: application to Searles Lake, California. *Geochim. Cosmochim. Acta*, 50, 2771, 1986.
106. **Hershey, J. P., Fernandez, M., Milne, P. J., and Millero, F. J.**, The ionization of boric acid in  $\text{NaCl}$ ,  $\text{Na-Ca-Cl}$ , and  $\text{Na-Mg-Cl}$  solutions at 25°C. *Geochim. Cosmochim. Acta*, 50, 143, 1986.
107. **Hershey, J. P. and Millero, F. J.**, The dependence of the acidity constants of silicic acid on  $\text{NaCl}$  concentration using Pitzer's equations. *Mar. Chem.*, 18, 101, 1986.
108. **Thurmond, J. V. and Millero, F. J.**, Ionization of carbonic acid in sodium chloride solutions at 25°C. *J. Solution Chem.*, 11, 447, 1982.
109. **Millero, F. J. and Thurmond, J. V.**, Ionization of carbonic acid in  $\text{Na-Mg-Cl}$  solutions at 25°C. *J. Solution Chem.*, 12, 401, 1990.
110. **Clegg, S. L. and Brimblecombe, P.**, Estimated mean activity coefficients of aqueous  $\text{BeCl}_2$  and properties of solution mixtures containing  $\text{Be}^{2+}$  ions. *J. Chem. Soc. Faraday Trans. 1*, 85, 157, 1989.
111. **Thurmond, J. V. and Brass, G. W.**, Activity and osmotic coefficients of  $\text{NaCl}$  in concentrated solutions from 0 to -40°C. *J. Chem. Eng. Data*, 33, 411, 1988.
112. **Downes, C. J. and Pitzer, K. S.**, Thermodynamics of electrolytes. Binary mixtures formed from aqueous  $\text{NaCl}$ ,  $\text{Na}_2\text{SO}_4$ ,  $\text{CuCl}_2$  and  $\text{CuSO}_4$  at 25°C. *J. Solution Chem.*, 5, 389, 1976.



113. **Reardon, E. J. and Armstrong, D. K.**, Celestite ( $\text{SrSO}_4$ ) solubility in water, seawater, and NaCl solution, *Geochim. Cosmochim. Acta*, 51, 63, 1987.
114. **Reardon, E. J.**, Ion interaction parameters for Al-SO<sub>4</sub> and application to the prediction of metal sulfate solubility in binary salt systems, *J. Phys. Chem.*, 92, 6426, 1988.
115. **Rard, J. A.**, Isopiestic determination of the osmotic and activity coefficients of aqueous  $\text{Lu}_2(\text{SO}_4)_3$  at 25°C, *J. Solution Chem.*, 19, 525, 1990.
116. **Del Re, G., DiGiacomo, G., and Fantauzzi, F.**, Enthalpy of dilution of aqueous  $\text{CaCl}_2$  at 298.15 K, *Thermochim. Acta*, 161, 201, 1990.
117. **Connaughton, L. M., Hershey, J. P., and Millero, F. J.**, PVT properties of concentrated aqueous electrolytes. V. Densities and apparent molal volumes of the four major sea salts for dilute solution to saturation and from 0 to 100°C, *J. Solution Chem.*, 15, 989, 1986. (In Table IV the signs of entries  $c_4$  and  $c_5$  for  $\text{MgCl}_2$  should be reversed and for  $\text{MgSO}_4$ ,  $d_2 = 6.1103123\text{E}-1$ .)
118. **Simonson, J. M. and Ryther, R. J.**, Volumetric properties of aqueous sodium hydroxide from 273.15 to 348.15 K, *J. Chem. Eng. Data*, 34, 57, 1989.
- 119a. **Monnin, C.**, An ion interaction model for the volumetric properties of natural waters: density of the solution and partial molal volumes of electrolytes to high concentration at 25°C, *Geochim. Cosmochim. Acta*, 53, 1177, 1989.
- 119b. **Monnin, C.**, The influence of pressure on the activity coefficients of the solutes and on the solubility of minerals in the system Na-Ca-Cl-SO<sub>4</sub>-H<sub>2</sub>O to 200°C and 1 kbar, and to high NaCl concentration, *Geochim. Cosmochim. Acta*, 54, 3265, 1990.
120. **Kumar, A.**, Volume properties of aqueous electrolytes. I. Examination of apparent molal volume data by the Pitzer method, *J. Chem. Eng. Data*, 32, 106, 1987.
121. **Pogue, R. F. and Atkinson, G.**, Solution thermodynamics of first row transition elements. II. Apparent molal volumes of aqueous  $\text{MnCl}_2$ ,  $\text{Mn}(\text{ClO}_4)_2$ ,  $\text{CoCl}_2$ ,  $\text{Co}(\text{ClO}_4)_2$ ,  $\text{FeCl}_2$ ,  $\text{Fe}(\text{ClO}_4)_2$  from 15 to 55°C, *J. Chem. Eng. Data*, 34, 227, 1989.
122. **Greenberg, J. P. and Møller, N.**, The prediction of mineral solubilities in natural waters: a chemical equilibrium model for the Na-K-Ca-Cl-SO<sub>4</sub>-H<sub>2</sub>O system to high concentration from 0 to 250°C, *Geochim. Cosmochim. Acta*, 53, 2503, 1989.
123. **Spencer, R. J., Møller, N., and Weare, J. H.**, The prediction of mineral solubilities in natural waters: a chemical equilibrium model for the Na-K-Ca-Mg-Cl-SO<sub>4</sub>-H<sub>2</sub>O system at temperatures below 25°C, *Geochim. Cosmochim. Acta*, 54, 575, 1990.
124. **Gates, J. A., Tillett, D. M., White, D. E., and Wood, R. H.**, Apparent molar heat capacities of aqueous NaCl solutions from 0.05 to 3.0 mol·kg<sup>-1</sup>, 350 to 600 K, and 2 to 18 MPa, *J. Chem. Thermodyn.*, 19, 131, 1987.
125. **de Lima, M. C. P. and Pitzer, K. S.**, Thermodynamics of saturated electrolyte mixtures of NaCl with Na<sub>2</sub>SO<sub>4</sub> and MgCl<sub>2</sub>, *J. Solution Chem.*, 12, 187, 1983.
126. **Holmes, H. F., Baes, C. F., and Mesmer, R. E.**, Isopiestic studies of aqueous solutions at elevated temperatures. I. KCl, CaCl<sub>2</sub> and MgCl<sub>2</sub>, *J. Chem. Thermodyn.*, 10, 983, 1978.
127. **Phutela, R. C., Pitzer, K. S., and Saluja, P. P. S.**, Thermodynamics of aqueous magnesium chloride, calcium chloride and strontium chloride at elevated temperatures, *J. Chem. Eng. Data*, 32, 76, 1987.
128. **Holmes, H. F. and Mesmer, R. E.**, Thermodynamics of aqueous solutions of the alkali metal sulfates, *J. Solution Chem.*, 15, 495, 1986.
129. **Simonson, J. M., Mesmer, R. E., and Rogers, P. S. Z.**, The enthalpy of dilution and apparent molar heat capacity of NaOH(aq) to 523 K and 40 MPa, *J. Chem. Thermodyn.*, 21, 561, 1989.
130. **Holmes, H. F. and Mesmer, R. E.**, Thermodynamic properties of aqueous solutions of the alkali metal chlorides to 250°C, *J. Phys. Chem.*, 87, 1242, 1983.
131. **Thiessen, W. E. and Simonson, J. M.**, Enthalpy of dilution and thermodynamics of NH<sub>4</sub>Cl(aq) to 523 K and 35 MPa, *J. Phys. Chem.*, 94, 7794, 1990.
132. **Saluja, P. P. S., Pitzer, K. S., and Phutela, R. C.**, High-temperature thermodynamic properties of several 1:1 electrolytes, *Can. J. Chem.*, 64, 1328, 1986.
133. **Pitzer, K. S.**, Theory: ion interaction approach, in *Activity Coefficients in Electrolyte Solutions*, Vol. 1, Pytkowicz, R. M., Ed., CRC Press, Boca Raton, FL, 1979, chap. 7.
134. **Filippov, V. K., Barkov, D. S., and Federov, Yu. A.**, Application of the Pitzer equations to the solubility of ternary aqueous nitrate solutions at 25°C, *J. Solution Chem.*, 15, 611, 1986.
135. **Filippov, V. K. and Kalinkin, A. M.**, The Li<sub>2</sub>SO<sub>4</sub>-Na<sub>2</sub>SO<sub>4</sub>-H<sub>2</sub>O system at 25°C, *Russ. J. Inorg. Chem.*, 32, 120, 1987.
136. **Filippov, V. K., Charykova, M. V., and Trofimov, Yu. M.**, Thermodynamic study of the systems Na<sup>+</sup>, NH<sub>4</sub><sup>+</sup>||SO<sub>4</sub><sup>2-</sup>-H<sub>2</sub>O and Na<sup>+</sup>, NH<sub>4</sub><sup>+</sup>||H<sub>2</sub>PO<sub>4</sub><sup>-</sup>-H<sub>2</sub>O at 25°C, *J. Appl. Chem. U.S.S.R.*, 60, 237, 1987.
137. **Filippov, V. K., Charykova, M. V., and Trofimov, Yu. M.**, Phase equilibria in the system Na, NH<sub>4</sub>||SO<sub>4</sub>, H<sub>2</sub>PO<sub>4</sub> at 25°C, *J. Appl. Chem. U.S.S.R.*, 60, 1160, 1987.

138. **Filippov, V. K. and Charykova, M. V.**, Die anwendung der Pitzer-gleichungen für die berechnung der phasengleichgewichte in quaternären system  $\text{Na}^+ \cdot \text{NH}_4^+ \parallel \text{Cl}^- \cdot \text{SO}_4^{2-} \cdot \text{H}_2\text{O}$  bei 25°C. *Z. Phys. Chem. Leipzig*, 270, 49, 1989.
139. **Filippov, V. K., Kalinkin, A. M., and Vasin, S. K.**, Thermodynamics of phase equilibria of aqueous (lithium sulfate + alkali-metal sulfate) (alkali metal: Na, K, and Rb), and (sodium sulfate + rubidium sulfate) at 298.15 K using Pitzer's model. *J. Chem. Thermodyn.*, 21, 935, 1989.
140. **Roy, R. N., Gibbons, J. J., Ovens, L. K., Bliss, G. A., and Hartley, J. J.**, Activity coefficients for the system  $\text{HCl}-\text{CaCl}_2-\text{H}_2\text{O}$  at various temperatures. *J. Chem. Soc. Faraday Trans. 1*, 78, 1405, 1981.
141. **Roy, R. N., Gibbons, J. J., Roy, L. N., and Greene, M. A.**, Thermodynamics of the unsymmetrical mixed electrolyte  $\text{HCl}-\text{SrCl}_2$ . Applications of Pitzer's equations. *J. Phys. Chem.*, 90, 6242, 1986.
142. **Roy, R. N., Roy, L. N., Farwell, G. D., Smith, K. A., and Millero, F. J.**, Thermodynamics of the unsymmetrical mixed electrolyte  $\text{HCl}-\text{NiCl}_2$ . Application of Pitzer's equations. *J. Phys. Chem.*, 94, 7321, 1990.
143. **Roy, R. N., Rice, S. A., Vogel, K. M., Roy, L. M., and Millero, F. J.**, Activity coefficients for  $\text{HCl}-\text{BaCl}_2-\text{H}_2\text{O}$  at different temperatures and effects of higher order electrostatic terms. *J. Phys. Chem.*, 94, 7706, 1990.
144. **Roy, R. N., Wood, M. D., Johnson, D., Roy, L. N., and Gibbons, J. J.**, Activity coefficients for hydrogen bromide + calcium bromide + water at various temperatures. Application of Pitzer's equations. *J. Chem. Thermodyn.*, 19, 307, 1987.
145. **Roy, R. N., Lawson, M. L., Nelson, E., Roy, L. N., and Johnson, D. A.**, Activity coefficients in (hydrogen bromide + magnesium bromide) (aq) at several temperatures. Application of Pitzer's equations. *J. Chem. Thermodyn.*, 22, 727, 1990.
146. **Esteso, M. A., Fernandez-Merida, L., Hernandez-Luis, F. F., and Gonzales-Diaz, O. M.**, Activity coefficients in the system  $\text{NaCl} + \text{Na succinate} + \text{H}_2\text{O}$  at 25°C. *Ber. Bunsenges. Phys. Chem.*, 93, 213, 1989.
147. **Maeda, M., Hisada, O., Ikedo, K., Masuda, H., Ito, K., and Kinjo, Y.**, Prediction of dissociation constants of ammonium ion in aqueous lithium chloride solutions in terms of the Pitzer approach. *J. Phys. Chem.*, 92, 6404, 1988.
148. **Clegg, S. L. and Brimblecombe, P.**, The solubility of ammonia in pure aqueous and multicomponent solutions. *J. Phys. Chem.*, 93, 7237, 1989.
149. **Filippov, V. K. and Cheremnykh, L. M.**, Calculation of phase equilibria of the system  $\text{Na.K} \parallel \text{Cl.SO}_4-\text{H}_2\text{O}$  at 25°C. *J. Appl. Chem. U.S.S.R.*, 60, 34, 1986.
150. **Filippov, V. K. and Charykov, N. A.**, Phase equilibria in the system  $\text{Na.Co} \parallel \text{Cl.SO}_4-\text{H}_2\text{O}$  at 25°C. *J. Appl. Chem. U.S.S.R.*, 59, 2255, 1986.
151. **Filippov, V. K., Cheremnykh, L. M., and Shestakov, N. E.**, Phase equilibria in the system  $\text{K.Mg} \parallel \text{Cl.SO}_4-\text{H}_2\text{O}$  at 25°C. *J. Appl. Chem. U.S.S.R.*, 60, 1831, 1986.
152. **Filippov, V. K., Prieto, M. S., and Charykova, M. V.**, Utilizacion de la ecuacion de Pitzer para el calculo de solubilidad del sistema  $\text{NH}_4.\text{Mg} \parallel \text{SO}_4-\text{H}_2\text{O}$  a 25° y 30°C. *Rev. Cubana Quim.*, 3, 37, 1987.
153. **Filippov, V. K. and Charykov, N. A.**, Phase equilibria in the  $\text{Na}^+ \cdot \text{Mn}^{2+} \parallel \text{Cl}^- \cdot \text{SO}_4^{2-} \cdot \text{H}_2\text{O}$  system at 25°C. *Russ. J. Inorg. Chem.*, 34, 916, 1989.
154. **Reardon, E. J.**, Ion interaction model applied in the  $\text{NiSO}_4-\text{H}_2\text{SO}_4-\text{H}_2\text{O}$  system. *J. Phys. Chem.*, 93, 4630, 1989.
155. **Millero, F. J., Connaughton, L. M., Vinokurova, F., and Chetirkin, P. V.**, PVT properties of aqueous electrolytes. III. Volume changes for mixing the major sea salts at  $I = 1.0$  and  $I = 3.0$  at 25°C. *J. Solution Chem.*, 14, 837, 1985.
156. **Connaughton, L. M. and Millero, F. J.**, The PVT properties of aqueous electrolytes. VIII. The volume changes for mixing the major sea salts at ionic strength 3.0 from 5 to 95°C. *J. Solution Chem.*, 16, 491, 1987.
157. **Connaughton, L. M., Millero, F. J., and Pitzer, K. S.**, Volume changes for mixing the major sea salts: equations valid to ionic strength 3.0 and temperature 95°C. *J. Solution Chem.*, 18, 1007, 1989. (In Equation 1 there should be a minus sign before  $A_\phi$  and the factor  $m_i$  in the final sum; also the sign before  $B_{\lambda\lambda}^2$  in Equation 11 should be +.)
158. **Oakes, C. S., Simonson, J. M., and Bodnar, R. J.**, The system  $\text{NaCl}-\text{CaCl}_2-\text{H}_2\text{O}$  II. Densities for ionic strengths of 0.1–19.2 mol · kg<sup>-1</sup> at 298.15 and 308.15 K and at 0.1 MPa. *J. Chem. Eng. Data*, 35, 304, 1990.
159. **Plummer, L. N., Parkhurst, D. L., Fleming, G. W., and Dunkle, S. A.**, A Computer Program Incorporating Pitzer's Equations for Calculation of Geochemical Reactions in Brines, U. S. Geological Survey, Water-Resources Investigations Report 88-4153, Reston, VA, 1988.
160. **Kirkwood, J. G.**, Theory of solutions of molecules containing widely separated charges with special application to zwitterions. *J. Chem. Phys.*, 2, 351, 1934.
161. **Haar, L., Gallagher, J. S., and Kell, G. S.**, *NBS NRC Steam Tables: Thermodynamic and Transport Properties and Computer Programs for Vapor and Liquid States of Water in SI Units*, Hemisphere Publishing, Washington, D.C., 1984.

162. **Silvester, L. F. and Pitzer, K. S.**, Thermodynamics of electrolytes. VIII. High temperature properties, including enthalpy and heat capacity, with application to sodium chloride, *J. Phys. Chem.*, 81, 1822, 1977.
163. **Archer, D. G. and Wang, P.**, The dielectric constant of water and Debye-Huckel limiting law slopes, *J. Phys. Chem. Ref. Data*, 19, 371, 1990.
164. **Archer, D. G.**, The effect of revisions of Debye-Huckel limiting law coefficients on the thermodynamic parameters for strong electrolyte solutions, *J. Chem. Eng. Data*, 35, 340, 1990.
165. **Melchior, D. C. and Bassett, R. L.**, *Chemical Modeling of Aqueous Systems II*, A.C.S. Symp. Ser. 416, American Chemical Society, Washington, D.C., 1990.
166. **Filippov, V. K., Charykov, N. A., and Federov, Yu. A.**, Application of Pitzer's equations to the calculation of solution-vapor equilibrium in the  $\text{MnCl}_2\text{-HCl-H}_2\text{O}$  system, *Dokl. Akad. Nauk SSSR Fiz. Khim.*, 307, 916, 1989; English transl., 307, 630, 1989.
167. **Anstiss, R. G. and Pitzer, K. S.**, to be published.
168. **Goldberg, R. N.**, Evaluated activity and osmotic coefficients for aqueous solutions: bi-univalent compounds of zinc, cadmium, and ethylene bis (trimethylammonium) chloride and iodide, *J. Phys. Chem. Ref. Data*, 10, 1, 1981.
169. **Pitzer, K. S. and Simonson, J. M.**, Thermodynamics of multicomponent, miscible, ionic systems: theory and equations, *J. Phys. Chem.*, 90, 3005, 1986. (Equation 26c of this chapter corrects an error in the corresponding equation of this reference.)
170. **Pitzer, K. S.**, Electrolytes: from dilute solutions to fused salts, *J. Am. Chem. Soc.*, 102, 2902, 1980.
171. **Pitzer, K. S. and Li, Y.-G.**, Thermodynamics of aqueous sodium chloride to 823 K and 1 kilobar, *Proc. Natl. Acad. Sci. U.S.A.*, 80, 7689, 1983.
172. **Laity, R. W.**, *Reference Electrodes*, Ives, D. J. G. and Janz, G. J., Eds., Academic Press, New York, 1961, 544.
173. **Blander, M.**, *Molten Salt Chemistry*, Interscience, New York, 1964, 130.
174. **Prausnitz, J. M., Lichtenthaler, R. N., and de Azevedo, E. G.**, *Molecular Thermodynamics of Fluid-Phase Equilibria*, 2nd ed., Prentice-Hall, Englewood Cliffs, NJ, 1986.
175. **Wohl, K.**, Thermodynamic evaluation of binary and ternary systems, *Trans. Am. Inst. Chem. Eng.*, 42, 215, 1946.
176. **Wohl, K.**, Thermodynamic evaluation of binary and ternary systems, *Chem. Eng. Prog.*, 46, 218, 1953.
177. **Adler, S. B., Friend, L., and Pigford, R. L.**, Application of the Wohl equation to ternary vapor-liquid equilibria, *AIChE J.*, 12, 629, 1966.
178. **Clegg, S. L. and Brimblecombe, P.**, Equilibrium partial pressures and mean activity and osmotic coefficients of 0–100% nitric acid as a function of temperature, *J. Phys. Chem.*, 94, 5369, 1990.
179. **Scatchard, G., Rush, R. M., and Johnson, J. S.**, Osmotic and activity coefficients for binary mixtures of sodium chloride, sodium sulfate, magnesium sulfate, and magnesium chloride in water at 25°C. III. Treatment with ions as components, *J. Phys. Chem.*, 74, 3786, 1970.
180. **Weres, O. and Tsao, L.**, Activity of water mixed with molten salts at 317°C, *J. Phys. Chem.*, 90, 3014, 1986.



## Chapter 4

**EXPERIMENTAL METHODS: POTENTIOMETRIC**

James N. Butler and Rabindra N. Roy

**TABLE OF CONTENTS**

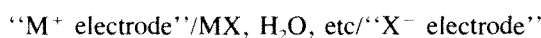
I.	Introduction: Principles of Potentiometry .....	156
II.	Hydrogen Electrode .....	157
	A. Method .....	157
	B. Typical Data .....	158
III.	The Glass pH Electrode .....	159
	A. Method .....	159
	B. Typical Results .....	165
IV.	Amalgam Electrodes .....	166
	A. Methods .....	166
	B. Typical Results .....	167
	C. Alkaline Earth Amalgams .....	168
	D. Other Metal Amalgams .....	168
V.	Cation-Selective Glass Electrodes .....	169
	A. Methods .....	169
	B. Selectivity .....	169
	C. Typical Results .....	170
VI.	Liquid and Polymer-Based Ion-Exchange Electrodes .....	175
	A. Introduction — Liquid Ion Exchange .....	175
	B. Activity Coefficient Measurements .....	175
	C. Ion Pairing and Stability Constants .....	177
	D. PVC Membranes .....	178
	E. Other Potential Tools .....	179
VII.	Neutral Carrier-Based Electrodes .....	181
	A. Methods .....	181
	B. Activity Coefficient Measurements .....	181
	C. Potential Tools .....	181
VIII.	Cells with Transference: Electrodes of the Second Kind .....	182
	A. Method .....	182
	B. Results .....	183
	C. Potential Tools .....	183
IX.	Solid-State Membrane Electrodes .....	184
	A. Methods .....	184
	B. Activity Coefficient Measurements .....	185
	C. Stability Constants .....	185
	D. Potential Tools .....	185

X.	Enzyme and Other Biologically Based Electrodes .....	186
A.	Methods .....	186
B.	Potential Tools .....	187
XI.	Gas-Sensitive Membrane Electrodes .....	187
A.	Methods .....	187
B.	Published Results .....	188
C.	Potential Tools .....	188
	Acknowledgments .....	188
	References .....	189

## I. INTRODUCTION: PRINCIPLES OF POTENTIOMETRY

Potentiometry has been an essential tool for experimental studies of electrolytes since the earliest quantitative work in the field.<sup>39,342</sup> As direct measures of salt chemical potential, potentiometric data have provided an ideal complement to isopiestic measurements, which determine water activity. They thus provide an independent check not only on the experimental accuracy of other methods, but also on the validity of the thermodynamic relations used to calculate salt activity from water activity.

In a multicomponent solution, the activity of a salt may be measured if an electrode reversible to  $M^+$  (and affected by the concentration of no other ion in the solution) can be found, and if an electrode reversible to  $X^-$  (and affected by the concentration of no other ion in the solution) can be found. Then the cell



has a potential given by

$$E = E^\circ - \frac{RT}{nF} \ln (a_{MX})$$

For a 1:1 electrolyte, with  $n = 1$ , this becomes

$$E = E^\circ - \frac{RT}{F} \ln (m_M m_X \gamma_{\pm}^2)$$

Here  $m_M$  and  $m_X$  = molal concentrations of ions  $M^+$  and  $X^-$ ;  $\gamma_{\pm}$  = mean activity coefficient of salt  $MX$ ;  $E^\circ$  = standard potential of the cell;  $R$  = gas constant (8.314 J/mol K);  $T$  = absolute temperature;  $F$  = Faraday constant (96497 C/mol).  $E^\circ$  is determined by measurements in solutions of known  $MX$  activity or by extrapolation to infinite dilution.

For polyvalent electrolytes  $n$  may be 2 or (rarely) greater; the expression for the argument

of the natural logarithm must be altered accordingly. For example,

$$a_{MX_2} = m_M (m_X)^2 \gamma_{\pm}^3 \quad \text{and } n = 2$$

Examples of cation-reversible electrodes are the hydrogen electrode (Section II), metal amalgam electrodes (Section IV), glass electrodes (Sections III and V), liquid ion-exchange electrodes (Section VI), and neutral carrier electrodes (Section VII).

Examples of anion-reversible electrodes of the second kind are silver-silver halide and lead amalgam-lead sulfate electrodes (Section VIII). Other electrodes reversible to anions include liquid ion-exchange (Section VI) and solid-state membrane electrodes (Section IX) made of  $Ag_2S$  (with additives) or  $LaF_3$ .

As ion-selective electrodes became commonly used during the 1970s, efforts were made to establish standard scales, analogous to the pH scale, for various ions.<sup>18,20,22,120</sup>

The most accurate electrochemical systems (e.g., hydrogen-silver chloride) give results reproducible to  $\pm 0.02$  mV, corresponding to an error of about 2 in the fourth decimal place of  $\log \gamma$ , or  $\pm 0.05\%$  in  $\gamma$  itself. This accuracy is limited by the accuracy with which solution concentrations can be determined, by the accuracy of temperature control, and by the noise inherent in electrical measurements.<sup>18,211</sup> Other systems give less accurate data, but even an accuracy of  $\pm 1$  mV will give  $\gamma$  to within  $\pm 2.5\%$ , often sufficient to test theoretical premises, and certainly an improvement over the approximation that all activity coefficients are unity.

Many of the basic studies of activity coefficients in single salt electrolytes have used cells with transport. Such cells are discussed briefly in Section VIII of this review. For further information, the reader is referred to the classic monographs.<sup>182,384</sup>

## II. HYDROGEN ELECTRODE

### A. METHOD

The hydrogen electrode was chosen as the zero of the potential scale for good reason. Properly constructed and operated, hydrogen electrodes are probably as close in accuracy to the practical limits of potentiometry as one can expect to achieve.<sup>211</sup> The electrode itself consists of a catalytic metal phase (platinum covered with platinum black), a solution phase (solvent, acidic solute, salts, dissolved hydrogen gas), and a gas phase (hydrogen bubbling through the solution):  $Pt/H_2/H^+$  etc.

Variants on this theme include a palladium membrane electrode through which hydrogen can diffuse.<sup>297</sup> Palladium and some other metals can dissolve hydrogen.<sup>169,338</sup> Palladium oxide on palladium,<sup>251</sup> as well as oxides of Pt, Ir, and Ti,<sup>252</sup> respond reversibly to the  $H_2/H^+$  couple.

The limitations of the hydrogen electrode arise primarily from two sources: (1) reducible solutions (especially  $O_2$ ) that react directly at the electrode — by doing so, they modify the equilibrium potential to a steady-state potential at which the solute is being reduced in addition to  $H^+$ ; and (2) solute-solvent combinations which produce so few solvated protons ( $H^+$ ) that the electrode cannot achieve equilibrium.

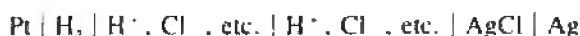
When equilibrium is attained, however, the potential is given by

$$E = E^\circ + \frac{RT}{F} \ln (m_H \gamma_{\pm} P_{H_2}^{-1/2}) - E_{ref} + E_j$$

Here  $E^\circ = 0$  for all temperatures by definition,  $m_H$  is the concentration of hydrogen ions ( $= m_{HX}$  for a strong acid HX), and  $\gamma_{\pm}$  is the activity coefficient of hydrogen ion in the solution. In a practical system, electrolytic connection with the solution phase of this half-cell must be made by a liquid junction and a reference electrode of some kind. Even if  $E_{ref}$

is held constant,  $E$  will depend somewhat on the composition of the solution phase in the hydrogen electrode, and thus  $\gamma_{\pm}$  and  $E_1$  are for practical purposes not separable to the accuracy implied by the measurement accuracy.<sup>18</sup>

However, when the hydrogen electrode is used to measure the mean activity of a salt, a cell can be set up in which the liquid junction potentials are essentially negligible. Such a cell was exploited by Harned and co-workers<sup>182</sup> for a long series of studies on the activity of HCl in a wide variety of solvent and solute mixtures:



The solution in the left-hand compartment is saturated with  $\text{H}_2$  gas at a concentration<sup>211</sup> of about  $8 \times 10^{-4} M$  for a gas pressure of 1 atm (1 atm = 1.0325 bars); the solution in the right-hand compartment is saturated with AgCl at about  $10^{-5} M$  if HCl is about 0.1  $M$ . The liquid junction potential between these two solutions is 0.01 mV or less (depending on assumptions about the mobility of the anionic silver chloride complexes).<sup>55</sup> Normally, this liquid junction potential is neglected, and the cell is referred to as "being without liquid junction".<sup>18,182,211</sup>

The potential of this "Harned cell" is given by

$$E = E^\circ + \frac{RT}{F} \ln (m_{\text{HCl}} \gamma_{\pm}^2 P_{\text{H}_2}^{-1/2})$$

which can be rearranged to put all experimentally accessible quantities on the left side and the parameters  $E^\circ$  and  $\gamma_{\pm}$  on the right:

$$E' = E + \frac{2RT}{F} \ln (m_{\text{HCl}}) - \frac{RT}{2F} \ln (P_{\text{H}_2}) = E^\circ - \frac{2RT}{F} \ln (\gamma_{\pm})$$

Typically, a series of values is obtained for  $E'$  over as wide a range of  $m_{\text{HCl}}$  concentrations as possible. These are extrapolated to  $m_{\text{HCl}} = 0$ , at which point  $E' = E^\circ$  by definition. Although  $E^\circ$  should be independent of the choice of extrapolation function, it is not entirely free from such errors. The accepted method is to use a Debye-Hückel function to determine  $\gamma_{\pm}$ , so that only a small residual term, nearly linear in  $m_{\text{HCl}}$ , is left for the extrapolation, as shown in Figure 1.<sup>24,180</sup>

## B. TYPICAL DATA

Typical data for 25°C are given in Table 1. These imply that the absolute accuracy with which potentiometric measurements can be made under the best circumstances is of the order of  $\pm 0.05$  mV.

Studies in many aqueous, nonaqueous, and partly aqueous solvents have yielded  $E^\circ$  for AgCl/Ag, AgBr/Ag, and AgI/Ag.<sup>57,211,219,220</sup> Some recent ones are listed in Table 2. Values of  $E^\circ$  have been obtained over the entire range from 1 to 100°C,<sup>124,180,183</sup> and some data have been obtained at elevated temperatures (to 275°C) where the aqueous phase is under pressures as great as 60 atm.<sup>173,275</sup>

The Harned cell has been used to measure the activity coefficient of HCl in aqueous electrolyte mixtures, electrolytes containing partly organic and partly aqueous solvent, and in nonaqueous electrolytes. Measurements in the presence of various standard buffers comprise the empirical foundations of the pH scale.<sup>18,82</sup>

Some recent examples of measurements in Harned-type cells are listed in Table 2. Proposed standard values for the mean activity coefficient of HCl between 0 and 60°C are given in Table 3.<sup>26</sup> These values can be used, with a standard 0.01-mol/kg solution of HCl, instead of the extrapolation method, to calibrate the Harned cell directly.



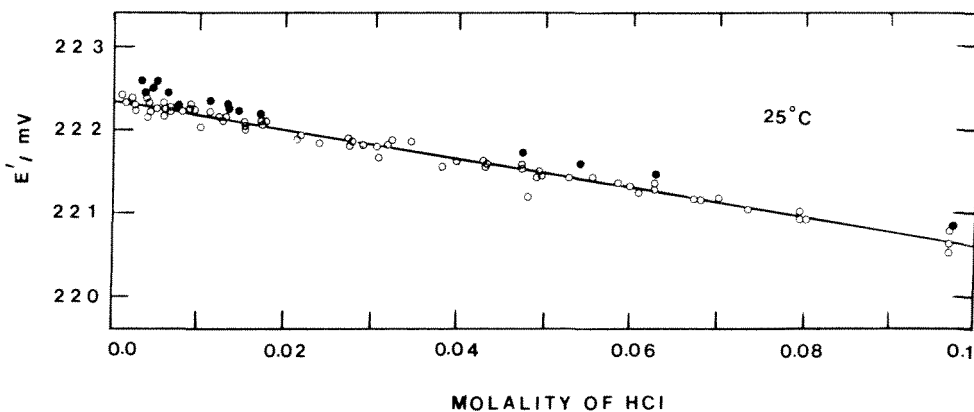


FIGURE 1. Provisional *standard potential*  $E'$  defined by  $E' = E + \frac{2RT}{F} \ln(m_{\text{HCl}}) - \frac{RT}{2F} \ln(P_{\text{H}_2}) = E^\circ - \frac{2RT}{F} \ln(\gamma_-)$  vs. molality of HCl.  $\circ$  Bates and Bower<sup>24</sup>,  $\bullet$  Harned and Ehlers<sup>180</sup>. Extrapolation to  $m_{\text{HCl}} = 0$  and  $P_{\text{H}_2} = 1.0$  atm gives  $E^\circ = 222.34$  mV.

**TABLE I**  
**Standard Potential of the Silver Chloride Electrode at 25°C**

Workers	Date	$E^\circ$ (mV)	Note	Ref.
Harned and Ehlers	1933	222.46	a	180
Bates and Bower	1954	222.34	a	24
Harned and Paxton	1953	222.39		183
Ahluwalia and Cobble	1964	222.38		1
Lietzke and Stoughton	1964	222.0	b	275
Dickson	1987	222.40	c	118
Bates and Macaskill	1978	222.42	c	25
Roy, Gibbons, Trower, and Lee	1980	222.59	c	400
Bates and Erickson	1986	222.58	c	30
Roy, Rice, Vogel, Roy, Millero	1990	222.58	c	422
Roy, Vega, Millero	1991	222.47	c	unpublished

<sup>a</sup> Data plotted in Figure 1.

<sup>b</sup> Lower accuracy than other data.

<sup>c</sup> Based on 0.01 *m* HCl only.

### III. THE GLASS pH ELECTRODE

#### A. METHOD

The use of the glass electrode for acidity measurements is so common<sup>18,211</sup> that the slow development of its use in measuring activity coefficients was surprising. Part of the reluctance of physical chemists to trust the glass electrode came from two well-known properties: (1) failure to obey the Nernst equation perfectly — a glass electrode standardized in phthalate buffer at  $\text{pH} = 4.01$  may read more than 0.02 units ( $>1$  mV) low in the standard borax buffer at  $\text{pH} = 9.18$ , whereas a hydrogen electrode would give perfect agreement; and (2) a tendency to drift in potential by millivolts over periods of minutes to days — thus,  $E^\circ$  is not constant in time.

Although a glass electrode cell cannot be used in the same way as a hydrogen electrode cell to make a primary standard, it can be used to measure the change in activity between two solutions of different composition.<sup>535</sup> The important change in method is to use the

**TABLE 2**  
**Recent Hydrogen Electrode Studies**

System	Ionic strength	Temp (K)	Ref.
<b>Hydrochloride Acid, Aqueous (See also Table 1)</b>			
HCl — std Ag/AgCl	0.01	273—333	28
	0.01	273—318	118
	0.01		400
		298	335
HCl, H <sub>2</sub> SO <sub>4</sub> , std Ag/AgCl	0.1—1.0	273—318	115,361
HCl, NaCl	0.1—0.9	278—318	296
HCl, NaCl, Harned coeff	High	Var	383
HCl, NaCl, KCl, NH <sub>4</sub> Cl	0.01—1.0	298	71
HCl, NaCl, MgCl <sub>2</sub>	0.1—0.87	278—318	526
HCl, NaNO <sub>3</sub>	1.0—4.0	288—308	431
HCl, KCl	0.1—3.0	298	294
	0.1—1.5	278—318	295
		298	70
HCl, KCl, NH <sub>4</sub> Cl	0.5	298	240
HCl, CsCl	0.1—3.0	278—323	438
HCl, MgCl <sub>2</sub>	0.1—3.0	298	241
	0.1—5.0	278—318	398
HCl, CaCl <sub>2</sub>	0.1—3.0	398	241
	0.1—5.0	278—318	405
			334
HCl, SrCl <sub>2</sub>	0.1—5.0	278—318	415
HCl, BaCl <sub>2</sub>	0.1—3.0	298	242
	0.005—4.0	278—318	422
HCl, MnCl <sub>2</sub>	0.1—5.0	278—318	400
HCl, NiCl <sub>2</sub>	0.1—3.0	298	239
HCl, CoCl <sub>2</sub>	0.1—3.0	278—318	423
	0.1—3.0	298	243
	0.1—4.0	278—318	429
HCl, LaCl <sub>3</sub>	0.1—3.0	298	246
	0.1—5.0	288—318	406
HCl, choline, acetylcholine	0.1—3.0	278—308	299
HCl, PIPES, H <sub>2</sub> O	0.16	298—310	402
HCl, quat ammonium salts			298
<b>Hydrochloric Acid, Nonaqueous and Mixed Solvents</b>			
HCl, acetonitrile, H <sub>2</sub> O	Std pot	288—308	289
	0.01—0.1	263—298	510
HCl, <i>t</i> -BuOH, H <sub>2</sub> O	Std pot		125
HCl, 50% diglyme in H <sub>2</sub> O	0.01—0.1	278—328	404
HCl, DMF, EG/AgCl	Std pot	298	97
HCl, DMSO, H <sub>2</sub> O/AgCl	Std pot	261—298	488
	Std pot	298	135
HCl, DMSO, H <sub>2</sub> O, bicine	0.01—0.1	253—298	409
HCl, DMSO, BES, tricine	0.01—0.1	253—298	412
HCl, DMSO, EG, MOPS, H <sub>2</sub> O	0.01—0.1	253—298	414
HCl, DMSO, EG, HEPES, H <sub>2</sub> O	0.01—0.1	253—298	413
HCl, dioxan, H <sub>2</sub> O/AgCl	Std pot		138
HCl, EG, H <sub>2</sub> O/AgCl	Std pot	288—328	136
HCl, EG, BES, H <sub>2</sub> O	0.01—0.1	253—298	417
HCl, EG, bicine, tricine	0.01—0.1	253—298	418
HCl, EtOH, H <sub>2</sub> O/AgCl	Std pot	263—298	436
	Std pot	288—328	133
HCl, EtOH, H <sub>2</sub> O	0.01—0.1	263—318	284
HCl, 2-ethoxyethanol, H <sub>2</sub> O	Std pot		123

**TABLE 2 (continued)**  
**Recent Hydrogen Electrode Studies**

System	Ionic strength	Temp (K)	Ref.
HCl, formamide, DMF/AgCl			259
HCl, formamide, H <sub>2</sub> O/AgCl			260
HCl, formic acid, H <sub>2</sub> O/AgCl	Std pot		3
HCl, formic, acetic acid	Std pot		4
HCl, glycerol, H <sub>2</sub> O/AgCl	Std pot		130
HCl, glycerol, H <sub>2</sub> O, MOPS	0.01—0.1	253—298	411
HCl, HMPA/AgCl			75
HCl, MeOH, H <sub>2</sub> O/AgCl	Std pot		130
HCl, NH <sub>4</sub> Cl, MeOH, H <sub>2</sub> O	1	298	237
HCl, var org solv, H <sub>2</sub> O	Std pot	273—318	450
HCl, var org solv, H <sub>2</sub> O	0.01—0.16	298	102
HCl, 2-propanol, H <sub>2</sub> O/AgCl	Std pot		131,100
HCl, 2-propanol, H <sub>2</sub> O	0.01—0.1	278—323	511
HCl, PC, H <sub>2</sub> O/AgCl	Std pot	298	132
HCl, propylene glycol	0.005—0.05	288—318	439
HCl, THF, H <sub>2</sub> O/AgCl	Std pot		128
<b>Hydrobromic Acid, Aqueous</b>			
HBr, MgBr <sub>2</sub> /AgBr	0.1—4.0	278—318	421
HBr, CaBr <sub>2</sub> /AgBr	0.25—5.0	278—318	416
	0.1—2.0	298	245
HBr, SrBr <sub>2</sub> /AgBr	0.1—3.0	278—318	421
		298	278
HBr, BaBr <sub>2</sub> /AgBr	0.1—3.0	278—318	421
	0.1—2.0	298	244
HBr, Et <sub>4</sub> NBr, H <sub>2</sub> O/AgBr	0.05—1.5	278	395
HBr, Pr <sub>4</sub> NBr, H <sub>2</sub> O/AgBr	0.05—2.0	298	395
HBr, PIPES, H <sub>2</sub> O/AgBr	0.02—0.1	278—328	399
<b>Hydrobromic Acid, Nonaqueous and Mixed Solvents</b>			
HBr, 2-butanol, H <sub>2</sub> O/AgBr	Std pot		316
HBr, <i>t</i> -butanol, BES/AgBr	0.01—0.1	278—308	410
HBr, 2-butanone, H <sub>2</sub> O/AgBr	0.003—0.1	288—308	493
HBr, DMSO, H <sub>2</sub> O/AgBr	Std pot	298	135
HBr, dioxan, H <sub>2</sub> O/AgBr		Var	98
HBr, EG, H <sub>2</sub> O/AgBr	Std pot	288—328	135
HBr, EtOH, H <sub>2</sub> O/AgBr	0.001—0.09	298—318	382
HBr, MeOH, BES, H <sub>2</sub> O/AgBr	0.02—0.2	278—328	394
HBr, MeOH, H <sub>2</sub> O/AgBr	Std pot		127
HBr, MG, H <sub>2</sub> O, glycine/AgBr	0.01—0.2	278—328	392
HBr, NMA, H <sub>2</sub> O/AgBr	0.01—0.1	278—318	450
HBr, var org solv, H <sub>2</sub> O	0.01—0.16	298	450
HBr, PC, H <sub>2</sub> O/AgBr	Std pot	298	132
HBr, THF, H <sub>2</sub> O, glycine/AgBr	0.01—0.1	278—328	392
HBr, THF, H <sub>2</sub> O, BES/AgBr	0.01—0.1	278—318	393
<b>Hydroiodic and Hydrofluoric Acids</b>			
HI, DMSO, H <sub>2</sub> O/AgI	Std pot	298	135
HI, Dioxan, H <sub>2</sub> O			325
HI, Dioxan, H <sub>2</sub> O/AgI	Std pot	298	134
HI, EtOH, PrOH, H <sub>2</sub> O/AgI	Std pot	298, var	100
HI, MeOH, H <sub>2</sub> O/AgI	Std pot		126
HI, EG, H <sub>2</sub> O/AgI	Std pot	288—328	135

**TABLE 2 (continued)**  
**Recent Hydrogen Electrode Studies**

System	Ionic strength	Temp (K)	Ref.
HI, var org solv, H <sub>2</sub> O	0.01—0.16	298, var	227
HI, PC, H <sub>2</sub> O/AgI	Std pot	298	132
HI, prop glycol, H <sub>2</sub> O/AgI	Std pot		124
HF, superacid media			110
<b>Borate</b>			
B(OH) <sub>3</sub> , B(OH) <sub>4</sub> <sup>-</sup> , pK*	0—6.0	298	195
B(OH) <sub>3</sub> , NaB(OH) <sub>4</sub> , NaCl	0.01—3.0	278—328	464
B(OH) <sub>3</sub> , NaB(OH) <sub>4</sub>	0.1—1.5	273—318	113
B(OH) <sub>3</sub> , KB(OH) <sub>4</sub> , KCl	0.01—3.0	278—328	464
B(OH) <sub>3</sub> , NaB(OH) <sub>4</sub> , CaCl <sub>2</sub>	0.15—3.1	278—328	463
B(OH) <sub>3</sub> , NaB(OH) <sub>4</sub> , MgCl <sub>2</sub>	0.15—3.1	278—328	463
B(OH) <sub>3</sub> , NaB(OH) <sub>4</sub> , SrCl <sub>2</sub>	0.1—3.0	278—328	427
B(OH) <sub>3</sub> , NaB(OH) <sub>4</sub> , BaCl <sub>2</sub>	0.1—3.0	278—328	430
B(OH) <sub>3</sub> , B(OH) <sub>4</sub> <sup>-</sup> , seawater	0.7	273—318	114
Borate, AgI/Ag, diethylene glycol		278—308	227
<b>Carbonate</b>			
CO <sub>2</sub> , NaHCO <sub>3</sub> , NaCl	0.01—6.0	278—318	393
CO <sub>2</sub> , NaHCO <sub>3</sub> , seawater	Var	275—308	117
CO <sub>2</sub> , KHCO <sub>3</sub> , KCl	0.002—0.25	278—318	407
CO <sub>2</sub> , Mg(HCO <sub>3</sub> ) <sub>2</sub> , MgCl <sub>2</sub>	0.003—3.0	298	362
CO <sub>2</sub> , Ca(HCO <sub>3</sub> ) <sub>2</sub> , CaCl <sub>2</sub>	0.003—3.0	298	362
CO <sub>2</sub> , NH <sub>4</sub> HCO <sub>3</sub> , NH <sub>4</sub> Cl	0.07—1.0	278—318	419
NaHCO <sub>3</sub> , Na <sub>2</sub> CO <sub>3</sub> , NaCl	To 5.0	323—523	354
	0.1—6.0	273—323	356
KHCO <sub>3</sub> , K <sub>2</sub> CO <sub>3</sub> , KCl	0.03—7.0	278—318	408
	0.2—6.3	368	465
<b>Other Aqueous Buffers</b>			
ADA	0.16	278—328	403
Amino acid pK	0.025—0.5	298	376
2-Aminopyridinium	0.01—0.1	278—313	534
2-AMP <sup>-</sup> , pH std	Seawater	278—313	30
BisH <sup>+</sup> , Cl <sup>-</sup>	Seawater	278—313	27
Diglycolate buffer	0.05	278—338	87
HEPES buffer pK	0.01—0.16	273—323	147
MOPS buffer	0.01—0.16	278—328	411
Morpholinium ion	Seawater	278—313	90
Tris H <sup>+</sup>	0.57—0.77	278—313	374
Tris H <sup>+</sup> , estuarine	0.002—0.6	298	323
Tris H <sup>+</sup> , brines, pK*	0.5—6.0	298	374
Seawater, Ag/AgCl	Std pot	278—313	241
Silicate, polysil NaCl	0.1—5.0	To 573	52
Strong acid pH	0.005—0.7	298	530
Tetrovalate buffer	0.05	373—473	303
Tartrate buffer	0.05	373—473	303
Phthalate buffer	0.05	373—473	303
Various, pH buffers	0.01—0.16	298	531
Various, pH scale	Seawater	298	112

**TABLE 2 (continued)**  
**Recent Hydrogen Electrode Studies**

System	Ionic strength	Temp (K)	Ref.
<b>Nonaqueous</b>			
Acetate, phosphate, EtOH/H <sub>2</sub> O	0.05—0.10	263—298	31
Acetate and tris in 2-MeO-EtOH, H <sub>2</sub> O		283—323	454
Ag/AgCl, Ag/AgBr std pot in 1,2-ethanediol-2,2-oxydiethanol		298	468
AgCl, AgBr, AgI, AgCNS, EtOH		298	102
BisH <sup>+</sup> , MeOH	0.015—0.0053	283—313	29
Deutero-phthalate, D <sub>2</sub> O	0.02—0.07	278—323	529
Phosphate, TES, phthalate, DMSO	0.005—0.2	261—298	489
Phthalate, organic	0.05	278—323	283
Phthalate, EtOH, H <sub>2</sub> O	0.005—0.03	268—318	288
Propylene carbonate		273—298	473
<b>Other</b>			
Kw and ioniz enthalpy of H <sub>2</sub> O		Var	83
Single ion activity coeff			20
<b>Codes for organic compounds</b>			
ADA	<i>N</i> -(2-Acetamido) iminodiacetate		
BES	<i>N,N</i> -Bis(2-hydroxyethyl)-2-aminoethane-sulfonic acid		
Bicine	<i>N,N</i> -bis(2-hydroxyethyl)glycine		
Bis	2-Amino-2-methyl-1,3-propanediol		
Diglycolate	2,2'-Oxydiacetate		
Diglyme	Bis(2-methoxyethyl) ether		
DMF	Dimethylformamide		
DMSO	Dimethyl sulfoxide		
DTAB	Decyl trimethylammonium bromide		
EG	Ethylene glycol		
Et <sub>4</sub> NBr	Tetraethylammonium bromide		
HEPES	<i>N</i> -(2-Hydroxyethyl)piperazine- <i>N'</i> -ethanesulfonic acid		
MG (Monoglyme)	1,2-Dimethoxyethane		
MOPS	3-( <i>N</i> -Morpholino)propanesulfonic acid		
NMA	<i>N</i> -Methylacetamide		
PC	Propylene carbonate		
PIPES	Piperazine- <i>N,N</i> -bis(2-ethanesulfonic acid) monosodium monohydrate		
Pr <sub>4</sub> NBr	Tetrapropylammonium bromide		
SDDS	Sodium dodecylsulfate		
TES	<i>N</i> -Tris(hydroxymethyl)methyl-2-aminoethane sulfonate		
THF	Tetrahydrofuran		
Tricine	<i>N</i> -[Tris(hydroxyoxyethyl)-methyl]glycine		
Tris	<i>N</i> -Tris(hydroxymethylamino)methane		

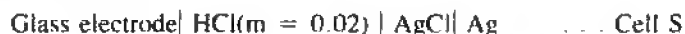
*Note:* Cell is Pt/H<sub>2</sub> . . . AgCl/Ag except where noted. Codes for organic chemical names are at the end of the table.

**TABLE 3**  
**Proposed Values for the**  
**Mean Activity Coefficient of**  
**0.01 M HCl<sup>28</sup>**

Temp (°C)	$\gamma_{\pm}$
0	0.9081
5	0.9074
10	0.9067
15	0.9060
20	0.9051
25	0.9042
30	0.9033
35	0.9024
40	0.9014
45	0.9003
50	0.8992
55	0.8980
60	0.8968

same glass electrode with two matched reference electrodes in the two solutions to be compared. The glass electrode is transferred back and forth between the two cells while the potential is recorded continuously. With a noise-free electrometer, proper shielding, and temperature matching of cells,<sup>161</sup> measurements accurate to a few hundredths of a millivolt, comparable in accuracy to the hydrogen electrode, can be achieved.<sup>78,79</sup>

An assessment of the accuracy of glass electrode response was made by Serjeant and Warner<sup>83</sup> using the two cells:



Cell S was used for standardization assuming

$$p(a_{\text{H}^+} \gamma_{\text{Cl}^-}) = \text{pH} - \log(\gamma_{\text{Cl}^-}) = -\log(m_{\text{H}^+} \gamma_{\text{Cl}^-}^{\pm}) = 1.815$$

(This value is from Bates.<sup>19</sup> Note that in Table 3,  $\gamma_{\pm} = 0.9042$  at 25°C,<sup>28</sup> which gives  $p(a_{\text{H}^+} \gamma_{\text{Cl}^-}) = 1.786$ . This is a significant difference, but not one which affects the error analysis.)

Cell X contained the solution whose acidity function was to be measured. Values of  $p(a_{\text{H}^+} \gamma_{\text{Cl}^-})$  and range within each of ten data sets for  $m_1 = 0.002$  to 0.05 and phosphate concentrations  $m_1 = m_2$  as given below were

$m_1 = m_2$	$p(a_{\text{H}^+} \gamma_{\text{Cl}^-})$	Range within a set
0.02	6.940 to 6.991	$\pm 0.001$ to 0.003
0.0025	6.989 to 7.113	$\pm 0.001$ to 0.003
0.001	7.000 to 7.142	$\pm 0.002$ to 0.008
0.0005	6.991 to 7.145	(Not given)

The errors in  $p(a_{\text{H}^+} \gamma_{\text{Cl}^-})$  extrapolated to  $m_{\text{Cl}^-} = 0$  at phosphate concentrations 0.001 to 0.02  $m$  were equal to or less than ( $\pm 0.003$ ), approaching that of the hydrogen electrode ( $\pm 0.001$ ).

Experimentally simpler, because elaborate precautions for eliminating oxygen are not necessary, the glass electrode method can provide detailed activity coefficient data more

**TABLE 4**  
**Thermodynamic Studies Using Glass pH**  
**Electrodes**

System	Ref.
<b>Activity Coefficients</b>	
HCl	13
HCl, LiCl, NaCl, KCl, CaCl <sub>2</sub> , etc.	516—518
HCl and chlorides	300, 301
HCl, HBr in brines	253
Trichloroacetic acid	143
<i>N</i> -Tris(hydroxymethyl)-aminomethane perchlorate	212
<b>Acidity Constants</b>	
Trichloroacetic acid	143
Boric acid and polymers	264
Carbonic acid in NaCl	492
Phosphoric acid in EtOH-H <sub>2</sub> O	37
Phosphoric acid in seawater	116
Phosphoric acid in NaCl	317
Ammonia in seawater	45
Ammonia in seawater	223
HS <sup>-</sup> -S <sup>=</sup>	273
H <sup>+</sup> , K <sup>+</sup> , citrate	92
Aliphatic dicarboxylic acids	108
Amino acids in isopropanol-H <sub>2</sub> O	111
Malonic etc. acids in dioxan-H <sub>2</sub> O	386
3-Butylacetylacetone, dioxan-H <sub>2</sub> O	458
Aromatic carboxylic acids in DMSO	166
Methoxybenzoic acids, dioxan-H <sub>2</sub> O	357
3,5-Dinitrosalicylic acid	177
<b>Stability Constants</b>	
Cu <sup>2+</sup> — histamine in PrOH-H <sub>2</sub> O	94
Ni <sup>2+</sup> -Cl <sup>-</sup> -imidazole	153
H <sup>+</sup> -H <sub>2</sub> VO <sub>4</sub> — C <sub>2</sub> O <sub>4</sub> <sup>2-</sup>	121
Al <sup>3+</sup> —CO <sub>2</sub> (g)—OH <sup>-</sup>	193
Fe(CN) <sub>6</sub> <sup>4-</sup>	109
Fe <sup>3+</sup> -3,5-dinitrosalicylate	177

rapidly, and can work under some circumstances (e.g., reducible solutes) where the hydrogen electrode cannot be used. For example, the standard potential of the Co<sup>3+</sup>/Co<sup>2+</sup> couple was measured using a gold redox electrode and a glass electrode as reference.<sup>38</sup>

The temperature range can be extended using ceramic membranes.<sup>196,347</sup> The corrosive action of HF solutions can be overcome by using lithium phosphate glasses.<sup>348</sup> Both acid errors<sup>312,313</sup> and alkaline errors<sup>272</sup> can be corrected if the electrode is calibrated in solutions of known activity. With enough data over a wide range of pH and ion composition, electrode parameters can be determined along with pK<sub>a</sub> or activity coefficient parameters.<sup>314,366</sup> See Section V for further discussion.

## B. TYPICAL RESULTS

A wide range of studies in both aqueous and nonaqueous<sup>57,487,489</sup> (see Table 4) media have employed the glass pH electrode to determine activity coefficients, acidity constants, and complex stability constants.

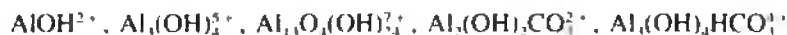
For example, a glass pH electrode and silver chloride electrode with double junction were used to determine activity coefficients and Pitzer parameters for "tris" buffer [*N*-tris(hydroxymethyl)amino methane] with perchlorate ion as well as the acidity constant of this buffer.<sup>212</sup>

Similarly, the activity coefficients of trichloroacetic acid and its anion, together with ionic association constants, were measured using a glass electrode, a 3 *M* KCl salt bridge, and a silver chloride electrode.<sup>144</sup>

The first and second acidity constants of sulfurous acid were determined over the NaCl ionic strength range 0.1 to 6.0 and temperature range 278 to 298 K using glass and silver chloride electrodes, by Millero et al.<sup>324</sup> The effects of MgCl<sub>2</sub>, NiCl<sub>2</sub>, CdCl<sub>2</sub>, MnCl<sub>2</sub>, and CoCl<sub>2</sub> in NaCl on these constants were investigated by Roy et al.<sup>424,425</sup>

A more complicated system involved multicomponent polyanions in the H<sup>+</sup>-H<sub>2</sub>VO<sub>4</sub> - C<sub>2</sub>O<sub>4</sub><sup>2-</sup> system in 0.6 *M* NaCl medium. A glass electrode and reference electrode with liquid junction were calibrated to determine E<sub>i</sub> in solutions with known [H<sup>+</sup>] for each titration, and hence used as the basis of a hydrogen ion activity scale; E<sub>j</sub> was found to be approximately -76 [H<sup>+</sup>] mV. Measurements of hydrogen ion activity over a wide range of acidity, vanadate and chromate, were analyzed to find stability constants for the ternary complexes (H<sup>+</sup>)<sub>p</sub>(H<sub>2</sub>VO<sub>4</sub>)<sub>q</sub>(C<sub>2</sub>O<sub>4</sub><sup>2-</sup>)<sub>r</sub>, where p, q, r = 2, 1, 2 and 2, 1, 1.<sup>121</sup> This particular study could not have used a hydrogen electrode because of the oxidizing nature of the vanadate and chromate ions.

A potentiometric study of speciation and equilibria in the Al<sup>3+</sup>-CO<sub>2</sub>(g)-OH<sup>-</sup> system employed a glass pH electrode with a double junction AgCl/Ag reference, to evaluate hydrolytic aluminum and carbonate species in 3.0 *M* NaCl):



pK<sub>a</sub> for HCO<sub>3</sub><sup>-</sup> was found to be 7.820 at 3 *M* NaCl and 7.619 at 0.1 *M* NaCl.<sup>193</sup>

A number of additional examples are listed in Table 4. A more comprehensive survey is beyond the scope of this work, but much information can be found in the stability constant literature.<sup>310,360,361</sup>

## IV. AMALGAM ELECTRODES

### A. METHODS

For a reversible electrode to be effective in cells used for thermodynamic measurements, three primary criteria must be satisfied: (1) the exchange current (rate at the equilibrium potential) for the desired reaction must be high; (2) the concentrations of reactants must be either constant or accurately known; and (3) no other reaction must take place at appreciable rates at the electrode.

The requirement of high exchange current is well satisfied by the amalgams of all the alkali metals. For example, under conditions where the sodium amalgam electrode has been used to determine the activity coefficients of NaCl,<sup>161</sup> the exchange current for the reversible reaction<sup>308</sup>



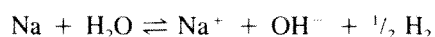
is of the order of 1 A/cm<sup>2</sup>, comparable to that of the platinum-hydrogen and silver-silver chloride electrodes.<sup>211</sup>

The second criterion is more difficult to satisfy. The electrolyte composition can be accurately analyzed, but because of the possibility of contamination by traces of oxygen, the composition of amalgams (prepared by electrolysis, or by mixing weighed quantities of



mercury and alkali metal) can be accurately determined only with great difficulty. For this reason, virtually all workers have used two identical cells fed from the same amalgam supply, with one containing a solution of known activity (as we described for the glass electrode) and the other the solution under study.<sup>181</sup>

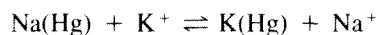
The final criterion, absence of side reactions, is the most difficult to satisfy and is the primary cause of experimental errors with amalgam electrodes. Even though the activity of an alkali metal in a dilute amalgam (0.5% by weight) may be  $10^{-14}$  that of the pure metal,<sup>36</sup> the dissolution reaction



may still take place at the amalgam-electrolyte interface.<sup>47,157,256</sup>

Dissolution of the amalgam affects the measured potential in two important ways: (1) it shifts the zero-current potential from the reversible value because the additional electrode process of hydrogen evolution adds cathodic current but not anodic current; and (2) it increases the concentration of sodium ion (and decreases the concentration of sodium in amalgam) in the diffusion layer immediately adjacent to the electrode surface, and thus shifts the electrode potential by concentration polarization. Both of these shifts are to more positive values: the first depending on pH, but not strongly on salt concentration, and the second becoming most important at low salt or low amalgam concentrations.

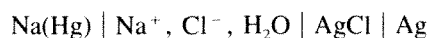
In addition to hydrogen evolution, reaction can also take place between the amalgam and another solute. For example, in NaCl-KCl electrolytes, the reaction



can shift the potential of a sodium amalgam electrode by several millivolts.<sup>63</sup> These various effects are discussed quantitatively elsewhere.<sup>55</sup>

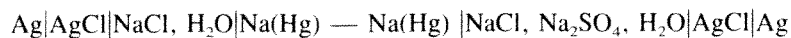
## B. TYPICAL RESULTS

The most careful early work done with sodium amalgam electrodes was probably the measurement by Smith and Taylor<sup>470</sup> of the standard electrode potential of sodium. Working in a completely air-free system, they obtained the potential of the cell



reproducible within  $\pm 0.02$  mV. Their results imply that the large ( $\pm 0.5$  mV) random deviations observed by other workers may have been caused by failure to exclude oxygen from the system rigorously.

Later work<sup>62</sup> confirmed this. For the pair of cells



with salt concentrations all at 1.000 *m*, both solutions 0.01 *m* in NaOH, and an amalgam containing 0.365% by weight of Na, potentials measured on successive changes of solution were

$$\begin{aligned} &22.25 \pm 0.05 \text{ mV} \\ &21.85 \pm 0.05 \text{ mV} \\ &21.65 \pm 0.01 \text{ mV} \end{aligned}$$

The last value was constant for over an hour without appreciable drift.

**TABLE 5**  
**Studies Using Alkali Amalgam**  
**Electrodes**

System	Ref.
LiCl	286
	387
	388
Li <sup>+</sup> (salt?) in THF	33
NaCl	181, 182
NaCl in seawater	363
NaCl	149
NaCl-MgSO <sub>4</sub>	364
NaCl-LiCl, NaCl-KCl	63
NaCl-CaCl <sub>2</sub> , NaCl-MgCl <sub>2</sub>	59
NaCl-NaF	53
NaCl-NaHCO <sub>3</sub> , NaCl-Na <sub>2</sub> CO <sub>3</sub>	61
NaBF <sub>4</sub>	107
Na <sup>+</sup> (salt?) in THF	34
NaCl and brine	16
Na <sub>2</sub> SO <sub>4</sub> in seawater	365
KBr, KI in ethylenediamine	302
LiCl, NaCl, KCl in EtOH-H <sub>2</sub> O and MeOH-H <sub>2</sub> O	315

Some studies of activity coefficients using sodium amalgam electrodes are listed in Table 5.

Lithium, potassium, cesium, and rubidium amalgams in principle can be used in the same type of measurements as sodium amalgams. Some examples are listed in Table 5.

### C. ALKALINE EARTH AMALGAMS

A word should be said about alkaline earth amalgams. Although some of the basic activity coefficient data for the alkaline earth chlorides were first obtained using amalgam electrodes, these have been supplanted by more accurate isopiestic and ion-selective membrane electrode data (see below).

Part of the reason for the lack of success of the alkaline earth amalgam electrodes is their much smaller exchange current, resulting from the necessity for two-electron transfers, as well as their more negative standard potentials (Mg:  $-2.1$  V, compared to Na:  $-1.96$  V).<sup>59</sup> A review of the literature on calcium amalgams<sup>64</sup> led to a "best" value for its standard potential of  $-1.996 \pm 0.002$  V. The experimental errors of individual measurements were of the order of 1 mV, which is not nearly so accurate as the data obtained with alkali amalgam electrodes discussed above.

Recent work has established standard potentials for magnesium amalgam electrodes in the aprotic solvents dimethylformamide, propylene carbonate, and acetonitrile.<sup>60</sup>

### D. OTHER METAL AMALGAMS

Amalgams of other metals have frequently been used in thermodynamic studies, especially cadmium and zinc, but also indium and thallium. The same principles as discussed above apply — the more positive the standard potential and the higher the exchange current, the more precise is the measurement. In many cases, amalgams saturated with the pure metal (e.g., Zn, Cd) are used so that the activity of the metal in the amalgam is equal to that of the pure metal and the amalgam does not need to be separately analyzed. Amalgams are used instead of the pure solid metal because the liquid surface is easily renewable and not subject to the formation of electroactive oxide or salt films.

Some examples are given in Table 6.

**TABLE 6**  
**Examples of Studies Using Other Metal**  
**Amalgam Electrodes**

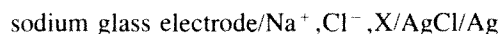
System	Ref.
In(Hg), InCl <sub>3</sub>	68
In(Hg), In(ClO <sub>4</sub> ) <sub>3</sub>	509
Tl(Hg), TlCl, KCl	73
Tl(Hg), TlBr, KBr, KNO <sub>3</sub>	175
Tl(Hg), TlCl, KCl	290
Tl(Hg), TlI, R <sub>4</sub> NI	14
Cu(Hg), CuSO <sub>4</sub>	2
	226
Zn(Hg), ZnSO <sub>4</sub> (activity)	202
Zn(Hg), ZnCl <sub>2</sub> , ethylenediamine	302
Zn(Hg), ZnCl <sub>2</sub> , dioxan, acetone, acetic acid, H <sub>2</sub> O	268
Zn(Hg), ZnCl <sub>2</sub> , NaClO <sub>4</sub> , LiClO <sub>4</sub> , Mg(ClO <sub>4</sub> ) <sub>2</sub> , Mg(NO <sub>3</sub> ) <sub>2</sub>	309
Cd(Hg), Cd <sup>2+</sup> -bipyridyl, Cd <sup>2+</sup> -citrate	95
Cd(Hg), Cd <sup>2+</sup> -I <sup>-</sup> complexes	293
Hg, Hg <sub>2</sub> <sup>2+</sup> , Hg <sup>2+</sup>	435
	525

## V. CATION-SELECTIVE GLASS ELECTRODES

### A. METHODS

Like glass pH electrodes, cation-selective glass electrodes were only recently used to determine activity coefficients. These electrodes are based on sodium aluminum silicate ("cation") or lithium aluminum silicate ("sodium") glasses which have little interference from hydrogen ion if the pH is near neutrality.

The activity coefficients of NaCl measured by the cell<sup>266,267</sup>



(where X stands for any set of noninterfering anions or cations) agree with values obtained using the corresponding amalgam electrode cell,<sup>59,62,63</sup> and with the isopiestic method<sup>226,227,442</sup> (see Figure 2).

To obtain accuracy better than  $\pm 0.1$  mV it is necessary to record the cell potential continuously as the electrode is transferred between a test and reference cell. Transients<sup>122</sup> lasting 10 to 100 ms resulting from charging the ion-exchange surface of the glass, transients of the order of 30 s resulting from diffusion of solutions of different concentrations into the hydrated glass layer, and transients of the order of hours resulting from changes in the deeper structure of the glass are all compensated by extrapolating the recorded traces to the same point in time.<sup>535</sup>

Most reliable work has been done with the standard commercial "Na-selective" and "K-selective" glasses — but the universe of possible glasses is very large and it has not been thoroughly explored yet.<sup>122</sup> Chalcogenide glasses have generated considerable interest.<sup>351</sup> A glass composed of AgAs<sub>2</sub> and PbI<sub>2</sub> responds in a Nernstian fashion to Pb<sup>2+</sup> and Ag<sup>+</sup>.<sup>43</sup> A lithium/lanthanum glass has been used as sensor for Na<sup>+</sup> and NH<sub>4</sub><sup>+</sup> in liquid ammonia solutions; activity coefficients of NaNO<sub>3</sub> and NH<sub>4</sub>NO<sub>3</sub> agreed with those measured by transference methods.<sup>72</sup>

### B. SELECTIVITY

With mixed electrolytes, the glass electrode potential may depend on the concentration

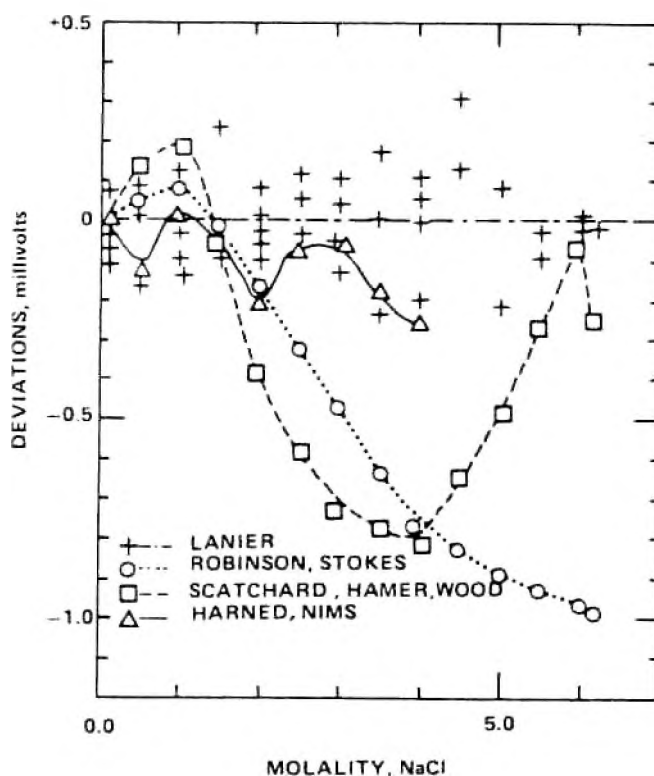


FIGURE 2. Precision of glass electrode-silver chloride cell in comparison with other determinations of the activity coefficient of NaCl: glass<sup>206</sup> + · — · — ·, amalgam<sup>201</sup> △ —, isopiestic and other methods<sup>142, 164, 172</sup> (—), ○ —.

of more than one cation.<sup>122</sup> Typically this dependence is described in terms of a selectivity ratio  $K_j$ :

$$E = E^{\circ} + \frac{RT}{F} \ln (a_{Na} + \sum_j K_j a_j)$$

where  $a_j$  is the activity of an ion that interferes with the sodium-selective electrode. If the cell is without liquid junction (e.g., reference electrode selective for Cl<sup>-</sup>) the activity of the ion is replaced by  $m_j m_{Cl} \gamma_{Cl}^2$ , where  $\gamma_{Cl}$  is the mean activity coefficient of the metal chloride. If polyvalent ions are to be included, their activity is raised to the power  $(1/z_j)$ , where  $z_j$  is the charge on the cation.

Selectivity ratios defined in this way are more or less characteristic of the glass composition, and in dilute solutions, relatively independent of solution composition. In concentrated solutions, however, interaction of ions in the hydrated glass layer leads to quite a complicated dependence of  $K_j$  on solution composition and the time scale of measurement;<sup>513, 524</sup> unfortunately the theory of glass electrodes is not adequate to predict this dependence *a priori*. It is thus necessary to verify glass electrode measurements by other methods.

### C. TYPICAL RESULTS

Studies of aqueous sodium chloride by this technique have been frequent (see Table 7) and all workers report satisfactory agreement with data obtained by other methods (Figure

2). Together, these studies cover the concentration range from below 0.01 to over 6 *m*, and the temperature range from 273 to 323 K.

In part because of its importance both in physiological systems and in the chemistry of seawater, the CaCl<sub>2</sub>-NaCl multicomponent electrolyte system has been studied by ion-selective electrodes more than any other. Moore and Ross<sup>328</sup> provided the rationale: “. . . it is calcium ion activity rather than stoichiometric concentration which is physiologically meaningful. No thermodynamic data are available, however, which allow estimation of mean ionic CaCl<sub>2</sub> activity in mixed electrolytic solutions with composition similar to that of extracellular fluid.” Their work employed a sodium-selective glass electrode. Its results were verified<sup>269</sup> by additional work with glass electrodes,<sup>168,266,267</sup> by the isopiestic method,<sup>385</sup> and by sodium amalgam electrodes.<sup>59</sup> These studies have verified that Harned’s rule is not fully obeyed: although  $\log \gamma_{\pm}$  for CaCl<sub>2</sub> is linearly dependent on the ionic strength fraction of NaCl,  $\log \gamma_{\pm}$  for NaCl is *not* linear with the ionic strength fraction of CaCl<sub>2</sub>.<sup>6</sup>

These results are in generally good agreement with isopiestic studies<sup>184,432</sup> and with amalgam electrode measurements<sup>55</sup> where such comparisons can be made. In particular, verification by amalgam electrodes has been obtained for

- NaCl-Na<sub>2</sub>SO<sub>4</sub> <sup>62</sup>
- NaCl-KCl and NaCl-LiCl <sup>63</sup>
- NaCl-MgCl<sub>2</sub> <sup>59</sup>
- NaCl-CaCl<sub>2</sub> <sup>59</sup>
- NaCl-NaHCO<sub>3</sub> <sup>61</sup>
- NaCl-Na<sub>2</sub>CO<sub>3</sub> <sup>61</sup>
- NaCl-NaF <sup>53</sup>

In this last system, a LaF<sub>3</sub> membrane electrode (see Section IX) was used as a reference electrode, together with sodium-selective glass and sodium amalgam electrodes.

Attention should be called, however, to an unexplained systematic error obtained with sodium-selective glass electrodes in NaCl-NaHCO<sub>3</sub> electrolytes (Figure 6).<sup>61</sup>

Ion pairing in K<sub>2</sub>SO<sub>4</sub> has been inferred<sup>497</sup> from measurements of salt activity using a cation-selective glass electrode. Similar measurements have been made in Na<sub>2</sub>SO<sub>4</sub> solutions using a sodium-selective glass electrode.<sup>233,235,370</sup>

As part of determining the second acidity constant of H<sub>2</sub>S in concentrated KOH solutions, corrections for potassium were established using cation-selective glass electrode.<sup>272,273</sup>

Sodium ferrocyanide<sup>462</sup> required use of a Pb(Hg)/Pb<sub>2</sub>Fe(CN)<sub>6</sub> electrode together with a sodium-selective glass electrode.

Sodium-selective glass electrodes have also been used to obtain the free energy of transfer of NaCl between H<sub>2</sub>O and H<sub>2</sub>O-D<sub>2</sub>O mixtures.<sup>292</sup> The LaF<sub>3</sub> membrane electrode (see Section IX) has been used with the cation glass electrode to determine the free energy of transfer of NaF from H<sub>2</sub>O to H<sub>2</sub>O-H<sub>2</sub>O<sub>2</sub> mixtures.<sup>84</sup>

These and other multicomponent systems studied using the sodium-selective glass electrode together with various reference electrodes in cells without liquid junction are listed in Table 7. Examples are shown in Figures 3 and 4. Note that Harned’s rule is not always obeyed (Figure 5).

Nonaqueous as well as aqueous solutions have been studied using glass electrodes. For example, a wide variety of measurements on alkali halides in acetone-water mixtures have been reported.<sup>146</sup> Sodium glass electrodes have been used in propylene carbonate to measure the complexation of uranyl ion with 18-crown-6 cyclic ether.<sup>159</sup> The possibilities are vast and have been only slightly explored.

**TABLE 7**  
**Cation-Selective Glass Electrode Measurements of**  
**Activity Coefficients in Multicomponent**  
**Electrolyte Solutions**

System	Ref. electrode	Ref.
NaCl	AgCl/Ag	266,267
	AgCl/Ag	199
	AgCl/Ag	276
	AgCl/Ag	496
	AgCl/Ag	446
	AgCl/Ag	455
	AgCl/Ag	358
NaCl, D <sub>2</sub> O	AgCl/Ag	292
NaCl-KCl	AgCl/Ag	122
	AgCl/Ag	266
	AgCl/Ag	329
	AgCl/Ag	318
NaCl-Na <sub>2</sub> SO <sub>4</sub>	AgCl/Ag	204
	AgCl/Ag.Pb(Hg)/PbSO <sub>4</sub>	267
	AgCl/Ag.Pb(Hg)/PbSO <sub>4</sub>	168
	AgCl/Ag.Pb(Hg)/PbSO <sub>4</sub>	370
	AgCl/Ag.Pb(Hg)/PbSO <sub>4</sub>	235
AgCl/Ag.Pb(Hg)/PbSO <sub>4</sub>	480	
NaCl-seawater		441
NaCl-NaHCO <sub>3</sub>	AgCl/Ag	61
NaCl-Na <sub>2</sub> CO <sub>3</sub>	AgCl/Ag	61
NaCl-NaClO <sub>4</sub>	AgCl/Ag	267
NaCl-NaNO <sub>3</sub>	AgCl/Ag	267
	AgCl/Ag	304
	AgCl/Ag	306
	AgCl/Ag	306
NaCl-NaAcetate	AgCl/Ag	267
	AgCl/Ag. Na-glass	307
NaCl-NaF	AgCl/Ag. LaF <sub>3</sub>	53
NaCl-LiClO <sub>4</sub>	AgCl/Ag	446
NaCl-MgCl <sub>2</sub>	AgCl/Ag	267
	AgCl/Ag	234
NaCl-MgSO <sub>4</sub>	AgCl/Ag	168
	AgCl/Ag	234
	AgCl/Ag	235
NaCl-Mg(ClO <sub>4</sub> ) <sub>2</sub>	AgCl/Ag	446
NaCl-CaCl <sub>2</sub>	AgCl/Ag	328
	AgCl/Ag	269
	AgCl/Ag	266
	AgCl/Ag	267
	AgCl/Ag	168
	AgCl/Ag	62
	AgCl/Ag	6
NaCl-SrCl <sub>2</sub>	AgCl/Ag	267
NaCl-BaCl <sub>2</sub>	AgCl/Ag	267
NaCl-Al(ClO <sub>4</sub> ) <sub>3</sub>	AgCl/Ag	446
NaCl-Ba(ClO <sub>4</sub> ) <sub>2</sub>	AgCl/Ag	446
NaCl-glycine	AgCl/Ag	358
NaCl-Na <sub>2</sub> Fer(CN) <sub>6</sub>	Hg <sub>2</sub> Cl <sub>2</sub> /Hg/Pb(Hg)/Pb <sub>2</sub> Fer(CN) <sub>6</sub>	462
NaF. H <sub>2</sub> O <sub>2</sub>	LaF <sub>3</sub>	84
NaBr. 2-propanol	AgBr/Ag	172
Na <sub>2</sub> SO <sub>4</sub>	fibre jet	370
	AgCl/Ag	235

**TABLE 7 (continued)**  
**Cation-Selective Glass Electrode Measurements of**  
**Activity Coefficients in Multicomponent**  
**Electrolyte Solutions**

System	Ref. electrode	Ref.
KCl-KNO <sub>3</sub>	AgCl/Ag	352
	AgCl/Ag	308
KCl-KF	AgCl/Ag, LaF <sub>3</sub>	221
KCl-K <sub>4</sub> Fe(CN) <sub>6</sub>	AgCl/Ag, K-glass?	109
KCl-CaCl <sub>2</sub>	AgCl/Ag, K-glass	305
K <sub>2</sub> SO <sub>4</sub>		497
KOH, K <sub>2</sub> S		272
		273

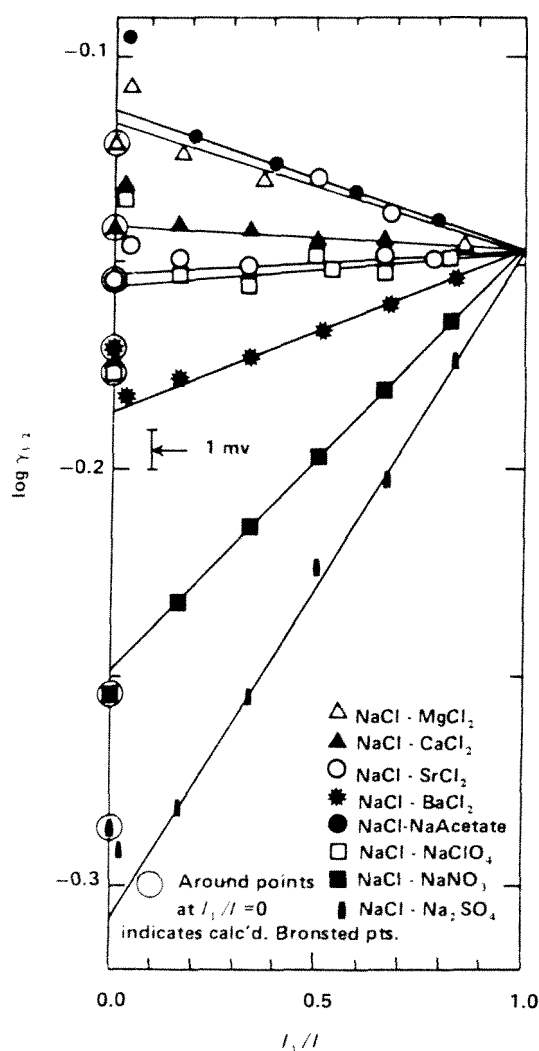


FIGURE 3. Activity coefficients of NaCl in mixtures at total ionic strength 3.0 m. (Reprinted with permission from Lanier, R. D., *J. Phys. Chem.*, 69, 3992, 1965. Copyright by the American Chemical Society.)

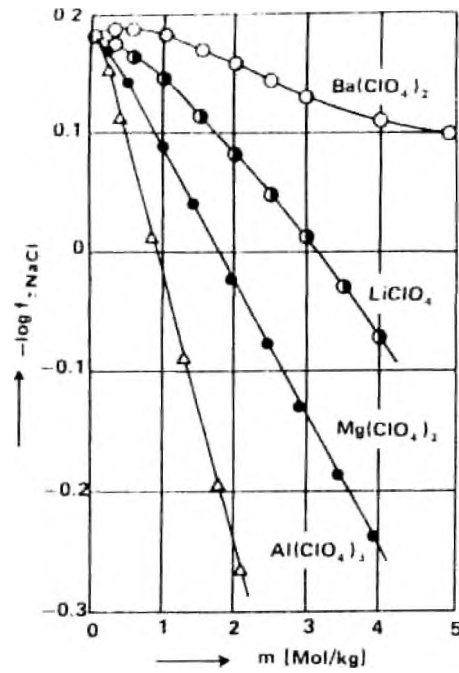


FIGURE 4. Activity coefficient of 1 m NaCl in the presence of other salts at concentration  $m$ . (From Schwabe, K. and Dwojak, J., *Z. Phys. Chem. (Frankfurt am Main)*, 64, 1, 1969. With permission.)

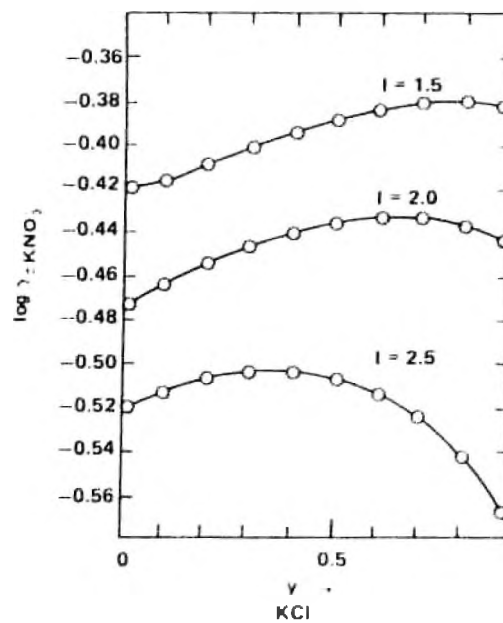


FIGURE 5. Activity coefficient of KNO<sub>3</sub> in KNO<sub>3</sub>-KCl electrolytes at constant ionic strength. (Reprinted with permission from Padova, J., *J. Phys. Chem.*, 26, 4587, 1970. Copyright by the American Chemical Society.)



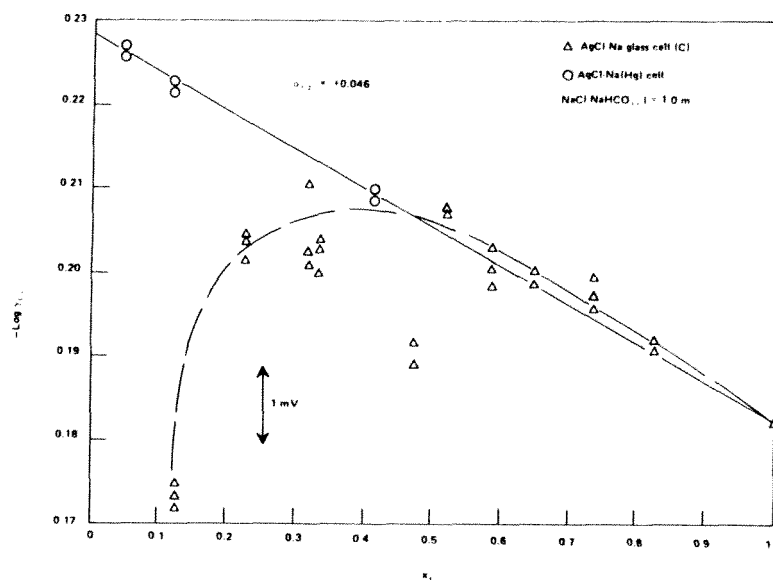


FIGURE 6. Activity coefficients of NaCl in NaCl-NaHCO<sub>3</sub> electrolytes at ionic strength 1.0 *m* (note deviations of glass electrode data). (Reprinted with permission from Butler, J. N. and Huston, R., *J. Phys. Chem.*, 74, 2976, 1970. Copyright by the American Chemical Society.)

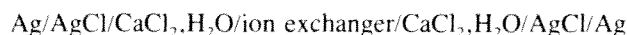
## VI. LIQUID AND POLYMER-BASED ION-EXCHANGE ELECTRODES

### A. INTRODUCTION — LIQUID ION EXCHANGE

The development since 1965 of liquid ion-exchange electrodes<sup>389,390</sup> that were selective for various cations and anions, particularly Ca<sup>2+</sup>, Mg<sup>2+</sup>, Cu<sup>2+</sup>, Pb<sup>2+</sup>, K<sup>+</sup>, NO<sub>3</sub><sup>-</sup>, ClO<sub>4</sub><sup>-</sup>, Cl<sup>-</sup>, and BF<sub>4</sub><sup>-</sup>, was motivated primarily by the need for easily automated analytical methods and not by the need to measure thermodynamic properties of electrolytes. These electrodes are subject to electrostatic instability of the membrane surface charge, which produces irregular drifts in potential. As might be expected, the ion exchangers are not perfectly selective — selectivity depends on site mobility as well as ion-exchange equilibrium<sup>476</sup> — and so measurements in multicomponent solutions must be interpreted with caution. Nevertheless, a number of studies relating cell potential to activity coefficients have been made.

### B. ACTIVITY COEFFICIENT MEASUREMENTS

The earliest such studies were of calcium chloride using the ion exchanger calcium didecyl phosphate dissolved in dioctylphenyl phosphonate,<sup>389</sup> in a cell such as



Examples<sup>56</sup> are the work of Huston and Butler<sup>203</sup> in the concentration range 0.01 to 6 *m*, Cachaza and Casal<sup>65</sup> in the range 0.001 to 1.6 *m*, a student laboratory experiment,<sup>265</sup> and the recent careful work of Briggs and Lilley<sup>48</sup> over the range from 0.001 to 0.3 *m* at 25°C, which established agreement within 0.15 mV with values calculated from cells with transport and from vapor pressure measurements (Table 8).

Early work with the calcium-selective liquid ion-exchange electrode in concentrated NaCl-CaCl<sub>2</sub> solutions<sup>203,389</sup> showed that although the response of the electrode was Nernstian in pure CaCl<sub>2</sub> electrolytes, the selectivity with respect to Na<sup>+</sup> became so poor at high ionic

TABLE 8  
Accuracy of Calcium Liquid in  
Exchange Electrode

$10^3(\text{Ca}^{2+})$ (mol/kg)	$\Delta E_{\text{exp}}$ (mV)	$\Delta E_{\text{exp}} - \Delta E_{\text{calc}}$ (mV)
1.0275	119.49	-0.07
3.2519	78.42	+0.10
10.165	39.05	-0.16
33.081	0.00	0.00
99.104	-35.68	-0.03
295.89	-72.64	+0.19

Note: Orion 92-02 calcium liquid ion exchanger. Measurements are by Briggs and Lilley;<sup>26</sup> activity coefficients for  $\Delta E_{\text{calc}}$  are from Lietzke and Stoughton.<sup>27a</sup>

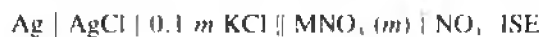
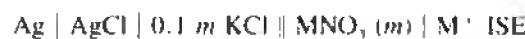
After Covington.<sup>69</sup>

strengths that no useful activity coefficients could be determined in mixed electrolytes. At low ionic strengths (0.03 to 0.12), however, satisfactory results were obtained,<sup>65,203</sup> and at ionic strength 0.3, satisfactory results were obtained with  $\text{CaCl}_2\text{-NaNO}_3$ ,  $\text{CaCl}_2\text{-KCl}$ , and  $\text{CaCl}_2\text{-KNO}_3$  mixtures, although not with  $\text{CaCl}_2\text{-NaCl}$ .<sup>65</sup>

An explanation for this behavior was proposed by Whitfield and Leyendekkers,<sup>537</sup> who developed a quantitative theory of the liquid ion-exchange electrode based on extraction equilibria, under the assumption that regular solution theory applies within the ion exchanger. Data on  $\text{CaCl}_2\text{-NaCl}$ ,<sup>269</sup>  $\text{CaCl}_2\text{-MgCl}_2$ ,<sup>270</sup> and  $\text{CaCl}_2\text{-SrCl}_2$ <sup>270</sup> were used to test the theory over the range of ionic strengths up to 6 with success (Figures 7 and 8).

More recent studies of the calcium ion-exchange electrode process have evaluated not only the zero-current potential,<sup>505</sup> but also the dissociation of the ion exchanger<sup>507</sup> and the mechanism of transport under nonzero current conditions.<sup>506</sup>

Activity coefficients of  $\text{NaNO}_3$ ,  $\text{KNO}_3$ , and  $\text{Ca(NO}_3)_2$  at molalities up to 4 *m* were measured using cells with a nitrate-selective liquid ion-exchange electrode, such as<sup>26</sup>



where the left half of the cell is a commercial double-junction reference electrode. The difference in potential between these two cells corresponds to

$$E = E^0 - (S_1 + S_2) \log m - (S_1 + S_2) \log \gamma_+$$

where  $E^0$  is a constant,  $S_1$  and  $S_2$  are the empirical "Nernst slopes" of the two cells above, and  $\gamma_+$  is the activity coefficient of  $\text{MNO}_3$  at concentration *m*. A number of cation-selective electrodes were used:

- A sodium-selective glass electrode
- A cation-selective glass electrode
- A commercial valinomycin-based  $\text{K}^+$  electrode (see Section VII)
- A valinomycin-PVC electrode (see Section VII)
- A neutral carrier (ETH 1001)  $\text{Ca}^{2+}$  electrode (see Section VII)

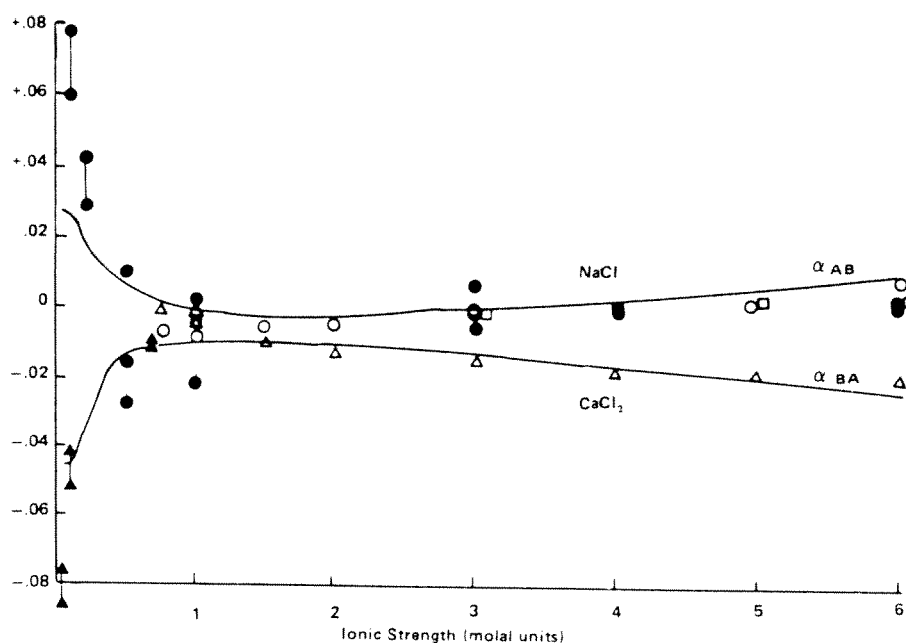
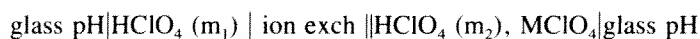


FIGURE 7. Harned rule coefficients for NaCl-CaCl<sub>2</sub> electrolytes. Curves are theoretical.<sup>269</sup> Experimental points obtained with sodium-selective glass electrode: ○ Moore and Ross,<sup>328</sup> □ Lanier;<sup>267</sup> with sodium amalgam electrode: ⊙ Butler and Huston<sup>59</sup>; with isopiestic vapor pressure method: ○, △ Robinson and Bower;<sup>385</sup> with calcium-selective liquid ion-exchange electrode: ▲ Leyendekkers and Whitfield.<sup>269</sup>  $\alpha_{AB}$  is the slope of the plot of sodium chloride activity vs. ionic strength fraction, divided by the (constant) ionic strength of the mixture. See Figure 3 for some of the data used.

- A PVC electrode based on the Orion 93-20-02 ion exchanger
- An Orion liquid ion-exchange electrode for Ca<sup>2+</sup>
- An Orion liquid ion-exchange electrode for divalent ions

An important conclusion reached by this study was that even if the Nernst plot for an electrode is strictly linear, satisfactory activity coefficient values can only be obtained when random errors do not exceed 0.5 mV; otherwise a strong correlation between parameters such as the Nernst slope and the Debye-Hückel linear term renders the results inaccurate.<sup>26</sup>

A perchlorate-selective liquid ion exchanger, 0.001 *m* tetraheptylammonium perchlorate in ethyl bromide, was used in the cell



to determine the activity coefficients of perchloric acid at concentrations from 0.001 to 1.5 *m*, and the activity coefficient of HClO<sub>4</sub> in solutions containing NaClO<sub>4</sub>.<sup>495</sup> This study is particularly important because it verifies isopiestic studies of a "noncomplexing" electrolyte used in thousands of stability constant measurements.

### C. ION PAIRING AND STABILITY CONSTANTS

A few studies have used the liquid ion exchangers to determine stability constants and related thermodynamic quantities.

- Ion association in MgSO<sub>4</sub> was measured using a divalent ion-selective liquid ion-exchange electrode.<sup>233,234,235</sup>

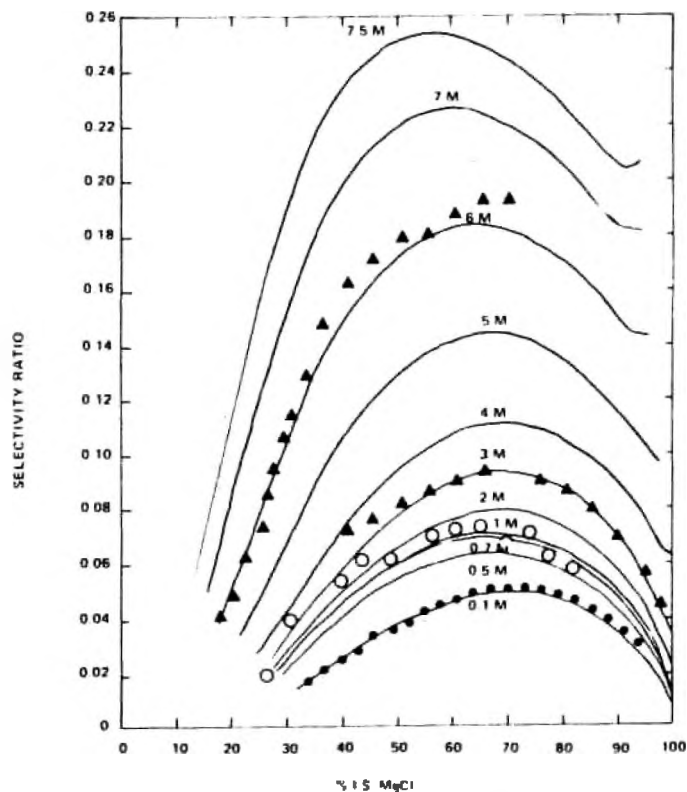


FIGURE 8. Solvent-extraction model of selectivity for calcium-selective liquid ion exchange electrodes, in mixtures with  $\text{MgCl}_2$ . Points are experimental results, curves are calculated theoretically. (Reprinted with permission from Leyendekers, J. V. and Whitfield, M., *Anal. Chem.*, 43, 322, 1971. Copyright by the American Chemical Society.)

- Ion association of  $\text{CaSO}_4$  has been studied using a calcium-selective liquid ion-exchange electrode.<sup>233,235</sup>
- The Orion 92-32 divalent cation-selective liquid ion-exchange electrode was used to study the association between  $\text{Mg}^{2+}$  and  $\text{SO}_4^{2-}$ , and  $\text{Ca}^{2+}$  and  $\text{SO}_4^{2-}$ , in  $\text{NaCl}$  of varying ionic strength and temperatures from 15 to 35°C.<sup>139,140</sup>
- The  $\text{CaCl}_2$ - $\text{CaSO}_4$  system and the  $\text{CaSO}_4$  system have been carefully studied by Briggs and Lilley.<sup>49,277</sup>
- The ion association of  $\text{Ca}^{2+}$  and  $\text{Mg}^{2+}$  with *m*-hydroxy-, 3,5-dihydroxy-, and 3,4,5-trihydroxybenzoate were measured at 25 to 45°C in aqueous  $\text{NaCl}$  or tetramethylammonium chloride electrolytes using the Orion 92-32 divalent cation electrode.<sup>142</sup>
- Cells consisting of a glass electrode and a 3,5-dinitrosalicylate (DNS) selective membrane<sup>179</sup> were used to determine both the second ionization constant of  $\text{DNSH}_2$  and the stability constant of  $\text{DNSFe}^+$ .<sup>177</sup>
- The  $\text{pK}_a$  of *N*-chloro-*p*-toluenesulfonamide, the acid of "chloramine-*t*" (CAT), was measured with a CAT-ion-selective membrane electrode and a glass electrode at ionic strengths 0.15 to 0.75 and 25°C, in close agreement with reported values.<sup>258</sup>

Other association equilibria have been inferred and their stability constants measured by similar methods. (See Martell and Smith<sup>310</sup> for a more complete bibliography.)

#### D. PVC MEMBRANES

The other popular way of using ion exchangers is to support them in a polyvinyl chloride

(PVC) membrane.<sup>326,355,501</sup> Such electrodes are easier to construct, more robust, and in some cases more precise than liquid ion exchangers.

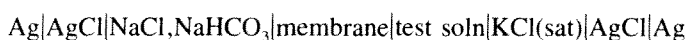
Electrodes selective for  $\text{Ca}^{2+}$ ,  $\text{Ba}^{2+}$ , divalent ions,  $\text{UO}_2^{2+}$ ,  $\text{K}^+$ ,  $\text{Li}^+$ ,  $\text{Na}^+$ , and substituted ammonium ions have been constructed and tested. They mostly exhibit Nernstian or near-Nernstian behavior over several orders of magnitude in concentration.<sup>326</sup> However, other than the work of Bates et al.,<sup>26</sup> no rigorous studies of activity coefficients have apparently been made using this type of electrode.

Thermodynamic studies using PVC membrane electrodes have been more numerous and apparently satisfactory. For example, a calcium electrode based on calcium bis[di(4-octyl-phenyl)phosphate] was used in solutions of  $10^{-7}$  to  $10^{-3}$  *m*  $\text{Ca}^{2+}$  with citrate, malate, malonate, oxalate, EDTA, NTA,  $\text{SO}_4^-$ ,  $\text{HPO}_4^-$ , tripolyphosphate, and pyrophosphate. Stability constants agreed with the literature, and phosphates were found not to interfere with the electrode (aside from the known calcium-phosphate complexing in solution).<sup>88</sup>

### E. OTHER POTENTIAL TOOLS

Many electrodes have been tested for selectivity and Nernstian behavior, which might easily be applied to activity coefficient or stability constant measurements. Here are some examples; others are briefly referenced in Table 9:

- A hydrogen ion-selective electrode stable in fluoride media was composed of iron (III) chloride hexahydrate in 1-decanol and tetrahydrofuran, and fabricated into a PVC membrane, which showed a linear pH response from 0 to 5 with a slope of 56 mV.<sup>522</sup>
- A PVC matrix containing Ca bis{di[4-(1,1,3,3-tetramethylbutyl) phenyl]phosphate}, with dioctyl phenylphosphonate, tripentyl phosphate, or trioctyl phosphate as solvent mediator as tested for calcium response in 0.15 *m* NaCl, and interference from various materials was found in body fluids: starch, sucrose, uric acid, creatinine, and bilirubin produced changes of <0.5 mV; cholic acid, cholesterol, lecithin, and vitamin D<sub>2</sub> produced larger changes. The electrode employing trioctyl phosphate showed the greatest resistance to interferences.<sup>236</sup>
- The ion exchanger tetradecylammonium carbonate, incorporated in PVC membranes plasticized by hexyl trifluoroacetylbenzoate and *o*-nitrophenyl octyl ether, was tested in the cell



for its response to  $\text{CO}_3^-$  activity.<sup>469</sup>

- A liquid membrane based on a lipophilic derivative of vitamin B<sub>12</sub> was tested for selectivity and found to have preference for nitrite over nitrate ( $K_{\text{sel}} > 10^{4.2}$ ) and chloride ( $10^{4.8}$ ).<sup>445</sup>
- A periodate-selective liquid ion-exchange electrode based on the perchlorate ion exchanger was used in a kinetic study of the tartaric acid-periodate reaction. The selectivity factor is  $> 10^5$  for most anions other than perchlorate.<sup>186</sup>
- Perchlorate-selective electrodes were made from the natural lacquer Urushi with tri-*n*-octylmethylammonium perchlorate to form a hard, lustrous surface with response ranges and selectivity similar to the commercial liquid ion-exchange electrodes.<sup>197</sup>
- Ionic activities in aqueous solution have reportedly been measured using ion exchangers based on epoxy resins.<sup>225</sup>
- Another  $\text{ClO}_4^-$ -selective ion exchanger was based on the nitron-perchlorate ion pair in nitrobenzene. (Nitron is 4,5-dihydro-1,4-diphenyl-3,5-phenylimino-1,2,4-triazole.) It had a near-Nernstian response over the concentration range  $2 \times 10^{-5}$  to 0.01 *m*, pH range 2.5 to 8.5, with slope 56 mV. Selectivity with respect to 27 organic and inorganic ions was measured; periodate, permanganate, and thiocyanate interfere most.<sup>191</sup>

TABLE 9  
Some Potentially Useful Ion-Exchange Electrodes

Selective to	Exchanger	Ref.
Li <sup>+</sup>	Ba polyalkoxylates	162
	Li polyalkoxylates	162
Cs <sup>+</sup>	K <sub>2</sub> ZnFe(CN) <sub>6</sub> — PVC	91
Alkali	Polypropylene glycol	213
Tetraalkyl cations		471
Tl <sup>+</sup>	$\alpha$ -Picolinium molybdoarsenate	216
		483
Ca <sup>2+</sup>		176
		207
	Organophosphate	76
	Bicyclic polyether amide	250
NaCl-CaCl <sub>2</sub>	HNU-ISE 20-20-00 <sup>a</sup>	6
Ba <sup>2+</sup>	In acetonitrile	340
Alkaline earth	Polypropylene glycol	213
Cu <sup>2+</sup>		485
		515
Bi <sup>3+</sup>		484
NO <sub>3</sub> <sup>-</sup>	2,2'-Bipyridine etc	206
	Nitrobenzene aliquat	311
PF <sub>6</sub> <sup>-</sup>	Quaternary phosphonium salts	254
TiCl <sub>4</sub>	Quaternary phosphonium salts	255
Au in CN <sup>-</sup>		456
Tetraphenylborate		230
Benzoate		35
46 univalent anions	Nitrobenzene-based	451
CO <sub>3</sub> <sup>2-</sup>		448
	Ion exchange/PVC	469
Thiobarbiturates		77
$\beta$ -Adrenergic blockers		89
Ca blockers		89
Nomonic surfactants	Ca and Ba tetraphenylborates with poly(oxyethylene) mono(6-methyl-heptyl)phenyl ether	479

<sup>a</sup> This electrode is probably a liquid ion-exchange type, but no details were given in the original paper.

- The nitron-tetrafluoroborate complex in nitrobenzene shows a rapid Nernstian response to BF<sub>4</sub><sup>-</sup> over the range from 10<sup>-5</sup> to 0.1 *m* and pH 3 to 9. Selectivity was measured with respect to 21 anions and cations.<sup>190</sup>
- An ephedrine-flavianate ion pair in 1-octanol shows near-Nernstian response to ephedrine from 10<sup>-5</sup> to 10<sup>-2</sup> *m*, pH 4 to 7; and this concept was extended to produce electrodes responsive to other neurotransmitters containing the  $\beta$ -ethanolamine moiety: epinephrine and norepinephrine.<sup>189</sup>
- Both liquid and PVC membrane electrodes based on the ion pair of glycopyrronium with dicyclohexyl naphthalenesulphonate, di-isopentyl naphthalenesulphonate, di-isobutyl naphthalenesulphonate, and tetraphenylborate show near-Nernstian response to glycopyrronium ion over the range pH 4 to 8 and concentrations as low as 10<sup>-6</sup> *m*.<sup>511</sup>
- The nafronyl-dinonylnaphthalenesulphonic acid ion pair in a PVC matrix exhibited near-Nernstian response to protonated nafronyl activity from 10<sup>-5</sup> to 10<sup>-2</sup> *m*. Nafronyl oxalate [2-(1-naphthyl)methyl-3-(2-furyl)propanoic acid 2-(diethylamino)ethyl ester oxalate] is a well-known vasodilator.<sup>209</sup>

## VII. NEUTRAL CARRIER-BASED ELECTRODES

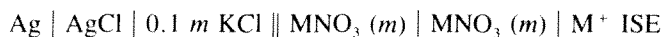
### A. METHODS

Ion exchangers based on neutral carriers such as the macrocyclic antibiotic valinomycin<sup>80,474</sup> and the synthetic crown ethers<sup>145,375,434</sup> have been used as the basis for electrodes selective for  $H^+$ ,  $Li^+$ ,  $Na^+$ ,  $Ca^{2+}$ ,  $Mg^{2+}$ , and a variety of other ions. Both liquid ion-exchange membranes and PVC-based membranes have been employed.<sup>326</sup> Neutral carrier electrodes have proved particularly useful in designing microelectrodes (as small as 45 nm diameter) for physiological studies.<sup>5</sup> However, few studies of activity coefficients have been published.

### B. ACTIVITY COEFFICIENT MEASUREMENTS

Shortly after the neutral carrier electrodes were first developed, activity coefficients in the NaCl-KCl system were measured using a potassium-selective valinomycin-based electrode,<sup>58</sup> and the results were within 10 mV of the predicted values based on isopiestic activity coefficient measurements at ionic strengths up to 4.2 *m*. The deviations were systematically in the direction of poorer selectivity and measurable  $Cl^-$  transport through the membrane.<sup>150,359</sup> More precise results can be obtained by using fresh, carefully purified ion-exchange materials.

As described in Section VI.B, activity coefficients of  $NaNO_3$ ,  $KNO_3$ , and  $Ca(NO_3)_2$  at molalities up to 4 *m* were measured using cells such as<sup>26</sup>



where the left half of the cell is a commercial double-junction reference electrode, and a similar cell was used to measure the activity of nitrate in another sample of the solution. Three neutral carrier-based cation-selective electrodes were used:

- A commercial valinomycin-based  $K^+$  electrode
- A valinomycin-PVC electrode
- A neutral carrier (ETH 1001)  $Ca^{2+}$  electrode

Comparison of calculated and observed values over the full range of concentrations (e.g., 0.001 to 2.00 *m*  $NaNO_3$ , 3.00 *m*  $KNO_3$ , 4.00 *m*  $Ca(NO_3)_2$ ) showed a root-mean-square deviation of the order of 2 mV.

As with the liquid ion-exchange electrodes, the literature on neutral carrier electrodes is dominated by analytical method development, particularly in the medical area. For instance, the 346-page monograph on ion-selective microelectrodes by Amman<sup>5</sup> with 840 references contains only two citations of experimental activity coefficient measurements — one of which has been cited here — Bates et al.<sup>26</sup> Most items in the text indexed under "activity coefficient" were general and theoretical.

### C. POTENTIAL TOOLS

Here are some examples of how neutral carrier electrodes have been used in analytical chemistry and in the determination of stability constants — which may suggest applications to activity coefficient measurements. Further references are given in Table 10.

- Lipophilic neutral carriers in PVC membranes were designed to be selective for lithium. Best selectivity for  $Li^+$  over  $Na^+$  was obtained with the diamide: *N,N*-dicyclohexyl-*N',N'*-diisobutyl-*cis*-cyclohexane-1,2-dicarboxamide; and the 14-crown-4 ether: 3-dodecyl-3-methyl-1,5,8,12-tetraoxacyclotetradecane.<sup>161</sup>
- Calcium-selective neutral carriers (cyclic polyether amides) were synthesized. Their

**TABLE 10**  
**Some Potentially Useful Neutral Carrier Electrodes**

Selective to	Exchanger	Ref.
Na <sup>+</sup>	Synthetic, intracellular microelec- trodes	5,475
	PVC-electron-transfer solid contact design	459
K <sup>+</sup> (impedance)	Valinomycin	8
K <sup>+</sup>	Bis-crown ether/PVC	158
K <sup>+</sup>	Valinomycin	262
K <sup>+</sup>		198
		200
K <sup>+</sup> in seawater		440
Li <sup>+</sup>	1,4,7,10-Tetraoxacyclodode- cane (12-crown-4)	160
Cs <sup>+</sup>	Bis-crown ether/PVC	158
Cs <sup>+</sup>	Bis(crown ether)/PVC	248
NH <sub>4</sub> <sup>+</sup>		287
K <sup>+</sup> , Rb <sup>+</sup> , Cs <sup>+</sup> , Tl <sup>+</sup> , Ag <sup>+</sup> , NH <sub>4</sub> <sup>+</sup>	PVC-valinomycin	520
Ba <sup>2+</sup> in acetonitrile	Macrocyelic polyether	340
Guanidinium	Crown ether/PVC	40
Cations	Macrocyelic lactones	42
	Macrocyelic lactonelactams	42

selectivity for Ca<sup>2+</sup> relative to H<sup>+</sup>, Na<sup>+</sup>, K<sup>+</sup>, and Mg<sup>2+</sup> was good enough to promise accurate determination of Ca<sup>2+</sup> activity in blood serum.<sup>250</sup>

- Another calcium-selective neutral carrier is *N,N,N',N'*-tetracyclohexyl-3-oxapentanediamide. This compound forms an almost ideal coordination sphere of nine oxygen atoms around a calcium ion, resulting in selectivity of 10<sup>7.4</sup> and 10<sup>8</sup> with respect to Na<sup>+</sup> and K<sup>+</sup>.<sup>443</sup> This represents a substantial improvement in ability to measure calcium activity in serum, soils, and other natural mixed electrolytes; it should also provide an improvement in measurement of activity coefficients in multicomponent salt solutions (compare Bates et al.<sup>26</sup>).
- A lead-selective electrode was developed using lipophilic amides which select for PbX<sup>+</sup> species. The neutral carrier *N,N*-dioctadecyl-*N',N'*-dipropyl-3,6-dioxaoctanediamide was found to reject alkali metal cations by a factor of at least 10<sup>1</sup> and alkaline earth metal ions by at least 10<sup>4</sup>.<sup>280</sup>
- Thioethers 1,4-dithia-12-crown-4 and 1,4-dithia-15-crown-5 showed response to Hg<sup>2+</sup> and Ag<sup>+</sup> over concentrations 10<sup>-6</sup> to 10<sup>-2</sup> and 10<sup>-1</sup>, respectively, and were applied as sensors in titration procedures for Br<sup>-</sup> and Cl<sup>-</sup> with Ag<sup>+</sup> and of I<sup>-</sup> and Cr<sub>2</sub>O<sub>7</sub><sup>2-</sup> with Hg<sup>2+</sup>.<sup>261</sup>
- Hasegawa et al.<sup>187</sup> report lithium salt effects on the extraction of 15-crown-5, 18-crown-6, or their silver(I) complexes as picrates

## VIII. CELLS WITH TRANSFERENCE: ELECTRODES OF THE SECOND KIND

### A. METHOD

In addition to the direct potentiometric measurement of activity coefficients as described in the previous sections, it is possible to measure activity coefficients in a cell with transference at a liquid junction between two solutions of different concentration.<sup>182,184</sup> The two identical reversible electrodes are almost always Ag/AgCl. (The silver halide electrode



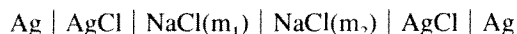
**TABLE 11**  
**Results from Cell with Transference Using**  
**CsCl at 25°C**

$10^2 m_1$ (mol/kg)	$10^2 m_2$ (mol/kg)	E (mV)	(Eobs-Ecalc) (mV)
10.723	8.8261	4.46	-0.01
10.723	7.9822	6.78	0.00
10.723	6.8737	10.21	-0.03
10.723	5.9933	13.41	-0.02
10.723	3.0204	29.72	+0.13
6.0436	4.9880	4.47	-0.02
6.0436	4.0329	9.45	-0.04
6.0436	2.9810	16.66	+0.01
3.0242	2.0042	9.85	-0.01
3.0242	1.6924	13.92	-0.02
3.0242	1.0139	26.38	-0.03

After Kelley and Lilley.<sup>232</sup>

literature was reviewed in Section II. See especially Bates and Macaskill,<sup>25</sup> Mussini,<sup>335</sup> and Bates and Robinson.<sup>28</sup>)

For example, the potential of the cell:



is given by (Reference 384, pp. 201 to 204)

$$E = - \frac{2RT}{F} \int_{m_1}^{m_2} t_+ d \ln (m\gamma)$$

where  $m_1$  and  $m_2$  are the two salt concentrations,  $\gamma$  is the corresponding activity coefficient, and  $t_+$  is the corresponding cation transport number — determined by a separate conductance experiment.

## B. RESULTS

Differences between observed and calculated values approach the reproducibility of the electrode potential measurements. For example, recent results obtained with cesium chloride<sup>232</sup> are given in Table 11. Similar results were obtained for LiCl.<sup>231</sup> The HCl-BaCl<sub>2</sub> liquid junction was thoroughly studied both experimentally and theoretically.<sup>349,350</sup>

Alkali halide solutions were studied in a cell with transference<sup>15</sup> employing the LaF<sub>3</sub> electrode as well as the Ag<sub>2</sub>S/AgCl and Ag<sub>2</sub>S/AgBr electrodes (see Section IX):



For their studies,  $m_1$  and  $m_2$  ranged from 0.001 to 6 *m* NaCl, 4 *m* KCl, 4 *m* KBr, 3 *m* KF, and 1 *m* LiCl. The results were consistent with other literature and with their model for the operation of crystal membrane electrodes.

Das et al.<sup>99</sup> measured the transference number of hydrochloric acid in dioxane + water mixtures by this technique. Activity coefficients for transfer of single ions between dipolar aprotic solvents were obtained from cells with liquid junction.<sup>170</sup>

## C. POTENTIAL TOOLS

Although silver/silver halide electrodes are virtually standard for cells with transference,

**TABLE 12**  
**Electrodes of the Second Kind**

Electrode	Ref.
Ag/Ag benzoate	106
Ag/AgCl (high temp)	96
Ag/Ag <sub>2</sub> CrO <sub>4</sub>	101
Ag/Ag <sub>2</sub> SO <sub>4</sub> , Na <sub>2</sub> SO <sub>4</sub>	457
Hg/Hg benzoate	433
Hg/Hg(IO <sub>3</sub> ) <sub>2</sub>	341
Hg/HgO	481
	482
Hg/Hg picrate	229
Hg/Hg propionate	17
Hg/Hg <sub>2</sub> SO <sub>4</sub>	226
	322

amalgam, glass, and ion-exchange electrodes could in principle be used. These have been reviewed in Sections IV to VII. Some other systems based on metal-solid phase equilibria (electrodes of the "second kind") are listed in Table 12 (see also Ives and Janz<sup>211</sup> and Janz and Tomkins<sup>210,211</sup>).

Other systems in this general style include the redox-based quinhydrone<sup>229,477</sup> and chloranil electrodes,<sup>129</sup> which were classic pre-glass-electrode pH sensors. Another is a sensor for Al employing a glass pH electrode:<sup>44</sup>



Bromide interference with anodized Ag/AgCl electrodes was studied by impedance measurement.<sup>377,378</sup>

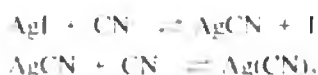
## IX. SOLID-STATE MEMBRANE ELECTRODES

### A. METHODS

This type of electrode includes both crystals and pellets made of pressed powder. Like the other membrane electrodes, selectivity is established by a combination of ion-exchange reactions at the interfaces and transport through the membrane bulk. It was made popular by the Frant and Ross<sup>151</sup> fluoride-selective electrode, which used a LaF<sub>3</sub> crystal as a membrane.

Related solid-state electrodes use a pressed mixture of Ag<sub>2</sub>S (which provides transport) with a silver halide or sulfide salt, such as AgCl, AgBr, PbS, or CdS (which provide the ion-exchange reactions). These electrodes are thermodynamically equivalent to the classic Ag/AgX or metal amalgam electrodes, but with the advantage of freedom from interference by oxidizing or reducing components.<sup>51,188</sup>

AgI/Ag<sub>2</sub>S electrodes are selective for CN<sup>-</sup>, or any other ligand which complexes more strongly with Ag than does I<sup>-</sup>.<sup>151,188,208</sup> The surface reactions



release I<sup>-</sup> in proportion to the (flow) surface concentration of CN<sup>-</sup>, which in turn determines the potential of the electrode.

**TABLE 13**  
**Activity Coefficient Studies Using Solid**  
**State Membrane Electrodes**

System	Electrode	Ref.
NaF:	LaF <sub>3</sub>	21
NaCl-NaF	LaF <sub>3</sub>	53
KF (and alkali halides?)	LaF <sub>3</sub>	15
NaF, acetone	LaF <sub>3</sub>	146
KCl-KF	LaF <sub>3</sub>	221
HCl	AgCl/Ag <sub>2</sub> S	253
NaCl-KCl	AgCl/Ag <sub>2</sub> S	253
NaCl-NaOH	AgCl/Ag <sub>2</sub> S	253
NaCl-NaBr	AgBr/Ag <sub>2</sub> S	253
NH <sub>4</sub> Br	AgBr/Ag <sub>2</sub> S	285

Selectivity of these electrodes depends on many factors, including concentration, solution mixing, measurement duration, and electrode history.<sup>51,201,369,377</sup>

Selectivity coefficients have been tabulated for LaF<sub>3</sub>, AgCl/Ag<sub>2</sub>S, and AgBr/Ag<sub>2</sub>S electrodes;<sup>201,327</sup> CdS/Ag<sub>2</sub>S.<sup>504</sup>

## B. ACTIVITY COEFFICIENT MEASUREMENTS

Some measurements of activity coefficients using solid-state ion-selective electrodes are outlined in Table 13.

NaF was a natural first choice.<sup>21</sup> We have already mentioned in Section IV the studies of NaCl-NaF electrolyte mixtures where the LaF<sub>3</sub> membrane electrode was used as a reference electrode in addition to the Ag/AgCl electrode.<sup>53</sup> The transference cell studies by Bagg and Rechnitz,<sup>15</sup> employing the LaF<sub>3</sub> electrode in place of the usual Ag/AgCl electrode, were mentioned in Section VIII. Free energies of transfer for NaF from water to mixtures containing up to 60 wt% acetone were obtained using a sodium-selective glass and LaF<sub>3</sub> electrode.<sup>146</sup>

Knauss et al.<sup>253</sup> compared potentials measured by pH-glass, Na-glass, AgCl-Ag<sub>2</sub>S and AgBr-Ag<sub>2</sub>S solid state, and K-selective membrane electrodes with activity functions (pH + pCl, pH + pBr, pH - pNa, pH - pK) calculated using the Pitzer<sup>360,361</sup> equations for activity coefficients in the geochemical modeling program EQ3/6.<sup>214</sup>

## C. STABILITY CONSTANTS

The rapid response of the fluoride-selective LaF<sub>3</sub> membrane electrode making it possible to measure the rate of formation of the complexes FeF<sup>2+</sup> and AlF<sup>2+</sup> was demonstrated soon after the electrode was first developed.<sup>472</sup>

The LaF<sub>3</sub> membrane electrode in conjunction with the glass pH electrode was used to determine the pK<sub>a</sub> of HF, in solutions with ionic strength 0.05 to 0.5, and total fluoride 10<sup>-5</sup> to 10<sup>-3</sup> m. The Nernstian behavior in 1.0 m NaClO<sub>4</sub>, and agreement of that pK<sub>a</sub> with other methods showed that the fluoride electrode continues to measure fluoride activity even in acidic solutions.<sup>508</sup>

Many more studies of solution equilibria using these electrodes have been published. Table 14 lists a few. See also Sillen and Martell,<sup>460,461</sup> Martell and Smith,<sup>310</sup> and Butler.<sup>56</sup>

## D. POTENTIAL TOOLS

A number of electrodes have been developed which might be used for activity coefficients or other thermodynamic studies. Table 15 lists some examples.

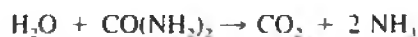
**TABLE 14**  
**Some Examples of Stability Constant**  
**Measurements Using Solid State**  
**Membrane Electrodes**

System	Electrode	Ref.
pKa of HF	LaF <sub>3</sub>	194
SiO <sub>2</sub> -F	LaF <sub>3</sub>	380
Sulfide ion pairs	Ag <sub>2</sub> S	178
Cd-EDTA	CdS/Ag <sub>2</sub> S	504
Cd-NTA	CdS/Ag <sub>2</sub> S	504
Cd-trien	CdS/Ag <sub>2</sub> S	504
Cd-tetren	CdS/Ag <sub>2</sub> S	504
CdCl <sub>2</sub>	CdS/Ag <sub>2</sub> S	333
Cu-EDTA etc. (12 different ligands)	CuAgSe	343, 344

## X. ENZYME AND OTHER BIOLOGICALLY BASED ELECTRODES

### A. METHODS

Enzyme electrodes consist of an enzyme immobilized in a layer adjacent to an ion-selective or pH electrode. Typically, an organic molecule in solution undergoes an enzyme-catalyzed reaction which produces a species to which the electrode responds.<sup>257,502</sup> For example, in the presence of urease, urea is hydrolyzed to CO<sub>2</sub> and NH<sub>3</sub>:



NH<sub>3</sub> is in equilibrium with NH<sub>4</sub><sup>+</sup>, which can be measured using a cation-selective electrode. Urea can be determined over the concentration range 5 × 10<sup>-5</sup> to 10<sup>-2</sup> M.<sup>224</sup> Oxalate (which produces CO<sub>2</sub>) can be determined using oxalate oxidase over concentrations from 3 × 10<sup>-6</sup> to 2 × 10<sup>-4</sup>.<sup>46,174</sup>

Other enzyme electrode systems are amperometric: β-glucose oxidase. β-glucose reacts with oxygen to produce gluconic acid and hydrogen peroxide:



Both O<sub>2</sub> and H<sub>2</sub>O<sub>2</sub> are electroactive.

Some important materials determinable by enzyme electrodes include

- Urea
- Glucose
- Amino acids
- Amygdalin
- Penicillin
- Creatinine
- Uric acid
- 5' Adenosine monophosphate

Substrate and electrode also can be used to measure enzyme activity. See the review by Koryta<sup>257</sup> which covers enzyme electrodes suitable for measuring alcohols, amines, amino acids, carboxylic acids, carbohydrates, cofactors, inorganic ions, and gases.

**TABLE 15**  
**Solid-State Membrane Electrodes: Potential Tools**

Selective to	Membrane material	Ref.
Ag <sup>+</sup>	Sulfide	218
Ag <sup>+</sup> , Hg <sup>2+</sup>	Cation exchange	353
	Sulfur nitride	371
Ag <sup>+</sup> (low conc)	Ag <sub>2</sub> S	185
Ca <sup>2+</sup>	CaF <sub>2</sub> crystal	167
Cd <sup>2+</sup>	Ag <sub>2</sub> S/CdS?	69
Cd <sup>2+</sup> , Cu <sup>2+</sup> , Mg <sup>2+</sup> mixtures		332
Cl <sup>-</sup> (cf. AgCl/Ag <sub>2</sub> S)	Hg <sub>2</sub> Cl <sub>2</sub> /HgS	279
CN <sup>-</sup>	Ag <sub>2</sub> S/AgI	172
	Ag <sub>2</sub> S/AgI	368
Cu <sup>2+</sup>	CuAgSe ternary alloy	44
	Polycrystalline	69
	Ag <sub>2</sub> S/CuS <sup>†</sup>	339
	Sulfide	343—345
	Ag <sub>2</sub> S/CuS?	346
	β-V <sub>2</sub> O <sub>5</sub> bronzes	500
	CuAgSe ternary alloy	519
F <sup>-</sup> (dynamics)	LaF <sub>3</sub>	67
F <sup>-</sup>	LaF <sub>3</sub>	148
F <sup>-</sup> (dynamics)	LaF <sub>3</sub>	165
F <sup>-</sup> (dynamics, flow)	LaF <sub>3</sub>	192
F <sup>-</sup>	Fluoride electrode	449
F <sup>-</sup>		499
F <sup>-</sup>	LaF <sub>3</sub>	503
F <sup>-</sup> (OH <sup>-</sup> interference)	LaF <sub>3</sub>	513
F <sup>-</sup>	LaF <sub>3</sub>	521
Halide (interference)	Ag halides	330
Hg <sup>2+</sup>	Iodide electrode	7
NH <sub>4</sub> <sup>+</sup>	Solid ion exchange	514
Pb <sup>2+</sup>	Sulfide	210
	Sulfide	339
Pb <sup>2+</sup> complexes*	PbS/AgS	478
Phosphate		319
Quat ammonium	Halide halide electrode	171
SO <sub>4</sub> <sup>2-</sup> , SO <sub>3</sub> <sup>2-</sup> , S <sub>2</sub> O <sub>6</sub> <sup>2-</sup>		467
S <sub>2</sub> O <sub>3</sub> <sup>2-</sup> , thiourea		66
Tl <sup>+</sup>		215
	Cu-hexacyanoferrate(III)	217

\* Titration of Ni<sup>2+</sup>, Co<sup>2+</sup>, Zn<sup>2+</sup>, and Vanadium(IV) with EDTA, CDTA, and DTPA, was conducted using a PbS/Ag<sub>2</sub>S electrode in the presence of a small amount of the corresponding lead complex. Stability constants of lead complexes could also be determined in such systems.

## B. POTENTIAL TOOLS

In principle, if diffusion rates and enzyme-catalyzed reaction rates are steady, these electrodes should measure the thermodynamic activity of the substrate molecule. However, no studies in which the activity coefficient was specifically mentioned were encountered in this survey. Some recent papers which could provide ideas for thermodynamic studies are noted in Table 16.

## XI. GAS-SENSITIVE MEMBRANE ELECTRODES

### A. METHODS

Electrodes are constructed using a membrane through which a particular gas can diffuse, with an electrode on the inside which responds to the gas or a reaction product. For example,

**TABLE 16**  
**Enzyme and Other Biologically Based Electrodes**

Selective to	System	Ref.
Urea	Urease	224
	Urease	494
Oxalate	Oxalate oxidase	46
	Oxalate oxidase	373
	Immobilized enzyme	336
	Glucose oxidase	490
Glucose	Glucose oxidase	282
	Glucose oxidase	444
	Glucose mutarotase	444
	Glucose oxidase	271
	Acetylcholine	Acetylcholinesterase
$\beta$ -Blocker	(cf. Table 9)	89
Creatinine	NH <sub>3</sub> and enzyme (cf. Section XI)	528
Ca-blocker	(cf. Table 9)	89
Penicillin G		494
Vitamin B <sub>6</sub>		188
Pyridoxal 5'-phosphate	CO <sub>2</sub> and enzyme (cf. Section XI)	188
Proteolytic enzyme-modified IrO <sub>2</sub> and RuO <sub>2</sub> -coated Ti		381

NH<sub>3</sub> can diffuse through a microporous membrane; on the inside is a solution of NH<sub>4</sub>Cl and a pH-glass electrode. The equilibrium reaction



with NH<sub>4</sub><sup>+</sup> activity held constant by the internal solution, guarantees that a change in NH<sub>3</sub> partial pressure produces a proportional change in H<sup>+</sup>, which can be measured by the pH-glass electrode.

## B. PUBLISHED RESULTS

Electrodes responsive to NH<sub>3</sub>, SO<sub>2</sub>, H<sub>2</sub>S, CO<sub>2</sub>, NO<sub>2</sub>, HF, and other gases have been developed. Ammonia and carbon dioxide electrodes have found particular use as elements of enzyme electrodes.<sup>379</sup>

Even though it seems reasonable that gas membrane electrodes could be used to measure the activity of the various uncharged species listed above, this review did not turn up any instances where gas-selective membrane electrodes were used in activity coefficient or thermodynamic stability constant studies.

## C. POTENTIAL TOOLS

The references listed in Table 17 indicate the range of systems studied, and may suggest ideas for possible thermodynamic studies using gas membrane electrodes.

## ACKNOWLEDGMENTS

The authors thank Dr. David A. Johnson of Spring Arbor College for conducting a heroic literature search, which made this review possible. Ms. Patricia Van Ness, Ms. Susan Costello, and Ms. Shanti Rabindran at Harvard, and Mr. Lakshmi N. Roy at Drury College assisted in collating references and preparing the manuscript.

This work was supported in part by the U.S. National Science Foundation, Grant No. CTS-8805882, and the American Chemical Society Petroleum Research Fund, Grant No. ACS-PRF-18137-B5-C.

TABLE 17  
Gas-Sensing Electrodes

Selective to	System	Log conc	Ref.
Cl <sub>2</sub>	Static and flow inj.	-5 to -2	74
	Pyridoxal 5'-phosphate	-9	188
CO <sub>2</sub>	Bovine serum albumin consumption by biocatalytic membrane	11	
	Microbial assay of gentamycin, streptomycin, neomycin		466
	Organic acid	-3.3 to -2.1	291
	Carbonate in seawater		337
	Interfer SO <sub>2</sub> , NO <sub>x</sub> , H <sub>2</sub> S	-4 to -2	331
	Dynamics		281
	NH <sub>3</sub>	PVC membrane, amines	-5 to -2
Teflon membranes			9
Bilayer lipid membrane			491
Salt media			523
Dynamics		High	11
Microsensor		-3 to -1	261
Fiber-optic probe		-0.6 to +0.2	10
Creatinine det'n			528

## REFERENCES

1. Ahluwalia, J. C. and Cobble, J. W., The thermodynamic properties of high temperature aqueous solutions. III. The partial molal heat capacities of hydrochloric acid from 0° to 100° and the third law potentials of the Ag-AgCl and calomel electrodes from 0° to 100°, *J. Am. Chem. Soc.*, 86, 5381, 1964.
2. Ajayi, S. O. and Wigwe, F. E. W., The standard potential of copper amalgam electrode and the activity coefficient of copper sulphate in aqueous solution. *J. Inorg. Nucl. Chem.*, 40, 825, 1978.
3. Aleksand, V. V. and Kireev, A. A., Standard e.m.f. of the cell Pt(H<sub>2</sub>)|HCl|AgCl|Ag in the formic acid + water system, *Sov. Electrochem.*, 15, 921, 1979.
4. Aleksand, V. V. and Kireev, A. A., Standard e.m.f. of the cell Pt(H<sub>2</sub>)|HCl|AgCl|Ag in the formic acid + acetic acid system, *Sov. Electrochem.*, 15, 1570, 1979.
5. Ammann, D., *Ion-Selective Microelectrodes*, Springer-Verlag, New York, 1986.
6. Ananthaswamy, J. and Atkinson, G., Thermodynamics of concentrated electrolyte mixtures. I. Activity coefficients in aqueous NaCl-CaCl<sub>2</sub> at 25°C, *J. Solution Chem.*, 11, 509, 1982.
7. Aomi, T., The determination of the mercuric ion with an iodide ion-selective electrode, *Denki Kagaku*, 48, 491, 1980.
8. Armstrong, R. D., Covington, A. K., and Evans, G. P., Mechanistic studies of the valinomycin-based potassium-selective electrode using ac impedance methods, *J. Electroanal. Chem.*, 159, 33, 1983.
9. Arnold, M. A., Improved dynamic response of potentiometric ammonia sensors using pure Teflon membranes, *Anal. Chim. Acta*, 154, 33, 1983.
10. Arnold, M. A. and Ostler, T. J., Fiber optic ammonia gas sensing probe, *Anal. Chem.*, 58, 1137, 1986.
11. Arnold, M. A. and Rechnitz, G. A., Dynamic behavior of potentiometric ammonia-sensing probes in samples of high osmolality, *Anal. Chim. Acta*, 158, 379, 1984.
12. Arnold, M. A. and Solsky, R. L., Ion-selective electrodes, *Anal. Chem.*, 58, 84R, 1986.
13. Awakura, Y., Mitsuda, S., and Majima, H., Measurements of HCl activity by using a glass electrode and chloride-ion selective electrode, *Denki Kagaku*, 50, 979, 1982.
14. Bag, B. C. and Das, M. N., Behaviour of Tl(Hg)-TlI electrode in tetraalkylammonium iodide solutions, *Indian J. Chem.*, A23, 639, 1984.
15. Bagg, J. and Rechnitz, G. A., Activity measurements at high ionic strengths using halide-selective membrane electrodes, *Anal. Chem.*, 45, 271, 1973.
16. Balej, J., Theoretical background of brine electrolysis: the standard e.m.f. of the cell Pt|Cl<sub>2</sub>|NaCl||Na(Hg) at elevated temperatures, *Electrochim. Acta*, 26, 719, 1981.

17. Basu, A. K. and Aditya, S., Mercury-mercurous propionate electrode: standard potentials at different temperatures and related thermodynamic quantities, *Electrochim. Acta*, 23, 1341, 1978.
18. Bates, R. G., Determination of pH, in *Theory and Practice*, 2nd ed., John Wiley & Sons, New York, 1973.
19. Bates, R. G., The modern meaning of pH, *CRC Crit. Rev. Anal. Chem.*, 10, 247, 1981.
20. Bates, R. G., Pursuit of the elusive single ion activity, in *Electrochemistry, Past and Present*, Stock and Orna, Eds., American Chemical Society, Washington, D.C., 1989, chap. 10.
21. Bates, R. G. and Alfenaar, M., Activity standards for ion-selective electrodes, in *Ion-Selective Electrodes*, Durst, R. A., Ed., NBS Spec. Publ. 314, National Bureau of Standards, Washington, D.C., 1969, 191.
22. Bates, R. G. and Robinson, R. A., An approach to conventional scales of ionic activity for the standardization of ion-selective electrodes, *Pure Appl. Chem.*, 37, 575, 1974.
23. Bates, R. G., Ion activity scales for use with selective ion-sensitive electrodes, *Pure Appl. Chem.*, 36, 407, 1973.
24. Bates, R. G. and Bower, V. E., Standard potential of the silver-silver chloride electrode from 0°C to 95°C and the thermodynamic properties of dilute hydrochloric acid solutions, *J. Res. Natl. Bur. Stand.*, 53, 283, 1954.
25. Bates, R. G. and Macaskill, J. B., Standard potential of the silver-silver chloride electrode, *Pure Appl. Chem.*, 50, 1701, 1978.
26. Bates, R. G., Dickson, A. G., Gratzl, M., Hrabeczy-Pall, A., Lindner, E., and Pungor, E., Determination of mean activity coefficients with ion-selective electrodes, *Anal. Chem.*, 55, 1275, 1983.
27. Bates, R. G. and Calais, J. G., Thermodynamics of the dissociation of  $\text{BisH}^+$  in seawater from 5 to 40°C, *J. Solution Chem.*, 10, 269, 1981.
28. Bates, R. G. and Robinson, R. A., Standardization of silver-silver chloride electrodes from 0 to 60°C, *J. Solution Chem.*, 9, 455, 1980.
29. Bates, R. G. and Tanaka, K., The solvent effect of methanol on the dissociation of  $\text{bis-H}^+$  from 10 to 40°C, *J. Solution Chem.*, 10, 155, 1981.
30. Bates, R. G. and Erickson, W. P., Thermodynamics of the dissociation of 2-aminopyridinium ion in synthetic seawater and a standard for pH in marine systems, *J. Solution Chem.*, 15, 891, 1986.
31. Bates, R. G., Benneto, H. P., and Sankar, M., Dissociation constants of acetic acid and primary phosphate ion and standards for pH in 10, 20, and 40 wt% ethanol/water solvents at 25, 0, -5, and -10°C, *Anal. Chem.*, 52, 1598, 1980.
32. Belusti, A. A., Shults, M. M., Peshekh, N. V., Ivanova, L. I., Shugalov, A. L., Mogileva, V. V., and Ivanovsky, I. S., Dynamics of glass electrode potential establishment and ion concentration distribution in glass surface layers, *Dokl. Akad. Nauk SSSR*, 240, 1376, 1978.
33. Belyakov, E. A. and Tikhonov, K. I., Electrochemical behavior of lithium and lithium amalgam in tetrahydrofuran, *Sov. Electrochem.*, 14, 1336, 1978.
34. Belyakov, E. A., Tikhonov, K. I., and Rotinyan, A. L., Electrochemical behavior of sodium amalgam in tetrahydrofuran, *Sov. Electrochem.*, 14, 1342, 1978.
35. Benignat, M. T., Campanel, L., and Ferri, T., Benzoate liquid-membrane ion-selective electrode, *Z. Anal. Chem.*, 296, 412, 1979.
36. Bent, H. F. and Swift, E., The activity of sodium in dilute sodium amalgams, *J. Am. Chem. Soc.*, 58, 2216, 1936.
37. Bhattach, A., Mandal, A. K., and Lahiri, S. C., Acid ionization constants of phosphoric acid in ethanol + water mixtures, *Indian J. Chem.*, A19, 532, 1980.
38. Biedermann, G., Orecchio, S., Romano, V., and Zingales, R., On the formal potential of the  $\text{Co}^{3+}/\text{Co}^{2+}$  couple at -5°C in 6.5 molal  $\text{HClO}_4$  medium, *Acta Chem. Scand. Ser. A*, 40, 161, 1986.
39. Bjerrum, N., Selected papers (transl.), E. Munksgaard, Copenhagen, 1949.
40. Bochenska, M. and Biernat, J. F., Guanidinium-selective PVC membrane electrodes based on crown ethers, *Anal. Chim. Acta*, 162, 369, 1984.
41. Body, P. E., Stimburys, P., and Mulcahy, D. E., A potentiometric sensing system for aluminum, *Anal. Lett.*, 18, 1999, 1985.
42. Bogatsky, A. V., Lukyanenko, N. G., Golubev, V. N., Nazarova, N. Y., Karpenko, I. P., Popkov, Y. A., and Shapkin, V. A., Cation selectivity of liquid-membrane electrodes based on macrocyclic lactones and lactonolactams, *Anal. Chim. Acta*, 157, 151, 1984.
43. Bohnke, C., Saida, A., and Robert, G.,  $\text{Pb(II)}$ -selective glass electrode in aqueous solution, *C. R. Acad. Sci. Ser. C*, 290, 97, 1980.
44. Bourgoigne, H., Fombon, J. J., Lancelot, F., Paris, J., Roubin, M., and Tacussel, J., Development of copper ion-selective electrodes with solid-state polycrystalline membrane, *Analyst*, 8, 296, 1980.
45. Bower, C. E. and Bidwell, J. P., Ionization of ammonia in seawater. Effects of temperature, pH, and salinity, *J. Fish. Res.*, 35, 1012, 1978.



46. **Bradley, C. R. and Rechnitz, G. A.**, Comparison of oxalate oxidase enzyme electrodes for urinary oxalate determinations, *Anal. Lett.*, 19, 151, 1986
47. **Brauer, K. and Strehlow, H.**, Effect of corrosion on the electrode potential of alkali amalgam electrodes, *Z. Phys. Chem. (Frankfurt am Main)*, 17, 336, 1958.
48. **Briggs, C. C. and Lilley, T. H.**, A rigorous test of a Ca ion exchange membrane electrode, *J. Chem. Thermodyn.*, 6, 599, 1974.
49. **Briggs, C. C. and Lilley, T. H.**, Thermodynamic studies on aqueous solutions containing  $\text{CaCl}_2 + \text{CaSO}_4$ , *J. Chem. Thermodyn.*, 8, 151, 1976.
50. **Brown, O. R. and McIntyre, R.**, Standard potential determinations for the Mg and Mg(Hg) electrodes and conductance data for Mg salts in aprotic solvents, *Electrochim. Acta*, 29, 995, 1984.
51. **Buck, R. P.**, Crystalline and pressed powder solid membrane electrodes, in *Ion-Selective Electrode Methodology*, Vol. 1, Covington, A. K., Ed., Plenum Press, New York, 1979, 175.
52. **Busey, R. H. and Mesmer, R. E.**, Ionization equilibria of silicic acid and polysilicate formation in aqueous sodium chloride solutions to 300°C, *Inorg. Chem.*, 16, 2444, 1977.
53. **Butler, J. N. and Huston, R.**, Potentiometric studies of multicomponent activity coefficients in the NaCl-NaF-H<sub>2</sub>O system using the LaF<sub>3</sub> membrane electrode, *Anal. Chem.*, 42, 1308, 1970.
54. **Butler, J. N.**, The standard potential of the calcium amalgam electrode, *J. Electroanal. Chem.*, 17, 309, 1968.
55. **Butler, J. N.**, The Use of Amalgam Electrodes to Measure Activity Coefficients in Multicomponent Salt Solutions, Office of Saline Water, Research and Development Progress Reports 388, U.S. Department of the Interior, 1968, 175.
56. **Butler, J. N.**, Thermodynamic Studies, Ion-Selective Electrodes, NBS Spec. Publ. 314, Durst, R. A., Ed., National Bureau of Standards, Washington, D.C., 1969, 143.
57. **Butler, J. N.**, Reference electrodes in aprotic organic solvents, in *Advances in Electrochemistry and Electrochemical Engineering*, Vol. 7, Delahay, P. and Tobias, C., Eds., 1970, 77.
58. **Butler, J. N. and Huston, R.**, Activity measurements using a potassium-selective liquid ion exchange electrode, *Anal. Chem.*, 42, 676, 1970.
59. **Butler, J. N. and Huston, R.**, Activity coefficient measurements in aqueous NaCl-CaCl<sub>2</sub> and NaCl-MgCl<sub>2</sub> electrolytes using sodium amalgam electrodes, *J. Phys. Chem.*, 71, 4479, 1967.
60. **Butler, J. N. and Huston, R.**, The Use of Amalgam Electrodes to Measure Activity Coefficients in Multicomponent Salt Solutions, Office of Saline Water, Research and Development Progress Report 486, U.S. Department of the Interior, 1969, 142.
61. **Butler, J. N. and Huston, R.**, Activity coefficients and ion pairs in the systems NaCl-NaHCO<sub>3</sub>-H<sub>2</sub>O and NaCl-Na<sub>2</sub>CO<sub>3</sub>-H<sub>2</sub>O, *J. Phys. Chem.*, 74, 2976, 1970.
62. **Butler, J. N., Hsu, P. T., and Synnott, J. C.**, Activity coefficient measurements in aqueous sodium chloride-sodium sulfate electrolytes using sodium amalgam electrodes, *J. Phys. Chem.*, 71, 910, 1967.
63. **Butler, J. N., Huston, R., and Hsu, P. T.**, Activity coefficient measurements in aqueous NaCl-LiCl and NaCl-KCl electrolytes using sodium amalgam electrodes, *J. Phys. Chem.*, 71, 3294, 1967.
64. **Butler, J. N., Synnott, J. C., and Huston, R.**, The Use of Amalgam Electrodes to Measure Activity Coefficients in Multicomponent Salt Solutions, Office of Saline Water, Research and Development Progress Report 606, U.S. Department of the Interior, 1970, 109.
65. **Cachaza, J. M. and Casal, R.**, Determination of the activity coefficient of calcium chloride in solution using a membrane electrode, *Quim. Anal.*, 69, 959, 1973.
66. **Calokeri, A. C. and Hadjiioanou, T. P.**, Direct potentiometric titration of thiosulphate, thiourea, and ascorbic acid with iodate using an iodide ion-selective electrode, *Microchem. J.*, 28, 464, 1983.
67. **Campbell, A. D. and Graham, P. B.**, Determination of fluoride with a fluoride-selective ion electrode by using a standard addition method, *N.Z. J. Sci.*, 26, 433, 1983.
68. **Campbell, A. N.**, Electromotive force measurements of the cell  $\text{In}|\text{InCl}_2|\text{In-Hg}$ , together with the derived thermodynamic quantities, *Can. J. Chem.*, 56, 2550, 1978.
69. **Cavallaro, N. and McBride, M. B.**, Response of the  $\text{Cu}_2^{2+}$  and  $\text{Cd}^{2+}$  ion-selective electrodes to solutions of different ionic strength and composition, *Soil Sci. Soc. Am.*, 44, 881, 1980.
70. **Chan, C.-Y. and Khoo, K. H.**, Re-determination of mean ionic activity coefficients for the system  $\text{HCl} + \text{KCl} + \text{water}$  at 298.15 K and correlations between Harned and Pitzer equations, *J. Chem. Soc. Faraday Trans. 1*, 75, 1371, 1979.
71. **Chan, C.-Y., Khoo, K. H., and Lim, T. K.**, Specific ionic interactions in the quaternary systems  $\text{HCl}-\text{NaCl}-\text{KCl}-\text{water}$  and  $\text{HCl}-\text{NH}_4\text{Cl}-\text{KCl}-\text{water}$  at 25°C, *J. Solution Chem.*, 8, 41, 1979.
72. **Check, Y. M., Gill, J. B., Balt, S., and Renkema, W. E.**, Electrochemistry of solutions in liquid ammonia. VII, *J. Solution Chem.*, 12, 829, 1983.
73. **Chiaramo, M., Longhi, P., Mussini, F., and Rondinini, S.**, Standard aqueous potentials of the thallium amalgam + thallic chloride electrode over the temperature range from 283.15 K to 343.15 K, *Ann. Chim. Milan*, 68, 497, 1978.

74. Coetzee, J. F. and Gunaratna, C., Potentiometric gas sensor for the determination of free chlorine in static or flow injection analysis systems, *Anal. Chem.*, 58, 650, 1986.
75. Contreras-Ortega, C. H. and Rock, P. A., Electrochemistry in hexamethylphosphorotriamide (HMPA). I. The  $H_2(g)|Pt|HCl(HMPA)|TlCl(s)|Tl(Hg)$  cell, *J. Electrochem. Soc.*, 127, 881, 1980.
76. Corfield, G. C., Ebdon, L., and Ellis, A. T., Calcium ion-selective electrodes with covalently bound organophosphate sensor groups, *Polym. Sci. Technol.*, 21, 341, 1983.
77. Cosofret, V. V. and Bunaciu, A. A., Determination of some thiobarbiturates with ion-selective membrane electrodes, *Anal. Lett.*, B12, 617, 1979.
78. Covington, A. K., Precise measurements with the glass electrode. III. The cell: glass electrode|HCl|AgCl|Ag at 0°, *J. Chem. Soc.*, p. 4441, 1960.
79. Covington, A. K., Precise measurements with the glass electrode. IV. The activity coefficient of hydrochloric acid in mixtures with calcium or manganous chloride at 25°C, *J. Chem. Soc.*, p. 4906, 1965.
80. Covington, A. K. and Davison, P., Liquid ion exchanger types, in *Ion-Selective Electrode Methodology*, Vol. 1, Covington, A. K., Ed., CRC Press, Boca Raton, FL, 1979, 85.
81. Covington, A. K. and Prue, J. E., Precise measurements with the glass electrode. I. The cell: glass electrode|HCl|AgCl|Ag, *J. Chem. Soc.*, p. 3696, 1955.
82. Covington, A. K., Bates, R. G., and Durst, R. A., Definition of pH scales, standard reference values, measurement of pH and related terminology, *Pure Appl. Chem.*, 57, 531, 1985.
83. Covington, A. K., Ferra, M. I. A., and Robinson, R. A., Ionic product and enthalpy of ionization of water from electromotive force measurements, *J. Chem. Soc. Faraday Trans. 1*, 73, 1721, 1977.
84. Covington, A. K., Newman, K. E., and Wood, M., Free energies of transfer of sodium fluoride from water to hydrogen peroxide-water mixtures using ion-selective electrodes, *J. Chem. Soc. Chem. Commun.*, p. 1234, 1972.
85. Covington, A. K., *Ion-Selective Electrode Methodology*, Vol. 2, CRC Press, Boca Raton, FL, 1979.
86. Covington, A. K., *Ion-Selective Electrode Methodology*, Vol. 1, CRC Press, Boca Raton, FL, 1979.
87. Covington, A. K. and Cairns, J., Determination of standard pH values for sodium hydrogen diglycolate buffer (0.05 m) from 5–65°C, *J. Solution Chem.*, 9, 517, 1980.
88. Craggs, A., Moody, G. J., and Thomas, J. D. R., Calcium ion-selective electrode measurements in the presence of complexing ligands, *Analyst*, 104, 961, 1979.
89. Cunningham, L. and Freiser, H., Ion-selective electrodes for some beta-adrenergic and calcium blockers, *Anal. Chim. Acta*, 157, 157, 1984.
90. Czerminski, J. F., Dickson, A. G., and Bates, R. G., Thermodynamics of the dissociation of morpholinium ion in seawater from 5 to 40°C, *J. Solution Chem.*, 11, 79, 1982.
91. D'Olieslager, W. and Heerman, L., Cesium ion-selective electrode. Potassium zinc ferrocyanide in a PVC matrix, *J. Electrochem. Soc.*, 126, 347, 1979.
92. Daniele, P. G., Rigano, C., and Sammartà, S., The formation of proton and alkali-metal complexes with ligands of biological interest in aqueous solution. Potentiometric study of the  $H^+ - K^+$  citrate system at 37°C, *Ann. Chim. Milan*, 70, 119, 1980.
93. Daniele, P. G., Rigano, C., and Sammartà, S., Studies on sulphate complexes. I. Potentiometric investigation of lithium, sodium, potassium, rubidium and caesium complexes at 37°C, *Inorg. Chim. Acta*, 63, 267, 1982.
94. Daniele, P. G., Amico, F., and Ostacoli, G., Potentiometric study of proton, copper(II) histamine complexes in water-1-propanol solvent mixtures, *Ann. Chim. Milan*, 70, 255, 1980.
95. Daniele, P. G., Amico, P., and Ostacoli, G., Ternary cadmium(II) complexes with 2-2'-bipyridyl and citric acid in aqueous solution. Studied by glass and Cd-Hg electrodes, *Ann. Chim. Milan*, 69, 61, 1979.
96. Danielson, M. J., A long-lived external Ag-AgCl reference electrode for use in high temperature and pressure environments, *Corrosion*, 39, 202, 1983.
97. Das, A. K. and Kundu, K. K., Studies in isodielectric media. I. Standard potential of the silver-silver chloride electrode in dimethyl formamide + ethylene glycol mixtures at 25°C, *Electrochim. Acta*, 23, 685, 1978.
98. Das, B. K. and Das, P. K., Thermodynamics of hydrobromic acid in dioxan + water mixtures from electromotive force measurements at different temperatures, *J. Chem. Soc. Faraday Trans. 1*, 74, 22, 1978.
99. Das, B. K., Mishra, U. C., and Das, P. K., Transference number of hydrochloric acid in dioxane + water mixtures from electromotive force measurements, *J. Indian Chem. Soc.*, 55, 140, 1978.
100. Das, K., Bose, K., Das, A. K., and Kundu, K. K., Standard potentials of the silver-silver iodide electrode in aqueous mixtures of ethanol and propan-2-ol at different temperatures. Free energies and entropies of transfer of hydroiodic acid at 25°, *Electrochim. Acta*, 23, 159, 1978.
101. Das, R. C., Dash, U. N., and Panda, K. N., Thermodynamics of the silver-silver chromate electrode in water + 10, 20, 30, and 40 mass % of dioxane at different temperatures, *Electrochim. Acta*, 24, 99, 1979.

102. **Dash, U. M., Das, B. B., Biswal, U. K., and Panda, T.**, Standard potentials of silver-silver ion electrode and thermodynamic solubility product constants of AgX (X = Cl, Br, I or CNS) in glycerol + water mixtures at 25°C (298.15 K), *Electrochim. Acta*, 28, 1273, 1983.
103. **Dash, U. N., Das, B. B., Biswal, U. K., and Panda, T.**, Thermodynamics of the silver-silver ion electrode and thermodynamic solubility products of silver chloride in water + D-glucose and D-fructose mixtures at 25°C, *Thermochim. Acta*, 70, 383, 1983.
104. **Dash, U. M., Das, B. B., Biswal, U. K., Panda, T., Purohit, N. K., Rath, D. K., and Bhattacharya, S.**, Thermodynamic properties of the silver ion in alcohol + water solvent mixtures from electromotive force measurements and thermodynamic solubility product constants of AgCl, AgBr, AgI, AgCNS at different temperatures, *Thermochim. Acta*, 63, 261, 1983.
105. **Dash, U. N., Das, B. B., Biswal, U. K., Panda, T., Purohit, N. K., Rath, D. K., and Bhattacharya, S.**, Thermodynamics of the silver-silver ion electrode in dioxane-water mixtures, *Thermochim. Acta*, 71, 199, 1983.
106. **Dash, U. N., Nayak, U. K., Nayak, S. K., and Pattnaik, S. P.**, Thermodynamics of silver benzoates and the standard electrode potentials of the silver-silver benzoate electrodes in aqueous medium, *Thermochim. Acta*, 34, 171, 1979.
107. **DeBattisti, A. and Trasatti, S.**, The electrical double layer between mercury and aqueous NaBF<sub>4</sub> solutions. I. Activity of aqueous NaBF<sub>4</sub> from e.m.f. measurements, *J. Chim. Phys. Phys. Chim. Biol.*, 70, 395, 1973.
108. **Delben, F. and Crescenzi, V.**, The ionization of aliphatic dicarboxylic acids in water, *J. Solution Chem.*, 7, 597, 1978.
109. **DeRobertis, A., Rigano, C., and Sammartano, S.**, Studies on hexacyanoferrate(II) complexes, *Ann. Chim. Milan*, 74, 33, 1984.
110. **Devynck, J., Hadid, A. B., and Fabre, P. L.**, The hydrogen electrode as pH indicator in hydrogen fluoride and super-acid media, *J. Inorg. Nucl. Chem.*, 41, 1159, 1979.
111. **Dey, B. P., Dutta, S., and Lahiri, S. C.**, Dissociation constants of amino acids in isopropanol + water mixtures, *Indian J. Chem.*, A21, 886, 1982.
112. **Dickson, A. G.**, pH scales and proton transfer reactions in saline media such as seawater, *Geochim. Cosmochim. Acta*, 48, 2299, 1984.
113. **Dickson, A. G.**, Thermodynamics of the dissociation of boric acid in KCl solutions from 273.15 to 318.15°K, *J. Chem. Eng. Data*, 35, 253, 1990.
114. **Dickson, A. G.**, Thermodynamics of boric acid in synthetic seawater from 273.15 to 318.15°K, *Deep Sea Research*, 37, 755, 1990.
115. **Dickson, A. G.**, Standard potential of the reaction  $\text{AgCl(s)} + 1/2 \text{H}_2 \text{(g)} = \text{Ag(s)} + \text{HCl(aq)}$  and the standard acidity constant of the ion  $\text{HSO}_4^-$  in synthetic seawater from 273.15 to 318.15°K, *J. Chem. Thermodyn.*, 22, 113, 1990.
116. **Dickson, A. G. and Riley, J. P.**, Estimation of acid dissociation constants in seawater media from potentiometric titrations with strong base. II. Dissociation of phosphoric acid, *Mar. Chem.*, 7, 101, 1979.
117. **Dickson, A. G. and Millero, F. J.**, A comparison of the equilibrium constants for the dissociation of carbonic acid in seawater media, *Deep Sea Res.*, 37, 755, 1987.
118. **Dickson, A. G.**, Standardization of the  $(\text{AgCl} + 1/2 \text{H}_2 = \text{Ag} + \text{HCl})$  cell from 273.15 to 318.15°K, *J. Chem. Thermodyn.*, 19, 993, 1987.
119. **Doe, H., Wakamiya, K., and Kitagawa, T.**, Comparison of stability constants of alkaline earth chlorides between conductometric and potentiometric studies, *Bull. Chem. Soc. Jpn.*, 60, 2231, 1987.
120. **Durst, R. A., Staples, B. R., and Paabo, M.**, Activity standards for ion-selective electrodes, *Biol. Aspects Electrochem. Exp. Suppl.*, 18, 275, 1971.
121. **Ehde, P. M., Andersson, I., and Pettersson, L.**, A potentiometric and 51V NMR study of equilibria in the  $\text{H}^+ - \text{H}_2\text{VO}_4^{2-} - \text{C}_2\text{O}_4^{2-}$  system in 0.6 M NaCl medium, *Acta Chem. Scand. Ser. A*, 40, 489, 1986.
122. **Eisenman, G.**, *Glass Electrodes for Hydrogen and Other Cations*, Marcel Dekker, New York, 1967.
123. **El-Harakany, A. A., Sadek, H., and El-Loboudy, A. S.**, Standard potentials of the Ag-AgCl electrode in water + 2-ethoxyethanol mixtures, *J. Electroanal. Chem.*, 142, 121, 1982.
124. **Elsemongy, M. M., Abdelkhan, A. A., and Hussein, M. A.**, Standard potentials of the silver-silver iodide electrode and the thermodynamic properties of hydriodic acid in propylene glycol + water solvents, *Thermochim. Acta*, 68, 187, 1983.
125. **Elsemongy, M. M.**, Solvent effect on standard electrode potential. V. Silver-silver chloride electrode in tert-butyl alcohol + water mixtures, *J. Electroanal. Chem.*, 90, 87, 1978.
126. **Elsemongy, M. M.**, Solvent effect on standard electrode potential. I. Silver-silver iodide electrode in methanol-water mixtures, *J. Electroanal. Chem.*, 90, 49, 1978.
127. **Elsemongy, M. M.**, Solvent effect on standard electrode potential. II. Silver-silver bromide electrode in methanol-water mixtures, *J. Electroanal. Chem.*, 90, 57, 1978.
128. **Elsemongy, M. M.**, Thermodynamics of hydrochloric acid in tetrahydrofuran-water mixtures, *Electrochim. Acta*, 23, 881, 1978.

129. **Elsemongy, M. M.**, Solvent effect on standard electrode potential. III. Silver-silver chloride electrode in methanol-water mixtures. *J. Electroanal. Chem.*, 90, 67, 1978.
130. **Elsemongy, M. M.**, Solvent effect on standard electrode potential. IV. Silver-silver chloride electrode in glycerol-water mixtures. *J. Electroanal. Chem.*, 90, 77, 1978.
131. **Elsemongy, M. M. and Fouda, A. S.**, Standard potentials of silver-silver chloride electrode and related thermodynamic quantities in 2-propanol + water. *J. Electroanal. Chem.*, 114, 25, 1980.
132. **Elsemongy, M. M.**, Thermodynamic properties of single ions in propylene glycol and its aqueous mixtures. *Thermochim. Acta*, 108, 133, 1986.
133. **Elsemongy, M. M. and Fouda, A. S.**, Standard potentials of the (silver + silver chloride) electrode and the thermodynamic behaviour of hydrochloric acid in (ethanol + water) at 288.15 to 328.15°K. *J. Chem. Thermodyn.*, 13, 725, 1981.
134. **Elsemongy, M. M. and Elnader, H. M.**, Absolute electrode potentials in dioxane-water solvent mixtures and transfer-free energies of individual ions. *Thermochim. Acta*, 120, 261, 1987.
135. **Elsemongy, M. M. and Reicha, F. M.**, Standard potentials of  $M;M'$  and  $Ag;AgX;X$  electrodes in ethylene glycol + water solvents and related transfer-free energies. *Thermochim. Acta*, 106, 309, 1986.
136. **Elsemongy, M. M. and Reicha, F. M.**, Absolute electrode potentials in dimethylsulfoxide-water mixtures and transfer free energies of individual ions. *Thermochim. Acta*, 108, 115, 1986.
137. **Elsemongy, M. M. and Reicha, F. M.**, Solvent effects on single electrode potential and related thermodynamic quantities. *Thermochim. Acta*, 103, 371, 1988.
138. **Elsemongy, M. M., Fouda, A. S., and Amira, M. F.**, Thermodynamics of hydrochloric acid in dioxan + water mixtures from electromotive force measurements. *J. Chem. Soc. Faraday Trans. 1*, 77, 1157, 1981.
139. **Emara, M. M., Lin, C. T., and Atkinson, G.**, The spectrophotometric and ion-selective electrode determinations of  $MgSO_4$  association at high ionic strengths. *Bull. Soc. Chim. Fr.*, p. 173, 1980.
140. **Emara, M. M., Farid, N. A., and Atkinson, G.**, An ion-selective electrode study of calcium and magnesium sulfate in aqueous solution. *Anal. Lett.*, A11, 797, 1978.
141. **Emara, M. M., Farid, N. A., and Atkinson, G.**, An ion-selective electrode study of calcium and magnesium sulfate in aqueous solution. *Anal. Lett.*, A11, 797, 1978.
142. **Emara, M. M., Farid, N. A., Wasfi, A. M., Bahr, M. M., and Abd-Elbary, H. M.**, Thermodynamics of ion association in aqueous solutions of calcium- and magnesium-substituted hydroxybenzoates using an ion-selective electrode technique. *J. Phys. Chem.*, 88, 3345, 1984.
143. **Esteso, M. A., Fernandes-Merida, L., and Hernandez-Luis, F. F.**, Determination of activity coefficients in aqueous solutions of trichloroacetic acid from EMF measurements at 25°C. *J. Electroanal. Chem.*, 230, 77, 1987.
144. **Esteso, M. A., Fernandes-Merida, L., and Hernandez-Luis, F. F.**, Activity coefficients for aqueous  $Na_2Succ$  solutions from EMF measurements. *J. Electroanal. Chem.*, 230, 69, 1987.
145. **Eyal, E. and Rechnitz, G. A.**, Mechanistic studies on the valinomycin-based potassium electrode. *Anal. Chem.*, 43, 1090, 1971.
146. **Feakins, D., Knox, M., and Hickey, B. E.**, Studies in ion solvation in non-aqueous solvents and their aqueous mixtures. XXI. *J. Chem. Soc. Faraday Trans. 1*, 80, 961, 1984.
147. **Feng, D., Koch, W. F., and Wu, Y. C.**, Second dissociation constant and pH of N-(2-hydroxyethyl)piperazine-N'-2-ethanesulfonic acid from 0 to 50°C. *Anal. Chem.*, 61, 1400, 1989.
148. **Ferry, D., Machting, M., and Bauer, D.**, Fluoride ion selective electrode study of the hydroxide ion interference. *Analyst*, 12, 90, 1984.
149. **Ferse, A.**, Die mittleren aktivitätskoeffizienten an NaOH in NaCl-Lösungen. *Z. Phys. Chem. (Frankfurt am Main)*, 229, 51, 1965.
150. **Ficklin, W. H. and Gottschall, W. C.**, Potentiometric measurements in nonaqueous media using bromide and iodide ion-selective membrane electrodes. *Anal. Lett.*, 6, 217, 1973.
151. **Fleet, B., and von Stopp, H.**, Analytical evaluation of a cyanide ion selective membrane electrode under flow-stream condition. *Anal. Chem.*, 43, 1575, 1971.
152. **Fogh Andersen, N., Wimerley, P. D., Thode, J., and Siggaard-Andersen, O.**, Determination of sodium and potassium with ion-selective electrodes. *Clin. Chem.*, 30, 433, 1984.
153. **Forsling, W.**, Metal complexes with mixed ligands. XVIII. A potentiometric and spectrophotometric study of the systems  $Ni^{2+}-Cl^-$ ,  $Ni^{2+}$ -imidazole and  $Ni^{2+}$ -imidazole in 3.0 M  $(Na)ClO_4 + Cl^-$  media. *Acta Chem. Scand. Ser. A*, 32, 471, 1978.
154. **Frant, M. S. and Ross, J. W., Jr.**, Electrode for sensing fluoride ion activity in solution. *Science*, 154, 1553, 1966.
155. **Fraser, R. R., Bresse, M., and Mansour, T. S.**,  $pK_a$  measurements in tetrahydrofuran. *J. Chem. Soc. Chem. Commun.*, p. 620, 1983.
156. **Fraticelli, Y. M. and Meyerhoff, M. E.**, Selectivity characteristics of ammonia-gas sensors based on a polymer membrane electrode. *Anal. Chem.*, 53, 1857, 1981.

157. **Frumkin, A. N., Korshunov, V. N., and Iofa, Z. A.**, Decomposition of alkali metal amalgams in buffer solutions, *Dokl. Akad. Nauk SSSR*, 141, 413, 1961.
158. **Fung, K. W. and Wong, K. H.**, Potassium- and caesium-selective PVC membrane electrodes based on bis-crown ethers, *J. Electroanal. Chem.*, 111, 359, 1980.
159. **Fux, P., Lagrange, J., and Lagrange, P.**, Sodium glass electrode in propylene carbonate for study of uranyl ion complexed to 18-crown-6 and substituted derivatives, *Anal. Chem.*, 56, 160, 1984.
160. **Gadzekpo, V. P. Y. and Christian, G. D.**, 1,4,7,10-Tetraoxacyclododecane (12-crown-4) as neutral carrier for lithium ion in lithium ion-selective electrode, *Anal. Lett.*, A16, 1371, 1983.
161. **Gadzekpo, V. P. Y., Hungerford, J. M., Kadry, A. M., Ibrahim, Y. A., Xie, R. Y., and Christian, G. D.**, Comparative study of neutral carriers in polymeric lithium ion selective electrodes, *Anal. Chem.*, 58, 1948, 1986.
162. **Gadzekpo, V. P. Y., Moody, G. J., and Thomas, J. D. R.**, Coated-wire lithium ion-selective electrodes based on polyalkoxylate complexes, *Analyst*, 110, 1381, 1985.
163. **Galster, H.**, Evaluation of measurements for the temperature matching of glass-electrode measuring cells, *Tech. Mess. Atm.*, 46, 81, 1979.
164. **Gamble, D. S.**, Potentiometric measurement of  $H^+$  concentration for aluminum orthophosphate titration curves, *Can. J. Chem.*, 58, 2150, 1980.
165. **Geissler, M. and Kunze, R.**, Error sources and regeneration of fluoride ion-selective electrodes, *Z. Chem.*, 24, 269, 1984.
166. **Georgieva, M., Velinov, G., and Budevsky, O.**, Acid-base equilibria in the mixed solvent 80% dimethylsulfoxide-20% water. II. Determination of pK values and investigation of the conditions for titration of some aromatic carboxylic acids and their conjugate bases, *Anal. Chim. Acta*, 101, 139, 1978.
167. **Ghosh, M., Dhaneshwar, M. R., Dhaneshwar, R. G., and Ghosh, B.**, Response to calcium ions of calcium fluoride crystal-membrane electrode, *Analyst*, 103, 768, 1978.
168. **Gieskes, J. M. T. M.**, Activity coefficients of sodium chloride in mixed electrolyte solutions at 25°C, *Z. Phys. Chem. (Frankfurt am Main)*, 50, 78, 1966.
169. **Goffe, R. A. and Tseung, A. C.**, Internally charged palladium hydride reference electrode. I. Effects of charging current density on long-term stability, *Med. Biol. Eng. Comp.*, 16, 670, 1978.
170. **Goldberg, S. S. and Popovych, O.**, Estimation of transfer activity coefficients for single ions between dipolar aprotic solvents from the e.m.f. of cells with liquid junction, *Aust. J. Chem.*, 36, 1767, 1983.
171. **Gomathi, H., Subramanian, G., Chandra, N., and Rao, G. P.**, Solid state halide ion selective electrodes. Studies of quaternary ammonium halide solutions and determination of surfactants, *Talanta*, 30, 861, 1983.
172. **Gratzl, M., Rakias, F., Horvai, G., Toth, K., and Pungor, E.**, Effect of pH on the response of a cyanide ion-selective electrode, *Anal. Chim. Acta*, 102, 85, 1978.
173. **Greeley, R. S., Smith, W. T., Lietzke, M. H., and Stoughton, R. W.**, Electromotive force studies in aqueous solutions at elevated temperatures. I. The standard potential of the Ag-AgCl electrode, *J. Phys. Chem.*, 64, 652, 1960.
174. **Greeley, R. S., Smith, W. T., Lietzke, M. H., and Stoughton, R. W.**, Electromotive force measurements in aqueous solutions at elevated temperatures. II. Thermodynamic properties of hydrochloric acid, *J. Phys. Chem.*, 64, 1445, 1960.
175. **Griffini, E., Longhi, P., Mussini, T., and Rondinini, S.**, Standard potentials for the (thallium amalgam + aqueous thallos bromide) electrode, *J. Chem. Thermodyn.*, 13, 843, 1981.
176. **Grima, J. M. and Brand, M. J. D.**, Activity and interference effects in measurement of ionized calcium with ion-selective electrodes, *Clin. Chem.*, 23, 2048, 1977.
177. **Gritzapis, P. C., Diamandis, E. P., and Hadjiioannou, T. P.**, Determination of the second ionization constant of 3,5-dinitrosalicylic acid (DNSH<sub>2</sub>) and the instability constant of [DNSFe]<sup>-</sup> and titrimetric determination of thiourea with a 3,5-dinitrosalicylate-selective electrode, *Microchem. J.*, 33, 62, 1986.
178. **Guterman, H., Ben-Yaakov, S., and Abeliovich, A.**, Determination of total dissolved sulfide in the pH range 7.5 to 11.5 by ion-selective electrodes, *Anal. Chem.*, 55, 1731, 1983.
179. **Hadjiioannou, T. P. and Gritzapis, P. C.**, Development and analytical applications of a new liquid-membrane 3,5-dinitrosalicylate-selective electrode, *Anal. Chim. Acta*, 126, 51, 1981.
180. **Harned, H. S. and Ehlers, R. W.**, The thermodynamics of aqueous hydrochloric acid solutions from electromotive forces, *J. Am. Chem. Soc.*, 55, 2179, 1933.
181. **Harned, H. S. and Nims, L. F.**, The thermodynamic properties of aqueous sodium chloride solutions from 0° to 40°, *J. Am. Chem. Soc.*, 54, 423, 1932.
182. **Harned, H. S. and Owen, B. B.**, *The Physical Chemistry of Electrolytic Solutions*, 3rd ed., Reinhold, New York, 1958.
183. **Harned, H. S. and Paxton, T. R.**, The thermodynamics of ionized water in SrCl<sub>2</sub> solutions from electromotive force measurements, *J. Phys. Chem.*, 57, 531, 1953.
184. **Harned, H. S. and Robinson, R. A.**, *Multicomponent Electrolyte Solutions*, Pergamon Press, Oxford, 1968.

185. Harsanyi, E. G., Toth, K., and Pungor, E., The behaviour of the silver sulphide precipitate-based ion-selective electrode in the low concentration range, *Anal. Chim. Acta*, 161, 333, 1984.
186. Hartofylax, V. H., Efsthathiou, C. E., and Hadji Ioannou, T. P., Kinetic study of the tartaric acid-periodate reaction: determination of the tartaric acid using an improved periodate-selective electrode, *Microchem. J.*, 33, 9, 1986.
187. Hasegawa, Y., Nakano, T., Odori, Y., and Ishikawa, Y., Lithium salt effects on extraction of 15-crown-5, 18-crown-6, or their silver(I) complexes as picrates, *Bull. Chem. Soc. Jpn.*, 57, 8, 1984.
188. Hassan, S. S. M. and Rechnitz, G. A., Enzyme amplification for trace level determination of pyridoxal 5'-phosphate with a pCO<sub>2</sub> electrode, *Anal. Chem.*, 53, 512, 1981.
189. Hassan, S. S. M. and Rechnitz, G. A., New liquid membrane electrode for the determination of ephedrine, epinephrine, and norepinephrine, *Anal. Chem.*, 58, 1052, 1986.
190. Hassan, S. S. M. and Elmosalami, M. A. F., A new tetrafluoroborate liquid membrane electrode for selective determination of boron, *Fresenius Z. Anal. Chem.*, 325, 178, 1986.
191. Hassan, S. S. M. and Elsaied, M. M., A new liquid-membrane electrode for selective determination of perchlorate, *Talanta*, 33, 679, 1986.
192. Hawkings, R. C., Corriveau, L. P. V., Kushnerluk, S. A., and Wong, P. Y., Dynamic response of the fluoride ion-selective electrode, *Anal. Chim. Acta*, 102, 61, 1978.
193. Hedlund, T., Sjöberg, S., and Öhman, L.-O., Equilibrium and structural studies of silicon (IV) and aluminum (III) in aqueous solution. XV. A potentiometric study of speciation and equilibria in the Al<sup>3+</sup>-CO<sub>2</sub>(g)-OH-system, *Acta Chem. Scand. Ser. A*, 41, 197, 1987.
194. Hefter, G. T., Acidity constant of hydrofluoric acid, *J. Solution Chem.*, 13, 457, 1984.
195. Hershey, P. J., Fernandez, M., Milne, P. J., and Millero, F. J., The ionization of boric acid in NaCl, Na-Ca-Cl and Na-Mg-Cl solutions at 25°C, *Geochim. Cosmochim. Acta*, 50, 143, 1986.
196. Hettiarachchi, S. and Macdonald, D. D., Ceramic membranes for precise pH measurements in high temperature aqueous environments, *J. Electrochem. Soc.*, 131, 2206, 1984.
197. Hiro, K., Kawahara, A., and Tanaka, T., Perchlorate-selective electrodes with urushi as the membrane matrix, *Anal. Chim. Acta*, 110, 321, 1979.
198. Hopirtean, E. and Stefanig, E., Liquid membrane electrodes. XV. Potassium-selective liquid membrane-electrode, *Chem. Anal.*, 22, 845, 1977.
199. Hostetler, P. B., Truesdell, A. H., and Christ, C. L., Activity coefficients of aqueous potassium chloride measured with a potassium-selective glass electrode, *Science*, 155, 1537, 1967.
200. Huang, D. P., Zhang, J. G., Zhe, C. S., Wang, D. F., Hu, H. W., Fu, T. Z., Ou, H. C., Shen, Z. C., and Yu, Z. X., Preparation of bis-crown ether potassium ion-selective electrode, *Acta Chim. Sin.*, 42, 101, 1984.
201. Hulanicki, A. and Lewanstan, A., Model for treatment of selectivity coefficients for solid-state ion-selective electrodes, *Anal. Chem.*, 53, 1401, 1981.
202. Hurlen, T. and Breivik, T. R., Ion activities and zinc electrode reactions in aqueous sulfate solutions, *Acta Chem. Scand. Ser. A*, 32, 447, 1978.
203. Huston, R. and Butler, J. N., Calcium activity measurements using a liquid ion exchange electrode in concentrated aqueous solutions, *Anal. Chem.*, 41, 200, 1969.
204. Huston, R. and Butler, J. N., Activity measurements in concentrated NaCl-KCl electrolytes using cation sensitive glass electrodes, *Anal. Chem.*, 41, 1695, 1969.
205. Huston, R. and Butler, J. N., Erratum: activity measurements in concentrated NaCl-KCl electrolytes using cation sensitive glass electrodes, *Anal. Chem.*, 42, 256, 1970.
206. Hwang, T. L. and Cheng, H. S., Nitrate ion-selective electrodes based on complexes of 2,2'-bipyridine and related compounds as ion exchangers, *Anal. Chim. Acta*, 106, 341, 1979.
207. Hulanicki, A., Trojanow, M., and Augustow, Z., Anion interferences of calcium selective electrodes, *Chem. Anal. Warsaw*, 26, 115, 1981.
208. Imai, H. and Delahay, P., Kinetics of discharge of the alkali metals on their amalgams as studied by Faradaic rectification, *J. Phys. Chem.*, 66, 1683, 1962.
209. Ionescu, M. S., Badea, V., Balulescu, G. E., and Cusofret, V. V., Nafronyl ion-selective membrane electrodes and their use in pharmaceutical analysis, *Talanta*, 33, 101, 1986.
210. Ito, K., Matsuda, S., Maeda, T., Ikeda, S., Iida, Y., and Nakagawa, G., Sulfide active materials for lead(II) ion selective electrodes, *Denki Kagaku*, 47, 220, 1979.
211. Ives, D. J. G. and Janz, G. J., *Reference Electrodes: Theory and Practice*, Academic Press, New York, 1961.
212. Izaguirre, M. and Millero, F. J., The pK\* for the dissociation of TRISH<sup>+</sup> in NaClO<sub>4</sub> media, *J. Solution Chem.*, 16, 827, 1987.
213. Jaber, A. M. Y., Moody, G. J., and Thomas, J. D. R., Alkali and alkaline-earth metal ion adducts of poly(propylene glycol) as sensors for ion-selective electrodes, *Analyst*, 102, 943, 1977.
214. Jackson, K. J. and Wolery, T. J., Extension of the EQ3/6 computer codes to geochemical modeling of brines, *Mat. Rev. Soc. Symp. Proc.*, 44, 507, 1985.

- 215 Jain, A. K., Agrawal, S., and Singh, R. P., Thallium(I) selective solid membrane electrode. *Anal. Lett.*, A12, 995, 1979.
- 216 Jain, A. K., Singh, R. P., and Agrawal, S., Membranes of  $\alpha$ -picolinium molybdoarsenate in araldite as Tl(I) ion-selective electrode. *Z. Anal. Chem.*, 302, 407, 1980.
- 217 Jain, A. K., Singh, R. P., and Bala, C., Solid membranes of copper hexacyanoferrate(III) as thallium(I) sensitive electrodes. *Anal. Lett.*, A19, 1557, 1982.
- 218 Jain, A. K., Srivastava, S. K., Singh, R. P., and Agrawal, S., Silver selective solid membrane electrode. *Anal. Chem.*, 51, 1093, 1979.
- 219 Janz, G. J. and Tomkins, R. P. T., et al., *Nonaqueous Electrolytes Handbook*, Vol. 1, Academic Press, New York, 1972.
- 220 Janz, G. J. and Tomkins, R. P. T., et al., *Nonaqueous Electrolytes Handbook*, Vol. 2, Academic Press, New York, 1973.
- 221 Jensen, J. B., Jaskula, M., and Sørensen, T. S., Mean activity coefficients in aqueous electrolyte mixtures. I. EMF studies at 25°C on the KCl-KF system. *Acta Chem. Scand. Ser. A*, 41, 461, 1987.
- 222 Jensen, M. A. and Rechnitz, G. A., Response time characteristics of the pCO<sub>2</sub> electrode. *Anal. Chem.*, 51, 1972, 1979.
- 223 Johansson, O. and Wedborg, M., The ammonia-ammonium equilibrium in seawater at temperatures between 5 and 25°C. *J. Solution Chem.*, 9, 37, 1980.
- 224 Joseph, J. P., A miniature enzyme electrode sensitive to urea. *Mikrochim. Acta (Wien)*, 2, 473, 1984.
- 225 Joshi, K. M. and Ganu, G. M., Measurement of ionic activities in aqueous solutions using epoxy-based ion-exchange membrane electrode. *Indian J. Technol.*, 16, 53, 1978.
- 226 Jund, R., Koenig, J. F., and Brenet, J., Cell for electrochemical studies under pressure. Application to the study of the EMF of the cell Cu(Hg)|CuSO<sub>4</sub>|Hg<sub>2</sub>SO<sub>4</sub>|Hg. *Electrochim. Acta*, 25, 1555, 1980.
- 227 Kalidas, C. and Rao, V. S., Standard potentials of the silver-silver iodide electrode in diethylene glycol-water mixtures at different temperatures and the related thermodynamic quantities. *J. Chem. Eng. Data*, 24, 255, 1979.
- 228 Kaminski, M. and Schiendewolf, U., Normal potentials of silver, thallium, lead and zinc, and thermodynamics of their ions in liquid ammonia. *Z. Phys. Chem. (Neue Folge)*, 149, 191, 1986.
- 229 Kampmeier, D. T. and Reardon, J. F., Standard potential of the mercury + mercury(I) picrate electrode from 188.15 to 303.15 K. *J. Chem. Thermodyn.*, 11, 733, 1979.
- 230 Katoaka, M., Kudoh, M., and Kambara, T., Liquid membrane type tetraphenylborate ion-selective electrode. *Denki Kagaku*, 46, 548, 1978.
- 231 Kelley, B. P. and Lilley, T. H., The activity coefficients of lithium chloride in water at 298.15°K. *J. Chem. Thermodyn.*, 9, 99, 1977.
- 232 Kelley, B. P. and Lilley, T. H., The activity coefficients of caesium chloride in water at 298.15°K. *J. Chem. Thermodyn.*, 12, 401, 1980.
- 233 Kester, D. R. and Pytkowicz, R. M., Sodium, magnesium, and calcium sulfate ion-pairs in sea water at 25°. *Limnol. Oceanogr.*, 14, 686, 1969.
- 234 Kester, D. R. and Pytkowicz, R. M., Magnesium sulfate association at 25°C in synthetic sea water. *Limnol. Oceanogr.*, 13, 670, 1968.
- 235 Kester, D. R. and Pytkowicz, R. M., Effect of temperature and pressure on sulfate ion association in sea water. *Geochim. Cosmochim. Acta*, 34, 1039, 1970.
- 236 Khalil, S. A. H., Moody, G. J., and Thomas, J. D. R., Studies of calcium ion-selective electrodes in the presence of biochemical materials. *Analyst*, 110, 353, 1985.
- 237 Khoo, K. H., Chan, C.-Y., and Lim, T.-K., Electromotive-force studies of mixed electrolytes in mixed solvents HCl + NH<sub>4</sub>Cl in methanol + water solvents at 25°C. *J. Solution Chem.*, 7, 349, 1978.
- 238 Khoo, K. H., Chan, C.-Y., and Lim, T. K., Thermodynamics of electrolyte solutions. The System HCl + CaCl<sub>2</sub> + H<sub>2</sub>O at 298.15°K. *J. Solution Chem.*, 6, 651, 1977.
- 239 Khoo, K. H., Lim, T.-K., and Chan, C.-Y., Activity coefficients for HCl + NiCl<sub>2</sub> + H<sub>2</sub>O at 298.15°K and effects of higher-order electrostatic terms. *J. Solution Chem.*, 7, 291, 1978.
- 240 Khoo, K. H. and Chan, C.-Y., Activity coefficient of hydrochloric acid in the system HCl-NH<sub>4</sub>Cl-KCl-H<sub>2</sub>O at constant total molality 0.5 mol kg<sup>-1</sup> at 298.15 K. *J. Chem. Eng. Data*, 24, 28, 1979.
- 241 Khoo, K. H., Chan, C.-Y., and Lim, T. K., Activity coefficients in binary electrolyte mixtures HCl + MgCl<sub>2</sub> + H<sub>2</sub>O at 298.15 K. *J. Solution Chem.*, 6, 855, 1977.
- 242 Khoo, K. H., Chan, C.-Y., and Lim, T. K., Activity coefficients for the system HCl + BaCl<sub>2</sub> + H<sub>2</sub>O at 298.15°K. *J. Chem. Soc. Faraday Trans. 1*, 74, 837, 1978.
- 243 Khoo, K. H., Lim, T. K., and Chan, C. Y., Activity coefficients for the system HCl + CoCl<sub>2</sub> + H<sub>2</sub>O at 298.15°K — effects of higher order electrostatic terms. *J. Chem. Soc. Faraday Trans. 1*, 74, 2037, 1978.
- 244 Khoo, K. H., Lim, T. K., and Chan, C. Y., Ionic interactions in the system HBr + BaBr<sub>2</sub> + H<sub>2</sub>O at 298.15 K. *J. Solution Chem.*, 8, 277, 1979.

- 245 **Kho, K. H., Lim, T. K., and Chan, C. Y.**, Activity coefficients for the system  $\text{HBr} + \text{CaBr}_2 + \text{H}_2\text{O}$  at 298.15°K, *J. Chem. Soc. Faraday Trans. 1*, 75, 1067, 1979.
- 246 **Kho, K. H., Lim, T. K., and Chan, C. Y.**, Activity coefficients in aqueous mixtures of hydrochloric acid and lanthanum chloride at 25°C, *J. Solution Chem.*, 10, 683, 1981.
- 247 **Kho, K. H., Rainette, R. W., Culberson, C. H., and Bates, R. G.**, Determination of hydrogen ion concentrations in seawater from 5 to 40°C. Standard potentials at salinities from 20 to 40 [‰], *Anal. Chem.*, 49, 29, 1977.
- 248 **Kimura, K., Tamura, H., and Shono, T.**, Calcium-selective PVC membrane electrodes based on bisterown ethers, *J. Electroanal. Chem.*, 105, 335, 1979.
- 249 **Kimura, K., Maeda, T., Tamura, H., and Shono, T.**, Potassium-selective PVC membrane electrodes based on bis- and poly-crownethers, *J. Electroanal. Chem.*, 95, 91, 1979.
- 250 **Kimura, K., Kumami, K., Kitazawa, S., and Shono, T.**, Calcium-selective polymeric membrane electrodes based on bicyclic polyether amide derivatives, *Anal. Chem.*, 56, 2369, 1984.
- 251 **Kinoshita, E., Ingman, F., Edwall, G., and Glab, S.**, An examination of the palladium-palladium oxide system and its utility for pH-sensing electrodes, *Electrochim. Acta*, 31, 29, 1986.
- 252 **Kinoshita, K. and Madou, M. J.**, Electrochemical measurements on Pt, Ir, and Ti oxides as pH probes, *J. Electrochem. Soc.*, 131, 1089, 1984.
- 253 **Knauss, K., Wolery, T. J., and Jackson, K. J.**, A new approach to measuring pH in brines and other concentrated electrolytes, *Geochim. Cosmochim. Acta*, 54, 1519, 1990.
- 254 **Kopytin, A. V., Gabor-Klatsmanyi, P., Izvekov, V. P., Pungor, E., and Hlyin, E. G.**, Investigation of ion-selective electrodes based on quaternary phosphonium salts. III. An ion selective electrode for hexafluorophosphate, *Anal. Chim. Acta*, 162, 133, 1984.
- 255 **Kopytin, A. V., Gabor-Klatsmanyi, P., Izvekov, V. P., Pungor, E., and Yagodin, G. A.**, Investigation of ion-selective electrodes based on quaternary phosphonium salts. II. A tetrachlorothallate(III) ion-selective electrode, *Anal. Chim. Acta*, 162, 123, 1984.
- 256 **Korshunov, V. N. and Iofa, Z. A.**, Decomposition kinetics of alkali metal amalgams in alkaline solutions of electrolytes, *Dokl. Akad. Nauk SSSR*, 141, 143, 1961.
- 257 **Koryta, J.**, Electrochemical sensors based on biological principles, *Electrochim. Acta*, 31, 515, 1986.
- 258 **Koupparis, M. A. and HadjiIoannou, T. P.**, Evaluation of the chloramine-T membrane electrode response in acidic solutions. The determination of the pK<sub>a</sub> of m-chloro-p-toluene sulfonamide (chloramine-T acid), *Microchem. J.*, 23, 178, 1978.
- 259 **Kozłowski, Z., Kinart, C., and Bald, A.**, Studies on galvanic cells  $\text{Pt.H}_2/\text{HCl}/\text{AgCl}/\text{Ag}$  in formamide — N,N-dimethyl-formamide mixtures, *Pol. J. Chem.*, 59, 113, 1978.
- 260 **Kozłowski, Z. and Wasiak, A. M.**, Electrochemical studies on HCl solutions in formamide + water mixtures, *Pol. J. Chem.*, 57, 497, 1983.
- 261 **Kubo, I., Kurube, I., Morizumi, T.**, Micro ammonia sensor, *Anal. Lett.*, 19, 697, 1986.
- 262 **Kumakura, M., Kaetsu, I., and Adachi, S.**, A new electrochemical determination of potassium ion concentration with immobilized valinomycin disk, *J. Electrochem. Soc.*, 131, 1272, 1984.
- 263 **Lai, M.-T. and Shih, J.-S.**, Mercury(II) and silver(I) ion-selective electrodes based on ditra crown ethers, *Analyst*, 111, 891, 1986.
- 264 **Lajunen, K., Hakkinen, P., and Purokoski, S.**, A potentiometric study on the complex formation of boric acid and tetrahydroxyborate ion with polyhydroxy compounds in aqueous solution, *Finn. Chem. Lett.*, 13, 21, 1986.
- 265 **Lamb, R. E., Natusch, D. F. S., O'Reilly, J. E., and Watkins, N.**, Laboratory experiments with ion-selective electrodes, *J. Chem. Educ.*, 50, 432, 1973.
- 266 **Lanier, R. D.**, Properties of organic-water mixtures. III. Activity coefficients of sodium chloride by cation-sensitive glass electrodes, *J. Phys. Chem.*, 69, 2697, 1965.
- 267 **Lanier, R. D.**, Activity coefficients of NaCl in aqueous 3-component solutions by cation-sensitive glass electrodes, *J. Phys. Chem.*, 69, 3992, 1965.
- 268 **Lewandowski, A. and Klecak, S.**, Thermodynamic studies of zinc chloride in mixed aqueous solvents from electromotive force measurements. II. Dioxan, acetone and acetic acid mixtures with water, *Electrochim. Acta*, 26, 89, 1981.
- 269 **Leyendekkers, J. V. and Whitfield, M.**, Measurement of activity coefficients with liquid ion-exchange electrodes for the system calcium(II)-sodium(I)-chloride(1)-water, *J. Phys. Chem.*, 75, 957, 1971.
- 270 **Leyendekkers, J. V. and Whitfield, M.**, Liquid ion exchange electrodes in mixed electrolyte solutions, *Anal. Chem.*, 43, 322, 1971.
- 271 **Leyoldt, J. K. and Gough, D. A.**, Model of a two-substrate enzyme electrode for glucose, *Anal. Chem.*, 56, 2896, 1984.
- 272 **Licht, S.**, pH measurement in concentrated alkaline solutions, *Anal. Chem.*, 57, 514, 1985.
- 273 **Licht, S. and Manussen, J.**, The second dissociation constant of  $\text{H}_2\text{S}$ , *J. Electrochem. Soc. Electrochem. Sci. Technol.*, 134, 918, 1987.



274. Lietzke, M. H. and Stoughton, R. S., The calculation of activity coefficients from osmotic coefficient data, *J. Phys. Chem.*, 66, 508, 1962.
275. Lietzke, M. H. and Stoughton, R. W., Electromotive force studies in aqueous solutions at elevated temperatures. V. The thermodynamic properties of DCl solutions, *J. Phys. Chem.*, 68, 3043, 1964.
276. Lietzke, M. H., Shea, R., and Stoughton, R. W., Correlation of sea salt concentration with the EMF response of a cation-sensitive glass electrode, *J. Tenn. Acad. Sci.*, 42, 123, 1967.
277. Lilley, T. H. and Briggs, C. C., Activity coefficients of calcium sulfate in water at 25°C, *Proc. R. Soc. London Ser. A*, 349, 355, 1976.
278. Lim, T.-K., Khoo, K. H., and Chan, C.-Y., Activity coefficients for the system HBr + SrBr<sub>2</sub> + H<sub>2</sub>O at 25°C, *J. Solution Chem.*, 9, 785, 1980.
279. Lima, J. L. F. C. and Machado, A. A. S. C., Preparation of a chloride-selective electrode based on mercury(I) chloride-mercury(II) sulphide on an electrically conductive epoxy support, *Analyst*, 111, 151, 1986.
280. Lindner, E., Toth, K., Pungor, E., Behm, F., Oggenfuss, P., Welti, D. H., Ammann, D., Morf, W. E., Pretsch, E., and Simon, W., Lead-selective neutral carrier based liquid membrane electrode, *Anal. Chem.*, 56, 1127, 1984.
281. Livansky, K., Simple model of equilibration dynamics of a membrane electrode for determination of CO<sub>2</sub>, *Collection Czech. Chem. Commun.*, 52, 582, 1987.
282. Lobel, E. and Rishpon, J., Enzyme electrode for the determination of glucose, *Anal. Chem.*, 53, 51, 1981.
283. Longhi, P., Mussini, T., and Rondinini, S., Predicting standard pH values for reference buffer solutions in solvent mixtures with water, *Anal. Chem.*, 58, 2290, 1986.
284. Longhi, P., Mussini, P. R., Mussini, T., and Rondinini, S., Thermodynamics of the hydrogen-silver chloride cell in ethanol-water mixtures from -10 to +40°C, *J. Solution Chem.*, 17, 417, 1988.
285. Longhi, P., Mussini, T., Nardi, F. M., and Rondinini, S., Activity coefficients of aqueous ammonium bromide over a range of concentrations and temperatures from e.m.f.s of cells with ammonium-selective heterogeneous-membrane electrodes, *Ann. Chim. Milan*, 70, 315, 1980.
286. Longhi, P., Rondinini, S., Ardizzoni, S., and Mussini, T., Lithium and lithium amalgams. I. Standard potential of lithium amalgam electrode and its temperature coefficient, *Ann. Chim. Milan*, 67, 177, 1977.
287. Longhi, P., Mussini, T., Nardi, F. M., and Rondinini, S., New NH<sub>4</sub><sup>+</sup>-sensing heterogenous-membrane electrode, *Nouv. J. Chim.*, 3, 649, 1979.
288. Longhi, P., Mussini, P. M., Mussini, T., and Rondinini, S., Reference value standards for pH measurements, and first ionization constants of o-phthalic acid, in ethanol/water solvent mixtures at temperatures from -5 to +40°C, *J. Chem. Eng. Data*, 34, 64, 1989.
289. Longhi, P., Mussini, T., Penotti, F., and Rondinini, S., Thermodynamics of the cell H<sub>2</sub>/HCl/AgCl/Ag in (acetonitrile + water) solvents, *J. Chem. Thermodyn.*, 17, 355, 1985.
290. Longhi, P., Mussini, T., Rondinini, S., and Sala, B., Standard potentials for the thallium amalgam electrode and for the thallium amalgam/thallic chloride electrode, *J. Chem. Thermodyn.*, 11, 73, 1979.
291. Lopez, M. E., Selectivity of the potentiometric carbon dioxide gas-sensing electrode, *Anal. Chem.*, 56, 2360, 1984.
292. Lowe, B. M. and Smith, D. G., Measurement of solvent isotope effects with cation selective glass electrodes, *J. Chem. Soc. Chem. Commun.*, p. 989, 1972.
293. Lutfullah and Paterson, R., Stability constants for cadmium iodide complexes in aqueous cadmium iodide (298.15 K), *J. Chem. Soc. Faraday Trans. 1*, 74, 484, 1978.
294. Macaskill, J. B. and Bates, R. G., Activity coefficient of hydrochloric acid in the system HCl-KCl-H<sub>2</sub>O at 25°C and ionic strengths from 0.1 to 3 mol kg<sup>-1</sup>, *J. Solution Chem.*, 7, 423, 1978.
295. Macaskill, J. B., Vega, C. A., and Bates, R. G., Activity coefficients of hydrochloric acid in HCl-KCl-H<sub>2</sub>O mixtures at ionic strengths up to 1.5 mol kg<sup>-1</sup> and temperatures from 5 to 45°C, *J. Chem. Eng. Data*, 23, 314, 1978.
296. Macaskill, J. B., Robinson, R. A., and Bates, R. G., Activity coefficients of hydrochloric acid in aqueous solutions of sodium chloride, *J. Solution Chem.*, 6, 385, 1977.
297. Macdonald, D. D., Wentreck, P. R., and Scott, A. C., The measurement of pH in aqueous systems at elevated temperatures using palladium hydride electrodes, *J. Electrochem. Soc.*, 127, 1745, 1980.
298. Mahapatra, P. and Sengupta, M., Activity measurements in aqueous mixed electrolyte solutions. I. Hydrochloric acid-quaternary ammonium chloride mixtures of constant total ionic strength, *J. Chem. Eng. Data*, 23, 281, 1978.
299. Mahapatra, P. and Sengupta, M., Activity measurements in aqueous mixed electrolyte solutions. II. Hydrochloric acid-choline chloride and hydrochloric acid-acetylcholine chloride mixtures of constant total ionic strength, *J. Chem. Eng. Data*, 26, 204, 1981.
300. Majima, H., Awakura, Y., and Sato, T., Measurements of activities of electrolytes in concentrated hydrochloric acid solutions, *Denki Kag.*, 48, 597, 1980.

- 301 **Majima, Y., Awakura, Y., Sato, T., and Michimot, T.**, Activities of hydrogen and chloride ions in concentrated acidic chloride solutions, *Denki Kagaku*, 50, 934, 1982.
- 302 **Makhija, S. P.**, Determination of the standard electrode potential of potassium amalgam in ethylenediamine, *Anal. Chem.*, 50, 1049, 1978.
- 303 **Manning, G. D.**, pH calibration of tetroxalate, tartrate and phthalate buffer solutions at above 100°C, *J. Chem. Soc. Faraday Trans. 1*, 74, 2434, 1978.
- 304 **Manohar, S. and Ananthaswamy, J.**, Thermodynamics of electrolyte solutions: an EMF study of the activity coefficients of the ternary system NaCl-NaNO<sub>3</sub>-H<sub>2</sub>O at 25°C, *J. Electrochem. Soc. India*, 37, 299, 1988.
- 305 **Manohar, S., Sarada, S., and Ananthaswamy, J.**, Thermodynamics of electrolyte solutions: an EMF study of the activity coefficients of KCl in the system KCl-CaCl<sub>2</sub>-H<sub>2</sub>O at 25, 34 & 45°C, *J. Chem. Thermodyn.*, 19, 969, 1989.
- 306 **Manohar, S. and Ananthaswamy, J.**, Thermodynamics of electrolyte solutions: an EMF study of the activity coefficients of the ternary system NaCl-NaNO<sub>3</sub>-H<sub>2</sub>O at 35 and 45°C, *Bull. Electrochem.*, in press.
- 307 **Manohar, S. and Ananthaswamy, J.**, Thermodynamics of NaCl in the mixture NaCl-NaOAc-H<sub>2</sub>O at 25, 35, and 45°C, *Can. J. Chem.*, in press.
- 308 **Manohar, S. and Ananthaswamy, J.**, Thermodynamic properties of electrolyte solutions: an EMF study of the activity coefficients of KCl in the system KCl-KNO<sub>3</sub>-H<sub>2</sub>O at 25, 34 & 45°C, *J. Solution Chem.*, 19, 1125, 1990.
- 309 **Marcos, E. S., Burgos, F. S., and Alvarez, A. M.**, Activity coefficients of zinc chloride in the presence of lithium, sodium, and magnesium perchlorates, and magnesium nitrate in aqueous solution at 25°C, *J. Solution*, 11, 889, 1982.
- 310 **Martell, A. E. and Smith, R. M.**, *Critical Stability Constants*, Vol. 1 to 6, Plenum Press, New York, 1974 to 1989.
- 311 **Mathis, D. E., Freeman, R. M., Clark, S. T., and Buck, R. P.**, Ion-transport in free and supported nitrobenzene aliquot nitrate liquid membrane ion-selective electrodes. III. Potentiometric limits of detection and selectivity, *J. Membr. Sci.*, 5, 103, 1979.
- 312 **Mauger, R., Chopin-Dumas, J., and Pariaud, J. C.**, Study of the acid error of the glass electrode in aqueous organic media, *J. Electroanal. Chem.*, 85, 345, 1977.
- 313 **Mauger, R., Chopin-Dumas, J., and Pariaud, J. C.**, Study of the acid error of the glass electrode in aqueous organic media. III. Mixed solutions of acid and alkali metal salt, *J. Electroanal. Chem.*, 86, 369, 1978.
- 314 **May, P. M.**, Simultaneous determination of glass electrode parameters and protonation constants, *Talanta*, 30, 899, 1983.
- 315 **Mazzarese, J. and Popovych, O.**, Standard potentials of Li, Na, and K electrodes and transfer free energies of LiCl, NaCl, and KCl in selected ethanol-water and methanol-water solvents, *J. Electrochem. Soc.*, 130, 2032, 1983.
- 316 **Mekjavic, I. and Tominic, I.**, Standard potentials of silver-silver bromide electrode and related thermodynamic quantities in (5, 10 and 15 wt%) 2-butanol-water mixtures, *J. Electroanal. Chem.*, 89, 1, 1978.
- 317 **Melardi, M.-R., Geroni, G., and Galea, J.**, Potentiometric study of the association and dissociation equilibria of orthophosphoric acid in the water-sodium chloride system, at 25°C, for a neutralisation rate value between 0 and 3, *Bull. Soc. Chim. Fr.*, p. 1004, 1978.
- 318 **Mesmer, R. E.**, Lanthanum fluoride electrode response in aqueous chloride media, *Anal. Chem.*, 40, 443, 1968.
- 319 **Midgley, D.**, Solid state ion-selective electrodes for the potentiometric determination of phosphate, *Talanta*, 26, 261, 1979.
- 320 **Midgley, D.**, Reference electrodes for use in the potentiometric determination of chloride. III. Chloranil electrodes, *Analyst*, 109, 749, 1984.
- 321 **Midgley, D.**, Reference electrodes for use in the potentiometric determination of chloride. II, *Analyst*, 109, 445, 1984.
- 322 **Midgley, D.**, Reference electrodes for use in the potentiometric determination of chloride. I, *Analyst*, 109, 439, 1984.
- 323 **Millero, F. J.**, The pH of estuarine waters, *Limnol. Oceanogr.*, 31, 839, 1986.
- 324 **Millero, F. J., Hershey, J. P., Johnson, G., and Zhang, J. Z.**, The solubility of SO<sub>2</sub> and the dissociation of H<sub>2</sub>SO<sub>3</sub> in NaCl solutions, *J. Atmos. Chem.*, 8, 377, 1989.
- 325 **Mishra, U. C., Das, B. K., and Das, P. K.**, Thermodynamic studies of hydrogen iodide in dioxan + water mixtures from electromotive force measurements, *Thermochim. Acta*, 28, 277, 1979.
- 326 **Moody, G. J. and Thomas, J. D. R.**, Polyvinyl chloride matrix membrane ion-selective electrodes, in *Ion-Selective Electrode Methodology*, Vol. 1, Covington, A. K., Ed., CRC Press, Boca Raton, FL, 1979, 111.

327. **Moody, G. J., Rigdon, L. P., Meisenheimer, R. G., and Frazer, J. W.**, Selectivity parameters of homogeneous solid-state chloride ion-selective electrodes and the surface morphology of silver chloride-silver sulphide discs under simulated interference conditions, *Analyst*, 106, 547, 1981.
328. **Moore, E. W. and Ross, J. W., Jr.**, NaCl and CaCl<sub>2</sub> activity coefficients in mixed aqueous solutions, *J. Appl. Physiol.*, 20, 1332, 1965.
329. **Moore, E. W. and Ross, J. W., Jr.**, Cationic glass electrode response in aqueous solution of sodium chloride and potassium chloride, *Science*, 148, 71, 1965.
330. **Morf, W. E.**, Time dependent selectivity behavior and dynamic response of silver halide membrane electrodes to interfering ions, *Anal. Chem.*, 55, 1165, 1983.
331. **Morf, W. E., Mostert, I. A., and Simon, W.**, Time response of potentiometric gas sensors to primary and interfering species, *Anal. Chem.*, 57, 1122, 1985.
332. **Motonaka, J., Ikeda, S., and Tanaka, N.**, Potentiometric titration of mixtures of cadmium, calcium, and magnesium ions with a cadmium ion-selective electrode, *Bunseki Kagaku*, 33, 551, 1984.
333. **Motonaka, J., Konishi, H., Ikeda, S., and Tanaka, N.**, Behavior of the cadmium ion-selective electrode in alcohol-water mixtures, *Bull. Chem. Soc. Jpn.*, 59, 737, 1986.
334. **Mukherjee, A. and Sengupta, M.**, Activity measurements in aqueous mixed electrolyte solutions. III. HCl-CaCl<sub>2</sub> mixtures of constant total ionic strength, *Electrochim. Acta*, 26, 1569, 1981.
335. **Mussini, T.**, Standard potential of the silver-silver chloride electrode, *Chim. Ind. (Milan)*, 61, 399, 1979.
336. **Nabi Rahni, M. A., Guilbault, G. G., and Graciliana de Olivera, N.**, Immobilized enzyme electrode for the determination of oxalate in urine, *Anal. Chem.*, 58, 523, 1986.
337. **Nagashima, K., Washio, Y., and Suzuki, S.**, Continuous determination of carbonate in sea water with gas sensitive electrode, *Bunseki Kagaku*, 33, T108, 1984.
338. **Nagy, Z. and Yonco, R. M.**, Palladium/hydrogen membrane electrode for high temperature/high pressure aqueous solutions, *J. Electrochem. Soc.*, 133, 2232, 1986.
339. **Nakagawa, G., Wada, H., and Sako, T.**, Performance of lead and copper (II) ion-selective electrodes in metal buffer solutions and the determination of the stability constants of lead and copper (II) complexes, *Bull. Chem. Soc. Jpn.*, 53, 1303, 1980.
340. **Nakamura, T. and Rechnitz, G. A.**, Barium ion selective membrane electrode for use in acetonitrile, *Anal. Chem.*, 56, 357, 1984.
341. **Nash, C. P.**, Standard potential of Hg/Hg(IO<sub>3</sub>)<sub>2</sub> electrode, *J. Electrochem. Soc.*, 125, 875, 1978.
342. **Nernst, W.**, *Theoretical Chemistry*, (transl. from the 10th German ed.), Macmillan, New York, 1923.
343. **Neshkova, M. and Sheytanov, H.**, On the anomalous behaviour of two types of solid-state copper(II)-ion-selective electrodes in presence of complexones — a possible explanation, *Mikrochim. Acta (Wien)*, 11, 161, 1985.
344. **Neshkova, M. and Sheytanov, H.**, The behaviour of two types of copper ion-selective electrodes in different copper(II)-ligand systems, *Talanta*, 32, 937, 1985.
345. **Neshkova, M. and Havas, J.**, The ternary copper-silver selenide. A new homogeneous solid state ion-selective electrode for copper (II), *Anal. Lett.*, A20, 1567, 1984.
346. **Neshkova, M. and Sheytanov, H.**, Ion-selective electrodes with sensors of electrolytically plated chalcogenide coatings. I. Copper ion-selective electrode based on plated copper selenide, *J. Electroanal. Chem.*, 102, 189, 1979.
347. **Niedrach, L. W. and Stoddard, W. H.**, Development of a high temperature pH electrode for geothermal fluids, *J. Electrochem. Soc.*, 131, 1017, 1984.
348. **Nomura, T. and Nakagawa, G.**, Development of hydrogen ion selective electrode with lithium phosphate glasses for the use in solutions containing hydrofluoric acid, *Bull. Chem. Soc. Jpn.*, 56, 3632, 1983.
349. **Østerberg, N. O., Jensen, J. B., and Sorensen, T. S.**, EMF of concentration cells with liquid-liquid junction established by free diffusion. I. Experimental results for HCl/BaCl<sub>2</sub> junctions at various concentrations, *Acta Chem. Scand. Ser. A*, 32, 721, 1978.
350. **Østerberg, N. O., Jensen, J. B., Sorensen, T. S., and Caspersen, L. D.**, EMF of concentration cells with liquid-liquid junction established by free diffusion. II. Applicability of some theoretical models on experimental results for BaCl<sub>2</sub>-HCl junctions, *Acta Chem. Scand. Ser. A*, 34, 523, 1980.
351. **Owen, A. E.**, Chalcogenide glasses as ion-selective materials for solid-state electrochemical sensors, *J. Noncryst. Solids*, 35 and 36, 999, 1980.
352. **Padova, J.**, Thermodynamics of mixed chloride-nitrate systems from glass electrode measurements, *J. Phys. Chem.*, 74, 4587, 1970.
353. **Pandey, S. D. and Tripathi, P.**, Investigation of some new solid cation exchange membrane electrodes for activity determination of monovalent cations, *Electrochim. Acta*, 27, 1715, 1982.
354. **Patterson, C. S., Busey, R. H., and Mesmer, R. E.**, Second ionization of carbonic acid in NaCl media to 250°C, *J. Solution Chem.*, 13, 647, 1984.
355. **Pavlik, V., Ujec, E., and Machek, J.**, Electrical parameters and electrochemical properties of miniature, ion-selective, plastic membrane electrodes (Crytur), *Physiol. Bohemoslov.*, 33, 278, 1984.

356. **Peiper, J. C. and Pitzer, K. S.**, Thermodynamics of aqueous carbonate solutions including mixtures of sodium carbonate, bicarbonate and chloride. *J. Chem. Thermodyn.*, 14, 613, 1982.
357. **Pethe, I. D. and Mali, B. D.**, Acid dissociation of some methoxybenzoic acids in dioxane + water medium. *Indian J. Chem.*, A16, 364, 1978.
358. **Phang, S. and Steel, B. J.**, Activity coefficients from e.m.f. measurements using cation-responsive glass electrodes. NaCl + glycine + water at 273.15, 283.15, 298.15, and 323.15°K. *J. Chem. Thermodyn.*, 6, 537, 1974.
359. **Pioda, I. A. R., Stankova, V. A., and Simon, W.**, Highly selective potassium ion responsive liquid membrane electrode. *Anal. Lett.*, 2, 665, 1969.
360. **Pitzer, K. S.**, Thermodynamics of electrolytes. I. Theoretical equations and general basis. *J. Phys. Chem.*, 77, 268, 1973.
361. **Pitzer, K. S.**, Theory: interaction approach. in *Activity Coefficients in Electrolyte Solutions*. Vol. 1, Pytkowicz, R. M., Ed., CRC Press, Boca Raton, FL, 1979, 157; Vol. 2, chup. 3.
362. **Pitzer, K. S., Olsen, J., Simonson, J. M., Roy, R. N., Gibbons, J. J., and LeAnn Rowe, L.**, Thermodynamics of aqueous magnesium and calcium bicarbonates and mixtures with chloride. *J. Chem. Eng. Data*, 30, 14, 1985.
363. **Platford, R. F.**, The activity coefficient of sodium chloride in seawater. *J. Mar. Res.*, 23, 55, 1965.
364. **Platford, R. F.**, Activity coefficients in the system H<sub>2</sub>O-NaCl-MgSO<sub>4</sub> at 25°C. *Can. J. Chem.*, 45, 821, 1967.
365. **Platford, R. F. and Dafoe, T.**, The activity coefficient of sodium sulfate in seawater. *J. Mar. Res.*, 23, 63, 1965.
366. **Powell, H. K. J. and Taylor, M. C.**, A comment on the simultaneous determination of glass electrode parameters and protonation constants. *Talanta*, 30, 885, 1983.
367. **Pungor, E., Hrabeczyi, A., Lindner, E., Gratzl, M., and Bates, R. G.**, Ion-selective electrodes for the determination of mean ionic activity coefficients. *Magy. Kem. Foly.*, 89, 337, 1983.
368. **Pungor, E., Gratzl, M., Polos, L., Toth, K., Evel, M. F., Ebel, H., Zuba, G., and Wernisch, J.**, Surface studies on precipitate-based cyanide electrodes. *Anal. Chim. Acta*, 156, 9, 1984.
369. **Pungor, E. and Umezawa, Y.**, Response time in electrochemical cells containing ion-selective electrodes. *Anal. Chem.*, 55, 1432, 1983.
370. **Pytkowicz, R. M. and Kester, D. R.**, Harned's rule behavior of sodium chloride-sodium sulfate solutions explained by an ion association model. *Am. J. Sci.*, 267, 217, 1969.
371. **Radic, N., Mulligan, K. J., and Mark, H. B., Jr.**, Ion-selective behavior of a polymeric sulphur nitride electrode for the measurement of silver(I). *Analyst*, 109, 963, 1984.
372. **Radosevic, J. and Mekjavic, I.**, Thermodynamic studies of sodium bromide in 2-propanol-water mixtures (10, 30 and 50 wt. %) from electromotive force measurements. *Electrochim. Acta*, 28, 1435, 1983.
373. **Rahnental, Oxalate detn. in urine with oxalate enzyme electrode.** *Anal. Chem.*, 1986.
374. **Ramette, R. W., Culherson, C. H., and Bates, R. G.**, Acid base properties of Tris(hydroxymethyl)aminomethane (Tris) buffers in seawater from 5 to 40°C. *Anal. Chem.*, 49, 867, 1977.
375. **Rechnitz, G. A. and Eyal, E.**, Selectivity of cyclic polyether type liquid membrane electrodes. *Anal. Chem.*, 44, 370, 1972.
376. **Rey, F., Varela, A., Antelo, J. M., and Arce, F.**, Influence of the ionic strength on the ionization of amino acids. *J. Chem. Eng. Data*, 34, 35, 1989.
377. **Rhodes, R. K. and Buck, R. P.**, Competitive ion-exchange evaluation of the bromide interference on anodized silver/silver chloride electrodes. *Anal. Chim. Acta*, 113, 67, 1980.
378. **Rhodes, R. K. and Buck, R. P.**, Impedance characterization of anodized silver/silver chloride electrodes. *Anal. Chim. Acta*, 113, 55, 1980.
379. **Riley, M.**, Gas-sensing probes. in *Ion Selective Electrode Methodology*, Vol. 2, Covington, A. K., Ed., CRC Press, Boca Raton, FL, 1979, 1.
380. **Roberson, C. E. and Barnes, R. B.**, Stability of fluoride complex with silica and its distribution in natural water systems. *Chem. Geol.*, 21, 239, 1978.
381. **Roberts, D. C., Osborn, J. A., Yacynych, A. M.**, Proteolytic enzyme modified metal oxide electrodes as potentiometric sensors. *Anal. Chem.*, 58, 140, 1986.
382. **Robinett, A. F. and Amis, E. S.**, Electromotive force and thermodynamic functions of the cell Pt|H<sub>2</sub>|HBr(m), X% alcohol, Y% H<sub>2</sub>O|AgBr|Ag in pure and mixed solvents. *Am. Chem. Soc. Adv. Chem. Ser.*, 177, 355, 1979.
383. **Robinson, R. A.**, The temperature variation of the Harned coefficient in the system HCl-NaCl. *J. Solution Chem.*, 9, 449, 1980.
384. **Robinson, R. A. and Stokes, R. H.**, *Electrolyte Solutions*, 2nd ed., Butterworths, London, 1959.
385. **Robinson, R. A. and Bower, V. E.**, Properties of aqueous mixtures of pure salts: thermodynamics of the ternary system H<sub>2</sub>O-NaCl-CaCl<sub>2</sub> at 25°C. *J. Res. Natl. Bur. Stand. Sect. A*, 70, 313, 1966.
386. **Rulletto, E. and Zelano, V.**, Potentiometric study of dissociation equilibria of malonic, dimethylmalonic and di-n-butylmalonic acids in water-dioxan mixtures. *J. Chim. Phys.*, 74, 1126, 1977.

387. **Rondinini, S., Longhi, P., and Mussini, T.**, Lithium and lithium amalgams. II. Standard potential of lithium electrode and related thermodynamic functions. *Ann. Chim. Milan*, 67, 305, 1977.
388. **Rondinini, S., Longhi, P., and Mussini, T.**, Lithium and lithium amalgams. III. Temperature-coefficient of standard potential of lithium electrode and related thermodynamic functions. *Ann. Chim. Milan*, 67, 467, 1977.
389. **Ross, J. W., Jr.**, Calcium-selective electrode with liquid ion exchanger. *Science*, 156, 1378, 1967.
390. **Ross, J. W., Jr.**, Solid state and liquid membrane ion-selective electrodes, in *Ion-Selective Electrodes*, Durst, R. A., Ed., NBS Spec. Publ. 314, National Bureau of Standards, Washington, D.C., 1969, 57.
391. **Roy, R. N., Gibbons, J. J., and Snelling, R.**, Thermodynamics of the dissociation of glycine in 50 mass % aqueous monoglyme from 5 to 55°C. *J. Solution Chem.*, 6, 475, 1977.
392. **Roy, R. N., Gibbons, J. J., Buechter, K., and Faszholz, S.**, A study of solute-solvent interactions: the  $pK_1$  and  $pK_2$  of glycine in 10, 30, and 50 mass % tetrahydrofuran-water mixtures from 5 to 55°C. *Am. Chem. Soc. Adv. Chem. Ser.*, 177, 277, 1979.
393. **Roy, R. N., Gibbons, J. J., Buechter, K., and Faszholz, S.**, Second stage dissociation of N,N-bis(2-hydroxyethyl)-2-aminoethanesulfonic acid (BES) in water + 10, 30, and 50 mass % tetrahydrofuran from 278.15 to 328.15°K. *J. Chem. Thermodyn.*, 14, 1011, 1982.
394. **Roy, R. N., Gibbons, J. J., Krueger, C., and La Cross, G., Jr.**, Second-stage dissociation of N,N-bis(2-hydroxyethyl)-2-aminoethanesulfonic acid ("BES") in water and in 50 mass % methanol + water from 278.15 to 328.15°K. *J. Chem. Thermodyn.*, 9, 325, 1977.
395. **Roy, R. N., Gibbons, J. J., Snelling, R., Moeller, J., and White, T.**, The system HBr + Pr<sub>4</sub>NBr + H<sub>2</sub>O at 25°C. Application of Pitzer's equations. *J. Phys. Chem.*, 81, 391, 1977.
396. **Roy, R. N., Gibbons, J. J., Snelling, R., and White, T.**, The system HBr + Et<sub>4</sub>NBr + H<sub>2</sub>O at 25°C. Application of Pitzer's equations. *Am. Chem. Soc. Adv. Chem. Ser.*, 177, 263, 1979.
397. **Roy, R. N., Gibbons, J. J., Trower, J. K., Lee, G. A., Hartley, J. J., and Mack, J. G.**, The ionization constant of carbonic acid in solutions of sodium chloride from EMF measurements at 278.15, 298.15, and 318.15°K. *J. Chem. Thermodyn.*, 14, 473, 1982.
398. **Roy, R. N., Gibbons, J. J., Bliss, D. P., Jr., Casebolt, R. G., and Baker, B. K.**, Activity coefficients for ternary systems. VI. The system HCl + MgCl<sub>2</sub> + H<sub>2</sub>O at different temperatures: application of Pitzer's equations. *J. Solution Chem.*, 9, 911, 1980.
399. **Roy, R. N., Gibbons, J. J., Padron, J. L., Buechter, K., and Faszhold, S.**, Sodium 1,4-piperazine diethane sulfonate monohydrate (PIPES) for measurement of pH of blood and other physiological media. *Clin. Chem.*, 26, 1919, 1980.
400. **Roy, R. N., Gibbons, J. J., Trower, J. K., and Lee, G. A.**, Applications of Pitzer's equation on the system HCl + MnCl<sub>2</sub> + H<sub>2</sub>O at various temperatures. *J. Solution Chem.*, 9, 535, 1980.
401. **Roy, R. N., Gibbons, J. J., Padron, J. L., and Casebolt, R. G.**, Thermodynamics of the second stage dissociation of N-(2-acetamido)iminodiacetic acid in water from 5 to 55°C. *Anal. Chim. Acta*, 129, 247, 1981.
402. **Roy, R. N., Gibbons, J. J., Padron, J. L., Buechter, K., Faszhold, S., and Doan, H.**, Revised values of the pH of monosodium 1,4-piperazine diethanesulfonate ("PIPES") in water and other buffers in isotonic saline at various temperatures. *Clin. Chem.*, 27, 1787, 1981.
403. **Roy, R. N., Gibbons, J. J., Padron, J. L., and Casebolt, R. G.**, Thermodynamics of the second-stage dissociation of N-(2-acetamido)iminodiacetic acid in water from 5 to 55°C. *Anal. Chim. Acta*, 129, 247, 1981.
404. **Roy, R. N., Gibbons, J. J., Buechter, K., and Faszholz, S.**, Thermodynamic behavior of hydrochloric and hydrobromic acid in [water + 50 mass percent bis-2-methoxyethyl]. *J. Chem. Thermodyn.*, 13, 537, 1981.
405. **Roy, R. N., Gibbons, J. J., Owens, L. K., Bliss, G. A., and Hartley, J. J.**, Activity coefficients for the system HCl + CaCl<sub>2</sub> + H<sub>2</sub>O at various temperatures. Application of Pitzer's equations. *J. Chem. Soc. Faraday Trans. 1*, 78, 1405, 1981.
406. **Roy, R. N., Gibbons, J. J., Pelper, J. C. and Pitzer, K. S.**, Thermodynamics of the unsymmetrical mixed electrolyte HCl-LaCl<sub>3</sub>. *J. Phys. Chem.*, 87, 2365, 1983.
407. **Roy, R. N., Gibbons, J. J., Wood, M. D., Williams, R. W., Peiper, J. C., and Pitzer, K. S.**, The first ionization of carbonic acid in aqueous solutions of potassium chloride including the activity coefficients of potassium bicarbonate. *J. Chem. Thermodyn.*, 15, 37, 1983.
408. **Roy, R. N., Gibbons, J. J., Williams, R., Godwin, L., Baker, G., Simonson, J. M., and Pitzer, K. S.**, The thermodynamics of aqueous carbonate solutions. II. Mixtures of potassium carbonate, bicarbonate, and chloride. *J. Chem. Thermodyn.*, 16, 303, 1984.
409. **Roy, R. N., Gibbons, J. J., Baker, G., and Bates, R. G.**, Standard EMF of the H<sub>2</sub>-AgCl: Ag cell in 30, 40, and 50 mass % dimethylsulfoxide-water from -20 to 25°C.  $pK_2$  and pH values for a standard "Bicine" buffer solution at subzero temperatures. *Cryobiology*, 21, 672, 1984.

410. Roy, R. N., Gibbons, J. J., Buechter, K., and Faszholz, S., Thermodynamic study of second-stage dissociation of *N,N*-bis-(2-hydroxyethyl)-2-aminoethanesulfonic acid (BES) in water + 10, 30, and 50 mass % *tert*-butyl alcohol from 278 to 308°K. *J. Chem. Soc. Faraday Trans. 1*, 80, 3167, 1984.
411. Roy, R. N., Gibbons, J. J., McGinnis, T., and Woodmansee, R., Electromotive force standard of the  $H_2$ -AgCl cell in 30, 40, and 50 mass % glycerol-water from -20 to 25°C.  $pK_2$  and pH values for a standard "MOPS" buffer in 50 mass % glycerol-water. *Cryobiology*, 22, 578, 1985 (and references cited therein).
412. Roy, R. N., Gibbons, J. J., and Baker, G. E., Acid dissociation constant and pH values for standard "BES" and "Tricine" buffer solution in 30, 40, and 50 mass % dimethylsulfoxide/water between 25 and -20°C. *Cryobiology*, 22, 589, 1985.
413. Roy, R. N., Gibbons, J. J., and Baker, G. E., Acid ionization constants and pH values of the physiological buffer "HEPES" in 50% (w/w) DMSO/water and ethylene glycol/water from 25 to -20°C. *Cryoletters*, 6, 285, 1985.
414. Roy, R. N., Gibbons, J. J., and Pogue, R., Acid dissociation constants and pH values of the biological buffer "MOPS" in 50 mass % DMSO/water and ethylene glycol/water from 25 to -20°C. *Cryoletters*, 6, 139, 1985.
415. Roy, R. N., Gibbons, J. J., Roy, L. N., and Greene, M. A., Thermodynamics of the unsymmetrical mixed electrolyte HCl-SrCl<sub>2</sub>. Applications of Pitzer's equations. *J. Phys. Chem.*, 90, 6242, 1986.
416. Roy, R. N., Wood, M. D., Johnson, D., Roy, L. N., and Gibbons, J. J., activity coefficients for (hydrogen bromide + calcium bromide + water) at various temperatures. Application of Pitzer's equations. *J. Chem. Thermodyn.*, 19, 307, 1987.
417. Roy, R. N., Baker, G. E., Pogue, R., and Roy, L. N., Standard electrode potentials of silver-silver chloride electrodes in 10, 20, 30, and 50 mass % ethylene glycol water at subzero temperatures.  $pK_1$  and pH values of BES buffers in 50 mass % ethylene glycol-water at subzero temperatures. *Cryoletters*, 9, 172, 1988.
418. Roy, R. N., Baker, G. E., Rowe, L., and Roy, L. N.,  $pK_1$  and pH values of Bicine and Tricine buffers in 20, 30, and 50 mass % ethylene glycol at subzero temperatures. *Cryoletters*, 9, 186, 1988.
419. Roy, R. N., Hufford, K., Lord, P. J., Mrad, D. R., Roy, L. N., and Johnson, D. A., The first acidity constant of carbon dioxide in solutions of ammonium chloride from e.m.f. measurements at 278.15 to 318.15°K. *J. Chem. Thermodyn.*, 20, 63, 1988.
420. Roy, R. N., Pogue, R. F., Burchfield, T. E., and Woolley, E. M., Determination of activity coefficients of HBr in aqueous surfactant solutions. in *Surfactants in Solution*, Vol. 7, Nital, K. L., Ed., Plenum Press, New York, 1989, 289.
421. Roy, R. N., Lawson, M. L., Nelson, E., Roy, L. N., and Johnson, D. A., Activity coefficients for HBr + MgBr<sub>2</sub> + H<sub>2</sub>O at various temperatures. Application of Pitzer's equations. *J. Chem. Thermodyn.*, 22, 727, 1990.
422. Roy, R. N., Rice, S. A., Vogel, K. M., and Roy, L. N., Millero, F. J., Activity coefficients for HCl + BaCl<sub>2</sub> + H<sub>2</sub>O at different temperatures and effects of higher order electrostatic terms. *J. Phys. Chem.*, 94, 7706, 1990.
423. Roy, R. N., Roy, L. N., Farwell, G. D., Smith, K. A., and Millero, F. J., Thermodynamics of the unsymmetrical mixed electrolyte HCl-NiCl<sub>2</sub>. Application of Pitzer's equations. *J. Phys. Chem.*, 94, 7321, 1990.
424. Roy, R. N., Zhang, J. Z., and Millero, F. J., The ionization of sulfurous acid in Na-Mg-Cl [NaCl-MgCl<sub>2</sub>] solutions at 25°C. *J. Solution Chem.*, 20, 1, 1991.
425. Roy, R. N., Zhang, J. Z., Sibbles, M. A., and Millero, F. J., The ionization of sulfurous acid in Na-Ni-Cl, Na-Mn-Cl, Na-Co-Cl and Na-Cd-Cl solutions at 25°C. *J. Solution Chem.*, 20, 467, 1991.
426. Roy, R. N., Ingle, A., Larkin, D., Davis, W., Roy, L. N., and Millero, F. J., Activity coefficients in hydrogen bromide + strontium bromide from 278.15 to 318.15°K. Application of Pitzer's equations. *J. Chem. Thermodyn.*, in press.
427. Roy, R. N., Ingle, A., Mrad, D., Johnson, M., Roy, L. N., Johnson, D. A., and Millero, F. J., Thermodynamics of boric acid in aqueous solutions of strontium chloride at different temperatures. *Geochim. Cosmochim. Acta*, to be submitted.
428. Roy, R. N., Larkin, D., Davis, W., Helderbrandt, C., Mackay, D., Roy, L. N., Johnson, D. A., and Millero, F. J., The system HBr + BaBr<sub>2</sub> + H<sub>2</sub>O at different temperatures. *J. Chem. Thermodyn.*, submitted.
429. Roy, R. N., Lehr, Q., Moore, P., White, M., Roy, L. N., Johnson, D. A., and Millero, F. J., Thermodynamics of HCl + CoCl<sub>2</sub> + H<sub>2</sub>O system at 5 to 55°C. Application of Pitzer's equations. *J. Phys. Chem.*, in press.
430. Roy, R. N., Lord, P. J., Rose, L. A., Roy, L. N., Johnson, D. A., and Millero, F. J., The thermodynamics of aqueous borate solutions. Mixtures of boric acid with barium chloride at various temperatures. *J. Solution Chem.*, submitted.
431. Rudra, S., Talukdar, H., Chakrabarti, B. P., and Kundu, K. K., Ion-ion-solvent interactions in aqueous ionic cosolvent systems. I. Transfer thermodynamics of hydrogen chloride in aqueous sodium nitrate solutions from EMF. *Indian J. Chem.*, 64, 1960, 1986.

- 432 **Rush, R. M.**, Parameters for the Calculation of Osmotic and Activity Coefficients, Report ORNL-4402, Oak Ridge National Laboratory, Oak Ridge, TN, 1969, 71
- 433 **Russell, T. P. and Reardon, J. F.**, Standard potential of the mercury-mercurous benzoate electrode at 20°C, *J. Chem. Eng. Data*, 22, 370, 1977.
- 434 **Ryba, O., Knizakova, E., and Petranek, J.**, Potassium polymeric membrane electrodes based on neutral carriers, *Collect. Czech. Chem. Commun.*, 38, 497, 1973.
- 435 **Sanemasa, I. and Hirata, T.**, The disproportionation constants of mercury(II) in dilute solutions, *Bull. Chem. Soc. Jpn.*, 50, 3255, 1977.
- 436 **Sankar, M., Macaskill, J. B., and Bates, R. G.**, Standard potential of the silver-silver chloride electrode in 10, 20, and 40 wt. % ethanol-water solvents at 25, 0, -5 and -10°C, *J. Solution Chem.*, 8, 887, 1979.
- 437 **Sankar, M., Macaskill, J. B., and Bates, R. G.**, Activity coefficients of hydrochloric acid and ionic interactions in the system HCl-LiCl-H<sub>2</sub>O from 5 to 45°C, *J. Solution Chem.*, 14, 333, 1985.
- 438 **Sankar, M., Macaskill, J. B., and Bates, R. G.**, Activity coefficients of hydrochloric acid and ionic interactions in the system HCl-CsCl-H<sub>2</sub>O from 5 to 50°C, *J. Solution Chem.*, 10, 169, 1981.
- 439 **Sastry, V. V. and Kalidas, C.**, Thermodynamics of hydrogen chloride in propylene glycol-water mixtures from electromotive force measurements, *J. Chem. Eng. Data*, 28, 5, 1983.
- 440 **Savenko, V. S.**, Potassium determinations in sea water with aid of membrane selective electrode, *Okeanologiya*, 17, 1123, 1977.
- 441 **Savenko, V. S.**, Determination of sodium chloride activity in sea-water, *Okeanologiya*, 18, 632, 1978.
- 442 **Scatchard, G., Hamer, W. J., and Wood, S. E.**, Isotonic solutions. I. The chemical potential of water in aqueous solutions of NaCl, KCl, H<sub>2</sub>SO<sub>4</sub>, sucrose, urea, and glycerol at 25°C, *J. Am. Chem. Soc.*, 60, 3061, 1938.
- 443 **Schefer, U., Ammann, D., Pretsch, E., Oesch, U., and Simon, W.**, Neutral carrier based Ca<sup>2+</sup>-selective electrode with detection limit in the sub-nanomolar range, *Anal. Chem.*, 58, 2282, 1986.
- 444 **Scheller, F., Pfeiffer, D., Seyer, I., Kirstein, D., Schulmel, T., and Nentwig, J.**, Degree of glucose conversion in amperometric glucose-oxidase (-mutarotase) membrane electrodes, *Bioelectrochem. Bioenerg.*, 11, 155, 1983.
- 445 **Schulthess, P., Ammann, D., Krautler, B., Cadenas, C., Stepanek, R., and Simon, W.**, Nitrite-selective liquid membrane electrode, *Anal. Chem.*, 57, 1397, 1985.
- 446 **Schwabe, K. and Dwojak, J.**, Bestimmung der Aktivitaten von Natriumchloridlosungen mit Fremdsalzzusatz aus Kettenspannung mit Na<sup>+</sup>-sensitiven Glaselektroden, *Z. Phys. Chem. (Frankfurt am Main)*, 64, 1, 1969.
- 447 **Schwabe, K., Andreis, B., Schwarzbach, M., and Suschke, H. D.**, Der einfluss hoher fremdsalz-gehalte auf den aktivitätskoeffizienten verdünnter elektrolyte, *Electrochim. Acta*, 13, 1837, 1968.
- 448 **Scott, W., Chapotea, E., Jensen, M., Johnson, R., and Runck, A.**, Carbonate ion-selective membrane electrode with improved characteristics, *Clin. Chem.*, 30, 966, 1984.
- 449 **Selig, W. S.**, the potentiometric titration of fluoride without fluoride ion-selective electrodes, *Microchem. J.*, 28, 489, 1983.
- 450 **Sen, B., Roy, R. N., Johnson, D. A., and Adcock, L. H.**, Computational techniques of ionic processes in water-organic mixed solvents, *Am. Chem. Soc. Adv. Chem. Ser.*, 177, 215, 1979 (see also p. 249).
- 451 **Senkyr, J. and Kouril, K.**, Selectivity coefficients of univalent anions for liquid ion-exchange membrane electrodes based on nitrobenzene, *J. Electroanal. Chem.*, 180, 383, 1984.
- 452 **Serjeant, E. P.**, Potentiometry and potentiometric titration, in *Analytical Chemistry Series 69*, John Wiley & Sons, New York, 1984.
- 453 **Serjeant, E. P. and Warner, A. G.**, Accuracy of the hydrogen ion-selective glass electrode, *Anal. Chem.*, 50, 1724, 1978.
- 454 **Shanbhag, P. M. and Bates, R. G.**, Dissociation constants of acetic acid and protonated tris(hydroxymethyl)aminomethane in 80-mass % 2-methoxyethanol-20-mass % water in the range 10–50°C, *Bull. Soc. Chim. Belg.*, 90, 1, 1981.
- 455 **Shatkay, A. and Lerman, A.**, Individual activities of sodium and chloride ions in aqueous solutions of NaCl, *Anal. Chem.*, 41, 514, 1969.
- 456 **Shavnya, Y. V., Bychkov, A. S., Petrukhi, O. M., Zarinski, V. A., Bakhtino, L. V., and Zolotov, Y. A.**, Determination of gold in cyanide solutions by means of a liquid ion-selective electrode, *Russ. J. Anal. Chem.*, 33, 1194, 1978.
- 457 **Shores, D. A. and John, R. C.**, Study of the Ag(s)-Ag<sub>2</sub>SO<sub>4</sub>/Na<sub>2</sub>SO<sub>4</sub> reference electrode, *J. Appl. Electrochem.*, 10, 275, 1980.
- 458 **Shukla, J. P., Ravi, P. M., and Subramanian, M. S.**, Studies on the proton-ligand dissociation equilibria in mixed solvents: thermodynamic ionization constants of 3-butylacetylacetonate in aqueous dioxane media, *Z. Phys. Chem. (Heidelberg)*, 265, 1245, 1984.
- 459 **Shumilova, G. I., Alagova, Z. S., Materova, E. A., and Suvorova, O. K.**, Solid contact sodium-selective electrode based on a neutral complexing agent, *Elektrokhimiya*, 20(5), 711, 1984.

460. **Sillen, L. G. and Martell, A. E.**, Stability constants of metal-ion complexes, Special Publ. 17. The Chemical Society, 1964.
461. **Sillen, L. G. and Martell, A. E.**, Stability constants of metal-ion complexes, Special Publ. 25. The Chemical Society, 1971.
462. **Silvester, L. F. and Rock, P. A.**, Activity coefficients of  $\text{Na}_4\text{Fe}(\text{CN})_6$  in water and in  $\text{Na}_4\text{Fe}(\text{CN})_6(\text{aq}) + \text{NaCl}(\text{aq})$  solutions at 25°C. *J. Chem. Eng. Data*, 18, 314, 1973.
463. **Simonson, J. M., Roy, R. N., Mrad, D., Lord, P., Roy, L. N., and Johnson, D. A.**, The thermodynamics of aqueous borate solutions. II. Mixtures of boric acid with calcium or magnesium borate and chloride. *J. Solution Chem.*, 17, 435, 1988.
464. **Simonson, J. M., Roy, R. N., Connole, J., Roy, L. N., and Johnson, D. A.**, The thermodynamics of aqueous borate solutions. I. Mixtures of boric acid with sodium or potassium borate and chloride. *J. Solution Chem.*, 17, 791, 1987.
465. **Simonson, J. M., Roy, R. N., and Gibbons, J. J.**, Thermodynamics of aqueous mixed potassium carbonate, bicarbonate and chloride solutions to 368 K. *J. Chem. Eng. Data*, 32, 41, 1987.
466. **Simpson, D. L. and Kobos, R. K.**, Potentiometric microbiological assay of gentamycin, streptomycin and neomycin with a  $\text{CO}_2$  gas-sensing electrode. *Anal. Chem.*, 55, 1974, 1983.
467. **Siskos, P. A., Diamandis, E. P., Gilliero, E., and Colbert, J. C.**, Potentiometric titration of sulphate, sulphite, and dithionate mixtures with use of a lead ion-selective electrode. *Talanta*, 30, 980, 1983.
468. **Sivaprasad, P. and Kalidas, C.**, Studies in isodielectric media. The standard potentials of Ag-AgCl and Ag-AgBr electrodes in 1,2-ethanediol-2,2-oxydiethanol mixtures at 25°C. *Bull. Chem. Soc. Jpn.*, 51, 2710, 1978.
469. **Smirnova, A. L., Grekovich, A. L., and Materova, E. A.**, Investigation of the properties of carbonate selective electrodes as a function of the ratio between the exchanger and the neutral chelating agent in the membrane. *Elektrokimiya*, 21, 1221, 1985.
470. **Smith, E. R. and Taylor, J. K.**, Standard electrode potential of sodium. *J. Res. Natl. Bur. Stand.*, 25, 731, 1940.
471. **Smolyakov, B. S. and Kokovkin, V. V.**, Ion-selective electrodes sensitive to tetraalkyl cations. III. Membrane-potential and concentration of electrochemically active components of membranes. *Izv. Sib. Otd. Akad. Nauk. Khim.*, 4, 11, 1984.
472. **Srinivasan, K. and Rechnitz, G. A.**, Reaction rate measurements with fluoride ion-selective membrane electrode. Formation kinetics of ferrous fluoride and aluminum fluoride complexes. *Anal. Chem.*, 40, 1818, 1968.
473. **Srivastava, A. K. and Mukherjee, L. M.**, Some potentiometric studies in propylene carbonate. Application of hydrogen and quinhydrone electrodes and evaluation of proton medium effect from ferrocene assumption. *J. Electroanal. Chem.*, 160, 209, 1984.
474. **Stefanac, Z. and Simon, W.**, A highly selective cation electrode system based on in vitro behavior of macroretrolides in membranes. *Chimia*, 20, 436, 1966.
475. **Steiner, R. A., Oehme, M., Ammann, D., and Simon, N.**, Neutral carrier sodium ion-selective microelectrode for intracellular studies. *Anal. Chem.*, 51, 351, 1979.
476. **Stover, F. S. and Buck, R. P.**, The role of site mobility in determining potentiometric selectivity of liquid ion-exchange membranes. *J. Phys. Chem.*, 81, 2105, 1977.
477. **Struck, B. D., Percec, M., and Triefenbach, D.**, Temperature dependence of the ionisation constants and evaluation of the related thermodynamic parameters for salicylic acid and metahydroxybenzoic acid. *J. Electroanal. Chem.*, 214, 473, 1986.
478. **Suarez, M. L., Calvo, A., and Leon, L. E.**, Complexometric titration of metals using a lead selective electrode. *Anal. Lett.*, 19, 1219, 1986.
479. **Sugawara, M., Nagasawa, S., and Ohashi, N.**, Potentiometric sensors based on tetraphenylborates of calcium and barium complexes with poly(oxyethylene) mono(6-methyl-heptyl)phenyl ether for the determination of nonionic surfactants. *J. Electroanal. Chem.*, 176, 183, 1984.
480. **Synnott, J. C. and Butler, J. N.**, The mean activity coefficient of sodium sulfate in aqueous sodium sulfate-sodium chloride electrolytes. *J. Phys. Chem.*, 72, 2474, 1968.
481. **Szabo, Z. G., Palfalvi, M., and Orban, M.**, Application of mercury-mercury oxide electrode to measurement of hydroxide ion activity in concentrated alkali solutions. *Magy. Kem. Foly.*, 84, 178, 1978.
482. **Szabo, Z. G., Rozsaheg, M., and Orban, M.**, Measurement of hydroxide ion activity in concentrated alkaline solutions using a Hg-HgO electrode. *Acta Chim. Hung.*, 97, 327, 1978.
483. **Szczepan, W. and Ren, K.**, Analytical application of thallium(I) sensitive membrane-electrode. *Chem. Anal. Warsaw*, 25, 449, 1980.
484. **Szczepan, W. and Ren, M.**, Liquid state membrane electrode sensitive to bismuth(III). *Talanta*, 30, 945, 1983.
485. **Szczepan, W., Ren, M., and Ren, K.**, Metal chelates as membrane active components in ion-selective electrodes. IV. New Cu(II)-selective liquid state membrane electrode. *Chem. Anal.*, 24, 51, 1979.



- 486 **Tanaka, K. and Bates, R. G.**, Measurement of pK for weak bases with the aid of sodium ion-selective electrodes. *Inorg. Chim. Acta*, 40, X56, 1980
- 487 **Taylor, M. J.**, Response of glass-calomel pH-cell in aqueous solutions containing dimethylsulphoxide at 25° and 12°C. *Cryobiology*, 15, 340, 1978.
- 488 **Taylor, M. J.**, Standard electromotive forces of the cell Pt:H<sub>2</sub>(1 atm), HCl(m), AgCl:Ag containing mixtures of dimethyl sulfoxide and water between +25 and -12°C. *J. Chem. Eng. Data*, 23, 308, 1978.
- 489 **Taylor, M. J.**, Assignment of standard pH values (pH°(S)) to buffers in 20 and 30% (w/w) dimethyl sulfoxide-water mixtures at normal and subzero temperatures. *J. Chem. Eng. Data*, 24, 230, 1979.
- 490 **Thevenot, D. R., Coulet, P. R., Sternberg, R., and Gauthero, D. C.**, Highly sensitive glucose electrode using glucose oxidase-collagen film. *Bioelectr. Bioeng.*, 5, 548, 1978
- 491 **Thompson, M., Krull, U. J., and Bendelly, L. I.**, The bilayer lipid membrane as a basis for a selective sensor for ammonia. *Talanta*, 30, 919, 1983
- 492 **Thurmond, V. and Millero, F. J.**, Ionization of carbonic acid in sodium chloride solutions at 25°C. *J. Solution Chem.*, 11, 447, 1982
- 493 **Tominic, I. and Mekjavic, I.**, Thermodynamics of hydrobromic acid in 2-butanone + water mixtures (5, 10, and 15 mass percent) from e.m.f. measurements. *J. Chem. Thermodyn.*, 11, 167, 1979.
- 494 **Tor, R. and Freeman, A.**, New enzyme membrane for enzyme electrodes. *Anal. Chem.*, 58, 1042, 1986
- 495 **Torrent, J., Sanz, F., and Virgili, J.**, Activity coefficients of aqueous perchloric acid. *J. Solution Chem.*, 15, 363, 1986
- 496 **Truesdell, A. H.**, Activity coefficients of aqueous sodium chloride from 15° to 50°C measured with a glass electrode. *Science*, 161, 884, 1968.
- 497 **Truesdell, A. H. and Husteller, P. B.**, Dissociation constants of KSO<sub>3</sub> from 10–50°. *Geochim. Cosmochim. Acta*, 32, 1019, 1968
- 498 **Tuhtar, D.**, Selectivity coefficients of a cyanide ion electrode. *Anal. Chem.*, 55, 2205, 1983.
- 499 **Tyman, V.**, Selectivity and sensitivity of fluoride ion-selective electrodes. *Chem. Listy*, 78, 992, 1984.
- 500 **Uemasu, I. and Umezawa, Y.**, Analysis of response for Cu(II) ion-selective electrode. *Denki Kagaku Oyoji Kogyo Butsuri Kagaku*, 51, 99, 1983.
- 501 **Ujcek, E., Pavlik, V., and Muchek, J.**, A technique for measuring small and fast ion concentration changes by means of miniature ion-selective electrodes with plastic membranes (Crytur). *Physiol. Bohemoslov.*, 33, 288, 1984.
- 502 **Vadgama, P.**, Enzyme electrodes. in *Ion Selective Electrode Methodology*, Vol. 2. Covington, A. K., Ed., CRC Press, Boca Raton, FL, 1979, 23.
- 503 **Van den Winkel, P., de Backer, G., Vandeputte, M., Mertens, N., Dryon, L., and Massart, D. L.**, Performance and characteristics of the fluoride-selective electrode in a flow injection system. *Anal. Chim.*, 145, 207, 1983.
- 504 **van der Linde, W. E. and Ostervink, R.**, The formation and properties of mixed cadmium sulfide-silver sulfide, and mixed mercury sulfide-silver sulfide membranes for electrodes selective to cadmium(II) and mercury(II). *Anal. Chim. Acta*, 108, 169, 1979
- 505 **Van Mau, N. D. and Gavache, C.**, A study of the mechanism of response of liquid ion exchanger calcium selective electrodes. I. Zero current potential of commercial and modified electrodes. *J. Electroanal. Chem.*, 97, 151, 1979.
- 506 **Van Mau, N. D. and Gavache, C.**, A study of the mechanism of response of liquid ion exchanger calcium selective electrodes. III. Membrane behaviour under non-zero current conditions. *J. Electroanal. Chem.*, 97, 171, 1979.
- 507 **Van Mau, N. D. and Gavache, C.**, A study of the mechanism of response of liquid ion exchanger calcium selective electrodes. II. Conductimetric investigation of the ionic dissociation in liquid ion exchangers. *J. Electroanal. Chem.*, 97, 163, 1979.
- 508 **Vandenborgh, N.**, Evaluation of the lanthanum fluoride membrane electrode response in acidic solutions. The determination of the pK<sub>a</sub> of hydrofluoric acid. *Talanta*, 15, 1009, 1968
- 509 **Vanhees, J., Francois, J.-P., and Van Poucke, L. C.**, Standard reduction potential of the indium-indium(III) electrode. *J. Phys. Chem.*, 85, 1713, 1981
- 510 **Vega, C. A. and Muniz, M. D. L. A.**, Standard potential of the (Ag + AgCl) electrode in (acetonitrile + water). *J. Chem. Thermodyn.*, 17, 1163, 1985
- 511 **Vega, C. A., Perez, B., and Torres, C.**, Standard potential of Ag-AgCl electrode in 25 and 50 wt % 2-propanol-water solvents from 5 to 50°C. *J. Chem. Eng. Data*, 29, 129, 1984.
- 512 **Vitiello, J. D., Kearney, S. D., Czaban, J. D., and Cormier, A. D.**, Transient response of the sodium glass electrode. Characterization of errors due to K<sup>+</sup> and electrode hydration. *Chim. Chem.*, 26, 1021, 1980
- 513 **Vlasov, Y. G., Ermolenko, Y. E., Kolodnikov, V. V., and Miloshov, M. S.**, Fluoride selective electrodes on the basis of calcium activated lanthanum fluoride single crystals. *Russ. J. Anal. Chem.*, 35, 463, 1980
- 514 **Vlasov, Y. G., Miloshova, M. W., Antonov, P. P., Efa, A. Y., and Bychkov, E. A.**, Solid phase ion selective electrode which is sensitive to ammonium ions. Electrochemical properties. *Sov. Electrochem.*, 10, 1054, 1983

515. **Vlasova, G. E., Zolotov, Y. A., Rybakova, E. V., Zarinskaya, V. A., Shpigun, L. K., and Volubaeva, I. V.**, Liquid ion-selective electrode for the determination of copper(II), *Russ. J. Anal. Chem.*, 38, 480, 1983.
516. **Volk, V. I. and Rozen, A. M.**, Interpretation of pH measurements in salt solutions. II. Correlation between pH and  $H^+$  activity in salt solutions (determination by extraction method), *Zh. Fiz. Khim.*, 51, 3159, 1977.
517. **Volk, V. I. and Rozen, A. M.**, Interpretation of pH measurements in salt solutions. I. Effect of salting out agents on pH determination of hydrogen ion activities, *Zh. Fiz. Khim.*, 51, 3156, 1977.
518. **Volk, V. I. and Rozen, A. M.**, Interpretation of pH meter readings in salt solutions. III. Determination by pH meter reading of hydrogen ion concentration, ionic and stoichiometric activity coefficients in salt solutions, *Zh. Fiz. Khim.*, 51, 2685, 1977.
519. **Volkov, V. L. and Manakova, L. I.**, Copper selective electrodes based on type beta-vanadium oxide bronzes, *Russ. J. Anal. Chem.*, 38, 594, 1983.
520. **Vytras, K.**, Titration of organic cations with sodium tetraphenylborate indicated by  $K^+$  ion-selective electrode "Crytur", *Collect. Czech. Chem. Commun.*, 42, 3168, 1977.
521. **Wagner, R. and Richter, T.**, Investigations on the time response of a fluoride sensitive electrode, *Z. Wasser Abwasser Forsch.*, 15, 296, 1982.
522. **Wakida, S., Tanaka, T., Kawahara, A., and Hiuro, K.**, Hydrogen ion selective electrode based on an iron-hydroxo-complex, *Fresenius Z. Anal. Chem.*, 323, 142, 1986.
523. **Walters, F. H., Griffin, K. B., and Keeley, D. F.**, Use of ammonia-sensing electrodes in salt media, *Analyst*, 109, 663, 1984.
524. **Wangsa, J. and Arnold, M. A.**, Selectivity properties of sodium glass membrane electrodes under non-steady conditions, *Anal. Chem.*, 59, 1604, 1987.
525. **Watters, J. I. and Dunnigan, P.**, The equilibrium constant and formal potentials of the mercury electrode in equilibrium with mercury(I) and mercury(II) at unit ionic strength and 25°C, *Anal. Chim. Acta*, 153, 341, 1983.
526. **White, D. R., Robinson, R. A., and Bates, R. G.**, Activity coefficient of hydrochloric acid in HCl/MgCl<sub>2</sub> mixtures and HCl/NaCl/MgCl<sub>2</sub> mixtures from 5 to 45°C, *J. Solution Chem.*, 9, 457, 1980.
527. **Whitfield, M. and Leyendekkers, J. V.**, Selectivity characteristics of a Ca-selective ion exchange electrode in the system Ca(II)-Na(I)-Cl(I)-water, *Anal. Chem.*, 42, 444, 1970.
528. **Winqvist, F., Lundstrom, I., and Danielsson, B.**, Determination of creatinine by an ammonia-sensitive semiconductor structure and immobilized enzymes, *Anal. Chem.*, 58, 145, 1986.
529. **Wu, Y. C. and Koch, W. F.**, First and second dissociation constants of deuterio-o-phthalic acid in D<sub>2</sub>O from 5 to 50°C, *J. Solution Chem.*, 15, 481, 1986.
530. **Wu, Y. C., Feng, D., and Koch, W. F.**, Evaluation of liquid junction potentials and determination of pH values of strong acids at moderate ionic strengths, *J. Solution Chem.*, 18, 641, 1989.
531. **Wu, Y. C., Koch, W. F., and Marinenko, G.**, A report on the National Bureau of Standards pH standards, *J. Res. Natl. Bur. Stand.*, 89, 395, 1984.
532. **Yang, N. F., Kapur, V., and Schloerb, P. R.**, Bromide analysis with a bromide ion-selective electrode, *Fed. Proc.*, 43, 915, 1984.
533. **Yao, S.-Z. and Liu, G.-H.**, Glycopyrrolonium-selective electrodes, *Talanta*, 32, 1113, 1985.
534. **Yoshio, M. and Bates, R. G.**, Dissociation constant and related thermodynamic quantities for 2-aminopyridinium ion from 5 to 40°C, *J. Chem. Eng. Data*, 26, 246, 1981.
535. **Zielen, A. J.**, The elimination of liquid junction potentials with the glass electrode, *J. Phys. Chem.*, 67, 1474, 1963.

## Chapter 5

**EXPERIMENTAL METHODS: ISOPIESTIC**

Joseph A. Rard and Robert F. Platford

**TABLE OF CONTENTS**

I.	Introduction .....	210
II.	Gibbs Energy, Osmotic Coefficients, Activities, Fugacities, and Vapor Pressures .....	214
III.	Isopiestic Reference Standards .....	220
	A. Isopiestic Standards for Aqueous Solutions at 298.15 K .....	222
	B. Isopiestic Standards for Aqueous Solutions at Other Temperatures .....	226
	C. Self-Consistency Among Isopiestic Reference Standards by use of the Isopiestic Molality Ratios .....	229
	D. Tertiary ("Working") Standards for Aqueous Solutions .....	230
	E. Standards for Nonaqueous Solutions .....	231
	F. Comments on the Publication of Isopiestic Data .....	231
IV.	Historical Development, Basic Features, Main Sources of Error, and Evolution of the Isopiestic Method .....	232
	A. Historical Development of the Isopiestic Method for Measurements Around Room Temperature, and Understanding Errors Inherent in the Chamber Design .....	232
	B. Historical Development of the Isopiestic Technique for Measurements from 273.15 to about 383 K .....	245
	C. Isopiestic Measurements above 373 K: Oak Ridge National Laboratory .....	246
	D. Related Experimental Techniques .....	249
V.	Sources of Error in Isopiestic Experiments .....	251
	A. Sample Sizes, Reuse of Samples, and Equilibration Times .....	252
	B. Systems with Special Difficulties .....	254
	C. Corrosion of Sample Cups .....	256
	D. Purity of Chemical Reagents .....	256
	E. The Effect of the Accuracy of Chemical Analysis .....	258
	F. Discrepancies Due to Changes in the Reference Standards .....	259
	G. Weighing Errors and Various Weight Corrections .....	259
	H. Summary of Errors .....	262
VI.	Solubility Determinations by the Isopiestic Method .....	262
VII.	Sources of Isopiestic Data .....	263

VIII.	Suitable Materials for Construction of an Isopiestic Apparatus.....	264
A.	Materials for the Isopiestic Chamber Walls.....	264
B.	Materials for the Heat-Transfer Block.....	266
C.	Materials for the Sample Cups.....	266
IX.	Representing Isopiestic Data with Equations.....	268
	Acknowledgments.....	272
	References.....	273

## I. INTRODUCTION

Experimental values are required of the Gibbs energy as a function of temperature and pressure for the complete thermodynamic characterization of an electrolyte solution and of any solid or vapor phase that is in thermodynamic equilibrium with it. This characterization can be accomplished either by measuring the Gibbs energy as a function of composition, temperature, and pressure, or by measuring the Gibbs energy as a function of composition at one or more temperatures under essentially isobaric conditions. These isothermal Gibbs energy values are then supplemented with measurements of enthalpies of dilution, heat capacities, molar volumes, etc. When this is done, thermodynamic consistency among the various properties can then be examined, and uncertainties assigned to the various quantities.

For some thermodynamic properties, experimental measurements yield thermodynamic information for the total solution (e.g., for molar volumes, heat capacities, thermal expansion, compressibilities, combustion enthalpies, etc.). Differentiation of these results must then be performed in order to obtain results for the individual components of the solution. Gibbs energy measurements for vapor phases generally yield a quantity related to the total Gibbs energy of the gaseous components, the total vapor pressure, but Gibbs energies of individual components in a mixture can be measured in some cases as when a membrane is available that is selective to one of these gases (e.g., palladium at higher temperatures is selective for hydrogen). However, in general for condensed phases, Gibbs energy measurements yield a quantity that is directly related to the partial molar Gibbs energy of one of the components in a solution. The Gibbs-Duhem equation can then be used to derive Gibbs energies for the other components of that solution.

Activity coefficients of solute components can be determined in many cases by direct measurement of the e.m.f. of an appropriate reversible redox couple, by the variation of the solubility of one component with changes in molality of the other components of that solution, and, in some cases, by liquid-liquid extraction.

The most precise of these techniques involves measurements of the e.m.f. for an electrochemical cell, but satisfactory reversible electrodes are not always available as for the ammonium, acetate, and alkali metal ions (alkali metal amalgam electrodes are difficult to work with and not especially reproducible). Electrode solubility can sometimes be a problem. Measurements with the e.m.f. method can be done in cells in which one electrode is reversible to an anion and the other is reversible to a cation, and this yields the activity of a solute directly. Two such cells can be combined to produce a concentration cell without transference, and this yields solute activities that are relative to some fixed experimental molality. Only

a single type of reversible electrode is required for concentration cells with transport, but to analyze such data requires accurate transference numbers and they are frequently not available.

In recent years ion-reversible electrodes have become available for some of these ions and for many ions for which no redox electrodes were previously available. However, these ion-reversible electrodes are usually not responsive to just one single type of ion, and corrections must be made for certain other ions if they are present in the solution by means of selectivity coefficients. In addition, ion-reversible electrodes must be calibrated with a standard electrolyte whose ionic activities are "known", and this involves partitioning the activities of that total solute into ionic contribution by some nonrigorous procedure, which yields increasing uncertainties as the molality increases. In addition, this method cannot be used for nonelectrolytes.

Solubility measurements for the saturating component in a solution can be used to derive reliable values of activity coefficients for that component, but this is limited to composition regions involving saturated solutions. These measurements are most readily used for sparingly soluble components in solution, although they have also been made for highly soluble solutes.

Liquid-liquid extraction measurements are more limited in application because they require use of an appropriate pair of immiscible solvents with a clearly identified extractable chemical species, and are generally less precise. There are unfortunately cases where the postulated species undergoing extraction turned out to be incorrect, which led to misinterpretation of the extraction results.

The concentration dependence of diffusion coefficients can be used to derive values for the concentration derivative of the logarithm of the mean molar activity coefficient. However, this method is restricted to 1-1 electrolytes below about  $0.01 \text{ mol} \cdot \text{dm}^{-3}$ , and it is not applicable to higher-valence electrolytes, due to uncertainty in the theoretical treatment of the electrophoretic effect for electrolyte solutions. In addition, the required precise diffusion coefficients are available only for very few (usually aqueous) systems and then usually only at 298.15 K.

The alternative to characterizing the activity coefficient of a solute or solutes is to measure the activity of the solvent. This can be done by a variety of techniques including measurement of its freezing temperature depression or boiling temperature elevation, by direct vapor pressure measurements, by vapor pressure osmometry, or by isopiestic measurements.

Freezing temperature depression measurements can be done very precisely, but only for temperatures at which a solution is in thermodynamic equilibrium with the pure solid solvent at a particular solute molality. These measurements yield the activity of the solvent as a function of composition but each value is at a different temperature. Consequently, such measurements have to be converted to a common temperature before the Gibbs-Duhem equation can be applied to derive activity coefficients for the solute(s), and this requires enthalpy and heat capacity data. Boiling temperature elevations can also be used to determine solvent activities and, in principle, this method is more flexible than freezing temperature measurements because the confining pressure on the solution can be varied to yield activities over a wider temperature range. However, the molal elevation of the boiling temperature is generally less than the molal depression of the freezing temperature (about a factor of 3.6 less for aqueous solutions), which requires that the boiling temperatures be measured even more accurately and precisely than the freezing temperatures. Inasmuch as precise boiling temperature experiments are more difficult to perform, this type of measurement is rarely utilized.

The most general methods of determining solvent activities involve the measurement of the vapor pressure of volatile components of a solution, and are simplest to interpret if only one component of the solution ("the solvent") is volatile. In that case the observed vapor pressure of the solvent can be directly used to calculate the solvent activity.

Direct measurement of the vapor pressure of the solvent in a solution can be done by either static or dynamic methods, and both are capable of high accuracy. However, accurate vapor pressure measurements by the static method require an essentially complete removal of dissolved air from the solution and vapor phase (this is usually done by freezing the solution, evacuating the vapor phase under high vacuum, thawing the solution and allowing it to outgas, refreezing the solution, reevacuating the vapor phase, etc., until complete removal of air has been effected). Also required is a very precise control of the temperature of the system because of the rapid variation of the vapor pressure of the solvent with temperature. Vapor pressure measurements by the dynamic method do not require this degassing, but they do require very careful temperature control, well-controlled gas flow rates that produce solvent-vapor saturated carrier gas, and a careful measurement of the mass of solvent swept out by the flowing carrier gas. The amount of solvent swept out by the flowing carrier gas divided by the volume of flowing gas is a measure of the vapor pressure of the solvent. Because the relative lowering of the vapor pressure of the solvent becomes less as the molality of solute decreases, direct vapor pressures for molalities below about  $1 \text{ mol} \cdot \text{kg}^{-1}$  generally yield solvent activities much less precise than most other techniques.

Solvent activities are also sometimes measured by vapor pressure osmometry, a technique originally developed for estimation of molecular masses and for which it is well suited. The commercial thermistor-type vapor pressure osmometers yield solvent activities rapidly, but they generally yield much less precise results than other vapor-pressure methods. In a vapor pressure osmometry experiment a drop of solvent is placed on one thermistor and a drop of solution on a second. These two thermistors are then suspended in a chamber with a solvent-saturated vapor phase, and this chamber is placed in a thermostat. Solvent evaporates from the pure solvent drop and is absorbed by the solution drop; this causes the solution drop to warm and the solvent drop to cool. These temperature differences are measured and then related to vapor pressures. However, the steady-state temperature difference may not be the equilibrium temperature difference because of heat conduction between the solution drop and the thermistor, and the molality of the solution is not accurately known. Consequently, the resulting calculated solvent activity will not be accurately known. In fact, at low molalities it may be more accurate in some cases to estimate the solvent activity from Raoult's law than by use of vapor pressure osmometry.

An experimental method that has been used for the determination of solvent activities for hundreds of binary and ternary electrolyte solutions (and some higher-order systems) is the isopiestic method. In brief, this method consists of placing samples of different solutions into separate open containers, keeping them isothermally at an essentially identical temperature by putting them in good thermal contact (usually, by placing the containers in recesses in a large copper block), and then allowing the samples to exchange solvent in a sealed chamber through a common vapor phase until thermodynamic equilibrium is reached. When these samples are at thermodynamic equilibrium, they will have identical solvent activities and thus equal vapor pressures. One or more of these solutions are used as isopiestic reference standards, and those are chosen to be systems whose solvent activities are accurately known as a function of molality at that temperature. Then, if the molality of each solution is determined after isopiestic equilibration has occurred, and if the solvent activity of the standard is calculated from its experimental molality, the solvent activity of each of the other solutions will also be known. By doing a series of such measurements as a function of molality, solvent activities of each of these solutions can be determined over a wide composition range.

Isopiestic measurements have many advantages over other methods of measurement and have been widely used, especially for aqueous electrolyte solutions. However, there is nothing inherent in the method that limits it to aqueous solutions or to electrolyte solutions. For example, it is as easy to use it for a solution of an electrolyte as for a solution of a

sugar, for a mixture of electrolytes, for a mixture of sugars, or for mixtures of electrolytes and sugars.

There is also no fundamental reason that limits this method to a single volatile component. However, if more than one volatile component is transported through the vapor phase, then each solution must be chemically analyzed after each isopiestic equilibration. This is in contrast to the ease and simplicity of the method when only one volatile component is present; in that case molalities are determined by weighing of the samples, and these samples can be reused by adding or removing solvent to change the molalities. In this regard we note that solvent mixtures can be easily studied if all but one of the solvents are relatively nonvolatile, e.g., dibutylphthalate or glycerol. The nonvolatile solvents are then formally treated as solutes. In all subsequent discussions of the isopiestic method we will assume that only a single volatile component is present in any system, and that component is referred to as the solvent.

Isopiestic experiments require several days or longer to reach equilibrium (see below), in contrast to methods such as e.m.f. where temperature equilibrations of an hour are generally more than sufficient. However, by using an isopiestic chamber with a number of sample containers, the water activity of a number of different electrolytes or mixtures can be determined simultaneously. An isopiestic experiment is also much less sensitive to temperature variation than a direct pressure measurement. The vapor pressure of a solution changes rapidly with temperature due to the large enthalpy of vaporization of the solvent from that solution. In contrast, the isopiestic experiments yield solvent activities whose temperature dependences are proportional to the relative partial molar enthalpies  $L_s$  of the solvent in the solution; this  $L_s$  is related to the difference between the enthalpies of vaporization of the solvent in the solution and the pure solvent, and this difference is considerably smaller than the vaporization enthalpies themselves. In addition, isopiestic equilibrations are considerably less sensitive to incomplete degassing than static vapor pressure measurements, and can even be done in an air-filled chamber with vapor stirring.

Although the isopiestic method does have wide applicability and great flexibility, it does have a few limitations. The precision of the determination of isopiestic molalities begins to decrease for molalities below several tenths, and the method is generally unsatisfactory below  $0.1 \text{ mol} \cdot \text{kg}^{-1}$ . Inasmuch as solvent activities need to be integrated from infinite dilution to the molality of interest for the calculation of the activity coefficients of solutes, the isopiestic experiments need to be supplemented by some other technique at low molalities such as e.m.f. measurements. This is especially important for higher-valence electrolytes and associated electrolytes, which have large deviations from the Debye-Hückel equation. In addition, e.m.f. measurements offer a distinct advantage if another component of the solution can become volatile at high molalities (e.g., HCl, HBr, HI, acetic acid,  $\text{CO}_2$ , etc.). The e.m.f. method is described in detail in the preceding chapter by Professors Butler and Roy.

As we have just noted, isopiestic measurements are simpler to perform and generally more accurate than direct vapor pressure measurements. However, the isopiestic method does not completely eliminate the need for direct pressure measurements since reference standards are required, and these reference standards still must be characterized by "absolute" methods such as e.m.f. and direct vapor pressure measurements. However, the isopiestic method does simplify the situation since the more difficult direct pressure measurements need only be performed on a few selected systems, and the simpler isopiestic method can be used for the majority of systems of interest. Accurate reference standards are available for aqueous solutions, but they are generally less reliable or unavailable for most nonaqueous solutions.

The history and basic features of the isopiestic method were discussed by one of the authors in the first edition of this book,<sup>1</sup> and the application of the isopiestic method to

solubility determinations was reviewed by the other author<sup>2</sup> at the first I.U.P.A.C. sponsored solubility symposium. In the present review this material has been combined, numerous additional historical and experimental details have been added, and more recent advances in the experimental methods are described.

## II. GIBBS ENERGY, OSMOTIC COEFFICIENTS, ACTIVITIES, FUGACITIES, AND VAPOR PRESSURES

Consider a liquid solution with a single solvent and an arbitrary number of solutes. The total Gibbs energy of this system is given by

$$G = n_s \mu_s + n_1 \mu_1 + n_2 \mu_2 + \dots \quad (1)$$

where  $n_s$  is the number of moles of solvent and  $n_i$  is the number of moles of solute  $i$ . Each partial molar Gibbs energy  $\mu_j$  (chemical potential) can be expressed in terms of a reference-state or standard-state value and a thermodynamic activity term

$$\mu_j = \mu_j^\circ + RT \ln a_j \quad (2)$$

where  $j$  denotes both solvents and solutes.

In the case of a solvent, the standard state is chosen to be the pure liquid solvent, and activities are defined on the basis of Raoult's law:

$$a_s = x_s f_{x,s} \quad (3)$$

where  $x_s$  is the mole fraction of solvent in the solution and  $f_{x,s}$  is the activity coefficient on that concentration scale. For a solution containing one or more dissociating electrolytes, the mole fraction of the solvent is defined as

$$x_s = \frac{n_s}{n_s + \sum_i \nu_i n_i} \quad (4)$$

where  $\nu_i$  is the number of ions formed by the complete dissociation of one formula unit of that electrolyte ( $\nu_i = 1$  for nonelectrolytes). The molal concentration scale is most commonly used for electrolyte solutions. In this case Equation 4 becomes

$$x_s = \frac{m_s}{m_s + \sum_i \nu_i m_i} \quad (5)$$

where the molality is in units of moles per kilogram of solvent. The molality of the solvent in a solution is constant and independent of composition. For water,

$$m_s = \frac{1000 \text{ g} \cdot \text{kg}^{-1}}{18.0153 \text{ g} \cdot \text{mol}^{-1}} = 55.5084 \text{ mol} \cdot \text{kg}^{-1} \quad (6)$$

We note that  $m_s$  is sometimes denoted by  $\Omega$ .

Activity coefficients were originally defined to describe the variation of the Gibbs energy of each component in a solution, because the activity value itself is not a sensitive-enough measure of nonideal behavior at low molalities. However, the activity coefficient of the



solvent  $f_{x,s}$  as defined by Equation 3 is also not a very sensitive measure of deviations from ideality at low solute molalities. Osmotic coefficients have been defined to exaggerate these deviations for the solvent from ideal behavior. One kind of osmotic coefficient is  $\Phi_x$ , which is defined by<sup>3</sup>

$$\ln a_s = \Phi_x \ln x_s \quad (7)$$

and a second kind by

$$\Phi = -\left(m_s / \sum_i \nu_i m_i\right) \ln a_s = \frac{m_s(\mu_s^\circ - \mu_s)}{RT \sum_i \nu_i m_i} \quad (8)$$

They are then related by

$$\Phi = -\left(\frac{m_s \Phi_x}{\sum_i \nu_i m_i}\right) \ln x_s \quad (9)$$

Both  $\Phi$  and  $\Phi_x$  are dimensionless quantities. We note that  $\Phi_x$  is also sometimes denoted by  $g$ .

The quantity  $\Phi$  is almost universally used and will be the osmotic coefficient discussed in the remainder of this chapter. However, the function  $\Phi_x$  does have an advantage for systems in which the solute is completely soluble in the solvent (e.g., the  $\text{H}_2\text{SO}_4\text{-H}_2\text{O}$  system).

The osmotic coefficient  $\Phi$  is usually referred to as the ‘‘practical’’ osmotic coefficient and  $\Phi_x$  as the ‘‘rational’’ osmotic coefficient. This is based on the consideration that the mole fraction concentration scale is more ‘‘rational’’ than the molality scale owing to the early definition of ideal solutions on the basis of mole fraction statistics. However, electrolyte solutions show large deviations from such ideal behavior even at low mole fractions of solute, so there is no reason to consider mole fractions to be more ‘‘rational’’. Thus we prefer the more descriptive terms molal osmotic coefficient for  $\Phi$  and mole fraction osmotic coefficient for  $\Phi_x$ .

An ideal solution can be defined for any particular concentration scale (molality, molarity, mole fraction, etc.) so that all activity coefficients are unity for all components on that scale. Since the activity of the solvent is almost always defined on the basis of Equation 3, for an ideal solution defined by mole fraction mixing statistics this amounts to setting  $f_{x,s} = 1$  for all compositions. Then, Equation 8 becomes

$$\Phi^{\text{id}} = -\left(m_s / \sum_i \nu_i m_i\right) \ln x_s \quad (10)$$

Thus  $\Phi$  for an ideal solution is not constant but varies with composition (however,  $\Phi_x = 1$  for an ideal solution). This equation can be used to derive the limiting value for  $\Phi$  at infinite dilution of the solutes, since  $f_{x,s} \rightarrow 1$  as  $x_s \rightarrow 1$ . First we rearrange Equation 5 into the form

$$x_s = \frac{1}{1 + \left(\sum_i \nu_i m_i\right) / m_s} \quad (11)$$

and then expand  $\ln x_s$  in a series

$$\begin{aligned}\ln x_s &= -\ln\left(1 + \left(\sum_i \nu_i m_i\right)/m_s\right) \\ &= -\left[\left(\sum_i \nu_i m_i\right)/m_s - \frac{1}{2} \left(\sum_i \nu_i m_i\right)^2/m_s^2 + \dots\right]\end{aligned}\quad (12)$$

As we approach infinite dilution only the first term in this expansion need be retained, and Equation 10 then becomes

$$\lim_{x_s \rightarrow 1} \Phi = -\left(m_s/\sum_i \nu_i m_i\right)\left(-\sum_i \nu_i m_i/m_s\right) = 1 \quad (13)$$

Like the activity coefficients of the solutes,  $\Phi$  has a limiting value of unity for all electrolyte valence types.

Equation 13 was derived based on the use of stoichiometric molalities, and it is strictly true only if the solute does not react chemically with the solvent. If such a reaction does occur, for example by hydrolysis, then the mole fraction statistics in Equation 10 should be applied with the actual speciation and not with the stoichiometric molalities, and then the limiting values of  $\Phi$  are then still one. However, the values of  $\Phi$  at infinite dilution will be greater than unity if calculated from the stoichiometric molalities. See Section IX for more details.

If an ideal solution is defined instead on the basis of molality statistics for the solutes, i.e., all mean molal activity coefficients equal to 1, then  $\Phi^{\text{id}}$  becomes equal to 1.

The activity of the solvent in a solution is also given by its relative fugacity

$$a_s = f_s/f_s^{\circ} \quad (14)$$

where  $f_s^{\circ}$  is the fugacity of the pure solvent at the same temperature as the solution, and both solution and solvent are at a reference-state pressure equal to the vapor pressure of the pure solvent. The fugacity of a volatile solvent can be computed from its vapor pressure after correction for the nonideal behavior of that phase. The fundamental equation relating the fugacity to pressure<sup>4</sup> is

$$\left(\frac{\partial \ln f_s}{\partial P}\right)_{T,s} = \frac{V_s}{RT} \quad (15)$$

where  $V_s$  is the molar volume of the solvent if a pure solvent is being considered; for a solution  $V_s$  will be its partial molar volume.

We have just commented that the fugacity of a gas is related to its vapor pressure. It is convenient to consider the ratio  $(f_s/P_s)$  to emphasize the differences:

$$\begin{aligned}RT \, d \ln (f_s^g/P_s^g) &= RT \, d \ln f_s^g - RT \, d \ln P_s^g \\ &= \left[ RT \left(\frac{\partial \ln f_s^g}{\partial P_s^g}\right)_{T,s} - \frac{RT}{P_s^g} \right] dP_s^g \\ &= \left( V_{s,g} - \frac{RT}{P_s^g} \right) dP_s^g\end{aligned}\quad (16)$$

where  $V_{s,g}$  is the gas phase molar volume of the solvent. This can be rearranged and integrated to yield

$$\int_0^{P_s} d \ln (f_s'/P_s') = \int_0^{P_s} \left( \frac{V_{s(g)}}{RT} - \frac{1}{P_s'} \right) dP_s' \quad (17)$$

As  $P_s' \rightarrow 0$ ,  $f_s' \rightarrow P_s'$  so the integral on the left-hand side vanishes at  $P_s' = 0$ . Thus

$$\ln (f_s/P_s) = \int_0^{P_s} \left( \frac{V_{s(g)}}{RT} - \frac{1}{P_s'} \right) dP_s' \quad (18)$$

The integration variable is  $P_s'$ , so an analytical representation of  $V_{s(g)}$  as a function of  $P_s'$  is required. A convenient and accurate expression for  $V_{s(g)}$  is the virial equation

$$\frac{V_{s(g)}}{RT} = \frac{1}{P} + \frac{B_2(T)}{RT} + \frac{B_3(T)P}{RT} + \frac{B_4(T)P^2}{RT} + \dots \quad (19)$$

where the virial coefficients  $B_i(T)$  are defined to be functions of temperature but not of pressure. Then, Equation 18 becomes

$$\begin{aligned} \ln (f_s/P_s) &= \frac{1}{RT} \int_0^{P_s} [B_2(T) + B_3(T)P_s' + B_4(T)P_s'^2 + \dots] dP_s' \\ &= \frac{B_2(T)}{RT} P_s + \frac{B_3(T)}{2RT} (P_s)^2 + \frac{B_4(T)}{3RT} (P_s)^3 + \dots \end{aligned} \quad (20)$$

If more than one gas is present in the vapor phase,  $P_s$  would be the partial pressure due to the solvent. An equation similar to this also holds for the pure solvent,

$$\ln (f_s^0/P_s^0) = \frac{B_2(T)}{RT} P_s^0 + \frac{B_3(T)}{2RT} (P_s^0)^2 + \frac{B_4(T)}{3RT} (P_s^0)^3 + \dots \quad (21)$$

We now compute the relative fugacity of the solvent

$$\begin{aligned} \ln(f_s/f_s^0) &= \ln(f_s/P_s) - \ln(f_s^0/P_s^0) + \ln(P_s/P_s^0) \\ &= \ln(P_s/P_s^0) + \frac{1}{RT} \left[ B_2(T)(P_s - P_s^0) + \frac{B_3(T)}{2} \{ P_s^2 - (P_s^0)^2 \} + \dots \right] \end{aligned} \quad (22)$$

Under the pressure conditions generally encountered for isopiestic experiments, contributions of the third and higher virial coefficients can generally be neglected. In this case Equation 22 becomes

$$\ln (f_s/f_s^0) \approx \ln(P_s/P_s^0) + B_2(T)(P_s - P_s^0)/RT \quad (23)$$

For many common solvents such as water, the data do not yield values of  $B_2(T)$  or higher-order coefficients, and even values of  $B_1(T)$  are highly uncertain.

We note that there is an alternative virial expansion to Equation 19 in which  $PV_{s(g)}$  is represented by a series in the inverse of  $V_{s(g)}$ . The first virial coefficient is  $RT$  in both cases, and the second virial coefficients for the expansions in terms of volume or pressure just differ by a factor of  $RT$ . The relationships between the third- and higher-order virial coefficients in these two treatments are more complex. We restricted our discussion to the expansion in terms of pressure, Equation 19, because it is more useful for fugacity calculations. However, the third virial coefficients for solvent vapor are sometimes better characterized for the volume form of the virial expansion than for the pressure form.

As the temperature and molality of the solution change, the confining pressure on the solution also changes. This pressure will also be affected by the presence or absence of air. Equation 15 can be used directly in this case:

$$\begin{aligned} d \ln (f'_s/f_s^\circ) &= d \ln f'_s - d \ln f_s^\circ \\ &= \frac{\{V_{s(l)} - V_{s(l)}^\circ\}}{RT} dP' \end{aligned} \quad (24)$$

where  $V_{s(l)}$  is the partial molar volume of the solvent in the solution and  $V_{s(l)}^\circ$  is the molar volume of the pure solvent.

Performing the integration yields

$$\begin{aligned} \ln \left\{ a_s(P_s^\circ) / \left( f_s(P_1)/f_s^\circ(P_2) \right) \right\} &= \frac{1}{RT} \left\{ \int_{P_1}^{P_s} V_{s(l)} dP' - \int_{P_2}^{P_s} V_{s(l)}^\circ dP' \right\} \\ &\approx \frac{V_{s(l)}}{RT} (P_s^\circ - P_1) - \frac{V_{s(l)}^\circ}{RT} (P_s^\circ - P_2) \\ &\approx V_{s(l)}^\circ (P_2 - P_1)/RT \end{aligned} \quad (25)$$

assuming that the liquid solution can be treated as incompressible under conditions normally used for isopiestic measurements. Here  $P_1$  is the confining (total) pressure on the solution and  $P_2$  is the confining pressure on the solvent. The last approximation,  $V_{s(l)} \approx V_{s(l)}^\circ$ , can be made because they are generally within  $1 \text{ cm}^3 \cdot \text{mol}^{-1}$  and rarely differ by as much as  $2 \text{ cm}^3 \cdot \text{mol}^{-1}$ .

By combining the relationship between  $\Phi$  and  $a_s$ , Equation 8, with Equations 23 and 25, we obtain the equation for the osmotic coefficient as a function of pressure

$$\Phi = -\frac{\left( m_s / \sum_i v_i m_i \right)}{RT} \left\{ RT \ln \left( P_s/P_s^\circ \right) + B_2(T) (P_s - P_s^\circ) + V_{s(l)}^\circ (P_2 - P_1) \right\} \quad (26)$$

If only the solvent is present in the vapor phase, then replace  $P_1$  with  $P_s$ ,  $P_2$  with  $P_s^\circ$  and  $V_{s(l)}^\circ$  with  $V_{s(l)}$ .

The isopiestic method has been most widely applied to aqueous solutions. Consequently, values of  $B_2(T)$  will be analyzed for water. Le Fevre et al.<sup>5</sup> have given an equation for  $B_2(T)$  for water vapor based on experimental data over the wide temperature range of 293 to 1100 or 1200 K. Their equation was given in units of  $\text{m}^3 \cdot \text{kg}^{-1}$ , which we have converted into the more common units of  $\text{cm}^3 \cdot \text{mol}^{-1}$ . In terms of these units their equation is

$$B_2(T) = \frac{27.02}{(1 + 10^{-4}T)} - \frac{13193}{T} - 16.9704 \left( 1 - e^{-1500/T} \right)^{5.2} e^{1500/T} \left( \frac{T}{1500} \right)^{1.2} \quad (27)$$

Values of  $B_2(T)$  were calculated at 5 K intervals by us from 273.15 to 373.15 K (0 to 100°C) and are given in Table 1. Also given are values of  $V_{s(l)}^\circ$  at these same temperatures as reported by Kell<sup>6</sup> for pressures corresponding to that of the vapor pressure of pure solvent, and the vapor pressure of water at these temperatures from Wexler and Greenspan.<sup>7</sup> For comparison, the volume of 1 mol of ideal gas is given at the vapor pressure of water.

**TABLE 1**  
**Vapor Pressure, Molar Volume, and Virial Coefficients of**  
**Water at Various Temperatures (IPTS-68)**

T (°C)	P <sup>*</sup> (Pa)	V <sub>sl</sub> <sup>o</sup> <sup>b</sup> (cm <sup>3</sup> · mol <sup>-1</sup> )	B <sub>2</sub> (T) <sup>c</sup> (cm <sup>3</sup> · mol <sup>-1</sup> )	V <sub>lg</sub> <sup>id</sup> <sup>d</sup> (cm <sup>3</sup> · mol <sup>-1</sup> )
0	610.75	18.019	-1.761	3,718.557
5	872.04	18.017	-1.609	2,652.036
10	1,227.57	18.022	-1.475	1,917.816
15	1,705.03	18.032	-1.357	1,405.152
20	2,338.34	18.049	-1.252	1,042.363
25	3,168.62	18.069	-1.157	782.350
30	4,245.15	18.095	-1.073	593.747
35	5,626.45	18.124	-998	455.370
40	7,381.29	18.157	-930	352.742
45	9,589.84	18.194	-868	275.840
50	12,344.73	18.234	-812	217.650
55	15,752.16	18.277	-761	173.208
60	19,932.93	18.324	-715	138.965
65	25,023.54	18.373	-673	112.356
70	31,177.15	18.425	-635	91.513
75	38,564.54	18.481	-599	75.061
80	47,374.98	18.539	-567	61.979
85	57,817.10	18.599	-537	51.505
90	70,119.59	18.663	-509	43.061
95	84,531.93	18.729	-484	36.211
100	101,324.97	18.798	-460	30.620

<sup>a</sup> Saturation vapor pressure of water from Wexler and Greenspan.<sup>7</sup>

<sup>b</sup> From Kell,<sup>6</sup> molar volume of liquid water at the actual vapor pressure of water at that temperature.

<sup>c</sup> Calculated from the equation given by Le Fevre et al.<sup>5</sup>

<sup>d</sup> Molar volume of an ideal gas at the vapor pressure of water.

It is obvious that  $V_{lg}^{id} \gg -B_2(T) \gg V_{sl}^o$ . However, as T increases  $V_{lg}^{id}$  drops rapidly,  $-B_2(T)$  also drops but much less rapidly, and  $V_{sl}^o$  increases slowly. For example, between 273.15 and 373.15 K,  $V_{lg}^{id}$  drops 121-fold,  $-B_2(T)$  decreases by a factor of 3.8, and  $V_{sl}^o$  increases by 4%. Values of  $B_2(T)$  were tabulated by Le Fevre et al.<sup>5</sup> at 25 K intervals up to 1523.15 K. Values of  $B_2(T)$  become smaller to  $-116 \text{ cm}^3 \cdot \text{mol}^{-1}$  at 573.15 K, to  $-50 \text{ cm}^3 \cdot \text{mol}^{-1}$  at 773.15 K, and to  $-24 \text{ cm}^3 \cdot \text{mol}^{-1}$  at 973.15 K. However,  $V_{sl}^o$  slowly increases with temperature until close to the critical temperature.

Volumes and  $B_2(T)$  are given in units of  $\text{cm}^3 \cdot \text{mol}^{-1}$  in Table 1, and  $P_s^o$  is in Pa. Noting that  $1 \text{ J} = 1 \text{ Pa} \cdot \text{m}^3 = 1 \times 10^6 \text{ Pa} \cdot \text{cm}^3$ , the value of R in consistent units is  $8.31451 \times 10^6 \text{ Pa} \cdot \text{cm}^3 \cdot \text{mol}^{-1} \cdot \text{K}^{-1}$ . Consider a solution with  $a_s = 0.9$ , then  $\ln a_s = -0.1054$ . At 298.15 K,  $(B_2(T)/RT) (P_s - P_s^o) = 0.00015$ , at 373.15 K it is 0.00150, but at 273.15 K it is only 0.00005. Clearly the  $B_2(T)$  term makes an all but negligible contribution to  $\Phi$  at low temperatures, but it makes a contribution comparable to the precision of high-quality vapor pressure measurements by room temperature, and it makes a significant contribution to  $\Phi$  at higher temperatures. The corresponding term for compression of the liquid,  $(V_{sl}^o/RT) (P_s^o - P_s)$ , is  $5 \times 10^{-7}$  at 273.15 K,  $2 \times 10^{-6}$  at 298.15 K, and  $6 \times 10^{-5}$  at 373.15 K.

We note that nonideal vapor corrections involving  $B_2(T)$  are usually ignored when vapor pressures are analyzed to yield  $\Phi$  or  $a_s$  at 298.15 K, but this term should not be neglected when data are of high quality. This is especially true if the data are being used to derive  $\Phi$  values for the isopiestic reference standards, since results of the highest quality are required in that case.

The osmotic pressure of a solution  $\Pi$  can be related to  $\Phi$  by<sup>3</sup>

$$\Pi = \frac{RT\Phi}{m_s V_{s(l)}} \left( \sum_i \nu_i m_i \right) \quad (28)$$

for an incompressible solvent. It is because of this direct relationship to osmotic pressure that  $\Phi$  is called an osmotic coefficient.

### III. ISOPIESTIC REFERENCE STANDARDS

The isopiestic method is a relative method for measuring solvent activities, which involves equilibrating two or more different solutions through a common vapor phase until the activities of the solvent become equal in all of the solutions. This requires that reference standards be used whose solvent activities have been determined by one or more direct techniques. This, in turn, requires that thermodynamic data for these reference standard solutions be critically evaluated and combined with appropriate statistical weighting to yield values of  $\Phi$  as a function of composition.

The reference standards should be chosen so as to be systems with high quality activity data. These data can be from e. m. f. measurements; freezing temperature depression or boiling temperature elevation measurements combined with enthalpies of dilution and heat capacities; and direct vapor pressure measurements. They may also include isopiestic intercomparison to other well-characterized standards. Preferably, thermodynamic data from two or more independent studies and two or more different methods should be available, so that thermodynamic consistency can be examined.

The earliest evaluations of isopiestic standards involved graphical analysis of experimental data to yield smoothed values of  $\Phi$  at various constant temperatures, and results were given in tabular form at various molality values.<sup>3</sup> Later evaluations involved least-squares equations for  $\Phi$  as a function of molality, which are more convenient to use for interpolation to the experimental molalities of the reference standards. These equations were generally given as separate fits for a single temperature, and usually contain few enough terms that  $\Phi$  can be computed with a hand calculator. More recently, "global" fits have been performed in which a variety of thermodynamic data are included at their temperature of measurement, and both temperature and molality (and, sometimes pressure) dependences of  $\Phi$  are modeled simultaneously by use of a multiparameter equation. Although these more complex equations can be evaluated with a programmable hand calculator, this is more conveniently done with a personal or main frame computer for these more complex equations.

The condition of isopiestic equilibrium is

$$a_i = \text{constant} \quad (29)$$

for each of the separate solutions involved in an equilibration. Isopiestic standards have always been chosen to be binary solutions, i.e., one solute in one solvent. Let a superscript asterisk denote the reference standard (a sub R is also sometimes used), and let the "test" solution be an arbitrary mixture of electrolytes in the same solvent. The condition for isopiestic equilibrium can then be written as

$$\ln a_i = \ln a_i^* \quad (30)$$

By using the definition of  $\Phi$ , Equation 8, this result can be rewritten as

$$-\left( \sum_i \nu_i m_i / m_s \right) \Phi = -(\nu^* m^* / m_s) \Phi^* \quad (31)$$

from which we obtain the fundamental equation for isopiestic equilibrium

$$\Phi = \frac{\nu^* m^* \Phi^*}{\sum_i \nu_i m_i} \quad (32)$$

Thus, given the molalities of the solutes in these two solutions at isopiestic equilibrium, the  $\Phi$  value of the test solution can be readily computed. The isopiestic molality ratio is sometimes denoted by  $R$ , but we will refrain from using that symbol in this review because of possible confusion with the gas constant. The quantity  $\sum_i \nu_i m_i$  is sometimes called the osmolality.

The overwhelming number of isopiestic experiments have been performed for aqueous solutions and are predominantly for electrolyte solutions. The following discussion will therefore emphasize the reference standards for aqueous solutions.

Isopiestic reference standards most commonly used for aqueous solutions are NaCl, KCl, H<sub>2</sub>SO<sub>4</sub>, and CaCl<sub>2</sub>. Both NaCl and KCl are obvious choices since they are inexpensive reagents, they are widely available in high purity, they are easy to work with, they require no special handling techniques, and their solutions are easily and accurately analyzed for molality. However, because of solubility limitations, they are only suited for high and moderate water activity measurements, and additional standards are required for lower water activities.

Sulfuric acid has been used as the primary isopiestic standard at high molalities (low water activities). Again, it is an obvious choice since it is completely miscible with water, and water activities can be achieved that span the entire range  $0 < a_w < 1$ . It is an inexpensive reagent available in high purity, and it is only slightly more difficult to analyze for molality than NaCl or KCl. However, many isopiestic experiments have been performed with sample containers made of silver or gold-plated silver, and H<sub>2</sub>SO<sub>4</sub> is too corrosive for these materials. There is also a limitation for extremely high concentrations of H<sub>2</sub>SO<sub>4</sub>, especially at higher temperatures, where transport of SO<sub>3</sub> can occur through the vapor phase. Sulfuric acid molalities of 30 mol · kg<sup>-1</sup> can easily be studied at 298.15 K without any such problems.

The most widely used standard at lower water activities has been aqueous CaCl<sub>2</sub>. Not only is it fairly soluble, but it forms fairly "stable" supersaturated solutions and can be used as an isopiestic reference standard up to 10 or 11 mol · kg<sup>-1</sup>. It should be noted that even purportedly pure CaCl<sub>2</sub> frequently contains 0.1% of more SrCl<sub>2</sub>. Fortunately, the presence of this amount of SrCl<sub>2</sub> has little effect on  $a_w$  of CaCl<sub>2</sub>, but its presence can add uncertainty to the molar mass needed for calculating molalities.

Activities of aqueous CaCl<sub>2</sub> are based on a number of e.m.f. studies for low molalities, and freezing temperature depression measurements are available to moderate molalities.<sup>8</sup> Unfortunately, there are very few reliable direct vapor pressure measurements available for aqueous CaCl<sub>2</sub>, even at 298.15 K. Consequently, the solute activities of aqueous CaCl<sub>2</sub> have been largely determined by isopiestic intercomparison to aqueous NaCl, KCl, and H<sub>2</sub>SO<sub>4</sub>. Because of this, CaCl<sub>2</sub> should be viewed as a secondary rather than a primary standard.

For water activity measurements at moderate and low molalities, CaCl<sub>2</sub> has been much more widely used than H<sub>2</sub>SO<sub>4</sub>. One reason for this preference for CaCl<sub>2</sub> has already been given: it is less corrosive than H<sub>2</sub>SO<sub>4</sub>. The second reason for this is historical in nature. In the precomputer age most analyses of experimental activity data for electrolyte solutions were performed with graphical techniques. The isopiestic molality ratio for most higher-valence electrolytes relative to a CaCl<sub>2</sub> reference standard varies much less rapidly with the molalities than does the analogous ratio for a H<sub>2</sub>SO<sub>4</sub> reference standard. A slower varying isopiestic molality ratio allowed graphical smoothing of data to be made more easily and accurately.

**TABLE 2**  
**Various Critically Assessed Osmotic Coefficients**  
**for Aqueous NaCl at 298.15 K**

$m$ (mol · kg <sup>-1</sup> )	$\Phi^a$	$\Phi^b$	$\Phi^c$	$\Phi^d$
0.05		0.9440		0.9436
0.1	0.9324	0.9328	0.9338	0.9325
0.2	0.9245	0.9237	0.9249	0.9239
0.3	0.9215	0.9207	0.9220	0.9212
0.4	0.9203	0.9203	0.9215	0.9211
0.5	0.9209	0.9212	0.9224	0.9222
0.6	0.9230	0.9231	0.9241	0.9243
0.7	0.9257	0.9256	0.9266	0.9269
0.8	0.9288	0.9285	0.9294	0.9300
0.9	0.9320	0.9319	0.9327	0.9335
1.0	0.9355	0.9356	0.9363	0.9373
1.2	0.9428	0.9437	0.9443	0.9457
1.4	0.9513	0.9527	0.9531	0.9549
1.5		0.9575	0.9578	0.9598
1.6	0.9616	0.9624	0.9627	0.9649
1.8	0.9723	0.9728	0.9730	0.9754
2.0	0.9833	0.9837	0.9838	0.9866
2.5		1.0131	1.0129	1.0164
3.0	1.0453	1.0452	1.0447	1.0485
3.5		1.0795	1.0785	1.0824
4.0	1.1158	1.1156	1.1141	1.1177
4.5		1.1530	1.1511	1.1542
5.0	1.1916	1.1915	1.1893	1.1916
5.5		1.2306	1.2286	1.2298
6.0	1.2706	1.2700	1.2687	1.2688

<sup>a</sup> Values from Robinson and Stokes.<sup>3</sup>

<sup>b</sup> Values from equation given by Hamer and Wu.<sup>9</sup>

<sup>c</sup> Values from Gibbard et al.<sup>10</sup>

<sup>d</sup> Values from Clarke and Glew.<sup>11</sup>

#### A. ISOPIESTIC STANDARDS FOR AQUEOUS SOLUTIONS AT 298.15 K

The first comprehensive evaluations of all four isopiestic reference standards were tabulated by Robinson and Stokes,<sup>3</sup> based on a critical analysis of direct vapor pressure, freezing temperature depression (in some cases), e.m.f., and isopiestic data. These values of  $\Phi$  were reported at 298.15 K only, although some values were also given for NaCl in the temperature range 333 to 373 K from analysis of boiling temperature elevation data. Several additional critical evaluations have since been reported for these reference standards, but except for NaCl they are generally restricted to 298.15 K. We now describe and compare the major evaluations.

Values of  $\Phi$  of aqueous NaCl have been reported by Robinson and Stokes,<sup>3</sup> Hamer and Wu,<sup>9</sup> Gibbard et al.,<sup>10</sup> and Clarke and Glew.<sup>11</sup> These results at 298.15 K are summarized in Table 2. Hamer and Wu<sup>9</sup> gave an isothermal equation for  $\Phi$  at 298.15 K only. Gibbard et al.<sup>10</sup> gave an equation they considered to be reliable to 473 K, and Clarke and Glew's equation is valid to about 427 K. Robinson and Stokes's values were given as a numerical tabulation only. Corrections for the nonideal behavior of water vapor were neglected in the first two evaluations,<sup>3,9</sup> but this correction would only change their results by about 0.1% at 298.15 K.

Values of  $\Phi$  from the first three of these evaluations<sup>3,9,10</sup> for NaCl agree to within 0.0019 up to 4.5 mol · kg<sup>-1</sup>, and to within 0.0023 at higher molalities. The results of Clarke and



**TABLE 3**  
**Various Critically Assessed**  
**Osmotic Coefficients for Aqueous**  
**KCl at 298.15 K**

<b>m</b> (mol · kg <sup>-1</sup> )	<b>Φ<sup>a</sup></b>	<b>Φ<sup>b</sup></b>
0.05		0.9404
0.1	0.9266	0.9266
0.2	0.9130	0.9132
0.3	0.9063	0.9065
0.4	0.9017	0.9025
0.5	0.8989	0.9001
0.6	0.8976	0.8986
0.7	0.8970	0.8979
0.8	0.8970	0.8976
0.9	0.8971	0.8977
1.0	0.8974	0.8981
1.2	0.8986	0.8997
1.4	0.9010	0.9020
1.5		0.9034
1.6	0.9042	0.9049
1.8	0.9081	0.9083
2.0	0.9124	0.9121
2.5		0.9231
3.0	0.9367	0.9359
3.5		0.9499
4.0	0.9647	0.9649

<sup>a</sup> Values taken from Robinson and Stokes.<sup>3</sup>

<sup>b</sup> Values from equation given by Hamer and Wu.<sup>9</sup>

Glew<sup>11</sup> agree with the other three sets of  $\Phi$  values to within 0.0016 up to 0.9 mol · kg<sup>-1</sup>, their values are approximately 0.003 higher than those from the other reviews from 1.0 to 4.0 mol · kg<sup>-1</sup>, but the agreement improves at higher molalities. These systematic differences in the latter study<sup>11</sup> were due to inclusion of  $\Phi$  data at other temperatures along with related calorimetric values.

These differences in  $\Phi$  of NaCl are small enough, <0.1 to 0.3%, that any set could be used as an isopiestic reference standard without introducing any serious inconsistencies. The results of Clarke and Glew<sup>11</sup> are probably slightly more accurate because of their larger data base along with their careful attention to consistency between data sets. However, they did include some of the isopiestic data available then at 298.15 K for NaCl with H<sub>2</sub>SO<sub>4</sub> as reference standard. Inasmuch as  $\Phi$  of H<sub>2</sub>SO<sub>4</sub> is largely determined by isopiestic comparison to NaCl and KCl, and thus is not independent of NaCl, the inclusion of such data can be questioned. However, those values were given a relatively low weight in the least-squares fits and only had a slight effect on the derived results. The equation of Clarke and Glew<sup>11</sup> is also quite complex (35 parameters). Fortunately, they tabulated values of  $\Phi$  at numerous molalities and temperatures, so it should be possible to do reliable interpolations from these tabulated values.

Values of  $\Phi$  for aqueous KCl at 298.15 K have been critically assessed by Robinson and Stokes<sup>3</sup> and Hamer and Wu,<sup>9</sup> and their results are summarized in Table 3. These two sets of  $\Phi$  values are in excellent agreement, with a maximum difference of 0.0012. Neither of these two sets was corrected for the nonideal behavior of water vapor, which introduces an uncertainty of the order of 0.1%.

**TABLE 4**  
**Various Critically Assessed Osmotic Coefficients for Aqueous H<sub>2</sub>SO<sub>4</sub> at 298.15 K**

$m$ (mol · kg <sup>-1</sup> )	$\Phi^a$	$\Phi^b$	$\Phi^c$	$m$ (mol · kg <sup>-1</sup> )	$\Phi^a$	$\Phi^b$	$\Phi^c$
0.1	0.680	(0.675)	0.6605	9.5	1.841	1.8433	1.8390
0.2	0.668	0.6650	0.6481	10.0	1.884	1.8872	1.8817
0.3	0.668	0.6635	0.6547	10.5		1.9281	1.9218
0.4		0.6656	0.6651	11.0	1.964	1.9662	1.9593
0.5	0.676	0.6713	0.6760	11.5		2.0016	1.9945
0.6		0.6788	0.6864	12.0	2.030	2.0345	2.0272
0.7	0.689	0.6872	0.6965	12.5		2.0650	2.0576
0.8		0.6965	0.7062	13.0	2.088	2.0933	2.0857
0.9		0.7065	0.7158	13.5		2.1196	2.1115
1.0	0.721	0.7179	0.7255	14.0	2.140	2.1440	2.1351
1.2		0.7417		14.5		2.1667	2.1565
1.4		0.7659		15.0	2.187	2.1878	2.1758
1.5	0.780	0.7784	0.7776	15.5		2.2076	2.1930
1.6		0.7909		16.0	2.228	2.2260	2.2082
1.8		0.8169		16.5		2.2433	2.2216
2.0	0.846	0.8439	0.8400	17.0	2.262	2.2595	2.2334
2.5	0.916	0.9149	0.9118	17.5		2.2748	2.2435
3.0	0.991	0.9906	0.9897	18.0	2.292	2.2893	2.2523
3.5	1.071	1.0678	1.0707	18.5		2.3029	2.2599
4.0	1.150	1.1479	1.1520	19.0	2.318	2.3159	2.2665
4.5	1.226	1.2295	1.2319	19.5		2.3282	2.2723
5.0	1.303	1.3035	1.3090	20.0	2.341	2.3400	2.2775
5.5	1.376	1.3738	1.3827	21.0	2.361	2.3618	2.2866
6.0	1.445	1.4440	1.4525	22.0	2.381	2.3814	2.2951
6.5	1.512	1.5111	1.5185	23.0	2.401	2.3987	2.3030
7.0	1.576	1.5749	1.5805	24.0	2.407	2.4134	2.3096
7.5	1.636	1.6353	1.6389	25.0		2.4249	2.3121
8.0	1.691	1.6923	1.6936	26.0	2.426	2.4326	2.3057
8.5	1.744	1.7460	1.7451	27.0		2.4353	2.2827
9.0	1.793	1.7962	1.7935				

<sup>a</sup> Values of Robinson and Stokes.<sup>3</sup>

<sup>b</sup> Values of Rard et al.<sup>12</sup> corrected as recommended by Rard.<sup>14</sup> The values at 4.5 and 5.0 mol · kg<sup>-1</sup> were adjusted so as to make the lower molality and higher molality  $\Phi$  merge smoothly. The value at 0.1 mol · kg<sup>-1</sup> is fairly uncertain, by about 0.004.

<sup>c</sup> Values of Staples.<sup>13</sup>

Critically assessed values of  $\Phi$  for aqueous H<sub>2</sub>SO<sub>4</sub> were reported at 298.15 K by Robinson and Stokes,<sup>3</sup> Rard et al.,<sup>12</sup> and Staples.<sup>13</sup> The  $\Phi$  values of Robinson and Stokes<sup>3</sup> were not corrected for the nonideal behavior of water vapor, and were given as a table of numerical values. Results from the other two evaluations<sup>12,13</sup> were corrected for nonideal vapor behavior and were represented as a function of molality by least-squares equations valid to 28 mol · kg<sup>-1</sup> or higher. Rard<sup>14</sup> subsequently remeasured the NaCl-H<sub>2</sub>SO<sub>4</sub> isopiestic ratio, and tabulated numerical correction factors to be applied to the earlier recommended values of Rard et al.<sup>12</sup> Table 4 is a listing of  $\Phi$  from these various evaluations. Larger thermodynamic data bases were available for the later evaluations<sup>12,14</sup> than were available to Robinson and Stokes.<sup>3</sup>

Values of  $\Phi$  given by Rard et al.<sup>12,14</sup> are in excellent agreement with those of Robinson and Stokes,<sup>3</sup> with a maximum difference of 0.006 from 0.1 to 27 mol · kg<sup>-1</sup>, but with agreement to 0.001 to 0.003 over most of this molality range. In contrast, the  $\Phi$  values of Staples<sup>13</sup> are up to 0.02 lower than the other two evaluations at low molalities (3%); they are in reasonable agreement at intermediate molalities (0.01); but they are considerably lower

by up to 0.152 (6%) by  $27 \text{ mol} \cdot \text{kg}^{-1}$ . These large differences were attributed by Staples to inclusion of freezing temperature depression and e.m.f. results in his evaluations.

There are three objections to the recommended  $\Phi$  values of Staples<sup>13</sup> for  $\text{H}_2\text{SO}_4$ . First, freezing temperature depression values for  $\text{H}_2\text{SO}_4$  from each source are highly scattered and discrepant from other published sets. Of the ten sets of freezing temperature depressions analyzed by Staples, three of them were rejected entirely, and for three of the other sets most of the individual  $\Phi$  values were given zero weight. For the remaining four sets, from 18 to 38% of the points were rejected. This high rejection rate, together with the fact that the  $\Phi$  values that were retained were scattered by several percent, indicates that these values were of low quality. Including them in least-squares fits, even at reduced weights, gives distortion to the final results. Calculation of  $\Phi$  from freezing temperature depression values involves the assumption that the solid phase was always pure ice. It is quite possible that the solid phases in most or all of the freezing temperature depression studies were actually dilute  $\text{H}_2\text{SO}_4$  solutions of variable composition, and this could have given rise to the discrepant results. Second, the recommended values of Staples for  $\Phi$  of  $\text{H}_2\text{SO}_4$  above  $16 \text{ mol} \cdot \text{kg}^{-1}$  are based entirely on direct vapor pressure measurements and isopiestic data relative to  $\text{NaOH}$ , and the same is true for the other evaluations.<sup>3,12</sup> However, the recommended smoothed values for  $\text{H}_2\text{SO}_4$  reported by Staples<sup>13</sup> are systematically lower than all of the input data used by him in that molality region. For example, the experimental  $\Phi$  are about 2.23 at  $16 \text{ mol} \cdot \text{kg}^{-1}$ , about 2.34 at  $20 \text{ mol} \cdot \text{kg}^{-1}$ , and about 2.43 at  $27 \text{ mol} \cdot \text{kg}^{-1}$ . In contrast, the recommended values of Staples at these molalities are 2.2082, 2.2775, and 2.2827, respectively. Since the recommended  $\Phi$  values of Staples do not even come close to any of the input data above  $16 \text{ mol} \cdot \text{kg}^{-1}$ , his least-squares equation must be unreliable. Third, between about 4 and  $15 \text{ mol} \cdot \text{kg}^{-1}$  for  $\text{H}_2\text{SO}_4$ , most of the data used by Staples were isopiestic relative to  $\text{CaCl}_2$ , but these same data were also used by him in the reverse direction to determine  $\Phi$  of  $\text{CaCl}_2$ . Since there are virtually no other data than this to fix  $\text{CaCl}_2$  above  $3 \text{ mol} \cdot \text{kg}^{-1}$ , this was equivalent to using  $\text{H}_2\text{SO}_4$  as a standard to determine its own  $\Phi$  values.

Because of these serious objections to the Staples evaluation of  $\Phi$  of  $\text{H}_2\text{SO}_4$ ,<sup>13</sup> we cannot recommend his values for use as an isopiestic reference standard. The best  $\Phi$  values at this time for  $\text{H}_2\text{SO}_4$  at 298.15 K are those of Rard et al.<sup>12</sup> as corrected by Rard.<sup>14</sup> However, the difference between these values and those recommended by Robinson and Stokes<sup>3</sup> are small enough that no serious inconsistency will result if they are used instead. Rard and Miller<sup>15</sup> stated that  $\Phi$  for  $\text{H}_2\text{SO}_4$  were too low by 0.2 to 0.4% between 4 and  $6 \text{ mol} \cdot \text{kg}^{-1}$  based on the critical evaluation of Rard et al.,<sup>12</sup> and the later revision<sup>14</sup> included recommending higher  $\Phi$  values in this molality region. Some additional accurate direct vapor pressure measurements between 4 and  $6 \text{ mol} \cdot \text{kg}^{-1}$  would still be desirable. The uncertainty for  $\Phi$  of  $\text{H}_2\text{SO}_4$  is generally about 0.2 to 0.3% for 0.1 to  $28 \text{ mol} \cdot \text{kg}^{-1}$ .

Values of  $\Phi$  for aqueous  $\text{CaCl}_2$  at 298.15 K have been critically assessed by Robinson and Stokes,<sup>3</sup> Rard et al.,<sup>8</sup> and Staples and Nuttall,<sup>16</sup> and these values are compared in Table 5. The first two of these studies are generally in reasonably good agreement, 0.005, except around 3 to  $3.5 \text{ mol} \cdot \text{kg}^{-1}$  and above about  $8 \text{ mol} \cdot \text{kg}^{-1}$  where differences are somewhat larger. Most of the input data for  $\Phi$  of  $\text{CaCl}_2$  above  $0.3 \text{ mol} \cdot \text{kg}^{-1}$  are isopiestic data relative to  $\text{NaCl}$ ,  $\text{KCl}$ , and  $\text{H}_2\text{SO}_4$  reference standards. The larger differences for  $\text{CaCl}_2$  around 3 to  $3.5 \text{ mol} \cdot \text{kg}^{-1}$  are due to the changeover of isopiestic standards from  $\text{NaCl}$  to  $\text{H}_2\text{SO}_4$ . Osmotic coefficients of Staples and Nuttall<sup>16</sup> are generally in agreement with the other two evaluations, but the deviation function shown in their Figure 4 indicates that their least-squares equation cycles slightly above the experimental data around 4.0 to  $4.5 \text{ mol} \cdot \text{kg}^{-1}$ , and below the data around  $6 \text{ mol} \cdot \text{kg}^{-1}$ , and their  $\Phi$  differ from their input values by about 0.005 in these narrow molality regions.

Subsequent to these evaluations, Rard and Miller<sup>15</sup> measured additional isopiestic data

**TABLE 5**  
**Various Critically Assessed Osmotic**  
**Coefficients for Aqueous CaCl<sub>2</sub> at**  
**298.15 K**

m (mol · kg <sup>-1</sup> )	Φ <sup>a</sup>	Φ <sup>b</sup>	Φ <sup>c</sup>
0.05		0.8617	0.8619
0.1	0.854	0.8525	0.8516
0.2	0.862	0.8594	0.8568
0.3	0.876	0.8752	0.8721
0.4	0.894	0.8943	0.8915
0.5	0.917	0.9154	0.9134
0.6	0.940	0.9381	0.9370
0.7	0.963	0.9622	0.9621
0.8	0.988	0.9878	0.9884
0.9	1.017	1.0146	1.0159
1.0	1.046	1.0426	1.0444
1.2	1.107	1.1021	
1.4	1.171	1.1656	
1.5		1.1987	1.2004
1.6	1.237	1.2327	
1.8	1.305	1.3028	
2.0	1.376	1.3756	1.3754
2.5	1.568	1.5670	1.5660
3.0	1.779	1.7678	1.7685
3.5	1.981	1.9738	1.9781
4.0	2.182	2.1807	2.1885
4.5	2.383	2.3830	2.3926
5.0	2.574	2.5739	2.5826
5.5	2.743	2.7457	2.7515
6.0	2.891	2.8907	2.8932
6.5	3.003	3.0032	3.0041
7.0	3.081	3.0815	3.0833
7.5	3.127	3.1299	3.1332
8.0	3.151	3.1576	3.1592
8.5	3.165	3.1739	3.169
9.0	3.171	3.1746	3.171

<sup>a</sup> Values of Robinson and Stokes.<sup>3</sup>

<sup>b</sup> Values of Rard et al.<sup>8</sup>

<sup>c</sup> Values of Staples and Nuttall.<sup>16</sup>

for aqueous CaCl<sub>2</sub> relative to H<sub>2</sub>SO<sub>4</sub> and NaCl. Including these new results in the critical evaluations<sup>8,16</sup> would raise Φ of CaCl<sub>2</sub> by about 0.1%, not including changes in standards NaCl, KCl, and H<sub>2</sub>SO<sub>4</sub> which would also affect CaCl<sub>2</sub>. Present values of Φ for CaCl<sub>2</sub> should be reliable to about 0.3% over most of the molality range, except around 3 to 4 mol · kg<sup>-1</sup> where the uncertainty is larger.

We note that experimental values of Φ extend to very high molalities for CaCl<sub>2</sub> and H<sub>2</sub>SO<sub>4</sub>, and that both of these electrolytes exhibit a flat maximum followed initially by a slow decrease and then by a more rapid decrease in Φ at higher molalities. Although the published least-squares equations<sup>8,12,16</sup> do follow this behavior, they generally turn down too sharply at higher molalities. Thus they should not be used for extrapolations to higher molalities.

## B. ISOPIESTIC STANDARDS FOR AQUEOUS SOLUTIONS AT OTHER TEMPERATURES

Of the four electrolytes used as isopiestic reference standards for aqueous solutions at

**TABLE 6**  
**Osmotic Coefficients for Aqueous NaCl at Various Temperatures<sup>a</sup>**

$m$ (mol · kg <sup>-1</sup> )	$\Phi$ 273.15 K	$\Phi$ 293.15 K	$\Phi$ 313.15 K	$\Phi$ 333.15 K	$\Phi$ 353.15 K	$\Phi$ 373.15 K
0.05	0.9441	0.9438	0.9425	0.9404	0.9378	0.9346
0.1	0.9318	0.9326	0.9315	0.9292	0.9261	0.9222
0.2	0.9206	0.9237	0.9234	0.9213	0.9178	0.9133
0.3	0.9153	0.9207	0.9215	0.9197	0.9162	0.9112
0.4	0.9125	0.9202	0.9220	0.9207	0.9172	0.9120
0.5	0.9113	0.9210	0.9239	0.9230	0.9196	0.9142
0.6	0.9110	0.9228	0.9266	0.9262	0.9228	0.9173
0.7	0.9115	0.9251	0.9299	0.9299	0.9266	0.9209
0.8	0.9125	0.9279	0.9336	0.9340	0.9309	0.9250
0.9	0.9141	0.9311	0.9377	0.9385	0.9354	0.9294
1.0	0.9161	0.9347	0.9421	0.9432	0.9402	0.9341
1.2	0.9212	0.9426	0.9514	0.9533	0.9504	0.9440
1.4	0.9276	0.9514	0.9616	0.9639	0.9611	0.9544
1.5	0.9312	0.9561	0.9668	0.9695	0.9667	0.9598
1.6	0.9351	0.9610	0.9723	0.9751	0.9723	0.9653
1.8	0.9436	0.9713	0.9835	0.9866	0.9838	0.9764
2.0	0.9530	0.9822	0.9951	0.9985	0.9955	0.9877
2.5	0.9798	1.0116	1.0257	1.0293	1.0256	1.0166
3.0	1.0105	1.0435	1.0580	1.0611	1.0564	1.0458
3.5	1.0443	1.0774	1.0915	1.0936	1.0874	1.0748
4.0	1.0808	1.1130	1.1259	1.1264	1.1182	1.1033
4.5	1.1193	1.1499	1.1610	1.1593	1.1486	1.1312
5.0	1.1598	1.1879	1.1965	1.1921	1.1784	1.1580
5.5	1.2020	1.2270	1.2323	1.2244	1.2074	1.1838
6.0	1.2459	1.2669	1.2682	1.2562	1.2353	1.2083

<sup>a</sup> Values from Clarke and Glew.<sup>11</sup>

298.15 K, NaCl is the only one with a sufficiently wide array of reliable thermodynamic data such that it can be used as a standard from the freezing temperatures of the solutions up to about 600 K. Table 6 lists values of  $\Phi$  for NaCl from 273.15 to 373.15 K from Clarke and Glew.<sup>11</sup> They appear to be comparable in accuracy to the values of  $\Phi$  at 298.15 K.

The only reliable published isopiestic measurements much above 373 K are those from the high-temperature group at Oak Ridge National Laboratory.<sup>17</sup> Inasmuch as they have used the evaluation of Silvester and Pitzer<sup>18</sup> for NaCl as their reference standard in nearly all cases, it is probably best to continue to do so at this time in order to maintain thermodynamic consistency. However, more reliable evaluations of the thermodynamic properties of aqueous NaCl have since been reported by Pitzer and colleagues, and references to those evaluations can be found in Chapter 3 by Pitzer on the ion interaction approach.

Platford<sup>19</sup> and Childs and Platford<sup>20</sup> have performed isopiestic intercomparisons of the four main isopiestic reference standards at 273.15 and 288.15 K, using both aqueous H<sub>2</sub>SO<sub>4</sub> and urea as reference standards. Their results are given in Table 7, and they have not been corrected for changes in  $\Phi$  values for H<sub>2</sub>SO<sub>4</sub> at 298.15 K. Holmes and Mesmer<sup>17</sup> gave an equation for the osmotic coefficients of aqueous KCl that is valid to 523 K. These values can be used as provisional standards and are probably reliable to about 0.5%.

Unfortunately, there are no comprehensive critical reviews of the thermodynamic properties of aqueous H<sub>2</sub>SO<sub>4</sub> or CaCl<sub>2</sub> over wide temperature and composition ranges that yield  $\Phi$  values comparable in accuracy to those for NaCl. Thus no primary standards are now available that can be recommended without reservations for both low water activities and high temperatures. However, Giaouque et al.<sup>21</sup> have published comprehensive tables of the

**TABLE 7**  
**Osmotic Coefficients for Aqueous KCl, CaCl<sub>2</sub>, and H<sub>2</sub>SO<sub>4</sub> at 273.15 and 288.15 K<sup>a</sup>**

m (mol · kg <sup>-1</sup> )	KCl		CaCl <sub>2</sub>		H <sub>2</sub> SO <sub>4</sub>	
	Φ 273.15 K	Φ 288.15 K	Φ 273.15 K	Φ 288.15 K	Φ 273.15 K	Φ 288.15 K
0.1	0.926	0.927	0.862	0.861	0.680	0.680
0.2	0.911	0.914	0.866	0.865	0.669	0.668
0.3	0.912	0.906	0.874	0.876	0.670	0.669
0.4	0.897	0.901	0.882	0.892	0.674	0.673
0.5	0.892	0.897	0.895	0.913	0.679	0.677
0.6	0.888	0.894	0.922	0.936	0.685	0.684
0.7	0.885	0.892	0.951	0.962	0.693	0.691
0.8	0.883	0.891	0.980	0.990	0.704	0.702
0.9	0.881	0.891	1.011	1.019	0.716	0.713
1.0	0.879	0.891	1.042	1.048	0.728	0.724
1.5	0.876	0.895	1.208	1.206	0.791	0.786
2.0	0.883	0.903	1.393	1.382	0.864	0.855
2.5	0.892	0.913	1.600	1.577	0.946	0.929
3.0	0.901	0.926	1.828	1.782	1.036	1.009
3.5	0.912	0.939	2.063	1.996	1.130	1.094
4.0	0.926	0.952	2.300	2.219	1.226	1.180
4.5			2.542	2.453	1.322	1.262
5.0			2.777	2.656	1.416	1.344
5.5			2.995	2.836	1.502	1.422
6.0			3.197	2.993	1.584	1.496
6.5			3.341	3.124	1.661	1.567
7.0			3.455	3.210	1.733	1.634
7.5					1.801	1.697
8.0					1.862	1.754
8.5					1.920	1.809
9.0					1.972	1.860
9.5					2.018	
10.0					2.066	

<sup>a</sup> Values of Platford<sup>19</sup> and Childs and Platford.<sup>20</sup> These are provisional values and have not been adjusted for changes in the standards at 298.15 K.

relative partial molar enthalpy of water, the partial molar heat capacity of water, and the temperature derivative of this heat capacity for aqueous H<sub>2</sub>SO<sub>4</sub> solutions at 298.15 K over the entire composition range. These can be combined with our recommended Φ at 298.15 K, Table 4, to yield accurate values of Φ from about 273 to 323 K and, with a slight loss of accuracy, to 373 K.

We note that at very high molalities of aqueous H<sub>2</sub>SO<sub>4</sub>, SO<sub>3</sub> becomes volatile and that this volatility increases with increasing temperature. Thus SO<sub>3</sub> can be transported into the other solutions during an isopiestic experiment which makes the measurements unreliable. However, H<sub>2</sub>SO<sub>4</sub> can be used as an isopiestic reference standard without problems up to about 30 mol · kg<sup>-1</sup> at 298.15 K, and to about 20 mol · kg<sup>-1</sup> at 373.15 K. This useful molality range decreases rapidly as the temperature is increased further.

Values of Φ of aqueous CaCl<sub>2</sub> have been tabulated by Garvin et al. as a function of temperature in the CODATA prototype tables.<sup>22</sup> They accepted the Staples and Nuttall<sup>16</sup> values of Φ at 298.15 K, and used thermal data to compute Φ at other temperatures. Their assigned uncertainties in Φ are quite large above 298.15 K, e.g., 0.05 for 1.0 mol · kg<sup>-1</sup> and 0.12 at 5 mol · kg<sup>-1</sup>. Thus the calorimetric data for aqueous CaCl<sub>2</sub> were obviously inadequate at that time (1987) to allow CaCl<sub>2</sub> to be recommended by us for use as an

isopiestic standard above room temperature. However, this situation will improve as more enthalpy of dilution and heat capacity measurements become available for that system.

As we have just noted, the osmotic coefficients of the four main isopiestic standards are fairly well characterized at 298.15 K, but only NaCl is also well characterized at significantly higher temperatures. It is clear that "global" treatments of thermodynamic values for aqueous solutions, such as are available for aqueous NaCl,<sup>11,18</sup> are also needed for KCl, H<sub>2</sub>SO<sub>4</sub>, and CaCl<sub>2</sub> in order that their  $\Phi$  values can be used with confidence as reference standards for isopiestic experiments at higher and lower temperatures. This will be more difficult to accomplish for aqueous H<sub>2</sub>SO<sub>4</sub> because the sulfate-bisulfate equilibrium also needs to be included, as does the increased volatility of SO<sub>3</sub> at high molalities and temperatures.

It was in recognition of the enormous amount of labor required to produce an accurate global representation of thermodynamic data that motivated one of the present authors (J. A. R., while attending the first I.U.P.A.C.-sponsored solubility symposium) to write the following limerick:

Two fellows, Clarke and Glew,  
thought they knew what to do.  
So they spent eight years,  
with sodium chloride up to their ears,  
and they used Pitzer's equations, too!

Actually, a different word than "ears" was used in the original, but the same rhyming scheme was present.

### C. SELF-CONSISTENCY AMONG ISOPIESTIC REFERENCE STANDARDS BY USE OF THE ISOPIESTIC MOLALITY RATIOS

We noted in the previous section that isopiestic measurements are available for the intercomparison of the four major isopiestic reference standards at 273.15, 288.15, and 298.15 K. In principle, all four isopiestic reference standards could be independently evaluated using directly measured (nonisopiestic) thermodynamic data only, and then adjusted to complete self-consistency by use of the experimental isopiestic ratios. Although some of the reference standards would be improved by this procedure, certain other ones would suffer a reduction in quality if this were done.

We consider the following to be reasonable criteria for deciding whether to use the isopiestic molality ratios to refine a particular pair of isopiestic reference standards. First, the isopiestic molality ratios should be accurately known and of good precision. Preferably, at least two independent determinations should be available. Second, the osmotic coefficients of each of these reference standards should be known to comparable accuracy if they are to be used in adjusting each other. Third, there should be a significant amount of "absolute" thermodynamic data for each reference standard under consideration (i.e., e.m.f., direct vapor pressure, freezing temperature depression), and isopiestic data should not have been included in the preliminary evaluations unless these isopiestic data are relative to a different standard that is largely or entirely independent of the two standards undergoing adjustment.

Based on these considerations, the  $\Phi$  of NaCl and KCl solutions can be made self-consistent, and this was done in some previous evaluations.<sup>9,11</sup> However, it would be ill advised to use  $\Phi$  of H<sub>2</sub>SO<sub>4</sub> or CaCl<sub>2</sub> to adjust  $\Phi$  of NaCl or KCl, because  $\Phi$  of H<sub>2</sub>SO<sub>4</sub> and CaCl<sub>2</sub> have been largely determined by isopiestic comparison to NaCl and KCl rather than by direct measurements. In addition,  $\Phi$  of H<sub>2</sub>SO<sub>4</sub> and CaCl<sub>2</sub> could be made more or less self-consistent at 298.15 K for  $1 < a_{\pm} < 0.75$  since their isopiestic molality ratio is fairly well characterized, and  $\Phi$  of both H<sub>2</sub>SO<sub>4</sub> and CaCl<sub>2</sub> have been determined to similar accuracy

by isopiestic comparison to NaCl and KCl. This definitely should not be done for aqueous  $\text{H}_2\text{SO}_4$  and  $\text{CaCl}_2$  at higher molalities. There are several sets of high quality direct vapor pressure measurements for aqueous  $\text{H}_2\text{SO}_4$ , but few such data for  $\text{CaCl}_2$ . Thus  $\Phi$  of  $\text{CaCl}_2$  at high molalities are largely determined by isopiestic comparison to  $\text{H}_2\text{SO}_4$ , and to reverse the procedure would seriously degrade the quality of the results for  $\text{H}_2\text{SO}_4$ .

#### D. TERTIARY (“WORKING”) STANDARDS FOR AQUEOUS SOLUTIONS

In Section III.A we described the four main isopiestic reference standards for aqueous electrolyte solutions. Three of these, aqueous NaCl, KCl, and  $\text{H}_2\text{SO}_4$ , had been characterized by direct measurements of their thermodynamic activities and were deemed to be primary reference standards. The other electrolyte,  $\text{CaCl}_2$ , had its activities determined mainly by isopiestic comparison to the primary reference standards, and was termed a secondary reference standard. In principle, these four electrolytes are suited to be reference standards for virtually all isopiestic measurements involving aqueous electrolyte solutions. In practice, this is close to being true, with the majority of isopiestic measurements having been made relative to those four reference standards.

In a few studies, other electrolytes or even nonelectrolytes have been used as “working” standards. We have already noted that Platford<sup>19</sup> and Childs and Platford<sup>20</sup> used aqueous urea solutions (along with aqueous  $\text{H}_2\text{SO}_4$ ) as reference standards for their determination of the osmotic coefficients of aqueous NaCl, KCl, and  $\text{CaCl}_2$  at 273.15 and 288.15 K. Other electrolytes have also been used as “working” standards, presumably to avoid use of  $\text{H}_2\text{SO}_4$  solutions which are too corrosive for some isopiestic sample containers. For example, LiBr solutions were used as a “working” standard by Covington et al.<sup>23</sup> at 298.15 K; Braunstein and Braunstein<sup>24</sup> used LiCl solutions at 373.4 to 422.6 K; Bonner<sup>25</sup> used LiCl solutions presumably at 298.15 K; and Libuś et al.<sup>26</sup> used aqueous  $\text{Mg}(\text{ClO}_4)_2$  at 298.15 K.

Although there are thermodynamic data for LiCl and LiBr in addition to isopiestic measurements relative to the main reference standards,<sup>9</sup> their values of  $\Phi$  lack the precision and accuracy available for the primary and secondary standards NaCl, KCl,  $\text{H}_2\text{SO}_4$ , and  $\text{CaCl}_2$ . Thus we consider LiCl, LiBr, and  $\text{Mg}(\text{ClO}_4)_2$  to be tertiary or “working” reference standards. As additional thermodynamic data become available for their solutions, it will be possible to refine their  $\Phi$  values and thus derive more reliable  $\Phi$  values for other solutions that were equilibrated with them under isopiestic conditions. It is best to keep the number of these “working” standards to a minimum, to reduce the effort required to characterize them by a variety of direct thermodynamic measurements.

Aqueous LiCl and LiBr were obvious choices as “working” reference standards because of their considerable solubilities, which means they can be used to fairly low water activities. For another reason, however, the use of them is unfortunate. Natural lithium is a mixture of  $^6\text{Li}$  and  $^7\text{Li}$  with an atomic mass of  $6.941 \pm 0.002 \text{ g} \cdot \text{g-atom}^{-1}$ .<sup>27</sup> However,  $^6\text{Li}$  is used as a source material for tritium production and as a neutron absorber for fusion reactions. Thus salts of lithium that are highly depleted in  $^6\text{Li}$  are sometimes sold commercially and are generally not identified as having an anomalous molar mass. Depleted lithium has an atomic mass closer to  $7.0 \text{ g} \cdot \text{g-atom}^{-1}$ .<sup>27</sup>

Consider, for example, a solution of LiCl that is analyzed for Cl<sup>-</sup> content, and the water content calculated by difference assuming a certain molar mass for LiCl. The numbers of moles of LiCl will be known correctly, but the amount of water will be uncertain. Around  $6 \text{ mol} \cdot \text{kg}^{-1}$  the calculated molality will be uncertain by 0.035%, around  $12 \text{ mol} \cdot \text{kg}^{-1}$  the uncertainty will be 0.071%, and at  $18 \text{ mol} \cdot \text{kg}^{-1}$  the uncertainty will be 0.106%. Inasmuch as isopiestic equilibrium molalities are generally determined to about  $\pm 0.05$  to  $\pm 0.1\%$ , it is clear that equilibrium molalities for lithium salt solutions will be inherently about twice as uncertain as the molalities for other reference standards.

There is a method that can be used to obtain the correct molality of lithium salt solutions.



The number of moles of LiCl or LiBr can be obtained by analysis for chloride or bromide, and the mass of water determined directly by thermal dehydration of weighed samples. The calculated molality will then be correct. This would also work for other lithium salts such as  $\text{Li}_2\text{SO}_4$ , since the number of moles of salt can be obtained by analysis for sulfate.

Robinson<sup>28</sup> reported the results of isopiestic equilibrations for NaCl, KCl, and their mixtures in 99.8 mol%  $\text{D}_2\text{O}$  at 298.15 K. Concentrations were reported as aquamolalities, or moles of salt per 55.508 mol of solvent. By assuming that  $\Phi$  of KCl was the same in  $\text{H}_2\text{O}$  and  $\text{D}_2\text{O}$  for the same aquamolality, he derived values of  $\Phi$  for NaCl and for the mixtures of NaCl and KCl. When this was done, the resulting  $\Phi$  of NaCl in  $\text{D}_2\text{O}$  were larger than those in  $\text{H}_2\text{O}$  by 0.0030 times the NaCl molality (aquamolality). Because  $\Phi$  of NaCl changes when  $\text{H}_2\text{O}$  is replaced by  $\text{D}_2\text{O}$ , it is likely that the same will be true for KCl and other electrolytes, also. Thus, an experimentally significant solvent isotope effect is present, and  $\Phi$  of electrolyte solutions in  $\text{D}_2\text{O}$  are not the same as in  $\text{H}_2\text{O}$ . Consequently,  $\Phi$  values for reference standards in  $\text{H}_2\text{O}$  cannot be used as reference standards in  $\text{D}_2\text{O}$  except as a rough approximation. Robinson also found that deviations of  $\Phi$  for NaCl and KCl mixtures from the Scatchard neutral-electrolyte binary-solution mixing approximation were essentially the same in  $\text{H}_2\text{O}$  or in  $\text{D}_2\text{O}$ . This could mean that  $\Phi$  for NaCl and KCl in  $\text{D}_2\text{O}$  are shifted roughly equal amounts from their corresponding  $\text{H}_2\text{O}$  solution values.

#### E. STANDARDS FOR NONAQUEOUS SOLUTIONS

Very few isopiestic measurements have been made for electrolytes in nonaqueous solvents. However, Platford<sup>29</sup> studied solutions of  $\text{AgClO}_4$  in benzene at 293 K, by using benzil as an isopiestic reference standard. As expected,  $\text{AgClO}_4$  behaved as a polymerized nonelectrolyte (mainly as dimers and trimers) in that solvent. Osmotic coefficients for the standard were not tabulated.

Bonner<sup>30</sup> has reported isopiestic data for LiCl,  $\text{NaNO}_3$ , tetramethylguanidinium perchlorate, and urea in methanol at 298.15 K, by using NaI solutions as the primary reference standard and 1,3-dimethylurea as a secondary standard. Values of  $\Phi$  for the primary standard NaI were tabulated by Bonner, based on his reanalysis of two sets of published direct vapor pressure measurements. Bonner estimated that his tabulated  $\Phi$  values for NaI were uncertain by about 1%.

Critically assessed values of  $\Phi$  for a reference standard are unavailable for the majority of nonaqueous solvents. Even for those that are available the  $\Phi$  values are uncertain by 1% or even more. This is about five to ten times larger than the uncertainty in the primary aqueous standards at 298.15 K. However, the lack of accurate reference standards for nonaqueous solutions should not hinder the application of the isopiestic method to such systems, because the isopiestic method is a relative method. Values of  $\Phi$  can easily be recalculated as more accurate results become available for the reference standards (provided, of course, that the experimental equilibrium molalities have been tabulated). In fact, the existence of a large body of isopiestic data for a particular nonaqueous solvent is very likely to stimulate interest in more accurate experimental characterization of the reference standards by direct thermodynamic measurements.

Although outside the scope of this review, we note that Wang et al.<sup>31</sup> have extended the isopiestic method to include solutions of various metals (Bi, Ga, In, and Sn) in mercury at 600 K, by using cadmium amalgam as a reference standard.

#### F. COMMENTS ON THE PUBLICATION OF ISOPIESTIC DATA

As discussed in the above sections, isopiestic reference standards for nonaqueous solutions are fairly uncertain, at least 1% for  $\Phi$ ; this is also true for aqueous standards at fairly high temperatures, especially for water activities lower than those achievable with NaCl as reference standard. Even the better-characterized aqueous solution primary reference stan-

dards at 298.15 K could undergo revisions in the future of 0.1 to 0.3% depending on the standard and the molality range under consideration.

Under favorable conditions, an individual isopiestic molality at equilibrium can be determined to  $\pm 0.05$  to  $\pm 0.1\%$ , and molality ratio of the reference standard to the test solution determined to  $\pm 0.1$  to  $\pm 0.2\%$ . Because values of  $\Phi^*$  for the reference standards generally have a comparable or larger uncertainty than this, it is clear that most if not all  $\Phi$  obtained from isopiestic data will ultimately require some revision to reflect an improvement in  $\Phi^*$  of the reference standards. This revision will be possible only if the actual experimental isopiestic equilibrium molalities have been published rather than smoothed results.

As will be discussed later in this chapter, values of  $\Phi$  from isopiestic experiments sometimes have larger differences from other published thermodynamic data than are to be expected from the estimated errors reported in those studies. It is therefore important that adequate experimental details be given in a thermodynamic study, so that this information can be used in resolving potential discrepancies between different sources of published data. This information should include the purity of solutes and solvents, methods of molality analyses and their precision, molar masses assumed for calculating molalities, and the temperatures used for the measurements and their uncertainty.

Isopiestic data should therefore be published in journals, books, or conference proceedings that allow a full listing of experimental results and experimental details. Correspondingly, experimentalists should be discouraged from publishing thermodynamic results in any journal or medium that restricts the amount of experimental information that can be given in order to save space, because this information is of potential importance to reevaluation of thermodynamic data. Even putting the primary data in a microfilm supplement is better than having it lost forever.

#### **IV. HISTORICAL DEVELOPMENT, BASIC FEATURES, MAIN SOURCES OF ERROR, AND EVOLUTION OF THE ISOPIESTIC METHOD**

##### **A. HISTORICAL DEVELOPMENT OF THE ISOPIESTIC METHOD FOR MEASUREMENTS AROUND ROOM TEMPERATURE, AND UNDERSTANDING ERRORS INHERENT IN THE CHAMBER DESIGN**

In 1917 Bousfield<sup>32</sup> first described the basic experimental technique that is generally known as the isopiestic method. Bousfield used the term isopiestic to describe solutions that had been allowed to reach equilibrium with regard to transfer of solvent through a vapor phase. The name was derived from the Greek *ισος πιεζειν* which literally means equal compressible or equal pressure. Our English word pressure was derived from the second Greek word.

Scatchard and co-workers,<sup>33</sup> however, argued that the term isotonic was more appropriate to describe solutions that had been equilibrated in this fashion. Their first argument was historical in nature. They stated that de Vries in 1882 used the term isotonic to describe solutions that were in equilibrium with regard to solvent transfer, although de Vries used that term in a conceptual sense only. In addition, Scatchard et al. noted that the term isotonic emphasizes equilibrium conditions, whereas vapor pressure does not. The "tonic" refers to vapor tension, which is an archaic term for saturation vapor pressure. However, the term isotonic has undergone a change in meaning over time and now refers to solutions that have equal osmotic pressures. Although the condition of equal osmotic pressure is true of solutions that are in equilibrium with regard to solvent transfer, it is not directly related to the experimental technique being considered and thus is irrelevant.

The fundamental characteristic of thermodynamic equilibrium for systems in equilibrium

with regard to transfer of solvent is the equality of Gibbs energy of the solvent (chemical potential), and thus the equality of the solvent activities for each of the solutions. The terms isoactive solutions and isoactive method could be used to describe this type of equilibrium, but they are ambiguous in the sense that solutions can be equilibrated so as to be isoactive in one of the solutes (e.g., in liquid-liquid extraction). Thus it seems best to retain the nomenclature isopiestic solutions, isopiestic equilibrium, and isopiestic method, which are the accepted terms for everyone except Scatchard and his students.

For the initial application of the isopiestic method, Bousfield<sup>32</sup> put cylindrical glass vessels containing dry salts on a tin stand inside a desiccator, added water, evacuated the air, maintained the desiccator at 291 K, and determined the mole ratio of solvent to solute at (typically) 2- to 4-day intervals until equilibrium was reached. However, as noted by Sinclair,<sup>34</sup> the use of glass sample containers with their poor thermal conductivity, and the absence of a medium for facilitating equilization of temperatures, gave a very slow approach to equilibrium and fairly inaccurate results for the relative lowering of solvent vapor pressure (up to 10% errors).

Sinclair<sup>34</sup> tested an isopiestic apparatus similar in design to that of Bousfield. He placed two samples in glass containers, one 1 mol · dm<sup>-3</sup> KCl and the other pure water, evacuated air from the chamber, and found that the approach to equilibrium was so slow as to be almost undetectable; even floating the dishes on mercury (to assist in heat transfer) caused very little improvement. Inasmuch as samples with much closer initial  $a_s$  values than used in this test are commonly used in isopiestic experiments, the approach to equilibrium would be even slower, and the prototype apparatus of Bousfield<sup>32</sup> would be incapable of giving meaningful results.

As noted both by Bousfield<sup>32</sup> and Sinclair,<sup>34</sup> the quality of the attainment of isopiestic equilibrium is highly dependent upon the equalization of temperatures between solutions being equilibrated. When the isopiestic chamber is sealed and the air removed, there will be temperature inhomogeneities initially present that need to be eliminated for isothermal conditions to occur. Sinclair<sup>34</sup> mentioned that the evaporation of water involves an enthalpy of vaporization of 2.436 kJ · g<sup>-1</sup> (2.442 kJ · g<sup>-1</sup> is a more modern value for 298.15 K). If two surfaces of the isopiestic chamber differed initially by  $7 \times 10^{-4}$  K, then, according to Sinclair's calculations, the time required for 1 g of water to be transported (which depends on the heat transfer medium) is 10 years for glass, 17 years for water, 500 years for various gases, 1.25 years for mercury, and 10 d for copper. It now appears that these calculations for solvent transfer times were overly pessimistic. However, Sinclair did make an important point: unless the sample containers and the heat conduction medium in an isopiestic apparatus are good thermal conductors, the equilibration times could be so long as to make the method impractical to use.

Both Sinclair<sup>34</sup> and Scatchard et al.<sup>33</sup> have performed elementary calculations of the magnitude of error that would occur for vapor pressures if small temperature differences were present in an isopiestic chamber. We now give a new derivation, in which we derive the error in the osmotic coefficient  $\Phi$ , because this is the quantity of most direct interest in isopiestic experiments.

The relationship between the molal osmotic coefficient and the activity of the solvent is given by Equation 8. If two solution samples are in isopiestic equilibrium but are at different temperatures due to a temperature gradient in the isopiestic apparatus, then they will still have the same vapor pressure. However, they will have different solvent activities because  $P_s^\circ$  will be for a different temperature in each case. Thus at equilibrium

$$\ln P_s(T_1) = \ln P_s^*(T_2) \quad (33)$$

where the pressures are treated formally as if they were dimensionless, the test solution is

at temperature  $T_1$ , and the reference standard is at temperature  $T_2$ . The activities are given by (neglecting the nonideal vapor correction):

$$\ln a_s(T_1) = \ln P_s(T_1) - \ln P_s^\circ(T_1) \quad (34)$$

and

$$\ln a_s^*(T_2) = \ln P_s^*(T_2) - \ln P_s^\circ(T_2) \quad (35)$$

The equation for isopiestic equilibrium is then

$$\ln a_s(T_1) + \ln P_s^\circ(T_1) = \ln a_s^*(T_2) + \ln P_s^\circ(T_2) \quad (36)$$

This can be rearranged into the form

$$\ln \left\{ a_s(T_1)/a_s^*(T_2) \right\} = \ln \left\{ P_s^\circ(T_2)/P_s^\circ(T_1) \right\} \quad (37)$$

By using the definition of the osmotic coefficient, Equation 8, we obtain

$$-\left( \sum_i \nu_i m_i \right) \Phi(T_1) + \nu^* m^* \Phi^*(T_2) = m_s \ln \left\{ P_s^\circ(T_2)/P_s^\circ(T_1) \right\} \quad (38)$$

and then rearrange this to

$$\Phi(T_1) = \frac{\nu^* m^* \Phi^*(T_2)}{\sum_i \nu_i m_i} + \frac{m_s}{\sum_i \nu_i m_i} \ln \left\{ P_s^\circ(T_1)/P_s^\circ(T_2) \right\} \quad (39)$$

A similar equation could be derived for two samples of the same electrolyte that are at different temperatures. The first term on the right-hand side of Equation 39 is of the form encountered for isopiestic equilibrium under isothermal conditions (Equation 32).

If the experimentalist were unaware that a temperature gradient was present, then Equation 32 would have been used for the calculations. Thus the difference between the correct value and the calculated value would be

$$\Delta\Phi = \frac{m_s}{\sum_i \nu_i m_i} \ln \left\{ P_s^\circ(T_1)/P_s^\circ(T_2) \right\} \quad (40)$$

Consider the example of aqueous solutions with  $T_1 = 298.15$  K and a temperature difference of only 0.001 K. Then

$$\Delta\Phi = 0.0033 / \left( \sum_i \nu_i m_i \right) \quad (41)$$

where the vapor pressures of water were taken from Wexler and Greenspan.<sup>7</sup> For a concentrated solution, say saturated NaCl where  $\nu m = 12.3 \text{ mol} \cdot \text{kg}^{-1}$ ,  $\Delta\Phi = 0.00027$  so a residual temperature difference of 0.001 K has little effect on  $\Phi$ . However, for dilute NaCl with  $\nu m = 0.2$ , a temperature difference of 0.001 K will give  $\Delta\Phi = 0.0165$ , which would be a serious error. This is one reason why isopiestic equilibrium molalities and derived  $\Phi$

become significantly less precise at low molalities. It is clear that temperature differences need to be reduced to about  $1 \times 10^{-4}$  K to obtain accurate  $\Phi$  at low molalities.

Sinclair<sup>34</sup> introduced several innovations to facilitate the equalization of temperature of each sample during an isopiestic equilibration. These changes include placing the solution samples into silver-plated copper sample containers (square prismatic in shape) and placing these containers against each other in the same recess in a large 2.5-cm-thick silver-plated copper block that is then inserted into a desiccator. Copper has a thermal conductivity approximately 400 times greater than the glass sample containers used by Bousfield.<sup>32</sup> Sinclair's experiments were performed at 298.15 K and the constant temperature bath was controlled to  $\pm 0.01$  K. Sinclair noted that the thick glass walls of the desiccator would tend to dampen out the effect of temperature variations in the temperature bath, and that the large copper block would allow rapid heat transfer so as to dampen out internal temperature variations. Most workers since then consider it to be adequate to control the bath temperature to  $\pm 0.01$  K to maintain the necessary highly uniform internal temperature inside the apparatus.

Sinclair<sup>34</sup> also added a film of aqueous NaOH between the sample containers and the copper block to improve thermal contact. Although evacuating air from the chambers helped increase the rate at which solutions reached equilibrium, the complete removal of air was found to be unnecessary. The chambers were rocked back and forth to keep the solutions stirred and thus insure that both uniform temperature and concentration were present in any sample container.

Although Sinclair<sup>34</sup> covered the tops of the sample containers after they were removed from the chamber and while the NaOH solution was being rinsed off and the containers dried, there were no individual caps for the containers. Thus they were weighed with their tops open, which gave rise to evaporation losses of up to several milligrams of water. Even with this significant source of error, Sinclair's results were at least 10 to 20 times more accurate than those of Bousfield.<sup>32</sup>

Robinson and Sinclair<sup>35</sup> took the obvious next step and added hinged flap-lids to each sample container. These lids were held up by wires during the equilibrations, and were then allowed to fall into place before the sample containers were removed for weighing. Although this was a definite improvement over weighing the equilibrated samples in open containers, flap-lids are only held in place by gravity and do not provide a tight seal. Thus, weight losses on the order of several tenths of a milligram can still occur before and while a sample is being weighed. It is possible to compensate for this weight loss by weighing each sample container several times, and then extrapolating the weights back to the time when the chamber was opened. However, this is inconvenient and time consuming.

Mason<sup>36</sup> introduced the use of metal equilibration chambers, both brass and monel, and introduced two other innovations. The first was the use of individual fitted caps for the sample containers after they were removed from the chamber, which prevented evaporation from occurring before they were weighed. Mason also added folded strips of platinum gauze to the solutions, and found that doing so decreased the minimum time required to reach equilibrium by about 50%. Although this was not discussed by Mason, it appears that the platinum gauze serves to help transfer heat between the sample container and the solution; it helps to give turbulent mixing when the chambers are rocked back and forth; and it helps to break the surface tension on the solution. Downes<sup>37</sup> and Ellerton et al.<sup>38</sup> found that adding small stainless steel ball bearings to each sample container similarly reduced the equilibration times by about 50%. However, stainless steel is corroded by some electrolyte solutions, so balls of a more inert metal such as platinum or gold might be more generally useful.

Scatchard et al.<sup>33</sup> introduced several additional refinements to the isopiestic technique. One was the use of platinum sample containers, which are much more chemically resistant than the silver-plated copper or silver sample containers used previously. However, the

thermal conductivity of Pt is only about one sixth that of Ag and Cu, so the heat transfer rates are less. Scatchard et al. also made their chamber of metal, stainless steel in this case, which has a thermal conductivity only about one tenth that of brass used by Mason.<sup>36</sup> A lower thermal conductivity is desirable because the chamber walls also function as a thermal buffer to dampen out temperature fluctuations from the constant temperature bath. In addition, Scatchard et al. reduced the area of contact between the copper block and the stainless steel walls to further buffer the inside of the chamber from external temperature changes. They<sup>33</sup> also rotated their chamber at an angle of 45° from the vertical in their constant temperature bath, which kept their solutions well mixed. This is an alternative to back-and-forth rocking of chambers which was introduced slightly earlier.<sup>34-36</sup>

When air is evacuated from an isopiestic chamber, a too rapid change in pressure can give rise to air bubble formation or even boiling of the solution, with its concomitant danger of having some of the solution splatter out of the sample containers. Scatchard et al.<sup>33</sup> described a technique that greatly reduced the danger of splattering: a hollow vessel is attached to the isopiestic chamber and to a vacuum pump with, for example, a three-way stopcock. This "ballast" is evacuated, and then the stopcock is rotated so as to slowly bleed air from the chamber to the ballast. The chamber is then isolated from the ballast, the ballast is reevacuated, and this process is repeated until the desired level of vacuum is obtained in the chamber. A fairly good removal of air is desirable at low molalities to get good equilibration rates. However, we note that it is usually adequate to use an aspirator at higher molalities, inasmuch as the equilibration rates there are much less sensitive to incomplete degassing.

Janis and Ferguson<sup>39</sup> performed isopiestic experiments with sample containers made of silver and silver-plated copper. They found in some cases that when NaCl solutions were equilibrated in silver-plated copper containers, the resulting solutions were turbid, presumably due to formation of a small amount of colloidal silver chloride. This implies that chloride solutions, even those as innocuous as alkali metal chlorides, either corrode silver metal or dissolve the surface layer of oxide. Thus silver sample containers are probably too reactive to be used with halide solutions and many other electrolytes. However, gold-plated silver dishes<sup>36</sup> retain the high thermal conductivity of silver while being much more resistant to chemical attack, and are thus much better suited for isopiestic experiments.

Phillips et al.<sup>40</sup> performed isopiestic measurements by using nickel metal sample containers and a steel heat-transfer equilibration block, and put a layer of mercury between the sample containers and the metal block to assist in heat transfer. To reduce corrosion of the nickel containers by their electrolyte solutions, they gold plated the inside of the cups. However, to reduce problems with amalgamation of this gold by mercury vapor, they covered the inside walls of the sample containers with a baked-resin varnish. This was not done to the bottom of the sample containers, presumably to retain good thermal contact with the solution. They observed significant weight gains for the sample containers during isopiestic equilibrations as the exposed gold became amalgamated, which means that the observed weight changes were not due solely to transport of water. In addition, some electrolyte solutions could react with mercury metal. Thus we consider the use of mercury metal as a heat transfer medium for isopiestic experiments involving electrolyte solutions to cause more problems than benefits, and its use should be avoided.

We have emphasized the importance of good thermal contact between solution samples, sample containers, and the metal (heat-transfer) block in order to have rapid heat transfer and equilization of temperature. Most workers have used an indirect criterion for determining when this occurs: the time required for the molalities of replicate solutions to become equal with certain limits of precision (typically  $\pm 0.1\%$ ), when their initial molalities differed by somewhat larger amounts from each other. The only study that we are aware of in which the uniformity of temperature was directly examined was done by Miller and Porter.<sup>41</sup> They

used an isopiestic chamber of fairly typical design which was made from a glass desiccator, and it contained a gold-plated copper heat-transfer block which was separated from the desiccator by means of a plastic stand. Their experiments were performed at  $298.15 \pm 0.01$  K. By means of a thermocouple inserted in the copper block, they found that *at least 48 hours were required to reach thermal equilibrium when a vacuum was present in the chamber*. Isopiestic experiments are frequently done with 1- to 3-day equilibrations. It is clear that with equilibrations less than 3 days in length, at least around room temperature, the reliability of the resulting data can be questioned as having been measured under nonisothermal conditions.

There are three types of sources of heat that need to be redistributed in an isopiestic apparatus in order for the solution samples to reach identical temperatures and for the entire chamber to be at the desired overall temperature, which corresponds to the mean temperature of the constant-temperature bath into which the chamber is inserted. First, when the chamber is placed in the temperature bath, its temperature will be essentially that of the laboratory in which it was stored previously and the internal temperature may not be completely uniform. We note that the chamber will actually be slightly cooler than the laboratory temperature because of cooling that occurs when the chamber is degassed (Joule-Thomson effect plus evaporation of some solvent from the solutions). Temperature inhomogeneities initially present inside the chamber will rapidly even out by heat transport through the metal heat-transfer block and the walls of the sample containers. Second, heat will flow either from the temperature bath into the chamber walls if the chamber was initially cooler than the constant temperature bath, or from the chamber walls into the temperature bath if the chamber was initially warmer. It is these two heat effects that the temperature equilization times of Miller and Porter<sup>41</sup> refer to.

In addition to these two factors, there will be enthalpy changes due to evaporation or condensation of solvent due to solvent exchange between solutions. These enthalpies of vaporization and condensation ("latent heats") will approximately cancel each other out, but they will provide local sources or sinks of heat inside the chamber as the solutions are being equilibrated.

The driving force "compelling" the solutions in an isopiestic chamber to reach isopiestic equilibrium is related to the chemical potential of the solvent  $\mu_s$ , because that is the quantity that must be equal for all solutions. At the start of an equilibration, inside the chamber there will initially be differences in temperature between individual solutions, and between the temperature bath, the samples, and the chamber. The vapor pressure will be slightly different from the equilibrium vapor pressure, and the concentrations will also be different from the equilibrium values. The differential difference of  $\mu_s$  for a particular solution from its equilibrium value then will be

$$\delta\mu_s = \left(\frac{\partial\mu_s}{\partial T}\right)_{P,n_s} \delta T + \left(\frac{\partial\mu_s}{\partial P}\right)_{T,n_s} \delta P + \left(\frac{\partial\mu_s}{\partial n_s}\right)_{T,P} \delta n_s \quad (42)$$

There are no terms for the derivative of  $\mu_s$  with regard to the number of moles of the solutes because the  $n_i$  do not change for an individual sample being used in an isopiestic experiment. We will now derive expressions for these partial derivatives and consider the relative sizes of the various terms in this equation and the temperature and pressure derivatives of  $\Phi$ .

From Equation 8 we know that

$$\frac{\mu_s - \mu_s^\circ}{T} = - \frac{R \sum_i \nu_i m_i}{m_s} \Phi \quad (43)$$

Taking the temperature derivative then gives

$$\begin{aligned}
 \frac{\partial}{\partial T} \left\{ \frac{\mu_s - \mu_s^\circ}{T} \right\}_{P,n_s} &= \frac{-H_s + H_s^\circ}{T^2} \\
 &= -\frac{L_s}{T^2} \\
 &= -\frac{R \sum_i \nu_i m_i}{m_s} \left( \frac{\partial \Phi}{\partial T} \right)_{P,n_s}
 \end{aligned} \tag{44}$$

where  $H_s$  and  $H_s^\circ$  are the partial molar enthalpy of the solvent in the solution and the molar enthalpy of the pure solvent, respectively, and  $L_s = H_s - H_s^\circ$  is the relative partial molar enthalpy of the solvent in the solution. Rearranging this equation gives

$$\left( \frac{\partial \Phi}{\partial T} \right)_{P,n_s} = \frac{m_s L_s}{RT^2 \sum_i \nu_i m_i} \tag{45}$$

For an aqueous solution at 298.15 K,

$$\left( \frac{\partial \Phi}{\partial T} \right)_{P,n_s} = 7.51 \times 10^{-5} \frac{L_s}{\sum_i \nu_i m_i} \tag{46}$$

where  $L_s$  is in units of  $\text{J} \cdot \text{mol}^{-1}$ . Using values of  $L_s$  for aqueous NaCl from Clarke and Glew<sup>11</sup> at 298.15 K we compute that this derivative is  $-4.1 \times 10^{-5} \text{K}^{-1}$  at  $\nu m = 0.2 \text{ mol} \cdot \text{kg}^{-1}$ ,  $+1.9 \times 10^{-4} \text{K}^{-1}$  at  $\nu m = 12.3 \text{ mol} \cdot \text{kg}^{-1}$  (saturation), and it falls between these values at intermediate molalities. Thus, even if the isopiestic sample containers were 1 K away from their correct temperature (as long as they were all at that temperature), the effect for  $\Phi$  of NaCl would not be noticeable.

Enthalpy effects are larger for some cases such as aqueous  $\text{H}_2\text{SO}_4$  solutions. Using the enthalpy values at 298.15 K tabulated by Giauque et al.<sup>21</sup> we computed that the derivative given by Equation 46 is  $-0.0005 \text{K}^{-1}$  at  $m = 1 \text{ mol} \cdot \text{kg}^{-1}$ ,  $-0.0070 \text{K}^{-1}$  at  $11.1 \text{ mol} \cdot \text{kg}^{-1}$ , and  $-0.0086 \text{K}^{-1}$  at  $27.75 \text{ mol} \cdot \text{kg}^{-1}$ . Thus in this case a temperature error of only about 0.1 K could be tolerated.

The temperature derivative of  $\mu_s$ ,  $\left( \frac{\partial \mu_s}{\partial T} \right)_{P,n_s}$ , is equal to the negative of the entropy of the solvent in the solution. Values of  $S_s$  have been reported for aqueous  $\text{H}_2\text{SO}_4$  at 298.15 K by Giauque et al.<sup>21</sup> They reported  $S_s = 70.16 \text{ J} \cdot \text{K}^{-1} \cdot \text{mol}^{-1}$  for  $1 \text{ mol} \cdot \text{kg}^{-1}$ ,  $69.30 \text{ J} \cdot \text{K}^{-1} \cdot \text{mol}^{-1}$  at  $11.1 \text{ mol} \cdot \text{kg}^{-1}$ , and  $68.45 \text{ J} \cdot \text{K}^{-1} \cdot \text{mol}^{-1}$  at  $27.75 \text{ mol} \cdot \text{kg}^{-1}$ . Multiplying these values by the temperature difference then gives the Gibbs energy differences. For a temperature difference of 0.02 K, for example, there is a Gibbs energy difference of about  $1.4 \text{ J} \cdot \text{mol}^{-1}$  or  $0.08 \text{ J} \cdot \text{g}^{-1}$  for the solvent. Since isopiestic samples typically have around 1 g of solvent, a temperature difference of 0.02 K provides only a small Gibbs energy change.

The pressure derivative can be obtained also by differentiating Equation 43:

$$\begin{aligned}
 \frac{\partial}{\partial P} (\mu_s - \mu_s^\circ)_{T,n_s} &= V_{s(\text{d})}^{\text{ex}} \\
 &= -\frac{RT \sum_i \nu_i m_i}{m_s} \left( \frac{\partial \Phi}{\partial P} \right)_{T,n_s}
 \end{aligned} \tag{47}$$



This can be rearranged to yield

$$\left(\frac{\partial \Phi}{\partial P}\right)_{T,n_s} = -\frac{m_s V_{sd}^{\text{ex}}}{RT \sum_i \nu_i m_i} \quad (48)$$

Between 273.15 and 373.15 K, the molar volume of pure water varies between 18.017 and 18.798 cm<sup>3</sup> · mol<sup>-1</sup> (see Table 1). The partial molar volume of water in a solution starts out at the pure water value at infinite dilution, but it generally decreases regularly with increasing molality. Thus, from 273.15 to 373.15 K,  $V_{sd} \leq 18.8 \text{ cm}^3 \cdot \text{mol}^{-1}$ . The pressure coefficient of the chemical potential of the solvent from Equation 47 is equal to  $V_{sd}^{\text{ex}}$ , and thus is  $18.8 \times 10^{-6} \text{ J} \cdot \text{Pa}^{-1} \cdot \text{mol}^{-1}$  ( $1 \text{ cm}^3 = 1 \times 10^{-6} \text{ J} \cdot \text{Pa}^{-1}$ ).

Initially, when the isopiestic solution samples are added to the chamber and the chamber is degassed, the vapor pressure inside the chamber will approximately equal that for the vapor pressure of the solutions at the temperature of the laboratory. Once the chambers are put into a constant temperature bath, the pressure inside the chamber will rapidly approach that for the solutions at the temperature of the constant temperature bath. Subsequent vapor pressure changes will be quite small, and the resulting chemical potential changes will be less than 0.01 J · mol<sup>-1</sup> which is insignificant compared to the effect of temperature differences.

The negative of the pressure coefficient of  $\Phi$  for an aqueous solution, as given by Equation 48, is equal to

$$(6.7 \times 10^{-6} V_{sd}^{\text{ex}}/T \sum_i \nu_i m_i)$$

in units of Pa<sup>-1</sup>. For binary aqueous solutions at 298.15 K,  $-(\partial\Phi/\partial P)_{T,n_s} = 2.24 \times 10^{-8}$  ( $V_{sd}^{\text{ex}}/\sum_i \nu_i m_i$ ). The excess volume of the solvent  $V_{sd}^{\text{ex}}$  typically ranges from 0 to -1 or -2 cm<sup>3</sup> · mol<sup>-1</sup>.

In the initial stages of an isopiestic equilibration, if the molalities of the solutions are somewhat different from their ultimate equilibrium values, then the last term on the right-hand side of Equation 42 can dominate. In this case we will calculate the derivative of the chemical potential of the solvent with regard to the number of moles of solvent. As the starting point, we use Equation 2 for the case of the solvent,

$$\mu_s = \mu_s^\circ + RT \ln a_s \quad (49)$$

and differentiate it to obtain

$$\begin{aligned} \left(\frac{\partial \mu_s}{\partial n_s}\right)_{T,P,n_i} &= \left(\frac{\partial \mu_s^\circ}{\partial n_s}\right)_{T,P,n_i} + RT \left(\frac{\partial \ln a_s}{\partial n_s}\right)_{T,P,n_i} \\ &= RT \left(\frac{\partial \ln a_s}{\partial n_s}\right)_{T,P,n_i} \end{aligned} \quad (50)$$

where  $n_i$  refers to the number of moles of a solute.

Water activities, osmotic coefficients, and solute activity coefficients are generally modeled as functions of molality rather than of  $n_s$ . Thus it is more convenient to express the derivative on the right-hand side of Equation 50 in the ‘‘chain-rule’’ form

$$\left(\frac{\partial \ln a_s}{\partial n_s}\right)_{T,P,n_i} = \sum_k \left(\frac{\partial \ln a_s}{\partial m_k}\right)_{T,P,n_i} \left(\frac{\partial m_k}{\partial n_s}\right)_{T,P,n_i} \quad (51)$$

for  $k \neq s$ . We then have

$$\left(\frac{\partial \mu_s}{\partial n_s}\right)_{T,P,n_i} = RT \sum_k \left(\frac{\partial \ln a_s}{\partial m_k}\right)_{T,P,n_i} \left(\frac{\partial m_k}{\partial n_s}\right)_{T,P,n_i} \quad (52)$$

The molality of salt  $i$  is given by the number of moles of salt  $i$  divided by the number of kilograms of solvent, and the number of kilograms of solvent is given by  $n_s M_s$ , where  $M_s$  is the molar mass in  $\text{kg} \cdot \text{mol}^{-1}$ . Thus,

$$m_k = \frac{n_k}{n_s M_s} \quad (53)$$

and performing the differentiation yields

$$\begin{aligned} \left(\frac{\partial m_k}{\partial n_s}\right)_{T,P,n_i} &= -\frac{n_k}{n_s^2 M_s} \\ &= -\frac{m_k}{n_s} \end{aligned} \quad (54)$$

This can be inserted into Equation 52 to yield

$$\left(\frac{\partial \mu_s}{\partial n_s}\right)_{T,P,n_i} = -\frac{RT}{n_s} \sum_k m_k \left(\frac{\partial \ln a_s}{\partial m_k}\right)_{T,P,n_i} \quad (55)$$

If only one solute is present the  $i$  and  $k$  subscripts can be dropped. In addition, if we restrict this to a binary aqueous solution at 298.15 K,

$$\begin{aligned} \left(\frac{\partial \mu_s}{\partial n_s}\right)_{T,P,n_i} &= \frac{-RTm}{n_s} \left(\frac{\partial \ln a_s}{\partial m}\right)_{T,P} \\ &= \frac{\nu RTm}{n_s m_s} \left(\frac{\partial (m\Phi)}{\partial m}\right)_{T,P} \\ &= \frac{0.044659\nu m}{n_s} \left(\frac{\partial (m\Phi)}{\partial m}\right)_{T,P} \end{aligned} \quad (56)$$

where the units are in  $\text{kJ} \cdot \text{mol}^{-2}$ .

The activity of the solvent in a solution changes very slowly at low molalities, and much more rapidly at high molalities. Thus the driving force "pushing" the solutions to reach equilibrium by means of transport of solvent through the vapor phase is small at low molalities but much larger at high molalities. That is, the chemical potential gradient "drives" the solutions to reach equilibrium much more strongly at high molalities than at low. Some numerical values of this chemical potential gradient are given in Table 8, and they were calculated with use of equations and parameters given by Hamer and Wu<sup>9</sup> and Rard et al.<sup>8,12</sup>

The quantity taken from Equation 56 and given in Table 8 is the "driving force" for isopiestic equilibrium.

$$0.044659\nu m \left(\frac{\partial (m\Phi)}{\partial m}\right)_{T,P}$$

**TABLE 8**  
**Driving Force for Solvent Transport in Aqueous**  
**NaCl, CaCl<sub>2</sub>, and H<sub>2</sub>SO<sub>4</sub> at 298.15 K<sup>a</sup>**

<b>m</b> (mol · kg <sup>-1</sup> )	<b>NaCl<sup>b</sup></b> (kJ · mol <sup>-1</sup> )	<b>CaCl<sub>2</sub><sup>c</sup></b> (kJ · mol <sup>-1</sup> )	<b>H<sub>2</sub>SO<sub>4</sub><sup>d</sup></b> (kJ · mol <sup>-1</sup> )
0.1	0.0082	0.0114	0.0087
1.0	0.0870	0.178	0.110
3.0	0.334	1.20	0.586
6.0	0.934	3.57	1.82
9.0		3.47	3.22
15.0			5.63
20.0			7.50
25.0			8.94
27.75			8.53

<sup>a</sup> These are values of  $-2.4790 \text{ m} \left( \frac{\partial \ln a_s}{\partial m} \right)_{T,P} = 0.044659$   
 $\text{vm} \left( \frac{\partial(m\Phi)}{\partial m} \right)_{T,P}$ .

<sup>b</sup> Values calculated from equation given by Hamer and Wu.<sup>9</sup>

<sup>c</sup> Values calculated from equation given by Rard et al.<sup>8</sup>

<sup>d</sup> Values calculated from equation given by Rard et al.<sup>12</sup>

The gain or loss of  $\delta n_s$  moles of solvent from a solution containing  $n_s$  moles of solvent will result in a chemical potential change for that solution equal to this quantity multiplied by  $(\delta n_s/n_s)$ . Examination of the values given in Table 8 indicates that the driving force increases by two or three orders of magnitude in going from dilute solutions to high molalities, and that at very high molalities some electrolytes have a maximum in this value followed by a slow decrease. These values indicate that there is a large driving force “pushing” the solutions toward isopiestic equilibrium at high molalities, but only a weak driving force at low molalities. This accounts, at least in part, for the decreased rates of approach to equilibrium as the solutions become dilute.

Consider a sample of electrolyte solution containing 1.0 g of water, and which is 0.1 mol · kg<sup>-1</sup> from its equilibrium molality. If the molality change is from 0.2 to 0.1 mol · kg<sup>-1</sup>, 1.0 g of solvent must be transported to this solution. However, from 6.1 to 6.0 mol · kg<sup>-1</sup> only 0.017 g of solvent is involved, and from 15.1 to 15.0 mol · kg<sup>-1</sup> involves 0.0067 g of solvent. Thus, very little solvent needs to be transported at high molalities (where the driving force is large) relative to low molalities (where the driving force is small). Therefore, at low molalities a lot more solvent needs to be transported but the driving force is very small. This suggests that although the kinetics of the approach to isopiestic equilibrium is largely determined by the efficiency of heat transport over most of the molality range, it should shift to a mass transport-dominated regime at very low molalities.

So far we have been noncommittal in our use of the term to describe the containers used to hold individual solution samples in an isopiestic experiment. This is because there is no single established name for them. Among the experimental papers already cited and in a few additional ones, we have found the following terms. The term cups has been used by Scatchard et al.,<sup>33</sup> Phillips et al.,<sup>40</sup> Humphries et al.,<sup>42</sup> Kirgintsev and Luk'yanov,<sup>43</sup> Holmes and Mesmer,<sup>17</sup> Libuś et al.,<sup>26</sup> Rard,<sup>2</sup> and Macaskill and Bates;<sup>44</sup> the term dishes has been used by Sinclair,<sup>34</sup> Robinson and Sinclair,<sup>35</sup> Janis and Ferguson,<sup>39</sup> Childs and Platford,<sup>20</sup> Rush and Johnson,<sup>45</sup> Ellerton et al.,<sup>38</sup> Covington et al.,<sup>23</sup> Downes,<sup>37</sup> and Miller and Porter;<sup>41</sup> the term vessels was also used by Miller and Porter;<sup>37</sup> the term bottles was used by Mason;<sup>36</sup> the term cuvettes by Kirgintsev and Luk'yanov,<sup>43</sup> Michimoto et al.,<sup>46</sup> and Yamauchi and

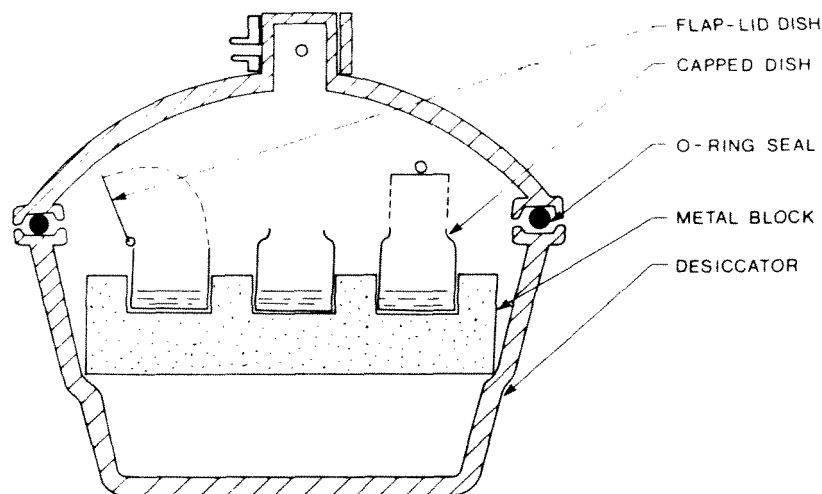


FIGURE 1. Diagram of a typical isopiestic apparatus constructed from a glass vacuum desiccator. Two common types of sample cup are illustrated. This apparatus is usually placed on a platform in a constant temperature bath and rotated or rocked back and forth.

Sakao;<sup>47</sup> Robinson<sup>48</sup> used the term boxes; Wang et al.<sup>31</sup> called them crucibles; Bousfield<sup>32</sup> called them glasses; and Braunstein and Braunstein<sup>24</sup> called them pans.

Some of these differences in nomenclature arise from the fact that there are some differences in shape between sample containers being used in different investigations (or they reflect the original name for a container that is being adapted for a new application), but such a plethora of names is obviously undesirable. The terms cups and dishes are the most widely used, and it seems best to retain them and reject the others. We propose that the term cups be used for sample containers that are cylindrical in shape, including those with tapered tops, and that the term dishes be used for containers with other shapes such as those with square cross-sections. Either term could be used in the generic sense, as when the function of the container is being described and its shape is unimportant.

There is also some variation in the name given to the total isopiestic unit (outer vessel, lid, metallic heat-transfer block). Among the experimental papers just cited, the most common name is desiccator,<sup>20,35,36,39-41,44</sup> although chamber,<sup>2,45</sup> apparatus,<sup>23,31,33,42,43,46,47</sup> and vessel<sup>17,26,33,43</sup> have also been used.

The use of the term desiccator is not surprising, inasmuch as a number of isopiestic "apparatuses" have been constructed out of glass desiccators, and several of the ones made out of metal have been roughly comparable in shape. In a sense, however, this term is unfortunate because it emphasizes an alternative function of a part of the apparatus that is not utilized in isopiestic experiments. However, the term desiccator is so widely used that it probably should be retained, although it should be restricted in meaning to refer to the outer container only. We do not recommend that any of the alternate names be selected over the others.

Figure 1 is a diagram of a generic isopiestic apparatus, based on the use of a modified vacuum desiccator. We note that no commercial models are available, and all isopiestic units have been individually made. This diagram illustrates two of the most common types of sample cups: a simple cylindrical shape with a hinged flap-lid, and a cup with a tapered top which has a tight-fitting cap that is put into position after the chamber is opened at the end of an experiment. Some of the metal equilibration chambers described in the literature have this same basic shape, whereas others are rectangular in shape. Detailed drawings are available for several of these chambers constructed out of metal,<sup>2,33,36,40</sup> including the apparatus used for study of metal amalgams at 600 K.<sup>31</sup>

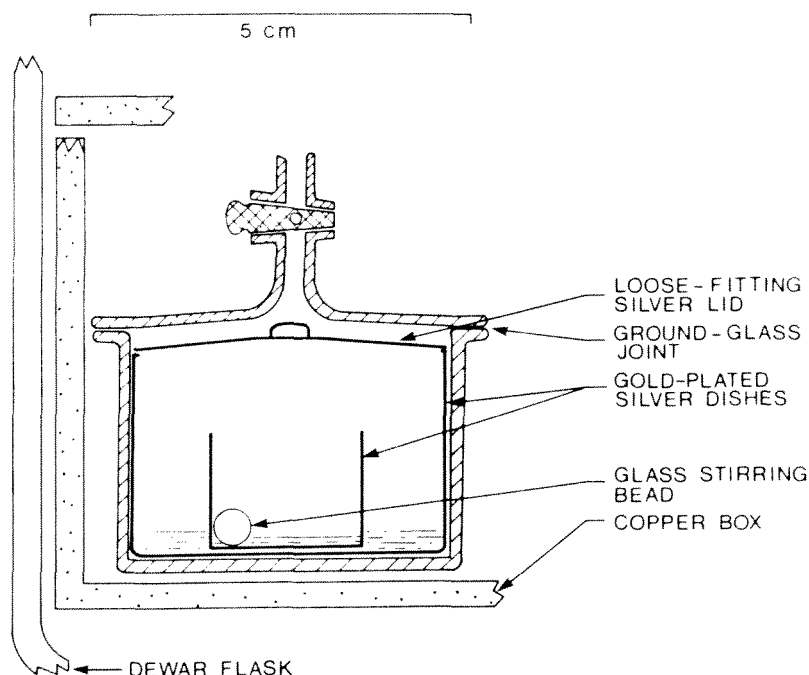


FIGURE 2. Diagram of an isopiestic apparatus designed for operation at very low molalities. The central dish containing a glass ball holds the solution being equilibrated with solution in the larger dish in which it sets. (Adapted with permission from Gordon, A. R., *J. Am. Chem. Soc.*, 65, 221, 1943. Copyright 1943 by the American Chemical Society.)

Gordon<sup>49</sup> performed isopiestic experiments for aqueous NaCl and KCl solutions from 0.032 to 0.100 mol · kg<sup>-1</sup>, and these are the lowest molalities investigated successfully by the isopiestic method. Gordon's apparatus is illustrated in Figure 2. It has a fairly complex design, and it was constructed to maintain a highly uniform internal temperature. Gordon used a chamber with a silver sample cup inside another silver dish that fitted tightly within a glass vessel that could be evacuated. This glass vessel was placed within a copper box that in turn was placed within a Dewar flask. Gordon added a glass ball to the solutions to provide stirring as the apparatus was rocked. Even with this elaborate design, Gordon reported that some experiments were unsuccessful due to condensation of water vapor or splattering during degassing, and of the 14 sets of data that were reported, 4 were inconsistent by 0.4 to 0.6%, presumably because of failure to reach equilibrium. Although the bulk of Gordon's data does appear to be accurate, these experiments were difficult enough that no one since then has been tempted to repeat them. Following Gordon, we note that 0.1 mol · kg<sup>-1</sup> should be considered the lower limit for isopiestic measurements under normal circumstances.

Gordon<sup>49</sup> mentioned that H. Sheffer had performed some (unpublished) experiments for aqueous solutions around 0.1 mol · kg<sup>-1</sup> in which a hinged copper paddle was suspended above the isopiestic cups, and it was used to stir the water vapor. Sheffer did find that this caused an improvement in the rate at which these solutions reached equilibrium. This suggested to them that the rate of diffusion of water vapor may have been the dominant factor in producing equilibrium at these low molalities. This empirical observation is in agreement with our deduction given earlier in this section, from purely thermodynamic arguments, that the rate of attainment of equilibrium should become mass-transport limited at very low concentrations. An apparatus utilizing vapor stirring has been described by Pan.<sup>50</sup>

An air-filled isopiestic apparatus was described by Kirgintsev and Luk'yanov,<sup>43</sup> and

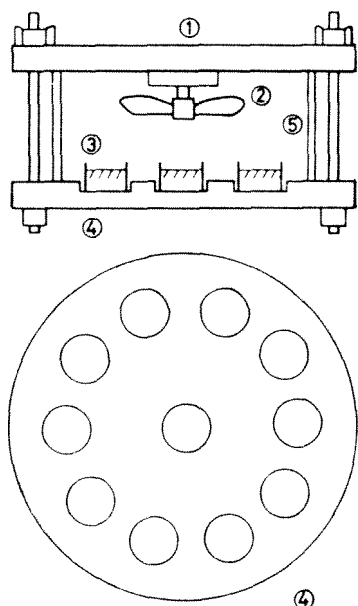


FIGURE 3. Diagram of an air-filled isopiestic apparatus: (1) lid of chamber made of stainless steel; (2) propeller-type vapor stirrer with electromagnetic transmission drive; (3) sample cups of glass; (4) bottom of chamber made of stainless steel; and (5) cylindrical glass walls of chamber. (Reprinted with permission from Majima, H. and Awakura, Y., *Metall. Trans.*, 16B, 433, 1985. Copyright 1985 by Metallurgical Transactions.)

similar designs have been used more recently by workers in Japan.<sup>46,47,51</sup> In each case a propeller-type stirrer protruded through the top of the chamber and was used to stir the vapor phase. This vapor stirring helps to compensate for the reduced rates of vapor diffusion caused by the presence of air. In all cases glass sample cups were used to hold the solutions, but using glass does reduce the efficiency of temperature equilization. The goal of using this type of apparatus is to simplify the experiments (no vacuum pump is required) and to eliminate the expense of machining cups of inert metal. The apparatus of Majima and Awakura<sup>51</sup> is illustrated in Figure 3. However, the use of an air-filled chamber does give rise to a new problem that seems to have been overlooked by these workers.<sup>43,46,47,51</sup>

The new problem arises because the mechanical energy of the spinning propeller will be converted into kinetic energy of the air, and this will give rise to a small but continuous heat source within the chamber. Thus the temperature inside the chamber will be slightly higher than the mean temperature of the constant temperature bath and a slight temperature gradient will be present inside the chamber that will not disappear with time. The magnitude of this problem is not obvious and might well be negligible, but the amount of heat added to the chamber will be related to the rate at which the propeller rotates. Intermittent rather than continuous vapor stirring might reduce the magnitude of this potential source of error.

Kirgintsev and Luk'yanov<sup>43</sup> controlled their temperature bath to better than  $\pm 0.01$  K, whereas in the other studies<sup>46,47,51</sup> it was only controlled to  $\pm 0.1$  K. This poorer temperature control for those air-filled chambers does seem to have caused a reduction in the precision of the isopiestic results at lower molalities.<sup>46</sup>

By far the majority of isopiestic apparatuses have recesses for the isopiestic cups machined into the metal heat-transfer block.<sup>1,2,31,33,26,39,40,41,43,46,47,50,51</sup> These recesses not only serve to increase the area of contact between the isopiestic cups and the heat-transfer block, but they also prevent the cups from sliding about as the chamber is rocked or rotated in the constant temperature bath. However, there were several studies in which flat-bottomed isopiestic cups were placed directly on top of the heat-transfer block.<sup>17,35,38,42,45,48</sup> The high-temperature isopiestic apparatus at ORNL<sup>17</sup> is not rocked or rotated during the equilibrations, so there is no difficulty with the cups sliding around. Humphries et al.<sup>42</sup> used a plexiglas plate to hold their isopiestic cups in place, and Rush and Johnson<sup>45</sup> had threads on the outside of their isopiestic cups, which allowed them to be screwed into a socket plate that

was positioned on the heat-transfer block. The apparatuses used by Robinson<sup>35,48</sup> and by Stokes did not have any device to hold the isopiestic cups in place. Rather, the bottoms of their cups and the heat-transfer block were hand-lapped to be flat, and a drop of electrolyte solution was placed between the bottom of each cup and the heat-transfer block to improve thermal contact and to help the cups adhere to the block (private communications from R. H. Stokes, February 19 and 22, 1991).

## **B. HISTORICAL DEVELOPMENT OF THE ISOPIESTIC TECHNIQUE FOR MEASUREMENTS FROM 273.15 TO ABOUT 383 K**

The basic experimental techniques and chamber features that we have just described are well suited for operation around room temperature (i.e., around 290 to 305 K). However, some rather minor changes in techniques or apparatus are all that is necessary to extend this technique to a temperature range of about 273 to 373 K.

For experiments in the vicinity of room temperature it is adequate to open the chamber first and then add tight-fitting caps by hand to the sample cups. With practice, this can be done typically in less than 1 min, and solvent evaporation losses are generally just several tenths of a milligram. For typical sample masses of 1 to 2 g, this is not a major source of error. Evaporation losses are even smaller at lower temperatures because the vapor pressures of the solutions are much less. However, for experiments around 273 K the opposite problem can occur: moisture from the air can condense on the surface of the cold isopiestic cups. If the sample cups are rapidly capped after the isopiestic chamber is opened at the end of a run, and the isopiestic cups then immediately transferred to a desiccator containing a desiccant, the cups will rapidly warm up to room temperature without any problem with condensation. Thus isopiestic measurements below 298.15 K are only slightly more complicated and should be no less precise.<sup>1</sup>

A different problem occurs above room temperature; the vapor pressure of a solvent in a solution increases rapidly with temperature in an approximately exponential manner. Thus, evaporation losses from solution samples (either because of a loose fitting flap-lid or while open containers are being capped after removal from the chamber) can be large enough that they give rise to serious errors in the resulting data. Consequently, a change is required in the way that isopiestic cups are capped.

The earliest report of the use of the isopiestic method over a fairly wide temperature range was by Robinson<sup>52</sup> in 1939, but, unfortunately, no experimental details were given except to note that a metal desiccator was used above 313 K. Only derived values of the activity coefficients were given, instead of actual data.

Hellams et al.<sup>53</sup> performed isopiestic measurements for aqueous solutions at 318 K by using an isopiestic apparatus of conventional design, but with a disk of plate glass suspended above the isopiestic cups. This glass plate was lowered on top of the isopiestic cups before the samples were removed from the chamber. Immediately after the chamber was opened, the isopiestic cups were placed on a cold brass plate with the glass plate on top of the cups, and the samples were allowed to cool for 3 or 4 min. Individual caps were then placed on the cups before they were weighed. The imprecision of their results, as determined by agreement between molalities of replicate samples, was <0.5% for 61 runs, 0.5 to 1.0% for 14 runs, and >1% in four other cases. Inasmuch as this is about three to six times the scatter usually obtained at lower temperatures, and because of the likelihood of some solvent loss, the accuracy may be even less.

Fortunately, soon afterward, they<sup>42</sup> modified their apparatus by adding a lid holder that could be screwed down to force tight-fitting caps onto the cups before they were removed from the chamber at the end of an equilibration period. A detailed drawing of this apparatus has been published.<sup>42</sup> This new method of capping gave equilibrium molalities precise to about 0.1% for the temperature range of 318 to 353 K,<sup>42,54,55</sup> which is similar to the precision usually obtained at 298.15 K.

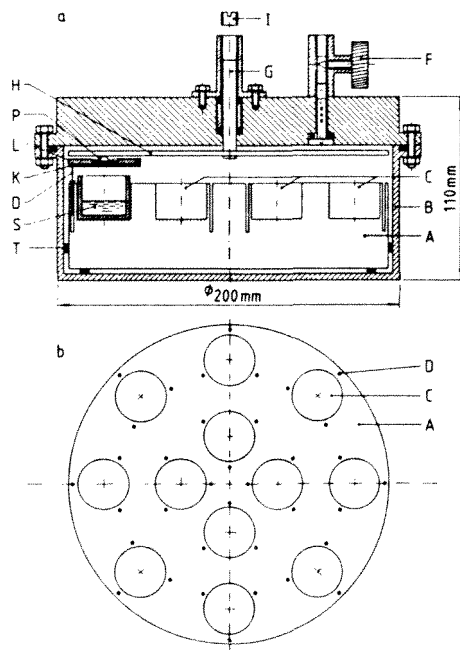


FIGURE 4. Diagram of isopiestic apparatus designed for operation around 373 K: (A) aluminum heat-transfer block; (B) aluminum chamber; (C) holes in block for sample cups; (D) wire for heat transfer; (F) needle valve for evacuation of air; (G) steel bolt; (H) stainless steel plate; (I) screw; (K) silicone rubber gasket; (L) cap for cup; (P) spring to push cap into place; (S) sample cup; and (T) PTFE shims to restrict contact between the chamber walls and heat-transfer block. (Reprinted from Grjotheim, K., Voigt, W., Haugsdal, B., and Dittrich, D., *Acta Chem. Scand. Ser. A*, 42, 470, 1988. With permission of the journal and authors.)

Isopiestic experiments have also been reported for aqueous solutions of several non-electrolytes at 310 and 333 K,<sup>56</sup> but no experimental details were given. Presumably, they used some type of internal capping device to seal the cups before they were removed from the chamber. Rush and Johnson<sup>45</sup> similarly used a device to position caps onto the sample cups at 298.15 K while they were still in the chamber.

Grjotheim et al.<sup>57</sup> have described an isopiestic apparatus designed for operation around 373 K. Their chamber was made from aluminum, as was the heat-transfer block, and the cups were of aluminum or vitreous carbon. The schematic of their apparatus is given in Figure 4. It is similar in design to isopiestic chambers for lower temperatures, except that the caps for the isopiestic cups are forced into place by lowering a stainless steel plate. Required equilibrium periods were from 20 to 72 h, which is slightly less than required at room temperature. Results have been published for several binary and ternary aqueous electrolytes,<sup>57-59</sup> and values of  $\Phi$  from these experiments appear to be of good precision.

### C. ISOPIESTIC MEASUREMENTS ABOVE 373 K: OAK RIDGE NATIONAL LABORATORY

The only isopiestic apparatus designed for operation to well above 373 K is the high-temperature unit constructed and operated at Oak Ridge National Laboratory (ORNL). The prototype model was described in detail by Soldano et al. in a chapter in *The Structure of Electrolytic Solutions*,<sup>60</sup> and it was used for isopiestic measurements in the temperature range of 373 to 438 K.<sup>61-64</sup>

A major problem with isopiestic measurements using chambers of conventional design at high temperatures is solvent loss when the samples cups are removed from the chamber for weighing. This was avoided in the ORNL high-temperature unit<sup>60</sup> by the inclusion of an electromagnetic balance within the chamber, which allowed the samples to be weighed *in situ* while still at the equilibrium temperature. By injecting more water into the system, additional equilibrations could be performed with the same samples.

The solution samples were equilibrated in silver dishes that were placed on a copper block within the stainless steel chamber, and a remote-controlled device was used to move



the sample cups from the copper block to the balance. Standard weights were enclosed in the chamber, and they were also weighed at the equilibrium temperatures. These additional weights allowed them<sup>60</sup> to calibrate the balance and to correct for nonlinear readout on their potentiometer. The silver dishes were replaced by titanium dishes in their subsequent studies.

Because of the complicated design of their apparatus, it was not possible to rock the chamber to mix a solution. Thus, mixing in a solution occurred only by diffusion. Test experiments for  $\approx 1 \text{ mol} \cdot \text{kg}^{-1}$  solutions at 318, 358, and 378 K indicated that required equilibration times were about 60, 10, and 3 days, respectively, at these temperatures. At lower temperatures these equilibration times are excessively long, but they are quite reasonable above 378 K. The temperature of their experiments was controlled with an air-bath thermostat.

Later more accurate isopiestic measurements by Holmes and co-workers indicated that most if not all of the earlier measurements<sup>60-64</sup> were inaccurate, with the size of the error increasing with temperature. See, for example, the comparison given by Holmes et al.<sup>65</sup> for aqueous KCl.

The problems with the earlier experiments appear to have been of two types. First, the electromagnetic balance used by Soldano et al.<sup>60</sup> was not as sensitive as required for the measurements. Second, it is very difficult to control the temperature of an air-bath thermostat to better than  $\pm 0.05 \text{ K}$ , and an even larger temperature gradient may have been present in their system.

McDuffie and Bien<sup>66</sup> made some modifications to the high-temperature apparatus, and rebuilt the outer part of the chamber. They replaced the original electromagnetic balance with a more sensitive one, and replaced some components with more corrosion-resistant parts. This modified apparatus was used by Braunstein and Braunstein<sup>24</sup> for various binary and ternary electrolyte solutions at 373.4, 393.2, and 422.6 K.

Further improvements to this high-temperature isopiestic apparatus were described by Holmes et al.,<sup>65</sup> and these changes have resulted in a major improvement in the quality of the resulting data. Among these changes was the addition of several "trim" heaters to various positions in the air-bath thermostat, which improved the temperature control to  $\pm 0.015 \text{ K}$ . In addition, they monitored the temperature of the copper heat-transfer block in several positions to check for gradients. They have used this modified apparatus to measure high quality isopiestic data for a number of aqueous binary and ternary electrolyte solutions.<sup>17,65,67-75</sup> Their initial paper<sup>65</sup> should be read by anyone contemplating high-temperature isopiestic measurements.

A few comments about these high-temperature experiments are in order. First, even with the improved temperature control, there was still a temperature gradient of about 0.02 K present across the copper heat-transfer block.<sup>65</sup> This gradient manifests itself by giving systematic differences to the equilibrium molalities, which then depend on the location of the individual sample cup on the heat-transfer block. Above about  $1 \text{ mol} \cdot \text{kg}^{-1}$  this gradient has little effect on the quality of the isopiestic data, but at lower molalities the resulting error in  $\Phi$  increases rapidly. This is understandable in terms of Equations 39 and 40, which indicate that the error in  $\Phi$  depends on  $(\sum_i \nu_i m_i)^{-1}$  for any fixed pair of temperatures. Second, because of the danger of splattering of the solutions when the temperature is changed rapidly from room temperature to a higher temperature, the isopiestic sample containers were added to the chamber with dry salts in them. Analyzed stock solutions can still be used provided the samples are evaporated to dryness before they are put into the apparatus. Injection of water into the system at these high temperatures readily converts the dry solids into aqueous solutions.

Figure 5 is a schematic of the ORNL high-temperature isopiestic unit in its present state of refinement; Figure 6 is a photograph of the electromagnetic balance, and Figure 7 is a photograph of the assembled apparatus in the air thermostat. The photographs were supplied to us by Dr. Howard F. Holmes.

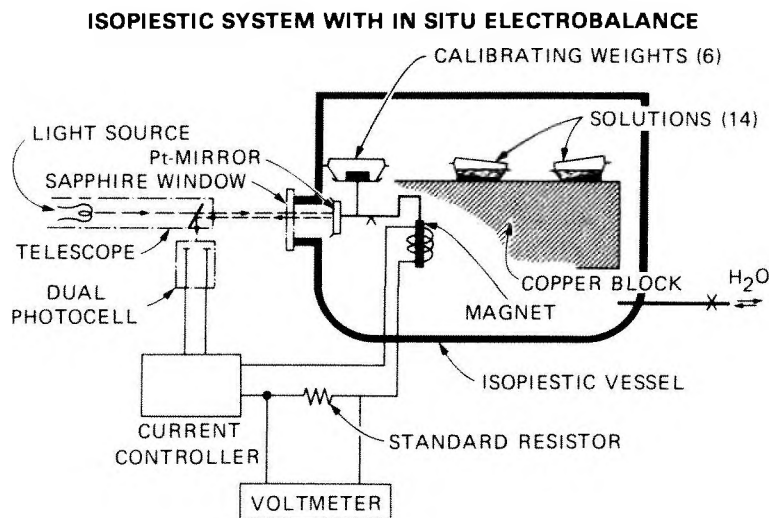


FIGURE 5. Diagram of the high-temperature isopiestic apparatus at Oak Ridge National Laboratory (ORNL). This figure was supplied by Dr. Howard F. Holmes.

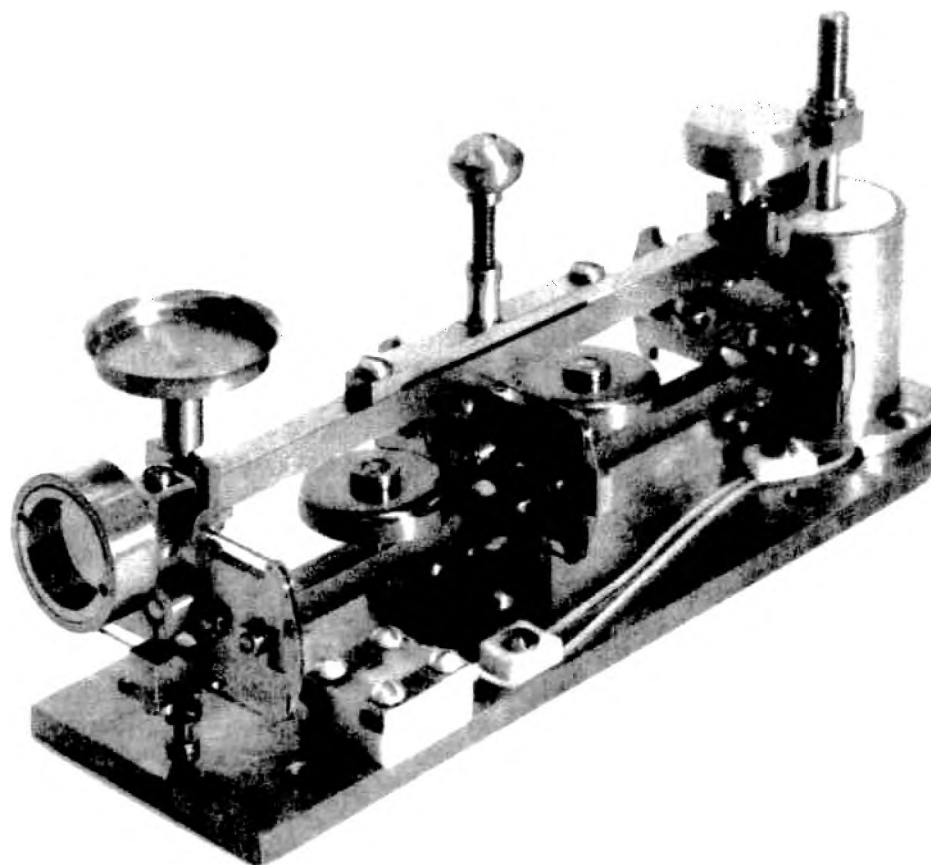


FIGURE 6. Photograph of the electromagnetic balance used for *in situ* weighing in the ORNL high-temperature isopiestic apparatus. This photograph was supplied by Dr. Howard F. Holmes.

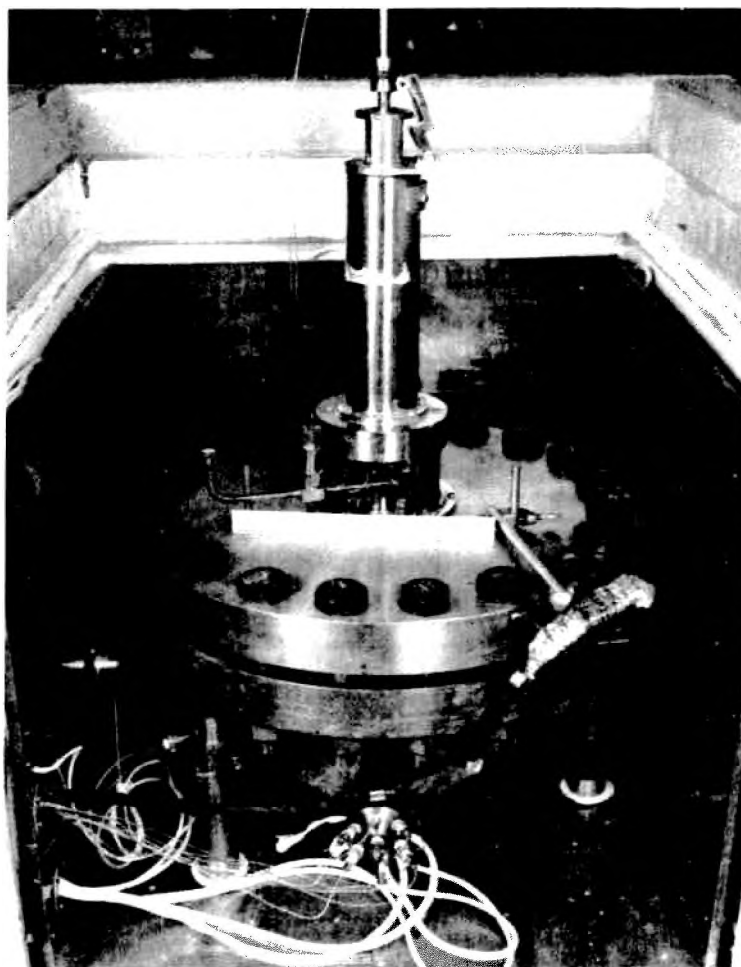


FIGURE 7. Photograph of the ORNL high-temperature isopiestic apparatus in place in the air-bath thermostat. This photograph was supplied by Dr. Howard F. Holmes.

In most of the papers by Holmes et al.,<sup>17,65,67-73</sup> the NaCl reference standard  $\Phi^*$  values were calculated from the equation given by Silvester and Pitzer.<sup>18</sup> In their more recent work<sup>74,75</sup> they used the NaCl evaluation by Pitzer et al.<sup>76</sup>

#### D. RELATED EXPERIMENTAL TECHNIQUES

In this subsection we will describe three experimental techniques that can be used for determining the solvent vapor pressures of electrolyte solutions, and which share some common features with the isopiestic method, but which were not mentioned in the introduction.

The first of these techniques is the bithermal equilibrium method that was used by Stokes<sup>77</sup> for his determination of vapor pressures of aqueous NaCl, NaOH, and  $\text{CaCl}_2$  at 298.15 K. Figure 8 is a redrawing of this apparatus. One copper "dome" contained a cup holding the electrolyte solution being investigated, and the other "dome" contained a sample of pure water. The solvent and solution were then degassed; the solution was maintained at 298.15 K; and the pure solvent sample was cooled in temperature until distillation of solvent ceased. The vapor pressure of the solvent in a solution is then equal to that of the pure solvent at the cooler "equilibrium" temperature; the vapor pressure can be calculated from

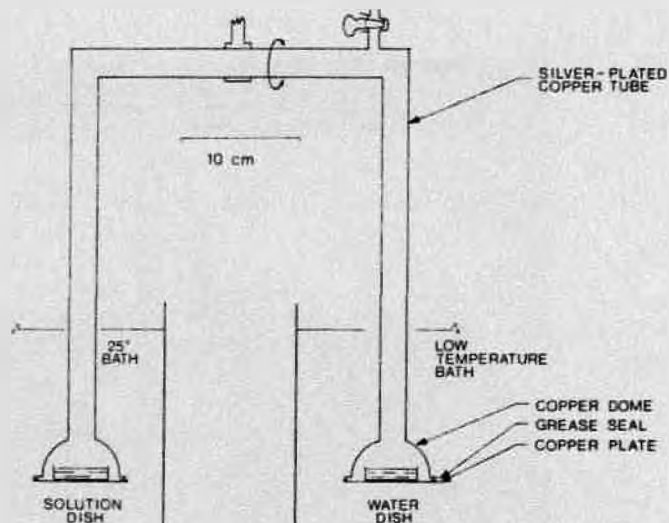


FIGURE 8. Diagram of the bi-thermal equilibrium vapor pressure apparatus of R. H. Stokes. (Adapted with permission from Stokes, R. H., *J. Am. Chem. Soc.*, 69, 1291, 1947. Copyright 1947 by the American Chemical Society.)

that temperature and the equation of state of water. By replacing the solvent sample with an electrolyte solution, or by cooling the solvent until it freezes, even lower water activities could have been investigated by this method.

Because a large temperature gradient is present in these experiments thermal diffusion can occur. This will give rise to a small amount of mass fractionation of the trace amounts of air from the water vapor, and of water containing different isotopes ( $\text{H}_2^{16}\text{O}$  and  $\text{H}_2^{18}\text{O}$ ). Under the experimental conditions used by Stokes,<sup>77</sup> this mass fractionation should have caused an error in the measured water activities of only a few hundredths of a percent. This is less than the error introduced from the uncertainty in determining the temperature of the solvent sample.

The second technique we mention involves the use of a porous-disk osmometer or "isothermal still", whose operation has been described by Williamson.<sup>78</sup> The classical type of osmometer involves a semipermeable membrane, with solution on one side and pure solvent on the other. Solvent is transported through the membrane from the pure solvent to the solution, until the hydrostatic pressure head on the solution side becomes large enough that it causes the movement of solvent to cease and equilibrium is reached.

For the porous-disk osmometer, however, the solution and solvent are not in direct physical contact, but they do exchange solvent through a common vapor phase. A sealed bulb contains the solution and a vapor phase, but into this bulb protrudes a column of solvent with a porous-disk cap on the end, and this column extends above the level of the solution so as to avoid direct liquid-liquid contact. In this case a negative hydrostatic pressure is applied to the pure solvent to change its Gibbs energy to equal that of the solution (in contrast to the classical osmometer where a positive hydrostatic head is applied to the solution) until distillation of solvent ceases. This method generally gives significantly less accurate vapor pressures than direct vapor pressure measurements.

Williamson<sup>78</sup> noted that distillation of solvent from the pure solvent to the solution causes the solvent to cool and the solution to warm, and this temperature difference will oppose the distillation process. Thus good heat conduction is essential for equilibrium to be reached in a reasonable time period. This is also true for an isopiestic apparatus.

The third of these methods for determining vapor pressures was refined by Richardson and Spann<sup>79</sup> and applied by Cohen et al.<sup>80</sup> to a variety of aqueous electrolytes at 293 K. In this method a single particle of solid is electrically charged and then suspended between electrodes. When this is done, the electrical force required to keep the particle motionless will balance the gravitational force, and thus will provide a measure of the mass of the particle. Water vapor is then admitted into the cell until the particle deliquesces, and the electric field is continually changed to keep the particle in balance. Another way of stating this is the charged particle or droplet is suspended in and weighed in an electrodynamic balance. By measuring the change in mass of the particle due to absorption of moisture, the molality can be calculated. Since the relative humidity of the moisture admitted to the cell is known,<sup>80</sup> and the water vapor pressure of the droplet at equilibrium is the same as the humidity used in the experiment, the water activity is thus known. By varying the humidity within the cell, a number of measurements can be done with the same droplet.

Because of the small particle sizes, typically about 20  $\mu\text{m}$  in diameter, and the absence of a physical container for the solution, the particles are much less likely to nucleate than in a bulk sample. Consequently, degrees of supersaturation can be achieved that are considerably higher than can be obtained in an experiment in which macroscopic-sized samples are used. This technique is not capable of anywhere near the precision of direct vapor pressure or isopiestic measurements, but is capable of yielding data at extreme degrees of supersaturation that cannot be studied by the other techniques.

There are two potential sources of inaccuracy in the electrodynamic balance experiments: the Kelvin effect, or change in vapor pressure for small particles due to surface energy contributions; and the change in Gibbs energy due to an electrical charge. Cohen et al.<sup>80</sup> concluded that these two factors were not a significant source of error under their experimental conditions.

## V. SOURCES OF ERROR IN ISOPIESTIC EXPERIMENTS

We have given a fair amount of detail in discussing the historical development of the isopiestic method, and we were very detailed in our discussion of errors that can result from failure to obtain a uniform temperature within the isopiestic chamber. The conclusion we reached was that 3 days should be an adequate equilibrium time in most cases for equilibrations at high and moderate molalities, but somewhat longer equilibrations may be required at low molalities as a consequence of the weak driving force combined with the large amounts of solvent to be transferred between solutions in different cups.

If the rates of heat and mass transfer were the only significant factors affecting the error of isopiestic experiments, then isopiestic data should be reproducible within the precision of the determination of isopiestic equilibrium molalities: within about 0.2% for the isopiestic equilibrium molality ratio and 0.2 to 0.3% for the osmotic coefficients. Although this agreement has been observed for some systems, deviations of several times this amount are frequently encountered between studies from different laboratories. It is therefore obvious that other sources of error may be present that were not always recognized or at least not discussed by the experimentalists.

We will now give a few typical examples of the magnitude of disagreement that may be encountered when comparing isopiestic data from different laboratories. As a source of information for this comparison we will use available critical evaluations of thermodynamic data at 298.15 K for several binary aqueous electrolyte solutions.<sup>81-85</sup> The errors that we mention will be the maximum errors for these systems, and in some cases it was obvious that a single set of results contained the major errors and the remaining sets of data were in much better agreement.

Rard<sup>81</sup> compared isopiestic data from different studies for aqueous  $\text{MnCl}_2$ ,  $\text{MnSO}_4$ , and

RbCl at 298.15 K. The maximum variation in  $\Phi$  was 0.5% for  $\text{MnCl}_2$ , 1.4% for  $\text{MnSO}_4$ , and 1% for RbCl. Similarly, Rard and Miller found that the variation in published  $\Phi$  was about 1% for CsCl and 2% for  $\text{SrCl}_2$ ,<sup>82</sup> and about 0.7% for  $\text{ZnCl}_2$ .<sup>83</sup> A large number of systems have been critically compared by Goldberg et al.<sup>84</sup> and Goldberg,<sup>85</sup> but we will mention only a few. Published  $\Phi$  of  $\text{CoCl}_2$  differ by about 2.3% at high molalities;<sup>84</sup> this difference is also about 2.5% for  $\text{CoBr}_2$ <sup>84</sup> and 1.5% for  $\text{Na}_2\text{SO}_4$ .<sup>85</sup>

In some cases the explanation for this discrepancy is obvious, such as for CsCl. Contamination of CsCl with NaCl is sometimes encountered in commercial material, and which, if present, causes large differences in  $\Phi$ . Unfortunately, in many cases it is impossible to assign realistic errors to a published set of data because of inadequate documentation of experimental details.

It is our hope that a better understanding of the sources and magnitude of various errors for isopiestic experiments will lead to an improvement in the quality and reproducibility of data yet to be measured. With this in mind we will now discuss the sources of errors and imprecision for isopiestic experiments, not including those due to temperature gradients which were discussed in Section IV.A.

#### A. SAMPLE SIZES, REUSE OF SAMPLES, AND EQUILIBRATION TIMES

It is common in isopiestic experiments to use sample sizes in the range 0.8 to 2.0 g, and occasionally samples as large as 3 g are used. However, as we have noted earlier, heat-transfer rates limit the attainment of equilibrium at moderate and high molalities, whereas mass-transport rates may be more important at low molalities. Consequently, it is advantageous to limit sample sizes to those necessary for good experimental precision. Small sample sizes (<1 g) are most important for low molalities where mass-transport rates are inherently lower due to the small chemical potential gradients. These statements are intended to apply for experiments in the temperature range of about 273 to 373 K. At temperatures of 373 K and higher, sample sizes several times this large can be used (e.g., the ORNL high-temperature unit) because of more favorable diffusion and heat-transfer rates.

Isopiestic samples are usually weighed out as liquid samples of an analyzed stock solution, although an anhydrous solid can be used in a few favorable cases. Thus the number of moles of solute that was added to each isopiestic cup should be known accurately. Provided that the solutes are nonvolatile and chemically stable, then simply weighing the samples after an isopiestic equilibrium has occurred will allow the molalities to be calculated because all of the weight gain or loss will be due to solvent. Isopiestic samples can also be reused: more solvent can be added to the cups and the samples reequilibrated. This can be repeated a number of times until the sample sizes become too large; then a new set of smaller samples can be weighed out for use at lower molalities. Alternatively, the solutions can be concentrated and then reequilibrated. Concentrating the solutions can be done either by removing the sample cups from the chamber and putting them into a desiccator with a desiccant, or by adding another cup to the isopiestic chamber with a solution in it that absorbs water. For example, a few drops of concentrated  $\text{H}_2\text{SO}_4$  makes an excellent "sink" for water vapor.

In a few exceptional cases there may be difficulties with the slow evaporation of a supposedly nonvolatile solute, a slow change in pH due to hydrolysis, or slow reaction between the electrolyte solutions and the isopiestic cups. In these cases the results would become progressively less accurate as the samples are reequilibrated. We note, however, that the presence or absence of any of these effects can easily be detected. If a number of equilibrations have been performed with the same solutions, for example, by sequential dilution of a given set of samples, then these samples could be concentrated and then reequilibrated to check whether earlier values of molality ratios are reproduced within their uncertainty limits.

We have already noted that 2- or 3-day isopiestic equilibrations are usually considered

to be adequate, but that somewhat longer times may be required at low molalities. If the kinetics of the approach to isopiestic equilibrium are very favorable, then it should be next to impossible to fail to reach equilibrium and all isopiestic data should be reliable. Unfortunately, this is not the case. To emphasize this point we refer to the very low molality isopiestic study of Gordon.<sup>49</sup> Gordon adjusted his starting molalities to differ by about 10% from the expected molality ratio:

*"This precaution is essential when dealing with dilute solutions, since if the initial concentrations have been chosen near some preconceived idea of the isopiestic ratio and if air has not been completely removed the final concentrations will not have altered appreciably from the initial, and thus may suggest erroneously that equilibrium has been attained."*

Equilibration times are not always given in experimental papers reporting isopiestic data. The traditional equilibration times for 298.15 K in the earlier isopiestic studies was 1 day at high molalities, 2 days at intermediate molalities, and 3 days at low molalities of about 0.1 to 0.2 mol · kg<sup>-1</sup>.<sup>33,35,39-41,48</sup> In several cases a solution of NaCl,<sup>33,36,39,41</sup> KCl,<sup>36</sup> or NaOH<sup>34</sup> was added to the chamber between the metal cups and the heat-transfer block to improve thermal contact, although this needs to be washed off before the cups are weighed. Robinson and Sinclair<sup>35</sup> reported the results of two equilibrations that seemed to indicate that these equilibration periods were sufficient to achieve precise equilibrium molalities.

Scatchard et al.<sup>34</sup> did a number of repeat experiments using these equilibration times, in which aqueous NaCl, KCl, and H<sub>2</sub>SO<sub>4</sub> were equilibrated against each other and against solutions of various organic compounds (sucrose, urea, glycerol). We used these equilibrium molalities and the reference standard  $\Phi^*$  of Hamer and Wu<sup>11</sup> for NaCl and KCl to recalculate  $\Phi$  of H<sub>2</sub>SO<sub>4</sub>. These resulting  $\Phi$  of H<sub>2</sub>SO<sub>4</sub> for molalities of 0.09079 to 0.09095 mol · kg<sup>-1</sup> range from 0.678 to 0.685 which is a 1.0% variation, whereas they should be essentially constant. The scatter in  $\Phi$  is about 0.5% around 0.19 mol · kg<sup>-1</sup>, but the precision is significantly better at higher molalities. This strongly suggests that 3 days is far from adequate to achieve isopiestic equilibrium at these low molalities, and that much longer equilibrations should be used.

In more recent studies, longer equilibrium periods have generally been used. At 298.15 K, for example, Rush and Johnson<sup>45</sup> used 2 to 7 days, Ellerton et al.<sup>36</sup> used 5 days to 2 weeks, Macaskill and Bates<sup>44</sup> used 2 days to 4 weeks, and Libuř et al.<sup>26</sup> used 3 to 21 days. Gordon<sup>49</sup> used 7 to 18 days for very low molalities. Required minimum equilibration times should depend on the materials used to construct the chambers, as well as the solution molalities. Equilibration periods of 1 to 3 days are definitely sufficient above 1 mol · kg<sup>-1</sup> for temperatures above and about 373 K,<sup>57,65</sup> but 2 weeks are required by 0.5 mol · kg<sup>-1</sup> if chambers are not rocked.

The prototype model of the isopiestic chamber used at Livermore<sup>2</sup> was that originally described by Saeger and Spedding.<sup>36</sup> This original setup used gold-plated silver equilibration cups, but these were later replaced by tantalum cups which have superior resistance to corrosion and can even be used for H<sub>2</sub>SO<sub>4</sub> solutions (but, alas, they have only 1/7 of the thermal conductivity of silver). However, these tantalum cups were smaller than the silver cups, so brass retainers had to be added to the recesses in the copper block to give a tight fit with good metal-to-metal contact. The required equilibrium periods at 298.15 K were essentially unaffected by these changes for molalities above 1 mol · kg<sup>-1</sup>, for which 3 to 4 days was adequate. For the silver cups about 2 weeks was required below 0.2 mol · kg<sup>-1</sup>, but for the tantalum cups 4 to 6 weeks was now necessary. This brings up the point that when corrosion-resistant metals such as platinum or tantalum are used to replace the more reactive silver and copper cups, the reduced heat transfer efficiency will require an increase in equilibration times for low molalities.

We noted four paragraphs above that aqueous NaOH or NaCl solutions are sometimes

added to the crevices between the sample cups and the recesses in the heat-transfer block, to serve as an intermediate heat-transfer medium that provides better thermal contact. This procedure has been reported to give better rates of equilibrium for solutions at low molalities.<sup>33,34,36,39,41</sup> However, this technique gives rise to some new problems that need to be discussed.

First, as the sample cups are removed from the chamber they need to be rinsed off and dried to remove this heat-transfer solution. This is somewhat time consuming, and there is the potential for evaporation of solvent from the solutions if the caps on the cups are not tight fitting. In addition, there is no guarantee that this will produce reproducible conditions of surface moisture and thus the weights of the cups may be altered slightly.

Second, the heat-transfer liquid will "attempt" to equilibrate with the solutions in the sample cups by solvent transfer, so extra sources or sinks of heat are present that need to be dissipated for thermal equilibrium to occur. This equilibration of the heat-transfer liquid with the solutions in the cups will be incomplete due to restricted contact with the vapor phase. Thus concentration gradients will build up in the heat-transfer liquid that will dissipate only very slowly by diffusion, and true equilibrium is not likely to be present.

Based on these considerations, we cannot recommend the use of an intermediate heat-transfer liquid unless the fits of the sample cups in the recesses of the heat-transfer block are so poor so as to seriously impede thermal equilibration.

We suggest the following "rule of thumb" in deciding on what equilibrium periods to use for a particular isopiestic chamber and a fixed set of solution cups. First do some preliminary experiments with solutions whose molalities are changed to cover a wide range of water activities. At each water activity equilibrate several replicate samples whose original molalities differ by several percent, and determine the minimum equilibration time required for the molalities to equalize to better than  $\pm 0.1\%$ . This gives the minimum time required for heat and mass transfer to reach equilibrium (or at least steady state) inside the chamber. Then add 50% more time to make sure the temperature inside the chamber is in equilibrium with the constant temperature bath. This procedure should greatly reduce the likelihood of systematic errors being present in low molality isopiestic data.

It is advantageous to adjust these initial molality differences so that equilibrium is approached both from higher and lower molalities for each type of test and reference solution. In this case good agreement between molalities after equilibration is an indicator of thermodynamic equilibrium and not an artifact of the adjustment of the initial molalities.

We note that there are a few aqueous electrolytes that seem to be inherently more sluggish than others in their approach to equilibrium at low molalities. For example, Robinson et al.<sup>87</sup> reported that they were unable to get good equilibrations for aqueous  $\text{Ba}(\text{ClO}_4)_2$  below  $1 \text{ mol} \cdot \text{kg}^{-1}$ , and Rard<sup>88</sup> reported that at about  $0.1 \text{ mol} \cdot \text{kg}^{-1}$  solutions of  $\text{Lu}_2(\text{SO}_4)_3$  did not equilibrate well even when 3-month equilibrations were used.

## B. SYSTEMS WITH SPECIAL DIFFICULTIES

The isopiestic method is simplest to use when only one component is volatile and the solvent and solutes are chemically stable. A few systems have been investigated in which these conditions are not true, and in which the measurements were more difficult and generally less accurate.

For example, Kharchenko et al.<sup>89</sup> did isopiestic measurements for mixtures of benzene and water containing one or more solutes. They referred to this as the double isopiestic method. Aqueous NaCl was used as one reference standard and diphenylmethane in benzene as the other, and the activities of both solvents were determined simultaneously. Kharchenko et al. noted that for this method to work the two solvents must be essentially immiscible in each other. One of the components of the reference standard, diphenylmethane, and one of the solutes, tri-*n*-butylphosphate, were slightly volatile, so the equilibration periods had to be restricted to reduce transport of the solutes.



Bonner<sup>91</sup> performed isopiestic measurements for aqueous solutions of methyl-substituted ammonium chlorides at 298.15 K. He found that  $(\text{CH}_3)_3\text{NHCl}$  was too volatile to allow accurate measurements. However, he performed a few measurements at high molalities as a function of time and then extrapolated the isopiestic molality ratio to zero equilibrium time.

Lantzke et al.<sup>91</sup> performed isopiestic experiments for three molalities of aqueous  $\text{Na}_2\text{SO}_3$  at 298.15 K. In spite of precautions to avoid exposure to air, from 4.4 to 8.5 mol% of the  $\text{Na}_2\text{SO}_3$  was oxidized to  $\text{Na}_2\text{SO}_4$  during the isopiestic equilibrations. Because of the need to correct for the presence of  $\text{Na}_2\text{SO}_4$ , values of  $\Phi$  for  $\text{Na}_2\text{SO}_3$  are fairly uncertain.

Bonner<sup>92</sup> reported isopiestic measurements for aqueous  $\text{K}_4\text{P}_2\text{O}_7$ ,  $\text{Na}_4\text{P}_2\text{O}_7$ , and  $\text{K}_2\text{H}_2\text{P}_2\text{O}_7$  at 298.15 K. Bonner found that  $\text{K}_2\text{H}_2\text{P}_2\text{O}_7$  underwent hydrolysis at a rate of about 1%/week. He measured results for the molality ratio relative to the reference standard as a function of time, and extrapolated the data back to zero hydrolysis (zero time). Inasmuch as it is difficult to reproduce a particular molality in an isopiestic experiment, the extrapolation adds some additional uncertainty to the derived  $\Phi$  values.

Robinson and Lim<sup>93</sup> found that for aqueous  $\text{UO}_2\text{Cl}_2$  molalities above  $3 \text{ mol} \cdot \text{kg}^{-1}$  at 298.15 K, evacuation of air from the isopiestic chamber caused HCl to volatilize from the  $\text{UO}_2\text{Cl}_2$  solutions, and this HCl was then transported to the  $\text{CaCl}_2$  reference standard solutions. Thus measurements at higher molalities were unreliable. Holmes and Mesmer<sup>94</sup> attempted to perform isopiestic measurements for aqueous  $\text{CoCl}_2$  at 413.36 K, but they found that  $\text{CoCl}_2$  solutions irreversibly lost HCl and precipitation of insoluble  $\text{Co}(\text{OH})_2$  occurred.

Platford<sup>94</sup> found that boric acid,  $\text{H}_3\text{BO}_3$ , was slightly volatile under the usual conditions for isopiestic experiments. His  $\text{NaBF}_4$  may have volatilized to a lesser degree, but hydrolysis also occurred.

The remaining systems to be discussed here are not especially difficult to study by the isopiestic technique, but they are systems for which isopiestic data from different investigations show remarkably large differences. They are all heavy metal perchlorates.

Goldberg<sup>95</sup> has critically reviewed isopiestic values for  $\text{UO}_2(\text{ClO}_4)_2$  at 298.15 K. The experimental sets of  $\Phi$  show systematic differences of up to 0.08 by  $4.3 \text{ mol} \cdot \text{kg}^{-1}$ , which is a 2% variation.

Rard et al.<sup>96</sup> and Libuř et al.<sup>96</sup> have reported isopiestic data for various aqueous rare earth perchlorate solutions at 298.15 K, and they studied 11 salts in common. At  $4.0 \text{ mol} \cdot \text{kg}^{-1}$ , for example, there were differences in  $\Phi$  for the same salt of up to 1.8%, although for 8 salts the agreement was to 1.0% or better. Curiously, their data for  $\text{Gd}(\text{ClO}_4)_3$  and for  $\text{Dy}(\text{ClO}_4)_3$  solutions were in essentially complete agreement, but the  $\Phi$  values of Libuř et al. are generally lower than those of Rard et al. for lighter rare earths and higher for heavier rare earths.

Robinson et al.<sup>97</sup> and Rush<sup>97</sup> reported isopiestic data for aqueous  $\text{Ba}(\text{ClO}_4)_2$  at 298.15 K, and their  $\Phi$  values differ by more than 5% at  $5.5 \text{ mol} \cdot \text{kg}^{-1}$ .

Heavy metal perchlorates have very high molar masses, and thus the experimental molalities are quite sensitive to uncertainties in concentration analyses. It is also quite possible that for uranyl and rare earth perchlorates, hydrolysis may not have been properly suppressed in one or more of the studies, and therefore these differences in  $\Phi$  may be due in part to hydrolytic effects. We note that hydrolysis is generally not extensive for rare earth salts, and it can easily be suppressed completely. However, the reaction of hydrolyzed rare earth perchlorates with  $\text{HClO}_4$  is fairly slow, and several days of heating with periodic pH adjustments are required to completely eliminate hydrolysis.

The discrepancies in  $\Phi$  for  $\text{Ba}(\text{ClO}_4)_2$  are extremely large,<sup>97,97</sup> yet we do not expect hydrolysis to be significant for that system. In fact, the differences are so large as to make one wonder whether the same salt was studied.

### C. CORROSION OF SAMPLE CUPS

Up to now our main interest with the isopiestic sample cups has been in regard to their heat-transfer characteristics. However, corrosion of the cup material was noted in a few cases for solutions of certain electrolytes, which casts a doubt on isopiestic data that were measured with those cups. Our main concern with corrosion is because it changes the chemistry of the solution phase and thus its water activity. However, the weight of the cup will also change if the cup is partially dissolved.

In some of the earliest isopiestic studies copper or silver-plated copper was used to construct the isopiestic cups, and silver became the favored material shortly after that. Generally no problems were reported. However, Robinson<sup>48</sup> found that aqueous KI, RbI, and CsI all corroded silver cups, but that chromium plating on the silver cups allowed KI to be studied. The RbI and CsI solutions could also be studied with the chromium-plated cups, but only if contact time between the cup and the solution was kept to a minimum.

Lindenbaum and Boyd<sup>98</sup> performed isopiestic measurements for aqueous tetraalkyl ammonium chlorides, bromides, and iodides at 298.15 K. They reported that some of these solutions caused severe corrosion of the silver isopiestic cups, but they did not specify which of these solutions were involved. Gold-plating the silver cups eliminated that problem. Corrosion of silver cups by alkali metal chlorides and bromides has also been reported at higher temperatures.<sup>60</sup>

Janis and Ferguson<sup>39</sup> attempted to perform isopiestic measurements for aqueous KCl and NaCl solutions in copper cups, but they found that some slight corrosion occurred. They also found that if silver-plated copper cups were used instead for these same solutions, these solutions usually became turbid, presumably from AgCl formation.

It is clear that a silver metal cup without any protective coating is not resistant to corrosion by bromide or iodide solutions, and all data that have been measured in them for these salts must be considered to be suspect. In addition, it is not clear whether silver cups are completely inert to all chloride solutions.

The dishes used in Robinson's earliest measurements<sup>48</sup> were square-shaped in cross section, and were made from sheets of silver that were attached together with silver solder. However, this silver solder was more easily corroded than the silver walls. These "boxes" were therefore replaced with dishes of a circular cross section, which were spun on a lathe from a single disk of silver (private communication, R. H. Stokes, February 22, 1991).

Mason<sup>36</sup> tested stainless steel sample cups with aqueous solutions of various trivalent metal chlorides and found that these cups were easily corroded.

A common procedure that is used for making silver cups more chemically resistant while still retaining their high thermal conductivity is to gold-plate the inner surfaces of the cup. This is a satisfactory solution to the corrosion problem in most cases, but care must be taken to insure that this plating is complete so that no "pinholes" remain to serve as sites for localized corrosion. A more nearly foolproof method is to replace the cups with ones made out of platinum or some other hard and inert metal, but this usually results in a significant lowering of the thermal conductivity.

When investigating a new system of a potentially reactive material, a corrosion test should be done beforehand. This need not be done with the actual isopiestic cups, but it can be easily performed by using an extra piece of the cup material and a few drops of the electrolyte solution. Several weeks of such a test should be sufficient; if present, corrosion is usually obvious from color changes in the solution or pitting of the metal slab.

### D. PURITY OF CHEMICAL REAGENTS

It should be obvious that a prerequisite for measuring accurate isopiestic data is to use electrolytes of high chemical purity. These chemicals may need to be recrystallized in some cases, and it is always a good policy to filter stock solutions to remove insoluble matter

from the starting material. It may be surprising how little experimental detail is typically reported in papers on the isopiestic method with regard to the quality and purity of materials being used. Unfortunately this is also true of most papers in thermodynamics.

In a number of reports on isopiestic data, the only information given about the solutes was their chemical names or formulas. Occasionally either the source of the material or the "grade" of the material was listed (reagent grade, analytical reagent, ultrapure, etc.). In a few cases the manufacturer's claims of impurities were given, but these are not always complete or reliable. It is the exception rather than the rule when actual experimental analyses have been done for the impurity content.

The lack of analytical determinations for the impurity contents is unfortunate but not really surprising, because having these analyses done is an added expense for the research, and thermodynamic research is usually not well funded. In addition, when many of the earlier isopiestic studies were performed, the analytical techniques may not have been refined enough to yield reliable impurity contents.

Professor F. H. Spedding used to tell a classic "horror story" about chemical purity. A supply of ultrapure calcium metal had been purchased for his research group. However, when they melted this calcium they discovered the head of a sledgehammer imbedded in it; it had been lost during a fire at the chemical plant. Although this type of macroscopic impurity is unlikely to be found in a bottle of chemical reagent, sufficient contamination may be present in some cases that vitiates the experimental results.

The presence of a contaminant in an electrolyte solution will affect the derived values of  $\Phi$  in two ways. First, it will affect  $\Phi$  directly because the chemical properties of the contaminant will differ more or less from the major component (such as from differences in ionic hydration or ionic association). Second, it will affect the computed solution molalities if the presence of the impurity or impurities was unknown, because the wrong molar mass will be used when calculating molalities.

Cases of gross chemical contamination of reagents are probably uncommon, and many of the common chemical reagents such as NaCl, KCl, Na<sub>2</sub>SO<sub>4</sub>, sucrose, etc. are generally obtained in high purity. However, there are a few electrolytes for which the presence of significant contamination is the rule rather than the exception, and these impurities may or may not be acknowledged by the company supplying the chemical. The presence of impurities in the solutes may account for some of the larger discrepancies in published isopiestic results, but, because of inadequate chemical characterization or no information at all, it may not be possible to judge with certainty which of the discrepant investigations is in error. We will now give a few examples of the effect of impurities on  $\Phi$  where the presence and concentration of these impurities was well known.

Samples of RbCl, even purportedly pure RbCl, are commonly contaminated with significant amounts of KCl. For example, Rard<sup>81</sup> had two different batches of commercial "99.9%" RbCl analyzed spectroscopically for impurities: one sample actually contained 0.58 mol% KCl and 0.053 mol% NaCl, whereas the other contained 3 mol% KCl and 0.4 mol% NaCl. Osmotic coefficients were also determined for a sample of RbCl to which 1.06 mol% KCl was intentionally added. The presence of this KCl changed  $\Phi$  by about 0.3% or less, depending on molality, as long as the correct molar mass was used in computing molalities. Similarly, the presence of 0.1 mass% Sr in CaCl<sub>2</sub> changed the observed  $\Phi$  by only about 0.1%.<sup>15</sup>

Rard and Miller<sup>14,81</sup> gave examples of supposedly pure divalent metal chlorides that actually had impurities of alkali metal chlorides present. They calculated values of  $\Phi$  for these solutions as if the impurities were not present, in order to determine the errors that would occur if the presence of these impurities had not been known. Such contamination had a large effect on the observed  $\Phi$  values. Both examples given below are for aqueous solutions at 298.15 K.

A sample of  $\text{MgCl}_2$  was studied that contained about 0.2 mass% Na, along with 0.02% Ca and 0.02% Fe.<sup>15</sup> Several equilibrations were performed from 3.3640 to 4.6615 mol · kg<sup>-1</sup>, and the derived values of  $\Phi$  were about 0.6% lower than those obtained with high-purity  $\text{MgCl}_2$ . Rard and Miller<sup>83</sup> also found that values of  $\Phi$  for  $\text{ZnCl}_2$  were very sensitive to small amounts of impurities; they studied a sample with 0.07 mol% of NaCl, along with much smaller amounts Si, Ca, and Mg. For the molality range of 10.335 to 11.133 mol · kg<sup>-1</sup>, the apparent values of  $\Phi$  were about 0.5% higher than values obtained with very high-purity  $\text{ZnCl}_2$ . In this case the major effect seems to have arisen from Na interfering with their method of analyzing the  $\text{ZnCl}_2$  stock solution molality, rendering it unreliable.

In general, the presence of alkali metal impurities in a solution of electrolytes of the type  $\text{MX}_2$  or  $\text{MX}_3$  will significantly lower the observed values of  $\Phi$ . However, the presence of impurities of the same valence type (for example, KCl in RbCl,  $\text{SrCl}_2$  in  $\text{CaCl}_2$ ) usually produces much smaller errors, especially if their presence is known and is taken into consideration when computing molalities.

As one last example, we note that Mason<sup>36</sup> reported isopiestic data for several aqueous rare earth chlorides including  $\text{YCl}_3$ ,  $\text{LaCl}_3$ ,  $\text{CeCl}_3$ ,  $\text{PrCl}_3$ , and  $\text{NdCl}_3$ . Prior to the development of ion-exchange and liquid-liquid extraction methods in the 1950s for the purification and separation of rare earths from each other, samples of rare earths generally contained several percent of the neighboring rare earths. Values of  $\Phi$  for  $\text{RCl}_3$  at a constant molality are more or less S-shaped<sup>99</sup> as a function of atomic number with values for the light and heavy rare earths slowly increasing with atomic number, but those in the middle of the series vary much more rapidly with their atomic number. Consequently, we anticipate that the error of  $\Phi$  for  $\text{RCl}_3$  solutions from the presence of other rare earths will depend on which rare earth was being studied and not just on the impurity levels present.

One thing that should be clear from this discussion is that it is essential to use electrolytes of high purity, and to have them analyzed for impurity content whenever possible. The danger of not doing this is to have an occasional set of very carefully measured isopiestic data rejected by future workers when results become available for material of higher purity.

### E. THE EFFECT OF THE ACCURACY OF CHEMICAL ANALYSIS

We have already mentioned that the molalities of solutions in isopiestic equilibrium are routinely measured with a precision of  $\pm 0.05$  to 0.1%, and thus the molality ratio of the "test" solution to the reference standard will be known to  $\pm 0.1$  to 0.2%. If there were no other sources of error, then isopiestic molality ratios should agree within this precision, and this is sometimes the case. However, this does not mean that the derived  $\Phi$  values will agree within the same limit.

If a number of different solutions are allowed to exchange solvent until isopiestic equilibrium is reached, then they will all have the same solvent activity. Values of

$$\left(\sum_i \nu_i m_i\right)\Phi$$

will thus be identical for all of these solutions. Now suppose that a chemical analysis was performed for the stock solution used for weighing out one of these samples, but that the analysis yielded molalities that were too low by 0.1%. Let  $m_i$  be the correct molality and  $m_i^a$  be the apparent molality calculated from the analysis results. For simplicity we will assume that the molality and osmotic coefficient of the reference standard are accurately known, and that the test solution is a binary solution. Then

$$\begin{aligned} \nu_i m_i \Phi &= \nu_i m_i^a \Phi^a \\ &= 0.999 \nu_i m_i \Phi^a \end{aligned} \quad (57)$$

and thus  $\Phi^a = \Phi/0.999 = 1.001 \Phi$ . This simple calculation indicates that if the molality is too small by 0.1% then  $\Phi^a$  will be too large by 0.1%. However,  $\Phi$  generally increases with molality over most of the molality range (except for low molalities before the minimum in  $\Phi$  is reached, and at very high molalities where a few systems have a maximum). Thus the ‘‘correct’’  $\Phi^a$  at  $m_1^a$  should be even lower. Consequently the error in  $\Phi$  that was calculated from  $m_1^a$  will be about 0.2% at low molalities and 0.25 to 0.3% at high molalities.

It should be clear from this example that when osmotic coefficients are being compared for the same chemical system but from different studies, and that if each test solution and reference standard have molality errors of  $\pm 0.05\%$ , then the isopiestic molality ratios could systematically differ by 0.2% and the derived  $\Phi$  by 0.5%. Clearly, accurate analysis of stock solutions is very important for isopiestic measurements.

We have used  $\pm 0.05\%$  as typical analytical uncertainties for stock solution molalities. These are random errors, and they will partially cancel in many cases so that the corresponding systematic differences may be much smaller. In addition, some solutions like NaCl and KCl can be analyzed with much better precision, so the agreement in  $\Phi$  values could be even better. In fact, the agreement in  $\Phi$  values between different studies is sometimes better than 0.2%, commonly better than 0.3%, and usually better than 0.5 to 0.6%. Larger differences than this sometimes occur but are rare.

#### F. DISCREPANCIES DUE TO CHANGES IN THE REFERENCE STANDARDS

When we discussed the various isopiestic reference standards we noted that their  $\Phi^*$  have uncertainties of 0.1 to 0.3%, depending on the electrolyte and the molality. Suppose isopiestic data were measured for a specific electrolyte solution relative to two or more different standards. Even if the solution molalities are all known very accurately, the derived  $\Phi$  can agree to 0.1% or disagree by 0.3 or 0.4%, and the differences will depend on the molalities of the reference standards. These discrepancies must be considered when assigning absolute errors to derived quantities such as Gibbs energies of solution. However, as long as the equilibrium molalities have been tabulated, the derived results can be corrected later when more accurate  $\Phi^*$  become available for the standards used, and the discrepancies will be reduced or eliminated.

#### G. WEIGHING ERRORS AND VARIOUS WEIGHT CORRECTIONS

The isopiestic method is essentially a gravimetric method provided only one volatile component is present. Weighed samples of electrolyte solution or, occasionally, dry solid are added to the sample cups. Thus the number of moles of electrolyte in each sample cup is known along with the mass of the cup when it was empty. Consequently, any gains or losses in mass during isopiestic equilibrations are due to gains or losses of solvent. The observed changes in mass can then be used in the calculation of the solution molalities at isopiestic equilibrium.

Analytical balances are generally used to weight the sample cups and solution samples, usually to about  $1 \times 10^{-4}$  g. For typical isopiestic sample sizes of 0.8 to 2.0 g, this weighing error affects the calculated molalities only by about 0.01% at low molalities and by 0.02 to 0.03% at high molalities. This is the lower limit of precision that one can normally expect from the isopiestic method. However, some workers have used glass equilibration cups; glass can have an additional problem with buildup of static charge and a significant drift in the apparent weight of the cup with time. This can cause errors in the calculated molality values, and this problem varies in size with different weather conditions. The static electricity on glass can be reduced by special techniques such as wiping the cups with a damp cloth or a cloth moistened with ethanol shortly before weighing them, or by using a radioactive ‘‘static ionizer’’ to counteract the static charge. Even with these precautions, it is likely that weighing errors for glass cups will be several times larger than for metal cups. Being electrical conductors, metal cups do not suffer from this problem.

The process of weighing a sample cup with solution gives a weight not a mass, and the mass of water is really what is required for calculation of molalities. For aqueous solutions around room temperature, making the buoyancy correction reduces the calculated molalities by about 0.1%. For high-temperature isopiestic experiments, the vapor density of water increases rapidly with temperature, and these buoyancy corrections become considerably larger. Thus buoyancy corrections should definitely be made for *in situ* weighing at high temperatures, since to neglect them would result in large errors.

In the first edition of this book Platford<sup>1</sup> observed that buoyancy corrections are frequently neglected when the weighings are done around room temperature. Neglecting buoyancy corrections under these conditions does not result in a serious error because of a certain degree of cancellation when isopiestic molality ratios are used for calculating osmotic coefficients. For example, Rard<sup>2</sup> determined that the equilibrium molality ratio of saturated  $\text{Ho}(\text{NO}_3)_3$  relative to a  $\text{CaCl}_2$  reference standard was 0.9892, but if buoyancy corrections were neglected this ratio only changed to 0.9893. However, neglecting the buoyancy correction did give an absolute error of 0.12% in the calculated saturation molality, and this is several times larger than the precision of the solubility determination. We always make the buoyancy corrections at Livermore, and recommend that they be made. We also note that solution densities only need to be known to a percent or two for the purpose of making buoyancy corrections, and that it is accurate enough to estimate densities for mixtures from densities of the limiting binary solutions at the same ionic strength, by using ionic strength fraction weighting.

If isopiestic sample cups are capped while still inside the chamber at the equilibrium temperature, or if the sample cups are rapidly capped after the chamber has been opened, then some extra solvent will be trapped inside the cups as a solvent-vapor-saturated vapor head. For experiments that are performed at elevated temperatures, some of this solvent will condense and become part of the solution phase as the samples cool to the temperature of the laboratory. For each sample, however, the total mass of the cup plus solution also includes this extra solvent from the vapor head of the cup. The amount of solvent trapped in the vapor head will obviously depend on the vapor pressures of the solutions and will thus increase rapidly with temperature.

We will now estimate the magnitude of the correction (or error, if the presence of the vapor head is neglected). The total mass of solvent vapor in the vapor head will obviously depend on the size of the isopiestic cup and the proportion of the cup not occupied by liquid solution. In some of the early studies somewhat larger cups were used: those of Sinclair<sup>34</sup> and Robinson and Sinclair<sup>35</sup> were 28 or 29  $\text{cm}^3$  in volume. For experiments with air-filled isopiestic chambers, small sample cups with a volume of about 5  $\text{cm}^3$  are typical.<sup>43,46,47</sup> However, for the majority of the studies in which the dimension of the sample cups were reported,<sup>33,38,40,41,45,48,50</sup> the volume of the sample cups ranged from 14 to 19  $\text{cm}^3$ . The cups used at Livermore have an internal volume of 20  $\text{cm}^3$ , but this is reduced to about 18  $\text{cm}^3$  after the platinum gauze is added and the cap put into place.

We will perform our calculations for a typical sample cup with a volume of 16.5  $\text{cm}^3$  containing 1.5  $\text{cm}^3$  of solution. We now calculate the mass of water vapor that would be trapped in this 15- $\text{cm}^3$  vapor head at temperatures of 273.15, 298.15, and 373.15 K. For the case of a vapor-saturated cup containing some pure water as liquid phase, the mass of water vapor in grams will be given by

$$\frac{(15 \text{ cm}^3)(18.0153 \text{ g} \cdot \text{mol}^{-1})}{V_{\text{s(g)}} \text{ cm}^3 \cdot \text{mol}^{-1}} = 270.2/V_{\text{s(g)}}$$

By using the ideal gas volumes for water vapor at saturation as given in Table 1, we calculate

that the 15-cm<sup>3</sup> vapor head contains  $7 \times 10^{-5}$ ,  $3.5 \times 10^{-4}$ , and  $8.8 \times 10^{-3}$  g of water at 273.15, 298.15, and 373.15 K, respectively.

The actual mass of water vapor trapped in the vapor head at the temperature of the isopiestic experiment will be less than this since the vapor pressure of a solution is less than that of the pure solvent. In addition, the mass of the empty cup is generally determined while filled with laboratory air which already contains some water vapor, and we should not count this water twice. For simplicity we will assume that the isopiestic cup is always weighed in air at 298.15 K at 50% relative humidity. Thus the "empty weight" of the cup will include  $1.7 \times 10^{-4}$  g of water vapor. The correction for excess water in the vapor head will be

$$\text{correction in grams} = \frac{270.2}{V_{\text{v(g)}}} \left( P_s(T)/P_s^\circ(T) \right) - 1.7 \times 10^{-4} \quad (58)$$

We will now calculate this mass of water for  $a_s \approx P_s(T)/P_s^\circ(T) = 0.9$  and the same three temperatures. At 273.15 K this correction becomes  $-1.1 \times 10^{-4}$  g, at 298.15 K it is  $1.4 \times 10^{-4}$  g, but at 373.15 K it becomes  $77.7 \times 10^{-4}$  g. Clearly, the correction for the water vapor trapped in the vapor head is very small in the temperature range 273.15 to 298.15 K, on the order of the weighing error, and can usually be neglected. However, at higher temperatures this correction must be made, or serious systematic errors will result.

The isopiestic cups can also absorb small amounts of water vapor on their walls and this absorption error should vary with the vapor pressure of the solutions being investigated. However, we expect this absorption error should be small and essentially cancel when experimental isopiestic molality ratios are used for calculation of osmotic coefficients. We have seen no published reports on this surface absorption of moisture by isopiestic cups. However, we have done a few check experiments at Livermore (unpublished) for our 20-cm<sup>3</sup> cups of tantalum metal. Empty cups were stored in a desiccator above CaSO<sub>4</sub>, weighed while empty, placed in an isopiestic chamber with other sample cups containing aqueous solutions and allowed to equilibrate for several days, and then removed from the chamber and reweighed. No detectable mass change was observed. In addition, empty sample cups were removed from the desiccator and weighed with their polyethylene caps in place. They were then allowed to sit in the laboratory air for 40 to 45 min at 36 to 42% humidity and were reweighed. Weight gains due to moisture absorption were 1 to  $3 \times 10^{-4}$  g, which is fairly small.

Individual isopiestic chambers typically contain around 6 to 18 sample cups. Some workers use duplicate or triplicate samples of each electrolyte in an equilibration because that allows the precision of the experiments to be checked, and to detect and avoid the possibility of using insufficient equilibration times at low molalities. However, some workers use only single samples of each electrolyte so that a larger variety of solutions can be studied in a single experiment. If a weighing error is made when one of the original samples is weighed into the cup, then a large amount of data will be measured that is precise but very inaccurate. It is important to use at least two samples of each electrolyte to detect and avoid such problems.

If two samples of the same electrolyte solution are used for sequential isopiestic equilibrations, and if they consistently have significant differences in their equilibrium molalities, then an initial weighing error is the likely cause. However, if duplicate samples of all of the solutions show a similar discrepancy, then a temperature gradient may be present in the isopiestic chamber. This can be tested for by moving the isopiestic cups from their original locations on the heat-transfer block to recesses on the opposite side of the block; if the discrepancies are pretty much the same after this change is made, then a weighing error is indicated, but if the direction of the molality discrepancies is reversed, then a temperature

gradient is indicated. This brings up the point that if replicate samples of each electrolyte are used, the cups containing them should be placed symmetrically on opposite sides of the heat-transfer block. Persistent temperature gradients are unlikely to be found in isopiestic chambers in a liquid-filled thermostat, but can occur in an air thermostat.

The remaining type of weighing error occurs only for chambers that are opened before the sample cups are capped. Evaporation can occur during this time interval, and the amount of solvent lost will depend on the temperature of the solution relative to the laboratory temperature and on the size of the opening at the top of the isopiestic cups. This error will be quite small for the sample cups capped first and larger for the samples capped last, and will depend on how fast the cups are capped. Evaporation can produce serious errors at high temperatures. At 298.15 K Rard<sup>2</sup> found that with 30 to 45 s required to cap eight sample cups, maximum evaporation errors were 5 to  $6 \times 10^{-4}$  g at low molalities, and 1 to  $2 \times 10^{-4}$  g at high molalities. This corresponded to molality errors of 0.02 to 0.04%. Similarly, Pan<sup>50</sup> reported solvent losses of 1 to  $4 \times 10^{-4}$  g due to evaporation while capping seven sample cups. We note that this evaporation error is opposite in sign to the error from neglecting water vapor trapped in the vapor head, so some cancellation of errors will result.

#### H. SUMMARY OF ERRORS

We have just discussed a number of potential errors for isopiestic experiments, and it is clear that large errors can sometimes occur. However, if some attention is given to using good technique and simple precautions, data of high quality can be obtained. For example, there are four independent sets of isopiestic data for aqueous CsCl and SrCl<sub>2</sub> at 298.15 K that agree with each other to 0.2 or 0.3%,<sup>82</sup> which indicates that highly reproducible results can be obtained (especially since some of these small differences are due to using different isopiestic reference standards).

### VI. SOLUBILITY DETERMINATIONS BY THE ISOPIESTIC METHOD

Our discussion of the isopiestic method has so far been concerned with solvent activity determinations without the presence of a solid phase. Isopiestic measurements are usually done on unsaturated solutions, but it is as easy to do them on supersaturated solutions provided the supersaturated solutions show little tendency to crystallize. For example, Rard<sup>100</sup> performed isopiestic measurements for aqueous La(NO<sub>3</sub>)<sub>3</sub> at 298.15 K up to 8.4591 mol · kg<sup>-1</sup>, which is considerably above the 4.6147-mol · kg<sup>-1</sup> solubility of La(NO<sub>3</sub>)<sub>3</sub> · 6H<sub>2</sub>O. Of the 29 experiments performed in the supersaturated molality region, crystallization only occurred in two cases and even then only one out of two duplicate samples underwent crystallization.

It has long been recognized that the isopiestic method could also be used for the simultaneous determination of the solvent activity and solubility of a saturated solution.<sup>33</sup> Rard<sup>2</sup> has reviewed this application of the isopiestic method with emphasis on binary aqueous electrolyte solutions. The following paragraph was adapted from his discussion.

When an isopiestic solubility determination is to be performed, an extra cup that contains both saturated solution and crystals is added to the chamber. Typically, the amount of solution and crystals in this cup is several times larger than the amount normally used in isopiestic experiments, because this cup functions as a reservoir to absorb or "donate" solvent to the test and reference standard solutions as required. First consider a test solution that is initially below saturation. Once the equilibration is started, the test solution will begin to lose solvent which will be absorbed by the reservoir solution, and some of the crystals will dissolve to maintain saturation. Next consider a test solution that was initially supersaturated; upon the start of the experiment the test solution will absorb solvent vapor from the reservoir, and more crystals will precipitate in the reservoir cup to maintain saturation.



At equilibrium the test solution will have the same solvent activity and molality as the saturated solution in the reservoir cup. Because the test solution contains no solid phase, simply weighing it will give the solubility molality. (Occasionally crystallization may occur in one or more of the test solution cups; even so, as long as that sample does not become completely dry the reference standard solution molality will at least give the solvent activity for saturation of the test solution.)

Consider the dissolution of a hydrated binary electrolyte



for which the thermodynamic solubility product is given by

$$K^\circ = x^x y^y (m/m^\circ)^{(x+y)} \gamma_{\pm}^{(x+y)} a_s^n \quad (60)$$

Here  $m$  is the molality at saturation,  $m^\circ = 1 \text{ mol} \cdot \text{kg}^{-1}$ , and  $\gamma_{\pm}$  is the mean molal activity coefficient of the solute. Both  $m$  and  $a_s$  are obtained directly from an isopiestic solubility experiment, and  $\gamma_{\pm}$  can be calculated from isopiestic data if  $\Phi$  is measured as a function of molality and then extrapolated to infinite dilution. The Gibbs energy of solution can be calculated from this solubility product:

$$\Delta_{\text{sol}}G^\circ = -RT \ln K^\circ \quad (61)$$

The isopiestic solubility determinations should be done at two or more different equilibration times to make sure that the experimental solubility refers to a thermodynamically stable hydrate. Rard<sup>101</sup> gave results for aqueous  $\text{NiCl}_2$  at 298.15 K; this temperature is close to the  $\text{NiCl}_2 \cdot 6\text{H}_2\text{O}/\text{NiCl}_2 \cdot 4\text{H}_2\text{O}$  transition temperature. He did five solubility determinations for different periods ranging from 4 to 13 days, and found that the experimental solubility asymptotically approached the solubility of pure  $\text{NiCl}_2 \cdot 6\text{H}_2\text{O}$  at long equilibration times. For most systems the solubility does not vary with time, so fewer experiments are required.

The application of the isopiestic method to solubilities of aqueous ternary electrolyte solutions has been described in detail by Platford.<sup>102</sup> In this case the reservoir cup must contain one or both of the solid phases, depending on the composition region being studied. Platford noted that the approach to equilibrium can occur very slowly under these conditions, and the precision may be less than for normal isopiestic experiments, because of the presence of solid-solid equilibria such as changes in hydration of crystals.

The most extensive series of sets of experiments for solubilities of ternary and higher-order systems have been performed by V. K. Filippov and colleagues at Leningrad State University. In most cases isopiestic data were measured for unsaturated solutions, and these results were used to predict thermodynamic solubility products. We reference a few of his papers<sup>103-105</sup> and note that additional references to his work can be found in Chapter 3.

## VII. SOURCES OF ISOPIESTIC DATA

A search throughout *Chemical Abstracts* will usually be adequate to tell whether isopiestic data have been published for a particular system, and whether thermodynamic activity data of other types are also available. However, there are various places where one can find numerous papers on the isopiestic method, and some of them will be mentioned in this section.

Throughout the 1930s, 1940s, and 1950s a large amount of isopiestic data and other thermodynamic data for aqueous electrolytes were published in the *Journal of the American Chemical Society* and the *Transactions of the Faraday Society*. In more recent years a large

fraction of isopiestic data has appeared in the *Journal of Chemical and Engineering Data*, the *Journal of Chemical Thermodynamics*, the *Journal of Solution Chemistry*, and the *Russian Journal of Physical Chemistry*. Much useful data can be found in these journals.

Early isopiestic data have been summarized in the extensive tables given in the appendices of the book *Electrolyte Solutions*.<sup>3</sup> Goldberg et al.<sup>106</sup> have provided a very useful bibliography with numerous references to the literature up through the mid-1970s. More recent references to isopiestic studies are given in Chapter 3.

Various members of the Electrolyte Data Center at the National Institute of Standards and Technology (formerly the U.S. National Bureau of Standards) have published critical reviews of osmotic and activity coefficients for a number of aqueous electrolyte solutions at 298.15 K.<sup>9,13,16,84,85,95,107,108</sup> All of these reviews were published in the *Journal of Physical and Chemical Reference Data*, and these articles contain an extensive survey of the published literature. The *Handbook of Aqueous Electrolyte Solutions* by Horvath<sup>109</sup> contains extensive references to experimental thermodynamic data and provides references for numerous review articles and textbooks on electrolyte solution thermodynamics. Horvath's appendices 1 through 5 are particularly useful in this regard.

## VIII. SUITABLE MATERIALS FOR CONSTRUCTION OF AN ISOPIESTIC APPARATUS

We have discussed in Section IV (from the historical viewpoint) the materials from which isopiestic apparatuses have been constructed. Important considerations were mentioned, such as low thermal conductivities for chamber walls, high thermal conductivities for the metal heat-transfer block, and high thermal conductivities and corrosion resistance for the sample cups. In this section we will survey some of the available materials in terms of these properties.

### A. MATERIALS FOR THE ISOPIESTIC CHAMBER WALLS

The outer walls of the isopiestic chamber should be poor thermal conductors in order to dampen out thermal fluctuations in the constant temperature bath. In addition, for measurements with aqueous solutions, the inside of the chamber walls will be subjected to a humid environment, and the chamber may well be equilibrated in a water-filled constant temperature bath. Thus, moisture resistance is also an important property.

Glass desiccators have been the most commonly used material for the construction of isopiestic chambers. They are of a desirable size; they are also designed to allow air to be evacuated, and they are fairly inexpensive. However, chambers of various metals have also been used. Scatchard et al.,<sup>33</sup> Phillips et al.,<sup>40</sup> Soldano et al.,<sup>60</sup> and Rard<sup>2</sup> used stainless steel; Mason<sup>36</sup> and Libuř et al.<sup>26</sup> used brass; and Mason<sup>36</sup> also used monel metal. Rush and Johnson<sup>45</sup> used lucite. The air-filled isopiestic chambers have been constructed out of glass cylinders with tops and bottoms made of metal, usually stainless steel.<sup>43,46,47,51</sup>

Table 9 contains values of the thermal conductivities of various metals and nonmetals that might be considered for construction of an isopiestic apparatus. Values of  $k$  for elements were taken from the critical review of Ho et al.,<sup>110</sup> those for selected alloys are from the *Metals Handbook*<sup>111</sup> or *Building Scientific Apparatus*,<sup>112</sup> those for glasses are from *CRC Handbook of Chemistry and Physics*<sup>113</sup> or *Building Scientific Apparatus*,<sup>112</sup> and those for polymers are from *Building Scientific Apparatus*.<sup>112</sup> The *CRC Handbook* also lists values for many additional types of glasses. Only those elements that had the more desirable chemical properties are listed here. The others were not included for obvious reasons (i.e., they are air or water reactive, they are radioactive, they are easily corroded, they produce toxic corrosion products, or they are too friable).

A thermal conductivity range of about  $0.01$  to  $0.2 \text{ W} \cdot \text{cm}^{-1} \cdot \text{K}^{-1}$  appears to be most

**TABLE 9**  
**Thermal Conductivities (k) of Elements, Selected Alloys, and**  
**Certain Glasses and Polymers at 298.15 K**

Substance	k (W · cm <sup>-1</sup> · K <sup>-1</sup> )	Substance	k (W · cm <sup>-1</sup> · K <sup>-1</sup> )
<b>Elements<sup>a</sup></b>			
Ag	4.29	Mo*	1.38
Al	2.37	Ni	0.909
Au*	3.18	Nb*	0.537
B (polycryst.)	0.274	Pd	0.718
Bi (polycryst.)	0.079	Pt	0.716
C (amorphous)	0.016	Re (polycryst.)	0.480
C (diamond)	9.00, 23.2, 13.6	Rh*	1.50
C (graphite)	0.8—2.2	Ru (polycryst.)*	1.17
Co (polycryst.)	1.00	Si	1.49
Cr (polycryst.)	0.939	Ta*	0.575
Cu	4.01	Sn (polycryst.)	0.668
Ge	0.602	Ti (polycryst.)*	0.219
Hf (polycryst.)	0.230	V*	0.307
In (polycryst.)	0.818	W	1.73
Ir*	1.47	Zn (polycryst.)	1.16
Mg (polycryst.)	1.56	Zr (polycryst.)*	0.23
<b>Metallic Alloys<sup>b</sup></b>			
Red brass	1.6	Stainless steel	0.14
Yellow brass	1.2	Manganin	0.21
Low brass	1.4	Monel	0.19—0.26
Aluminum bronzes	0.38—0.83	Hastalloys	0.1—0.2
Carbon steels	0.45—0.52		
<b>Glasses<sup>c</sup></b>			
Vitreous silica	0.013	Pyrex-type glass	0.011
Vycor glass	0.013	Soda lime	~0.01
Flint glass	0.005—0.008	Fiberglass	0.00002—0.004
<b>Polymers<sup>d</sup></b>			
Nylon	0.0024	Teflon TFE	0.004

<sup>a</sup> Thermal conductivities of the elements are from the review by Ho et al.<sup>110</sup> Only the values for polycrystalline samples are reported for those elements exhibiting anisotropy for single crystals. The three values for diamond are for types I, IIa, and IIb, respectively. An asterisk indicates the metal is fairly corrosion resistant.

<sup>b</sup> Values for alloys were taken from the *Metals Handbook*<sup>111</sup> and from the book *Building Scientific Apparatus*.<sup>112</sup>

<sup>c</sup> Values for glasses were taken from the *CRC Handbook of Chemistry and Physics*<sup>113</sup> with an approximate adjustment to 298.15 K. They also tabulate values for many other types of glasses. Value for fiberglass is from *Building Scientific Apparatus*.<sup>112</sup>

<sup>d</sup> Values for polymers were taken from *Building Scientific Apparatus*.<sup>112</sup>

appropriate for the chamber walls of an isopiestic apparatus. Although brass has occasionally been used, its high thermal conductivity ( $\geq 1.2 \text{ W} \cdot \text{cm}^{-1} \cdot \text{K}^{-1}$ ) indicates it will do an inefficient job of dampening out temperature variations, and thus less precise isopiestic data will likely be produced. It is also likely that the thermal conductivity of some types of fiberglass is too low to make a good chamber material; such a low thermal conductivity

would insure that a very uniform temperature was present in the heat-transfer block but it would greatly increase the time required for the inside of the chamber to reach the mean temperature of the constant temperature bath.

Glass has the advantage of low cost, and glass desiccators do not require any machining to adapt them for isopiestic measurements, but they are breakable. If a glass desiccator were cracked or dropped while under vacuum, there is a danger of implosion. Plastic desiccators are available and have the advantage of being less breakable, although they are unsatisfactory for some organic solvents. Metal chambers have the advantage of being unbreakable, although most pure metals and alloys have thermal conductivities that are too high. Of the metals and metallic alloys listed in Table 9, only a few such as stainless steel and hastalloys have low-enough thermal conductivities. Stainless steel is also resistant to water and many electrolyte solutions.

When consideration is given to all of the important factors (low thermal conductivity, low cost, water resistance, convenience), it appears that the two most suitable materials are glass and stainless steel, although some organic polymers may also be satisfactory.

## **B. MATERIALS FOR THE HEAT-TRANSFER BLOCK**

By far the majority of isopiestic apparatuses have been constructed with a thick slab (2 cm or more) of copper as the heat-transfer block, although brass,<sup>36</sup> and aluminum<sup>57</sup> have also been used. The air-filled isopiestic chambers<sup>43,46,47,51</sup> do not contain a heat-transfer block, but depressions for the isopiestic cups are machined directly into the metal bottom of the chamber. Using the bottom of the chamber for heat transfer is likely to allow larger temperature variation between samples than a conventional design, and thus give lower precision to the resulting data.

Examination of the thermal conductivities listed in Table 9 indicates that the most suitable materials, in decreasing order of their thermal conductivities, are diamond, Ag, Cu, Au, Al, W, brass, Rh, and Si. Such a large slab of diamond is unavailable (and would be unworkable), and Ag, Au, and Rh are much too expensive for such an application. Thus the most satisfactory materials for a heat-transfer block, in decreasing order of preference, are Cu, Al, and brass. We note that high-purity copper and aluminum should be used because certain impurities can greatly reduce their thermal conductivities.

The three most desirable materials for the heat-transfer block, Cu, Al, and brass, are slowly corroded by water vapor, and are more readily attacked by many electrolyte solutions (as might occur, for example, if the solutions splattered during a too-rapid degassing of the chamber). Thus they need to be protected from their environment.

To protect the copper block from corrosion, Sinclair,<sup>34</sup> Braunstein and Braunstein,<sup>24</sup> Janis and Ferguson,<sup>39</sup> and Ellerton et al.<sup>38</sup> used silver plating. However, as we have noted earlier, silver is not completely inert to many common electrolyte solutions and it slowly tarnishes in air. Gold plating of the copper block is more commonly used<sup>33,41,42,44,45,53,98</sup> and it is more satisfactory. We have used a less expensive method for protecting the copper blocks for the chambers used at Livermore:<sup>2,86</sup> only the surfaces of the copper block that are in contact with the sample cups are gold plated, and the rest of the copper block is coated with a clear lacquer.

## **C. MATERIALS FOR THE SAMPLE CUPS**

Although a high thermal conductivity is very desirable for the material used to construct an isopiestic sample cup, it is not the only important factor. Obviously, being resistant to corrosion by the electrolyte solutions is even more important if the resulting isopiestic molalities are to be reliable. In addition, the weight of the "empty cup" should remain constant with time during a series of equilibrations, since all weight gains and losses are assumed to be due to solvent exchange when equilibrium molalities are being calculated.

**TABLE 10**  
**Hardness of Elements, Selected Alloys, and**  
**Glass (Mohs's Hardness Scale)**

Substance	Hardness	Substance	Hardness
<b>Elements*</b>			
Ag	2.5—4	Mo	
Al	2—2.9	Ni	
Au	2.5—3	Nb	
B	9.5 (?)	Pd	4.8
Bi	2.5	Pt	4.3
C (amorphous)		Re	
C (diamond)	10	Rh	
C (graphite)	0.5—1	Ru	6.5
Co		Si	7.0
Cr	9.0	Ta	
Cu	2.5—3	Sn	1.5—1.8
Ge		Ti	
Hf		V	
In	1.2	W	
Ir	6—6.5	Zn	2.5
Mg	2.0	Zr	
<b>Metallic Alloys</b>			
Brasses	3—4	Steels	5—8.5
Platinum-iridium	6.5		
<b>Glass</b>			
Glasses	4.5—6.5		

\* Values for the metallic alloys, glass, and elements were taken from the *CRC Handbook of Chemistry and Physics*.<sup>113</sup> The structural polymorph of boron was not identified, but it is probably the  $\beta$ -rhombohedral form.

Thus there should be no significant change in the mass of the cup due to corrosion, due to surficial oxidation of the cup by atmospheric oxygen, or due to abrasion as the isopiestic cup is repeatedly removed and returned to the recesses in the heat-transfer block. Any such problems will be exaggerated by sequential equilibrations with the same solution samples.

There are several numerical scales that have been proposed for assigning values of hardness to various materials, and these values differ considerably in changing from one scale to another. Many of these differences occur because several different properties are actually being measured. For example, the Mohs scale measures the ease or difficulty of scratching the material, whereas the Vickers hardness scale is a measure of the force required to penetrate the solid with a diamond pyramid penetrator. In addition, the hardness of a particular metal or metallic alloy can change with time due to age hardening or work hardening.

Table 10 contains values of Mohs hardness.<sup>113</sup> Unfortunately, these values are not available for all of the metals of interest. However, O'Neill<sup>114</sup> has given a plot of Vickers hardness for various solid elements at room temperature. The highest values are for diamond,  $\alpha$ -Mn, Si, Ge, Tc, Np, and Os. O'Neill's graph suggests that nearly all of the elements in columns 4 through 10 in the I.U.P.A.C. 18-column periodic table should be sufficiently hard for use as isopiestic cups. For comparison we note that the human fingernail is usually assigned a Mohs hardness of 2.5, and a copper coin a hardness of about 3.5.

Both silver-plated copper<sup>34</sup> and pure silver have been used for constructing isopiestic cups, but as we have mentioned previously, they are not especially resistant to corrosion by halide solutions and can undergo slight weight changes due to tarnishing. It is thus best to avoid these materials.

One of the most common materials for isopiestic cups is gold-plated silver, which retains the high thermal conductivity of silver while giving superior corrosion resistance. Isopiestic cups of this type are quite satisfactory for most applications provided the layer of gold plating that is in contact with the electrolyte solutions is complete and free of "pinholes". However, gold is a fairly soft metal, and thus gold plating can be rubbed off the cups as they are removed and returned to the heat-transfer block. Thus it is best to avoid gold-plating the outside of the silver cups. Pure gold cups were used by Pan,<sup>50</sup> but they are too soft for us to recommend.

Platinum is the next most widely used material for isopiestic cups:<sup>23,26,33,37,41,45</sup> it is fairly inert chemically, it is quite hard, but its thermal conductivity is somewhat lower than silver or gold. Adding a few extra days to the equilibrium times compensates for the lower thermal conductivity. Of the platinum-group metals, both rhodium and iridium or their alloys would be even better for constructing isopiestic cups, because they have higher thermal conductivities and better corrosion resistance, but they do not seem to have been used for this purpose, presumably due to high cost.

Cups of titanium metal are used by the high-temperature group at ORNL,<sup>17</sup> and cups of tantalum metal are used at Livermore.<sup>2</sup> Both metals are highly resistant to corrosion by most electrolyte solutions (but no fluoride solutions should be used in tantalum cups), although they do have lower thermal conductivities and require slightly longer equilibration times than silver. We have also found that cups of tantalum metal undergo almost no weight loss with time due to corrosion or abrasion; weight changes of  $1$  to  $3 \times 10^{-4} \text{ g} \cdot \text{year}^{-1}$  are quite typical for our 44- to 45-g cups.

Because of the lower thermal conductivities of platinum, tantalum, and titanium, the thickness of the walls of these cups should be kept to a minimum consistent with their structural integrity. This should reduce the thermal lag between the heat-transfer block and the solutions in the cups.

Glass sample cups are sometimes still used in isopiestic experiments; however, because of their very poor thermal conductivity, low molality data measured in such cups are not always reliable.

Grjotheim et al.<sup>57</sup> used vitreous carbon for isopiestic measurements at 373 K. Vitreous carbon is a very poor thermal conductor and is extremely soft, so it cannot be recommended for general use. They also used cups of aluminum metal but coated the inside walls with silicone lacquer to make them corrosion resistant. A lacquer coating would be undesirable for room temperature isopiestic measurements because of the resulting poor thermal contact between solution and cup, but it does not appear to be a problem at higher temperatures where equilibrium is reached much more rapidly.

If we had to pick a "perfect" material for an isopiestic cup it would be diamond, perhaps with the inside surface coated with a metal like Ir, Rh, Au, or Pt. Unfortunately such a cup cannot now be constructed.

To summarize this subsection, corrosion resistance is the single most important criterion for choosing which material to use for making isopiestic cups. Of the metals that have been hitherto used for this purpose, Pt, Ta, and Ti seem to be the best. However, silver cups with their internal surface gold plated give more rapid equilibrations because they are better thermal conductors, and are recommended when the likelihood of corrosion is less.

## IX. REPRESENTING ISOPIESTIC DATA WITH EQUATIONS

Numerous equations have been proposed to represent the composition dependence of

activity data for binary and ternary electrolyte solutions. These are equations for  $\Phi$ ,  $\ln \gamma_{\pm}$ , or the excess Gibbs energy for the total solution. It is outside the scope of the present article to discuss all of these equations. However, we note that much information on this subject can be found in Robinson and Stokes's book<sup>3</sup> and in Chapter 1 by Stokes and Chapter 3 by Pitzer in this book. They are well worth reading for the valuable information they contain. Also see the article by Platford in the first edition of this book.<sup>1</sup> A fairly comprehensive listing of published equations for binary solutions is given in the *Handbook of Aqueous Electrolyte Solutions* by Horvath,<sup>109</sup> and that book contains an extensive bibliography of relevant publications. We will conclude our review with a brief discussion of the Debye-Hückel equation and some of its extensions, and give a few comments about excess quantities.

Virtually all representations of activity data for electrolyte solutions include a leading term from some form of the Debye-Hückel equation. We will now derive the equivalent expression for  $\Phi$  from the Debye-Hückel equation for  $\ln \gamma_{\pm}$ .

The Gibbs-Duhem equation for the Gibbs energy can be obtained by differentiating Equation 1 for the case of 1 kg of solvent:

$$dG = 0 = m_s d\mu_s + m_1 d\mu_1 + m_2 d\mu_2 + \dots \quad (62)$$

at constant temperature and pressure. Our discussion will be restricted to a single electrolyte, so only the first two terms on the right-hand side need to be considered. Thus

$$d\mu_s = -\frac{m_1}{m_s} d\mu_1 \quad (63)$$

By using the definitions of  $\Phi$  (Equation 8) and  $\ln \gamma_{\pm}$ , this equation can be recast into the form

$$\Phi = 1 + \frac{1}{m} \int_0^m m \, d \ln \gamma_{\pm} \quad (64)$$

See, for example, p. 34 of Robinson and Stokes.<sup>3</sup>

The Debye-Hückel equation can be written in the form

$$\ln \gamma_{\pm} = -\frac{A|z_a z_c| \sqrt{I_m}}{1 + B\sqrt{I_m}} \quad (65)$$

where  $I_m$  is the molal ionic strength, and  $z_a$  and  $z_c$  are the charges on the anion and cation, respectively. (Actually, this equation should be written on the molar ionic strength scale, but molality is more convenient for most applications.) The Gibbs-Duhem equation is in terms of molality, whereas the Debye-Hückel equation is in terms of ionic strength. These two concentration scales are related by

$$\begin{aligned} I_m &= \frac{1}{2} \sum_i z_i^2 m_i \\ &= m \left( \frac{\sum_i z_i^2 \nu_i}{2} \right) \end{aligned} \quad (66)$$

where  $i$  now denotes an anion or cation. We rewrite the Debye-Hückel equation as

$$\ln \gamma_{\pm} = -\frac{A^*(B^*/B)m^{1/2}}{1 + B^*m^{1/2}} \quad (67)$$

where  $A^* = |z_a z_c| A$  and  $B^* m^{1/2} = B I_m^{1/2}$ .

We differentiate this equation to yield

$$\frac{d \ln \gamma_{\pm}}{d m^{1/2}} = -\frac{A^*(B^*/B)}{(1 + B^* m^{1/2})^2} \quad (68)$$

The equation for  $\Phi$  can then be recast into the form

$$\Phi^{\text{DH}} = 1 - \frac{A^* B^*}{B m} \int_0^m \frac{m \, d m^{1/2}}{(1 + B^* m^{1/2})^2} \quad (69)$$

This integral can be rewritten in the standard form

$$\int_0^u \frac{u^2 du}{(1 + u)^2} = \left[ (1 + u) - (1 + u)^{-1} - 2 \ln(1 + u) \right] \quad (70)$$

where  $u = B^* m^{1/2}$ , and the Debye-Hückel equation for  $\Phi$  is then

$$\Phi^{\text{DH}} = 1 - \frac{A^*}{B(B^*)^2 m} \left[ (1 + B^* m^{1/2}) - (1 + B^* m^{1/2})^{-1} - 2 \ln(1 + B^* m^{1/2}) \right] \quad (71)$$

In various analyses of activity data,  $B$  has either been used as an adjustable parameter for each electrolyte which is related to a distance of closest approach of ions, or "universal" values of  $B$  have been assigned to all electrolytes ( $B$  is usually fixed at between 1 and 1.6 for aqueous solutions). Equation 71 is strictly applicable just for dilute solutions, so higher-order empirical terms are also added on to represent  $\Phi$  at higher molalities. These higher-order terms also compensate for the difference between molar and molal concentrations.

The Debye-Hückel limiting law for  $\ln \gamma_{\pm}$  can be obtained by setting  $B = 0$  in Equation 65. The Debye-Hückel limiting for  $\Phi$  can be obtained by using the Taylor series expansions

$$(1 + u)^{-1} = 1 - u + u^2 - u^3 + u^4 - \dots \quad (72)$$

and

$$\ln(1 + u) = u - \frac{u^2}{2} + \frac{u^3}{3} - \frac{u^4}{4} + \dots \quad (73)$$

for  $u < 1$ . If we now apply these expansions to Equation 70, the terms in square brackets can be rewritten as  $u^3/3 - u^4/4 + \dots$ . If we retain only the term in  $u^3$ , we obtain the Debye-Hückel limiting law:

$$\Phi^{\text{DH,1}} = 1 - \frac{A^*}{3} I_m^{1/2} \quad (74)$$



Lietzke and Stoughton<sup>115</sup> found that the Debye-Hückel equation could be extended to represent isopiestic data to high molalities by adding on a series of terms with  $I_m$  raised to integer powers,

$$\Phi = \Phi^{\text{DH}} + \sum_i A_i' I_m^i \quad (75)$$

where  $\Phi^{\text{DH}}$  is given by Equation 71. This equation has been successfully used to represent the osmotic coefficients of a variety of aqueous 1-1 and 2-1 electrolytes. See, for example, the papers by Hamer and Wu,<sup>9</sup> Downes,<sup>37</sup> Ellerton et al.,<sup>38</sup> Rush and Johnson,<sup>45</sup> and Goldberg and Nuttall.<sup>107,108</sup>

Lietzke and Stoughton<sup>115</sup> also used their equation to represent available isopiestic data for aqueous 2-2 sulfates. However, these data only extend down to about  $0.9 \text{ mol} \cdot \text{kg}^{-1}$ . When data at lower molalities are included, the Lietzke-Stoughton equation is unable to represent the real negative deviations from the DHLL caused by ionic association. For example, values of  $(1 - \Phi)/m^{1/2}$  plotted against  $m^{1/2}$  for aqueous  $\text{CuSO}_4$  have a pronounced maximum that is not reproduced by Equation 75.<sup>116</sup> However, the Pitzer equations can represent this behavior;<sup>116</sup> see Chapter 3 by Pitzer in this book.

As an alternative, an extended form of the Debye-Hückel limiting law can be used:

$$\Phi = \Phi^{\text{DHLL}} + \sum_i A_i' m^i \quad (76)$$

We have found that series in  $m^{1/2}$  and  $m^{1/4}$  are capable of representing  $\Phi$  accurately for a variety of associated electrolytes such as  $\text{MnSO}_4$ ,<sup>81</sup>  $\text{Lu}_2(\text{SO}_4)_3$ ,<sup>88</sup> and  $\text{ZnCl}_2$ ,<sup>83</sup> this equation works equally well for stronger electrolytes such as  $\text{CsCl}$ ,  $\text{SrCl}_2$ ,<sup>82</sup>  $\text{MnCl}_2$ ,<sup>81</sup> and  $\text{NiCl}_2$ ,<sup>101</sup> and for higher-valence salts like rare earth nitrates.<sup>100,101</sup> In general, these series in  $m^{1/2}$  and  $m^{1/4}$  represent  $\Phi$  values as well or better than integer powers in  $I_m$ , and usually fewer coefficients are required.

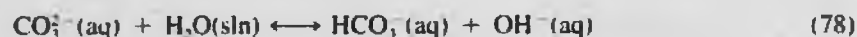
Equations 10, 13, and 71 are generally valid for any valence type of electrolyte, but they are not correct for systems in which chemical reactions occur between the solvent and solute. For example, if an electrolyte is hydrolyzed by water, then some of the solvent will become part of the solutes, and the number of ions present per mole of solute will change. That is, although the system is still formally a single solute in water, hydrolysis will cause it to change into a multicomponent system.

Let quantities that are based on the actual equilibrium speciation be denoted by a superscript *e* and let unsuperscripted quantities denote those calculated using the stoichiometric molalities. A solvent activity measurement yields a solvent activity that is independent of any assumption about speciation. However, the definition of the osmotic coefficient, Equation 8, indicates that it depends on the assumed speciation. Thus the value of  $\Phi^e$  calculated with the actual equilibrium molalities of the various chemical species is given by

$$\Phi^e = \frac{\left( \sum_i \nu_i m_i \right) \Phi}{\sum_i \nu_i^e m_i^e} \quad (77)$$

The effect of hydrolysis on  $\Phi$  and activity coefficients was considered in detail by Peiper and Pitzer<sup>117</sup> and Vanderzee,<sup>118</sup> and discussed later by Goldberg.<sup>119</sup> In each case they studied aqueous  $\text{Na}_2\text{CO}_3$ .

Solutions of carbonates undergo the following reactions:



and



Thus,  $\text{Na}_2\text{CO}_3$  solutions will contain a mixture of  $\text{Na}_2\text{CO}_3$ ,  $\text{NaHCO}_3$ ,  $\text{NaOH}$ , and dissolved  $\text{CO}_2$ , and some of the  $\text{CO}_2$  will appear in the vapor phase. The limiting value of  $\Phi$  for this system at infinite dilution was given as  $\approx 1.33$  by Peiper and Pitzer<sup>117</sup> and 1.395 by Vanderzee.<sup>118</sup> However,  $\Phi^e$  has a limiting value of 1. A more detailed discussion can be found in the two source papers.<sup>117,118</sup> We also note that the isopiestic method is not especially well suited to measurements for carbonate solutions because of the volatility of  $\text{CO}_2$ .

The excess Gibbs energy for a component in a solution is defined as the difference between the actual value and that for an ideal solution, which for the solvent is based on Raoult's law. For 1 mol of solvent using mole fraction statistics to define an ideal solution,

$$\begin{aligned} \mu_i^{\text{ex}} &= RT \ln (a_i/x_i) \\ &= RT \ln f_{i,s} \end{aligned} \quad (80)$$

It should also be possible to define an excess osmotic coefficient by

$$\Phi^{\text{ex}} = \Phi - \Phi^{\text{id}} = -\frac{m_s \ln f_{s,s}}{\sum_i \nu_i m_i} \quad (81)$$

where  $\Phi$  is defined by Equation 8 and  $\Phi^{\text{id}}$  was given by Equation 10. Thus,

$$\Phi^{\text{ex}} = -\frac{m_s \mu_s^{\text{ex}}}{RT \sum_i \nu_i m_i} \quad (82)$$

We are not aware if  $\Phi^{\text{ex}}$  has been defined previously. It contains the same information as  $\mu_s^{\text{ex}}$ , and it is an obvious concept once  $\mu_s^{\text{ex}}$  has been defined.

If  $\Phi^{\text{ex}}$  were defined instead on the basis of molality statistics, i.e.,  $\gamma_{\pm} = 1$ , then  $\Phi^{\text{ex}}$  would be equal to  $\Phi - 1$ .

## ACKNOWLEDGMENTS

This work was supported under the auspices of the Office of Basic Energy Sciences (Geosciences) of the U.S. Department of Energy by the Lawrence Livermore National Laboratory under Contract No. W-7405-ENG-48, and the authors also thank Dr. Lee Younker for some additional support from the Earth Sciences Department at LLNL. The authors thank Karen Roland for the typing of this manuscript with some assistance from Tonya Fletcher, Jackie Oberg, and Susan Ulhorn.

We thank the following individuals for critically reviewing our draft manuscript: Dr. Donald G. Miller (Lawrence Livermore National Laboratory), Dr. Robert N. Goldberg (National Institute of Standards and Technology), Professor Kenneth S. Pitzer (University of California, Berkeley), and Dr. Howard F. Holmes (Oak Ridge National Laboratory). Their suggestions were invaluable for turning our comprehensive review into a comprehensible review.

## REFERENCES

1. **Platford, R. F.**, Experimental methods: isopiestic, in *Activity Coefficients in Electrolyte Solutions*, Vol. 1, 1st ed., Pytkowicz, R. M., Ed., CRC Press, Boca Raton, FL, 1979, chap. 3.
2. **Rard, J. A.**, Solubility determinations by the isopiestic method and application to aqueous lanthanide nitrates at 25°C, *J. Solution Chem.*, 14, 457, 1985; text of talk presented at the I.U.P.A.C. sponsored 1st Int. Symp. on Solubility Phenomena, August 21 to 23, 1984.
3. **Robinson, R. A. and Stokes, R. H.**, *Electrolyte Solutions*, 2nd ed. (revised), Butterworths, London, 1965.
4. **Lewis, G. N., Randall, M., Pitzer, K. S., and Brewer, L.**, *Thermodynamics*, 2nd ed., McGraw-Hill, New York, 1961.
5. **Le Fevre, E. J., Nightingale, M. R., and Rose, J. W.**, The second virial coefficient of ordinary water substance: a new correlation, *J. Mech. Eng. Sci.*, 17, 243, 1975.
6. **Kell, G. S.**, Density, thermal expansivity, and compressibility of liquid water from 0° to 150°C: correlations and tables for atmospheric pressure and saturation reviewed and expressed on 1968 temperature scale, *J. Chem. Eng. Data*, 20, 97, 1975.
7. **Wexler, A. and Greenspan, L.**, Vapor pressure equation for water in the range 0 to 100°C, *J. Res. Natl. Bur. Stand. Sect. A*, 75, 213, 1971.
8. **Rard, J. A., Habenschuss, A., and Spedding, F. H.**, A review of the osmotic coefficients of aqueous CaCl<sub>2</sub> at 25°C, *J. Chem. Eng. Data*, 22, 180, 1977.
9. **Hamer, W. J. and Wu, Y.-C.**, Osmotic coefficients and mean activity coefficients of uni-univalent electrolytes in water at 25°C, *J. Phys. Chem. Ref. Data*, 1, 1047, 1972.
10. **Gibbard, H. F., Jr., Scatchard, G., Rousseau, R. A., and Creek, J. L.**, Liquid-vapor equilibrium of aqueous sodium chloride, from 298 to 373 K and from 1 to 6 mol kg<sup>-1</sup>, and related properties, *J. Chem. Eng. Data*, 19, 281, 1974.
11. **Clarke, E. C. W. and Glew, D. N.**, Evaluation of the thermodynamic functions for aqueous sodium chloride from equilibrium and calorimetric measurements below 154°C, *J. Phys. Chem. Ref. Data*, 14, 489, 1985.
12. **Rard, J. A., Habenschuss, A., and Spedding, F. H.**, A review of the osmotic coefficients of aqueous H<sub>2</sub>SO<sub>4</sub> at 25°C, *J. Chem. Eng. Data*, 21, 374, 1976.
13. **Staples, B. R.**, Activity and osmotic coefficients of aqueous sulfuric acid at 298.15 K, *J. Phys. Chem. Ref. Data*, 10, 779, 1981.
14. **Rard, J. A.**, Isopiestic determination of the osmotic coefficients of aqueous H<sub>2</sub>SO<sub>4</sub> at 25°C, *J. Chem. Eng. Data*, 28, 384, 1983.
15. **Rard, J. A. and Miller, D. G.**, Isopiestic determination of the osmotic and activity coefficients of aqueous MgCl<sub>2</sub> solutions at 25°C, *J. Chem. Eng. Data*, 26, 38, 1981.
16. **Staples, B. R. and Nuttall, R. L.**, The activity and osmotic coefficients of aqueous calcium chloride at 298.15 K, *J. Phys. Chem. Ref. Data*, 6, 385, 1977.
17. **Holmes, H. F. and Mesmer, R. E.**, Thermodynamic properties of aqueous solutions of the alkali metal chlorides to 250°C, *J. Phys. Chem.*, 87, 1242, 1983.
18. **Silvester, L. F. and Pitzer, K. S.**, Thermodynamics of electrolytes. VIII. High-temperature properties, including enthalpy and heat capacity, with application to sodium chloride, *J. Phys. Chem.*, 81, 1822, 1977.
19. **Platford, R. F.**, Osmotic coefficients of aqueous solutions of seven compounds at 0°C, *J. Chem. Eng. Data*, 18, 215, 1973.
20. **Childs, C. W. and Platford, R. F.**, Excess free energies of mixing at temperatures below 25°. Isopiestic measurements on the systems H<sub>2</sub>O-NaCl-Na<sub>2</sub>SO<sub>4</sub> and H<sub>2</sub>O-NaCl-MgSO<sub>4</sub>, *Aust. J. Chem.*, 24, 2487, 1971.
21. **Giauque, W. F., Hornung, E. W., Kunzler, J. E., and Rubin, T. R.**, The thermodynamic properties of aqueous sulfuric acid solutions and hydrates from 15 to 300°K, *J. Am. Chem. Soc.*, 82, 62, 1960.
22. **Garvin, D., Parker, V. B., and White, H. J., Jr., Eds.**, *CODATA Thermodynamic Tables. Selections for Some Compounds of Calcium and Related Mixtures: A Prototype Set of Tables*, Hemisphere Publishing Corporation, Washington, D.C., 1987.
23. **Covington, A. K., Robinson, R. A., and Thompson, R.**, Osmotic and activity coefficients for aqueous methane sulfonic acid solutions at 25°C, *J. Chem. Eng. Data*, 18, 422, 1973.
24. **Braunstein, H. and Braunstein, J.**, Isopiestic studies of very concentrated aqueous electrolyte solutions of LiCl, LiBr, LiNO<sub>3</sub>, Ca(NO<sub>3</sub>)<sub>2</sub>, LiNO<sub>3</sub> + KNO<sub>3</sub>, LiNO<sub>3</sub> + CsNO<sub>3</sub>, and Ca(NO<sub>3</sub>)<sub>2</sub> + CsNO<sub>3</sub>, at 100 to 150°C, *J. Chem. Thermodyn.*, 3, 419, 1971.
25. **Bonner, O. D.**, Osmotic and activity coefficients of the sodium salts of formic, acetic and propionic acids, *J. Solution Chem.*, 17, 999, 1988.
26. **Libuś, Z., Sadowska, T., and Trzaskowski, J.**, Osmotic coefficients of aqueous rare-earth perchlorates and nitrates, *J. Chem. Thermodyn.*, 11, 1151, 1979.
27. **Holden, N. E., Martin, R. L., et al.**, (I.U.P.A.C. commission on atomic weights and isotopic abundances), Atomic weights of the elements 1983, *Pure Appl. Chem.*, 56, 653, 1984.

28. **Robinson, R. A.**, An isopiestic vapor pressure study of the system potassium chloride-sodium chloride in deuterium oxide solutions at 25°, *J. Phys. Chem.*, 73, 3165, 1969.
29. **Platford, R. F.**, Behavior of  $\text{AgClO}_4$  in water and in benzene, *J. Chem. Eng. Data*, 24, 70, 1979.
30. **Bonner, O. D.**, The colligative properties of certain electrolytes and non-electrolytes in methanol, *J. Solution Chem.*, 16, 307, 1987.
31. **Wang, Z.-C., Zhang, X.-H., He, Y.-Z., and Bao, Y.-H.**, A new form of the high-temperature isopiestic technique and its application to mercury-bismuth, mercury-cadmium, mercury-gallium, mercury-indium and mercury-tin binary amalgams, *J. Chem. Soc. Faraday Trans. 1*, 84, 4369, 1988.
32. **Bousfield, W. R.**, Iso-piestic solutions, *Trans. Faraday Soc.*, 13, 401, 1917.
33. **Scatchard, G., Hamer, W. J., and Wood, S. E.**, Isotonic solutions. I. The chemical potential of water in aqueous solutions of sodium chloride, potassium chloride, sulfuric acid, sucrose, urea and glycerol at 25°, *J. Am. Chem. Soc.*, 60, 3061, 1938.
34. **Sinclair, D. A.**, A simple method for accurate determinations of vapor pressures of solutions, *J. Phys. Chem.*, 37, 495, 1933.
35. **Robinson, R. A. and Sinclair, D. A.**, The activity coefficients of the alkali chlorides and of lithium iodide in aqueous solution from vapor pressure measurements, *J. Am. Chem. Soc.*, 56, 1830, 1934.
36. **Mason, C. M.**, The activity and osmotic coefficients of trivalent metal chlorides in aqueous solution from vapor pressure measurements at 25°, *J. Am. Chem. Soc.*, 60, 1638, 1938.
37. **Downes, C. J.**, Osmotic and activity coefficients for mixtures of potassium chloride and strontium chloride in water at 298.15 K, *J. Chem. Thermodyn.*, 6, 317, 1974.
38. **Ellerton, H. D., Reinfelds, G., Mulcahy, D. E., and Dunlop, P. J.**, Activity, density, and relative viscosity data for several amino acids, lactamide, and raffinose in aqueous solution at 25°, *J. Phys. Chem.*, 68, 398, 1964.
39. **Janis, A. A. and Ferguson, J. B.**, Sodium chloride solutions as an isopiestic standard, *Can. J. Res.*, 17B, 215, 1939.
40. **Phillips, B. A., Watson, G. M., and Felsing, W. A.**, Activity coefficients of strontium chloride by an isopiestic method, *J. Am. Chem. Soc.*, 64, 244, 1942.
41. **Miller, G. and Porter, A. S.**, Activity coefficients of some polyphosphates in aqueous solution, *Trans. Faraday Soc.*, 63, 335, 1967.
42. **Humphries, W. T., Kohrt, C. F., and Patterson, C. S.**, Osmotic properties of some aqueous electrolytes at 60°C, *J. Chem. Eng. Data*, 13, 327, 1968.
43. **Kirgintsev, A. N. and Luk'yanov, A. V.**, Non-vacuum apparatus for determining vapour pressure by the isopiestic method, *Russ. J. Phys. Chem.*, 37, 121, 1963.
44. **Macaskill, J. B. and Bates, R. G.**, Osmotic and activity coefficients of Tris sulfate from isopiestic vapor pressure measurements at 25°C, *J. Chem. Eng. Data*, 31, 416, 1986.
45. **Rush, R. M. and Johnson, J. S.**, Osmotic coefficients of synthetic sea-water solutions at 25°C, *J. Chem. Eng. Data*, 11, 590, 1966.
46. **Michimoto, T., Awakura, Y., and Majima, H.**, Isopiestic determination of the activity of water in aqueous sulfuric acid-sulfate systems, *Denki Kagaku*, 51, 373, 1983.
47. **Yamauchi, C. and Sakao, H.**, Determination of water and solute activities in  $\text{H}_2\text{SO}_4\text{-In}_2(\text{SO}_4)_3\text{-H}_2\text{O}$  system, *Trans. Jpn. Inst. Met.*, 28, 327, 1987.
48. **Robinson, R. A.**, The activity coefficients of the alkali bromides and iodides in aqueous solution from vapor pressure measurements, *J. Am. Chem. Soc.*, 57, 1161, 1935.
49. **Gordon, A. R.**, Isopiestic measurements in dilute solutions; the system potassium chloride-sodium chloride at 25° at concentrations from 0.03 to 0.10 molal, *J. Am. Chem. Soc.*, 65, 221, 1943.
50. **Pan, C.-F.**, Osmotic and Activity Coefficients in  $\text{BaCl}_2\text{-ZnCl}_2\text{-H}_2\text{O}$  at 25°C, Ph.D. dissertation, University of Kansas, Lawrence, May 1966.
51. **Majima, H. and Awakura, Y.**, Water and solute activities of  $\text{H}_2\text{SO}_4\text{-Fe}_2(\text{SO}_4)_3\text{-H}_2\text{O}$  and  $\text{HCl-FeCl}_3\text{-H}_2\text{O}$  solution systems. I. Activities of water, *Metall. Trans.*, 16B, 433, 1985.
52. **Robinson, R. A.**, The heat content and heat capacity of sodium chloride solutions, *Trans. Faraday Soc.*, 35, 1222, 1939.
53. **Hellams, K. L., Patterson, C. S., Prentice, B. H., III, and Taylor, M. J.**, Osmotic properties of some aqueous solutions at 45°C, *J. Chem. Eng. Data*, 10, 323, 1965.
54. **Moore, J. T., Humphries, W. T., and Patterson, C. S.**, Isopiestic studies of some aqueous electrolyte solutions at 80°C, *J. Chem. Eng. Data*, 17, 180, 1972.
55. **Davis, T. M., Duckett, L. M., Owen, J. F., Patterson, C. S., and Saleeby, R.**, Osmotic coefficients of aqueous LiCl and KCl from their isopiestic ratios to NaCl at 45°C, *J. Chem. Eng. Data*, 30, 432, 1985.
56. **Bonner, O. D. and Breazeale, W. H.**, Osmotic and activity coefficients of some nonelectrolytes, *J. Chem. Eng. Data*, 10, 325, 1965.
57. **Grjotheim, K., Voigt, W., Haugsdal, B., and Dittrich, D.**, Isopiestic determination of osmotic coefficients at 100°C by means of a simple apparatus, *Acta Chem. Scand. Ser. A*, 42, 470, 1988.

58. **Voigt, W., Dittrich, A., Haugsdal, B., and Grjotheim, K.**, Thermodynamics of aqueous reciprocal salt systems. II. Isopiestic determination of the osmotic and activity coefficients in  $\text{LiNO}_3\text{-NaBr-H}_2\text{O}$  and  $\text{LiBr-NaNO}_3\text{-H}_2\text{O}$  at  $100.3^\circ\text{C}$ , *Acta Chem. Scand.*, 44, 12, 1990.
59. **Voigt, W., Haugsdal, B., and Grjotheim, K.**, Thermodynamics of reciprocal salt systems. III. Isopiestic determination of the osmotic and activity coefficients of the system  $\text{Li}^+, \text{Na}^+/\text{Cl}^-, \text{NO}_3^- \text{-H}_2\text{O}$  at  $100.3^\circ\text{C}$ , *Acta Chem. Scand.*, 44, 311, 1990.
60. **Soldano, B. A., Stoughton, R. W., Fox, R. J., and Scatchard, G.**, A high-temperature isopiestic unit, in *The Structure of Electrolytic Solutions*, Hamer, W. J., Ed., John Wiley & Sons, New York, 1959, chap. 14.
61. **Patterson, C. S., Gilpatrick, L. O., and Soldano, B. A.**, The osmotic behavior of representative aqueous salt solutions at  $100^\circ$ , *J. Chem. Soc.*, p. 2730, 1960.
62. **Soldano, B. A. and Patterson, C. S.**, Osmotic behavior of aqueous salt solutions at elevated temperatures. II, *J. Chem. Soc.*, p. 937, 1962.
63. **Soldano, B. A. and Meek, M.**, Isopiestic vapour-pressure measurements of aqueous salt solutions at elevated temperatures. III, *J. Chem. Soc.*, p. 4424, 1963.
64. **Soldano, B. A. and Bien, P. B.**, Osmotic behavior of aqueous salt solutions at elevated temperatures. IV, *J. Chem. Soc. A.* p. 1825, 1966.
65. **Holmes, H. F., Baes, C. F., Jr., and Mesmer, R. E.**, Isopiestic studies of aqueous solutions at elevated temperatures. I.  $\text{KCl}$ ,  $\text{CaCl}_2$ , and  $\text{MgCl}_2$ , *J. Chem. Thermodyn.*, 10, 983, 1978.
66. **McDuffie, H. F. and Bien, P. B.**, High-temperature isopiestic studies, in *Reactor Chemistry Division Annual Progress Report for Period Ending December 31, 1967*, ORNL-4229, 1967, 102.
67. **Holmes, H. F., Baes, C. F., Jr., and Mesmer, R. E.**, Isopiestic studies of aqueous solutions at elevated temperatures. II.  $\text{NaCl} + \text{KCl}$  mixtures, *J. Chem. Thermodyn.*, 11, 1035, 1979.
68. **Holmes, H. F., Baes, C. F., Jr., and Mesmer, R. E.**, Isopiestic studies of aqueous solutions at elevated temperatures. III.  $\{(1-y)\text{NaCl} + y\text{CaCl}_2\}$ , *J. Chem. Thermodyn.*, 13, 101, 1981.
69. **Holmes, H. F. and Mesmer, R. E.**, Isopiestic studies of aqueous solutions at elevated temperatures. IV.  $\text{NiCl}_2$  and  $\text{CoCl}_2$ , *J. Chem. Thermodyn.*, 13, 131, 1981.
70. **Holmes, H. F. and Mesmer, R. E.**, Isopiestic studies of aqueous solutions at elevated temperatures. V.  $\text{SrCl}_2$  and  $\text{BaCl}_2$ , *J. Chem. Thermodyn.*, 13, 1025, 1981.
71. **Holmes, H. F. and Mesmer, R. E.**, Isopiestic studies of aqueous solutions at elevated temperatures. VI.  $\text{LiCl}$  and  $\text{CsCl}$ , *J. Chem. Thermodyn.*, 13, 1035, 1981.
72. **Holmes, H. F. and Mesmer, R. E.**, Isopiestic studies of aqueous solutions at elevated temperatures. VII.  $\text{MgSO}_4$  and  $\text{NiSO}_4$ , *J. Chem. Thermodyn.*, 15, 709, 1983.
73. **Holmes, H. F. and Mesmer, R. E.**, Isopiestic studies of aqueous solutions at elevated temperatures. VIII. The alkali-metal sulfates, *J. Chem. Thermodyn.*, 18, 263, 1986.
74. **Holmes, H. F. and Mesmer, R. E.**, Isopiestic studies of aqueous solutions at elevated temperatures. IX.  $\{(1-y)\text{NaCl} + y\text{LiCl}\}$ , *J. Chem. Thermodyn.*, 20, 1049, 1988.
75. **Holmes, H. F. and Mesmer, R. E.**, Isopiestic studies of aqueous solutions at elevated temperatures. 10.  $\{(1-y)\text{NaCl} + y\text{CsCl}\}(\text{aq})$ , *J. Phys. Chem.*, 94, 7800, 1990.
76. **Pitzer, K. S., Peiper, J. C., and Busey, R. H.**, Thermodynamic properties of aqueous sodium chloride solutions, *J. Phys. Chem. Ref. Data*, 13, 1, 1984.
77. **Stokes, R. H.**, The measurement of vapor pressures of aqueous solutions by bi-thermal equilibration through the vapor phase, *J. Am. Chem. Soc.*, 69, 1291, 1947.
78. **Williamson, A. T.**, The mechanism of isothermal distillation in the porous-disk osmometer, *Proc. R. Soc. London Ser. A*, 195, 97, 1948.
79. **Richardson, C. B. and Spann, J. F.**, Measurement of the water cycle in a levitated ammonium sulfate particle, *J. Aerosol Sci.*, 15, 563, 1984.
80. **Cohen, M. D., Flagan, R. C., and Seinfeld, J. H.**, Studies of concentrated electrolyte solutions using the electrodynamic balance. I. Water activities for single-electrolyte solutions, *J. Phys. Chem.*, 91, 4563, 1987.
81. **Rard, J. A.**, Isopiestic determination of the osmotic and activity coefficients of aqueous  $\text{MnCl}_2$ ,  $\text{MnSO}_4$ , and  $\text{RbCl}$  at  $25^\circ\text{C}$ , *J. Chem. Eng. Data*, 29, 443, 1984.
82. **Rard, J. A. and Miller, D. G.**, Isopiestic determination of the osmotic and activity coefficients of aqueous  $\text{CsCl}$ ,  $\text{SrCl}_2$ , and mixtures of  $\text{NaCl}$  and  $\text{CsCl}$  at  $25^\circ\text{C}$ , *J. Chem. Eng. Data*, 27, 169, 1982.
83. **Rard, J. A. and Miller, D. G.**, Isopiestic determination of the osmotic and activity coefficients of  $\text{ZnCl}_2(\text{aq})$  at  $298.15\text{ K}$ , *J. Chem. Thermodyn.*, 21, 463, 1989.
84. **Goldberg, R. N., Nuttall, R. L., and Staples, B. R.**, Evaluated activity and osmotic coefficients for aqueous solutions: iron chloride and the bi-univalent compounds of nickel and cobalt, *J. Phys. Chem. Ref. Data*, 8, 923, 1979.
85. **Goldberg, R. N.**, Evaluated activity and osmotic coefficients for aqueous solutions: thirty-six uni-bivalent electrolytes, *J. Phys. Chem. Ref. Data*, 10, 671, 1981.

86. **Saeger, V. W. and Spedding, F. H.**, Some Physical Properties of Rare-Earth Chlorides in Aqueous Solution. IS-338. Ames Laboratory, November 1960.
87. **Robinson, R. A., Lim, C. K., and Ang, K. P.**, The osmotic and activity coefficients of calcium, strontium and barium perchlorate at 25°, *J. Am. Chem. Soc.*, 75, 5130, 1953.
88. **Rard, J. A.**, Isopiestic determination of the osmotic and activity coefficients of aqueous  $\text{Lu}_2(\text{SO}_4)_3$  at 25°C, *J. Solution Chem.*, 19, 525, 1990.
89. **Kharchenko, S. K., Luk'yanov, A. V., and Mikhailov, V. A.**, Method of double isopiestic measurements, *Russ. J. Phys. Chem.*, 42, 977, 1968.
90. **Bonner, O. D.**, Osmotic and activity coefficients of methyl-substituted ammonium chlorides, *J. Chem. Soc. Faraday Trans. 1*, 77, 2515, 1981.
91. **Lantzke, I. R., Covington, A. K., and Robinson, R. A.**, Osmotic and activity coefficients of sodium dithionate and sodium sulfite at 25°C, *J. Chem. Eng. Data*, 18, 421, 1973.
92. **Bonner, O. D.**, The osmotic and activity coefficients of some pyrophosphates, *J. Chem. Thermodyn.*, 11, 559, 1979.
93. **Robinson, R. A. and Lim, C. K.**, The osmotic and activity coefficients of uranyl nitrate, chloride, and perchlorate at 25°, *J. Chem. Soc.*, p. 1840, 1951.
94. **Platford, R. F.**, Osmotic and activity coefficients of some simple borates in aqueous solutions at 25°, *Can. J. Chem.*, 47, 2271, 1969.
95. **Goldberg, R. N.**, Evaluated activity and osmotic coefficients for aqueous solutions: bi-univalent compounds of lead, copper, manganese, and uranium, *J. Phys. Chem. Ref. Data*, 8, 1005, 1979.
96. **Rard, J. A., Weber, H. O., and Spedding, F. H.**, Isopiestic determination of the activity coefficients of some aqueous rare earth electrolyte solutions at 25°C. 2. The rare earth perchlorates, *J. Chem. Eng. Data*, 22, 187, 1977.
97. **Rush, R. M.**, Isopiestic measurements of the osmotic and activity coefficients for the system  $\text{HClO}_4\text{-Ba}(\text{ClO}_4)_2\text{-H}_2\text{O}$  at 25°C, *J. Chem. Eng. Data*, 31, 478, 1986.
98. **Lindenbaum, S. and Boyd, G. E.**, Osmotic and activity coefficients for the symmetrical tetraalkyl ammonium halides in aqueous solution of 25°, *J. Phys. Chem.*, 68, 911, 1964.
99. **Spedding, F. H., Weber, H. O., Saeger, V. W., Petheram, H. H., Rard, J. A., and Habenschuss, A.**, Isopiestic determination of the activity coefficients of some aqueous rare earth electrolyte solutions at 25°C. 1. The rare earth chlorides, *J. Chem. Eng. Data*, 21, 341, 1976.
100. **Rard, J. A.**, Osmotic and activity coefficients of aqueous  $\text{La}(\text{NO}_3)_3$  and densities and apparent molal volumes of aqueous  $\text{Eu}(\text{NO}_3)_3$  at 25°C, *J. Chem. Eng. Data*, 32, 92, 1987.
101. **Rard, J. A.**, Isopiestic determination of the osmotic and activity coefficients of aqueous  $\text{NiCl}_2$ ,  $\text{Pr}(\text{NO}_3)_3$ , and  $\text{Lu}(\text{NO}_3)_3$  and solubility of  $\text{NiCl}_2$  at 25°C, *J. Chem. Eng. Data*, 32, 334, 1987.
102. **Platford, R. F.**, Isopiestic determination of solubilities in mixed salt solutions. Two salt system, *Am. J. Sci.*, 272, 959, 1972.
103. **Filippov, V. K. and Cheremnykh, L. N.**, The thermodynamic study of the  $\text{Mg} \parallel \text{Cl}, \text{SO}_4\text{-H}_2\text{O}$  system at 25°, *Sov. Prog. Chem.*, 50(10), 20, 1984.
104. **Filippov, V. K., Charykova, M. V., and Trofimov, Yu. M.**, Thermodynamic study of the systems  $\text{Na}^+, \text{NH}_4^+ \parallel \text{SO}_4^{2-}\text{-H}_2\text{O}$  and  $\text{Na}^+, \text{NH}_4^+ \parallel \text{H}_2\text{PO}_4^-\text{-H}_2\text{O}$  at 25°C, *J. Appl. Chem. U.S.S.R.*, 60, 237, 1987.
105. **Filippov, V. K., Kalinkin, A. M., and Vasin, S. K.**, Thermodynamics of phase equilibria of aqueous (lithium sulfate + alkali-metal sulfate) (alkali metal: Na, K, and Rb) and (sodium sulfate + rubidium sulfate), at 298.15 K using Pitzer's model, *J. Chem. Thermodyn.*, 21, 935, 1989.
106. **Goldberg, R. N., Staples, B. R., Nuttall, R. L., and Arbuckle, R.**, A Bibliography of Sources of Experimental Data Leading to Activity or Osmotic Coefficients for Polyvalent Electrolytes in Aqueous Solution, NBS Special Publ. 485, U.S. Government Printing Office, Washington, D.C., 1977.
107. **Goldberg, R. N. and Nuttall, R. L.**, Evaluated activity and osmotic coefficients for aqueous solutions: the alkaline earth metal halides, *J. Phys. Chem. Ref. Data*, 7, 263, 1978.
108. **Goldberg, R. N.**, Evaluated activity and osmotic coefficients for aqueous solutions: bi-univalent compounds of zinc, cadmium, and ethylene bis(trimethylammonium) chloride and iodide, *J. Phys. Chem. Ref. Data*, 10, 1, 1981.
109. **Horvath, A. L.**, *Handbook of Aqueous Electrolyte Solutions. Physical Properties, Estimation and Correlation Methods*, Ellis Horwood, Chichester, U.K., 1985.
110. **Ho, C. Y., Powell, R. W., and Liley, P. E.**, Thermal conductivity of the elements, *J. Phys. Chem. Ref. Data*, 1, 279, 1972.
111. **Lyman, T., Ed.**, *Metals Handbook*. Vol. 1, 8th ed., American Society for Metals, Metals Park, OH, 1961.
112. **Moore, J. H., Davis, C. C., and Coplan, M. A.**, *Building Scientific Apparatus*, 2nd ed., Addison-Wesley, Redwood City, CA, 1989.
113. **Weast, R. C., Astle, M. J., and Beyer, W. H., Eds.**, *CRC Handbook of Chemistry and Physics*, 68th ed., CRC Press, Boca Raton, FL, 1987.

114. **O'Neill, H.**, *Hardness Measurement of Metals and Alloys*, 2nd ed., Chapman and Hall, London, 1967.
115. **Lietzke, M. H. and Stoughton, R. W.**, The calculation of activity coefficients from osmotic coefficient data, *J. Phys. Chem.*, 66, 508, 1962.
116. **Miller, D. G., Rard, J. A., Eppstein, L. B., and Robinson, R. A.**, Mutual diffusion coefficients, electrical conductances, osmotic coefficients, and ionic transport coefficients  $I_{ij}$  for aqueous  $\text{CuSO}_4$  at 25°C, *J. Solution. Chem.*, 9, 467, 1980.
117. **Peiper, J. C. and Pitzer, K. S.**, Thermodynamics of aqueous carbonate solutions including mixtures of sodium carbonate, bicarbonate, and chloride, *J. Chem. Thermodyn.*, 14, 613, 1982.
118. **Vanderzee, C. E.**, Thermodynamic properties of solutions of a hydrolyzing electrolyte: relative partial molar enthalpies and heat capacities, solvent activities, osmotic coefficients, and solute activity coefficients of aqueous sodium carbonate, *J. Chem. Thermodyn.*, 14, 1051, 1982.
119. **Goldberg, R. N.**, An equilibrium model for the calculation of activity and osmotic coefficients in aqueous solutions, *J. Res. Natl. Bur. Stand.*, 89, 251, 1984.





## Chapter 6

**ACTIVITY COEFFICIENTS IN NATURAL WATERS**

Simon L. Clegg and Michael Whitfield

**TABLE OF CONTENTS**

I.	Introduction .....	281
A.	The Composition of Natural Waters .....	281
1.	The Hydrological Cycle .....	281
2.	The Stoichiometry of Seawater — a Case Study .....	283
a.	The Salinity Concept and the Density of Seawater .....	283
b.	Seawater as a Multicomponent Electrolyte Solution .....	286
c.	The Stoichiometry of Sea Salt .....	289
B.	The Relevance of Equilibrium Thermodynamics .....	290
1.	Chemical Potential in Closed Systems .....	290
2.	Chemical Potential in Open Systems .....	292
II.	Calculation of Activity Coefficients .....	293
A.	Ion Association Models .....	293
B.	Ion Interaction Models .....	294
1.	The Pitzer Model .....	295
a.	Interaction Parameters .....	299
i.	Single Salt Solutions .....	299
ii.	Multicomponent Salt Solutions .....	301
iii.	Neutral Solutes .....	302
iv.	Neutral Solutes and Dissolved Salts .....	302
b.	Ion Pairing and Ion Association .....	304
c.	Parameter Values .....	306
III.	Applied Calculations in Natural Waters .....	313
A.	Solutions of Strong Electrolytes .....	313
1.	The Major Components of Seawater, and the Activity Coefficient of Sea Salt .....	315
2.	Mineral Solubilities .....	317
a.	Gypsum Solubility in Salt Solutions and Brines .....	318
3.	Solutions Containing Sulfuric Acid .....	322
4.	Solubility of Volatile Strong Electrolytes .....	324
5.	Supersaturated Solutions .....	327
6.	Thermodynamic Properties over the Entire Concentration Range — $\text{HNO}_3$ .....	328
B.	Neutral Solutes .....	329
1.	Empirical Representations of Solubility .....	332
2.	Theoretical Prediction of Setchenow Coefficients .....	334
3.	Solubility of Atmospheric Gases in Water and Seawater .....	335
a.	Application of the Pitzer Model .....	337
4.	Gas Solubility Data .....	346

C.	Weak Electrolytes .....	349
1.	Weak Acid-Base Equilibria in Natural Waters .....	350
2.	Potentiometry and the Definition of pH Scales in Saline Media .....	352
a.	Hydrogen Ion Concentration and Activity in Aqueous Solution .....	353
i.	NBS Scale .....	353
ii.	Total Hydrogen Ion Concentration Scale .....	354
iii.	Free Hydrogen Ion Concentration Scale .....	357
3.	Calculations of Ionic Equilibria Involving Weak Acids and Bases .....	359
a.	The Carbon Dioxide-Dissolved Carbonate System .....	360
i.	Dissolution of CO <sub>2</sub> and Ionization of Carbonic Acid in Solution .....	360
ii.	Stoichiometric Equilibrium Constants for the Carbonate System in Seawater .....	361
iii.	Carbonate Equilibria Involving the Solid Phase .....	365
iv.	Thermodynamic Solubility Products of Calcium Carbonate Minerals .....	365
v.	Stoichiometric Solubility Products of Calcium Carbonate Minerals in Seawater .....	365
vi.	Calculation of ${}^{\text{T}}K_{\text{CaCO}_3}^*$ from $K_{\text{CaCO}_3}$ .....	367
vii.	Application of the Pitzer Model to Systems Containing Carbonate .....	368
b.	Boric Acid .....	370
c.	Ammonia .....	373
d.	Hydrofluoric Acid .....	378
e.	Phosphoric Acid .....	380
f.	Hydrogen Sulfide .....	385
g.	Sulfur Dioxide .....	389
h.	Ion Product of Water in Seawater .....	391
D.	Complexation of Trace Species in Natural Waters .....	392
1.	Formation of Cu(II) Chloro-Complexes .....	399
2.	Formation of Pb Chloro-Complexes .....	400
3.	Formation of MgF <sup>+</sup> in Aqueous NaCl and Seawater .....	402
4.	Application of Ion Pairing Models .....	406
	Glossary of Symbols .....	419
	References .....	422

## I. INTRODUCTION

### A. THE COMPOSITION OF NATURAL WATERS

#### 1. The Hydrological Cycle

Natural waters are, as Lavoisier pointed out, the “rinsings of the earth”, and during their interminable cycling they interact with the air, with the rocks, and with the biota to form solutions of great complexity and variability. This can be illustrated by following the movement of water around the hydrological cycle.

Pure water is distilled from the oceans and is augmented by fine salt spray and the dissolution of atmospheric gases. In the atmosphere, most water exists in the vapor phase, thus controlling the aqueous phase concentrations of material dissolved in aerosols and cloud droplets. It is in this portion of the natural water cycle that the greatest concentrations are found, since the finely dispersed nature of the aerosol phase leads to high degrees of supersaturation being attainable under conditions of low relative humidity.<sup>1</sup> Condensation of water vapor upon aerosols acting as cloud nuclei, and precipitation scavenging, result in the dilution of the dissolved component so that rainwater is the purest of natural waters (Table 1). However, its composition is extremely variable, with significant differences occurring even within a single shower. Rainwater is a powerful weathering agent, since it is rendered acid by dissolved carbon dioxide and, to a lesser extent, by the oxides of sulfur and nitrogen. As it washes over the rocks and percolates through the soil, its load of dissolved constituents is enhanced, and it achieves a composition that is set by the local geology and by the seasonal and geographical patterns of the biota.<sup>2,3</sup> Most of these primary rinsings drain off the land surface, first into streams and then into rivers. The weathering and breakdown of rock fragments and of organic debris continue within the rivers, further enhancing the content of dissolved solids (Table 1). Where larger volumes of water accumulate in lakes, residence times are increased and the temporal variability in composition is reduced somewhat, although considerable variations will occur between one lake and the next.<sup>4,5</sup>

Within estuaries, river and coastal ocean water mix, and the ionic strength changes encountered will significantly shift equilibria that have been established between the water and suspended particles on the passage to the sea.<sup>6</sup> In contrast to surface waters inland, the oceans have a remarkably uniform composition (Table 2), and it has been suggested that this composition is maintained, so far as the major cations are concerned, by reactions occurring in or near the mouths of estuaries. It is likely, also, that the oceans owe their relatively high ionic strengths to the accumulation of volatile acids (such as HCl and H<sub>2</sub>SO<sub>4</sub>) from volcanic activity, and that these acids have reacted over the millennia with basic components (e.g., carbonates and oxides) brought down by the rivers, to form seawater according to the classic reaction: acid + base = salt + water.

A number of deviations can occur from this simple cycle that produce waters with distinctive compositions. Where water becomes stagnant, dissolved oxygen is rapidly utilized in the oxidative breakdown of dissolved or suspended organic matter. If the rate of supply of organic matter outstrips the rate of supply of oxygen, then anoxic water is produced, and alternative electron acceptors such as nitrate, sulfate, and ferric iron are used by bacteria in the oxidation of organic matter. The reduced inorganic components [e.g., S<sup>2-</sup>, NH<sub>4</sub><sup>+</sup>, Fe(II)] remain in solution, and a number of unusual gaseous components (e.g., H<sub>2</sub>S, CH<sub>4</sub>, and H<sub>2</sub>) may be found dissolved in the water. Such conditions frequently occur in the interstitial waters of silty sediments, and in the summer months, the anoxic layer can invade the water column of productive lakes and fjords.<sup>7,8</sup>

If water accumulates in enclosed basins on the earth's surface, then more water may be lost by evaporation than is received via runoff and direct precipitation. Under these circumstances, hypersaline waters will be produced with ionic strengths far in excess of those that

**TABLE 1**  
**Major Ion Composition of Selected Natural Waters with Ionic Strengths  $<0.1 \text{ mol dm}^{-3}$** <sup>306</sup>

Property <sup>a</sup>	Rain water <sup>b</sup>	Stream runoff			Freshwater lakes			
		c	d	e	f	g	h	i
Na <sup>+</sup>	0.083	0.274	0.223	0.45	0.139	0.43	5.29	2.83
Mg <sup>2+</sup>	0.008	0.169	0.058	0.10	0.013	0.12	3.58	1.73
Ca <sup>2+</sup>	0.008	0.374	0.126	2.45	0.09	0.59	0.12	0.17
K <sup>+</sup>	0.005	0.059	0.011	0.03	0.007	0.04	2.49	0.79
Cl	0.093	0.220	0.240	0.30	0.151	0.42	1.55	0.62
SO <sub>4</sub> <sup>2-</sup>	0.033	0.117	0.075	0.30	0.060	0.19	0.25	0.04
HCO <sub>3</sub>	0.007	0.958	0.194	4.60	0.061	1.08	12.5	6.24
pH	4.5	7.0	6.6	8.0	6.7	—	—	—
Ionic strength	0.21	2.08	0.85	8.4	0.51	2.5	18.8	9.1

<sup>a</sup> Concentrations in  $\text{mmol dm}^{-3}$  ( $\approx \text{mmol kg}^{-1} \text{H}_2\text{O}$  at these low ionic strengths).

<sup>b</sup> Shows considerable variation from sample to sample.

<sup>c</sup> Mean river water.<sup>1b</sup>

<sup>d</sup> Crosby Gill (tributary of R. Duddon, U.K.).

<sup>e</sup> Bere Stream, U.K.

<sup>f</sup> Thirlmere, U.K.

<sup>g</sup> Whin's Pond, U.K.

<sup>h</sup> Lake Kivu, East Africa.

<sup>i</sup> Lake Tanganyika, East Africa.

From Davison, W. and Whitfield, M., *J. Electroanal. Chem.*, 75, 763, 1977. With permission.

**TABLE 2**  
**Concentration of Major Sea Salt Constituents in Oceanic Seawater Expressed on the Molality Scale at 35 S‰ Conventional Salinity**

Constituent	Molality ( $m_i$ , $\text{mol kg}^{-1}$ water)			
	Natural seawater		Artificial seawater	
	a	b	c	d
Na <sup>+</sup>	0.48586	0.48525	0.48532	0.48527
Mg <sup>2+</sup>	0.05520	0.05519	0.05522	0.05529
Ca <sup>2+</sup>	0.01065	0.01064	0.01071	0.01049
K <sup>+</sup>	0.01058	0.01058	0.01026	0.01013
Sr <sup>2+</sup>	0.00009	0.00009	0.00009	0.00016
Cl	0.56572	0.56579	0.56579	0.56572
SO <sub>4</sub> <sup>2-</sup>	0.02927	0.02927	0.02925	0.02914
Br	0.00087	0.00087	0.00086	0.00085
F	0.00007	0.00006	0.00005	0.00007
HCO <sub>3</sub>	0.00241	0.00241	0.00241	0.00241
B(OH) <sub>3</sub>	0.00044	0.00044	0.00044	0.00046

<sup>a</sup> Riley and Skirrow.<sup>307</sup>

<sup>b</sup> Millero.<sup>26</sup>

<sup>c</sup> Kester et al.<sup>308</sup>

<sup>d</sup> Lyman and Fleming.<sup>309</sup>

**TABLE 3**  
**Major Ion Composition of Selected Natural Waters with Ionic**  
**Strengths  $>1 \text{ mol dm}^{-3}$**

Property	Dead Sea brines <sup>a</sup>		Red Sea brines <sup>b</sup>	Deep-seated groundwaters <sup>b</sup>		
	Upper	Lower		NE Mecklenberg <sup>c</sup>	Lausitz <sup>c</sup>	SSGB <sup>d</sup>
Na <sup>+</sup>	1.7519	1.7919	5.4265	1.1688 <sup>e</sup>	2.0470 <sup>e</sup>	3.1115
Mg <sup>2+</sup>	1.5552	1.8110	0.0448	3.3440	1.7224	0.0006
Ca <sup>2+</sup>	0.4274	0.4448	0.1577	1.7496	0.2755	0.9698
K <sup>+</sup>	0.1739	0.2014	0.0739	0.6920	0.6998	0.5696
Cl <sup>-</sup>	5.8098	6.4173	5.8869	12.0278	6.6781	5.9012
SO <sub>4</sub> <sup>2-</sup>	0.0063	0.0045	0.0105	—	0.0085	—
Br <sup>-</sup>	0.0602	0.0684	—	0.0340	0.0342	—
HCO <sub>3</sub> <sup>-</sup>	0.0039	0.0038	—	0.0112	0.0133	—
<i>I</i>	7.88	8.76	6.12	17.15	8.75	7.12
Density	1.205	1.233	—	1.309	1.282	—

Note: Concentrations are expressed in mol kg<sup>-1</sup> H<sub>2</sub>O.

<sup>a</sup> Neev and Emery.<sup>310</sup>

<sup>b</sup> Riley.<sup>311</sup>

<sup>c</sup> Rosler and Lange,<sup>312</sup> recalculated.

<sup>d</sup> Salton Sea geothermal brine, Cramer.<sup>313</sup>

<sup>e</sup> Adjusted to maintain charge balance.

would result from natural weathering on the earth's surface. Under extreme conditions, evaporation of a fresh water body will yield a soda lake, and evaporation of an enclosed area of the sea will produce concentrated brines (Table 3).

Hypersaline conditions can also be produced in pore waters percolating through the rocks, not because of the selective removal of the water, but because the high temperatures and pressures encountered at depth render the water more corrosive.<sup>9</sup> Spectacular increases in salt content are observed where these groundwaters encounter the remnants of earlier salt deposits.

Although geochemical processes control the composition of the major dissolved components in natural waters, biological processes frequently play an important role in establishing their pH and redox potential and in fixing the concentrations of trace metals and of the minor nutrient components. These effects superimpose a diurnal and seasonal variability on natural water chemistry that is impossible to summarize in such a brief introduction.

The diversity of natural waters is therefore immense, and in this chapter we intend to select a few representative examples to illustrate strategies that can be used to calculate activity coefficients over the whole range of ionic strengths encountered naturally. Although most of the elements in the periodic table have been identified as occurring in natural waters, the concentrations of only a handful of elements have been sufficiently well characterized to be considered in the recipes of various natural waters (Tables 1 to 3). The stoichiometry of seawater, which has been particularly well studied, will be considered in some detail to illustrate the problems inherent in specifying the exact composition of natural waters.

## 2. The Stoichiometry of Seawater — a Case Study

### a. The Salinity Concept and the Density of Seawater

The overwhelming bulk of sea salt (>99.95% of the total dissolved solids) is contributed by the 11 major constituents (Table 2). These major constituents interact with each other

TABLE 4  
Chlorinity Ratios (g/Cl‰) for the Major  
Seawater Constituents in Open Ocean Water

Constituent	g/Cl‰			
	a	b	c	d
Na <sup>+</sup>	0.55625 0.5561 <sup>a</sup>	0.55556	0.55559	0.5560
Mg <sup>2+</sup>	0.06682	0.06680	0.06684	0.06693
Ca <sup>2+</sup> <sup>f</sup>	0.02127	0.02125	0.02137	0.02093
K <sup>+</sup>	0.02060	0.02060	0.01997	0.01972
Sr <sup>2+</sup>	0.00042	0.00041	0.00041	0.00068
Cl <sup>-</sup>	0.99880 0.99896 <sup>a</sup>	0.99894	0.99882	0.99883
SO <sub>4</sub> <sup>2-</sup>	0.14003	0.14000	0.13992	0.13943
Br <sup>-</sup>	0.00346 0.00347 <sup>a</sup>	0.00348	0.00341	0.00340
F <sup>-</sup>	0.00007	0.00006	0.00005	0.00007
HCO <sub>3</sub> <sup>-</sup> <sup>g</sup>	0.00733	0.00735	0.00733	0.00735
B(OH) <sub>3</sub> <sup>h</sup>	0.00133	0.00132	0.00134	0.00139
Σ <sub>i</sub> g <sub>i</sub> /Cl‰ =	1.81638 1.81639 <sup>a</sup>	1.81577	1.81505	1.81434
k =	1.00544	1.00510	1.00471	1.00431

<sup>a</sup> Natural seawater.<sup>107</sup>

<sup>b</sup> Natural seawater.<sup>26</sup>

<sup>c</sup> Artificial seawater.<sup>108</sup>

<sup>d</sup> Artificial seawater.<sup>109</sup>

<sup>e</sup> Wilson.<sup>10</sup>

<sup>f</sup> Concentrations markedly affected by biological processes.

<sup>g</sup> Concentrations possibly influenced by submarine vulcanism.

<sup>h</sup> About 10% of this total present as CO<sub>3</sub><sup>2-</sup> at pH 8.

<sup>i</sup> About 20% of this total present as B(OH)<sub>4</sub><sup>-</sup> at pH 8.

predominantly via weak electrostatic forces so that they have long residence times in the oceans. As a consequence, they are well mixed and their concentrations exhibit an almost constant ratio to one another throughout the oceans, although the total concentration of dissolved constituents may vary from place to place. This constancy of composition greatly simplifies the task of describing the thermodynamics of seawater, since it implies that, for many purposes, the major dissolved constituents can be seen as a composite sea salt. The composition of the sea salt component (Tables 2 and 4) can be determined directly by the tedious and painstaking chemical analysis of the 11 dominant constituents.<sup>10,11</sup>

However, in situations where constancy of composition is observed, it has become the convention to estimate the total halide concentration (excluding fluoride) by titration with silver nitrate and to use the *chlorinity* determined in this way to calculate the concentrations of the individual conservative constituents. The mass of each constituent can be conveniently expressed in terms of its ratio to chlorinity, i.e., as g/Cl‰ (Table 4). The total salt content ( $S_T$ , g kg<sup>-1</sup> seawater) of the seawater is given by (recipe a, Table 4)

$$S_T = \sum_i g_i = 1.81638 \times \text{Cl‰} \quad (1)$$

Unfortunately, this simple definition of the total salt content is seldom used because of the obvious difficulties involved in the direct analysis of all of the major ionic constituents. An early definition of the total salt content was based on a procedure where the seawater,

following pretreatment with chlorine water and hydrochloric acid, was evaporated to dryness for 72 h at 480°C and the residual salt weighed.<sup>11</sup> This led to the definition of salinity<sup>12</sup> ( $S_K$ ) as ‘‘the weight in grams of dissolved inorganic matter in 1 kg of seawater, after all bromide and iodide have been replaced by an equivalent amount of chloride and all carbonate converted to oxide’’. For the seawater recipe **a**, in Table 4, this gives<sup>13</sup>

$$\begin{aligned} S_K &= S_T + [g\text{Br}(w\text{Br} - 1) + g\text{HCO}_3(w\text{O}/2w\text{HCO}_3 - 1)] \\ &= 35.000 - 0.160 = 34.840 \end{aligned} \quad (2)$$

where  $wX$  is the molar mass of  $X$ .

For many years the Knudsen salinity ( $S_K$ ) was used to define the total salt content of seawater and was related to the chlorinity by the equation:

$$S_K = 0.03 + 1.805 \times \text{Cl}\%_c \quad (3)$$

which gives, for recipe **a** (Table 4),  $S_K = 34.811$ . The discrepancy between this value and the one calculated from Equation 2 is significant. The parameters in Equation 3 were derived from a series of nine seawater samples, most of which were taken from the Baltic Sea, an extensive estuary. To minimize the estuarine bias in the definition of salinity and still maintain a similar relationship between salinity and chlorinity, it was decided to define the salinity *arbitrarily*,<sup>14</sup> so that

$$S\%_c = 1.80655 \times \text{Cl}\%_c \quad (4)$$

For recipe **a** (Table 4), the salinity is now 34.811‰ by definition. The salinity defined in this way does *not* specify the number of grams of salt present in each kilogram of seawater ( $S_T$ ). The conventional salinity ( $S\%_c$ ) is related to this quantity in open ocean waters by the equation

$$S_T = k \times S\%_c \quad (5)$$

where  $k = \sum_i g_i / (1.80655 \text{ Cl}\%_c)$ . Values of  $\sum_i g_i / \text{Cl}\%_c$  and  $k$  are given in Table 4 for a variety of seawater recipes.

In coastal and estuarine waters, the dissolved solids contributed by river runoff must be taken into account by readopting the form of the equation used by Knudsen (Equation 3) in place of Equation 5, so that<sup>15</sup>

$$S_T(\text{estuarine}) = a + bS\%_c \quad (6)$$

where  $a = S_T(\text{river})$  and  $b = [S_T(\text{oceanic}) - S_T(\text{river})] / S\%_c(\text{oceanic})$ .  $S\%_c(\text{oceanic})$  is the conventional salinity of the oceanic end member. For mean world river water<sup>16</sup>  $S_T(\text{river}) = 0.120 \pm 0.01 \text{ g kg}^{-1}$ . This value is valid for present-day inputs to the Baltic,<sup>15</sup> although at the time of Knudsen's work<sup>17</sup> the value was probably closer to  $0.073 \text{ g kg}^{-1}$ .

The chemical estimation of salinity via chlorinity is now rarely used outside laboratories that specialize in preparing standard seawater samples for intercomparison purposes. The conventional salinity is currently defined in terms of the conductivity of the seawater sample<sup>10</sup> relative to such a standard for which  $S = 35.000\%_c$ .

The relationship between salinity and density at 1 atm (101,325 Pa) pressure may be summarized by the equation<sup>18</sup>

$$d_{(s)} = d_0 + AS + BS^{3/2} + CS^2 \quad (7a)$$

$$A = 8.24493 \times 10^{-1} - 4.0899 \times 10^{-3} t + 7.6438 \times 10^{-5} t^2 \\ - 8.2467 \times 10^{-7} t^3 + 5.3875 \times 10^{-9} t^4 \quad (7b)$$

$$B = -5.72466 \times 10^{-3} + 1.0277 \times 10^{-4} t - 1.6546 \times 10^{-6} t^2 \quad (7c)$$

$$C = 4.8314 \times 10^{-4} \quad (7d)$$

where  $t$  is temperature ( $^{\circ}\text{C}$ ) and  $d_{(s)}$  and  $d_0$  ( $\text{kg m}^{-3}$ ) are the relative densities of seawater and pure water, respectively, at the appropriate temperature. The relative density is defined by

$$d_x = \rho_x / \rho_{\text{max}} \quad (8)$$

where  $\rho_x$  is the absolute density of solution “ $x$ ” and  $\rho_{\text{max}}$  is the absolute maximum density of pure water at 1 atm pressure. The value of  $\rho_{\text{max}}$  will depend on the isotopic composition of the water used in the measurements. For standard mean oceanic water (SMOW),  $\rho_{\text{max}} = 999.975 \text{ kg m}^{-3}$  at  $4^{\circ}\text{C}$ .<sup>18</sup> Natural variations in the isotopic composition are not likely to introduce any significant errors into the calculations considered in this chapter. The relative density of pure water at 1 atm pressure may be described by the equation<sup>18,19</sup>

$$d_0 = 999.842594 + 6.793952 \times 10^{-2} t - 9.909529 \times 10^{-3} t^2 \\ + 1.001685 \times 10^{-4} t^3 - 1.120083 \times 10^{-6} t^4 + 6.536332 \times 10^{-9} t^5 \quad (9)$$

These equations are valid for 1 atm total pressure. Millero<sup>18,20</sup> gives further expressions enabling densities and other PVT and thermochemical properties to be calculated as functions of both temperature and pressure. Seawater densities calculated using the equations above (Appendix Table A1) will prove useful in the interconversion of concentration scales, which will be discussed in the following section.

The densities of other natural waters are equal, within experimental error, to those of seawater diluted with pure water (Equation 7) when compared at the same value of  $S_T$ <sup>15,21</sup> (Equation 5 or 6). Thus the density equations can be used even in situations where the concept of constancy of composition is no longer valid. Since many important biological and geological processes are associated with (and indeed are responsible for) areas where constant composition is not observed, this is an important generalization.

### ***b. Seawater as a Multicomponent Electrolyte Solution***

Four distinct scales have been used to express the concentrations of dissolved constituents in seawater<sup>13</sup> (Tables 5 and 6). The molinity scale ( $\text{mol kg}^{-1}$  of seawater) has been widely used by chemical oceanographers, because it provides the simplest means for expressing analytical results in a medium of unknown composition. As our detailed chemical knowledge has improved and the description of seawater properties put on a sound thermodynamic basis, the molality scale ( $\text{mol kg}^{-1}$  of water) has become the principal unit. Most of the conversion factors are provided (Appendix Tables A2 and A3) for those wishing to use other scales or to convert other values to molalities.

Although the ten major ions are the principal constituents of seawater, they cannot be described as solution *components*, in the strict thermodynamic sense, since the electroneutrality condition prevents their concentrations from being varied independently. Since it is



**TABLE 5**  
**Concentration Scales Used in Marine Chemistry<sup>13</sup>**

Scale	Symbols <sup>a</sup>	Units	Remarks
Molarity	<i>c</i>	mol dm <sup>-3</sup>	Dependent on temperature and pressure; natural scale for development of electrostatic theories of electrolyte solution
	<i>y</i>	—	
Molality	<sup>c</sup> <i>a</i>	mol dm <sup>-3</sup>	Independent of temperature and pressure; most widely used in physical chemistry
	<i>m</i>	mol kg <sup>-1</sup> water	
	$\gamma$	—	
Mole fraction	<i>a</i>	mol kg <sup>-1</sup> water	Independent of temperature and pressure, convenient for theoretical work since it gives an immediate grasp of the mole ratios in solution; covers entire concentration range
	<i>x</i>	mol/total moles	
	<i>f</i>	—	
	<sup>c</sup> <i>a</i>	mol/total moles	
Molality <sup>b</sup>	<i>k</i>	mol kg <sup>-1</sup> solution	Independent of temperature and pressure; useful in situations where the solution composition is unknown
	<sup>k</sup> $\gamma$	—	
	<sup>k</sup> <i>a</i>	mol kg <sup>-1</sup> solution	

<sup>a</sup> Concentration, activity coefficient, and activity, respectively. The molal scale is used throughout this work.

<sup>b</sup> This term is used rather than "mokal", suggested by MacIntyre,<sup>13</sup> since it immediately signifies that the use of this scale implies the same degree of chemical ignorance as is inherent in the salinity and chlorinity concepts.

**TABLE 6**  
**Concentrations of Major Sea Salt Constituents in Artificial Seawater at 35 S‰, 25°C, and 1 atm Pressure<sup>308</sup>**

Constituent	a	b	c	d	e
Na <sup>+</sup>	0.46825	8.56408	0.47926	0.48532	10.7650
Mg <sup>2+</sup>	0.05328	0.97448	0.05453	0.05522	1.2950
Ca <sup>2+</sup>	0.01033	0.18891	0.01057	0.01071	0.4140
K <sup>+</sup>	0.00990	0.18103	0.01013	0.01026	0.3871
Sr <sup>2+</sup>	0.00009	0.00166	0.00009	0.00009	0.0079
Cl <sup>-</sup>	0.54589	9.98385	0.55871	0.56579	19.3534
SO <sub>4</sub> <sup>2-</sup>	0.02822	0.51617	0.02889	0.02925	2.7102
Br <sup>-</sup>	0.00083	0.01511	0.00085	0.00086	0.0663
F <sup>-</sup>	0.00005	0.00097	0.00005	0.00005	0.0009
HCO <sub>3</sub> <sup>-</sup>	0.00233	0.04256	0.00238	0.00241	0.1422
B(OH) <sub>3</sub>	0.00042	0.00770	0.00043	0.00044	0.0260

<sup>a</sup> Molality (mol kg<sup>-1</sup> seawater).

<sup>b</sup> Mole fraction (10<sup>3</sup> *x*<sub>i</sub>), Equation 11.

<sup>c</sup> Molarity (mol dm<sup>-3</sup>).

<sup>d</sup> Molality (mol kg<sup>-1</sup> water).

<sup>e</sup> g kg<sup>-1</sup> seawater.

not possible to estimate the thermodynamic properties of individual ions directly, it is often more convenient to express the composition of artificial seawater in terms of the component neutral salts that could be used in its preparation (Table 7). However, it introduces a rather artificial restriction when dealing with natural seawaters, since there is no unique way of pairing the analytically determined single ion concentrations. Nevertheless, the salt component approach has, in the past, provided a useful means for predicting the thermodynamic properties of seawater from what is known about the component single electrolyte solutions.

**TABLE 7**  
**The Composition of an Artificial Seawater<sup>308</sup>**  
**Expressed in Terms of the Component Neutral**  
**Salts<sup>25</sup>**

Component	$w_j$	$m_j$	$y_j$	$\nu_j$	$y_j w_j$
NaCl	58.4428	0.424310	0.796440	2	46.5462
Na <sub>2</sub> SO <sub>4</sub>	142.0372	0.029245	0.054895	3	7.7971
NaHCO <sub>3</sub>	84.0070	0.002418	0.004539	2	0.3813
NaF	41.9882	0.000074	0.000139	2	0.0058
KCl	74.5550	0.009412	0.017666	2	1.3166
KBr	119.0060	0.000854	0.001602	2	0.1906
MgCl <sub>2</sub>	95.2110	0.055211	0.103630	3	9.8667
CaCl <sub>2</sub>	110.9860	0.010707	0.020098	3	2.2306
SrCl <sub>2</sub>	158.5260	0.000093	0.000173	3	0.0274
H <sub>2</sub> BO <sub>3</sub>	61.8322	0.000436	0.000818	2	0.0506

Some care must be exercised when using the term ‘‘mole fraction’’, since it is employed in at least three different ways in natural water chemistry. The general definition, for the mole fraction of component  $i$ , may be written as:

$$x_i = C_i / \sum_i C_i \quad (10)$$

where  $x_i$  and  $C_i$  are general terms for the mole fraction and the concentration, respectively, of component  $i$ . MacIntyre<sup>13</sup> adopted a mole fraction concentration scale that gives direct insight into the molecular reality in the solution. According to his definition, the summation in Equation 10 is over all molecular species, including water, so that

$$x_i = m_i / (\sum_i m_i + 55.50837) \quad (11)$$

if concentrations are expressed on the molality scale (since  $m_{H_2O} = 1000/w_{H_2O} = 1000/18.0153 = 55.50837$ ). The mole fraction  $x_i$  is dependent on the salinity of the seawater at constant composition. This definition (Equation 11) corresponds to the convention for describing concentration in electrolyte solutions, where it is usual to assume complete dissociation into ions<sup>22,23</sup> so that, for example,  $x_{Na^+}$  in a  $1 \text{ mol kg}^{-1}$  NaCl solution is equal to  $1.0 / (2 \times 1.0 + 55.50837) = 0.01739$ .

The term mole fraction may also be used to describe the relative contributions of the solutes to the properties of the solution.<sup>15,24</sup> Leyendekkers<sup>25</sup> prefers to express the composition of the solution in terms of the component neutral salts and to define a mole fraction ( $y_j$ ), so that

$$y_j = m_j / \sum_j m_j \quad (12)$$

where the summation is over all the component neutral salts  $J$ . If the individual ions are treated as the solution constituents, then this relationship could be adapted to give

$$y_i = m_i / \sum_i m_i \quad (13)$$

Millero and Kremling<sup>15</sup> treat the anions and cations separately, thus:

$$y_c^+ = m_c / \sum_c m_c \quad (14)$$

and

$$y_a^- = m_a / \sum_a m_a \quad (15)$$

The boric acid molecule is included in the anionic summation. The mole fractions expressed in Equations 12 to 15 are independent of the salinity at constant composition and are unaffected by the concentration scale used for the individual components. They, therefore, provide a particularly convenient means of expressing the contributions of the individual solutes to the properties of seawater.

*c. The Stoichiometry of Sea Salt*

The molinity of sea salt ( $k_{(s)}$ ) may be defined as

$$\begin{aligned} k_{(s)} &= 0.5(\sum_i k_i - k\text{B(OH)}_3) + k\text{B(OH)}_3 \\ &= 0.5(\sum_i k_i + k\text{B(OH)}_3) \end{aligned} \quad (16)$$

where the summation is over the molinities ( $k_i$ ) of all ionic or molecular constituents  $i$ , including boric acid. The molinity  $k_{(s)}$  can be expressed as a function of chlorinity and salinity, so that for Millero's seawater recipe<sup>26</sup>

$$k_{(s)} = 28.9099 \times 10^{-3} \text{ Cl}\%_o \quad (17a)$$

$$= 16.0028 \times 10^{-3} \text{ S} \quad (17b)$$

The molality of sea salt ( $m_{(s)}$ ) for this recipe is given by

$$m_{(s)} = k_{(s)}/(1000 - \sum_i k_i w_i) \quad (18a)$$

$$= 28.9099 \text{ Cl}\%_o/(1000 - 1.81578 \text{ Cl}\%_o) \quad (18b)$$

$$= 16.0028 \text{ S}/(1000 - 1.00511 \text{ S}) \quad (18c)$$

where  $w_i$  is the molar mass (g) of constituent  $i$ . The ionic strength of this seawater on the molinity scale is defined by

$$I_{k(s)} = 0.5 \sum_i k_i z_i^2 \quad (19a)$$

$$= 35.9997 \times 10^{-3} \text{ Cl}\%_o \quad (19b)$$

and on the molal scale by

$$I_{(s)} = I_{k(s)}/(1000 - \sum_i k_i w_i) \quad (20a)$$

$$= 35.9997 \text{ Cl}\%_o/(1000 - 1.81578 \text{ Cl}\%_o) \quad (20b)$$

$$= 19.9273 \text{ S}/(1000 - 1.00511 \text{ S}) \quad (20c)$$

Values of  $k_{(s)}$ ,  $m_{(s)}$ ,  $I_{k(s)}$ , and  $I_{(s)}$  for Millero's recipe are given in Table 8. The effective molality of the sea salt may be defined as:

$$m_{(s)} = \sum_J m_J \quad (21)$$

where the summation is over all the neutral salts  $J$ . The molar mass of sea salt may be obtained from the equation

$$w_{(s)} = \sum_J w_J y_J \quad (22)$$

**TABLE 8**  
**The Concentration and Ionic Strength**  
**of the Sea Salt Component in the**  
**Model Oceanic Seawater of Millero<sup>26</sup>**

S‰	$k_{(s)}$ <sup>a</sup>	$m_{(s)}$ <sup>b</sup>	$I_{(s)}$ <sup>c</sup>	$I_{(s)}$ <sup>d</sup>
5	0.08001	0.08042	0.09964	0.10014
10	0.16003	0.16165	0.19927	0.20130
15	0.24004	0.24372	0.29891	0.30349
20	0.32006	0.32662	0.39855	0.40672
25	0.40007	0.41038	0.49818	0.51102
30	0.48008	0.49501	0.59782	0.61641
35	0.56010	0.58052	0.69746	0.72289
40	0.64011	0.66693	0.79709	0.83048

<sup>a</sup> Equation 17.

<sup>b</sup> Equation 18.

<sup>c</sup> Equation 19.

<sup>d</sup> Equation 20.

For the seawater recipe shown in Table 7,  $w_{(s)} = 68.4131$ . For the more recent recipe used by Millero<sup>18</sup> and Millero and Leung,<sup>27</sup>

$$m_{(s)} = 16.0030 \text{ S}/(1000 - 1.00488 \text{ S}) \quad (23)$$

for which the valence factor (from  $I_{(s)}/m_{(s)}$ ) is equal to 1.245 and the molar mass of sea salt 62.793g.

## B. THE RELEVANCE OF EQUILIBRIUM THERMODYNAMICS

### 1. Chemical Potential in Closed Systems

According to the concepts of equilibrium thermodynamics, a component present in a closed system in a thermodynamically unstable state will progress, possibly via a series of metastable intermediates, to the equilibrium state of minimum free energy. The influence of solution composition on the free energy of a component J in an ideal solution is defined by the relative partial molal free energy ( $G_J$ ), so that

$$G_J = \mu_J - \mu_J^\ominus = RT \ln(m_J/m_J^\ominus) \quad (24)$$

where  $\mu_J (= (\partial G_J/\partial n_J)_{n_{k \neq J, P}})$  is the chemical potential of the solute J and  $m_J$  is its molal concentration. The superscript  $\ominus$  refers to the properties of some arbitrarily defined standard state. To maintain the formal simplicity of Equation 24 in nonideal systems, a correction factor known as the activity coefficient  $\gamma_J$  is defined, so that

$$\begin{aligned} G_J &= RT \ln(m_J \gamma_J / m_J^\ominus \gamma_J^\ominus) \\ &= RT \ln(a_J / a_J^\ominus) \end{aligned} \quad (25)$$

where  $a_J$  is the solute activity and it has the dimensions of concentration. The most convenient choice of a standard state for the solute is a hypothetical ideal solution of unit concentration, where  $a_J^\ominus = m_J^\ominus = \gamma_J^\ominus = 1$ , so that Equation 25 becomes

$$G_J = RT \ln(m_J \gamma_J) = RT \ln(a_J) \quad (26)$$

Under any given experimental conditions the value of  $\mu_j$  will be fixed, but the following parameters must be defined before unique values can be assigned to  $G_j$ ,  $\gamma_j$ , or  $\mu_j^\ominus$ :

1. The concentration scale used to define  $m_j$
2. The temperature and pressure of the standard state
3. The composition of the standard state

In the following discussion we will employ a standard state for the solutes where the molal concentration scale is used, and the standard state has the same temperature and pressure as the sample solution. In physicochemical studies it is normally assumed that the standard state is defined for an ideal solution of the component  $J$  in *pure water*. In natural water chemistry, however, it is sometimes convenient to consider a solution, containing the major salts, as the solvent for the component  $J$ . The standard state is then defined as a hypothetical solution of unit molality of component  $J$  in the specified salt solution. Every change in the composition or the total concentration of the major salt component produces a new solvent and consequently results in a shift in the definition of  $\mu_j^\ominus$  and  $\gamma_j$ .

The infinitely dilute solution of  $J$ , either in pure water or in the appropriate ionic medium, is usually selected as the reference state for the solute. Although this reference solution cannot be attained experimentally, it can be approached and extrapolated to with some confidence, using mechanistic theories of electrolyte solution behavior for guidance.

Both the standard and reference states of *water* in the solution are taken as pure water at the same temperature and pressure as the solution. This provides identical reference states for both the solute and solvent and therefore simplifies the experimental determination of chemical potentials. It does imply, however, that the standard state for water in the solution is defined on the mole fraction scale where  $x_{\text{H}_2\text{O}}^\ominus = a_{\text{H}_2\text{O}}^\ominus = 1$ . Since standard states are defined at the convenience of the experimenter, the fact that different concentration scales are used in their definition for solute and solvent does not cause any problems in practice. The water activity is related to the (molal) osmotic coefficient  $\phi$  of a solution by

$$a_{\text{H}_2\text{O}} = \exp(-[w_{\text{H}_2\text{O}}/1000] \phi \sum_i m_i) \quad (27)$$

The most useful application of chemical potentials in marine chemistry is in the prediction of the distribution of reactants and products in a system at equilibrium.

The overall free energy change accompanying a particular reaction is given by

$$\Delta G = \sum_i \mu_i n_i - \sum_j \mu_j n_j \quad (28)$$

where  $n$  is the stoichiometric number of moles of the subscripted component represented in the reaction equation. Subscript  $i$  refers to reactants and subscript  $j$  to products. From Equations 26 and 28 we can write:

$$\Delta G = (\sum_i \mu_i^\ominus n_i - \sum_j \mu_j^\ominus n_j) + RT [\sum_i n_i \ln(a_i) - \sum_j n_j \ln(a_j)] \quad (29)$$

At equilibrium  $\Delta G = 0$ , so that

$$\Delta G^\ominus = \sum_i \mu_i^\ominus n_i - \sum_j \mu_j^\ominus n_j = -RT [\sum_i n_i \ln(a_i) - \sum_j n_j \ln(a_j)] \quad (30)$$

The equilibrium constant for the reaction ( $K$ ) is defined as

$$\ln(K) = -\Delta G^\ominus/RT = \ln(K^*) + \ln(\Gamma) \quad (31)$$

where  $\ln(K^*) = \sum_i n_i \ln(m_i) - \sum_j n_j \ln(m_j)$ , and  $\ln(\Gamma) = \sum_i n_i \ln(\gamma_i) - \sum_j n_j \ln(\gamma_j)$ . Symbol  $K^*$  represents the stoichiometric equilibrium constant and  $\Gamma$  is the activity coefficient quotient. The value of  $K$  will depend on the temperature and pressure at which the reaction is taking place and on the standard used to define  $\mu_i^0$  and  $\mu_j^0$ . As an example, consider an equilibrium in solution between components A and B, and C (where the numbers of moles present are given "per kilogram" of  $H_2O$ , and are therefore equivalent to  $m$ ):



The equilibrium constant  $K$  is given by

$$\begin{aligned} K &= a_C / (a_A a_B) = m_C \gamma_C / (m_A \gamma_A m_B \gamma_B) \\ &= m_C / (m_A m_B) \cdot \gamma_C / (\gamma_A \gamma_B) \\ &= K^* \cdot \Gamma \end{aligned} \quad (33)$$

where one of the reactants is a (pure) solid phase, then its activity ( $a$ ) is unity.

## 2. Chemical Potential in Open Systems

In natural waters a number of effects might prevent the attainment of equilibrium. The real system is open to a flux of material, and the throughput might be far more rapid than the rate of conversion to more stable forms, so that metastable components can persist indefinitely. The chemistry of these components is then determined by a supply-and-demand economy, rather than by equilibrium thermodynamics. The rate of conversion to the more stable form will also be related inversely and exponentially to the activation energy for the conversion from one form to another. The largest activation barriers, found for reactions occurring at solid-solid or solid-liquid interfaces, can often slow reactions down to such an extent that equilibrium will not be reached even over millions of years. Many natural reactions involving heterogeneous or nonstoichiometric solid phases are therefore difficult to deal with in equilibrium terms, and there are many instances of chemical processes being dominated by the slow precipitation or dissolution of solid phases. However, there are numerous homogeneous reactions in natural waters proceeding at rates that are very rapid when compared to the residence times of the reacting components. Under these circumstances, equilibrium thermodynamics, which strictly only applies to closed systems, can be used to good effect. In other instances, equilibrium models will provide clearly defined base lines against which to judge the importance of kinetic and biological factors in controlling the chemistry of natural waters. Where composition gradients occur, activities, rather than concentrations, should be used in the definition of diffusion equations<sup>28</sup> and in the elucidation of chemical kinetics.<sup>29</sup>

The real system is also open to an influx of energy from the sun, and it is likely that somewhere in the biological web this energy will be used to maintain particular components in a nonequilibrium form. However, the energy resources of the biota are hard won, and there is always a fine balance between income and expenditure. Consequently, organisms tend to make use of thermodynamically economic processes wherever possible. In addition, studies of the uptake of toxic components by marine organisms have indicated that for both ionic<sup>30,31</sup> and nonionic<sup>32,34</sup> components, the response is correlated with solute activities rather than solute concentrations. The student of natural water chemistry must, therefore, find ways of estimating activity coefficients in complex electrolyte mixtures.

Precise statistical mechanical theories of electrolyte solutions are highly complicated and are largely restricted to single electrolyte solutions with ionic strength less than  $1 \text{ mol dm}^{-3}$ . Consequently, the procedures and models available for estimating activity coefficients

are, at least partly, empirically based. It is also inevitable that, since this chapter has been written by marine chemists, greatest emphasis will be given to treatments of seawater as an electrolyte solution. There are good scientific reasons for this, too. Seawater is the most abundant electrolyte solution on the earth's surface. It has a remarkably uniform composition and its ionic strength ( $\approx 0.72 \text{ mol kg}^{-1}$ ) is high enough to provide a reasonable test for the methods used to calculate activity coefficients. Furthermore, it has received a considerable amount of attention in recent years, so that it is probably the most thoroughly "modeled" of all natural waters.

## II. CALCULATION OF ACTIVITY COEFFICIENTS

To determine speciation and other equilibrium properties, such as distribution between solid and aqueous phases in solution, it is necessary to calculate the osmotic coefficient (hence water activity) and activity coefficients of the dissolved components. In the present state of knowledge of aqueous solution behavior, thermodynamic models used to estimate these properties in real mixtures are necessarily partly empirical. That is to say, while their starting points may derive from some fundamental observations of the character of the aqueous solutions to be modeled, and their form be guided by theory, there usually remain empirical parameters that must be determined by fitting to thermodynamic data (e.g., osmotic or activity coefficients) for pure aqueous solutions or simple mixtures.

Historically, there have been two classes of model used to estimate activity coefficients in natural waters: ion association and ion interaction. It is usually assumed that most conventional strong electrolytes such HCl and NaCl are completely dissociated in aqueous solution over a wide range of concentrations. This view can probably be explained simply by the fact that covalent molecules are much more difficult to detect in solution than ions. Ion interaction models treat deviations from ideal solution behavior as being caused by interactions (usually a function of concentration or ionic strength) among the free ions and neutral components. However, there is considerable direct evidence that ion pairs form in aqueous solutions. Ion association has been demonstrated in solutions by measurements of sound attenuation<sup>35</sup> and by Raman spectroscopy.<sup>36</sup> It has long been known to occur in solutions of certain electrolytes such as the bivalent metal sulfates;<sup>37</sup> thus, a model based on the principle of ion association has a basis in molecular terms. In such models, the concentrations of the ions are determined from their association constants, and the free ion activity coefficients depend only on the effective ionic strength of the solution.<sup>38</sup>

### A. ION ASSOCIATION MODELS

Ion association models have played an important role in understanding the chemical nature of seawater, beginning with the pioneering work of Garrels and Thompson.<sup>39</sup> These authors presented a major-ion seawater model which was used to calculate individual ion activity coefficients and the distribution of dissolved species. Their model is typical of ion association models in general in its basic assumption that specific interactions between ions in the solution occur solely as association. They also assumed that the alkali metal and alkaline earth chlorides are unassociated salts. These serve as a baseline against which the extent of ion association in the solution can be assessed. Ion association models have been particularly successful in predicting the activities of the geochemically important trace elements.<sup>40-41</sup> Millero and Schreiber<sup>42</sup> have evaluated activity coefficients of the ionic components of natural waters estimated using ion association models. Ion association, and the calculation of activity coefficients, was discussed in the previous edition of this book by Johnson and Pytkowicz,<sup>43</sup> and has recently been examined within the context of currently available geochemical (computer) models by Parkhurst.<sup>44</sup>

Two practical difficulties with ion association models are lack of association constant data and the increasing complexity of the systems of equations to be solved as more species

are added to the solution. The assumption of Garrels and Thompson<sup>39</sup> that alkali metal and alkaline earth chlorides are unassociated cannot account for their observed behavior in solution mixtures.<sup>45,46</sup> Indeed, ion association has been measured in pure solutions of these salts.<sup>38</sup> Other serious objections are the lack of conventions to specify, first, the properties of individual ions in solution at high ionic strengths, and second, to assign values to the thermodynamic properties of the ion pairs themselves.<sup>46</sup> Ion association models are therefore both difficult to use and, in addition, cannot make any unique claims to represent the molecular reality of the solution.

## B. ION INTERACTION MODELS

By contrast, ion interaction models treat conventional strong electrolytes as completely dissociated, and the properties of the solutions are described in terms of interactions between free ions. These models, in their most basic form, therefore take an opposite view of the state of a solution mixture to ion association models, though one that is equally based upon a set of conventions. The simplest models only consider interactions between pairs of ions of opposite sign as these attractive forces are strongest.<sup>47-50</sup> The models are often based on a linear summation of the properties of the component single electrolyte solutions — in terms of single electrolyte activity coefficients, for example<sup>48</sup> — and adequately describe osmotic and activity coefficients in dilute mixed solutions. The model of Pitzer<sup>51</sup> (Chapter 3, this volume) and also those of other workers<sup>52,53</sup> are more comprehensive, and treat interactions between pairs of ions of like sign and also triplets of ions. This enables calculations to be extended to multicomponent solutions at high ionic strength.<sup>54</sup> The properties of neutral solutes are simply incorporated in such models, yielding expressions similar to the empirical Setchenow relationship<sup>55,56</sup> (see Section III.B.1), but with the advantage of being incorporated into a self-consistent thermodynamic framework. Ion interaction models have in the past been most successful in predicting the behavior of the major components of electrolyte solutions such as seawater.<sup>46,57,58</sup> In unmodified form they are less accurate than ion association models when dealing with trace components, particularly in cases where ion pairing is known to occur.<sup>58</sup> However, association reactions can readily be incorporated into the ion interaction scheme, as has been done for the model of Pitzer,<sup>59</sup> enabling its usefulness to be extended to a very wide range of systems.<sup>56,60,61</sup> This aspect of the Pitzer model, particularly as it applies to the treatment of  $\text{CaSO}_4$  solubility and the formation of polymeric boron species in solution, has been discussed by Weare.<sup>62</sup>

In the previous edition of this book, a variety of approaches to the calculation of activity coefficients in natural waters were illustrated, ranging from extended Debye-Hückel expressions at very low ionic strengths, the application of Young's rules of mixing, and the use of Setchenow coefficients for neutral species, to an evaluation of the more elaborate models of Scatchard et al.,<sup>53</sup> Reilly et al.,<sup>52</sup> and Pitzer.<sup>51</sup> More recently, Zemaitis and others<sup>63</sup> have reviewed in depth some of the principal models available for calculating activity coefficients, beginning with the work of Guggenheim,<sup>47</sup> and including the equations of Bromley,<sup>48</sup> Pitzer,<sup>51</sup> Meissner and Kusik,<sup>49</sup> and Chen et al.<sup>64</sup> Tests of the models (except that of Chen et al., for which an error in the multicomponent formulation was found) predicting salt solubilities in ternary ion systems generally demonstrated the superiority of the Pitzer model, where adequately parameterized.

During the past decade, the ion interaction model of Pitzer has achieved wide acceptance and has been applied successfully in a number of areas that are important geochemically, notably association reactions between aqueous species,<sup>59,65</sup> the equilibria of multicomponent brines with solid phases,<sup>54,66</sup> and the solubility of atmospheric gases in natural waters.<sup>67,68</sup> The model has been extended to include neutral solutes, and incorporated into established geochemical computer models such as PHREEQE<sup>69</sup> (now PHRQPITZ) and EQ3/6.<sup>70</sup> There is now considerable experience in the application of the Pitzer thermodynamic model to



natural aqueous systems, and consequently a substantial database of model parameters available in the literature, although it is important to realize that these are not all compatible, as will be discussed later.

While the Pitzer model has been used successfully for calculations of solubility in brines to ionic strengths of 10 to 15 mol kg<sup>-1</sup>, atmospheric aerosols (whose water content is controlled by the ambient relative humidity) may exist at higher concentrations and be supersaturated with respect to major constituents such as NaCl.<sup>71,72</sup> For such solutions, and especially those consisting chiefly of H<sub>2</sub>SO<sub>4</sub> which is liquid over the entire concentration range, it may be necessary to adopt alternative approaches based on a mole fraction concentration scale,<sup>23</sup> as described by Pitzer<sup>51</sup> (Chapter 3, this volume). Initial applications of such a model to three component aqueous solutions<sup>73</sup> and aqueous HNO<sub>3</sub><sup>74</sup> have been quite successful, and some example calculations will be presented later in this chapter. However, in view of the widespread and still increasing use of the *molal* Pitzer model, this formalism has been adopted here as the principal means of calculating activity coefficients, and is described below.

### 1. The Pitzer Model

The Pitzer model equations for the osmotic coefficient ( $\phi$ ) and the logarithms of the activity coefficients of cations (M), anions (X), and neutral species (N) are given below for a solution containing an indefinite number of both neutral and ionic solutes. In each case the summations of terms arising from the presence of individual salts, neutral species, and their mixtures are indicated.

$$\begin{aligned}
 (\phi - 1) = & (2/\sum_i m_i)[-A^\phi I^{3/2}/(1 + 1.2I^{1/2})] & \text{(i) } \geq 1 \text{ salt} \\
 & + \sum_c \sum_a m_c m_a (B_{ca}^\phi + Z C_{ca}) \\
 & + \sum_{c < c'} m_c m_{c'} (\Phi_{cc'}^\phi + \sum_a m_a \psi_{cc'a}) & \text{(ii) } \geq 2 \text{ cations} \\
 & + \sum_{a < a'} m_a m_{a'} (\Phi_{aa'}^\phi + \sum_c m_c \psi_{aa'c}) & \text{(iii) } \geq 2 \text{ anions} \\
 & + 1/2 \sum_n m_n^2 \lambda_{nn} + \sum_n m_n^3 \mu_{nnn} & \text{(iv) } \geq 1 \text{ neutral} \\
 & + \sum_{n < n'} m_n m_{n'} \lambda_{nn'} + 3 \sum_{n < n'} m_n^2 m_{n'} \mu_{nnn'} & \text{(v) } \geq 2 \text{ neutrals} \\
 & + 6 \sum_{n < n' < n''} m_n m_{n'} m_{n''} \mu_{nn'n''} & \text{(vi) } \geq 3 \text{ neutrals} \\
 & + \sum_{n < c} m_n m_c \lambda_{nc} + 3 \sum_{n < c} m_n^2 m_c \mu_{nnc} & \text{(vii) } \geq 1 \text{ cation, } \geq 1 \text{ neutral} \\
 & + \sum_{n < a} m_n m_a \lambda_{na} + 3 \sum_{n < a} m_n^2 m_a \mu_{nna} & \text{(viii) } \geq 1 \text{ anion, } \geq 1 \text{ neutral} \\
 & + \sum_n \sum_c \sum_a m_n m_c m_a \zeta_{nca} & \text{(ix) } \geq 1 \text{ cation, } \geq 1 \text{ anion, } \geq 1 \text{ neutral} \\
 & + \sum_{n < c} \sum_{c' < c} m_n m_c m_{c'} \eta_{ncc'} & \text{(x) } \geq 2 \text{ cations, } \geq 1 \text{ neutral} \\
 & + \sum_{n < a} \sum_{a' < a} m_n m_a m_{a'} \eta_{naa'} & \text{(xi) } \geq 2 \text{ anions, } \geq 1 \text{ neutral} \\
 & + 6 \sum_c \sum_{n < n'} m_c m_n m_{n'} \mu_{cnn'} & \text{(xii) } \geq 1 \text{ cation, } \geq 2 \text{ neutrals} \\
 & + 6 \sum_a \sum_{n < n'} m_a m_n m_{n'} \mu_{ann'} & \text{(xiii) } \geq 1 \text{ anion, } \geq 2 \text{ neutrals} \quad (34)
 \end{aligned}$$

$$\begin{aligned}
\ln \gamma_M &= z_M^2 F + \sum_a m_a (2B_{Ma} + Z C_{Ma}) & (i) \geq \text{salt} \\
&+ |z_M| \sum_c \sum_a m_c m_a C_{ca} \\
&+ \sum_c m_c (2\Phi_{Mc} + \sum_a m_a \psi_{Mca}) & (ii) \geq 2 \text{ cations} \\
&+ \sum_{a < a'} \sum_{a'} m_a m_{a'} \psi_{Maa'} & (iii) \geq 2 \text{ anions} \\
&+ 2 \sum_n m_n \lambda_{Mn} + 3 \sum_n m_n^2 \mu_{Mnn} & (iv) \geq 1 \text{ neutral} \\
&+ 6 \sum_n \sum_{n'} m_n m_{n'} \mu_{Mnn'} & (v) \geq 2 \text{ neutrals} \\
&+ 6 \sum_n \sum_a m_n m_a \zeta_{Mna} & (vi) \geq 1 \text{ anion, } \geq 1 \text{ neutral} \\
&+ 6 \sum_n \sum_c m_n m_c \eta_{Mnc} & (vii) \geq 2 \text{ cations, } \geq 1 \text{ neutral} \quad (35)
\end{aligned}$$

$$\begin{aligned}
\ln \gamma_X &= z_X^2 F + \sum_c m_c (2B_{cX} + Z C_{cX}) & (i) \geq 1 \text{ salt} \\
&+ |z_X| \sum_c \sum_a m_c m_a C_{ca} \\
&+ \sum_a m_a (2\Phi_{Xa} + \sum_c m_c \psi_{cXa}) & (ii) \geq 2 \text{ anions} \\
&+ \sum_c \sum_{c'} m_c m_{c'} \psi_{cc'X} & (iii) \geq 2 \text{ cations} \\
&+ 2 \sum_n m_n \lambda_{Xn} + 3 \sum_n m_n^2 \mu_{Xnn} & (iv) \geq 1 \text{ neutral} \\
&+ 6 \sum_n \sum_{n'} m_n m_{n'} \mu_{Xnn'} & (v) \geq 2 \text{ neutrals} \\
&+ 6 \sum_n \sum_c m_n m_c \zeta_{ncX} & (vi) \geq 1 \text{ cation, } \geq 1 \text{ neutral} \\
&+ 6 \sum_n \sum_a m_n m_a \eta_{Xna} & (vii) \geq 2 \text{ anions, } \geq 1 \text{ neutral} \quad (36)
\end{aligned}$$

$$\begin{aligned}
\ln \gamma_N &= 2 \sum_n \lambda_{Nn} m_n + 3 \sum_n m_n^2 \mu_{Nnn} & (i) \geq 1 \text{ neutral} \\
&+ 6 \sum_n' m_n m_{nn} \mu_{Nnn} & (ii) \geq 2 \text{ neutrals} \\
&+ 6 \sum_n \sum_{n'} m_n m_{n'} \mu_{Nnn'} & (iii) \geq 3 \text{ neutrals} \\
&+ 2 \sum_c \lambda_{Nc} m_c + 2 \sum_a \lambda_{Na} m_a + \sum_c \sum_a m_c m_a \zeta_{Nca} & (iv) \geq 1 \text{ cation, } \geq 1 \text{ anion} \\
&+ \sum_c \sum_{c'} m_c m_{c'} \eta_{Ncc'} & (v) \geq 2 \text{ cations} \\
&+ \sum_{a < a'} \sum_{a'} m_a m_{a'} \eta_{Naa'} & (vi) \geq 2 \text{ anions} \\
&+ 6 \sum_n \sum_c m_n m_c \mu_{Nnc} + 6 \sum_n \sum_a m_n m_a \mu_{Nna} & (vii) \geq 1 \text{ neutral, } \geq 1 \text{ cation, } \geq 1 \text{ anion} \\
& & (37)
\end{aligned}$$

The water activity ( $a_{H_2O}$ ) is related to the osmotic coefficient ( $\phi$ ) by Equation 27. In the equations above,  $A^\phi$  is the Debye-Hückel parameter (0.3915, at 25°C),  $I$  (mol kg<sup>-1</sup>) is ionic strength,  $m_i$  is the molality of species  $i$ , and subscripts c, a, and n represent cations, anions, and neutrals.

Terms  $B_{ca}$ ,  $B_{ca}^\phi$ ,  $Z$ ,  $C_{ca}$ ,  $F$ ,  $\Phi_{cc'}$ , and  $\Phi_{cc'}^\phi$  (and corresponding ones for anion pairs) are functions given in full by Pitzer<sup>51</sup> (Chapter 3, this volume) and therefore not reproduced here. The B and C functions incorporate ion interaction parameters obtained from pure electrolyte data, ( $\beta_{ca}^{(0)}$ ,  $\beta_{ca}^{(1)}$ ,  $\beta_{ca}^{(2)}$ , and  $C_{ca}^\phi$ ). Functions  $\Phi_{cc'}^\phi$ ,  $\Phi_{cc'}$  (and those for anions) contain parameters ( $\theta_{cc'}$  and  $\theta_{aa'}$ ) for interactions between ions of like sign and an unsymmetrical

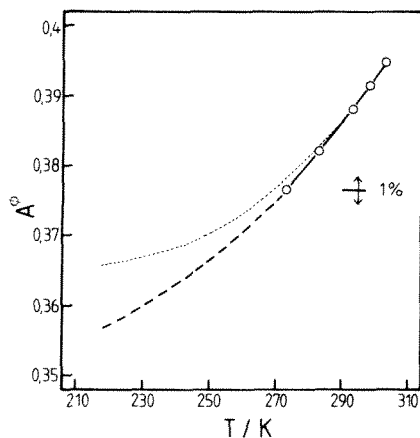


FIGURE 1. Estimates of the Debye-Hückel parameter  $A^\phi$  below 273.15 K. Symbols — 273 to 303 K values listed by Pitzer;<sup>51</sup> full line — calculated Equation 39 (valid 273 to 373 K); dashed line —  $A^\phi$  ( $T < 273$  K) estimated by Clegg and Brimblecombe<sup>74</sup> from extrapolated Debye-Hückel heat capacity parameter  $A_j$  (Equation 38); dotted line —  $A^\phi$  ( $T < 273$  K) estimated by Spencer et al.<sup>76</sup> from isothermal model fits to data for systems at 268, 263, and 253 K and including tabulated values<sup>51</sup> of  $A^\phi$  above 273 K. Note discrepancy between  $A^\phi$  used by Spencer et al.<sup>76</sup> and established values for  $T \geq 273$  K.

mixing term. The parameters  $\psi_{cc'a}$  and  $\psi_{aa'c}$  account for interactions between one ion of one sign, and two dissimilar ions of opposite sign. These ion parameters arise from the grouping of observable combinations of the virial coefficients  $\lambda_{ij}$  and  $\mu_{ijk}$ .

Double (or triple) summation indices such as  $c < c'$ ,  $a < a'$ , and  $n < n'$  denote sums over all distinguishable pairs (or triplets) of cations, anions, or neutrals. For the primed summations  $\Sigma'$ ,  $n$  (or  $n'$  as indicated) cannot equal  $N$ . All interactions are assumed to be symmetrical, thus  $\theta_{ij}$  is equal to  $\theta_{ji}$  and  $\lambda_{ij}$  is equal to  $\lambda_{ji}$  with corresponding relations applying to other binary and all triplet interactions.

The value of the Debye-Hückel parameter  $A^\phi$  as a function of temperature and pressure is well established (Pitzer,<sup>51</sup> Chapter 3, this volume), at least above 0°C. Where model calculations are extended below the freezing point of water, empirical extensions have been employed<sup>74,75</sup> or estimates obtained indirectly using the model itself.<sup>76</sup> Unless they are supercooled, solutions are maintained in a liquid state below 0°C by freezing point depression. Consequently, at temperatures significantly below zero, solutions are too concentrated for activity coefficients to approach the Debye-Hückel limiting slope. However, the dilute solution component of the osmotic and activity coefficient equations does make an (approximately constant) contribution, which is dependent upon  $A^\phi$ , to  $(\phi - 1)$  and  $\ln(\gamma_\pm)$  at higher aqueous phase concentrations. Consequently, the value of  $A^\phi$  used must be consistent with the other parameters. Thurmond and Brass,<sup>75</sup> when calculating model parameters for aqueous NaCl to  $-40^\circ\text{C}$  (using heat capacity data), extrapolated  $A^\phi$  and the associated heat capacity constant  $A_j$  from values above 0°C. Although the precise method is not given, the result is presumably similar to that obtained by Clegg and Brimblecombe,<sup>74</sup> who extrapolated  $A_j$  linearly below 0°C and integrated twice to yield the Debye-Hückel enthalpy parameter  $A_L$ , then  $A^\phi$ . The difference between the values obtained in this way and those estimated by Spencer et al. from salt solubility data<sup>76</sup> is about 3% in  $A^\phi$  at  $-60^\circ\text{C}$ , and is illustrated in Figure 1 for temperatures below 30°C. For practical calculations two equations are given below for  $A^\phi$  at temperatures up to 100°C:

for  $T \leq 273$  K:

$$A^\phi = 0.13422(0.0368329 T - 14.62718 \ln(T) - 1530.1474/T + 80.40631) \quad (38)$$

for  $273 \leq T \leq 373$  K:

$$A^\phi = 0.13422(4.1725332 - 0.1481291 T^{0.5} + 1.5188505 \times 10^{-5} T^2 - 1.8016317 \times 10^{-8} T^3 + 9.3816144 \times 10^{-10} T^{3.5}) \quad (39)$$

**TABLE 9**  
**Pure Electrolyte Pitzer Model Parameters ( $\beta^{(0)}$ ,  $\beta^{(1)}$ ,  $\beta^{(2)}$ , and  $C^\phi$ ), Their**  
**Partial Derivatives with Respect to Temperature and Pressure, and**  
**Relationship to Measurable Properties**

Parameter	Relationship to $\beta^{(i)}$ , $C^\phi$	Used in equation for	Principal data	Ref. and equation no.
$\beta^{(i)}$ , $C^\phi$	--	Activity ( $\gamma_i$ ) and osmotic coefficient ( $\phi$ )	EMF, freezing point depression, vapor pressure	Pitzer (Chapter 3, this volume), 62—64; this work, 34—37
$\beta^{(i)h}$ , $C^{\phi h}$	$(\partial/\partial T)_P$	Apparent molal enthalpy ( $^hL$ )	Heat of dilution	Pitzer (Chapter 3, this volume), 81
$\beta^{(i)h}$ , $C^{\phi h}$	$(\partial^2/\partial T^2)_P$	Apparent molal heat capacity ( $^hC_p$ )	Heat capacity	Pitzer (Chapter 3, this volume), 91
$\beta^{(i)V}$ , $C^{\phi V}$	$(\partial/\partial P)_T$	Apparent molal volume ( $^hV$ )	Density	Pitzer (Chapter 3, this volume), 96
$\beta^{(i)\kappa}$ , $C^{\phi\kappa}$	$(\partial^2/\partial P^2)_T$	Apparent molal compressibility ( $\kappa$ )	Compressibility, speed of sound	Millero et al., <sup>81</sup> 5 (with substitutions)

Equation 39 reproduces values of  $A^\phi$  listed by Pitzer<sup>51</sup> (Chapter 3, this volume) to within 0.01%. (Note that the corresponding parameter on a mole fraction basis,  $A_i$ , may be obtained by removing the factor of 0.13422 from each equation.)

The classical equations<sup>77</sup> (and see Stokes,<sup>78</sup> Chapter 1, this volume) relating activities at some reference temperature and pressure (usually 298.15 K and 1 atm) to values at other (T, P) via the partial molal functions allow osmotic and activity coefficients to be determined as  $f(T, P)$  where the necessary data are available. However, calculations can become quite cumbersome since empirical representations of the partial molal properties, as functions of concentration, are also required. In the case of aqueous  $\text{HNO}_3$ ,<sup>74</sup> for example, Chebychev polynomials of up to 12 coefficients were required to represent partial molal enthalpies and heat capacities of solute and solvent as functions of  $\text{HNO}_3$  concentration. However, partial differentiation of the Pitzer model expression for the Gibbs energy (Equation 59; Pitzer,<sup>51</sup> Chapter 3, this volume) with respect to temperature and pressure leads to corresponding expressions for the apparent molal properties of aqueous solutions (Equations 81, 91, 96; Pitzer,<sup>51</sup> Chapter 3, this volume). These equations are readily extended to mixtures,<sup>79-81</sup> in the same way as those for osmotic and mean activity coefficients. The model parameters in the expressions for apparent molal enthalpy ( $\beta^{(i)h}$ ,  $C^{\phi h}$ ), heat capacity ( $\beta^{(i)h}$ ,  $C^{\phi h}$ ), volume ( $\beta^{(i)V}$ ,  $C^{\phi V}$ ), and compressibility ( $\beta^{(i)\kappa}$ ,  $C^{\phi\kappa}$ ) for single electrolyte solutions are equivalent to the first and second differentials of parameters ( $\beta^{(i)}$ ,  $C^\phi$ ) with respect to temperature and pressure, respectively. There are similar correspondences for the derivatives of the mixture parameters  $\theta_{ij}$  and  $\psi_{ijk}$ . Using this approach, the effects of temperature and pressure on activity can be quite simply determined. The relationships are summarized in Table 9.

The Pitzer model only considers interactions between pairs and triplets of solute species. Thus, in principle, all interaction parameters can be determined from measurements on solutions containing no more than three dissolved components. For example, most  $\theta_{ij}$  and  $\psi_{ijk}$  parameters are obtained from isopiestic, EMF, or salt solubility data for ternary ion systems — solutions containing two salts with a common ion.<sup>54,82</sup> Even considering only binary and ternary interactions results in a very large number of parameters for an arbitrarily complex system, as can be seen in Equations 34 to 37. However, most of the summations involve some combination of ions and neutral species — hence for a solution containing only ionic components, the expressions for osmotic and single ion activity coefficients involve

only lines (i to iii) of Equations 34 to 36. Most solutions of geochemical interest are likely to be constrained in that the neutral species are atmospheric gases whose concentrations are too low at normal temperature and pressure to affect the activities of the solvent, and other solutes. In such cases, all summations involving  $m_n$ ,  $m_n'$ , and  $m_n''$  can be neglected. Thus, in natural waters the activity coefficient of  $\text{CO}_2$  or  $\text{O}_2$  can be described using only line (iv) of Equation 37, and the effect of these components on the osmotic coefficient and activity coefficients of dissolved ions is negligible.

An extensive database of model parameters has been evaluated by Pitzer and co-workers from data for binary and ternary ion mixtures, much of which is listed by Pitzer<sup>51</sup> (Tables 2 to 11, Chapter 3, this volume). Ideally, the expansion of the database, to include a larger number of pure solutes and their mixtures, and the variation of their properties as  $f(T,P)$ , should occur in a self-consistent way. However, this is not always the case, partly because of the necessary revision and updating of thermodynamic data. More importantly, in a number of geochemical applications, treatments of ion pairing or association reactions and the temperature functionality of associated parameters have varied between groups of workers.<sup>76,83,84</sup> In some cases empirical extensions to the model have also been used for specific systems.<sup>85,86</sup> Because of this it is important to consider first how the model parameters are obtained, and second the areas of inconsistency between the main datasets of geochemical interest.

### a. Interaction Parameters

#### i. Single Salt Solutions

Pure electrolyte solution parameters  $\beta^{(i)}$ ,  $C^\phi$  ( $i = 0, 1, 2$ ) are determined by fitting Equations 34, or 35 and 36 to osmotic or mean activity coefficient data, respectively, usually at 25°C. The temperature variation of these parameters is obtained either from further direct measurements [yielding  $\phi$  or  $\ln(\gamma_{\pm})$ ], or from heats of dilution and heat capacities which yield the first ( $\beta^{(i)L}$ ,  $C^{\phi L}$ ) and second ( $\beta^{(i)J}$ ,  $C^{\phi J}$ ) partial differentials of the model parameters with respect to temperature (see Table 9). Accurate estimation of the variation of  $\beta^{(i)}$  and  $C^\phi$  as functions of temperature requires at least  $\phi$  or  $\ln(\gamma_{\pm})$ , apparent molal enthalpy at a single temperature, and heat capacities measured at different temperatures over the range of interest. This enables the model parameters  $\beta^{(i)}$ ,  $C^\phi$  to be calculated as continuous functions of temperature by integration. Fitting equations for these parameters are available for a number of important solutes (see Table 10). The sources of the equations used for calculations in this chapter are indicated in Table 11. Where heat capacities, heats of dilution, and osmotic or mean activity coefficients are available only at a single temperature  $T_r$  (typically 298.15 K), then the pure electrolyte parameters  $p^{(i)}$  can be calculated for temperatures  $T$  not too far from  $T_r$  by the equation:

$${}_T p^{(i)} = {}_{T_r} p^{(i)} + (T - T_r)(p^{(i)L} - {}_{T_r} p^{(i)J}) + 0.5(T^2 - T_r^2)p^{(i)J} \quad (40)$$

An analogous equation applies for the pressure effect on parameter  $p^{(i)}$ , in which case the reference pressure  $P_r$  would usually be 1 atm. Values of  $\beta^{(i)L}$  and  $C^{\phi L}$  for many electrolytes are listed by Pitzer<sup>51</sup> (Tables 12 and 13 of Chapter 3, this volume). Second derivatives ( $\beta^{(i)J}$ ,  $C^{\phi J}$ ) are obtained from heat capacities, and have been determined for KCl,<sup>87</sup> NaCl,<sup>88</sup> and for some strong acids.<sup>68</sup>

Close to 25°C the change in  $\theta_{cc}$  and  $\psi_{caa}$  (also  $\theta_{aa}$  and  $\psi_{cc'a}$ ) can probably be neglected, although applications of the model to salt solubilities in brines have shown that it is necessary, over a very large range of temperature, to treat such variations explicitly.<sup>76,83,89</sup> Work involving the neutral solute  $\text{O}_2$  has yielded neutral-ion interaction parameters ( $\lambda_{\text{O}_2,i}$ ) as functions of temperature for many ions.<sup>90</sup> From this work it appears that  $\zeta_{nca}$  can be treated as constant except over extended ranges of temperature, in a similar way to the mixture parameters for ions.

**TABLE 10**  
**Availability of Fitting Equations Giving Pure Electrolyte Parameters**  
**( $\beta^{(0)}$ ,  $\beta^{(1)}$ ,  $\beta^{(2)}$ , and  $C^\phi$ ) as Functions of Temperature**

Solute	Temperature range	Pressure	Ref.	Solute	Temperature range	Pressure	Ref.
H <sub>2</sub> SO <sub>4</sub>	273—323		111	K <sub>2</sub> SO <sub>4</sub> <sup>h</sup>	298—498		84
HCl	273—523		85	CsF	298—373		317
LiCl	273—523		314	CsCl	273—523		314
Li <sub>2</sub> SO <sub>4</sub>	273—498		260	CsI	298—373		317
NaCl	273—573	→1 kbar	315	Cs <sub>2</sub> SO <sub>4</sub>	273—523		260
NaCl <sup>a</sup>	273—573		89	MgCl <sub>2</sub>	298—473		318
NaCl <sup>b</sup>	228—298		76	MgCl <sub>2</sub>	298—473		319
NaCl <sup>c</sup>	233—298		75	MgCl <sub>2</sub> <sup>l</sup>	221—298		76
NaOH	273—623	→400 bar	316	MgSO <sub>4</sub>	298—473		320
Na <sub>2</sub> SO <sub>4</sub>	273—498		260	MgSO <sub>4</sub>	268—298		76
Na <sub>2</sub> SO <sub>4</sub> <sup>d</sup>	298—523		89	CaCl <sub>2</sub> <sup>l</sup>	298—473		321
Na <sub>2</sub> SO <sub>4</sub> <sup>e</sup>	251—298		76	CaCl <sub>2</sub>	298—473		319
KCl	273—523		314	CaCl <sub>2</sub> <sup>k</sup>	298—523		89
KCl <sup>f</sup>	273—523		84	CaCl <sub>2</sub> <sup>l</sup>	273—523		84
KCl <sup>g</sup>	249—298		76	CaCl <sub>2</sub> <sup>m</sup>	223—298		76
KCl	298—598	→500 bar	87	CaSO <sub>4</sub> <sup>n</sup>	298—523		89
K <sub>2</sub> SO <sub>4</sub>	273—498		260	SrCl <sub>2</sub>	298—473		319

<sup>a</sup> Parameter values of Pitzer et al.<sup>315</sup> refitted to alternative equation.

<sup>b</sup> Parameters at low temperatures estimated partly from solubilities in ternary ion solutions. Above 25°C parameter values merge smoothly with those of Moller.<sup>89</sup>

<sup>c</sup> Temperature variation of parameters estimated from heat capacity data.

<sup>d</sup>  $\beta^{(0)}$  and  $\beta^{(1)}$  from 25—200°C same as Rogers and Pitzer.<sup>322</sup>  $C^\phi$  (25—200°C) and  $\beta^{(0)}$  and  $\beta^{(1)}$  (>200°C) were evaluated from solubilities in Na-Cl-SO<sub>4</sub>-H<sub>2</sub>O aqueous solutions.

<sup>e</sup> Parameters at low temperatures estimated partly from solubilities in ternary ion solutions.

<sup>f</sup> Parameter values of Holmes and Mesmer<sup>314</sup> were refitted to alternative equation.

<sup>g</sup> Parameters at low temperatures estimated partly from solubilities in ternary ion solutions.

<sup>h</sup> Parameter values of Holmes and Mesmer<sup>260</sup> were refitted to alternative equation. Also used by Spencer et al.<sup>76</sup> to estimate activity coefficients below 0°C.

<sup>i</sup> Parameter values merge with those given by equation of Phutela et al.<sup>319</sup> above 25°C.

<sup>l</sup> Concentration range 0—4.3 mol kg<sup>-1</sup>.

<sup>k</sup> Concentration range 0—4 mol kg<sup>-1</sup>.

<sup>l</sup>  $C^\phi$  refitted, to extend treatment of Moller<sup>89</sup> to 0°C.

<sup>m</sup> Parameters at low temperatures estimated partly from solubilities in ternary ion solutions.

<sup>n</sup> Treatment includes formation of ion pair CaSO<sub>4</sub><sup>0</sup>, with temperature variation of formation constant given by two equations 25—150 and 150—250°C.  $\beta^{(0)}$ ,  $\beta^{(1)}$ , and  $C^\phi$  set constant at all temperatures ( $C^\phi = 0$ ), while  $\beta^{(2)}$  varies with temperature from 25—50°C and is set to zero for T > 50°C.

Millero<sup>91</sup> has reviewed the effect of pressure on activity coefficients in seawater (data to 1983) and includes partial molal volumes and compressibilities for both ions and non-electrolytes in the medium. The effect of pressure on the thermodynamic properties of seawater itself is also well characterized.<sup>18,20,92</sup> More recently, Millero and co-workers<sup>80,81,93,94</sup> have studied in detail the PVT properties of the major components of sea salt (NaCl, Na<sub>2</sub>SO<sub>4</sub>, MgCl<sub>2</sub>, MgSO<sub>4</sub>, KCl, and K<sub>2</sub>SO<sub>4</sub>) and their mixtures, leading to values of  $\beta^{(i)V}$ ,  $C^{\phi V}$  as f(T) for all solutes, and also further differentials with respect to pressure ( $\beta^{(i)K}$ ,  $C^{\phi K}$ ) for some of these components. Densities of Na<sup>+</sup> and K<sup>+</sup> chloride and sulfate mixtures have yielded estimates of  $\theta_{Na,K}^V$ ,  $\theta_{Na,Mg}^V$ , and  $\theta_{Cl,SO_4}^V$  as functions of temperature.<sup>80,94</sup> In Appendix Tables A4 and A5 are listed equations giving the pressure effect on the activity coefficients of the major constituents of sea salt. Values of ( $\beta^{(i)}$ ,  $C^\phi$ ) at a given temperature and pressure may be obtained by applying Equation 40, or by integration.

**TABLE 11**  
**Sources of Fitting Equations for Pure Electrolyte Parameters ( $\beta^{(0)}$ ,  $\beta^{(1)}$ ,  $\beta^{(2)}$ , and  $C^\phi$ ) Used for Calculations Carried Out in the Present Study**

Solute	Temperature range	Pressure	Ref.
H <sub>2</sub> SO <sub>4</sub>	273—323		111
HCl	273—523		85
NaCl	273—573	→1 kbar	315
NaOH	273—623	→400 bar	316
Na <sub>2</sub> SO <sub>4</sub>	273—498		260
KCl	273—523		314
K <sub>2</sub> SO <sub>4</sub>	273—498		260
MgCl <sub>2</sub>	298—473		318
MgSO <sub>4</sub>	298—473		320
CaCl <sub>2</sub>	298—523		89

*Note:* The fitting equations, with the exception of those for H<sub>2</sub>SO<sub>4</sub>, are given in Appendix B of Pitzer.<sup>323</sup>

### ii. Multicomponent Salt Solutions

In multicomponent solution mixtures, the additional parameters  $\theta_{cc'}$ ,  $\theta_{aa'}$ ,  $\psi_{cc'a}$ , and  $\psi_{aa'c}$  arise, describing interactions between pairs of dissimilar cations, anions, and one anion and cation, respectively. As described by Pitzer<sup>51</sup> (Chapter 3, this volume), these parameters can best be determined from  $\phi$  or  $\ln(\gamma_{\pm})$  data for ternary ion systems. An alternative source of these parameters, particularly important for geochemical applications, is salt solubilities in ternary and other multicomponent systems. For example, consider a salt solution containing the ions  $M^{a+}$ ,  $N^{b+}$ , and  $X^{c-}$  which is saturated with respect to the solid phase  $M_{\nu_+}X_{\nu_-} \cdot zH_2O$ . (It is assumed that only the pure solution model parameters for the two salts are known.) The chemical potential of the salt is related to the activity product of its components in solution by the following equation:<sup>95</sup>

$$\mu_{\text{solid}}^{\ominus} = \nu_+ \mu_M^{\ominus} + \nu_- \mu_X^{\ominus} + z\mu_{H_2O}^{\ominus} + RT \ln[\gamma_{\pm}^{\nu} \cdot m_M^{\nu_+} \cdot m_X^{\nu_-} \cdot (aH_2O)^z] \quad (41)$$

thus:

$$(\mu_{\text{solid}}^{\ominus} - \nu_+ \mu_M^{\ominus} - \nu_- \mu_X^{\ominus} - z\mu_{H_2O}^{\ominus})/RT = \ln[\gamma_{\pm}^{\nu} \cdot m_M^{\nu_+} \cdot m_X^{\nu_-} \cdot (aH_2O)^z] \quad (42)$$

where  $\mu_i^{\ominus}$  is the standard chemical potential of component  $i$ ,  $\gamma_{\pm}$  is the mean activity coefficient of salt  $M_{\nu_+}X_{\nu_-}$ , and  $\nu$  is equal to  $(\nu_+ + \nu_-)$ . Where the standard chemical potentials are known, the difference between the model-calculated activity product  $\gamma_{\pm}^{\nu} \cdot m_M^{\nu_+} \cdot m_X^{\nu_-} \cdot (aH_2O)^z$  and that calculated from the standard chemical potentials (Equation 42) can be attributed to the unknown parameters  $\theta_{MN}$  and  $\psi_{MNX}$ . These are then fitted as unknowns to bring the calculated activity product into agreement with the theoretical value. This procedure has been used most extensively in studies of salt solubility in multicomponent brines by Weare and co-workers,<sup>54,56,61</sup> who have determined not only the values of mixture parameters, but also the chemical potentials of some solid phases where these also were unknown.

Ion-ion mixture parameters  $\theta_{ij}$  and  $\psi_{ijk}$  vary with temperature to a lesser extent than the pure salt parameters ( $\beta^{(i)}$ ,  $C^\phi$ ). From laboratory measurements of HCl activity in H-Mg-Cl-H<sub>2</sub>O solutions, Roy et al.<sup>96</sup> have determined the temperature variation of both  $\theta_{H,Mg}$  and  $\psi_{H,Mg,Cl}$  from 5 to 40°C. However, in an application of the model to salt solubilities in Na-

K-Ca-Cl-SO<sub>4</sub>-H<sub>2</sub>O brines from 0 to 250°C Greenberg and Moller<sup>84</sup> were able to set several  $\theta_{ij}$  and  $\psi_{ijk}$  constant at all temperatures. Similarly, Pabalan and Pitzer<sup>83</sup> set  $\theta_{ij}$  constant, while allowing  $\psi_{ijk}$  to vary with temperature, when determining ternary ion parameters for the system Na-K-Mg-Cl-SO<sub>4</sub>-OH-H<sub>2</sub>O to 200°C from solubility data. These choices for the functionality of  $\theta_{ij}$  and  $\psi_{ijk}$  are unlikely to represent the true temperature variation of the interactions, and are made rather on the basis of the minimum number of parameters required to reproduce the input data. Also, any inaccuracies in the description of the binary cation-anion interactions, likely to be greatest at high concentration and temperatures far from 25°C, are subsumed into the mixture parameters. The possibility of different parameter choices and the question of where to include ion association or ion pairing (e.g., formation of CaSO<sub>4</sub><sup>0</sup>) lead to problems of consistency between parameter sets as described above.

### iii. Neutral Solutes

Neutral-neutral (self) interaction parameters ( $\lambda_{NN}$ ) and  $\mu_{NNN}$  have been obtained for phosphoric acid (H<sub>3</sub>PO<sub>4</sub>), which in aqueous solution is only 10 to 20% dissociated, from osmotic coefficients and data for buffer solutions containing H<sub>3</sub>PO<sub>4</sub>.<sup>59</sup> A similar self-interaction is also implicit in a treatment of CH<sub>4</sub> solubility in water and aqueous solutions at high pressure, based on the Pitzer formalism.<sup>97</sup> More direct determinations have been made for aqueous NH<sub>3</sub>, for solutions concentrated ( $\leq 20$  mol kg<sup>-1</sup>) far in excess of those found in natural waters.<sup>98</sup> These were obtained from equilibrium measurements of  $p\text{NH}_3$ , from the equation

$$K'_H = \gamma_{\text{NH}_3} m_{\text{NH}_3} / f_{\text{NH}_3} \quad (43)$$

where  $K'_H$  (mol kg<sup>-1</sup> atm<sup>-1</sup>) is the thermodynamic Henry's law constant,  $m_{\text{NH}_3}$  is the molal NH<sub>3</sub> concentration, and  $f_{\text{NH}_3}$  (atm) the equilibrium gas phase fugacity, assumed to be equivalent to partial pressure. For pure solutions sufficiently concentrated for dissociation to be negligible (e.g., NH<sub>3(aq)</sub> is about 1.4% dissociated at a total concentration of 0.1 mol kg<sup>-1</sup> at 25°C), and for which the triplet interaction ( $\mu_{\text{NH}_3, \text{NH}_3, \text{NH}_3}$ ) can be neglected,  $\gamma_{\text{NH}_3}$  is equal to  $\exp(2\lambda_{\text{NH}_3, \text{NH}_3} \cdot m_{\text{NH}_3})$ . The variation of  $\lambda_{\text{NH}_3, \text{NH}_3}$  with temperature was estimated from both equilibrium partial pressures as  $f(T)$  and apparent molal enthalpies in a similar way to the variation for pure electrolytes.

For major atmospheric gases such as O<sub>2</sub>, the equilibrium concentrations in water are sufficiently low (e.g.,  $m_{\text{O}_2}$  at 298.15 K = 0.00026 for a partial pressure of 0.2 atm) that self-interactions can be neglected. Thus, as previously stated, the estimation of their activity coefficients in natural waters requires only the ion-neutral interactions given in line (iv) of Equation 37, and possibly those in lines (v) and (vi) in concentrated brines.

There are few estimates of parameters  $\lambda_{nr}$  for dissimilar neutral species, which are at present confined to interactions between dissolved CO<sub>2</sub> and some Mg and Ca ion pairs,<sup>56</sup> and  $\lambda_{\text{NH}_3, \text{CO}_2}$ .<sup>90</sup>

### iv. Neutral Solutes and Dissolved Salts

Where a neutral species, such as O<sub>2</sub>, CO<sub>2</sub>, or NH<sub>3</sub>, is a gas at normal temperature and pressure, the activity coefficient  $\gamma_N$  is most simply obtained from the solubility of the gas in salt solutions (Equation 42), for which a great deal of compiled data are available (see Table 12). Analogously, the activity coefficient can be determined from measurements of partitioning into a second solvent, whereupon the Henry's law constant is replaced by an "infinite dilution" partition coefficient. In a solution of a single salt M<sub>v</sub>X<sub>v</sub>, the activity coefficient of the neutral species N (for which self-interactions are negligible) is given by

$$\ln(\gamma_N) = 2(\lambda_{NM}m_M + \lambda_{NX}m_X) + m_Mm_X\zeta_{NMX} \quad (44)$$



**TABLE 12**  
**Some Sources of Compiled Data for Gas Solubilities in**  
**Aqueous Solutions**

Gas	Year	Ref.	Gas	Year	Ref.
Ar	1980	324	CH <sub>4</sub>	1987	325
He, Ne	1979	326	C <sub>2</sub> H <sub>6</sub>	1982	327
Kr, Xe, Rn	1979	328	C <sub>3</sub> H <sub>8</sub> , C <sub>4</sub> H <sub>10</sub>	1986	329
H <sub>2</sub> , D <sub>2</sub>	1981	330	Hydrocarbons C5—C7	1989	331
N <sub>2</sub> , air	1982	332	Hydrocarbons C8—C36	1989	333
N <sub>2</sub> O, NO	1981	334	Alcohols	1984	335
O <sub>2</sub> , O <sub>3</sub>	1981	192	Halogenated benzenes, toluenes and phenols	1985	336
SO <sub>2</sub> , Cl <sub>2</sub> , F <sub>2</sub>	1983	288	Polychlorinated biphenyls	1986	338
CO	1990	337	“Chemicals of environ- mental interest	1981	339

*Note:* See also Tables A7—A9.

Because of the constraint of electroneutrality, parameters  $\lambda_{NM}$  and  $\lambda_{NX}$  can only be determined as the sum ( $\nu_+ \lambda_{NM} + \nu_- \lambda_{NX}$ ). To simplify practical calculations it is usual to set  $\lambda_{Ni}$  for some ion  $i$  to zero at all temperatures — such as the chloride parameter  $\lambda_{N,Cl}$  in the cases of H<sub>3</sub>PO<sub>4</sub>, O<sub>2</sub> and NH<sub>3</sub>.<sup>59,90,98</sup> However, while Harvie et al.<sup>56</sup> set  $\lambda_{H,CO_2}$  to zero in a study of brine solubility in systems containing dissolved CO<sub>2</sub>, the choice of “baseline” parameter may be very simply changed. For example, the parameters listed by Harvie et al.<sup>56</sup> for cations  $c$  and anions  $a$  can be adjusted to a scale on which  $\lambda_{CO_2,Cl}$  is equal to zero, using the following relationships:

$${}^Cl\lambda_{CO_2,c} = {}^H\lambda_{CO_2,c} + (z_c/z_{Cl}) {}^Cl\lambda_{CO_2,Cl} \quad (45)$$

$${}^Cl\lambda_{CO_2,a} = {}^H\lambda_{CO_2,a} + (z_a/z_{Cl}) {}^Cl\lambda_{CO_2,Cl} \quad (46)$$

where  ${}^Cl\lambda_{CO_2,i}$  is the binary interaction parameter for CO<sub>2</sub> with ion  $i$  on the “chloride scale”,  ${}^H\lambda_{CO_2,i}$  the same parameter but on the “hydrogen ion scale”, and  $z_i$  the charge on ion  $i$ . However, retaining existing values does not result in any incompatibility as long as mean ion activity coefficients, rather than single ion values, are the desired quantity. It is clear from line (vii) of Equation 37 that a similar question arises with regard to the triplet parameters  $\mu_{Nnc}$  and  $\mu_{Nna}$ . In a study of NH<sub>3</sub>, Clegg and Brimblecombe<sup>98</sup> set  $\mu_{NH_3,NH_3,Cl}$  to zero.

Where the concentration of the neutral component can be sufficiently high to affect ion activity coefficients (as is the case in aqueous NH<sub>3</sub>), then ion-neutral interaction parameters can be determined from measured salt solubilities in solutions containing the neutral species. Such data are extensive for aqueous NH<sub>3</sub>.<sup>99</sup> The fundamental relationship is again Equation 41, where the difference between the activity product of the salt calculated by the model (using pure electrolyte parameters only) and that known from the chemical potential of the solid phase is attributed to interactions with the neutral species — given (for a single electrolyte) by lines (iv) and (vi) of Equations 35 and 36, and also by lines (vii to ix) of Equation 34 where the solid phase is hydrated.

The temperature variation of the binary ion-neutral interaction parameter  $\lambda_{N,i}$  can be determined straightforwardly. For example, for O<sub>2</sub> this was obtained from gas solubilities in salt solutions at different temperatures. In many cases, where a further term in  $m_M \cdot m_X \cdot \zeta_{O_2,M,X}$  in the expression for the activity coefficient was required, this could be made temperature invariant where the range was not too great.

Values of  $\partial\lambda_{NH_3,i}/\partial T$  estimated for a few ions  $i$  from salt solubilities in aqueous NH<sub>3</sub> are less certain since they incorporate any inaccuracies in both modeled ion-ion interactions and

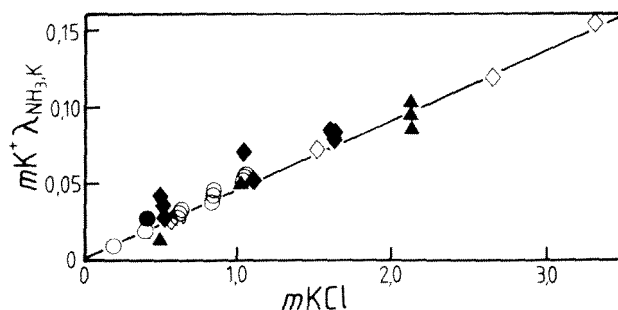


FIGURE 2. Comparison of the  $\lambda_{\text{NH}_3, \text{K}}$  interaction parameter (slope of line) determined from different data types, leading to either  $\gamma_{\text{NH}_3}$  or  $\gamma_{\text{KCl}}$  in aqueous solution at 25°C: circle —  $\text{KCl}_{(\text{aq})}/\text{CHCl}_3$  partitioning data;<sup>380</sup> open diamonds —  $\text{KCl}$  solubility in  $\text{NH}_3(\text{aq})$ ;<sup>99</sup> closed diamonds —  $p\text{NH}_3$ ;<sup>381</sup> dots —  $p\text{NH}_3$ ;<sup>382</sup> triangles —  $p\text{NH}_3$  for systems containing  $>10 \text{ mol kg}^{-1} \text{ NH}_3$ .<sup>383</sup>

the variation of the solubility product with temperature. Also, the variation of solubility with temperature is influenced more by the change in ion-ion interactions than by the ion- $\text{NH}_3$  interaction. Consequently,  $\partial\lambda_{\text{NH}_3, \text{SO}_4}/\partial T$  could only be estimated (from  $\text{Na}_2\text{SO}_4$ ,  $\text{Na}_2\text{SO}_4 \cdot 10\text{H}_2\text{O}$ , and  $\text{K}_2\text{SO}_4$  solubilities in aqueous  $\text{NH}_3$ ) to lie between  $-0.0005$  and  $-0.0009$  for a 25°C value of  $\lambda_{\text{NH}_3, \text{SO}_4}$  of 0.14.<sup>98</sup>

It is clear from the above discussion that model parameters can be determined from a variety of data that lead either to the activity of the solvent or one of the solutes. This is one of the principal advantages of a self-consistent model describing the activities of all solution components and their variation with temperature and pressure, over the more empirical approaches used in the past — such as extended Debye-Hückel expressions for ionic solutes or the Setchenow equation for neutral species. As an example of the use of different kinds of data for parameter evaluation we now compare the  $\text{K}^+$ - $\text{NH}_3$  interaction, in terms of the binary parameter  $\lambda_{\text{NH}_3, \text{K}}$ , determined from measurements of  $p\text{NH}_3$  above  $\text{NH}_3$ - $\text{KCl}$ - $\text{H}_2\text{O}$  solutions (containing up to  $8 \text{ mol dm}^{-3} \text{ NH}_3$ ),  $\text{KCl}$  solubilities in aqueous  $\text{NH}_3$  ( $m\text{NH}_3 \leq 25 \text{ mol kg}^{-1}$ ), and partitioning of  $\text{NH}_3$  between aqueous  $\text{KCl}$  and  $\text{CHCl}_3$  ( $m\text{NH}_3 \leq 1 \text{ mol kg}^{-1}$ ). Figure 2 shows that  $\lambda_{\text{NH}_3, \text{K}}$  obtained from all these experimental data agree well.

### b. Ion Pairing and Ion Association

The Pitzer model treats all interactions in solutions of conventional strong electrolytes as occurring between free ions. For solutions of single electrolytes this approach is satisfactory even for solutes such as the 2:2 metal sulfates, where ion pairing is known to occur at low concentrations<sup>37</sup> ( $0.03$  to  $0.1 \text{ mol kg}^{-1}$ ), and for aqueous  $\text{HNO}_3$  which Raman spectroscopy has shown to be about 20% associated at a stoichiometric concentration of  $6 \text{ mol kg}^{-1}$ .<sup>100</sup> For stronger association reactions, such as that between  $\text{Mg}^{2+}$  and  $\text{F}^-$  in saline media, a choice of approaches is possible. Millero<sup>60</sup> has calculated stability constants of  $\text{MgF}^+$  and  $\text{CaF}^+$  in  $0.7 \text{ mol kg}^{-1} \text{ NaCl}$  of 18.8 and  $4.2 \text{ kg mol}^{-1}$ , respectively. Alternatively, it is possible to describe the influence of complex formation on  $\text{F}^-$  activity in seawater solutions as due to strong interactions between free  $\text{Mg}^{2+}$  and  $\text{F}^-$ , using parameters  $\beta^{(i)}$  and  $C^{\text{fb}}$  as an alternative to the formation of species such as  $\text{MgF}^+$ . This can also be done for the interaction of major seawater cations with a number of weak acid anions (A) such as  $\text{B}(\text{OH})_3^{2-}$ ,  $\text{HCO}_3^-$ , and  $\text{H}_2\text{PO}_4^-$ , yielding parameters that are specific to a seawater medium.<sup>60</sup> The results also show that the stoichiometric stability constants  $\text{p}K_{\text{HA}}^{\text{st}}$  for the weak acids (HA) in seawater can be satisfactorily predicted, using the model to estimate the activity coefficients of the free  $\text{H}^+$  and acid anion A. However, this approach is limited both in the

range of solution concentration that can be covered and in the strength of the (real) association that can be described. Measurements of  $\gamma_{\text{NaF}}$  using ion-specific electrodes in NaCl media have shown that in a concentrated brine where  $m\text{Mg}^{2+}$  would greatly exceed its seawater concentration, it is necessary to consider the formation of  $\text{MgF}^+$  explicitly.<sup>101</sup>

Where there is strong association over a wide range of concentration, for example, for  $\text{H}_2\text{SO}_4$ ,  $\text{H}_2\text{CO}_3$ , and  $\text{H}_3\text{PO}_4$  aqueous solutions, then the different species ( $\text{H}^+$ ,  $\text{HSO}_4^-$ ,  $\text{SO}_4^{2-}$ ,  $\text{CO}_2^*$ ,  $\text{HCO}_3^-$ ,  $\text{CO}_3^{2-}$ ,  $\text{H}_3\text{PO}_4$  and  $\text{H}_2\text{PO}_4^-$ ) are recognized explicitly, and the appropriate equations iterated to determine activity coefficients simultaneously with dissolved speciation. It is worthwhile to consider here how this can be done. Where only acid-base equilibria are to be determined (i.e., reactions involving  $\text{H}^+$  or  $\text{OH}^-$  and any cation or anion), then equilibrium speciation in the solution can be obtained by calculating the zero of the following function:

$$\mathbf{F} = m\text{H}_{(\text{F})}^+ - m\text{OH}_{(\text{F})}^- + (\Sigma m\text{H}_{\text{assoc.}}^+) - (\Sigma m\text{OH}_{\text{assoc.}}^-) - m\text{H}_{\text{total}}^+ \quad (47)$$

where  $m\text{H}_{\text{total}}^+$  is the total concentration of hydrogen ion initially present in, or added to, the solution. In this definition hydroxide is equated to a negative hydrogen ion concentration. Thus, in a neutral solution (or pure water)  $m\text{H}_{\text{total}}^+ = 0.0 \text{ mol kg}^{-1}$ , in a solution of  $1 \text{ mol kg}^{-1} \text{ H}_2\text{SO}_4$   $m\text{H}_{\text{total}}^+ = 2.0 \text{ mol kg}^{-1}$ , and in a solution of  $1 \text{ mol kg}^{-1} \text{ NaOH}$   $m\text{H}_{\text{total}}^+ = -1.0 \text{ mol kg}^{-1}$ . Subscript (F) in Equation 47 refers to the free, unbound ions and assoc. to  $\text{H}^+$  or  $\text{OH}^-$  present in associated form — as  $\text{HSO}_4^-$  or  $\text{MgOH}^+$ , for example. Consider the reaction:



The concentration of bound  $\text{H}^+$  ( $m\text{H}_{\text{assoc.}}^+$ ), present as HX, is given by:

$$m\text{H}_{\text{assoc.}}^+ = m\text{HX} = m\text{X}_{(\text{F})}^- (K_{\text{HX}}/\Gamma) m\text{H}_{(\text{F})}^+ \quad (49)$$

where:

$$m\text{X}_{(\text{F})}^- = m\text{X}_{(\text{T})}^- / (1 + (K_{\text{HX}}/\Gamma) m\text{H}_{(\text{F})}^+) \quad (50)$$

where  $K_{\text{HX}}$  is the equilibrium constant for the reaction in Equation 48,  $\Gamma$  is the activity coefficient quotient as defined in Equation 31, and the stoichiometric concentration  $m\text{X}_{(\text{T})}^-$  is known from the overall composition of the solution. Analogous expressions can be derived for reactions involving  $\text{OH}^-$ . Concentrations of free  $\text{H}^+$  and  $\text{OH}^-$  are of course related via the ionic product of water:

$$K_{\text{H}_2\text{O}} = m\text{H}_{(\text{F})}^+ m\text{OH}_{(\text{F})}^- \cdot (\gamma_{\text{H}}\gamma_{\text{OH}}/a\text{H}_2\text{O}) \quad (51)$$

Equation 47 is solved for  $\mathbf{F} = \text{zero}$  by starting with an initial estimate (or estimates) of  $m\text{H}_{(\text{F})}^+$  and iterating Equations 47 to 51 until a sufficiently close approach to the zero is obtained. Press et al.<sup>102</sup> discuss a number of iteration procedures, and include FORTRAN code. Brent's method, which requires that the interval within which the solution for  $m\text{H}_{(\text{F})}^+$  lies must first be determined, is reliable and converges rapidly.

An interesting case where an association reaction is not found to be necessary for the representation of thermodynamic properties is aqueous  $\text{HNO}_3$ . Its speciation at  $25^\circ\text{C}^{100}$  is shown in Figure 3. Clegg and Brimblecombe<sup>103</sup> have shown that equilibrium partial pressures of  $\text{HNO}_3$ , proportional to the activity of the undissociated acid molecule in solution, can be satisfactorily predicted in acidified multicomponent solutions of up to  $6.0 \text{ mol kg}^{-1}$  ionic

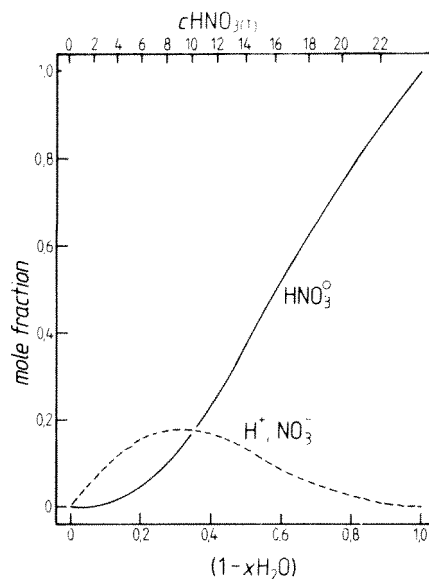


FIGURE 3. Speciation in pure aqueous HNO<sub>3</sub> at 25°C, from tabulated values of Davis and DeBruin.<sup>100</sup> Note use of mole fraction scale. Here "mole fraction" is defined so that:  $x\text{HNO}_3^0 = n\text{HNO}_3^0 / (n\text{HNO}_3^0 + n\text{NO}_3^- + n\text{H}_2\text{O})$ , and  $x\text{NO}_3^- (= x\text{H}^+) = n\text{NO}_3^- / (n\text{HNO}_3^0 + n\text{NO}_3^- + n\text{H}_2\text{O})$ . The molar concentration on the abscissa is a stoichiometric (total) value.

strength using the Pitzer model without treating H<sup>+</sup>-NO<sub>3</sub><sup>-</sup> association. Indeed it is possible, at least for pure aqueous HNO<sub>3</sub>, to describe solute and solvent activities over the entire concentration range using a (mole fraction-based) ion interaction model without association.<sup>74</sup> One important advantage of this approach is that, in addition to simplicity of calculation, no assumptions need be made about the individual activity coefficients in solution where insufficient information is available to determine those of both charged and uncharged species independently.<sup>104</sup>

There are no rules implicit in the Pitzer model to decide whether an ion pairing or ion association reaction should be recognized. The decision is essentially an empirical one, based on achieving the best fit to the available thermodynamic data, rather than most closely reflecting the molecular reality of the solution. Association and ion pairing reactions treated in studies of geochemical interest are listed in Table 13.

In practical calculations this flexible modeling approach presents few difficulties, but does have one significant drawback already referred to: based on the choices made, inconsistencies can arise between sets of parameters describing the same geochemical system. This requires great care in the use of the model.

### c. Parameter Values

Pure electrolyte solution parameters determined from laboratory data for a wide range of electrolytes, and mixed solution parameters  $\theta_{ij}$  and  $\psi_{ijk}$ , are listed by Pitzer<sup>51</sup> (Chapter 3, this volume). In addition, Plummer et al.<sup>69</sup> have compiled a database of parameters, evaluated from single and mixed inorganic salt data to March 1988, with an accompanying bibliography. The most recent large-scale evaluation of ion-ion interaction parameters for binary and ternary ion systems is by Kim and Frederick.<sup>105,106</sup> As noted here by Pitzer,<sup>51</sup> caution should be exercised when using these parameters, since in most cases the pure electrolyte solution data (osmotic or activity coefficients) have been fitted to the concentration limit of

**TABLE 13**  
**Association and Ion-Pairing Reactions Treated**  
**Explicitly in Laboratory and Geochemical Modeling**  
**Studies Using the Pitzer Model**

Reaction	Temperature	Ref.
$\text{CO}_{2(\text{aq})} + \text{H}_2\text{O} = \text{H}^+ + \text{HCO}_3^-$	298	56 <sup>a</sup>
$\text{H}^+ + \text{CO}_3^{2-} = \text{HCO}_3^-$	298	56
$\text{H}^+ + \text{SO}_4^{2-} = \text{HSO}_4^-$	298	56 <sup>b</sup>
$\text{H}^+ + \text{H}_2\text{PO}_4^- = \text{H}_3\text{PO}_4$	298	59
$\text{B}(\text{OH})_3 + \text{H}_2\text{O} = \text{H}^+ + \text{B}(\text{OH})_4^-$	298	61 <sup>c</sup> , 246
$\text{Mg}^{2+} + \text{B}(\text{OH})_4^- = \text{MgB}(\text{OH})_4^+$	298	61
$\text{Ca}^{2+} + \text{B}(\text{OH})_4^- = \text{CaB}(\text{OH})_4^+$	298	61
$\text{H}^+ + \text{F}^- = \text{HF}$	298	264 <sup>d</sup> , 101
$\text{HF} + \text{F}^- = \text{HF}_2^-$	298	264 <sup>d</sup>
$\text{NH}_3 + \text{H}_2\text{O} = \text{NH}_4^+ + \text{H}^+$	298	255, 258, 259
$\text{H}^+ + \text{HS}^- = \text{H}_2\text{S}$	298	281, 278, 285
$\text{SO}_{2(\text{aq})} + \text{H}_2\text{O} = \text{H}^+ + \text{HSO}_3^-$	298	286
$\text{H}^+ + \text{SO}_3^{2-} = \text{HSO}_3^-$	298	286
$\text{Cu}^{2+} + n\text{Cl}^- = \text{CuCl}_n^{(2-n)+}$	298	264 <sup>d</sup>
$\text{Mg}^{2+} + \text{CO}_3^{2-} = \text{MgCO}_3^0$	298	56
$\text{Ca}^{2+} + \text{CO}_3^{2-} = \text{CaCO}_3^0$	298	56
$\text{Ca}^{2+} + \text{SO}_4^{2-} = \text{CaSO}_4^0$	298—523	89 <sup>e</sup>

*Note:* The reference list is not exhaustive, and gives geochemical applications (where available) in preference to purely laboratory studies.

- <sup>a</sup> For the carbonate system there have been numerous studies of the two equilibria since the work of Harvie et al.<sup>56</sup> that improve the thermodynamic database and extend it to temperatures other than 298.15 K. However, to maintain self-consistency, parameters determined in such studies should not be substituted for those of Harvie et al.<sup>56</sup> (see text).
- <sup>b</sup> Parameters determined for model incorporating unsymmetrical mixing terms (see Pitzer,<sup>51</sup> Chapter 3, this volume) after original work of Pitzer et al.<sup>65</sup> More recently, Reardon and Beckie<sup>111</sup> have determined the temperature variation of the ion-interaction parameters for aqueous  $\text{H}_2\text{SO}_4$  0—6 mol kg<sup>-1</sup>, 0—55°C.
- <sup>c</sup> Formation and interactions of  $\text{B}_3\text{O}_3(\text{OH})_4^-$  and  $\text{B}_4\text{O}_5(\text{OH})_4^{2-}$  also treated by Felmy and Weare.<sup>61</sup>
- <sup>d</sup> In pure aqueous solution.
- <sup>e</sup> Ion pairing constant varies as f(T), while  $\text{Ca}^{2+}$ - $\text{SO}_4^{2-}$  interaction parameters are constant (see also notes to Table 10). Inconsistent with study of Harvie et al.<sup>56</sup> at 298.15 K, which assumes no  $\text{CaSO}_4^0$  ion pair is formed.

the measurements. For many solutes — such as HCl — activity coefficients are available to much higher concentrations than the model is able to fit within the experimental uncertainty (normally about 6 mol kg<sup>-1</sup>). It seems unlikely that such parameters can be used to determine the effects of ion-ion interactions on activity coefficients in multicomponent mixtures with any degree of reliability. Where the thermodynamic properties of a solution of a single electrolyte are required to high concentration, it seems best to use either a more appropriate model (e.g., see Appendix I of Pitzer<sup>51</sup>), or a purely empirical representation such as used in the critical evaluations of Hamer and Wu<sup>107</sup> and Goldberg and Nuttall.<sup>108</sup>

Model parameters evaluated in the chemical literature and listed by Pitzer<sup>51</sup> (Chapter 3, this volume) were obtained chiefly from direct measurements of solute or solvent activities. In studies of phase equilibria in brines, a complete parameterization of the model with regard to ternary interactions  $\theta_{ij}$  and  $\psi_{ijk}$  has been found to be essential due to the high concentration of the solutions.<sup>54</sup> The most complete study using the Pitzer model is that of Harvie et al.<sup>56</sup> (incorporating that of Harvie and Weare<sup>54</sup>) at 25°C for the system Na-K-Mg-Ca-H-Cl-SO<sub>4</sub>-OH-HCO<sub>3</sub>-CO<sub>3</sub>-CO<sub>2</sub>-H<sub>2</sub>O. Here salt solubilities in ternary ion systems were used to obtain mixture parameters  $\theta_{ij}$  and  $\psi_{ijk}$ , and also the chemical potentials of some solid phases where these were unknown. The results were tested by predicting solubilities in more complex solutions. Felmy and Weare<sup>61</sup> have extended this 25°C parameterization to include borate equilibria. The treatment of these fundamental systems, which include the major ions of seawater and dissolved CO<sub>2</sub> over a wide range of H<sup>+</sup> concentration, has, as yet, been only partially extended with respect to temperature. Pabalan and Pitzer<sup>83</sup> have treated the system Na-K-Mg-Cl-SO<sub>4</sub>-OH-H<sub>2</sub>O from 0°C to high temperature, Moller<sup>89</sup> has studied the system Na-Ca-Cl-SO<sub>4</sub>-H<sub>2</sub>O to high temperature, and Greenberg and Moller<sup>84</sup> have extended this to solutions containing K<sup>+</sup> ion over the temperature range 0 to 250°C. Below 25°C and at subzero temperatures Spencer et al.<sup>76</sup> have successfully modeled the system Na-K-Mg-Ca-Cl-SO<sub>4</sub>-H<sub>2</sub>O. When calculating activity and osmotic coefficients using parameters derived in these studies it is important to be aware that, first, ion-pair or association equilibria recognized in these treatments may not be the same, and furthermore that parameter values often differ even at 25°C. For example, while Harvie et al.<sup>56</sup> did not consider the formation of the CaSO<sub>4</sub><sup>0</sup> ion pair in their studies of brines at 25°C, the species has been incorporated in later works covering both subzero<sup>76</sup> and high temperatures.<sup>84</sup> Because of these factors, the studies referred to above should, in some respects, be viewed as different models rather than extensions of the same model.

Substitution of revised parameters, even from more accurate data, can lead to dramatic worsening of predicted activity coefficients rather than an improvement. For example, Plummer et al.<sup>69</sup> have shown that, for the solubility of NaHCO<sub>3</sub> in aqueous Na<sub>2</sub>CO<sub>3</sub> at 25°C, substitution of parameters ( $\beta^{(0)}$ ,  $\beta^{(1)}$ , and  $C^{\phi}$ ) obtained from recent data for the system Na-HCO<sub>3</sub>-CO<sub>3</sub>-CO<sub>2</sub>-H<sub>2</sub>O<sup>109</sup> for those of Harvie et al.<sup>56</sup> leads to gross inaccuracies in predicted NaHCO<sub>3</sub> solubility in Na<sub>2</sub>CO<sub>3</sub> solutions. This is in spite of the fact that the difference in activity coefficients (in pure aqueous NaHCO<sub>3</sub>) calculated from the two sets of parameters is only about 8% up to 1 mol kg<sup>-1</sup> concentration. Consequently, it is desirable to clarify the differences between the sets of parameters determined in the studies referred to above, and others, to avoid possible errors in calculation. A few specific comments are worthwhile concerning the NaHCO<sub>3</sub> calculation of Plummer et al.<sup>69</sup> The values of  $\beta^{(0)}$  and  $\beta^{(1)}$  determined by Sarbar et al.<sup>109</sup> fall far outside the general relationship found for 1:1 electrolytes (Figure 3, Pitzer,<sup>51</sup> Chapter 3, this volume), and it is possible<sup>108</sup> that isopiestic equilibrium was not achieved in their experiments. It is therefore emphasized that, in addition to maintaining the integrity of a particular set of model parameters, the validity of new data should be considered very carefully before inclusion in the model.

Table 14 lists the sources of Pitzer model parameters used in major studies of phase equilibria in brines by Pabalan and Pitzer,<sup>83</sup> Greenberg and Moller,<sup>84</sup> and Weare and co-workers.<sup>54,56,76</sup> Although restricted to 25°C, the treatment of Harvie et al.<sup>56</sup> is the most comprehensive in terms of composition, including acid-base equilibria for systems containing both sulfate and carbonate. (This has been further extended to include borate to high concentration.<sup>61</sup>) The sources of parameters adopted by Harvie et al.<sup>56</sup> are indicated in Table 14a and 14b. This study includes many new parameters determined from salt solubilities, in addition to those obtained from the earlier evaluations of Pitzer and co-workers. The parameterization of Harvie et al.<sup>56</sup> has been included in the PHRQPITZ geochemical model,<sup>69,110</sup> and has been adopted as the basis for most of the calculations presented in this chapter. The

**TABLE 14**  
**Compatibility of Parameters Derived from Applications of the**  
**Pitzer Model to Salt Solubilities in Brines**

(Symbols denote sources of parameters used in each of the studies. Parameters set to zero (—) are either redundant or could not be determined from the available data.)

(a) Harvie and Weare,<sup>54</sup> System Na-K-Mg-Ca-Cl-SO<sub>4</sub>-H<sub>2</sub>O  
 (298.15 K)

Ions		$\theta_{cc'}$	$\psi_{cc'Cl}$	$\psi_{cc'SO_4}$
Na	K	P	P	P
Na	Mg	P	1	1
Na	Ca	P	1	1
K	Mg	—	1	1
K	Ca	P	P	—
Mg	Ca	P	1	1

Ions		$\theta_{aa'}$	$\psi_{aa'Na}$	$\psi_{aa'K}$	$\psi_{aa'Mg}$	$\psi_{aa'Ca}$
Cl	SO <sub>4</sub>	P	P	—	1	—

*Note:* Symbols: P — obtained from Pitzer and Kim<sup>82</sup> or Pitzer;<sup>340</sup> 1 — determined by Harvie and Weare,<sup>54</sup> “—” — parameter set to zero. All pure electrolyte solution parameters for this system (not listed here) were taken from Pitzer and Mayorga.<sup>191,292</sup>

(b) Harvie et al.,<sup>56</sup> System Na-K-Mg-Ca-H-Cl-SO<sub>4</sub>-OH-HCO<sub>3</sub>-CO<sub>3</sub>-  
 CO<sub>2</sub>-H<sub>2</sub>O (298.15 K)

Ion	Cl	SO <sub>4</sub>	HSO <sub>4</sub>	OH	CO <sub>3</sub>	HCO <sub>3</sub>
Na	P	P	3	P	3	PP
K	P	P	3	P	3	3
Mg	P	P	3	—	—	3
Ca	P	2	3	3	—	3
MgOH	3	—	—	—	—	—
H	P	3	3	—	—	—

Ions		$\theta_{cc'}$	$\psi_{cc'Cl}$	$\psi_{cc'SO_4}$	$\psi_{cc'HSO_4}$	$\psi_{cc'OH}$	$\psi_{cc'HCO_3}$	$\psi_{cc'CO_3}$
Na	K	P	P	P	—	—	3	3
Na	Ca	P	2	2	—	—	—	—
Na	Mg	P	—	2	—	—	—	—
Na	MgOH	—	—	—	—	—	—	—
Na	H	P	P	—	3	—	—	—
K	Ca	P	P	1	—	—	—	—
K	Mg	1	1	1	—	—	—	—
K	MgOH	—	—	—	—	—	—	—
K	H	P	3	3	3	—	—	—
Ca	Mg	P	P	1	—	—	—	—
Ca	MgOH	—	—	—	—	—	—	—
Ca	H	3	3	—	—	—	—	—
Mg	MgOH	—	3	—	—	—	—	—
Mg	H	3	3	—	3	—	—	—
MgOH	H	—	—	—	—	—	—	—

**TABLE 14 (continued)**  
**Compatibility of Parameters Derived from Applications of the Pitzer Model to Salt Solubilities in Brines**

Ions		$\theta_{\text{Na}^+}$	$\psi_{\text{Na}^+\text{Na}}$	$\psi_{\text{Na}^+\text{K}}$	$\psi_{\text{Na}^+\text{Ca}}$	$\psi_{\text{Na}^+\text{Mg}}$	$\psi_{\text{Na}^+\text{MgOH}}$	$\psi_{\text{Na}^+\text{H}}$
Cl	SO <sub>4</sub>	P	P	—	2	1	—	—
Cl	HSO <sub>4</sub>	3	3	—	—	—	—	3
Cl	OH	P	P	3	3	—	—	—
Cl	HCO <sub>3</sub>	PP	3	—	—	3	—	—
Cl	CO <sub>3</sub>	3	3	3	—	—	—	—
SO <sub>4</sub>	HSO <sub>4</sub>	—	3	3	3	3	—	—
SO <sub>4</sub>	OH	3	3	3	—	—	—	—
SO <sub>4</sub>	HCO <sub>3</sub>	3	3	—	—	3	—	—
SO <sub>4</sub>	CO <sub>3</sub>	3	3	3	—	—	—	—
HSO <sub>4</sub>	OH	—	—	—	—	—	—	—
HSO <sub>4</sub>	HCO <sub>3</sub>	—	—	—	—	—	—	—
HSO <sub>4</sub>	CO <sub>3</sub>	—	—	—	—	—	—	—
OH	HCO <sub>3</sub>	—	—	—	—	—	—	—
OH	CO <sub>3</sub>	3	3	—	—	—	—	—
HCO <sub>3</sub>	CO <sub>3</sub>	3	3	3	—	—	—	—

Note: Symbols: P — obtained from Pitzer and Kim<sup>82</sup> or Pitzer;<sup>140</sup> PP — Peiper and Pitzer;<sup>113</sup> 1 — determined by Harvie and Weare;<sup>84</sup> 2 — values revised by Harvie et al.;<sup>86</sup> 3 — determined by Harvie et al.;<sup>86</sup> — — — parameter set to zero. Harvie et al.<sup>86</sup> assumed the formation of MgCO<sub>3</sub><sup>0</sup> and CaCO<sub>3</sub><sup>0</sup>, and also determined binary interaction parameters  $\lambda_{\text{CO}_3}$  for H<sup>+</sup>, Na<sup>+</sup>, K<sup>+</sup>, Ca<sup>2+</sup>, Mg<sup>2+</sup>, Cl<sup>-</sup>, SO<sub>4</sub><sup>2-</sup>, and HSO<sub>4</sub><sup>-</sup>.

(c) Pabalan and Pitzer,<sup>83</sup> System Na-K-Mg-Cl-OH-SO<sub>4</sub>-H<sub>2</sub>O (273.15—473.15 K)

Ions	Cl	SO <sub>4</sub>	OH
Na	Pitzer et al. <sup>115</sup>	Holmes and Mesmer <sup>69</sup>	Pabalan and Pitzer <sup>116</sup>
K	Holmes and Mesmer <sup>114</sup>	Holmes and Mesmer <sup>69</sup>	—
Mg	De Lima and Pitzer <sup>118</sup>	Phutela and Pitzer <sup>120</sup>	—

Ions		$\theta_{\text{Na}^+}$	$\psi_{\text{Na}^+\text{Cl}}$
Na	K	<sup>a</sup> 3	<sup>b</sup> 3
Na	Mg	<sup>a</sup> 3	<sup>b</sup> 3
K	Mg	<sup>a</sup> 3	<sup>b</sup> 3

Ions		$\theta_{\text{Na}^+}$	$\psi_{\text{Na}^+\text{Na}}$	$\psi_{\text{Na}^+\text{K}}$	$\psi_{\text{Na}^+\text{Mg}}$
Cl	SO <sub>4</sub>	4	—	<sup>a</sup> 4	<sup>b</sup> 4
Cl	OH	<sup>a</sup> 3	<sup>a</sup> 3	—	—
SO <sub>4</sub>	OH	<sup>a</sup> 3	<sup>a</sup> 3	—	—

Note: For pure electrolyte parameters the sources of the fitting equations [giving values as f(T)] are listed. Symbols: 3 — value at 298.15 K as Harvie et al.;<sup>86</sup> 4 — estimated by Pabalan and Pitzer.<sup>83</sup> Not all binary and ternary solutions were investigated.

<sup>a</sup> Invariant with temperature.  
<sup>b</sup> Proportional to T or 1/T.



**TABLE 14 (continued)**  
**Compatibility of Parameters Derived from Applications of the**  
**Pitzer Model to Salt Solubilities in Brines**

(d) Greenberg and Moller,<sup>84</sup> System Na-K-Ca-Cl-SO<sub>4</sub>-H<sub>2</sub>O  
 (273.15—523.15 K)<sup>a</sup>

Ions	Cl	SO <sub>4</sub>
Na	Moller <sup>89</sup> b	Moller <sup>89</sup> c
K	5 <sup>d</sup>	5 <sup>e</sup>
Ca	Moller <sup>89</sup> f	Moller <sup>89</sup> g

*Note:* With the exception of  $\psi_{\text{Cl},\text{SO}_4,\text{Na}}$  (set constant to 298.15 K value of Harvie et al.<sup>56</sup>) all mixture parameters are given as functions of temperature over some or all of the range 273—523 K, and differ from those determined by both Pabalan and Pitzer<sup>83</sup> and the two earlier studies at 298.15 K. Symbols: 5 — determined by Greenberg and Moller.<sup>84</sup>

- <sup>a</sup> Incorporates earlier study of Moller,<sup>89</sup> on the subsystem Na-Ca-Cl-SO<sub>4</sub>-H<sub>2</sub>O, over the same temperature range.  
<sup>b</sup> Parameters of Pitzer et al.<sup>315</sup> refitted (273—578 K) to alternative equation.  
<sup>c</sup>  $\beta^{(0)}$  and  $\beta^{(1)}$  (298—473 K) as in Rogers and Pitzer,<sup>322</sup> C<sup>\*</sup> (298—523 K) and  $\beta^{(0)}$  and  $\beta^{(1)}$  (>473 K) were estimated from ternary solution solubilities.  
<sup>d</sup> Parameter values of Holmes and Mesmer<sup>314</sup> refitted to alternative equation.  
<sup>e</sup> Results of Holmes and Mesmer<sup>260</sup> refitted to be consistent with the standard value (2.0) of model parameter  $\alpha$  (see Pitzer,<sup>51</sup> this volume).  
<sup>f</sup>  $\beta^{(1)}$  (298—523 K) from Phutela and Pitzer,<sup>321</sup>  $\beta^{(0)}$  and C<sup>\*</sup> fit to water vapor pressures (>473 K) and values from Phutela and Pitzer<sup>321</sup> (298—473 K).  
<sup>g</sup> Formation of ion pair CaSO<sub>4</sub><sup>0</sup> incorporated into treatment. Two equations given for temperature variation of ion pairing constant: 298—423 and 423—523 K.  $\beta^{(0)}$  and  $\beta^{(1)}$  invariant with temperature, C<sup>\*</sup> set to zero, and  $\beta^{(2)}$  given as f(T) from 298—323 K but set to zero at higher temperatures.

(e) Spencer et al.,<sup>76</sup> System Na-K-Ca-Mg-Cl-SO<sub>4</sub>-H<sub>2</sub>O  
 (213—298 K)

Ions	Cl	SO <sub>4</sub>
Na	6 <sup>a</sup>	6
K	6 <sup>b</sup>	5 <sup>c</sup>
Ca	6 <sup>d</sup>	5 <sup>e</sup>
Mg	6 <sup>f</sup>	6

Ions	$\theta_{\text{cc}'}$	$\theta_{\text{cc}'\text{Cl}}$	$\psi_{\text{cc}'\text{SO}_4}$
Na K	6	6	6
Na Ca	5 <sup>f</sup>	6	5 <sup>f</sup>
Na Mg	4 <sup>f</sup>	6	6
K Ca	6	6	—
K Mg	6 <sup>f</sup>	6	6
Ca Mg	6	6	—

Ions	$\theta_{\text{aa}'}$	$\psi_{\text{aa}'\text{Na}}$	$\psi_{\text{aa}'\text{K}}$	$\psi_{\text{aa}'\text{Ca}}$	$\psi_{\text{aa}'\text{Mg}}$
Cl SO <sub>4</sub>	5 <sup>f</sup>	6	6	5 <sup>f</sup>	6

*Note:* The authors estimate the value of the Debye-Hückel parameter A<sup>h</sup> below 273 K from solubility data. Symbols: 6 — estimated by Spencer et al.<sup>76</sup>

**TABLE 14 (continued)**  
**Compatibility of Parameters Derived from Applications of the**  
**Pitzer Model to Salt Solubilities in Brines**

- <sup>a</sup> Model parameter values generated by the fitting equation of Spencer et al. merge smoothly with those of Moller<sup>89</sup> above 298 K.
- <sup>b</sup> Parameter values merge smoothly with those of Greenberg and Moller<sup>84</sup> above 298 K.
- <sup>c</sup> Equation of Greenberg and Moller<sup>84</sup> extrapolated below 273 K.
- <sup>d</sup> Parameters discontinuous with those estimated by Moller<sup>89</sup> above 298 K.
- <sup>e</sup> Treatment of Greenberg and Moller<sup>84</sup> adopted unchanged.
- <sup>f</sup> Invariant with temperature.

parameters of Greenberg and Moller<sup>84</sup> and Spencer et al.<sup>76</sup> for more restricted systems as  $f(T)$  are largely inconsistent with the 25°C study of Harvie et al.<sup>56</sup> (Table 14d and 14e). This is certainly true for the mixture terms  $\theta_{ij}$  and  $\psi_{ijk}$ , and probably also for the pure electrolyte parameters which have been extensively refitted. Consequently, these model treatments should be regarded as essentially independent of one another, and of the work of Harvie et al.<sup>56</sup>

How can calculations best be extended to temperatures other than 25°C? The study of Pabalan and Pitzer<sup>83</sup> of the system Na-K-Mg-Cl-SO<sub>4</sub>-H<sub>2</sub>O (Table 14c) from 0 to 200°C is more compatible with the work of Harvie et al.<sup>56</sup> Most of the mixture parameters are equal, at 25°C, to those of Harvie et al.<sup>56</sup> (the exceptions being  $\theta_{\text{Cl},\text{SO}_4}$ ,  $\psi_{\text{Cl},\text{SO}_4,\text{K}}$ , and  $\psi_{\text{Cl},\text{SO}_4,\text{Mg}}$ ). Comparison of pure solution activity coefficients calculated using ( $\beta^{(1)}$ ,  $C^{(b)}$ ) of Harvie et al.<sup>56</sup> with those derived from the fitting equations used by Pabalan and Pitzer<sup>83</sup> yields agreement to within 1% or better at 25°C. This is also the case for most other salts included in the study of Harvie et al.<sup>56</sup> for which ( $\beta^{(1)}$ ,  $C^{(b)}$ ) are available as continuous functions of temperature (Table 10).

Two further studies, not listed in Table 14, are also relevant to the problem of calculating activity coefficients over a range of temperatures. Reardon and Beckie<sup>111</sup> have determined the parameters necessary to describe sulfuric acid equilibria from 0 to 50°C, while retaining consistency with the treatment of Harvie et al.<sup>56</sup> Monnin and Schott<sup>112</sup> have studied the system Na-Cl-HCO<sub>3</sub>-CO<sub>3</sub>-OH-H<sub>2</sub>O from 5 to 50°C, using a broader array of data than Harvie et al.<sup>56</sup> but basing the parameterization on their work and that of Peiper and Pitzer.<sup>113</sup> Monnin and Schott<sup>112</sup> used constant values of the mixture parameters that, with the exceptions of  $\theta_{\text{OH},\text{CO}_3}$  and  $\psi_{\text{Na},\text{OH},\text{CO}_3}$  (set to zero), differ negligibly from those of Harvie et al.<sup>56</sup> Equilibrium constants for the carbonate system were calculated from equations of Peiper and Pitzer,<sup>113</sup> who also list first ( $\beta^{(1)}$ ,  $C^{(d)}$ ) and second ( $\beta^{(2)}$ ,  $C^{(f)}$ ) differentials of the pure electrolyte parameters for NaHCO<sub>3</sub> and Na<sub>2</sub>CO<sub>3</sub>.

Thus, adopting the parameterization of Harvie et al.<sup>56</sup> as the basis for estimating activity coefficients in brines, calculations can be extended to other temperatures, not too far from 25°C, in the following way. Opposite sign interactions should be calculated using parameters ( $\beta^{(1)}$ ,  $C^{(b)}$ ) valid for the temperature of interest and obtained using the fitting equations referred to in Table 10. Where mixture parameters  $\theta_{ij}$  and  $\psi_{ijk}$  are available as  $f(T)$  and are equal to the Harvie et al.<sup>56</sup> values at 298 K, this temperature functionality may be used. Otherwise 25°C values of Harvie et al.<sup>56</sup> should be retained. Experience suggests that this results in little error over a restricted temperature range.

We have examined the question of model parameterization in some detail; as for many practical problems it will inevitably remain incomplete, thus involving the researcher in parameter determination or at least requiring that the limitations of the model, and its possible pitfalls, be understood. We now turn to practical examples of the calculation of activity coefficients.

**TABLE 15**  
**Availability of Ion Interaction Parameters, at 25°C and**  
**as Functions of Temperature, for the Components of**  
**Sea Salt**

Ions	Cl	SO <sub>4</sub>	HCO <sub>3</sub>	Br	CO <sub>3</sub>	B(OH) <sub>4</sub>	F	B(OH) <sub>3</sub>
Na	f	f	2	1	2	*	1	*
Mg	f	f	*	1	* <sup>a</sup>	—	*	—
Ca	f	1	*	*	* <sup>a</sup>	*	*	—
K	f	f	1	1	1	*	*	*
Sr	1	*	*	1	—	—	—	—
B(OH) <sub>3</sub>	*	*	—	—	—	—	—	—

*Note:* f — fitting equation giving pure electrolyte model parameters as  $f(T)$ ; <sup>32,3</sup> \* — only 25°C parameters available; 1 — parameters and first differential with respect to temperature (both at 25°C) available; 2 — parameters and both first and second differentials with respect to temperature (both at 25°C) available.

<sup>a</sup> Harvie et al.<sup>56</sup> parameterized the  $Mg^{2+}-CO_3^{2-}$  and  $Ca^{2+}-CO_3^{2-}$  interactions as ion pair formation. In this work the earlier ion interaction treatment of Millero<sup>60</sup> is used.

### III. APPLIED CALCULATIONS IN NATURAL WATERS

The temperature and pressure ranges of the oceans are from  $-2$  to  $40^\circ\text{C}$  and up to 1000 bars applied pressure. In geothermal solutions much higher values are attained,  $600^\circ\text{C}$  and perhaps  $2 \times 10^4$  bars pressure, while in the atmosphere, although the variation of pressure is for many purposes negligible, temperatures as low as  $-60^\circ\text{C}$  occur in the upper troposphere. It would not be possible to cover the whole range of natural aqueous systems in a single study, or indeed with a single method. Here we largely restrict ourselves to conditions attainable in the oceans. Millero<sup>91</sup> has reviewed in great detail what is known about the effect of pressure on chemical processes in the sea, and uses partial molal volume and compressibility data to estimate the influence of pressure on the thermochemical properties of seawater, and on acid-base, solid-liquid, gas-liquid, and ion pair equilibria. Therefore we do not explicitly consider the effects of pressure here, beyond drawing attention to the method of calculating its effect on activity coefficients within the Pitzer model (Section II.B.1.a, and Tables A4 and A5).

Natural waters in the ionic strength range  $0.1$  to  $1.0 \text{ mol kg}^{-1}$  result almost exclusively from the concentration of seawater by evaporation or from its dilution by land runoff in estuaries — which for most calculations it is sufficiently accurate to consider as a series of dilutions of seawater with pure water. Much of the following discussion will focus on seawater. At  $25^\circ\text{C}$  the Pitzer model is fully parameterized with respect to the major components of seawater, and in Table 15 the availability of pure electrolyte solution parameters, including their temperature functionality, is indicated.

#### A. SOLUTIONS OF STRONG ELECTROLYTES

The calculation of  $\phi$ ,  $\gamma_M$ , and  $\gamma_X$  in mixtures of strong electrolytes is straightforward, involving only lines (i) to (iii) of Equations 34 to 36, respectively. In dilute solutions of less than about  $0.1 \text{ mol kg}^{-1}$  ionic strength, activity coefficients are determined chiefly by long-range electrostatic interactions between ions of opposite sign. At extreme dilution these may be thought of as being dependent only upon charge and ionic strength. In such solutions, where activity coefficients approach the Debye-Hückel limiting law, there is very little

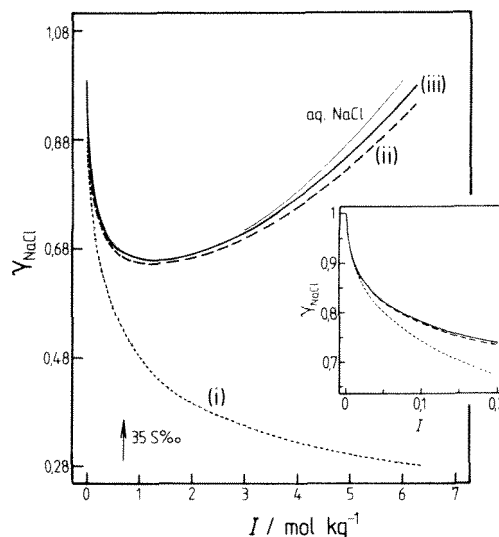


FIGURE 4. Contributions of extended Debye-Hückel, binary (opposite sign), and mixture expressions to the model calculated  $\gamma_{\text{NaCl}}$  in seawater, as a function of ionic strength. (i) Extended Debye-Hückel term  $z_i^2 F$  (for expansion of  $F$ , see Pitzer<sup>51</sup>); (ii) extended Debye-Hückel term plus binary interactions  $z_i^2 F + \sum_i m_i (2B_{ii} + Z C_{ii}) + |z_i| \sum_i \sum_j m_i m_j C_{ij}$ ; (iii) all terms including mixture parameters ( $\theta_{ij}$ ,  $\psi_{ijk}$ ), as given in Equations 35 and 36. The mean activity coefficient of NaCl in pure aqueous NaCl at the same ionic strength as the seawater is also shown for  $3 \leq I \leq 6 \text{ mol kg}^{-1}$ . Inset shows detail at low concentration.

difference between values estimated with the Pitzer model, and earlier, simpler equations. As an example, calculated values of  $\gamma_{\text{NaCl}}$  in seawater solutions at 25°C are shown in Figure 4, together with the contributions of the Debye-Hückel function ( $F$  in Equations 35 and 36), opposite sign interactions (functions  $B_{ca}$  and  $C_{ca}$ ), and like sign interactions (involving  $\Phi_{\text{Na},c}$ ,  $\Phi_{\text{Cl},a}$ ,  $\psi_{\text{Na},c,a}$ , and  $\psi_{\text{Cl},a,c}$ ). The effect of the like-sign interactions changes  $\gamma_{\text{NaCl}}$  by only 1% at  $I = 0.5 \text{ mol kg}^{-1}$  (24.5 S‰), and even at  $I = 6 \text{ mol kg}^{-1}$  (233 S‰) is only 3.5% of the total. This shows that the large number of possible like-sign interactions that arise in a multicomponent system (many of which are likely to be unknown) may be ignored without introducing significant error, at least in dilute solutions. For example, Whitfield<sup>46</sup> has shown that the osmotic coefficient and mean ion activity coefficients of the major components of seawater can be satisfactorily predicted by the Pitzer model, assuming that only interactions between ions of opposite sign are significant (i.e.,  $\theta_{ij}$  and  $\psi_{ijk}$  are equal to zero), a result consistent with the calculations shown in Figure 4 for NaCl. Finally, we note that since NaCl constitutes about 90 mol% of sea salt,  $\gamma_{\text{NaCl}}$  in a pure aqueous solution of NaCl is quite similar to that in seawater at the same ionic strength (see Figure 4).

While the temperature variation of the pure electrolyte model parameters ( $\beta^{(i)}$ ,  $C^{\phi}$ ) is well known for many salts (Table 10), the temperature variation of like-sign interactions is more poorly understood. As noted in the previous section, the *ad hoc* way in which some of these have been estimated is one of the greatest sources of incompatibility between parameter sets (Table 14). However, the relative weakness of these interactions, in all but the most concentrated solutions, means that like-sign interactions may be considered temperature invariant without introducing serious error. For example, Pabalan and Pitzer<sup>83</sup> found it an adequate approximation in their studies of mineral solubility (system Na-K-Mg-Cl-SO<sub>4</sub>-OH-H<sub>2</sub>O from 0 to 200°C) to retain existing 25°C values of  $\theta_{ij}$  (see Table 14c) and allow only  $\psi_{ijk}$  to vary as a function of temperature. Even so, a parameter such as  $\psi_{\text{Na},\text{K},\text{Cl}}$  only changes from  $-0.0021$  to  $-0.00155$  from 0 to 40°C.

**TABLE 16**  
**Mean Ion Activity Coefficients of NaCl, Na<sub>2</sub>SO<sub>4</sub>, KCl, and K<sub>2</sub>SO<sub>4</sub> in Seawater over a Range of Ionic Strength and Temperature**

T(°C)	<i>I</i>	$\gamma_{\text{NaCl}}$ (experiment) <sup>a</sup>	$\gamma_{\text{NaCl}}$ (model)	$\gamma_{\text{Na}_2\text{SO}_4}$ (experiment) <sup>b</sup>	$\gamma_{\text{Na}_2\text{SO}_4}$ (model)
35	0.718	0.685 ± 0.007	0.664	0.408 ± 0.016	0.345
25	0.718	0.672 ± 0.007	0.665	0.378 ± 0.016	0.345 (0.352)
25	0.718	0.668 ± 0.003 <sup>b</sup>	0.665		
15	0.718	0.679 ± 0.007	0.663	0.385 ± 0.016	0.344
0	0.718	0.650 ± 0.007	0.654	0.440 ± 0.016	0.338
25	0.511	0.690 ± 0.01	0.680	0.405 ± 0.016	0.378 (0.385)
25	0.303	0.730 ± 0.01	0.708	0.435 ± 0.016	0.433 (0.439)
25	0.100	0.795 ± 0.01	0.777	0.620 ± 0.016	0.559 (0.563)

T(°C)	<i>I</i>	$\gamma_{\text{NaCl}}$ (experiment) <sup>c</sup>	$\gamma_{\text{NaCl}}$ (model) <sup>d</sup>
25	0.10	0.799	0.788
25	0.30	0.711	0.710
25	0.50	0.682	0.682
25	0.70	0.667	0.667
25	0.723	0.677	

T(°C)	<i>I</i>	$\gamma_{\text{KCl}}$ (experiment)	$\gamma_{\text{KCl}}$ (model)	$\gamma_{\text{K}_2\text{SO}_4}$ (experiment)	$\gamma_{\text{K}_2\text{SO}_4}$ (model)
25	0.700	0.645 ± 0.008	0.639	0.352 ± 0.018	0.336

*Note:* Results for KCl are unpublished data of Whitfield. Model values of  $\gamma_{\text{Na}_2\text{SO}_4}$  are given both for pure electrolyte parameters ( $B_{\text{Na}_2\text{SO}_4}^{\text{Na}_2\text{SO}_4}$ ,  $C_{\text{Na}_2\text{SO}_4}^{\text{Na}_2\text{SO}_4}$ ) calculated from the fitting equation listed in Table 11 (in parentheses), and as listed by Pitzer<sup>51</sup> (altered using temperature derivatives where  $T \neq 25^\circ\text{C}$ ).

<sup>a</sup> Experimental data of Platford<sup>114</sup> (NaCl) and Platford and Dafoe<sup>116</sup> (Na<sub>2</sub>SO<sub>4</sub>), in artificial seawater of composition: 0.424 *m*NaCl, 0.0553 *m*MgCl<sub>2</sub>, 0.0291 *m*Na<sub>2</sub>SO<sub>4</sub>, 0.0105 *m*CaCl<sub>2</sub>, 0.0094 *m*KCl for ionic strength (*I*) 0.718 mol kg<sup>-1</sup>.

<sup>b</sup> Experimental data and model calculation of Johnson and Pytkowicz.<sup>117</sup>

<sup>c</sup> Estimate of Gieskes.<sup>115</sup>

### 1. The Major Components of Seawater, and the Activity Coefficient of Sea Salt

At 25°C, activity coefficients of major sea salt components have been measured by a number of workers.<sup>114-116</sup> In Table 16 modeled values are compared with measurement. There is good agreement in the cases of KCl and K<sub>2</sub>SO<sub>4</sub>, and with the measurements of  $\gamma_{\text{NaCl}}$  by Johnson and Pytkowicz.<sup>117</sup> Platford<sup>114</sup> and Platford and Dafoe<sup>116</sup> measured  $\gamma_{\text{NaCl}}$  and  $\gamma_{\text{Na}_2\text{SO}_4}$  using Na amalgam, and Ag-AgCl and Pb amalgam-PbSO<sub>4</sub> electrodes, respectively, being unable to obtain satisfactory results with a Na<sup>+</sup>-specific glass electrode. Their results differ by about 3% (for NaCl) and up to 18% (for Na<sub>2</sub>SO<sub>4</sub>) from modeled values of the activity coefficients. Comparisons of measured and calculated activity coefficients of a number of other ions, including trace components, have been made by Millero<sup>66,118</sup> and show satisfactory agreement.

A more stringent test is possible in terms of overall solute and solvent activity in seawater. Millero and Leung<sup>27</sup> have determined the thermochemical properties of seawater from measurements of water vapor pressure, freezing point depression, enthalpy, and heat capacity. The mean activity coefficient of sea salt ( $\gamma_{\pm(\text{ss})}$ ) is defined as

$$\ln(\gamma_{\pm(\text{ss})}) = (1/2m_{(\text{ss})})\sum_i m_i \ln(\gamma_i) \quad (52)$$

**TABLE 17**  
**Contribution of Sea Salt Components to the Total Molality ( $m_{(s)}$ ) and Ionic Strength ( $I_{(s)}$ ) of Sea Salt for the Seawater Recipe of Millero<sup>18,27</sup>**

Solute	$m_i/m_{(s)}$	$I_i/I_{(s)}$	Solute	$m_i/m_{(s)}$	$I_i/I_{(s)}$	Solute	$m_i/m_{(s)}$	$I_i/I_{(s)}$
Na	0.85226	0.67269	Sr	$1.578 \times 10^{-4}$	$5.2 \times 10^{-4}$	Br	$1.5254 \times 10^{-3}$	0.001206
Mg	0.095976	0.30302	Cl	0.95690	0.78295	CO <sub>3</sub>	$3.5066 \times 10^{-4}$	0.001112
Ca	0.018690	0.05899	SO <sub>4</sub>	0.05132	0.16200	B(OH) <sub>4</sub>	$1.578 \times 10^{-4}$	0.000119
K	0.01855	0.01464	HCO <sub>3</sub>	$3.3838 \times 10^{-3}$	0.002668	F	$1.230 \times 10^{-4}$	$9.7 \times 10^{-5}$
						B(OH) <sub>3</sub>	$5.96 \times 10^{-4}$	—

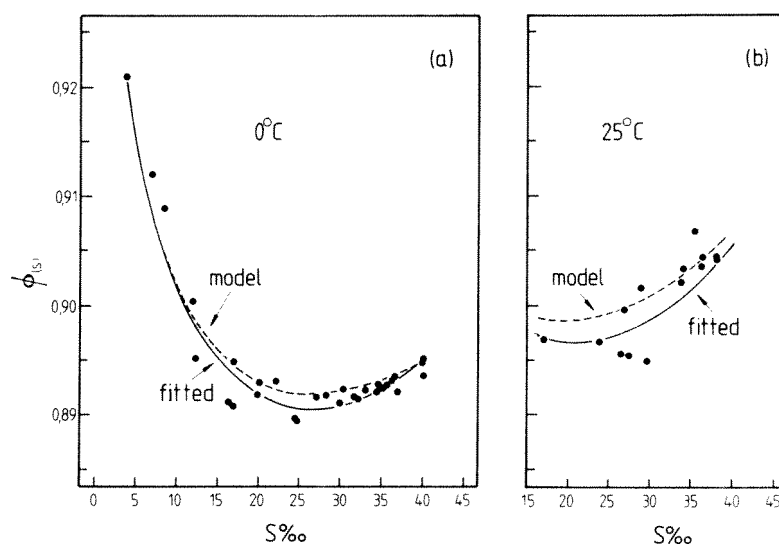


FIGURE 5. Measured and calculated osmotic coefficients ( $\phi_{(s)}$ ) of seawater at 0°C (a) and 25°C (b). Dashed line — calculated using the Pitzer model; full line — fitted equation of Millero and Leung.<sup>27</sup> Measured values (symbols) are from Robinson<sup>384</sup> (273.15 K) and Doherty and Kester<sup>385</sup> (298.15 K), as listed by Millero and Leung.<sup>27</sup>

where  $\gamma_i$  is the conventional single ion activity coefficient (calculated from Equations 35 and 36),  $m_i$  the molality of ion  $i$ , and  $m_{(s)}$  the total molality of sea salt, given by

$$m_{(s)} = (1/2)\sum_i m_i \quad (53)$$

For the seawater recipe used by Millero<sup>18</sup> and Millero and Leung<sup>27</sup> the molal ionic strength ( $I_{(s)}$ ) of seawater is related to salinity (S‰) by

$$I_{(s)} = 19.9201 S/(1000 - 1.00488 S) \quad (54)$$

The concentrations of the individual ions are related to  $m_{(s)}$  and  $I_{(s)}$  by the factors listed in Table 17. As a test of the multicomponent model, calculated values of the osmotic coefficient of seawater and mean activity coefficient of sea salt ( $\gamma_{\pm, (s)}$ ) have been compared with available data, and with the work of Millero and Leung.<sup>27</sup> (The speciation of the weak acids H<sub>2</sub>CO<sub>3</sub> and B(OH)<sub>3</sub> was assumed not to vary from 25°C estimates.) Figure 5 shows the results of these calculations for  $\phi$  at 0 and 25°C. At both temperatures the estimated osmotic coefficient is in satisfactory agreement with the data, within the experimental uncertainty, and differs by no more than about 0.3% from the best-fit equation of Millero and Leung.<sup>27</sup> A more

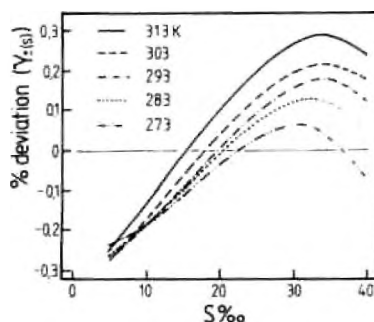


FIGURE 6. Percentage deviation of the mean activity coefficient of sea salt ( $\gamma_{\pm(s)}$ ), calculated using the Pitzer model, from that obtained from the fitted equation of Millero and Leung,<sup>27</sup> from 5–40 S‰, and 273–313 K.

extensive comparison in terms of  $\gamma_{\pm(s)}$ . Figure 6, demonstrates a similar level of agreement over the entire temperature and concentration range. These results, for sea salt as a whole, suggest that mean ion activity coefficients of the individual sea salts estimated using the model are likely to be more reliable than some of the available data with which they have been compared (see Table 16). The osmotic coefficient of seawater and conventional single ion activity coefficients of the major components (5 to 40 S‰, 273 to 313 K) are listed in Appendix Table A6.

## 2. Mineral Solubilities

Perhaps the most extensive geochemical application of the Pitzer model has been to studies of mineral solubilities in brines.<sup>95</sup> These concentrated, highly nonideal solutions have not been previously amenable to a generalized thermodynamic treatment. We have already shown, in Section II.B.1.a.ii, how laboratory solubility measurements have been used to determine model parameters for a number of important brine systems. In general, the approach is first to determine unknown parameters from solubilities in ternary ion systems, then verify the results by predicting solubilities in quaternary and quinary systems. Numerous examples of this may be seen in the works of Harvie and Weare<sup>54</sup> and Harvie et al.<sup>56</sup> These parameterization and validation exercises have served as stepping stones to applications to real problems, such as the evaporation sequence of seawater.<sup>66,119</sup> For a multicomponent solution such as seawater, a purely empirical method of analysis, such as the use of phase diagrams, is limited by the number of degrees of freedom that can be simultaneously represented and by lack of sufficient data to cover the compositional variations that occur naturally. The use of a model avoids these difficulties by drawing on a very wide range of data to achieve the necessary parameterization, and predicting directly the thermodynamic quantities that control solubility. Weare<sup>62</sup> has described in some detail the application of the Pitzer model to solubility studies, including field observations. He discusses the merits of the ion association vs. ion interaction approaches, the basis for the various parameter choices and some of the pitfalls — such as transfer of parameters and control of the size of the ternary mixture parameters (as large values lead to unstable behavior in regions of high concentration).

Applications of the model to the calculation of salt solubilities are widespread, and include gypsum and halite solubility in Dead Sea waters,<sup>120,121</sup> alkaline earth sulfate solubilities in deep brines,<sup>122</sup> scale mineral formation in oilfield brines,<sup>86,123,124</sup> carbonate mineral solubilities in Lake Magadi,<sup>112</sup> equilibria in acid mine drainage waters,<sup>111</sup> and solubilities in fluid inclusions in ice.<sup>76</sup> Perhaps the most interesting and demanding application has been to the study of evaporite sequences,<sup>61, 66, 119, 125</sup> where the model together with the observed

sequence may be used to infer information about the conditions of formation of the deposit. For example, Harvie et al.<sup>66,119</sup> used the parameterization of the Ca-Na-K-Mg-Cl-SO<sub>4</sub>-H<sub>2</sub>O system at 25°C to calculate mineral sequences for the evaporation of seawater, and have compared these to the Permian Zechstein deposit in Germany. The results clarify a number of mineralogical discrepancies, by providing the equilibrium evaporation path, and, for example, emphasizing the role of back reactions of the evolving brine with previously deposited minerals. These are important in the case of minerals containing Ca<sup>2+</sup>, for example. This ion had not been included in the early studies of the seawater system by Van't Hoff,<sup>126</sup> who assumed that it would quickly be removed in calcite and gypsum and could afterward be neglected.

Brantley et al.<sup>125</sup> have used the model to establish the processes controlling the formation of a modern marine evaporite (Peru), and Felmy and Weare<sup>61</sup> used it to study the Searles Lake deposit. Felmy and Weare<sup>61</sup> compared observations with calculated mineral sequences, and concluded that the deposit could be formed from the evaporation of water from its major source (with present-day composition). By comparing the observed mineral sequence with that predicted for various precipitation schemes, Felmy and Weare<sup>61</sup> concluded that calcium and magnesium carbonate minerals were prevented from equilibrating with the overlying brine, and presented a plausible mechanism for this. This, as Weare<sup>62</sup> has stated, is an important example of how thermodynamic constraints may be linked to field observations.

#### a. Gypsum Solubility in Salt Solutions and Brines

In the previous edition of this book, gypsum precipitation in natural waters was considered as an example of the difficulties of estimating mineral solubilities. In practical terms, this translates into the problem of calculating  $a_{\text{H}_2\text{O}}$ ,  $\gamma_{\text{Ca}^{2+}}$ , and  $\gamma_{\text{SO}_4^{2-}}$  (or the activity coefficients of other minerals being precipitated) in a multicomponent ionic medium such as seawater. For CaSO<sub>4</sub> and other sparingly soluble salts, the total ionic strength of the background medium (e.g., seawater) is invariably much greater than that attainable in a solution of pure CaSO<sub>4</sub> (0.061 mol kg<sup>-1</sup> at 298 K). In terms of the Pitzer model, this means that the functionality of  $B_{\text{CaSO}_4}$  [as  $f(I)$  to high concentration] cannot be determined from data for pure solutions of aqueous CaSO<sub>4</sub>. Therefore it must be estimated indirectly from ternary solution data. Harvie et al.<sup>66</sup> used the result of Rogers<sup>127</sup> for  $\beta^{(1)}$ , set  $C^b$  to zero, and found that solubilities could be satisfactorily described using these parameters in combination with ternary terms  $\psi_{\text{Ca},\text{SO}_4,\text{a}^-}$  or  $\psi_{\text{SO}_4,\text{Ca},\text{e}^-}$  in solutions containing Ca<sup>2+</sup>, SO<sub>4</sub><sup>2-</sup>, and either cation c or anion a. (Note that the parameters  $\theta_{\text{Ca},\text{e}^-}$  and  $\theta_{\text{SO}_4,\text{a}^-}$  are obtained from solutions *not* containing the salt CaSO<sub>4</sub>.) At 25°C, in common with other 2:2 metal sulfates which show some association, the  $\beta^{(2)}$  parameter is used as a convenient alternative to assuming the formation of an ion pair CaSO<sub>4</sub><sup>0</sup>. However, over the more extended range of temperature studied by Moller<sup>89</sup> and Greenberg and Moller<sup>84</sup> an ion pair *is* included — and  $\beta^{(2)}$  set to zero.

For gypsum the solubility equilibrium may be written as



If the activity of the (pure) solid phase is unity, the thermodynamic solubility product may be defined as

$$K_{\text{gypsum}} = a_{\text{Ca}^{2+}} a_{\text{SO}_4^{2-}} (a_{\text{H}_2\text{O}})^2 = K_{\text{gypsum}}^* \Gamma_{\text{gypsum}} \quad (56)$$

where the stoichiometric solubility product  $K_{\text{gypsum}}^* = m_{\text{Ca}^{2+}} m_{\text{SO}_4^{2-}}$  and the activity coefficient product  $\Gamma_{\text{gypsum}} = \gamma_{\text{Ca}^{2+}} \gamma_{\text{SO}_4^{2-}} (a_{\text{H}_2\text{O}})^2$ . Since the dissolution of gypsum in seawater and other ionic media has a significant effect on the ionic strength and therefore activity coef-



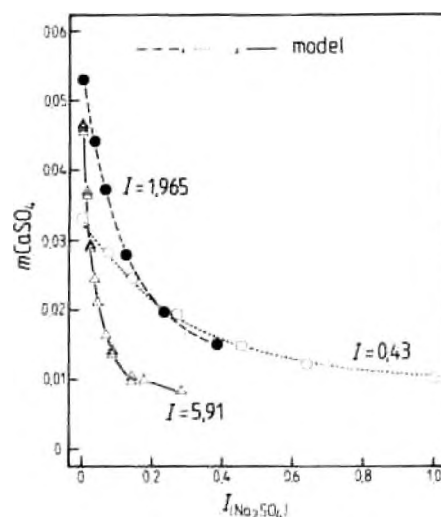


FIGURE 7. Measured and calculated gypsum ( $\text{CaSO}_4 \cdot 2\text{H}_2\text{O}$ ) solubilities in aqueous  $\text{NaCl}/\text{Na}_2\text{SO}_4$  mixtures at  $25^\circ\text{C}$ , as a function of the ionic strength fraction of  $\text{Na}_2\text{SO}_4$  ( $I(\text{Na}_2\text{SO}_4)$ ). Symbols — experimental data of Yeatts and Marshall;<sup>129</sup> lines — model calculated values. The ionic strengths ( $I$ ) given for the three sets of data are the *initial* values for the solutions before addition of  $\text{CaSO}_4$ . The discontinuities in the modeled curves are due to the fact that the (starting) ionic strengths are not constant, but vary over the following ranges:  $I = 5.91$ , from 5.69 to 6.13  $\text{mol kg}^{-1}$ ;  $I = 1.965$ , from 1.96 to 2.02  $\text{mol kg}^{-1}$ ;  $I = 0.43$ , from 0.392 to 0.48  $\text{mol kg}^{-1}$ .

ficients, the solubility must be calculated by an iterative procedure. For the most generalized calculations, where equilibria between ions and associated species in solution and with multiple solid phases are being considered, a Gibbs free energy minimization routine such as that used by Weare<sup>138</sup> and co-workers is probably most suitable. However, for the example here we require only the solution of Equation 56, thus,

$$(m\text{Ca}^{2+} \cdot m\text{SO}_4^{2-} \Gamma_{\text{gypsum}}) / K_{\text{gypsum}} - 1 = 0 \quad (57)$$

where  $m\text{Ca}^{2+}$  and  $m\text{SO}_4^{2-}$  are the equilibrium concentrations of the two ions at saturation. In a solution initially containing no  $\text{Ca}^{2+}$  or  $\text{SO}_4^{2-}$ ,  $m\text{Ca}^{2+}$  and  $m\text{SO}_4^{2-}$  are equivalent to the added moles of  $\text{CaSO}_4$  per kilogram of  $\text{H}_2\text{O}$ ,  $\Delta$ , which is to be determined. In solutions already containing  $\text{Ca}^{2+}$  and  $\text{SO}_4^{2-}$ ,  $m\text{Ca}^{2+}$  and  $m\text{SO}_4^{2-}$  in Equation 57 then become  $(m\text{Ca}^{2+} + \Delta)$  and  $(m\text{SO}_4^{2-} + \Delta)$ . There are a number of straightforward techniques for determining the zero of a function in one variable ( $\Delta$ ), from an initial guess to final estimate of desired accuracy.<sup>102</sup> At each iteration the activity coefficient quotient  $\Gamma_{\text{gypsum}}$  is calculated using the Pitzer equations.

How much do solutions of differing composition affect gypsum solubility? As an example we first consider gypsum solubility in  $\text{NaCl}/\text{Na}_2\text{SO}_4$  solutions. Yeatts and Marshall<sup>129</sup> have measured equilibrium gypsum and anhydrite solubilities in a number of ternary ion systems at  $25^\circ\text{C}$ , in the case of  $\text{NaCl}/\text{Na}_2\text{SO}_4$  making 30 determinations at initial ionic strengths of approximately 0.43, 1.97, and 5.91  $\text{mol kg}^{-1}$ . Using the parameterization of Harvie et al.,<sup>56</sup> we show measured and calculated solubilities as a function of ionic strength fraction of  $\text{Na}_2\text{SO}_4$  in Figure 7. There is satisfactory agreement at all ionic strengths and compositions. A clearer idea of the effect of the composition of the same ionic medium on gypsum solubility can be gained from Figure 8, where calculated gypsum solubilities in the system  $\text{Na-Ca-Cl}$

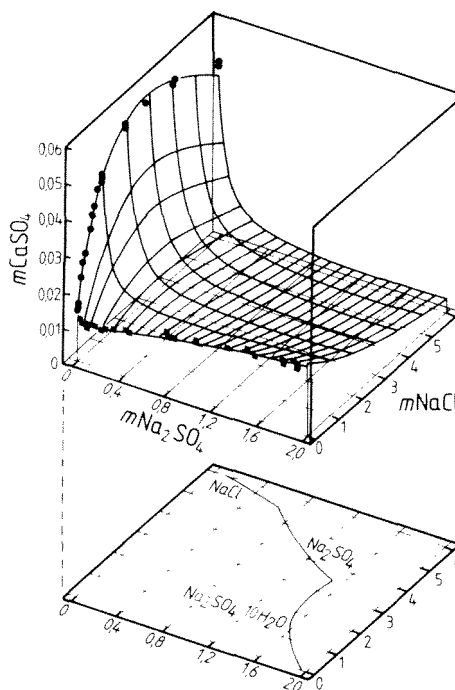


FIGURE 8. Gypsum solubility in the system Na-Ca-Cl-SO<sub>4</sub>-H<sub>2</sub>O at 25°C. The surface represents calculated gypsum solubility in mixtures of aqueous NaCl/Na<sub>2</sub>SO<sub>4</sub>. Measured solubilities are plotted for solutions of the two end members; data from Linke.<sup>386</sup> The compositions of saturated solutions (with respect to NaCl, Na<sub>2</sub>SO<sub>4</sub>, and Na<sub>2</sub>SO<sub>4</sub> · 10H<sub>2</sub>O), for systems not containing Ca<sup>2+</sup>, are marked on the lower projection. These approximately indicate the range of solution composition for which the calculations are valid.

SO<sub>4</sub>-H<sub>2</sub>O at 25°C are plotted. Measurements for the two pure components (aqueous NaCl and Na<sub>2</sub>SO<sub>4</sub>) are also shown. The relationship is quite complex, gypsum solubility being increased in pure NaCl at all concentrations because of decreased  $\gamma_{Ca^{2+}}$ ,  $\gamma_{SO_4^{2-}}$ , and  $a_{H_2O}$ ; while in pure Na<sub>2</sub>SO<sub>4</sub>, solubility at first decreases sharply, then rises with  $mNa_2SO_4$  despite the high concentration of added SO<sub>4</sub><sup>2-</sup>. Note that, in these calculations, we have not included back reactions with the precipitated gypsum that could lead to the formation of glauberite [Na<sub>2</sub>Ca(SO<sub>4</sub>)<sub>2</sub>].

The solubility of gypsum in seawater (both concentrated and diluted) has been measured by Schaffer<sup>130</sup> and Marshall and Slusher<sup>131</sup> over a range of temperatures, and by Krungalz and Millero<sup>120</sup> in mixtures of Dead Sea and Mediterranean water at 25°C. (For a complete review of the literature on gypsum and anhydrite solubility, see Raju and Atkinson.<sup>124</sup>) Marshall and Slusher comment that the stoichiometric solubility product ( $K_{\text{gypsum}}^*$ ) in synthetic concentrated seawaters to 60°C (and for  $I < 2$  mol kg<sup>-1</sup>) is essentially the same as in aqueous NaCl at the same ionic strength. Krungalz and Millero<sup>120</sup> have shown their experimental gypsum solubilities to be in good agreement with calculated values (Pitzer model) at all concentrations. In Figure 9 we show the measured gypsum solubility products ( $K_{\text{gypsum}}^*$ ) of Krungalz and Millero<sup>120</sup> and Marshall and Slusher<sup>131</sup> at 30°C (uncorrected for the 5° temperature difference), together with the calculated gypsum saturation index, defined by

$$\Omega_{\text{gypsum}} = mCa^{2+} mSO_4^{2-} \Gamma_{\text{gypsum}} / K_{\text{gypsum}} \quad (58)$$

Again it can be seen that the model agrees with observation to very high ionic strength.

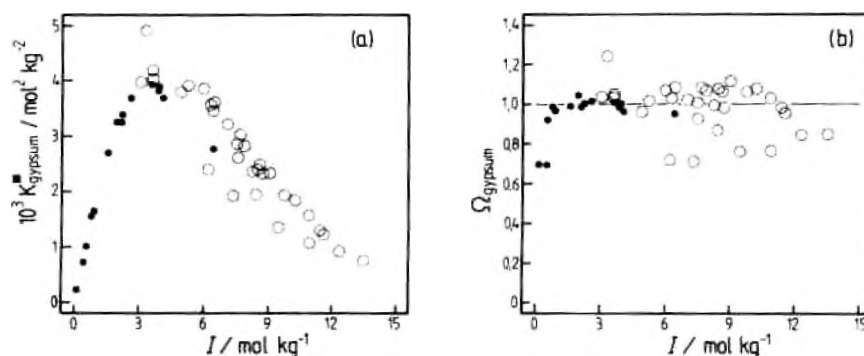


FIGURE 9. The solubility of gypsum in natural brines. (a) The stoichiometric solubility product of gypsum ( $K_{\text{gypsum}}^*$ ) in concentrated seawater (points) at 30°C and Dead Sea/Mediterranean waters (circles) at 25°C; (b) the calculated gypsum saturation index ( $\Omega_{\text{gypsum}}$ ) in concentrated seawater (points) and Dead Sea/Mediterranean waters (circles); data same as part (a). Experimental measurements are from Marshall and Slusher<sup>111</sup> (seawater) and Katz et al.<sup>107</sup>

What of gypsum solubilities at other temperatures? Marshall and Slusher<sup>111</sup> present empirical equations (and FORTRAN code) for calculating gypsum, anhydrite, and hemihydrate solubility as functions of temperature and seawater ionic strength. The studies of Moller<sup>109</sup> and Greenberg and Moller<sup>104</sup> apply the Pitzer model to the system Na-K-Ca-Cl-SO<sub>4</sub>-H<sub>2</sub>O from 0 to 250°C, and Spencer et al.<sup>76</sup> to Na-K-Ca-Mg-Cl-SO<sub>4</sub>-H<sub>2</sub>O below 25°C. However, the parameter sets are mutually incompatible both with each other and with that of Harvie et al.<sup>66</sup> (used here) at 25°C. Raju and Atkinson<sup>106,123,124</sup> have studied CaSO<sub>4</sub>, BaSO<sub>4</sub>, and SrSO<sub>4</sub> solubility in NaCl (as an analogue of oilfield brines) as a function of temperature, and present useful literature reviews of available data including comparisons of  $K_{\text{sp}}^*$  for these salts obtained by different workers. Raju and Atkinson<sup>106</sup> describe solute and solvent activities using the Pitzer formalism, but with an empirical extension replacing functions involving  $\psi_{ij,k}$  and  $\theta_{ij}$  parameters. Their analysis of the data for gypsum agrees closely with the work of Marshall and Slusher.<sup>111</sup>

The application of the model to describing laboratory solubility data has been shown to be successful in both pure and multicomponent solutions to high ionic strengths. However, in real systems the conditions under which reactions take place are likely to be both less well constrained and less accurately known. Comparisons of model predictions with observations of both present<sup>125</sup> and past<sup>61,66</sup> evaporite deposits, referred to above, show satisfactory agreement. We now consider such an example.

McCaffrey et al.<sup>112</sup> have analyzed samples of brines obtained at a solar salt production facility from successive evaporation ponds. Dissolved ion concentrations (mol dm<sup>-3</sup>) were determined by ion chromatography, and molal concentrations estimated from an empirical relationship between Mg<sup>2+</sup> concentration and specific gravity. The average temperature of the samples was 31.2°C. In Figure 10 the calculated saturation indices  $\Omega$ , (see Equation 58) for NaCl and MgSO<sub>4</sub> · 6H<sub>2</sub>O are plotted against degree of evaporation, together with sample ionic strength. As can be seen, the observed onset of NaCl precipitation (marked) occurs when the solution is within 10% of model-estimated saturation. The onset of large-scale sulfate and magnesium precipitation, observed at about 68% evaporation, coincides with the calculated saturation with respect to MgSO<sub>4</sub> · 6H<sub>2</sub>O (and MgSO<sub>4</sub> · 7H<sub>2</sub>O, not shown as it differs very little from MgSO<sub>4</sub> · 6H<sub>2</sub>O). Overall, McCaffrey et al.<sup>112</sup> found the evaporation sequence of the brines to be largely consistent with that predicted by Harvie et al.<sup>66</sup> and Eugster et al.<sup>133</sup> for the fractionated evaporation of seawater, where there are no back reactions with precipitated minerals. This is the appropriate mode, since precipitation was carried out sequentially, thus separating the evolved brines from earlier formed minerals.

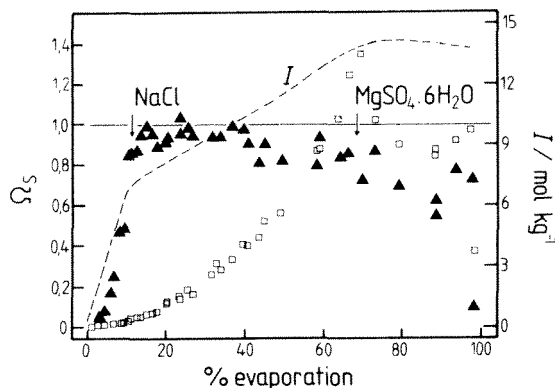


FIGURE 10. Total ionic strength ( $I$ ) and saturation indices  $\Omega_s$  of NaCl (triangles) and  $\text{MgSO}_4 \cdot 6\text{H}_2\text{O}$  (squares) in evaporated brine samples, from data of McCaffrey et al.<sup>132</sup> For each salt the observed onset of salt precipitation is indicated with an arrow.

### 3. Solutions Containing Sulfuric Acid

Of what are conventionally regarded as strong acids,  $\text{HNO}_3$  has already been shown to undergo measurable association (Figure 3), but this does not require explicit treatment within the Pitzer formalism. However, this is not the case for  $\text{H}_2\text{SO}_4$ , for which we must consider the formation of the bisulfate ion:



(The first dissociation of  $\text{H}_2\text{SO}_4$  is essentially complete at stoichiometric concentrations less than 50 mol%, about 60 mol kg<sup>-1</sup>.)<sup>134</sup> Pitzer et al.<sup>65</sup> have successfully treated the thermodynamics of aqueous  $\text{H}_2\text{SO}_4$  as a mixture of the ions  $\text{H}^+$ ,  $\text{HSO}_4^-$ , and  $\text{SO}_4^{2-}$  to a stoichiometric concentration of 6 mol kg<sup>-1</sup> at temperatures close to 25°C. Harvie et al.<sup>56</sup> have updated this treatment (at 298.15 K) for the model including unsymmetrical mixing terms — the normal mode of use. While retaining consistency with the treatment of Harvie et al.,<sup>56</sup> Reardon and Beckie<sup>111</sup> have determined the parameter values from 0 to 50°C, given by the following expressions:

$$\beta_{\text{H},\text{SO}_4}^{(0)} = 0.0217 + 58.33(1/T - 1/298) \quad (60)$$

$$C_{\text{H},\text{SO}_4}^{\phi} = 0.0411 - 58.65(1/T - 1/298) \quad (61)$$

$$\beta_{\text{H},\text{HSO}_4}^{(0)} = 0.2106 + 48.01(1/T - 1/298) \quad (62)$$

$$\beta_{\text{H},\text{HSO}_4}^{(1)} = 0.5320 + 1183(1/T - 1/298) + 2.364 \ln(T/298) \quad (63)$$

These are to be used in conjunction with the following equation for  $K_{\text{HSO}_4}$  (kg mol<sup>-1</sup>) derived by Pitzer et al.:<sup>65</sup>

$$\ln(K_{\text{HSO}_4}) = 14.0321 - 2825.2/T \quad (64)$$

Note that the possible interaction parameters  $\theta_{\text{HSO}_4,\text{SO}_4}$  and  $\psi_{\text{HSO}_4,\text{SO}_4,\text{H}}$  that arise for pure aqueous sulfuric acid are set to zero. Equation 64 assumes that  $\Delta C_p^\circ$  for the association

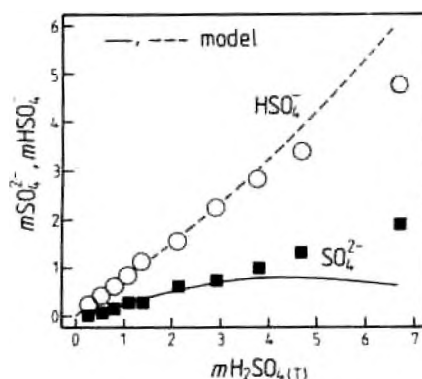


FIGURE 11. Molal concentrations of  $\text{HSO}_4^-$  and  $\text{SO}_4^{2-}$  in pure aqueous  $\text{H}_2\text{SO}_4$  at 298.15 K. Symbols — determinations of Chen and Irish;<sup>177</sup> lines — calculated using the Pitzer model. Comparisons of the model with the earlier data of Young et al.<sup>124</sup> at 0 and 50°C show similar behavior.

reaction is zero. Hovey and Hepler<sup>135</sup> have measured apparent molal heat capacities and volumes of aqueous  $\text{H}_2\text{SO}_4$  from 10 to 33°C, leading to a revised temperature functionality of  $K_{\text{HSO}_4}$ . However, the corresponding model parameters for the osmotic and activity coefficients were determined without including unsymmetrical mixing terms in the model, and so cannot be used here. Dickson et al.<sup>136</sup> have measured the dissociation of  $\text{HSO}_4^-$  in aqueous NaCl to high temperature. Their equation for the temperature variation of  $K_{\text{HSO}_4}$ , incorporating the measurements of Hovey and Hepler,<sup>135</sup> agrees well with Equation 64 above about 15°C, but at 0°C there is a difference of 0.06 in  $\log_{10}(K_{\text{HSO}_4})$ , suggesting that the  $K_{\text{HSO}_4}$  of Pitzer et al.<sup>65</sup> is too high by 15%. However, until the model parameters are redetermined to be consistent with the best estimates of the equilibrium constant as  $f(T)$ , then  $K_{\text{HSO}_4}$  together with parameters given by Equations 60 to 64 should be used.

In fitting the model equations to the osmotic coefficient and cell data,<sup>65</sup> there are no independent constraints on the sulfate speciation. It is of some interest to compare modeled concentrations with  $m\text{SO}_4^{2-}$  and  $m\text{HSO}_4^-$  obtained by Raman spectroscopy<sup>177</sup> (see Figure 11). There is satisfactory agreement up to a stoichiometric concentration of about 3 mol kg<sup>-1</sup>, but increasing deviations beyond this. However, since total activities are correctly reproduced — including those in multicomponent solutions containing  $\text{H}_2\text{SO}_4$  — this does not result in errors in most practical calculations. Adequate prediction of  $\text{HSO}_4^-$  formation in seawater is important as, for example, this enables measurements of dissociation constants and pH on the free and total hydrogen ion scales to be compared (see Section III.C.2.a). Dickson<sup>138</sup> has measured the standard potential of the reaction ( $\text{AgCl}_{(s)} + \frac{1}{2}\text{H}_{2(g)} = \text{Ag}_{(s)} + \text{HCl}_{(aq)}$ ), leading to the dissociation constant of  $\text{HSO}_4^-$  in artificial seawater as a function of salinity from 273 to 318 K. The determination of the dissociation constant from the measured EMFs required estimates of  $\gamma_{\text{HCl}}$  in the cell. A change equivalent to 0.1 in  $\log_{10}(K_{\text{HSO}_4}^*)$  (where  $K_{\text{HSO}_4}^*$  is the stoichiometric formation constant of  $\text{HSO}_4^-$ ) is quoted for a difference of 1.6 mV for the cell reaction. In Figure 12, values of  $\log_{10}(K_{\text{HSO}_4}^*)$  from the best-fit equation of Dickson<sup>138</sup> are plotted against seawater ionic strength  $I_{(s)}$  together with corresponding estimates using the Pitzer model. It is clear that modeled values are higher, by a factor that increases below 25°C. Part of this difference, however, is probably due to the fact that  $K_{\text{HSO}_4}$  calculated from Equation 64 is too great at low temperatures, as described above. Recalculation of the model parameters for  $\text{H}^+ - \text{HSO}_4^- - \text{SO}_4^{2-}$  interactions to be consistent with the best estimates of  $K_{\text{HSO}_4}$  would be particularly worthwhile for this application of the model. Stability constants at three ionic strengths and 25°C from results of Khoo et

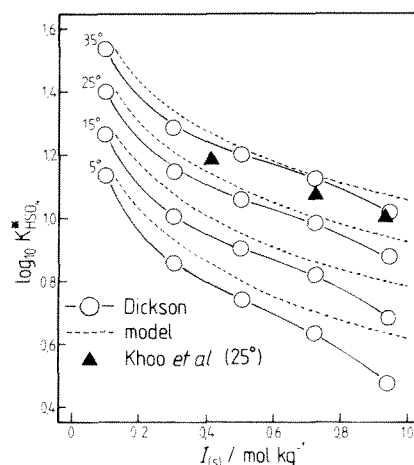


FIGURE 12. Measured and calculated values of the stoichiometric formation constant of  $\text{HSO}_4^-$  as a function of seawater ionic strength  $I_{(s)}$  from 5 to 35°C. Dashed lines — calculated using the Pitzer model; circles with full lines — from best fit equation of Dickson.<sup>138</sup> The circles indicate those concentrations at which measurements were made. The triangles are 25°C values of Khoo *et al.*<sup>139</sup> For the artificial seawater used here, the ionic strength is related to salinity “S” by:  $I_{(s)} = 19.919 \text{ S}/(1000 - 1.00198 \text{ S})$ .

al.<sup>139</sup> are also shown in Figure 12, but are in poor agreement with both the results of Dickson<sup>138</sup> and calculations using the Pitzer model.

While sulfuric acid does not occur in appreciable concentrations in what are usually regarded as “natural waters”, it is a major component of both natural marine and anthropogenic aerosols, being produced by the oxidation of  $\text{SO}_2$  and DMS (dimethyl sulfide). Consequently, a knowledge of  $\text{H}^+$  activity is essential for determining the chemical transformations in cloud/aerosol systems, for example, fluxes of acid gases such as HF, HCl, and  $\text{HNO}_3$  between gas and aqueous phases. This is discussed below.

#### 4. Solubility of Volatile Strong Electrolytes

For nondissociating neutral solutes, such as  $\text{O}_2$  and  $\text{N}_2$ , gas solubility is treated straightforwardly as an equilibrium between vapor and aqueous phase molecules (see Section III.B). For a weakly dissociating solute, such as  $\text{NH}_3$ ,  $\text{SO}_2$ , or  $\text{CO}_2$ , there is, in addition, the effect of dissociation to take into account, which complicates the treatment somewhat. However, for strong acid gases such  $\text{HNO}_3$  and the hydrogen halides (excepting HF), the significant equilibrium is<sup>134,140</sup>



leading to a thermodynamic Henry’s law constant ( $\text{K}_{\text{H}}/\text{mol}^2 \text{ kg}^{-2} \text{ atm}^{-1}$ ) defined as

$$\text{K}_{\text{H}} = m\text{H}^+ m\text{X}^- \gamma_{\text{HX}}^2 / f\text{HX} \quad (66)$$

where  $f\text{HX}$  (atm) is the fugacity of HX. (For convenience we have retained the atmosphere “atm” as the unit of pressure throughout this work. For conversion to S.I. units,  $\text{atm} = 101,325 \text{ Pa} = 1.01325 \text{ bar}$ .) Thus, if it is assumed that fugacity is equivalent to partial pressure for these gases under normal atmospheric conditions, then the gas solubility (or

TABLE 18  
Henry's Law Constants ( $K_H$ ) from 0–40°C

Species	$K_H$ (25°C)	$e^{-\Delta G^{\circ}/RT}$	a	b	c
HCl*	$2.04 \times 10^6$	$1.97 \times 10^6$	4.6187	5977.5014	-0.03401
HBr*	$1.32 \times 10^9$	$7.06 \times 10^8$	7.60095	7117.0552	-0.03512
HI	$2.5 \times 10^9$	$2.15 \times 10^9$	9.70617	6689.1418	-0.03522
HNO <sub>3</sub>	$2.45 \times 10^6$	$2.51 \times 10^6$	2.70104	6137.3984	-0.02876

Note: Value of  $K_H$  for MSA (methane sulphonic acid) is  $6.5 \times 10^{11}$  at 25°C.<sup>141</sup> Values at 25°C determined from partial pressure data. Estimates calculated from available free energy data<sup>37b</sup> are also shown. Temperature dependence given by:  $\ln(K_H) = a + b/T + cT$  where T/K.

\*  $K_H$  of  $2.04 \times 10^6$  also derived thermodynamically,<sup>142</sup> although the lower  $1.97 \times 10^6$  may be marginally preferred.

<sup>b</sup> Due to uncertainty in  $\gamma_{\text{HBr}}$  at high concentrations (compare Hamer and Wu<sup>37c</sup> and Macaskill and Bates<sup>41</sup>)  $K_H$  may be lower than that given here. For calculations of  $p\text{HBr}$  at low concentrations the value  $7.064 \times 10^8$  may be more accurate (for which "a" is 6.9759, and other parameters are unchanged).

conversely partial vapor pressure) at equilibrium can be calculated from a knowledge of the Henry's law constant and the use of the thermodynamic model to calculate aqueous phase activity coefficients. Henry's law constants, evaluated as a function of temperature from partial pressure, enthalpy, and heat capacity data, are listed in Table 18 for the gases of interest.

The water content of atmospheric aerosols containing soluble material, such as sea salt or H<sub>2</sub>SO<sub>4</sub>, is controlled by the surrounding atmosphere: thus aqueous phase water activity is equivalent to ambient relative humidity. At relative humidities below 80% or so, aqueous aerosols are therefore highly concentrated multicomponent solutions.<sup>141,142</sup>

Figure 13 shows a schematic mass distribution of a marine tropospheric aerosol (after Heintzenberg<sup>143</sup>), consisting of two components: sea salt and a smaller mass of H<sub>2</sub>SO<sub>4</sub> partially neutralized by NH<sub>3</sub>. The latter may be broadly characterized as NH<sub>4</sub>HSO<sub>4</sub>, although the ratio of NH<sub>4</sub><sup>+</sup> to H<sup>+</sup> is quite variable.<sup>144</sup> This acidic component, and also HNO<sub>3</sub> in more polluted atmospheres, interacts with the larger sea salt particles and droplets to displace HCl and HF to the gas phase.<sup>67,145,146</sup> The chemical thermodynamics of the fine mode (NH<sub>4</sub>HSO<sub>4</sub>) aerosol is also of interest because of its role in cloud formation.<sup>1,147</sup>

Clegg and Brimblecombe<sup>103,148</sup> have made an extensive series of measurements at 298.15 K of equilibrium  $p\text{HNO}_3$  and  $p\text{HCl}$  over acidified salt solutions at high ionic strength. This was done, first, to validate the Pitzer model for use in gas solubility calculations, and second, to estimate unknown interaction parameters. The basic set of parameters used in this work, as elsewhere, is that of Harvie et al.<sup>76</sup> Figure 14 shows measured and calculated  $p\text{HCl}$  over H-Na-NH<sub>4</sub>-Cl-H<sub>2</sub>O solutions at 5 mol kg<sup>-1</sup> ionic strength and constant  $m\text{H}^+$  and  $m\text{Cl}^-$ , and illustrates some purely compositional influences on equilibrium partial pressure. The effect of replacing Na<sup>+</sup> entirely by NH<sub>4</sub><sup>+</sup>, where in all cases  $m\text{Na}^+ + m\text{NH}_4^+ = 3.5 \text{ mol kg}^{-1}$ , is to decrease  $\gamma_{\text{HCl}}$  (also shown) and cause a reduction in  $p\text{HCl}$  by a factor of 2. (Note that additional parameters  $\theta_{\text{H,NH}_4} = -0.01$  and  $\psi_{\text{H,NH}_4,\text{Cl}} = -0.009$  were estimated from activity coefficient data for H-NH<sub>4</sub>-Cl-H<sub>2</sub>O and H-NH<sub>4</sub>-Br-H<sub>2</sub>O solutions.) A more realistic example is shown in Figure 15 for a seawater/H<sub>2</sub>SO<sub>4</sub> mixture. This represents the acidification of a natural marine aerosol, in equilibrium with an atmosphere of about 85% relative humidity,

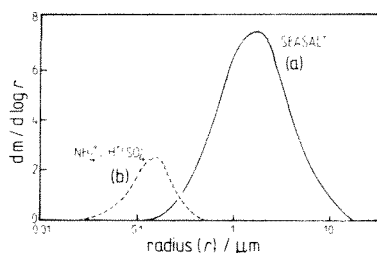


FIGURE 13. Schematic representation of bimodal marine aerosol mass distribution, after Heintzenberg<sup>143</sup> and Clarke et al.<sup>144</sup> The major component (a) with most mass (m) residing in the 1–10  $\mu\text{m}$  size range, is sea salt. The fine component of the aerosol (b) consists chiefly of  $\text{H}_2\text{SO}_4$ , partially neutralized by  $\text{NH}_3$ .

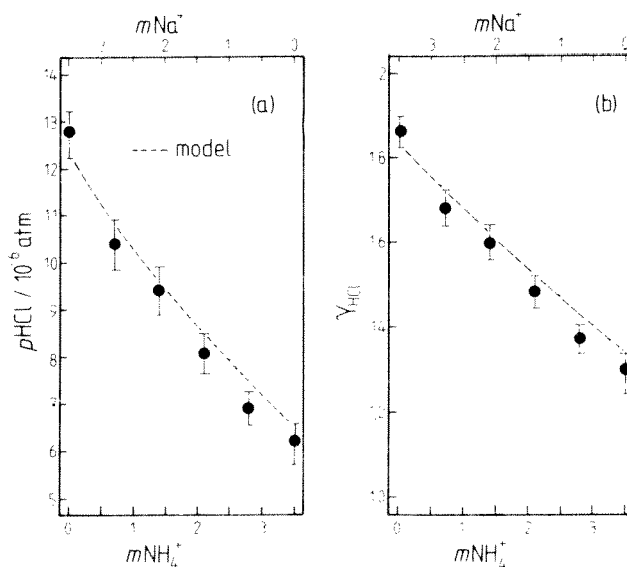


FIGURE 14. (a) Measured and predicted partial pressures of HCl over H-Na-NH<sub>4</sub>-Cl-H<sub>2</sub>O solutions at  $I = 5.0 \text{ mol kg}^{-1}$ ,  $m\text{H}^+ \approx 1.5 \text{ mol kg}^{-1}$ , and  $m\text{Cl}^- \approx 5.0 \text{ mol kg}^{-1}$ ; (b) the mean activity coefficient of HCl ( $\gamma_{\text{HCl}}$ ) derived from the partial pressure data [ $\gamma_{\text{HCl}} = [p_{\text{HCl}} \cdot K_{\text{HCl}}(m\text{H}^+ m\text{Cl}^-)]^{1/2}$ ] compared with values calculated using the Pitzer model. Data from Clegg and Brimblecombe.<sup>148</sup>

by the accumulation of  $\text{H}_2\text{SO}_4$  either through scavenging of smaller particles or by oxidation of the dissolved precursor  $\text{SO}_2$ . The measured equilibrium  $p_{\text{HCl}}$  ranges from  $0.43 \times 10^{-6}$  to  $22 \times 10^{-6}$  atm, and agrees well with values estimated using the model. While the experimental concentrations of  $\text{H}_2\text{SO}_4$  are much greater than might be found in a natural sea salt aerosol, these results for highly nonideal solutions suggest that the model can be used for equilibrium calculations involving real aerosol systems. For acidified solutions containing  $\text{SO}_4^{2-}$ , the bisulfate-sulfate speciation is obtained as part of the activity coefficient calculations. For the solutions shown in Figure 15, about 53% of total  $\text{H}^+$  is calculated to exist as the free ion.

A similar level of agreement between measurement and calculation is found for salt solutions acidified by nitric acid,<sup>103</sup> important in more polluted areas, where, for example,  $\text{NO}_3^-$  has been found to almost completely displace aerosol  $\text{Cl}^-$ .<sup>146</sup>

For calculations involving aerosols under realistic atmospheric conditions, activity coefficients must be estimated over a range of temperatures. For pure aqueous HCl, model parameters are available from  $0^\circ\text{C}$  to high temperature,<sup>85</sup> and for  $\text{HNO}_3$  to subfreezing temperatures<sup>74</sup> — principally because of the importance of  $\text{HNO}_3$  in the chemistry of the stratosphere.<sup>149</sup> In view of the success of the model at 298 K using the parameters of Harvie



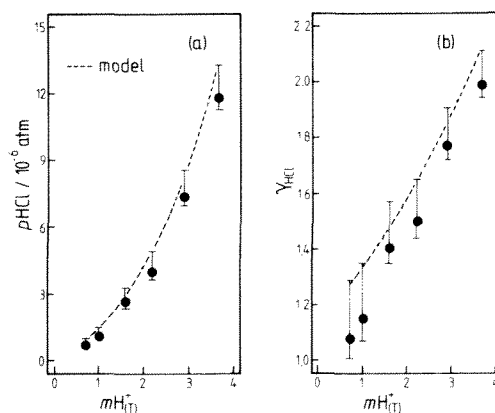


FIGURE 15. (a) Measured and predicted partial pressures of HCl over concentrated artificial seawater (stoichiometric  $I = 5 \text{ mol kg}^{-1}$ ) acidified with sulfuric acid, plotted against total  $\text{H}^+$  concentration; (b) the mean activity coefficient of HCl ( $\gamma_{\text{HCl}}$ ) derived from the partial pressure data ( $\gamma_{\text{HCl}} = [p_{\text{HCl}} \cdot K_{\text{H}} / (m\text{H}^+ m\text{Cl}^-)]^{1/2}$ ) compared with values calculated using the Pitzer model. Data from Clegg and Brimblecombe.<sup>148</sup>

et al.<sup>56</sup> and the relatively small variations in the mixture parameters with temperature, for  $T \neq 298 \text{ K}$  simply using ( $\beta^{(i)}$ ,  $C^{\text{b}}$ ) at the temperature of interest and 298 K values of  $\theta_{ij}$  and  $\psi_{ijk}$  should yield satisfactory results. Perhaps the most widespread, and for cloud nucleation the most important aerosol components, are acid sulfate mixtures containing  $\text{NH}_4^+$ . At present these remain difficult to treat using the Pitzer model, since model parameters ( $\beta^{(i)}$ ,  $C^{\text{b}}$ ) are available for  $(\text{NH}_4)_2\text{SO}_4$  only at 298 K, valid to  $5.5 \text{ mol kg}^{-1}$  (Table 7 of Pitzer,<sup>51</sup> Chapter 3, this volume). However, there are some early measurements of enthalpy and heat capacity from which temperature derivatives could be derived.<sup>150</sup> More recently, measurements of water vapor pressure over aqueous  $(\text{NH}_4)_2\text{SO}_4$ , and its mixtures with NaCl, have been extended to extreme concentration.<sup>151,152</sup> Water vapor pressures<sup>153</sup> and sulfate-bisulfate speciation<sup>154-156</sup> have also been measured for  $\text{NH}_4\text{HSO}_4$  solutions.

## 5. Supersaturated Solutions

For activity calculations involving aerosols, the Pitzer model's practical concentration limit of about 10 to 15  $\text{mol kg}^{-1}$  ionic strength in mixtures is a more serious limitation than in most mineral solubility work. There are two reasons for this. First, extremes of concentration compared to terrestrial brines are possible since relative humidity (equivalent to aerosol water activity) may routinely fall below about 75% (which corresponds to a saturated solution of aqueous NaCl at 298 K). Second, the size of the aerosol particles (submicron to about 10  $\mu\text{m}$  radius) means that very high degrees of supersaturation are possible, with respect even to soluble constituents, before nucleation takes place. A substantial literature exists regarding these "hysteresis" effects for both natural and artificial aerosols,<sup>1,71,72</sup> and experiments on micron-sized droplets have yielded much of the available thermodynamic data for supersaturated salt solutions.<sup>151,153,157</sup>

It is of some interest to compare measured water activities for supersaturated solutions of single salts to previously estimated values. We exclude simple extrapolations of fitting equations as these are rarely likely to lead to reliable predictions. Lenzi et al.<sup>158</sup> have estimated  $a_{\text{H}_2\text{O}}$  for supersaturated solutions of NaCl, KCl, and  $\text{K}_2\text{SO}_4$  at 25°C by reverse application of the Reilly-Wood-Robinson<sup>52</sup> and Zdanovskii-Stokes-Robinson<sup>159</sup> solution models. The former equations require, in order to predict multicomponent solution properties,  $a_{\text{H}_2\text{O}}$  (for example) of at least the single salt solutions at the ionic strength of the mixture. The

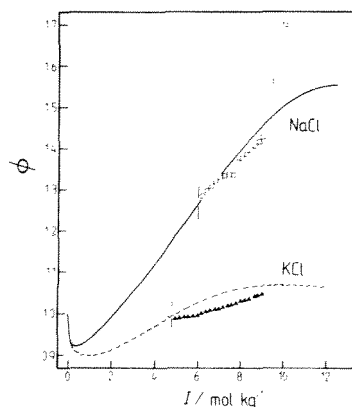


FIGURE 16. Osmotic coefficients of pure aqueous NaCl and KCl at 25°C, to supersaturation. Symbols — tabulated estimates of Lenzi et al.;<sup>158</sup> lines — best-fit equation of Tang et al.<sup>160</sup> to data obtained from water activity measurements on single aerosol particles. The concentrations of the saturated solutions are marked by vertical lines.

Zdanovskii-Stokes-Robinson equations require the molality  $m$  of the binary solutions at the water activity of the mixed solution. Lenzi et al.,<sup>158</sup> using various data for concentrated ternary solutions containing the above salts, have used the models to estimate self-consistent values of  $a_{\text{H}_2\text{O}}$  for the supersaturated binary constituents. In Figure 16 we compare the values of the osmotic coefficient  $\phi$  for supersaturated aqueous NaCl and KCl, from  $a_{\text{H}_2\text{O}}$  tabulated by Lenzi et al.,<sup>158</sup> with the best-fit equations to  $a_{\text{H}_2\text{O}}$  data obtained using an electrodynamic balance.<sup>160</sup> It can be seen that the model estimates are quite substantially in error, although this is less apparent when expressed in terms of  $a_{\text{H}_2\text{O}}$ .

## 6. Thermodynamic Properties over the Entire Concentration Range — $\text{HNO}_3$

We have already noted that, for an aqueous solution of a single salt, the Pitzer molality-based model is unable to represent osmotic and mean activity coefficients within the experimental precision at concentrations greater than about 6 mol kg<sup>-1</sup> (and only about 3 mol kg<sup>-1</sup> in the case of some lithium salts). One of the most important aerosol components is  $\text{H}_2\text{SO}_4$ . While for pure sulfuric acid solutions several empirical representations of thermodynamic properties are available,<sup>161-163</sup> solute activity coefficients and water activities in mixtures involving  $\text{H}_2\text{SO}_4$  are also desirable, over wide ranges of temperature and concentration. Consequently, a different form of model is required. In view of the success of the (molal) Pitzer ion interaction model, a similar formalism transferred to the mole fraction scale appears to be an obvious choice. The basis for such a model is described by Pitzer<sup>51</sup> (Chapter 3, this volume). Still at an early stage of development, it has so far been applied to ternary ion systems of uniform charge<sup>73,164</sup> and to pure aqueous  $\text{HNO}_3$ ,<sup>74</sup> which is an important component of stratospheric aerosols.<sup>149</sup> Whether such an approach will prove as successful in unsymmetrical mixtures remains to be seen. However, its application to the thermodynamics of aqueous  $\text{HNO}_3$  demonstrates that it can be used at all concentrations (infinitely dilute  $\text{HNO}_{3(\text{aq})}$  to pure liquid  $\text{HNO}_3$ ) and over a large temperature range. This does, however, require that quaternary interactions between solute and solvent be considered, thus extending the Margules expansion given by Pitzer<sup>51</sup> (Chapter 3, this volume) and Pitzer and Simonson<sup>23</sup> to include terms in  $a_{ijkl}$ . Very considerable complications would arise should this also prove necessary for solution mixtures, as thermodynamic data for quaternary systems are sparse.

For  $\text{HNO}_3$ , the activity of water  $a_{\text{H}_2\text{O}}$  is given by

$$\ln(a_{\text{H}_2\text{O}}) = \ln(x_1) + 2A_1 I_1^{1/2} / (1 + \rho I_1^{1/2}) + x_1^2 \{W_{1,\text{HNO}_3} + (2x_1 - 1)U_{1,\text{HNO}_3}\} \quad (67)$$

where  $A_1 = (1000/w_{\text{H}_2\text{O}})^{1/2} A^\phi$  is the Debye-Hückel constant on a mole fraction basis, subscript 1 denotes the solvent  $\text{H}_2\text{O}$ ,  $\rho$ ,  $W_{1,\text{HNO}_3}$ , and  $U_{1,\text{HNO}_3}$  are adjustable parameters, and  $I_1$  is the mole fraction ionic strength given by

$$I_1 = 1/2 \sum_i z_i^2 x_i \quad (68)$$

where  $z_i$  is the magnitude of the charge on ionic component  $i$ , and the sum is over all ionic components. We also define the composition variable  $x_1$ , the total mole fraction of ions, here equivalent to  $(1 - x_1)$ , or  $2I_1$  if all ions are of unit charge. The mean activity coefficient  $f_{\text{HNO}_3}^\infty$  (infinite dilution standard state) on the mole fraction scale is given by

$$\ln(f_{\text{HNO}_3}^*) = -A_1 \{ (2/\rho) \ln(1 + \rho I_1^{1/2}) + (I_1^{1/2} - 2I_1^{3/2}) / (1 + \rho I_1^{1/2}) \} + x_1^2 (W_{1,\text{HNO}_3} + 2x_1 U_{1,\text{HNO}_3}) - W_{1,\text{HNO}_3} \quad (69)$$

The fitted equations are valid for  $x_1 < 0.6$  at  $25^\circ\text{C}$ . When extended with a further interaction term  $V$  (Equations 41 and 42 of Clegg and Brimblecombe<sup>74</sup>) the equations, perhaps surprisingly, give a satisfactory representation of  $p\text{HNO}_3$  even over pure liquid  $\text{HNO}_3$ . This is in spite of the fact that molecular  $\text{HNO}_3$  is the dominant solution component of the acid at all stoichiometric concentrations greater than  $10 \text{ mol dm}^{-3}$  (Figure 3).

Water and solute activities for  $T \neq 298 \text{ K}$  may be calculated, first, from empirical expressions yielding model parameters  $\rho$ ,  $U_{1,\text{HNO}_3}$ , and  $W_{1,\text{HNO}_3}$  as functions of temperature (determined by applying corresponding model expressions for apparent molal enthalpy and heat capacity to available data).<sup>74</sup> Second, they may be obtained using the activity coefficients at  $25^\circ\text{C}$  together with the partial molal enthalpy and heat capacity functions. Both approaches have been used for  $\text{HNO}_3$ ; determining parameters  $\rho$ ,  $U_{1,\text{HNO}_3}$ , and  $W_{1,\text{HNO}_3}$  as  $f(T)$  for a fitted model valid to a maximum concentration ( $x_1$ ) of 0.24; and using an extended parameter set  $\omega$ ,  $U$ ,  $W$ , and  $V$  at  $298.15 \text{ K}$  only, and determining activities at other temperatures directly from the partial molal functions.<sup>74</sup> The additional (empirical) parameter  $V$  is related to a quaternary term  $V_{1,\text{HNO}_3}$ , for the Pitzer and Simonson model, arising for single salt solutions. Model fits to activity and osmotic coefficients of a variety of very soluble 1:1 electrolytes, such as  $\text{HCl}$ , show that the additional parameter  $V_{1,\text{cr}}$  is often required. In Figure 17 the mole fraction activity coefficient  $f_{\text{HNO}_3}^*$  and rational osmotic coefficient  $g = \ln(a_{\text{H}_2\text{O}})/\ln(x_1)$  of aqueous  $\text{HNO}_3$  at  $25^\circ\text{C}$  are shown for the entire concentration range.

Extrapolation of the mole fraction model to supercooled solutions of  $\text{HNO}_3$  at temperatures 210 to 250 K agrees well with available experimental determinations.<sup>165</sup> However, it is worth recalling that, in calculations of gas solubility, the principal determinant of the temperature variation of the partial pressure (assuming constant aqueous phase composition) is the Henry's law constant. For example, the Henry's law constant of  $\text{HNO}_3$  changes by more than an order of magnitude from 5 to  $35^\circ\text{C}$ , whereas  $f_{\text{HNO}_3}^*$  varies by a factor of 3 at most (for pure liquid  $\text{HNO}_3$ ), and very much less at moderate aqueous phase concentrations.<sup>165</sup>

## B. NEUTRAL SOLUTES

The principal neutral solutes of interest in natural waters, apart from ion pairs, are atmospheric gases such as  $\text{O}_2$  and  $\text{N}_2$ , the noble gases, and the undissociated forms of weak

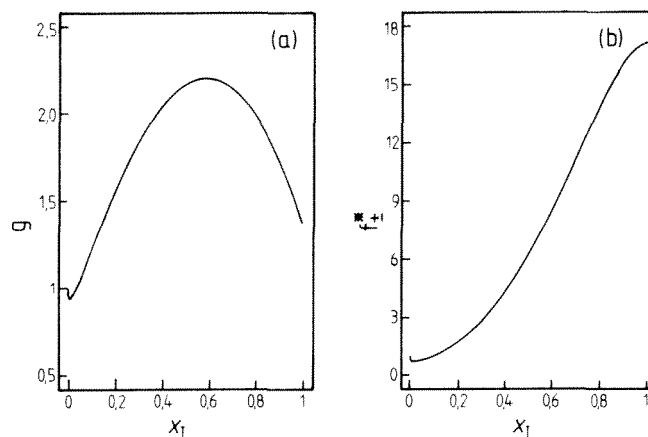


FIGURE 17. Rational osmotic coefficient  $g$  (a) and mean activity coefficient  $f_{\pm}^*$  (mole fraction scale) (b) of aqueous  $\text{HNO}_3$  at  $25^\circ\text{C}$ , from infinitely dilute solution ( $x_1 = 0$ ) to pure liquid  $\text{HNO}_3$  ( $x_1 = 1$ ).

acids and bases such as  $\text{CO}_2$ ,  $\text{H}_2\text{S}$ ,  $\text{SO}_2$ , and  $\text{NH}_3$ . The latter gases, which undergo hydrolysis or dissociation in solution, are considered further in the section on weak electrolytes below. Here we restrict ourselves to nondissociating solutes. Consider a volatile nonelectrolyte N, for example  $\text{O}_2$ , partitioned between the gaseous and solution phases:

$$N_{(g)} = N_{(aq)} \quad (70)$$

at equilibrium:

$$K_H' = m_N \gamma_N / f_N \quad (71)$$

where  $K_H'$  ( $\text{mol kg}^{-1} \text{atm}^{-1}$ ) is the Henry's law constant,  $f_N$  is the fugacity of N in the gas phase, and  $m_N$  and  $\gamma_N$  its molality and aqueous phase activity coefficient, respectively. The Henry's law constant is dependent only on temperature and pressure. The fugacity  $f_N$  is defined relative to a standard state where N forms an ideal gas at 1 atm total pressure, and is measured relative to a reference state where  $f_N \rightarrow p_N$  as  $p_N \rightarrow 0.0$  (where  $p_N$  is the partial pressure of N in the gas phase). For ideal gases, the partial pressure exerted by a mixture contained in a volume  $V$  at a temperature  $T$  is given by

$$p_N = n_N RT / V_i \quad (72)$$

where  $n_N$  is the total number of moles of N in the volume  $V_i$  and  $R$  is the gas constant. For nonideal gases, the van der Waals equation provides a useful approximation:

$$(p_N + n_N^2 a / V^2)(V - b n_N) = n_N RT \quad (73)$$

The volume occupied by 1 mol of a gas at standard temperature and pressure (STP:  $0^\circ\text{C}$ , 1 atm total pressure), calculated from Equation 73 and using the appropriate values of  $a$  and  $b$  (Table 19), gives a measure of the deviation of that gas from ideal behavior. For most of the common atmospheric gases, assuming ideal behavior and replacing  $f_N$  by  $p_N$  in Equation 71 will produce an error of no more than a few tenths of a percent (Table 19). However, much larger errors may arise for  $\text{CO}_2$ ,  $\text{N}_2\text{O}$ , and Xe and possibly the higher hydrocarbons.

TABLE 19  
Fundamental Properties of Gases Commonly Dissolved in  
Natural Waters<sup>344</sup>

Gas	Mole fraction in dry air $x_{\text{g}}$ <sup>a</sup>	van der Waals coefficients <sup>b</sup>		Molar volume at STP (dm <sup>3</sup> mol <sup>-1</sup> ) <sup>c</sup>	Deviation from ideality (%) <sup>c</sup>
		a	b		
N <sub>2</sub>	0.78080	1.390	0.03913	22.391	-0.10
O <sub>2</sub>	0.20952	1.360	0.03183	22.385	-0.13
Ar	$9.34 \times 10^{-4}$	1.345	0.03219	22.386	-0.12
CO <sub>2</sub>	$3.3 \times 10^{-4}$	3.592	0.04267	22.296	-0.53
Ne	$1.818 \times 10^{-5}$	0.2107	0.01709	22.421	+0.03
He	$5.24 \times 10^{-6}$	0.03412	0.02370	22.436	+0.10
CH <sub>4</sub>	$2 \times 10^{-6}$	2.253	0.04278	22.356	-0.26
Kr	$1.14 \times 10^{-6}$	2.318	0.03978	22.350	-0.29
CO	$0.1-0.2 \times 10^{-6}$	1.485	0.03985	22.387	-0.12
N <sub>2</sub> O	$5 \times 10^{-7}$	3.782	0.04415	22.288	-0.56
Xe	$8.7 \times 10^{-8}$	4.194	0.05105	22.277	-0.61

<sup>a</sup>  $x_{\text{g}} = n_{\text{g}}/\sum_{\text{N}} n_{\text{N}}$ .

<sup>b</sup> For Equation 73.

<sup>c</sup> Relative to the ideal value of 22.414 dm<sup>3</sup> mol<sup>-1</sup>.

Adapted with permission from Kester, D. R., *Chemical Oceanography*, Vol. 1, Riley, J. P. and Skirrow, G., Eds., Academic Press, London, 1975, 497.

Deviations from ideality have been examined in some detail for carbon dioxide,<sup>166,167</sup> and the results have been summarized in terms of the virial equation of state:<sup>168,169</sup>

$$PV = RT + B_2P + C_2P^2 + \dots \quad (74)$$

so that,<sup>170</sup> using only the first term in the expansion,

$$V = V_1 + B_2 \quad (75)$$

and<sup>170</sup>

$$\ln(f_{\text{N}}^{\circ}/p_{\text{N}}^{\circ}) = B_2P/RT \quad (76)$$

Here  $V_1$  is the volume occupied by 1 mol of an ideal gas under these conditions, and  $P$  is the total pressure at the liquid-gas interface. The superscript <sup>o</sup> has been introduced to emphasize that the ratio calculated here refers to a gas phase containing N only. For carbon dioxide (265 to 320 K):

$$B_2 = -1636.75 + 12.0408 T - 3.27957 \times 10^{-2} T^2 + 3.16528 \times 10^{-5} T^3 \quad (77)$$

where  $B_2$  is expressed in cm<sup>3</sup> mol<sup>-1</sup>. Values of  $V$  and  $f_{\text{N}}^{\circ}/p_{\text{N}}^{\circ}$  are summarized in Table 20. Values of the ratio  $f_{\text{N}}^{\circ}/p_{\text{N}}^{\circ}$  calculated in this way for the pure gas can be applied with errors of less than 10% to gaseous mixtures, since, according to the Lewis fugacity rule,  $f_{\text{N}}^{\circ}/p_{\text{N}}^{\circ} = f_{\text{N}}/p_{\text{N}}$ , i.e., the ratio is independent of the gas composition.

Generally, it is reasonable to assume ideal behavior for most of the volatile solutes in

**TABLE 20**  
**Deviation of Gaseous Carbon**  
**Dioxide from Ideal Behavior**  
**at 1 atm Total Pressure**

T(°C)	V <sub>l</sub> <sup>a</sup>	V <sup>b</sup>	f <sub>N</sub> <sup>c</sup> /p <sub>N</sub> <sup>c</sup>
0	22.414	22.263	0.9933 <sup>d</sup>
5	22.823	22.679	0.9937
10	23.233	23.095	0.9941
15	23.644	23.511	0.9944
20	24.054	23.926	0.9947
25	24.464	24.341	0.9950
30	24.874	24.756	0.9952

<sup>a</sup> Equation 72, with R = 0.082053 dm<sup>3</sup> atm mol<sup>-1</sup>.

<sup>b</sup> Equations 75 and 77.

<sup>c</sup> Equations 76 and 77.

<sup>d</sup> For comparison, the corresponding value for nitrogen is 0.99955.

natural systems (Table 19), so that partial pressure, rather than fugacity, can be used in Equation 71 and

$$K'_H = m_N \gamma_N / p_N \quad (78)$$

so that the dissolution of a gas, for example, O<sub>2</sub>, into aqueous solution is described by

$$K'_H = m_{O_2} \gamma_{O_2} / p_{O_2} \quad (79)$$

In multicomponent solutions such as seawater, the influence of major solution components on the activity coefficient of a neutral solute is represented by the Pitzer model as a summation of the effects of the individual species present. This approach can only be of value where there are sufficient data for single salt solutions to parameterize the model adequately. The analysis of such data, so far carried out comprehensively for NH<sub>3</sub><sup>98</sup> and O<sub>2</sub><sup>90</sup> (with some parameters also available for CO<sub>2</sub><sup>56</sup>) is probably only worthwhile in the two following situations: first, where the activity coefficient is required in a multicomponent solution for which no direct determinations have been made, and which cannot be satisfactorily approximated by a pure salt solution; second, where the concentration of the neutral species is so great that it affects the activities of the solvent and/or other solutes, which are also required. Both cases are straightforwardly handled by the Pitzer model.

### 1. Empirical Representations of Solubility

If two vessels containing pure solvent (superscript °) and a salt solution s, respectively, are subjected to the same partial pressure of N at the same temperature, the values of the activity coefficient of N (γ<sub>N</sub>) in the two solutions can be related through the Henry's law expression (Equations 71 and 78):

$$\gamma_N^s / \gamma_N^\circ = m_N^\circ / m_N^s \quad (80)$$

where for a sparingly soluble gas γ<sub>N</sub><sup>°</sup> is equal to unity, thus m<sub>N</sub><sup>°</sup>/m<sub>N</sub><sup>s</sup> is equivalent to γ<sub>N</sub><sup>s</sup>. The empirically determined Setchenow relationship, giving the influence of dissolved salt concentration upon nonelectrolyte solubility, is<sup>77</sup>

$$\log_{10}(S^{\circ}/S^s) = {}^s k_s c_s \quad (81)$$

where  $S^{\circ}$  and  $S^s$  are the solubilities of the neutral molecule in the pure solvent and salt solution, respectively,  $c_s$  is the salt concentration in  $\text{mol dm}^{-3}$ , and  ${}^s k_s$  is a constant — the Setchenow coefficient on the molar scale. Alternatively, on a molal basis and using natural logarithms, we can write:

$$\ln(\gamma_N^s/\gamma_N^{\circ}) = \ln(m_N^{\circ}/m_N^s) = k_s m_s \quad (82)$$

where  $m_s$  is the molality of salt  $s$ , and  $k_s$  is on the molal scale. The above expressions are related to theories of the salt effect by Long and McDevit,<sup>171</sup> and also by Gordon.<sup>172</sup> It can be seen that (where  $\gamma_N^{\circ} = 1$ ) the Setchenow relationship, as given in Equation 82, is equivalent to an expression for the activity coefficient of the neutral molecule in terms of the salt concentration. The relationship is found to hold up to salt concentrations of a few  $\text{mol dm}^{-3}$  for many salts (above which nonlinear terms need to be added). When  $S^{\circ}$  is sufficiently large that  $\gamma_N^{\circ} \neq 1$ , the self-interaction of the nonelectrolyte must be taken into account:

$$\log(S^{\circ}/S^s) = {}^s k_s c_s + {}^s k_N(S^s - S^{\circ}) \quad (83)$$

where  ${}^s k_N$  is the self-interaction parameter of  $N$  on the molar scale. Comparisons with the Pitzer model expression for  $\gamma_N$  in a multicomponent solution (Equation 37) show that it may be viewed as an elaboration of Equation 82 or 83, allowing for self-interactions, interactions with multiple ions (instead of salts), and for deviations from linearity ( $\zeta_{Nca}$ ,  $\eta_{Nca}$ , and  $\eta_{Naa}$  terms).

If the salting coefficient  $k_s$  (or  ${}^s k_s$ ) is positive, the solubility of  $N$  is decreased by the presence of the dissolved salt  $s$  (i.e., the activity coefficient increases and  $N$  is salted out), and if it is negative, the solubility of  $N$  is increased by the presence of the salt (i.e., the activity coefficient of  $N$  decreases and  $N$  is salted in). In natural waters the salting coefficients are invariably positive. Since the logarithmic form of Equation 81 makes the experimental salting out coefficient particularly sensitive to errors in the measured gas solubility at low salt concentrations, it is somewhat surprising that the Setchenow equation has proved to be such a useful way of representing gas solubilities in salt solutions.

This description of gas solubility in salt solutions has been elaborated by Schumpe et al.,<sup>173</sup> and used by Lang and Zander<sup>174</sup> for  $O_2$ , expressing a salting coefficient  $k_{s, O_2}$  in terms of individual ion contributions:

$$k_{s, O_2} = (1/2)\sum_i H_i \nu_i z_i^2 \quad (84)$$

where  $H_i$  is the  $O_2$  solubility parameter for ion  $i$  (relative to  $H_{Na} = 0$ ),  $\nu_i$  is the number of moles of ion  $i$  per mole of salt  $M_s X_{\nu}$ , and  $z_i$  the charge on ion  $i$ . The salting parameter  $k_{s, O_2}$  is related to the measured solubility by

$$\log(\beta^{\circ}/\beta^s) = k_{s, O_2} c_s \quad (85)$$

where  $\beta^{\circ}$  and  $\beta^s$  are the Bunsen coefficients (defined in Section III.B.4) for  $O_2$  solubility in the salt solution and pure solvent, respectively. The quotient  $(\beta^{\circ}/\beta^s)$  is equivalent to the molar activity coefficient  $\gamma_{O_2}$ . Note that, in Equations 84 and 85, gas solubility is treated as being dependent upon ionic strength rather than ion concentration, as in the Pitzer model. Lang and Zander<sup>174</sup> tabulate  $H_i$  at 310 K for 21 cations and 5 anions (including the major ions of seawater), and obtain agreement between measured and fitted  $k_{s, O_2}$  (Equation 84) to

about 3.5%. The same data have also recently been used to determine parameters for the Pitzer model equation for  $\gamma_{\text{O}_2}$ .<sup>90</sup>

Van Krevelen and Hofstijzer<sup>175</sup> adopted the Setchenow relationship to express salt effects on gas solubility, considering the salting parameter  $h$  as the sum of three terms:

$$\log(\alpha^2/\alpha^*) = hI_r \quad (86)$$

where  $I_r$  is the molar ionic strength, and the salting parameter  $h$  is equal to the sum of cation ( $h_c$ ), anion ( $h_a$ ), and gas ( $h_N$ ) terms (i.e.,  $h = h_c + h_a + h_N$ ). This equation implies that the ionic effect ( $h_c + h_a$ ) is the same for all gases, the salt effect on the solubility of two gases  $N_1$  and  $N_2$  differing only by ( $h_{N_1} - h_{N_2}$ ). More seriously, Equation 86 neglects the differing ionic contributions to  $I_r$  in solutions of salts of different stoichiometries. This strictly renders the equation invalid, as noted by Schumpe et al.<sup>173</sup> Despite this, Equation 86 has been applied with some success to the solubilities of a number of gases.<sup>176,177</sup> Onda et al.<sup>178</sup> have extended Equation 86 to include solution mixtures, and applied it to their measurements of the solubility of  $\text{CO}_2$ ,  $\text{C}_2\text{H}_2$ , and  $\text{C}_2\text{H}_4$  in multicomponent salt solutions at 25°C and molar ionic strengths of up to about 6 mol dm<sup>-3</sup>.

From a study of the solubility of naphthalene in seawater, Gordon and Thorne<sup>179,180</sup> have also suggested that the Setchenow equation could be extended to a multicomponent mixture, by assuming that the effects of the individual salts (rather than ions) in the electrolyte mixture are approximately additive (Young's first rule). Thus

$$\ln(S^0/S^*) = c_{(T)} \sum_j y_j {}^1k_j \quad (87)$$

where  $c_{(T)}$  is the sum of the concentrations of the individual salt components (mol dm<sup>-3</sup>) and  $y_j$  is the mole fraction of the salt  $J$  in the mixture (Equation 12). The Young's rule estimate of naphthalene solubility in seawater is in good agreement with experimental values in both artificial and natural seawaters (Table 21).

## 2. Theoretical Prediction of Setchenow Coefficients

The scaled particle theory has been applied to the calculation of Setchenow coefficients in multicomponent solutions by Masterton and co-workers.<sup>181-183</sup> According to this theory, the salting coefficient  ${}^1k$  consists of three components, i.e.,

$${}^1k = {}^1k_c + {}^1k_b + {}^1k_s \quad (88)$$

where  ${}^1k_c$  represents the work required to create cavities in the solution large enough to accommodate the nonelectrolyte molecules, and  ${}^1k_b$  represents the energy required to place the nonelectrolyte molecules in these cavities in the face of interactions with the water molecules and the ions of the electrolyte. The coefficient  ${}^1k_c$  is a salting-out term, indicating that it is easier to form the cavity in pure water than it is in an electrolyte solution, and  ${}^1k_b$  is a salting-in term, suggesting that the presence of the ions reduces the energy required to fill the cavity with the nonelectrolyte molecule (Table 22). The coefficient  ${}^1k_s$  is a statistical term representing a standard-state correction that disappears when concentrations are expressed on the molar scale. In general, the calculated and observed values agree to within  $\pm 0.014$  units, although the theory predicts  ${}^1k$  values for aromatic hydrocarbons that are at least 50% too small.

From the point of view of the natural water chemist, the main virtue of the scaled particle theory is that, because it is based on the concept of ionic additivity, it is readily extended to electrolyte mixtures and has been applied to the calculation of gas solubilities in seawater with moderate success (see Table 23).



**TABLE 21**  
**Application of Young's First Rule to the Solubility**  
**of Naphthalene in Seawater at 25°C<sup>a</sup>**

Salt	${}^c k_j(c_j)$	$y_j$	$y_j {}^c k_j(c_j)$
NaCl	$0.507 \pm 0.009$	0.79644	0.4038
MgCl <sub>2</sub>	$0.693 \pm 0.014$	0.10363	0.0718
Na <sub>2</sub> SO <sub>4</sub>	$1.603 \pm 0.032$	0.05489	0.0880
CaCl <sub>2</sub>	$0.741 \pm 0.013$	0.02010	0.0149
KCl	$0.428 \pm 0.010$	0.01767	0.0076
NaHCO <sub>3</sub>	$0.735 \pm 0.032$	0.00454	0.0033
			$\Sigma = 0.5894$

Note: From Equation 87  $\ln S^{(s)} = a_1 + a_2 c_{(T)}$ , where naphthalene solubilities " $S^{(s)}$ " in seawater are on the molar scale.

Parameters for this equation are given by:

Computed <sup>a</sup>	Experimental <sup>a</sup>		
	Artificial seawater	Natural seawater	
$-a_1$	$8.2663 \pm 0.0076$	$8.2789 \pm 0.0143$	$8.2697 \pm 0.0173$
$-a_2$	$0.5894 \pm 0.0078$	$0.5828 \pm 0.0230$	$0.5948 \pm 0.0309$

<sup>a</sup> Data from Gordon and Thorne<sup>180</sup> corrected to natural logarithms and to the seawater recipe shown in Table 7.

**TABLE 22**  
**Calculated Values of  ${}^c k_\alpha$ ,  ${}^c k_\beta$ , and  ${}^c k_\gamma$  in the**  
**Scaled Particle Theory for Several Salt-**  
**Nonelectrolyte Pairs at 25°C**

Components	${}^c k_\alpha$	${}^c k_\beta$	${}^c k_\gamma$	${}^c k$
H <sub>2</sub> — NaCl <sup>a</sup>	0.2901	-0.0530	0.0184	0.2556
H <sub>2</sub> — KI <sup>a</sup>	0.2648	-0.0714	-0.0092	0.1842
CH <sub>4</sub> — NaCl <sup>a</sup>	0.4674	-0.1842	0.0184	0.3016
CH <sub>4</sub> — KI <sup>a</sup>	0.4191	-0.2349	-0.0092	0.1750
SF <sub>6</sub> — NaCl <sup>a</sup>	0.8911	-0.4467	0.0207	0.4651
SF <sub>6</sub> — KI <sup>a</sup>	0.7898	-0.5204	-0.0092	0.2602
He — SW <sup>b</sup>	0.2523	-0.0247	—	0.2276
Ne — SW <sup>b</sup>	0.2793	-0.0507	—	0.2286
Ar — SW <sup>b</sup>	0.4095	-0.1267	—	0.2828
O <sub>2</sub> — SW <sup>b</sup>	0.4236	-0.1135	—	0.3101
N <sub>2</sub> — SW <sup>b</sup>	0.4587	-0.1281	—	0.3306

Note: All values are adjusted to natural logarithms.

<sup>a</sup> Masterton and Lee.<sup>182</sup> It is not clear from the paper why  ${}^c k_\gamma$  corrections were included, since  $c_N$  is in mol dm<sup>-3</sup>.

<sup>b</sup> Masterton.<sup>183</sup> SW = seawater.  ${}^c k_\gamma$  corrections were neglected since  $c_N$  is in mol dm<sup>-3</sup>.

### 3. Solubility of Atmospheric Gases in Water and Seawater

The solubilities of both major and trace atmospheric gases have been studied extensively and determined as functions of both temperature and salinity (see Table 12 for sources of compiled data). Parameters leading to the solubility of a number of gases in pure water, as

**TABLE 23**  
**Setchenow Coefficients [ $k(I_c)$ ] for the Major**  
**Atmospheric Gases in Seawater and Sodium Chloride**  
**Solutions at 25°C**

Gas	Seawater		NaCl	
	Experimental <sup>a</sup>	Calculated <sup>b</sup>	Experimental <sup>c</sup>	Calculated <sup>b</sup>
He	0.212	0.228	0.192, 0.137	0.230
Ne	0.235	0.228	0.229	0.230
Ar	0.281	0.283	0.314, 0.307	0.281
O <sub>2</sub>	0.281	0.311	0.312	0.309
N <sub>2</sub>	0.304	0.332	0.309	0.329

*Note:* In his equation for the Setchenow coefficient, Masterton<sup>183</sup> expressed salt concentration (in seawater) in terms of the molar ionic strength  $I_c$ , where:  $I_c = 0.019924\rho_{\text{sea}}S\%$ , and solubilities were expressed as Bunsen coefficients (Equations 102 and 103).

<sup>a</sup> Calculated from fitting equations, Table 24.

<sup>b</sup> Masterton.<sup>183</sup> His value has been multiplied by  $\ln(10)$ .

<sup>c</sup> Masterton et al.<sup>181</sup> Corrected, assuming that salt molarities are approximately equal to salt molalities at this concentration.

a function of temperature, are listed in Appendix Table A7. The availability of salting coefficients for atmospheric gases in salt solutions is indicated in Appendix Table A8. Solubilities have often been presented in the form of empirical fitting equations. For example, Weiss<sup>184</sup> assumed that atmospheric gases obeyed the Setchenow equation in seawater and expressed their solubility using

$$\ln\{\text{solubility}\} = A_1 + A_2S \quad (89)$$

where  $S$  is salinity ( $\%$ ). The integral form of the Van't Hoff equation is used to express  $A_1$  as a function of temperature, and a simple quadratic form is used for  $A_2$ , so that

$$\begin{aligned} \ln\{\text{solubility}\} = & [a_1 + a_2(100/T) + a_3\ln(T/100) + a_4(T/100)] \\ & + S[b_1 + b_2(T/100) + b_3(T/100)^2] \end{aligned} \quad (90)$$

Equation 90 and similar expressions have been used to represent so-called "air solubilities" for a sea salt solution equilibrated with a gas phase at 1 atm total pressure, exerting the natural partial pressure of gas  $N$ , at 100% relative humidity. Where  $N$  is a trace gas whose concentration in air is variable, it is also necessary to specify its vapor phase mole fraction or fugacity. Since the work of Weiss on the solubilities of N<sub>2</sub>,<sup>184</sup> O<sub>2</sub>,<sup>184</sup> CO<sub>2</sub>,<sup>167</sup> He,<sup>185</sup> Ne,<sup>185</sup> Ar,<sup>186</sup> Kr,<sup>187</sup> and N<sub>2</sub>O,<sup>188</sup> data have become available for other solutes and there have been slight revisions to the equations for a few gases (O<sub>2</sub>, N<sub>2</sub>, and Ar). Equations and associated parameters giving the best available estimates of air solubilities on both a "per liter of seawater" and "per kilogram of seawater" basis are presented in Tables 24 and 25. In Figure 18 the salt effect is illustrated for some of the principal atmospheric gases, calculated from the equations given in Table 25, and shows that solubilities are reduced, in normal seawater, by 15 to 35%.

To convert these values to molal solubilities for a known partial pressure of the dissolving gas,  $p_N$  (or  $f_N$  as appropriate) must first be determined from the volume composition of dry air and values of the equilibrium  $p\text{H}_2\text{O}$  over the solutions (given, for example, by Millero

and Leung<sup>77</sup>). Then aqueous phase concentrations must be converted to mol kg<sup>-1</sup> (H<sub>2</sub>O), using seawater densities where concentrations are expressed in volume units as in Table 24. We have carried out these conversions for N<sub>2</sub> and some of the noble gases, and in Figure 19 show their activity coefficients from 5 to 35°C as a function of salinity. It can be seen that the temperature effect is quite small, for example  $\gamma_{N_2}$  varying by only about  $\pm 4\%$  from its 20°C value at 40 S‰.

While expressions such as that given above are satisfactory for media of constant composition, such as seawater, it is desirable to extend the treatment to a more generalized form and so enable gas solubilities to be calculated in brines of arbitrary composition and temperature.

#### a. Application of the Pitzer Model

Equation 37 is the basic expression for the activity coefficient of a neutral species, such as a dissolved gas, in an aqueous solution. Barta and Bradley<sup>97</sup> have applied an analogous expression, also based on the Pitzer formalism, to the solubilities of H<sub>2</sub>S, CH<sub>4</sub>, and CO<sub>2</sub> in aqueous NaCl, and earlier Chen et al.<sup>109</sup> have treated HCl, NH<sub>3</sub>, and CO<sub>2</sub> solubility in systems of industrial interest. The form of Equation 37 can be considerably simplified for gases dissolved in natural waters. Here, as an example, we apply the Pitzer model to the description of O<sub>2</sub> solubility in saline solutions including seawater. Since O<sub>2</sub> is only weakly soluble in water at normal atmospheric pressure, self-interactions can be neglected, as can other neutral-neutral interactions, since other similar gases will only be present at trace concentrations. Thus we obtain from lines (iv to vi) of Equation 37:

$$\begin{aligned} \ln \gamma_N = & 2 \sum_c \lambda_{Nc} m_c + 2 \sum_a \lambda_{Na} m_a + \sum_c \sum_a m_c m_a \zeta_{Nca} \\ & + \sum_c \sum_c m_c m_c \eta_{Ncc} + \sum_a \sum_a m_a m_a \eta_{Naa} \end{aligned} \quad (91)$$

where the final two terms only occur for multicomponent solutions, and would be expected to be significant only at high salt concentrations. For O<sub>2</sub> there are insufficient data available to determine any values of  $\eta_{O_2cc}$  and  $\eta_{O_2aa}$ . The remaining parameters  $\lambda_{Nc}$ ,  $\lambda_{Na}$ , and  $\zeta_{Nca}$  are determined from O<sub>2</sub> activities in single electrolyte solutions — obtained from measurements of O<sub>2</sub> solubility in salt solutions — using Equation 79. The Henry's law constant of O<sub>2</sub> is very precisely known as a function of temperature from the work of Benson and Krause.<sup>100</sup> For oxygen, fugacity corrections (at  $p_{O_2} = 1$  atm) range from 0.1% at 273 K to 0.05% at 373 K, and so may be neglected without significant loss of accuracy. This is not always the case for other gases of geochemical interest, such as CO<sub>2</sub>. Also, the range of techniques and experimental conditions employed by different workers (sometimes inadequately characterized) often renders such corrections difficult.

As an illustration of the effects of different salts on gas solubility, in Figure 20  $\log_{10}(\gamma_{O_2})$  is shown in solutions of the alkali metal chlorides. With the exception of LiCl, for low salt concentrations there is decreased salting-out (lower activity coefficients) as ion size increases (inset to Figure 20). At higher salt concentrations, there are deviations from the linear Setchenow relationship, particularly for KCl. Aqueous LiCl (and also other Li<sup>+</sup> salts) are a clear exception to the trend, with a relatively small effect on the activity coefficient of O<sub>2</sub>.<sup>90</sup> There appear to be some analogies here with the values of certain ion-ion interaction parameters for salts containing Li<sup>+</sup>, which may be explained in terms of "structure making" and "structure breaking" effects of the ions.<sup>191</sup>

Clegg and Brimblecombe<sup>90</sup> have used O<sub>2</sub> solubility data for a wide range of salts, obtained from the IUPAC compilation<sup>192</sup> plus a few additional sources,<sup>174</sup> to determine ion-O<sub>2</sub> interaction parameters for ions of geochemical importance. The results show that the data for a

**TABLE 24**  
**Parameters for Equations Giving the Solubility of Atmospheric Gases in Water and Seawater, per Unit Volume of Solution**

Gas	Equation	$a_1$	$a_2$	$a_3$	$a_4$	$b_1$	$b_2$	$b_3$	Note	Ref.
N <sub>2</sub>	2	-29.1410	53.3161	7.499	1.8299	0.007365	-0.04038	—	a	332
O <sub>2</sub>	1	-1268.9782	36063.19	220.1832	-0.351299	0.006229	-3.5912	$3.44 \times 10^{-6}$	b	192
CO <sub>2</sub>	2	-58.0931	90.5069	22.2940	—	0.027766	-0.025888	0.0050578	c	167
He	2	-152.9405	196.884	126.8015	-20.6767	-0.040543	0.021315	-0.0030732	d	185
Ne	2	-160.263	211.0969	132.1657	-21.3165	-0.122883	0.077055	-0.0125568	e	185
Ar	1	-1304.2075	36686.68	226.1517	-0.364328	0.006118	-3.5438	—	f	324
Kr	2	-109.9329	149.8152	72.8393	-9.9217	-0.006953	-0.004085	0.0014759	g	328
H <sub>2</sub>	3	-314.3572	455.8526	297.5313	-49.2778	-0.070143	0.041069	-0.0063763	h	330
N <sub>2</sub> O	2	-62.7062	97.3066	24.1406	—	-0.05842	0.033193	-0.0051313	i	188
CO	3	-169.4951	263.5657	159.2552	-25.4967	0.051198	-0.044591	0.0086462	j	337
CH <sub>4</sub>	3	-412.171	596.8104	379.2599	-62.0757	-0.05916	0.032174	-0.0048198	k	325

Equations:

$$(1) \ln(C) = a_1 + a_2/T + a_3 \ln(T) + a_4 T + S(b_1 + b_2/T) + b_3 S^2$$

$$(2) \ln(C) = a_1 + a_2(100/T) + a_3 \ln(T/100) + a_4(T/100) + S[b_1 + b_2(T/100) + b_3(T/100)^2]$$

$$(3) \ln(C) = x_N + a_1 + a_2(100/T) + a_3 \ln(T/100) + a_4(T/100) + S[b_1 + b_2(T/100) + b_3(T/100)^2]$$

T is in Kelvin, S is the conventional salinity (ppt), and  $x_N$  is the mole fraction of gas N in dry air.

Note: The pressure effect on the solubility of He, CO<sub>2</sub>, N<sub>2</sub>, O<sub>2</sub>, and Ar has been determined by Enns et al.<sup>345</sup>

<sup>a</sup> C = ml (STP) N<sub>2</sub> dm<sup>-3</sup> (solution), at the temperature of measurement, from water-saturated atmosphere at 1 atm total pressure.

<sup>b</sup> C = ml (STP) O<sub>2</sub> dm<sup>-3</sup> (solution), at the temperature of measurement, from water-saturated atmosphere at 1 atm total pressure. Validity 0—35.5°C, 0—40 S‰.

<sup>c</sup> C = mol dm<sup>-3</sup> (solution) atm<sup>-1</sup> (CO<sub>2</sub>). Gas phase CO<sub>2</sub> is expressed as the fugacity  $f_{CO_2}$ . Validity 0—40°C, 0—40 S‰.

<sup>d</sup> C = cm<sup>3</sup> (STP) He dm<sup>-3</sup> (solution), at the temperature of measurement, from water-saturated atmosphere at 1 atm total pressure. He is treated as an ideal gas, with mole fraction  $5.24 \times 10^{-6}$  in dry air.

- <sup>c</sup>  $C = \text{cm}^3 \text{ (STP) Ne dm}^{-3}$  (solution), at the temperature of measurement, from water-saturated atmosphere at 1 atm total pressure. Ne is treated as an ideal gas, with mole fraction  $1.818 \times 10^{-5}$  in dry air. Validity 0—40°C, 0—40 S%.
- <sup>d</sup>  $C = \text{cm}^3 \text{ (STP) Ar dm}^{-3}$  (solution), at the temperature of measurement, from water-saturated atmosphere at 1 atm total pressure; 1 mol Ar assumed to occupy 22,400 cm<sup>3</sup> at STP. Atmospheric Ar concentration = 0.934% by volume in dry air. Validity 0—40°C, 0—40 S%.
- <sup>e</sup>  $C = \text{cm}^3 \text{ (STP) Kr dm}^{-3}$  (solution), at the temperature of measurement, from water-saturated atmosphere at 1 atm total pressure. Kr mole fraction in dry air =  $1.141 \times 10^{-6}$ . Results corrected for deviations from ideality in the gas phase. Validity 0—40°C, 0—40 S%.
- <sup>f</sup>  $C = 10^{-9} \text{ dm}^3 \text{ (STP) H}_2 \text{ dm}^{-3}$  (solution), at the temperature of measurement, from water-saturated atmosphere at 1 atm total pressure (for a "dry air" mole fraction  $\text{H}_2$  of  $x\text{H}_2$ ). Validity 0—40°C, 0—40 S%.
- <sup>g</sup>  $C = \text{mol N}_2\text{O dm}^{-3}$  (solution)  $\text{atm}^{-1}$  ( $\text{N}_2\text{O}$ ). Gas phase  $\text{N}_2\text{O}$  is expressed as fugacity  $f\text{N}_2\text{O}$ . Validity 0—40°C, 0—40 S%.
- <sup>h</sup>  $C = 10^{-9} \text{ dm}^3 \text{ (STP) CO dm}^{-3}$  (solution), at the temperature of measurement, from a water-saturated atmosphere at 1 atm total pressure (for a "dry air" mole fraction of  $x\text{CO}$ ).
- <sup>i</sup>  $C = 10^{-9} \text{ dm}^3 \text{ (STP) CH}_4 \text{ dm}^{-3}$  (solution), at the temperature of measurement, from a water-saturated atmosphere at 1 atm total pressure (for a "dry air" mole fraction of  $x\text{CH}_4$ ). Validity 0—30°C, 0—40 S%.

**TABLE 25**  
**Parameters for Equations Giving the Solubility of Atmospheric Gases in Water and Seawater, per Unit Mass of Solution**

Gas	Equation	$a_1$	$a_2$	$a_3$	$a_4$	$b_1$	$b_2$	$b_3$	Note	Ref.
N <sub>2</sub>	2	-29.2710	58.6753	10.3401	1.5045	0.007116	-0.04186	—	a	332
O <sub>2</sub>	1	-1282.870	36619.96	223.1396	-0.354707	0.005957	-3.7353	$3.68 \times 10^{-6}$	b	192
CO <sub>2</sub>	2	-60.2409	93.4517	23.3585	—	0.023517	-0.023656	0.0047036	c	167
He	2	-167.2178	216.3442	139.2032	-22.6202	-0.044781	0.023541	-0.0034266	d	185
Ne	2	-170.6018	225.1946	140.8863	-22.6290	-0.127113	0.079277	-0.0129095	e	185
Ar	1	-1313.707	37125.99	228.3402	-0.366478	0.005855	-3.6872	—	f	324
Kr	2	-112.684	153.5817	74.469	-10.0189	-0.011213	-0.001844	0.0011201	g	328
H <sub>2</sub>	3	-320.3079	459.7398	299.26	-49.3946	-0.074474	0.043363	-0.006742	h	330
N <sub>2</sub> O	2	-64.8539	100.252	25.2049	—	-0.062544	0.035337	-0.0054699	i	188
CO	3	-175.6092	267.6796	161.0862	-25.6218	0.046103	-0.041767	0.0081890	j	337
CH <sub>4</sub>	3	-417.5053	599.8626	380.3636	-62.0764	-0.06423	0.03498	-0.0052732	k	325
C <sub>2</sub> H <sub>6</sub>	4	-671.5248	31696.51	99.97065	—	-145.3127	6137.061	21.8756	l	346

Equations:

$$(1) \ln(C) = a_1 + a_2/T + a_3 \ln(T) + a_4 T + S(b_1 + b_2/T) + b_3 S^2$$

$$(2) \ln(C) = a_1 + a_2(100/T) + a_3 \ln(T/100) + a_4(T/100) + S[b_1 + b_2(T/100) + b_3(T/100)^2]$$

$$(3) \ln(\bar{C}) = \lambda_N + a_1 + a_2(100/T) + a_3 \ln(T/100) + a_4(T/100) + S[b_1 + b_2(T/100) + b_3(T/100)^2]$$

$$(4) \ln(H) = a_1 + a_2/T + a_3 \ln(T) + W[b_1 + b_2/T + b_3 \ln(T)]$$

T is in Kelvin. S is the conventional salinity (ppt).  $\lambda_N$  is the mole fraction of gas N in dry air, and W is weight % of NaCl or sea salt.

Note: The pressure effect on the solubility of He, CO<sub>2</sub>, N<sub>2</sub>, O<sub>2</sub>, and Ar has been determined by Enns et al.<sup>345</sup>

<sup>a</sup>  $C = \mu\text{mol N}_2 \text{ kg}^{-1}$  (solution), at the temperature of measurement, from water-saturated atmosphere at 1 atm total pressure.

<sup>b</sup>  $C = \mu\text{mol O}_2 \text{ kg}^{-1}$  (solution), at the temperature of measurement, from water-saturated atmosphere at 1 atm total pressure. Validity 0–35.5°C, 0–40 S‰. A factor of 22.393 cm<sup>3</sup> mol<sup>-1</sup> was used to convert volume of O<sub>2</sub> to  $\mu\text{mol}$ .

<sup>c</sup>  $C = \text{mol kg}^{-1}$  (solution) atm<sup>-1</sup> (CO<sub>2</sub>). Gas phase CO<sub>2</sub> is expressed as the fugacity  $f\text{CO}_2$ . Validity 0–40°C, 0–40 S‰.

- 4  $C = \text{cm}^3 (\text{STP}) \text{He kg}^{-1}$  (solution), at the temperature of measurement, from water-saturated atmosphere at 1 atm total pressure. He is treated as an ideal gas, with mole fraction  $5.24 \times 10^{-6}$  in dry air.
- 7  $C = \text{cm}^3 (\text{STP}) \text{Ne kg}^{-1}$  (solution), at the temperature of measurement, from water-saturated atmosphere at 1 atm total pressure. Ne is treated as an ideal gas, with mole fraction  $1.818 \times 10^{-5}$  in dry air. Validity 0—40°C, 0—40 S‰.
- 1  $C = \mu\text{mol Ar kg}^{-1}$  (solution), at the temperature of measurement, from water-saturated atmosphere at 1 atm total pressure; 1 mol Ar assumed to occupy 22,400 cm<sup>3</sup> at STP. Atmospheric Ar concentration = 0.934% by volume in dry air. Validity 0—40°C, 0—40 S‰.
- 6  $C = \text{cm}^3 (\text{STP}) \text{Kr kg}^{-1}$  (solution), at the temperature of measurement, from water-saturated atmosphere at 1 atm total pressure. Kr mole fraction in dry air =  $1.141 \times 10^{-6}$ . Results corrected for deviations from ideality in the gas phase. Validity 0—40°C, 0—40 S‰.
- 8  $C = 10^{-4} \text{ mol H}_2 \text{ kg}^{-1}$  (solution), at the temperature of measurement, from water-saturated atmosphere at 1 atm total pressure (for a "dry air" mole fraction  $\text{H}_2$  of 1H<sub>2</sub>). Validity 0—40°C, 0—40 S‰.
- 11  $C = \text{mol N}_2\text{O kg}^{-1}$  (solution) atm<sup>-1</sup>. Gas phase N<sub>2</sub>O is expressed as fugacity  $f\text{N}_2\text{O}$ . Validity 0—40°C, 0—40 S‰. See Weiss and Price<sup>186</sup> for ideality correction.
- $C = 10^{-9} \text{ mol CO kg}^{-1}$  (solution), at the temperature of measurement, from a water-saturated atmosphere at 1 atm total pressure (for a "dry air" mole fraction of  $\alpha\text{CO}$ ). In the derivation of the equation CO was assumed to behave as an ideal gas.
- 12  $C = 10^{-4} \text{ mol CH}_4 \text{ kg}^{-1}$  (solution), at the temperature of measurement, from a water-saturated atmosphere at 1 atm total pressure (for a "dry air" mole fraction  $\text{CH}_4$  of  $\alpha\text{CH}_4$ ). Validity 0—30°C, 0—40 S‰. In the derivation of the equation CH<sub>4</sub> was assumed to behave as an ideal gas.
- $\text{H}^+ = \text{ppm (by weight)} \text{C}_6\text{H}_{10} \text{ atm}^{-1} (\text{C}_6\text{H}_6)$ . Valid 0—10% by weight of dissolved solids (NaCl or sea salt), 0—20°C. See Bajolle et al.<sup>187</sup> for solubilities at higher temperatures.

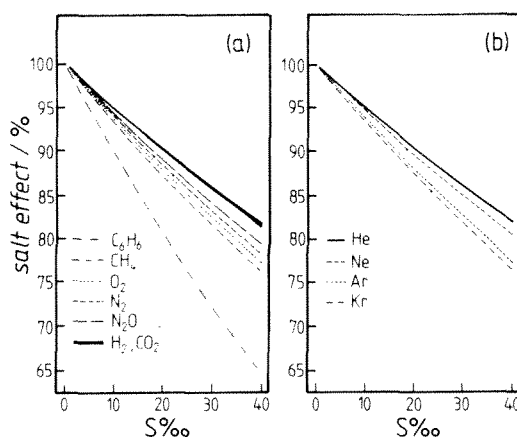


FIGURE 18. Effect of salinity on gas solubility (per kilogram of solution) in seawater at 25°C, from equations listed in Table 25. Vertical axis represents the percentage of the pure water solubility (expressed in the units given in Table 25) for the following gases: (a)  $H_2$ ,  $CO_2$ ,  $N_2O$ ,  $N_2$ ,  $O_2$ ,  $CH_4$ , and  $C_6H_6$  (at 20°C); (b) He, Ne, Ar, and Kr.

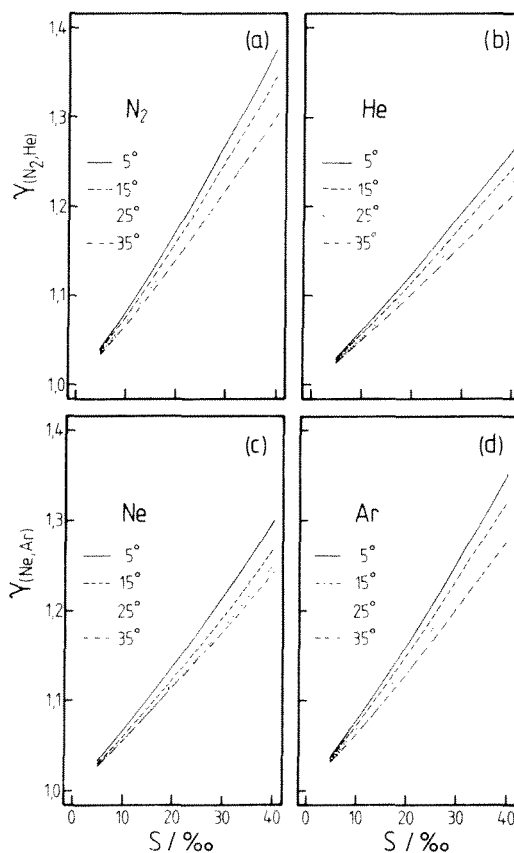


FIGURE 19. Activity coefficients ( $\gamma_N$ ) of  $N_2$ , Ar, He, and Ne from 5 to 35°C as a function of salinity. Values were calculated from equations in Tables 24 and 25, with appropriate conversions to obtain molal solubilities. (a)  $N_2$ ; (b) He; (c) Ne; (d) Ar.



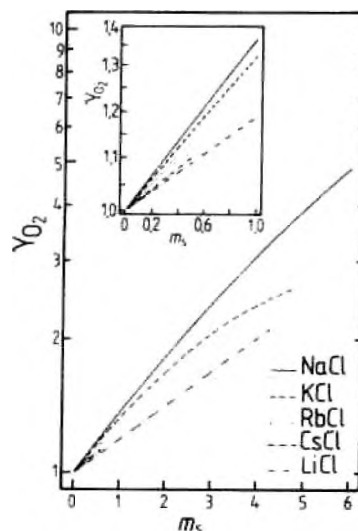


FIGURE 20. Activity coefficient of  $O_2$  ( $\gamma_{O_2}$ ) in aqueous solutions of the alkali metal chloride(s) at 25°C (except LiCl, for which most reliable data are for 37°C<sup>174</sup>), calculated using the Pitzer model.<sup>91</sup> Activity coefficients are given to the limits of fit of the available data. For aqueous RbCl and CsCl, model parameters derived from 37°C data of Lang and Zander<sup>174</sup> to 3 and 6 mol dm<sup>-3</sup> agree well with those used in these calculations (to 0.5 mol kg<sup>-1</sup> at 25°C). Inset gives detail at low concentration.

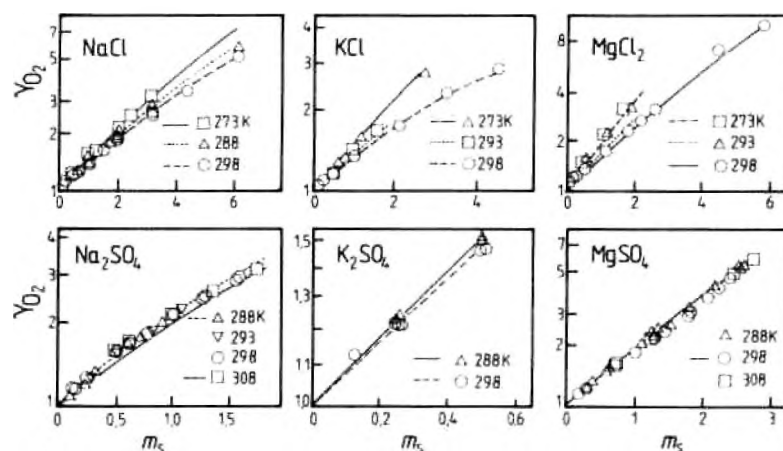


FIGURE 21. Measured (symbols) and fitted values of  $\gamma_{O_2}$ , obtained from  $O_2$  solubilities in pure aqueous salt solutions. Note logarithmic scale for  $\gamma_{O_2}$ . Activity coefficients are plotted against salt concentration " $m_s$ " (mol kg<sup>-1</sup>).

wide variety of salt solutions can be satisfactorily described using the Pitzer interaction model. In Figure 21, measured and fitted values of  $\gamma_{O_2}$  in solutions of a number of salts are shown. Model parameter values are listed in Table 26. In view of the fact that NaCl is often the major component of natural brines, the following equation for  $\gamma_{O_2}$  in aqueous NaCl is provided, valid for  $273 \leq T \leq 570$  K:

$$\begin{aligned} \ln(\gamma_{O_2}) = & 2mNaCl(-0.38316 + 132.4246/T + 0.108392 \times 10^{-6} T^2) \\ & + mNaCl^2(-0.028771 + 6.15316/T) \end{aligned} \quad (92)$$

**TABLE 26**  
**Interaction Parameters  $\lambda_{O_2^i}$ ,  $\lambda_{O_2^a}$ , and  $\zeta_{O_2^{ca}}$  Determined from  $O_2$  Solubilities in Pure Aqueous Salt Solutions**

Ion	$\lambda_{O_2^i}$				$^{298}\lambda_{O_2^i}$
	<i>a</i>	<i>b</i>	<i>c</i>	<i>d</i>	
Na	-0.39548	141.307	—	$9.19882 \times 10^{-7}$	0.1602
K	-0.51698	199.431	—	—	0.1519
Mg	-0.79489	305.513	—	—	0.2298
Ca	0.2497	—	—	—	0.2497
Cl	0	0	0	0	0.0
Br	-0.0347	—	—	—	-0.0347
OH	0.93318	-430.552	49860.8	—	0.0500
SO <sub>4</sub>	1.00706	-274.085	—	—	0.0878
NH <sub>4</sub>	(0.0751)	—	—	—	0.0751
Ba	0.285	—	—	—	0.285
CO <sub>3</sub>	1.0258	-277.074	—	—	0.0964

Ions	$\zeta_{O_2^{ca}}$			$^{298}\zeta_{O_2^{ca}}$
	<i>a</i>	<i>b</i>	<i>c</i>	
Na Cl	—	-2.739	—	-0.00919
Na Br	-0.00909	—	—	-0.00909
Na OH	-0.0125	—	—	-0.0125
Na SO <sub>4</sub>	-0.0460	—	—	-0.0460
Na CO <sub>3</sub>	-0.0181	—	—	-0.0181
K Cl	-0.0211	—	—	0.0211
K Br	-0.00541	—	—	-0.00541
K OH	0.002342	—	836.15	-0.00706
K SO <sub>4</sub>	0.0	—	—	—
NH <sub>4</sub> SO <sub>4</sub>	(-0.028)	—	—	(-0.028)
Mg Cl	0.00565	—	—	0.00565
Mg SO <sub>4</sub>	0.0	—	—	—
Ca Cl	-0.0169	—	—	-0.0169
Ba Cl	0.0	—	—	0.0

*Note:* For all  $\zeta_{O_2^{ca}}$ , *d* is equal to zero. Values of the parameters at 298.15 K are also listed. The following parameter values have been determined from the solubility data of Lang and Zander<sup>124</sup> at 37°C:  $\lambda_{O_2, NH_4} = 0.0564$ ;  $\lambda_{O_2, Ca} = 0.205$ ;  $\lambda_{O_2, Ba} = 0.274$ ;  $\zeta_{O_2, NH_4, SO_4} = -0.0173$ .

(Each parameter “*P*” is given as the following function of temperature:  $P = a + b/T + c/T^2 + d/T^3$ .)

When the  $O_2$ -ion interaction parameters ( $\lambda_{O_2^i}$  and  $\zeta_{O_2^{ca}}$ ) are determined simultaneously from data for salts with common ions, the model provides a useful test of consistency. For example, the data of MacArthur<sup>193</sup> and Yasunishi<sup>194</sup> for aqueous KCl at 25°C were found to be discordant. However, by comparison with data for other salts containing the K<sup>+</sup> ion it was clear that only the MacArthur<sup>193</sup> data were consistent with  $\lambda_{O_2, K}$  determined from the other data sets. In this way the results of Yasunishi<sup>194</sup> were rejected.

To be of practical benefit for calculating solubilities in natural waters, it should be possible to calculate the solubility of  $O_2$  in seawater and other brines using the Pitzer model together with the thermodynamic Henry's law constant. Figure 22 shows calculated  $\gamma_{O_2}$  in seawater over a range of temperatures compared with measured values. Calculated  $\gamma_{O_2}$  in pure aqueous NaCl at the same total concentration is also included. Clearly, model calculations are in excellent agreement with experimental data. Detailed comparison with the data

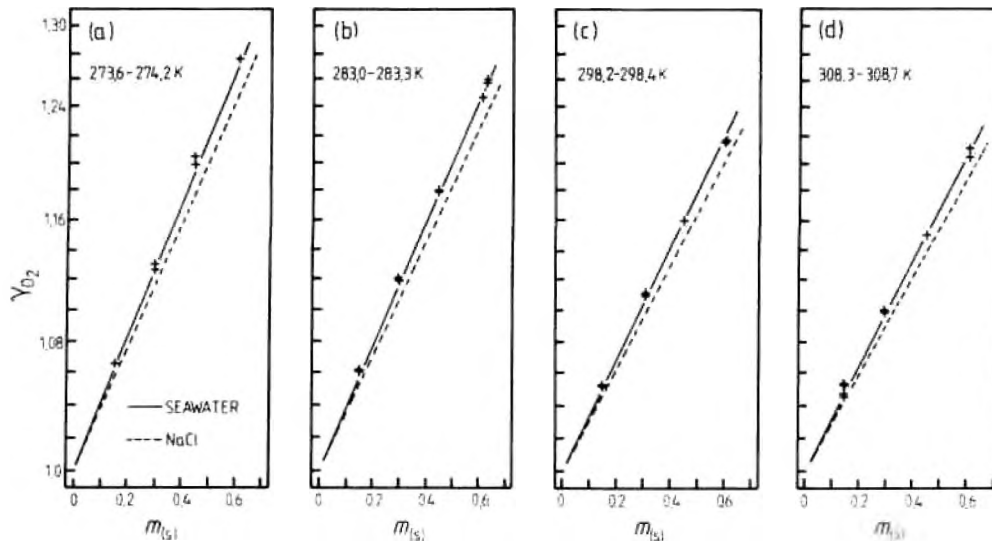


FIGURE 22 Activity coefficient of  $O_2$  ( $\gamma_{O_2}$ ) in seawater at four different temperatures, as a function of molality  $m_{(s)}$  (e.g., see Equation 23). Symbols — data of Carpenter;<sup>195</sup> full lines — calculated using Pitzer model parameterized from single salt data; dashed lines — calculated for pure aqueous NaCl at the same total salt concentration. In each case the calculated activity coefficients were determined at the mean temperature of the experimental range (listed on each graph).

of Carpenter<sup>195</sup> and Murray and Riley<sup>196</sup> shows that deviations are no more than 0.65% from 0 to 40°C, 0 to 40 S‰. In more concentrated solutions the lack of ternary mixture parameters  $\eta_{(O_2)Na}$  and  $\eta_{(O_2)Mg}$  begins to tell, as can be seen in Figure 23 for concentrated seawaters to salinity 255 S‰ ( $m_{(s)} \approx 5 \text{ mol kg}^{-1}$ ). There is a similar overprediction of the activity coefficient when modeling  $\gamma_{O_2}$  in the Salton Sea geothermal brine (ionic strength 7.06 mol  $\text{kg}^{-1}$ ),<sup>90</sup> although the temperature variation of the activity coefficient is quite well predicted as the brine is composed chiefly of NaCl. Model calculated values of  $\gamma_{O_2}$  in the lower ionic strength (0.6 mol  $\text{kg}^{-1}$ ) East Mesa geothermal brine<sup>90</sup> agree better with measured values.

As an alternative to using the Weiss equation for  $O_2$  solubility in seawater, or the rather cumbersome summation procedure involved in calculating the numerous ion- $O_2$  interactions, the Pitzer interaction parameters have been determined for "sea salt" by fitting Equation 91 directly to the solubility data of Carpenter,<sup>195</sup> Murray and Riley,<sup>196</sup> Green,<sup>197</sup> and Kinsman et al.<sup>198</sup> The resulting expression is given below together with the Henry's law constant determined by Benson et al.<sup>199</sup>

$$\ln(K_H^O) = 0.298399 - 5.59617 \times 10^{-5}/T + 1.049668 \times 10^{-6}/T^2 \quad (93)$$

$$\ln(\gamma_{O_2}) = 2m(S)\lambda_{(O_2)S} + m(S)_+m(S)_-\zeta_{(O_2)S} \quad (94)$$

where  $m(S)$  is equal to the sum of the molal concentrations of all seawater components (equivalent to  $2m_{(s)}$  listed in recipe a of Table 2),  $m(S)_+$  is the sum of concentrations of all cations, and  $m(S)_-$  the corresponding sum of all anions. (Note that, for simplicity, total borate [B(OH)<sub>3</sub> in Table 7] is counted as an anion.)

$$\lambda_{(O_2)S} = 0.4341 - 255.5911/T + 45132.321/T^2 \quad (95)$$

$$\zeta_{(O_2)S} = -0.0187 \quad (96)$$

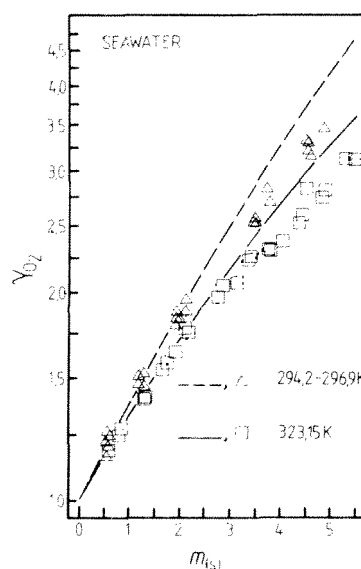


FIGURE 23. Activity coefficient of  $O_2$  in concentrated seawater at 323.15 and 294.2 to 296.9 K. Symbols — data of Kinsman et al.<sup>198</sup> lines — calculated using Pitzer model parameterized from single salt data. For measurements where  $294.2 < T < 296.9$  K the calculated activity coefficients were determined at the mean temperature only (295.55 K).

$$m(S)_c = 0.484334m(S) \quad (97)$$

$$m(S)_a = 0.515662m(S) \quad (98)$$

Comparing Equation 94 with 91, the combined seawater interaction parameters  $\lambda_{O_2,S}$  and  $\zeta_{O_2,S}$  are related to those for individual ions by

$$\lambda_{O_2,S} = (1/m(S)) \left( \sum_c m_c \lambda_{O_2,c} + \sum_a m_a \lambda_{O_2,a} \right) \quad (99)$$

$$\zeta_{O_2,S} = (1/m(S)_c m(S)_a) \sum_c \sum_a m_c m_a \zeta_{O_2,ca} \quad (100)$$

Where the solubilities of other gases are to be calculated in brines, similar analyses of solubility data for single salt solutions may also be worthwhile.

#### 4. Gas Solubility Data

Measurements of gas solubility in salt solutions have been made for over a century, and it is still the case for quite a few systems that very early determinations are the only data available. Measurements to 1924 of the solubility of  $O_2$ ,  $H_2$ ,  $N_2$ ,  $N_2O$ ,  $CO_2$ ,  $H_2S$ ,  $NH_3$ , and  $C_2H_2$  in electrolyte solutions are summarized by Randall and Failey,<sup>199</sup> and the availability of data for a much larger range of gases by Long and McDevit<sup>171</sup> (to 1952). Where available (see Table 12), modern critical compilations of solubility data should be used as sources of coefficients, and as means of parameterizing solution models. In Appendix Table A9, salting parameters (from the work of Krishnan and Friedman<sup>200</sup> and Masterton et al.<sup>181</sup> only) are listed for many atmospheric gases. The availability of solubility data for hydrocarbons in aqueous NaCl and seawater is indicated in Appendix Table A10.

The numerical value of the salting coefficient will depend on the scales used to express the concentrations of the salt S and dissolved neutral species N, and considerable care must be exercised when using published salting coefficients. A number of units are commonly used for expressing gas solubilities. The Ostwald coefficient L is defined as the ratio of the volume of gas absorbed to the volume of the absorbing liquid, all at the temperature of measurement. If the gas is ideal and Henry's law is applicable, then the Ostwald coefficient is independent of the partial pressure. It is necessary, in practice, to state the temperature and total pressure for which the Ostwald coefficient is measured. It is related to the molal solubility by

$$m_N/p_N = (L/RT)(1000/(d_s - c_s w_s)) \quad (101)$$

where  $m_N$  (mol kg<sup>-1</sup>) is the solubility of gas N,  $p_N$  (atm) is its partial pressure, L is the Ostwald coefficient, R (dm<sup>3</sup> atm mol<sup>-1</sup> K<sup>-1</sup>) is the gas constant,  $d_s$  (g dm<sup>-3</sup>) the density of the solution,  $c_s$  (mol dm<sup>-3</sup>) the molar salt concentration, and  $w_s$  (g) the molar mass of the salt.

The Bunsen coefficient  $\beta$  is defined as the volume of gas reduced to 273.15 K and 1 atm pressure which is absorbed by a unit volume of solution (at the temperature of measurement) under a partial pressure of 1 atm. The Bunsen coefficient is therefore related to the Ostwald coefficient by

$$\beta = L(273.15/T) \quad (102)$$

and to molal gas solubility, for a partial pressure of 1 atm, by

$$m_N = \beta/(273.15 RT)(1000/(d_s - c_s w_s)) \quad (103)$$

where the symbols have the same meaning as before. The solubilities can then be transformed, knowing the molar volume of the dissolving gas and solution density. Note that, when using Setchenow coefficients to express gas solubilities in aqueous solutions, a number of different conventions are used for expressing the dissolved salt concentration, so the procedure used must be clearly identified.

The definition of mole fraction solubility would appear to be straightforward, but may, however, be expressed in two different ways. Solution chemists commonly treat the mole fraction composition of salt solutions on the basis of complete dissociation. Thus, the mole fraction of neutral species N in a solution also containing  $m_s$  mol kg<sup>-1</sup> of salt  $M_\nu X_\nu$  under this convention is given by

$$x_N = n_N/(n_N + \nu m_s + \nu m_s + nH_2O) \quad (104)$$

where prefix  $n$  indicates the number of moles of the component present, and  $nH_2O$  is equal to  $1000/wH_2O$ . On the alternative convention, *not* treating the salt as dissociated, the term  $(\nu m_s + \nu m_s)$  in Equation 104 above would simply be replaced by  $m_s$ .

Parameters summarizing the solubility of a wide range of gases in pure water are given in Appendix Table A7, where some recent general reviews are also listed. These data can be used for calculating Setchenow coefficients from measurements of gas solubility in natural waters. The permanent gases (Table 19) are relatively insoluble in water, hence their activity coefficients  $\gamma_N^0$  are unity in pure water, and activity coefficients in salt solutions may be determined from (Equation 82):

$$\gamma_N = \exp(k_s m_s) \quad (105)$$

When estimating activity coefficients from Setchenow coefficients, it is important to remember that  $\gamma_N^\circ$  and  $\gamma_N$  refer to solutions of N in pure water and in the salt solution subjected to the same partial pressure of N.

For volatile liquid solutes such as ethanol, concentrations are more conveniently expressed in the mole fraction scale. The activity coefficient of N on this scale ( $f_N$ ), assuming that partial pressure can be treated as equivalent to fugacity, is related to the composition of the solution by

$$f_N = (p_N/p_N^\circ)/x_N \quad (106)$$

where  $p_N^\circ$  is the vapor pressure of the pure solute at the same temperature. In a pure liquid,  $p_N = p_N^\circ$ , hence:

$$f_N = x_N^{-1} \quad (107)$$

so that  $a_N = 1$ .

The activity coefficients of organic compounds in seawater and estuarine waters are of considerable importance, since it has been clearly shown<sup>32-34,201</sup> that the physical toxicity of these compounds is directly related to their thermodynamic activity in solution.

The Setchenow coefficients for hydrocarbons in seawater (Table 27) are considerably larger than those observed for the atmospheric gases under similar circumstances, indicating more vigorous salting out. Even larger values are found for the polychlorinated biphenyls (PCBs) in seawater (Table 28). For these compounds, the Setchenow coefficients change by less than 30%, although the individual solubilities range over two orders of magnitude. The activity coefficients of the PCBs calculated from Equation 106 appear unusually large (Table 28), because they refer to pure liquid solute as the standard state, rather than to a hypothetical ideal solution of unit concentration.

Linear correlations have been demonstrated between the solubility and the molar volume of organic solutes in distilled water.<sup>202,203</sup> The form of the Setchenow equation suggests that similar correlations are to be expected in seawater. This will simplify the task of estimating activity coefficients where no experimental data are available. Care must be taken to correct the solubilities for Henry's law artifacts arising from the marked changes in vapor pressure that occur as the molecular weight increases in the homologous series.<sup>204</sup> In addition, there is evidence of hydrocarbon-hydrocarbon interactions in seawater (Table 27), which will complicate attempts to predict the behavior of natural hydrocarbon mixtures resulting from the spillage of oil and oil wastes.

Activity coefficients on molar ( $y$ ), molal ( $\gamma$ ), and mole fraction ( $f$ ) scales for each solute in a single or multicomponent solution may be calculated from the following equations:<sup>22</sup>

$$f = \gamma(1 + 0.001 w_{H_2O} \sum_i m_i) \quad (108)$$

$$f = (y/d_0)(d + 0.001(w_{H_2O} \sum_i c_i - \sum_i c_i w_i)) \quad (109)$$

$$\gamma = (y/d_0)(d - 0.001 \sum_i c_i w_i) = (c/m d_0)y \quad (110)$$

$$y = (\gamma d_0/d)(1 + 0.001 \sum_i m_i w_i) = (m d_0/c)\gamma \quad (111)$$

where  $d$  is solution density,  $d_0$  the density of the pure solvent,  $w_i$  the molar mass of species  $i$ , and  $w_{H_2O}$  the molar mass of water. Note that the equations for  $f$  apply only to values for which the standard state is one of infinite dilution. These equations apply to both the activity

TABLE 27  
Setchenow Coefficients for Hydrocarbons in Seawater at  
25°C and 1 atm Total Pressure

Component	Pure water $c_i^0$	Seawater (35 S‰) $c_i^0$ <sup>†</sup>	Setchenow coefficient <sup>a</sup> $k_{s,i}$	Ref.
Dodecane (C <sub>12</sub> )	$2.18 \times 10^{-8}$	$1.71 \times 10^{-8}$	0.425	348
Tetradecane (C <sub>14</sub> )	$1.11 \times 10^{-8}$	$8.59 \times 10^{-9}$	0.450	348
Hexadecane (C <sub>16</sub> )	$3.98 \times 10^{-9}$	$1.77 \times 10^{-9}$	1.415	348
Octadecane (C <sub>18</sub> )	$8.27 \times 10^{-9}$	$3.15 \times 10^{-9}$	1.684	348
Eicosane (C <sub>20</sub> )	$6.74 \times 10^{-9}$	$2.84 \times 10^{-9}$	1.509	348
Hexacosane (C <sub>26</sub> )	$4.64 \times 10^{-9}$	$2.73 \times 10^{-10}$	4.942	348
Toluene	$5.81 \times 10^{-3}$	$4.12 \times 10^{-3}$	0.602	204
Ethyl benzene	$1.52 \times 10^{-3}$	$1.05 \times 10^{-3}$	0.650	204
<i>o</i> -Xylene	$1.61 \times 10^{-3}$	$1.22 \times 10^{-3}$	0.482	204
<i>m</i> -Xylene	$1.38 \times 10^{-3}$	$1.00 \times 10^{-3}$	0.560	204
<i>p</i> -Xylene	$1.47 \times 10^{-3}$	$1.05 \times 10^{-3}$	0.596	204
Isopropyl benzene	$5.44 \times 10^{-4}$	$3.54 \times 10^{-4}$	0.747	204
1,2,4-Trimethyl benzene	$4.92 \times 10^{-4}$	$3.30 \times 10^{-4}$	0.698	204
1,2,3-Trimethyl benzene	$6.27 \times 10^{-4}$	$4.05 \times 10^{-4}$	0.764	204
1,3,5-Trimethyl benzene	$4.02 \times 10^{-4}$	$2.61 \times 10^{-4}$	0.753	204
<i>n</i> -Butyl benzene	$8.81 \times 10^{-5}$	$5.29 \times 10^{-5}$	0.891	204
<i>s</i> -Butyl benzene	$1.31 \times 10^{-4}$	$8.88 \times 10^{-5}$	0.681	204
<i>t</i> -Butyl benzene	$2.20 \times 10^{-4}$	$1.58 \times 10^{-4}$	0.578	204
Naphthalene	$2.54 \times 10^{-4}$	$1.88 \times 10^{-4}$	0.516 <sup>b</sup>	179
	$2.50 \times 10^{-4}$	$1.76 \times 10^{-4}$	0.613	349
	$2.43 \times 10^{-4}$	$1.72 \times 10^{-4}$	0.603 <sup>c</sup>	349
Biphenyl	$0.51 \times 10^{-4}$	$0.32 \times 10^{-4}$	0.841	349
	$0.39 \times 10^{-4}$	$0.25 \times 10^{-4}$	0.776 <sup>c</sup>	349
Phenanthrene	$0.64 \times 10^{-5}$	$0.41 \times 10^{-5}$	0.786	349
	$0.53 \times 10^{-5}$	$0.33 \times 10^{-5}$	0.806 <sup>c</sup>	349

<sup>a</sup> Setchenow coefficient on molar scale such that, for each compound  $N$ ,  $\ln(c_i^0/c_i^0) = k_{s,i} \cdot c_{s,i}$ , where  $c_{s,i}$  is the molarity of seawater. The molar mass of sea salt ( $w_{s,i}$ ) is 62.793 g, hence at 35 S‰  $c_{s,i} = 0.573$ . (In the original work,<sup>40,179,204,349</sup>  $c_{s,i} = 0.504$  at 35 S‰.)

<sup>b</sup> Mean of experimental values.

<sup>c</sup> Solubility when naphthalene, biphenyl, and phenanthrene are all present together.

coefficients of neutral species, and either conventional single ion or mean activity coefficients of pairs of cations and anions. The concentration terms  $c$  and  $m$  without subscripts in Equations 110 and 111 refer to those of the species of interest.

### C. WEAK ELECTROLYTES

Thermodynamic stability constants ( $K$ ) for the ion pair and weak electrolyte equilibria most commonly encountered in natural waters are listed in Table 29, together with Henry's law constants for species (such as  $\text{NH}_3$  and  $\text{CO}_2$ ) which also occur in the gas phase. These values must be divided by the activity coefficient quotient  $\Gamma$  (Equation 31) to determine the stoichiometric constant  $K^*$  relevant to the natural water of interest.

Where the equilibrium (or equilibria) involve only trace species, in a solution dominated by strong electrolytes, then the activity coefficients of the trace species will be determined solely by interactions with the major ions present. In such a case, the activity coefficient

**TABLE 28**  
**Solubility of Polychlorinated Biphenyls**  
**(C<sub>12</sub>H<sub>10-n</sub>Cl<sub>n</sub>) in 30 S% Seawater at 11.5°C**

n	Mol. mass	10 <sup>6</sup> c <sub>N</sub> <sup>o</sup>	10 <sup>7</sup> c <sub>N</sub> <sup>(s)</sup>	k <sub>(s)</sub> <sup>a</sup>
2	223.10	1.488	2.030	4.06
3	257.55	0.462	0.700	3.85
4	291.99	0.183	0.254	4.01
5	326.44	0.063	0.107	3.63
6	360.88	0.028	0.062	3.04
7	395.33	0.016	0.039	2.85

Note: Values were recalculated from Dexter and Pavlou.<sup>202</sup>

<sup>a</sup> Setchenow coefficient on molar scale such that, for each compound N,  $\ln(c_N^o/c_N^{(s)}) = k_{(s)} \cdot c_{(s)}$ , where  $c_{(s)}$  is the molarity of seawater. The molar mass of sea salt ( $w_{(s)}$ ) is 62.793 g, hence at 30 S%  $c_{(s)} = 0.491$ .

quotient and stoichiometric association constant may first be calculated for each reaction, and then the equilibrium equation, together with equations defining the mass and charge balances, are solved simultaneously to calculate the distribution of the various species in solution. Where the association reaction involves the major ions or neutral species present, such that the composition of the solution, in terms of these species, will be significantly changed by considering the equilibrium, then a different procedure must be followed. The equilibrium, mass balance, and activity coefficient equations must be iterated to determine a solution, as described in Section III.A.3 on aqueous sulfuric acid.

Although pressure in the deep ocean can rise as high as 1000 atm, information on the influence of pressure on mineral equilibria and on the ionization of weak acids in seawater is sparse. Millero<sup>91</sup> has extensively reviewed the available data, including pressure effects on ion pair and gas-liquid equilibria. More recent data leading to the influence of pressure on the major ions of seawater have already been referred to (see Section II.B.1.a.i). For the pressure dependence of stoichiometric dissociation constants of H<sub>2</sub>CO<sub>3</sub>, HCO<sub>3</sub><sup>-</sup>, and B(OH)<sub>3</sub> see Section III.C.3.a.ii and Table 32. The pressure effect on the ionic product of water in seawater has recently been considered by Kumar.<sup>205</sup>

### 1. Weak Acid-Base Equilibria in Natural Waters

The pH of natural waters is buffered in the short term by equilibria involving weak acid-base reactions in solution. Such reactions exert a fundamental influence on trace metal speciation and on the interaction of dissolved components with the solid phase. The generic dissociation reaction for acid-base equilibria may be written as



so that the thermodynamic acid dissociation constant ( $K_X$ ) is given, on the molal concentration scale, by

$$\begin{aligned} K_X &= (mX^- mH^+ / mHX) \cdot (\gamma_X \gamma_H / \gamma_{HX}) \\ &= K_X^* \cdot \Gamma \end{aligned} \quad (113)$$

The stoichiometric dissociation constants ( $K_X^*$ ) for acids of interest can be determined experimentally in the ionic medium under consideration. While this has proved to be a viable



**TABLE 29**  
**Thermodynamic Association Constants for the Weak Acid, Ion Pair, and**  
**Gas/Liquid Equilibria Considered in Models of Natural Waters at 25°C,**  
**1 atm Pressure**

Reaction	$\Delta H^\circ$ (kJ mol <sup>-1</sup> )	$\log_{10}(K)^a$ 298 K	$\log_{10}(K)^b$ 298 K	Ref.	As f(T)
H <sub>2</sub> O = H <sup>+</sup> + OH <sup>-</sup>	-55.907	-14.000	-13.997	56	See below
H <sup>+</sup> + F <sup>-</sup> = HF	13.3	3.18	3.165	267	
H <sup>+</sup> + 2F <sup>-</sup> = HF <sub>2</sub> <sup>-</sup>	19.04	3.76	—		
CO <sub>2(aq)</sub> + H <sub>2</sub> O = H <sup>+</sup> + HCO <sub>3</sub> <sup>-</sup>	9.109	-6.352	-6.337	56	Equation 168
HCO <sub>3</sub> <sup>-</sup> = H <sup>+</sup> + CO <sub>3</sub> <sup>2-</sup>	14.9	-10.329	-10.34	56	Equation 169
B(OH) <sub>3</sub> + H <sub>2</sub> O = B(OH) <sub>4</sub> <sup>-</sup> + H <sup>+</sup>	—	—	9.239	61	Equation 188
NH <sub>4</sub> <sup>+</sup> = NH <sub>3</sub> + H <sup>+</sup>	—	—	-9.246	98	Equation 195
H <sup>+</sup> + SO <sub>4</sub> <sup>2-</sup> = HSO <sub>4</sub> <sup>-</sup>	16.11	1.988	1.979	65	Equation 64
H <sub>2</sub> S = H <sup>+</sup> + HS <sup>-</sup>	—	—	-6.980	285	Equation 227
SO <sub>2(aq)</sub> + H <sub>2</sub> O = H <sup>+</sup> + HSO <sub>3</sub> <sup>-</sup>	—	—	-1.860	286	Equation 235b
HSO <sub>3</sub> <sup>-</sup> = H <sup>+</sup> + SO <sub>3</sub> <sup>2-</sup>	—	—	-7.17	286	Equation 236b
H <sub>2</sub> PO <sub>4</sub> <sup>-</sup> = H <sup>+</sup> + H <sub>2</sub> PO <sub>3</sub> <sup>2-</sup>	—	—	-2.148	276	Equation 208b <sup>c</sup>
H <sub>2</sub> PO <sub>4</sub> <sup>-</sup> = H <sup>+</sup> + HPO <sub>4</sub> <sup>2-</sup>	—	—	-7.206	276	Equation 209b <sup>c</sup>
HPO <sub>4</sub> <sup>2-</sup> = H <sup>+</sup> + PO <sub>4</sub> <sup>3-</sup>	—	—	-12.34	276	Equation 210b <sup>c</sup>
Mg <sup>2+</sup> + OH <sup>-</sup> = MgOH <sup>+</sup>	—	2.56	2.188	56	
Mg <sup>2+</sup> + F <sup>-</sup> = MgF <sup>+</sup>	13.39	1.82	1.822	350	
Ca <sup>2+</sup> + F <sup>-</sup> = CaF <sup>+</sup>	17.24	0.94	—		
Ca <sup>2+</sup> + H <sub>2</sub> O = CaOH <sup>+</sup> + H <sup>+</sup>	—	-12.78	—		
Mg <sup>2+</sup> + CO <sub>3</sub> <sup>2-</sup> = MgCO <sub>3</sub> <sup>0</sup>	11.35	2.98	2.928	56	
Ca <sup>2+</sup> + CO <sub>3</sub> <sup>2-</sup> = CaCO <sub>3</sub> <sup>0</sup>	14.83	3.224	3.151	56	
Mg <sup>2+</sup> + B(OH) <sub>4</sub> <sup>-</sup> = MgB(OH) <sub>4</sub> <sup>+</sup>	—	—	1.399	61	
Ca <sup>2+</sup> + B(OH) <sub>4</sub> <sup>-</sup> = CaB(OH) <sub>4</sub> <sup>+</sup>	—	—	1.65	61	
CO <sub>2(g)</sub> = CO <sub>2(aq)</sub>	-19.98	1.468	1.482	56	Table 33
NH <sub>3(g)</sub> = NH <sub>3(aq)</sub>	—	—	1.7833	98	Equation 190
H <sub>2</sub> S <sub>(g)</sub> = H <sub>2</sub> S <sub>(aq)</sub>	—	—	-0.987	281	Equation 221
SO <sub>2(g)</sub> = SO <sub>2(aq)</sub>	—	—	0.0898	286	Equation 238b
HF <sub>(g)</sub> = HF <sub>(aq)</sub>	—	—	4.155	67	Equation 200

*Note:* For further equilibrium constants involving the carbonate system, including CaCO<sub>3</sub> mineral solubilities, see Tables 31—33, and Table 4 of Harvie et al.<sup>56</sup>

<sup>a</sup> Equilibrium constants and  $\Delta H^\circ$  values taken from tabulation of Nordstrom et al.<sup>56</sup>

<sup>b</sup> Equilibrium constants from Harvie et al.,<sup>56</sup> or other workers using the Pitzer model (reference given in following column).

<sup>c</sup> Valid in seawater only.

The dissociation constant of water is given by  $\log_{10}(K_{H_2O}) = 283.971 + 13323/T - 0.05069842T + 102.24447 \log_{10}(T) - 1119669/T^2$ .<sup>176</sup>

approach for studies in seawater which has a relatively constant composition and covers 70% of the planet's surface, it is more useful to be able to calculate  $K_x^*$  from  $K_x$  if the medium has variable composition (e.g., estuarine waters, brine evaporites), is of unusual composition, or is of local interest only (e.g., saline pore waters).

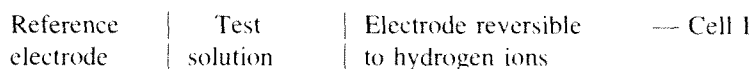
Numerous attempts have been made to relate the activity coefficient quotient ( $\Gamma$ ) to empirical functions of ionic strength in simple media.<sup>166</sup> Such approaches are, however, of very limited use for studying acid-base equilibria in natural saline solutions. More accurate

estimates of  $\Gamma$  can be calculated from ionic interaction or ion pair models if the necessary parameters are available. These values of  $\Gamma$  can then be used in conjunction with the appropriate  $K_x$  to obtain  $K_x^*$  for ionic media for which experimental measurements are not available.

In practical situations, the total anion concentration ( $mHX + mX^-$ ) can be determined by chemical analysis and it is the concentration ratio of the acid to the base component ( $mHX/mX^- = mH^+/K_x^*$ ) that is required to calculate buffer capacity or chemical speciation in solution. In principle, where  $K_x^*$  is known this simply requires the experimental determination of the hydrogen ion concentration  $mH^+$ . In fact, the universal application of sensitive and highly specific potentiometric techniques for sensing hydrogen ions, particularly in complex natural media, has introduced some subtleties into the determination and application of acid-base dissociation constants.<sup>206</sup>

## 2. Potentiometry and the Definition of pH Scales in Saline Media

In the potentiometric determination of acidity constants and the practical measurement of  $mH^+$ , use is made of the cell



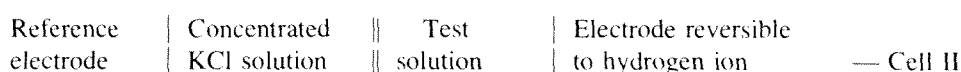
whose EMF is given by

$$E = E^\circ + gT \log_{10}(mH^+ f_H) \quad (114)$$

or:

$$(E - E^\circ)/gT = \log_{10}(mH^+ f_H) \quad (115)$$

where  $g = R \ln(10)/F = 0.19841 \times 10^{-3} \text{ V K}^{-1}$ . The activity coefficient term  $f_H$  contains some imponderables whose exact identity will depend on the nature of the cell. The most commonly encountered experimental configuration is represented by



A hydrogen ion-selective glass electrode is used in combination with a chloride-selective reference electrode, which is held in a solution of constant chloride concentration. A liquid junction provides the electrical connection between the chloride reference solution and the test solution. For such a cell,

$$\begin{aligned} (E - E^\circ)/gT &= E_j + \log_{10}(\gamma_H) + \log_{10}(mH^+) \\ &= E_j - p(aH^+) \end{aligned} \quad (116)$$

$E_j$ , the potential generated at the liquid junction, is a complicated function of the activities and mobilities of the ions that are intermixed at the junction, which will depend on the physical structure of the junction as well as composition of the test solution. Several simplified formulations have been proposed for idealized junctions.<sup>207</sup> The most widely used form is the Henderson<sup>208</sup> (1908) equation for the special case where a continuous mixture is formed between the KCl solution and the sample (see, for example, p. 40 to 43 of Whitfield and Jagner<sup>209</sup>).

The liquid junction potential cannot be calculated exactly, although the use of electrolyte solution models can refine the estimation of the ion activity contribution to  $E_j$ . Experimental procedures must therefore be adopted that either minimize its variation between standard and test solutions, or ensure that the related terms cancel out when the measured pH values are used in conjunction with the appropriate stability constants. To this end three distinct pH scales have been proposed for use in seawater and other saline brines.<sup>206,210</sup>

#### a. Hydrogen Ion Concentration and Activity in Aqueous Solution

##### i. NBS Scale

The most widely used pH scale is that proposed by Bates<sup>211</sup> for the National Bureau of Standards pH(NBS). The pH values of low ionic strength ( $<0.01 \text{ mol dm}^{-3}$ ) standard buffers are assigned according to the convention

$$\text{pH(NBS,S)} = \text{p}(a\text{H}^+ \gamma_Z)^\circ - A I_c^{1/2}/(1 + B a I_c^{1/2}) \quad (117)$$

where Z represents a halide ion and a is an adjustable parameter. A and B are Debye-Hückel constants and  $I_c$  is the molar ionic strength. The activity term  $\text{p}(a\text{H}^+ \gamma_Z)^\circ$  is obtained by extrapolation to  $mZ = 0$  from measurements with Cell I where the reference is a halide-selective electrode immersed in the test solution. By arbitrarily fixing a value of "a" for each buffer, a conventional pH(NBS) scale is defined which is internally consistent to within  $\pm 0.005$  pH units. The relationship between pH(NBS) and the properties of hydrogen ions in concentrated salt solutions is by no means clear-cut. If a standard solution (S) and a test solution (X) are placed in Cell II in turn, then the conventional pH of the test solution, yielding an apparent  $\text{H}^+$  ion activity ( $a'\text{H}^+$ ), is given by

$$-\log_{10}(a'\text{H}^+) = \text{pH(NBS,X)} = \text{pH(NBS,S)} + [E^*(\text{S}) - E^*(\text{X})]/gT \quad (118)$$

The observed potential difference  $[E^*(\text{S}) - E^*(\text{X})]$  contains two components. The first is related to the potential shift due to the change in hydrogen ion activity and the second is due to the change in liquid junction potential, so that

$$\text{pH(NBS,X)} = \text{pH(NBS,S)} + [E(\text{S}) - E(\text{X})]/gT + \Delta E_j/gT \quad (119)$$

The final term will depend on the construction of the cell and the composition of the test solution. A difference in  $\Delta E_j$  of  $\pm 1$  mV will result in a change in pH of  $\pm 0.017$  units at  $25^\circ\text{C}$ . Cells without a liquid junction of the form

Reference electrode selective to $\text{M}^+$ or X	Solution containing $\text{H}^+$ and $\text{M}^+$ or X	Electrode selective to hydrogen ions
---	---	---

have been used by Biedermann et al.<sup>212</sup> for very precise potentiometric studies, and have been proposed as a means of avoiding liquid junction problems for pH measurements in saline solutions.<sup>213</sup> Difficulties will clearly arise if the activity of the ion selected by the reference electrode also varies in the sample solution,<sup>214</sup> but the extent of such variations can be calculated much more accurately from ionic interaction models than the associated changes in potential of a cell containing a liquid junction.

If the liquid junction effects are to cancel in applying the NBS convention to saline media, the measured pH(NBS) values must be combined with hybrid or "apparent" dissociation constants ( $K_X'$  for reaction  $\text{HX} = \text{H}^+ + \text{X}^-$ ) defined as<sup>215</sup>

$$K_X' = mB (a'\text{H}^+)/m\text{HX} \quad (120)$$

where  $(a'H^+)$  is defined by Equation 118. The cell design must be optimized to reduce variations in  $\Delta E_j$ . These apparent constants proved extremely useful in the development of a quantitative approach to ionic equilibria in seawater prior to the development of comprehensive ionic interaction models.

In practice, it is found that  $\Delta E_j$  values in saline media vary both with electrode design and between electrodes of the same design (see, for example, Whitfield et al.<sup>210</sup> and Johnson et al.<sup>216</sup>). While these effects can be minimized by the use of free-diffusion liquid junctions,<sup>217,218</sup> problems are still encountered with drifts in the glass electrode potentials on transferring the cells from the low ionic strength buffers to high ionic strength samples. These problems can be largely overcome by the use of saline buffers.

#### ii. Total Hydrogen Ion Concentration Scale

A pH scale based on saline buffers, and with a clearer conceptual significance, can be defined in terms of the total hydrogen ion concentration ( $CH_{(T)}^+$ ) so that, on the molal concentration scale,

$$pH_{(T)} = -\log_{10}(mH_{(T)}^+) \quad (121)$$

For seawater  $mH_{(T)}^+$  is defined by:

$$\begin{aligned} mH_{(T)}^+ &= mH_{(F)}^+ + mHSO_4^- + mHF \\ &= mH_{(F)}^+(1 + {}^tK_{HSO_4}^* mSO_4^{2-} + {}^tK_{HF}^* mF_{(T)}^-) \\ &= mH_{(F)}^+ \alpha_{(s)} \end{aligned} \quad (122)$$

where  $mH_{(F)}^+$  is the free hydrogen ion concentration and  $\alpha_{(s)}$  is the total side reaction coefficient for hydrogen ions in seawater on the molal scale (see also Section III.D). The superscript lower case t indicates the use of free  $H^+$  concentration, but total anion concentration in the expressions for  $mHSO_4^-$  and  $mHF$ . [At 25°C and 35 S‰ the values of ( ${}^tK_{HSO_4}^* mSO_4^{2-}$ ) and ( ${}^tK_{HF}^* mF_{(T)}^-$ ) are about 0.29 and 0.021, respectively.] To set up the pH scale it is necessary to define solutions of known  $mH_{(T)}^+$  in the appropriate ionic medium.

Hansson,<sup>219</sup> using the molality concentration scale, proposed the use of TRIS [tris-(hydroxymethyl) amino methane] buffers in an artificial seawater medium to reduce  $\Delta E_j$  to a negligible value. In saline solutions dilute with respect to the buffer and containing equal concentrations of TRIS and  $TRIS^+$ , we find (from Equation 113) that:

$$\begin{aligned} {}^tK_{TRIS}^* &= kTRIS \, kH_{(T)}^+ / kTRIS^+ \\ &\approx kH_{(T)}^+ \\ \therefore p({}^tK_{TRIS}^*) &= -pH(SWS) \end{aligned} \quad (123)$$

where prefix  $k$  and associated constant  $K^*$  indicate concentrations on the molality scale, and in this instance superscript t denotes the use of a total  $H^+$  concentration but free TRIS and  $TRIS^+$  concentrations. In a buffer made up in an artificial seawater, and where *both* buffer and sample (and consequent side reaction coefficients) either include or exclude  $F^-$ ,  $pH(SWS)$  is equivalent to  $pH_{(T)}$  with concentrations of the latter expressed on the molality ( $\text{mol kg}^{-1}$  seawater) scale. Hansson<sup>219</sup> prepared his buffers in a fluoride-free seawater medium with a total TRIS concentration of  $0.005 \text{ mol kg}^{-1}$  (seawater) (see Table 30), and measured

**TABLE 30**  
**Artificial Seawater Recipes (35 S‰) Used in the**  
**Preparation of pH Buffers and in the Development of**  
**Models**

Species	Hansson <sup>219</sup>		Millero <sup>220</sup>		Harvie et al. <sup>26</sup>
	Normal seawater	Seawater buffer	Artificial seawater*	Standard buffer	
Na <sup>+</sup>	468.04	463	485.16	425.16	486.95
K <sup>+</sup>	10.00	10	10.58	10.58	10.63
Mg <sup>2+</sup>	53.27	54	55.18	55.18	55.16
Ca <sup>2+</sup>	10.33	10	10.77	10.77	10.73
Sr <sup>2+</sup>	0.10	—	—	—	—
Cl <sup>-</sup>	545.88	550	569.12	569.12	568.17
SO <sub>4</sub> <sup>2-</sup>	28.20	28	29.26	29.26	29.39
Br <sup>-</sup>	0.83	—	—	—	—
F <sup>-</sup>	0.07	—	—	—	—
HCO <sub>3</sub> <sup>-</sup>	2.40	—	—	—	1.85 <sup>b</sup>
TB	0.43	—	—	—	0.276
H <sup>+</sup>	—	—	—	—	—
TRIS	—	5	—	60	—
TRISH <sup>+</sup>	—	5	—	60	—

Note. TB = total borate.

\* Identical values were used by Khoo et al.<sup>225</sup>

<sup>b</sup> pCO<sub>2</sub> = 3.3 × 10<sup>-4</sup> atm.

p(K<sub>TRIS</sub><sup>\*</sup>) from 20 to 40 S‰ salinity and 5 to 25°C. For this medium, the side reaction coefficient <sup>4</sup>α<sub>IM</sub> is defined as

$${}^4\alpha_{IM} = kH_{(T)}^+(1 + {}^4K_{HSO_4}^* kSO_{(T)}^2) \quad (124)$$

His pH(SWS) values (mol kg<sup>-1</sup> of seawater) may be summarized by the equation

$$\begin{aligned} \text{pH(SWS)} = & (2559.7 + 4.5 S)/T - 0.5523 \\ & - 0.01391 S \end{aligned} \quad (125)$$

Millero<sup>220</sup> took advantage of the almost linear variation of p(K<sub>TRIS</sub><sup>\*</sup>) with salinity to obtain more accurate values of pH<sub>(T)</sub> (molal concentration scale) at salinities below those investigated by Hansson,<sup>219</sup> thereby extending the total hydrogen ion concentration scale to estuarine waters. For TRIS concentrations from 0.005 to 0.06 mol kg<sup>-1</sup>, salinities from 0 to 40 S‰, and temperatures from 5 to 40°C, he expressed the p(K<sub>TRIS</sub><sup>\*</sup>) values (molal concentration scale) via the equation (σ = 0.003):

$$\text{p}(K_{\text{TRIS}}^*) = \text{p}K_{\text{TRIS}} + A_1 + B_1/T \quad (126)$$

where

$$A_1 = -2.3755 \times 10^{-2} S + 6.165 \times 10^{-5} S^2$$

$$B_1 = 6.313 S$$

and

$$\begin{aligned} \text{p}K_{\text{TRIS}} = & -22.5575 + 3477.5496/T \\ & + 3.32867 \ln(T) \end{aligned} \quad (127)$$

Millero<sup>220</sup> gives particularly clear instructions for the preparation of the TRIS buffers.

The practical problems of using total hydrogen ion concentration scales in estuarine waters have been considered in some detail.<sup>210,218</sup> Very precise measurements are possible but the accuracy can be compromised, particularly at low salinities, if saline buffers are used. Under such circumstances, the NBS scale is preferable if stable, free-diffusion junctions are employed and the cell is properly characterized across the salinity range.<sup>218</sup>

The total hydrogen ion concentration scale can be extended to higher salt concentrations and to other media, if the appropriate Pitzer model coefficients can be determined, by measuring  $\text{p}(K_{\text{TRIS}}^*)$  in mixed salt solutions. A study by Millero et al.<sup>221</sup> indicates the potential of this approach, but there are insufficient experimental data to allow systematic calculation in the variety of ionic media encountered in natural waters.

Values of pH on the total hydrogen ion concentration ( $\text{pH}_{\text{CTI}}$ ) and NBS scales [ $\text{pH}(\text{NBS})$ ] can be related by the equation (both scales expressed in molal concentrations):

$$\begin{aligned} \text{pH}(\text{NBS}) &= \text{pH}_{\text{CTI}} - \log_{10}(\gamma_{\text{H}^+}) - \Delta E_j/gT \\ &= \text{pH}_{\text{CTI}} - \log_{10}(f_{\text{H}}) \end{aligned} \quad (128)$$

where, we recall,  $f_{\text{H}}$  is a conversion factor which may be seen as an apparent activity coefficient on the NBS scale. For seawater with a salinity of 35 S‰ at a temperature of 25°C, Bates<sup>222</sup> estimated that  $\gamma_{\text{H}^+} = 0.83$ ,  $\Delta E_j = 4.5$  mV, so that

$$\text{pH}(\text{NBS}) = \text{pH}_{\text{CTI}} + 0.134 \quad (129)$$

in molal units. If the concentrations are on the molinity scale then:

$$\text{pH}(\text{NBS}) = \text{pH}(\text{SWS}) + 0.149 \quad (130)$$

Experimental measurements by Hansson<sup>219</sup> using Cell II give a conversion constant of 0.159 for Equation 130.

The interconversion parameter  $f_{\text{H}}$  can be determined experimentally by the direct transfer of the cell between a standardized NBS buffer and a standardized TRIS buffer in the appropriate ionic medium.<sup>218</sup> Alternatively, the ionic medium can be titrated with hydrochloric acid and the pH measured by an electrode standardized in NBS buffers. Plotting  $\text{pH}(\text{NBS})$  against  $m\text{H}_{\text{CTI}}^+$  according to the equation

$$10^{-\text{pH}(\text{NBS})} = f_{\text{H}} m\text{H}_{\text{CTI}}^+ \quad (131)$$

gives  $f_{\text{H}}$  from the slope of the resulting straight line. The variations in  $f_{\text{H}}$  values observed for commercial electrodes are considerable<sup>210,217</sup> (see Figure 24). Culberson<sup>217</sup> summarizes his experimental values with the relationship ( $\sigma = \pm 0.03$  pH units, dashed lines, Figure 24):

$$\begin{aligned} \log_{10}(f_{\text{H}}) = & -A I_{\text{S}}^{1/2}/(1 + 2.16 I_{\text{S}}^{1/2}) + (0.1681 + 6.26 \times 10^{-4} I_{\text{S}}) \\ & - \log_{10}(1 + m\text{SO}_{\text{CTI}}^2/K_{\text{HSO}_2}^*) \end{aligned} \quad (132)$$

where  $t$  is in °C and seawater ionic strength  $I_{\text{S}} = 19.927S/(1000 - 1.0051 S)$ . A similarly

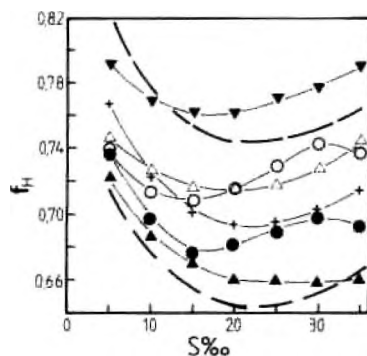


FIGURE 24. Mean  $f_{H^+}$  values determined from measurements in NBS and saline buffers as a function of salinity at 25°C. Dashed lines — the upper and lower confidence limits of Equation 132; symbols — the results obtained with various electrode pairs (glass electrode — reference electrode) listed in Table 1 of Whitfield et al.<sup>210</sup>

wide spread of values is reported by Millero.<sup>220</sup> The range of variability can be reduced to  $\pm 0.01$  pH if a free-diffusion liquid junction is employed.<sup>210,217</sup>

The contribution of the liquid junction potential to  $f_{H^+}$  (see Equation 128) can be approximated by the Henderson equation.<sup>219</sup> This can be written, for KCl salt bridges in a seawater medium at 25°C, in a simplified form:<sup>223</sup>

$$E_j/gT = (xm - XS)/(ym - YS) \log_{10}(\{ym\}/\{YS\}) \quad (133)$$

where  $x = -2.85$ ,  $X = -0.476$ ,  $y = 149.85$ ,  $Y = 2.261$ , and  $m$  is the molality of the KCl salt bridge. Values of  $\gamma_{HCl}$  can be calculated from Equation 122 by first using the seawater ion pair model of Dickson and Whitfield<sup>224</sup> (at 25°C) to obtain

$$\ln(\gamma_{HCl}) = -1.176 I_{\text{eff}}^{1/2}/(1 + 1.670 I_{\text{eff}}^{1/2}) + 0.525 I_{\text{eff}} \quad (134)$$

where  $I_{\text{eff}}$  ( $= 0.0029 + 0.018575 S + 1.639 \times 10^{-5} S^2$ ) is an effective ionic strength including ion pairing. Values of the side reaction coefficient  $\alpha_{\text{SM}}$ , taken from Khoo et al.,<sup>225</sup> yield  $\gamma_{HCl}$  from:  $\gamma_{HCl} = (mH_{\text{Cl}}^*/mH_{\text{Cl}}^0)\gamma_{HCl}$ . The resulting  $\Delta\text{pH}$  values ( $\log_{10} f_{H^+}$ ) are of the same order as those observed experimentally when the pH values of seawater buffers were measured relative to a seawater buffer with a salinity of 20 S‰ (Table 3 of Whitfield et al.<sup>210</sup>).

### iii. Free Hydrogen Ion Concentration Scale

A pH scale can be defined in terms of the concentration of the free (uncomplexed) hydrogen ions in solution:

$$\text{p}(m\text{H}) = -\log_{10}(mH_{\text{Cl}}^0) \quad (135)$$

The interconversion between the  $\text{p}(m\text{H})$  and  $\text{pH}_{\text{Cl}}$  concentration scales will depend on the determination of the side reaction coefficient  $\alpha_{\text{SM}}$  (Equation 122). The TRIS buffer system can also be used to establish standards for the  $\text{p}(m\text{H})$  scale.<sup>226</sup> An equation analogous to Equation 123 can be written so that

$$\begin{aligned} \text{p}K_{\text{TRIS}}^* &= m\text{TRIS} \cdot mH_{\text{Cl}}^0/m\text{TRISH}^* \\ &\approx mH_{\text{Cl}}^0 \end{aligned} \quad (136)$$

where the stoichiometric dissociation constant (molal scale) is expressed on the basis of free ion concentrations. A relationship analogous to Equation 126 can be defined<sup>220</sup> where for seawater media ( $\sigma = 0.0012$ )

$$A_F = 2.065 \times 10^{-3} \text{ S} - 1.770 \times 10^{-4} \text{ S}^2 \quad (137)$$

$$B_F = 0.64 \text{ S} \quad (138)$$

These relationships are valid over the salinity range 0 to 40 ‰, the temperature range 5 to 40°C, and  $m_{\text{TRIS}} = 0.005$  to  $0.06 \text{ mol kg}^{-1}$ . Millero<sup>220</sup> suggests that the major difference between the  $p(m\text{H})$  and  $p\text{H}_{(\text{F})}$  scales (expressed in molal concentrations) is provided by interaction with sulfate ions. The values of  $K_{\text{HSO}_4}^*$  to be employed (where superscript  $*$  indicates the use of free  $\text{H}^+$  but total  $\text{SO}_4^{2-}$ ) can be summarized by the equation ( $\sigma = 0.03$ ):

$$\log_{10}(K_{\text{HSO}_4}^*) = A/T + B \quad (139)$$

where

$$A = -1226.969 + 65.6 \text{ S}^{1/2}$$

and

$$B = 6.09405 - 0.4502 \text{ S}^{1/2} + 1.3525 \times 10^{-2} \text{ S}$$

The  $p\text{H}_{(\text{F})}$  scale is very convenient for measurements in seawater where the side reaction coefficient ( $\alpha_{(\text{F})}$ ) is dominated by the relatively high and constant concentrations of sulfate. However, in strong brines, sulfate concentrations are reduced to very low values by gypsum precipitation and a variety of proton acceptors can become significant.<sup>214</sup> Under these circumstances a free hydrogen ion scale may be more convenient.

The differences between the pH values assigned on the  $p\text{H}(\text{NBS})$  and  $p(m\text{H})$  scales are small.<sup>220,226</sup> For seawater of 35 ‰ salinity at a temperature of 25°C, Bates<sup>222</sup> quotes the relationship

$$p\text{H}(\text{NBS}) = p(m\text{H}) + 0.004 \quad (140)$$

We can write:

$$p\text{H}(\text{NBS}) = p(m\text{H}) - \log_{10}(\alpha_{(\text{F})}) - \log_{10}(\gamma_{\text{H}(\text{F})}) - \Delta E/gT \quad (141)$$

The almost complete cancellation in seawater of the final three terms on the right-hand side is fortuitous.

Recently Knauss et al.<sup>213</sup> have proposed the use of a (free hydrogen) pH scale using a liquid junction free cell, which consists of an ion-specific electrode for  $\text{H}^+$  and another for a major ion such as  $\text{Cl}^-$  or  $\text{Na}^+$ . Standard solutions, for calibration, need contain only those ions whose activities are to be measured (and for which mean activity coefficients are known). Measurements yield the mean activity coefficient (e.g.,  $\gamma_{\text{H}(\text{Cl})}$ ) or activity coefficient quotient (e.g.,  $\gamma_{\text{H}}/\gamma_{\text{Na}}$ ) directly. This procedure requires that the concentration of the second ion in the test solution be known, and the use of a model to estimate its activity coefficient if this has not previously been measured directly. Thus, for an  $\text{H}^+, \text{Cl}^-$  electrode pair:

$$p\text{H} = -\log_{10}(a\text{H}^+) = -\log_{10}(a\text{H}^+ a\text{Cl}^-) + \log_{10}(\gamma_{\text{Cl}} m\text{Cl}^-) \quad (142)$$

where the measured quantity is  $(a\text{H}^+ a\text{Cl}^-)$ . This approach has the advantage of being without liquid junction, and ties pH directly to the activity coefficient model employed to estimate the activity coefficient of the second ion ( $\text{Cl}^-$  in Equation 142). A disadvantage is that for



systems incompletely parameterized with respect to the “reference” ion, model uncertainties are reflected in the derived pH. Practical problems associated with this approach are chiefly interferences to the reference electrode, as discussed by Knauss et al.<sup>213</sup> In seawater, an  $\text{Na}^+$  or  $\text{Cl}^-$  electrode (with corrections for the constant proportion of  $\text{Br}^-$  present) would be a suitable reference. In the Dead Sea,  $\text{Br}^-$  concentrations are much higher, about  $0.01 \times m\text{Cl}^-$ . While it might be thought that a  $\text{Br}^-$  electrode (which suffers no interference from  $\text{Cl}^-$ ) could be paired with a  $\text{H}^+$  electrode here, the Pitzer model is quite poorly parameterized for interactions involving this ion. Consequently, an  $\text{H}^+, \text{Na}^+$  electrode pair might be more suitable, although the latter suffers interference from  $\text{H}^+$  for  $\text{pH} < 6$ .<sup>213</sup>

Harvie et al.,<sup>56</sup> in their work on brines containing  $\text{CO}_3^{2-}$ , converted the unscaled single ion activity coefficients obtained from Pitzer model Equations 35 and 36 to the MacInnes convention under which  $\gamma_{\text{Cl}}$  is defined as equal to that in a pure aqueous KCl solution of the same ionic strength. Even such a simple convention is not without its problems, since at  $25^\circ\text{C}$  the solubility of KCl is only about  $4.3 \text{ mol dm}^{-3}$ . Extrapolations of various fitting equations to high ionic strengths yield very different results. (Note that  $25^\circ\text{C}$  osmotic and activity coefficient data are available to  $12 \text{ mol kg}^{-1}$ <sup>160</sup> [see Figure 16].) Plummer et al.<sup>69</sup> point out that the problems of pH and activity coefficient scales are most critical when pH is introduced into calculations of chemical equilibria. Even if measured pH is placed on the same scale as the activity coefficient model, uncertainties such as those due to the presence of liquid junctions may introduce inconsistencies. The dependence of thermodynamic properties on pH scale is greatest for the carbonate system, where both aqueous phase speciation and gas/liquid and solid/liquid equilibria depend on  $\text{H}^+$  activity. The use of an  $\text{H}^+, \text{Cl}^-$  electrode pair by Knauss et al.<sup>213</sup> to determine calcite solubility in solutions at equilibrium with the atmosphere, and the Pitzer model to estimate aqueous phase activity coefficients, is significant here as it demonstrates what can be achieved when measurements are closely linked to a geochemical model that is well parameterized for the system being studied.

### 3. Calculations of Ionic Equilibria Involving Weak Acids and Bases

The seawater system has received thorough experimental investigation and, although some inconsistencies still remain when analytical data of the highest precision are being processed, there is now a reasonable consensus concerning the principal weak acid-base equilibria. However, there are many brines associated with seawater evaporites<sup>56,66</sup> or with the evaporation of inland waters, to form alkali lakes,<sup>61,112</sup> where high ionic strengths are experienced and a wide range of mineral phases can be precipitated. The solubilities of minerals in many such systems (especially those representative of evaporite sequences from seawater) have been determined experimentally, but the measurement of pH and the determination of stoichiometric acid-base equilibrium constants have not been investigated as thoroughly as in seawater.

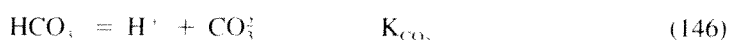
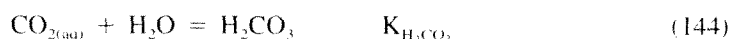
To tackle such complex and diverse systems in a coherent way it is necessary to establish a comprehensive theoretical approach for the estimation of conventional single-ion activity coefficients. Models based on ion pairing have not proved adequate for treating solutions with ionic strengths greater than  $1 \text{ mol dm}^{-3}$ , while the Pitzer model, as implemented by Harvie et al.<sup>56</sup> and Felmy and Weare,<sup>61</sup> successfully predicts acid-base equilibria in brines. It is important to bear in mind that the parameterizations that have been built up in the various studies are independent and often mutually exclusive; see, for example, Table 14. Thus the model is only effective if all the parameters derived in its initial construction, for a particular system, are used together. This effectively “freezes” the model in time, so that it is not a simple matter to introduce new parameters if subsequent experimental studies result in significant improvements in the data. Furthermore, any misconceptions concerning, for example, the application of pH measurements must be accounted for when comparing model predictions to observed solution behavior.

**a. The Carbon Dioxide-Dissolved Carbonate System**

The precipitation and dissolution of calcium carbonate is in large measure responsible for the distribution of carbonate alkalinity in the oceans of the world. The surface layers of the ocean are supersaturated with respect to calcite and aragonite. Precipitation occurs near the ocean surface and is almost invariably triggered by microscopic organisms that use either calcite or aragonite to form intricate shells. Inorganic precipitation of calcium carbonate is rare in seawater, but can occur in warm shallow lagoons after the onset of evaporation. The calcium carbonate falls into the deep ocean where it encounters progressively more corrosive waters as the pressure rises and the temperature falls. Eventually a depth is reached (the lysocline) where the surrounding water is no longer supersaturated, first with respect to aragonite and further down with respect to calcite. Above the lysocline, calcium carbonate can accumulate in the sediment and provide a valuable indicator of oceanic productivity patterns. If the calcium carbonate deposition rate below the lysocline is faster than the dissolution rate, then deposition can still occur. However, a depth is eventually reached (the compensation depth) where accumulation can no longer be observed at the most rapid deposition rates that can be sustained by the biota. The importance of this sequence of events for understanding oceanic productivity and its influence on atmospheric CO<sub>2</sub> levels has resulted in intensive study of calcium carbonate solubility.

*i. Dissolution of CO<sub>2</sub> and Ionization of Carbonic Acid in Solution*

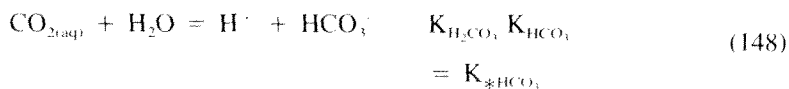
The chemistry of carbon dioxide is controlled primarily by the following equilibria:



The equilibrium partial pressure of dissolved carbon dioxide in solution is given by

$$p\text{CO}_2 = m\text{CO}_2/K'_{\text{H}} \quad (147)$$

Most of the undissociated dissolved CO<sub>2</sub> gas is in the CO<sub>2(aq)</sub> form so that it is conventional (hydrate convention) to combine Equations 144 and 145 to give<sup>169</sup>



The precipitation and dissolution of calcium carbonate effectively control the alkalinity in many saline waters and are described by the relationship



The stability constant equations can be written according to Equation 113. For example, for the ionization of bicarbonate ions we can write

$$K_{\text{CO}_3} = [m\text{CO}_3^{2-} (\text{H}^+) / m\text{HCO}_3^-] [\gamma_{\text{CO}_3^{2-}} / \gamma_{\text{HCO}_3^-}] \quad (150)$$

where ( $H^+$ ) serves as a remainder that there are several options for specifying the involvement of the hydrogen ion in such equilibria. In the saline media the numerical values assigned to dissociation constants will depend on the pH scale adopted in their determination.

The definition of the experimentally accessible parameters of carbonate alkalinity (CA/ mol kg<sup>-1</sup>),

$$CA = mHCO_3^- + 2mCO_3^{2-} \quad (151)$$

and total carbon dioxide concentration (TCO<sub>2</sub>/mol kg<sup>-1</sup>):

$$TCO_2 = mCO_2 + mHCO_3^- + mCO_3^{2-} \quad (152)$$

helps to constrain the system further. By combining these equations with the appropriate stability constants it is possible to establish a set of relationships<sup>227,228</sup> that enable the equilibrium characteristics of the CO<sub>2</sub> system ( $mHCO_3^-$ ,  $mCO_3^{2-}$ ,  $pCO_{2(aq)}$ , pH) to be calculated from any pair of four experimentally determined parameters (CA, TCO<sub>2</sub>,  $pCO_{2(aq)}$ , pH). The error propagation characteristics of these calculations in seawater media have been considered in some detail.<sup>215,229</sup> To relate CA to total alkalinity (TA) in seawater we must take into account the equilibria



so that:

$$CA = TA - TB/(1 + (H^+)/K_{B(OH)_4}^*) - mOH^- + mH^+ \quad (155)$$

Total borate (TB) is defined as:

$$TB = mB(OH)_3 + mB(OH)_4^- \quad (156)$$

where  $K_{B(OH)_4}^*$  is the stoichiometric formation constant on the appropriate  $H^+$  concentration scale. In seawater TB is less than  $5 \times 10^{-4}$  mol kg<sup>-1</sup> (Table 2). For titrimetric analyses where the error in TA exceeds  $5 \times 10^{-6}$  mol kg<sup>-1</sup> the final two terms in Equation 155 can be ignored.<sup>229</sup>

It is interesting to note that the analytical method which involves the determination of TCO<sub>2</sub> and TA makes use of equations in which the ratio  $K_{*HCO_3^-}^*/K_{*CO_3^{2-}}^*$ , rather than the individual constants, appears. In this case the analysis of the carbon dioxide system is independent of the pH scale used.

Procedures have been developed for measuring the four experimental parameters (TA, TCO<sub>2</sub>,  $pCO_{2(aq)}$ , pH) to a high precision on board ship, and the CO<sub>2</sub> system in seawater plays a crucial role in controlling the air-sea exchange of gaseous carbon dioxide. In view of the central importance of this process in predicting atmosphere CO<sub>2</sub> levels, and hence the pace of climate change, much attention has been paid to the determination of accurate  $pK^*$  values for the reactions involved, using the various pH scales.

#### ii. Stoichiometric Equilibrium Constants for the Carbonate System in Seawater

The most careful and complete set of measurements of "apparent" constants using the pH(NBS) scale are those of Mehrbach et al.<sup>230</sup> determined in a natural seawater medium.

Their data, as refitted by Plath et al.,<sup>231</sup> may be summarized by (mol kg<sup>-1</sup> seawater):

$$p({}^t\mathbf{K}_{*HCO_3}^{*'}) = 17.788 - 0.073104 T - 0.005187 S \\ + 0.00011463 T^2 \quad (157)$$

$$p({}^t\mathbf{K}_{CO_3}^{*'}) = 20.919 - 0.064209 T - 0.011887 S \\ + 0.000087313 T^2 \quad (158)$$

where the prime indicates the use of an apparent concentration scale for H<sup>+</sup>, and the superscript lower case t total CO<sub>3</sub><sup>2-</sup> and HCO<sub>3</sub><sup>-</sup> (*k*CO<sub>3(T)</sub><sup>2-</sup> and *k*HCO<sub>3(T)</sub><sup>-</sup>). Fortunately, Mehrbach et al.<sup>230</sup> measured the *f*<sub>H</sub> values of the electrode pairs that they used and reported the values along with the constants defined above. Subsequently, Dickson and Millero<sup>232</sup> corrected their stability constants to the pH(SWS) scale (mol kg<sup>-1</sup> solution) using equations of the form

$$p({}^t\mathbf{K}_a^*) = -\log_{10}({}^t\mathbf{K}_a^{*'} / f_H) \quad (159)$$

where superscript T indicates the use of total HCO<sub>3</sub><sup>-</sup>, CO<sub>3</sub><sup>2-</sup>, and H<sup>+</sup> (= *k*H<sup>+</sup> + *k*HSO<sub>4</sub><sup>-</sup> + *k*HF). The recalculated constants (Table 31) were fitted to equations of the form<sup>232</sup>

$$p({}^t\mathbf{K}_a^*) = A/T + B + C \ln(T) + DS + ES^2 \quad (160)$$

The most thorough set of measurements on the pH(SWS) scale are those of Hansson<sup>233</sup> in an artificial seawater medium in the absence of fluoride ions. His data were later refitted by Johansson and Wedborg<sup>234</sup> to the equations (mol kg<sup>-1</sup> seawater, 20 to 40 S‰):

$$p({}^t\mathbf{K}_{*HCO_3}^{*'}) = 841.2/T + 3.2762 - 0.010382 S \\ + 0.00010287 S^2 \quad (161)$$

$$p({}^t\mathbf{K}_{CO_3}^{*'}) = 1376.4/T + 4.8256 - 0.018232 S \\ + 0.00011839 S^2 \quad (162)$$

where total H<sup>+</sup> is equivalent to (*k*H<sup>+</sup> + *k*HSO<sub>4</sub><sup>-</sup>). Dickson and Millero<sup>232</sup> also reassessed this data set and corrected the measurements to allow for the differences between Hansson's artificial medium and natural seawater using the relationship

$$p({}^t\mathbf{K}_a^*) = p({}^t\mathbf{K}_a^*)(\text{experimental}) - \log_{10}({}^k\alpha_{(s)}/{}^k\alpha_{(M)}) \quad (163)$$

where the seawater side reaction coefficient on the molality scale (<sup>k</sup>α<sub>(s)</sub>) is given by

$${}^k\alpha_{(s)} = 1 + {}^t\mathbf{K}_{HSO_4}^* {}^k\text{SO}_4^{2-} + {}^t\mathbf{K}_{HF}^* {}^k\text{F}_{(T)} \quad (164)$$

and the ionic medium side reaction coefficient by:

$${}^k\alpha_{(M)} = 1 + {}^t\mathbf{K}_{HSO_4}^* {}^k\text{SO}_4^{2-} \quad (165)$$

**TABLE 31**  
**Fitting Parameters for the Variation of Stoichiometric**  
**Stability Constants for Carbonic Acid with Temperature and**  
**Salinity, Corrected to the Total Hydrogen Ion Concentration**  
**Scale in a Seawater Range<sup>232</sup>**

Constant	A	B	C	D	10 <sup>4</sup> E	$\sigma$
<b>pH(NBS), Mehrbach et al.<sup>230</sup> (Salinity 20 to 40 S‰)</b>						
$p^{\dagger}K_{*HCO_3}^{\circ}$	3670.7	-62.008	9.7944	-0.0118	1.16	0.011
$p^{\dagger}K_{CO_2}^{\circ}$	1394.7	4.777	—	-0.0184	1.18	0.020
<b>pH(SWS), Hansson<sup>233</sup> (Salinity 20 to 40 S‰)</b>						
$p^{\dagger}K_{*HCO_3}^{\circ}$	851.4	3.237	—	-0.0106	1.05	0.013
$p^{\dagger}K_{CO_2}^{\circ}$	-3885.4	125.844	-18.141	-0.0192	1.32	0.017
<b>Combined Data Set (Salinity 20 to 40 S‰)</b>						
$p^{\dagger}K_{*HCO_3}^{\circ}$	845.0	3.248	—	-0.0098	0.87	0.017
$p^{\dagger}K_{CO_2}^{\circ}$	1377.3	4.824	—	-0.0185	1.22	0.026

*Note:* Fitting equation:  $pK = A/T + B + C \ln T + DS + ES^2$ . The stoichiometric constants are defined on the molality concentration scale, for a total hydrogen ion concentration equivalent to  $([H^+] + [HSO_4^-] + [HF])$ . The association constants for  $HSO_4^-$  and  $HF$  were obtained from the work of Khoo et al.<sup>225</sup> and Dickson and Riley,<sup>226</sup> respectively.<sup>232</sup>

where prefix  $k$  denotes a concentration on the molality scale. The corrected constants were fitted to Equation 160 (see Table 31). The two sets of constants, once adjusted to the same pH scale and the same ionic medium, agree well. Consequently, a set of constants based on the pooled data has been recommended<sup>229,232</sup> for use in seawater. For the salinity range 0 to 40 S‰ and 0 to 35°C the combined data set is represented by the following equations (mol kg<sup>-1</sup> seawater, SWS pH scale):

$$p^{\dagger}K_{*HCO_3}^{\circ} - pK_{*HCO_3} = (-840.39/T + 19.894 - 3.0189 \ln(T))S^{1/2} + 0.0068 S (\pm 0.017) \quad (166)$$

$$p^{\dagger}K_{CO_2}^{\circ} - pK_{CO_2} = (-690.59/T + 17.176 - 2.6719 \ln(T))S^{1/2} + 0.0217 S (\pm 0.032) \quad (167)$$

(Recall that at infinite dilution  $K_x = K_x^{\circ}$ .) The fitting parameters for  $pK_{*HCO_3}$  and  $pK_{CO_2}$  are given by

$$pK_{*HCO_3} = 6320.81/T - 126.3405 + 19.568(\ln T) \quad (168)$$

$$pK_{CO_2} = 5143.69/T - 90.1833 + 14.613(\ln T) \quad (169)$$

**TABLE 32**  
**Parameters Describing the Influence of Pressure on the Ionic Equilibria**  
**Controlling the Speciation of the CO<sub>2</sub> System (and Total Borate) in Seawater**  
**S = 20—40 S‰, t = 0—30°C<sup>229</sup>**

$$X = a + bt + ct^2 + d(S - 34.8)$$

Constant	X =						
	-ΔV			-10 <sup>3</sup> Δκ			
	a	b	10 <sup>3</sup> c	d	a	b	d
	<b>Ionization</b>						
B(OH) <sub>3</sub> ( <sup>1</sup> K <sub>B(OH)<sub>3</sub>}<sup>*</sup>)</sub>	29.48	-0.1622	2.608	-0.295	2.84	—	-0.354
H <sub>2</sub> CO <sub>3</sub> ( <sup>1</sup> K <sub>H<sub>2</sub>CO<sub>3</sub>}<sup>*</sup>)</sub>	25.50	-0.1271	—	0.151	3.08	-0.0877	0.578
HCO <sub>3</sub> <sup>-</sup> ( <sup>1</sup> K <sub>HCO<sub>3</sub>}<sup>*</sup>)</sub>	15.82	0.0219	—	-0.321	-1.13	-0.1475	0.314
	<b>Solubility</b>						
Calcite ( <sup>1</sup> K <sub>Calcite}</sub> <sup>*</sup> )	48.76	-0.5304	—	—	11.76	-0.3692	—
Aragonite ( <sup>1</sup> K <sub>Aragonite}</sub> <sup>*</sup> )	45.96	-0.5304	—	—	11.76	-0.3692	—

Note: Equations 170—172 (see text) give the pressure effect on the equilibrium constants.

This careful analysis confirmed the indications of Bates and Culberson<sup>226</sup> that the stability constants measured on the NBS and SWS pH scales were in good agreement. Uncertainties in the variability of liquid junction potentials make the use of the pH(NBS) scale impractical for the most precise measurements, and the pH(SWS) scale is recommended.

For the effect of pressure on <sup>1</sup>K<sub>HCO<sub>3</sub>}<sup>\*</sup> and <sup>1</sup>K<sub>CO<sub>2</sub>}<sup>\*</sup>, there is good agreement<sup>235</sup> between the direct potentiometric measurements of Disteché and Disteché<sup>236</sup> and Culberson and Pytkowicz.<sup>237</sup> The pressure dependence of the stoichiometric acid dissociation constants (molality concentration scale, and total H<sup>+</sup> concentration (= *k*H<sup>+</sup> + *k*H<sub>2</sub>SO<sub>4</sub> + *k*HF) may be summarized by the following equation:<sup>229,235</sup></sub></sub>

$$\ln(^1K_a^{*p}/^1K_a^{*o}) = -(\Delta V/RT)P + (0.5\Delta\kappa/RT)P^2 \quad (170)$$

where <sup>1</sup>K<sub>a</sub><sup>\*p</sup> is the stoichiometric acid dissociation constant (mol kg<sup>-1</sup> solution) at pressure *P* (atm), and <sup>1</sup>K<sub>a</sub><sup>\*o</sup> is its value at 1 atm pressure. The partial molal volume (Δ*V*) and compressibility (Δκ) terms are themselves expressed as functions of temperature and salinity by

$$-\Delta V = a + bt + ct^2 + d(S - 34.8) \quad (171)$$

$$-\Delta\kappa = a + bt + d(S - 34.8) \quad (172)$$

*t* is in °C. The parameters are summarized in Table 32. See Millero<sup>91</sup> for a fuller treatment of the effect of pressure on chemical equilibria in the ocean.

Although Equations 166 to 172 represent the best analysis so far of the carbonic acid stability constants, the errors incurred in their use may be significant in relation to the high analytical precision that can now be achieved.<sup>229</sup> In particular, it is apparent that calculations of *p*CO<sub>2</sub> can deviate in a systematic way from those measured directly.<sup>238</sup> Further refinements in the determination of the stability constants will be required as the analytical methods continue to improve and the practical demands placed on them become more critical.

### iii. Carbonate Equilibria Involving the Solid Phase

Calcium carbonate production, dissolution, and deposition in the oceans are important for understanding oceanic productivity and its influence on atmospheric CO<sub>2</sub> levels, and have resulted in intensive study of calcium carbonate solubility. Provision of unequivocal solubility data has been hampered by, first, the long equilibration times required; second, the presence of high magnesium concentrations in seawater that can give rise to the formation of mixed magnesium-calcium carbonates (especially if precipitation is rapid); and last, by the presence of several calcium carbonate phases (calcite, aragonite, vaterite). The development of models to predict the true equilibrium solubility of calcium carbonate has also proved difficult because some of the major interactions involved (notably Ca<sup>2+</sup>-HCO<sub>3</sub><sup>-</sup>, Ca<sup>2+</sup>-CO<sub>3</sub><sup>2-</sup>) lie in the uneasy area between those systems that can be most simply treated by ionic interaction models and those that require the explicit recognition of ion pairing. We will tackle the problem in stages by considering:

1. The procedures used to determine thermodynamic solubility constants (K<sub>sp</sub>) in CO<sub>2</sub>-H<sub>2</sub>O solutions
2. The consistency of determinations of stoichiometric constants for the solubility equilibria in seawater (K<sub>sp</sub><sup>\*</sup>)
3. The methods used to calculate K<sub>sp</sub><sup>\*</sup> from K<sub>sp</sub> to check the validity of the measurements

### iv. Thermodynamic Solubility Products of Calcium Carbonate Minerals

In a thorough reassessment of the CaCO<sub>3</sub>-CO<sub>2</sub>-H<sub>2</sub>O system, Plummer and Busenberg<sup>239</sup> critically analyzed earlier determinations of K<sub>sp</sub> for calcite, aragonite, and vaterite and contributed over 300 new solubility measurements in the temperature range 0 to 90°C. They paid careful attention to the correction of pH measurements and were able to obtain consistent results using the Henderson equation to calculate liquid junction potentials at the low ionic strengths encountered. Care was taken to ensure full equilibration by using finely divided solids in agitated systems and by allowing several days before analysis when working at low pCO<sub>2</sub> values.

Taking advantage of their own measurements, and a critical assessment of earlier data, Plummer and Busenberg<sup>239</sup> were able to provide fitting parameters for the solubilities of all three carbonate minerals using equations of the form (Table 33)

$$\log_{10}(K_{sp}) = A + BT + C/T + D \log_{10}(T) + ET^2 \quad (173)$$

They also used the same form of equation to fit critically assessed stability constants for the Henry's law solubility of CO<sub>2</sub> (Equation 143) and for the first and second ionization constants of carbonic acid (K<sub>#HCO<sub>3</sub></sub> and K<sub>c(t)</sub>, Equations 148 and 146, respectively). The fitting parameters cover a much wider temperature range (0 to 250°C) than those listed in Equations 168 and 169. In the course of their analysis they confirmed the need to treat CaCO<sub>3</sub> and CaHCO<sub>3</sub><sup>+</sup> formation, and estimated the values of the stoichiometric stability constants over a wide temperature range (0 to 90°C, Equation 173, Table 33).

### v. Stoichiometric Solubility Products of Calcium Carbonate Minerals in Seawater

The stoichiometric solubility product of calcium carbonate in seawater, on a total concentration basis (molal units), may be defined as

$$\begin{aligned} {}^tK_{CaCO_3}^* &= mCa_{(T)}^{2+} \cdot mCO_{3(T)}^{2-} \\ &= K_{CaCO_3} / (\gamma_{Ca^{2+}} \gamma_{CO_3^{2-}}) \end{aligned} \quad (174)$$

The determination of  ${}^tK_{CaCO_3}^*$  in seawater has been bedeviled by the slow equilibration

**TABLE 33**  
**Fitting Parameters for the Thermodynamic Equilibrium**  
**Constants in the CaCO<sub>3</sub>-H<sub>2</sub>O-CO<sub>2</sub> System<sup>239</sup>**

Constant	log <sub>10</sub> (K) at 25°C	A	B	C	D	E
K <sub>CaCO<sub>3</sub></sub> (calcite) <sup>a</sup>	-8.480	-171.9065	-0.077993	2839.319	71.595	
K <sub>CaCO<sub>3</sub></sub> (aragonite) <sup>a</sup>	-8.336	-171.9773	-0.077993	2903.293	71.595	
		-171.9450 <sup>b</sup>				
K <sub>CaCO<sub>3</sub></sub> (vaterite) <sup>a</sup>	-7.913	-172.1295	-0.077993	3074.688	71.595	
Constant	log <sub>10</sub> (K) at 25°C	A	B	C	D	E
K <sub>H<sup>+</sup></sub> <sup>c</sup>	-1.468	108.3865	0.01985076	-6919.53	-40.45154	669365
K <sub>H<sub>2</sub>CO<sub>3</sub>*</sub>	-6.352	-356.3094	-0.06091964	21834.37	126.8339	-1684915
	(-6.350) <sup>d</sup>					
K <sub>CO<sub>3</sub><sup>2-</sup></sub>	-10.319	-107.8771	-0.03252849	5151.79	38.92561	-563713.9
	(-10.327) <sup>d</sup>					
K <sub>CaHCO<sub>3</sub><sup>-</sup></sub> <sup>d</sup>	1.11	1209.120	0.31294	-34765.05	-478.782	---
K <sub>CaCO<sub>3</sub><sup>0</sup></sub> <sup>e</sup>	3.22	-1228.732	-0.299444	35512.75	485.818	---

Fitting equation:  $\log_{10}(K) = A + BT + C/T + D \log_{10}(T) + E/T^2$

Note: Constants are for molal concentrations, 1 atm total pressure.

<sup>a</sup> 0–90°C.

<sup>b</sup> From Mucci.<sup>241</sup>

<sup>c</sup> 0–250°C — for 1 atm total pressure from 0–100°C and following the vapor pressure curve for water at higher temperatures.

<sup>d</sup> From Millero.<sup>235</sup>

<sup>e</sup> 5–80°C.

between the solid and solution phases, and by the possibility of the formation of mixed (Mg,Ca)CO<sub>3</sub> solid phases, because of the relatively high concentrations of magnesium in the solution phase.<sup>240</sup> Attention to detail and the use of equilibration times ranging from 5 days to 2 years resulted in the determination of <sup>1</sup>K<sub>CaCO<sub>3</sub></sub><sup>\*</sup> (calcite) values by different workers that agree within ±5%.<sup>229,240,241</sup> The range of error has been much greater for aragonite because longer equilibration times are required, but here, too, <sup>1</sup>K<sub>CaCO<sub>3</sub></sub><sup>\*</sup> (aragonite) values have now converged to give close agreement.<sup>229,240,242</sup> It is important in such experiments that the composition of the medium should not be significantly altered during the equilibration process; otherwise true equilibrium may not be attained. The most complete set of measurements is that of Mucci,<sup>241</sup> who estimated *m*Ca<sub>2</sub><sup>2+</sup> and CA by precise titrimetric methods. Measurements of pH were made on the pH(NBS) scale but no details were given from which correction factors *f<sub>H</sub>* can be calculated, although the Gran titration methods used to estimate CA can give *f<sub>H</sub>* values from Equation 128. Total carbonate on the molality scale (*k*CO<sub>3(T)</sub><sup>2-</sup>) was then calculated from the equation

$$k\text{CO}_{3(T)}^{2-} = \text{CA}/[2 + (10^{-\text{pH(NBS)}/\text{p}K_{\text{CO}_3^*}^{\prime}})] \quad (175)$$

The constant <sup>1</sup>K<sub>CO<sub>3</sub><sup>2-</sup></sub><sup>\*</sup> was estimated from the data of Mehrbach et al.<sup>230</sup> so that the calculations are internally consistent. Mucci<sup>241</sup> used equilibration times of up to 2 years (for some aragonite solubility studies) with the *p*CO<sub>2</sub> maintained at 360 ± 10 ppm. His measurements, converted



to molal units, can be fitted to an equation of the form (5 to 45 S‰, 5 to 40°C, 1 atm total pressure):

$$\log_{10}({}^T K_{CaCO_3}^*) - \log_{10}(K_{CaCO_3}) = (a_1 + a_2 T + a_3/T)S^{0.5} + bS + cS^{1.5} \quad (176)$$

yielding for calcite:

$$\log_{10}({}^T K_{CaCO_3}^*) - \log_{10}(K_{CaCO_3}) = (-0.77712 + 2.8426 T + 178.34/T)S^{0.5} - 0.07711 S + 4.1249 S^{1.5} \quad (177)$$

and aragonite:

$$\log_{10}({}^T K_{CaCO_3}^*) - \log_{10}(K_{CaCO_3}) = (-0.068393 + 1.7276 T + 88.135/T)S^{0.5} - 0.10018 S + 5.9415 S^{1.5} \quad (178)$$

The calculated  ${}^T K_{CaCO_3}^*$  values at 35 S‰ salinity and 25°C are 6.35 and 6.17, respectively, for calcite and aragonite. The influence of pressure on the solubility of calcite and aragonite in seawater can be estimated from Equations 171 and 172 using the parameters listed in Table 32.<sup>235</sup>

vi. *Calculation of  ${}^T K_{CaCO_3}^*$  from  $K_{CaCO_3}$*

To ascertain the consistency of the experimental stoichiometric and thermodynamic solubility products via Equation 174 it is necessary to estimate values of the activity coefficient product ( $\gamma_{Ca(T)} \gamma_{CO_3(T)} = \Gamma$ ). This task has been undertaken by Plummer and Sundquist.<sup>242</sup> In terms of experimentally accessible parameters they derived the following relationship:

$$\Gamma = K_{*HCO_3} K_{CO_3} \gamma_{CO_2} a_{H_2O} \gamma_{CaSO_4}^2 \gamma_{MCl}^4 \theta^2 / ({}^T K_{*HCO_3}^* {}^T K_{CO_3}^* \gamma_{M_2SO_4}^3 \gamma_{HCl}^4) \quad (179)$$

where the stoichiometric dissociation constants  ${}^T K_{*HCO_3}^*$  and  ${}^T K_{CO_3}^*$  are on the molality scale (data of Hansson<sup>233</sup>), and  $\theta^2$  is a factor to correct these values to molal units.  $M = Na^+$  or  $K^+$ , and stability constants and activity coefficients (based on total concentrations) are expressed on the molal scale. The mean ion activity coefficients used are experimental values in the seawater medium (Table 3 of Plummer and Sundquist<sup>242</sup>) and  $\gamma_{CO_2}$  represents the correction from carbon dioxide concentration to carbon dioxide activity at 1 atm total pressure. With  $M = Na^+$  Equation 176 gives  $\Gamma = 0.00661$ , and with  $M = K^+$ , 0.00666 at 25°C and 35 S‰ salinity. The mean value gives  $\log_{10}(\Gamma) = -2.177$ . Combined with the thermodynamic constants from Table 33 this yields:

$$\begin{aligned} \log_{10}({}^T K_{CaCO_3}^*) \text{ (calcite)} &= -8.480 + 2.177 & (180) \\ &= -6.303 \text{ (experimental } -6.35, \text{ Equation 176)} \end{aligned}$$

$$\begin{aligned} \log_{10}({}^T K_{CaCO_3}^*) \text{ (aragonite)} &= -8.336 + 2.177 & (181) \\ &= -6.159 \text{ (experimental } -6.17, \text{ Equation 176)} \end{aligned}$$

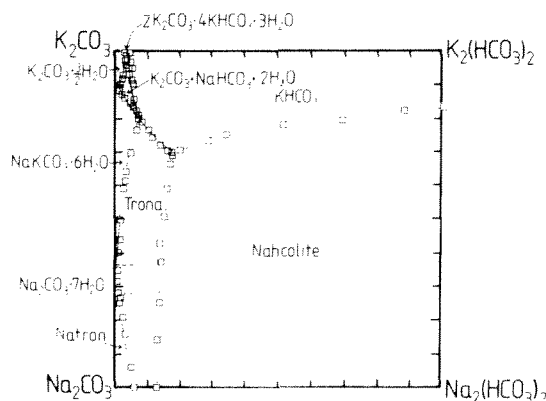


FIGURE 25. Equilibrium solid phases at 25°C for the reciprocal closed system Na-K-HCO<sub>3</sub>-CO<sub>2</sub>-H<sub>2</sub>O, calculated using the Pitzer model as parameterized by Harvie et al.<sup>56</sup> (Redrawn from Harvie et al.<sup>56</sup>)

Using this model they have calculated  $\log_{10}(K_{ac}^*_{CaCO_3})$  (calcite) =  $-6.303$  on the molal concentration scale at 35 S‰ salinity and 25°C. Together these results suggest that the calcium carbonate solubilities measured by Morse et al.<sup>240</sup> and Mucci<sup>241</sup> represent true equilibrations between the solid and solution phases. It therefore seems unlikely that stable (Mg,Ca)CO<sub>3</sub> coatings play a significant role in defining the solubility of CaCO<sub>3</sub> provided that sufficient time is allowed for equilibration between the solution and solid phases.

#### vii. Application of the Pitzer Model to Systems Containing Carbonate

As stated earlier, Harvie et al.<sup>56</sup> have used the Pitzer equations to develop a model for the Na-K-Mg-Ca-H-Cl-SO<sub>4</sub>-OH-HCO<sub>3</sub>-CO<sub>3</sub>-CO<sub>2</sub>-H<sub>2</sub>O system at 25°C. In the work of Harvie et al.<sup>56</sup> the formation of HCO<sub>3</sub><sup>-</sup>, HSO<sub>4</sub><sup>-</sup>, MgOH<sup>+</sup>, MgCO<sub>3</sub><sup>0</sup>, and CaCO<sub>3</sub><sup>0</sup> is treated explicitly, whereas the "formation" of CaHCO<sub>3</sub><sup>+</sup>, CaOH<sup>+</sup>, CaSO<sub>4</sub><sup>0</sup>, and MgSO<sub>4</sub><sup>0</sup> is parameterized as strong interactions between free ions. Also, the standard chemical potentials that define the equilibrium constants are sometimes used as adjustable parameters in fitting the experimental data, e.g., for CaCl<sub>2</sub> · 4H<sub>2</sub>O in fitting the Ca-H-Cl-H<sub>2</sub>O system.<sup>56</sup> Equilibrium constants usually reflect relatively small net differences between the large total chemical potentials of the reactants and the products. Even if more accurate values become available at a later stage they cannot be substituted into the model without a reassessment of the other parameters.

Where experimental data are sparse there can be some degeneracy in the fitted single electrolyte parameters,<sup>62</sup> which are therefore sometimes optimized to fit the data. Thus the ternary parameters ( $\theta_{ij}$  and  $\psi_{ijk}$  in Equations 34 to 36) are intimately interlinked with the single electrolyte parameters employed. As previously noted, single ion activity coefficients determined in the work of Harvie et al.<sup>56</sup> are scaled according to the MacInnes convention.

The model is able to predict accurately the solubility relationships in the system Na-K-HCO<sub>3</sub>-CO<sub>2</sub> (Figure 25) and water and CO<sub>2</sub> activities in the system Na-Cl-HCO<sub>3</sub>-CO<sub>2</sub>-H<sub>2</sub>O (Table 34). The model is also able to predict the solubility of Ca(OH)<sub>2</sub>, and with rather less success CaCO<sub>3</sub>, in salt solutions. In the work of Harvie et al.<sup>56</sup> the CaHCO<sub>3</sub><sup>+</sup> parameters were determined from the data of Jacobson and Langmuir<sup>243</sup> for CaCO<sub>3</sub> solubility in water to 1 atm. These data agree well with the more complete analysis of Plummer and Busenberg.<sup>249</sup>

No explicit mention is made of the source of the chemical potential data used to calculate the ion pairing constant for the Ca<sup>2+</sup>-CO<sub>3</sub><sup>2-</sup> interaction, although it is indicated (Harvie et al.,<sup>56</sup> p. 741) that the Mg<sup>2+</sup>-CO<sub>3</sub><sup>2-</sup> and Mg<sup>2+</sup>-HCO<sub>3</sub><sup>-</sup> parameters were estimated from

TABLE 34  
Comparison of Calculated and Experimental Water Activities and Equilibrium  $p\text{CO}_2$  for Solutions at Equilibrium with the Specified Phase Assemblages in the Na-Cl-HCO<sub>3</sub>-CO<sub>2</sub>-CO<sub>2</sub>-H<sub>2</sub>O System at 25°C

System	Water activity		10 <sup>3</sup> pCO <sub>2</sub>		
	Calculated	Experimental <sup>a</sup>	Calculated	Experimental <sup>b</sup>	Experimental <sup>a</sup>
Na-HCO <sub>3</sub> -CO <sub>2</sub> -H <sub>2</sub> O + nahcolite + trona	0.906	0.899—0.903	1.87	1.80—1.95	2.02
Na-HCO <sub>3</sub> -CO <sub>2</sub> -H <sub>2</sub> O + natron + trona	0.888	0.868—0.872	0.37	—	0.3—0.34
Na-HCO <sub>3</sub> -CO <sub>2</sub> -Cl-H <sub>2</sub> O + nahcolite + trona + halite	0.746	0.765—0.771	1.54	1.45—1.60	1.72—1.77
Na-HCO <sub>3</sub> -CO <sub>2</sub> -Cl-H <sub>2</sub> O + natron + Na <sub>2</sub> CO <sub>3</sub> · 7H <sub>2</sub> O	0.756	0.756 <sup>c</sup>			
Na-HCO <sub>3</sub> -CO <sub>2</sub> -Cl-H <sub>2</sub> O + thermonatrite + Na <sub>2</sub> CO <sub>3</sub> · 7H <sub>2</sub> O	0.697	0.705 <sup>c</sup>			

Note: Nahcolite = NaHCO<sub>3</sub>, trona = Na<sub>2</sub>H(CO<sub>3</sub>)<sub>2</sub> · 2H<sub>2</sub>O, thermonatrite = Na<sub>2</sub>CO<sub>3</sub> · H<sub>2</sub>O. This table reproduced from Harvie et al.<sup>56</sup>

<sup>a</sup> Data from Hatch.<sup>101</sup>

<sup>b</sup> Data from Eugster.<sup>102</sup>

<sup>c</sup> Extrapolated to 25°C.

Hansson's<sup>233</sup> data. The reassessment of Ca<sup>2+</sup>-CO<sub>3</sub><sup>2-</sup> ion pairing by Plummer and Busenberg,<sup>239</sup> the measurement of the interactions in the Na-Mg-CO<sub>3</sub>-HCO<sub>3</sub>-Cl-H<sub>2</sub>O system by Millero and Thurmond,<sup>234</sup> and the Na-CO<sub>3</sub>-HCO<sub>3</sub>-Cl-H<sub>2</sub>O system by Peiper and Pitzer<sup>111</sup> provide relevant and carefully assessed data sets that postdate the establishment of the parameterization of Harvie et al. The experimental data on CaCO<sub>3</sub> solubility are subject to the artefacts discussed earlier and the usefulness of the model should be reassessed using the more reliable data for seawater.

The Pitzer model as parameterized by Harvie et al.<sup>56</sup> has been applied by Monnin and Schott<sup>112</sup> to Lake Magadi, a soda lake in Kenya. Their parameterization of the Na-Cl-HCO<sub>3</sub>-CO<sub>3</sub>-OH-H<sub>2</sub>O system differs from that of Harvie et al.<sup>56</sup> in a few respects. The interaction parameters  $\theta_{\text{Cl},\text{HCO}_3}$  and  $\psi_{\text{Na},\text{OH},\text{CO}_3}$  were not required even though the brines exhibited pH values as high as 11. Significantly different values were used for  $\beta_{\text{NaCO}_3}^{(0)}$ ,  $\beta_{\text{NaCO}_3}^{(1)}$ ,  $\theta_{\text{Cl},\text{HCO}_3}$  and  $\psi_{\text{Cl},\text{HCO}_3,\text{Na}}$ . Nonetheless the model was able to provide an accurate account of the equilibrium solubility fields. The variation of mineral solubility with temperature was also investigated in this study and it was shown that the determination of temperature coefficients for the binary interaction parameters was sufficient to account for the observed behavior over the temperature range 5 to 50°C.

As discussed above, empirical fitting equations are available yielding  $^1K_{\text{HCO}_3}^*$  and  $^1K_{\text{Cl}}^*$  as functions of temperature and salinity. While the extensive use of mineral solubility data in the parameterization of the model of Harvie et al.<sup>56</sup> means that it is likely to be biased somewhat toward high ionic strength systems, it is of interest to compare calculated  $^1K_{\text{HCO}_3}^*$  and  $^1K_{\text{Cl}}^*$  with measured values at 25°C. This is done in Figure 26, retaining the use of the molality concentration scale and total H<sup>+</sup> concentration defined as:  $k\text{H}_4^+(1 + ^1K_{\text{HSO}_4}^* k\text{SO}_4^{2-} + ^1K_{\text{HT}}^* k\text{F}_T)$ . Values of  $^1K_{\text{HCO}_3}^*$  predicted using the model are 7 to 10% too high, while  $^1K_{\text{Cl}}^*$  agree well over the range of salinities for which measurements were made. Since the values of both constants predicted from Equations 166 to 169 at salinities <20 ‰ are essentially interpolations between the seawater measurements and infinite dilution values, it may be worthwhile exploring the use of theoretical models (such as that of Pitzer) to obtain improved estimates of the two dissociation constants in very dilute solutions.

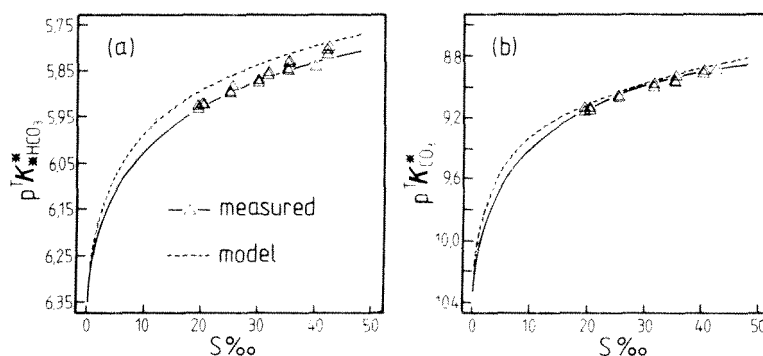
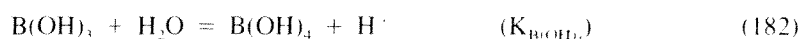


FIGURE 26. Comparison of measured and calculated stoichiometric dissociation constants of carbonic acid. (a)  $pK_{\text{HCO}_3}^*$ . Symbols — adjusted data of Mehrbach et al.<sup>230</sup> and Hansson<sup>231</sup> as listed by Dickson and Millero;<sup>232</sup> solid line — Equations 166 and 168; dashed line — calculated using  $K_{\text{H}_2\text{CO}_3}^* = 4.47 \times 10^{-7}$  and Pitzer model to determine  $a_{\text{H}_2\text{O}}$  and activity coefficients of  $\text{CO}_2$ ,  $\text{H}^+$ , and  $\text{HCO}_3^-$ . (b)  $pK_{\text{CO}_3}^*$ . Symbols — adjusted data of Mehrbach et al.<sup>230</sup> and Hansson<sup>231</sup> as listed by Dickson and Millero;<sup>232</sup> solid line — Equations 167 and 169; dashed line — calculated using  $K_{\text{CO}_3}^* = 4.70 \times 10^{-11}$  and Pitzer model to determine activity coefficients of  $\text{H}^+$ ,  $\text{CO}_3^{2-}$ , and  $\text{HCO}_3^-$ .

### b. Boric Acid

Boric acid,  $\text{B}(\text{OH})_3$ , dissociates in water according to the following equation:



where  $K_{\text{B}(\text{OH})_4^-}$  is equal to  $5.802 \times 10^{-10} \text{ mol kg}^{-1}$  at  $25^\circ\text{C}$ .<sup>245</sup> (Note that Felmy and Weare<sup>61</sup> use a slightly lower value of  $5.77 \times 10^{-10} \text{ mol kg}^{-1}$ .) Millero<sup>60</sup> has estimated the values of model coefficients  $\beta^{(0)}$  to parameterize the interaction of  $\text{Mg}^{2+}$  and  $\text{Ca}^{2+}$  with  $\text{B}(\text{OH})_3$ , and has used  $pK_{\text{B}(\text{OH})_4^-}^*$  data to estimate model parameters for the interaction of borate with  $\text{Na}^+$  and  $\text{K}^+$ . Hershey et al.<sup>246</sup> have measured the ionization of  $\text{B}(\text{OH})_3$  at  $25^\circ\text{C}$  in  $\text{NaCl}$ ,  $\text{Na-Ca-Cl-H}_2\text{O}$ , and  $\text{Na-Mg-Cl-H}_2\text{O}$  solutions at  $25^\circ\text{C}$ , while Simonson et al.<sup>247</sup> have determined  $\text{Na}^+-\text{B}(\text{OH})_4^-$  and  $\text{K}^+-\text{B}(\text{OH})_4^-$  interaction parameters ( $\beta^{(0)}$ ,  $C^\phi$ ) from 0 to  $55^\circ\text{C}$ . The most comprehensive study of borate equilibria in multicomponent solutions is that of Felmy and Weare<sup>61</sup> at  $25^\circ\text{C}$ , which is an extension of the earlier work of Harvie et al.<sup>56</sup> Model parameters for systems at low total borate concentrations are given in Table 35, and these are adopted in the present calculations. For interactions of the borate anion with  $\text{Mg}^{2+}$  and  $\text{Ca}^{2+}$ , complex formation [i.e.,  $\text{MgB}(\text{OH})_4^-$ ,  $\text{CaB}(\text{OH})_4^-$ ] is assumed rather than an ion-ion interaction. It should be noted that the values of the parameters are very sensitive to the assumptions that are made concerning the speciation in solution. Later assessments<sup>247</sup> of  $C_{\text{NaB}(\text{OH})_4^-}^\phi$ ,  $\beta_{\text{KB}(\text{OH})_4^-}^{(0)}$ , and  $C_{\text{KB}(\text{OH})_4^-}^\phi$  differ considerably from those deduced by Felmy and Weare.<sup>61</sup> Total borate concentrations of  $0.05 \text{ mol kg}^{-1}$  were used by Simonson et al.,<sup>247</sup> which is somewhat above the  $0.03 \text{ mol kg}^{-1}$  threshold normally considered as the limit beyond which polymeric boron species become significant. By their own reckoning some 13% of the total boron should be present in polymeric form at  $0.05 \text{ mol kg}^{-1}$  and their fitting parameters, which are unusually large, might reflect this influence. Careful analysis of data from systems at higher total boron concentrations by Felmy and Weare<sup>61</sup> indicated the importance of the  $\text{B}_3\text{O}_3(\text{OH})_4^-$  and  $\text{B}_4\text{O}_5(\text{OH})_7^-$  species. Here, as was the case for the  $\text{CO}_2$  system, solubility data were fitted to give, simultaneously, values for the interaction parameters and for the chemical potentials of the solid phases involved. In some instances quite complex systems had to be employed to derive the triplet interaction parameters. For example, the  $\theta_{\text{B}_3\text{O}_3(\text{OH})_4^-, \text{SO}_4^{2-}}$  term was derived from sodium pentaborate solubilities in the system  $\text{Na}_2\text{B}_4\text{O}_7-$

TABLE 35  
Ion-Ion Interaction Parameters for Borate Species at 25°C<sup>61</sup>

Species		$\beta^{(0)}$	$\beta^{(1)}$	$C^6$
Na <sup>+</sup>	B(OH) <sub>3</sub>	-0.0427	0.089	0.0114
K <sup>+</sup>	B(OH) <sub>3</sub>	0.035	0.14	0.0
MgB(OH) <sub>4</sub> <sup>-</sup>	Cl	0.16	0.0	0.0
CaB(OH) <sub>4</sub> <sup>-</sup>	Cl	0.12	0.0	0.0

Species		$\lambda_{\text{B(OH)}_3, \text{Cl}}$	$\zeta_{\text{B(OH)}_3, \text{Cl}}$	$\zeta_{\text{B(OH)}_3, \text{Na}}$
B(OH) <sub>3</sub>	Cl	0.0	-0.0102	—
B(OH) <sub>3</sub>	SO <sub>4</sub> <sup>2-</sup>	-0.262	—	0.046
B(OH) <sub>3</sub>	Na <sup>+</sup>	-0.006	—	—
B(OH) <sub>3</sub>	K <sup>+</sup>	-0.049	—	—

Species		$\theta_{\text{B(OH)}_3, \text{Cl}}$	$\psi_{\text{B(OH)}_3, \text{Na}}$
B(OH) <sub>3</sub>	Cl	-0.065	-0.0073
B(OH) <sub>3</sub>	SO <sub>4</sub>	-0.012	—

Note. See text for thermodynamic stability constants of MgB(OH)<sub>4</sub><sup>-</sup> and CaB(OH)<sub>4</sub><sup>-</sup>.

B(OH)<sub>3</sub>-Na<sub>2</sub>SO<sub>4</sub>-H<sub>2</sub>O, the other parameters required to describe this system having been deduced at an earlier stage. The model proved successful in predicting solubility relationships in the Na<sub>2</sub>B<sub>4</sub>O<sub>7</sub>-Na<sub>2</sub>CO<sub>3</sub>-H<sub>2</sub>O and Na<sub>2</sub>B<sub>4</sub>O<sub>7</sub>-Na<sub>2</sub>CO<sub>3</sub>-NaHCO<sub>3</sub>-H<sub>2</sub>O systems at 25°C, but gave a poor representation of NaBO<sub>2</sub>-Na<sub>2</sub>CO<sub>3</sub>-H<sub>2</sub>O systems. On application to the Searle's Lake evaporite deposit, the model gave a good account of the occurrence of minerals in the bed deposits, although the sequence of deposition predicted from the model differed from that observed in some significant respects. Nonetheless, the success of the model is encouraging given the complexity of the mineral sequences and the fact that total boron concentrations approach 0.5 mol kg<sup>-1</sup> at total ionic strengths of 6 mol kg<sup>-1</sup> or more.

For the relatively low boron concentrations encountered in seawater (less than 0.5 millimolal) the boron chemistry can be adequately described by a simple ionization equilibrium (Equation 154). However, when boron concentrations exceed 30 millimolal the involvement of polymeric boron species has to be taken into account.

The equilibria involving boric acid in seawater have not been studied as extensively as those concerning carbonic acid. The early measurements based on the NBS buffer scale (e.g., Lyman<sup>248</sup>) used electrode couples that were inadequately characterized. Hansson<sup>249</sup> measured  $K_{\text{B(OH)}_3}^*$  (SWS pH scale) over a limited salinity range (20 to 40 S‰) from 5 to 30°C in the fluoride-free synthetic seawater medium that he employed for his measurements on carbonic acid. These values have been refitted as a function of salinity and ionic strength by Millero.<sup>255</sup> Recent measurements on the total hydrogen ion concentration scale by Dickson<sup>255</sup> are much more extensive and employ a high precision potentiometric system using a hydrogen gas electrode and a silver-silver chloride electrode in a cell without a liquid junction.<sup>250</sup> A fluoride-free artificial seawater similar in composition to that employed by Millero<sup>250</sup> was used (see Table 30). The stoichiometric dissociation constant  $K_{\text{B(OH)}_3}^*$  is related to the thermodynamic value by

$${}^1K_{\text{B(OH)}_3}^* = m\text{H}_{\text{Cl}}^+ m\text{B(OH)}_{3,\text{Cl}} / m\text{B(OH)}_3 \quad (183a)$$

$$= K_{\text{B(OH)}_3} a_{\text{H}_2\text{O}} \gamma_{\text{B(OH)}_3} / (\gamma_{\text{H}^+} \gamma_{\text{B(OH)}_3, \text{Cl}}) \quad (183b)$$

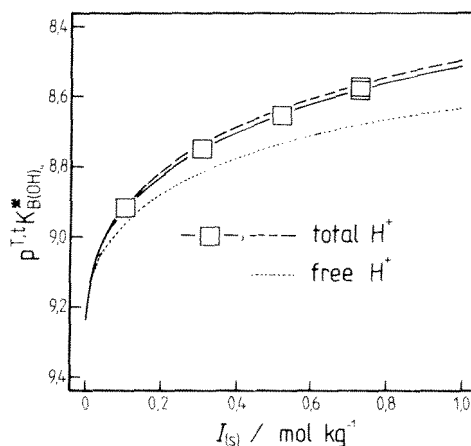


FIGURE 27. Stoichiometric acid dissociation constant  $K_{B(OH)_4}^*$  of boric acid in seawater at 25°C, on both a "total" ( ${}^tK_{B(OH)_4}^*$ ) and "free" ( ${}^fK_{B(OH)_4}^*$ ) hydrogen ion basis. Borate concentrations are total values in both cases. Symbols — data of Dickson<sup>245</sup> (total  $H^+$  scale); dashed line — calculated using Pitzer model with parameters listed in Table 35 (total  $H^+$  scale); full line — empirical fitting equation of Dickson<sup>245</sup>; dotted line — calculated using the Pitzer model on a free  $H^+$  (but total borate) basis.

where the superscript T indicates that the constant is calculated using total concentrations of both  $H^+$  and  $B(OH)_4$ . The "total" and "free" ion activity coefficients for  $H^+$  and  $B(OH)_4$  are related by

$$\gamma_{H(T)} = \gamma_{H(F)} / (1 + mSO_{4(F)}^2 {}^tK_{HSO_4}^*) \quad (184)$$

$$\gamma_{B(OH)_4(T)} = \gamma_{B(OH)_4(F)} / (1 + mMg^{2+} {}^tK_{MgB(OH)_4}^* + mCa^{2+} {}^tK_{CaB(OH)_4}^*) \quad (185)$$

Here the superscript lower case t indicates the use of total  $Mg^{2+}$  and  $Ca^{2+}$ , but free  $B(OH)_4$  concentrations, in the artificial seawater medium. The two stoichiometric association constants are given by

$${}^tK_{MgB(OH)_4}^* = K_{MgB(OH)_4} \gamma_{Mg(T)} \gamma_{B(OH)_4(F)} / \gamma_{MgB(OH)_4} \quad (186)$$

$${}^tK_{CaB(OH)_4}^* = K_{CaB(OH)_4} \gamma_{Ca(T)} \gamma_{B(OH)_4(F)} / \gamma_{CaB(OH)_4} \quad (187)$$

The thermodynamic values of  $K_{MgB(OH)_4}$  and  $K_{CaB(OH)_4}$  are 25.1 and 44.7  $\text{kg mol}^{-1}$ , respectively, at 25°C.<sup>61</sup>

Using the parameters in Table 35, we have calculated  ${}^tK_{B(OH)_4}^*$  in seawater as a function of ionic strength at 25°C and compared these values with the measurements of Dickson<sup>245</sup> (see Figure 27). It can be seen that there is quite good agreement, the maximum difference in  $\log_{10}({}^tK_{B(OH)_4}^*)$  being about 0.02 units — due perhaps to a poor prediction of  ${}^tK_{HSO_4}^*$  or lack of parameters for the interaction of  $SO_4^{2-}$  with the calcium and magnesium orthoborate complexes. Calculated values of the individual ion activity coefficients in seawater are listed in Appendix Table A11. Due to the lack of model parameters covering a wide range of temperatures, the following fitting equation of Dickson<sup>245</sup> should be used to obtain  ${}^tK_{B(OH)_4}^*$  from 0 to 45 S‰, 0 to 45°C:

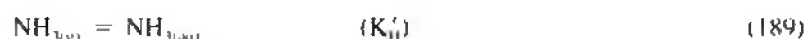
$$\begin{aligned} \ln({}^tK_{B(OH)_4}^*) = & (-8966.9 - 2890.51 S^{1/2} - 77.942 S + 1.726S^{3/2} - 0.0993 S^2)/T \\ & + (148.0248 + 137.194 S^{1/2} + 1.62247 S) \\ & + (-24.4344 - 25.085 S^{1/2} - 0.247 S) \ln(T) + 0.053105 S^{1/2} T \end{aligned} \quad (188)$$

The pressure effect on the dissociation of borate in seawater has been estimated by Millero,<sup>251,250</sup> and may be calculated using Equations 171 and 172 and parameters listed in Table 32.

### c. Ammonia

The toxicity of ammonium salts to freshwater life has been shown to be strongly dependent on pH, in a manner consistent with un-ionized  $\text{NH}_3$  being the most lethal fraction.<sup>251</sup> The free base ( $\text{NH}_3$ ) has a relatively high lipid solubility because it carries no charge and is therefore able to diffuse quite readily across cell membranes.<sup>252</sup> In upwelling areas at the ocean margins where nutrient concentrations, and therefore total dissolved ammonia, are high there is indirect evidence of ocean-to-atmosphere transfer.<sup>144</sup> A significant atmospheric sink for  $\text{NH}_3$  is neutralization by strong acids, particularly  $\text{H}_2\text{SO}_4$  (in aerosols), followed by removal in rain.<sup>253</sup>

Since in most natural waters  $\text{NH}_3$  only undergoes a partial dissociation in solution, the equilibrium between gas and aqueous phase  $\text{NH}_3$  is described as for a nondissociating solute:



where (for  $273 \leq T \leq 313 \text{ K}$ ):

$$\ln(K'_H) = -8.09694 + 3917.507/T - 0.00314 T \quad (190)$$

followed by base dissociation:



where:

$$K_{\text{NH}_3} = (m\text{NH}_4^+ m\text{OH}^- / m\text{NH}_3) \cdot (\gamma_{\text{NH}_4^+} \gamma_{\text{OH}^-} / \gamma_{\text{NH}_3} \theta_{\text{H}_2\text{O}}) \quad (192)$$

At 298.15 K the values of  $K'_H$  and  $K_{\text{NH}_3}$  are  $60.72 \text{ mol kg}^{-1} \text{ atm}^{-1}$  and  $1.774 \times 10^{-5} \text{ mol kg}^{-1}$ , respectively. Alternatively, the reaction may be expressed as



$$K_{\text{NH}_4^+} = (m\text{H}^+ m\text{NH}_3 / m\text{NH}_4^+) \cdot (\gamma_{\text{H}^+} \gamma_{\text{NH}_3} / \gamma_{\text{NH}_4^+}) \quad (194)$$

$K_{\text{NH}_4^+}$  is given as a function of temperature by:

$$\ln(K_{\text{NH}_4^+}) = \ln(^{\circ\circ}K_{\text{NH}_4^+}) + (1/R)\{52220(1/T_1 - 1/T) + 4.1185(T_1/T - (1 + \ln(T_1/T)))\} \quad (195)$$

where the dissociation constant at 298.15 K ( $^{\circ\circ}K_{\text{NH}_4^+}$ ) is equal to  $5.6825 \times 10^{-10} \text{ mol kg}^{-1}$ ,  $R$  is the gas constant ( $8.314 \text{ J K}^{-1} \text{ mol}^{-1}$ ), and  $T_1$  is the reference temperature of 298.15 K.

The ion-neutral interaction parameters ( $\lambda_{\text{NH}_4^+, \text{NH}_3}$ ,  $\lambda_{\text{NH}_4^+, \text{H}^+}$  and triplet terms) leading to values of  $\gamma_{\text{NH}_4^+}$  in salt solutions have been determined by Clegg and Brimblecombe<sup>26</sup> from available experimental measurements of equilibrium  $p\text{NH}_3$ , salt solubilities in aqueous  $\text{NH}_3$ , and  $\text{NH}_3$ ,

**TABLE 36**  
**Interaction Parameters for NH<sub>3</sub> at 25°C.<sup>98</sup>**  
 (See Text Concerning Self-Consistency of Data Set)

Species i	$\lambda_{\text{NH}_3,i}$	$\mu_{\text{NH}_3,\text{NH}_3,i}$	Species i	$\lambda_{\text{NH}_3,i}$	$\mu_{\text{NH}_3,\text{NH}_3,i}$
NH <sub>4</sub> <sup>a</sup>	0.01472	—	F	0.091	—
Mg <sup>2+</sup> · b	-0.21	—	Cl	0.0	0.0
Ca <sup>2+</sup> · b	-0.081	—	Br	-0.022	—
Sr <sup>2+</sup> · b	-0.041	—	I	-0.051	—
Ba <sup>2+</sup> · b	-0.021	—	OH	0.103	—
Li <sup>+</sup>	-0.038	—	NO <sub>3</sub>	-0.01	-0.000437
Na <sup>+</sup> · c	0.0175	-0.000311	S <sup>2-</sup>	0.174	—
K <sup>+</sup> · d	0.0454	-0.000321	SO <sub>4</sub> <sup>2-</sup>	0.158	—
NH <sub>4</sub> <sup>e</sup>	0.0	-0.00075	SO <sub>3</sub> <sup>2-</sup> · f	0.140	—
			CO <sub>3</sub> <sup>2-</sup>	0.180	0.000625

Additional parameter values:

$\zeta_{\text{NH}_4,\text{K},\text{OH}}$	0.0231
$\zeta_{\text{NH}_4,\text{NH}_4,\text{SO}_4}$	-0.00918
$\zeta_{\text{NH}_4,\text{Ca},\text{Cl}}$	-0.00804

<sup>a</sup> Temperature variation over the range 0–40°C given by the equation:  
 $\lambda_{\text{NH}_3,\text{NH}_4} = 0.033161 - 21.12816/T + 4665.1461/T^2$  where T/K.

<sup>b</sup> These values tentative only.

<sup>c</sup> Partial pressure and solubility data suggest  $\lambda_{\text{NH}_4,\text{Na}}$  is equal to about 0.031 — see text.

<sup>d</sup>  $\partial\lambda_{\text{NH}_4,\text{K}}/\partial T$  equal to -0.000141 obtained from KCl solubility data.

<sup>e</sup>  $\partial\mu_{\text{NH}_4,\text{NH}_4,\text{NH}_4}/\partial T$  equal to  $2.3 \times 10^{-5}$  estimated from partial pressure data.

<sup>f</sup>  $\partial\lambda_{\text{NH}_4,\text{SO}_4}/\partial T$  estimated from salt solubility data to lie in the range -0.0005 to -0.00095.

partitioning between salt solutions and CHCl<sub>3</sub>. The most recent data are those of Maeda and co-workers, who have determined  $\gamma_{\text{NH}_4}$  in solutions of various 1:1 salts<sup>254-257</sup> including NaCl<sup>255</sup> and measured the pK\* of NH<sub>3</sub> in aqueous LiCl,<sup>258</sup> Na-Li-Cl-H<sub>2</sub>O solutions,<sup>259</sup> and artificial seawater<sup>255</sup> at 25°C. Maeda and co-workers have also applied the Pitzer model to their results. Available ion-NH<sub>3</sub> interaction parameters of geochemical interest are listed in Table 36.

There is some uncertainty regarding the value of  $\lambda_{\text{NH}_4,\text{Na}}$  — which is unfortunate in view of the fact that NaCl is the principal constituent of seawater. The listed value of 0.0175 was obtained from NaCl solubilities in aqueous NH<sub>3</sub>.<sup>98</sup> Partial pressure data, including those of Maeda et al.,<sup>255</sup> and NaCl<sub>(aq)}/CHCl<sub>3</sub> partitioning data both suggest a higher value of about 0.031. Very little information is available concerning the temperature variation of the ion-NH<sub>3</sub> interaction parameters, though a few estimates are listed in the notes to Table 36.</sub>

In common with other (inorganic) compounds that undergo dissociation in solution, the variation of  $\gamma_{\text{NH}_3}$  with solution concentration is likely to be much less than that of the product  $\gamma_{\text{NH}_4}\gamma_{\text{OH}}$  (Equation 192), or quotient  $\gamma_{\text{H}^+}/\gamma_{\text{NH}_4}$  (Equation 194). Successful modeling of the degree of dissociation therefore depends chiefly on obtaining an adequate description of  $\gamma_{\text{NH}_4}$  and  $\gamma_{\text{OH}}$  in solution, or alternatively if Equation 194 is being used,  $\gamma_{\text{NH}_4}$  and  $\gamma_{\text{H}^+}$ . Model parameters for the principal NH<sub>4</sub><sup>+</sup> salts [NH<sub>4</sub>Cl and (NH<sub>4</sub>)<sub>2</sub>SO<sub>4</sub>] are known at 298.15 K, as are those of hydroxide salts NaOH and KOH (Tables 2 and 7, Pitzer,<sup>51</sup> Chapter 3, this volume). For the interaction of Mg<sup>2+</sup> with OH<sup>-</sup> Harvie et al.<sup>56</sup> adopt an ion pair MgOH<sup>+</sup> with a formation constant of 154 kg mol<sup>-1</sup> at 298.15 K, while for Ca<sup>2+</sup>-OH<sup>-</sup> an interaction



TABLE 37  
Mixture Parameters  $\theta_{ij}$  and  $\psi_{ijk}$  Involving the  $\text{NH}_4^+$  Ion

Cation c	$\theta_{\text{NH}_4,c}$	$\psi_{\text{NH}_4,c,\text{Cl}}$	$\psi_{\text{NH}_4,c,\text{SO}_4}$	$\psi_{\text{NH}_4,c,\text{Br}}$	Ref.
$\text{H}^+$ <sup>a</sup>	-0.01	-0.009	—	-0.0104	148
$\text{H}^+$ <sup>a</sup>	-0.019	0.0	0.0	0.0	51
$\text{H}^+$ <sup>a</sup>	-0.0127	-0.0091	—	—	353
$\text{Li}^+$	-0.027	-0.011	—	—	258
$\text{Na}^+$	0.004	0.0005	—	—	259
$\text{Na}^+$	0.0	-0.0003	-0.0013	—	51
$\text{Be}^{2+}$ <sup>b</sup>	0.012	—	-0.0199	—	354

Note: Parameters  $\theta_{\text{NH}_4,\text{Mg}}$  and  $\psi_{\text{NH}_4,\text{Mg}/\text{SO}_4}$  have also been derived, but for the model *without* unsymmetrical mixing terms  ${}^t\theta$  and  ${}^t\theta'$ .<sup>51</sup> The following temperature derivatives of pure electrolyte parameters ( $\beta_{\text{NH}_4,\text{Cl}}^0$ ,  $C_{\text{NH}_4,\text{Cl}}^0$ ) have been determined and are used in all calculations:  $10^3\beta^{\text{NH}_4,\text{Cl}}$  1.11,  $10^3\beta^{\text{NH}_4,\text{Cl}}$  13.1,  $10^3C^{\text{NH}_4,\text{Cl}}$  0.137,  $10^3\beta^{\text{NH}_4,\text{Cl}}$  -1.31,  $10^3\beta^{\text{NH}_4,\text{Cl}}$  1.415,  $10^3C^{\text{NH}_4,\text{Cl}}$  0.2668.

<sup>a</sup> Parameters of Chan et al.<sup>51</sup> adopted here.

<sup>b</sup> See Clegg and Brimblecombe<sup>51</sup> for model parameters ( $\beta^0$ ,  $C^0$ ) and coefficients ( $\alpha_1$  and  $\alpha_2$ ) required for  $\text{BeCl}_2$  and  $\text{BeSO}_4$ .

between the free ions is retained. Interaction parameters for NaOH and KOH are available as functions of temperature (Table 11). First temperature derivatives of parameters ( $\beta^0$ ,  $C^0$ ) are available for the  $\text{NH}_4^+$ -Cl<sup>-</sup> interaction (Table 12, Pitzer,<sup>51</sup> Chapter 3, this volume). There appear to be no data from which to estimate the temperature variation of the strong  $\text{Mg}^{2+}$ -OH<sup>-</sup> and  $\text{Ca}^{2+}$ -OH<sup>-</sup> interactions. Because of this it is probably better to estimate ammonia equilibrium in aqueous solution via the acid dissociation given in Equation 194, thus avoiding some of the problems of poorly known ion pairing reactions and ion-ion interactions. Interaction parameters for aqueous HCl are available as a function of temperature, as are those for interactions of  $\text{H}^+$  with  $\text{SO}_4^{2-}$  (Table 11). The reaction of  $\text{H}^+$  with  $\text{F}^-$  to form  $\text{HF}_{(\text{aq})}$  is adequately understood<sup>101</sup> in NaCl media at 298.15 K (see Section III.C.3.d), as is the equilibrium with borate in multicomponent solutions<sup>61</sup> (again at 298.15 K). Currently available mixture parameters ( $\theta_{ij}$  and  $\psi_{ijk}$ ) involving  $\text{NH}_4^+$ ,  $\text{H}^+$ , and the major ions of seawater are listed in Table 37, together with new estimates of both first and second temperature derivatives of the pure electrolyte  $\text{NH}_4\text{Cl}$  parameters. There is no information regarding the temperature variation of  $\theta_{ij}$  and  $\psi_{ijk}$ , but it is likely that constant 25°C values will be adequate over the normal range of temperature of about 0 to 40°C.

As an initial test of the model, applied to the dissociation of  $\text{NH}_4$  in salt solutions, we have calculated  $\text{pK}_{\text{NH}_4}^*$ , [as  $-\log_{10}(\text{K}_{\text{NH}_4}/\Gamma)$ ] in aqueous NaCl at 15, 25, and 35°C. The results are shown in Figure 28a, together with the measured values of Maeda et al.<sup>259</sup> at 25°C. There is good agreement at all concentrations. Note that the model calculations were carried out using  $\lambda_{\text{NH}_4,\text{Na}}$  equal to 0.031. In the most concentrated solutions, the lower value of 0.0175 resulted in  $\text{K}_{\text{NH}_4}^*$  values which were too great. This comparison strongly suggests that the higher value of  $\lambda_{\text{NH}_4,\text{Na}}$  is more nearly correct, and that for a self-consistent parameter set other  $\lambda_{\text{NH}_4,i}$  should be reestimated from the original determinations of ( $\nu_+ \lambda_{\text{NH}_4,+} + \nu_- \lambda_{\text{NH}_4,-}$ ) tabulated by Clegg and Brimblecombe.<sup>50</sup> Figure 28b shows the activity coefficient quotient  $\Gamma$  for the acid dissociation, at each temperature.

Whitfield<sup>261</sup> has used a number of simple theoretical procedures to estimate the  $\text{pK}_{\text{NH}_4}^*$  at 298.15 K of  $\text{NH}_4$  in seawater, which are in surprisingly good agreement with the mea-

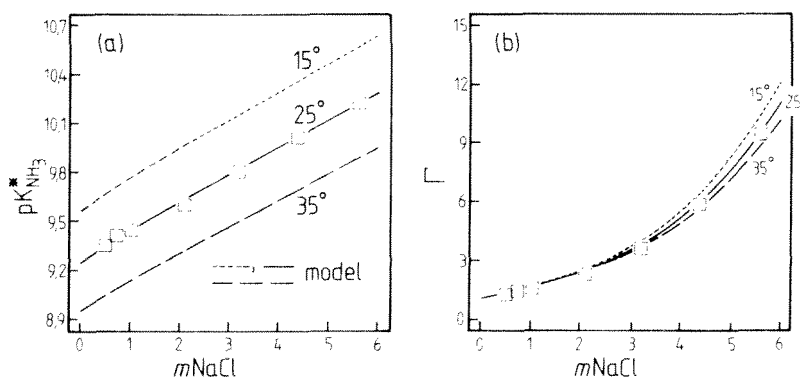


FIGURE 28. Measured and calculated values of the stoichiometric acid dissociation constant ( $K_{NH_4}^*$ ), and activity coefficient quotient  $\Gamma$  ( $\gamma_{NH_3}/\gamma_{NH_4^+}$ ) of  $NH_3$  at 15, 25, and 35°C in pure aqueous NaCl. (a)  $pK_{NH_4}^*$ ; (b) activity coefficient quotient  $\Gamma$ . Lines --- calculated using the thermodynamic dissociation constant given by Equation 195 and the Pitzer model; symbols — data of Maeda et al.<sup>255</sup>

measurements of Khoo et al.<sup>225</sup> in artificial seawater (Na-Mg-Ca-K-Cl-SO<sub>4</sub>-H<sub>2</sub>O), carried out using an ionic medium pH scale based on sulfate-free buffers. Maeda et al.<sup>255</sup> have also determined the dissociation constant of  $NH_4^+$  in artificial seawater by potentiometry. They compared their results with calculations using the Pitzer model, though without mixture parameters  $\theta_{ij}$  and  $\psi_{ijk}$  or allowing for the formation of  $HSO_4^-$ . They concluded that the model was in satisfactory agreement with observation at most seawater concentrations.

In Figure 29 we compare calculated  $pK_{NH_4}^*$  in seawater (recipe of Khoo et al.<sup>225</sup>) from 5 to 35°C with the results of Khoo et al.<sup>225</sup> at all temperatures, and those of Maeda et al.<sup>255</sup> at 25°C. The empirical best-fit lines of Khoo et al. are also shown, and at 25°C the effect of using  $\lambda_{NH_4,Na}$  equal to 0.0175 on predicted  $pK_{NH_4}^*$  is indicated. We note that the quoted uncertainty of the results of Maeda et al.<sup>255</sup> is about  $\times 10$  greater than that of Khoo et al.<sup>225</sup> Although there is some suggestion that at 35°C the model yields a  $pK_{NH_4}^*$  that is too low, in general the predicted values agree well with the measurements.

Johansson and Wedborg<sup>262</sup> have measured the  $pK_{NH_4}^*$  of  $NH_3$  in artificial seawater (Na-Mg-Ca-Cl-SO<sub>4</sub>-H<sub>2</sub>O) by potentiometric titration, expressing the results on a total  $H^+$  (T) ion scale: thus  $mH_{(T)}^+ = mH_{(F)}^+ + mHSO_4^-$ , where subscript (F) indicates a free ion concentration. For their definition of pH, the stoichiometric acid dissociation constant  ${}^T K_{NH_4}^*$  is given by

$${}^T K_{NH_4}^* = (mH_{(F)}^+ + mHSO_4^-)mNH_3/mNH_4^+ \quad (196)$$

This is readily related to  $K_{NH_4}^*$ :

$${}^T K_{NH_4}^* = mH_{(F)}^+(1 + mSO_{4(F)}^{2-} {}^T K_{HSO_4}^*)mNH_3/mNH_4^+ \quad (197)$$

Hence:

$${}^T K_{NH_4}^* = K_{NH_4}^*(1 + mSO_{4(F)}^{2-} {}^T K_{HSO_4}^*) \quad (198)$$

Using Equation 198 and model estimates of  ${}^T K_{HSO_4}^*$ , the results of Johansson and Wedborg<sup>262</sup> have been converted to  $K_{NH_4}^*$  and are compared with calculated values in Figure 30a. While

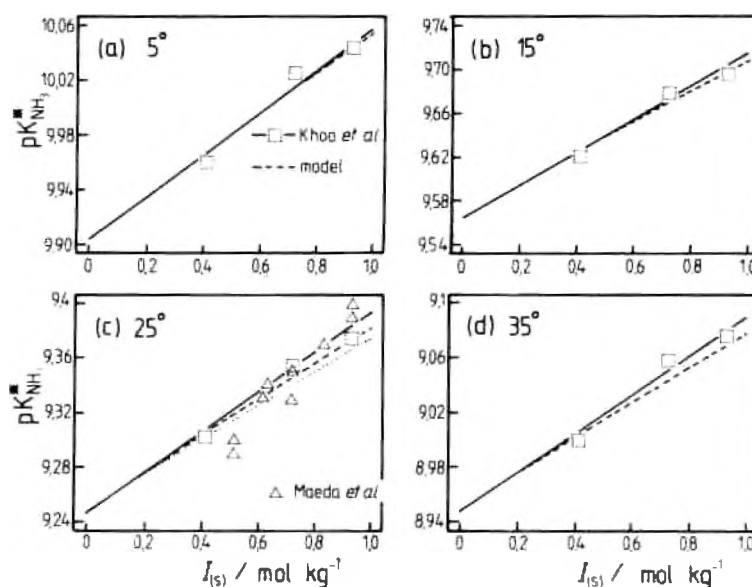


FIGURE 29 Measured and calculated values of the stoichiometric acid dissociation constant ( $K_{NH_4}^*$ ) of  $NH_4$  from 5 to 35°C in artificial seawater, as a function of ionic strength. Open squares — data of Khoo *et al.*;<sup>225</sup> triangles — data of Maeda *et al.*<sup>255</sup> at 25°C; dashed lines — calculated using the Pitzer model and the thermodynamic dissociation constant given by Equation 195; full lines — best-fit equation of Khoo *et al.*<sup>225</sup> (Dotted line at 25°C calculated using  $\lambda_{NH_4,Na} = 0.0175$ .)

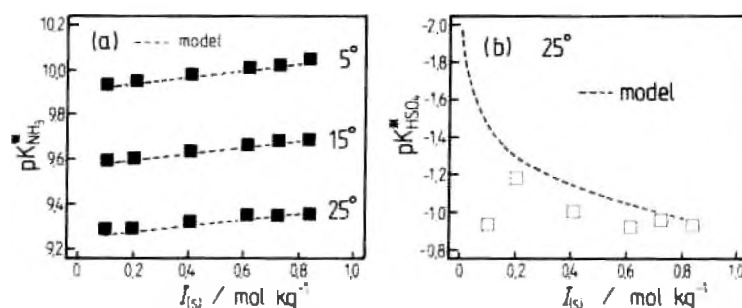


FIGURE 30. (a) Measured and calculated values of the stoichiometric acid dissociation constant ( $K_{NH_4}^*$ ) of  $NH_4$  at 5, 15 and 25°C in artificial seawater, as a function of ionic strength ( $I_{(s)}$ ). Symbols — data of Johansson and Wedborg,<sup>262</sup> corrected from the “total” to “free” hydrogen ion scale; dashed lines — calculated using the Pitzer model and the thermodynamic dissociation constant given by Equation 195. (b) Stoichiometric formation constant of  $HSO_4$  ( $K_{HSO_4}^*$ ) at 25°C. Symbols — estimated from the  $K_{NH_4}^*$  data of Johansson and Wedborg<sup>262</sup> at 25°C; dashed line — calculated using the Pitzer model.

the trend of  $pK_{NH_4}^*$  with ionic strength is well predicted, the  $pK_{NH_4}^*$  derived from measurements are consistently greater than calculated values. Could this be related to the model estimates of  $K_{HSO_4}^*$ ? In Figure 30b  $\log_{10}(K_{HSO_4}^*)$  calculated using the model are compared with values inferred from measured  $K_{NH_4}^*$  using Equation 198 at 25°C and calculated  $K_{NH_4}^*$ , which have already been shown to be in good agreement with the work of Khoo *et al.*<sup>225</sup> It is clear that the measurements fail to match the rapid rise in  $\log_{10}(K_{HSO_4}^*)$  with decreasing ionic strength, to the thermodynamic value of 1.979.

It is concluded from these comparisons that the stoichiometric dissociation constant of  $\text{NH}_4$  in seawater may be satisfactorily estimated by taking the thermodynamic  $K_{\text{NH}_4}$  and using the Pitzer model to estimate the activity coefficient quotient  $\Gamma$  for the reaction. In Appendix Table A11 are listed values of  $\gamma_{\text{H}^+}$ ,  $\gamma_{\text{NH}_4^+}$ , and  $\gamma_{\text{NH}_3}$  (and the activity coefficients of other trace species in seawater) at 25°C to enable stoichiometric association or dissociation constants to be obtained.

#### d. Hydrofluoric Acid

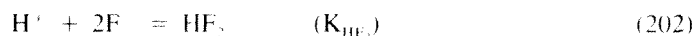
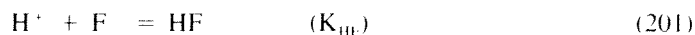
The solubility of the weak acid HF is expressed by the equation



where ( $273 \leq T \leq 313$  K):

$$\ln(K'_{\text{H}}) = 6.61712 + 3360.464/T - 0.02789 T \quad (200)$$

There are two association reactions involving  $\text{H}^+$  and  $\text{F}^-$  ions in aqueous solution:



where the thermodynamic association constants  $K_{\text{HF}}$  and  $K_{\text{HF}_2}$  take the values  $1.462 \times 10^3 \text{ kg mol}^{-1}$  and  $3.837 \times 10^4 \text{ kg}^2 \text{ mol}^{-2}$ , respectively, at 298.15 K,<sup>263</sup> and the enthalpy changes for the reactions  $\Delta H^\circ$  are 13.3 kJ mol<sup>-1</sup> ( $K_{\text{HF}}$ ) and 19.04 kJ mol<sup>-1</sup> ( $K_{\text{HF}_2}$ ) (Table 29). Haung<sup>264</sup> has applied the Pitzer model to activity and osmotic coefficients of pure aqueous solutions of HF, including both the above reactions explicitly. However, in most natural waters such as seawater, both  $\text{H}^+$  and  $\text{F}^-$  are present at trace concentrations in solutions relatively concentrated with respect to other dissolved constituents ( $m\text{Cl}^- = 7.61 \times 10^3 \text{ mF}_{(\text{H})}$  in seawater, Table 2). Consequently, for our purposes the second association above may be neglected, as the formation of  $\text{HF}_2^-$  is insignificant. Also, the activity coefficients of free  $\text{H}^+$  and  $\text{F}^-$  will be controlled by other ions present, and their own "interaction" can be treated as association to form HF.

Determinations of stoichiometric values of  $K_{\text{HF}}$  are available for a number of salt solutions<sup>265,266</sup> including NaCl, of which the most recent are measurements at 298.15 K by Clegg and Brimblecombe.<sup>101</sup> Here mean activity coefficients of HF were measured using a  $\text{H}^+$  (glass),  $\text{F}^-$  ( $\text{LaF}_3$ ) electrode pair in aqueous NaCl solutions containing small amounts of  $\text{H}^+$  and  $\text{F}^-$ . The decrease in activity from that calculated using total concentrations and activity coefficients estimated using the Pitzer model, fully parameterized for the system excluding the  $\text{H}^+$ - $\text{F}^-$  reaction, was attributed to the formation of HF. The association constant in NaCl at 298.15 K is given as a function of ionic strength ( $I$ ) by the following equation:

$$\log_{10}(K_{\text{HF}}^*) = 3.165 - 1.81I^{1/2} (1 + 3.73I^{1/2}) + 0.06I + 0.0136I^2 \quad (203)$$

The infinite dilution value of  $K_{\text{HF}}$  is 1462.3.<sup>167</sup> In Figure 31 measured and fitted (Equation 203)  $K_{\text{HF}}^*$  are shown. Estimates of  $K_{\text{HF}}^*$  made using the thermodynamic value, and  $\gamma_{\text{H}^+}$  and  $\gamma_{\text{F}^-}$  calculated using the Pitzer model with  $\gamma_{\text{HF}}$  equal to unity, are also plotted. These show a small positive deviation from the measured values, which may be attributed to the activity coefficient of undissociated HF:

$$\gamma_{\text{HF}} = (K_{\text{HF}}/K_{\text{HF}}^*) \gamma_{\text{H}^+} \gamma_{\text{F}^-} \quad (204)$$

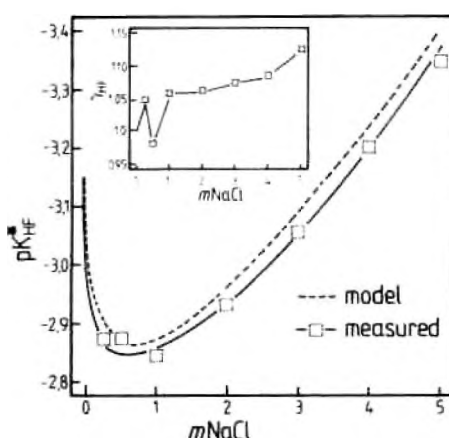


FIGURE 31 The stoichiometric association constant ( $K_{HF}^*$ ) of HF in aqueous NaCl at 25°C. Symbols — measured values; full line — fitted (Equation 203); dashed line — obtained from the thermodynamic constant  $K_{HF}$ , and  $\gamma_H$  and  $\gamma_F$  calculated using the Pitzer model ( $\gamma_{HF} = 1.0$ ) Inset:  $\gamma_{HF}$  estimated from fitted  $K_{HF}^*$ , thermodynamic  $K_{HF}$ , and model-calculated  $\gamma_H$  and  $\gamma_F$ .

where  $\gamma_{H(F)}$  and  $\gamma_{F(H)}$  are free ion activity coefficients, calculated using the Pitzer model. Values of  $\gamma_{HF}$ , shown in the inset to Figure 31, are offset from unity at the lowest ionic strength by 0.05, which is most likely due to experimental error. If so, this suggests that  $K_{HF}^*$  given by Equation 203 is about 5% too low. Increases in the derived value of  $\gamma_{HF}$  with ionic strength indicate salting out of HF, although the effect appears to be small. Certainly, at seawater ionic strength ( $\approx 0.73 \text{ mol kg}^{-1}$ )  $\gamma_{HF}$  differs negligibly from unity.

It is possible, using the Pitzer model, to calculate the stoichiometric formation constant of HF in seawater on both free and total concentration scales. Millero<sup>60</sup> has determined the dissociation constants of several weak acids in seawater on the basis of "total" concentrations. Thus, we can define an equivalent association constant,  ${}^tK_{HF}^*$ :

$${}^tK_{HF}^* = mHF / (mH_{(T)}^+ mF_{(T)}^-) \quad (205a)$$

$$= mHF / (mH_{(F)}^+ + mHSO_4^-) (mF_{(F)}^- + mMgF^+ + mCaF^+) \quad (205b)$$

where the total hydrogen ion concentration  $mH_{(T)}^+$  is equivalent to the free hydrogen ion concentration plus that of bisulfate, and similarly  $mF_{(T)}^-$  is equivalent to free fluoride plus the concentrations of  $MgF^+$  (see Section III.D.3) and  $CaF^+$ . Note that in seawater,  $mHF$  is small compared to both  $mF_{(T)}^-$  and  $mH_{(T)}^+$ . Dickson and Riley<sup>268</sup> defined a stoichiometric stability constant of HF in terms of free hydrogen ion, but total fluoride:

$${}^sK_{HF}^* = mHF / (mH_{(F)}^+ mF_{(T)}^-) \quad (206)$$

We have used the Pitzer model and a thermodynamic  $K_{HF}$  of  $1462 \text{ kg mol}^{-1}$  at 25°C to calculate  $K_{HF}^*$  (free ions),  ${}^tK_{HF}^*$  (total  $H^+$  and total  $F^-$ ), and  ${}^sK_{HF}^*$  (free  $H^+$  and total  $F^-$ ) as functions of seawater ionic strength. These quantities are plotted in Figure 32 together with values of  $K_{HF}^*$  estimated by Perez and Fraga<sup>269</sup> and  ${}^tK_{HF}^*$  (measured and predicted) listed by Millero.<sup>60</sup> The equation of Dickson and Riley<sup>268</sup> for  ${}^sK_{HF}^*$  is based on only two measurements, and yields values  $>0.1 \log_{10}$  units greater than those shown in the figure. The free ion association constants estimated by Perez and Fraga<sup>269</sup> appear to be unrealistically high, while

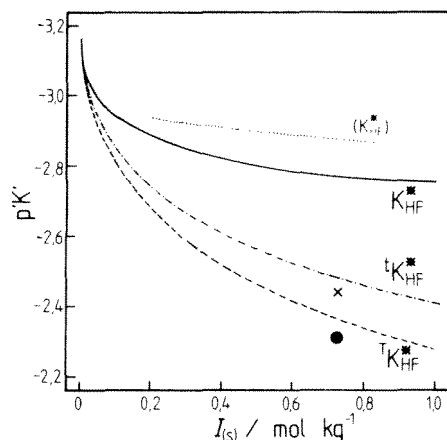


FIGURE 32. Values of the stoichiometric association constant of HF in seawater media at 25°C as a function of ionic strength ( $I_{(s)}$ ). Lines — association constants, defined in Equations 205 and 206, calculated using the Pitzer model — except that marked “ $(K_{HF}^*)$ ”, which is due to Perez and Fraga;<sup>269</sup>  $K_{HF}^*$  — free  $H^+$  and free  $F^-$  concentrations;  $K_{HF}^*$  — free  $H^+$  and total  $F^-$  concentrations;  $tK_{HF}^*$  — total  $H^+$  and total  $F^-$  concentrations. Symbols — measured (cross) and calculated (circle) values of  $K_{HF}^*$  listed by Millero.<sup>60</sup>

the  $K_{HF}^*$  listed by Millero<sup>60</sup> are in reasonable agreement with calculated values. In calculations such as these, it is necessary to ensure that consistency is maintained, particularly with regard to stability constants of associated species such as  $HSO_4^-$  and  $MgF^+$ . For example, Millero<sup>60</sup> used a seawater stability constant of  $HSO_4^-$  determined by Khoo et al.,<sup>139</sup> which has already been shown to differ from that estimated from the Pitzer model by about 15% (Figure 12).

#### e. Phosphoric Acid

Pitzer and Silvester<sup>59</sup> have applied the model equations to solvent and solute activities in aqueous  $H_3PO_4$  at 298.15 K, to a total concentration of  $6 \text{ mol kg}^{-1}$ , including the following association:



where  $K_{H_3PO_4}$  is equal to  $140 \text{ kg mol}^{-1}$  at 25°C. Volumetric properties of the acid have been considered by Barta and Bradley,<sup>270</sup> and first and second pressure derivatives of the pure solution interaction parameters determined. In natural waters, further equilibria with  $HPO_4^{2-}$  and  $PO_4^{3-}$  ions must also be considered. The thermodynamic values of the equilibrium constants are listed in Table 29.

Interaction parameters are available for  $Na^+$  and  $K^+$  salts of  $H_2PO_4^-$ ,  $HPO_4^{2-}$ , and  $PO_4^{3-}$  (Tables 2 and 9 of Pitzer,<sup>51</sup> Chapter 3, this volume). Both  $Mg^{2+}$  and  $Ca^{2+}$  associate strongly with the phosphate anions — chiefly  $PO_4^{3-}$  — so much so that the need to avoid precipitation of their salts becomes a practical limitation in the determination of stoichiometric dissociation constants of phosphoric acid in seawater media.<sup>271,272</sup> Association constants of  $Mg^{2+}$  and  $Ca^{2+}$  with phosphate species in seawater have been measured by Atlas et al.,<sup>273</sup> and also estimated by Johansson and Wedborg.<sup>274</sup> Millero<sup>60</sup> has used these data to determine interaction parameters ( $\beta^{(0)}$ ) for  $Mg^{2+}$  and  $Ca^{2+}$  with the three principal phosphate species in seawater at 35 S‰ and 25°C, thus avoiding the need to calculate the concentrations of the associated forms ( $MgH_2PO_4^+$ ,  $CaH_2PO_4^+$ , etc.) explicitly in order to account for the ion

**TABLE 38**  
**Ion-Ion Interaction Parameters Involving Phosphate Species**  
 **$\text{H}_2\text{PO}_4^-$ ,  $\text{HPO}_4^{2-}$ , and  $\text{PO}_4^{3-}$  at 25°C**

Species	$\beta^{00}$	$\beta^{01}$	$C^*$	Note	Ref.
Na <sup>+</sup> $\text{H}_2\text{PO}_4^-$	-0.0533	0.0396	0.00795		51
	(-0.0651	0.091	0.01138)		105
K <sup>+</sup> $\text{H}_2\text{PO}_4^-$	-0.0678	-0.1042	0.0		51
	(-0.1128	0.0606	0.02012)		105
NH <sub>4</sub> <sup>+</sup> $\text{H}_2\text{PO}_4^-$	-0.07043	-0.4156	0.00669		355
Mg <sup>2+</sup> $\text{H}_2\text{PO}_4^-$	-0.41	0.0	0.0	a	60
	(-3.55	16.9	0.0)		274
Ca <sup>2+</sup> $\text{H}_2\text{PO}_4^-$	-0.29	0.0	0.0	a	60
Na <sup>+</sup> $\text{HPO}_4^{2-}$	-0.05828	1.4655	0.02938		51
K <sup>+</sup> $\text{HPO}_4^{2-}$	0.02475	1.2743	0.01639		51
Mg <sup>2+</sup> $\text{HPO}_4^{2-}$	-3.6	0.0	0.0	a	60
	-4.1	0.0	0.0	b	60
	(-17.5	27.4	0.0)		274
Ca <sup>2+</sup> $\text{HPO}_4^{2-}$	-1.6	0.0	0.0	a	60
	-2.0	0.0	0.0	b	60
Na <sup>+</sup> $\text{PO}_4^{3-}$	0.17813	3.8513	-0.05154		51
K <sup>+</sup> $\text{PO}_4^{3-}$	0.37293	3.972	-0.08679		51
Mg <sup>2+</sup> $\text{PO}_4^{3-}$	-62.0	0.0	0.0	a	60
	-43.0	0.0	0.0	b	60
Ca <sup>2+</sup> $\text{PO}_4^{3-}$	-67.0	0.0	0.0	a	60
	-56.0	0.0	0.0	b	60
Species	$\theta_{aa}$	$\psi_{aa,Na}$	$\psi_{aa,K}$		
Cl <sup>-</sup> $\text{PO}_4^{3-}$	(-0.59	0.110)			274
Cl <sup>-</sup> $\text{HPO}_4^{2-}$	(-0.105	-0.003)			274
Cl <sup>-</sup> $\text{H}_2\text{PO}_4^-$	0.100	0.0	-0.010		51
	(0.107	-0.0147	-0.016)		105
	(0.100	-0.028)			274
Na <sup>+</sup> $\text{H}_2\text{PO}_4^- (\lambda_{00})$	0.075				274

*Note.* Values are of Kim and Frederick<sup>105</sup> and Hershey et al.,<sup>274</sup> ( ), not used here (see comments in text). Kim and Frederick<sup>105</sup> have also obtained estimates of  $\psi_{Ca,K,H_2PO_4^-}$ , but this is inconsistent with the  $\theta_{Ca,K}$  used throughout this work. Millero<sup>60</sup> has derived alternative values for Mg<sup>2+</sup> and Ca<sup>2+</sup> interactions with HPO<sub>4</sub><sup>2-</sup> and PO<sub>4</sub><sup>3-</sup> from the data of (a) Atlas et al.<sup>275</sup> and (b) Johansson and Wedborg.<sup>271</sup> Those of Johansson and Wedborg<sup>271</sup> were used here, where available.

pair formation. These two alternative approaches, applied to Mg<sup>2+</sup>-F<sup>-</sup> association in seawater, are discussed in more detail in Section III.D.3. More recently, Hershey et al.<sup>274</sup> have determined dissociation constants in aqueous NaCl and Na-Mg-Cl-H<sub>2</sub>O solutions to high ionic strengths, and used the results to estimate a number of interaction parameters. The parameters for interactions involving phosphates are listed in Table 38, drawn from the compilation of Plummer et al.<sup>60</sup> and more recent publications.

In natural waters, total phosphate is generally present at  $\leq 1 \mu\text{mol kg}^{-1}$ . In seawater, stoichiometric dissociation constants of phosphate have been determined by Kester and Pytkowicz,<sup>276</sup> Johansson and Wedborg,<sup>271</sup> and Dickson and Riley.<sup>272</sup> As can be seen from Table 38, the Pitzer model is quite poorly parameterized with respect to the various phosphate

species, especially in terms of mixture parameters  $\theta_{ij}$  and  $\psi_{ijk}$ , although these only make a small contribution to activity coefficients at seawater ionic strengths. Dickson and Riley<sup>272</sup> give the following equations for the dissociation of phosphoric acid in seawater as functions of concentration and temperature:



$${}^1K_{\text{H}_3\text{PO}_4}^* = -75/T + 2.16 - 0.35I_{\text{M}}^2 \quad (208b)$$



$${}^1K_{\text{HPO}_4}^* = 737.6/T + 4.176 - 0.851I_{\text{M}}^2 \quad (209b)$$



$${}^1K_{\text{PO}_4}^* = 2404/T + 1.31 - 0.87I_{\text{M}}^2 \quad (210b)$$

Equations 208 to 210 are valid from 5 to 30°C and 0.3 to 0.9 mol kg<sup>-1</sup> of seawater. These equations do not extrapolate to the infinite dilution values of the constants, which are as follows:  $K_{\text{H}_3\text{PO}_4} = 7.11 \times 10^{-3}$ ,  $K_{\text{HPO}_4} = 6.23 \times 10^{-8}$ , and  $K_{\text{PO}_4} = 4.55 \times 10^{-13}$  mol kg<sup>-1</sup>.<sup>276</sup> Note that the seawater ionic strengths are expressed in moles per kilogram of solution, and the molal concentration of total H<sup>+</sup> ion is defined as

$$m\text{H}_{\text{f}}^+ = m\text{H}_{\text{t}}^+ (1 + {}^1K_{\text{HSO}_4}^* m\text{SO}_{4(\text{f})}^{2-} + {}^1K_{\text{HF}}^* m\text{F}_{(\text{f})}) \quad (211)$$

where  $m\text{H}_{\text{f}}^+$  is the concentration of free hydrogen ion,  ${}^1K_{\text{HSO}_4}^*$  and  ${}^1K_{\text{HF}}^*$  are association constants of  $\text{HSO}_4^-$  and HF, respectively (on the basis of free H<sup>+</sup> ion and total anion), and  $m\text{SO}_{4(\text{f})}^{2-}$  and  $m\text{F}_{(\text{f})}$  the total concentrations of sulfate and fluoride. The stoichiometric dissociation constants of Johansson and Wedborg<sup>271</sup> are similarly defined, except that they exclude HF formation from  $m\text{H}_{\text{f}}^+$  (Equation 211). However, this makes only a small difference in calculations involving normal seawater.

Millero<sup>60</sup> has compared measured stoichiometric dissociation constants (total hydrogen ion basis) for phosphates in seawater at 35 S‰ with values calculated using the Pitzer model, including parameters listed in Table 38, and obtained reasonable agreement. Of the available stability constants for the formation of Mg<sup>2+</sup> and Ca<sup>2+</sup> ion pairs with  $\text{H}_3\text{PO}_4$ ,  $\text{HPO}_4^{2-}$ , and  $\text{PO}_4^{3-}$ , Millero<sup>60</sup> has used those of Atlas et al.<sup>273</sup> ( $\text{H}_3\text{PO}_4$ ) and Johansson and Wedborg<sup>271</sup> ( $\text{HPO}_4^{2-}$  and  $\text{PO}_4^{3-}$ ) to parameterize the Pitzer model ( $\beta^{(0)}$ ) for seawater at 25°C. The same values are used here.

The stoichiometric dissociation constants  ${}^1K^*$  (defined in Equations 208 to 210) at 25°C have been estimated as functions of seawater ionic strength using the model, to compare them with measured values. This was done as follows. Taking  ${}^1K_{\text{HPO}_4}^*$  as an example, the stoichiometric constant is related to the thermodynamic value by

$${}^1K_{\text{HPO}_4}^* = K_{\text{HPO}_4} \gamma_{\text{H}^+} \gamma_{\text{HPO}_4^{2-}} / (\gamma_{\text{H}_2\text{O}} \gamma_{\text{HPO}_4^{2-}}) \quad (212)$$

Using the  $\beta^{(0)}$  parameters for the interactions of phosphate anions with Mg<sup>2+</sup> and Ca<sup>2+</sup> means that the anion activity coefficients are obtained on a "total" basis, as required. For the H<sup>+</sup> ion the model yields the free ion activity coefficient  $\gamma_{\text{Hf}}^+$ , which is related to that on a total basis by

$$m\text{H}_{\text{f}}^+ \gamma_{\text{Hf}}^+ = m\text{H}_{\text{t}}^+ \gamma_{\text{Ht}}^+ \quad (213)$$



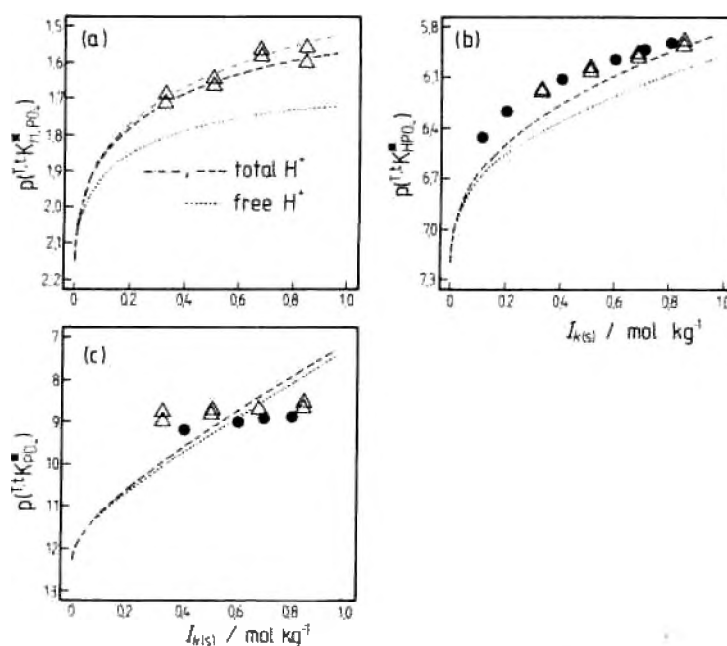


FIGURE 33. Stoichiometric dissociation constants  ${}^1K^*$  of phosphoric acid in a seawater medium at 25°C. Anion concentrations are total values. (a)  ${}^1K_{H_2PO_4}^*$ . Symbols — data of Dickson and Riley;<sup>272</sup> dashed line — calculated using Pitzer model with  $\gamma_{H_2PO_4} = 1$ ; dot/dash line — calculated using Pitzer model with  $\gamma_{H_2PO_4} = \exp(0.12I)$ ; dotted line — calculated dissociation constant on “free”  $H^+$  ion basis ( ${}^1K_{H_2PO_4}^*$ ). (b)  ${}^1K_{HPO_4}^*$ . Symbols: triangles — data of Dickson and Riley;<sup>272</sup> circles — data of Johansson and Wedborg;<sup>271</sup> dashed line — calculated using Pitzer model; dotted line — calculated dissociation constant on free  $H^+$  ion basis. (c)  ${}^1K_{PO_4}^*$ . Symbols: triangles — data of Dickson and Riley;<sup>272</sup> circles — data of Johansson and Wedborg;<sup>271</sup> dashed line — calculated using Pitzer model; dotted line — calculated dissociation constant on free  $H^+$  ion basis.

Hence, from Equation 211:

$$\gamma_{H_2F} / \gamma_{HF} = 1 / (1 + {}^1K_{HSO_4}^* mSO_{4(T)}^2 + {}^1K_{HF}^* mF_{(T)}) \quad (214)$$

We note that in calculating the terms in parenthesis in Equation 214, the concentration of total  $SO_4^{2-}$  is negligibly reduced by  $HSO_4^-$  formation in seawater. Also, since  ${}^1K_{HF}^*$  is expressed on the basis of total  $F^-$  concentration (free +  $MgF^+$  +  $CaF^+$ ), model parameters for  $Mg^{2+}$ - $F^-$  and  $Ca^{2+}$ - $F^-$  interactions must be used when estimating  ${}^1K_{HF}^*$  from the thermodynamic association constant and the activity coefficients of  $H^+$ ,  $F^-$ , and  $HF$  in the seawater medium. Using the relationships above, dissociation constants  ${}^1K^*$  were calculated as functions of seawater ionic strength, and are compared with measured values in Figure 33. For the first dissociation constant there is good agreement over the range of ionic strengths covered. Two estimates of  ${}^1K_{H_2PO_4}^*$  were made, first using  $\gamma_{H_2PO_4}$  equal to unity, and a second consistent with Millero's<sup>269</sup> assumption of  $\gamma_{H_2PO_4}$  equal to 1.09 at 35 S‰. Values of the dissociation constant on the basis of free  $H^+$ , but total  $H_2PO_4$  ( ${}^1K_{H_2PO_4}^*$ ), are also shown.

Similar comparisons of  ${}^1K_{HPO_4}^*$  and  ${}^1K_{PO_4}^*$  with the data of both Dickson and Riley<sup>272</sup> and Johansson and Wedborg,<sup>271</sup> appear in Figure 33c and d. At about  $I_{(s)} = 0.7 \text{ mol kg}^{-1}$  (solution) there is reasonable agreement, considering the uncertainties concerning the strength of the interactions of the phosphate anions with  $Mg^{2+}$  and  $Ca^{2+}$ , but at lower ionic strengths

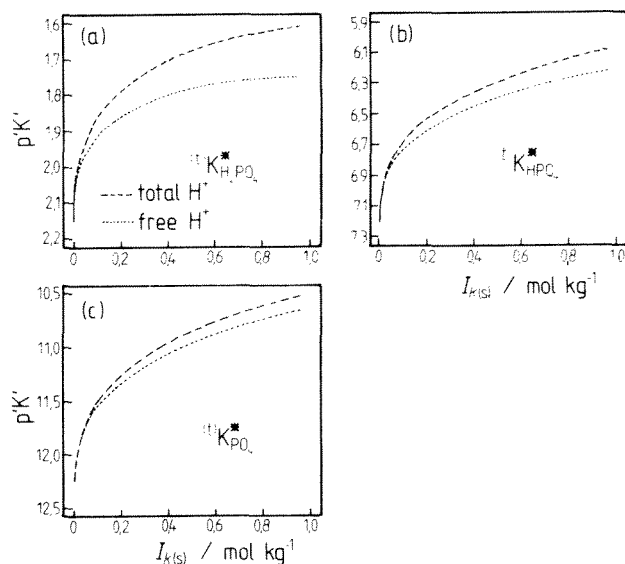


FIGURE 34. Stoichiometric dissociation constants  ${}^{\circ}K^*$  of phosphoric acid, on a free ion basis (the three phosphate anions), in a seawater medium at 25°C. (a)  $K_{H_2PO_4}^*$ ; (b)  $K_{HPO_4}^*$ ; (c)  $K_{PO_4}^*$ . Lines: dashed — calculated using Pitzer model with  $\gamma_{H_2PO_4} = 1$  on a total “H<sup>+</sup>” ion basis ( ${}^{\circ}K^*$ ); dotted — for “free” H<sup>+</sup> concentration ( ${}^{\circ}K^*$ ).

the differences between measured and calculated values become much greater. In particular, the variation with ionic strength of  ${}^{\circ}K_{PO_4}^*$  appears unrealistic, and is related to the way in which  $\beta_{MgPO_4}^{(0)}$  and  $\beta_{CaPO_4}^{(0)}$  are estimated. From Equation 31 of Millero<sup>60</sup> it can be seen that  $\ln(mAnion_{(F)}/mAnion_{(I)})$  is treated as being linearly related to  $mMg^{2+}$  (or  $mCa^{2+}$ ) in solution — hence the form of  $p({}^{\circ}K_{PO_4}^*)$  in Figure 33c where these very strong interactions dominate all other effects. This is unlikely to be realistic, and the parameters should only be considered valid close to normal seawater ionic strength. For practical calculations involving  ${}^{\circ}K_{HPO_4}^*$  and  ${}^{\circ}K_{PO_4}^*$ , the measured constants of Dickson and Riley<sup>272</sup> or Johansson and Wedborg<sup>271</sup> should be used in preference to a model parameterization of their effects.

The results shown in Figure 33 were obtained using the Pitzer model without the interaction parameters determined by Hershey et al.,<sup>274</sup> as these are optimized for high ionic strength solutions. Test calculations using this parameter set yielded estimates of the stoichiometric dissociation constants in seawater in much poorer agreement with measured values than those shown in the figure. Use of those mixture parameters determined for Na-Cl- $H_3PO_4$ - $H_2O$  solutions only (given in Table 38) yielded a small improvement in the calculated  ${}^{\circ}K_{HPO_4}^*$  — an increase of about 0.075 log units. While Hershey et al.<sup>274</sup> obtained  $\lambda_{Na,H_3PO_4}$  equal to 0.075 (currently the only available estimate), for calculations in seawater media a value of about 0.03 gives the best agreement with the measured  ${}^{\circ}K_{H_2PO_4}^*$ .

Stoichiometric dissociation constants on the basis of free anion concentrations have also been calculated (Figure 34), so that these may be combined with new estimates of association constants (with  $Mg^{2+}$  and  $Ca^{2+}$ ), as available. Again taking the second dissociation constant as an example,

$$K_{HPO_4}^* = \frac{mH_{(F)}^+ mHPO_{4(F)}^{2-}}{mH_{2(4F)}PO_4} = K_{HPO_4} \gamma_{H_2PO_4(F)} / \gamma_{H(F)} \gamma_{HPO_4(F)} \quad (215)$$

We also have for each anion:

$$m\text{H}_2\text{PO}_{4(\text{F})} \gamma_{\text{H}_2\text{PO}_{4(\text{F})}} = m\text{H}_2\text{PO}_{4(\text{T})} \gamma_{\text{H}_2\text{PO}_{4(\text{T})}} \quad (216)$$

$$m\text{HPO}_{4(\text{F})}^{2-} \gamma_{\text{HPO}_{4(\text{F})}^{2-}} = m\text{HPO}_{4(\text{T})}^{2-} \gamma_{\text{HPO}_{4(\text{T})}^{2-}} \quad (217)$$

Total anion concentrations are related to the "free" values by:

$$m\text{H}_2\text{PO}_{4(\text{T})} = m\text{H}_2\text{PO}_{4(\text{F})} (1 + K_{\text{MgH}_2\text{PO}_4}^* m\text{Mg}^{2+} + K_{\text{CaH}_2\text{PO}_4}^* m\text{Ca}^{2+}) \quad (218)$$

$$m\text{HPO}_{4(\text{T})}^{2-} = m\text{HPO}_{4(\text{F})}^{2-} (1 + K_{\text{MgHPO}_4}^* m\text{Mg}^{2+} + K_{\text{CaHPO}_4}^* m\text{Ca}^{2+}) \quad (219)$$

Thus the stoichiometric dissociation constant on a free ion basis ( $K_{\text{HPO}_4}^*$ ) is related to that on the "total" scale ( ${}^tK_{\text{HPO}_4}^*$ ) by

$$\begin{aligned} {}^tK_{\text{HPO}_4}^* &= K_{\text{HPO}_4}^* (1 + {}^tK_{\text{HSO}_4}^* m\text{SO}_{4(\text{T})}^{2-} + {}^tK_{\text{HF}}^* m\text{F}_{(\text{T})}^-) \\ &\quad \times (1 + K_{\text{MgHPO}_4}^* m\text{Mg}^{2+} + K_{\text{CaHPO}_4}^* m\text{Ca}^{2+}) \\ &\quad / (1 + K_{\text{MgH}_2\text{PO}_4}^* m\text{Mg}^{2+} + K_{\text{CaH}_2\text{PO}_4}^* m\text{Ca}^{2+}) \end{aligned} \quad (220)$$

Free ion activity coefficients of dissolved phosphate species in seawater, calculated as a function of salinity, are listed in Appendix Table A11.

#### f. Hydrogen Sulfide

The solubility of  $\text{H}_2\text{S}$  in water and seawater has been measured by Douabul and Riley<sup>277</sup> (2 to 30°C, 0 to 40 S‰), and the results presented in the form of the Weiss equation. Millero<sup>278</sup> gives the following equation for the Henry's law constant  $K_{\text{H}}$  (mol kg<sup>-1</sup> atm<sup>-1</sup>), from 25 to 260°C, based on the work of Clarke and Glew:<sup>279</sup>

$$\log_{10}(K_{\text{H}}) = -102.325 + 4423.11/T + 36.6296(\log_{10} T) + 0.1387 T \quad (221)$$

The more recent measurements of Carrol and Mather<sup>280</sup> are in satisfactory agreement with Equation 221 above. Pure water solubilities of Douabul and Riley<sup>277</sup> are slightly higher than those of other workers, and deviate from the results of Carroll and Mather<sup>280</sup> by 1 to 4%. From the measured seawater solubilities, it would appear that  $\gamma_{\text{H}_2\text{S}}$  is little different from unity in this medium; Millero<sup>278</sup> estimated a salting coefficient  $k_{\text{H}_2\text{S}}$  (such that  $\log_{10}(\gamma_{\text{H}_2\text{S}}) = k_{\text{H}_2\text{S}}/f_{\text{H}_2\text{S}}$ ) for  $\text{H}_2\text{S}$  of 0.02, much lower than the value of 0.121 for  $\text{O}_2$ , for example. We have used the original data of Douabul and Riley<sup>277</sup> to determine  $\gamma_{\text{H}_2\text{S}}$  as a function of temperature and salinity, given by the following equation:

$$\ln(\gamma_{\text{H}_2\text{S}}) = 2m_{\text{cs}}\lambda_{\text{H}_2\text{S}(\text{s})} + m_{\text{ca}}m_{\text{sa}}\zeta_{\text{H}_2\text{S}(\text{s})} \quad (222)$$

$$\lambda_{\text{H}_2\text{S}(\text{s})} = 2.03276 - 0.012837 T + 0.00002043 T^2 \quad (223)$$

$$\zeta_{\text{H}_2\text{S}(\text{s})} = -0.0294777 \quad (224)$$

where  $m_{\text{cs}}$  is the molality of sea salt, defined in Equation 18, and  $m_{\text{ca}}$  and  $m_{\text{sa}}$  the molalities of cations (0.484334 $m_{\text{cs}}$ ) and anions (0.515662 $m_{\text{cs}}$ ), respectively. (Note the factor of 2

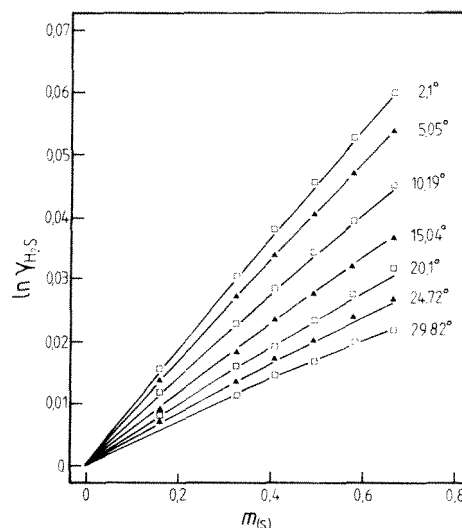
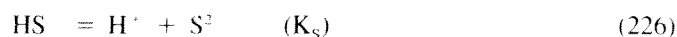
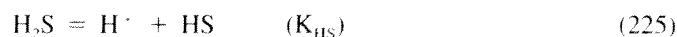


FIGURE 35. Measured and fitted activity coefficients of  $\text{H}_2\text{S}$  in seawater as functions of concentration and temperature. Symbols — from data of Douabul and Riley;<sup>277</sup> lines — fitted values (Equations 222 to 224).

difference from values used in the corresponding Equations 94 to 98 for  $\text{O}_2$  solubility.) The results of the fit are shown in Figure 35. It is of some interest to compare these values with activity coefficients in pure aqueous NaCl, both because NaCl is the principal component of sea salt and because  $\gamma_{\text{H}_2\text{S}}$  in  $\text{NaCl}_{\text{aq}}$  has been used by Millero<sup>278</sup> and Hershey et al.<sup>281</sup> in their studies of the first dissociation constant of  $\text{H}_2\text{S}$  in ionic media. Hydrogen sulfide solubilities in NaCl solutions have been measured by Gamsjager and Schindler<sup>282</sup> (0.51 to 3.20  $m\text{NaCl}$ , 25°C), Barrett et al.<sup>283</sup> (1 to 5  $m\text{NaCl}$ , 25 to 95°C), and Barta and Bradley<sup>97</sup> (0 to 6  $m\text{NaCl}$ , 25 to 350°C). Barta and Bradley<sup>97</sup> apply a form of the Pitzer model to their results, in which parameters  $\Delta_{\text{Na,H}_2\text{S,Cl}}$  and  $\chi_{\text{Na,H}_2\text{S,Cl}}$  are directly equivalent to  $\lambda_{\text{H}_2\text{S,Na}}$  and  $(1/3)\zeta_{\text{H}_2\text{S,Na,Cl}}$ , respectively. The results of Barta and Bradley are in reasonable agreement with those of Barrett et al.<sup>283</sup> at 60°C and above, but anomalously low (as equilibrium  $m\text{H}_2\text{S}$ ) at 25°C.<sup>283</sup> In Figure 36 we compare  $\gamma_{\text{H}_2\text{S}}$  at 25°C determined by Gamsjager and Schindler<sup>282</sup> and Barrett et al.,<sup>283</sup> together with  $\gamma_{\text{H}_2\text{S}}$  in seawater for  $m_{\text{Cl}}$  equal to  $m\text{NaCl}$ . The fitted line through the data of Gamsjager and Schindler<sup>282</sup> was determined by Hershey et al.<sup>281</sup> These results yield model interaction parameters  $\lambda_{\text{H}_2\text{S,Na}}$  equal to 0.0777 and  $\zeta_{\text{H}_2\text{S,Na,Cl}}$  equal to -0.00806 (with  $\lambda_{\text{H}_2\text{S,Cl}}$  set to zero). It is clear from the figure that while the two data sets for NaCl are in moderate agreement,  $\gamma_{\text{H}_2\text{S}}$  in seawater is extremely low considering the fact that NaCl constitutes some 90% of sea salt. Without further measurements in seawater media it does not appear possible to resolve this discrepancy directly. The data of Douabul and Riley<sup>277</sup> must be considered doubtful.

Hydrogen sulfide undergoes a two-stage dissociation in solution:



In natural waters at normal pH (6 to 9) the formation of  $\text{S}^{2-}$  may be neglected ( $\text{p}K_{\text{S}}$  is equal to at least 14.6,<sup>278</sup> with an even higher value probable<sup>284</sup>). The value of the first dissociation constant is given by<sup>281</sup>

$$\log_{10}(K_{\text{H}_2\text{S}}) = 98.08 - 5765.4/T - 15.00455(\ln T) \quad (227)$$

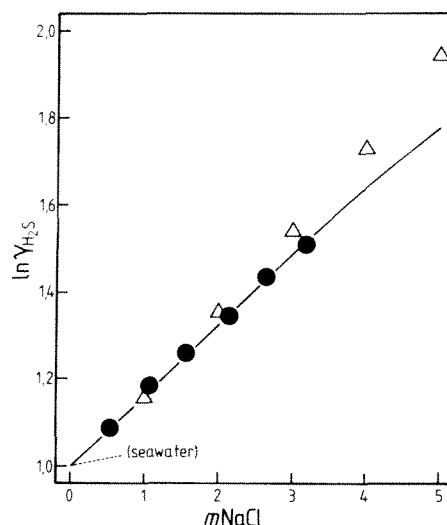


FIGURE 36. Activity coefficients of H<sub>2</sub>S in pure aqueous NaCl at 25°C. Symbols: circles — data of Gamsjager and Schindler;<sup>282</sup> triangles — tabulated values of Barrett et al.;<sup>283</sup> full line — equation of Hershey et al.;<sup>281</sup> dotted line — activity coefficients in seawater (for  $m_{(s)} = m\text{NaCl}$ ) from Equations 222 to 224.

where  $T/K$  and the equation is valid from 0 to 300°C. The stoichiometric value of the dissociation constant on the molality (mol kg<sup>-1</sup> seawater) scale has been determined by Millero<sup>285</sup> as a function of salinity (5 to 40 S‰) from 5 to 25°C:

$$p^T K_{\text{HS}}^* = pK_{\text{HS}} - 0.1498 S^{1/2} + 0.0119 S \quad (228)$$

To convert dissociation constants obtained from Equation 228 to the molal scale, multiply by the factor  $1/(1 - 0.001005 S)$ . The constant  ${}^T K_{\text{HS}}^*$  is on the total hydrogen ion pH scale, thus in molal units

$${}^T K_{\text{HS}}^* = m\text{H}_{(\text{T})}^+ m\text{HS}_{(\text{T})}^- / m\text{H}_2\text{S} \quad (229)$$

For HS<sup>-</sup> and H<sub>2</sub>S the meaning of the “total” concentrations is straightforward; for H<sup>+</sup> the total concentration is again related to the free hydrogen ion concentration by

$$m\text{H}_{(\text{T})}^+ = m\text{H}_{(\text{F})}^+ + m\text{HSO}_4^- + m\text{HF} \quad (230)$$

where the species concentrations are estimated from the stoichiometric stability constants (see Equation 211).

Hershey et al.<sup>281</sup> and earlier Millero<sup>278</sup> have determined  $K_{\text{HS}}^*$  of H<sub>2</sub>S in NaCl, KCl, and their mixtures with MgCl<sub>2</sub> and CaCl<sub>2</sub>, to determine model interaction parameters for these major seawater ions with HS<sup>-</sup>. These are listed in Table 39. Note that these values are to some degree dependent upon the (assumed) relationship of  $\gamma_{\text{H}_2\text{S}}$  with ionic strength obtained from solubilities in aqueous NaCl solutions (Equation 18, Hershey et al.<sup>281</sup>).

Hershey et al.<sup>281</sup> have compared  ${}^T K_{\text{HS}}^*$  in seawater, as measured by Millero et al.,<sup>285</sup> with that calculated using the Pitzer model and obtain agreement to within 0.02 pK<sub>HS</sub><sup>\*</sup> units. Using the parameters listed in Table 39, we have also calculated  ${}^T K_{\text{HS}}^*$  (molal concentrations) for comparison with the measurements of Millero et al.<sup>285</sup> which were used to parameterize

**TABLE 39**  
**Ion-Ion Interaction Parameters Involving**  
**HS<sup>-</sup> at 25°C<sup>281</sup>**

Species		$\beta^{(0)}$	$\beta^{(1)}$	$C^\phi$
Na <sup>+</sup>	HS	0.1396	0.0	-0.0127
K <sup>+</sup>	HS	0.1674	0.0	-0.0194
Mg <sup>2+</sup>	HS	0.17	2.78	0.0
Ca <sup>2+</sup>	HS	-0.105	3.43	0.0

*Note:* The activity coefficient of undissociated H<sub>2</sub>S in pure aqueous NaCl is given by:  $\ln(\gamma_{\text{H}_2\text{S}}) = [(0.1554 - 0.00806I) - 0.002532(t - 25) + 3.1984 \times 10^{-5}(t^2 - 625)]/t$ , where  $t$  is in centigrade. This equation also yields  $\lambda_{\text{Na,H}_2\text{S}} = 0.0777$  and  $\zeta_{\text{H}_2\text{S,NaCl}} = -0.00806$  at 25°C. Equations 222—224 in the text give  $\gamma_{\text{H}_2\text{S}}$  in seawater, but the result appears to be inconsistent with the NaCl values. Pure electrolyte parameters  $\beta^{(0)}$  for NaHS and KHS are given as functions of temperature by:  $\beta_{\text{Na,HS}}^{(0)} = 0.366 - 67.5/T$ ,  $\beta_{\text{K,HS}}^{(0)} = 0.637 - 140/T$ .

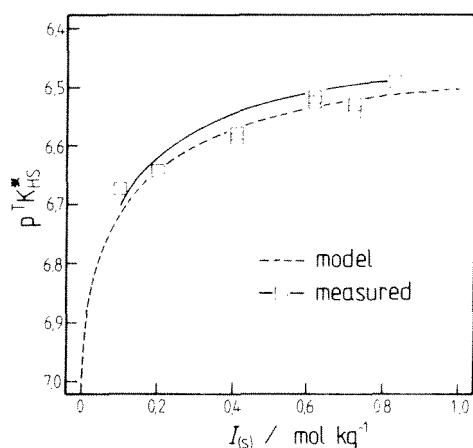


FIGURE 37. Stoichiometric dissociation constant of H<sub>2</sub>S ( ${}^1K_{\text{HS}}^*$ ) in seawater at 25°C. Symbols — data of Millero et al.<sup>285</sup> (converted to molal units); dashed line — calculated using the Pitzer model and a thermodynamic value of the dissociation constant of  $1.046 \times 10^{-7}$  mol kg<sup>-1</sup>; full line — fitted equation of Millero et al.<sup>285</sup> (Equations 227 and 228), again converted to molal units.

Equation 228. Two different sets of activity coefficients of undissociated H<sub>2</sub>S were used in the calculations: first, those given by Equations 222 to 224, from the seawater solubilities measured by Douabul and Riley,<sup>227</sup> and second, values based on solubilities in pure aqueous NaCl (see Table 39 for equation) for which it was assumed that  $m_{\text{Na}} \equiv I$  (in aqueous NaCl). The latter approach yielded better agreement with measured  ${}^1K_{\text{HS}}^*$ , suggesting that activity coefficients derived from the data of Douabul and Riley<sup>227</sup> are indeed too low, and that aqueous NaCl is a satisfactory analog of seawater. Measured and predicted  ${}^1K_{\text{HS}}^*$  at 25°C are shown in Figure 37, together with values calculated using Equation 228. The Pitzer model, together with a thermodynamic  $K_{\text{HS}}$  equal to  $1.046 \times 10^{-7}$  mol kg<sup>-1</sup>, yields stoichiometric dissociation constants in excellent agreement with measured values. Comparisons by Hershey et al.<sup>281</sup> down to 5°C are similarly satisfactory.

*g. Sulfur Dioxide*

Sulfur dioxide is a precursor of atmospheric  $\text{H}_2\text{SO}_4$ , which is formed by the (largely aqueous phase) oxidation of  $\text{SO}_2$ , which is highly soluble. Sulfur dioxide dissociates on dissolution in aqueous solution to form sulfite and bisulfite:



The following stoichiometric constants can be defined and related to the thermodynamic constants ( $K_{\text{HSO}_3}$  and  $K_{\text{SO}_3}$ ) above:

$$K_{\text{HSO}_3}^* = m\text{H}^+ m\text{HSO}_3^- / m\text{SO}_{2(\text{T})} = K_{\text{HSO}_3} (a_{\text{H}_2\text{O}} \gamma_{\text{SO}_{2(\text{T})}} / \gamma_{\text{H}} \gamma_{\text{HSO}_3}) \quad (233)$$

$$K_{\text{SO}_3}^* = m\text{H}^+ m\text{SO}_3^{2-} / m\text{HSO}_3^- = K_{\text{SO}_3} (\gamma_{\text{HSO}_3} / \gamma_{\text{H}} \gamma_{\text{SO}_3}) \quad (234)$$

where  $m\text{SO}_{2(\text{T})}$  is equal to  $m\text{SO}_2 + m\text{H}_2\text{SO}_3$ . Millero et al.<sup>286</sup> have determined values of  $K_{\text{HSO}_3}^*$  and  $K_{\text{SO}_3}^*$  in aqueous NaCl at 5 and 25°C. The variation of both  $K_{\text{HSO}_3}^*$  and  $K_{\text{SO}_3}^*$  with ionic strength appears to be independent of temperature within this range. Results extrapolated to zero ionic strength agree closely with thermodynamic values of the equilibrium constants, determined by Goldberg and Parker,<sup>287</sup> so that the variation of  $\text{p}K_{\text{HSO}_3}^*$  and  $\text{p}K_{\text{SO}_3}^*$  can be described (from 5 to 25°C) by the equations

$$\text{p}K_{\text{HSO}_3}^* = \text{p}K_{\text{HSO}_3} - 0.485I^{1/2} + 0.3I \quad (235a)$$

where

$$\ln(K_{\text{HSO}_3}) = 554.963 - 16700.1/T - 93.67(\ln T) + 0.1022 T \quad (235b)$$

$$\text{p}K_{\text{SO}_3}^* = \text{p}K_{\text{SO}_3} - 1.052I^{1/2} + 0.36I \quad (236a)$$

where

$$\ln(K_{\text{SO}_3}) = -358.57 + 5477.1/T + 65.31(\ln T) - 0.1624 T \quad (236b)$$

Solubility data for  $\text{SO}_2$ ,<sup>288</sup> in both seawater and aqueous NaCl, prior to the work of Millero et al.<sup>286</sup> appear to be of doubtful quality. While Douabul and Riley<sup>289</sup> have determined  $\text{SO}_2$  solubilities in seawater, their salting coefficients appear to be anomalously low<sup>286</sup> in much the same way as those for  $\text{H}_2\text{S}$  (see previous section). Consequently, for calculations involving seawater, activity coefficients will be assumed to be the same as those in aqueous NaCl at the same total molality. Millero et al.<sup>286</sup> obtained the following relationship for the solubility of total  $\text{SO}_2$  ( $m\text{SO}_{2(\text{T})}$ ) in aqueous NaCl to 6 mol  $\text{kg}^{-1}$  NaCl:

$$\log_{10}(m\text{SO}_{2(\text{T})}) = \log_{10}(m\text{SO}_{2(\text{T})}^0) + (-0.0997 + 22.3T)I \quad (237)$$

where  $m\text{SO}_{2(\text{T})}^0$  is the equilibrium solubility in pure water, related to the apparent Henry's law constant  $K_{\text{H}}'$  (determined by Goldberg and Parker<sup>287</sup>) by

$$m\text{SO}_{2(\text{T})}^0 = \text{pSO}_2 K_{\text{H}}' \quad (238a)$$

where

$$\ln(K_{\text{H}}') = -142.679 + 8988.76/T + 19.8967(\ln T) - 0.0021 T \quad (238b)$$

**TABLE 40**  
**Ion-Ion Interaction Parameters Involving**  
**HSO<sub>3</sub><sup>-</sup> and SO<sub>3</sub><sup>2-</sup> Ions at 25°C<sup>286</sup>**

Species		$\beta^{(0)}$	$\beta^{(1)}$	$C^{\phi}$
Na <sup>+</sup>	HSO <sub>3</sub> <sup>-</sup>	0.1527	0.3197	-0.02459
Na <sup>+</sup>	SO <sub>3</sub> <sup>2-</sup>	0.08015	1.185	-0.00434
		$\theta_{\text{Cl},\text{SO}_3}$	$\psi_{\text{Na},\text{Cl},\text{SO}_3}$	
Cl <sup>-</sup>	SO <sub>3</sub> <sup>2-</sup>	0.099	-0.0156	

*Note:* Parameters for Na<sub>2</sub>SO<sub>3</sub> at 25°C are same as those of Kim and Frederick.<sup>105</sup> Parameters for interaction of Mg<sup>2+</sup> and Ca<sup>2+</sup> with SO<sub>3</sub><sup>2-</sup> and HSO<sub>3</sub><sup>-</sup> were assumed by Millero et al.<sup>286</sup> to be the same as those for SO<sub>4</sub><sup>2-</sup> and HSO<sub>4</sub><sup>-</sup> (e.g., see Pitzer,<sup>51</sup> Chapter 3, this volume). Model parameters for Na<sub>2</sub>SO<sub>3</sub> and NaHSO<sub>3</sub> are the following functions of temperature:

$$\begin{aligned} \text{Na}_2\text{SO}_3: \\ \beta^{(0)} &= 5.88444 - 1730.55/T, \\ \beta^{(1)} &= -19.4549 + 6153.78/T \\ C^{\phi} &= -1.2355 + 367.07/T \end{aligned}$$

$$\begin{aligned} \text{NaHSO}_3: \\ \beta^{(0)} &= 4.3407 - 1248.66/T, \\ \beta^{(1)} &= -13.146 + 4014.80/T \\ C^{\phi} &= -0.9565 + 277.85/T \end{aligned}$$

The activity coefficient of SO<sub>2(aq)</sub> in the aqueous phase may be derived from the solubility relationships given in the text (Equation 239).

The empirical representation of solubility in Equations 237 and 238 has not been used to estimate Pitzer model parameters, as this would require both fugacity corrections to be considered and probably some estimate of the self-interaction of SO<sub>2</sub> in solution, since the solubility is about 1 mol kg<sup>-1</sup> for an experimental partial pressure of 1 atm. The effective activity coefficient for total SO<sub>2</sub> in aqueous solution is given by

$$\log_{10}(\gamma_{\text{SO}_2(\text{aq})}) = \log_{10}(m\text{SO}_{2(\text{CT})}^{\circ}/m\text{SO}_{2(\text{CT})}) = (0.0997 - 22.3/T)I \quad (239)$$

To assist more generalized calculations, Millero et al.<sup>286</sup> have determined model parameters for the interaction of HSO<sub>3</sub><sup>-</sup> and SO<sub>3</sub><sup>2-</sup> with Na<sup>+</sup> (including ternary terms  $\theta_{\text{Cl},\text{SO}_3}$  and  $\psi_{\text{Na},\text{Cl},\text{SO}_3}$  for NaCl solutions) as functions of temperature (see Table 40). The results, including values of  $\gamma_{\text{SO}_2(\text{aq})}$  estimated from Equation 239, can be used to satisfactorily reproduce the values of the stoichiometric dissociation constants in aqueous NaCl.<sup>286</sup>

What of more complex natural waters, such as seawater? The principal additional interactions that need to be considered, to determine activity coefficients of SO<sub>3</sub><sup>2-</sup> and HSO<sub>3</sub><sup>-</sup>, are with Mg<sup>2+</sup> and Ca<sup>2+</sup>. At present there appear to be no data available from which to estimate their values. However, in view of the rough similarity between Na<sup>+</sup> interactions with HSO<sub>4</sub><sup>-</sup> and SO<sub>4</sub><sup>2-</sup>, and HSO<sub>3</sub><sup>-</sup> and SO<sub>3</sub><sup>2-</sup>, Millero et al.<sup>286</sup> have suggested setting the unknown Mg<sup>2+</sup> and Ca<sup>2+</sup> interaction parameters (with HSO<sub>3</sub><sup>-</sup> and SO<sub>3</sub><sup>2-</sup>) to the values for



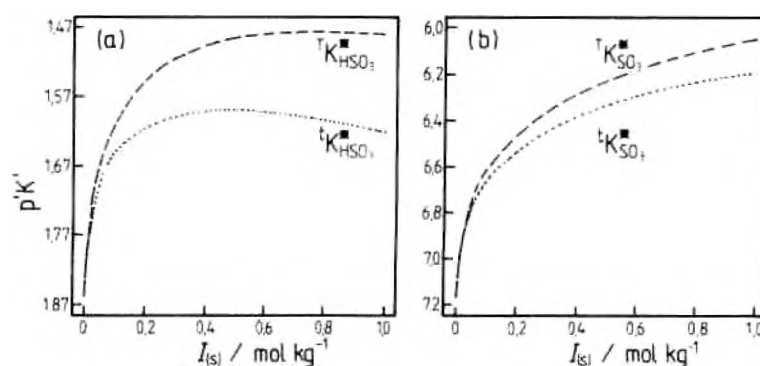


FIGURE 38. Stoichiometric dissociation constants of  $\text{SO}_2$  in seawater at  $25^\circ\text{C}$ , calculated on both a "free"  $\text{H}^+$  ( ${}^t\text{K}_{\text{HSO}_3^-}^*$  and  ${}^t\text{K}_{\text{SO}_3^{2-}}^*$ ) and "total"  $\text{H}^+$  ( ${}^t\text{K}_{\text{HSO}_3^-}^*$  and  ${}^t\text{K}_{\text{SO}_3^{2-}}^*$ ) basis, using the Pitzer model with parameters for  $\text{HSO}_3^-$  and  $\text{SO}_3^{2-}$  interactions given in Table 34 (a) First dissociation (Equation 233); (b) second dissociation (Equation 234).

the corresponding S(VI) anions in order to estimate dissociation constants in natural brines. Comparisons with single measurements of  $\text{pK}_{\text{HSO}_3^-}^*$  and  $\text{pK}_{\text{SO}_3^{2-}}^*$  in seawater at  $25^\circ\text{C}$  confirm that this substitution gives reasonable results. Calculated values of the two dissociation constants in seawater at  $25^\circ\text{C}$  are shown in Figure 38.

#### h. Ion Product of Water in Seawater

Dickson and Riley<sup>268</sup> have measured the ion product of water in seawater over a range of temperature and salinity on a total (SWS) pH scale such that, in molal units,

$${}^t\text{K}_{\text{H}_2\text{O}}^* = m\text{H}_{(\text{T})}^+ m\text{OH}_{(\text{T})}^- \quad (240)$$

where:

$$m\text{H}_{(\text{T})}^+ = m\text{H}_{(\text{F})}^+ + m\text{HSO}_3^- + m\text{HF} \quad (241)$$

$$m\text{OH}_{(\text{T})}^- = m\text{OH}_{(\text{F})}^- + m\text{MgOH}^+ + m\text{CaOH}^+ + m\text{SrOH}^+ \quad (242)$$

Dickson and Riley<sup>268</sup> have compared their results with earlier measurements of Culberson and Pytkowicz<sup>269</sup> and also Hansson.<sup>291</sup> While small systematic differences were evident, the variation of  ${}^t\text{K}_{\text{H}_2\text{O}}^*$  with temperature and salinity was found to be similar in the three studies.

Within the context of the Pitzer model, the formation of  $\text{HSO}_3^-$ ,  $\text{HF}$ , and  $\text{MgOH}^+$  are treated explicitly, while the influence of  $\text{Ca}^{2+}$  and  $\text{Sr}^{2+}$  upon  $\text{OH}^-$  activity is treated as an interaction between the free ions at  $25^\circ\text{C}$ . For seawater media the greatest obstacle to direct calculations of  $\text{K}_{\text{H}_2\text{O}}^*$  (on any scale) for temperatures other than  $25^\circ\text{C}$  lies in the lack of information concerning the temperature variability of  $\text{MgOH}^+$  formation, which accounts for a large proportion of total  $\text{OH}^-$  in seawater.

We have calculated  ${}^t\text{K}_{\text{H}_2\text{O}}^*$  in seawater as

$$\text{K}_{\text{H}_2\text{O}}^* a\text{H}_2\text{O} / (\gamma_{\text{H}^+} \gamma_{\text{OH}^-}) \quad (243)$$

where the total activity coefficients  $\gamma_{\text{H}^+}$  and  $\gamma_{\text{OH}^-}$  take into account  $\text{HSO}_3^-$ ,  $\text{MgOH}^+$ , and  $\text{HF}$  formation, using the seawater recipe of Dickson and Riley.<sup>268</sup> Results at  $25^\circ\text{C}$  are shown in Figure 39 together with calculated concentrations of free and associated  $\text{H}^+$  and  $\text{OH}^-$  for a solution in which  $m\text{H}_{(\text{F})}^+ = m\text{OH}_{(\text{F})}^-$ . It is clear that the Pitzer model calculations are

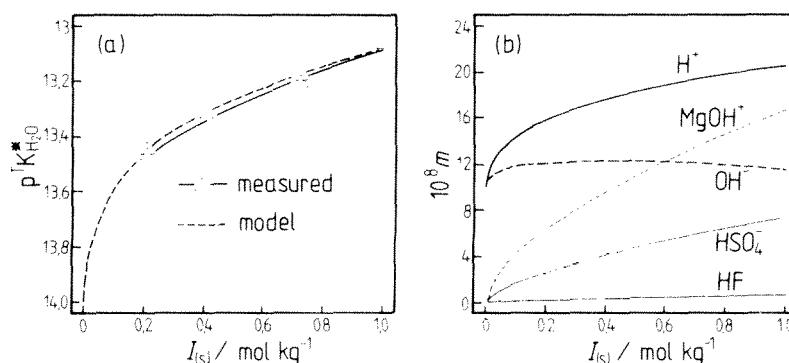


FIGURE 39. (a) Comparison of measured and calculated ionic product of water ( ${}^1K_{\text{H}_2\text{O}}^*$ ) in artificial seawater at 25°C. Symbols — data of Dickson and Riley;<sup>268</sup> full line — empirical fitting equation of Dickson and Riley; dashed line — calculated using the Pitzer model. (b) Calculated species concentrations of free and associated  $\text{H}^+$  and  $\text{OH}^-$  as a function of seawater ionic strength at 25°C.

in excellent agreement with the data, and are likely to provide reliable estimates of  ${}^1K_{\text{H}_2\text{O}}^*$  to zero salinity (which the empirical fitting equation of Dickson and Riley<sup>268</sup> does not do). The calculated species concentrations shown in Figure 39 confirm the importance of the  $\text{Mg}^{2+}$ - $\text{OH}^-$  interaction in determining the ionic product of water.

Comparisons of calculated and measured  ${}^1K_{\text{H}_2\text{O}}^*$  for  $T \neq 298 \text{ K}$  showed positive errors at 5, 10, and 15°C (i.e., calculated  ${}^1K_{\text{H}_2\text{O}}^*$  too great), but negative errors at 35°C. Since the  $\text{H}^+$ - $\text{HSO}_4^-$  equilibrium and ion-ion interactions (opposite sign) are quite well parameterized as functions of temperature, it is likely that these systematic deviations are chiefly due to the fact that a constant  $K_{\text{MgOH}}$  ( $154 \text{ kg mol}^{-1}$ <sup>56</sup>) is used. To aid model calculations of the ionic product of water over a range of temperatures, we have fitted  $K_{\text{MgOH}}$  as a function of temperature [ $\ln(K_{\text{MgOH}}) \propto 1/T$ ] to obtain optimum agreement between measured and calculated  ${}^1K_{\text{H}_2\text{O}}^*$  from 5 to 35°C, with the following result:

$$\ln(K_{\text{MgOH}}) = -1155/T + 8.9108 \quad (244)$$

Use of this equation yields a calculated  ${}^1K_{\text{H}_2\text{O}}^*$  in excellent agreement with the data of Dickson and Riley<sup>268</sup> at all temperatures. Since all differences between measured and calculated  ${}^1K_{\text{H}_2\text{O}}^*$  at  $T \neq 25^\circ\text{C}$  have been subsumed into  $K_{\text{MgOH}}$ , use of Equation 244 should be restricted to calculations of the ion product of water in saline solutions.

#### D. COMPLEXATION OF TRACE SPECIES IN NATURAL WATERS

Complex formation in solutions of single electrolytes (such as pure aqueous  $\text{ZnCl}_2$ ,  $\text{CuCl}$ , and  $\text{H}_3\text{PO}_4$ ), and the activity coefficients of the various species that arise, have been reviewed by Zemaitis et al.<sup>63</sup> These authors also consider methods of identifying complex formation in aqueous solution, and the application of activity coefficient models to describing their behavior. They conclude that, over the range of attainable temperatures and pressures, most electrolytes form complexes in pure solution or with other compounds dissolved in water. It has been shown earlier that these effects can be treated as strong interactions between free ions, where ion pairing or complex formation is not too great. For example, this is the case for ion pair formation in solutions of bivalent metal sulfates,<sup>292</sup> and dissociation to produce  $\text{HPO}_4^-$  and  $\text{PO}_4^{2-}$  in pure aqueous  $\text{H}_3\text{PO}_4$  (for which only the first dissociation is treated explicitly using the Pitzer model).<sup>59</sup> Millero<sup>60</sup> has presented Pitzer model parameters that enable the effects of numerous acid-base equilibria on trace component activities to be simply calculated, although their validity is mostly restricted to 25°C and  $\approx 35 \text{ S\%}$ .

Metals belonging to the transition series and the B subgroups of the periodic table form relatively strong complexes ( $K > 20 \text{ kg mol}^{-1}$ ) with  $\text{Cl}^-$ ,  $\text{OH}^-$ ,  $\text{HCO}_3^-$ , and  $\text{CO}_3^{2-}$ . Thus, it is impossible to calculate the total activity coefficients of these constituents in natural waters without an extensive consideration of chemical equilibria. The metals are also present at such low concentrations ( $10^{-7} \text{ mol kg}^{-1}$  or less) that the complexes they form will have a negligible effect on the concentrations of the major components. Against this constant ionic background, we can define for the reaction between metal M and ligand L



a parameter,  $\sigma_{\text{L},n}$ , such that

$$\sigma_{\text{L},n} = K_{\text{ML}_n}^* m\text{L}^n = m\text{ML}_n/m\text{M}_{\text{TF}} \quad (246)$$

where  $K_{\text{ML}_n}^*$  is the overall stoichiometric formation constant, and  $m\text{M}_{\text{TF}}$  is the concentration of free, uncomplexed metal. The percentage of metal present as  $\text{ML}_n$  is given by

$$\%(\text{ML}_n) = 100 \times m\text{ML}_n/m\text{M}_{\text{TF}} \quad (247)$$

where the total metal concentration,  $m\text{M}_{\text{TF}}$ , is related to the free concentration by

$$m\text{M}_{\text{TF}} = m\text{M}_{\text{F}} \left( 1 + \sum_1 \sum_n \sigma_{\text{L},n} \right) = m\text{M}_{\text{F}} \alpha_{\text{M}} \quad (248)$$

The summations account for all complexes involving metal M, and  $\alpha_{\text{M}}$  is known as the overall side reaction coefficient.<sup>293,294</sup> From Equation 246 we obtain

$$m\text{ML}_n = m\text{M}_{\text{TF}} \sigma_{\text{L},n} \quad (249)$$

so that, substituting Equations 248 and 249 into Equation 247:

$$\%(\text{ML}_n) = 100 \times \sigma_{\text{L},n}/\alpha_{\text{M}} \quad (250)$$

Similarly, the percentage of free metal ion at equilibrium can be calculated from

$$\%(\text{M}_{\text{F}}) = 100/\alpha_{\text{M}} \quad (251)$$

Organisms are believed to respond to the free metal ions in solution rather than to that in complexed form. Equation 251 has been used to estimate free copper ion concentrations in seawater media, and these concentrations have been used to correlate the behavior of phytoplankton cultures with varying background copper levels.<sup>30,31</sup> The use of the term "free cupric ion activity" in this context is a misnomer, since the activity of any ion in solution depends only on the temperature, pressure, and standard state employed.

Equation 250 can be used to determine the distribution of the metal between the various complexes. Equation 251, together with free-ion activity coefficients ( $\gamma_{\text{M}_{\text{F}}}$ ), can be used to calculate conventional total ion activity coefficients ( $\gamma_{\text{M}_{\text{TF}}}$ ) from

$$\gamma_{\text{M}_{\text{TF}}} = \gamma_{\text{M}_{\text{F}}}/\alpha_{\text{M}} \quad (252)$$

The most difficult problem encountered in the preparation of a speciation model of a particular solution is undoubtedly the selection of conditional stability constants ( $K_{\text{ML}_n}^*$ ) to describe the

**TABLE 41**  
**Calculated Speciation of Copper(II) and Lead in Seawater (25°C, 1 atm**  
**Pressure,  $I_c = 0.70 \text{ mol dm}^{-3}$ , pH 8)**

Complex	Total copper (%)				Total lead (%)					
	a	b	c	d	a	b	c	e	f	g
$M^{2+}$	2.5	1.6	1.8	3	2	1.0	4.5	4	2	—
$MCl^+$	39	27.7	29.2	34	11	8.8	18.9	13	7	2.4
$MCl_2^0$	51	30.3	37.5	51	3	12.2	42.3	8	10	1.0
$MCL_3^-$	6	26.3	27.9	12	—	5.3	9.2	3	4	—
$MCl_4^{2-}$	—	0.1	—	—	—	1.5	3.6	—	2	—
$MOH^+$	—	4.0	—	0.1	—	1.3	10.2	30	4	—
$M(OH)_2^0$	—	<0.1	—	—	1	<0.1	—	2	—	—
$MOHCl^0$	—	—	2.9	—	—	—	8.8	—	2	—
$MCO_3^0$	—	0.7	0.2	0.4	80	67.8	0.4	40	53	64.6
$MHCO_3^-$	—	0.1	—	—	—	0.2	1.4	—	—	—
$MSO_4^0$	—	0.3	0.2	0.3	—	1.9	0.5	—	1	—

<sup>a</sup> Zirino and Yamamoto.<sup>356</sup>

<sup>b</sup> Florence and Batley.<sup>357</sup>

<sup>c</sup> Dyrssen and Wedborg.<sup>40</sup>

<sup>d</sup> Ahrland.<sup>358</sup>

<sup>e</sup> Stumm and Brauner.<sup>359</sup>

<sup>f</sup> Whitfield and Turner,<sup>360</sup> where lead speciation is reviewed. Includes the species  $Pb(CO_3)_2^2-$  (2%),  $Pb(CO_3Cl)^-$  (12%), and  $Pb(CO_3OH)^-$  (1%).

<sup>g</sup> Lu and Chen,<sup>36</sup> includes the species  $PbCl_3^-$  (28.7%) and  $Pb(CO_3)_2^2-$  (2%).

complexation reactions that occur. Table 41, for example, shows widely varying estimates of the speciation of Cu(II) and Pb in seawater, using stability constants drawn from available compilations.

Owing to the complexity of natural systems it is necessary to adapt stability constants determined in simple ionic media, chiefly aqueous solutions of single salts, for use in a speciation model of a more complex medium such as seawater. The most rigorous procedure would undoubtedly be to correct the  $K_{ML_n}^*$  values measured in simple media to infinite dilution ( $K_{ML_n}$ ) using the Pitzer equations or some other suitable formalism. The same theoretical approach could then be used to adjust  $K_{ML_n}$  to provide a conditional constant appropriate for the medium under consideration, by accounting for the effects of all the ion-ion and ion-complex interactions on the activity coefficients:

$$K_{ML_n}^* = K_{ML_n} \gamma_M \gamma_L^n / \gamma_{ML_n} \quad (253)$$

Unfortunately, there are few systems for which the necessary ionic interaction parameters are available, especially those involving complexes rather than just free ions. Also, the measurements for only a small minority of the tabulated  $K_{ML_n}^*$  (in simple ionic media) are presented in sufficient detail for the initial extrapolations to infinite dilution to be made.

The necessary alternative approach is to make some simplifying assumptions concerning the interactions in both the ionic medium and the natural system, thus enabling the measured  $K_{ML_n}^*$  to be used for speciation calculations with the minimum of manipulation. In applying such a procedure it is customary to assume the following:

1. Any strong specific interactions between the medium ions and the trace element ion or ligand have been taken into account in the interpretation of the original measurement of  $K_{ML_n}^*$ .

2. The activity coefficients of the free metal ion, free ligand, and complex are unaffected by changes in the medium composition at constant ionic strength.
3.  $K_{ML_n}^*$  can be reliably corrected for the difference in ionic strength between the medium in which the original measurement was carried out and the system which is being modeled.

These assumptions become more tenable the more closely the ionic medium corresponds to the natural system. However, most experimental measurements are made in perchlorate or nitrate media. In the introduction to their critical compilation of stability constants, Smith and Martell<sup>295</sup> state that the constants listed are uncorrected for the interaction of trace components with the medium ions, since, in the majority of cases, insufficient data are available. Turner et al.<sup>296</sup> have taken the measured values compiled by Smith and Martell<sup>295</sup> and fitted them directly as functions of ionic strength. The original compilation of  $K_{ML_n}^*$  values is necessarily a rather heterogeneous collection of data, gathered by numerous authors using different experimental techniques. The fitting parameters obtained are best considered as providing a summary of available data. Turner et al.<sup>296</sup> fitted measured stability constants, on a molar basis, to the empirical relationship

$$\log_{10}(K_{ML_n}^*) = \log_{10}(K_{ML_n}) + S\Delta z^2 I^{1/2} / (1 + B I^{1/2}) \quad (254)$$

where  $S$  is the Debye-Hückel slope (0.511) and:

$$\Delta z^2 = \sum z^2(\text{products}) - \sum z^2(\text{reactants}) \quad (255)$$

This operational approach still provides the most comprehensive summary of the stability constants of trace metal complexes as functions of ionic strength, although more recent studies have improved our detailed knowledge of the complexation behavior of a number of metals. It should also be kept in mind that complexation by organic compounds plays an important role in natural waters such as seawater. For example, it appears that dissolved Cu(II) in surface seawater is present mostly in the form of organic complexes<sup>297</sup> rather than carbonate as would be predicted by considering only interactions with inorganic ligands.

In Table 42 are listed values of the stoichiometric stability constants at 25°C and 35 S‰ for complexes of 49 metals with the major anions present in seawater, derived from the work of Turner et al.<sup>296</sup> It should be noted first that concentrations are in molar units, and second that the original calculations were carried out using an ion pair model to determine the activities (and speciation) of the major ions. Thus the ligand concentrations and ionic strength of 0.65 mol dm<sup>-3</sup> are lower than the total ion concentrations given elsewhere in this chapter (see the notes to Table 42). Turner et al.<sup>296</sup> list the calculated speciation of cations in model seawater (excluding organic ligands). A similar approach has previously been taken in modeling chemical speciation in estuarine waters.<sup>298</sup>

As the experimental data base expands and theoretical procedures improve, a more rigorous method may be adopted and the inconsistencies of this simple treatment removed. For example, the Pitzer formalism has been used to model activity coefficients and speciation in aqueous solutions of HF,<sup>299</sup> AgCl and its mixtures with a number of chloride salts,<sup>300</sup> aqueous CuCl (on a molar basis),<sup>301</sup> aqueous CuCl<sub>2</sub>,<sup>264, 301, 302</sup> and the formation of MgF<sup>+</sup> in saline media.<sup>101</sup> Most of these applications are not relevant to the study of natural waters — the complexation of Cu(II) by Cl<sup>-</sup> is of little importance and the activity coefficients of both H<sup>+</sup> and F<sup>-</sup> are determined entirely by interactions with major ions. However, they do illustrate the difficulties that the more rigorous approach entails, notably the very large number of (unknown) ion interactions that arise for systems in which multiple complexes are formed. The case of MgF<sup>+</sup> formation is more relevant here, and demonstrates how both

**TABLE 42**  
**Logarithms of the Stability Constants for  $\text{Cl}^-$ ,  $\text{F}^-$ ,  $\text{SO}_4^{2-}$ , and  $\text{OH}^-$ , and  $\text{CO}_3^{2-}$**   
**Complexes of Trace Metals in 35 S% Seawater at 25°C, for the Reaction:**  

$$\text{M}^{x+} + n\text{A}^{y-} = \text{MA}_n^{(x-ny)+}$$
 296

Cl <sup>-</sup> complexes							Cl <sup>-</sup> complexes				
n =	1	2	3	4	5	6	n =	1	2	3	4
Ag	3.21	5.16	5.80	3.53	—	—	Lu	-0.38	-2.14	—	—
Al	—	—	—	—	—	—	Mn	0.04	—	—	—
Am	—	—	—	—	—	—	Nb	—	—	—	—
As	—	—	—	—	—	—	Nd	-0.08	-2.14	—	—
Ba	-0.75	—	—	—	—	—	Ni	0.10	—	—	—
Be	-0.30	-1.43	—	—	—	—	NpO <sub>2</sub>	-0.056	—	—	—
Bi	2.00	3.39	5.03	5.69	6.16	5.89	Pb	0.92	1.25	1.24	1.29
Cd	1.35	1.70	1.48	1.36	—	—	Pm	-0.08	-2.14	—	—
Ce	-0.08	-0.47	—	—	—	—	Pr	-0.08	-2.14	—	—
Cf	—	—	—	—	—	—	Pu	0.31	—	—	—
Co	-0.05	—	—	—	—	—	Ra	-0.75	—	—	—
Cr	-0.46	—	—	—	—	—	Sb	—	—	—	—
Cs	-0.86	—	—	—	—	—	Sc	0.04	-0.09	—	—
Cu	-0.22	—	—	—	—	—	Sm	-0.08	-2.14	—	—
Dy	-0.08	-2.14	—	—	—	—	Sn	—	—	—	—
Er	-0.08	-2.14	—	—	—	—	Ta	—	—	—	—
Eu	-0.08	-0.67	—	—	—	—	Tb	-0.08	-2.14	—	—
Fe(II)	-0.30	—	—	—	—	—	Th	0.24	-1.32	—	—
Fe(III)	0.63	0.78	-0.74	—	—	—	TiO	—	—	—	—
Ga	0.011	—	—	—	—	—	Tl(III)	6.68	11.65	14.38	16.19
Gd	-0.08	-2.14	—	—	—	—	Tl(I)	0.043	-0.139	—	—
Hf	0.50	-0.254	-1.026	—	—	—	Tm	-0.08	-2.14	—	—
Hg	6.72	13.20	14.10	15.20	—	—	U(IV)	0.31	—	—	—
Ho	-0.08	-2.14	—	—	—	—	U(VI)	-0.056	—	—	—
In	2.30	3.72	4.10	—	—	—	Y	-0.078	—	—	—
La	-0.08	-2.14	—	—	—	—	Yb	-0.18	-2.14	—	—
Li	—	—	—	—	—	—	Zn	-0.21	-0.11	-0.61	0.09
							Zr	0.42	-0.33	-1.10	—

F <sup>-</sup> complexes							F <sup>-</sup> complexes						
n =	1	2	3	4	5	6	n =	1	2	3	4	5	6
Ag	-0.22	—	—	—	—	—	Lu	3.63	—	—	—	—	—
Al	6.10	11.07	14.98	17.98	19.40	19.84	Mn	0.07	—	—	—	—	—
Am	—	—	—	—	—	—	Nb	—	—	—	—	—	—
As	—	—	—	—	—	—	Nd	3.11	—	—	—	—	—
Ba	-0.30	—	—	—	—	—	Ni	0.50	—	—	—	—	—
Be	4.99	8.79	11.55	12.54	—	—	NpO <sub>2</sub>	4.54	7.96	10.50	11.90	—	—
Bi	1.40	—	—	—	—	—	Pb	1.44	2.53	—	—	—	—
Cd	0.46	0.52	—	—	—	—	Pm	3.13	—	—	—	—	—
Ce	3.03	—	—	—	—	—	Pr	3.03	—	—	—	—	—
Cf	—	—	—	—	—	—	Pu	9.08	14.50	19.60	—	—	—
Co	0.40	—	—	—	—	—	Ra	-0.30	—	—	—	—	—
Cr	4.33	7.65	10.18	—	—	—	Sb	—	—	—	—	—	—
Cs	—	—	—	—	—	—	Sc	6.15	11.41	15.48	18.38	—	—
Cu	0.90	—	—	—	—	—	Sm	3.14	—	—	—	—	—
Dy	3.48	—	—	—	—	—	Sn	—	—	—	—	—	—
Er	3.56	—	—	—	—	—	Ta	—	—	—	—	—	—
Eu	3.21	—	—	—	—	—	Tb	3.44	—	—	—	—	—
Fe(II)	0.80	—	—	—	—	—	Th	7.53	13.32	17.90	20.10	—	—
Fe(III)	5.17	9.10	12.10	—	—	—	TiO	—	—	—	—	—	—
Ga	4.40	7.95	10.10	—	—	—	Tl(III)	—	—	—	—	—	—
Gd	3.36	—	—	—	—	—	Tl(I)	-0.367	—	—	—	—	—
Hf	9.08	15.30	21.50	26.90	32.10	32.80	Tm	3.58	—	—	—	—	—
Hg	1.01	—	—	—	—	—	U(IV)	9.08	14.50	19.64	—	—	—

TABLE 42 (continued)  
 Logarithms of the Stability Constants for  $\text{Cl}^-$ ,  $\text{F}^-$ ,  $\text{SO}_4^{2-}$ , and  $\text{OH}^-$ , and  $\text{CO}_3^{2-}$   
 Complexes of Trace Metals in 35 ‰ Seawater at 25°C, for the Reaction:  
 $\text{M}^{x+} + n\text{A}^{y-} = \text{MA}_n^{(x-ny)+ 296}$

$\text{F}^-$ complexes							$\text{F}^-$ complexes						
n =	1	2	3	4	5	6	n =	1	2	3	4		
Ho	3.54	—	—	—	—	—	U(VI)	4.54	7.96	10.50	11.90	—	
In	3.72	6.44	8.57	9.82	—	—	Y	3.80	7.08	10.28	—	—	
La	2.67	—	—	—	—	—	Yb	3.60	—	—	—	—	
Li	—	—	—	—	—	—	Zn	0.75	—	—	—	—	
							Zr	8.78	16.10	22.00	27.60	21.60 26.10	

$\text{SO}_4^{2-}$ complexes						$\text{SO}_4^{2-}$ complexes				
n =	1	2	3	4	5	n =	1	2	3	4
Ag	0.524	0.447	-2.20	—	—	Lu	1.45	2.16	—	—
Al	—	—	—	—	—	Mn	0.87	—	—	—
Am	—	—	—	—	—	Nb	—	—	—	—
As	—	—	—	—	—	Nd	1.75	2.57	—	—
Ba	0.77	1.62	—	—	—	Ni	0.95	1.62	—	—
Be	0.65	1.98	—	—	—	NpO <sub>2</sub>	1.89	2.70	4.01	—
Bi	2.20	3.79	3.95	6.05	5.13	Pb	1.36	2.93	—	—
Cd	1.06	1.86	2.40	1.77	—	Pm	1.76	2.62	—	—
Ce	1.67	2.74	—	—	—	Pr	1.73	2.39	—	—
Cf	—	—	—	—	—	Pu	4.11	6.86	—	—
Co	0.97	—	—	—	—	Ra	0.77	1.62	—	—
Cr	2.72	—	—	—	—	Sb	—	—	—	—
Cs	—	—	—	—	—	Sc	2.51	3.80	—	—
Cu	1.06	—	—	—	—	Sm	1.78	2.67	—	—
Dy	1.73	2.27	—	—	—	Sn	—	—	—	—
Er	1.70	2.57	—	—	—	Ta	—	—	—	—
Eu	1.68	2.57	—	—	—	Tb	1.75	2.62	—	—
Fe(II)	0.81	—	—	—	—	Th	3.91	6.57	—	—
Fe(III)	2.15	2.85	—	—	—	TiO	1.84	—	—	—
Ga	—	—	—	—	—	Tl(III)	2.486	—	—	—
Gd	1.80	2.68	—	—	—	Tl(I)	0.594	—	—	—
Hf	3.73	6.48	—	—	—	Tm	1.70	2.61	—	—
Hg	1.27	2.28	—	—	—	U(IV)	4.11	6.86	—	—
Ho	1.70	2.37	—	—	—	U(VI)	1.89	2.70	4.01	—
In	1.967	2.90	3.14	—	—	Y	1.58	2.77	—	—
La	1.57	2.76	—	—	—	Yb	1.69	2.67	—	—
Li	-0.135	—	—	—	—	Zn	0.94	1.67	2.01	1.67
						Zr	4.36	7.44	8.37	—

$\text{OH}^-$ complexes						$\text{OH}^-$ complexes					
n =	1	2	3	4	5	n =	1	2	3	4	5
Ag	-12.13	-23.82	—	—	—	Lu	-8.22	-16.61	-24.60	-32.50	—
Al	-5.50	-10.30	-16.10	-23.70	—	Mn	-10.90	-22.60	-34.90	-47.60	—
Am	-8.12	-17.41	-27.43	-37.73	—	Nb	-7.34	—	—	—	—
As	-9.035	—	—	—	—	Nd	-8.62	-17.80	-27.40	-37.80	—
Ba	-13.89	—	—	—	—	Ni	-10.20	-19.40	-30.10	-43.30	—
Be	-5.71	-14.05	-23.29	-36.65	—	NpO <sub>2</sub>	-5.89	—	—	—	—
Bi	-1.51	-4.87	-9.81	-22.4	—	Pb	-7.78	-17.21	-27.82	—	—
Cd	-11.14	-20.75	-33.30	-46.78	—	Pm	-8.57	-17.63	-26.95	-36.71	—
Ce	-8.92	-18.01	-27.73	-38.33	—	Pr	-8.72	-17.90	-27.53	-37.90	—
Cf	-8.12	-17.41	-27.43	-37.73	—	Pu	1.267	-3.60	-7.36	-11.88	-17.35
Co	-9.98	-19.19	-31.59	-45.61	—	Ra	-14.00	—	—	—	—
Cr	-4.55	-10.81	-19.24	-28.25	—	Sb	-11.56	—	—	—	—
Cs	-14.70	—	—	—	—	Sc	-4.87	-10.76	-17.21	-26.78	—

TABLE 42 (continued)  
 Logarithms of the Stability Constants for Cl<sup>-</sup>, F<sup>-</sup>, SO<sub>4</sub><sup>2-</sup>, and OH<sup>-</sup>, and CO<sub>3</sub><sup>2-</sup>  
 Complexes of Trace Metals in 35 S‰ Seawater at 25°C, for the Reaction:  
 $M^{x+} + nA^{y-} = MA_n^{(x-ny)+}$  296

OH <sup>-</sup> complexes							OH <sup>-</sup> complexes				
n =	1	2	3	4	5	6	n =	1	2	3	4
Cu	-8.29	-17.63	-27.83	-38.79	—	Sm	-8.52	-17.50	-26.70	-36.40	—
Dy	-8.62	-17.11	-25.63	-34.23	—	Sn	0.93	0.59	0.53	-0.75	—
Er	-8.52	-16.81	-25.10	-33.30	—	Ta	-9.54	—	—	—	—
Eu	-8.42	-17.50	-26.50	-36.00	—	Tb	-8.52	-17.21	-26.03	-35.03	—
Fe(II)	-9.80	-21.00	-31.10	-45.30	—	Th	-4.08	-7.65	-12.94	-17.16	—
Fe(III)	-2.73	-6.39	-12.65	-21.96	—	TiO	-2.69	-5.26	—	—	—
Ga	-3.25	-7.01	-11.54	-17.45	—	Tl(III)	-1.02	-2.29	-4.11	-15.50	—
Gd	-8.62	-17.30	-26.10	-35.10	—	Tl(I)	-13.223	—	—	—	—
Hf	-1.13	-3.12	-7.24	-12.00	-18.20	Tm	-8.32	-16.81	-25.03	-33.33	—
Hg	-3.68	-6.34	-21.10	—	—	U(IV)	1.267	-3.60	-7.36	-11.88	-17.35
Ho	-8.62	-17.01	-25.53	-34.13	—	U(VI)	-5.89	—	—	—	—
In	-4.09	-8.47	-13.14	-22.50	—	Y	-8.32	-17.31	-26.93	-37.23	—
La	-9.12	-18.30	-28.40	-39.50	—	Yb	-8.32	-16.71	-25.03	-33.43	—
Li	-13.75	—	—	—	—	Zn	-9.18	-17.20	-28.40	-40.40	—
						Zr	0.58	-2.42	-6.34	-10.96	-17.04

CO <sub>3</sub> <sup>2-</sup> complexes				CO <sub>3</sub> <sup>2-</sup> complexes			
n =	1	2	3	n =	1	2	3
Ag	2.62	—	—	Lu	5.68	—	—
Al	6.54	—	—	Mn	2.71	—	—
Am	4.11	7.47	10.62	Nb	—	—	—
As	—	—	—	Nd	4.83	—	—
Ba	1.39	—	—	Ni	3.98	—	—
Be	3.74	—	—	NpO <sub>2</sub>	6.11	15.10	20.20
Bi	—	—	—	Pb	5.61	8.71	—
Cd	2.96	—	—	Pm	4.91	—	—
Ce	4.89	—	—	Pr	4.73	—	—
Cf	4.11	7.47	10.62	Pu	—	—	—
Co	3.52	—	—	Ra	1.391	—	—
Cr	—	—	—	Sb	—	—	—
Cs	—	—	—	Sc	8.21	—	—
Cu	5.36	9.11	—	Sm	4.97	—	—
Dy	5.28	—	—	Sn	—	—	—
Er	5.43	—	—	Ta	—	—	—
Eu	4.94	—	—	Tb	5.04	—	—
Fe(II)	3.34	—	—	Th	7.60	—	—
Fe(III)	7.83	—	—	TiO	—	—	—
Ga	6.90	—	—	Tl(III)	—	—	—
Gd	5.40	—	—	Tl(I)	—	—	—
Hf	—	—	—	Tm	5.19	—	—
Hg	9.55	—	—	U(IV)	—	—	—
Ho	5.34	—	—	U(VI)	6.11	15.10	20.20
In	4.10	—	—	Y	5.05	—	—
La	4.27	—	—	Yb	5.71	—	—
Li	—	—	—	Zn	3.36	—	—
				Zr	—	—	—

Note: Free concentrations (in mol dm<sup>-3</sup>) of the major ions in model seawater, to be used with the above complexation constants, are taken from Table 1 of Turner et al.<sup>296</sup> and are as follows:

Ion	Conc.	Ion	Conc.
Na <sup>+</sup>	0.4677	Cl <sup>-</sup>	0.5623
Mg <sup>2+</sup>	0.04365	F <sup>-</sup>	3.31 × 10 <sup>-5</sup>
Ca <sup>2+</sup>	0.00851	SO <sub>4</sub> <sup>2-</sup>	9.55 × 10 <sup>-3</sup>
K <sup>+</sup>	0.0102	CO <sub>3</sub> <sup>2-</sup>	3.16 × 10 <sup>-5</sup>
Sr <sup>2+</sup>	6.31 × 10 <sup>-6</sup>		

pH is equal to 8.20, and the model seawater has an effective ionic strength (*I<sub>e</sub>*) of 0.65 mol dm<sup>-3</sup>.



**TABLE 43**  
**Pitzer Model Parameters for Cu(II) Salts and Their Binary Mixtures<sup>302</sup>**

Salt	Conc.	$\beta^{(0)}$	$\beta^{(1)}$	$\beta^{(2)}$	$C^\phi$
CuSO <sub>4</sub>	0.005—1.6 <i>m</i>	0.2340	2.527	-48.33	0.0044
CuCl <sub>2</sub>	0.19—2.25 <i>m</i>	0.2966	1.391	—	-0.0360

*Note:* For CuSO<sub>4</sub>, model parameter  $b = 1.2$ ,  $\alpha_1 = 1.4$ ,  $\alpha_2 = 12.0$ . For CuCl<sub>2</sub>,  $b = 1.2$ ,  $\alpha_1 = 2.0$ , and  $\alpha_2$  is not required.

System	Maximum $I$	Like charge ( $\theta_{Cu,e}$ )	Triplet ( $\psi_{Cu,c,a}$ )
NaCl-CuCl <sub>2</sub>	7.3	0.00	-0.014
Na <sub>2</sub> SO <sub>4</sub> -CuSO <sub>4</sub>	5.5	0.00	-0.011
CuCl <sub>2</sub> -CuSO <sub>4</sub>	7.2	-0.02	0.043
NaCl-Na <sub>2</sub> SO <sub>4</sub>	9.0	-0.02	0.004

*Note:* These parameters also give a good account of the osmotic coefficients in the mixtures without common ions, viz., NaCl-CuSO<sub>4</sub>-H<sub>2</sub>O and CuCl<sub>2</sub>-Na<sub>2</sub>SO<sub>4</sub>-H<sub>2</sub>O.

ion association and ion interaction treatments can be used to obtain  $F^-$  activities in seawater (see Section III.D.3 below). Where primary interest lies in the behavior of trace species and their complexes, and ionic strength is not too high; the ion pairing approach to modeling activities has much to offer and is well proven for estuarine systems. Some of the examples of the Pitzer approach are given below, followed by a discussion of the use of ion association models.

### 1. Formation of Cu(II) Chloro-Complexes

Copper forms relatively weak complexes with chloride ions, and a number of treatments of activity coefficients in chloride media containing copper have been carried out using the Pitzer formalism.<sup>264,301,302</sup>

The simplest approach is that taken by Downes and Pitzer<sup>302</sup> who measured the osmotic coefficients of the five copper-containing binary mixtures of NaCl, Na<sub>2</sub>SO<sub>4</sub>, CuCl<sub>2</sub>, and CuSO<sub>4</sub> using the isopiestic technique. They summarized their results using the Pitzer equations without any explicit recognition of complex formation (Table 43). The ionic interaction equations were able to account for the experimental data to ionic strengths  $>6 \text{ mol kg}^{-1}$  (Table 43). Indeed, the osmotic coefficients predicted using the single electrolyte solution parameters alone agree well with the experimental data, even for mixtures without a common ion.

A much more elaborate approach was taken by Haung<sup>264</sup> who accounted explicitly for the stepwise formation of four copper chloro-complexes, in mixtures of CuCl<sub>2</sub> with NaCl or HCl, according to the equation



His analysis was comprehensive and treated all possible pairwise interactions and all triplet interactions except those involving the neutral complex CuCl<sub>2</sub><sup>0</sup>. In all, 37 interaction parameters and 3 stability constants were required to describe the binary CuCl<sub>2</sub> system — in contrast to the three parameters required by Downes and Pitzer<sup>302</sup> for the same system. For the ternary Na-Cu-Cl-H<sub>2</sub>O system, 54 parameters were required, compared to the 3 or 4 needed for the simpler treatment. This is not an economical way of describing activity

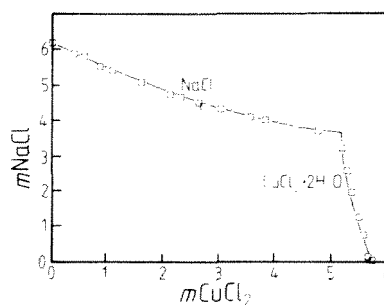


FIGURE 40. Measured and calculated salt solubilities in the system Na-Cu-Cl-H<sub>2</sub>O at 25°C. Symbols — experimental data; lines — calculated by Haung.<sup>264</sup> (Redrawn from Haung.<sup>264</sup>)

coefficients in electrolyte mixtures, but does illustrate a more general approach for situations where the complexes themselves are of interest, or their influence cannot be incorporated readily into a pure "ion interaction" scheme.

In dealing with such complicated systems, extensive experimental data are required to obtain a unique set of parameters. In the system treated by Haung,<sup>264</sup> only 53 data points were used to characterize the binary CuCl<sub>2</sub>-H<sub>2</sub>O system, and only a further 36 data points were available to describe the ternary Na-Cu-Cl-H<sub>2</sub>O system. Consequently, although the fitted model parameters are able to give a good account of the solubilities of CuCl<sub>2</sub> · 2H<sub>2</sub>O and NaCl to high ionic strengths (Figure 40), the parameter values owe as much to the fitting procedures used (and any simplifying assumptions made) as to the real magnitudes of the interactions in solution. This point may be illustrated by comparing the parameters obtained by Haung<sup>264</sup> with those employed by Furst et al.<sup>301</sup> to describe the extraction of Cu(II) from aqueous chloride media (NaCl, LiCl, or MgCl<sub>2</sub>) by the organic solvent LIX 65N.

Furst et al.<sup>301</sup> considered only pairwise interactions between ions of opposite sign, and did not incorporate interactions involving the neutral complex CuCl<sub>2</sub><sup>0</sup>. Rather than fitting the full suite of parameters required for pairwise interactions, Furst et al.<sup>301</sup> used correlations between  $\beta^{(0)}$  and  $\beta^{(1)}$  to further reduce the number of unknowns. Despite this considerable simplification they still had to employ their experimental measurements to determine 33 Pitzer model parameters, 24 molar extraction coefficients, and 4 stability constants. While the experimental data are satisfactorily described, the parameter values obtained using this truncated Pitzer approach are quite different to those derived by Haung,<sup>264</sup> and are in some instances unusually large (see Table 44). It is therefore emphasized that the parameters tabulated do not provide a unique description of the interactions occurring in solution, and great care must be taken in using them to model related systems.

## 2. Formation of Pb Chloro-Complexes

Although there are large discrepancies between the published values of the stability constants for lead chloro-complexes, the critical compilation of Smith and Martell<sup>275</sup> indicates that  $1 < \log_{10}(K_{\text{PbCl}_n}) < 2$ . It should therefore be feasible to account for the activity coefficient of lead, in solutions where chloro-complexes dominate, by using Pitzer parameters derived in a manner analogous to that used by Downes and Pitzer<sup>302</sup> for copper chloride. However, the study of lead chloro-complexes by Miller and Byrne,<sup>303</sup> which takes explicit account of the presence of chloro-complexes, provides a further example of the way in which the Pitzer treatment has been modified to include stepwise complex formation. The stability constants for the reaction



**TABLE 44**  
**Interaction Parameters for the System Cu(II)-Na-Cl-H<sub>2</sub>O at 25°C and 1 atm Pressure**

Interaction	Note	$\beta^{0a}$	$\beta^{1a}$	$\beta^{2a}$	C*
Cu <sup>2+</sup> -Cl <sup>-</sup>	a	0.448	1.316		0.002
	b	0.272	1.862		
Cu <sup>2+</sup> -CuCl <sub>2</sub>	a	0.005	-0.353		0.352
	b	0.797	2.687		
Cu <sup>2+</sup> -CuCl <sub>2</sub> <sup>-</sup>	a	0.793	1.520	2.529	0.293
	b	0.852	24.978		
CuCl <sup>+</sup> -CuCl <sub>2</sub>	a	0.601	0.147		0.700
	b	2.279	3.382		
CuCl <sup>+</sup> -CuCl <sub>2</sub> <sup>-</sup>	a	0.298	0.437		0.341
	b	2.305	5.055		
CuCl <sup>+</sup> -Cl <sup>-</sup>	a	0.083	0.147		0.340
	b	0.197	0.384		
CuCl <sub>2</sub> <sup>-</sup> -Na <sup>+</sup>	a	0.151	0.400		-0.012
	b	0.449	0.746		
CuCl <sub>2</sub> <sup>-</sup> -Na <sup>+</sup>	a	-0.006	0.051		0.004
	b	0.124	1.630		

The following  $\ln(K_{c,w})$  values were also obtained from the experimental data:

Note	$\ln(K_{c,wCl})$	$\ln(K_{c,wCl_2})$	$\ln(K_{c,wCl_3})$	$\ln(K_{c,wCl_4})$
a	0.480	-0.641	-2.512	-6.253
b	0.191	-2.938	-5.339	-7.849

\* Haung,<sup>304</sup>  $\theta_{ij}$ ,  $\psi_{ij}$ , and  $\lambda_{ij}$  terms also fitted.

<sup>b</sup> Furst et al.,<sup>305</sup> only  $\beta^{(0)}$  terms considered.

are given by:

$$K_{PbCl_2} = (K_{PbCl_2}^* \gamma_{PbCl_2}) / (\gamma_{Pb} \gamma_{Cl}^2) \quad (258)$$

Millero and Byrne<sup>303</sup> assumed that the parameters describing the interactions of the free lead and chloride ions in solution were identical to those for zinc chloride solutions at the same total ionic strength. On this basis they were able to calculate the free ion activity coefficients  $\gamma_{Pb^{2+}}$  and  $\gamma_{Cl^-}$  as a function of ionic strength in various chloride media. Furthermore they ignored interactions *between* the complex ions since the lead chloride was only present at trace concentration. Rearranging Equation 257 and inserting the appropriate interaction coefficients, the following relationships were obtained in ternary chloride mixtures:

$$\begin{aligned} \ln(K_{PbCl_2}^*) &= \ln(K_{PbCl_2}^*) - \ln(\gamma_{PbCl_2}) - \ln(\gamma_{Cl^-}) \\ &= \ln(K_{PbCl_2}^*) - 2mCl \beta_{PbCl_2,Cl}^{(0)} - 2mM^{2+} \theta_{M,PbCl_2} \end{aligned} \quad (259)$$

$$\begin{aligned} \ln(K_{PbCl_2}^*) &= \ln(K_{PbCl_2}^*) - \ln(\gamma_{PbCl_2}) - 2\ln(\gamma_{Cl^-}) \\ &= \ln(K_{PbCl_2}^*) - 2mM^{2+} \lambda_{M,PbCl_2} - 2mCl \lambda_{Cl,PbCl_2} \end{aligned} \quad (260)$$

$$\begin{aligned} \ln(K_{PbCl_2}^*) &= \ln(K_{PbCl_2}^*) - \ln(\gamma_{PbCl_2}) - 3\ln(\gamma_{Cl^-}) \\ &= \ln(K_{PbCl_2}^*) - 2mM^{2+} \beta_{M,PbCl_2}^{(0)} - 2mCl \theta_{Cl,PbCl_2} \end{aligned} \quad (261)$$

**TABLE 45**  
**Pitzer Model Parameters for Lead Chloro-Complex Interactions**  
**in Chloride and Perchlorate Media<sup>303</sup>**

Interaction	Note	$\beta^{(0)}$	$\beta^{(1)}$	$C^{\phi}$	$\theta_j$
$\text{Pb}^{2+} \text{-Cl}$	a	0.2602	1.6425	0.0880	
$\text{Pb}^{2+} \text{-ClO}_4$		0.3332	1.7220	-0.0088	
$\text{PbCl}^+ \text{-Cl}$	b	0.15			
$\text{PbCl}^+ \text{-ClO}_4$		0.22			
$\text{Na}^+ \text{-PbCl}_3$		-0.19			
$\text{H}^+ \text{-PbCl}_3$		-0.01			
$\text{Mg}^{2+} \text{-PbCl}_3$		0.30			
$\text{Ca}^{2+} \text{-PbCl}_3$		0.40			
$\text{Ca}^{2+} \text{-PbCl}^+$					-0.37
$\text{Mg}^{2+} \text{-PbCl}^+$					-0.37
$\text{Cl}^- \text{-PbCl}_3$	c				-0.03

Interaction parameters ( $\lambda_{M, \text{PbCl}_3}$ ) for neutral  $\text{PbCl}_3^0$  species:

$M'^+$ =	$\text{H}^+$	$\text{Na}^+$	$\text{Mg}^{2+}$	$\text{Ca}^{2+}$	$\text{Cl}^-$	$\text{ClO}_4$
$\lambda_{M, \text{PbCl}_3}$	0 (assumed)	-0.14	-0.20	-0.20	-0.11	-0.04

<sup>a</sup> Assumes the parameters are identical to those for  $\text{ZnCl}_2$ .

<sup>b</sup> Assumes  $\theta_{\text{Na}, \text{PbCl}} = \theta_{\text{H}, \text{PbCl}} = 0$ .

<sup>c</sup> Assumes  $\theta_{\text{Cl}, \text{PbCl}_3} = \theta_{\text{ClO}_4, \text{PbCl}_3}$ .

**TABLE 46**  
**Thermodynamic Formation Constants of Lead**  
**Chloro-Complexes at 25°C (from the Work of**  
**Millero and Byrne<sup>303</sup>)**

$\log_{10}(K_{\text{PbCl}})$	Note	$\log_{10}(K_{\text{PbCl}_2})$	Note	$\log_{10}(K_{\text{PbCl}_3})$	Note
1.48	a	2.03	a	1.86	a
1.1—1.62	b	1.78—2.44	b	1.68—1.86	b

<sup>a</sup> Millero and Byrne.<sup>303</sup>

<sup>b</sup> Range of previous values obtained from the literature and listed by Millero and Byrne.<sup>303</sup>

where  $M'^+$  represents the medium cation. From plots of  $\ln(K'_{\text{PbCl}_n})$  vs.  $m\text{Cl}^-$  for the various media, values for the interaction terms in Equations 259 to 261 can be derived (Table 45). Parameters involving  $\text{PbCl}^+$  were obtained by assuming that  $\theta_{\text{Na}, \text{PbCl}} = \theta_{\text{H}, \text{PbCl}} = 0$  and  $\theta_{\text{Mg}, \text{PbCl}} = \theta_{\text{Ca}, \text{PbCl}}$ . The stoichiometric stability constants determined from the data were corrected using the tabulated parameters to obtain thermodynamic stability constants which were in reasonable agreement with values obtained from other studies (see, for example, Table 46).

### 3. Formation of $\text{MgF}^+$ in Aqueous NaCl and Seawater

In seawater, the magnesium fluoride ion pair accounts for about 49% of total dissolved fluoride, compared with about 2%  $\text{CaF}^+$ .<sup>58</sup> The association constant, with an infinite dilution value of 66.4,<sup>267</sup> is greater than the *circa* 20  $\text{kg mol}^{-1}$  limit above which association should

**TABLE 47**  
**Pitzer Interaction Parameters for Na-Mg-Cl-F-H<sub>2</sub>O**  
**Solutions at 25°C**

Ions		$\beta^{(0)}$	$\beta^{(1)}$	$C^\phi$	$\theta_{\text{Na,Mg}}$	$\psi_{\text{Na,Mg,Cl}}$	$\psi_{\text{Na,Mg,F}}$
Na	Cl	0.0765	0.2664	0.00127	0.07	-0.012	—
Na	F	0.0215	0.2107	0.0			
Mg	Cl	0.3523	1.6815	0.0			
					$\theta_{\text{Cl,F}}$	$\psi_{\text{Cl,F,Na}}$	$\psi_{\text{Cl,F,Mg}}$
					0.01 <sup>a</sup>	0.0023 <sup>a</sup>	—

*Note:* The seawater recipe of Dickson,<sup>138</sup> used here, is as follows for a solution of total salt content  $S_T$  equal to 35‰, and ionic strength 0.7225 mol kg<sup>-1</sup>:  $m\text{NaCl}$  0.42764,  $m\text{Na}_2\text{SO}_4$  0.02927,  $m\text{KCl}$  0.01058,  $m\text{MgCl}_2$  0.05474, and  $m\text{CaCl}_2$  0.01075 mol kg<sup>-1</sup>.

<sup>a</sup> Determined by ion-selective electrode measurement, as described in text. Other parameters are as listed by Harvie and Weare<sup>54</sup> and Pitzer<sup>51</sup> (Chapter 3, this volume).

be recognized explicitly in the Pitzer model.<sup>56</sup> Nonetheless, it is possible, at least for the  $\text{Mg}^{2+}$  concentrations present in seawater, to represent the  $\text{Mg}^{2+}$ - $\text{F}^-$  interaction either as occurring between free ions or in terms of the formation of the complex  $\text{MgF}^+$ . The two alternative analyses are now described as an example of how these calculations may be carried out.

The association of  $\text{Mg}^{2+}$  and  $\text{F}^-$  has been measured potentiometrically in NaCl media by Clegg and Brimblecombe<sup>101</sup> from 0 to 6 mol kg<sup>-1</sup> ionic strength at 25°C. Aqueous NaCl is the simplest medium that may be considered an adequate analog of seawater and, in terms of a comprehensive thermodynamic treatment, has the advantage that the interactions of  $\text{Mg}^{2+}$  and  $\text{F}^-$  with  $\text{Na}^+$  and  $\text{Cl}^-$  are well established (Table 47), with the exception of two mixture parameters ( $\theta_{\text{Cl,F}}$  and  $\psi_{\text{Na,Cl,F}}$ ) which it was first necessary to determine.

The unknown parameters were obtained by measuring the mean activity coefficient  $\gamma_{\text{NaF}}$  and quotient  $\gamma_{\text{F}}/\gamma_{\text{Cl}}$  in Na-Cl-F-H<sub>2</sub>O solutions from 1 to 6 mol kg<sup>-1</sup> ionic strength.<sup>101</sup> All experiments were carried out using glass  $\text{Na}^+$  and solid-state  $\text{F}^-$  and  $\text{Cl}^-$  electrodes, thus avoiding the problem of liquid junction potentials. Both series of results were combined to determine  $\theta_{\text{Cl,F}}$  and  $\psi_{\text{Na,Cl,F}}$  by the usual graphical method.<sup>82</sup>

It is worth noting here that, although the system contains only three ions and the pure solution activity coefficients of  $\text{NaCl}_{(\text{aq})}$  (to 6 mol kg<sup>-1</sup>) and  $\text{NaF}_{(\text{aq})}$  (to 1 mol kg<sup>-1</sup>) are well known, the treatment above is not the only one possible within the context of the model. This is because the saturation concentration of aqueous NaF is only 0.983 mol kg<sup>-1</sup>,<sup>107</sup> thus the variation of the function  $B_{\text{NaF}}$  above this concentration, the limit for which activity coefficient data are available, may be poorly predicted in solutions of greater ionic strength. A possible alternative treatment would therefore be to use the measurements described above, together with pure solution  $\gamma_{\text{NaF}}$ , to redetermine the parameters  $\beta_{\text{NaF}}^{(0)}$ ,  $\beta_{\text{NaF}}^{(1)}$ , and  $C_{\text{NaF}}^\phi$  to high ionic strength together with  $\theta_{\text{Cl,F}}$  and  $\psi_{\text{Na,Cl,F}}$  if needed.

Knowing all interactions for the Na-Mg-F-Cl-H<sub>2</sub>O system except those involving  $\text{Mg}^{2+}$  and  $\text{F}^-$ ,  $\gamma_{\text{NaF}}$  was then measured in the full mixture. Since both  $\text{Mg}^{2+}$  and  $\text{F}^-$  concentrations were maintained sufficiently low that the influence of  $\text{Na}^+$ - $\text{Mg}^{2+}$ - $\text{F}^-$  and  $\text{Mg}^{2+}$ - $\text{Cl}^-$ - $\text{F}^-$  interactions on  $\gamma_{\text{F}}$  ( $\psi_{\text{Na,Mg,F}}$  and  $\psi_{\text{Mg,Cl,F}}$ ) were likely to be small, the difference between the measured  $\ln(\gamma_{\text{NaF}})$  and that calculated by the model ( $\text{Mg}^{2+}$ - $\text{F}^-$  interactions set to zero) can be attributed to parameters  $\beta_{\text{MgF}}^{(0)}$ ,  $\beta_{\text{MgF}}^{(1)}$ , and  $C_{\text{MgF}}^\phi$ ; thus,

$$\ln(\gamma_{\text{NaF}}) = m\text{Mg}^{2+}(\beta_{\text{MgF}}^{(0)} + g(2I^{1/2})\beta_{\text{MgF}}^{(1)} + C_{\text{MgF}}^\phi(Z/2 + mF)) + \ln(\gamma'_{\text{NaF}}) \quad (262)$$

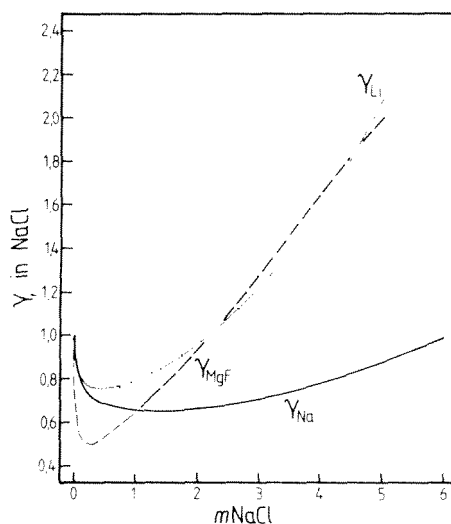


FIGURE 41. The activity coefficient of  $\text{MgF}^+$  ( $\gamma_{\text{MgF}}$ ) in aqueous NaCl, estimated from the stability constant  $K_{\text{MgF}}^*$  (Equation 264), and compared with calculated activity coefficients of  $\text{Na}^+$  ( $\gamma_{\text{Na}}$ ) and trace  $\text{Li}^+$  ( $\gamma_{\text{Li}}$ ) in the same solution.

where  $g(x)$  and  $Z$  are model functions given by Pitzer (Chapter 3, this volume). By fitting the experimental data to this equation, the following parameter values were determined:  $\beta_{\text{MgF}}^{(0)}$ , 3.932;  $\beta_{\text{MgF}}^{(1)}$ , -25.17;  $C_{\text{MgF}}^{\phi}$ , -5.294. These parameters should be valid at all ionic strengths to 5 mol  $\text{kg}^{-1}$  and  $m\text{Mg}^{2+}$  to *circa* 0.06 mol  $\text{kg}^{-1}$  (the concentration of  $\text{Mg}^{2+}$  in seawater is 0.0556 mol  $\text{kg}^{-1}$  at 35 S%). The large magnitudes of the parameters, particularly that of  $C_{\text{MgF}}^{\phi}$ , suggest that they should not be used outside of these ranges of concentration.

The alternative approach is to associate the decrease in measured NaF activity in the experiments, as  $\text{Mg}^{2+}$  is added to the solution, with the formation of  $\text{MgF}^+$  (i.e., a decrease in  $m\text{F}^-$ , rather than in  $\gamma_{\text{NaF}}$ ), leading to

$$K_{\text{MgF}}^* = m\text{MgF}^+ / (m\text{Mg}^{2+} m\text{F}^-) \quad (263)$$

where  $K_{\text{MgF}}^*$  ( $\text{kg mol}^{-1}$ ) is the stoichiometric stability constant of  $\text{MgF}^+$  at 298.15 K, and the concentrations in Equation 263 are those of the free ions. The stability constant in the NaCl medium is given by the following equation, as a function of ionic strength:

$$\log_{10}(K_{\text{MgF}}^*) = 1.822 - 0.9821I^{1/2}/(1 + 0.328I^{1/2}) + 0.0713I + 0.0169I^2 \quad (264)$$

From this equation the activity coefficient of  $\text{MgF}^+$  in the solutions can also be inferred. Assuming that the activity coefficients of  $\text{Mg}^{2+}$  and  $\text{F}^-$  are determined only by interactions with  $\text{Na}^+$  and  $\text{Cl}^-$ , then

$$\gamma_{\text{MgF}} = \gamma_{\text{Mg}} \gamma_{\text{F}} K_{\text{MgF}} / K_{\text{MgF}}^* \quad (265)$$

where  $K_{\text{MgF}}$  is the thermodynamic value of the stability constant, and both  $\gamma_{\text{Mg}}$  and  $\gamma_{\text{F}}$  are estimated using the Pitzer model with  $\text{Mg}^{2+}$ - $\text{F}^-$  interactions set to zero. The resulting activity coefficient ( $\gamma_{\text{MgF}}$ ) is shown in Figure 41, compared with values of  $\gamma_{\text{Na}}$  and  $\gamma_{\text{Li}}$  (calculated for trace  $\text{Li}^+$  in the same solution). Of the two singly charged ions,  $\gamma_{\text{MgF}}$  most closely resembles that of  $\text{Li}^+$  at moderate to high ionic strength. Values at low concentration ( $I < 1$

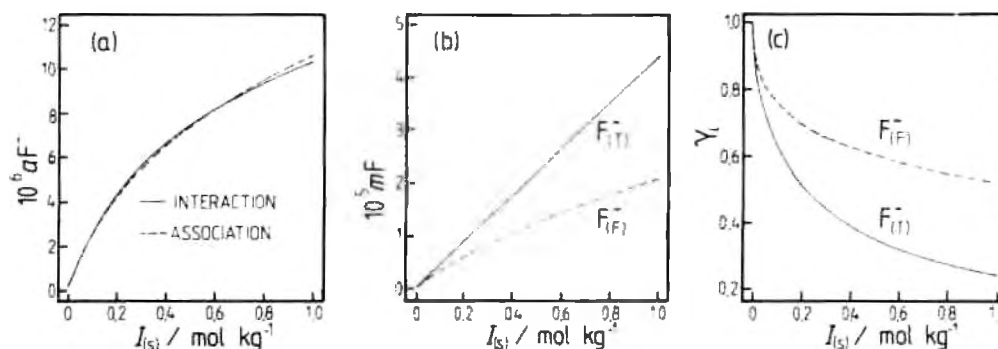


FIGURE 42 The activity and free concentration of  $F^-$  in seawater at  $25^\circ C$ . (a) Activity of  $F^-$  as a function of ionic strength  $I_{(s)}$ . Solid line — calculated using the ion interaction parameters ( $\beta_{MgF}^{(s)}, C_{MgF}^{(s)}$ ) listed in the text; dashed line — estimated using the stability constant  $K_{MgF}^*$  given by Equation 264 and the activity coefficient of *free*  $F^-$  determined using the model with ( $\beta_{MgF}^{(s)}, C_{MgF}^{(s)}$ ) set to zero. (b) Comparison of total ( $mF_{(T)}$ ) and free ( $mF_{(F)}$ ) fluoride concentration (for which formation of  $MgF^+$  is assumed). (c) Comparison of the activity coefficients of free  $F^-$  ( $\gamma_{(F)}$ ), and total  $F^-$  ( $\gamma_{(T)}$ ) — where  $MgF^+$  is assumed not to exist and the decrease in  $F^-$  activity is attributed to strong interaction with  $Mg^{2+}$ .

$\text{mol kg}^{-1}$ ) depend strongly on the nature of the empirical fitting equation, and may therefore be subject to large errors.

It is possible to go some way to estimating how  $K_{MgF}^*$  in seawater might differ from that in NaCl, by assuming  $\gamma_{MgF}$  retains the same value as in aqueous NaCl (at the same ionic strength), but allowing for the changed activity coefficients of  $Mg^{2+}$  and  $F^-$ . The stoichiometric stability constant in seawater,  $K_{MgF(s)}^*$ , is therefore given by

$$K_{MgF(s)}^* = K_{MgF}^* (\gamma_{Mg^{2+}} \gamma_{F(s)}) / (\gamma_{Mg} \gamma_F) \quad (266)$$

where quantities with the subscript (s) refer to values in a seawater medium. A comparison of the two sets of stoichiometric constants suggests that  $K_{MgF(s)}^* < K_{MgF}^*(\text{NaCl})$  as both  $\gamma_{Mg}$  and  $\gamma_F$  are reduced in seawater relative to NaCl — probably due to the strong interactions with  $SO_4^{2-}$  and  $Ca^{2+}$ , respectively. However, the change (15% at  $I = 0.7 \text{ mol kg}^{-1}$ ) is probably less than the uncertainty in the data from which  $K_{MgF}^*$  has been derived.

Finally, as a comparison, we estimate the activity of  $F^-$  in seawater as a function of ionic strength, using both the stability constant and purely ion interaction approaches. The artificial seawater recipe of Dickson<sup>100</sup> was used (see Table 47), in which a ratio  $mF^-/mNa^+$  of  $1.029 \times 10^{-4}$  was assumed (see Table 6), the equivalent amount of NaCl being replaced by NaF. First the activity of  $F^-$  ( $aF^-$ ) was estimated using the Pitzer model, with parameters  $\beta^{(m)}, \beta^{(1)}$ , and  $C^\phi$  for the  $Mg^{2+}-F^-$  interaction taking the values listed above, and using *total*  $F^-$  concentration ( $mF_{(T)}$ ) in the calculation. The alternative approach involved first calculating the *free*  $F^-$  concentration, using the stability constant given by Equation 264 above and the  $Mg^{2+}$  concentration at each ionic strength. Then the activity coefficient of the free  $F^-$  was calculated using the Pitzer model with parameters for the  $Mg^{2+}-F^-$  interaction set to zero, and the quantities multiplied together to obtain a second estimate of the activity. The results of both approaches are shown in Figure 42. Both methods give similar results at all seawater ionic strengths to  $1 \text{ mol kg}^{-1}$ . In more concentrated solutions the stability constant (given by Equation 264 to  $5 \text{ mol kg}^{-1}$ ) should be used in preference to the pure ion interaction method, as  $mMg^{2+}$  will exceed the maximum concentration used in the original fit.<sup>100</sup> Figure 42b shows total and free  $F^-$  concentrations in the solutions. At  $I_{(s)}$  equal to 0.722 free  $F^-$  constitutes 52% of the total, in satisfactory agreement with earlier estimates. Calculated  $F^-$  activity coefficients on both a “free ion” and stoichiometric basis are shown in Figure 42c.

#### 4. Application of Ion Pairing Models

The incorporation of ion pair equilibria within the formalism of the Pitzer model, described in the sections above, is rendered complex by the need to consider specific interactions between each of the species formed and the other (major) ions present. Ion association models necessarily involve many more equilibria than are required by the ion interaction approach. However, a great simplification is that the activity coefficients of the free (charged) solute species are considered to be functions of effective ionic strength only, and not solution composition. Ion association models therefore have much to offer where the behavior of complexed species is of interest and ionic strengths are relatively low. (This last restriction arises because of the use of simple extended Debye-Hückel expressions to determine activity coefficients, and the lack of specific interactions which become more important as solution concentration is increased.)

The ion association model for seawater introduced by Garrels and Thompson<sup>39</sup> has proved to be generally useful. The original model has been updated and extended over the years (see Whitfield<sup>57</sup> and Johnson and Pytkowicz<sup>43</sup>), but is not readily applied to solutions of high ionic strength ( $>1 \text{ mol kg}^{-1}$ ) for the reasons given above. Calculations using the ion association formalism within various geochemical modeling codes are described by Parkhurst.<sup>44</sup>

The key to the approach is to combine the existing stability constant data with conventional but consistent estimates of single ion activity coefficients to provide a simplified model of ionic interactions in solution. The ion association model assumes that pairwise interactions between ions of opposite charge sign are dominant and that a fraction of the anion-cation couples lose their electrolyte properties when their coulombic attraction is strong. The free ions and the ion pairs are assumed to be in equilibrium. In such a situation the ionic strength is defined in terms of the actual charges of the components assumed to exist in solution. An effective ionic strength ( $I_{\text{eff}}$ ), as opposed to the conventional stoichiometric ionic strength, is defined such that

$$I_{\text{eff}} = 0.5 \left( \sum_i z_i^2 m_{\text{free}} + \sum_j z_j^2 m_j(\text{IP}) \right) \quad (267)$$

where the subscript (F) refers to the free, unpaired component of ion  $i$  in solution and (IP) refers to the (charged) ion pairs  $j$ . It is assumed that the activity coefficients of the ions and the ion pairs in such a solution depend only on the effective ionic strength and *not* on solution composition. To establish such a model, it is necessary to specify

1. The components of the solution (including the complexes and ion pairs that are assumed to exist)
2. Activity data for all the model species, considered as a function of effective ionic strength
3. Stability constants ( $I = 0$ ) for the ion pairs considered
4. Stability constants ( $I = 0$ ) for the other equilibria in solution

The definition of activity coefficients is conventionally based on the following assumptions:

1. There are solutions where no ion association occurs.
2. The free ion activity coefficients of  $\text{K}^+$  and  $\text{Cl}^-$  are equal in solutions of pure aqueous KCl at all ionic strengths (extended MacInnes convention).
3. These free ion activity coefficients are independent of solution composition.

We note here, first, that the aqueous speciation, stability constants, and activity coefficients



**TABLE 48**  
**Fitting Parameters for the Activity Coefficients of the Various**  
**Species, for the Equation:**

$$\ln(\gamma_i) = -1.176 z_i^2 I_{(e)}^{1/2} / (1 + B I_{(e)}^{1/2}) + C I_{(e)}^{2/3} \quad (268)$$

Species	B	C	$10^3 a$	Source
H <sup>+</sup>	1.670	0.525	2.4	$\gamma_{H^+}^0 / \gamma_{KCl}$
Na <sup>+</sup>	1.541	0.126	1.9	$\gamma_{Na^+}^0 / \gamma_{KCl}$
Mg <sup>2+</sup>	1.790	0.454	3.9	$\gamma_{Mg^{2+}}^0 / \gamma_{KCl}$
Ca <sup>2+</sup>	1.729	0.321	1.9	$\gamma_{Ca^{2+}}^0 / \gamma_{KCl}$
K <sup>+</sup>	1.265	0.014	1.2	$\gamma_{K^+}$
Sr <sup>2+</sup>	1.781	0.268	3.7	$\gamma_{Sr^{2+}}^0 / \gamma_{KCl}$
Cl <sup>-</sup>	1.265	0.014	1.2	$\gamma_{Cl^-}$
Br <sup>-</sup>	1.376	0.033	1.1	$\gamma_{Br^-}^0 / \gamma_{KCl}$
OH <sup>-</sup>	0.988	0.475	1.9	$\gamma_{OH^-}^0 / \gamma_{KCl}$
HSO <sub>4</sub> <sup>-</sup>	1.347	-0.088	2.2	$\gamma_{NaHSO_4}^0, \gamma_{NaCl}^{a,b}$
SO <sub>4</sub> <sup>2-</sup>	2.876	-0.598	4.3	$\gamma_{K_2SO_4}^0, \gamma_{KCl}^b$
HCO <sub>3</sub> <sup>-</sup>	0.38	0.43	14	$\gamma_{NaHCO_3}^0, \gamma_{NaCl}^b$
CO <sub>3</sub> <sup>2-</sup>	1.811	-0.064	11.4	$\gamma_{Na_2CO_3}^0, \gamma_{NaCl}^b$
Bi(OH) <sub>3</sub>	1.438	0.011	9.5	$\gamma_{NaBi(OH)_3}^0, \gamma_{NaCl}^b$
F <sup>-</sup>	1.234	0.153	2.2	$\gamma_{KF}^0 / \gamma_{KCl}$
Ion pairs				
1/1		-0.3	?	Reardon and Langmuir <sup>601</sup>
2/2		-1.2	?	Reardon and Langmuir <sup>601</sup>
1/2	1.265	-0.0114	?	As for Cl <sup>-</sup> (see Reardon <sup>602</sup> )
Neutral species				
CO <sub>2</sub> <sup>*</sup>		0.22	2.4	Solubility data of Murray and Riley <sup>603</sup>
Bi(OH) <sub>3</sub>		0.02	3.0	
HF		0.2		Poor fit

*Note:* Sources of mean-ion activity data are KCl, HCl, NaCl, KF, KOH, KBr — Hamer and Wu;<sup>103</sup> MgCl<sub>2</sub>, SrCl<sub>2</sub>, K<sub>2</sub>SO<sub>4</sub>, Na<sub>2</sub>CO<sub>3</sub>, NaBi(OH)<sub>3</sub> — Pitzer and Mayorga;<sup>101</sup> CaCl<sub>2</sub> — Staples and Nuttall;<sup>104</sup> NaHCO<sub>3</sub> — Pitzer and Peiper.<sup>105</sup>

<sup>a</sup> Suggestion of Pitzer et al.<sup>65</sup>

<sup>b</sup> Iterative procedure.

derived using an ion association model are unlikely to be consistent with mineral solubility data. Second, the choice of complexes and the concentration dependence of activity coefficients within the ion pairing approach are not uniquely defined (many such choices are possible, and these are likely to depend upon the application).

In the absence of association, free ion activity coefficients for other ions can be obtained from suitably weighted ratios of the appropriate mean-ion activity coefficients, e.g.,

$$\gamma_{Ca^{2+}} = \gamma_{CaCl_2}^0 / \gamma_{KCl}^2 \quad (268)$$

For ions which exhibit strong pairwise interactions in all solutions (e.g., SO<sub>4</sub><sup>2-</sup>), an iterative procedure is required.<sup>234</sup> Conventional free-ion activity coefficients calculated in this way can be fitted to an equation of the form (Table 48)

$$\ln(\gamma_i) = -1.176 z_i^2 I_{(e)}^{1/2} / (1 + B I_{(e)}^{1/2}) + C I_{(e)}^{2/3} \quad (269)$$

**TABLE 49**  
**Log<sub>10</sub>(K) (*I*<sub>e1</sub> = 0) for those Association**  
**Equilibria which Represent Ionic Interactions<sup>224</sup>**

Anion/cation	Na <sup>+</sup>	Mg <sup>2+</sup>	Ca <sup>2+</sup>	K <sup>+</sup>	Sr <sup>2+</sup>
Cl	*	*	*	*	*
Br	**	**	**	*	**
OH <sup>-</sup>	-0.2 <sup>a</sup>	2.21 <sup>b</sup>	1.15 <sup>c</sup>	*	0.71 <sup>a</sup>
HSO <sub>4</sub> <sup>-</sup>	-0.7 <sup>a</sup>	0.4 <sup>c</sup>	0.3 <sup>c</sup>	*	0.5 <sup>c</sup>
SO <sub>4</sub> <sup>2-</sup>	0.82 <sup>d</sup>	2.25 <sup>e</sup>	2.31 <sup>f</sup>	0.85 <sup>d</sup>	2.55 <sup>g</sup>
HCO <sub>3</sub> <sup>-</sup>	-0.25 <sup>h</sup>	1.07 <sup>i</sup>	1.10 <sup>j</sup>	*	1.24 <sup>k</sup>
CO <sub>3</sub> <sup>2-</sup>	0.7 <sup>l</sup>	2.88 <sup>m</sup>	3.15 <sup>n</sup>	0.7 <sup>o</sup>	2.64 <sup>o</sup>
B(OH) <sub>3</sub>	0.00 <sup>p</sup>	1.44 <sup>p</sup>	1.70 <sup>p</sup>	*	1.7 <sup>q</sup>
F	-0.26 <sup>r</sup>	1.82 <sup>r</sup>	1.04 <sup>r</sup>	*	0.55 <sup>r</sup>

Note: (\*) — K is defined as zero by extended MacInnes convention for activity coefficients; (\*\*) — assumed K = 0 by analogy with the chloride values.

<sup>a</sup> Baes and Mesmer.<sup>366</sup>

<sup>b</sup> McGee and Hostetler.<sup>367</sup>

<sup>c</sup> Estimated by assuming that  $K_{NaCl}/K_{H_2SO_4} = K_{CaCl_2}/K_{HCO_3}$ .

<sup>d</sup> Reardon.<sup>362</sup>

<sup>e</sup> Nair and Nancollas.<sup>368</sup>

<sup>f</sup> Bell and George.<sup>369</sup>

<sup>g</sup> Smith and Martell.<sup>295</sup>

<sup>h</sup> Garrels and Thompson.<sup>39</sup>

<sup>i</sup> Seibert and Hostetler.<sup>170</sup>

<sup>j</sup> Reardon et al.<sup>371</sup>

<sup>k</sup> Nakayama and Rasmick.<sup>372</sup>

<sup>l</sup> Chosen for consistency with  $\gamma_{Na_2CO_3}$ .

<sup>m</sup> Reardon and Langmuir.<sup>373</sup>

<sup>n</sup> Assumed equal to K for NaCO<sub>3</sub>.

<sup>o</sup> Estimated from plot of log<sub>10</sub> K(CO<sub>3</sub><sup>2-</sup>) against log<sub>10</sub> K(Oxalate).<sup>226</sup>

<sup>p</sup> Estimated by correction to *I* = 0 of data of Byrne and Kester.<sup>374</sup>

<sup>q</sup> Assumed equal to K for CaBO<sub>3</sub>.

<sup>r</sup> Duer et al.<sup>375</sup>

<sup>s</sup> Connick and Tsao.<sup>376</sup>

<sup>t</sup> Estimated from plot of log<sub>10</sub> K(F<sup>-</sup>) against log<sub>10</sub> K(OH<sup>-</sup>).

The activity coefficients attributed to the ion pairs and complexes produced in solution are usually based on a variety of *ad hoc* assumptions. In the model of Dickson and Whitfield,<sup>224</sup> singly charged ion pairs were assumed to behave like K<sup>+</sup> or Cl<sup>-</sup>. Neutral ion pairs and neutral complexes N were treated via a Setchenow-type relationship:

$$\ln(\gamma_N) = aI_{e1} \quad (270)$$

where *a* = 1.2 for neutral 2:2 ion pairs and 0.3 for 1:1 ion pairs. The activity coefficients of neutral compounds, such as dissolved CO<sub>2</sub>, were calculated from the appropriate solubility data (see Section III.B).

In addition to these conventional definitions it is necessary to select stability constants (*I* = 0) to represent the equilibria involved. The constants selected for the ion pair equilibria will vary from model to model, but the values employed in the model of Dickson and Whitfield<sup>224</sup> are typical (Table 49). Such models have been shown to provide reasonable accounts of the activity coefficients and osmotic coefficients of seawater to ionic strength up to 1 mol kg<sup>-1</sup> (see Whitfield<sup>224</sup> in the previous edition of this book).

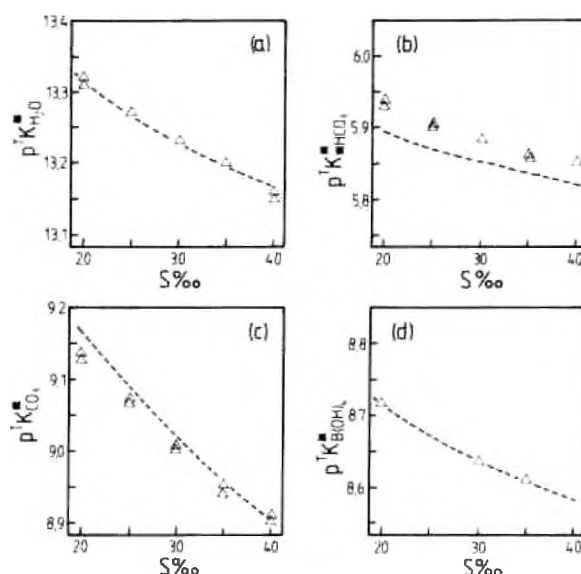


FIGURE 43. Stoichiometric equilibrium constants in seawater at 25°C, as a function of salinity, calculated using the ion association model of Dickson and Whitfield.<sup>224</sup> (a) The ionic product of water ( ${}^1K_{H_2O}^*$ ); (b) the first dissociation constant of carbonic acid ( ${}^1K_{H_2CO_3}^*$ ); (c) the second dissociation constant of carbonic acid ( ${}^1K_{CO_3}^*$ ); (d) the dissociation constant of boric acid ( ${}^1K_{B(OH)_3}^*$ ). Lines — model calculations; symbols — available data. (This diagram reproduced from Dickson and Whitfield.<sup>224</sup>)

The efficiency of such a model for calculating the stoichiometric stability constants of acid-base equilibria in seawater was tested by Dickson and Whitfield.<sup>224</sup> The values obtained were in reasonable agreement with the experimental data (total hydrogen ion pH scale) over the limited salinity range (20 to 30 S‰) for which accurate experimental values were available (see Figure 43). The calculated values for the first ionization constant for carbonic acid in seawater (Figure 43b) are consistently lower than the experimental values. This discrepancy (which was also noted for the calculations using the Pitzer model, Figure 26) is probably due to inaccuracies in the estimation of the stability constants for ion pair formation involving  $HCO_3^-$ . Since the model can accurately predict  $p({}^1K_{HCO_3}^*)$  in aqueous NaCl for  $I$ , up to 1 mol dm<sup>-3</sup>,<sup>223</sup> it is likely that the problem lies with the  $Mg^{2+}$  and  $Ca^{2+}$  ion pairs with bicarbonate. Predicted values of  ${}^1K_{H_2CO_3}^*$ ,  ${}^1K_{B(OH)_3}^*$ , and  ${}^1K_{CO_3}^*$  are in satisfactory agreement with available data. This simple form of the ion pair model therefore provides a tolerable description of ionic interactions in seawater.

The format of the model clearly lends itself to the incorporation of metal complexation equilibria. To follow up the examples considered during the discussion of the Pitzer treatment (Sections III.D.1 to III.D.3) we can look at the use of the ion pair model to estimate the activity coefficients of copper in saline media.<sup>405</sup> Since copper forms strong complexes with organic ligands, and since many of the ligands can be highly charged in natural systems, the equation describing conventional activity coefficients of the individual ionic components (Equation 269) is extended by the addition of the term  $D_i^{1,2}$ . The stability constants and fitting parameters required to describe the behavior of copper in seawater or estuarine waters containing no organic matter are summarized in Table 50. A full Pitzer model to cover all the possible interactions in this system would clearly be complex. Using the data in Table 50 in conjunction with the standard seawater model (Table 48) indicates that the chloro-complexes considered earlier are negligible in these natural waters. At a pH of 8.2, char-

**TABLE 50**  
**Thermodynamic Stability Constants and**  
**Activity Coefficient Fits for Inorganic**  
**Copper Complexes (Equation 269)<sup>305</sup>**

Complex	$\log_{10} K$	B	C	$\sigma$
$\text{Cu}^{2+}$	—	1.718	0.083	0.0016
$\text{CuOH}^+$	-7.98	1.5	-0.0426	—
$\text{Cu(OH)}_2^0$	-16.24	—	-0.0237	—
$\text{CuSO}_4^0$	2.36	—	-0.521	—
$\text{CuCO}_3^0$	6.77	—	-0.410	0.025
$\text{Cu(CO}_3)_2^{2-}$	10.51	1.5	-0.124	0.071
$\text{CuHCO}_3^+$	1.84	1.5	0.183	0.040

acteristic of seawater, the speciation is dominated by the formation of  $\text{CuCO}_3^0$  (78%) with less than 5% of the copper present in the free ionic form. By contrast, experimental measurements suggest that more than 90% of the copper in natural samples is, in fact, complexed by organic matter. Model organic ligands such as glycine and EDTA can be incorporated into the copper speciation models in a relatively straightforward manner, and the stoichiometric stability constants calculated for copper complexation reactions are in good agreement with the experimental values in a variety of ionic media.<sup>305</sup> The incorporation of a further range of trace metals into such a model will depend on the availability of the stability constants for the relevant complex formation reactions.

## APPENDIX

**TABLE A1**  
**The Relative Density ( $d_{(s)}/\text{kg m}^{-3}$ ) of Oceanic Seawater as a Function of Salinity and**  
**Temperature<sup>18</sup> (Equation 7)**

Temp (°C)	Salinity (S‰)							
	0	5	10	15	20	25	30	35
0	999.84	1003.91	1007.95	1011.99	1016.01	1020.04	1024.07	1028.11
5	999.97	1003.95	1007.91	1011.86	1015.81	1019.76	1023.71	1027.68
10	999.70	1003.61	1007.50	1011.39	1015.27	1019.16	1023.05	1026.95
15	999.10	1002.95	1006.78	1010.61	1014.44	1018.28	1022.12	1025.97
20	998.21	1002.01	1005.79	1009.58	1013.36	1017.15	1020.95	1024.76
25	997.05	1000.81	1004.56	1008.30	1012.05	1015.81	1019.57	1023.34
30	995.65	999.38	1003.10	1006.81	1010.53	1014.25	1017.99	1021.73
35	994.04	997.74	1001.43	1005.12	1008.81	1012.51	1016.22	1019.93

*Note:* In the equation given by Millero<sup>18</sup> for the relative density of pure water the sign of the term in  $t^3$  should be changed to correspond to Equation 9 in this work.

**TABLE A2**  
**Factors for the Interconversion of**  
**Concentration Scales Using the Equation**  
 $Y = X/E$

Y	X	E
$x_i$	$k_i$	$\sum_i k_i + (1000 - \sum_i k_i w_i)/w_{H_2O}$
$x_i$	$c_i$	$\sum_i c_i + (\rho - \sum_i c_i w_i)/w_{H_2O}$
$x_i$	$m_i$	$1000/w_{H_2O} + \sum_i m_i$
$m_i$	$k_i$	$1 - \sum_i k_i w_i$
$m_i$	$c_i$	$\rho - \sum_i c_i w_i$
$m_i$	$x_i$	$(1 - \sum_i x_i)10^{-3} w_{H_2O}$
$k_i$	$m_i$	$1 + 10^{-3} \sum_i m_i w_i$
$k_i$	$x_i$	$10^{-3}(x_{H_2O} w_{H_2O} + \sum_i x_i w_i)$
$k_i$	$c_i$	$10^{-3} \rho$
$c_i$	$m_i$	$(1000 + \sum_i m_i w_i)/\rho$
$c_i$	$k_i$	$10^3/\rho$
$c_i$	$x_i$	$[x_{H_2O} w_{H_2O} + \sum_i x_i w_i]/\rho$

*Note:* The symbols for the concentration scales are defined in Table 5.  $\rho$  = density ( $\text{g dm}^{-3}$ ),  $w_i$  = molar mass (g) of ion or neutral species "i" (excluding water, given as  $w_{H_2O}$ ). Summations are over all ionic and neutral species (again excluding  $H_2O$ ). The mole fraction  $x_i$  of ion or neutral species "i" corresponds to the definition in Equation 11.

**TABLE A3**  
**Selected Values for the Conversion**  
**Parameters Defined in Table A2 ( $Y =$**   
 **$X/E$ ) for Various Seawater Recipes**

Y	X	E		
		(a)	(b)	(c)
$x_i$	$k_i$	54.67544	54.67532	54.67613
$x_i$	$c_i$	55.95348	55.95353	55.96102
$x_i$	$m_i$	56.66899	56.60953	56.66907
$m_i$	$k_i$	0.964821	0.964810	0.964832
$m_i$	$c_i$	0.987374 <sup>d</sup>	0.987365	0.987506
$m_i$	$x_i$	0.017646	0.017646	0.017646
$k_i$	$m_i$	1.036462	1.036473	1.036540
$k_i$	$x_i$	0.0182897	0.018343	0.0182895
$k_i$	$c_i$	1.023375	1.023375	1.0235
$c_i$	$m_i$	1.012788	1.012799	1.012653
$c_i$	$k_i$	0.977159	0.977159	0.977040
$c_i$	$x_i$	0.0178720	0.017924	0.0178696

<sup>a</sup> Millero.<sup>26</sup>

<sup>b</sup> Riley and Skirrow,<sup>307</sup> assuming  $\rho = 1023.375 \text{ g dm}^{-3}$ .

<sup>c</sup> Recipe of Kester et al.<sup>308</sup> as calculated by MacIntyre,<sup>13</sup> assuming  $\rho = 1023.5 \text{ g dm}^{-3}$ .

<sup>d</sup> For groundwater brines (Table 3), this value can be as low as 0.8002.

**TABLE A4**  
**Coefficients for the Calculation of Pitzer Model Parameters  $\beta^{(0)\vee}$ ,  $\beta^{(1)\vee}$ ,  $\beta^{(2)\vee}$ ,**  
**and  $C^{\phi\vee}$  as Functions of Temperature from 0 to 100°C<sup>93,94</sup>**

	NaCl	Na <sub>2</sub> SO <sub>4</sub>	MgCl <sub>2</sub>	MgSO <sub>4</sub>
$b_0$	$-4.1090410 \times 10^{-1}$	-1.1644972	$-1.4118667 \times 10^{-2}$	$-7.8645669 \times 10^{-1}$
$b_1$	8.8045055	$2.4186443 \times 10^1$	$4.5783681 \times 10^{-1}$	$1.6105729 \times 10^1$
$b_2$	$7.7002565 \times 10^{-2}$	$2.1978590 \times 10^{-1}$	$2.3719202 \times 10^{-4}$	$1.4892797 \times 10^{-1}$
$b_3$	$-2.2505103 \times 10^{-4}$	$-6.6686839 \times 10^{-4}$	$-3.0501313 \times 10^{-6}$	$-4.5954181 \times 10^{-4}$
$b_4$	$1.0974488 \times 10^{-7}$	$3.3743240 \times 10^{-7}$	$-3.7549481 \times 10^{-11}$	$2.3590114 \times 10^{-7}$
$c_0$		$-6.1507685 \times 10^{-2}$	-7.9923583	$-8.5368752 \times 10^{-1}$
$c_1$		3.2577301	$1.6695782 \times 10^2$	$2.5326354 \times 10^1$
$c_2$		$8.9092747 \times 10^{-1}$	1.5056833	$1.4616910 \times 10^{-1}$
$c_3$			$-4.5164571 \times 10^{-1}$	$-2.1444963 \times 10^{-4}$
$c_4$			$-2.2510088 \times 10^{-6}$	
$d_0$				-4.1068422
$d_1$				$1.9093018 \times 10^{-2}$
$d_2$				$6.9103123 \times 10^{-1}$
$e_0$	$1.0679642 \times 10^{-2}$	$-3.7140974 \times 10^{-6}$	$2.9007867 \times 10^{-4}$	
$e_1$	$-3.0822989 \times 10^{-1}$		$-1.5248427 \times 10^{-2}$	
$e_2$	$-1.8372623 \times 10^{-1}$		$4.2278115 \times 10^{-5}$	
$e_3$	$2.7528745 \times 10^{-6}$			
	<b>KCl</b>	<b>K<sub>2</sub>SO<sub>4</sub></b>		
$b_0$	$0.507066 \times 10^{-2}$	$-0.212275165 \times 10^{-1}$		
$b_1$	$0.213420 \times 10^{-8}$	$0.1062023 \times 10^1$		
$b_2$	$-0.112814 \times 10^{-2}$	$0.3108538 \times 10^{-2}$		
$b_3$	$0.562678 \times 10^{-5}$			
$b_4$	$-0.345546 \times 10^{-8}$			
$c_0$		$-0.781281 \times 10^{-1}$		
$c_1$		0.2927024		
$c_2$				
$e_0$	$0.3614778 \times 10^{-1}$			
$e_1$	$-0.1840717 \times 10^{-1}$			
$e_2$	$-0.5274099 \times 10^{-4}$			

Note: The model parameters (kg bar<sup>-1</sup> mol<sup>-1</sup>) are given by the following equations:

$$\beta^{(0)\vee} (= \partial\beta^{(0)\vee}/\partial P) = b_0 + b_1/T + b_2 \ln(T) + b_3/T + b_4/T^2$$

$$\beta^{(1)\vee} (= \partial\beta^{(1)\vee}/\partial P) = c_0 + c_1/T + c_2 \ln(T) + c_3/T + c_4/T^2$$

$$\beta^{(2)\vee} (= \partial\beta^{(2)\vee}/\partial P) = d_0 + d_1/T + d_2 \ln(T)$$

$$C^{\phi\vee} (= \partial C^{\phi\vee}/\partial P) = e_0 + e_1/T + e_2 \ln(T) + e_3/T$$

The model parameters were obtained using a fit constrained to pass through the most reliable infinite dilution values of the partial molal volumes. For conversion to S.I. units: 1 bar = 10<sup>5</sup> Pa.

**TABLE A5**  
**Coefficients for the Calculation of Pitzer Model Parameters  $\beta^{(0)*}$ ,  $\beta^{(1)*}$ ,  $\beta^{(2)*}$ , and  $C^{\phi*}$  as Functions of Temperature from 0 to 100°C<sup>(1)</sup>**

	NaCl	Na <sub>2</sub> SO <sub>4</sub>	MgCl <sub>2</sub>	MgSO <sub>4</sub>
B <sub>0</sub>	$-0.944474 \times 10^{-5}$	$-0.487769 \times 10^{-4}$	$-0.100866 \times 10^{-4}$	$-0.376506 \times 10^{-4}$
B <sub>1</sub>	$0.111681 \times 10^{-6}$	$0.596173 \times 10^{-6}$	$0.121094 \times 10^{-6}$	$0.462335 \times 10^{-6}$
B <sub>2</sub>	$-0.499433 \times 10^{-9}$	$-0.273124 \times 10^{-8}$	$-0.545891 \times 10^{-9}$	$-0.212285 \times 10^{-8}$
B <sub>3</sub>	$0.500505 \times 10^{-12}$	$0.555388 \times 10^{-11}$	$0.109379 \times 10^{-11}$	$0.431564 \times 10^{-11}$
B <sub>4</sub>	$-0.379426 \times 10^{-15}$	$-0.422839 \times 10^{-14}$	$-0.821611 \times 10^{-15}$	$-0.327532 \times 10^{-14}$
C <sub>0</sub>		$-0.793395 \times 10^{-5}$	$-0.290546 \times 10^{-5}$	$0.134943 \times 10^{-4}$
C <sub>1</sub>		$0.484600 \times 10^{-7}$	$0.179985 \times 10^{-7}$	$-0.173557 \times 10^{-6}$
C <sub>2</sub>		$-0.738734 \times 10^{-10}$	$-0.276707 \times 10^{-10}$	$0.681185 \times 10^{-9}$
C <sub>3</sub>				$-0.847680 \times 10^{-12}$
D <sub>0</sub>				$-0.189028 \times 10^{-7}$
D <sub>1</sub>				$0.176629 \times 10^{-4}$
D <sub>2</sub>				$-0.549757 \times 10^{-7}$
D <sub>3</sub>				$0.568136 \times 10^{-10}$
E <sub>0</sub>	$0.137289 \times 10^{-6}$	$0.892502 \times 10^{-8}$	$0.893214 \times 10^{-9}$	
E <sub>1</sub>	$-0.838713 \times 10^{-9}$			
E <sub>2</sub>	$0.128245 \times 10^{-11}$			

Note: The model parameters (pressure in bars) are given by the following equations:

$$\begin{aligned}\beta^{(0)*} ( = \partial^2 \beta^{(0)*} / \partial P^2 ) &= B_0 + B_1 T + B_2 T^2 + B_3 T^3 + \dots \\ \beta^{(1)*} ( = \partial^2 \beta^{(1)*} / \partial P^2 ) &= C_0 + C_1 T + C_2 T^2 + C_3 T^3 + \dots \\ \beta^{(2)*} ( = \partial^2 \beta^{(2)*} / \partial P^2 ) &= D_0 + D_1 T + D_2 T^2 + D_3 T^3 + \dots \\ C^{\phi*} ( = \partial^2 C^{\phi*} / \partial P^2 ) &= E_0 + E_1 T + E_2 T^2 + E_3 T^3 + \dots\end{aligned}$$

**TABLE A6**  
**Osmotic and Major Ion Activity Coefficients in Seawater (5–40 S‰, 0–35°C) Calculated Using the Pitzer Model (Seawater Recipe<sup>28</sup> in Column b of Table 2)**

S	<i>T</i> <sub>m</sub>	ϕ	aH <sub>2</sub> O	γ <sub>+</sub>	γ <sub>Na</sub>	γ <sub>Ca</sub>	γ <sub>Mg</sub>	γ <sub>SO<sub>4</sub></sub>	γ <sub>Cl</sub>	γ <sub>CO<sub>3</sub></sub>	γ <sub>HCO<sub>3</sub></sub>	γ <sub>B</sub>	γ <sub>F</sub>	γ <sub>CO<sub>2</sub></sub>
5	0.1001	0.9141	0.997	25	0.770	0.356	0.348	0.759	0.345	0.785	0.294	0.789	0.616	0.761
10	0.2012	0.9030	0.995	25	0.721	0.285	0.277	0.702	0.270	0.745	0.211	0.753	0.496	0.705
15	0.3034	0.8943	0.992	25	0.692	0.251	0.243	0.667	0.233	0.724	0.169	0.735	0.424	0.672
20	0.4067	0.8985	0.990	25	0.672	0.232	0.223	0.641	0.211	0.710	0.143	0.725	0.373	0.648
25	0.5110	0.8994	0.987	25	0.658	0.219	0.210	0.620	0.195	0.702	0.125	0.719	0.335	0.630
30	0.6163	0.9013	0.984	25	0.647	0.211	0.201	0.604	0.184	0.696	0.111	0.717	0.306	0.616
35	0.7228	0.9039	0.981	25	0.638	0.205	0.194	0.589	0.175	0.692	0.100	0.716	0.281	0.605
40	0.8304	0.9070	0.978	25	0.631	0.201	0.189	0.577	0.168	0.689	0.092	0.717	0.260	0.595
5	0.1001	0.9146	0.9974	0	0.771	0.376	(0.361)	0.760	0.788	0.310				
10	0.2012	0.9015	0.9948	0	0.719	0.304	(0.287)	0.700	0.746	0.220				
15	0.3034	0.8958	0.9922	0	0.688	0.271	(0.251)	0.662	0.723	0.174				
20	0.4067	0.8932	0.9895	0	0.666	0.252	(0.229)	0.634	0.708	0.145				
25	0.5110	0.8922	0.9869	0	0.649	0.240	(0.214)	0.612	0.697	0.125				
30	0.6163	0.8924	0.9842	0	0.635	0.232	(0.204)	0.593	0.689	0.110				
35	0.7228	0.8934	0.9815	0	0.624	0.227	(0.196)	0.577	0.684	0.098				
40	0.8304	0.8950	0.9787	0	0.615	0.224	(0.189)	0.563	0.679	0.088				
5	0.1001	0.9148	0.9974	5	0.772	0.371	(0.359)	0.761	0.788	0.306				
10	0.2012	0.9023	0.9948	5	0.721	0.300	(0.287)	0.702	0.747	0.218				
15	0.3034	0.8972	0.9922	5	0.690	0.266	(0.252)	0.665	0.724	0.173				
20	0.4067	0.8951	0.9895	5	0.669	0.247	(0.231)	0.637	0.710	0.145				

TABLE A6 (continued)  
Osmotic and Major Ion Activity Coefficients in Seawater (5–40 S‰, 0–35°C) Calculated Using  
the Pitzer Model (Seawater Recipe<sup>26</sup> in Column b of Table 2)

S	$I_m$	$\phi$	$a_{H_2O}$	$t$	$\gamma_{Na}$	$\gamma_{Mg}$	$\gamma_{Ca}$	$\gamma_K$	$\gamma_{Cl}$	$\gamma_{SO_4}$	$\gamma_{NO_3}$	$\gamma_{HCO_3}$	$\gamma_{CO_3}$	$\gamma_{HPO_4}$	$\gamma_{SiO_4}$
25	0.5110	0.8947	0.9869	5	0.652	0.235	(0.217)	0.615	0.700	0.126					
30	0.6163	0.8954	0.9842	5	0.639	0.227	(0.207)	0.597	0.692	0.111					
35	0.7228	0.8968	0.9814	5	0.629	0.222	(0.199)	0.582	0.687	0.099					
40	0.8304	0.8989	0.9786	5	0.620	0.219	(0.194)	0.568	0.683	0.089					
5	0.1001	0.9148	0.9974	10	0.772	0.367	(0.357)	0.761	0.788	0.303					
10	0.2012	0.9028	0.9948	10	0.721	0.296	(0.285)	0.703	0.747	0.216					
15	0.3034	0.8982	0.9921	10	0.691	0.262	(0.250)	0.666	0.725	0.172					
20	0.4067	0.8965	0.9895	10	0.671	0.243	(0.230)	0.639	0.711	0.145					
25	0.5110	0.8965	0.9868	10	0.655	0.231	(0.216)	0.618	0.701	0.126					
30	0.6163	0.8976	0.9841	10	0.642	0.223	(0.206)	0.600	0.694	0.111					
35	0.7228	0.8994	0.9814	10	0.632	0.217	(0.199)	0.585	0.689	0.099					
40	0.8304	0.9019	0.9786	10	0.624	0.214	(0.194)	0.572	0.686	0.090					
5	0.1001	0.9147	0.9974	15	0.771	0.363	(0.354)	0.760	0.787	0.300					
10	0.2012	0.9031	0.9948	15	0.721	0.292	(0.282)	0.703	0.747	0.214					
15	0.3034	0.8988	0.9921	15	0.692	0.258	(0.248)	0.667	0.725	0.171					
20	0.4067	0.8975	0.9895	15	0.672	0.239	(0.228)	0.640	0.711	0.144					
25	0.5110	0.8979	0.9868	15	0.656	0.227	(0.215)	0.619	0.702	0.126					
30	0.6163	0.8993	0.9841	15	0.645	0.218	(0.205)	0.602	0.695	0.111					
35	0.7228	0.9014	0.9813	15	0.635	0.213	(0.198)	0.587	0.691	0.100					
40	0.8304	0.9041	0.9785	15	0.627	0.209	(0.193)	0.574	0.688	0.091					
5	0.1001	0.9144	0.9974	20	0.771	0.359	(0.351)	0.760	0.786	0.297					
10	0.2012	0.9032	0.9948	20	0.721	0.288	(0.280)	0.703	0.746	0.212					
15	0.3034	0.8992	0.9921	20	0.692	0.255	(0.246)	0.667	0.725	0.170					
20	0.4067	0.8982	0.9895	20	0.672	0.235	(0.226)	0.641	0.711	0.144					
25	0.5110	0.8988	0.9868	20	0.657	0.223	(0.212)	0.620	0.702	0.125					
30	0.6163	0.9004	0.9841	20	0.646	0.214	(0.203)	0.603	0.696	0.111					
35	0.7228	0.9028	0.9813	20	0.637	0.209	(0.196)	0.589	0.692	0.100					
40	0.8304	0.9058	0.9785	20	0.629	0.205	(0.191)	0.576	0.689	0.091					
5	0.1001	0.9137	0.9974	30	0.768	0.352	(0.344)	0.758	0.784	0.292					
10	0.2012	0.9028	0.9948	30	0.720	0.281	(0.274)	0.701	0.744	0.209					
15	0.3034	0.8992	0.9921	30	0.691	0.248	(0.240)	0.666	0.723	0.168					
20	0.4067	0.8987	0.9895	30	0.672	0.228	(0.221)	0.640	0.710	0.142					
25	0.5110	0.8997	0.9868	30	0.657	0.216	(0.207)	0.620	0.701	0.124					
30	0.6163	0.9017	0.9841	30	0.647	0.207	(0.198)	0.604	0.695	0.111					
35	0.7228	0.9045	0.9813	30	0.638	0.201	(0.192)	0.590	0.691	0.100					
40	0.8304	0.9078	0.9784	30	0.631	0.197	(0.187)	0.578	0.689	0.091					
5	0.1001	0.9132	0.9974	35	0.767	0.349	(0.341)	0.757	0.782	0.290					
10	0.2012	0.9024	0.9948	35	0.718	0.278	(0.270)	0.700	0.742	0.207					
15	0.3034	0.8990	0.9921	35	0.690	0.245	(0.237)	0.665	0.721	0.167					
20	0.4067	0.8986	0.9895	35	0.671	0.225	(0.218)	0.640	0.708	0.141					
25	0.5110	0.8997	0.9868	35	0.657	0.212	(0.205)	0.620	0.700	0.124					
30	0.6163	0.9019	0.9840	35	0.646	0.203	(0.196)	0.603	0.694	0.110					
35	0.7228	0.9048	0.9813	35	0.638	0.197	(0.189)	0.590	0.690	0.099					
40	0.8304	0.9083	0.9784	35	0.631	0.193	(0.184)	0.578	0.688	0.091					

Note. These activity and osmotic coefficients were calculated using constant (25°C) values of all ternary parameters  $\theta_{ij}$  and  $\phi_{ij}$  and full fitting equations [giving  $B^{\circ}$  and  $C^{\circ}$  as f(T)] for NaCl, Na<sub>2</sub>SO<sub>4</sub>, MgCl<sub>2</sub>, MgSO<sub>4</sub>, CaCl<sub>2</sub>, KCl, and K<sub>2</sub>SO<sub>4</sub>. Available  $\partial B^{\circ}/\partial T$ ,  $\partial C^{\circ}/\partial T$  were used for CaSO<sub>4</sub>. Activity coefficients of all ions are given at 25°C, but at other temperatures only those of ions whose interactions are well parameterized. The activity coefficient of F<sup>-</sup> at 25°C is a "total" value, taking into account complexation by Mg<sup>2+</sup> and Ca<sup>2+</sup>.



**TABLE A7**  
**The Solubility of Gases in Pure Water at 1 atm Pressure**  
**[ $R \ln(x_N) = A + B/T + C \ln(T) + DT$ ]<sup>a</sup>**

Gas	Temp. range (T/K)	A (cal K <sup>-1</sup> mol <sup>-1</sup> )	B (cal mol <sup>-1</sup> )	C (cal K <sup>-1</sup> mol <sup>-1</sup> )	D (cal K <sup>-2</sup> mol <sup>-1</sup> )
He	273—334	-233.163	8737.84	32.2652	-0.0119726
Ne	272—339	-310.827	12766.8	43.6185	-0.0127534
Ar	274—347	-336.760	16170.1	46.2117	-0.00608793
Kr	274—348	-270.967	15992.9	33.2892	0.0260485
Xe	285—345	-360.119	18744.6	49.0332	-0.00311323
Rn	276—370	-499.309	13897.5	52.2871	-0.00101227
H <sub>2</sub>	274—339	-357.802	13897.5	52.2871	-0.0298936
N <sub>2</sub>	273—346	-327.850	16757.6	42.8400	0.0167645
O <sub>2</sub>	274—348	-327.850	16757.6	42.8400	0.0187662
O <sub>3</sub>	277—293	-29.7374	3905.44 <sup>b</sup>	—	—
CO	273—353	-341.325	16487.3	46.3757	—
CO <sub>2</sub>	273—353	-317.658	17371.2	43.0607	-0.00219107
CH <sub>4</sub>	275—353	-365.183	18106.7	49.7554	-0.000285033
C <sub>2</sub> H <sub>6</sub>	275—353	-533.392	26565.0	74.6240	-0.00457313
Ethylene	287—346	-303.888	15817.6	40.7591	—
Acetylene	274—343	-311.014	16215.8	42.5305	—
Propane	273—347	-628.866	31638.4	88.0808	—
Propene	294—361	199.656	-3940.90	-35.8336	—
Propyne	273—361	-16821.1	45295.1	2933.82	-4.78664
Cyclopropane	298—361	649.616	-26880.3	-101.150	—
<i>n</i> -Butane	273—349	-639.209	32785.7	89.1483	—
Isobutane	278—343	190.982	-4912.98	-34.5102	—
1-Butene	311—378	-59.297	12730.6 <sup>b</sup>	—	—
2-Methylpropene	273—343	-475.781	25385.0	65.3599	—
1,3-Butadiene	298—363	-976.088	50382.7	138.778	—
Ethylacetylene	273—333	171.933	-5084.59	-29.4809	—
Vinylacetylene	273—333	-99.0059	6690.87	10.8969	—
Neopentane	288—353	-868.764	43323.6	122.986	—
CH <sub>3</sub> F	273—353	-270.079	15103.1	36.1231	—
CH <sub>3</sub> Cl	277—353	-342.796	194112.2	46.5481	—
CH <sub>3</sub> Br	278—535	-325.392	19159.9	43.7970	—
CF <sub>4</sub>	276—323	-644.690	30657.7	90.7528	—
CH <sub>2</sub> FCl	283—352	-276.044	16178.1	36.8643	—
CHF <sub>2</sub> Cl	297—352	-378.939	25999.6	—	0.0642996
CHF <sub>3</sub>	298—348	-37.9627	6386.96 <sup>b</sup>	—	—
CClF <sub>3</sub>	298—348	-32.5600	3204.55 <sup>b</sup>	—	—
CCl <sub>2</sub> F <sub>2</sub>	298—348	-31.8744	3480.07 <sup>b</sup>	—	—
CClF <sub>2</sub> CF <sub>3</sub>	298—348	-42.5189	5568.80 <sup>b</sup>	—	—
Vinyl chloride	273—348	-240.646	15080.2	30.8852	—
C <sub>2</sub> F <sub>4</sub>	273—343	-367.547	21547.6	45.9952	0.0416536
C <sub>2</sub> F <sub>6</sub>	278—343	-132.311	8925.54	13.7311	—
CH <sub>3</sub> NH <sub>2</sub>	298—333	-18.2657	5180.80 <sup>b</sup>	—	—
(CH <sub>3</sub> ) <sub>2</sub> NH	298—333	-28.0155	8000.71 <sup>b</sup>	—	—
C <sub>2</sub> H <sub>5</sub> NH <sub>2</sub>	298—333	-25.0844	7210.82 <sup>b</sup>	—	—
NH <sub>3</sub>	273—373	-162.446	2179.59	32.9085	-0.119722
N <sub>2</sub> O	273—313	-180.950	13205.8	20.0399	0.0238544
NO	273—353	-333.515	16358.8	45.3253	-0.0519354
H <sub>2</sub> S	273—333	-297.158	16347.7	40.2024	0.00257153
SO <sub>2</sub>	283—386	-29.8850	5709.15	0.601884	—
Cl <sub>2</sub>	283—313	215.390	-4826.15	-38.1252	0.0177270
Cl <sub>2</sub> O	273—293	-14.3490	3574.66 <sup>b</sup>	—	—
ClO <sub>2</sub>	283—333	112.751	284.523	-21.3532	—

**TABLE A7 (continued)**  
**The Solubility of Gases in Pure Water at 1 atm Pressure**  
 $[R \ln(x_N) = A + B/T + C \ln(T) + DT]^a$

Gas	Temp. range (T/K)	A (cal K <sup>-1</sup> mol <sup>-1</sup> )	B (cal mol <sup>-1</sup> )	C (cal K <sup>-1</sup> mol <sup>-1</sup> )	D (cal K <sup>-2</sup> mol <sup>-1</sup> )
H <sub>2</sub> Se	298—343	-147.799	16264.9	41.5653	—
PH <sub>3</sub>	298—323	-309.240	16364.9	41.5653	—
AsH <sub>3</sub>	273—299	-286.171	15437.9	38.0934	—
Air	273—373	-319.323	15492.6	43.0259	0.0196194

<sup>a</sup>  $x_N$  is the mole fraction solubility at 1 atm partial pressure of the gas.

<sup>b</sup> For the equation  $RT \ln(x_N) = B + AT$ .

Reprinted with permission from Wilhelm, E., Battino, R., and Wilcock, R. J., *Chem. Rev.*, 77, 219, 1977. Copyright by the American Chemical Society.

**TABLE A8**  
**Availability of Salting Coefficients (at the Indicated Centigrade Temperature) for Some Atmospheric Gases in Solutions of the Major Seawater Salts**

Salt	He	Ne	Ar	Kr	Xe	Rn	H <sub>2</sub>	O <sub>2</sub>	N <sub>2</sub>
NaCl	25	15—30	5—75	25—45	0—45	0—50	1—71	0—30 <sup>a</sup>	5—125
Na <sub>2</sub> SO <sub>4</sub>	—	—	—	25	—	—	15	15—35	25—30
Na <sub>2</sub> CO <sub>3</sub>	—	—	—	—	—	—	15	15—35	25
KCl	25	15—25	5—30	25	—	18	15—25	0—35	0—240
K <sub>2</sub> SO <sub>4</sub>	—	—	—	—	—	—	—	15—25	—
K <sub>2</sub> CO <sub>3</sub>	—	—	—	—	—	—	15	—	50—90
MgCl <sub>2</sub>	<sup>b</sup>	20	25	<sup>b</sup>	—	—	—	0—25	—
MgSO <sub>4</sub>	—	20	—	—	—	—	15	15—35	30
CaCl <sub>2</sub>	—	20	25	—	—	—	15	25	30
NaOH	—	—	—	—	—	—	25—250	15—250	0—240
KOH	25—80	20	25—80	—	—	—	21—200	15—100	—

Salt	N <sub>2</sub> O	NO	SO <sub>2</sub>	Cl <sub>2</sub>	CO	CH <sub>4</sub>	C <sub>2</sub> H <sub>6</sub>	C <sub>3</sub> H <sub>8</sub>	C <sub>4</sub> H <sub>10</sub>
NaCl	0—40	20	25	25	—	0—300	0—75	0—70	0—70
Na <sub>2</sub> SO <sub>4</sub>	5—20	—	25—50	—	25	20—25	—	—	—
Na <sub>2</sub> CO <sub>3</sub>	25	—	—	—	—	25	—	25	—
KCl	0—40	—	10—90	25	—	10—30	10—30	25	25—70
K <sub>2</sub> SO <sub>4</sub>	5—20	—	25	—	—	25	—	—	—
K <sub>2</sub> CO <sub>3</sub>	—	—	—	—	—	25	—	—	—
MgCl <sub>2</sub>	25	—	—	<sup>b</sup>	—	25	—	—	—
MgSO <sub>4</sub>	0—40	—	—	—	—	25	—	—	—
CaCl <sub>2</sub>	5—20	—	—	—	—	25—125	0	—	—
NaOH	—	—	—	—	—	—	—	—	—
KOH	10—25	—	—	—	—	25—80	—	—	—

*Note:* This table was compiled from IUPAC Solubility Data Series publications, and does not take into account any more recent data that may be available. The references and their years of publication are as follows: He — 326 (1979), Ne — 326 (1979), Ar — 324 (1980), Kr — 328 (1979), Xe — 328 (1979), Rn — 328 (1979), H<sub>2</sub> — 330 (1981), O<sub>2</sub> — 192 (1981), N<sub>2</sub> — 332 (1982), N<sub>2</sub>O — 334 (1981), NO — 334 (1981), SO<sub>2</sub> — 288 (1983), Cl<sub>2</sub> — 288 (1983), CO — 337 (1990), CH<sub>4</sub> — 325 (1987), C<sub>2</sub>H<sub>6</sub> — 327 (1982), C<sub>3</sub>H<sub>8</sub> — 329 (1986), C<sub>4</sub>H<sub>10</sub> — 329 (1986). See Tables 24 and 25 for fitting equations giving solubilities of some of these gases in seawater.

<sup>a</sup> See Cramer<sup>137</sup> for data to high temperature.

<sup>b</sup> Some data for barium salt available.

**TABLE A9**  
**Molal Setchenow Coefficients ( $k_s$ ) for Volatile Solutes in Single Electrolyte Solutions at 25°C<sup>a</sup>**

Salt	He	Ne	Ar	Kr	Xe	H <sub>2</sub>	O <sub>2</sub>	N <sub>2</sub>
LiCl	0.118	0.139	0.226	0.275	—	0.155	0.295	0.245
NaCl	0.192	0.229	0.314	0.344	0.356 <sup>b</sup>	0.219	0.312	0.309
NaBr	0.208	—	0.279	—	—	—	0.240	—
KF	—	—	0.330	—	—	—	—	—
KCl	0.155 <sup>b</sup>	—	0.135 <sup>b</sup>	0.295	—	0.187	0.298	—
KBr	—	—	0.263	—	—	—	0.249	—
KI	0.203	0.196	0.263	0.293	0.275	0.203	0.162	0.268
KOH	0.309	—	0.376	—	—	0.278 <sup>b</sup>	0.389 <sup>b</sup>	—
NaOH	—	—	—	—	—	0.325	0.422	—
NaNO <sub>3</sub>	0.148	—	0.166	—	—	0.201	—	—
KNO <sub>3</sub>	—	—	—	0.224	—	0.132	0.190	—
NH <sub>4</sub> Cl	0.067	—	0.157	0.157	—	—	—	—
Salt	N <sub>2</sub> O	CH <sub>4</sub>	C <sub>2</sub> H <sub>2</sub>	C <sub>2</sub> H <sub>4</sub>	C <sub>2</sub> H <sub>6</sub>	C <sub>3</sub> H <sub>8</sub>	C <sub>6</sub> H <sub>6</sub>	
LiCl	0.192	0.252	—	0.219	0.314	0.364	0.325	
NaF	—	—	—	—	—	—	0.585	
NaCl	0.245	0.333 <sup>b</sup>	0.222	0.309	0.391 <sup>b</sup>	0.461	0.449	
NaBr	0.199	—	0.171	—	—	—	—	
KCl	0.183 <sup>b</sup>	—	0.155	—	—	—	0.382	
KBr	0.157 <sup>b</sup>	—	0.123	—	—	—	0.290	
KI	0.143	0.261	—	0.157	0.263	0.249	0.152	
RbCl	—	—	—	—	—	—	0.322	
CsCl	—	—	—	—	—	—	0.203	
KOH	0.300	0.417	—	—	—	—	—	
NaNO <sub>3</sub>	0.188 <sup>b</sup>	—	0.123	—	—	—	—	
NaClO <sub>4</sub>	—	—	—	—	—	—	0.244	
KNO <sub>3</sub>	0.119 <sup>b</sup>	—	0.074	—	—	—	—	
NH <sub>4</sub> Cl	0.073 <sup>b</sup>	—	0.054	—	—	—	—	
NH <sub>4</sub> Br	0.056	0.127	0.033	—	0.153	—	—	

<sup>a</sup> Compiled from data given in Krishnan and Friedman<sup>200</sup> and Masterton et al.<sup>181</sup> Experimental values (expt.) of this second reference are related to  $k_s$  tabulated here by  $k_s = (k_s(\text{expt.}) - 0.0157) \ln(10)$ .  $k_s$  (expt.) is defined in terms of nonelectrolyte concentrations expressed as mole fractions.

<sup>b</sup> Mean value from Masterton et al.<sup>181</sup>

**TABLE A10**  
**Availability of Solubility Data (at the Indicated Centigrade Temperature) for Hydrocarbons in Seawater and Aqueous NaCl**

Hydrocarbon	Aqueous NaCl	Seawater	Note
Benzene	25	0—25	
Toluene	25	0—25	a
Methyl-cyclopentane (C <sub>6</sub> H <sub>12</sub> )	25	—	
Heptane (C <sub>7</sub> H <sub>16</sub> )	—	25	
Hexane (C <sub>6</sub> H <sub>14</sub> )	25	25	
Pentane (C <sub>5</sub> H <sub>12</sub> )	25	—	
Acenaphthalene (C <sub>12</sub> H <sub>10</sub> )	—	15—25	
Anthracene (C <sub>14</sub> H <sub>10</sub> )	8—30	25	
Benz[a]anthracene (C <sub>18</sub> H <sub>12</sub> )	—	25	

**TABLE A10 (continued)**  
**Availability of Solubility Data (at the Indicated Centigrade Temperature) for Hydrocarbons in Seawater and Aqueous NaCl**

Hydrocarbon	Aqueous NaCl	Seawater	Note
Butylbenzene (C <sub>10</sub> H <sub>14</sub> )	—	25	a
<i>o</i> -Xylene (C <sub>8</sub> H <sub>10</sub> )	—	25	a
<i>m</i> -Xylene (C <sub>8</sub> H <sub>10</sub> )	—	25	a
<i>p</i> -Xylene (C <sub>8</sub> H <sub>10</sub> )	—	25	a
<i>tert</i> -Butylbenzene (C <sub>10</sub> H <sub>14</sub> )	—	25	
Ethylbenzene (C <sub>10</sub> H <sub>8</sub> )	—	0—25	a
Cumene (C <sub>9</sub> H <sub>10</sub> )	—	25	
<i>sec</i> -Butylbenzene (C <sub>10</sub> H <sub>14</sub> )	—	25	
Benzo[ghi]perylene (C <sub>22</sub> H <sub>12</sub> )	—	25	
Benzo[b]triphenylene (C <sub>22</sub> H <sub>14</sub> )	—	25	
Benzo[a]pyrene (C <sub>20</sub> H <sub>12</sub> )	—	25	
Benzo[e]pyrene (C <sub>20</sub> H <sub>12</sub> )	9—30	25	
Biphenyl (C <sub>12</sub> H <sub>10</sub> )	25	25	a
Decane (C <sub>10</sub> H <sub>22</sub> )	—	25	
Dibenz[a,h]anthracene (C <sub>22</sub> H <sub>14</sub> )	—	25	
Dodecane (C <sub>12</sub> H <sub>26</sub> )	—	25	a
Eicosane (C <sub>20</sub> H <sub>42</sub> )	—	25	a
Hexacosane (C <sub>26</sub> H <sub>54</sub> )	—	25	a
Hexadecane (C <sub>16</sub> H <sub>34</sub> )	—	25	a
Napthalene (C <sub>10</sub> H <sub>8</sub> )	—	25	a
Nonane (C <sub>9</sub> H <sub>20</sub> )	—	25	
Octadecane (C <sub>18</sub> H <sub>38</sub> )	—	25	a
Octane (C <sub>8</sub> H <sub>18</sub> )	—	25	
Phenanthrene (C <sub>14</sub> H <sub>10</sub> )	11—32	25	a
Pyrene (C <sub>16</sub> H <sub>10</sub> )	—	15—25	
Tetradecane (C <sub>14</sub> H <sub>30</sub> )	—	25	a
Undecane (C <sub>11</sub> H <sub>24</sub> )	—	25	
2-Methylanthracene (C <sub>15</sub> H <sub>12</sub> )	25	—	
Benz[a]anthracene (C <sub>18</sub> H <sub>12</sub> )	25	—	
Chrysene (C <sub>18</sub> H <sub>12</sub> )	25	—	
Fluoranthene (C <sub>16</sub> H <sub>10</sub> )	25	—	
Fluorene (C <sub>13</sub> H <sub>10</sub> )	25	—	
Napthalene (C <sub>10</sub> H <sub>8</sub> )	9—32	—	a
1-Ethylnapthalene (C <sub>12</sub> H <sub>12</sub> )	8—29	—	
1-Methylnapthalene (C <sub>11</sub> H <sub>10</sub> )	8—29	—	
1-Methylphenanthrene (C <sub>15</sub> H <sub>12</sub> )	25	—	
Pyrene (C <sub>16</sub> H <sub>10</sub> )	9—31	—	

Note: Data are from compilations of Shaw (C<sub>1</sub>—C<sub>11</sub>)<sup>331</sup> and (C<sub>8</sub>—C<sub>36</sub>)<sup>332</sup>, both published in 1989.

<sup>a</sup> See Table 27 for pure water and seawater solubilities of these compounds. For the solubilities of further organic compounds, see also the following: References 335, 336, 338, 339, 378, and 379.

**TABLE A11**  
**Activity Coefficients of the Components of Weak Acids and Bases in Seawater at 25°C as a Function of Salinity (S), Calculated Using the Pitzer Model**

(See "Note" below for details of parameterization.)

S	$\gamma_{\text{H}^+}$	$\gamma_{\text{HSO}_4^-}$	$\gamma_{\text{MgOH}^+}$	$\gamma_{\text{MgB(OH)}_4^-}$	$\gamma_{\text{CaB(OH)}_4^-}$	$\gamma_{\text{OH}^-}$	$\gamma_{\text{B(OH)}_3}$	$\gamma_{\text{H}_2\text{PO}_4^-}$	$\gamma_{\text{HPO}_4^{2-}}$	$\gamma_{\text{CO}_3^{2-}}$
5	0.784	0.759	0.859	0.753	0.749	0.756	0.732	0.741	0.314	0.0581
10	0.749	0.702	0.862	0.697	0.688	0.697	0.655	0.672	0.219	0.0235
15	0.734	0.667	0.869	0.665	0.652	0.659	0.603	0.628	0.170	0.0123
20	0.727	0.641	0.875	0.643	0.627	0.631	0.562	0.595	0.138	0.00721
25	0.727	0.621	0.878	0.628	0.608	0.609	0.529	0.568	0.115	0.00454
30	0.730	0.605	0.880	0.618	0.594	0.591	0.500	0.546	0.0985	0.00300
35	0.735	0.592	0.879	0.610	0.583	0.575	0.475	0.528	0.0851	0.00204
40	0.743	0.580	0.875	0.605	0.575	0.561	0.452	0.512	0.0744	0.00143

S	$\gamma_{\text{HSO}_4^-}$	$\gamma_{\text{SO}_4^{2-}}$	$\gamma_{\text{HSO}_3^-}$	$\gamma_{\text{SO}_3^{2-}}$	$\gamma_{\text{HS}^-}$	$\gamma_{\text{HCO}_3^-}$	$\gamma_{\text{CO}_3^{2-}}$	$\gamma_{\text{B(OH)}_3}$	$\gamma_{\text{H}_2\text{PO}_4^-}$	$\gamma_{\text{CO}_2}$
5	0.792	0.300	0.799	0.308	0.781	0.761	0.291	0.998	1.00	1.02
10	0.756	0.218	0.770	0.229	0.739	0.705	0.189	0.995	1.00	1.03
15	0.737	0.177	0.759	0.190	0.717	0.672	0.136	0.993	1.01	1.05
20	0.725	0.150	0.755	0.165	0.703	0.648	0.103	0.991	1.01	1.07
25	0.716	0.132	0.755	0.148	0.694	0.630	0.0800	0.989	1.01	1.09
30	0.711	0.118	0.758	0.135	0.689	0.616	0.0633	0.987	1.01	1.11
35	0.706	0.106	0.763	0.125	0.685	0.604	0.0508	0.984	1.01	1.13
40	0.703	0.0972	0.769	0.117	0.684	0.595	0.0412	0.982	1.02	1.15

*Note:* Calculations were carried out using ternary ( $\theta_i$  and  $\psi_{ij}$ ) parameters as listed by Pitzer (Chapter 3, this volume), Harvie et al.,<sup>26</sup> and Tables 35, 36, and 38—40. Details are given below of where "ion pair" formation or association equilibria (usually with  $\text{Mg}^{2+}$ ,  $\text{Ca}^{2+}$ ,  $\text{SO}_4^{2-}$ , or  $\text{CO}_3^{2-}$ ) must be considered explicitly, or where ion interaction parameters have been used instead.  $\text{H}^+$  — free ion activity coefficient;  $\text{OH}^-$  —  $\text{Ca}^{2+}$ - $\text{OH}^-$  interaction parameterized in terms of ( $\beta^{\text{OH}}$ ,  $C^{\text{OH}}$ );  $\text{Mg}^{2+}$ - $\text{OH}^-$  interaction treated as  $\text{MgOH}^+$  formation and must be considered separately (see Harvie et al.<sup>26</sup>);  $\text{B(OH)}_3$  — interaction with  $\text{Mg}^{2+}$  and  $\text{Ca}^{2+}$  treated as ion pair formation (see Felmy and Weare<sup>27</sup>);  $\text{H}_2\text{PO}_4^-$  — interaction with  $\text{Mg}^{2+}$  and  $\text{Ca}^{2+}$  parameterized in terms of ( $\beta^{\text{H}_2\text{PO}_4}$ ,  $C^{\text{H}_2\text{PO}_4}$ );  $\text{HPO}_4^{2-}$  — interaction with  $\text{Mg}^{2+}$  and  $\text{Ca}^{2+}$  to be treated as ion pair formation, activity coefficient listed is for the *free* ion. For values of stability constants see Atlas et al.<sup>28</sup> and Johansson and Wedborg;<sup>29</sup>  $\text{PO}_4^{3-}$  — interaction with  $\text{Mg}^{2+}$  and  $\text{Ca}^{2+}$  to be treated as ion pair formation, activity coefficient listed is for the *free* ion. For values of stability constants see Atlas et al.<sup>28</sup> and Johansson and Wedborg;<sup>29</sup>  $\text{HS}^-$  — interaction with  $\text{Mg}^{2+}$  and  $\text{Ca}^{2+}$  parameterized in terms of ( $\beta^{\text{HS}}$ ,  $C^{\text{HS}}$ );  $\text{CO}_3^{2-}$  — interaction with  $\text{Mg}^{2+}$  and  $\text{Ca}^{2+}$  parameterized in terms of ( $\beta^{\text{CO}_3}$ ,  $C^{\text{CO}_3}$ ).<sup>30</sup>

## GLOSSARY OF SYMBOLS

Parentheses indicate table or equation where term is introduced.

$a$	(Subscript) anion "a" (15)
$a$	(Subscript, with K) an acid dissociation constant (in text)
$\alpha$	Activity (25)
$a'$	Apparent activity (118)
$A^\phi$	Debye-Hückel (activity coefficient) parameter (34)
$A_s$	Debye-Hückel (activity coefficient) parameter on mole fraction scale (67)

$B_2$	Virial coefficient (74)
$c$	(Subscript) cation "c" (14)
$c_i$	Molar concentration of species "i" (81)
$c$	(Subscript or superscript) quantity on molar concentration scale
$C_i$	General concentration (unspecified units) of component "i" (10)
$C_{ca}^\phi$	Pitzer model ion interaction parameter (34)
Cl% $c$	Chlorinity (1)
$d_0$	Relative density of pure water ( $\text{kg m}^{-3}$ ) (7)
$d_{(s)}$	Relative density of seawater ( $\text{kg m}^{-3}$ ) (7)
$E$	EMF (114)
$E^\circ$	Standard potential (114)
$E_i$	Liquid junction potential (116)
$f$	Activity coefficient on mole fraction scale (106)
$f_\pm^*$	Mean ion activity coefficient on the mole fraction scale, infinite dilution standard state (69)
$f_i$	Fugacity (atm) of component "i" (43)
$f_{ih}$	Activity coefficient correction factor (115)
(F)	(Subscript) free quantity (usually concentration or activity coefficient) (47)
$g_i$	Mass of component "i" in grams (1)
$G_J$	Relative chemical potential of component J (24)
$i$	(Subscript) component ion or neutral species (1)
$I$	Molal ionic strength ( $\text{mol kg}^{-1} \text{H}_2\text{O}$ ) (20)
$J$	(Subscript) component salt (12)
$J$	(Superscript) Pitzer model parameter for partial molal heat capacity expression (Table 9)
$k$	Constant (5)
$\mathbf{k}$	Setchenow coefficient for salt concentration in molal units (82)
$\mathbf{k}$	Setchenow coefficient for salt concentration in molar units (81)
$\mathbf{k}_{\text{setc}}$	Setchenow coefficient used by Lang and Zander (84)
$k$	(Subscript or superscript) quantity on molality concentration scale (19)
$k_i$	Molality of component "i" ( $\text{mol kg}^{-1}$ solution) (16)
$K$	Thermodynamic equilibrium constant (molal units) (31)
$K^*$	Stoichiometric equilibrium constant, free species concentrations in molal units (31)
$\mathbf{K}^*$	Stoichiometric equilibrium constant on molality concentration scale (123)
$K_H$	Henry's law constant ( $\text{mol}^2 \text{kg}^{-2} \text{atm}^{-1}$ ) of a volatile strong electrolyte, assuming complete dissociation in solution (66)
$K'_H$	Henry's law constant ( $\text{mol kg}^{-1} \text{atm}^{-1}$ ) of a gas, <i>not</i> including any dissociation that occurs in the aqueous phase (43)
$K_{\text{H}_2\text{O}}$	The thermodynamic dissociation constant of water (51)
$L$	Ostwald solubility coefficient (101)
$L$	(Superscript) Pitzer model parameter for partial molal enthalpy expression (Table 9)
$m_i$	Molality of component "i" ( $\text{mol kg}^{-1} \text{H}_2\text{O}$ ) (11)
$n$	(Subscript) neutral species "n" (34)
$n_i$	Number of moles of component "i" (28)
$p_i$	Partial pressure of species "i" (72)
$P$	Pressure (74)
$R$	The gas constant ( $8.314 \text{ J mol}^{-1} \text{K}^{-1}$ ) (24)
$s$	(Superscript or subscript) property relating to salt "s" (80)
(s)	(Subscript) property of sea salt or seawater (7)

sp	(Subscript) solubility product (173)
S	General term for gas solubility (81)
S <sup>°</sup>	Gas solubility in pure solvent (81)
S <sub>K</sub>	Knudsen salinity (2)
S <sub>T</sub>	Total salt content of seawater (g kg <sup>-1</sup> seawater) (1)
S‰	Conventional Salinity (4)
t	Temperature (°C) (7)
t	(Superscript) indicates a stoichiometric association constant calculated from one “free” and one “total” concentration of the two associating species (usually H <sup>+</sup> and a weak acid anion); for each constant, the “total” and “free” species used are indicated in the text (122)
T	Absolute temperature (K) (24)
T	(Superscript) indicates a stoichiometric association constant calculated from “total” concentrations of both associating species (159)
(T)	(Subscript) total, or stoichiometric, quantity (50)
U <sub>1,MX</sub>	Pitzer (mole fraction) activity coefficient model parameter (67)
V	(Superscript) Pitzer model parameter for partial molal volume expression (Table 9)
V <sub>i</sub>	Volume occupied by species “i” (72)
w <sub>i</sub>	Molar mass of component “i” in grams (2)
W <sub>1,MX</sub>	Pitzer (mole fraction) activity coefficient model parameter (67)
x <sub>i</sub>	Mole fraction concentration of component “i” (10)
x <sub>±</sub>	The total mole fraction of ions (67)
y	Mole fraction (alternate definition to x) (12)
z <sub>i</sub>	Charge on ion “i” (19)
α	Side reaction coefficient (122)
β	Bunsen solubility coefficient (85)
β <sub>ca</sub> <sup>(i)</sup>	Pitzer model ion interaction parameter (i = 0, 1, 2), defined in text following Equation 37
γ	The molal activity coefficient (25, and see Table 5)
γ <sub>±</sub>	Mean activity coefficient of neutral salt (41)
γ <sub>i</sub> <sup>°</sup>	Activity coefficient of species “i” in pure solvent (80)
Γ	Activity coefficient quotient (31)
ζ <sub>ijk</sub>	Pitzer model parameter involving neutral species (34)
η <sub>ijk</sub>	Pitzer model parameter involving neutral species (34)
θ <sub>ij</sub>	Pitzer model ion interaction parameter (cc’ and aa’) (34)
κ	(Superscript) Pitzer model parameter for partial molal compressibility expression (Table 9)
λ <sub>ij</sub>	Pitzer model parameter involving neutral species (34)
μ <sub>ijk</sub>	Pitzer model parameter involving neutral species (34)
μ <sub>J</sub>	Chemical potential of component J (24)
ν <sub>i</sub>	Stoichiometric number of ion “i” (41)
ν	Sum of stoichiometric numbers of cation (ν <sub>+</sub> ) and anion (ν <sub>-</sub> ) in salt M <sub>ν<sub>+</sub></sub> X <sub>ν<sub>-</sub></sub> (41)
ρ	Parameter for Pitzer mole fraction-based model (67)
ρ <sub>x</sub>	Absolute density of solution “x” (8)
ρ <sub>max</sub>	Maximum density of pure water at 1 atm pressure (8)
φ	The molal osmotic coefficient (27)
ψ <sub>ijk</sub>	Pitzer model ion interaction parameter (cc’a and aa’c) (34)
Ω	The saturation index of a solid phase (58)

## REFERENCES

1. Pruppacher, H. R. and Klett, J. D., *Microphysics of Clouds and Precipitation*, D. Reidel, Dordrecht, 1978.
2. Edwards, A. M. C., The variation of dissolved constituents with discharge in some Norfolk rivers, *J. Hydrol.*, 18, 219, 1973.
3. Caesar, J., Collier, R., Edmond, J., Frey, F., Matisoff, G., Ng, A., and Stallard, R., Chemical dynamics of a polluted watershed, the Merrimack River in northern New England, *Environ. Sci. Technol.*, 10, 697, 1976.
4. Golterman, H. L., *Physiological Limnology*, Elsevier, Amsterdam, 1975.
5. Wetzel, R. G., *Limnology*, W. B. Saunders, Philadelphia, 1975.
6. Burton, J. D. and Liss, P. S., *Estuarine Chemistry*, Academic Press, London, 1976.
7. Dueser, W. G., Reducing environments, in *Chemical Oceanography*, Riley, J. P. and Skirrow, G., Eds., Academic Press, London, 1975.
8. Grasshoff, K., The hydrochemistry of landlocked basins and fjords, in *Chemical Oceanography*, Vol. 2, Riley, J. P. and Skirrow, G., Eds., Academic Press, London, 1975.
9. Truesdell, A. H., Summary of section III, geochemical techniques in exploration, in Proc. 2nd U.N. Symp. on the Development and Use of Geothermal Resources, Vol. 1, U.S. Government Printing Office, Washington, D.C., 1976, 53.
10. Wilson, T. R. S., Salinity and the major elements of sea water, in *Chemical Oceanography*, Vol. 1, Riley, J. P. and Skirrow, G., Eds., Academic Press, London, 1975, 365.
11. Wallace, W. J., *The Development of the Chlorinity-Salinity Concept in Oceanography*, Elsevier, Amsterdam, 1974.
12. Knudsen, M., Deuxieme Conference International pour l'Exploration de la Mer, Kristiana, Norway, Report Suppl. 9, 1901.
13. MacIntyre, F., Concentration scales: a plea for physico-chemical data, *Mar. Chem.*, 4, 205, 1976.
14. Wooster, W. D., Lee, A. J., and Dietrich, G., Redefinition of salinity, *Limnol. Oceanogr.*, 14, 437, 1969.
15. Millero, F. J. and Kremling, K., The densities of Baltic Sea waters, *Deep Sea Res.*, 23, 1129, 1976.
16. Livingstone, D. A., The Data of Geochemistry, Professional Paper 440-G, U.S. Government Printing Office, Washington, D.C., 1963.
17. Millero, F. J., Gonzalez, A., and Ward, G. A., The density of sea water solutions at one atmosphere as a function of temperature and salinity, *J. Mar. Res.*, 34, 61, 1976.
18. Millero, F. J., The thermodynamics of seawater. I. The PVT properties, *Ocean Sci. Eng.*, 7, 403, 1982.
19. Bigg, P. H., Density of water in SI units over the range 0–40°C, *Br. J. Appl. Phys.*, 18, 521, 1967.
20. Millero, F. J., The thermodynamics of seawater. II. Thermochemical properties, *Ocean Sci. Eng.*, 8, 1, 1983.
21. Chen, C. T. and Millero, F. J., The use and misuse of pure water PVT properties for lake waters, *Nature*, 266, 707, 1977.
22. Robinson, R. A. and Stokes, R. H., *Electrolyte Solutions*, Butterworths, London, 1965.
23. Pitzer, K. S. and Simonson, J. M., Thermodynamics of multicomponent, miscible, ionic systems: theory and equations, *J. Phys. Chem.*, 90, 3005, 1986.
24. Makarov, I. L. and Stupin, D. Yu., Activity coefficient in concentrated aqueous solutions of KI-RbI at 25°C, *Russ. J. Phys. Chem.*, 35, 295, 1961.
25. Leyendekkers, J. V., *Thermodynamics of Sea Water (Part 1)*, Marcel Dekker, New York, 1976.
26. Millero, F. J., Sea water as a multicomponent electrolyte solution, in *The Sea*, Vol. 5, Goldberg, E. D., Ed., John Wiley & Sons, New York, 1974.
27. Millero, F. J. and Leung, W. H., The thermodynamics of seawater at one atmosphere, *Am. J. Sci.*, 276, 1035, 1976.
28. Bockris, J. O. and Reddy, A. K. N., *Modern Electrochemistry*, Vol. 1, MacDonald, London, 1970, 297.
29. Eyring, N. and Eyring, E. M., Reaction rates in solution, in *Principles and Applications of Water Chemistry*, Faust, S. D. and Hunter, J. V., Eds., John Wiley & Sons, New York, 1967, 1.
30. Sunda, W. and Guillard, R. R. L., The relationship between cupric ion activity and the toxicity of copper in phytoplankton, *J. Mar. Res.*, 34, 511, 1976.
31. Manahan, S. E. and Smith, M. J., Copper micronutrient requirement for algae, *Environ. Sci. Technol.*, 7, 829, 1973.
32. Christie, A. O. and Crisp, D. J., Activity coefficients of the n-primary, secondary and tertiary aliphatic amines in aqueous solution, *J. Appl. Chem.*, 17, 11, 1967.
33. Crisp, D. J. and Marr, D. H., Energy relationships in physical toxicity, in *Proc. 2nd Int. Congr. Surface Activity*, Butterworths, London, 1957, 310.
34. Ferguson, J., The use of chemical potentials as indices of toxicity, *Proc. R. Soc. London Ser. B*, 127, 387, 1939.



35. Fisher, F. H., Ion pairing of magnesium sulphate in seawater: determined by ultrasonic absorption, *Science*, 157, 823, 1967.
36. Daly, F. P., Brown, C. W., and Kester, D. R., Sodium and magnesium sulphate ion pairing: evidence from Raman spectroscopy, *J. Phys. Chem.*, 76, 3664, 1972.
37. Pitzer, K. S., Thermodynamic properties of aqueous solutions of bivalent sulphates, *J. Chem. Soc., Faraday Trans. 2*, 68, 101, 1972.
38. Johnson, K. S. and Pytkowicz, R. M., Ion association of  $\text{Cl}^-$  with  $\text{H}^+$ ,  $\text{Na}^+$ ,  $\text{K}^+$ ,  $\text{Ca}^{2+}$  and  $\text{Mg}^{2+}$  in aqueous solutions at 25°C, *Am. J. Sci.*, 278, 1428, 1978.
39. Garrels, R. M. and Thompson, M., A chemical model for seawater at 25°C and one atmosphere total pressure, *Am. J. Sci.*, 260, 57, 1962.
40. Dyrssen, D. and Wedborg, M., Equilibrium calculations of the speciation of elements in sea water, in *The Sea*, Vol. 5, Goldberg, E. D., Ed., John Wiley & Sons, New York, 1975, 181.
41. Millero, F. J., Thermodynamic models for the state of metal ions in seawater, in *The Sea*, Vol. 6, Goldberg, E. D., Ed., John Wiley & Sons, New York, 1977.
42. Millero, F. J. and Schreiber, D. R., Use of the ion pairing model to estimate activity coefficients of the ionic components of natural waters, *Am. J. Sci.*, 282, 1508, 1982.
43. Johnson, K. S. and Pytkowicz, R. M., Ion association and activity coefficients in multicomponent solutions, in *Activity Coefficients in Electrolyte Solutions*, Vol. 2, Pytkowicz, R. M., Ed., CRC Press, Boca Raton, FL, 1979.
44. Parkhurst, D. L., Ion-association models and mean activity coefficients of various salts, in *Chemical Modelling in Aqueous Systems II*, Melchior, D. C. and Bussett, R. L., Eds., American Chemical Society, Washington, D.C., 1990, 30.
45. Harned, H. S. and Robinson, R. A., *Multicomponent Electrolyte Solutions*, Pergamon Press, Elmsford, NY, 1968.
46. Whitfield, M., An improved specific interaction model for seawater at 25°C and 1 atmosphere pressure, *Mar. Chem.*, 3, 197, 1975.
47. Guggenheim, E. A., Thermodynamic properties of aqueous solutions of strong electrolytes, *Philos. Mag.*, 19, 588, 1935.
48. Bromley, L. A., Thermodynamic properties of strong electrolytes in aqueous solutions, *AIChE J.*, 19, 313, 1972.
49. Meissner, H. P. and Kusik, C. J., Aqueous solutions of two or more strong electrolytes, *Ind. Eng. Chem. Process Des. Dev.*, 12, 205, 1973.
50. Whitfield, M., A chemical model for the major electrolyte component of sea water based on the Bronstead-Guggenheim hypothesis, *Mar. Chem.*, 1, 251, 1973.
51. Pitzer, K. S., Ion interaction approach: theory and data correlation, in *Activity Coefficients in Electrolyte Solutions*, 2nd ed., Pitzer, K. S., Ed., CRC Press, Boca Raton, FL, 1991, chap. 3.
52. Reilly, P. J., Wood, R. H., and Robinson, R. A., The prediction of osmotic and activity coefficients in mixed electrolyte solutions, *J. Phys. Chem.*, 75, 1305, 1971.
53. Seatchard, G., Rush, R. M., and Johnson, J. S., Osmotic and activity coefficients for binary mixtures of sodium chloride, sodium sulphate, magnesium sulphate and magnesium chloride in water at 25°C. III. Treatment with the ions as components, *J. Phys. Chem.*, 74, 3786, 1970.
54. Harvie, C. E. and Weare, J. H., The prediction of mineral solubilities in natural waters: the Na-K-Mg-Ca-Cl-SO<sub>2</sub>-H<sub>2</sub>O systems from zero to high concentration at 25°C, *Geochim. Cosmochim. Acta*, 44, 981, 1980.
55. Randall, M. and Failey, C. F., Activity coefficients of the undissociated part of weak electrolytes, *Chem. Rev.*, 4, 291, 1927.
56. Harvie, C. E., Moller, N., and Weare, J. H., The prediction of mineral solubilities in natural waters: the Na-K-Mg-Ca-H-Cl-SO<sub>2</sub>-OH-HCO<sub>3</sub>-CO<sub>3</sub>-CO<sub>2</sub>-H<sub>2</sub>O system to high ionic strengths at 25°C, *Geochim. Cosmochim. Acta*, 48, 723, 1984.
57. Whitfield, M., The extension of chemical models for seawater to include trace components at 25°C and one atmosphere pressure, *Geochim. Cosmochim. Acta*, 39, 1545, 1975.
58. Millero, F. J., Use of models to determine ionic interactions in natural waters, *Thalassia Jugosl.*, 18, 253, 1982.
59. Pitzer, K. S. and Silvester, L. F., Thermodynamics of electrolytes. VI. Weak electrolytes including H<sub>2</sub>PO<sub>4</sub>, *J. Solution Chem.*, 5, 269, 1976.
60. Millero, F. J., The estimation of  $\text{pK}_{\text{a}}^{\text{app}}$  of acids in seawater using the Pitzer equations, *Geochim. Cosmochim. Acta*, 47, 2121, 1983.
61. Felmy, A. R. and Weare, J. H., The prediction of borate mineral equilibria in natural waters—application to Searles Lake, California, *Geochim. Cosmochim. Acta*, 50, 2771, 1986.
62. Weare, J. H., Models of mineral solubility in concentrated brines with application to field observations, *Rev. Mineral.*, 17, 143, 1987.

63. **Zemaitis, J. F., Clark, D. M., Rafal, M., and Scrivner, N. C.**, *Handbook of Aqueous Electrolyte Thermodynamics*, DIPPR, New York, 1985.
64. **Chen, C.-C., Britt, H. I., Boston, J. F., and Evans, L. B.**, Local composition model for excess Gibbs energy of electrolyte systems. I. Single solvent, single completely dissociated electrolyte systems, *AIChE J.*, 28, 588, 1982.
65. **Pitzer, K. S., Roy, R. N., and Silvester, L. F.**, Thermodynamics of electrolytes. VII. Sulphuric acid, *J. Am. Chem. Soc.*, 99, 4930, 1977.
66. **Harvie, C. E., Eugster, H. P., and Weare, J. H.**, Mineral equilibria in the six component seawater systems Na-K-Mg-Ca-SO<sub>4</sub>-Cl-H<sub>2</sub>O at 25°C. II. Compositions of the saturated solutions, *Geochim. Cosmochim. Acta*, 46, 1603, 1982.
67. **Brimblecombe, P. and Clegg, S. L.**, The solubility and behaviour of acid gases in the marine aerosol, *J. Atmos. Chem.*, 7, 1, 1988.
68. **Clegg, S. L. and Brimblecombe, P.**, The solubility of volatile electrolytes in multicomponent solutions, with atmospheric applications, in *Chemical Modelling in Aqueous Systems II*, Melchior, D. C. and Bassett, R. L., Eds., American Chemical Society, Washington, D.C., 1990, 58.
69. **Plummer, L. N., Parkhurst, D. L., Fleming, G. W., and Dunkle, S. A.**, A Computer Program Incorporating Pitzer's Equations for Calculation of Geochemical Reactions in Brines, Water-Resources Investigations Report 88-4153, U.S. Geological Survey, Reston, VA, 1988.
70. **Wolery, T. J., Jackson, K. J., Bourcier, W. L., Bruton, C. J., Viani, B. E., Knauss, K. G., and Delany, J. M.**, Current status of the EQ3/6 software package for geochemical modelling, in *Chemical Modelling in Aqueous Systems II*, Melchior, D. C. and Bassett, R. L., Eds., American Chemical Society, Washington, D.C., 1990, 104.
71. **Hanel, G.**, The properties of atmospheric aerosol particles as functions of the relative humidity at thermodynamic equilibrium with the surrounding moist air, *Adv. Geophys.*, 19, 73, 1976.
72. **Winkler, P.**, The growth of atmospheric aerosol particles as a function of the relative humidity. II. An improved concept of mixed nuclei, *Aerosol Sci.*, 4, 373, 1973.
73. **Simonson, J. M. and Pitzer, K. S.**, Thermodynamics of multicomponent, miscible, ionic systems: the system LiNO<sub>3</sub>-KNO<sub>3</sub>-H<sub>2</sub>O, *J. Phys. Chem.*, 90, 3009, 1986.
74. **Clegg, S. L. and Brimblecombe, P.**, Equilibrium partial pressures, and mean activity and osmotic coefficients of 0–100% nitric acid as a function of temperature, *J. Phys. Chem.*, 94, 5369, 1990.
75. **Thurmond, V. L. and Brass, G. W.**, Activity and osmotic coefficients of NaCl in concentrated solutions from 0 to –40°C, *J. Chem. Eng. Data*, 33, 411, 1988.
76. **Spencer, R. J., Moller, N., and Weare, J. H.**, The prediction of mineral solubilities in natural waters. A chemical equilibrium model for the Na-K-Ca-Mg-Cl-SO<sub>4</sub>-H<sub>2</sub>O system at temperatures below 25°C, *Geochim. Cosmochim. Acta*, 54, 575, 1990.
77. **Harned, H. S. and Owen, B. B.**, *The Physical Chemistry of Electrolytic Solutions*, Reinhold, New York, 1958.
78. **Stokes, R. H.**, Thermodynamics of solutions, in *Activity Coefficients in Aqueous Solutions*, 2nd ed., Pitzer, K. S., Ed., CRC Press, Boca Raton, FL, 1991, chap. 1.
79. **Phutela, R. C. and Pitzer, K. S.**, Thermodynamics of electrolyte mixtures. Enthalpy and the effect of temperature on the activity coefficient, *J. Solution Chem.*, 15, 649, 1986.
80. **Connaughton, L. M., Millero, F. J., and Pitzer, K. S.**, Volume changes for mixing the major sea salts: equations valid to ionic strength 3.0 and temperature 95°C, *J. Solution Chem.*, 18, 1037, 1989.
81. **Millero, F. J., Vinokurova, F., Fernandez, M., and Hershey, J. P.**, PVT properties of concentrated electrolytes. VI. The speed of sound and apparent molal compressibilities of NaCl, Na<sub>2</sub>SO<sub>4</sub>, MgCl<sub>2</sub>, and MgSO<sub>4</sub> solutions from 0 to 100°C, *J. Solution Chem.*, 16, 269, 1987.
82. **Pitzer, K. S. and Kim, J.**, Thermodynamics of electrolytes. IV. Activity and osmotic coefficients of mixed electrolytes, *J. Am. Chem. Soc.*, 96, 5701, 1974.
83. **Pabalan, R. T. and Pitzer, K. S.**, Thermodynamics of concentrated electrolyte mixtures and the prediction of mineral solubilities to high temperatures for mixtures in the system Na-K-Mg-Cl-SO<sub>4</sub>-OH-H<sub>2</sub>O, *Geochim. Cosmochim. Acta*, 51, 2429, 1987.
84. **Greenberg, J. P. and Moller, N.**, The prediction of mineral solubilities in natural waters: a chemical equilibrium model for the Na-K-Ca-Cl-SO<sub>4</sub>-H<sub>2</sub>O system to high concentration from 0 to 25°C, *Geochim. Cosmochim. Acta*, 53, 2503, 1989.
85. **Holmes, H. F., Busey, R. H., Simonson, J. M., Mesmer, R. E., Archer, D. G., and Wood, R. H.**, The enthalpy of dilution of HCl<sub>aq</sub> to 648K and 40MPa. Thermodynamic properties, *J. Chem. Thermodyn.*, 19, 863, 1987.
86. **Raju, K. and Atkinson, G.**, Thermodynamics of "scale" mineral solubilities. I. BaSO<sub>4</sub> in H<sub>2</sub>O and aqueous NaCl, *J. Chem. Eng. Data*, 33, 490, 1988.
87. **Pabalan, R. T. and Pitzer, K. S.**, Apparent molar heat capacity and other thermodynamic properties of aqueous KCl solutions to high temperatures and pressures, *J. Chem. Eng. Data*, 33, 354, 1988.

88. **Silvester, L. F. and Pitzer, K.**, Thermodynamics of electrolytes. VIII. High temperature properties, including enthalpy and heat capacity, with application to sodium chloride. *J. Phys. Chem.*, 81, 1822, 1977.
89. **Moller, N.**, The prediction of mineral solubilities in natural waters: a chemical equilibrium model for the Na-Ca-Cl-SO<sub>4</sub>-H<sub>2</sub>O system, to high temperature and concentration, *Geochim. Cosmochim. Acta*, 52, 821, 1988.
90. **Clegg, S. L. and Brimblecombe, P.**, The solubility and activity coefficient of oxygen in salt solutions and brines. *Geochim. Cosmochim. Acta*, 54, 3315, 1990.
91. **Millero, F. J.**, Influence of pressure on chemical processes in the sea, in *Chemical Oceanography*, Vol. 8, Riley, J. P. and Chester, R., Eds., Academic Press, New York, 1983, 2.
92. **Millero, F. J. and Schreiber, D. R.**, The effect of pressure on the thermodynamic properties of seawater, *J. Mar. Res.*, 41, 323, 1983.
93. **Connaughton, L. M., Hershey, J. P., and Millero, F. J.**, PVT properties of concentrated aqueous electrolytes. V. Densities and apparent molal volumes of the four major seasalts from dilute solution to saturation and from 0 to 100°C, *J. Solution Chem.*, 15, 989, 1986.
94. **Dedick, E. A., Hershey, J. P., Sotolongo, S., Stade, D. J., and Millero, F. J.**, The PVT properties of concentrated aqueous electrolytes. IX. The volume properties of KCl and K<sub>2</sub>SO<sub>4</sub> and their mixtures with NaCl and Na<sub>2</sub>SO<sub>4</sub> as a function of temperature, *J. Solution Chem.*, 19, 353, 1990.
95. **Pitzer, K. S.**, Theoretical considerations of solubility with emphasis on mixed aqueous electrolytes, *Pure Appl. Chem.*, 58, 1599, 1986.
96. **Roy, R. N., Gibbons, J. J., Bliss, D. P., Casebolt, R. G., and Baker, B. K.**, Activity coefficients for ternary systems. VI. The system HCl + MgCl<sub>2</sub> + H<sub>2</sub>O at different temperatures: application of Pitzer's equations, *J. Solution Chem.*, 9, 911, 1980.
97. **Barta, L. and Bradley, D. J.**, Extension of the specific interaction model to include gas solubilities in high temperature brines. *Geochim. Cosmochim. Acta*, 49, 195, 1985.
98. **Clegg, S. L. and Brimblecombe, P.**, Solubility of ammonia in pure aqueous and multicomponent solutions, *J. Phys. Chem.*, 93, 7237, 1989.
99. **Silcock, H. L.**, *Solubilities of Inorganic and Organic Compounds*, Vol. 3, Pergamon Press, Oxford, 1979.
100. **Davis, W. and DeBruin, H. J.**, New activity coefficients of 0-100 percent aqueous nitric acid, *J. Inorg. Nucl. Chem.*, 26, 1069, 1964.
101. **Clegg, S. L. and Brimblecombe, P.**, Hydrofluoric and hydrochloric acid behaviour in concentrated saline solutions, *J. Chem. Soc. Dalton Trans.*, p. 705, 1988.
102. **Press, W. H., Flannery, B. P., Teukolsky, S. A., and Vetterling, W. T.**, *Numerical Recipes*, Cambridge University Press, Cambridge, 1986.
103. **Clegg, S. L. and Brimblecombe, P.**, Equilibrium partial pressures of strong acids over concentrated saline solutions. I. HNO<sub>3</sub>, *Atmos. Environ.*, 22, 91, 1988.
104. **Clegg, S. L. and Brimblecombe, P.**, The dissociation constant and Henry's law constant of HCl in aqueous solution, *Atmos. Environ.*, 20, 2483, 1986.
105. **Kim, H.-T. and Frederick, W. J.**, Evaluation of Pitzer ion interaction parameters of aqueous mixed electrolyte solutions at 25°C. II. Ternary mixing parameters, *J. Chem. Eng. Data*, 33, 278, 1988.
106. **Kim, H.-T. and Frederick, W. J.**, Evaluation of Pitzer ion interaction parameters of aqueous electrolytes at 25°C. I. Single salt parameters, *J. Chem. Eng. Data*, 33, 177, 1988.
107. **Hamer, W. J. and Wu, Y.-C.**, Osmotic coefficients and mean activity coefficients of uni-univalent electrolytes in water at 25°C, *J. Phys. Chem. Ref. Data*, 1, 1047, 1972.
108. **Goldberg, R. N. and Nuttall, R. L.**, Evaluated activity and osmotic coefficients for aqueous solutions: the alkaline earth metal halides, *J. Phys. Chem. Ref. Data*, 7, 263, 1978.
109. **Sarbar, M., Covington, A. K., Nuttall, R. L., and Goldberg, R. N.**, The activity and osmotic coefficients of aqueous sodium bicarbonate solutions, *J. Chem. Thermodyn.*, 14, 967, 1982.
110. **Plummer, L. N. and Parkhurst, D. L.**, Application of the Pitzer equations to the PHREEQE geochemical model, in *Chemical Modelling in Aqueous Systems II*, Melchior, D. C. and Bassett, R. L., Eds., American Chemical Society, Washington, D.C., 1990, 128.
111. **Reardon, E. J. and Beckie, R. D.**, Modelling chemical equilibria of acid mine drainage: the FeSO<sub>4</sub>-H<sub>2</sub>SO<sub>4</sub>-H<sub>2</sub>O system, *Geochim. Cosmochim. Acta*, 51, 2355, 1987.
112. **Monnin, C. and Schott, J.**, Determination of the solubility products of sodium carbonate minerals and an application to irona deposition in Lake Magadi (Kenya), *Geochim. Cosmochim. Acta*, 48, 571, 1984.
113. **Peiper, J. C. and Pitzer, K. S.**, Thermodynamics of aqueous carbonate solutions including mixtures of sodium carbonate, bicarbonate and chloride, *J. Chem. Thermodyn.*, 14, 613, 1982.
114. **Platford, R. F.**, The activity coefficient of sodium chloride in seawater, *J. Mar. Res.*, 23, 55, 1965.
115. **Gieskes, J. M. T. M.**, The activity coefficients of sodium chloride in mixed electrolyte solutions, *Z. Phys. Chem. (Frankfurt am Main)*, 50, 78, 1966.
116. **Platford, R. F. and Dafeo, T.**, The activity coefficient of sodium sulphate in sea water, *J. Mar. Res.*, 23, 63, 1965.

117. Johnson, K. S. and Pytkowicz, R. M., The activity of NaCl in seawater of 10–40% salinity and 5–25°C at 1 atmosphere. *Mar. Chem.*, 10, 85, 1981.
118. Millero, F. J., The physical chemistry of natural waters. *Pure Appl. Chem.*, 57, 1015, 1985.
119. Harvie, C. E., Weare, J. H., Hardie, L. A., and Eugster, H. P., Evaporation of seawater: calculated mineral sequences. *Science*, 208, 498, 1980.
120. Krumgalz, B. S. and Millero, F. J., Physico-chemical study of Dead Sea waters. III. On gypsum saturation in Dead Sea waters and their mixtures with Mediterranean seawater. *Mar. Chem.*, 13, 127, 1983.
121. Krumgalz, B. S. and Millero, F. J., Halite solubility in Dead Sea waters. *Mar. Chem.*, 27, 219, 1989.
122. Langmuir, D. and Melchior, D., The geochemistry of Ca, Sr, Ba and Ra sulphates in some deep brines from the Palo Duro Basin, Texas. *Geochim. Cosmochim. Acta*, 49, 2423, 1985.
123. Raju, K. and Atkinson, G., Thermodynamics of "scale" mineral solubilities. II. SrSO<sub>4</sub> in aqueous NaCl. *J. Chem. Eng. Data*, 34, 361, 1989.
124. Raju, K. and Atkinson, G., Thermodynamics of "scale" mineral solubilities. III. CaSO<sub>4</sub> in H<sub>2</sub>O and aqueous NaCl. *J. Chem. Eng. Data*, 35, 361, 1990.
125. Brantley, S. L., Crerar, D. A., Moller, N. E., and Weare, J. H., Geochemistry of a modern marine evaporite: Bocana de Virvila, Peru. *J. Sediment. Petrol.*, 54, 447, 1984.
126. Braltsch, O., *Salt Deposits. Their Origin and Composition*. Springer-Verlag, New York, 1971.
127. Rogers, P. S. Z., Thermodynamics of Geothermal Fluids, Ph.D. thesis, University of California at Berkeley, Berkeley, 1981.
128. Harvie, C. E., Greenberg, J. P., and Weare, J. H., A chemical equilibrium algorithm for highly non-ideal multiphase systems: free energy minimization. *Geochim. Cosmochim. Acta*, 51, 1045, 1987.
129. Yeatts, L. B. and Marshall, W. L., Solubility of calcium sulphate dihydrate and association equilibria in several aqueous mixed electrolyte salt systems at 25°C. *J. Chem. Eng. Data*, 17, 163, 1972.
130. Schaffer, L. H., Solubility of gypsum in seawater and seawater concentrates at temperatures from ambient to 65°C. *J. Chem. Eng. Data*, 12, 183, 1967.
131. Marshall, W. L. and Stusher, R., Solubility to 200°C of calcium sulphate and its hydrates in sea water and saline water concentrates, and temperature-concentration limits. *J. Chem. Eng. Data*, 13, 83, 1968.
132. McCaffrey, M. A., Lazar, B., and Holland, H. D., The evaporation path of seawater and the coprecipitation of Br<sup>-</sup> and K<sup>+</sup> with halite. *J. Sediment. Petrol.*, 57, 928, 1987.
133. Eugster, H. P., Harvie, C. E., and Weare, J. H., Mineral equilibria in a six component seawater system, Na-K-Mg-Ca-SO<sub>4</sub>-Cl-H<sub>2</sub>O at 25°C. *Geochim. Cosmochim. Acta*, 44, 1335, 1980.
134. Young, T. F., Maraville, L. F., and Smith, H. M., Raman spectral investigations of ionic equilibria in solutions of strong electrolytes, in *Structure of Electrolytic Solutions*, Hamer, W. J., Ed., John Wiley & Sons, New York, 1959, 35.
135. Hovey, J. K. and Hepler, L. G., Thermodynamics of sulphuric acid: apparent and partial molar heat capacities and volumes of aqueous HSO<sub>4</sub><sup>-</sup> from 0–55°C and calculation of the second dissociation constant to 350°C. *J. Chem. Soc. Faraday Trans.*, 86, 2831, 1990.
136. Dickson, A. G., Wesolowski, D. J., Palmer, D. A., and Mesmer, R. E., Dissociation constant of the bisulphate ion in aqueous sodium chloride solutions to 523K. *J. Phys. Chem.*, 94, 7978, 1990.
137. Chen, H. and Irish, D. E., A Raman spectral study of bisulphate-sulphate systems. II. Constitution, equilibria, and ultrafast proton transfer in sulphuric acid. *J. Phys. Chem.*, 75, 2672, 1971.
138. Dickson, A. G., Standard potential of the (Ag<sub>11</sub> + 1/2H<sub>2</sub>, = Ag<sub>11</sub> + HCl<sub>1,10</sub>) cell and the dissociation constant of bisulphate ion in synthetic seawater from 273.15 to 318.15K. *J. Chem. Thermodyn.*, 22, 113, 1990.
139. Khoo, K. H., Ramette, R. W., Culberson, C. H., and Bates, R. G., Determination of hydrogen ion concentrations in seawater from 5 to 40°C: standard potentials at salinities from 20 to 45 ppt salinity. *Anal. Chem.*, 49, 29, 1977.
140. Denbigh, K., *The Principles of Chemical Equilibrium*, Cambridge University Press, Cambridge, 1971.
141. Pilinis, C., Seinfeld, J. H., and Grosjean, D., Water content of atmospheric aerosols. *Atmos. Environ.*, 23, 1601, 1989.
142. Koutrakis, P., Wolfson, J. M., Spengler, J. D., Stern, B., and Franklin, C. A., Equilibrium size of atmospheric aerosol sulphates as a function of relative humidity. *J. Geophys. Res.*, 94, 6442, 1989.
143. Heintzenberg, J., Fine particles in the global troposphere. *Tellus*, 41B, 149, 1989.
144. Clarke, A. D., Ahlquist, N. C., and Covert, D. S., The Pacific marine aerosol: evidence for natural acid sulphates. *J. Geophys. Res.*, 92, 4179, 1987.
145. Hitchcock, D. R., Spiller, J. L., and Wilson, W. E., Sulphuric acid aerosols and HCl release in coastal atmospheres: evidence of rapid formation of sulphuric acid particulates. *Atmos. Environ.*, 14, 165, 1980.
146. Martens, C. S., Wesolowski, J. J., Harriss, J. J., and Kalfer, R., Chlorine loss from Puerto Rican and San Francisco Bay area aerosols. *J. Geophys. Res.*, 78, 8778, 1973.
147. Charlson, R. J., Lovelock, J. E., Andreae, M. O., and Warren, S. G., Oceanic phytoplankton, atmospheric sulphur, cloud albedo and climate. *Nature*, 326, 655, 1987.

148. **Clegg, S. L. and Brimblecombe, P.**, Equilibrium partial pressures of strong acids over concentrated saline solutions. II. HCl, *Atmos. Environ.*, 22, 117, 1988.
149. **Hamill, P., Turco, R. P., and Toon, O. B.**, On the growth of nitric acid and sulphuric aerosol particles under stratospheric conditions, *J. Atmos. Chem.*, 7, 287, 1988.
150. **Smith-Magowan, D. and Goldberg, R. N.**, A Bibliography of Sources of Experimental Data Leading to Thermal Properties of Binary Aqueous Electrolyte Solutions, NBS Special Publ. 537, U.S. Government Printing Office, Washington, D.C., 1979.
151. **Cohen, M. D., Flagan, R. C., and Seinfeld, J. H.**, Studies of concentrated electrolyte solutions using the electrodynamic balance. I. Water activities for single electrolyte solutions, *J. Phys. Chem.*, 91, 4563, 1987.
152. **Richardson, R. A. and Spann, J. F.**, Measurement of the water cycle in a levitated ammonium sulphate particle, *J. Aerosol Sci.*, 15, 563, 1984.
153. **Tang, I. N. and Munkelwitz, H. R.**, Aerosol growth studies. III. Ammonium bisulphate aerosols in a moist atmosphere, *J. Aerosol Sci.*, 8, 321, 1977.
154. **Irish, D. E. and Chen, H.**, Equilibria and proton transfer in the bisulphate-sulphate system, *J. Phys. Chem.*, 74, 3796, 1970.
155. **Dawson, B. S. W., Irish, D. E., and Toogood, G. E.**, Vibrational spectral studies of solutions at elevated temperatures and pressures. VIII. A Raman spectral study of ammonium hydrogen sulphate solutions and the  $\text{HSO}_4^- - \text{SO}_4^{2-}$  equilibrium, *J. Phys. Chem.*, 90, 334, 1986.
156. **Balej, J., Hanousek, F., Pisarcik, M., and Sarka, K.**, Composition of aqueous solutions of ammonium sulphate and sulphuric acid, *J. Chem. Soc. Faraday Trans. 1*, 80, 521, 1984.
157. **Cohen, M. D., Flagan, R. C., and Seinfeld, J. H.**, Studies of concentrated electrolyte solutions using the electrodynamic balance. II. Water activities for mixed electrolyte solutions, *J. Phys. Chem.*, 91, 4575, 1987.
158. **Lenzi, F., Tran, T.-T., and Teng, T.-T.**, The water-activity of supersaturated aqueous solutions of NaCl, KCl, and  $\text{K}_2\text{SO}_4$  at 25°C, *Can. J. Chem.*, 53, 3133, 1975.
159. **Chen, H., Sangster, J., Teng, T. T., and Lenzi, F.**, General method of predicting the water activity of ternary aqueous solutions from binary data, *Can. J. Chem. Eng.*, 51, 234, 1973.
160. **Tang, I. N., Munkelwitz, H. R., and Wang, N.**, Water activity measurements with single suspended droplets: the NaCl-H<sub>2</sub>O and KCl-H<sub>2</sub>O systems, *J. Colloid Interface Sci.*, 114, 409, 1986.
161. **Bosen, A. and Engels, H.**, Description of the phase equilibrium of sulphuric acid with the NRTL equations and a solvation model in a wide concentration and temperature range, *Fluid Phase Equilibria*, 43, 213, 1988.
162. **Gmitro, J. I. and Vermeulen, T.**, Vapor-liquid equilibria for aqueous sulphuric acid, *AIChE J.*, 10, 740, 1964.
163. **Bolsaitis, P. and Elliot, J. F.**, Thermodynamic activities and equilibrium partial pressures for aqueous sulphuric acid solutions, *J. Chem. Eng. Data*, 35, 69, 1990.
164. **Weres, O. and Tsao, L.**, Activity of water mixed with molten salts at 317°C, *J. Phys. Chem.*, 90, 3014, 1986.
165. **Brimblecombe, P. and Clegg, S. L.**, Equilibrium partial pressures of strong acids over concentrated aqueous solutions. III. The temperature variation of HNO<sub>3</sub> solubility, *Atmos. Environ.*, 24A, 1945, 1990.
166. **King, E. J.**, *Acid-Base Equilibria*, Pergamon Press, Elmsford, NY, 1965.
167. **Weiss, R. F.**, Carbon dioxide in water and sea water: the solubility of a non-ideal gas, *Mar. Chem.*, 2, 203, 1974.
168. **Guggenheim, E. A.**, *Thermodynamics*, North-Holland, Amsterdam, 1967.
169. **Lewis, G. N. and Randall, M.**, *Thermodynamics*, McGraw-Hill, New York, 1961.
170. **Guggenheim, E. A. and Stokes, R. H.**, *Equilibrium Properties of Aqueous Solutions of Single Strong Electrolytes*, Pergamon Press, London, 1969.
171. **Long, F. A. and McDevit, W. F.**, Activity coefficients of nonelectrolyte solutes in aqueous salt solutions, *Chem. Rev.*, 51, 119, 1952.
172. **Gordon, J. E.**, *The Organic Chemistry of Electrolyte Solutions*, John Wiley & Sons, New York, 1975.
173. **Schumpe, A., Adler, I., and Deckwer, W. D.**, Solubility of oxygen in electrolyte solutions, *Biotechnol. Bioeng.*, 20, 145, 1978.
174. **Lang, W. and Zander, R.**, Salting-out of oxygen from aqueous electrolyte solutions: prediction and measurement, *Ind. Eng. Chem. Fundam.*, 25, 775, 1986.
175. **van Krevelen, D. W. and Hoftijzer, P. J.**, *Chimie et Industrie: Numero Speciale du XXIe Congr. Int. de Chimie Industrielle*, 1948, 168.
176. **Dankwerts, P. V.**, *Gas-Liquid Reactions*, McGraw-Hill, New York, 1970, 18.
177. **Onda, K., Sada, E., Kobayashi, T., Kito, S., and Ito, K.**, Salting-out parameters of gas solubility in aqueous salt solutions, *J. Chem. Eng. Jpn.*, 3, 18, 1970.
178. **Onda, K., Sada, E., Kobayashi, T., Kito, S., and Ito, K.**, Solubility of gases in aqueous solutions of mixed salts, *J. Chem. Eng. Jpn.*, 3, 137, 1970.

179. **Gordon, J. E. and Thorne, R. L.**, Salt effects on the activity coefficient of naphthalene in mixed aqueous electrolyte solutions. I. Mixtures of two salts, *J. Phys. Chem.*, 71, 4390, 1967.
180. **Gordon, L. I., Cohen, Y., and Standley, D. R.**, The solubility of molecular hydrogen in sea water, *Deep Sea Res.*, 24, 937, 1977.
181. **Masterton, W. L., Bolocofsky, D., and Lee, T. P.**, Ionic radii from scaled particle theory of the salt effect, *J. Phys. Chem.*, 75, 2809, 1971.
182. **Masterton, W. L. and Lee, T. P.**, Salting coefficients from scaled particle theory, *J. Phys. Chem.*, 74, 1776, 1970.
183. **Masterton, W. L.**, Salting coefficients for gases in seawater from scaled particle theory, *J. Solution Chem.*, 4, 523, 1975.
184. **Weiss, R. F.**, The solubility of nitrogen, oxygen and argon in water and sea water, *Deep Sea Res.*, 17, 721, 1970.
185. **Weiss, R. F.**, Solubility of helium and neon in water and sea water, *J. Chem. Eng. Data*, 16, 235, 1971.
186. **Weiss, R. F.**, The effect of salinity on the solubility of argon in sea water, *Deep Sea Res.*, 118, 225, 1971.
187. **Weiss, R. F. and Kyser, T. K.**, Solubility of krypton in water and seawater, *J. Chem. Eng. Data*, 23, 69, 1978.
188. **Weiss, R. F. and Price, B. A.**, Nitrous oxide solubility in water and seawater, *Mar. Chem.*, 8, 347, 1980.
189. **Chen, C., Britt, H. I., Boston, J. F., and Evans, L. B.**, Extension and application of the Pitzer equation for vapour-liquid equilibrium of aqueous electrolyte systems with molecular solutes, *AIChE J.*, 24, 820, 1979.
190. **Benson, B. B., Krause, D., and Peterson, M. A.**, The solubility and isotopic fractionation of gases in dilute aqueous solution. I. Oxygen, *J. Solution Chem.*, 8, 655, 1979.
191. **Pitzer, K. S. and Mayorga, G.**, Thermodynamics of electrolytes. II. Activity and osmotic coefficients for strong electrolytes with one or both ions univalent, *J. Phys. Chem.*, 77, 2300, 1973.
192. **Battino, R., Ed.**, *Oxygen and Ozone*, Vol. 7, IUPAC Solubility Data Series, Pergamon Press, Oxford, 1981, 515.
193. **MacArthur, C. G.**, Solubility of oxygen in salt solutions and the hydrates of these salts, *J. Phys. Chem.*, 20, 495, 1916.
194. **Yasunishi, A.**, Solubility of oxygen in aqueous electrolyte solutions, *Kagaku Kogaku Rombunshu*, 4, 185, 1978.
195. **Carpenter, J. H.**, New measurements of oxygen solubility in pure and natural water, *Limnol. Oceanogr.*, 11, 264, 1966.
196. **Murray, C. N. and Riley, J. P.**, The solubility of gases in distilled water and seawater. II. Oxygen, *Deep Sea Res.*, 16, 311, 1969.
197. **Green, E. J.**, A Redetermination of the Solubility of Oxygen in Seawater and the Thermodynamic Implications of the Solubility Relations, Ph.D. thesis, Massachusetts Institute of Technology, Cambridge, 1965.
198. **Kinsman, D. J. J., Boardman, M., and Borcsik, M.**, An experimental determination of the solubility of oxygen in marine brines, in *4th Symp. on Salt*, Vol. I, Coogan, A. H., Ed., Northern Ohio Geological Society, Cleveland, 1974, 325.
199. **Randall, M. and Failey, C. F.**, The activity coefficient of gases in aqueous salt solutions, *Chem. Rev.*, 4, 271, 1927.
200. **Krishnan, C. V. and Friedman, H. L.**, Model calculations of Setchenow coefficients, *J. Solution Chem.*, 3, 727, 1974.
201. **Crisp, D. J., Christie, A. O., and Ghobashy, A. F. A.**, Narcotic and toxic action of organic compounds on barnacle larvae, *Comp. Biochem. Physiol.*, 22, 629, 1967.
202. **Dexter, R. N. and Pavlou, S. P.**, Mass solubility and aqueous activity coefficients of stable organic chemicals in the marine environment: polychlorinated biphenyls, *Mar. Chem.*, 6, 41, 1978.
203. **McAuliff, C.**, Solubility in water of paraffin, cycloparaffin, olefin, acetylene, cycloolefin and aromatic hydrocarbons, *J. Phys. Chem.*, 70, 1267, 1966.
204. **Sutton, C. and Calder, J. A.**, Solubility of alkylbenzenes in distilled water and sea water at 25.0°C, *J. Chem. Eng. Data*, 20, 320, 1975.
205. **Kumar, A.**, Estimation of the ion product of water in sea water, *J. Chem. Eng. Data*, 33, 48, 1988.
206. **Dickson, A. G.**, pH scales and proton transfer reactions in saline media such as seawater, *Geochim. Cosmochim. Acta*, 48, 2299, 1984.
207. **Covington, A. K. and Rebello, M. J. F.**, Reference electrodes and liquid junction effects in ion-selective electrode potentiometry, *Ion Selective Electrode Rev.*, 5, 93, 1983.
208. **Henderson, P.**, Thermodynamic der flussigkeitskeffen, *Z. Phys. Chem.*, 63, 325, 1908.
209. **Whitfield, M. and Jagner, D.**, *Marine Electrochemistry*, John Wiley & Sons, Chichester, 1981.

210. Whitfield, M., Butler, R. A., and Covington, A. K., The determination of pH in estuarine waters. I. Definition of pH scales and the selection of buffers, *Oceanol. Acta*, 8, 423, 1985.
211. Bates, R. G., Ion activity scales for use with selective ion-sensitive electrodes, *Pure Appl. Chem.*, 36, 407, 1973.
212. Biedermann, G., Lagrange, J., and Lagrange, P., On the complex formation equilibria between the Cd(II) and Cl<sup>-</sup> ions, *Chem. Scr.*, 10, 153, 1974.
213. Knauss, K. G., Wolery, T. J., and Jackson, K. J., A new approach to measuring pH in brines and other concentrated electrolytes, *Geochim. Cosmochim. Acta*, 54, 1519, 1990.
214. Marcus, Y., Determination of pH in highly saline waters, *Pure Appl. Chem.*, 61, 1133, 1989.
215. Dickson, A. G. and Riley, J. P., The effect of analytical error on the evaluation of the components of the aquatic carbon dioxide system, *Mar. Chem.*, 6, 77, 1978.
216. Johnson, K. S., Voll, R., Curtis, C. S., and Pytkowicz, R. M., A critical examination of the NBS pH scale and the determination of titration alkalinity, *Deep Sea Res.*, 24, 915, 1977.
217. Culberson, C. H., Direct potentiometry, in *Marine Electrochemistry*, Whitfield, M. and Jagner, D., Eds., John Wiley & Sons, Chichester, 1981, 187.
218. Butler, R. A., Covington, A. K., and Whitfield, M., The determination of pH in estuarine waters. II. Practical considerations, *Oceanol. Acta*, 8, 433, 1985.
219. Hansson, I., A new pH scale and set of standard buffers for sea water, *Deep Sea Res.*, 20, 479, 1973.
220. Millero, F. J., The pH of estuarine waters, *Limnol. Oceanogr.*, 31, 839, 1986.
221. Millero, F. J., Hershey, J. P., and Fernandez, M., The pK<sup>a</sup> of TRISH<sup>+</sup> in Na-K-Mg-Ca-Cl-SO<sub>4</sub> brines — pH scales, *Geochim. Cosmochim. Acta*, 51, 707, 1987.
222. Bates, R. G., pH measurements in the marine environment, *Pure Appl. Chem.*, 54, 229, 1982.
223. Whitfield, M. and Turner, D. R., Seawater as an electrochemical medium, in *Marine Electrochemistry*, Whitfield, M. and Jagner, D., Eds., John Wiley & Sons, Chichester, 1981, 3.
224. Dickson, A. G. and Whitfield, M., An ion-association model for estimating acidity constants (at 25°C and 1 atm total pressure) in electrolyte mixtures related to seawater (ionic strength <1 mol kg<sup>-1</sup> H<sub>2</sub>O), *Mar. Chem.*, 10, 315, 1981.
225. Khoo, K. H., Culberson, C. H., and Bates, R. G., Thermodynamics of the dissociation of ammonium ion in seawater from 5 to 40°C, *J. Solution Chem.*, 6, 281, 1977.
226. Bates, R. G. and Culberson, C. H., Hydrogen ions and the thermodynamic state of marine systems, in *The Fate of Fossil Fuel CO<sub>2</sub> in the Oceans*, Andersen, N. R. and Malahoff, A., Eds., Plenum Press, New York, 1977, 45.
227. Park, K., The oceanic CO<sub>2</sub> system: an evaluation of ten methods of investigation, *Limnol. Oceanogr.*, 14, 179, 1969.
228. Skirrow, G., The dissolved gases — carbon dioxide, in *Chemical Oceanography*, Vol. 2, Riley, J. P. and Skirrow, G., Eds., Academic Press, New York, 1975, 1.
229. UNESCO, Thermodynamics of the carbon dioxide system in seawater, UNESCO Technical Papers in Marine Science No. 51, UNESCO, 1987.
230. Mehrbach, C., Culberson, C. H., Hawley, J. E., and Pytkowicz, R. M., Measurements of the apparent dissociation constants of carbonic acid in seawater at atmospheric pressure, *Limnol. Oceanogr.*, 18, 897, 1973.
231. Plath, C. C., Johnson, K. S., and Pytkowicz, R. M., The solubility of calcite — probably containing magnesium — in seawater, *Mar. Chem.*, 10, 9, 1980.
232. Dickson, A. G. and Millero, F. J., A comparison of the equilibrium constants for the dissociation of carbonic acid in seawater media, *Deep Sea Res.*, 34, 1733, 1987.
233. Hansson, I., A new set of acidity constants for carbonic acid and boric acid in sea water, *Deep Sea Res.*, 20, 461, 1973.
234. Johansson, O. and Wedborg, M., On the evaluation of potentiometric titrations in seawater with hydrochloric acid, *Oceanol. Acta*, 5, 209, 1982.
235. Millero, F. J., The thermodynamics of the carbonate system in seawater, *Geochim. Cosmochim. Acta*, 43, 1657, 1979.
236. Distèche, A. and Distèche, S., The effect of pressure on the dissociation of carbonic acid from measurements with buffered glass electrode cells, the effects of NaCl, KCl, Mg<sup>2+</sup>, Ca<sup>2+</sup>, SO<sub>4</sub><sup>2-</sup> and boric acid with special reference to seawater, *J. Electrochem. Soc.*, 114, 330, 1967.
237. Culberson, C. H. and Pytkowicz, R. M., The effect of pressure on carbonic acid, boric acid and the pH of seawater, *Limnol. Oceanogr.*, 13, 403, 1968.
238. Copine-Montegut, C., A new formula for the effect of temperature on the partial pressure of carbon dioxide in seawater, *Mar. Chem.*, 25, 29, 1988.
239. Plummer, L. N. and Busenberg, E., The solubilities of calcite, aragonite and witerite in CO<sub>2</sub>-H<sub>2</sub>O solutions between 0 and 90°C, and an evaluation of the aqueous model for the system CaCO<sub>3</sub>-CO<sub>2</sub>-H<sub>2</sub>O, *Geochim. Cosmochim. Acta*, 46, 1011, 1982.

240. **Morse, J. W., Mucci, A., and Millero, F. J.**, The solubility of calcite and aragonite in seawater of 35 ppt salinity at 25°C and atmospheric pressure. *Geochim. Cosmochim. Acta*, 44, 85, 1980.
241. **Mucci, A.**, The solubility of calcite and aragonite in seawater at various salinities, temperatures and one atmosphere pressure. *Am. J. Sci.*, 283, 789, 1985.
242. **Plummer, L. N. and Sundqvist, E. T.**, Total individual ion activity coefficients of calcium and carbonate in seawater at 25°C and 35 ppt salinity, implications for the agreement between apparent and thermodynamic constants of calcite and aragonite. *Geochim. Cosmochim. Acta*, 46, 247, 1982.
243. **Jacobson, R. L. and Langmuir, D.**, Dissociation constants of calcite and  $\text{CaHCO}_3^-$  from 0 to 50°C. *Geochim. Cosmochim. Acta*, 38, 301, 1974.
244. **Millero, F. J. and Thurmond, V.**, The ionization of carbonic acid in Na-Mg-Cl solutions at 25°C. *J. Solution Chem.*, 12, 401, 1983.
245. **Dickson, A. G.**, Thermodynamics of the dissociation of boric acid in synthetic seawater from 273.15 to 318.15K. *Deep Sea Res.*, 37, 755, 1989.
246. **Hershey, J. P., Fernandez, M., Milne, P. J., and Millero, F. J.**, The ionization of boric acid in NaCl, Na-Ca-Cl and Na-Mg-Cl solutions at 25°C. *Geochim. Cosmochim. Acta*, 50, 143, 1986.
247. **Simonson, J. M., Roy, R. N., Roy, L. N., and Johnson, D. A.**, The thermodynamics of aqueous borate solutions. I. Mixtures of boric acid with sodium or potassium borate and chloride. *J. Solution Chem.*, 16, 791, 1987.
248. **Lyman, J.**, Buffer Mechanism of Seawater, Ph.D. thesis, UCLA, Los Angeles, 1956.
249. **Hansson, I.**, Determination of the acidity constant of boric acid in synthetic sea water media. *Acta Chem. Scand.*, 27, 924, 1973.
250. **Owen, B. B. and King, E. J.**, The effect of sodium chloride upon the ionization of boric acid at various temperatures. *J. Am. Chem. Soc.*, 65, 1612, 1945.
251. **Kemp, H. T., Abrams, J. P., and Overbeck, R. C.**, Effects of chemicals on aquatic life, in *Water Quality Criteria Data Book*, Vol. 3, Environmental Protection Agency, U.S. Government Printing Office, Washington, D.C., 1971, A9.
252. **Fromm, P. O. and Gillette, J. R.**, Effect of ambient ammonia on blood ammonia and nitrogen excretion of rainbow trout (*Salmo gairdnerii* Richardson). *Comp. Biochem. Phys.*, 26, 887, 1968.
253. **Quinn, P. K., Charlson, R. J., and Zoller, W. H.**, Ammonia, the dominant base in the remote marine troposphere: a review. *Tellus*, 39B, 413, 1987.
254. **Maeda, M.**, Prediction of dissociation constants of ammonium ion in aqueous solutions containing different ionic media. *Denki Kagaku*, 55, 61, 1987.
255. **Maeda, M., Hayashi, M., Ikeda, S., Kinjo, Y., and Ito, K.**, Prediction of dissociation constants of ammonium ion in artificial seawaters and concentrated sodium chloride solutions. *Bull. Chem. Soc. Jpn.*, 60, 2047, 1987.
256. **Maeda, M., Hisada, O., and Ito, K.**, Estimation of Setchenow coefficients of ammonia in aqueous salt solutions. *Denki Kagaku*, 55, 778, 1987.
257. **Maeda, M., Nakagawa, G., and Blederman, G.**, Estimation of medium effect on dissociation constant of ammonium ion and formation of silver(I)-ammine complexes in aqueous solution. *J. Phys. Chem.*, 87, 121, 1983.
258. **Maeda, M., Hisada, O., Ikeda, K., Masuda, H., Ito, K., and Kinjo, Y.**, Prediction of dissociation constants of ammonium ion in aqueous lithium chloride solutions in terms of the Pitzer approach. *J. Phys. Chem.*, 92, 6404, 1988.
259. **Maeda, M., Hisada, O., Ito, K., and Kinjo, Y.**, Application of Pitzer's equations to dissociation constants of ammonium ion in lithium chloride-sodium chloride mixtures. *J. Chem. Soc. Faraday Trans. 1*, 85, 2555, 1989.
260. **Holmes, H. F. and Mesmer, R. E.**, Thermodynamics of aqueous solutions of the alkali metal sulphates. *J. Solution Chem.*, 15, 495, 1986.
261. **Whitfield, M.**, The hydrolysis of ammonium ions in sea water — a theoretical study. *J. Mar. Biol. Assoc. U.K.*, 54, 565, 1974.
262. **Johansson, O. and Wedborg, M.**, The ammonia-ammonium equilibrium in seawater at temperatures between 5 and 25°C. *J. Solution Chem.*, 9, 37, 1980.
263. **Nordstrom, D. K., Plummer, N. L., and Langmuir, D.**, Revised chemical equilibrium data for major water mineral reactions and their limitations, in *Chemical Modelling in Aqueous Systems II*, Melchior, D. C. and Bassett, R. L., Eds., American Chemical Society, Washington, D.C., 1990, 398.
264. **Haug, H.**, Estimation of Pitzer's ion interaction parameters for electrolytes involved in complex formation using a chemical equilibrium model. *J. Solution Chem.*, 18, 1069, 1989.
265. **Hogfeldt, E.**, *Stability Constants of Metal-Ion Complexes. A. Inorganic Ligands*, Pergamon Press, Oxford, 1982.
266. **Bond, A. M. and Hefter, G. T.**, *Critical Survey of Stability Constants and Related Thermodynamic Data of Fluoride Complexes in Aqueous Solution*, Pergamon Press, Oxford, 1980.



267. Hamer, W. J. and Wu, Y.-C., The activity coefficients of hydrofluoric acid in water from 0 to 35°C, *J. Res. Natl. Bur. Stand. Sect. A*, 74, 761, 1970.
268. Dickson, A. G. and Riley, J. P., The estimation of acid dissociation constants in seawater media from potentiometric titrations with strong base. I. The ionic product of water —  $K_w$ , *Mar. Chem.*, 7, 89, 1979.
269. Perez, F. F. and Fraga, F., Association constant of fluoride and hydrogen ions in seawater, *Mar. Chem.*, 21, 161, 1987.
270. Barta, L. and Bradley, D. J., Interaction model for the volumetric properties of weak electrolytes with application to  $H_3PO_4$ , *J. Solution Chem.*, 12, 631, 1983.
271. Johansson, O. and Wedborg, M., Stability constants of phosphoric acid in seawater of 5–40‰ salinity and temperatures of 5–25°C, *Mar. Chem.*, 8, 57, 1979.
272. Dickson, A. G. and Riley, J. P., The estimation of acid dissociation constants in seawater media from potentiometric titrations with strong base. II. The dissociation of phosphoric acid, *Mar. Chem.*, 7, 101, 1979.
273. Atlas, E., Culberson, C., and Pytkowicz, R. M., Phosphate association with  $Na^+$ ,  $Ca^{2+}$  and  $Mg^{2+}$  in seawater, *Mar. Chem.*, 4, 243, 1976.
274. Hershey, J. P., Fernandez, M., and Millero, F. J., The dissociation of phosphoric acid in NaCl and NaMgCl solutions at 25°C, *J. Solution Chem.*, 18, 875, 1989.
275. Kester, D. R. and Pytkowicz, R. M., Sodium, magnesium and calcium sulphate ion-pairs in sea water at 25°C, *Limnol. Oceanogr.*, 14, 686, 1968.
276. Wagman, D. D., Evans, W. H., Parker, V. B., Schumm, I. H., Bailey, S. M., Churney, K. L., and Nuttall, R. L., The NBS tables of chemical thermodynamic properties, *J. Phys. Chem. Ref. Data*, 11, 1, 1982.
277. Douahul, A. A. and Riley, J. P., The solubility of gases in distilled water and seawater — hydrogen sulphide, *Deep Sea Res.*, 26, 259, 1978.
278. Millero, F. J., The thermodynamics and kinetics of the hydrogen sulphide system in natural waters, *Mar. Chem.*, 18, 121, 1986.
279. Clarke, E. C. and Glew, D. N., Aqueous nonelectrolyte solutions. VIII. Deuterium and hydrogen sulphide solubilities in deuterium oxide and water, *Can. J. Chem.*, 49, 691, 1971.
280. Carroll, J. J. and Mather, A. E., The solubility of hydrogen sulphide in water from 0 to 90°C and pressure to 1 MPa, *Geochim. Cosmochim. Acta*, 53, 1163, 1989.
281. Hershey, J. P., Plese, T., and Millero, F. J., The  $pK^{\dagger}$  for the dissociation of  $H_2S$  in various ionic media, *Geochim. Cosmochim. Acta*, 52, 2047, 1988.
282. Gamsjäger, H. and Schindler, P., Solubilities and activity coefficients of  $H_2S$  in electrolyte mixtures, *Helv. Chim. Acta*, 52, 1395, 1969.
283. Barrett, T. J., Anderson, G. M., and Lugowski, J., The solubility of hydrogen sulphide in 0–5 mNaCl solutions at 25–95°C and one atmosphere, *Geochim. Cosmochim. Acta*, 52, 807, 1988.
284. Myers, R. J., The new low value for the second dissociation constant for  $H_2S$ , *J. Chem. Educ.*, 63, 687, 1986.
285. Millero, F. J., Plese, T., and Fernandez, M., The dissociation of hydrogen sulphide in seawater, *Limnol. Oceanogr.*, 33, 269, 1988.
286. Millero, F. J., Hershey, J. P., Johnson, G., and Zhang, J.-Z., The solubility of  $SO_2$  and the dissociation of  $H_2SO_3$  in NaCl solutions, *J. Atmos. Chem.*, 8, 377, 1989.
287. Goldberg, R. N. and Parker, V. B., Thermodynamics of solution of  $SO_{2(g)}$  in water and of aqueous sulphur dioxide solutions, *J. Res. Natl. Bur. Stand.*, 90, 341, 1985.
288. Young, C. L., Ed., *Sulphur Dioxide, Chlorine, Fluorine and Chlorine Oxides*, Vol. 12, IUPAC Solubility Data Series, Pergamon Press, Oxford, 1983, 473.
289. Douahul, A. A. and Riley, J. P., Solubility of sulphur dioxide in distilled water and decarbonated sea water, *J. Chem. Eng. Data*, 24, 274, 1979.
290. Culberson, C. H. and Pytkowicz, R. M., Ionization of water in sea water, *Mar. Chem.*, 1, 309, 1973.
291. Hansson, I., An Analytical Approach to the Carbonate System in Seawater, Ph.D. thesis, University of Göteborg, Göteborg, 1972.
292. Pitzer, K. S. and Mayorga, G., Thermodynamics of electrolytes. III. Activity and osmotic coefficients for 2:2 electrolytes, *J. Solution Chem.*, 3, 539, 1974.
293. Ringbom, A., *Complexation in Analytical Chemistry*, Wiley Interscience, New York, 1963.
294. Elder, J. F., Complexation side reactions involving trace metals in natural water systems, *Limnol. Oceanogr.*, 20, 96, 1975.
295. Smith, R. M. and Martell, A. E., *Critical Stability Constants (Inorganic Complexes)*, Vol. 4, Plenum Press, New York, 1976.
296. Turner, D. R., Whitfield, M., and Dickson, A. G., The equilibrium speciation of dissolved components in freshwater and seawater at 25°C and 1 atm pressure, *Geochim. Cosmochim. Acta*, 45, 855, 1981.
297. Coale, K. H. and Bruland, K. W., Copper complexation in the northeast Pacific, *Limnol. Oceanogr.*, 33, 1084, 1988.

298. **Dyrssen, D. and Wedborg, M.**, Major and minor elements. chemical speciation in estuarine waters, in *Chemistry and Biogeochemistry of Estuaries*, Olausson, E. and Cato, I., Eds., John Wiley & Sons, New York, 1980, 71.
299. **Fritz, J. J.**, Thermodynamic properties of chloro-complexes of silver chloride in aqueous solution, *J. Solution Chem.*, 14, 865, 1985.
300. **Fritz, J. J.**, Chloride complexes of CuCl in aqueous solution, *J. Phys. Chem.*, 84, 2241, 1980.
301. **Furst, W., Hachimi, S., and Renon, H.**, Representation of cupric chloride solutions with the Pitzer model — application to the extraction equilibrium of Cu(II) by LIX 65N, *J. Solution Chem.*, 17, 953, 1988.
302. **Downes, C. J. and Pitzer, K. S.**, Thermodynamics of electrolytes. Binary mixtures formed from aqueous NaCl, Na<sub>2</sub>SO<sub>4</sub>, CuCl<sub>2</sub>, and CuSO<sub>4</sub> at 25°C, *J. Solution Chem.*, 5, 389, 1976.
303. **Millero, F. J. and Byrne, R. H.**, Use of the Pitzer equations to determine the medium effect on the formation of lead chloro complexes, *Geochim. Cosmochim. Acta*, 48, 1145, 1984.
304. **Whitfield, M.**, Activity coefficients in natural waters, in *Activity Coefficients in Electrolyte Solutions*, Vol. 2, Pytkowicz, R. M., Ed., CRC Press, Boca Raton, FL, 1979, 153.
305. **Turner, D. R. and Whitfield, M.**, An equilibrium speciation model for copper in sea and estuarine waters at 25°C including complexation with glycine, EDTA and NTA, *Geochim. Cosmochim. Acta*, 51, 3231, 1987.
306. **Davison, W. and Whitfield, M.**, Modulated polarographic and voltammetric techniques in the study of natural waters, *J. Electroanal. Chem.*, 75, 763, 1977.
307. **Riley, J. P. and Skirrow, G.**, *Chemical Oceanography*, Vol. 1, Academic Press, London, 1975.
308. **Kester, D. R., Duedall, I. W., Connors, D. N., and Pytkowicz, R. M.**, Preparation of artificial sea water, *Limnol. Oceanogr.*, 12, 176, 1967.
309. **Lyman, J. and Fleming, R. H.**, Composition of sea water, *J. Mar. Res.*, 3, 134, 1940.
310. **Neev, D. and Emery, K. O.**, The Dead Sea. Depositional processes and environments of evaporites, *Isr. Geol. Surv. Bull.*, No. 41, 1967.
311. **Riley, J. P.**, The hot saline waters of the Red Sea bottom and their related sediments, *Oceanogr. Mar. Biol. Annu. Rev.*, 5, 141, 1967.
312. **Rosler, H. J. and Lange, H.**, *Geochemical Tables*, Elsevier, Amsterdam, 1973, 320.
313. **Cramer, S. D.**, The solubility of oxygen in brines from 0 to 300°C, *Ind. Eng. Chem. Process Des. Dev.*, 19, 300, 1980.
314. **Holmes, H. F. and Mesmer, R. E.**, Thermodynamic properties of aqueous solutions of the alkali metal chlorides to 250°C, *J. Phys. Chem.*, 87, 1242, 1983.
315. **Pitzer, K. S., Peiper, J. C., and Busey, R. H.**, Thermodynamic properties of aqueous sodium chloride solutions, *J. Phys. Chem. Ref. Data*, 13, 1, 1984.
316. **Pabalan, R. T. and Pitzer, K. S.**, Thermodynamics of NaOH<sub>(aq)</sub> in hydrothermal solutions, *Geochim. Cosmochim. Acta*, 51, 829, 1987.
317. **Saluja, P. P. S., Pitzer, K. S., and Phutela, R. C.**, High temperature thermodynamic properties of several 1:1 electrolytes, *Can. J. Chem.*, 64, 1328, 1986.
318. **De Lima, M. C. P. and Pitzer, K. S.**, Thermodynamics of saturated electrolyte mixtures of NaCl with Na<sub>2</sub>SO<sub>4</sub> and with MgCl<sub>2</sub>, *J. Solution Chem.*, 12, 187, 1983.
319. **Phutela, R. C., Pitzer, K. S., and Saluja, P. P. S.**, Thermodynamics of aqueous magnesium chloride, calcium chloride and strontium chloride at elevated temperatures, *J. Chem. Eng. Data*, 32, 76, 1987.
320. **Phutela, R. C. and Pitzer, K. S.**, Heat capacity and other thermodynamic properties of aqueous magnesium sulphate to 473K, *J. Phys. Chem.*, 90, 895, 1986.
321. **Phutela, R. C. and Pitzer, K. S.**, Thermodynamics of aqueous calcium chloride, *J. Solution Chem.*, 12, 201, 1983.
322. **Rogers, P. S. Z. and Pitzer, K. S.**, High temperature thermodynamic properties of sodium sulphate solutions, *J. Phys. Chem.*, 85, 2886, 1981.
323. **Pitzer, K. S.**, Thermodynamic model for aqueous solutions of liquid-like density, *Rev. Mineral.*, 17, 97, 1987.
324. **Clever, H. L., Ed.**, *Argon*, Vol. 4, IUPAC Solubility Data Series, Pergamon Press, Oxford, 1980, 329.
325. **Clever, H. L. and Young, C. L., Eds.**, *Methane*, Vol. 27/28, IUPAC Solubility Data Series, Pergamon Press, Oxford, 1987.
326. **Clever, H. L., Ed.**, *Helium and Neon — Gas Solubilities*, Vol. 1, IUPAC Solubility Data Series, Pergamon Press, Oxford, 1979, 392.
327. **Hayduk, W., Ed.**, *Ethane*, Vol. 9, IUPAC Solubility Data Series, Pergamon Press, Oxford, 1982.
328. **Clever, H. L., Ed.**, *Krypton, Xenon and Radon — Gas Solubilities*, Vol. 2, IUPAC Solubility Data Series, Pergamon Press, Oxford, 1979, 355.
329. **Hayduk, W., Ed.**, *Propane, Butane and 2-Methylpropane*, Vol. 24, IUPAC Solubility Data Series, Pergamon Press, Oxford, 1986.
330. **Young, C. L., Ed.**, *Hydrogen and Deuterium*, Vol. 5/6, IUPAC Solubility Data Series, Pergamon Press, Oxford, 1981.

331. Shaw, D. G., Ed., *Hydrocarbons with Water and Seawater Part I: Hydrocarbons C5 to C7*, Vol. 37, IUPAC Solubility Data Series, Pergamon Press, Oxford, 1989.
332. Battino, R., Ed., *Nitrogen and Air*, Vol. 10, IUPAC Solubility Data Series, Pergamon Press, Oxford, 1982, 565.
333. Shaw, D. G., Ed., *Hydrocarbons with Water and Seawater II: Hydrocarbons C8 to C16*, Vol. 38, IUPAC Solubility Data Series, Pergamon Press, Oxford, 1989.
334. Young, C. L., Ed., *Oxides of Nitrogen*, Vol. 8, IUPAC Solubility Data Series, Pergamon Press, Oxford, 1981, 367.
335. Barton, A. F. M., Ed., *Alcohols with Water*, Vol. 15, IUPAC Solubility Data Series, Pergamon Press, Oxford, 1984.
336. Horvath, A. L., Getzen, F. W., and Jancso, G., Eds., *Halogenated Benzenes, Toluenes and Phenols with Water*, Vol. 20, IUPAC Solubility Data Series, Pergamon Press, Oxford, 1985.
337. Cargill, R. W., Ed., *Carbon Monoxide*, Vol. 43, IUPAC Solubility Data Series, Pergamon Press, Oxford, 1990.
338. Shiu, W. Y. and Mackay, D., A critical review of aqueous solubilities, vapour pressures, Henry's law constants, and octanol-water partition coefficients of the polychlorinated biphenyls, *J. Phys. Chem. Ref. Data*, 15, 911, 1986.
339. Mackay, D. and Shiu, W. Y., Critical review of Henry's law constants for chemicals of environmental interest, *J. Phys. Chem. Ref. Data*, 10, 1175, 1981.
340. Pitzer, K. S., Thermodynamics of electrolytes. V. Effects of higher order electrostatic terms, *J. Solution Chem.*, 4, 249, 1975.
341. Clegg, S. L. and Brimblecombe, P., The Henry's law constant of methanesulphonic acid and its implications for atmospheric chemistry, *Environ. Technol. Lett.*, 6, 269, 1985.
342. Fritz, J. J. and Fuget, C. R., Vapour pressure of aqueous hydrogen chloride solutions, 0° to 50°C, *J. Chem. Eng. Data*, 10, 1956.
343. Macaskill, J. B. and Bates, R. G., Osmotic coefficients and activity coefficients of aqueous hydrobromic acid at 25°C, *J. Solution Chem.*, 12, 607, 1983.
344. Kester, D. R., Dissolved gases other than CO<sub>2</sub>, in *Chemical Oceanography*, Vol. 1, Riley, J. P. and Skirrow, G., Eds., Academic Press, London, 1975, 497.
345. Enns, T., Scholander, P. F., and Bradstreet, E. D., Effect of hydrostatic pressure on gases dissolved in water, *J. Phys. Chem.*, 69, 389, 1965.
346. Rice, P. A., Gale, R. P., and Barduhn, A. J., Solubility of butane in water and salt solutions at low temperatures, *J. Chem. Eng. Data*, 21, 204, 1976.
347. Bajolle, J.-E., Rice, P. A., and Barduhn, A. J., Vacuum stripping of butane from water in a packed column, *Desalination*, 9, 351, 1971.
348. Sutton, C. and Calder, J. A., Solubility of higher-molecular-weight n-paraffins in distilled water and seawater, *Environ. Sci. Technol.*, 8, 654, 1974.
349. Eganhouse, R. P. and Calder, J. A., The solubility of medium molecular weight aromatic hydrocarbons and the effects of hydrocarbon co-solutes and salinity, *Geochim. Cosmochim. Acta*, 40, 555, 1976.
350. Elgquist, B. and Wedborg, M., Stability constants of NaSO<sub>3</sub><sup>-</sup>, MgSO<sub>4</sub>, MgF<sup>-</sup>, MgCl<sup>-</sup> ion pairs at the ionic strength of seawater by potentiometry, *Mar. Chem.*, 6, 243, 1978.
351. Hatch, J. R., Phase Relationships in Part of the System, Sodium Carbonate-Calcium Carbonate-Carbon Dioxide-Water, at 1 atm Pressure, Ph.D. thesis, University of Illinois, Urbana, 1972.
352. Eugster, H. P., Sodium carbonate-bicarbonate minerals as indicators of P<sub>CO<sub>2</sub></sub>, *J. Geophys. Res.*, 71, 3369, 1966.
353. Chan, C. Y., Khoo, K. H., and Lim, T. K., Specific ionic interactions in the quaternary systems HCl-NaCl-KCl-water and HCl-NH<sub>4</sub>Cl-KCl-water at 25°C, *J. Solution Chem.*, 8, 41, 1979.
354. Clegg, S. L. and Brimblecombe, P., Estimated mean activity coefficients of aqueous BeCl<sub>2</sub> and properties of solution mixtures containing the Be<sup>2+</sup> ion, *J. Chem. Soc. Faraday Trans. 1*, 85, 157, 1989.
355. Filippov, V. K., Charykova, M. V., and Trofimov, Yu. M., Thermodynamics of the system NH<sub>4</sub>H<sub>2</sub>PO<sub>4</sub>-(NH<sub>4</sub>)<sub>2</sub>SO<sub>4</sub>-H<sub>2</sub>O at 25°C, *J. Appl. Chem. U.S.S.R.*, 58, 1807, 1986.
356. Zirino, A. and Yamamoto, S., A pH dependent model for the chemical speciation of copper, zinc, calcium and lead in sea water, *Limnol. Oceanogr.*, 17, 661, 1972.
357. Florence, T. M. and Batley, G. E., Trace metal species in sea water. I. Removal of trace metals from sea water by a chelating resin, *Talanta*, 23, 179, 1976.
358. Ahrland, S., Metal complexes present in sea water, in *The Nature of Sea Water*, Goldberg, E. D., Ed., Dahlem Konferenzen, Berlin, 1975.
359. Stumm, W. and Brauner, P. A., Chemical speciation, in *Chemical Oceanography*, Vol. 1, Riley, J. P. and Skirrow, G., Eds., Academic Press, New York, 1975, 173.
360. Whitfield, M. and Turner, D. R., Chemical speciation of lead in sea water, in *Lead Occurrence, Fate and Pollution in the Marine Environment*, Pergamon Press, Oxford, 1978.

361. **Reardon, E. J. and Langmuir, D.**, Activity coefficients of  $\text{MgCO}_3^0$  and  $\text{CaSO}_4^0$  ion pairs as a function of ionic strength, *Geochim. Cosmochim. Acta.* 40, 549, 1976.
362. **Reardon, E. J.**, Dissociation constants of some monovalent sulphate ion pairs at 25°C from stoichiometric activity coefficients, *J. Phys. Chem.*, 79, 422, 1975.
363. **Murray, C. N. and Riley, J. P.**, The solubility of gases in distilled water and sea water. IV. Carbon dioxide, *Deep Sea Res.*, 18, 533, 1971.
364. **Staples, B. R. and Nuttall, R. L.**, The activity and osmotic coefficients of aqueous calcium chloride at 298.15K, *J. Phys. Chem. Ref. Data.* 6, 385, 1977.
365. **Pitzer, K. S. and Peiper, J. C.**, The activity coefficient of aqueous  $\text{NaHCO}_3$ , *J. Phys. Chem.*, 84, 2396, 1980.
366. **Baes, C. F. and Mesmer, R. E.**, *The Hydrolysis of Cations*, Wiley Interscience, New York, 1976.
367. **McGee, K. A. and Hostetler, P. B.**, Studies in the system  $\text{MgO-SiO}_2\text{-CO}_2\text{-H}_2\text{O}$ . IV. The stability of  $\text{MgOH}^+$  from 10 to 90°C, *Am. J. Sci.*, 275, 304, 1975.
368. **Nair, V. S. K. and Nancollas, G. H.**, Thermodynamics of ion association. IV. Magnesium and zinc sulphates, *J. Chem. Soc.*, p. 3706, 1958.
369. **Bell, R. P. and George, J. H. B.**, The incomplete dissociation of some thalous and calcium salts at different temperatures, *Trans. Faraday Soc.*, 49, 619, 1953.
370. **Seibert, R. M. and Hostetler, P. B.**, The stability of the magnesium bicarbonate ion pair from 10 to 90°C, *Am. J. Sci.*, 227, 697, 1977.
371. **Reardon, E. J., Jacobson, R. L. and Langmuir, D.**, Dissociation constants of  $\text{CaHCO}_3^-$  and  $\text{MgHCO}_3^-$  ion pairs as a function of ionic strength, *Am. Geophys. Union Trans.*, 54, 260, 1973.
372. **Nakayama, F. S. and Rasnick, B. A.**, Bicarbonate complexes of barium and strontium, *J. Inorg. Nucl. Chem.*, 31, 3491, 1969.
373. **Reardon, E. J. and Langmuir, D.**, Thermodynamic properties of the ion pairs  $\text{MgCO}_3^0$  and  $\text{CaCO}_3^0$  from 10 to 50°C, *Am. J. Sci.*, 274, 599, 1974.
374. **Byrne, R. H. and Kester, D. R.**, Inorganic speciation of boron in sea water, *J. Mar. Res.*, 32, 119, 1974.
375. **Duer, W. C., Robinson, R. A. and Bates, R. G.**, Molar conductivity of sodium fluoride in aqueous solution at 25°C, *J. Chem. Soc. Faraday Trans. 1.* 68, 716, 1972.
376. **Connick, R. E. and Tsao, M. S.**, Complexing of magnesium ion by fluoride ion, *J. Am. Chem. Soc.*, 76, 5311, 1954.
377. **Cramer, S. D.**, Oxygen solubility in brines, *Ind. Eng. Chem. Process Des. Dev.*, 23, 618, 1984.
378. **Keeley, D. F., Hoffpauir, M. A., and Meriwether, J. R.**, Solubility of aromatic hydrocarbons in water and NaCl solutions of different ionic strengths: benzene and toluene, *J. Chem. Eng. Data*, 33, 87, 1988.
379. **Groves, F. R.**, Solubility of cycloparaffins in distilled water and salt water, *J. Chem. Eng. Data*, 33, 136, 1988.
380. **Dawson, H. M. and McCrae, J.**, Metal-ammonia compounds in aqueous solution. II. The absorptive powers of dilute solutions of salts of the alkali metals, *J. Chem. Soc.*, 79, 493, 1901.
381. **Abegg, R. and Reisenfeld, H.**, Über das Lösungsvermögen von Salzlösungen für Ammoniak nach Messungen seines Partialdrucks. I. *Z. Phys. Chem.*, 40, 84, 1902.
382. **Gaus, W.**, Über den Einfluss von Neutralsalzen auf die Tension des Ammoniaks aus wässriger Lösung, *Z. Anorg. Allg. Chem.*, 25, 236, 1900.
383. **Baldi, G. and Specchia, V.**, Solubilità dell'ammoniaca in soluzioni saline, *Chim. Ind. (Milan)*, 53, 1022, 1971.
384. **Robinson, R. A.**, The vapour pressure and osmotic equivalence of sea water, *J. Mar. Biol. Assoc. U.K.*, 33, 449, 1954.
385. **Doherty, L. A. and Kester, D. R.**, Freezing point of sea water, *J. Mar. Sci.*, 32, 285, 1974.
386. **Linke, W. F.**, *Solubilities of Inorganic and Metal Organic Compounds*, American Chemical Society, Washington, D.C., 1965.
387. **Katz, A., Starinsky, A., and Taitel-Goldman, N.**, Solubilities of gypsum and halite in the Dead Sea and in its mixtures with seawater, *Limnol. Oceanogr.*, 26, 709, 1981.
388. **Pitzer, K. S.**, personal communication.

**MINERAL SOLUBILITIES IN ELECTROLYTE SOLUTIONS****Roberto T. Pabalan and Kenneth S. Pitzer****TABLE OF CONTENTS**

I.	Introduction .....	436
II.	Basic Theory .....	437
III.	Modeling Approach .....	438
IV.	Solubility Calculations Using the Ion Interaction Model .....	440
	A. Solubilities at 25°C .....	441
	B. Solubilities at Variable Temperatures .....	453
	1. Choice of Standard-State Properties .....	453
	2. Choice of Ion Interaction Parameters and Calculated Solubilities in Binary Systems .....	458
	3. Solubilities in Ternary Systems .....	460
	4. Solubilities in Quaternary Systems .....	465
V.	Solubility Calculations Using the Margules Expansion Model .....	466
	A. Model Equations and Solubility Calculations in Binary Electrolyte + Water Systems .....	470
	B. Model Equations and Solubility Calculations in Ternary Systems .....	477
VI.	Conclusions .....	479
	Acknowledgment .....	480
	Appendix: Numerical Expressions for Temperature Dependency .....	480
	References .....	485

## I. INTRODUCTION

Chemical modeling designed to understand geochemical processes such as those related to hydrothermal brines, seawater systems, and evaporite formations, as well as industrial problems in such areas as desalination, steam power generation, and hydrometallurgy, requires a detailed knowledge of the thermodynamic properties of aqueous electrolyte solutions. The systems of interest in these studies can differ widely in terms of their physical and chemical characteristics; hence, it is essential to have chemical models that accurately describe electrolyte solution properties over wide ranges of temperature, pressure, and concentration. In addition, it is impractical to conduct measurements for a large number of different mixture compositions; thus, one needs models that allow the prediction of these properties for complex mixtures based on parameters evaluated from simple systems.

Various models of aqueous electrolyte thermodynamic properties have been proposed in the literature. Numerical comparisons of some of these models have been presented by Zemaitis et al.<sup>1</sup> Unfortunately, these authors failed to recognize the stated ranges of validity of the various models; hence, the comparisons can be misleading. The validity of alternate equations is also discussed in Chapter 6 of this book. The most frequently used model at present is the ion interaction or virial coefficient approach developed by Pitzer<sup>2</sup> and co-workers and discussed in detail in Chapter 3 of this volume. Success of this model when applied to complex and concentrated electrolyte mixtures was demonstrated for calculations of equilibria at room temperature between a brine phase and one or more solids by Harvie and Weare<sup>3</sup> and Harvie et al.<sup>4</sup> Model applications at high temperatures were later shown to be equally successful for calculations of solubility equilibria by Pabalan and Pitzer,<sup>5,6</sup> Møller,<sup>7</sup> and Greenberg and Møller,<sup>8</sup> as well as to calculations of vapor pressure depression and boiling point elevation by Pabalan and Pitzer.<sup>9,10</sup> More recently, the model has also been applied to solubility calculations at temperatures below 25°C (to near -60°C) by Spencer et al.<sup>11</sup>

There are, however, electrolytes of geochemical and industrial interest which become extremely soluble in water at high temperatures and pressures. Although the ion interaction model has been successful on systems from dilute to high (10 or even 20) molality,<sup>3,8</sup> application of that model to even higher concentrations by using additional virial terms<sup>12</sup> becomes complex and often unsatisfactory. In addition, the molality for a pure fused salt is infinite. An alternate approach to the molality-based model is the mole fraction-based model recently proposed by Pitzer and Simonson.<sup>13</sup> This is based on a Margules-type expansion. It can be applied to systems which extend from dilute solutions to the fused salt, and for other systems of very high, but limited solubility. Applications of the model on some ionic systems have been demonstrated by Simonson and Pitzer,<sup>14</sup> Weres and Tsao,<sup>15</sup> and Pabalan and Pitzer.<sup>16</sup> This model is also discussed in detail in Chapter 3 (Appendix I).

Prediction of mineral solubilities in aqueous electrolyte mixtures is an important use of chemical models. It is also a rigorous test of equations for the activity and osmotic coefficients of aqueous electrolytes. There is a large body of solubility data available in the literature, particularly near room temperature, from which model parameters can be derived, or on which model predictions can be validated. For example, an excellent compilation of solubility data is given by Linke.<sup>17</sup> In addition, the Russian literature on physical and inorganic chemistry provides a substantial source of solubility data, mostly at 25°C, but some extending to 100°C or higher.

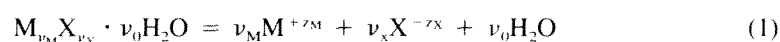
The objective of this chapter is to demonstrate the successful use of the molality-based ion interaction and the Margules expansion models to calculations of solubility equilibria on a wide variety of chemical systems which are of geochemical or industrial interest. In several cases, solubility calculations extend upward to high temperatures. We do not attempt to present here a comprehensive list of model parameters and systems for which solubility

data have been evaluated. Chapter 3 includes extensive tables of parameters for 25°C. It is anticipated that as better data on solubilities or on aqueous electrolyte thermodynamic properties become available, model parameters may have to be reevaluated. This is especially true at high temperatures and pressures, where more precise data on aqueous solution activities, enthalpies, and heat capacities are currently being measured (see, for example, Table 15 of Chapter 3).

In addition, solubility parameters determined by one investigator are not necessarily consistent with those determined by others. An extensive evaluation of experimental data is required to verify the internal consistency of a set of parameters for accurate modeling of solubilities in complex mixtures. As a result, although numerous studies have modeled solubilities using the ion interaction approach,<sup>3,11,18-53</sup> most of these have calculated solubilities in binary or ternary mixtures only. The most complex system for which an internally consistent set of model parameters has been generated is that of seawater<sup>3,4,7,8,11,18</sup> (also Chapter 6). For details of parameter evaluations on specific aqueous electrolyte mixtures which are not discussed in this chapter, the references cited here and in Chapters 3 and 6 should be consulted.

## II. BASIC THEORY

The basic theory for calculations of solubility equilibria is well known. Mineral solubilities in electrolyte solutions can be calculated from thermodynamic considerations provided that equilibrium constants are known and activity coefficients can be obtained. For a hydrated solid with a fixed composition  $M_{\nu_M}X_{\nu_X} \cdot \nu_0 H_2O$ , which consists of  $\nu_M$  positive ions, M, of charge  $z_M$ ,  $\nu_X$  negative ions, X, of charge  $z_X$ , and  $\nu_0$  molecules of water, the equilibrium constant, K, at a fixed temperature and pressure for the dissolution reaction



is given by

$$\ln K = \mu_i^\circ/RT - (\nu_M \mu_M^\circ + \nu_X \mu_X^\circ + \nu_0 \mu_{H_2O}^\circ)/RT \quad (2)$$

where the  $\mu_i^\circ$ 's represent the chemical potentials of the solid or of the aqueous species at their defined standard states. The standard states for the aqueous ions and electrolytes were taken to be the hypothetical 1-*m* ideal solution which is actually referenced to infinite dilution at any temperature and pressure. The solid and solvent standard states were taken to be the pure phases at the temperature and pressure of interest.

In terms of activities or molalities, the equilibrium constant for the solubility reaction is given by

$$\ln K = \nu_M \ln a_M + \nu_X \ln a_X + \nu_0 \ln a_{H_2O} \quad (3)$$

or

$$\ln K = \nu_M \ln (m_M \gamma_M) + \nu_X \ln (m_X \gamma_X) + \nu_0 \ln a_{H_2O} \quad (4)$$

where  $a_i$ ,  $m_i$ , and  $\gamma_i$  represent the activity, molality, and activity coefficient of the aqueous ion  $i$ , respectively, and  $a_{H_2O}$  is the activity of the solvent. Although absolute values of  $\gamma_i$ 's for individual ions cannot be determined by ordinary thermodynamic methods due to electroneutrality constraints, the mean activity coefficient,  $\gamma_{\pm}$ , can be defined unambiguously as

$$\ln \gamma_{\pm} = (\nu_M \ln \gamma_M + \nu_X \ln \gamma_X) / \nu \quad (5)$$

with  $\nu = (\nu_M + \nu_X)$ . It is shown in Chapter 3, however, that equations for  $\gamma_M$  and  $\gamma_X$  can be written where the only ambiguity is a term which cancels for the  $\gamma_{\pm}$  product for any charge type. Thus, one can either use equations for  $\gamma_{\pm}$  or those for  $\gamma_M$  and  $\gamma_X$ . In aqueous electrolyte mixtures of complex composition (e.g., seawater including minor components), it is advantageous to use the latter because the number of possible  $\gamma_{\pm}$  is much larger than the number of  $\gamma_M$  and  $\gamma_X$ .

The activity of water is related to the osmotic coefficient,  $\phi$ , by the equation

$$\ln a_{H_2O} = -\phi (M_w/1000) \sum_i m_i \quad (6)$$

where  $M_w$  is the molecular mass of water in  $\text{g} \cdot \text{mol}^{-1}$  and the sum covers all solute species. The Gibbs-Duhem equation relates the composition dependence of  $\phi$  or  $a_{H_2O}$  to various solute  $\gamma_i$  or  $\gamma_{\pm}$ . These activity and osmotic coefficients can be calculated from the ion interaction or Margules expansion models described in Chapter 3.

The equilibrium constant,  $K$ , can be calculated provided the standard-state chemical potentials of the solid and aqueous species are available at the temperature and pressure of interest. The relationships between the dependencies of the chemical potentials on pressure and temperature, and on volumes, entropies (or enthalpies), and heat capacities are well-known. At constant pressure the temperature dependence of the standard-state chemical potential of component  $i$  is given by

$$(\partial \mu_i^{\circ} / \partial T)_p = -S_i^{\circ} \quad (7)$$

or

$$\mu_{i,T_2}^{\circ} - \mu_{i,T_1}^{\circ} = -S_{i,T_1}^{\circ} (T_2 - T_1) + \int_{T_1}^{T_2} C_p^{\circ} dT - T_2 \int_{T_1}^{T_2} (C_p^{\circ}/T) dT \quad (8)$$

where  $S_i^{\circ}$  represents the standard-state entropy of component  $i$ , and  $C_p^{\circ}$  is the standard-state heat capacity (at constant pressure) which itself is expressed as a function of temperature.  $T_1$  and  $T_2$  represent the reference temperature and temperature of interest, respectively. An analogous expression for the temperature dependence of the chemical potential can be written in terms of the enthalpy and heat capacity.

The dependence of the chemical potential on pressure is given by the molar or partial molar volume and can be derived from density and compressibility data. At the saturation pressures considered in this study the effects of this pressure dependence on solubilities are usually small, but can be significant at moderate to high pressures.<sup>44,55</sup> When pressure dependency information is noted below or in the Appendix, it was included in the calculations. In other cases, primarily at relatively low temperatures and pressures, we assume that the pressure effects on the calculated solubilities are within the combined uncertainties of all the parameters.

### III. MODELING APPROACH

From the equations given above, it is apparent that calculations of mineral solubilities in electrolyte solutions require data on (1) standard-state chemical potentials of solids and of aqueous species at the temperature and pressure of interest, and (2) activity coefficients of aqueous species as functions of solution composition, as well as of temperature and



pressure. For many systems of geochemical or industrial interest, the former requirement has not been a major problem. There are extensive compilations of standard-state properties for solids and aqueous species, mostly for 25°C and 1 bar, but in many cases extending upward in temperature.<sup>56-59</sup> The database for aqueous species at temperatures above 25°C is less extensive, but there is now an increasing amount of experimental data at high temperatures for the most geochemically or industrially important electrolytes (see below and Table 15, Chapter 3). In addition, equations of state based in part on solvation theory have been useful in estimating the standard-state properties of aqueous species at elevated temperatures and pressures.<sup>60,61</sup> In the case of water, its chemical potential at the temperature and pressure of interest can be conveniently calculated from the equations of Haar et al.<sup>62</sup> Thus, equilibrium constants for important dissolution reactions can be readily calculated.

In practice, a computer database of 25°C standard-state chemical potentials of the solids and aqueous species of interest can be set up which the computer program can access to calculate the pertinent equilibrium constants. If calculations at temperatures other than 25°C will be performed, the database may include values of 25°C standard-state entropy (or enthalpy) and analytical expressions for the temperature dependence of the standard-state heat capacity of the solids and aqueous species.

Alternatively, a thermodynamic database consisting of equilibrium constants (or their temperature functions) for all the independent equilibrium reactions can be set up. This format is used in many of the existing geochemical modeling codes.<sup>63-69</sup> It is believed to introduce less errors in the equilibrium calculations because standard-state chemical potentials of individual phases or species are always derived values (e.g., EMF, solubility measurement), while equilibrium constants are based on reaction equilibria and are closest in their derivation to the actual measurements.<sup>70</sup> In addition, the flexibility afforded by being able to independently adjust equilibrium constants of individual reactions and to fit these as functions of temperature is advantageous in developing an internally consistent database of parameters for complex mixtures. In this study, however, we have opted to use a database consisting of standard-state properties of the solids and aqueous species. This avoids the necessity of fitting analytical expressions to the temperature dependence of the equilibrium constants. This approach is very dependent on standard-state properties, as well as activity coefficient model parameters, reported in the literature; hence, it provides a mechanism for checking the consistency between independently derived parameters.

The second data requirement listed above has presented a more challenging problem for solubility calculations in high ionic strength solutions. Prior to the development of the ion interaction model by Pitzer and co-workers (Chapter 3), equilibrium calculations of mineral solubilities have more or less been limited to dilute aqueous solutions. Successful prediction of mineral solubilities in concentrated electrolyte mixtures had been hampered by the lack of an adequate thermodynamic model for the properties of concentrated electrolyte solutions. This difficulty is largely due to the fact that the solubilities of many minerals become exceedingly dependent on the concentration of co-solutes in the concentrated range.<sup>71</sup> This behavior indicates that activity coefficients must correct for specific salt effects as well as for ionic strength. The application of the ion interaction approach in modeling aqueous activity coefficients has allowed solubilities to be calculated in aqueous solutions of high concentrations and complex compositions. For simpler systems, but those which extend over an even wider range of concentration, activity coefficients derived from a Margules expansion model have also been shown to be successful.<sup>16</sup>

It is important to recognize that equilibrium calculations are highly dependent on the thermodynamic data and model parameters used in the calculations. In modeling solubilities in complex systems, there is a need for both accuracy and internal consistency among all the model parameters and thermodynamic data for the chemical systems considered in the study. The approach we have taken here is to utilize as much as possible the standard-state

properties for solids and aqueous species recommended in various compilations,<sup>56-59</sup> as well as ion interaction parameters reported in the literature. Most of the reported ion interaction parameters are based on measurements of aqueous solution activities (e.g., EMF, isopiestic, vapor pressure); hence, these are derived independently of solubility data. In a majority of the cases studied here, the published standard-state properties and binary ion interaction parameters yield calculated mineral solubilities in pure water (i.e., binary electrolyte + water systems) which are in very good agreement with experimental data. In some cases, small adjustments to the values of the chemical potential of the solid phase were needed to improve the agreement between calculated and experimental solubilities in the binary systems. In a few cases where the thermodynamic data for a hydrated solid are not available, these were estimated from the data for the same solid of different hydration numbers,<sup>5</sup> or were estimated directly from solubility data. For calculations in ternary or more complex systems, the same standard-state chemical potentials and ion interaction parameters validated by solubility data in binary systems were used. However, mixing parameters for activity coefficients are required in these calculations. Solubility calculations in mixed electrolytes are particularly sensitive to the values of these mixing terms. For some systems the reported mixing parameters, which were evaluated from measured aqueous solution activities in ternary systems, were used successfully, although in a few cases slight adjustments were made to better fit the measured solubilities. For many mixtures of geochemical or industrial interest, however, the only data available are solubility measurements; hence, the evaluation of mixing terms had to rely on solubility data. Details of parameter evaluations for specific systems are given in the pertinent sections below, as well as in the comprehensive papers of Harvie and Weare<sup>3</sup> and Harvie et al.<sup>4</sup> together with other references given here and in Chapter 3.

Computationally, the approach taken in this study to calculate the equilibrium assemblage is based on solution of a set of nonlinear mass-action equations involving equilibrium constants for all the relevant equilibria and an auxiliary set of linear mass-balance and charge-balance equations. This is a standard technique used also by other computer codes such as WATEQ,<sup>63</sup> SOLMNEQ,<sup>64,65</sup> EQ3NR,<sup>66</sup> EQ3/6,<sup>67</sup> PHREEQE,<sup>68</sup> and PHRQPITZ.<sup>69</sup> As mentioned previously, the equilibrium constants at the temperature of interest were calculated from standard-state chemical potentials, entropies, and heat capacities of the solids and aqueous species. The solution to the set of mass-action, mass-balance, and charge-balance equations was solved iteratively by matrix inversion (see, for example, Frantz et al.<sup>72</sup>). Alternatively, the multiphase equilibria can be solved by means of a Gibbs free energy minimization algorithm such as that used by Harvie and Weare.<sup>3</sup>

It should be noted that computer programs for simulation of geochemical interactions and which utilize equations based on the ion interaction model are available. The program PHRQPITZ<sup>69</sup> contains most of the reaction-modeling capabilities of the original PHREEQE<sup>68</sup> code, but has replaced the aqueous model with the ion interaction approach. Latest versions of the programs SOLMNEQ<sup>65</sup> and EQ3/6<sup>67</sup> include options to calculate activity coefficients using the ion interaction model.

#### IV. SOLUBILITY CALCULATIONS USING THE ION INTERACTION MODEL

For systems ranging from dilute to moderately high concentrations, the ion interaction or virial coefficient model is the most commonly used representation of the thermodynamic properties of aqueous electrolytes. Its theoretical bases are extensively discussed in Chapter 3 of this volume. The model is based on a virial expansion of the excess Gibbs energy,  $G^{ex}/RT$ , i.e., the actual Gibbs energy of the solution minus the Gibbs energy of a reference solution of the same composition but with unit activity and osmotic coefficients. Expressions

for various thermodynamic properties, including osmotic coefficients, activity coefficients, excess enthalpies, and volumes, follow directly from the equation for  $G^{\text{ex}}/RT$  through the appropriate derivatives. Working equations for these thermodynamic functions are given in Chapter 3. For the purposes of solubility calculations, the expressions for osmotic and activity coefficients are of direct relevance. However, the expressions for excess enthalpies, heat capacities, and volumes are also important because they yield the temperature and pressure dependence of the model parameters for osmotic and activity coefficients. For convenience, the ion interaction model equations for osmotic and activity coefficients are summarized in Table 1. The terms in these equations for neutral species are not included because these species are not considered in the examples given below, but the full equations are given in Chapter 3.

In practical terms, the ion interaction model represents the osmotic and activity coefficients of most\* electrolyte mixtures in terms of six types of empirical parameters, namely,  $\beta_{\text{MX}}^{(0)}$ ,  $\beta_{\text{MX}}^{(1)}$ ,  $\beta_{\text{MX}}^{(2)}$ ,  $C_{\text{MX}}^{\phi}$ ,  $\theta_{ij}$ , and  $\psi_{ijk}$ . The values of  $\beta_{\text{MX}}^{(0)}$ ,  $\beta_{\text{MX}}^{(1)}$ ,  $\beta_{\text{MX}}^{(2)}$ , and  $C_{\text{MX}}^{\phi}$  can be determined from experimental data on single electrolyte solutions, whereas  $\theta_{ij}$  and  $\psi_{ijk}$ , which arise for mixtures of two or more electrolytes, can be evaluated from data on simple mixtures. Provided that their temperature and pressure dependencies are known, these parameters permit the calculation of solubilities in binary, ternary, and more complex mixtures at different temperatures and pressures.

In the following two sections, experimental data on mineral solubilities are compared with values calculated using the ion interaction model. The first section gives examples of mineral solubility calculations at 25°C. Calculations at variable temperatures are given in the second section, some at temperatures extending to 300°C. The symbols in the figures of the following sections represent experimental data from various sources, and the curves represent solubilities calculated using the model. The intersections of the curves are the calculated invariant points in the system.

### A. SOLUBILITIES AT 25°C

Numerous studies on solubility calculations at 25°C have been published in the past decade,<sup>3-11,18-53</sup> and it is beyond the scope of this chapter to give an extensive summary. For equilibrium modeling of mineral solubilities in natural waters, a comprehensive model has been developed by Harvie et al.<sup>4</sup> for the system Na-K-Mg-Ca-H-Cl-SO<sub>4</sub>-OH-HCO<sub>3</sub>-CO<sub>3</sub>-CO<sub>2</sub>-H<sub>2</sub>O, and this reference should be consulted for detailed discussions; many of the parameters tabulated in Chapter 3 are taken from this paper. In this section, we present some new solubility calculations for mixtures of different valence types as an example and an addition to earlier calculations at 25°C. The binary ion interaction parameters ( $\beta_{\text{MX}}^{(0)}$ ,  $\beta_{\text{MX}}^{(1)}$ ,  $\beta_{\text{MX}}^{(2)}$ ,  $C_{\text{MX}}^{\phi}$ ), mixing parameters ( $\theta_{ij}$ ,  $\psi_{ijk}$ ), and standard-state chemical potentials of the solids and aqueous species used in the calculations are given in Tables 2 to 4, respectively, together with their corresponding references.

For most of the systems considered here, measurements of aqueous mixture activities are not available; hence, evaluation of the values for the mixing parameters  $\theta_{ij}$  and  $\psi_{ijk}$  relied on solubility data. In these cases, however, it was impractical to evaluate both  $\theta_{ij}$  and  $\psi_{ijk}$  from measured solubilities, and satisfactory results were obtained when either  $\theta_{ij}$  or both  $\theta_{ij}$  and  $\psi_{ijk}$  were assumed to be zero. In addition, the inclusion of the terms  ${}^{\text{E}}\theta_{ij}$  and  ${}^{\text{E}}\theta'_{ij}$  was found to be unnecessary in fitting the solubility data, in agreement with studies done by Filippov and associates.<sup>19-39</sup> Therefore, for the solubility calculations illustrated in this section, these terms were omitted from the equations given in Table 1 for osmotic and activity

\* Additional terms apply to mixtures containing neutral species or to solutions of very high concentrations. See discussion in Chapter 3.

**TABLE 1**  
**Ion Interaction Model Equations for Osmotic and Activity Coefficients<sup>a</sup>**

The expression for the osmotic coefficient is given by

$$(\phi - 1) = (2/\sum_i m_i)[-A_\phi I^{3/2}/(1 + bI^{1/2}) + \sum_c \sum_a m_c m_a (B_{ca}^\phi + ZC_{ca}) + \sum_{c < c'} \sum_c m_c m_{c'} / (\Phi_{cc'}^\phi + \sum_a m_a \psi_{cc'a}) + \sum_a \sum_{a < a'} m_a m_{a'} (\Phi_{aa'}^\phi + \sum_c m_c \psi_{caa'})] \quad (9)$$

and activity coefficients are given by

$$\ln \gamma_M = z_M^2 F + \sum_a m_a (2B_{Ma} + ZC_{Ma}) + \sum_c m_c (2\Phi_{Mc} + \sum_a m_a \psi_{Mca}) + \sum_{a < a'} \sum_a m_a m_{a'} \psi_{Maa'} + |z_M| \sum_c \sum_a m_c m_a C_{ca} \quad (10a)$$

and

$$\ln \gamma_X = z_X^2 F + \sum_c m_c (2B_{cX} + ZC_{cX}) + \sum_a m_a (2\Phi_{Xa} + \sum_c m_c \psi_{cXa}) + \sum_{c < c'} \sum_c m_c m_{c'} \psi_{cc'X} + |z_X| \sum_c \sum_a m_c m_a C_{ca} \quad (10b)$$

where  $c$  and  $c'$  are cations and  $a$  and  $a'$  are anions. The charges are indicated by  $z_M$  and  $z_X$ . The  $B$  and  $C$  terms can be evaluated empirically from data on binary (electrolyte + water) systems, while the  $\Phi$  and  $\psi$  terms arise only for mixed electrolyte solutions and can best be determined from common ion mixtures. The quantity  $F$  includes the Debye-Hückel term and other terms as follows:

$$F = -A_\phi [I^{1/2}/(1 + bI^{1/2}) + (2/b)\ln(1 + bI^{1/2})] + \sum_c \sum_a m_c m_a B'_{ca} + \sum_{c < c'} \sum_c m_c m_{c'} \Phi'_{cc'} + \sum_a \sum_{a < a'} m_a m_{a'} \Phi'_{aa'} \quad (11)$$

Also,

$$Z = \sum_i m_i |z_i| \quad (12)$$

$$B_{ca}^\phi = B_{ca} + IB'_{ca} \quad (13)$$

$$\Phi_{cc'}^\phi = \Phi_{cc'} + I\Phi'_{cc'} \quad (14)$$

$B'$  and  $\Phi'$  are the ionic strength derivatives of  $B$  and  $\Phi$ . The sums over  $i$  include all solute species; uncharged species do not contribute to  $I$  or  $Z$ . The double summation indices,  $c < c'$  and  $a < a'$ , denote the sum over all distinguishable pairs of different cations or anions. The parameter  $C_{MX}$  is related to the commonly tabulated parameter  $C_{MX}^\phi$  by the equation:

$$C_{MX} = C_{MX}^\phi / (2|z_M z_X|^{1/2}) \quad (15)$$

**TABLE 1 (continued)**  
**Ion Interaction Model Equations for Osmotic and Activity Coefficients<sup>a</sup>**

The ionic strength dependence of the  $B$  terms is shown by the following equations:

$$B_{MX}^{\phi} = \beta_{MX}^{(0)} + \beta_{MX}^{(1)}\exp(-\alpha_1 I^{1/2}) + \beta_{MX}^{(2)}\exp(-\alpha_2 I^{1/2}) \quad (16a)$$

$$B_{MX} = \beta_{MX}^{(0)} + \beta_{MX}^{(1)}g(\alpha_1 I^{1/2}) + \beta_{MX}^{(2)}g(\alpha_2 I^{1/2}) \quad (16b)$$

$$B'_{MX} = [\beta_{MX}^{(1)}g'(\alpha_1 I^{1/2}) + \beta_{MX}^{(2)}g'(\alpha_2 I^{1/2})]/I \quad (16c)$$

where the functions  $g$  and  $g'$  are given by

$$g(x) = 2[1 - (1 + x)\exp(-x)]/x^2 \quad (17a)$$

$$g'(x) = -2[1 - (1 + x + x^2/2)\exp(-x)]/x^2 \quad (17b)$$

$\beta^{(0)}$ ,  $\beta^{(1)}$ , and  $\beta^{(2)}$  are solute-specific parameters fit to isothermal-isobaric experimental data on pure electrolytes at varying concentrations.  $\beta^{(2)}$  is important only for 2-2 or higher valence electrolytes that show a tendency toward electrostatic ion pairing. For electrolytes in which at least one of the ions is univalent,  $\alpha_1$  is usually taken to be  $2.0 \text{ kg}^{1/2}\text{mol}^{-1/2}$ . However, other values of  $\alpha_1$  can be used without undue complication. For 2-2 electrolytes at  $25^\circ\text{C}$ , the optimized values of  $\alpha_1$  and  $\alpha_2$  are 1.4 and  $12 \text{ kg}^{1/2}\text{mol}^{-1/2}$ , respectively. These values can be taken to be independent of  $T$  and  $P$  for many applications, but there are theoretical reasons for taking  $\alpha_2$  to be proportional to the Debye-Hückel parameter,  $A_{\phi}$  (see Chapter 3).

In the case of the  $\Phi$  terms there is a large ionic strength dependence for unsymmetrical mixing such as  $\text{Na}^+$  with  $\text{Mg}^{2+}$  or  $\text{Cl}^-$  with  $\text{SO}_4^{2-}$  arising from long-range electrostatic forces which is given by theory. The complete expressions for  $\Phi_{ij}$  are

$$\Phi_{ij} = \theta_{ij} + {}^E\theta_{ij}(I) \quad (18a)$$

$$\Phi'_{ij} = {}^E\theta'_{ij}(I) \quad (18b)$$

$$\Phi_{ij}^{\phi} = \theta_{ij} + {}^E\theta_{ij}(I) + I{}^E\theta'_{ij}(I) \quad (18c)$$

where  ${}^E\theta(I)$  and  ${}^E\theta'(I)$  account for electrostatic unsymmetrical mixing effects and depend only on the charges of the ions  $i$  and  $j$ , the total ionic strength, and on the density and dielectric constant of the solvent (hence, on the temperature and pressure). Equations for calculating these terms are given in Appendix B of Chapter 3. The remaining term  $\theta_{ij}$  arising from short-range forces is taken as a constant for any particular  $c, c'$  or  $a, a'$  at a given  $T$  and  $P$ . As explained in the text, the  ${}^E\theta$  and  ${}^E\theta'$  terms are often omitted for solubility calculations. They are omitted in Section IV.A, but are retained in Section IV.B of this chapter.

<sup>a</sup> Terms for neutral species are not included. The full equations including these terms are given in Chapter 3.

**TABLE 2**  
Single Electrolyte Parameters at 25°C

Cation	Anion	$\beta^{(0)}$	$\beta^{(1)}$	$\beta^{(2)}$	$C^\phi$	Ref.
Na	Cl	0.0765	0.2664		0.00127	73
H	Cl	0.1775	0.2945		0.00080	73
Mg	Cl	0.35235	1.6815		0.00519	73
Ni	Cl	0.34991	1.5300		-0.00471	75
Mn	Cl	0.32473	1.5146		-0.02269	76
Co	Cl	0.36428	1.4753		-0.01522	73
Na	SO <sub>4</sub>	0.01958	1.1130		0.00497	73
Li	SO <sub>4</sub>	0.13628	1.2705		-0.00399	73
Mg	SO <sub>4</sub>	0.2150	3.365	-32.74	0.0280	77
Fe	SO <sub>4</sub>	0.2568	3.063	-42.0	0.0209	40
Mn	SO <sub>4</sub>	0.2130	2.938	-41.91	0.01551	76
Ni	SO <sub>4</sub>	0.1702	2.907	-40.06	0.0366	74
Cu	SO <sub>4</sub>	0.2340	2.527	-48.33	0.00440	78
Co	SO <sub>4</sub>	0.1631	3.346	-30.7	0.03704	21
Cd	SO <sub>4</sub>	0.2053	2.617	-48.07	0.0114	74
Al	SO <sub>4</sub>	0.854	18.53	-500.0	-0.0911	44

**TABLE 3**  
Mixing Parameters for 25°C for Use without  ${}^E\theta_{ij}$  and  ${}^E\theta'_{ij}$

c	c'	$\theta_{cc'}$	$\psi_{cc'Cl}$	$\psi_{cc'SO_4}$	Ref.	
					$\theta$ value	$\psi$ value
H	Mn	0	-0.0128		79	This study
Na	Li	0.012		-0.007	79	This study
Na	Cu	0		-0.011	78	78
Na	Ni	0	-0.01	-0.015	This study	This study
Na	Co	-0.016	-0.003	-0.008	79	This study
Na	Mn	0		-0.009	79	This study
Mg	Ni	0	0.006		This study	This study
Mg	Cd	0		0	This study	This study
Mg	Al	0		0	This study	This study
Cu	Li	0		0	21	21
Ni	Li	0		0	This study	This study
Fe	Li	0		0	This study	This study
Fe	Al	0		-0.04	This study	This study

a	a'	$\theta_{aa'}$	$\psi_{aa'Ni}$	$\psi_{aa'Co}$	Ref.	
					$\theta$ value	$\psi$ value
Cl	SO <sub>4</sub>	-0.02	0.005	0.01	79	This study

coefficients. The mixing parameters given in Table 3 are *only* for use without the  ${}^E\theta_{ij}$  and  ${}^E\theta'_{ij}$  terms.

Experimental and calculated solubilities in aqueous mixtures of 1:1 and 2:1 electrolytes are given in Figures 1 to 3, for the ternary systems NaCl-NiCl<sub>2</sub>-H<sub>2</sub>O, NaCl-CoCl<sub>2</sub>-H<sub>2</sub>O, and HCl-MnCl<sub>2</sub>-H<sub>2</sub>O, respectively. The intersection of the curves in Figures 1 and 2 represents the calculated ternary invariant point, i.e., the coexistence of two solid phases and a saturated aqueous solution. For calculating the solubilities of NiCl<sub>2</sub> · 6H<sub>2</sub>O and MnCl<sub>2</sub> · 4H<sub>2</sub>O, the standard-state chemical potentials ( $\mu_i^\circ/RT$ ) of the solids were adjusted slightly from the values recommended by Wagman et al.<sup>58</sup> to better fit the solubility data. A value of -690.8 and -574.78 are used here for NiCl<sub>2</sub> · 6H<sub>2</sub>O and MnCl<sub>2</sub> · 4H<sub>2</sub>O, respectively, compared

**TABLE 4**  
**Standard-State Chemical Potentials of Aqueous Species**  
**and Solid Phases at 25°C**

Substance	Formula	$-\mu_i^0/RT$	Ref.
Water	H <sub>2</sub> O	95.6635	56
Chloride ion	Cl <sup>-</sup>	52.955	56
Sulfate ion	SO <sub>4</sub> <sup>2-</sup>	300.386	56
Hydrogen ion	H <sup>+</sup>	0	(Convention)
Sodium ion	Na <sup>+</sup>	105.651	56
Lithium ion	Li <sup>+</sup>	118.044	56
Magnesium ion	Mg <sup>2+</sup>	183.468	56
Cupric ion	Cu <sup>2+</sup>	26.42	58
Nickel ion	Ni <sup>2+</sup>	18.40	58
Cobalt ion	Co <sup>2+</sup>	21.94	58
Ferrous ion	Fe <sup>2+</sup>	31.83	58
Mangannous ion	Mn <sup>2+</sup>	92.02	58
Cadmium ion	Cd <sup>2+</sup>	31.309	58
Aluminum ion	Al <sup>3+</sup>	195.6	58
Halite	NaCl	154.99	56
Mirabilite	Na <sub>2</sub> SO <sub>4</sub> · 10H <sub>2</sub> O	1471.15	58
Epsomite	MgSO <sub>4</sub> · 7H <sub>2</sub> O	1157.74	5
Bischofite	MgCl <sub>2</sub> · 6H <sub>2</sub> O	853.1	56
	Li <sub>2</sub> SO <sub>4</sub> · H <sub>2</sub> O	631.13	This study
	Li <sub>2</sub> SO <sub>4</sub> · 3Na <sub>2</sub> SO <sub>4</sub> · 12H <sub>2</sub> O	3227.66	This study
Chalcanthite	CuSO <sub>4</sub> · 5H <sub>2</sub> O	758.315	56
	CuSO <sub>4</sub> · Na <sub>2</sub> SO <sub>4</sub> · 2H <sub>2</sub> O	985.99	25
	NiCl <sub>2</sub> · 4H <sub>2</sub> O	497.6	This study
	NiCl <sub>2</sub> · 6H <sub>2</sub> O	690.8	This study
Morenosite	NiSO <sub>4</sub> · 7H <sub>2</sub> O	993.51	20
	NiSO <sub>4</sub> · Na <sub>2</sub> SO <sub>4</sub> · 4H <sub>2</sub> O	1221.0	This study
	CoCl <sub>2</sub> · 6H <sub>2</sub> O	695.95	58
	CoSO <sub>4</sub> · 7H <sub>2</sub> O	997.02	21
	CoSO <sub>4</sub> · Na <sub>2</sub> SO <sub>4</sub> · 4H <sub>2</sub> O	1224.35	This study
Melanterite	FeSO <sub>4</sub> · 7H <sub>2</sub> O	1006.93	45
Halotrichite	FeSO <sub>4</sub> · Al <sub>2</sub> (SO <sub>4</sub> ) <sub>3</sub> · 22H <sub>2</sub> O	3752.79	Corrected from 45
	MnCl <sub>2</sub> · 4H <sub>2</sub> O	574.78	This study
	MnSO <sub>4</sub> · 4H <sub>2</sub> O	778.62	This study
	MnSO <sub>4</sub> · Na <sub>2</sub> SO <sub>4</sub> · 2H <sub>2</sub> O	1101.9	This study
	CdSO <sub>4</sub> · 8/3H <sub>2</sub> O	591.042	58
Alunogen	Al <sub>2</sub> (SO <sub>4</sub> ) <sub>3</sub> · 17H <sub>2</sub> O	2936.57	45
Pickeringite	Al <sub>2</sub> (SO <sub>4</sub> ) <sub>3</sub> · MgSO <sub>4</sub> · 22H <sub>2</sub> O	3903.02	45

to values of  $-691.11$  and  $-574.28$  tabulated by Wagman et al. The solubility data of Putivl'skii et al.<sup>81</sup> for this system extend to about  $13.5 m$  HCl. However, the ion interaction parameters for HCl were derived by Pitzer and Mayorga<sup>73</sup> from fitting solution activity data up to  $6 m$ ; hence, agreement between calculated and experimental solubilities does not extend much above  $6 m$  HCl, where a less hydrated solid,  $MnCl_2 \cdot 2H_2O$ , becomes stable in equilibrium with the aqueous solution.<sup>81</sup> It may be possible to calculate the solubilities over the whole concentration range studied by Putivl'skii et al. if the alternate treatment of HCl properties by Filippov et al.<sup>97</sup> is used. That treatment was successful in fitting HCl properties

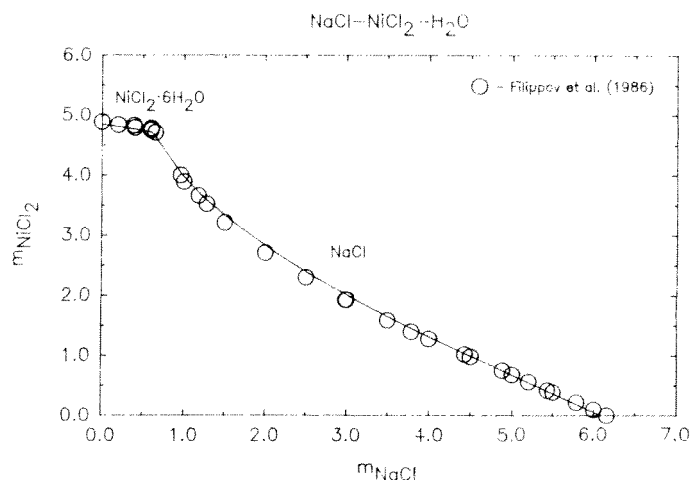


FIGURE 1. Solubilities in the system NaCl-NiCl<sub>2</sub>-H<sub>2</sub>O at 25°C. The symbols represent values tabulated by Filippov et al.,<sup>26</sup> and the solid curves represent values calculated using the ion interaction model. The intersection of the curves represents the calculated ternary invariant point, i.e., the coexistence of two solids (NaCl and NiCl<sub>2</sub> · 6H<sub>2</sub>O) and a saturated aqueous solution.

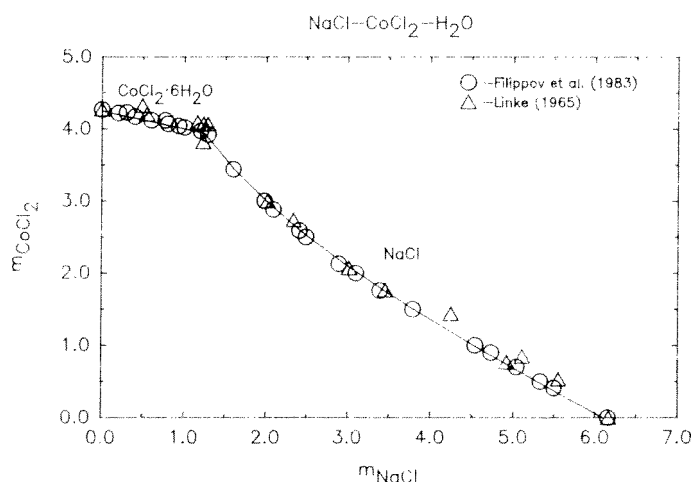


FIGURE 2. Solubilities in the NaCl-CoCl<sub>2</sub>-H<sub>2</sub>O system at 25°C. Values given by Linke<sup>1</sup> and Filippov et al.<sup>26</sup> are indicated by the symbols, and those calculated using the ion interaction model are represented by the solid curves.

up to 16  $m$  by including the  $\beta_{MX}^{(2)}$  term, which is not used for 1:1 electrolytes in the standard ion interaction model (see Chapter 3, Appendix H).

Figures 4 and 5, for the respective ternary systems Na<sub>2</sub>SO<sub>4</sub>-Li<sub>2</sub>SO<sub>4</sub>-H<sub>2</sub>O and MgCl<sub>2</sub>-NiCl<sub>2</sub>-H<sub>2</sub>O, show examples of calculated and experimental solubilities in mixtures of two 1:2 aqueous electrolytes. For calculating the solubility of Li<sub>2</sub>SO<sub>4</sub> · H<sub>2</sub>O in Figure 4, the  $\mu_i^\circ/RT$  of the solid was changed slightly from Wagman et al.'s recommended value of  $-631.53$  to  $-631.13$ . The standard-state chemical potential for the double salt Li<sub>2</sub>SO<sub>4</sub> · 3Na<sub>2</sub>SO<sub>4</sub> · 12H<sub>2</sub>O given in Table 4 was derived from a best fit to solubility data. The value for NiCl<sub>2</sub> · 4H<sub>2</sub>O was adjusted to better fit the solubility data. This was also done for NiCl<sub>2</sub> · 6H<sub>2</sub>O as discussed previously. Wagman et al. recommended a value of  $-498.16$  for NiCl<sub>2</sub>



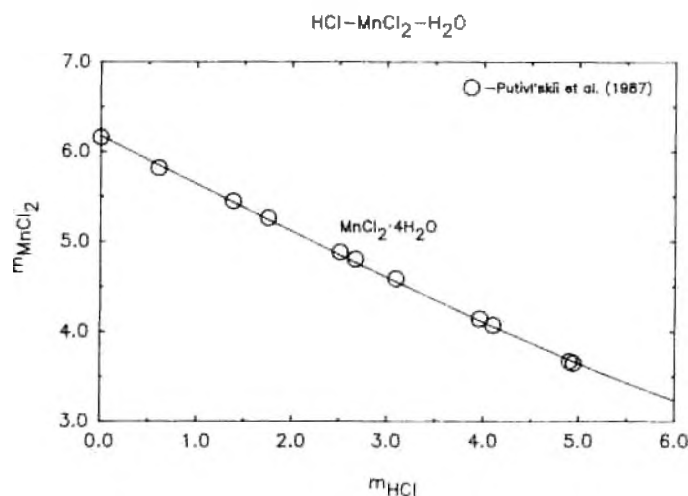


FIGURE 3. Calculated and experimental solubilities in the system HCl-MnCl<sub>2</sub>-H<sub>2</sub>O at 25°C. Experimental data are from Putivl'skii et al.<sup>31</sup>

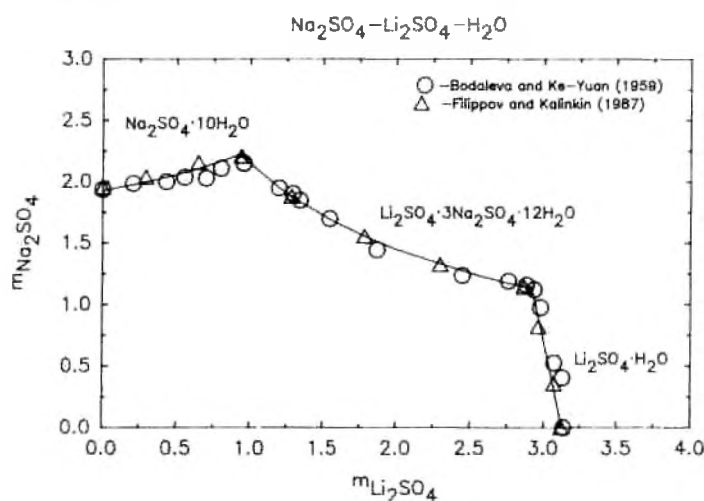


FIGURE 4. Calculated and experimental solubilities in the Na<sub>2</sub>SO<sub>4</sub>-Li<sub>2</sub>SO<sub>4</sub>-H<sub>2</sub>O system at 25°C. Experimental data from Filippov and Kalinkin<sup>30</sup> and Bodaleva and Ke-Yuan<sup>32</sup> are represented by the symbols.

· 4H<sub>2</sub>O, compared to -497.6 which was used in the calculations. Note that in the MgCl<sub>2</sub>-NiCl<sub>2</sub>-H<sub>2</sub>O system shown in Figure 5, the less hydrated NiCl<sub>2</sub> solid becomes stable at MgCl<sub>2</sub> molalities greater than about 3.6.

For mixtures involving 2:1 and 2:2 electrolytes, several examples are illustrated in Figures 6 to 14. Experimental and calculated solubilities are shown in Figures 6 to 9 for the ternary systems Na<sub>2</sub>SO<sub>4</sub>-CuSO<sub>4</sub>-H<sub>2</sub>O, Na<sub>2</sub>SO<sub>4</sub>-NiSO<sub>4</sub>-H<sub>2</sub>O, Na<sub>2</sub>SO<sub>4</sub>-CoSO<sub>4</sub>-H<sub>2</sub>O, and Na<sub>2</sub>SO<sub>4</sub>-MnSO<sub>4</sub>-H<sub>2</sub>O, respectively. These systems are characterized by the formation of hydrated double salts, the standard-state chemical potentials of which were evaluated from solubility data and are given in Table 4. The values of  $\mu_i^0/RT$  for NiSO<sub>4</sub>·7H<sub>2</sub>O and CoSO<sub>4</sub>·7H<sub>2</sub>O used in the calculations were derived from the equilibrium constants given by Filippov and Nokhrin<sup>30,31</sup> and are equal to -993.51 and -997.02, respectively. These are somewhat

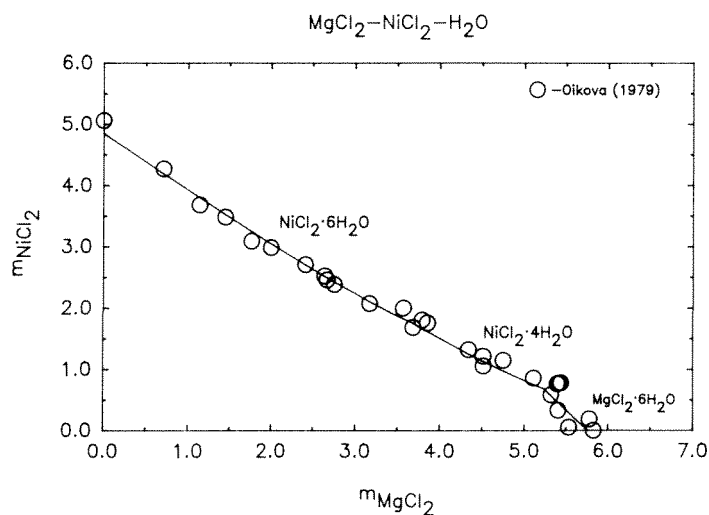


FIGURE 5. Experimental data at 25°C in the system  $\text{MgCl}_2\text{-NiCl}_2\text{-H}_2\text{O}$  from Oikova<sup>83</sup> compared with solubilities calculated using the ion interaction model. Note that a less hydrated  $\text{NiCl}_2$  solid is stable at  $\text{MgCl}_2$  molalities greater than about 3.6.

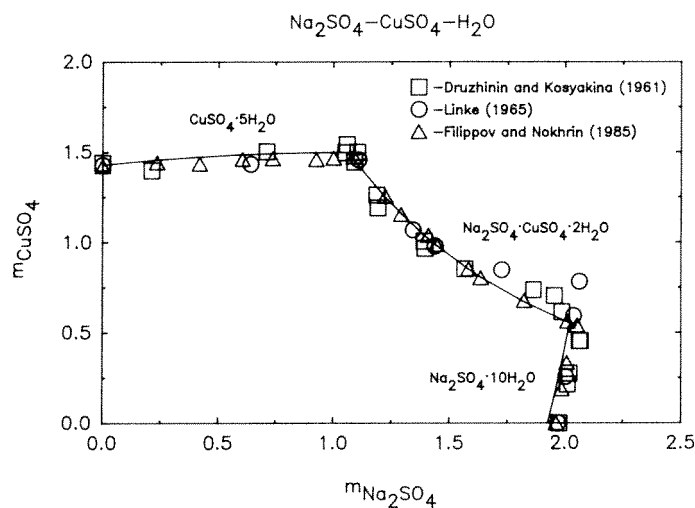


FIGURE 6. Solubilities at 25°C in the  $\text{Na}_2\text{SO}_4\text{-CuSO}_4\text{-H}_2\text{O}$  system. Experimental data are from Linke,<sup>17</sup> Filippov and Nokhrin,<sup>25</sup> and Druzhinin and Kosyakina.<sup>84</sup>

different from those of Wagman et al., who give values of  $-993.109$  and  $-997.784$  for  $\text{NiSO}_4 \cdot 7\text{H}_2\text{O}$  and  $\text{CoSO}_4 \cdot 7\text{H}_2\text{O}$ , respectively. The  $\mu_i^\circ/\text{RT}$  value for  $\text{MnSO}_4 \cdot 4\text{H}_2\text{O}$  given in Table 4 was fit to solubility data.

Figures 10 to 12 compare calculated and experimental values in the  $\text{Li}_2\text{SO}_4\text{-CuSO}_4\text{-H}_2\text{O}$ ,  $\text{Li}_2\text{SO}_4\text{-NiSO}_4\text{-H}_2\text{O}$ , and  $\text{Li}_2\text{SO}_4\text{-FeSO}_4\text{-H}_2\text{O}$  systems, respectively. Measured and calculated solubilities in the system  $\text{CoCl}_2\text{-CoSO}_4\text{-H}_2\text{O}$  are given in Figure 13, while those in the system  $\text{NiCl}_2\text{-NiSO}_4\text{-H}_2\text{O}$  are shown in Figure 14. An example of calculated and experimental solubilities in aqueous mixtures of two 2:2 electrolytes is given in Figure 15 for the ternary system  $\text{MgSO}_4\text{-CdSO}_4\text{-H}_2\text{O}$ .

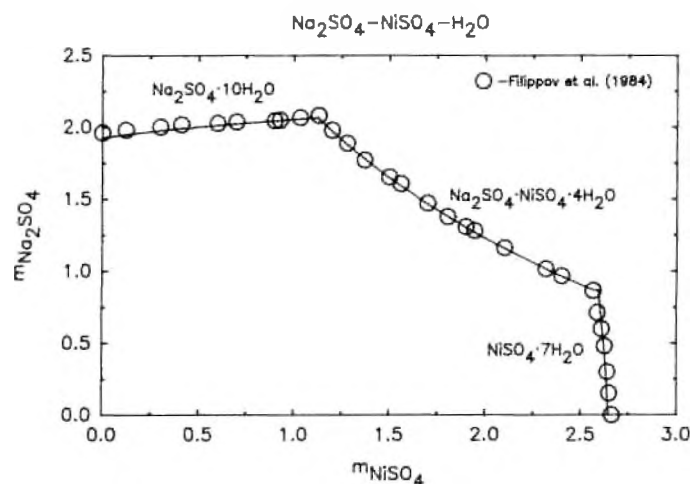


FIGURE 7. Solubilities in the system  $\text{Na}_2\text{SO}_4\text{-NiSO}_4\text{-H}_2\text{O}$  at  $25^\circ\text{C}$ . The symbols represent values tabulated by Filippov et al.,<sup>85</sup> and the curves represent values calculated using the ion interaction model.

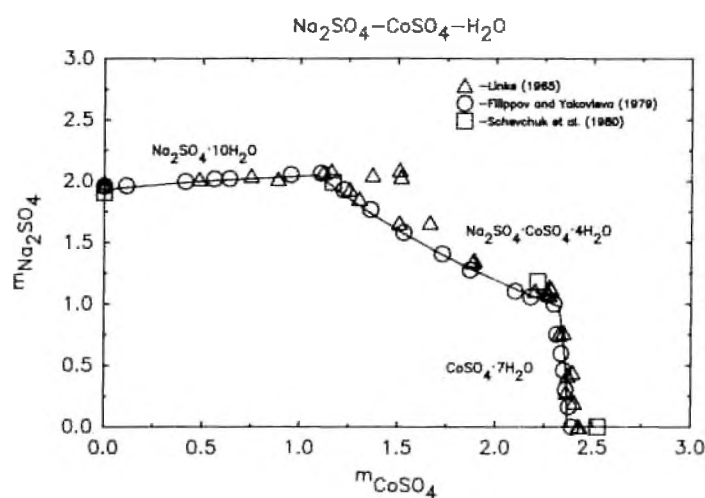


FIGURE 8. Solubilities in the system  $\text{Na}_2\text{SO}_4\text{-CoSO}_4\text{-H}_2\text{O}$  at  $25^\circ\text{C}$ . Solid curves represent calculated values, and symbols represent experimental data from Linke,<sup>17</sup> Filippov and Yakovleva,<sup>86</sup> and Schevchuk et al.<sup>87</sup>

Solubilities in some of the systems discussed above were also treated using the ion interaction model by Filippov and associates.<sup>21, 24, 25, 26, 30, 36, 80, 85, 90, 96</sup> Several of the mixing parameters derived in their studies differ from those determined here. For the sulfate systems this is due to their choice of different binary interaction parameters, or to differences in equilibrium constants for the dissolution reaction. For the chloride systems such as  $\text{NiCl}_2$ ,  $\text{CuCl}_2$ ,  $\text{CoCl}_2$ , and  $\text{MnCl}_2$ , it is largely due to their use of the  $\beta_{\text{MIX}}^{21}$  term to fit aqueous properties over an extended concentration range.<sup>26, 90</sup> The standard ion interaction model does not use the  $\beta_{\text{MIX}}^{21}$  term for 1:1 and 2:1 electrolytes, although its inclusion makes it possible to fit aqueous solution properties to very high concentrations (e.g., 16 *m*  $\text{HCl}$ <sup>97</sup>). Although the binary ion interaction parameters for  $\text{NiCl}_2$ ,  $\text{CuCl}_2$ ,  $\text{CoCl}_2$ ,  $\text{MnCl}_2$ , and  $\text{MgCl}_2$  used in this study were derived from solution data well below saturation concentrations,

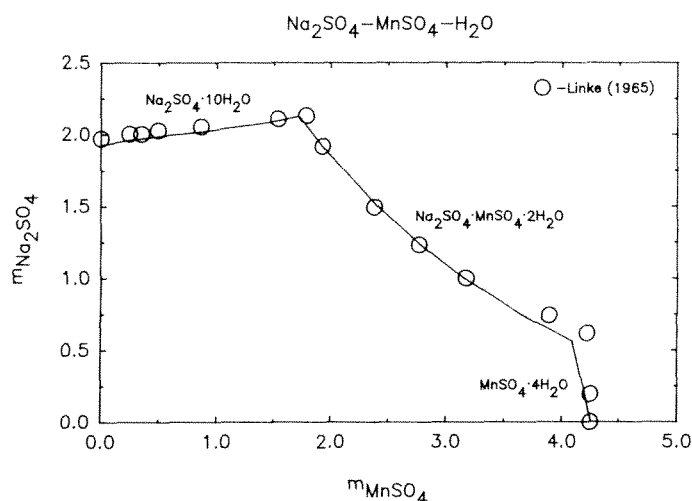


FIGURE 9. Experimental and calculated solubilities at 25°C in the system  $\text{Na}_2\text{SO}_4\text{-MnSO}_4\text{-H}_2\text{O}$ . The symbols represent experimental data from Linke.<sup>17</sup>

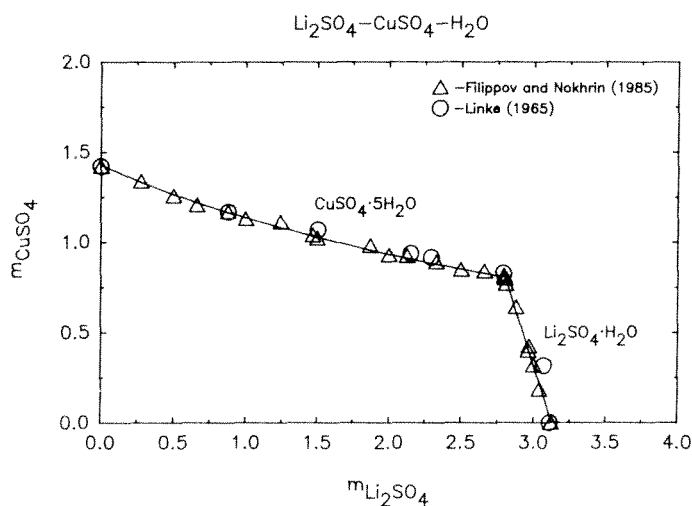


FIGURE 10. Solubilities in the  $\text{Li}_2\text{SO}_4\text{-CuSO}_4\text{-H}_2\text{O}$  system at 25°C. The symbols represent values tabulated by Linke<sup>17</sup> and Filippov and Nokhrin.<sup>21</sup>

they were found to be adequate in calculating aqueous electrolyte properties up to saturation values.

Comparisons of calculated and experimental solubilities in aqueous mixtures of 2:2 and 3:2 electrolytes are given in Figures 16 and 17 for the systems  $\text{MgSO}_4\text{-Al}_2\text{SO}_4\text{-H}_2\text{O}$  and  $\text{FeSO}_4\text{-Al}_2\text{SO}_4\text{-H}_2\text{O}$ , respectively. These systems and other electrolyte mixtures with  $\text{Al}_2\text{SO}_4$  were treated previously using the ion interaction approach by Reardon.<sup>44</sup> The calculations here used his binary ion interaction parameters for  $\text{Al}_2\text{SO}_4$ , which are based on the values  $\alpha_1 = 2.0$ ,  $\alpha_2 = 50$ , and the solid phase standard-state chemical potentials recommended in his study. However, his treatment of mixture properties used the full equations given in Table 1, including the higher-order terms for asymmetric mixing. To be consistent with the other examples given above, new values of the mixing parameters  $\theta_{ij}$  and  $\psi_{ijk}$  were derived from the solubility data for use without the  ${}^E\theta_{ij}$  and  ${}^E\theta'_{ij}$  terms. For these two systems, as

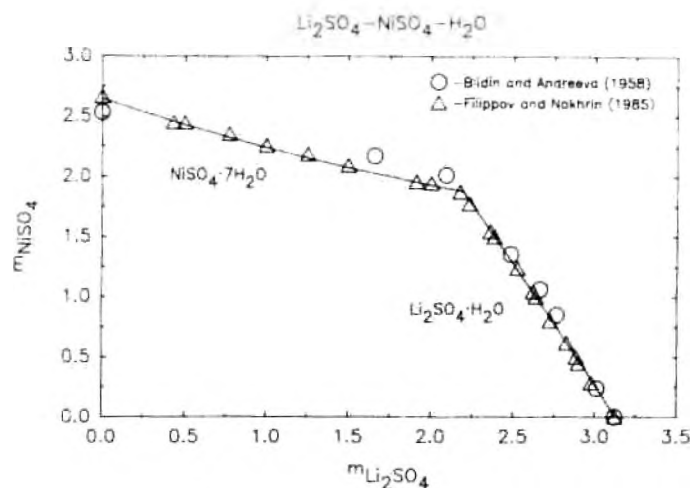


FIGURE 11. Solubilities in the system  $\text{Li}_2\text{SO}_4\text{-NiSO}_4\text{-H}_2\text{O}$  at 25°C. The symbols represent experimental values from Filippov and Nokhrin<sup>31</sup> and Blidin and Andreeva<sup>32</sup>.

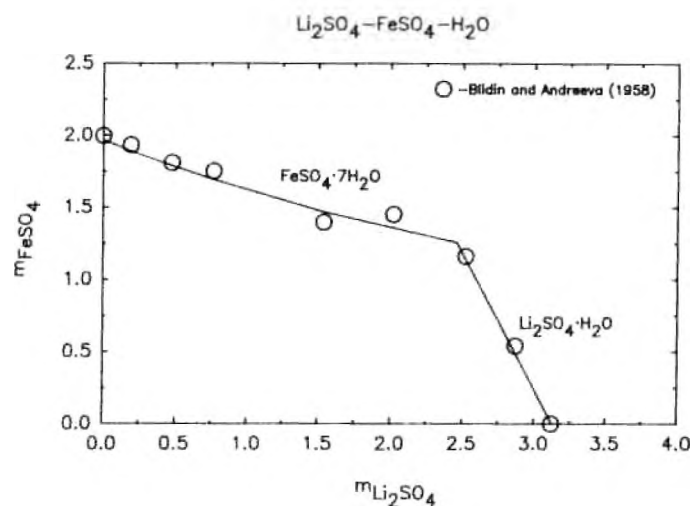


FIGURE 12. Experimental solubilities at 25°C in the system  $\text{Li}_2\text{SO}_4\text{-FeSO}_4\text{-H}_2\text{O}$  from Blidin and Andreeva<sup>32</sup> compared with calculated values.

well as for most of the other systems shown previously, it was sufficient for solubility calculations to set either  $\theta_{ij}$  or both  $\theta_{ij}$  and  $\psi_{ijk}$  equal to zero.

No additional parameters are needed by the ion interaction model to describe aqueous solution properties in quaternary or more complex systems. Hence, the parameters determined previously from simple mixtures can be used to predict solubilities in more complicated systems. Examples are given in the next two figures. Figure 18 shows experimental and calculated solubilities in the quaternary system  $\text{Na}_2\text{SO}_4\text{-Li}_2\text{SO}_4\text{-CuSO}_4\text{-H}_2\text{O}$ , and Figure 19 compares solubilities in the quaternary reciprocal system  $\text{Na-Co-Cl-SO}_4\text{-H}_2\text{O}$ . In Figure 18, the symbols inside the triangle represent quaternary invariant points (i.e., equilibrium between three solids and a saturated aqueous solution) experimentally determined by Filippov and Nokhrin,<sup>31</sup> and those at the edges of the triangle represent experimental ternary invariant

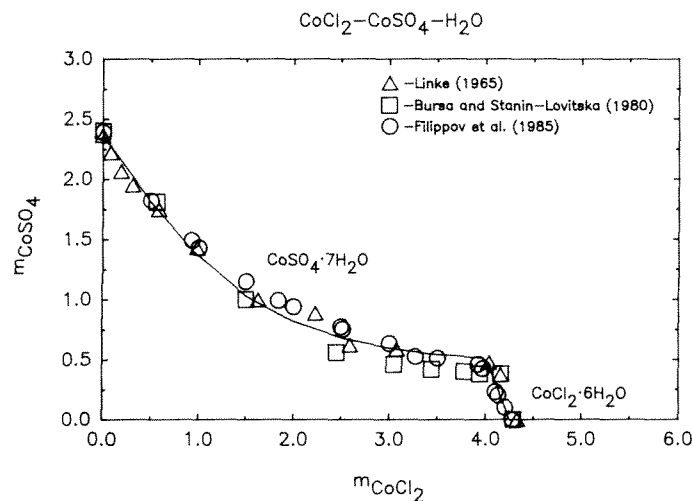


FIGURE 13. Calculated and experimental solubilities at 25°C in the system  $\text{CoCl}_2\text{-CoSO}_4\text{-H}_2\text{O}$ . The symbols represent values tabulated by Linke,<sup>17</sup> Bursa and Stanin-Lovitska,<sup>89</sup> and Filippov et al.<sup>90</sup>

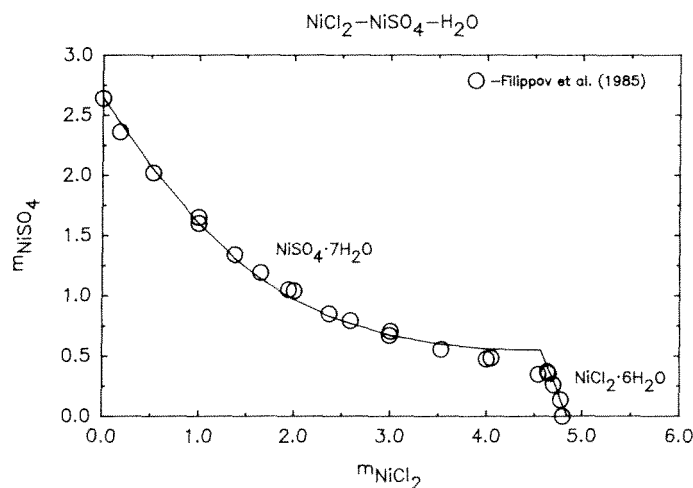


FIGURE 14. Solubilities in the  $\text{NiCl}_2\text{-NiSO}_4\text{-H}_2\text{O}$  system at 25°C. Values taken from Filippov et al.<sup>90</sup> are indicated by the symbols.

points (i.e., coexistence of two solids plus a saturated aqueous solution) taken from the references in Figures 4, 6, and 10. In Figure 19, the symbols inside the figure are experimental quaternary invariant points taken from Filippov and Charykov,<sup>36</sup> and those at the edges are experimental ternary invariant points from the references in Figures 2, 8, and 13. The solid curves represent values predicted using the ion interaction parameters derived from binary and ternary systems. These figures demonstrate that reliable predictions of solubilities in complex systems can be obtained using parameters determined from simple mixtures. It should be noted that Filippov and Charykov<sup>36</sup> also calculated solubilities in the reciprocal system  $\text{Na-Co-Cl-SO}_4\text{-H}_2\text{O}$  using the ion interaction model. They obtained better agreement with experimental data at higher  $\text{CoCl}_2$  concentrations by including the  $\beta_{MX}^{(2)}$  term in their treatment of aqueous  $\text{CoCl}_2$  properties.

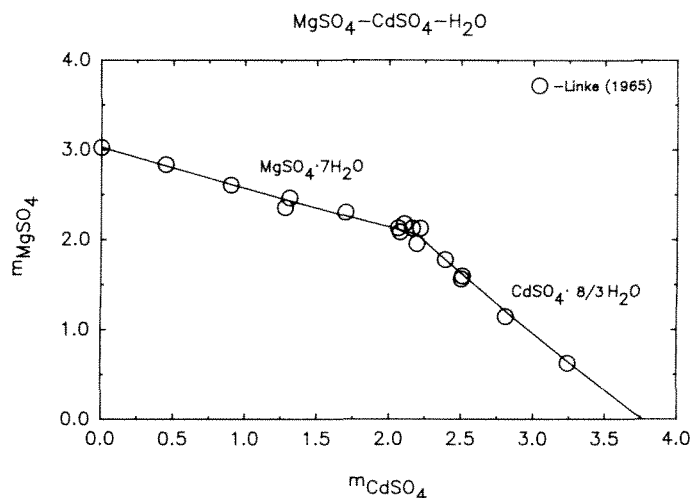


FIGURE 15. Calculated solubilities at 25°C in the system  $\text{MgSO}_4\text{-CdSO}_4\text{-H}_2\text{O}$  compared with experimental data from Linke.<sup>17</sup>

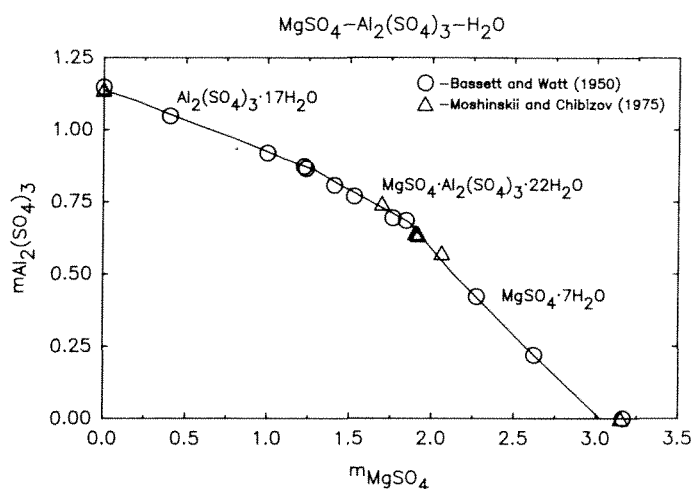


FIGURE 16. Solubilities in the system  $\text{MgSO}_4\text{-Al}_2(\text{SO}_4)_3\text{-H}_2\text{O}$  at 25°C. Experimental data are from Bassett and Watt<sup>91</sup> and Moshinskii and Chibizov.<sup>92</sup>

## B. SOLUBILITIES AT VARIABLE TEMPERATURES

### 1. Choice of Standard-State Properties

Mineral solubilities at variable temperatures can be calculated provided that standard-state chemical potentials of the solids and aqueous species and the ion interaction parameters are known at the temperature of interest. If the standard-state chemical potentials and entropies (or enthalpies) at a reference temperature and temperature functions for standard-state heat capacities are available, the standard-state chemical potential at the temperature of interest can be derived using Equation 8. For the examples given in this section, thermodynamic data for solids and aqueous species used in the calculations are given in Table 5. The values of  $\mu_i^\circ/RT$  at the reference temperature of 25°C were taken mostly from Robie et al.<sup>56</sup> Those for the solids  $\text{MgCl}_2 \cdot n\text{H}_2\text{O}$  were taken from Wagman et al.<sup>58</sup> The reference chemical potential of the solid  $\text{MgSO}_4 \cdot 7\text{H}_2\text{O}$  was adjusted slightly to fit the 25°C solubility

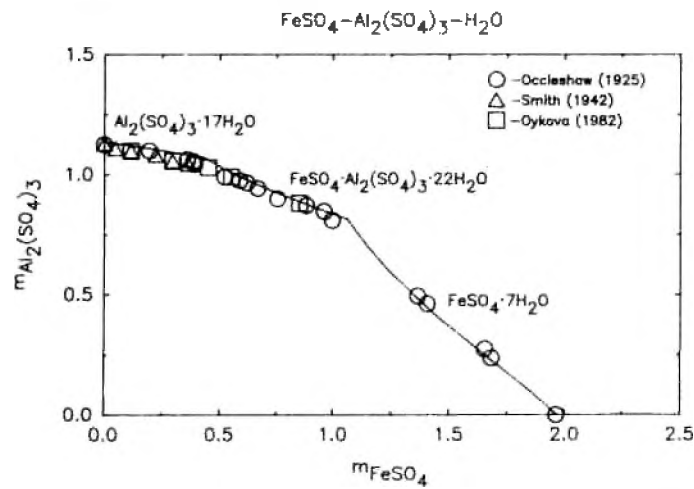


FIGURE 17. Solubilities in the system  $\text{FeSO}_4\text{-Al}_2(\text{SO}_4)_3\text{-H}_2\text{O}$  at  $25^\circ\text{C}$ . Experimental data are from Occlshaw,<sup>11</sup> Smith,<sup>12</sup> and Oykova.<sup>13</sup>

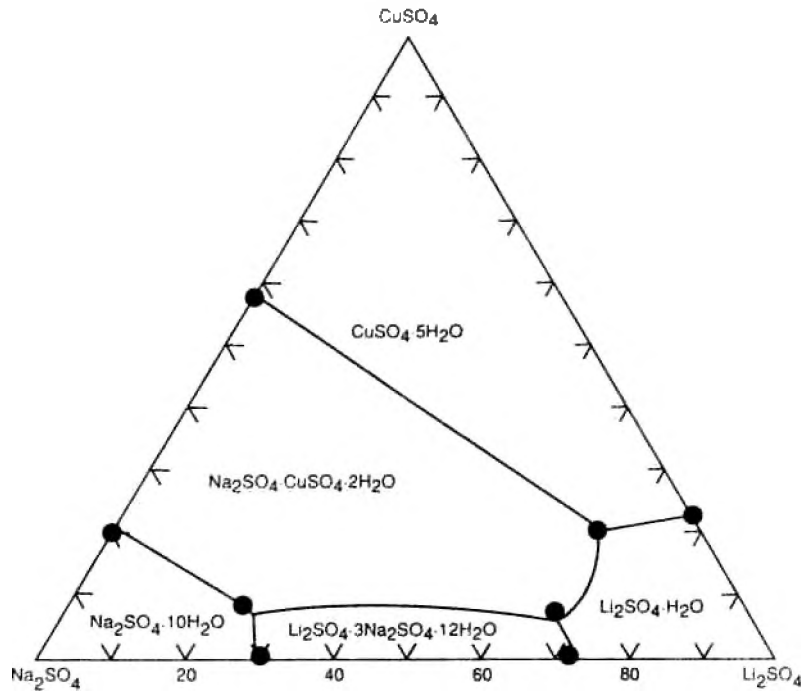


FIGURE 18. Solubilities at  $25^\circ\text{C}$  in the quaternary system  $\text{Na}_2\text{SO}_4\text{-Li}_2\text{SO}_4\text{-CuSO}_4\text{-H}_2\text{O}$ . The values are plotted in terms of the mole percent of the component ( $\text{Na}_2\text{SO}_4$ ,  $\text{Li}_2\text{SO}_4$ , or  $\text{CuSO}_4$ ) with respect to the total number of moles of  $\text{Na}_2\text{SO}_4 + \text{Li}_2\text{SO}_4 + \text{CuSO}_4$ . The symbols inside the triangle represent quaternary invariant points experimentally determined by Filippov and Nokhrin.<sup>14</sup> The symbols at the edges of the triangle represent experimental ternary invariant points from the references in Figures 4, 6, and 10. The curves represent values predicted from the ion interaction model using parameters derived previously from binary and ternary systems. The stability fields of the various solid phases are indicated on the figure.



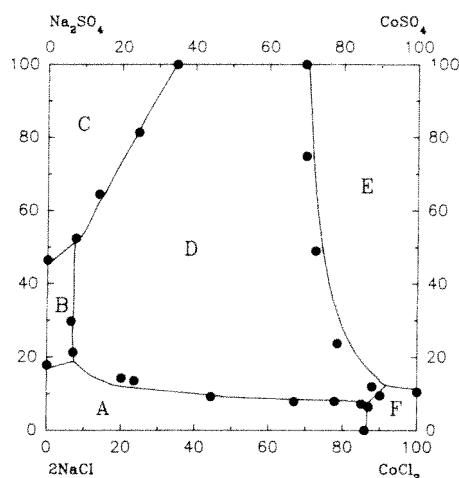


FIGURE 19. Solubilities in the quaternary reciprocal system Na-Co-Cl-SO<sub>4</sub>-H<sub>2</sub>O at 25°C. The values are plotted in terms of Janecke indices of the ions (Janecke index  $Y_i = m_i z_i / \sum m z$ ). The symbols inside the figure are experimental quaternary invariant points determined by Filippov and Charykov.<sup>36</sup> The symbols at the edges of the figure represent ternary invariant points for the systems NaCl-CoCl<sub>2</sub>-H<sub>2</sub>O, Na<sub>2</sub>SO<sub>4</sub>-CoSO<sub>4</sub>-H<sub>2</sub>O, and CoCl<sub>2</sub>-CoSO<sub>4</sub>-H<sub>2</sub>O from the references given in Figures 2, 8, and 13, respectively. The invariant points for the NaCl-Na<sub>2</sub>SO<sub>4</sub>-H<sub>2</sub>O system were taken from Linke.<sup>17</sup> The curves represent values predicted using ion interaction parameters derived from binary and ternary systems. The stability fields of the solid phases are labeled as: (A) NaCl, (B) Na<sub>2</sub>SO<sub>4</sub>, (C) Na<sub>2</sub>SO<sub>4</sub> · 10H<sub>2</sub>O, (D) Na<sub>2</sub>SO<sub>4</sub> · CoSO<sub>4</sub> · 4H<sub>2</sub>O, (E) CoSO<sub>4</sub> · 7H<sub>2</sub>O, and (F) CoCl<sub>2</sub> · 6H<sub>2</sub>O.

in the binary system. For MgSO<sub>4</sub> · 6H<sub>2</sub>O and MgSO<sub>4</sub> · H<sub>2</sub>O, which become stable at higher temperatures, the values were slightly adjusted to fit their lowest temperature solubility values in binary systems. The reference value of  $\mu_i^0/RT$  for the double-salt KCl · MgCl<sub>2</sub> · 6H<sub>2</sub>O (carnallite) was fit to solubility data by Harvie and Weare.<sup>3</sup> In the case of water, its standard-state chemical potential at T and P was calculated using the equations of state derived by Haar et al.<sup>62</sup>

Heat capacity ( $C_p$ ) data from calorimetric measurements are available for most of the solids considered here. Table 5 gives the parameters for the following equation for the heat capacity of a solid:

$$C_p = a + bT + c/T^2 \quad (19)$$

The range of validity is also indicated. These heat capacity parameters were taken mostly from Kelley.<sup>59</sup> The coefficients given by Kelley<sup>59</sup> for KCl(s) are incorrect, however, and the values listed are from Holmes and Mesmer,<sup>98</sup> who fit the values tabulated by Chase et al.<sup>57</sup> The values for Na<sub>2</sub>SO<sub>4</sub>(s) and Na<sub>2</sub>SO<sub>4</sub> · 10H<sub>2</sub>O(s) were fit by Pabalan and Pitzer<sup>5</sup> to data from Brodale and Giaque,<sup>99,100</sup> while those for MgSO<sub>4</sub>(s) were derived from JANAF data.<sup>57</sup> The equation for Na<sub>2</sub>SO<sub>4</sub>(s) is valid only to 241°C, which corresponds to a change in the stable form of the solid from Form IV to Form I.<sup>100</sup> In addition, there is an associated heat of transition in going from Form V to Form IV at 185°C equal to 75 cal/mol.<sup>100</sup> For calculations of Na<sub>2</sub>SO<sub>4</sub>(s) solubilities to 350°C, standard-state chemical potentials of Na<sub>2</sub>SO<sub>4</sub>(s) can be derived from the free energy functions tabulated by Brodale and Giaque.<sup>100</sup> The  $C_p$  coefficients for MgSO<sub>4</sub> · H<sub>2</sub>O(s) and MgSO<sub>4</sub> · 6H<sub>2</sub>O(s) were derived from linear fits to the low temperature data of Frost et al.<sup>101</sup> and Cox et al.,<sup>102</sup> respectively.

**TABLE 5**  
**Standard-State Chemical Potentials, Enthalpies of Formation, and Entropies at 298.15 K of Aqueous Species and Minerals, and Temperature Functions of the Heat Capacity of the Solids**

Substance	Formula	$-\mu_f^\circ/RT$	$-\Delta H_f^\circ/RT$	$S^\circ/R$	$C_p/R = a + bT + c/T^2$			T(K) range
					a	$10^3 b$	$10^{-5} c$	
Water	H <sub>2</sub> O(l)	95.6635	115.304	8.409				
Chloride ion	Cl <sup>-</sup> (aq)	52.955	67.432	6.778				
Sulfate ion	SO <sub>4</sub> <sup>2-</sup> (aq)	300.386	366.800	2.42				
Sodium ion	Na <sup>+</sup> (aq)	105.651	96.865	7.096				
Potassium ion	K <sup>+</sup> (aq)	113.957	101.81	12.33				
Magnesium ion	Mg <sup>2+</sup> (aq)	183.468	188.329	-16.64				
Halite	NaCl(s)	154.99	165.88	8.676	5.525	1.96 <sub>3</sub>	—	298—1073
Sylvite	KCl(s)	164.84	176.034	9.934	5.575	2.011	—	~298—~700
Carnallite	KCl · MgCl <sub>2</sub> · 6H <sub>2</sub> O(s)	1020.3	1184.85	55.53	96.11	-180.4	—	273—423
Arcanite	K <sub>2</sub> SO <sub>4</sub> (s)	532.39	580.01	21.12	14.48	11.98	-2.14 <sub>4</sub>	298—856
	MgSO <sub>4</sub> (s)	472.26	518.33	11.02	6.71	16.30	—	298—700
Kieserite	MgSO <sub>4</sub> · H <sub>2</sub> O(s)	579.18 <sub>4</sub>	649.34	(14.99)	6.89	31.05	—	~273—~473
Leonhardtite	MgSO <sub>4</sub> · 4H <sub>2</sub> O(s)	868.55	1007.13	(30.64)	9.39	74.8	—	~273—~473
Pentahydrate	MgSO <sub>4</sub> · 5H <sub>2</sub> O(s)	965.13	—	(35.7)	10.2	89.3	—	~273—~473
Hexahydrate	MgSO <sub>4</sub> · 6H <sub>2</sub> O(s)	1061.37	(1244.79)	41.87	10.9	104	—	~273—~473
Epsomite	MgSO <sub>4</sub> · 7H <sub>2</sub> O(s)	1157.74	(1366.27)	44.79	11.8	118	—	~273—~473
	MgCl <sub>2</sub> (s)	238.74	258.71	10.78	9.511	0.714 <sub>6</sub>	-1.03 <sub>3</sub>	298—987
	MgCl <sub>2</sub> · H <sub>2</sub> O(s)	347.66	389.94	16.505	10.95	9.788	—	298—650
	MgCl <sub>2</sub> · 2H <sub>2</sub> O(s)	451.06	516.24	21.64	15.05	13.74	—	298—500
	MgCl <sub>2</sub> · 4H <sub>2</sub> O(s)	654.93	766.06	31.75	22.56	21.65	—	298—450
Bischofite	MgCl <sub>2</sub> · 6H <sub>2</sub> O(s)	853.1	1008.11	44.03	29.08	29.56	—	298—385
Thenardite	Na <sub>2</sub> SO <sub>4</sub> (s)	512.39	559.55	17.99	12.667	13.900	-1.240	250—514
Mirabilite	Na <sub>2</sub> SO <sub>4</sub> · 10H <sub>2</sub> O(s)	1471.15	1475.75	71.21	10.65	196.0	—	~200—~333

Heat capacity data for  $\text{MgSO}_4 \cdot 4\text{H}_2\text{O}(\text{s})$ ,  $\text{MgSO}_4 \cdot 5\text{H}_2\text{O}(\text{s})$ , and  $\text{MgSO}_4 \cdot 7\text{H}_2\text{O}(\text{s})$  are not available. However, the contribution of each water molecule to the entropy or heat capacity of a hydrated solid is expected to be about the same. In fact, data on 25°C entropies and heat capacities of  $\text{MgCl}_2 \cdot n\text{H}_2\text{O}(\text{s})$  and  $\text{MgSO}_4 \cdot n\text{H}_2\text{O}(\text{s})$  plotted by Pabalan and Pitzer<sup>5</sup> shows a linear trend with the number of hydration waters. A linear relationship was also shown between hydration numbers and enthalpies of formation for a wide variety of solids by Hisham and Benson.<sup>103</sup> Thus the unknown  $C_p$  temperature functions for  $\text{MgSO}_4 \cdot 4\text{H}_2\text{O}(\text{s})$ ,  $\text{MgSO}_4 \cdot 5\text{H}_2\text{O}(\text{s})$ , and  $\text{MgSO}_4 \cdot 7\text{H}_2\text{O}(\text{s})$  were estimated on this basis. In the case of  $\text{KCl} \cdot \text{MgCl}_2 \cdot 6\text{H}_2\text{O}$ , the heat capacity parameters were estimated by Pabalan and Pitzer<sup>5</sup> from the temperature dependence of its solubility in the ternary system  $\text{KCl}-\text{MgCl}_2-\text{H}_2\text{O}$  from 0 to 150°C tabulated by Linke.<sup>17</sup>

The  $S^\circ/R$  values in Table 5 are mostly from Wagman et al.<sup>58</sup> Entropy values enclosed in parentheses were calculated from the corresponding  $\mu_f^\circ/RT$  and  $\Delta H_f^\circ/RT$ . For  $\text{MgSO}_4 \cdot 5\text{H}_2\text{O}(\text{s})$ , its entropy is not known independently and was estimated from the entropy of the other hydrous  $\text{MgSO}_4$  solids. For  $\text{KCl} \cdot \text{MgCl}_2 \cdot 6\text{H}_2\text{O}$ , its reference entropy was estimated from its solubility as a function of temperature.<sup>5</sup> With the exception of  $\text{MgSO}_4 \cdot \text{H}_2\text{O}(\text{s})$ , values of  $\Delta H_f^\circ/RT$  given in the table were calculated from  $\mu_f^\circ/RT$  and  $S^\circ/R$ , or were taken from Wagman et al.<sup>58</sup> when the value of  $S^\circ/R$  is in parentheses. For  $\text{MgSO}_4 \cdot \text{H}_2\text{O}(\text{s})$ ,  $\Delta H_f^\circ/RT$  at 25°C was taken from Ko and Daut.<sup>104</sup>

The thermodynamic data for aqueous species at the reference temperature of 25°C are given in Table 5 in terms of ionic properties. However, for the examples given in this section, equilibrium constants for dissolution reactions at variable temperatures were calculated using these reference values combined with temperature-dependent functions for standard-state heat capacities reported for neutral electrolytes (e.g.,  $C_{p,\text{NaCl}}^\circ$  for  $[\text{C}_{p,\text{Na}^+}^\circ + \text{C}_{p,\text{Cl}^-}^\circ]$ ). There is now an extensive array of experimental data for the most geochemically or industrially important aqueous electrolytes extending upward in temperature, as indicated in Table 15 of Chapter 3. It should be noted that there is currently little theoretical guidance for the temperature and pressure dependencies of standard-state heat capacities; hence, the references cited below used arbitrary analytical forms to describe these properties. The complexity of the empirical equations used by different investigators depends on the temperature and pressure range of experimental data that were used in the regression. Where convenient, the equations used in the examples here are given in Appendix I. Some studies (e.g., Tanger and Helgeson<sup>60</sup>) have shown that standard-state properties of aqueous species vary rapidly at high temperatures when the critical point of water is approached, and at low temperatures in the vicinity of an anomaly in the thermodynamic properties of supercooled water. Hence, some of these equations include terms in  $1/(647-T)$  and  $1/(T-227)$  or other similar terms to describe rapid variations in these temperature ranges.

For  $\text{NaCl}(\text{aq})$ , Pitzer et al.<sup>105</sup> evaluated calorimetric data and gave parameters for calculating standard-state heat capacities to 300°C and 1 kb. For  $\text{KCl}(\text{aq})$ , Holmes and Mesmer<sup>98</sup> presented a set of parameters for  $\text{KCl}(\text{aq})$  properties based on an evaluation of thermodynamic data on  $\text{KCl}$  solutions to 250°C. In addition, Pabalan and Pitzer<sup>9</sup> combined their heat capacity measurements on  $\text{KCl}$  solutions with other literature data to yield a thermodynamically consistent set of parameters for  $\text{KCl}(\text{aq})$  valid to 325°C and 500 bars. Although Holmes and Mesmer's parameters are valid only up to temperatures of 250°C and to pressures not much greater than the saturation pressure of water,<sup>98</sup> their equations are less complex and were used in the present examples.

In the case of  $\text{Na}_2\text{SO}_4(\text{aq})$  thermodynamic data including calorimetric measurements were evaluated by Holmes and Mesmer<sup>106</sup> to yield parameters valid to 225°C. Pabalan and Pitzer<sup>6</sup> extended to 300°C the heat capacity measurements on  $\text{Na}_2\text{SO}_4$  solutions and combined these with other data to develop a comprehensive treatment for the range to 300°C and to 200 bars. Their new equation for  $\text{Na}_2\text{SO}_4(\text{aq})$  standard-state heat capacities is more complex,

but results in very good agreement between calculated and observed solubilities up to at least 300°C.  $\text{MgSO}_4(\text{aq})$  heat capacities have been measured by Phutela and Pitzer<sup>107</sup> from 75 to 200°C. These authors combined their data with literature values at 25°C and reported the temperature dependence of  $\text{MgSO}_4(\text{aq})$  standard-state heat capacities from 25 to 200°C. A similar evaluation has been done by Phutela et al.<sup>108</sup> for  $\text{MgCl}_2(\text{aq})$  based on experimental data up to a temperature of 200°C.

For  $\text{K}_2\text{SO}_4(\text{aq})$ , heat capacity data at high temperatures are not available. Therefore, standard-state heat capacities for  $\text{K}_2\text{SO}_4(\text{aq})$  were calculated from the known values for  $\text{NaCl}(\text{aq})$ ,  $\text{KCl}(\text{aq})$ , and  $\text{Na}_2\text{SO}_4(\text{aq})$  as shown by

$$C_p^\circ(\text{K}_2\text{SO}_4) = 2C_p^\circ(\text{KCl}) + C_p^\circ(\text{Na}_2\text{SO}_4) - 2C_p^\circ(\text{NaCl}) \quad (20)$$

## 2. Choice of Ion Interaction Parameters and Calculated Solubilities in Binary Systems

Ion interaction parameters necessary to calculate osmotic and activity coefficients at 25°C are available for a wide variety of electrolyte solutions and are tabulated in Chapter 3. Recent measurements of the thermodynamic properties of electrolyte solutions have extended our knowledge of these parameters to higher temperatures.

For  $\text{NaCl}(\text{aq})$ , there is an extensive array of experimental data as reported by Pitzer et al.<sup>105</sup> Their evaluation of these data yielded a complete set of parameters valid in the region 0 to 300°C and saturation pressure to 1 kb.  $\text{NaCl}$  solubilities calculated using these parameters are compared with measured solubilities<sup>17,109</sup> in Figure 20. As shown in Figure 20, there is excellent agreement between calculated and experimentally determined values with a maximum deviation of 1.5% at 275°C.

For  $\text{KCl}(\text{aq})$ , the set of equations valid to 250°C and saturation pressure derived by Holmes and Mesmer<sup>98</sup> was used, instead of the more complex temperature and pressure functions valid to 325°C and 500 bars determined by Pabalan and Pitzer.<sup>9</sup> For solubility calculations, there is no great advantage in using the latter because of the very high solubility of  $\text{KCl}(\text{s})$  at high temperatures. The ion interaction parameters of  $\text{KCl}(\text{aq})$  derived by Holmes and Mesmer<sup>98</sup> and Pabalan and Pitzer<sup>9</sup> were fit to data up to a concentration of 6 *m*, whereas the solubility of  $\text{KCl}(\text{s})$  exceeds this value at a temperature less than 100°C. Figure 21 compares calculated and experimental<sup>17</sup> solubilities of  $\text{KCl}(\text{s})$  in water. Since Holmes and Mesmer's<sup>98</sup> equations are valid only to 250°C, the calculations above this temperature represent extrapolations of their temperature-dependent equations. As shown in Figure 21, there is excellent agreement between calculated and experimental solubilities up to 170°C. There is some deviation above this temperature, but the maximum difference of 6.5% at 250°C is quite acceptable.

For  $\text{NaOH}(\text{aq})$ , Pabalan and Pitzer<sup>110</sup> derived temperature functions for ion interaction parameters valid to 350°C. Their treatment did not consider measurements of heat capacities or enthalpies, hence, no equations for standard-state heat capacities were given. However, this does not present a problem for calculations where the solubility of  $\text{NaOH}(\text{s})$  is not of interest. Its solubility in aqueous solutions is very high and is beyond the concentration limit for valid treatment with the ion interaction model. A later study by Simonson et al.<sup>111</sup> incorporates recent measurements of heat capacities and heats of dilution, but is limited to a temperature range below 250°C and to moderate molality.

For  $\text{MgCl}_2(\text{aq})$ , ion interaction parameters were derived by de Lima and Pitzer<sup>112</sup> based on the isopiestic data of Holmes et al.<sup>113</sup> at high temperatures and Rard and Miller<sup>114</sup> at 25°C. However, the osmotic coefficient data of Holmes et al. extend only to 3.5 *m*  $\text{MgCl}_2$ , whereas the solubility of the various hydrates of  $\text{MgCl}_2$  is already 7.7 *m* at 100°C and rises to 14 *m* at 200°C. Hence, Pabalan and Pitzer<sup>5</sup> adjusted the trend of  $C_{\text{MX}}^\phi$  for  $\text{MgCl}_2(\text{aq})$  to better fit the solubility data. We used de Lima and Pitzer's temperature functions for  $\beta_{\text{MX}}^{(0)}$  and  $\beta_{\text{MX}}^{(1)}$ , and the equation of Pabalan and Pitzer for  $C_{\text{MX}}^\phi$ . Calculated and observed solubilities

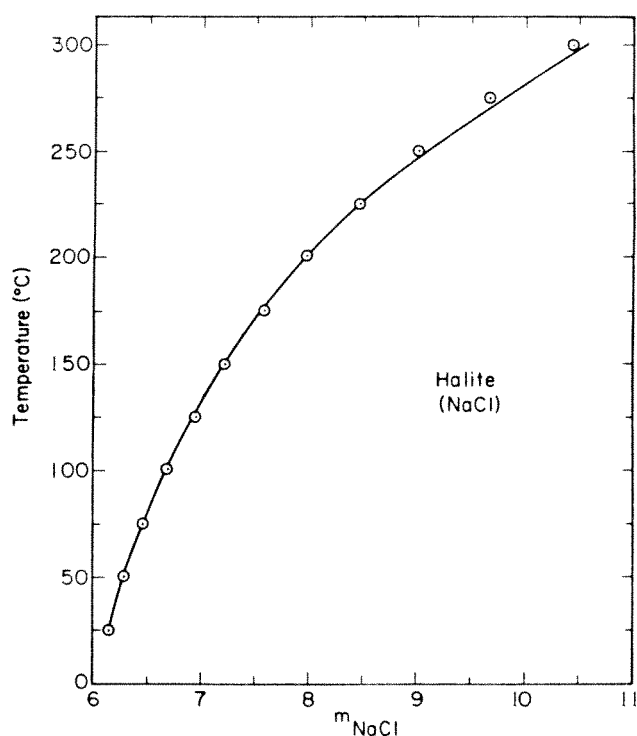


FIGURE 20. Calculated NaCl (halite) solubilities in the binary NaCl-H<sub>2</sub>O system compared to experimental data. The solubility data from 75 to 300°C are from Liu and Lindsay,<sup>109</sup> and those below 75°C are from Linke.<sup>17</sup> (Reproduced with permission from Pabalan, R. T. and Pitzer, K. S., *Geochim. Cosmochim. Acta*, 51, 2429, 1987. Copyright 1987 Pergamon Press.)

are compared in Figure 22, and show good agreement up to 200°C, with a maximum deviation of 4% at 150°C.

In the case of Na<sub>2</sub>SO<sub>4</sub>(aq), Holmes and Mesmer<sup>106</sup> presented temperature functions for ion interaction parameters based on experimental data to 225°C. Pabalan and Pitzer<sup>6</sup> measured heat capacities of Na<sub>2</sub>SO<sub>4</sub> solutions to 300°C and combined their results with various other data to develop a comprehensive treatment for the range to 300°C and to 200 bars. Figure 23 compares experimental solubilities of Na<sub>2</sub>SO<sub>4</sub> · 10H<sub>2</sub>O(s) and Na<sub>2</sub>SO<sub>4</sub>(s) with values calculated using the parameters derived by Pabalan and Pitzer. The symbols are observed values tabulated by Linke,<sup>17</sup> and the curves are our calculated values. The curves are dashed outside the temperature range of regression of aqueous solution properties.<sup>6</sup> While the calculated solubilities are greater than experimental values for Forms IV and V, the differences are not large, averaging 0.08 *m*. The maximum at 241°C corresponds to a change in the stable form of Na<sub>2</sub>SO<sub>4</sub>(s) from Form IV to Form I.<sup>100</sup> The agreement is remarkably good for the extrapolated curves below 25°C and from 300 to 320°C.

For K<sub>2</sub>SO<sub>4</sub>(aq), ion interaction coefficients are given by Holmes and Mesmer<sup>106</sup> up to 225°C. Figure 24 indicates relatively good agreement between experimental and calculated solubilities to 208°C, with a maximum deviation of 8% at 143°C.

In the case of MgSO<sub>4</sub>(aq), a comprehensive regression of heat capacity, enthalpy, and osmotic coefficient data by Phutela and Pitzer<sup>107</sup> yielded ion interaction parameters that are valid from 25 to 200°C. Figure 25 shows that calculated solubilities are in very good agreement with experimental data to 200°C.

The numerical functions for the temperature dependency of standard-state heat capacities and ion interaction parameters are given in the Appendix.

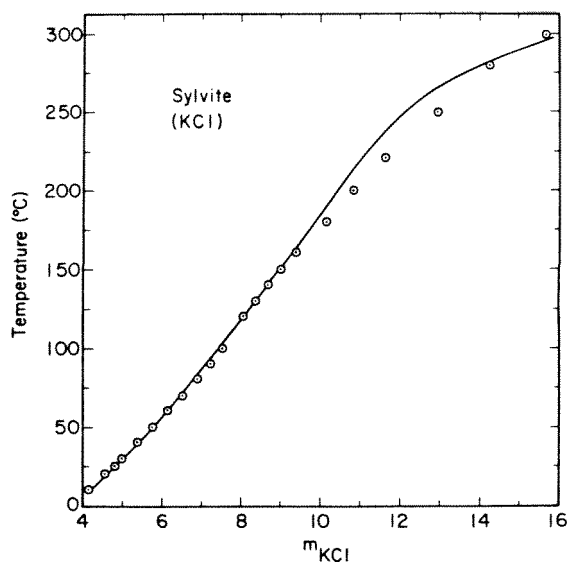


FIGURE 21. Calculated KCl (sylvite) solubilities in the binary KCl-H<sub>2</sub>O system compared to experimental data from Linke.<sup>17</sup> (Reproduced with permission from Pabalan, R. T. and Pitzer, K. S., *Geochim. Cosmochim. Acta*, 51, 2429, 1987. Copyright 1987 Pergamon Press.)

### 3. Solubilities in Ternary Systems

For ternary and more complex systems, the interaction coefficients  $\theta_{ij}$  and  $\psi_{ijk}$  complete the parameters necessary to describe the thermodynamic properties of electrolyte mixtures. These parameters are best evaluated from activity or osmotic coefficient data for common-ion mixtures. Because the terms which include  $\psi_{ijk}$  in the equations for activity and osmotic coefficients involve the second power of molality, this quantity is best determined by measurements at the highest concentration, i.e., in saturated solutions. Hence, some of the best values of  $\psi_{ijk}$  for many electrolyte mixtures come from solubility data.<sup>3,4</sup>

The values of  $\theta_{ij}$  and  $\psi_{ijk}$  at 25°C are available for a large number of systems and are summarized in Chapter 3. These quantities undoubtedly vary with temperature, and there are heat of mixing data which give their temperature derivatives at 25°C.<sup>115</sup> Until heats of mixing measurements become generally available at higher temperatures, we have to depend on isopiestic and solubility data for the values of  $\theta_{ij}$  and  $\psi_{ijk}$  at high temperatures. These quantities are both small, however, and for solubility calculations Pabalan and Pitzer<sup>5,6</sup> previously found that it was an adequate approximation to keep  $\theta_{ij}$  at its 25°C value and to assume simple temperature dependencies for  $\psi_{ijk}$ .

Comparisons of calculated and experimental solubilities in ternary systems for several systems are given below. Values of  $\theta_{ij}$  and the temperature functions for  $\psi_{ijk}$  used in the calculations are given in Table 6. The values of  $\theta_{ij}$  and  $\psi_{ijk}$  at 25°C were taken from various sources.  $\theta_{\text{Na,K}}$  and  $\psi_{\text{Na,K,Cl}}$  at 25°C are from Pitzer and Kim,<sup>116</sup> who derived the parameters from the isopiestic data of Robinson.<sup>117</sup>  $\theta_{\text{Cl,SO}_4}$ ,  $\psi_{\text{Cl,SO}_4,\text{Na}}$ , and  $\psi_{\text{Cl,SO}_4,\text{K}}$ , which were also reported by Pitzer and Kim,<sup>116</sup> were revised by Downes and Pitzer<sup>78</sup> based on their new osmotic coefficient data in the common-ion mixtures. The value of  $\psi_{\text{Cl,SO}_4,\text{Mg}}$  was fit to solubility data at 25°C by Pabalan and Pitzer.<sup>5</sup>  $\theta_{\text{Na,Mg}}$  reported by Pitzer<sup>118</sup> was used, but the value of  $-0.012$  for  $\psi_{\text{Na,Mg,Cl}}$  derived by Harvie and Weare<sup>3</sup> from solubility data was chosen instead of Pitzer's value of  $-0.010$ . For  $\theta_{\text{K,Mg}}$ ,  $\theta_{\text{Cl,OH}}$ ,  $\theta_{\text{SO}_4,\text{OH}}$ ,  $\psi_{\text{K,Mg,Cl}}$ ,  $\psi_{\text{Cl,OH,Na}}$ , and  $\psi_{\text{SO}_4,\text{OH,Na}}$ , the 25°C values are from Harvie et al.<sup>4</sup> who evaluated the parameters from solubility data. The temperature functions for  $\psi_{ijk}$  were evaluated from solubility data by Pabalan and Pitzer.<sup>5,6</sup>

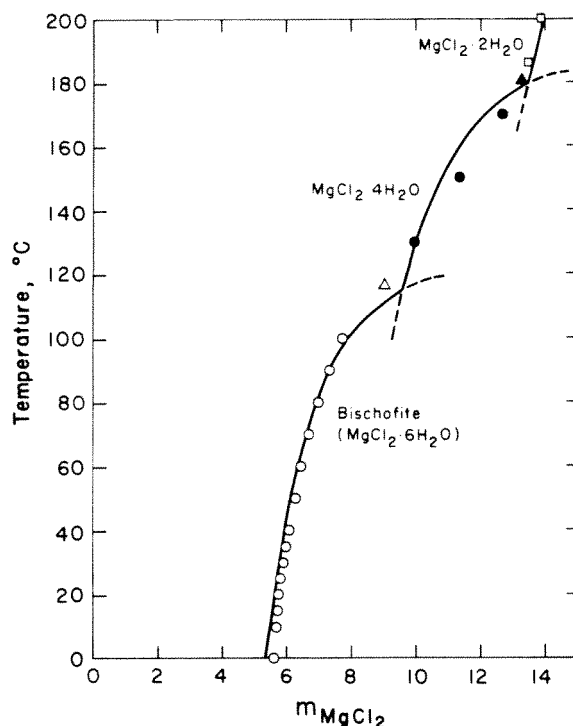


FIGURE 22. Calculated solubilities in the  $\text{MgCl}_2\text{-H}_2\text{O}$  binary system compared to experimental data from Linke.<sup>17</sup> The triangles represent experimental data at the triple points. The  $C_{\text{MX}}^\phi$  values for  $\text{MgCl}_2$  above  $100^\circ\text{C}$  were adjusted on the basis of the solubility data. (Reproduced with permission from Pabalan, R. T. and Pitzer, K. S., *Geochim. Cosmochim. Acta*, 51, 2429, 1987. Copyright 1987 Pergamon Press.)

It should be noted that, in the examples presented in this section, the full set of terms in the equations given in Table 1 were used, including  ${}^E\theta_{ij}$  and  ${}^E\theta'_{ij}$  for unsymmetrical mixing effects. Thus, the mixing parameters given in the previous section (Table 3) should not be used when the  ${}^E\theta_{ij}$  and  ${}^E\theta'_{ij}$  terms are present. There is also a small ionic strength effect on symmetrical mixing<sup>119</sup> which is negligible for present purposes and is omitted.

Experimental and calculated solubilities at variable temperatures in mixtures of two 1:1 electrolytes are shown in Figures 26 and 27 for the systems  $\text{NaCl-KCl-H}_2\text{O}$  and  $\text{NaCl-NaOH-H}_2\text{O}$ , respectively. In the case of the  $\text{NaCl-KCl-H}_2\text{O}$  system, Holmes et al.<sup>120</sup> reported that  $\psi_{\text{Na,K,Cl}}$  could be neglected and represented  $\theta_{\text{Na,K}}$  by the equation  $\theta_{\text{Na,K}} = 0.0039 - 6.726/T(\text{K})$ , based on their osmotic coefficient data for the system to a temperature of  $201^\circ\text{C}$ . These values fitted the observed solubilities tabulated by Linke<sup>17</sup> up to  $150^\circ\text{C}$ , but gave large deviations at higher temperatures and convergence problems at  $200^\circ\text{C}$ . For calculating solubilities in this system, it was found adequate<sup>5</sup> to keep  $\theta_{\text{Na,K}}$  at its  $25^\circ\text{C}$  value of  $-0.012$  and to use the temperature function for  $\psi_{\text{Na,K,Cl}}$  given in Table 6. Figure 26 shows that there is excellent agreement through  $150^\circ\text{C}$ , and that the small differences in the ternary system at  $200^\circ\text{C}$  are no larger than those of the  $\text{KCl-H}_2\text{O}$  binary. It should be pointed out that the binary ion interaction parameters for  $\text{KCl(aq)}$  were derived by fitting thermodynamic data to  $6\text{ m}$  only. Hence, solubility calculations at  $200^\circ\text{C}$  represent severe extrapolations beyond the experimentally constrained range.

Examples of solubilities in mixtures involving 1:1 and 2:1 electrolytes are illustrated in Figures 28 to 32. Figures 28 and 29 compare calculated and experimental<sup>17,121</sup> values in the ternary systems  $\text{KCl-K}_2\text{SO}_4\text{-H}_2\text{O}$  and  $\text{KCl-MgCl}_2\text{-H}_2\text{O}$ , respectively, and Figure 30 shows

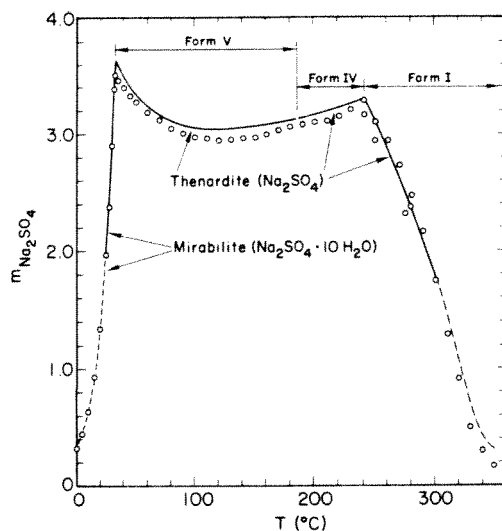


FIGURE 23. Calculated solubilities of  $\text{Na}_2\text{SO}_4 \cdot 10\text{H}_2\text{O}$  (mirabilite) and  $\text{Na}_2\text{SO}_4$  (thenardite) in water as a function of temperature. The symbols are experimental data tabulated by Linke,<sup>17</sup> and the curves are predicted values. The curves are dashed outside the temperature range used in the regression of  $\text{Na}_2\text{SO}_4(\text{aq})$  properties. (Reproduced with permission from Pabalan, R. T. and Pitzer, K. S., *Geochim. Cosmochim. Acta*, 52, 2393, 1988. Copyright 1988 Pergamon Press.)

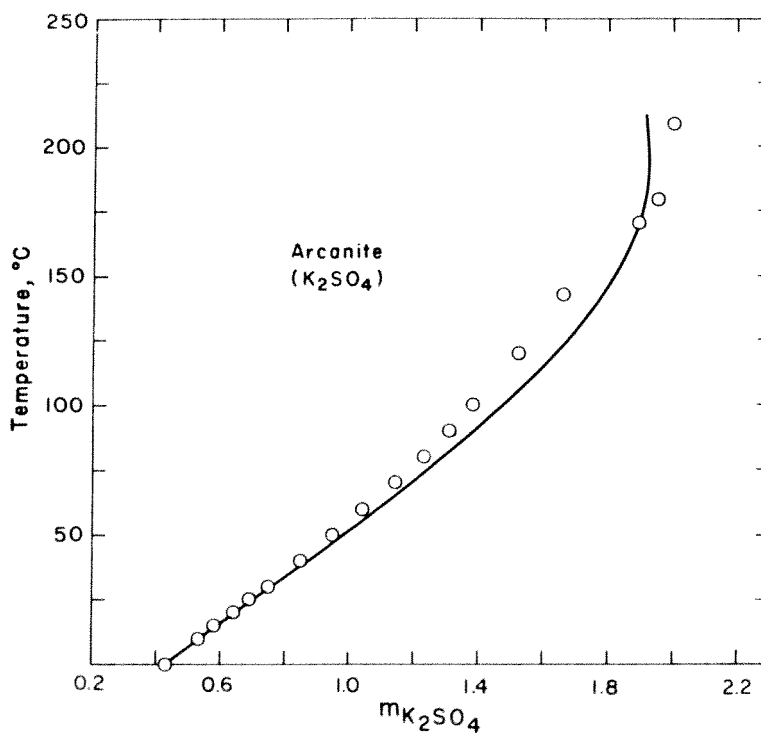


FIGURE 24. Calculated and experimental solubilities of  $\text{K}_2\text{SO}_4$  (arcanite) in water. The experimental data are from Linke.<sup>17</sup> (Reproduced with permission from Pabalan, R. T. and Pitzer, K. S., *Geochim. Cosmochim. Acta*, 51, 2429, 1987. Copyright 1987 Pergamon Press.)



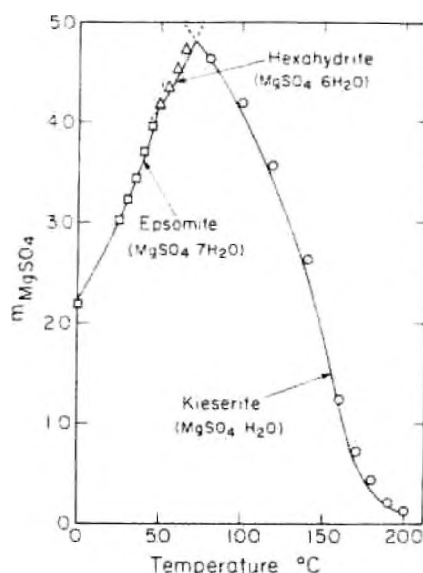


FIGURE 25. Calculated solubilities in the system  $\text{MgSO}_4\text{-H}_2\text{O}$  compared to experimental data from Linke.<sup>17</sup> (Reproduced with permission from Pabalan, R. T. and Pitzer, K. S., *Geochim. Cosmochim. Acta*, 51, 2429, 1987. Copyright 1987 Pergamon Press.)

**TABLE 6**  
Mixed Electrolyte Parameters for Variable Temperature Calculations and for Use with  ${}^{\circ}\theta_{ij}$  and  ${}^{\circ}\theta'_{ij}$  (Temperature T in K)

i	j	k	$\theta_{ij}$	$\psi_{ijk}$
Na	K	Cl	-0.012	$-6.809\text{E-}3 + 1.680\text{E-}5\text{T}$
Na	Mg	Cl	0.07	$1.99038\text{E-}2 - 9.51213/\text{T}$
K	Mg	Cl	0	$2.58557\text{E-}2 - 14.26819/\text{T}$
Cl	$\text{SO}_4$	Na	0.030	$-1.69580\text{E-}2 + 3.13544/\text{T} + 2.16352\text{E-}5\text{T} - 1.31254\text{E}5/(647\text{-T})^4$
Cl	$\text{SO}_4$	K	0.030	$-5.0\text{E-}3$
Cl	$\text{SO}_4$	Mg	0.030	$-1.17457\text{E-}1 + 32.6347/\text{T}$
Cl	OH	Na	-0.050	$7.93217\text{E-}2 - 1.89664\text{E}1/\text{T} - 7.28094\text{E-}5\text{T}$
$\text{SO}_4$	OH	Na	-0.013	$7.94135\text{E-}2 - 1.99387\text{E}1/\text{T} - 7.21586\text{E-}5\text{T} - 3.64900\text{E}5/(647\text{-T})^4$

solubilities in the system  $\text{NaCl-MgCl}_2\text{-H}_2\text{O}$ . Experimental data<sup>17</sup> in the  $\text{KCl-K}_2\text{SO}_4\text{-H}_2\text{O}$  system extend only to 100°C, and it was found sufficient to use the 25°C values of both  $\theta_{\text{Cl},\text{SO}_4}$  and  $\psi_{\text{Cl},\text{SO}_4,\text{K}}$  over the whole temperature range.

Observed<sup>122</sup> and calculated solubilities from 150 to 300°C are compared in Figures 31 and 32 for the systems  $\text{NaCl-Na}_2\text{SO}_4\text{-H}_2\text{O}$  and  $\text{NaOH-Na}_2\text{SO}_4\text{-H}_2\text{O}$ , respectively. These systems are particularly interesting because at very high temperatures, the solubility of  $\text{Na}_2\text{SO}_4(\text{s})$  increases with increasing  $\text{NaCl}$  or  $\text{NaOH}$  concentration. This is in contrast to the typical solubility behavior of salts which shows a decrease with increasing concentration of a common-ion solute. In the case of the system  $\text{NaCl-Na}_2\text{SO}_4\text{-H}_2\text{O}$ , the solubility of  $\text{Na}_2\text{SO}_4(\text{s})$  at 300°C initially decreases with an increase in  $\text{NaCl}$  concentration, but flattens out at the higher  $\text{NaCl}$  molalities as shown in Figure 31. The experimental data of Schroeder et al.<sup>122</sup> show that at 350°C its solubility increases with increasing  $\text{NaCl}$  concentration. This reversal in trend occurs at a lower temperature for the ternary system  $\text{NaOH-Na}_2\text{SO}_4\text{-H}_2\text{O}$  as illustrated in Figure 32, where the solubility of  $\text{Na}_2\text{SO}_4(\text{s})$  at 300°C increases with an increase in  $\text{NaOH}$  molality. Although it was found adequate to use constant values of  $\theta_{\text{Cl},\text{SO}_4}$  and  $\theta_{\text{OH},\text{SO}_4}$  to

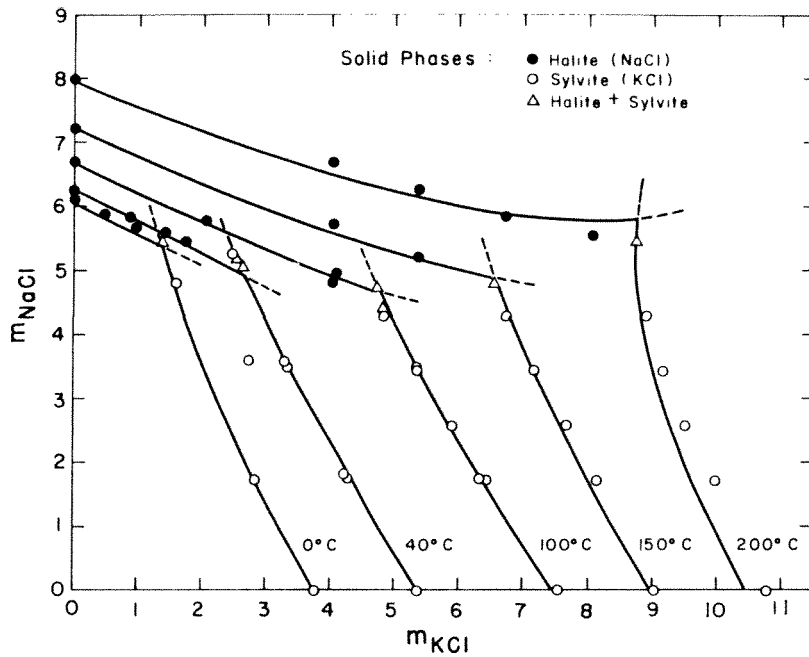


FIGURE 26. Calculated solubilities in the ternary mixture NaCl-KCl-H<sub>2</sub>O compared with experimental data taken from Linke.<sup>17</sup> The dashed curves are extrapolations of the solubilities of either NaCl or KCl into the supersaturated solution concentration of the other electrolyte. The intersections of isothermal curves represent calculated ternary invariant points. The values of  $\psi_{Na,K,Cl}$  above 25°C were fit to solubility data. (Reproduced with permission from Pabalan, R. T. and Pitzer, K. S., *Geochim. Cosmochim. Acta*, 51, 2429, 1987. Copyright 1987 Pergamon Press.)

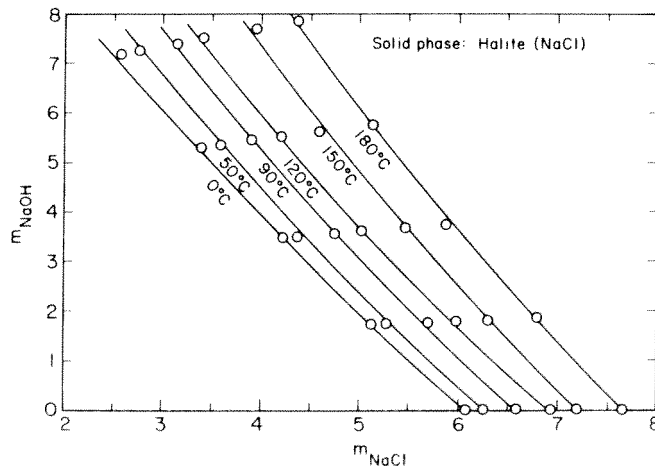


FIGURE 27. Calculated and experimental solubilities in the ternary system NaCl-NaOH-H<sub>2</sub>O. The experimental data were taken from Linke<sup>17</sup> and were used to adjust  $\psi_{Cl,OH,Na}$  above 25°C. (Reproduced with permission from Pabalan, R. T. and Pitzer, K. S., *Geochim. Cosmochim. Acta*, 51, 2429, 1987. Copyright 1987 Pergamon Press.)

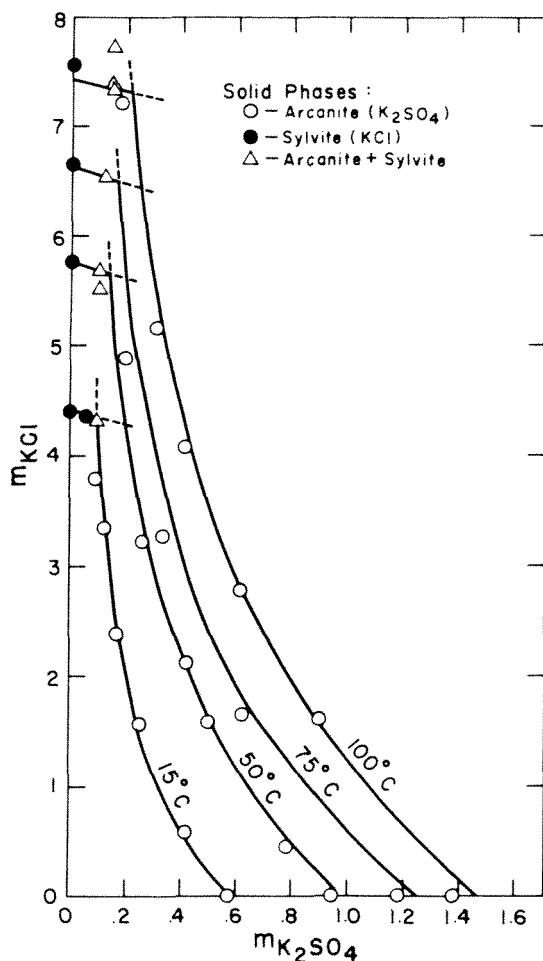


FIGURE 28. Calculated and experimental solubilities in the KCl-K<sub>2</sub>SO<sub>4</sub>-H<sub>2</sub>O system. The experimental data are from Linke.<sup>17</sup> (Reproduced with permission from Pabalan, R. T. and Pitzer, K. S., *Geochim. Cosmochim. Acta*, 51, 2429, 1987. Copyright 1987 Pergamon Press.)

300°C, it was necessary to use values of  $\psi_{\text{Cl},\text{SO}_4,\text{Na}}$  and  $\psi_{\text{OH},\text{SO}_4,\text{Na}}$  above 250°C which are more negative than those at lower temperatures in order to fit the solubility data.<sup>6</sup> The temperature functions derived for  $\psi_{\text{Cl},\text{SO}_4,\text{Na}}$  and  $\psi_{\text{OH},\text{SO}_4,\text{Na}}$  are given in Table 6. Figures 31 and 32 indicate that in both systems, there is very good agreement between calculated and observed solubilities from 150 to 300°C. The same agreement at lower temperatures down to 10°C was also shown by Pabalan and Pitzer.<sup>5</sup>

An example of solubilities in mixtures involving 1:2 and 2:2 electrolytes is shown in Figure 33. This figure compares experimental and calculated values in the ternary system MgCl<sub>2</sub>-MgSO<sub>4</sub>-H<sub>2</sub>O, and indicates very good agreement in the temperature range 0 to 100°C.

#### 4. Solubilities in Quaternary Systems

Ion interaction parameters and standard-state properties evaluated previously using data on simple mixtures can be used to predict solubility equilibria in quaternary or more complex systems. There are no new parameters in the equations for the more complex examples. Figures 34 and 35 and Table 7 present the results for the quaternary system NaCl-KCl-MgCl<sub>2</sub>-H<sub>2</sub>O. Figure 34 compares the predicted solubilities of NaCl(s) and/or KCl(s) at 20, 55, and 90°C and at various molalities of MgCl<sub>2</sub>(aq) with experimental data given by

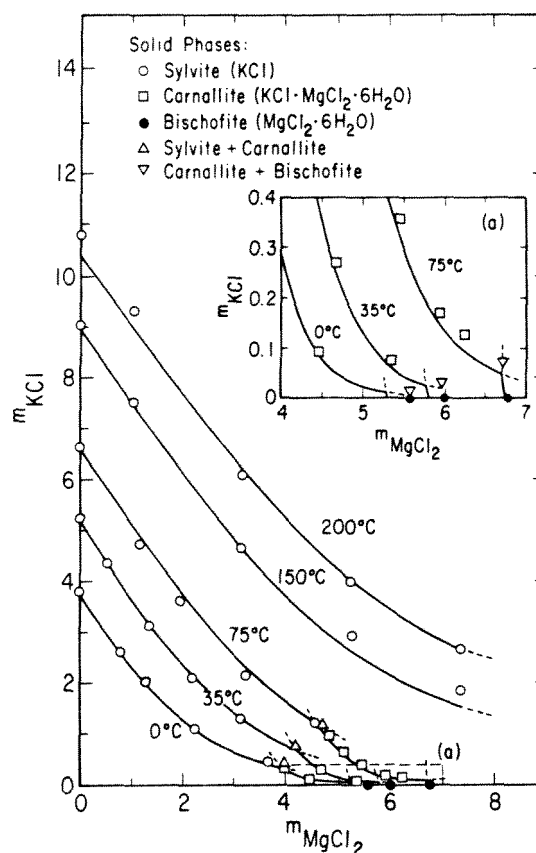


FIGURE 29. Calculated solubilities in the ternary system KCl-MgCl<sub>2</sub>-H<sub>2</sub>O compared with observed values tabulated by Linke.<sup>17</sup> The inset shows an expanded view of the area delineated by box (a). The values of  $\psi_{K,Mg,Cl}$  above 25°C were adjusted on the basis of the experimental data. (Reproduced with permission from Pabalan, R. T. and Pitzer, K. S., *Geochim. Cosmochim. Acta*, 51, 2429, 1987. Copyright 1987 Pergamon Press.)

Kayser.<sup>123</sup> Figure 35 compares predicted solubilities at 15, 40, 65, and 90°C with observed values taken from Boecke.<sup>124</sup> Table 7 compares the predicted solution compositions up to 105°C at the quaternary invariant point with the experimental values of Serowy.<sup>125</sup> The agreement between predicted and experimental values is quite acceptable considering the uncertainties in MgCl<sub>2</sub>(aq) ion interaction parameters and in the thermodynamic properties of KCl · MgCl<sub>2</sub> · 6H<sub>2</sub>O.

Additional examples are given in Figure 36, which compares experimental and calculated solubilities of Na<sub>2</sub>SO<sub>4</sub>(s) in the quaternary system NaCl-NaOH-Na<sub>2</sub>SO<sub>4</sub>-H<sub>2</sub>O at 150, 200, 250, and 300°C. Figure 36 indicates there is very good agreement between calculated and observed<sup>122</sup> solubilities up to 300°C.

## V. SOLUBILITY CALCULATIONS USING THE MARGULES EXPANSION MODEL

We now turn our attention to systems which may vary in concentration over the entire range from dilute solutions to the fused salt. While aqueous solutions miscible over the

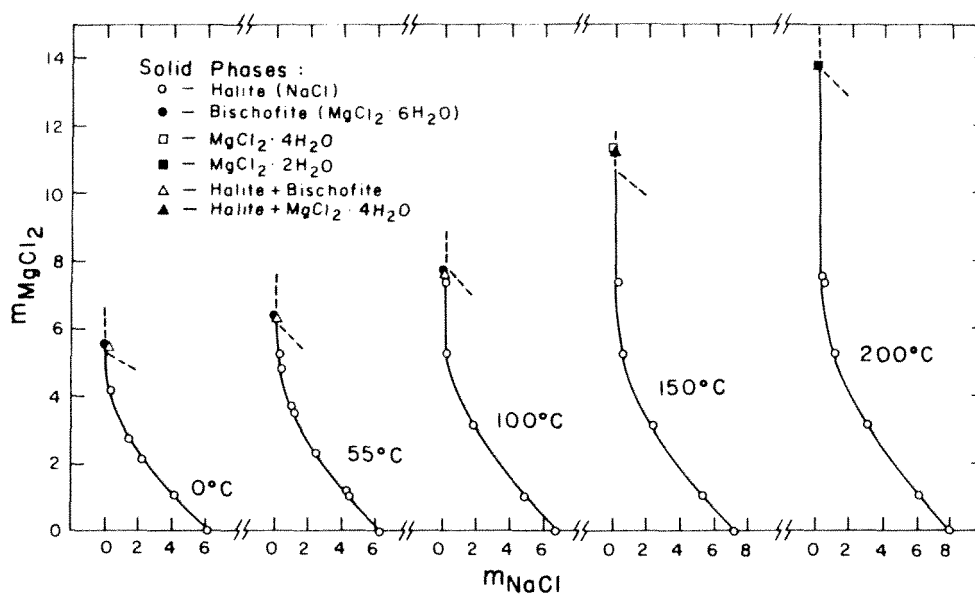


FIGURE 30. Calculated and experimental solubilities in the NaCl-MgCl<sub>2</sub>-H<sub>2</sub>O system. Experimental data below 100°C are from Linke,<sup>17</sup> whereas those above 100°C are from Akhumov and Vasil'ev.<sup>121</sup> Values of  $\psi_{\text{Na,Mg,Cl}}$  above 25°C were fit to solubility data. (Reproduced with permission from Pabalan, R. T. and Pitzer, K. S., *Geochim. Cosmochim. Acta*, 51, 2429, 1987. Copyright 1987 Pergamon Press.)

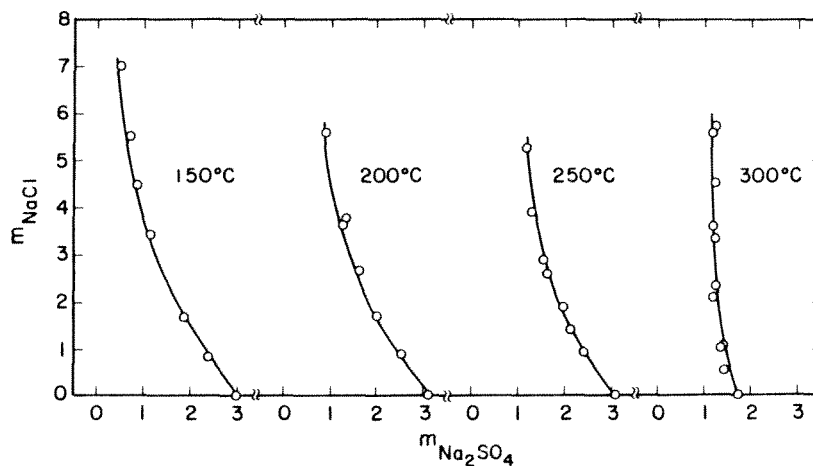


FIGURE 31. Calculated and experimental solubilities of Na<sub>2</sub>SO<sub>4</sub> (thenardite) in the NaCl-Na<sub>2</sub>SO<sub>4</sub>-H<sub>2</sub>O system. The experimental data are from Schroeder et al.<sup>122</sup> The values of  $\psi_{\text{Cl,SO}_4,\text{Na}}$  above 25°C were fit to solubility data. (Reproduced with permission from Pabalan, R. T. and Pitzer, K. S., *Geochim. Cosmochim. Acta*, 52, 2393, 1988. Copyright 1988 Pergamon Press.)

whole concentration range at moderate temperatures are relatively uncommon, there are electrolytes of geochemical and industrial interest which become extremely soluble in water at high temperatures and pressures. As discussed previously, an alternative approach to the molality-based ion interaction treatment is useful for systems extending to the fused salt and for other systems of very high but limited solubility. The model discussed below is essentially

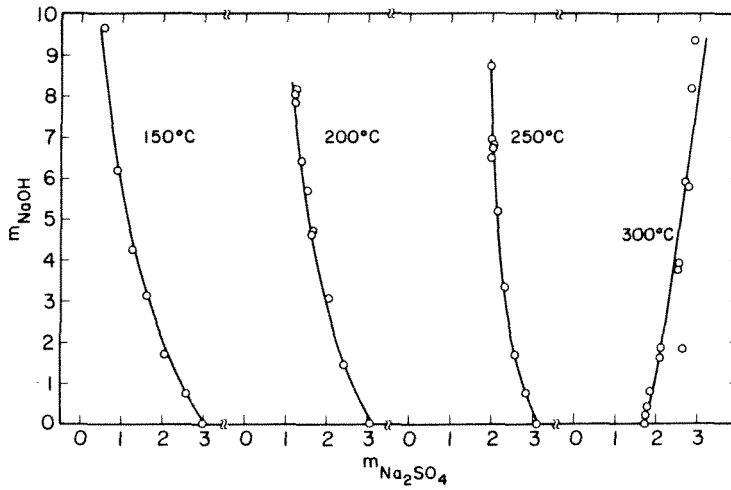


FIGURE 32. Calculated solubilities of  $\text{Na}_2\text{SO}_4$  (thenardite) in the  $\text{NaOH-Na}_2\text{SO}_4\text{-H}_2\text{O}$  system compared with experimental data from Schroeder et al.<sup>122</sup> The values of  $\psi_{\text{OH},\text{SO}_4,\text{Na}}$  above  $25^\circ\text{C}$  were fit to solubility data. (Reproduced with permission from Pabalan, R. T. and Pitzer, K. S., *Geochim. Cosmochim. Acta*, 52, 2393, 1988. Copyright 1988 Pergamon Press.)

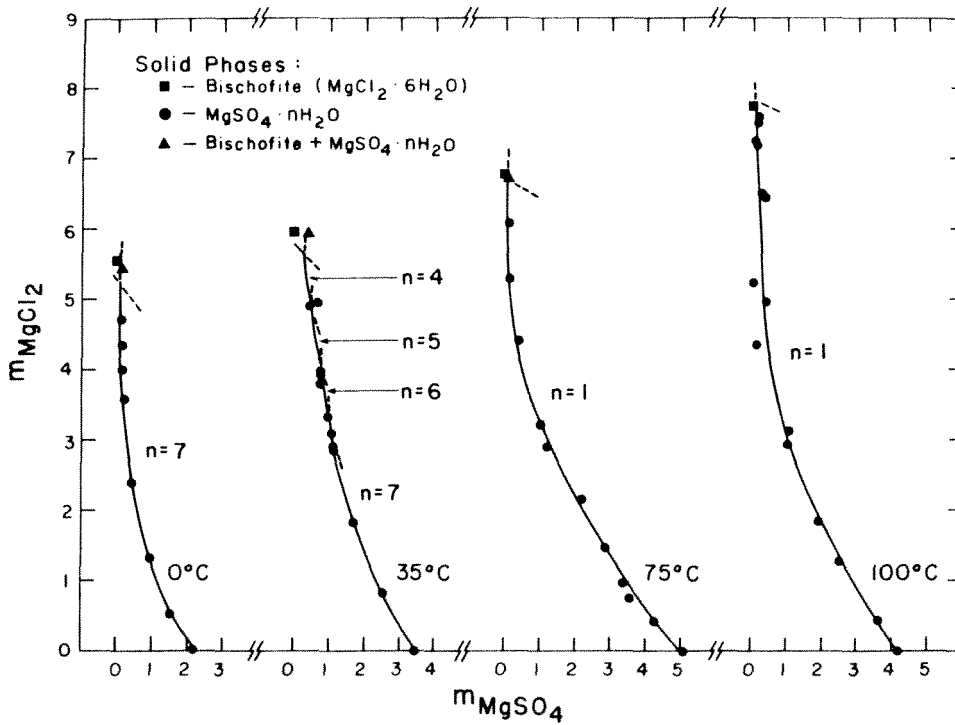


FIGURE 33. Calculated solubilities in the system  $\text{MgCl}_2\text{-MgSO}_4\text{-H}_2\text{O}$  compared with experimental data taken from Linke.<sup>17</sup> The experimental data were used to adjust the values of  $\psi_{\text{SO}_4,\text{Cl},\text{Mg}}$ . (Reproduced with permission from Pabalan, R. T. and Pitzer, K. S., *Geochim. Cosmochim. Acta*, 51, 2429, 1987. Copyright 1987 Pergamon Press.)

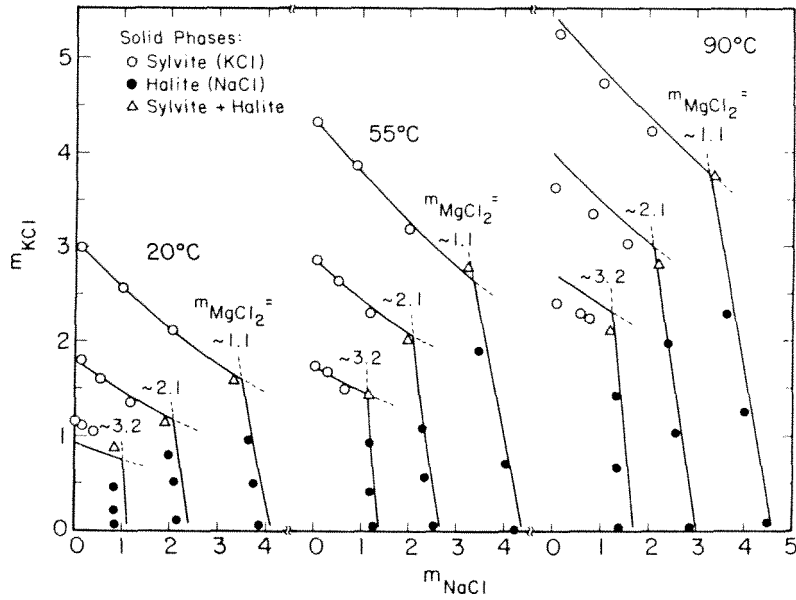


FIGURE 34. Predicted and experimental solubilities of NaCl (halite) or KCl (sylvite) in the quaternary system NaCl-KCl-MgCl<sub>2</sub>-H<sub>2</sub>O at 20, 55, and 90°C, and at MgCl<sub>2</sub> molalities of approximately 1.1, 2.1, and 3.2. Experimental data are from Kayser.<sup>123</sup> (Reproduced with permission from Pabalan, R. T. and Pitzer, K. S., *Geochim. Cosmochim. Acta*, 51, 2429, 1987. Copyright 1987 Pergamon Press.)

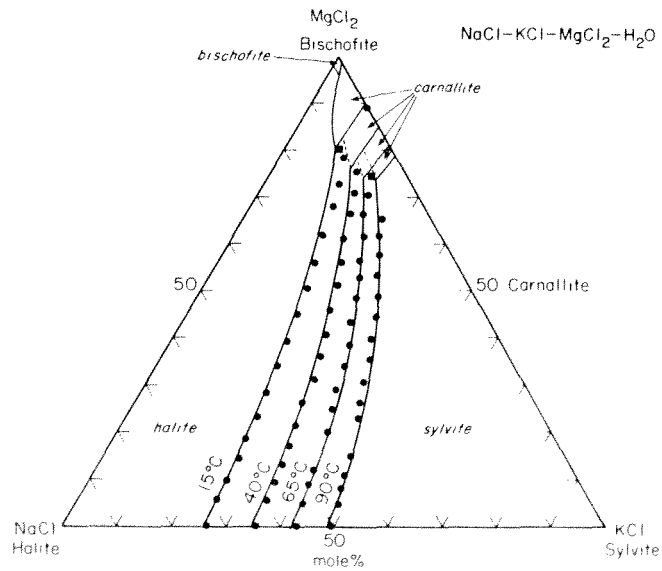


FIGURE 35. Predicted solubilities in the quaternary system NaCl-KCl-MgCl<sub>2</sub>-H<sub>2</sub>O at 15, 40, 65, and 90°C. The solid symbols represent experimental values from Boecke<sup>124</sup> for solutions saturated with both halite and sylvite.

**TABLE 7**  
**Experimental and Predicted Compositions of**  
**Solutions in the Quaternary System NaCl-KCl-**  
**MgCl<sub>2</sub>-H<sub>2</sub>O at Various Temperatures in**  
**Equilibrium with Halite + Sylvite + Carnallite.<sup>a</sup>**

T (°C)	Experimental			Calculated		
	m <sub>NaCl</sub>	m <sub>KCl</sub>	m <sub>MgCl<sub>2</sub></sub>	m <sub>NaCl</sub>	m <sub>KCl</sub>	m <sub>MgCl<sub>2</sub></sub>
0	0.50	0.35	3.77	0.50	0.31	3.83
10	0.46	0.45	3.84	0.50	0.40	3.89
15	0.45	0.49	3.88	0.51	0.45	3.92
20	0.44	0.54	3.92	0.51	0.50	3.95
25	0.43	0.59	3.97	0.51	0.56	3.98
30	0.42	0.64	4.02	0.52	0.61	4.02
40	0.40	0.73	4.13	0.52	0.73	4.09
50	0.39	0.83	4.26	0.51	0.85	4.18
55	0.39	0.88	4.34	0.51	0.91	4.23
60	0.38	0.93	4.41	0.50	0.98	4.29
70	0.39	1.03	4.58	0.49	1.10	4.42
80	0.39	1.13	4.72	0.47	1.21	4.57
83	0.41	1.15	4.78	0.46	1.24	4.63
90	0.46	1.22	4.90	0.44	1.31	4.76
95	0.49	1.27	4.99	0.43	1.35	4.87
100	0.55	1.32	5.10	0.41	1.39	4.99
105	0.60	1.37	5.20	0.39	1.43	5.12

<sup>a</sup> Experimental values are from Serowy.<sup>125</sup>

that of Pitzer and Simonson<sup>13</sup> and is analogous to those used for nonelectrolyte solutions. Various expressions have been used to describe the excess Gibbs energy of nonelectrolytes,<sup>126</sup> and the Margules expansion has been used successfully by Adler et al.<sup>127</sup> for several nonelectrolyte systems. The theoretical basis for using this approach on electrolyte solutions was discussed by Pitzer<sup>128</sup> (also Appendix I of Chapter 3). Briefly, in concentrated electrolyte solutions the substantial ionic concentration effectively screens the long-range interionic forces to short range. Thus all of the interparticle forces are effectively short range and the properties of the system can be calculated by methods similar to those for nonelectrolytes. In the dilute range, however, where ionic concentrations are very low, the screening effect is lost and the long-range nature of electrostatic forces must be considered. As with the molality-based ion interaction model, this effect is described by an extended Debye-Hückel treatment.

#### A. MODEL EQUATIONS AND SOLUBILITY CALCULATIONS IN BINARY ELECTROLYTE + WATER SYSTEMS

The excess Gibbs energy,  $g^{ex}$ , per mole of particles is given by the sum of a term for short-range interactions,  $g^s$ , and a Debye-Hückel term,  $g^{DH}$ :

$$G^{ex} \sum_i n_i = g^{ex} = g^s + g^{DH} \quad (21)$$

where  $G^{ex}$  is the excess Gibbs energy for any amount of material and  $n_i$  is the number of moles of component  $i$ . It should be noted that the base function from which  $G^{ex}$  is an "excess" is different in the molality and the mole fraction systems (see Chapters 1 and 3). The logarithms of the activity coefficients are similarly sums of terms for short-range forces and for the Debye-Hückel effect. A choice must be made for the reference state of the solute:



either the pure liquid (possibly supercooled), or the solute at infinite dilution in the solvent. The latter differs from the conventional solute standard state only in the use of mole fraction instead of molality units. For the activity coefficient of a symmetrical salt MX, one has either

$$\ln (\gamma_M \gamma_X) \rightarrow 0 \text{ as } x_1 \rightarrow 0 \quad (22)$$

or

$$\ln (\gamma_M^* \gamma_X^*) \rightarrow 0 \text{ as } x_1 \rightarrow 1 \quad (23)$$

where the symbol \* denotes the infinitely dilute reference state on a mole fraction basis and  $x_1$  is the mole fraction of the solvent on an ionized basis, i.e., for a symmetrical salt MX,

$$x_1 = n_1 / (n_1 + 2n_2) \quad (24)$$

with  $n_1$  and  $n_2$  the numbers of moles of solvent and solute, respectively. In addition, the mole fractions of the solute are defined as

$$x_M = x_X = n_2 / (n_1 + 2n_2) = (1 - x_1) / 2 \quad (25)$$

$$x_2 = x_M + x_X = 1 - x_1 \quad (26)$$

and the ionic strength on a mole fraction basis is given by:

$$I_x = (1/2) \sum_i x_i z_i^2 \quad (27)$$

with  $z_i$  the charge on the  $i$ th ion. For the present case with  $z = 1$ ,  $I_x = x_2 / 2 = x_M = x_X$ .

A system of equations for electrolytes based on the reference states expressed in Equations 22 and 23 was developed in detail for singly charged ions by Pitzer and Simonson.<sup>13</sup> Although they considered both types of reference states for the solute, most of their working equations are for the pure liquid reference state. This supercooled liquid basis was used for NaCl-H<sub>2</sub>O by Pitzer and Li<sup>129</sup> for a study extending to 550°C. However, for the examples given here, which are limited to 350°C, it seemed better to use the infinitely dilute reference state, and the equations below are derived on that basis.

The short-range contribution to the excess Gibbs energy of an aqueous solution with a single solute MX can be written in terms of the Margules expression:

$$g^s/RT = -x_2^2(W_{1,MX} - x_1 U_{1,MX}) \quad (28)$$

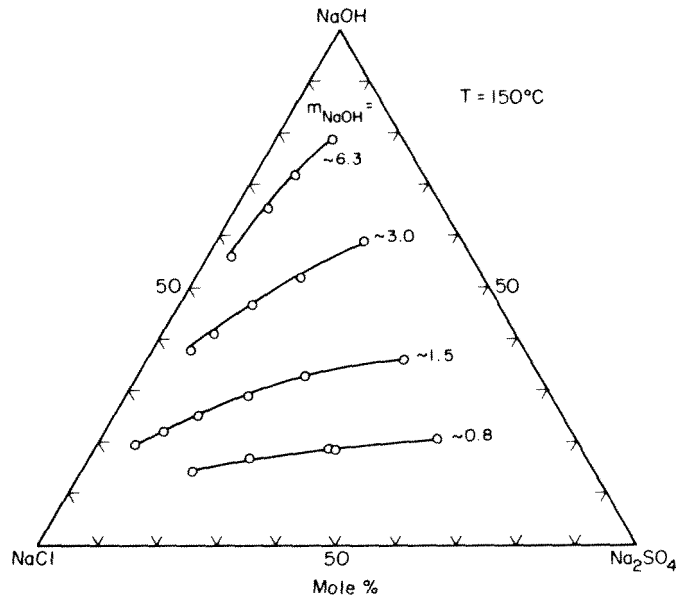
where  $W_{1,MX}$  and  $U_{1,MX}$  are specific to each solute MX and are functions of temperature and pressure. The Debye-Hückel term representing the long-range electrostatic contribution is given by

$$g^{DH}/RT = -(4A_x I_x / \rho) \ln(1 + \rho I_x^{1/2}) \quad (29)$$

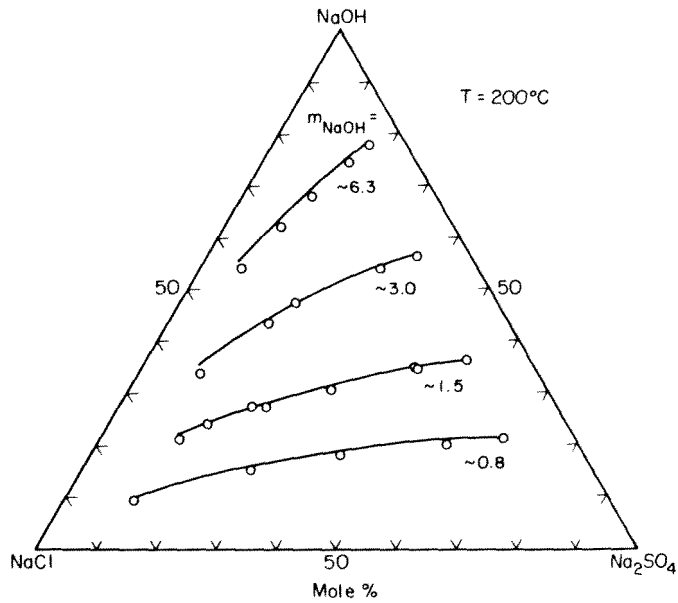
The Debye-Hückel parameter  $A_x$  is related to the usual parameter  $A_\phi$  (for the osmotic coefficient on a molality basis) by

$$A_x = \Omega^{1/2} A_\phi \quad (30)$$

where  $\Omega$  is the number of moles of solvent per kilogram ( $\sim 55.51$  for water).



A



B

FIGURE 36. Calculated and experimental solubilities of  $\text{Na}_2\text{SO}_4$  (thenardite) at fixed molalities of NaOH in the quaternary system  $\text{NaCl-NaOH-Na}_2\text{SO}_4\text{-H}_2\text{O}$  at temperatures of: (A)  $150^\circ\text{C}$ ; (B)  $200^\circ\text{C}$ ; (C)  $250^\circ\text{C}$ ; and (D)  $300^\circ\text{C}$ . The symbols are experimental data from Schroeder et al.<sup>122</sup> (Reproduced with permission from Pabalan, R. T. and Pitzer, K. S., *Geochim. Cosmochim. Acta*, 52, 2393, 1988. Copyright 1988 Pergamon Press.)

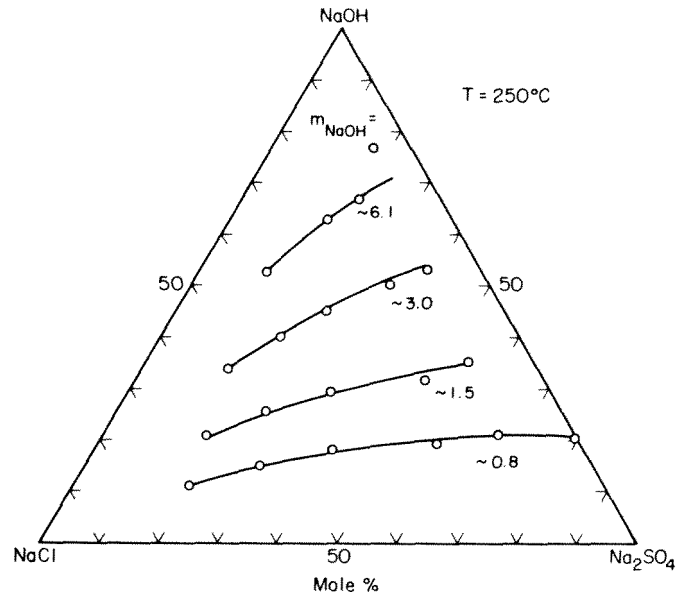


FIGURE 36C

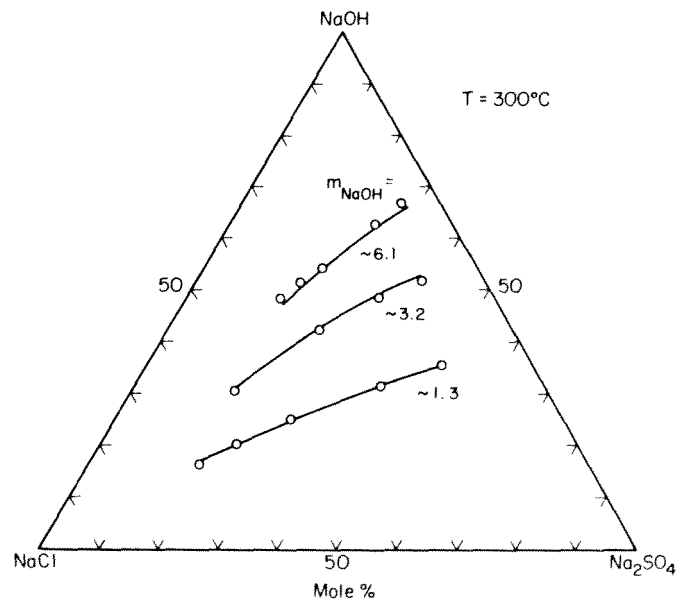


FIGURE 36D

Appropriate differentiations of the excess Gibbs energy with respect to the numbers of moles of the solvent and MX (at constant  $T$  and  $P$ ) yield the equations for the activity coefficients:

$$\ln \gamma_1 = 2A_x I_x^{3/2} / (1 + \rho I_x^{1/2}) + x_2^2 [W_{1,MX} + (1 - 2x_1)U_{1,MX}] \quad (31)$$

$$\begin{aligned} \ln(\gamma_{x_1}^* \gamma_{x_2}^*) = & -2A_x \{ (2/\rho) \ln(1 + \rho I_x^{1/2}) + I_x^{1/2} (1 - 2I_x) / (1 + \rho I_x^{1/2}) \} \\ & + 2(x_1^2 - 1)W_{1,MX} + 4x_2 x_1^2 U_{1,MX} \end{aligned} \quad (32)$$

The activities of the solvent and the solute are then given by

$$\ln a_1 = \ln(x_1\gamma_1) \quad (33)$$

$$\ln a_{MX} = \ln(x_M x_X \gamma_M^* \gamma_X^*) \quad (34)$$

The parameter  $\rho$  in Equations 29, 31, and 32 is related to the distance of closest approach of ions. To keep the equations for the thermodynamic properties of electrolyte mixtures simple, it is desirable to have the same value of  $\rho$  for a wide variety of salts and for a wide range of temperature and pressure. The functional forms of Equations 31 and 32 are relatively insensitive to variations in  $\rho$  values. It has been found satisfactory<sup>2,13</sup> to take a standard value for  $\rho$  and let the short-range force terms accommodate any differences in  $\rho$ . In calculations for metal nitrates in water<sup>14</sup> from 100 to 163°C,  $\rho$  was given a fixed value of 14.9. For systems considered here, a constant value of 15.0 was found to be satisfactory.<sup>16</sup>

The Margules expansion model has been tested on some ionic systems over very wide ranges of composition, but over limited ranges of temperature and pressure<sup>14,15</sup> (also Chapter f6). In the examples given here, the model is applied over a wider range of temperature and pressure, from 25 to 350°C and from 1 bar or saturation pressure to 1 kb. NaCl and KCl are major solute components in natural fluids and there are abundant experimental data from which their parameters can be evaluated. Models based on the ion interaction approach are available for NaCl(aq)<sup>105</sup> and KCl(aq),<sup>9,98</sup> but these are accurate only to about 6 *m*. Solubilities of NaCl and KCl in water, however, reach 12 and 20 *m*, respectively, at 350°C, and ionic strengths of NaCl-KCl solutions reach more than 30 *m* at this temperature.<sup>130</sup> Thus, the problem of describing accurately the thermodynamic properties of NaCl(aq) and KCl(aq) to saturation concentrations in binary salt-H<sub>2</sub>O mixtures and in ternary NaCl-KCl-H<sub>2</sub>O systems, and in calculating solubility equilibria to 350°C is a severe test of the Margules expansion model.

For solubility calculations, equations for osmotic and activity coefficients at saturation pressure are of direct relevance. However, for purposes of developing general equations for the thermodynamic properties of electrolyte solutions, it is useful to recalculate experimental values to a single reference pressure. This allows experimental data on different solution properties (e.g., activities, enthalpies, and heat capacities) whose relationships with each other are defined on an isobaric basis, to be considered in the overall regression of the model equations. The parameters required to recalculate thermodynamic data from the experimental to the reference pressure can be determined from a regression of volumetric data. For the Margules expansion model, the pressure dependence of the excess Gibbs energy, osmotic coefficient, and activity coefficient can be derived from volumetric data as shown below.

The total volume,  $V$ , of the solution is given by

$$V = n_1 V_1^\circ + n_2 \bar{V}_2^\circ + (\partial G^{\text{ex}}/\partial P)_T \quad (35)$$

where  $V_1^\circ$  is the molal volume of the solvent, and  $\bar{V}_2^\circ$  is the partial molal volume of the salt at infinite dilution. The apparent molal volume,  ${}^\phi V$ , of the solute is given by

$${}^\phi V = (V - n_1 V_1^\circ)/n_2 \quad (36)$$

so that

$${}^\phi V = \bar{V}_2^\circ + (1/n_2)(\partial G^{\text{ex}}/\partial P)_{T,n_1,n_2} \quad (37)$$

Equations 28 and 29 for the excess Gibbs energy, and Equation 37 then yield

$$\phi V = (A_{v,x}/\rho)\ln(1 + \rho I^{1/2}) + \bar{V}_2^\circ - 2RTx_2[W_{1,MX}^v - x_1 U_{1,MX}^v] \quad (38)$$

where

$$A_{v,x} = -4RT\Omega^{1/2}(\partial A_\phi/\partial P)_T \quad (39)$$

$$W_{1,MX}^v = (\partial W_{1,MX}/\partial P)_T \quad (40)$$

and

$$U_{1,MX}^v = (\partial U_{1,MX}/\partial P)_T \quad (41)$$

Equations 40 and 41 relate the volumetric parameters  $W_{1,MX}^v$  and  $U_{1,MX}^v$  to the pressure dependence of the parameters  $W_{1,MX}$  and  $U_{1,MX}$  for the excess Gibbs energy and osmotic/activity coefficients. For NaCl(aq), Pabalan and Pitzer<sup>16</sup> derived values of  $W_{1,MX}^v$  and  $U_{1,MX}^v$  for NaCl(aq) for temperatures 25 to 350°C and pressures from 1 bar or saturation pressure to 1 kb, based on volumetric data on NaCl solutions. Initially, they regressed Equation 38 to isothermal and isobaric sets of experimental values. They obtained excellent fits to isobaric-isothermal sets of data, which indicated the P and T dependence of  $\bar{V}_2^\circ$ ,  $W_{1,MX}^v$ , and  $U_{1,MX}^v$ . The next step was to perform a simultaneous regression of NaCl(aq) apparent molal volumes from 25 to 350°C. Over this wide range of temperature, however, and particularly above 300°C, standard-state properties based on the infinitely dilute reference state exhibit a very complex behavior,<sup>105,131</sup> which is related to various peculiarities of the solvent. For example, in modeling NaCl(aq) volumetric properties, Rogers and Pitzer<sup>131</sup> adopted a reference composition of a "hydrated fused salt", NaCl · 10H<sub>2</sub>O, in order to minimize the P and T dependence of the standard-state volume and to adequately fit volumetric data to 300°C and 1 kb. Thus, in an analogous manner, Pabalan and Pitzer<sup>16</sup> used the (supercooled) fused salt as the reference state. The equation for the apparent molal volume on this basis can be easily derived from that for the excess Gibbs energy of Pitzer and Simonson,<sup>13</sup> and is given by

$$\phi V = (A_{v,x}/\rho) \ln[(1 + \rho I_x^{1/2})/(1 + \rho(I_x^\circ)^{1/2})] + V_2^{\circ fs} + 2RTx_1(W_{1,MX}^v + x_2 U_{1,MX}^v) \quad (42)$$

where  $I_x^\circ$  represents  $I_x$  for a pure fused salt and is  $1/2$  for salts of singly charged ions, while  $V_2^{\circ fs}$  is the molal volume for a (supercooled) fused salt. Values for the infinitely dilute reference state can be calculated from  $V_2^{\circ fs}$  using the relation

$$\bar{V}_2^\circ = V_2^{\circ fs} + 2RTW_{1,MX}^v - (A_{v,x}/\rho) \ln[1 + \rho(I_x^\circ)^{1/2}] \quad (43)$$

Apparent molal volumes of NaCl solutions from 25 to 350°C were used to fit Equation 42 and the following P and T function for  $\bar{V}_2^\circ$ ,  $W_{1,MX}^v$ , and  $U_{1,MX}^v$ :

$$f(T,P) = A + BP + CP^2 \quad (44a)$$

where

$$A = q_1 + q_2/T + q_3T + q_4T^2 + q_5/(647 - T)^2 \quad (44b)$$

$$B = q_6 + q_7/T + q_8T + q_9T^2 + q_{10}/(647 - T)^2 \quad (44c)$$

$$C = q_{11} + q_{12}/T + q_{13}T + q_{14}T^2 + q_{15}/(647 - T)^2 \quad (44d)$$

**TABLE 8**  
**Parameters for Equations 42 and 44 Evaluated from**  
**Apparent Molal Volumes of NaCl Solutions up to 350°C**  
**and 1 kb**

	$V_2^s$	$W_{1,MX}$	$U_{1,MX}$
$q_1$	-6.434497E + 02	-1.724835E - 02	-2.9789818E - 02
$q_2$	0.0	3.347333E + 00	5.7872110E + 00
$q_3$	3.554544E + 00	1.996689E - 05	3.5321836E - 05
$q_4$	-4.612823E - 03	3.861388E - 09	6.7591836E - 09
$q_5$	-3.254781E + 05	4.273295E + 00	4.4639601E + 00
$q_6$	4.496614E - 01	3.318704E - 06	1.2359971E - 05
$q_7$	-2.830405E + 01	-6.183551E - 04	-2.0125079E - 03
$q_8$	-2.047906E - 03	0.0	-1.7757055E - 08
$q_9$	2.627796E - 06	-9.914615E - 12	0.0
$q_{10}$	1.948423E + 03	-2.048634E - 02	-2.9326904E - 02
$q_{11}$	-1.201087E - 04	0.0	0.0
$q_{12}$	1.327249E - 02	0.0	0.0
$q_{13}$	3.539774E - 07	0.0	0.0
$q_{14}$	-3.546851E - 10	0.0	0.0
$q_{15}$	1.263778E - 01	0.0	0.0

Up to 300°C, the overall regression included values at pressures to 1 kb. At 350°C, however, only volumetric data at pressures less than or equal to 200 bars were included because the simple pressure function given by Equation 44a is inadequate to fit the 350°C data over the whole pressure range. The parameters for Equation 44 for  $\bar{V}_2^{os}$ ,  $W_{1,MX}$  and  $U_{1,MX}$  evaluated from the volumetric data are given in Table 8. Using this set of parameters the various thermodynamic properties of NaCl(aq) solutions can be recalculated to a reference pressure, here chosen to be 200 bars. Because the volumetric data for KCl solutions are more limited in concentration range and are less precise than those for NaCl solutions,<sup>9</sup> a separate evaluation of KCl(aq) volumetric data was not done. Instead, the pressure dependence of KCl(aq) properties was approximated using the values for NaCl(aq). This procedure has been shown to be successful for Na<sub>2</sub>SO<sub>4</sub>(aq).<sup>6</sup>

Osmotic coefficients of NaCl and KCl solutions from various sources were recalculated to the reference pressure of 200 bars.<sup>16</sup> An overall regression to each isobaric set of data was done to determine values of  $W_{1,MX}$  and  $U_{1,MX}$  as functions of temperature using the equation

$$f(T) = q_1 + q_2/T + q_3 \ln T + q_4 T + q_5 T^2 + q_6/(647 - T) \quad (45)$$

The parameters for NaCl(aq) and KCl(aq) evaluated from the osmotic coefficients are given in Table 9. These parameters, together with those of Table 8, permit the calculation of osmotic and activity coefficients of NaCl and KCl solutions to saturation concentration at pressures to 1 kb from 25 to 300°C, and at pressures to 200 bars above 300°C.

For solubility calculations, standard-state chemical potentials for the solids and for the aqueous species are needed. The latter can be derived from equations for standard-state heat capacities given by Pitzer et al.<sup>105</sup> and Pabalan and Pitzer<sup>9</sup> for NaCl(aq) and KCl(aq), respectively, or from the equation of state for standard-state properties of electrolytes given by Tanger and Helgeson.<sup>60</sup> In the present calculations, the former equations were used to 300°C, and the latter above 300°C. Standard-state values for the solids can be derived as discussed previously in Section IV.B, or directly from the Gibbs energy functions tabulated by Chase et al.<sup>57</sup> Figures 37 and 38 compare predicted solubilities in water for NaCl and KCl, respectively, to 350°C with experimental values taken from various sources. The

**TABLE 9**  
**Parameters for Equation 45 for  $W_{1,MX}$  and  $U_{1,MX}$  for NaCl and KCl Solutions**  
**Evaluated from Osmotic Coefficients up to 350°C at a Reference Pressure of 200**  
**bars**

	$W_{1,NaCl}$	$U_{1,NaCl}$	$W_{1,KCl}$	$U_{1,KCl}$
$q_1$	1.0620140E + 03	2.2783431E + 03	1.870602E + 03	3.999606E + 03
$q_2$	-2.3263776E + 04	-5.5141510E + 04	-5.071750E + 04	-1.063245E + 05
$q_3$	-2.0149086E + 02	-4.2036595E + 02	-3.326169E + 02	-7.145462E + 02
$q_4$	6.1763652E - 01	1.1574638E + 00	7.159419E - 01	1.610570E + 00
$q_5$	-2.9491559E - 04	-5.3640257E - 04	-2.458959E - 04	-6.069845E - 04
$q_6$	0.0	2.5441911E + 01	-1.634611E + 01	0.0

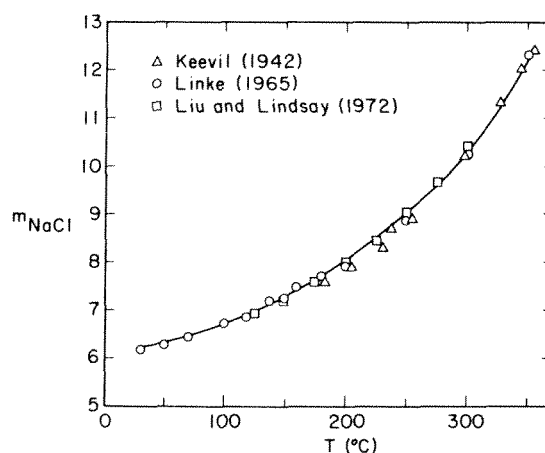


FIGURE 37. Solubilities of halite (NaCl) in water to 350°C. The curve represents values calculated using the Margules expansion model for activity coefficients (infinite dilution reference state), and standard-state chemical potentials for NaCl(aq) derived from the equations of Pitzer et al.<sup>105</sup> to 300°C, and of Tanger and Helgeson<sup>69</sup> above 300°C. (Reproduced with permission from Pabalan, R. T. and Pitzer, K. S., *Chemical Modeling of Aqueous Systems II*, Melchior, D. C. and Bassett, R. L., Eds., A.C.S. Symp. Series 416, American Chemical Society, Washington, D.C., 1990, chap. 4. Copyright 1990 American Chemical Society.)

agreement is very good, although there are substantial differences between various measurements for KCl.

## B. MODEL EQUATIONS AND SOLUBILITY CALCULATIONS IN TERNARY SYSTEMS

Of more interest are solubility calculations in the ternary system NaCl-KCl-H<sub>2</sub>O. The equations for the excess Gibbs energy and activity coefficients in a mixture of a solvent and two salts with a common ion, MX and NX, and with cation fraction F of M were derived by Pitzer and Simonson.<sup>13</sup> Their equation for the activity coefficient of the solute MX in the ternary mixture MX-NX-H<sub>2</sub>O based on a pure fused salt standard state, when converted to the infinitely dilute reference state (Appendix I, Chapter 3), is

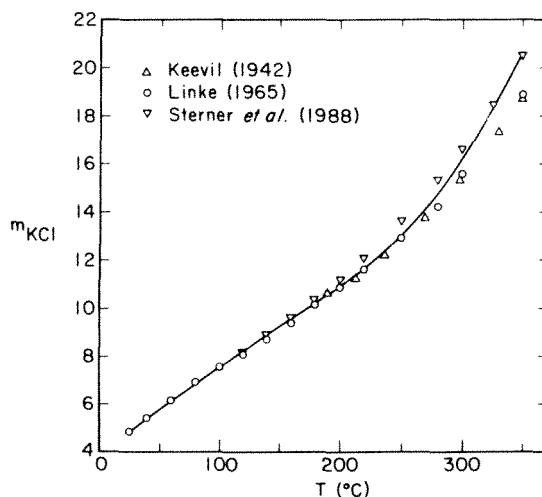


FIGURE 38. Solubilities of sylvite (KCl) in water to 350°C. The curve represents values calculated using the Margules expansion model for activity coefficients (infinite dilution reference state), and standard-state chemical potentials for KCl(aq) derived from the equations of Pabalan and Pitzer<sup>9</sup> to 300°C, and of Tanger and Helgeson<sup>60</sup> above 300°C. (Reproduced with permission from Pabalan, R. T. and Pitzer, K. S., *Chemical Modeling of Aqueous Systems II*, Melchior, D. C. and Bassett, R. L., Eds., A.C.S. Symp. Series 416, American Chemical Society, Washington, D.C., 1990, chap. 4. Copyright 1990 American Chemical Society.)

$$\begin{aligned} \ln(\gamma_M^* \gamma_X^*) = & -2A_x \{ (2/\rho) \ln(1 + \rho I_x^{1/2}) + I_x^{1/2} (1 - 2I_x) / (1 + \rho I_x^{1/2}) \} + 2[x_1(1 - x_1)F - 1]W_{1,MX} \\ & + 2x_1x_1\{ (1 - F + 2Fx_1)U_{1,MX} - (1 - F)[W_{1,NX} + (x_1 - x_1)U_{1,NX}] \} \\ & + x_1(1 - F)\{ (1 - x_1)F W_{MX,NX} + x_1[3F - 1 + 2x_1F(1 - 2F)]U_{M,N} + 2x_1(1 - 2x_1F)Q_{1,MX,NX} \} \end{aligned} \quad (46)$$

Here the total mole fraction of ions  $x_i = (1 - x_1)$ , whereupon  $x_M = Fx_i/2$ ,  $x_N = (1 - F)x_i/2$ , and  $x_X = x_i/2$ . The corresponding equation for  $(\gamma_M^* \gamma_X^*)$  can be obtained from Equation 46\* by interchanging subscripts M and N and interchanging F with  $(1 - F)$ ; note that  $W_{MX,NX}$  remains unchanged but that  $U_{N,M} = -U_{M,N}$ . In principle, all but one of the parameters of a ternary system MX-NX-H<sub>2</sub>O, namely,  $Q_{1,MX,NX}$ , can be determined from the binary systems. For NaCl-KCl-H<sub>2</sub>O, however, the temperatures of interest here are far below the melting points of NaCl and KCl which precludes the determination of  $W_{NaCl,KCl}$  and  $U_{Na,K}$  from that binary. Hence, these two parameters together with  $Q_{1,NaCl,KCl}$  must be evaluated from activity data in the ternary system. Values of  $W_{1,NaCl}$ ,  $W_{1,KCl}$ ,  $U_{1,NaCl}$ , and  $U_{1,KCl}$  have been previously determined from binary NaCl and KCl solutions.

Robinson<sup>117</sup> provided precise isopiestic data for the NaCl-KCl-H<sub>2</sub>O at 25°C, whereas Holmes et al.<sup>120</sup> provided data at 110, 140, 172, and 201°C. These measurements, however, extend only to ionic strengths of about 7.5 *m*, whereas the maximum solubility in the system already exceeds this value at  $T < 50^\circ\text{C}$ , and reaches more than 30 *m* at 350°C. It is apparent that a determination of the values of  $W_{NaCl,KCl}$ ,  $U_{Na,K}$ , and  $Q_{1,NaCl,KCl}$  should consider also the solubility data for mixtures of NaCl and KCl in solution. These are available from the

\* There is an error in this equation in Reference 16 and in the similar equation for  $\ln(\gamma_M \gamma_X)$  in References 13 and 14 in the location of the bracket which here precedes  $U_{M,N}$ .



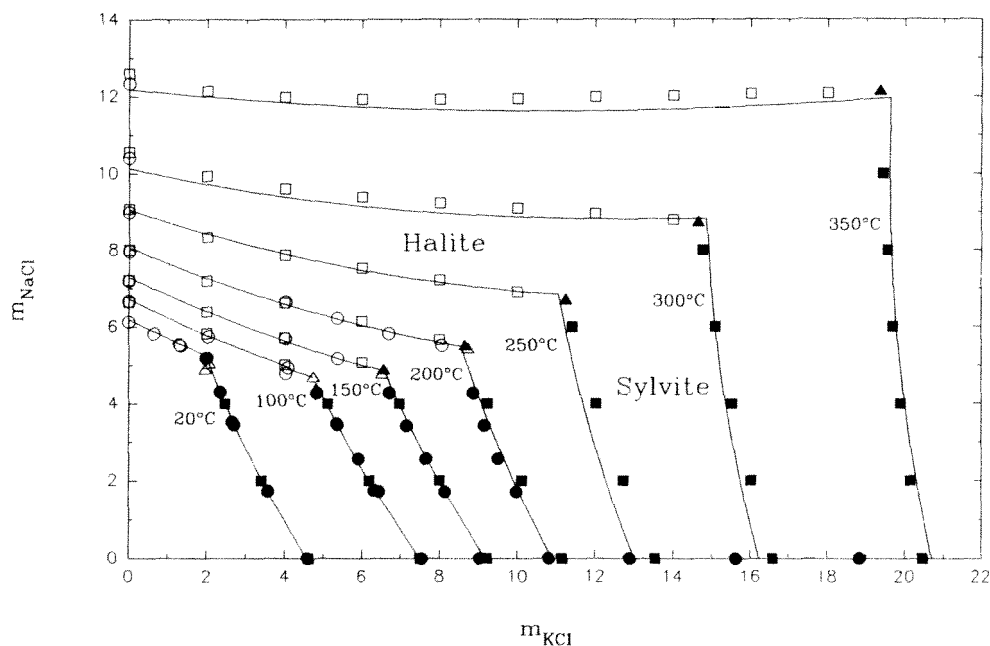


FIGURE 39. Solubilities of halite and/or sylvite in the NaCl-KCl-H<sub>2</sub>O system. The squares and circles are experimental data taken from Sterner et al.<sup>130</sup> and Linke,<sup>17</sup> respectively (open symbols for halite, closed symbols for sylvite). The open triangles are triple-point (halite + sylvite + saturated solution) data from Linke, and the closed triangles are triple-point data from Sterner et al. The curves are calculated as in Figures 37 and 38.

tabulation of Linke<sup>17</sup> and the extensive evaluation of Sterner et al.<sup>130</sup> Good agreement was obtained with the constant values  $U_{Na,K} = 1.250$  and  $Q_{1,NaCl,KCl} = 0.9547$ , together with a temperature-dependent expression for  $W_{NaCl,KCl}$  given by Equation 45 for which  $q_1, q_2, q_3, q_4, q_5,$  and  $q_6$  have values of 1779.00,  $-319.436, -46416.5, 0.73346, -0.00028096,$  and 0.0, respectively.\* Solubilities calculated from these parameters and those given in Tables 8 and 9 are compared to experimental data in Figure 39. The calculated values agree very well with those measured by Sterner et al.,<sup>130</sup> mostly within 2% and not exceeding 5%.\*\* Standard deviations between osmotic coefficients calculated using these parameters and experimentally determined values are 0.004, 0.003, 0.005, 0.006, and 0.008 for temperatures of 25, 110, 140, 172, and 201°C, respectively.

## VI. CONCLUSIONS

The calculation of mineral solubilities in electrolyte solutions requires models that accurately describe the thermodynamic properties of aqueous electrolytes over wide ranges of concentration as well as temperature and pressure. For practical applications to systems of geochemical or industrial importance, one needs thermodynamic models that can be generalized to multicomponent systems and which rely primarily on parameters that can be evaluated from simple systems. The examples given in this chapter clearly demonstrate that

\* The numerical value of  $U_{Na,K}$  in Reference 16 is different because of the error in the equation for  $\ln(\gamma_M^* \gamma_X^*)$ .

\*\* These calculations ignored the potential effects of solid solution formation. The very recent work of Sterner et al.<sup>135</sup> indicates that at temperatures above about 300°C, formation of NaCl-KCl solid solution becomes significant. This reduces KCl(s) and NaCl(s) activities from the values for the pure solids, and will result in slightly lower calculated solubilities at temperatures above 300°C if the Margules parameters given here are used.

two models based on general equations for the excess Gibbs energy of aqueous electrolyte mixtures meet these criteria. The ion interaction model has been shown to be successful in modeling mineral solubilities for a large variety of systems and over wide ranges of temperature conditions. The Margules expansion model is at a less mature stage of development, but the examples given in this chapter indicate that it is a useful alternative for systems which may extend to very high concentration and potentially to fused salt systems.

### ACKNOWLEDGMENT

Some of the research that forms the basis of this chapter was supported by the U.S. Department of Energy or the Nuclear Regulatory Commission.

### APPENDIX: NUMERICAL EXPRESSIONS FOR TEMPERATURE DEPENDENCY

Given below are expressions for the temperature dependency of the ion interaction parameters and the standard-state heat capacities for several important salts as well as HCl and NaOH. The functions are those actually used in the mineral solubility calculations reported above, together with comments and citations. Citations and comments are also included for two cases where new but more complex expressions have been published very recently. Alternate expressions are also given by Greenberg and Møller<sup>8</sup> and Møller<sup>7</sup> for several of these solutes for the range 273 to 523 K. For optimum accuracy, all ion interaction parameters for a particular solute should be taken from the same source.

Pressures are here designated by P and are in bars; standard-state heat capacities are in  $\text{J} \cdot \text{mol}^{-1} \cdot \text{K}^{-1}$ ;  $\beta^{(0)}$  and  $\beta^{(1)}$  are in  $\text{kg} \cdot \text{mol}^{-1}$ ; while  $C^\phi$  is in  $\text{kg}^2 \cdot \text{mol}^{-2}$ . T is in K and  $T_r = 298.15 \text{ K}$ .

#### NaCl(aq)

Ion interaction parameters — Pitzer et al.,<sup>105</sup> 273 to 573 K and saturation pressure to 1 kbar. P refers to pressure in bars.

$$\begin{aligned}
 f(T) = & Q1/T + Q2 + Q3 P + Q4 P^2 + Q5 P^3 + Q6 \ln(T) \\
 & + (Q7 + Q8P + Q9 P^2 + Q10 P^3)T + (Q11 + Q12 P + Q13 P^2)T^2 \\
 & + (Q14 + Q15 P + Q16 P^2 + Q17 P^3)/(T - 227) + (Q18 + Q19 P \\
 & + Q20 P^2 + Q21 P^3)/(680 - T)
 \end{aligned}$$

	$\beta^{(0)}$	$\beta^{(1)}$	$C^\phi = 2C$
Q1	-656.81518	119.31966	-6.1084589
Q2	24.86912950	-0.48309327	4.0217793E - 1
Q3	5.381275267E - 5	0	2.2902837E - 5
Q4	-5.588746990E - 8	0	0
Q5	6.589326333E - 12	0	0
Q6	-4.4640952	0	-0.075354649
Q7	0.01110991383	1.4068095E - 3	1.531767295E - 4
Q8	-2.657339906E - 7	0	-9.0550901E - 8
Q9	1.746006963E - 10	0	0
Q10	1.046261900E - 14	0	0
Q11	-5.307012889E - 6	0	-1.538600820E - 8
Q12	8.634023325E - 10	0	8.6926600E - 11
Q13	-4.178596200E - 13	0	0

	$\beta^{(0)}$	$\beta^{(1)}$	$C^{\Phi} = 2C$
Q14	-1.579365943	-4.2345814	0.3531041360
Q15	2.202282079E - 3	0	-4.3314252E - 4
Q16	-1.310550324E - 7	0	0
Q17	-6.3813688333E - 11	0	0
Q18	9.706578079	0	-0.09187145529
Q19	-0.02686039622	0	5.1904777E - 4
Q20	1.534474401E - 5	0	0
Q21	-3.215398267E - 9	0	0

Standard-state heat capacity — the following equation was fit to values from 273 to 573 K and at 1 bar or saturation pressure tabulated by Pitzer et al.,<sup>105</sup> Table A-4. For values at other pressures, the reader is referred to the tables and equations given by Pitzer et al.<sup>105</sup> which are valid in the range 273 to 573 K and to 1 kbar pressure.

$$C_p^{\circ} = -1.848175E6 + 4.411878E7/T + 3.390654E5 \ln(T) \\ - 8.893249E2T + 4.005770E - 1T^2 - 7.244279E4/(T - 227) \\ - 4.098218E5/(647 - T)$$

A computer program to calculate various properties of NaCl(aq) from the equations of Pitzer et al.<sup>105</sup> is available.<sup>132</sup>

#### KCl(aq)

Ion interaction parameters — Holmes and Mesmer,<sup>98</sup> 273 to 523 K.

$$f(T) = Q1 + Q2(1/T - 1/T_R) + Q3 \ln(T/T_R) + Q4(T - T_R) + Q5(T^2 - T_R^2) \\ + Q6 \ln(T - 260)$$

	$\beta^{(0)}$	$\beta^{(1)}$	$C^{\Phi} = 2C$
Q1	0.04808	0.0476	-7.88E - 4
Q2	-758.48	303.9	91.270
Q3	-4.7062	1.066	0.58643
Q4	0.010072	0	-0.0012980
Q5	-3.7599E - 6	0	4.9567E - 7
Q6	0	0.0470	0

Standard-state heat capacity — Holmes and Mesmer,<sup>98</sup> 273 to 523 K.

$$C_p^{\circ} = -991.51 + 5.56452 T - 0.00852996 T^2 - 686/(T - 270)$$

A more comprehensive and complex treatment including volumetric properties which yield the pressure dependencies of other parameters was presented very recently by Pabalan and Pitzer.<sup>9</sup>

#### MgCl<sub>2</sub>(aq)

Ion interaction parameters — de Lima and Pitzer,<sup>112</sup> with equation for  $C_{MX}^{\Phi}$  modified to fit the solubility data, 298 to 473 K.

$$f(T) = Q1 T^2 + Q2 T + Q3$$

	$\beta^{(0)}$	$\beta^{(1)}$	$C^\phi = 2^{3/2} C$
Q1	5.93915E - 7	2.60169E - 5	2.41831E - 7
Q2	-9.31654E - 4	-1.09438E - 2	-2.49949E - 4
Q3	0.576066	2.60135	5.95320E - 2

Standard-state heat capacity — Phutela et al.,<sup>108</sup> 298 to 453 K.

$$C_p^\circ = -7.39872E6/T + 7.96487E4 - 3.25868E2 T \\ + 5.98722E - 1 T^2 - 4.21187E - 4 T^3$$

### CaCl<sub>2</sub>(aq)

Ion interaction parameters — Greenberg and Møller,<sup>8</sup> 298 to 523 K, 0 to 4 mol · kg<sup>-1</sup>.

$$f(T) = Q1 + Q2 T + Q3/T + Q4 \ln T + Q5/(T - 263) + Q6 T^2 + Q7/(680 - T)$$

	$\beta^{(0)}$	$\beta^{(1)}$	$C^\phi = 2^{3/2} C$
Q1	-9.41895832E1	3.4787	1.93056024E1
Q2	-4.0475002E - 2	-1.5417E - 2	9.77090932E - 3
Q3	2.34550368E3	0	-4.28383748E2
Q4	1.70912300E1	0	-3.57996343
Q5	-9.22885841E - 1	0	8.82068538E - 2
Q6	1.51488122E - 5	3.1791E - 5	-4.62270238E - 6
Q7	-1.39082000	0	9.91113465

A simpler equation valid to 473 K and 4.3 mol · kg<sup>-1</sup> is given by Phutela and Pitzer.<sup>133</sup>

Standard-state heat capacity — Phutela et al.,<sup>108</sup> 298 to 373 K.

$$C_p^\circ = -1.26721E6/T + 7.41013E3 - 11.5222 T$$

### Na<sub>2</sub>SO<sub>4</sub>(aq)

Ion interaction parameters — Pabalan and Pitzer,<sup>6</sup> 298 to 573 K and 1 bar or saturation pressure,  $T_r = 298.15$  K. Note that these parameters are based on the value  $\alpha_1 = 1.4$  instead of the usual value of 2.0 for a 2-1 electrolyte.

$$f(T) = p_1 T^2/6 + p_2 T/2 + p_3 T^2 (\ln T - 5/6)/6 + p_4 T^3/12 \\ + p_5 T^4/20 + p_6 [T/2 + 3(227)^2/2 T + 227(1 - 227/T) \ln(T - 227)] \\ - p_7 [T/2 + 3(647)^2/2 T + 647(1 - 647/T) \ln(647 - T)] \\ - k_1/T - f_L(T_r)[T_r^2/T] + K_2 + f_G(T_r)$$

	$\beta^{(0)}$	$\beta^{(1)}$	$C = C^\phi/2^{3/2}$
$p_1$	2.1549644E - 02	3.6439508	-4.6590760E - 02
$p_2$	-7.6918219E - 01	-9.1962646E + 01	1.1711403
$p_3$	-3.5486084E - 03	-6.5961772E - 01	8.4319701E - 03
$p_4$	4.0811837E - 06	1.6043868E - 03	-2.0439550E - 05
$p_5$	0.0	-6.5972836E - 07	8.3348147E - 09
$p_6$	0.0	1.6491982E - 01	-1.3147008E - 03
$p_7$	0.0	2.2057312E - 01	-1.6797063E - 03
$f_L(T_r, 1 \text{ bar})$	1.738512E - 03	5.820066E - 03	-1.117462E - 04
$f_G(T_r, 1 \text{ bar})$	-1.255087E - 02	7.037660E - 01	3.808550E - 03
$K_1$	3.915.434531	708.447.986899	-6.717.929066
$K_2$	55.769488	5.768.102375	-68.202263

Standard-state heat capacity — Pabalan and Pitzer,<sup>6</sup> 200 bars, 298 to 573 K.

$$C_p^\circ = 1727842 - 4.643364E7/T - 307864.3 \ln T \\ + 680.2831 T - 0.2438667 T^2 + 100338.7/(T - 227) \\ - 252748.6/(647 - T) \text{ J} \cdot \text{mol}^{-1} \cdot \text{K}^{-1}$$

The change of heat capacity with pressure for  $\text{Na}_2\text{SO}_4(\text{aq})$  was assumed to be twice that for  $\text{NaCl}(\text{aq})$  in the absence of detailed volumetric data for  $\text{Na}_2\text{SO}_4(\text{aq})$ . A simpler equation from Holmes and Mesmer<sup>106</sup> valid from 276 to 498 K and 1 bar of saturation pressure may suffice; it is

$$C_p^\circ = -1206.2 + 7.6405 T - (1.23672E - 2)T^2 - 6045/(T - 263)$$

### $\text{K}_2\text{SO}_4(\text{aq})$

Ion interaction parameters — Holmes and Mesmer,<sup>106</sup> 273 to 498 K. Note: these parameters are consistent with using a value of  $\alpha_1 = 1.4$ , instead of the usual value of 2.0.

$$f(T) = Q1 + Q2(T_R - T_R^2/T) + Q3(T^2 + 2T_R^2/T - 3T_R^2) + Q4(T + T_R^2/T - 2T_R) \\ + Q5[\ln(T/T_R) + T_R/T - 1] + Q6\{1/(T - 263) + (263 T - T_R^2)/[T(T_R - 263)^2]\} \\ + Q7\{1/(680 - T) + (T_R^2 - 680 T)/[T(680 - T_R)^2]\}$$

	$\beta^{(0)}$	$\beta^{(1)}$	$C^\phi = 2^{3/2} C$
Q1	0	0.6179	9.1547E - 3
Q2	7.476E - 4	6.85E - 3	0
Q3	0	5.576E - 5	0
Q4	4.265E - 3	-5.841E - 2	-1.81E - 4
Q5	-3.088	0	0
Q6	0	-0.90	0
Q7	0	0	0

Standard-state heat capacity:

$$C_p^\circ(\text{K}_2\text{SO}_4) = 2C_p^\circ(\text{KCl}) + C_p^\circ(\text{Na}_2\text{SO}_4) - 2C_p^\circ(\text{NaCl})$$

### $\text{MgSO}_4(\text{aq})$

Ion interaction parameters — Phutela and Pitzer,<sup>107</sup> 298 to 473 K. Note that the final column gives the temperature coefficients for C. For  $\text{MgSO}_4$ , this is related to  $C^\phi$  by  $C^\phi = 4C$  (see Equation 15).

$$f(T) = Q1(T/2 + 298^2/2 T - 298) + Q2(T^2/6 + 298^3/3 T - 298^2/2) \\ + Q3(T^3/12 + 298^4/4 T - 298^3/3) + Q4(T^4/20 + 298^5/5 T - 298^4/4) \\ + (298 - 298^2/T)Q5 + Q6$$

	$\beta^{(0)}$	$\beta^{(1)}$	$\beta^{(2)}$	$C = C^\phi/4$
Q1	-1.0282	-2.9596E - 1	-1.3764E - 1	1.0541E - 1
Q2	8.4790E - 3	9.4564E - 4	1.2121E - 1	-8.9316E - 4
Q3	-2.33667E - 5	0	-2.7642E - 4	2.51E - 6
Q4	2.1575E - 8	0	0	-2.3436E - 9
Q5	6.8402E - 4	1.1028E - 2	-2.1515E - 1	-8.7899E - 5
Q6	0.21499	3.3646	-32.743	0.006993

Standard-state heat capacity — Phutela and Pitzer,<sup>107</sup> 298 to 473 K.

$$C_p^\circ = -6.2543E6/T + 6.5277E4 - 2.6044E2 T + 4.6930E - 1 T^2 \\ - 3.2656E - 4 T^3$$

### HCl(aq)

Ion interaction parameters — Holmes et al.,<sup>134</sup> 273 to 523 K. The equation and parameters listed are valid to  $7 \text{ mol} \cdot \text{kg}^{-1}$ , but this paper also includes more complex equations valid to 648 K and to  $16 \text{ mol} \cdot \text{kg}^{-1}$ ; also note that the equations use  $\rho$ , the density in  $\text{kg} \cdot \text{m}^{-3}$  of pure water at the particular P and T, and that they include pressure dependence to 400 bars.

$$f(T) = Q1 + Q2 \ln(\rho/997) + Q3(\rho - 997) + Q4(T - T_R) + Q5(P - 1)$$

	$\beta^{(0)}$	$\beta^{(1)}$	$C = C^*/2$
Q1	0.17690	0.2973	0.362E - 3
Q2	-9.140E - 2	16.147	0
Q3	0	-1.7631E - 2	0
Q4	-4.034E - 4	0	-3.036E - 5
Q5	6.20E - 6	7.20E - 5	0

Standard-state heat capacity — Holmes et al.,<sup>134</sup> 273 to 648 K.

$$C_p^\circ = 17.93 - 16.79 T/(T - 240) + 6.4579E5 TX_p$$

where

$$X_p = [(\partial^2 \ln \epsilon / \partial T^2)_p - (\partial \ln \epsilon / \partial T)_p^2] / \epsilon$$

with  $\epsilon$  the dielectric constant (relative permittivity).

### NaOH(aq)

Ion interaction parameters — Pabalan and Pitzer,<sup>110</sup> 0 to 350°C and saturation pressure to 400 bars. P refers to pressure in bars.

$$f(T) = Q1 + Q2 P + (Q3 + Q4 P)/T + Q5 \ln(T) + (Q6 + Q7 P)T \\ + (Q8 + Q9 P)T^2 + Q10/(T - 227) + (Q11 + Q12 P)/(647 - T)$$

	$\beta^{(0)}$	$\beta^{(1)}$	$C^* = 2C$
Q1	2.7682478E + 2	4.6286977E + 2	-1.6686897E + 1
Q2	-2.8131778E - 3	0	4.0534778E - 4
Q3	-7.3755443E + 3	-1.0294181E + 4	4.5364961E + 2
Q4	3.7012540E - 1	0	-5.1714017E - 2
Q5	-4.9359970E + 1	-8.5960581E + 1	2.9680772
Q6	1.0945106E - 1	2.3905969E - 1	-6.5161667E - 3
Q7	7.1788733E - 6	0	-1.0553037E - 6
Q8	-4.0218506E - 5	-1.0795894E - 4	2.3765786E - 6
Q9	-5.8847404E - 9		8.9893405E - 10
Q10	1.1931122E + 1	0	-6.8923899E - 1
Q11	2.4824963		-8.1156286E - 2
Q12	-4.8217410E - 3	0	0

A more precise treatment based in part on new measurements of heat capacities and enthalpies but for the more restricted range to 523 K has been published recently by Simonson et al.<sup>111</sup>

## REFERENCES

- Zemaitis, J. F., Jr., Clark, D. M., Rafal, M., and Scrivner, N. C., *Handbook of Aqueous Electrolyte Thermodynamics: Theory and Applications*, AIChE, New York, 1986.
- Pitzer, K. S., Thermodynamics of electrolytes. I. Theoretical basis and general equations, *J. Phys. Chem.*, 77, 268, 1973.
- Harvie, C. E. and Weare, J. H., The prediction of mineral solubilities in natural waters: the Na-K-Mg-Ca-Cl-SO<sub>4</sub>-H<sub>2</sub>O system from zero to high concentration at 25°C, *Geochim. Cosmochim. Acta*, 44, 981, 1980.
- Harvie, C. E., Møller, N., and Weare, J. H., The prediction of mineral solubilities in natural waters: the Na-K-Mg-Ca-H-Cl-SO<sub>4</sub>-OH-HCO<sub>3</sub>-CO<sub>3</sub>-CO<sub>2</sub>-H<sub>2</sub>O system to high ionic strengths at 25°C, *Geochim. Cosmochim. Acta*, 48, 723, 1984.
- Pabalan, R. T. and Pitzer, K. S., Thermodynamics of concentrated electrolyte mixtures and the prediction of mineral solubilities to high temperatures for mixtures in the system Na-K-Mg-Cl-SO<sub>4</sub>-OH-H<sub>2</sub>O, *Geochim. Cosmochim. Acta*, 51, 2429, 1987.
- Pabalan, R. T. and Pitzer, K. S., Heat capacity and other thermodynamic properties of Na<sub>2</sub>SO<sub>4</sub>(aq) in hydrothermal solutions and the solubilities of sodium sulfate minerals in the system Na-Cl-SO<sub>4</sub>-OH-H<sub>2</sub>O to 300°C, *Geochim. Cosmochim. Acta*, 52, 2393, 1988.
- Møller, N., The prediction of mineral solubilities in natural waters: a chemical equilibrium model for the CaSO<sub>4</sub>-NaCl-CaCl<sub>2</sub>-H<sub>2</sub>O system to high temperature and concentration, *Geochim. Cosmochim. Acta*, 52, 821, 1988.
- Greenberg, J. P. and Møller, N., The prediction of mineral solubilities in natural waters: a chemical equilibrium model for the Na-K-Ca-Cl-SO<sub>4</sub>-H<sub>2</sub>O system to high concentrations from 0 to 250°C, *Geochim. Cosmochim. Acta*, 53, 2503, 1989.
- Pabalan, R. T. and Pitzer, K. S., Apparent molar heat capacity and other thermodynamic properties of aqueous KCl solutions to high temperatures and pressures, *J. Chem. Eng. Data*, 33, 354, 1988.
- Pabalan, R. T. and Pitzer, K. S., Prediction of high-temperature thermodynamic properties of mixed electrolyte solutions including solubility equilibria, vapor pressure depression and boiling point elevation, in *Proc. 1987 Symp. on Chemistry in High-Temperature Water*, EPRI NP-6005, Electric Power Research Institute, Palo Alto, CA, 1990, D4f-1.
- Spencer, R. J., Møller, N., and Weare, J. H., The prediction of mineral solubilities in natural waters: a chemical equilibrium model for the Na-K-Ca-Mg-Cl-SO<sub>4</sub>-H<sub>2</sub>O system at temperatures below 25°C, *Geochim. Cosmochim. Acta*, 54, 575, 1990.
- Ananthaswamy, J. and Atkinson, G., Thermodynamics of concentrated electrolyte mixtures. V. A review of the thermodynamic properties of aqueous calcium chloride in the temperature range 273.15–373.15 K, *J. Chem. Eng. Data*, 30, 120, 1985.
- Pitzer, K. S. and Simonson, J. M., Thermodynamics of multicomponent, miscible, ionic systems: theory and equations, *J. Phys. Chem.*, 90, 3005, 1986.
- Simonson, J. M. and Pitzer, K. S., Thermodynamics of multicomponent miscible, ionic systems: the system LiNO<sub>3</sub>-KNO<sub>3</sub>-H<sub>2</sub>O, *J. Phys. Chem.*, 90, 3009, 1986.
- Weres, O. and Tsao, L., Activity of water mixed with molten salts at 317°C, *J. Phys. Chem.*, 90, 3014, 1986.
- Pabalan, R. T. and Pitzer, K. S., Models for aqueous electrolyte mixtures for systems extending from dilute solutions to fused salts, in *Chemical Modeling of Aqueous Systems II*, Melchior, D. C. and Bassett, R. L., Eds., A.C.S. Symp. Series 416, American Chemical Society, Washington, D.C., 1990, chap. 4.
- Linke, W. F., *Solubilities of Inorganic and Metal Organic Compounds*, Vol. 1 and 2, 4th ed., American Chemical Society, Washington, D.C., 1965.
- Harvie, C. E., Eugster, H. P., and Weare, J. H., Mineral equilibria in the six-component seawater system, Na-K-Mg-Ca-SO<sub>4</sub>-Cl-H<sub>2</sub>O at 25°C. II. Compositions of the saturated solutions, *Geochim. Cosmochim. Acta*, 46, 1603, 1982.
- Filippov, V. K., Dmitriev, G. V., and Yakovleva, S. I., Use of the Pitzer method for calculating the activity of components in mixed solutions of electrolytes according to data on solubility, *Dokl. Akad. Nauk SSSR Fiz. Khim.*, 252, 156, 1980; Engl. Transl., 252, 359, 1980.
- Filippov, V. K. and Nokhrin, V. I., The Li<sub>2</sub>SO<sub>4</sub>-MSO<sub>4</sub>-H<sub>2</sub>O systems (M = Mg, Ni, Zn) at 25°C, *Russ. J. Inorg. Chem.*, 30, 282, 1985.
- Filippov, V. K. and Nokhrin, V. I., Li<sub>2</sub>SO<sub>4</sub>-MSO<sub>4</sub>-H<sub>2</sub>O (M = Mn, Co, and Cu) systems at 25°C, *Russ. J. Inorg. Chem.*, 30, 289, 1985.
- Filippov, V. K., Barkov, D. S., and Federov, Ju. A., Die anwendung der Pitzergleichungen für die berechnung der löslichkeit im system Cu(NO<sub>3</sub>)<sub>2</sub>-Ni(NO<sub>3</sub>)<sub>2</sub>-H<sub>2</sub>O bei 25°C, *Z. Phys. Chem. Leipzig*, 266, 129, 1985.
- Filippov, V. K., Nokhrin, V. I., and Muzalevskaya, A. P., A thermodynamic study of the Na<sub>2</sub>SO<sub>4</sub>-ZnSO<sub>4</sub>-H<sub>2</sub>O and Na<sub>2</sub>SO<sub>4</sub>-CdSO<sub>4</sub>-H<sub>2</sub>O systems at 25°C, *Russ. J. Inorg. Chem.*, 30, 2407, 1985.

24. **Filippov, V. K., Charykova, M. V., and Trofimov, Yu. M.**, Thermodynamics of the system  $\text{NH}_4\text{H}_2\text{PO}_4$ - $(\text{NH}_4)_2\text{SO}_4$ - $\text{H}_2\text{O}$  at 25°C. *J. Appl. Chem. U.S.S.R.*, 58, 1807, 1985.
25. **Filippov, V. K. and Nokhrin, V. I.**, Solubility in the  $\text{Na}_2\text{SO}_4$ - $\text{CuSO}_4$ - $\text{H}_2\text{O}$  system at 25°C. *Russ. J. Inorg. Chem.*, 30, 1688, 1985.
26. **Filippov, V. K., Charykov, N. A., and Fedorov, Yu. A.**, The  $\text{NaCl}$ - $\text{NiCl}_2$ - $\text{H}_2\text{O}$  and  $\text{NaCl}$ - $\text{CuCl}_2$ - $\text{H}_2\text{O}$  systems at 25°C. *Russ. J. Inorg. Chem.*, 31, 1071, 1986.
27. **Filippov, V. K., Charykov, N. A., and Fedorov, Yu. A.**, The  $\text{NaCl}$ - $\text{NiCl}_2$ - $\text{H}_2\text{O}$  and  $\text{NaCl}$ - $\text{CuCl}_2$ - $\text{H}_2\text{O}$  systems at 25°C. *Russ. J. Inorg. Chem.*, 31, 1071, 1986.
27. **Filippov, V. K., Kalinkin, A. M., and Vasin, S. K.**, Thermodynamics of phase equilibria of aqueous ( $\text{Li}_2\text{SO}_4 + \text{Cs}_2\text{SO}_4$ ), ( $\text{Na}_2\text{SO}_4 + \text{Cs}_2\text{SO}_4$ ), and ( $\text{K}_2\text{SO}_4 + \text{Cs}_2\text{SO}_4$ ) at 298.15 K using Pitzer's model. *J. Chem. Thermodyn.*, 19, 185, 1987.
28. **Filippov, V. K., Charykov, N. A., and Rumyantsev, A. V.**, Application of Pitzer's method to water-salt systems with complex formation, *Dokl. Akad. Nauk SSSR Fiz. Khim.*, 296, 665, 1987; Engl. transl., 296, 936, 1987.
29. **Filippov, V. K., Barkov, D. S., and Federov, Yu. A.**, Application of the Pitzer equations to the solubility of ternary aqueous nitrate solutions at 25°C. *J. Solution Chem.*, 15, 611, 1986.
30. **Filippov, V. K. and Kalinkin, A. M.**, The  $\text{Li}_2\text{SO}_4$ - $\text{Na}_2\text{SO}_4$ - $\text{H}_2\text{O}$  system at 25°C. *Russ. J. Inorg. Chem.*, 32, 120, 1987.
31. **Filippov, V. K., Charykova, M. V., and Trofimov, Yu. M.**, Thermodynamic study of the systems  $\text{Na}^+$ ,  $\text{NH}_4^+$  ||  $\text{SO}_4^{2-}$ - $\text{H}_2\text{O}$  and  $\text{Na}^+$ ,  $\text{NH}_4^+$  ||  $\text{H}_2\text{PO}_4$ - $\text{H}_2\text{O}$  at 25°C. *J. Appl. Chem. U.S.S.R.*, 60, 237, 1987.
32. **Filippov, V. K., Charykova, M. V., and Trofimov, Yu. M.**, Phase equilibria in the system  $\text{Na}$ ,  $\text{NH}_4$  ||  $\text{SO}_4$ ,  $\text{H}_2\text{PO}_4$  at 25°C. *J. Appl. Chem. U.S.S.R.*, 60, 1160, 1987.
33. **Filippov, V. K. and Charykova, M. V.**, Die anwendung der Pitzer-gleichungen für die berechnung der phasengleichgewichte in quaternaren system  $\text{Na}^+$ ,  $\text{NH}_4^+$  ||  $\text{Cl}^-$ ,  $\text{SO}_4^{2-}$ - $\text{H}_2\text{O}$  bei 25°C. *Z. Phys. Chem. (Leipzig)*, 270, 49, 1989.
34. **Filippov, V. K., Kalinkin, A. M., and Vasin, S. K.**, Thermodynamics of phase equilibria of aqueous (lithium sulfate + alkali-metal sulfate) (alkali metal: Na, K, and Rb), and (sodium sulfate + rubidium sulfate) at 298.15 K using Pitzer's model. *J. Chem. Thermodyn.*, 21, 935, 1989.
35. **Filippov, V. K. and Cheremnykh, L. M.**, Calculation of phase equilibria of the system  $\text{Na}$ ,  $\text{K}$  ||  $\text{Cl}$ ,  $\text{SO}_4$ - $\text{H}_2\text{O}$  at 25°C. *J. Appl. Chem. U.S.S.R.*, 60, 34, 1986.
36. **Filippov, V. K. and Charykov, N. A.**, Phase equilibria in the system  $\text{Na}$ ,  $\text{Co}$  ||  $\text{Cl}$ ,  $\text{SO}_4$ - $\text{H}_2\text{O}$  at 25°C. *J. Appl. Chem. U.S.S.R.*, 59, 2255, 1986.
37. **Filippov, V. K., Cheremnykh, L. M., and Shestakov, N. E.**, Phase equilibria in the system  $\text{K}$ ,  $\text{Mg}$  ||  $\text{Cl}$ ,  $\text{SO}_4$ - $\text{H}_2\text{O}$  at 25°C. *J. Appl. Chem. U.S.S.R.*, 60, 1831, 1986.
38. **Filippov, V. K., Prieto, M. S., and Charykova, M. V.**, Utilizacion de la ecuacion de Pitzer para el calculo de solubilidad del sistema  $\text{NH}_4$ ,  $\text{Mg}$  ||  $\text{SO}_4$ - $\text{H}_2\text{O}$  a 25° y 30°C. *Rev. Cubana Quim.*, 3, 37, 1987.
39. **Filippov, V. K. and Charykov, N. A.**, Phase equilibria in the  $\text{Na}^+$ ,  $\text{Mn}^{2+}$  ||  $\text{Cl}^-$ ,  $\text{SO}_4^{2-}$ - $\text{H}_2\text{O}$  system at 25°C. *Russ. J. Inorg. Chem.*, 34, 916, 1989.
40. **Reardon, E. J. and Beckie, R. D.**, Modelling chemical equilibria of acid mine-drainage: the  $\text{FeSO}_4$ - $\text{H}_2\text{SO}_4$ - $\text{H}_2\text{O}$  system. *Geochim. Cosmochim. Acta*, 51, 2355, 1987.
41. **Felmy, A. R. and Weare, J. H.**, The prediction of borate mineral equilibria in natural waters: application to Searles Lake, California. *Geochim. Cosmochim. Acta*, 50, 2771, 1986.
42. **Clegg, S. L. and Brimblecombe, P.**, Estimated mean activity coefficients of aqueous  $\text{BeCl}_2$  and properties of solution mixtures containing  $\text{Be}^{2+}$  ions. *J. Chem. Soc. Faraday Trans. 1*, 85, 157, 1989.
43. **Reardon, E. J. and Armstrong, D. K.**, Celestite ( $\text{SrSO}_4$ ) solubility in water, seawater, and  $\text{NaCl}$  solution. *Geochim. Cosmochim. Acta*, 51, 63, 1987.
44. **Reardon, E. J.**, Ion interaction parameters for  $\text{Al}$ - $\text{SO}_4$  and application to the prediction of metal sulfate solubility in binary salt systems. *J. Phys. Chem.*, 92, 6426, 1988.
45. **Reardon, E. J.**, Ion interaction model applied in the  $\text{NiSO}_4$ - $\text{H}_2\text{SO}_4$ - $\text{H}_2\text{O}$  system. *J. Phys. Chem.*, 93, 4630, 1989.
46. **Monnin, C. and Galinier, C.**, The solubility of celestite and barite in electrolyte solutions and natural waters at 25°C: a thermodynamic study. *Chem. Geol.*, 71, 283, 1988.
47. **Chan, C.-Y. and Khoo, K. H.**, Calculation of activities and solubilities of alkali metal perchlorates at high ionic strengths in multicomponent aqueous systems. *J. Solution Chem.*, 17, 547, 1988.
48. **Felmy, A. R., Rai, D., and Amonette, J. E.**, The solubility of barite and celestite in sodium sulfate: evaluation of thermodynamic data. *J. Solution Chem.*, 19, 175, 1990.
49. **Langmuir, D. and Melchior, D.**, The geochemistry of Ca, Sr, Ba and Ra sulfates in some deep brines from the Palo Duro Basin, Texas. *Geochim. Cosmochim. Acta*, 49, 2423, 1985.
50. **Gueddari, M., Monnin, C., Perret, D., Fritz, B., and Tardy, Y.**, Geochemistry of the brines of Chott El Jerid in southern Tunisia: application of Pitzer's equations. *Chem. Geol.*, 39, 165, 1983.
51. **Meijer, J. A. M. and Van Rosmalen, G. M.**, Solubilities and supersaturation of calcium sulfate and its hydrates in seawater. *Desalination*, 51, 255, 1984.



52. **Monnin, C. and Schott, J.**, Determination of the solubility products of sodium carbonate minerals and application to trona deposition in Lake Magadi (Kenya), *Geochim. Cosmochim. Acta*, 48, 571, 1984.
53. **Williams-Jones, A. E. and Samson, I. M.**, Theoretical estimation of halite solubility in the system NaCl-CaCl<sub>2</sub>-H<sub>2</sub>O: applications to fluid inclusions, *Can. Mineral.*, 28, 299, 1990.
54. **Aggarwal, P. K., Gunter, W. D., and Kharaka, Y. K.**, Effect of pressure on aqueous equilibria, in *Chemical Modeling in Aqueous Systems II*, Melchior, D. C. and Bassett, R. L., Eds., American Chemical Society, Washington, D.C., 1990, chap. 7.
55. **Monnin, C.**, The influence of pressure on the activity coefficients of the solutes and on the solubility of minerals in the system Na-Ca-Cl-SO<sub>4</sub>-H<sub>2</sub>O to 200°C and 1 kbar, and to high NaCl concentration, *Geochim. Cosmochim. Acta*, 54, 3265, 1990.
56. **Robie, R. A., Hemingway, B. S., and Fischer, J. R.**, Thermodynamic properties of minerals and related substances at 298.15 K and 1 bar pressure and at higher temperatures, *U.S. Geol. Surv. Bull.*, 1452, 1, 1978.
57. **Chase, M. W., Jr., Davies, C. A., Downey, J. R., Jr., Frurip, D. J., McDonald, R. A., and Syverud, A. N.**, *JANAF Thermochemical Tables*, 3rd ed., *J. Phys. Chem. Ref. Data*, 14 (Suppl. 1), 1, 1985.
58. **Wagman, D. D., Evans, W. H., Parker, V. B., Schumm, R. H., Halow, I., Bailey, S. M., Churney, K. L., and Nuttall, R. L.**, The NBS tables of chemical thermodynamic properties. Selected values for C<sub>1</sub> and C<sub>2</sub> organic substances in SI units, *J. Phys. Chem. Ref. Data*, 11 (Suppl. 2), 1, 1982.
59. **Kelley, K. K.**, Contributions to the data on theoretical metallurgy. XIII. High-temperature heat-content, heat-capacity, and entropy data for the elements and inorganic compounds, *U.S. Bur. Mines Bull.*, 584, 1, 1960.
60. **Tanger, J. C., IV and Helgeson, H. C.**, Calculation of the thermodynamic and transport properties of aqueous species at high pressures and temperatures: revised equations of state for the standard partial molal properties of ions and electrolytes, *Am. J. Sci.*, 288, 19, 1988.
61. **Tanger, J. C., IV and Pitzer, K. S.**, Calculation of the thermodynamic properties of aqueous electrolytes to 1000°C and 5000 bar from a semicontinuum model for ion hydration, *J. Phys. Chem.*, 93, 4941, 1989.
62. **Haar, L., Gallagher, J. S., and Kell, G. S.**, *NBS/NRC Steam Tables: Thermodynamic and Transport Properties and Computer Programs for Vapor and Liquid States of Water in SI Units*, Hemisphere, Washington, D.C., 1984, 1.
63. **Truesdell, A. H. and Jones, B. F.**, WATEQ, a computer program for calculating chemical equilibria of natural waters, *J. Res. U.S. Geol. Surv.*, 2, 233, 1974.
64. **Kharaka, Y. K. and Barnes, I.**, SOLMNEQ: Solution-Mineral Equilibrium Computations, *U.S. Geol. Surv. Comput. Contrib.*, National Technical Information Service #PB-215-899, 1973.
65. **Perkins, E. H., Kharaka, Y. K., Gunter, W. D., and DeBraal, J. D.**, Geochemical modeling of water-rock interactions using SOLMINEQ.88, in *Chemical Modeling of Aqueous Systems II*, Melchior, D. C. and Bassett, R. L., Eds., A.C.S. Symp. Series 416, American Chemical Society, Washington, D.C., 1990, chap. 9.
66. **Wolery, T. J.**, *EQ3NR. A Computer Program for Geochemical Aqueous Speciation-Solubility Calculations: User's Guide and Documentation*, UCRL-53414, Lawrence Livermore National Laboratory, CA, 1983, 1.
67. **Wolery, T. J., Jackson, K. J., Bourcier, W. L., Bruton, C. J., Viani, B. E., Knauss, K. G., and Delany, J. M.**, Current status of the EQ3/6 software package for geochemical modeling, in *Chemical Modeling of Aqueous Systems II*, Melchior, D. C. and Bassett, R. L., Eds., A.C.S. Symp. Series 416, American Chemical Society, Washington, D.C., 1990, chap. 8.
68. **Plummer, L. N. and Parkhurst, D. L.**, Application of the Pitzer equations to the PHREEQE geochemical model, in *Chemical Modeling of Aqueous Systems II*, Melchior, D. C. and Bassett, R. L., Eds., A.C.S. Symp. Series 416, American Chemical Society, Washington, D.C., 1990, chap. 10.
69. **Plummer, L. N., Parkhurst, D. L., Fleming, G. W., and Dunkle, S. A.**, A computer program incorporating Pitzer's equations for calculation of geochemical reactions in brines, in U.S. Geological Survey, Water-Resources Investigations Report 88-4153, Reston, VA, 1988.
70. **Nordstrom, D. K., Plummer, L. N., Langmuir, D., Busenberg, E., May, H. M., Jones, B. F., and Parkhurst, D. L.**, Revised chemical equilibrium data for major water-mineral reactions and their limitations, in *Chemical Modeling of Aqueous Systems II*, Melchior, D. C. and Bassett, R. L., Eds., A.C.S. Symp. Series 416, American Chemical Society, Washington, D.C., 1990, chap. 31.
71. **Wood, J. R.**, Thermodynamics of brine-salt equilibria. I. The systems NaCl-KCl-MgCl<sub>2</sub>-CaCl<sub>2</sub>-H<sub>2</sub>O and NaCl-MgSO<sub>4</sub>-H<sub>2</sub>O at 25°C, *Geochim. Cosmochim. Acta*, 39, 1147, 1975.
72. **Frantz, J. D., Popp, R. K., and Boctor, N. Z.**, Mineral-solution equilibria. V. Solubilities of rock-forming minerals in supercritical fluids, *Geochim. Cosmochim. Acta*, 45, 69, 1981.
73. **Pitzer, K. S. and Mayorga, G.**, Thermodynamics of electrolytes. II. Activity and osmotic coefficients for strong electrolytes with one or both ions univalent, *J. Phys. Chem.*, 77, 2300, 1973; 78, 2698, 1974.
74. **Pitzer, K. S. and Mayorga, G.**, Thermodynamics of electrolytes. III. Activity and osmotic coefficients for 2-2 electrolytes, *J. Solution Chem.*, 3, 539, 1974.

75. **Rard, J. A.**, Isopiestic determination of the osmotic and activity coefficients of aqueous  $\text{NiCl}_2$ ,  $\text{Pr}(\text{NO}_3)_3$ , and  $\text{Lu}(\text{NO}_3)_3$  and solubility of  $\text{NiCl}_2$  at 25°C, *J. Chem. Eng. Data*, 32, 334, 1987.
76. **Rard, J. A.**, Isopiestic determination of the osmotic and activity coefficients of aqueous  $\text{MnCl}_2$ ,  $\text{MnSO}_4$ , and  $\text{RbCl}$  at 25°C, *J. Chem. Eng. Data*, 29, 443, 1984.
77. **Rard, J. A. and Miller, D. G.**, Isopiestic determination of the osmotic coefficients of aqueous  $\text{Na}_2\text{SO}_4$ ,  $\text{MgSO}_4$ , and  $\text{Na}_2\text{SO}_4\text{-MgSO}_4$  at 25°C, *J. Chem. Eng. Data*, 26, 33, 1981.
78. **Downes, C. J. and Pitzer, K. S.**, Thermodynamics of electrolytes. Binary mixtures formed from aqueous  $\text{NaCl}$ ,  $\text{Na}_2\text{SO}_4$ ,  $\text{CuCl}_2$  and  $\text{CuSO}_4$  at 25°C, *J. Solution Chem.*, 5, 389, 1976.
79. **Pitzer, K. S.**, Theory: ion interaction approach, in *Activity Coefficients in Electrolyte Solutions*, Vol. 1, Pytkowicz, R. M., Ed., CRC Press, Boca Raton, FL, 1979, chap. 7.
80. **Filippov, V. K., Fedorov, Yu. A., and Charykov, N. A.**, Solubilities in the systems  $\text{NaCl-MnCl}_2\text{-H}_2\text{O}$  and  $\text{NaCl-CoCl}_2\text{-H}_2\text{O}$  systems at 25°C, *Zh. Neorg. Khim.*, 28, 3166, 1983.
81. **Putiv'skii, V. V., Mil'ner, A. A., and Zapol'skii, A. K.**, Solubility in the  $\text{MnCl}_2\text{-HCl-H}_2\text{O}$  system at 25°C, *Russ. J. Inorg. Chem.*, 32, 293, 1987.
82. **Bodaleva, N. V. and Ke-Yuan, K.**, A study of solubility in the  $\text{Li}_2\text{SO}_4\text{-Na}_2\text{SO}_4\text{-H}_2\text{O}$  system, *Russ. J. Inorg. Chem.*, 4, 1303, 1959.
83. **Oikova, T.**, The  $\text{MgCl}_2\text{-NiCl}_2\text{-H}_2\text{O}$  and  $\text{CoCl}_2\text{-MgCl}_2\text{-H}_2\text{O}$  systems at 25°C, *Russ. J. Inorg. Chem.*, 24, 122, 1979.
84. **Druzhinin, I. G. and Kosyakina, O. A.**, Solubility and solid phases in the  $\text{CuCl}_2 + \text{Na}_2\text{SO}_4 = \text{CuSO}_4 + \text{Na}_2\text{Cl}_2$  aqueous reciprocal system at 25°C, *Russ. J. Inorg. Chem.*, 6, 868, 1961.
85. **Filippov, V. K., Veretennikova, G. A., and Nokhrin, V. I.**, Thermodynamic study of the system  $\text{Na}_2\text{SO}_4\text{-NiSO}_4\text{-H}_2\text{O}$  at 25°C, *J. Appl. Chem. U.S.S.R.*, 57, 1793, 1984.
86. **Filippov, V. K. and Yakovleva, S. I.**, The  $\text{CoSO}_4\text{-Na}_2\text{SO}_4\text{-H}_2\text{O}$  system at 25°C, *Russ. J. Inorg. Chem.*, 24, 1553, 1979.
87. **Schevchuk, V. G., Storozhenko, D. A., and Kisel, N. N.**, The  $\text{CoSO}_4\text{-Li}_2\text{SO}_4\text{-H}_2\text{O}$  and  $\text{CoSO}_4\text{-Na}_2\text{SO}_4\text{-H}_2\text{O}$  systems at 25–75°C, *Russ. J. Inorg. Chem.*, 25, 466, 1980.
88. **Blidin, V. P. and Andreeva, T. A.**, Solubility isotherms of the systems  $\text{Li}_2\text{SO}_4\text{-FeSO}_4\text{-H}_2\text{O}$ ,  $\text{Li}_2\text{SO}_4\text{-CoSO}_4\text{-H}_2\text{O}$ , and  $\text{Li}_2\text{SO}_4\text{-NiSO}_4\text{-H}_2\text{O}$  at 25°C, *Russ. J. Inorg. Chem.*, 3, 249, 1958.
89. **Bursa, S. and Stanin-Lovitska, M.**, Solubility in the system  $\text{CoSO}_4\text{-CoCl}_2\text{-H}_2\text{O}$  at 20, 25, 35, 45, 50, 55 and 60°C, *Zh. Neorg. Khim.*, 25, 2534, 1980.
90. **Filippov, V. K., Charykov, N. A., and Solechnik, N. D.**, Thermodynamics of the systems  $\text{Ni||Cl}_2\text{-SO}_4\text{-H}_2\text{O}$  and  $\text{Co||Cl}_2\text{-SO}_4\text{-H}_2\text{O}$  at 25°C, *J. Appl. Chem. U.S.S.R.*, 58, 1811, 1985.
91. **Bassett, H. and Watt, W.**, Pickeringite and the system  $\text{MgSO}_4\text{-Al}_2(\text{SO}_4)_3\text{-H}_2\text{O}$ , *J. Chem. Soc.*, 500, 1408, 1950.
92. **Moshinskii, A. S. and Chibizov, V. P.**, Polythermal solubility diagram (for 0–100°C) and double sulfate in the system  $\text{MgSO}_4\text{-Al}_2\text{SO}_4\text{-H}_2\text{O}$ , *Zh. Prikl. Khim.*, 48, 2186, 1975.
93. **Occleshaw, V. J.**, The equilibrium in the systems aluminium sulphate-copper sulphate-water and aluminium sulphate-ferrous sulphate-water at 25°C, *J. Chem. Soc.*, 127, 2598, 1925.
94. **Smith, N. O.**, The hydration of aluminum sulfate, *J. Am. Chem. Soc.*, 64, 41, 1942.
95. **Oykova, T.**, Die Veränderung der mittleren Ionenaktivitätskoeffizienten der Komponenten in dreistoffsystemen mit Doppelsalzbildung, *Z. Phys. Chem. (Leipzig)*, 263, 1153, 1982.
96. **Filippov, V. K. and Nokhrin, V. I.**, 25°C solubility diagram of the  $\text{Li}_2\text{SO}_4\text{-Na}_2\text{SO}_4\text{-CuSO}_4\text{-H}_2\text{O}$  system, *Russ. J. Inorg. Chem.*, 32, 440, 1987.
97. **Filippov, V. K., Charykov, N. A., and Federov, Yu. A.**, Application of Pitzer's equations to the calculation of solution-vapor equilibrium in the  $\text{MnCl}_2\text{-HCl-H}_2\text{O}$  system, *Dokl. Akad. Nauk SSSR Fiz. Khim.*, 307, 916, 1989; Engl. transl., 307, 630, 1989.
98. **Holmes, H. F. and Mesmer, R. E.**, Thermodynamic properties of aqueous solutions of the alkali metal chlorides to 250°C, *J. Phys. Chem.*, 87, 1242, 1983.
99. **Brodale, G. E. and Giauque, W. F.**, The heat of hydration of sodium sulfate. Low temperature heat capacity and entropy of sodium sulfate decahydrate, *J. Am. Chem. Soc.*, 80, 2042, 1958.
100. **Brodale, G. E. and Giauque, W. F.**, The relationship of crystalline forms I, III, IV, and V of anhydrous sodium sulfate as determined by the third law of thermodynamics, *J. Phys. Chem.*, 76, 737, 1972.
101. **Frost, G. B., Breck, W. G., Clayton, R. N., Reddoch, A. H., and Miller, C. G.**, The heat capacities of the crystalline and vacuum dehydrated form of magnesium sulphate monohydrate, *Can. J. Chem.*, 35, 1446, 1957.
102. **Cox, W. P., Hornung, E. W., and Giauque, W. F.**, The spontaneous transformation from macrocrystalline to microcrystalline phases at low temperatures. The heat capacity of  $\text{MgSO}_4 \cdot 6\text{H}_2\text{O}$ , *J. Am. Chem. Soc.*, 77, 3935, 1955.
103. **Hisham, M. W. M. and Benson, S. W.**, The enthalpies of formation of crystals of hydrates, ammoniates, and alcoholates, and some observations on heats of dilution, *J. Phys. Chem.*, 91, 5998, 1987.
104. **Ko, H. C. and Daut, G. E.**, Enthalpies of formation of  $\alpha$ - and  $\beta$ -magnesium sulfate and magnesium sulfate monohydrate, *U.S. Bur. Mines Rep. Invest.*, 8409, 1, 1979.

105. **Pitzer, K. S., Peiper, J. C., and Busey, R. H.**, Thermodynamic properties of aqueous sodium chloride solutions, *J. Phys. Chem. Ref. Data*, 13, 1, 1984.
106. **Holmes, H. F. and Mesmer, R. E.**, Thermodynamics of aqueous solutions of the alkali metal sulfates, *J. Solution Chem.*, 15, 495, 1986.
107. **Phutela, R. C. and Pitzer, K. S.**, Heat capacity and other thermodynamic properties of aqueous magnesium sulfate to 473 K, *J. Phys. Chem.*, 90, 895, 1986.
108. **Phutela, R. C., Pitzer, K. S., and Saluja, P. P. S.**, Thermodynamics of aqueous magnesium chloride, calcium chloride and strontium chloride at elevated temperatures, *J. Chem. Eng. Data*, 32, 76, 1987.
109. **Liu, C. and Lindsay, W. T., Jr.**, Thermodynamics of sodium chloride solutions at high temperatures, *J. Solution Chem.*, 1, 45, 1972.
110. **Pabalan, R. T. and Pitzer, K. S.**, Thermodynamics of NaOH(aq) in hydrothermal solutions, *Geochim. Cosmochim. Acta*, 51, 829, 1987.
111. **Simonson, J. M., Mesmer, R. E., and Rogers, P. S. Z.**, The enthalpy of dilution and apparent molar heat capacity of NaOH(aq) to 523 K and 40 MPa, *J. Chem. Thermodyn.*, 21, 561, 1989.
112. **de Lima, M. C. P. and Pitzer, K. S.**, Thermodynamics of saturated electrolyte mixtures of NaCl with Na<sub>2</sub>SO<sub>4</sub> and MgCl<sub>2</sub>, *J. Solution Chem.*, 12, 187, 1983.
113. **Holmes, H. F., Baes, C. F., and Mesmer, R. E.**, Isopiestic studies of aqueous solutions at elevated temperatures. I. KCl, CaCl<sub>2</sub> and MgCl<sub>2</sub>, *J. Chem. Thermodyn.*, 10, 983, 1978.
114. **Rard, J. A. and Miller, D. G.**, Isopiestic determination of the osmotic and activity coefficients of aqueous MgCl<sub>2</sub> solutions at 25°C, *J. Chem. Eng. Data*, 26, 38, 1981.
115. **Pitzer, K. S.**, Thermodynamics of unsymmetrical electrolyte mixtures: enthalpy and heat capacity, *J. Phys. Chem.*, 87, 2360, 1983.
116. **Pitzer, K. S. and Kim, J. J.**, Thermodynamics of electrolytes. IV. Activity and osmotic coefficients for mixed electrolytes, *J. Am. Chem. Soc.*, 96, 5701, 1974.
117. **Robinson, R. A.**, Activity coefficients of sodium chloride and potassium chloride in mixed aqueous solutions at 25°C, *J. Phys. Chem.*, 65, 662, 1961.
118. **Pitzer, K. S.**, Thermodynamics of electrolytes. V. Effects of higher-order electrostatic terms, *J. Solution Chem.*, 4, 249, 1975.
119. **Phutela, R. C. and Pitzer, K. S.**, Thermodynamics of electrolyte mixtures. Enthalpy and the effect of temperature on the activity coefficient, *J. Solution Chem.*, 15, 649, 1986.
120. **Holmes, H. F., Baes, C. F., and Mesmer, R. E.**, Isopiestic studies of aqueous solutions at elevated temperatures. II. NaCl + KCl mixtures, *J. Chem. Thermodyn.*, 11, 1035, 1979.
121. **Akhumov, E. I. and Vasil'ev, B. B.**, A study of aqueous solutions at elevated temperatures. II, *Zh. Obshch. Khim.*, 2, 282, 1932.
122. **Schroeder, W. C., Gabriel, A., and Partridge, E. P.**, Solubility equilibria of sodium sulfate at temperatures 150 to 350°C. I. Effect of sodium hydroxide and sodium chloride, *J. Am. Chem. Soc.*, 57, 1539, 1935.
123. **Kayser, E.**, Die ersatzzahlen inkonstanter Lösungen über Kaliumchlorid und Natriumchlorid, *Kali*, 17, 1, 1923.
124. **Boecke, H. E.**, Ein Schlüssel zur Beurteilung des Kristallisationsverlaufes der bei der Kalisalzverarbeitung vorkommenden Lösungen, *Kali*, 4, 271 and 300, 1910.
125. **Serowy, L.**, Die Polythermen der Viersalzpunkte des Chlorkaliumfeldes im quinären System ozeanischer Salzablagerungen: ihre teilweise Nachprüfung und Vervollständigung bis zu Temperaturen über 100°, *Kali*, 17, 345, 1923.
126. **Prausnitz, J. M., Lichtenthaler, R. N., and de Azevedo, E. G.**, *Molecular Thermodynamics of Fluid-Phase Equilibria*, 2nd ed., Prentice-Hall, Englewood Cliffs, NJ, 1986.
127. **Adler, S. B., Friend, L., and Pigford, R. L.**, Application of the Wohl equation to ternary vapor-liquid equilibria, *AIChE J.*, 12, 629, 1966.
128. **Pitzer, K. S.**, Thermodynamics of condensed ionic systems, in *Physics and Chemistry of Electrons and Ions in Condensed Matter*. Acrivos, J. V., Mott, N. F., and Yoffe, A. D., Eds., D. Reidel, Boston, 1984, 165.
129. **Pitzer, K. S. and Li, Y.-G.**, Thermodynamics of aqueous sodium chloride to 823 K and 1 kilobar, *Proc. Natl. Acad. Sci. U.S.A.*, 80, 7689, 1983.
130. **Sternner, S. M., Hall, D. L., and Bodnar, R. J.**, Synthetic fluid inclusions. V. Solubility relations in the system NaCl-KCl-H<sub>2</sub>O under vapor-saturated conditions, *Geochim. Cosmochim. Acta*, 52, 989, 1988.
131. **Rogers, P. S. Z. and Pitzer, K. S.**, Volumetric properties of aqueous sodium chloride solutions, *J. Phys. Chem. Ref. Data*, 11, 15, 1982.
132. **Weres, O., Peiper, J. C., Pitzer, K. S., and Pabalan, R. T.**, Documentation for computer code NACL, Lawrence Berkeley Laboratory Report 21859, Berkeley, CA, 1987.
133. **Phutela, R. C. and Pitzer, K. S.**, Thermodynamics of aqueous calcium chloride, *J. Solution Chem.*, 12, 201, 1983.

134. **Holmes, H. F., Busey, R. H., Simonson, J. M., Mesmer, R. E., Archer, D. G., and Wood, R. H.,** The enthalpy of dilution of HCl(aq) to 648 K and 40 MPa; thermodynamic properties, *J. Chem. Thermodyn.*, 19, 863. 1987.
135. **Sterner, S. M., Chou, I.-M., Downs, R. T., and Pitzer, K. S.,** Phase relations in the system NaCl-KCl-H<sub>2</sub>O. V. Thermodynamic-PX analysis of solid-liquid equilibria at high temperatures and pressures, *Geochim. Cosmochim. Acta.* submitted.

## Chapter 8

**ION ASSOCIATION AT HIGH TEMPERATURES AND PRESSURES**

Robert E. Mesmer, Donald A. Palmer, and J. M. Simonson

**TABLE OF CONTENTS**

I.	Introduction.....	492
A.	General.....	492
B.	Experimental Methods.....	492
	1.  Electrochemical Cells.....	492
	2.  Electrical Conductance.....	493
C.	Acid-Base Equilibria to 300°C.....	495
II.	Association Reactions to Form H <sub>2</sub> O, NH <sub>3</sub> (aq), HCl(aq), and NaCl(aq) to 800°C.....	496
A.	Model.....	496
B.	Thermodynamics of Association.....	498
C.	Driving Force for Ion Association Reactions.....	501
D.	Hydration Model.....	503
E.	Extrapolation of Association Constants.....	504
F.	Uncertainties in Extrapolated Equilibrium Constants.....	505
III.	Ion Association from Calorimetric Evidence.....	506
A.	Electrostatic Considerations.....	507
B.	Ion Association Evidence from Dilution Enthalpy Measurements.....	510
C.	Ion Association Evidence from Mixing Enthalpy Measurements.....	514
IV.	Metal Complexation.....	515
A.	Experimental Methods — Their Application and Limitations.....	515
	1.  General.....	515
	2.  Specific Methods.....	516
	a.  Electrochemical Cells.....	516
	b.  UV-Visible Spectrophotometry.....	518
	c.  Solubility Measurements.....	518
	d.  Raman Spectrometry.....	519
B.	Specific Equilibrium Results.....	519
	1.  Metal Hydroxide Complexes.....	519
	2.  Metal Chloride Complexes.....	522
	3.  Metal Acetate Complexes.....	524
	Acknowledgment.....	525
	References.....	525



electrolyte for controlling activity coefficients and minimizing liquid junction potentials. These cells operate well to 300°C as limited by the Teflon in liners, seals, and the porous plug junction. Routinely, the ionic strength is varied to determine salt effects and to permit derivation of infinite dilution log K values, often accurate to about 0.01 log units. Such cells have been operated in both titration<sup>7</sup> and flow<sup>8</sup> modes. In the former, equilibration permits wide variation of the test solution by admitting titrant to the system where complex speciation analysis is involved. In the latter, no vapor space is present and only short residence times are required. Details of considerations of the liquid junction potentials are discussed in some detail previously.<sup>7,9</sup>

The cell potential is given by

$$E = \frac{RT}{F} \ln \frac{[H^+]_r \gamma_r}{[H^+] \gamma} + ELJ \quad (2)$$

where r refers to the reference compartment, the bracketed terms are molal concentrations (including any associated acid HX formed with the medium electrolyte NaX), and  $\gamma$  and  $\gamma_r$  are the activity coefficients of the hydrogen ion in the two solutions and are assumed to be constant and equal in the presence of the supporting electrolyte. The liquid junction potential ELJ is approximated by use of the Henderson equation using limiting conductances for all ions present:<sup>7,9</sup>

$$ELJ = \sum D_i ([i] - [i]_r) \quad (3)$$

Here [i] represents each ion in the two solutions and the coefficients  $D_i$  in the presence of a supporting electrolyte are given by

$$D_i = \frac{RT}{F} \cdot \frac{z_i \lambda_i}{|z_i| \sum (|z_i| \lambda_i [i])} \quad (4)$$

where  $z_i$  is the charge and  $\lambda$  is the limiting conductance of the ion. Using supporting electrolytes ELJ can be easily kept <1 mV.

These concentration cells have been used to examine a number of ionization and hydrolysis reactions as summarized in Reference 6. Ionization constants derived from such cells are represented for simple weak acids and bases to 300°C in Figure 1.

## 2. Electrical Conductance

A number of studies of electrical conductances of electrolyte solutions in the supercritical range have been carried out at ORNL using a platinum-lined cell described by Quist and Marshall.<sup>10</sup> Results are available<sup>6</sup> for several of 1-1 electrolytes and for the ionization of H<sub>2</sub>O and NH<sub>3</sub>(aq). The conductance apparatus and procedures for data analysis are discussed by Marshall and Frantz.<sup>11</sup>

Briefly, the molar conductance  $\Lambda$  of an electrolyte solution is given by

$$\Lambda = a/R_0 M \quad (5)$$

where  $a$  is the cell constant that depends on cell geometry,  $R_0$  is the observed resistance of the solution, and  $M$  is the molar concentration of the electrolyte. The degree of ionization or dissociation of an electrolyte  $\theta$  is given by the ratio  $\Lambda/\Lambda'$ , where  $\Lambda'$  is the hypothetical conductance of a solution of completely dissociated solute. The latter quantity, at temper-

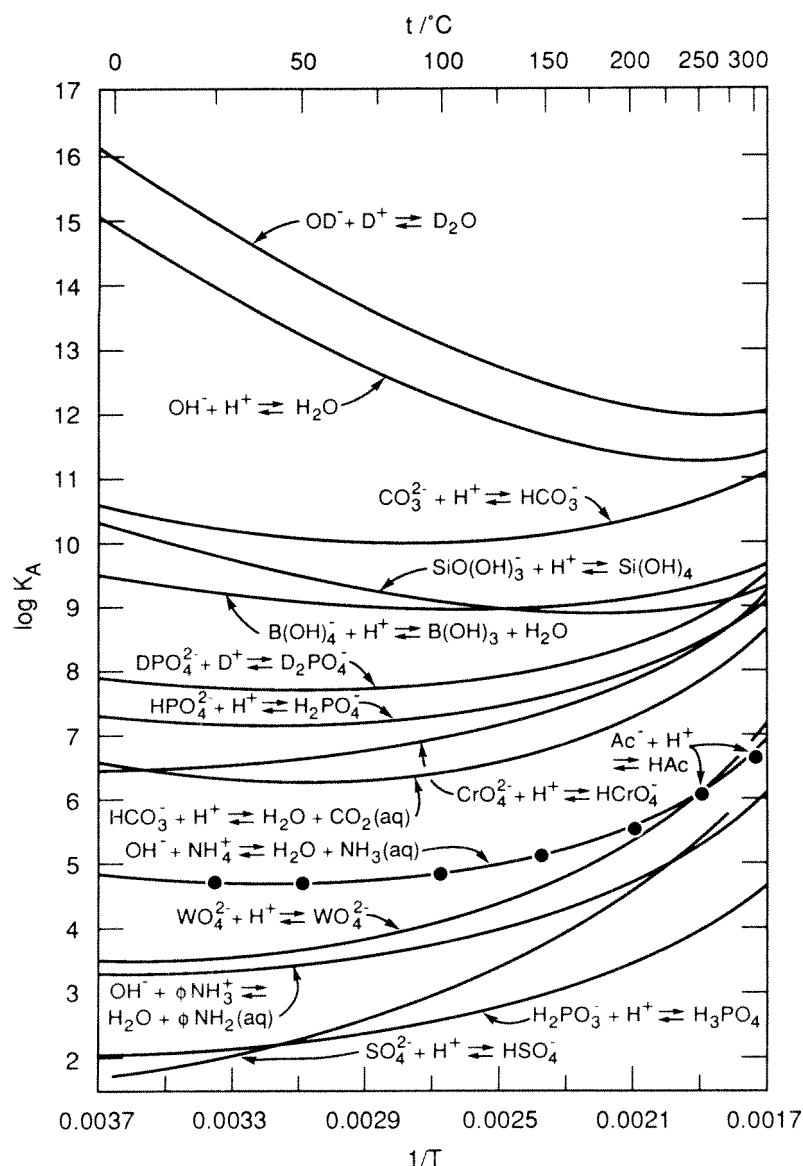


FIGURE 1. Temperature dependence of the association constants for the formation of weak acids and bases at the saturation vapor pressure of water to 300°C. All data are based on results from EMF measurements. The symbol  $\phi$  represents cyclohexyl- group.

atures and densities where no association occurs, obeys the Onsager relationship in dilute solutions:

$$\Lambda' = \Lambda_0 - (A + B\Lambda_0)M^{1/2} \quad (6)$$

Here  $A$  and  $B$  have theoretical values based on viscosity, dielectric constant, temperature, and ionic charge. By extrapolation of  $\Lambda_0$ , the limiting equivalent conductance, from temperature-density regions where complete dissociation occurs to regions of incomplete dis-



sociation,  $\Lambda'$  can be computed from Equation 6. The equilibrium constant (molar concentrations) is given by

$$K = \theta^2 M y_{\pm}^2 / (1 - \theta) \quad (7)$$

where  $y_{\pm}$ , the mean real ionic activity coefficient, is usually approximated by the extended Debye-Hückel relationship. Alternatively,  $K$  and  $\Lambda_0$  may be obtained from the Shedlovsky equation

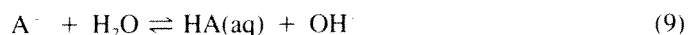
$$\frac{1}{\Lambda S(z)} = \frac{1}{\Lambda_0} + \frac{M \Lambda S(z) y_{\pm}^2}{K \Lambda_0^2} \quad (8)$$

where  $S(z)$  is treated as an empirical parameter and  $\Lambda_0$  and  $K$  are solved for simultaneously. At this time, it is not possible to assess properly the uncertainties in the derived values of  $K$ , but there is presently no better experimental method for their measurement in the supercritical region.

The ionization reactions of only two neutral species,  $H_2O$  and  $NH_3(aq)$ , have been studied by potentiometry<sup>12</sup> to 300°C and by conductivity<sup>13</sup> in the supercritical region. The accuracy of the results for  $H_2O$  were inherently limited in the supercritical region by the need to involve several other equilibrium constants in deriving  $K_w$  from the hydrolysis of  $NH_4Br(aq)$ .<sup>13</sup> Probably the ionization results for  $NH_3(aq)$  are more accurate since they could be derived directly from the measured conductance<sup>14</sup> of dilute  $NH_3(aq)$  solutions.

### C. ACID-BASE EQUILIBRIA TO 300°C

The temperature dependence of the association constants for the formation of 13 acids and bases along with light and heavy water are shown in Figure 1 at the saturation vapor pressure of water. All have been studied by the EMF method and the results were derived by a general analysis of selected literature data along with the EMF results. The results from recent work on acetic acid<sup>15</sup> and bisulfate<sup>16</sup> are shown along with the results presented previously.<sup>6</sup> All these results demonstrate similar curvature of  $1/T$  plots, which reflects a similar  $\Delta C_p^\circ$  for the association process. Of these systems,  $H_3PO_4$ ,  $H_2PO_4^-$ ,  $Si(OH)_4(aq)$ , and  $B(OH)_3(aq)$  were studied in cells in which the hydroxide ion concentration was actually determined, i.e., a reference of standard hydroxide solution was used. The free hydroxide concentration in equilibrium with the buffer mixture was observed for the following reaction:



All such reactions are found to have small  $\Delta C_p^\circ$  values over the range to 300°C. This was first observed in 1974 by Mesmer and Baes<sup>17</sup> for phosphate equilibria and was attributed to the small change in solvent electrostriction for reactions with only anions. In 1980 Lindsay<sup>18</sup> termed these reactions and the analogous ones involving cations as "isocoulombic". The isocoulombic form is convenient for extrapolation and as a basis for obtaining estimates where the change in heat capacity can be approximated as zero. Figure 2 shows several examples of  $\log(K_A/K_{H_2O})$  plots, where  $K_A$  represents the association constant for the acid. The value of  $\Delta C_p^\circ$  represented by the curvature of the  $1/T$  dependence for  $Si(OH)_4(aq)$  is  $-49.4 \text{ J} \cdot \text{mol}^{-1} \cdot \text{K}^{-1}$ .

Although the precise representation of the temperature dependence of equilibrium constants is model dependent, the high precision of these data sets ( $\pm 0.01$  log units) allows the derivation of accurate enthalpy and heat capacity changes for association by differentiation. Also, the availability of very accurate low temperature data as reference points provides a firm anchor for the temperature dependence. Figure 3 shows  $\Delta C_p^\circ$  values for

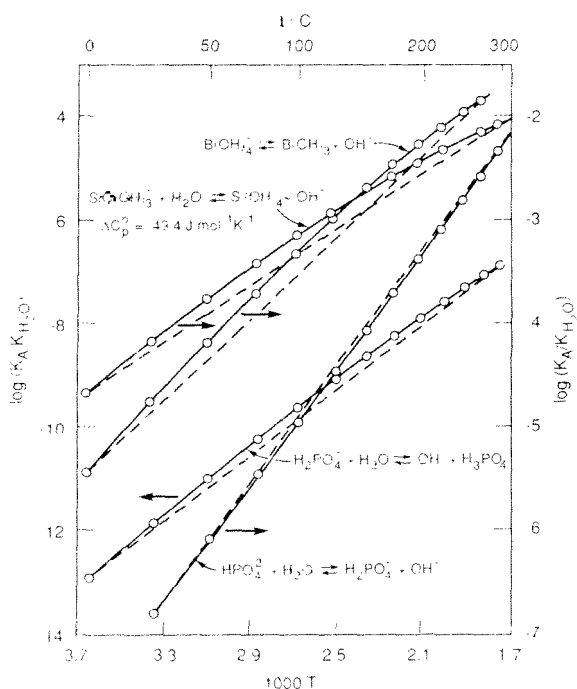


FIGURE 2.  $\log(K_A/K_{H_2O})$  for four acids to 300°C.

association reactions to form  $H_2O$ ,  $NH_3(aq)$ ,  $CO_2(aq)$ , and cyclohexylamine(aq), and for their isocoulombic reactions as well as that of  $Si(OH)_4(aq)$ . The  $\Delta C_p^\circ$  for ion association in all these cases approaches infinity as the critical temperature of water is approached, while  $[\Delta C_p^\circ - \Delta C_p^\circ(H_2O)]$  is small and relatively insensitive to temperature [ $\Delta C_p^\circ(H_2O)$  corresponds to the association reaction ( $H^+ + OH^- \rightleftharpoons H_2O$ )]. The results for  $\Delta V^\circ$  exhibit similar behavior. Such behavior reflects the fact that  $\bar{C}_{p,i}^\circ$  and  $\bar{V}_i^\circ$ , the partial molar quantities for the electrolyte, diverge toward negative infinity more rapidly for strong electrolytes than the same quantities for the neutral species (such as  $H_2O$ ) approach positive infinity. Data on  $\bar{C}_{p,i}^\circ$  for  $NaCl(aq)$  have been reported by Smith-Magowan and Wood<sup>11</sup> and on  $\bar{V}_i^\circ$  by Rogers and Pitzer<sup>12</sup> and by Hilbert.<sup>13</sup> The large variation of  $\Delta C_p^\circ$  for ion association is virtually eliminated by holding the density constant near  $1.0 \text{ g} \cdot \text{cm}^{-3}$ , as shown by Patterson et al.<sup>14</sup> for the formation of  $CO_2(aq)$  from the ions. This phenomenon will be discussed in general in the next section.

## II. ASSOCIATION REACTIONS TO FORM $H_2O$ , $NH_3(aq)$ , $HCl(aq)$ , AND $NaCl(aq)$ TO 800°C

### A. MODEL

It is observed empirically that the observation being made is that, for the association reactions,  $\Delta C_p^\circ$  approaches infinity as  $T \rightarrow T_c$  (Fig. 2). The empirical model of other ion association cases. Their results are in the class of the model of Al-Saber et al.<sup>15</sup> in which  $\Delta C_p^\circ$  is dependent on the formation of ion association in the liquid.

The expression selected by Al-Saber et al.<sup>15</sup> for representing the ion association constant of water to 1000°C and 10 kbar has been as given, representing ionization reactions in general. This density-based model has relatively few parameters to describe such widely ranging temperature-pressure conditions, and although it may not fit the data within experi-

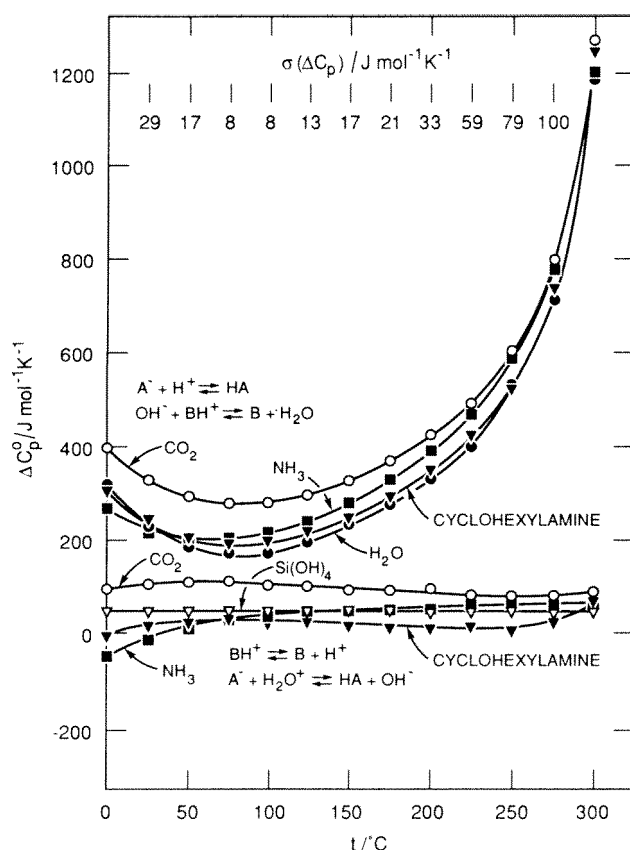


FIGURE 3.  $\Delta C_p^\circ$  as a function of temperature for association reactions representing water,  $\text{CO}_2(\text{aq})$ , cyclohexylamine, and  $\text{NH}_3(\text{aq})$  and isocoulombic reactions for the latter three and  $\text{Si}(\text{OH})_4(\text{aq})$ .<sup>6</sup> Uncertainties in  $\Delta C_p^\circ$  for the ion association reaction to form  $\text{H}_2\text{O}$  are indicated across the top of the figure.

imental uncertainty everywhere it represents accurately the principal variations. Such an analytical function affords the opportunity for evaluating and examining the thermodynamic quantities. The following relationships have been derived<sup>6</sup> from Equation 10a and are given in part by Marshall<sup>24</sup> and by Gates et al.<sup>25</sup>

$$\log K = a + b/T + c/T^2 + d/T^3 + k \log p \quad (10a)$$

$$k = (e + f/T + g/T^2)$$

$$\Delta H^\circ = -2.303R[(b + 2c/T + 3d/T^2) + (f + 2g/T) \log p] - RT^2 k \alpha \quad (10b)$$

$$\Delta S^\circ = 2.303R[(a - c/T^2 - 2d/T^3) + (e - g/T^2) \log p] - RT k \alpha \quad (10c)$$

$$\Delta C_p^\circ = -2.303R[(-2c/T^2 - 6d/T^3) - (2g/T^2) \log p]$$

$$-R\alpha(2eT - 2g/T) - RT^2 k(\partial \alpha / \partial T)_p \quad (10d)$$

$$\Delta V^\circ = -RT k \beta \quad (10e)$$

TABLE 1  
Parameters for Equation 10a,<sup>a</sup> Reference 6

Parameters	H <sub>2</sub> O	NH <sub>3</sub> (aq)	HCl(aq)	NaCl(aq)
a	4.098	5.50020	5.405	1.197
10 <sup>-3</sup> b	3.2452	-1.56787	-3.8749	-1.260
10 <sup>-5</sup> c	-2.2362	6.1790	0	0
10 <sup>-7</sup> d	3.984	-6.52561	0	0
10 <sup>-9</sup> e	-1.3957	-1.41095	-1.393	-0.920
10 <sup>-5</sup> f	1.2623	0.629378	0	0
10 <sup>-5</sup> g	-8.5641	-12.43	0	0

<sup>a</sup>Units: b and f, K; c and g, K<sup>2</sup>; d, K<sup>3</sup>.

$$\Delta\bar{\alpha}^\circ \equiv (1/\Delta V^\circ)(\partial\Delta V^\circ/\partial T)_p = (1/\beta)(\partial\beta/\partial T)_p + (e - g/T^2)(Tk) \quad (10f)$$

$$\Delta\bar{\beta}^\circ \equiv -(1/\Delta V^\circ)(\partial\Delta V^\circ/\partial p)_T = -(1/\beta)(\partial\beta/\partial p)_T \quad (10g)$$

where  $\rho$  is the density of water,  $\alpha$  is the expansivity coefficient,  $-(1/\rho)(\partial\rho/\partial T)_p$ , and  $\beta$  is the compressibility coefficient,  $(1/\rho)(\partial\rho/\partial p)_T$ .

The parameters for the four association reactions are given in Table 2. Note, the coefficients in Table 1 for the association reactions have the opposite signs to those in Reference 6; also the a parameter for NH<sub>3</sub> was incorrectly given and should be -5.50020 for the ionization reaction.

Equation 10a can be further simplified for the purpose of approximate fits to data over restricted regions of temperature and pressure and for extrapolations as was presented elsewhere:<sup>6, 26, 29</sup> Such a simple form having only a, b, and f as parameters has been successful in modeling several reaction types to about 300°C along the saturation pressure curve. This simple form requires only reference values of  $\log K$ ,  $\Delta H^\circ$ , and  $\Delta C_p^\circ$  at 25°C and 1 bar, for example, for the estimation of the temperature and pressure dependencies with useful accuracy. In this simple case,  $\Delta C_p^\circ = -fRT(\partial\alpha/\partial T)_p$  and  $\Delta V^\circ = -fR\beta$ . The uncertainty for such estimates is discussed in Section II.F.

## B. THERMODYNAMICS OF ASSOCIATION

Association constants for the four cases presented here are shown in Figure 4 at constant pressure, at constant density, and along the saturation vapor pressure curve for water. The simple nearly linear variation of  $\log K$  with  $1/T$  at constant density is common to all and suggests that maintaining a constant spatial relationship among the solutes and solvent is a source of this simplicity. Also, as was seen previously,<sup>6</sup> the variation of  $\log K_s/K_{H_2O}$  for HCl(aq) and NaCl(aq) with  $1/T$  shows very little curvature (small  $\Delta C_p^\circ$ ), since the reaction represented is in the anion-only form. In the supercritical region a small variation with pressure results from a small  $\Delta V^\circ$  for the reaction in this form. The general pattern observed for these association reactions is expected to apply to other charge pairing reactions.

The derivative quantities,  $\Delta S^\circ$  (Figure 5),  $\Delta V^\circ$  (Figure 6),  $\Delta H^\circ$  (Figure 7), and  $\Delta C_p^\circ$  (Figure 7), have similar overall features for the four cases. At the saturation pressure very large positive values are approached; values for  $\Delta V^\circ$  indicated at 370°C are equal to several liters per mole. Less variation with temperature is seen at constant density and also at constant pressures that are higher than the water vapor pressure.

The dependence of these four thermodynamic quantities on the volumetric properties of water in the density model leads to divergent values at the  $T_c$  and  $p_c$  for water, since the density derivatives with respect to temperature and pressure approach negative and positive infinity, respectively, at the critical point. These trends with increasing temperature can

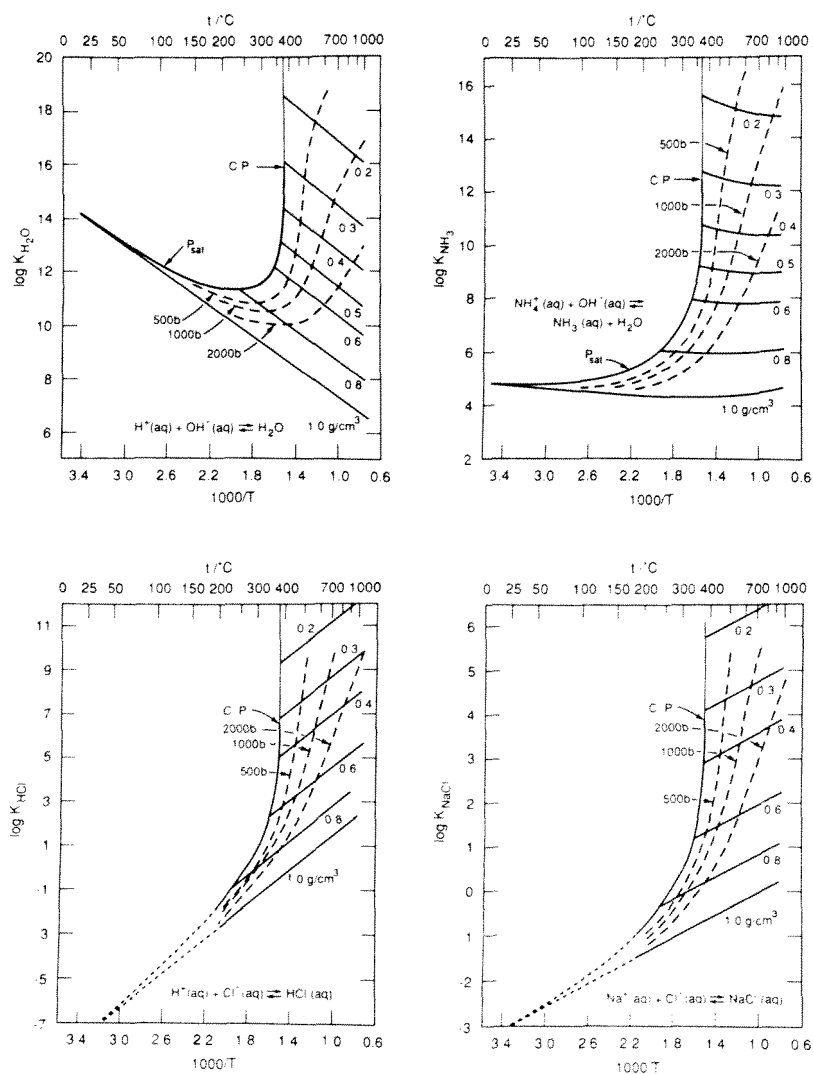


FIGURE 4. The log  $K$  for the association of ions to form  $\text{H}_2\text{O}$ ,  $\text{NH}_3(\text{aq})$ ,  $\text{HCl}(\text{aq})$ , and  $\text{NaCl}(\text{aq})$  to  $800^\circ\text{C}$ .<sup>6</sup> Conditions: saturation vapor pressure of water, bold curve; constant density, light lines; constant pressure, dashed curves.

result from the hydration sphere becoming increasingly more ordered, the solvent becoming increasingly more disordered, or from a combination of the two effects. On the other hand, all the thermodynamic quantities vary only slightly with temperature at high densities ( $0.8$  to  $1.0 \text{ g} \cdot \text{cm}^{-3}$ ). This suggests that under such conditions there is little change in the ordering or of the energy of the system. Likewise, the literature cited indicates strongly that the ionic strength effect on thermodynamic quantities for association reactions is analogous to increasing the pressure or density, i.e., it reduces the magnitude of the quantities and their dependence on temperature. Adding electrolytes makes further ordering of the solvent with increased pressure more difficult.

Cobble and Murray<sup>30</sup> first observed the rapid approach of  $\Delta\text{H}^\circ$  of solution of electrolytes to very large negative values at high temperatures. Later Gates et al.<sup>25</sup> derived  $\bar{C}_{p,2}^\circ$  and  $\bar{V}_2^\circ$  for the pair of ions ( $\text{H}^+$ ,  $\text{OH}^-$ ) from the  $\Delta\text{C}_p^\circ$  for the ionization of water and demonstrated the behavior shown in Figure 7. Here  $\Delta\text{C}_p^\circ$  shows even more interesting behavior than the

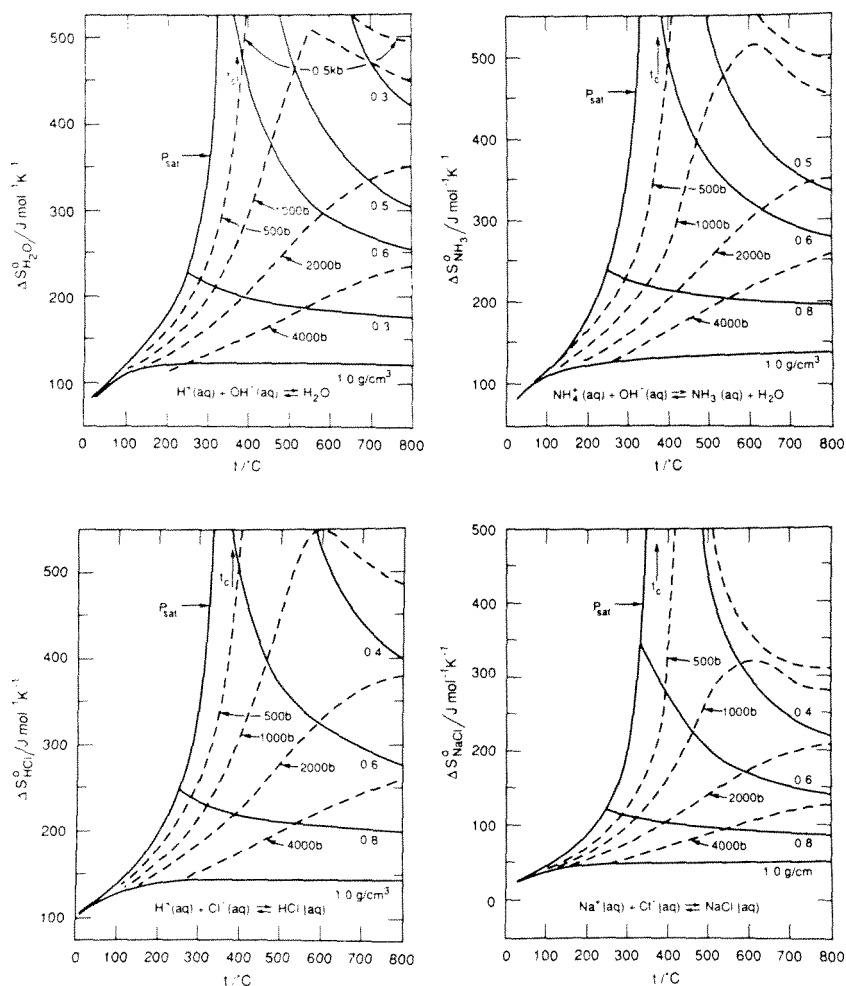


FIGURE 5. The change in entropy for association reactions to form  $\text{H}_2\text{O}$ ,  $\text{NH}_3(\text{aq})$ ,  $\text{HCl}(\text{aq})$ , and  $\text{NaCl}(\text{aq})$ .<sup>6</sup> Conditions: saturation vapor pressure of water, bold curve; constant density, light lines; constant pressure, dashed lines.

other quantities in that it approaches positive infinity with increasing temperature below the critical point and approaches negative infinity with decreasing temperature above the critical point. They also showed the approach to positive infinity for volumes on approaching the critical  $t_c$  and  $v_c$  from either direction. It is apparent that the reaction thermodynamics for association reactions are dominated by the partial molar quantities for the ions rather than by those quantities for the neutral species.

The Born equation for the solvation energy of electrolytes predicts the qualitative features of the behavior of electrolyte thermodynamics and this has been discussed by several groups: Cobble and Murray,<sup>30</sup> Helgeson and Kirkham,<sup>31</sup> Gates et al.,<sup>25</sup> and Wood et al.<sup>32</sup> However, this continuum model provides no molecular insight regarding the solvation process but suggests that electrostatic forces extend over greater distances as the dielectric constant of the medium declines. For thermodynamic quantities to become excessively large implies larger spheres of influence at high temperatures than at low temperatures, since individual bond strengths are finite and rarely exceed about  $400 \text{ kJ} \cdot \text{mol}^{-1}$  or molar volumes rarely exceed a few tens of cubic centimeters per mole of bonding unit.

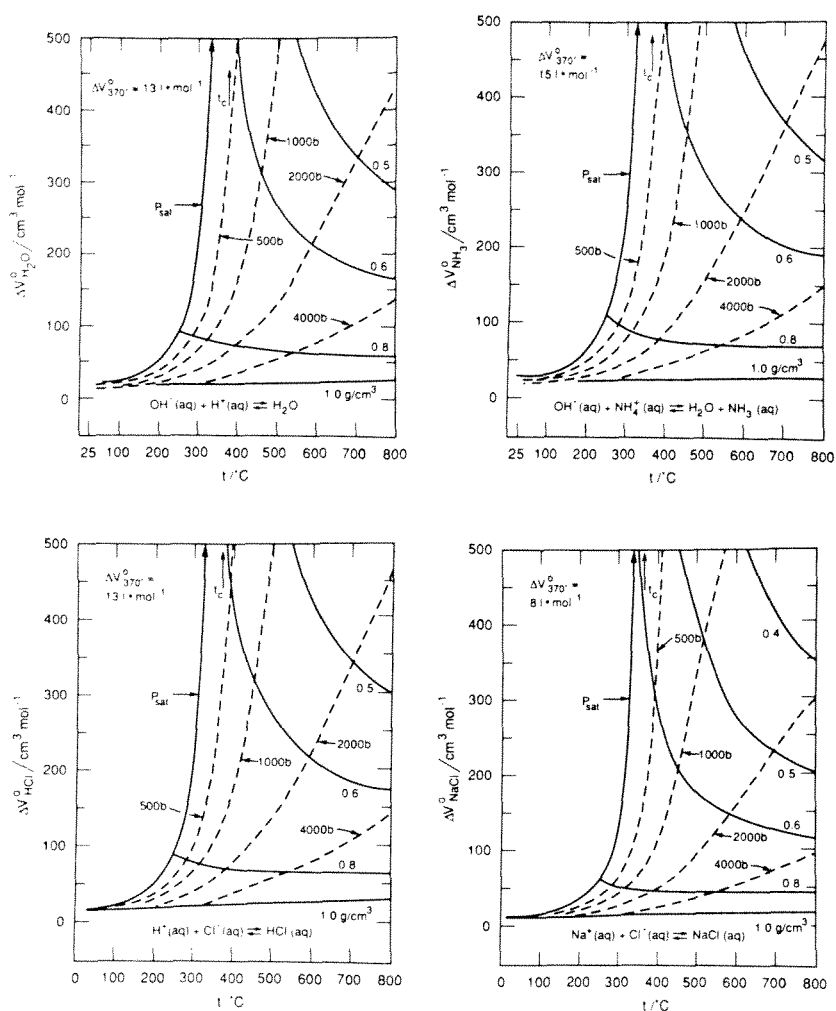


FIGURE 6. The change in volume for the association reactions to form  $\text{H}_2\text{O}$ ,  $\text{NH}_3(\text{aq})$ ,  $\text{HCl}(\text{aq})$ , and  $\text{NaCl}(\text{aq})$ .<sup>6</sup> Values at  $370^\circ\text{C}$  at the saturation vapor pressure are indicated at the upper left. Conditions: saturation vapor pressure of water, bold curve: constant density, light lines: constant pressure, dashed lines.

Another interesting consideration results from the Bjerrum model<sup>3</sup> for ion association as found by Simonson et al.<sup>33</sup> and discussed in more detail below. This model is also an electrostatic approach and it assumes ions are paired if separated by a distance less than a distance for which the interaction energy is  $2\text{ kT}$ ; those separated at greater distances are assumed to be dissociated. Qualitatively correct enthalpies and equilibrium constants were obtained for  $(\text{Ca}^{2+}, \text{Cl}^-)$  association with a value for the closest distance of approach of  $4\text{ \AA}$ . For example, the  $\Delta H^\circ$  extrapolated from conductance data at  $523\text{ K}$  is  $120\text{ kJ}\cdot\text{mol}^{-1}$ , and  $51\text{ kJ}\cdot\text{mol}^{-1}$  is given by the Bjerrum model.

### C. DRIVING FORCE FOR ION ASSOCIATION REACTIONS

Often the driving force for ion association reactions at ambient conditions is the  $T\Delta S^\circ$  term of  $\Delta G^\circ$ , although occasionally both the  $\Delta H^\circ$  and  $T\Delta S^\circ$  terms favor association. The results summarized in Table 2 demonstrate that in the four cases presented here the  $T\Delta S^\circ$  term is the driving force at temperatures greater than about  $200^\circ\text{C}$ . At these conditions  $\Delta H^\circ$

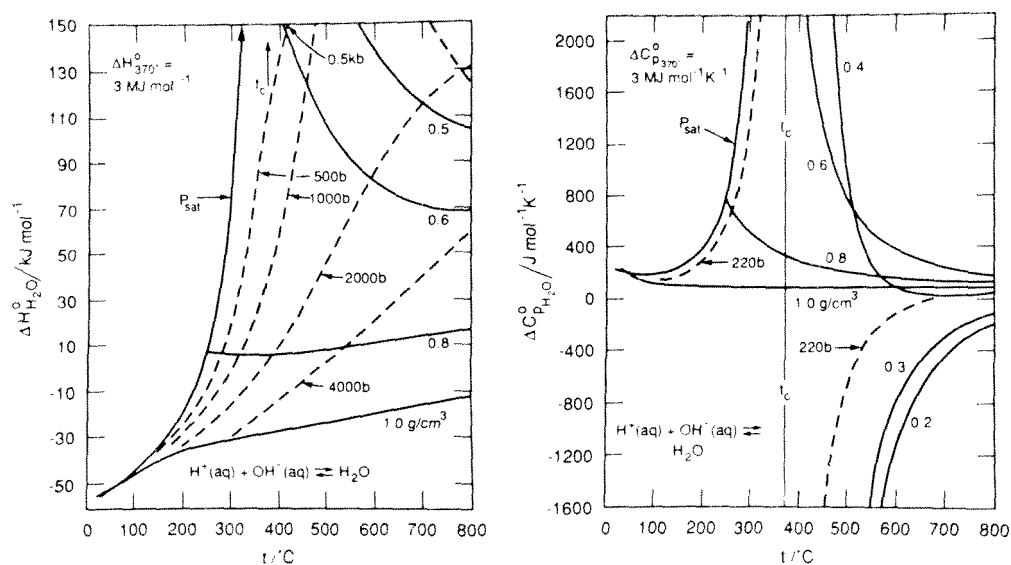


FIGURE 7. The changes in enthalpy and heat capacity for the association reaction to form water.<sup>6</sup> Conditions: saturation vapor pressure of water, bold curve; constant density, light lines; dashed curves, constant pressure.

TABLE 2  
Standard Enthalpies, Entropies, and Gibbs Energies for  
Association Reactions<sup>a</sup>

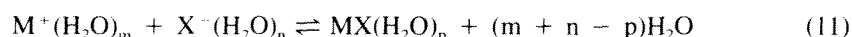
°C	p/bar	H <sub>2</sub> O(aq)			NH <sub>3</sub> (aq)		
		ΔH°	TΔS°	ΔG°	ΔH°	TΔS°	ΔG°
25	Sat.	-55.55	24.33	-79.88	-2.38	24.81	-27.19
100	Sat.	-42.27	45.35	-87.62	9.94	44.76	-34.82
200	Sat.	-18.36	83.39	-102.25	38.16	87.87	-49.71
300	Sat.	69.35	194.51	-125.16	139.82	214.13	-74.31
350	Sat.	412.0	558.7	-146.7	531.7	629.9	-98.1
374.1	Sat.	∞	∞		∞	∞	
400	500	197	350	-153	282	387	-104
500	500	417	656	-239	516	715	-199
600	500	191	497	-305	258	529	-271
800	500	122	531	-408	179	560	-380
		HCl(aq)			NaCl(aq)		
200	Sat.	110	93	17	48	40	8
300	Sat.	198	206	-8	106	110	-4
350	Sat.	540	570	-30	332	349	-17
374.1	Sat.	∞	∞		∞	∞	
400	500	331	369	38	194	213	-19
500	500	563	691	-128	347	421	-74
600	500	337	536	-199	198	314	116
800	500	264	575	311	150	331	-181

<sup>a</sup> Units: kJ · mol<sup>-1</sup>. Uncertainties in ΔH° and TΔS° for H<sub>2</sub>O and NH<sub>3</sub>(aq) are estimated for temperatures up to 300°C as cited in Reference 6. At temperatures near and above the critical temperature, the uncertainties for all four reactions are expected to vary from about 5 kJ · mol<sup>-1</sup> at the lower temperatures to about 15 at the highest temperatures. Also, strong correlation is expected for the nearly equal uncertainties in ΔH° and TΔS°.



opposes association and the predominance of the  $T\Delta S^\circ$  term increases as temperature increases, resulting from the contribution of an increasingly positive  $\Delta C_p^\circ$  to the two terms as demonstrated in Reference 6.

The implications of these facts have been discussed in terms of bonding changes and changes in the ordering in the system as ion association occurs. The overall process is



which takes account of hydration of the species in the reaction. The process can be viewed as three hypothetically separable steps: (1) a new bond or interaction is formed, M-X; (2) the  $(m + n - p)$  water molecules are liberated from the hydration spheres; and (3) these liberated waters become bound to bulk water. For step (1)  $\Delta H^\circ$ ,  $\Delta S^\circ$ , and  $\Delta V^\circ$  are all expected to be negative and  $\Delta V^\circ$  is quite small. For step (2) all are expected to be positive as bonds and structure are lost (the actual case for association thermodynamics at high temperatures is shown in Table 2), and for step (3) the opposite is expected. Step 2 leads to the condition that describes the high temperature results. The magnitude of the positive changes could increase if the number of waters liberated increases with temperature or conversely if the bulk solvent structure, or hydrogen bonding, decreases.

#### D. HYDRATION MODEL

The Figures 4 to 7 show that at densities near  $1.0 \text{ g} \cdot \text{cm}^{-3}$  all the thermodynamic quantities are both relatively small and essentially invariant from 25 to  $800^\circ\text{C}$ . Therefore, the differences in the environment of water molecules in the solvation spheres of the dissolved species and in the bulk solvent network are very small only at this density, while near the critical point very large differences exist. A simplified picture consisting of two states for water molecules, hydration spheres and bulk water, was given previously.<sup>6</sup> By this model the partial molar volumes for species (ions and neutral) are represented by only two terms as follows:

$$V_i^\circ = V_i^{\text{hc}} + n_i(V_i^{\text{hs}} - V^{\text{bw}}) \quad (12)$$

where  $V^{\text{hc}}$  represents the species hard core molar volume,  $n$  is the hydration number,  $V^{\text{hs}}$  is the molar volume of water in the hydration sphere of the species, and  $V^{\text{bw}}$  is the molar volume of (bulk) water. The molar volume change for an association reaction is given by

$$\Delta V = -\Delta n(\bar{V}^{\text{hs}} - V^{\text{bw}}) \quad (13)$$

where  $\Delta$  represents (products — minus — reactants) and  $\bar{V}^{\text{hs}}$  is an average for the hydration spheres of all species in the reaction. If the  $\Delta V^{\text{hc}}$  is assumed to be small and  $V^{\text{hs}}$  is  $18 \text{ cm}^3 \cdot \text{mol}^{-1}$ , the values of  $\Delta n$  listed in Table 3 are obtained from the observed  $\Delta V^\circ$  for association reactions. Very high  $\Delta n$  values are obtained near the critical point as the compressibility coefficient for water and  $\Delta V^\circ$  for the association reactions approach infinity. That fact is true no matter what finite value is assumed for  $\bar{V}^{\text{hs}}$ , since  $V^{\text{bw}}$  is finite at the critical point ( $56 \text{ cm}^3 \cdot \text{mol}^{-1}$ ). These values of  $\Delta n$  are, of course, dependent on the choice of  $\bar{V}^{\text{hs}}$  such that if a larger value of  $\bar{V}^{\text{hs}}$  is chosen  $\Delta n$  increases; the sensitivity of  $\Delta n$  to the choice of  $\bar{V}^{\text{hs}}$  is greatest at high solvent densities. No particular significance can be attributed to the actual magnitude of the  $\Delta n$  numbers, especially the smaller values, but the trends toward high values at low densities and temperatures near the critical temperature are of most interest. For  $\Delta V^\circ$  to approach infinity, the hydration number for ions must do so as well, a result which is also predicted by the model of Quint and Wood.<sup>34</sup>

**TABLE 3**  
**Changes in Hydration Numbers  $\Delta n$  for Association Reactions<sup>a</sup>**

°C	$\rho/g \cdot cm^{-3}$	H <sub>2</sub> O	NH <sub>3</sub> (aq)	HCl(aq)	NaCl(aq)
200	Sat.	19	23	17	11
250	Sat.	21	25	20	13
300	Sat.	30	35	29	19
350	Sat.	91	106	90	60
370	Sat.	588	674	582	384
374.1	Sat.	$\infty$	$\infty$	$\infty$	$\infty$
250	0.8	21	28	20	13
300	0.8	16	21	17	11
400	0.8	15	17	15	10
600	0.8	14	15	14	9
800	0.8	14	15	14	10
350	0.6	62	72	62	41
400	0.6	36	41	36	24
600	0.6	18	19	18	12
800	0.6	14	15	14	10
400	0.3	316	360	315	208
600	0.3	33	37	34	22
800	0.3	21	22	21	14

<sup>a</sup> Based on the assumption of an average molar volume for the hydration water of  $18 \text{ cm}^3 \cdot \text{mol}^{-1}$  at all temperatures and pressures.

### E. EXTRAPOLATION OF ASSOCIATION CONSTANTS

Extrapolation of association constants can be viewed as a matter of the precision of the reference quantities of  $\log K$ ,  $\Delta H^\circ$ , and  $\Delta C_p^\circ$  chosen and the temperature variation of  $\Delta C_p^\circ$ . The general case is given by the following relationship, where the  $\Delta C_p^\circ$  integrals are determined by the model that best represents the process at hand:

$$\log \left( \frac{K_T\{p\}}{K_{T_r}\{p_r\}} \right) = (1/(2.303R))[\Delta H_{T_r}^\circ\{p\} \left( \frac{1}{T_r} - \frac{1}{T} \right) - \frac{1}{T} \int \Delta C_p^\circ dT + \int \frac{\Delta C_p^\circ}{T} dT - \Delta V_{T_r}^\circ(p - p_r)] \quad (14)$$

Here, the reference temperature and pressure are 298.15 K and 1 bar. It is a very good approximation that  $\Delta H^\circ\{p\} = \Delta H^\circ\{p_r\}$  along the saturation pressure curve. Also,  $\Delta V^\circ$  is nearly independent of pressure at 298.15 K. The last term contributes only about +0.03 log units at 573 K and for the purpose of estimates can be ignored. With these approximations, the contribution of the two integrals in  $\Delta C_p^\circ$  to  $\log (K_T\{p\}/K_{T_r}\{p_r\})$  can be evaluated and, if  $\Delta H_{T_r}^\circ$  and  $K_{T_r}$  are known, the value of  $\log K_T\{p\}$  can be computed. The values of the integrals for some literature data are shown in Table 4. Listed are values of  $[\log (K_T\{p\}/K_{T_r}\{p_r\}) - (\Delta H_{T_r}^\circ\{p_r\}/(2.303R))(1/T_r - 1/T)]$ . The term in  $\Delta V^\circ$  is neglected. The contribution in log units from the  $\Delta C_p^\circ$  integrals becomes 0.24 to 0.37 at 100°C, 0.93 to 1.4 at 200°C, and 2.0 to 2.9 at 300°C, always in the direction of increasing association with increasing temperature. Thus, if the  $\Delta H_{T_r}^\circ$  were zero for an association reaction, then the increase in  $\log K$  for the reaction is indicated by these amounts.

It is also interesting to examine the magnitude of  $\Delta C_p^\circ$  for ion association reaction types from this point of view. The  $\Delta C_p^\circ$  values in Table 5 become increasingly positive for the association of ions;  $(-\bar{C}_{p,2}^\circ)$  for NaCl also shows quite similar increases. Results for the formation of the ferrous acetate complex,<sup>16</sup>  $\text{FeAc}^+$ , are also shown for comparison.

**TABLE 4**  
**Values of the Integrals**  $[-\frac{1}{T} \int \Delta C_p^\circ dT + \int \frac{\Delta C_p^\circ}{T} dT]$   $(1/(2.303R))$   
**for Ion Association Reactions from Equation 14**

t(°C)	H <sub>2</sub> CO <sub>3</sub>	NH <sub>3</sub> (aq)	H <sub>2</sub> O	$-\bar{C}_{p,2}^\circ(\text{NaCl})^a$	(FeAc <sup>+</sup> ) <sup>b</sup>
100	0.37 ± 0.01	0.24 ± 0.04	0.24 ± 0.01	0.09	0.07 ± 0.3
200	1.43 ± 0.02	1.03 ± 0.03	0.93 ± 0.02	0.69	0.28 ± 0.3
300	2.91 ± 0.06	2.27 ± 0.06	2.00 ± 0.05	2.14	1.20 ± 0.3

<sup>a</sup> Value at 200 bars is shown for comparison.<sup>35</sup>

<sup>b</sup> Reference temperature 50°C instead of 25°C.<sup>36</sup>

**TABLE 5**  
 **$\Delta C_p^\circ$  Values for Formation Reactions and  $\bar{C}_{p,2}^\circ$  (NaCl) at the Saturation Vapor Pressure of Water**

t (°C)	H <sub>2</sub> CO <sub>3</sub>	NH <sub>3</sub> (aq)	H <sub>2</sub> O	(FeAc <sup>+</sup> ) <sup>a</sup>	$-\bar{C}_{p,2}^\circ(\text{NaCl})^b$
100	278 ± 14	212 ± 10	174 ± 6	100 ± 100	77
200	430 ± 36	401 ± 40	342 ± 30	420 ± 60	245
300	1300 ± 150 <sup>b</sup>	1220 ± 100 <sup>b</sup>	1180 ± 100 <sup>b</sup>	1800 ± 200	1641

<sup>a</sup> Corrected as described in Reference 6.

<sup>b</sup> Values at 200 bars from Reference 31.

## F. UNCERTAINTIES IN EXTRAPOLATED EQUILIBRIUM CONSTANTS

Extrapolation of equilibrium constants beyond the range of experimental data has uncertainty associated with the failure of the chosen model to represent accurately physical reality, but also from random errors originating from the parameters in the model. Little can be done to assess the former, but the latter can and should be evaluated as a lower estimate of the error for the extrapolated value. In this discussion two cases will be evaluated: (1) a reaction for which a small and constant  $\Delta C_p^\circ$  is likely, e.g., a reaction for which only cations or only anions are present (the so-called isocoulombic case); and (2) a reaction for which  $\Delta C_p^\circ$  is expected to vary strongly with temperature and pressure such as in ion association or charge neutralization reactions.

The uncertainties associated with independent variables contribute to the variance<sup>37</sup> of the dependent variables  $X_i$  as

$$\sigma_{\log K}^2 = \sum (\partial \log K / \partial x_i)^2 \sigma_{x_i}^2 \quad (15)$$

with no cross terms.

For the case of constant  $\Delta C_p^\circ$  where  $\Delta V^\circ \sim 0$ ,

$$\log K_T = \log K_{T_r} + \frac{\Delta H_{T_r}^\circ}{2.303R} \left( \frac{1}{T_r} - \frac{1}{T} \right) + \frac{\Delta C_{p,T_r}^\circ}{2.303R} \times \left[ \ln \frac{T}{T_r} + T_r \left( \frac{1}{T} - \frac{1}{T_r} \right) \right] \quad (16)$$

Nominal uncertainties were assigned to the reference values of  $\Delta H^\circ$  and  $\Delta C_p^\circ$  ( $\sigma_{\Delta H} = 4 \text{ kJ} \cdot \text{mol}^{-1}$  and  $\sigma_{\Delta C_p} = 40 \text{ J} \cdot \text{mol}^{-1} \cdot \text{K}^{-1}$ ) and their contributions to  $\sigma_{\log K}$  are plotted in

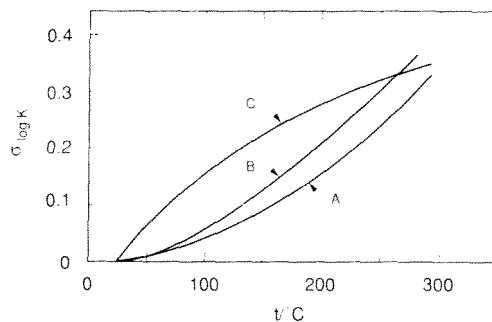


FIGURE 8. Contribution to the uncertainty in  $\log K$  computed from reference values of  $\log K$ ,  $\Delta H^\circ$ , and  $\Delta C_p^\circ$  at  $25^\circ\text{C}$  and 1 bar using two models and assigned uncertainties to  $\Delta H_{25^\circ}^\circ$  and  $\Delta C_p^\circ(25^\circ\text{C})$ . Cases: (A) using the density model in Equation 18 and assuming the sole error is  $\sigma_{\Delta C_p(25^\circ)} = 40 \text{ J} \cdot \text{mol}^{-1} \cdot \text{K}^{-1}$ ; (B) using the constant  $\Delta C_p$  model in Equation 16 and assuming the sole error is  $\sigma_{\Delta C_p(25^\circ)} = 40 \text{ J} \cdot \text{mol}^{-1} \cdot \text{K}^{-1}$ ; (C) using either model with the sole error assigned to  $\sigma_{\Delta H(25^\circ)} = 4 \text{ kJ} \cdot \text{mol}^{-1}$ .

Figure 8 as a function of temperature. Here we assume  $\log K_{T_r}$  is not a significant contributor to the  $\sigma_{\log K}$ . Similar quantities are shown for the second case for which  $\log K$  is represented by the simple form

$$\ln K = a + b/T + c/T \ln \rho \quad (17)$$

and  $\Delta C_p^\circ$  varies as given by Equation 10d. The dependence on reference values is given by

$$\log K\{T,p\} = \log K\{T_r,p_r\} + \frac{\Delta H^\circ\{T_r,p_r\}}{2.303R} \left( \frac{1}{T_r} - \frac{1}{T} \right) + \frac{\Delta C_p^\circ\{T_r,p_r\}}{2.303R} \left\{ \frac{\alpha_r}{T} (T_r - T) + \frac{1}{T} \ln \frac{\rho_r}{\rho} \right\} / (T_r (\partial \alpha / \partial T)_{p_r}) \quad (18)$$

where  $\alpha_r$  represents the expansivity coefficient and  $\rho_r$  the density of water at the reference conditions.

The  $\sigma_{\Delta H}(25^\circ)$  contributes the same amount to  $\sigma_{\log K}$  in both cases and its magnitude reaches 0.35 log units at  $300^\circ\text{C}$ . For the two cases  $\sigma_{\Delta C_p}(25^\circ)$  contributes nearly equally but slightly more for Equation 16 ( $\Delta C_p^\circ = \text{constant}$ ) and becomes 0.33 and 0.38 for the two cases at  $300^\circ\text{C}$ . At lower temperatures the contribution from the  $\sigma_{\Delta H}(25^\circ)$  is significantly greater than that for  $\sigma_{\Delta C_p}(25^\circ)$ . Of course, the uncertainties in  $\log K_{T_r}$  are proportional to the values assumed for  $\sigma_{\Delta H}$  and  $\sigma_{\Delta C_p}$  at the reference conditions.

### III. ION ASSOCIATION FROM CALORIMETRIC EVIDENCE

In contrast to spectroscopic and spectrophotometric methods, which give direct evidence for the presence of associated species at high temperatures, and conductance and electromotive-force measurements, which allow direct inference of the presence and concentration of the products of ion pairing or hydrolysis reactions, evidence for ion association at elevated temperatures from calorimetric methods is less direct. This is due to the fact that calorimetry

as a bulk thermodynamic technique yields no direct information on the molecular or ionic species present in a given solution, and that, for a particular solution model, both activities and enthalpies for the assumed species are needed to resolve observed heats. In the case of heat capacity measurements, the picture is even less clear: in addition to the needed activity, enthalpy, and heat capacity values for the species, there may be a significant contribution to the observed heat capacity from "chemical relaxation" effects due to changes in relative species concentrations over the temperature range of an individual measurement. Except for reactions which proceed essentially to completion, there is relatively strong model dependence of reaction thermodynamic properties and assignments of speciation obtained from the analysis of calorimetric measurements.

In spite of these limitations, calorimetry can give useful information on ion association in electrolyte solutions at higher temperatures and pressures. Calorimetry may be used as a tool for extending the temperature range of measurements of ion association reactions; in favorable cases, assignment of the association constants and enthalpies of association may be made solely on the basis of calorimetric measurements. Enthalpy measurements are used more often than heat capacities in studies of ion association in electrolyte solutions, and the following discussion will be limited in its treatment of heat-capacity techniques. Two distinct types of experiments have been used to obtain information on ion association in electrolyte solutions. Enthalpies of dilution, particularly when extended to low solute molalities (below  $0.01 \text{ mol} \cdot \text{kg}^{-1}$ ), provide evidence for association of electrolytes through marked departure of the observed enthalpies from the expected limiting-law behavior. Enthalpies of mixing, or titration experiments, may be useful in determining association constants for those cases where a product ion pair predominates over the levels of associated species contained in the two solutions to be mixed. Each of these experiments, with relevant examples, will be discussed in detail in the following sections.

### A. ELECTROSTATIC CONSIDERATIONS

The entropic basis for the enhanced formation of ion pairs in simple electrolytes at high temperatures has been discussed in detail above, where it was pointed out that the entropy increase on ion pair formation, due to the net release of hydrated water molecules to the bulk solvent, dominates the entropy decrease on formation of the ion pair from the component ions. It is also useful to consider a continuum-dielectric picture of the solvent, the Bjerrum model of ion association, in which simple electrostatic effects strongly favor ion association at high temperatures. In that model the Bjerrum length, which is taken to be that interionic separation defining the formation of an ion pair, is given by

$$q_{ij} = |z_i z_j| e^2 / (2DkT) \quad (19)$$

where  $z_i$  and  $z_j$  are the charges on the ions,  $e$  is the electronic charge, and  $k$  is the Boltzmann constant. This length increases as the product of the dielectric constant  $D$  and temperature  $T$  decreases with increasing temperature, suggesting increased formation of ion pairs at high temperatures. On this basis the degree of dissociation  $\theta$  may be written as<sup>3</sup>

$$\theta = 1 - \frac{4\pi N c_i}{1000} \frac{(|z_i z_j| e^2)^3}{(DkT)^3} \int_2^b y^{-4} \exp(y) dy \quad (20)$$

where  $y = -z_i z_j e^2 / DrkT$ ,  $b = -z_i z_j e^2 / Da_0 kT$ ,  $N$  is Avogadro's number,  $c_i$  is the molar concentration,  $r$  is the distance of ion  $i$  from the test charge  $j$ , and  $a_0$  is the distance of closest approach of the ions. The association constant  $K_A$  is the limiting value of Equation 20:

$$K_A = (4\pi N / 1000) (|z_i z_j| e^2 / DkT)^3 \cdot Q(b) \quad (21)$$

where  $Q(b)$  represents the integral in Equation 20. It should be noted that this constant has units ( $\text{l} \cdot \text{mol}^{-1}$ ), that is, reciprocal molarity units. Expressing  $K_A$  as the logarithmic quantity in molal units,

$$\log K_A = A - 3 \log (DT) + \log Q(b) + \log \rho \quad (22)$$

where  $A = \log \{(4\pi N_A/1000)(|z_+z_-|e^2/k)^3\} = 13.55$  for a 1-1 charge-type electrolyte. Temperature differentiation gives

$$\Delta H^\circ/RT^2 = \alpha - [3/(DT)] \{\partial(DT)/\partial T\}_p + \{\partial[\ln Q(b)]/\partial T\}_p \quad (23)$$

where  $\alpha$  is the thermal expansivity of water. Here the derivative  $\{\partial(DT)/\partial T\}_p$  is negative,  $\{\partial[\ln Q(b)]/\partial T\}_p$  and  $\alpha$  are positive, and the overall expression is positive-definite. Thus by this model ion association is endothermic and  $\Delta H^\circ$  diverges toward  $+\infty$  at the solvent critical conditions. The model predicts large exothermic differences from limiting-law behavior for dilution enthalpies at low molalities, where the fractional level of ion pairing decreases with decreasing molality. Also, since  $\Delta H^\circ$  for ion association is strongly positive, the model also points to the entropy as the driving force for association reactions. A quantitative example of the application of Equations 22 and 23 to hydrochloric acid is given below.

An assignment of ion pairing thermodynamic properties based on observed departures of dilution enthalpies at low molalities from the electrostatic limiting law presupposes that the limiting law is applicable at high temperatures. Two factors limit confidence in this analysis at high temperatures. Practically, the solvent dielectric constant and its temperature derivative, needed to compute the limiting slope for the relative enthalpy, are known less precisely with increasing temperature. Compilations based on the available measured dielectric constants have been made over wide ranges of temperature by Bradley and Pitzer,<sup>38</sup> Uematsu and Franck,<sup>39</sup> and Archer and Wang.<sup>40</sup> Limiting-law slopes as defined by Bradley and Pitzer<sup>38</sup> have been reported by Pitzer et al.<sup>35</sup> and by Archer and Wang.<sup>40</sup> In the former calculation, the equation of state for water of Haar et al.<sup>41</sup> was used to calculate the required values of solvent density and its temperature and pressure derivatives; Archer and Wang<sup>40</sup> used the equation of state of Hill,<sup>42</sup> noting that it does not include the apparent fitting artifacts in higher derivatives of  $\rho$  at low temperatures present in the equations of Haar et al. and of Saul and Wagner.<sup>43</sup> Archer<sup>44</sup> has given a simple set of parameters in the Pitzer model extending beyond the limiting-law term which may be used in interconversions between the various representations of limiting-law slopes. In work above 523 K, notably by Holmes et al.<sup>45</sup> and Simonson et al.,<sup>46</sup> the equation of state of Haar et al. has been used with the dielectric constant representation of Uematsu and Franck to calculate limiting-law slopes. Values of the limiting-law slopes for the osmotic coefficient and for the relative enthalpy calculated from the HGK equation of state and either the Bradley and Pitzer or the Uematsu and Franck correlations for the dielectric constant are compared in Figure 9 with the recent values of Archer and Wang, based on their dielectric constant and the equation of state of Hill. Agreement of  $A_\phi$  and  $A_H$  among the three treatments is reasonably good at temperatures between 298.15 and 523.15 K over the pressure range from the saturation vapor pressure to 100 MPa, with differences in  $A_\phi$  no larger than 1% and calculated  $A_H$  within 5% at all conditions considered. The disagreement of calculated values, particularly in the temperature and pressure derivative properties, at temperatures below 298.15 K has been noted previously.<sup>5</sup> Based on this comparison, limiting-slope values are relatively unambiguously known to 523 K. However, the departures from limiting-law behavior of the observed dilution enthalpies taken as an indication of the onset of ion association at high temperatures become pronounced only above 523 K. Even at these higher temperatures, the apparent uncertainty in the limiting slopes is not sufficiently large to account for the observed departures from theoretical behavior of the dilution enthalpy at low molalities.

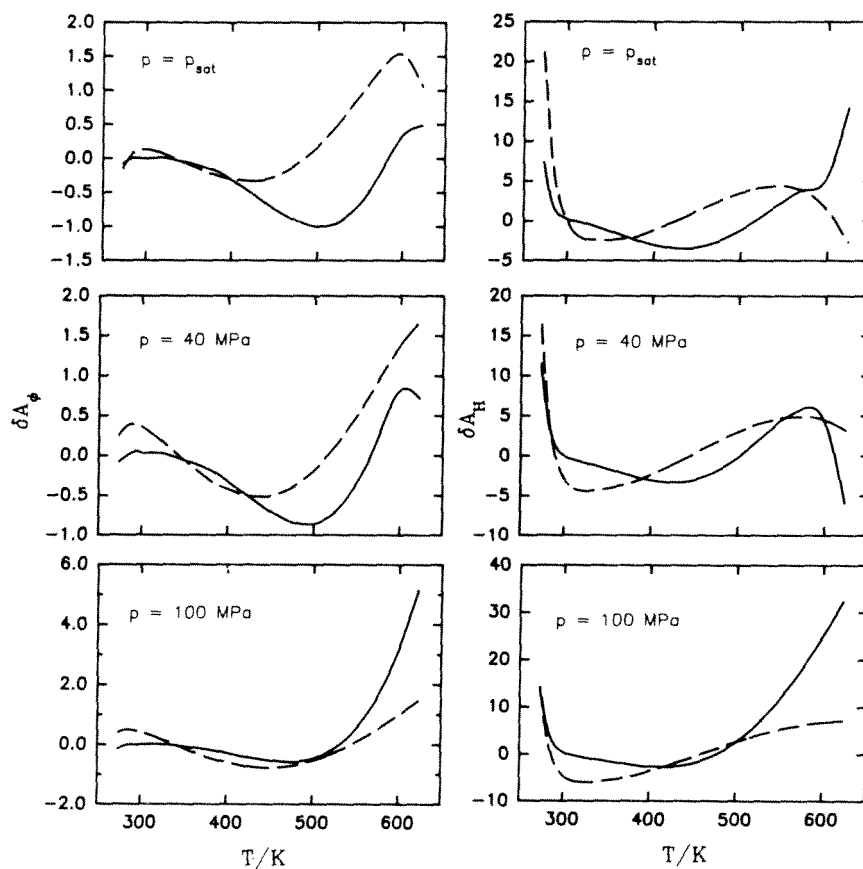


FIGURE 9. Comparison of Debye-Hückel limiting slopes  $A_\phi$  and  $A_H$  as defined by Bradley and Pitzer.<sup>38</sup> For both  $A_\phi$  and  $A_H$ ,  $\delta A = 100(A - A_{ref})/A_{ref}$ , where  $A$  is taken from the equation of state of Haar et al.<sup>33</sup> and the dielectric constant of Bradley and Pitzer<sup>38</sup> (solid curves) or of Uematsu and Franck<sup>39</sup> (dashed curves), and  $A_{ref}$  is taken from Archer and Wang.<sup>40</sup>

A more fundamental concern with this approach to the study of ion pair formation in high-temperature electrolyte solutions arises through consideration of the underlying assumptions of the application of the Debye-Hückel theory to Gibbs free energies at elevated temperatures. As the solvent compressibility increases, particularly near the saturation pressure curve above 573 K, treatment of the solvent as an incompressible continuum dielectric fluid becomes increasingly doubtful. This question has been addressed by Levelt Sengers and co-workers,<sup>47</sup> who have outlined a treatment of solution thermodynamics at high temperatures based on an expansion of the Helmholtz free energy in temperature, density, and composition about the solvent critical point. Also, Wood et al.<sup>34</sup> have described properties of an ionic solute in a compressible dielectric solvent. At the present time no quantitative limits have been set on the temperature and pressure limits of applicability for models such as the Pitzer ion interaction treatment, which reduce to the Debye-Hückel limiting law in the natural variables of the Gibbs free energy. Pitzer and Li<sup>48</sup> and others have introduced the relatively loose concept of "liquid-like" densities as a condition for applying Gibbs free energy electrostatic models at high temperatures. Simonson et al.<sup>46</sup> have shown that such a treatment may be used to represent quantitatively observed enthalpies of dilution of HCl(aq) to the solvent critical temperature at pressures well above the critical pressure provided an assumed ion association equilibrium is included in the analysis, and that the levels of ion

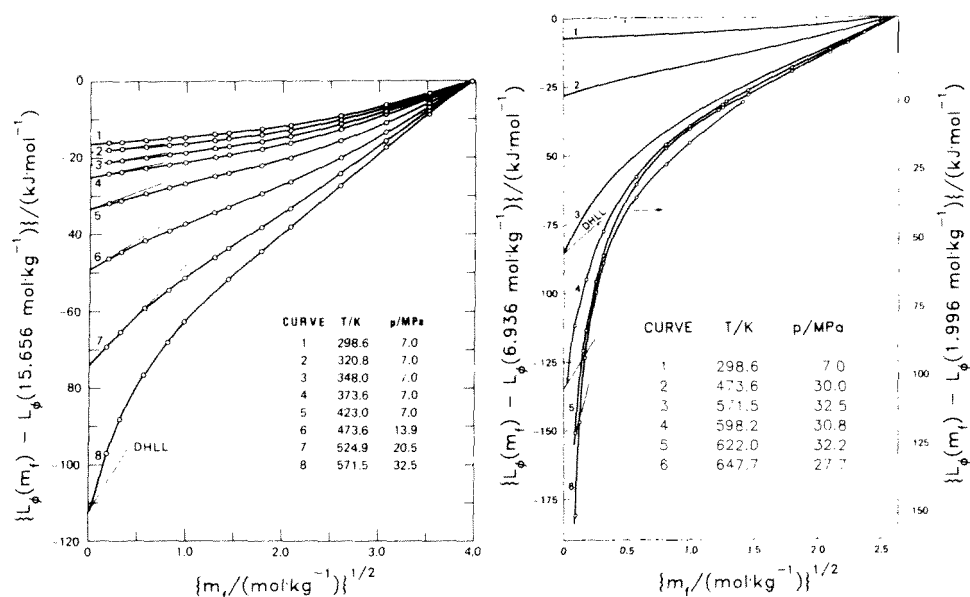


FIGURE 10. Dilution enthalpies of HCl(aq) at various temperatures from Holmes et al.<sup>45</sup> indicating departures from limiting-law slopes (light lines) at higher temperatures.

pairing calculated from conductance measurements in the supercritical region are consistent with the observed dilution enthalpies. With this in mind, the departure at low molalities and high temperatures of measured enthalpies of dilution of simple electrolytes from the limiting behavior predicted by the electrostatic limiting law in the Gibbs free energy may be assumed to be due to the dissociation of ion pairs, as outlined in Equations 20 and 21.

## B. ION ASSOCIATION EVIDENCE FROM DILUTION ENTHALPY MEASUREMENTS

Enthalpies of dilution have been measured, primarily at Oak Ridge, for a number of simple electrolyte solutions over wide ranges of temperature, pressure, and molality. Results reported to date include dilutions of NaCl(aq),<sup>49</sup> HCl(aq),<sup>45,46</sup> NH<sub>3</sub>Cl(aq),<sup>50</sup> CaCl<sub>2</sub>(aq),<sup>33</sup> and NaOH(aq),<sup>51</sup> at temperatures as high as 673 K. In these studies it has been noted that the observed dilution enthalpies  $\Delta_{\text{dil}}H_m$ , given for a simple electrolyte in terms of the relative apparent enthalpy  $L_\phi$ , as

$$\Delta_{\text{dil}}H_m = L_\phi(m_f) - L_\phi(m_i) \quad (24)$$

are consistent with the assumption of complete solute dissociation at temperatures to approximately 523 K. In the case of NaCl(aq), complete dissociation was assumed in the treatment of Pitzer et al.<sup>35</sup> at temperatures to 573 K. At higher temperatures, the observed  $\Delta_{\text{dil}}H_m$  at low molalities plotted against  $m^{1/2}$  are steeper than predicted by the Debye-Hückel limiting-law slope. Examples of this behavior as exhibited by HCl(aq) and CaCl<sub>2</sub>(aq) are illustrated in the dilution enthalpies shown in Figures 10 and 11.

This divergence from the theoretical slope for  $\Delta_{\text{dil}}H_m$  occurs in a molality range where it is not possible to account fully for the observed results with widely used models for short-range interparticle interactions such as the ion interaction model of Pitzer.<sup>35,52</sup> However, unless measurements of  $\Delta_{\text{dil}}H_m$  are available at very low molalities with very high precision, it is not possible to assign unambiguous values of  $K_A$  and  $\Delta H^\circ$  based on dilution enthalpy measurements. While this point has been discussed in detail by Simonson et al.,<sup>46</sup> it is useful to reconsider the primary considerations here.



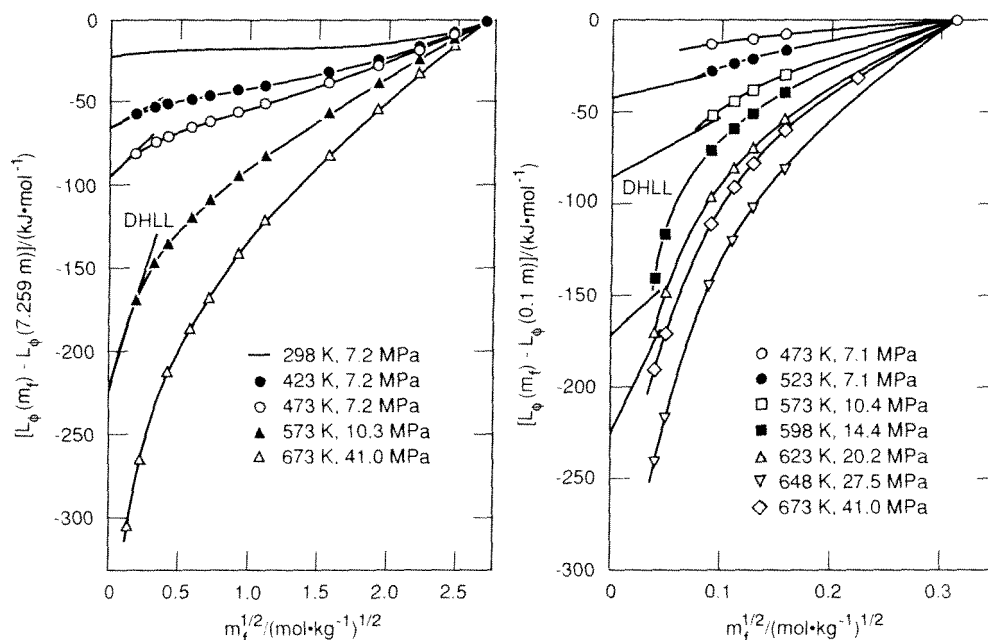
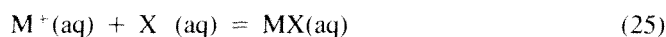


FIGURE 11. Dilution enthalpies of  $\text{CaCl}_2(\text{aq})$  to 673 K from Simonson et al.<sup>46</sup> indicating departure from limiting-law behavior at low molalities on the expanded scale of the right-hand plot.

For a solute MX which may undergo ion pairing according to



with

$$K_A = (m_{\text{MX}}/m_{\text{M}} \cdot m_{\text{X}})(\gamma_{\text{MX}}/\gamma_{\text{M}} \cdot \gamma_{\text{X}}) \quad (26)$$

and degree of dissociation  $\theta = m_{\text{MX}}/m$ , where  $m$  is the stoichiometric molality of the solute, the enthalpy of dilution from  $m_i$  to  $m_f$  may be written

$$\Delta_{\text{dil}}H_m = (\delta n)\Delta_A H^\circ + L_\phi^E(m_f) - L_\phi^E(m_i) \quad (27)$$

Here the  $L_\phi$  are apparent relative enthalpies of the mixed solutions  $[\text{M}^+(\text{aq}) + \text{X}^-(\text{aq}) + \text{MX}(\text{aq})]$  at their equilibrium mole ratios, relative to the hypothetical reference state  $L_\phi^E = 0$  at  $m = 0$  with  $\theta$  held fixed at the finite-molality equilibrium value. The quantity  $\delta n$  is the difference in the number of moles of ion pairs formed for a given total number of moles of solute between the initial and final solution molalities. In a usual case, i.e., where  $\theta$  increases with  $m$  at constant  $T$  and  $p$ ,  $\delta n < 0$ , and  $\Delta_A H^\circ \gg 0$ , the net  $\Delta_{\text{dil}}H_m$  observed is more negative than predicted based on assumed complete dissociation and the limiting-law slope even when the assumed smaller values of the  $L_\phi^E$  compared with the case of assumed complete dissociation are taken into account. The source of the ambiguity in the treatment lies in the coupling of excess and reaction thermodynamic properties. Given the assumed large differences in dilution enthalpies per mole of solute for charged and uncharged solutes, the  $L_\phi^E$  are strongly dependent on  $\theta$ , which is determined by the equilibrium constant, the species molalities, and their activity coefficients. The most appropriate conditions for determining reaction thermodynamic constants from dilution enthalpy results are very low

molalities, where activity coefficients of the charged species may be assumed to follow extended-limiting-law behavior and those for uncharged species may be assumed to be unity. The reaction quantities  $K_A$  and  $\Delta H^\circ$  may then be fitted to the observed dilution enthalpies over a range of temperatures, with appropriate forms chosen for the temperature dependence of  $K_A$  to give thermodynamic consistency of the resulting values. This method is most appropriate when  $K_A$  is large enough that  $\theta$  varies significantly over a relatively small range of low molalities. In practice, the idealized method described above has not been applied to actual experimental results due to limitations of the calorimetric techniques in reaching very low molalities with sufficiently high precision. A modification of this approach based on the assumption of model-substance behavior of excess thermodynamic properties of charged solutes has been applied in mixing-enthalpy studies, as discussed below.

Two methods to lift the covariance of excess- and reaction-thermodynamic quantities have been used in a recent analysis of enthalpies of dilution of  $\text{HCl}(\text{aq})$  to 648 K.<sup>46</sup> In one treatment, the values of  $K_A$  and  $\Delta H^\circ$  are assumed known from another source, e.g., extrapolation of conductance measurements at supercritical temperatures, and excess thermodynamic properties of all solute species are assigned by fitting to the observed dilution enthalpies as a function of temperature. In a second approach simplifying assumptions are made concerning the form of the expression for excess thermodynamic properties of the solute species; values of excess and reaction thermodynamic properties are then assigned by fitting the model to the available experimental results, without recourse to independently determined values of  $K_A$  and  $\Delta H^\circ$ .

In the case of  $\text{HCl}(\text{aq})$ , a third method may be used to evaluate  $K_A$  near ambient temperature. Following Marsh and McElroy,<sup>53</sup> if it is assumed that the distribution of unionized  $\text{HCl}$  to the vapor phase follows Raoult's law at those conditions below the solute critical temperature (324.6 K),

$$a_{\text{HCl}}(l) = a_{\text{HCl}}(v) \quad (28)$$

$$x_{\text{HCl}}g_{\text{HCl}} = f/f^\circ \approx p/p^\circ \quad (29)$$

At low stoichiometric liquid-phase  $\text{HCl}$  molalities,  $x_{\text{HCl}} \approx m_{\text{HCl}}/55.5$ ,  $g_{\text{HCl}} \approx 1$ ; these approximations give

$$m_{\text{HCl}} = 55.5 p/p^\circ \quad (30)$$

where  $p$  is the measured partial pressure of  $\text{HCl}$  over the solution and  $p^\circ$  is the corresponding vapor pressure of pure  $\text{HCl}$ ;  $K_A$  may then be calculated from Equation 26. The vapor pressure data of Fritz and Fuget,<sup>54</sup> calculated from emf measurements, combined with vapor pressures of pure  $\text{HCl}$ ,<sup>55</sup> were used to calculate molalities of unionized  $\text{HCl}$  in the liquid phase from 273.15 to 323.15 K along the saturation vapor pressure curve. Apparent  $K_A$  values were then calculated for a given stoichiometric molality using the activity coefficients tabulated by Holmes et al.;<sup>45</sup> the values were found to be independent of molality to  $m = 0.5 \text{ mol} \cdot \text{kg}^{-1}$ , indicating that the approximations introduced above are appropriate for the present set of results. The resulting  $K_A$  values, and those at higher temperatures where the other representations for  $K_A$  are in agreement, were fitted to a simple function of temperature and solvent density (slightly different from that of Section II):

$$\log K_A = 4.424 - 3149.9/T - 13.85 \log \rho \quad (31)$$

Values of  $K_A$  calculated from this fit are compared in Figure 12 with those extrapolated from the supercritical conductance measurements of Frantz and Marshall<sup>56</sup> and those for the

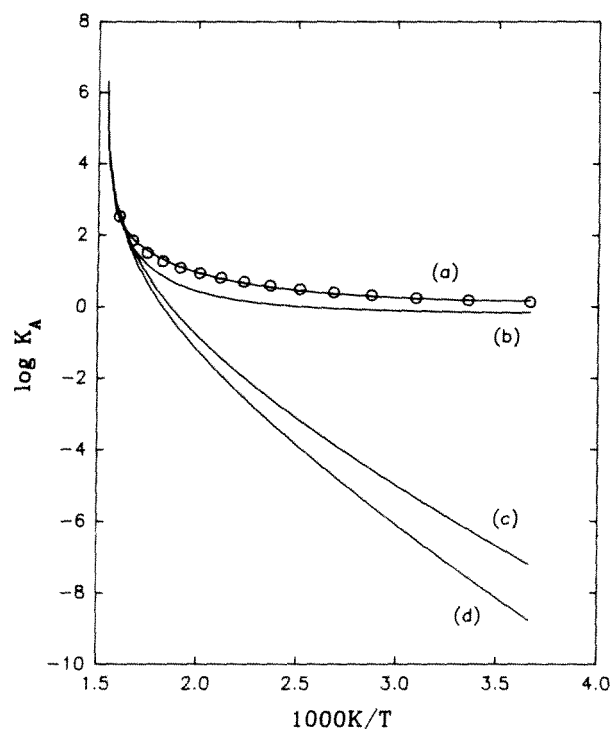


FIGURE 12. Ion association constant for HCl(aq) along the saturation vapor pressure curve. (a) Symbols calculated from Equation 22, curve fitted to the form of Equation 31; (b) calculated for the formation of the 1-1 ion pair from the CE model of Reference 46; (c) fitted to low-temperature partitioning data and high-temperature conductance data as described in the text; (d) extrapolated from fitted data of Frantz and Marshall.<sup>56</sup>

1-1 ion association reaction calculated from dilution enthalpies and the CE model of Simonson et al.<sup>46</sup> Another set of  $K_A$  values, reported from 298.15 to 623.15 K by Ruaya and Seward<sup>57</sup> from measurements of AgCl solubility, are in reasonable agreement (0.5 log units) with curve (b) of Figure 12, and are not shown in the plot.

Values of  $K_A$  may also be calculated for this temperature range from Equation 22, assuming a reasonable value (0.18 nm) for the ion pair radius for HCl. The resulting values are complex functions of temperature, density, and dielectric constant, but are well reproduced ( $\pm 0.05$  log units) with the functional form of Equation 31. This capability of the simple fitting function to represent results calculated from the more complex Equation 22 may account in part for the wide success of this temperature-density relation in representing measured  $K_A$ . These fitted values are shown as curve (a) in Figure 12, where it is clear that the use of a temperature-independent ion pair radius is insufficient to give agreement with any of the curves obtained from fitting experimental results. This failure is not surprising in view of the approximations involved in the Bjerrum treatment concerning short-range interactions; in particular, very small values of  $K_A$  calculated from the Bjerrum treatment would require unphysically large values of the ion pair contact radius. All equations for  $K_A$  are in good agreement for  $K_A \geq 50$ , but disagree widely at lower temperatures (lower  $K_A$ ) where the ambiguities in assignment of excess and reaction thermodynamic properties are pronounced. Reaction thermodynamic properties derived from dilution enthalpy measurements may differ significantly from more directly obtained values where association is

inconsequential, but should come into closer agreement as the effects of ion association become increasingly important.

### C. ION ASSOCIATION EVIDENCE FROM MIXING ENTHALPY MEASUREMENTS

Measurements of enthalpies of mixing of simple electrolytes at high temperatures have also been used to provide an experimental basis for the assignment of values of thermodynamic properties of assumed ion association reactions, notably by Oscarson et al.<sup>58,59</sup> in recent studies to 593 K. This method is a flow-calorimetric adaptation of the thermometric titration method widely applied in batch instruments near ambient temperature.<sup>60</sup> For single reactions which proceed to completion,  $\Delta H^\circ$  may be calculated straightforwardly from the limiting value of the observed enthalpy with one reactant in excess, with appropriate corrections for dilution enthalpies of products and reactants. Where the reaction does not proceed to completion, i.e., where  $K < +\infty$ , both  $K$  and  $\Delta H^\circ$  may be determined from the shape and magnitude of the observed enthalpies as a function of titrant added. It has been noted<sup>60</sup> that this method is most appropriate for  $1 < \log K < 4$ .

In cases where one association reaction is markedly favored over all other possible combinations in the experiment, the results are relatively unambiguous. Uncertainties in enthalpies of dilution of reactants and products, and in the levels of ion pairing of the electrolytes in the reactant solutions, may be negligible in comparison with the observed enthalpy of formation of the product ion pair. However, the reaction thermodynamic values must be extracted from modeling the observed enthalpies, with consideration of all possible reactions in a relatively complex electrolyte mixture at high temperatures; the resulting values may include a significant uncertainty due to covariance of multiple reactions in the mixture under unfavorable conditions.

The second ionization constant for sulfuric acid,



has been reported by Oscarson et al.<sup>58</sup> for temperatures from 423.15 to 593.15 K based on measured enthalpies of mixing of  $(\text{Na}_2\text{SO}_4 + \text{H}_2\text{SO}_4)$  and dilution enthalpies of  $\text{Na}_2\text{SO}_4$  and  $\text{H}_2\text{SO}_4$ . The reported  $\log K_2$  for association of  $\text{H}^+$  and  $\text{SO}_4^{2-}$  ranges from 3.56 at 423.15 K to 6.94 at 593.15 K, with the higher values somewhat outside the optimum range for the determination of  $\log K_2$  from analysis of mixing enthalpy curves with varying extent of reaction. Dilution enthalpy corrections to the observed enthalpies were made for all charged species, assuming that the excess thermodynamic properties of NaCl at high temperature reported by Liu and Lindsay,<sup>61</sup> with appropriate charge factors, could be used to represent the dilution enthalpies of product and reactant species. Values of  $K_2$  and  $\Delta H^\circ$  were fitted to each isothermal set of results, and brought into approximate thermodynamic consistency through a representation of the temperature dependence of these quantities which ignored the effects of changing experimental pressures with temperature. The resulting  $K_2$  values were in approximate agreement with the recent potentiometric study of Dickson et al.,<sup>16</sup> with  $\Delta(\log K_2)$  ranging from 0.02 log units at 523.15 K to 0.25 log units at 423.15 K. Differences in  $\Delta H^\circ$  were as large as  $15 \text{ kJ} \cdot \text{mol}^{-1}$  at 523 K.

A brief consideration of the data analysis techniques employed in the mixing enthalpy experiments will serve to illustrate important sources of the discrepancies between the calorimetrically determined values and the more precise potentiometric results. At 523.15 K, the reported  $\Delta H^\circ$  for the calorimetric study was  $105 \text{ kJ} \cdot \text{mol}^{-1}$ . Using the approximation (at  $\log K_2 = 5.34$ ) of complete reaction of  $\text{Na}_2\text{SO}_4$  with  $\text{H}_2\text{SO}_4$  gives a limiting value for the reaction enthalpy of  $54 \text{ J} \cdot \text{mol}^{-1}$  in the experiments where reactants were mixed at  $1 \text{ mol} \cdot \text{kg}^{-1}$ ; the observed heat production was near  $19 \text{ J} \cdot \text{mol}^{-1}$ , giving a total correction

of  $35 \text{ J} \cdot \text{min}^{-1}$  arising from dilution enthalpies and any assumed competing reactions. Assuming a 20% uncertainty introduced in the dilution enthalpy corrections from the use of NaCl as a model substance in calculating excess thermodynamic properties gives an uncertainty in  $\Delta H^\circ$  of  $14 \text{ kJ} \cdot \text{mol}^{-1}$ , approximately the difference between the  $\Delta H^\circ$  values calculated from the calorimetric and potentiometric studies.

The above example also serves to indicate that the thermodynamic quantities for competing minor reactions, e.g., the reaction



in the present case, must include very large uncertainties which are difficult to assess quantitatively. Thermodynamic properties for assumed competing reactions must be assigned on the basis of misfit of the observed mixing and dilution enthalpies using the NaCl model-substance assumption for excess thermodynamic properties. Since this assumption is inappropriate in most cases, incorrect values of  $K$  and  $\Delta H^\circ$  for secondary reactions will be obtained from the calorimetric results.

#### IV. METAL COMPLEXATION

Most of the early work on metal complexation was concentrated on chlorides,<sup>4,5,62</sup> which are of primary interest in geochemistry related to the mobility of metals in natural hydrothermal systems and the subsequent formation of ore deposits. Other applications include corrosion, hydrometallurgy, waste disposal, and oceanography. More recently, the emphasis has shifted to organic ligands<sup>63</sup> that may influence the transport of metal ions in groundwaters and play a similar role in the cycle chemistry of power-generating plants, and to those synthetic ligands that exhibit the potential for removal of metal ions from waste streams.

In general, four techniques have been used predominately to obtain quantitative information as to the stability of these complexes in solution, viz., spectrophotometry, conductivity, solubility, and potentiometry. More attention will be given to potentiometry in this section as the utilization of concentration cells to study metal complexation at high temperatures is relatively recent. Other methods such as solvent extraction and polarography have received more limited attention; Raman spectroscopy has proven to be a versatile tool in determining speciation and suggesting the relative stabilities of these species.<sup>64</sup> Neutron and X-ray diffraction<sup>65,66</sup> have been used to gain a direct measure of the structure, bond lengths, and angles in the first coordination sphere of aqueous metal ions. However, although these studies are critical to our understanding of solvation and solute-solute interactions, they are restricted to high concentrations, metal ions with a high neutron cross-section, and finally to ambient conditions for the present. NMR is another technique that is growing in use to elucidate structures of dissolved metal species, e.g., for such species as aluminum acetate.<sup>67</sup> NMR has been used effectively at high pressures and to high temperatures, although to a limited extent.<sup>68</sup> The above discussion focuses on those complexes that are amenable and practical for study at high temperatures as this is the theme of this chapter and therefore excludes the wealth of information available on coordination compounds of transition metals at ambient conditions.<sup>4,5,62,63</sup> Seward<sup>69</sup> reviewed the general topic of metal complexation at high temperatures in 1981 so that this section also serves to update the material formerly covered with some shift in emphasis.

#### A. EXPERIMENTAL METHODS — THEIR APPLICATION AND LIMITATIONS

##### I. General

The majority of complexes formed with mono- and bivalent metal cations involving geologically and industrially interesting ligands have low inherent stabilities at moderate



quotients for the metal complexation, as defined by the generalized equation for mononuclear species.

$$Q_n^T = [\text{MAc}_n^{m-n}]/[\text{M}^{m+}][\text{Ac}^-]^n \quad (36)$$

is related to the equilibrium constant,  $K_n^T$ , at infinite dilution,

$$K_n^T = Q_n^T \gamma_{\text{MAc}} / (\gamma_M \gamma_{\text{Ac}}) \quad (37)$$

where  $\gamma$  represents the activity coefficient of the appropriate species in solution and the superscript T serves to differentiate the overall thermodynamic quantity from the stepwise quantity preferred later in the discussion. Thus  $\bar{n}$  is related to  $Q_n^T$ , the derived hydrogen ion concentration,  $[\text{H}^+]$ , and the acetic acid concentration,  $[\text{HAc}]$ , as shown in Equation 38:

$$\begin{aligned} \bar{n} &= n \sum [(\text{MAc}_n)^{m-n}] / \{[\text{M}^{m+}] + \sum [(\text{MAc}_n)^{m-n}]\} \\ &= n \sum \{Q_n^T [\text{Ac}^-]^n\} / \{1 + \sum Q_n^T [\text{Ac}^-]^n\} \\ &= n \sum \{Q_n^T \{Q_{\text{HAc}} [\text{HAc}] / [\text{H}^+]\}^n\} / \{1 + \sum \{Q_n^T \{Q_{\text{HAc}} [\text{HAc}] / [\text{H}^+]\}^n\}\} \end{aligned} \quad (38)$$

The proton concentration is obtained in turn from the measured potential difference  $E$  as given in Equation 2. Given matching electrolytes of identical ionic strengths, substantial evidence exists supporting the effectiveness of the Henderson equation in accurately predicting the value of  $\text{ELJ}$ .<sup>76</sup> An iterative solution of Equations 2, 36, and 38, and the mass balance equations, ionic strength, and  $\text{ELJ}$ , yields the formation quotients,  $Q_n^T$ , of the principal species in solution.

The limitations of this potentiometric method involving competitive complexation are (1) there is a need to estimate liquid junction potentials (with the precautions mentioned, the uncertainty in  $\log Q_n^T$  amount to about  $\pm 0.002$ ); (2) the metal ions must be inert to reduction by hydrogen; (3) the minimum concentration of total metal ion in solution is *circa*  $10^{-3} \text{ mol} \cdot \text{kg}^{-1}$ ; (4) readily hydrolyzable metals present a problem, particularly at temperatures approaching  $300^\circ\text{C}$ , because the minimum pH of the solution is dictated by the buffer ratio of the hydrolyzable ligand; (5) the upper temperature limit is  $295^\circ\text{C}$ , due mainly to the presence of Teflon in the system, but also to the volatility of acetic acid; and (6) the assignment of formation quotients to complexes that represent  $<10\%$  of the total metal concentration is usually ambiguous without supporting information, or at least a knowledge of these quotients at other experimental conditions. The latter limitation is common to all techniques that do not distinguish species explicitly based on some directly measurable property, such as the assignment of a characteristic Raman vibrational mode.

It may be of interest to note that this method of competitive complexation has been taken a step further in the case of the ferrous acetate, whereby chloride ions are also titrated into the above cell configuration.<sup>77</sup> Thus both chloride and acetate ions compete as ligands and, from a knowledge of the thermodynamics of the acetate complexation, those for chloride can be extracted. However, the competing ligands cannot differ too greatly in their complexing abilities so as to ensure a meaningfully large potential change, and the equilibrium quotients obtained are necessarily less precise than those obtained for the "primary" ligand.

A cell of similar configuration to that described above, fitted with silver/silver chloride electrodes, has been tested successfully in this laboratory to measure chloride complexation with cadmium(II) up to  $200^\circ\text{C}$ .<sup>78</sup> This method shows great potential for the direct and precise measurement of the strength of a number of important metal chloride complexes as a function of temperature and ionic strength. The liquid junction potential is again minimized by

matching the ionic strength in both cell compartments and maintaining a low pH, because the mobility of hydrogen ions dominates the Henderson expression. The low pH is obviously an effective counter to contributions from metal ion hydrolysis. There is the usual need to restrict the chloride concentration to *circa* 10% of the total ionic strength to maintain a constant ionic medium, i.e., the approximation is made that the activity coefficients of the interacting species are constant throughout a titration. The limitations are, in common with concentration cells in general, as outlined in (1), (3), (5), and (6) above; however, (2) now restricts metals for study to those that are not oxidized by silver chloride or reduced by silver, and (4) an upper temperature limit of *circa* 250°C is imposed by the solubility of silver chloride which becomes so great in the presence of high chloride concentrations as to affect the stoichiometry to an, as yet, inestimable extent.

The more conventional cells without liquid junctions have been used in various forms, e.g., mercury-metal amalgam electrode vs. a silver chloride reference electrode<sup>79,80</sup> for chloride complexation measurements. These measurements can be made very precisely, but require calibration or a knowledge of the absolute potentials of each half-cell reaction. Although this criterion alone does not preclude their application to high temperatures, as demonstrated by Greeley et al.<sup>81</sup> in their use of a Harned cell to determine of hydrochloric acid activity coefficients to 250°C, this remains a virgin field.

#### ***b. UV-Visible Spectrophotometry***

Perhaps the majority of complexation equilibria involving transition metals and actinides has been investigated by this technique at ambient conditions. The measurements are convenient and relatively fast. In those idealized cases involving a single-step process where the starting material and final product have been independently identified and their spectra recorded, the interpretation of the intermediate spectra is unambiguous and explicit thermodynamic quantities can result. Most transition metal systems involve multistep equilibria and speciation is based on deconvolution routines of the broad absorption bands associated with d-d electronic transitions to obtain the individual extinction coefficients. A simultaneous fitting process is carried out isothermally with the assignment of corresponding formation quotients.

Seward and co-workers,<sup>82,83</sup> who have reported the thermodynamics of chloride complexation of lead(II) and iron(II), are pioneers in the application of spectrophotometry to high temperature environments. Their results extend to 350 and 200°C, respectively, and were performed in the absence of any supporting electrolyte, such that the activity coefficients of the ionic species were treated individually from available experimental data and/or from extended Debye-Hückel expressions.

#### ***c. Solubility Measurements***

Most of the information on complexation at high temperatures is derived from solubility measurements, which are intrinsically appropriate for poorly soluble metal ions that are often difficult to study by more convenient methods.<sup>84-87</sup> Solubility studies are in general tedious and often suffer in precision because of several problems: sampling (particularly for those metal ions having prograde solubility); analytical limitations at very low solubilities; slow equilibration kinetics (especially experiments conducted from supersaturation where nonequilibrium, and/or amorphous, phases are preferentially precipitated); adequate control and characterization of the solid phase(s) and the particle sizes present prior to and following the attainment of equilibrium; and other parameters such as temperature, pressure, redox potential, and pH at temperature. Other concerns result from the need for analysis of the sampled solutions in terms of the species actually present at temperature, and, particularly in the case of organic ligands at high temperature, the thermal stability of the species over the long time periods generally required for equilibration. Nevertheless, with careful control



of the experimental conditions and an appropriate choice of solid phase and solution composition, solubility studies often provide a unique vehicle for the study of complexation phenomena.

The solubility method infers that the solid phase contains the metal ion of interest as an oxide, sulfide, etc., or a more complex mineral assemblage. Ruaya and Seward<sup>88</sup> have investigated the enhancement in the solubility of silver chloride in the presence of metal ions to deduce the thermodynamics of the metal chloride species based on a prior knowledge of the inherent silver chloride solubility to 350°C. Thus, dealing with crystalline solids which exhibit rapid dissolution kinetics overcomes many of the potential difficulties outlined above.

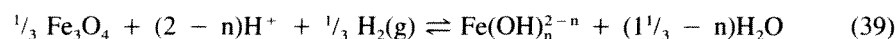
#### d. Raman Spectrometry

Raman spectrometry has developed into a powerful tool for the identification of aqueous species and a whole range of innovative high temperature cells has been designed. Measurements are normally restricted to concentrations in excess of  $0.1 \text{ mol} \cdot \text{kg}^{-1}$  and obviously to species with Raman active bond stretching or deformational modes. These measurements are particularly useful as an aid in confirming the configuration of metal complexes and can be carried out to extremes of temperature<sup>89</sup> and pressure,<sup>90</sup> as well as deal directly with natural microsize samples, such as fluid inclusions. However, despite the rapidly growing list of metal complexes that have been investigated by this technique, quantitative thermodynamic information is difficult to extract. Moreover, questions as to changes in stereochemistry from octahedral to tetrahedral configurations as a function of either temperature or ligand concentration (i.e., change in  $\bar{n}$ ) have not been answered unequivocally. Similarly, distinguishing between mono- and bidentate complexation by such ligands as acetate is speculative rather than definitive.

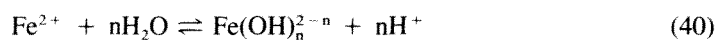
## B. SPECIFIC EQUILIBRIUM RESULTS

### 1. Metal Hydroxide Complexes

These complexes, which are normally categorized under the heading of hydrolysis reactions, have received considerable attention at elevated temperatures because of their obvious importance in natural and industrial environments. However, the almost universal insolubility of metal oxides and their hydrates has limited the applicability of most techniques, particularly potentiometry, leaving the majority of thermodynamic information to be gleaned from very difficult solubility studies. The solubility results are obtained from the primary dissolution reaction, which for the well-known case of magnetite,<sup>84,86</sup>  $\text{Fe}_3\text{O}_4$ , takes the form



Combining the equilibrium constants for the reaction for which  $n$  is zero, i.e., for the unhydrolyzed ferrous ion, with those for the successive hydrolyzed forms leads to the generalized reaction



For values of  $n \leq 2$ , this reaction involves only cationic species. In this sense, the reactions are "isocoulombic",<sup>6,18</sup> and as such are expected to have a minimal dependence on ionic strength and to exhibit a minimal change in heat capacity of reaction, because the change in solvation, or electrostriction, is minimized. Thus, to a first approximation, the enthalpy of reaction is temperature independent and the equilibrium constant for Reaction 40 may be represented as simply

$$\log K_{n,n}^T = a + b/T \quad (41)$$

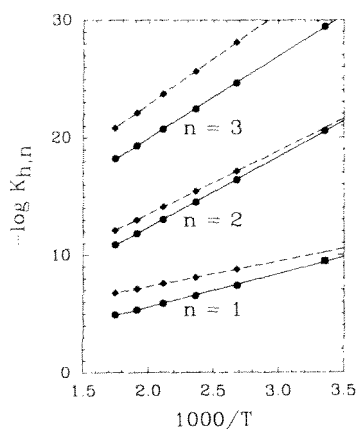


FIGURE 13. Temperature dependence of the overall formation constants of  $\text{Fe}(\text{OH})_n^{2-n}$ , according to Reaction 40, where the solid lines and  $\bullet$  symbols were calculated from the equation in Table 4 of Reference 84, while the dashed lines and  $\blacklozenge$  symbols were obtained from Table V in Reference 86, and the value symbolized by  $\blacksquare$  was taken from Mesmer.<sup>91</sup>

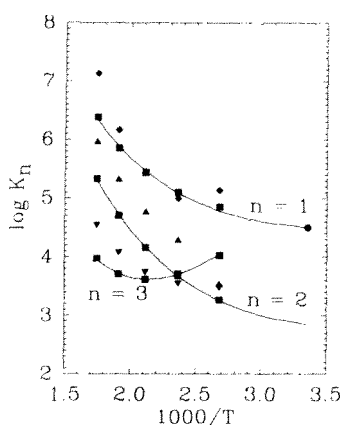


FIGURE 14. Temperature dependence of the stepwise formation constants of  $\text{Fe}(\text{OH})_n^{2-n}$ , according to Reaction 42, where the solid lines represent the regression curves for the results of Sweeton and Baes<sup>84</sup> symbolized as  $\blacksquare$  and Mesmer<sup>91</sup> symbolized as  $\bullet$ , while the remaining values were taken from Tremaine and LeBlanc<sup>86</sup> for  $n = 1$ ,  $\blacktriangledown$ ;  $n = 2$ ,  $\blacktriangle$ ; and  $n = 3$ ,  $\blacklozenge$ .

As a further consequence of the isocoulombic form, the  $\Delta V_{h,n}^0$  for the reaction is expected to be small so that changes in pressure along the saturation curve should have minimal effect on  $K_{h,n}$ . The results for Reaction 40 shown in Figure 13 are based on solubility data taken over the temperature ranges 50 to 300°C<sup>84</sup> and 100 to 300°C<sup>86</sup> and the results of potentiometric titrations at 25°C.<sup>91</sup> The latter was restricted to the determination of  $K_{h,1}^T$  by the solubility limit, but does show good agreement with the extrapolation of Sweeton and Baes.<sup>84</sup> However, expressing the formation of the higher-order hydroxoferrous(II) species in terms of overall equilibrium constants defined by Equation 40 does not allow for a direct comparison of these two sets of data. Moreover, Equation 40 can be reformulated to the hydroxide form using the known dissociation constant of water<sup>92</sup> (i.e.,  $K_n^T = K_{h,n}^T/K_w$ , where  $K_w = [\text{H}^+][\text{OH}^-]$ ) to a form more familiar to complexation reactions as exemplified by Equation 35. It is more instructive to present complexation equilibria as stepwise reactions in the general form



where  $\text{M}^{m+}$  and  $\text{L}^-$  represent  $\text{Fe}^{2+}$  and  $\text{OH}^-$  in the present example and the equilibrium quotient at infinite ionic strength,  $K_n$ , is then  $K_n^T/K_{n-1}^T$ . The stepwise formation constants for  $\text{Fe}(\text{OH})_n^{2-n}$  are given in Figure 14 as functions of temperature. Clearly, there is a marked disparity between the two sets of reported constants;<sup>84,86</sup> particularly noticeable is the reversal in the trend in the  $K_n$  values. This is notwithstanding the larger experimental uncertainties in the lower temperature values for  $n = 3$ . Stepwise formation constants generally decrease

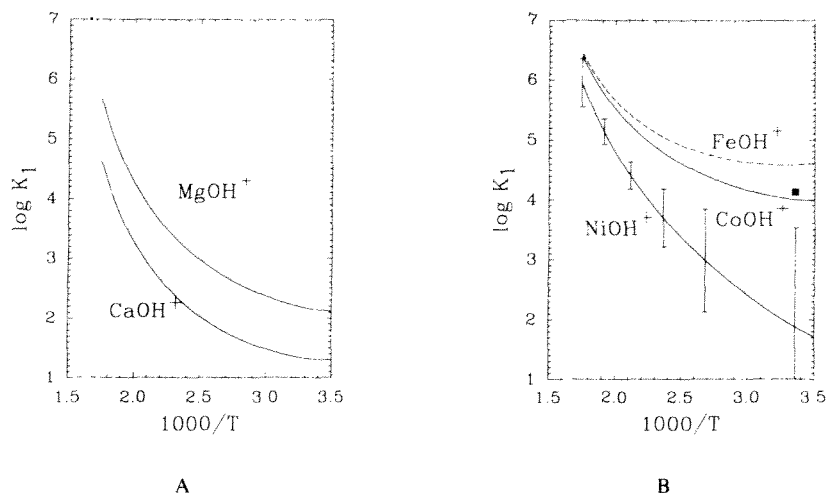


FIGURE 15. Temperature dependence of the first formation constant of (A) magnesium<sup>94</sup> and calcium;<sup>95</sup> (B) nickel(II),<sup>96</sup> cobalt(II),<sup>97</sup> and iron(II),<sup>84</sup> where ■ represents the value at 25°C of Perrin.<sup>98</sup>

as the number of ligands increases;<sup>4,5,6,3</sup> even when a "trans" effect is operative, the constants decrease, although in a more irregular, pairwise manner.<sup>93</sup> Therefore, at least based on this criterion and the excellent agreement with the 25°C constant of Mesmer,<sup>91</sup> the results of Sweeton and Baes<sup>25</sup> appear more consistent.

The hydrolysis of magnesium and calcium were investigated<sup>94,95</sup> in  $1 \text{ mol} \cdot \text{kg}^{-1}$  NaCl and KCl from 50 to 250°C and 50 to 200°C, respectively, using the high temperature hydrogen ion concentration cell. Solubility limited these experiments to a study of the first hydrolysis constant, which when written in the "proton form", Equation 40, is isocoulombic and can be converted to the "base form", Equation 42, at infinite dilution by the approximation:

$$K_1 = Q_{h,1} Q_w / K_w^2 \quad (43)$$

These results can be seen in Figure 15A. For ease of comparison, the corresponding  $\log K_1$  values are presented in Figure 15B for nickel(II),<sup>96</sup> cobalt(II),<sup>97</sup> and iron(II),<sup>84</sup> where the latter curve is that shown in Figure 14. The nickel(II) results were obtained from a study of the solubility of NiO for 150 to 300°C.<sup>96</sup> The first hydrolysis constant of cobalt(II) was measured in a hydrogen ion concentration cell from 25 to 200°C in HCl/KCl mixtures<sup>97</sup> where the maximum  $\bar{n}$  achievable was  $< 0.02$  such that the second hydrolysis product was negligible. These authors carried out the extrapolation to infinite dilution using a  $\log K_{h,1}$  vs.  $I^{1/2}$  plot and these results are presented here without modification.

The trend in stability of  $Mg(OH)^+ > Ca(OH)^+$  is expected based simply on ion size, which in turn is consistent with the similar shape of the curves, indicating that this difference is due primarily to a more positive entropy change for the former reaction, since  $\Delta H_1$  is virtually the same and  $\Delta C_{p,1}$  is related to that for the association of a proton and a hydroxide ion by virtue of Equation 43. Indeed, it is apparent that the  $\Delta H_1$  is comparable to the enthalpies for the hydrolysis reactions shown in Figure 1. Similarly, for cobalt(II), iron(II), and possibly nickel(II) considering the experimental errors imposed by this difficult study and the discrepancy with the precise value reported at 25°C<sup>98</sup> (see Figure 15B), it would appear that  $\Delta S_1$  controls the trend in  $\Delta G_1$  for the various metals. Specifically, the more tightly bound and extensive the solvating sheath, the larger the entropy change as these water molecules are lost to the bulk solvent. Figure 16 illustrates this point qualitatively, in

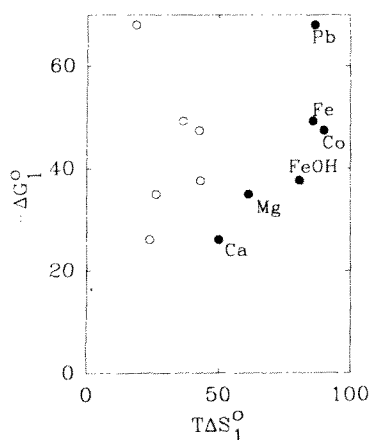


FIGURE 16. The relationship between the Gibbs energy change for Reaction 42 and the entropy change, symbolized by ●, at 200°C where the units are  $\text{kJ} \cdot \text{mol}^{-1}$ . The corresponding enthalpy changes are depicted (○) for comparison. The metals considered are  $\text{Ca}^{2+}$ ,<sup>95</sup>  $\text{Mg}^{2+}$ ,<sup>94</sup>  $\text{Fe}^{2+}$ ,<sup>84</sup>  $\text{Co}^{2+}$ ,<sup>97</sup> and  $\text{Pb}^{2+}$ .<sup>99</sup>

that variations in the entropy term at 200°C (this temperature is convenient as it lies near the center of the temperature ranges studied) are reflected directly in the free energy of reaction for those systems in which the bonding is predominantly electrostatic. By way of comparison, the more covalent character of the "softer" lead(II)<sup>99</sup> ion gives rise to an additional exothermic enthalpy contribution. Furthermore, as the change in charge becomes less of a factor as in the stepwise addition of hydroxide ions, the positive entropy contribution decreases until for divalent metal ions, the effect of temperature on the formation of higher-order species (i.e.,  $n > 2$ ) is less predictable.

## 2. Metal Chloride Complexes

As only the complexes of iron(II) have been studied to high temperatures for the three main ligands discussed here, viz., hydroxide, chloride, and acetate, initial focus will be placed on this metal. Ferrous chloride complexation, although very relevant to problems of corrosion, are nevertheless very weak and therefore many of the difficulties associated with such measurements as described above apply to this system. Consequently, there is a large disparity in the values reported at ambient conditions, as well as apparent discord at high temperatures. However, the results of a recent spectrophotometric investigation from 25 to 200°C involving chloride concentrations from 0.01 to 3.4  $\text{mol} \cdot \text{kg}^{-1}$  and those from potentiometric titrations alluded to in Section IV.A.2.a show good agreement within the experimental error limits and similar agreement with earlier solubility data at the highest temperature of 300°C (see Figure 17). The potentiometric results were determined at an ionic strength of unity and were assigned the same ionic strength dependence as the corresponding ferrous acetate complex to obtain the infinite dilution data depicted in the figure. Considering the two markedly different methods used in the extrapolations which most likely account for most of the uncertainties in the reported equilibrium constants, the agreement is satisfactory.

Lead and zinc chloride complexes have also been studied to high temperatures by spectrophotometry and solubility, respectively.<sup>82,88,101</sup> These results shown in Figure 18 indicate that Seward<sup>82</sup> has described well the behavior of  $K_1$  and  $K_2$  for the lead(II) system, whereas the zinc(II) data appear extraordinary both in the magnitude of  $K_1$  and in its relationship to the remaining equilibrium constants. Kaatze et al.<sup>102</sup> suggest that both the monochloro- and dichlorozinc(II) species maintain the octahedral geometry of the fully hydrated zinc(II) precursor, whereas the trichloro ion is five coordinate with a possible trigonal bipyramidal structure. The tetrachlorozinc(II), like most of the divalent 3d transition metal analogues, is known to be tetrahedral. These authors hypothesize, based on dielectric spectroscopic measurements, that the monochlorozinc(II) ion is an outer sphere, or water-

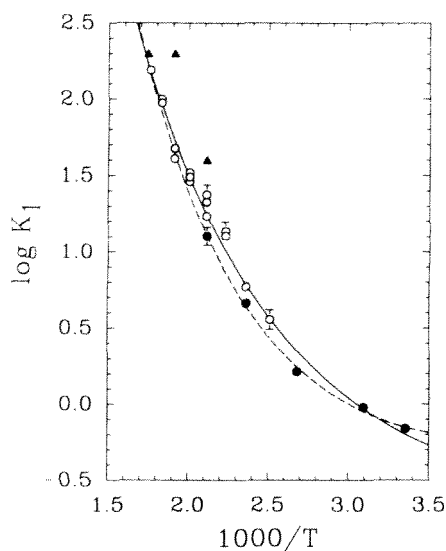


FIGURE 17. Temperature dependence of the formation constant of  $\text{FeCl}^+$ , where the symbols  $\bullet$ ,  $\circ$ , and  $\blacktriangle$  represent the results in References 83, 77, and 100, respectively. The solid and dashed curves result from the respective fits of the combined potentiometric and spectrophotometric data<sup>77,83</sup> and the spectrophotometric data alone.<sup>83</sup>

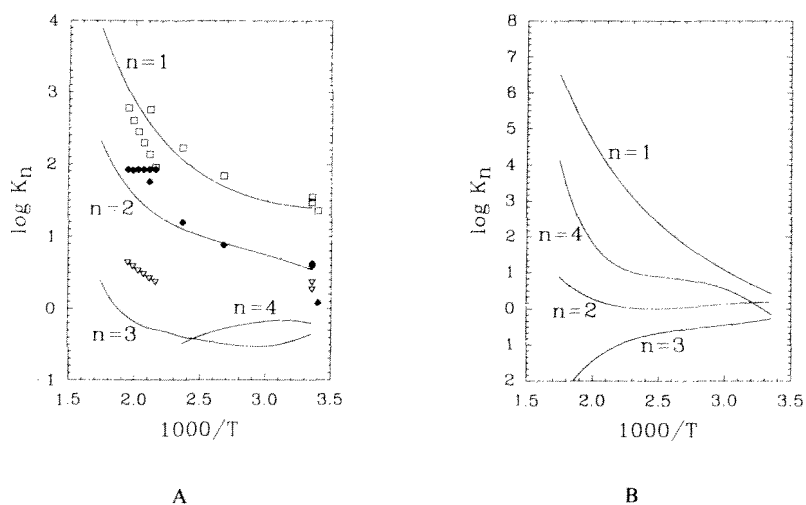


FIGURE 18. Temperature dependence of the formation constants of (A) the  $\text{Pb}(\text{Cl})_n^{2-n}$  complexes where the solid curves represent the regression fits of Seward,<sup>82</sup> while the symbols  $\square$  ( $n = 1$ ),  $\blacklozenge$  ( $n = 2$ ), and  $\nabla$  ( $n = 3$ ) were taken from Reference 101 and the references quoted therein; and (B) the  $\text{Zn}(\text{Cl})_n^{2-n}$  complexes.<sup>88</sup>

separated ion pair. While this may be the case at ambient conditions, there exists ample evidence to show that  $\text{ZnCl}^+$  is an inner sphere complex at high temperatures.<sup>82</sup> However, none of these observations suggests why the  $K_1$  values reported by Seward<sup>82</sup> for  $\text{ZnCl}^+$  should be so large relative to either the other divalent metal complexes or to the higher-order chlorozinc(II) complexes. Raman spectra indicate that at least at the  $1 \text{ mol} \cdot \text{L}^{-1}$

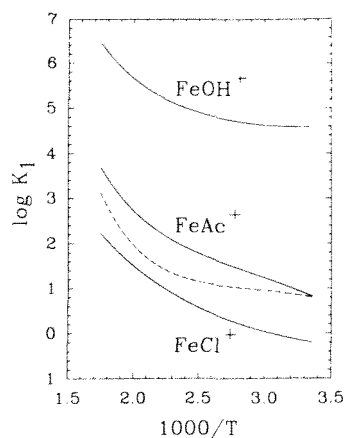


FIGURE 19. Temperature dependence of the formation constants of  $\text{FeOH}^+$ ,<sup>84</sup>  $\text{FeAc}^+$ ,<sup>36</sup>  $\text{FeCl}^+$  (see Figure 17), and  $\text{FeAc}_2$  (dashed curve).<sup>36</sup>

concentration level,  $\text{ZnCl}_2$  dominates at high temperatures.<sup>90</sup> In addition, the  $\text{ZnCl}^+$  ion shows anomalous behavior relative to  $\text{ZnAc}^+$  in that it is less stable at low temperatures, for a given  $[\text{Cl}^-]/[\text{Ac}^-]$  ratio, and more stable at high temperatures.<sup>75</sup> In the cases of iron(II)<sup>36</sup> (see Section IV.2.C) and lead(II),<sup>103</sup> the chloro-complex is systematically less stable than the corresponding acetate complex. Clearly, more experimental work is called for to clarify this important and interesting question.

In view of the above speculation as to changes in stereochemistry of chloroaquozinc(II) complexes, it is interesting to note that Angell and Gruen<sup>104</sup> were able to observe spectrophotometrically the transition from octahedral to tetrahedral symmetry for conversion of  $\text{NiCl}_6^{4-}$  to  $\text{NiCl}_4^{2-}$  with increasing temperature in concentrated magnesium chloride solutions. Similarly, the cobalt(II) complexes with chloride and bromide exhibit the same behavior<sup>105</sup> as they rearrange by strongly endothermic processes establishing that these changes are also entropy driven. The octahedral  $\text{CuCl}_6^{4-}$  analogue was not observed,<sup>104</sup> and only partial conversion of  $\text{Co}(\text{H}_2\text{O})_6^{2+}$  to a tetrahedral configuration was reported at 350°C.<sup>105</sup>

Frantz and Marshall<sup>106</sup> investigated the association of  $\text{Mg}^{2+}$  and  $\text{Ca}^{2+}$  by chloride ions from 25 to 600°C using conductivity. For the sake of comparison, the  $\log K_1$  values extrapolated to the arbitrarily chosen temperature of 200°C by means of density functions are  $-1.21$  and  $-0.49$ , respectively. Thus the order of increasing stability of the  $\text{MCl}^+$  species with respect to the hydrated metal ion,  $\text{M}^{2+}$ , is  $\text{Mg}(\text{II}) < \text{Ca}(\text{II}) < \text{Fe}(\text{II}) < \text{Pb}(\text{II}) < \text{Zn}(\text{II})$ , which, for the last three metals, reflects their increasing hardness.<sup>107</sup> Therefore, if it is assumed that interactions between the hard chloride ion and these metals are predominantly electrostatic as suggested, there is sufficient covalent character or ligand field stabilization of the metal-chloride bond to account for their enhanced stability.

### 3. Metal Acetate Complexes

Acetate complexation by ferrous(II)<sup>36</sup> and zinc(II)<sup>75</sup> ions was studied using the hydrogen ion concentration cell as referred to earlier and stepwise formation quotients of the former are presented in Figure 19 as a function of temperature and ionic strength. The dashed curve represents  $\log K_2$  as a function of temperature where the values at 25°C are uncertain to at least 0.5 log units, thus accounting for the usual behavior at low temperature.<sup>36</sup>

Considering the trend in stability of the ferrous complexes in Figure 19, the major contribution is from differences in entropy. For example, for the sequence  $\text{FeOH}^+$ ,  $\text{FeAc}^+$ ,  $\text{FeCl}^+$  at 200°C,  $\Delta H_1^\circ = 36, 44, \text{ and } 43 \text{ kJ mol}^{-1}$ , while  $T\Delta S_1^\circ = 86, 66, \text{ and } 53 \text{ kJ mol}^{-1}$ ,

respectively. Thus, it is again solvation changes associated with the formation of the  $\text{FeL}^+$  species that mainly dictate their relative stabilities, regardless of the suggestions of possible effects of chelation by the potentially bidentate acetate ion.<sup>36,75,89</sup> Moreover, solvation changes outweigh considerations of the ligand field stabilization effect, as the spectrochemical series would predict that the ligands fall in the order  $\text{Ac} > \text{OH} > \text{Cl}$ . Finally, the relative order of increasing stability,  $-\Delta G_1^\circ$ , in terms of the metals is  $\text{AlAc}^{2+ 108} > \text{PbCl}^{+ 103} > \text{ZnAc}^{+ 75} > \text{FeAc}^{+ 36}$ . The strength of the interaction of acetate with the very hard  $\text{Al}^{3+}$  ion is in full accord with these arguments.

## ACKNOWLEDGMENT

The work was sponsored by the Division of Chemical Sciences, Office of Basic Energy Sciences, U.S. Department of Energy under contract DE-AC05-84OR21400 with Martin Marietta Energy Systems, Inc.

## REFERENCES

1. Johnson, K. S. and Pytkowicz, R. M., Ion association and activity coefficients in multicomponent solutions, in *Activity Coefficients in Electrolyte Solutions*, Vol. 2, Pytkowicz, R. M., Ed., CRC Press, Boca Raton, FL, 1979, 1.
2. Nancollas, G. H., *Interactions in Electrolyte Solutions*, Elsevier, New York, 1966.
3. Davies, C. W., *Ion Association*, Butterworths, Washington, D.C., 1962.
4. Sillen, L. G. and Martell, A. E., *Stability Constants of Metal-Ion Complexes*, The Chemical Society, Burlington House, London, 1964; *Stability Constants Supplement*, No. 1, 1971.
5. Högfeltdt, E., *Stability Constants of Metal-Ion Complexes Part A. Inorganic Ligands*, Pergamon Press, Elmsford, NY, 1982.
6. Mesmer, R. E., Marshall, W. L., Palmer, D. A., Simonson, J. M., and Holmes, H. F., Thermodynamics of aqueous association and ionization reactions at high temperatures and pressures, *J. Solution Chem.*, 17, 699, 1988.
7. Mesmer, R. E., Baes, C. F., Jr., and Sweeton, F. H., Acidity measurements at elevated temperatures. IV. Apparent dissociation product of water in 1 m potassium chloride up to 295°C, *J. Phys. Chem.*, 74, 1937, 1970.
8. Sweeton, F. H., Mesmer, R. E., and Baes, C. F., Jr., A high temperature flowing EMF cell, *J. Phys. E*, 6, 165, 1973.
9. Baes, C. F., Jr., and Mesmer, R. E., *The Hydrolysis of Cations*, John Wiley & Sons, New York, 1976.
10. Quist, A. S. and Marshall, W. L., Electrical conductances of aqueous sodium chloride solutions from 0° to 800°C and at pressures to 4000 bars, *J. Phys. Chem.*, 72, 684, 1968.
11. Marshall, W. L. and Frantz, J. D., Electrical conductance measurements of dilute aqueous electrolytes at temperatures to 800°C and pressures to 4000 bars: techniques and interpretations, in *Research Techniques for High Pressures and Temperatures*, 2nd ed., Ulmer, G. C. and Barnes, H. L., Eds., John Wiley & Sons, New York, 1987.
12. Sweeton, F. H., Mesmer, R. E., and Baes, C. F., Jr., Acidity measurements at elevated temperatures. VIII. Dissociation of water, *J. Solution Chem.*, 3, 225, 1974.
13. Quist, A. S., The ionization of water to 800° and 4000 bars, *J. Phys. Chem.*, 74, 3396, 1970.
14. Quist, A. S. and Marshall, W. L., Ionization equilibria in ammonia-water solutions to 700°C and to 4000 bars of pressure, *J. Phys. Chem.*, 72, 3122, 1968.
15. Mesmer, R. E., Patterson, C. S., Busey, R. H., and Holmes, H. F., Ionization of acetic acid in NaCl(aq) media: a potentiometric study to 573 K and 130 bar, *J. Phys. Chem.*, 93, 2483, 1989.
16. Dickson, A., Wesolowski, D. J., Palmer, D. A., and Mesmer, R. E., The dissociation constant of bisulfate ion in aqueous sodium chloride solutions to 250°C, *J. Phys. Chem.*, 94, 7978, 1990.
17. Mesmer, R. E. and Baes, C. F., Jr., Phosphoric acid dissociation equilibrium in aqueous solutions to 300°C, *J. Solution Chem.*, 3, 307, 1974.
18. Lindsay, W. T., Estimation of concentration quotients for ionic equilibria in high temperature water: the model substance approach, in *Proc. 41st Int. Water Conf.*, Pittsburgh, 1980, 284.

19. **Smith-Magowan, D. and Wood, R. H.**, Heat capacity of aqueous sodium chloride from 320 to 600 K measured with a new flow calorimeter, *J. Chem. Thermodyn.*, 13, 1047, 1981.
20. **Rogers, P. S. Z. and Pitzer, K. S.**, Volumetric properties of aqueous sodium chloride solutions, *J. Phys. Chem. Ref. Data*, 11, 15, 1982.
21. **Hilbert, R.**, PVT-Daten von Wasser und von Wässrigen Natriumchlorid-Lösungen, Doctoral dissertation, University of Karlsruhe, Karlsruhe, West Germany, 1979.
22. **Patterson, C. S., Slocum, G. H., Busey, R. H., and Mesmer, R. E.**, Carbonate equilibria in hydrothermal systems: first ionization of carbonic acid in NaCl media to 300°C, *Geochim. Cosmochim. Acta*, 46, 1653, 1982.
23. **Marshall, W. L. and Franck, E. U.**, Ion product of water substance, 0–1000°C, 1–10,000 bars. New international formulation and its background, *J. Phys. Chem. Ref. Data*, 10, 295, 1981.
24. **Marshall, W. L.**, Complete equilibrium constants, electrolyte equilibria, and reaction rates, *J. Phys. Chem.*, 74, 346, 1970.
25. **Gates, J. A., Wood, R. H., and Quint, J. R.**, Experimental evidence for the remarkable behavior of the partial molar heat capacity at infinite dilution of aqueous electrolytes at the critical point, *J. Phys. Chem.*, 86, 4948, 1982.
26. **Mesmer, R. E.**, A model for estimation of thermodynamic quantities for reactions-uncertainties from such predictions, presented at 2nd Int. Symp. on Hydrothermal Reaction, Pennsylvania State University, State College, August 12, 1985.
27. **Mesmer, R. E., Marshall, W. L., Palmer, D. A., Simonson, J. M., and Holmes, H. F.**, Chemical equilibria and thermodynamics of reactions at high temperatures and pressure, presented at the Int. Conf. on Thermodynamics of Aqueous Systems with Industrial Applications, Airlie House, Warrenton, VA, May 11, 1987; also presented at Symp. on Chemistry in High Temperature Aqueous Solutions, Provo, UT, August 25, 1987.
28. **Mesmer, R. E.**, Aqueous chemistry and thermodynamics to high temperatures and pressure, presented at 41st Calorimetry Conf., Somerset, NJ, August 17, 1986.
29. **Anderson, G. M., Castet, S., Schott, J., and Mesmer, R. E.**, The density model for estimation of thermodynamic parameters for reactions at high temperatures and pressures, *Geochim. Cosmochim. Acta*, in press.
30. **Cobble, J. W. and Murray, R. C.**, Unusual ion solvation energies in high temperature water, *Faraday Discuss. Chem. Soc.*, 64, 144, 1977.
31. **Helgeson, H. C. and Kirkham, D. H.**, Theoretical prediction of the thermodynamic behavior of aqueous electrolytes at high pressures and temperatures. I. Summary of the thermodynamic/electrostatic properties of the solvent, *Am. J. Sci.*, 274, 1089, 1974.
32. **Wood, R. H., Smith-Magowan, D., Pitzer, K. S., and Rogers, P. S. Z.**, Comparison of experimental values of  $V^0$ ,  $C_{p2}^0$  for aqueous NaCl with predictions using the Born equation at temperatures from 300 to 573.15 K at 17.7 MPa, *J. Phys. Chem.*, 87, 3297, 1983.
33. **Simonson, J. M., Busey, R. H., and Mesmer, R. E.**, Enthalpies of dilution of aqueous calcium chloride to low molalities at high temperatures, *J. Phys. Chem.*, 89, 557, 1985.
34. **Quint, J. R. and Wood, R. H.**, Thermodynamics of a charged hard-sphere in a compressible dielectric fluid. II. Calculation of the ion-solvent pair correlation function, the excess solvation, the dielectric constant near the ion, and the partial molar volume of the ion in a water-like fluid above the critical point, *J. Phys. Chem.*, 89, 380, 1985.
35. **Pitzer, K. S., Peiper, J. C., and Busey, R. H.**, Thermodynamic properties of aqueous sodium chloride solutions, *J. Phys. Chem. Ref. Data*, 13, 1, 1984.
36. **Palmer, D. A. and Drummond, S. E.**, Potentiometric determination of the molal constants of ferrous acetate complexes in aqueous solutions to high temperatures, *J. Phys. Chem.*, 92, 6795, 1988.
37. **Young, H. D.**, *Statistical Treatment of Experimental Data*, McGraw-Hill, New York, 1962, 96.
38. **Bradley, D. J. and Pitzer, K. S.**, Thermodynamics of electrolytes. XII. Dielectric properties of water and Debye-Hückel parameters to 350°C and 1 kbar, *J. Phys. Chem.*, 83, 1599, 1979.
39. **Uematsu, M. and Franck, E. U.**, Static dielectric constant of water and steam, *J. Phys. Chem. Ref. Data*, 9, 1291, 1980.
40. **Archer, D. G. and Wang, P.**, The dielectric constant of water and Debye-Hückel limiting law slopes, *J. Phys. Chem. Ref. Data*, 19, 371, 1990.
41. **Haar, L., Gallagher, J. S., and Kell, G. S.**, *NBS/NRC Steam Tables*, Hemisphere, New York, 1984.
42. **Hill, P. G.**, A unified equation of state for H<sub>2</sub>O, written report to the International Association for the Properties of Steam, 1987, *J. Phys. Chem. Ref. Data*, submitted for publication.
43. **Saul, A. and Wagner, W.**, A fundamental equation for water covering the range from the melting line to 1273 K at pressures up to 25,000 MPa, *J. Phys. Chem. Ref. Data*, 18, 1537, 1989.
44. **Archer, D. G.**, Effect of revisions of Debye-Hückel limiting law coefficients on the thermodynamic parameters for strong-electrolyte solutions, *J. Chem. Eng. Data*, 35, 340, 1990.



45. Holmes, H. F., Busey, R. H., Simonson, J. M., Mesmer, R. E., Archer, D. G., and Wood, R. H., The enthalpy of dilution of HCl(aq) to 648 K and 40 MPa. Thermodynamic properties, *J. Chem. Thermodyn.*, 19, 863, 1987.
46. Simonson, J. M., Holmes, H. F., Busey, R. H., Mesmer, R. E., Archer, D. G., and Wood, R. H., Modeling of the thermodynamics of electrolyte solutions to high temperatures including ion association. Application to hydrochloric acid, *J. Phys. Chem.*, 94, 7675, 1990.
47. Levelt Sengers, J. M. H., Everhart, C. M., Morrison, G., and Pitzer, K. S., Thermodynamic anomalies in near-critical aqueous NaCl solutions, *Chem. Eng. Commun.*, 47, 315, 1986.
48. Pitzer, K. S. and Li, Y.-G., Thermodynamics of aqueous sodium chloride to 823 K and 1 kilobar (100 MPa), *Proc. Natl. Acad. Sci. U.S.A.*, 80, 7689, 1983.
49. Busey, R. H., Holmes, H. F., and Mesmer, R. E., The enthalpy of dilution of aqueous sodium chloride to 673 K using a new heat-flow and liquid-flow microcalorimeter. Excess thermodynamic properties and their pressure coefficients, *J. Chem. Thermodyn.*, 16, 343, 1984.
50. Thiessen, W. E. and Simonson, J. M., Enthalpy of dilution and the thermodynamics of NH<sub>4</sub>Cl(aq) to 523 K and 35 MPa, *J. Phys. Chem.*, 94, 7794, 1990.
51. Simonson, J. M., Mesmer, R. E., and Rogers, P. S. Z., The enthalpy of dilution and apparent molar heat capacity of NaOH(aq) to 523 K and 40 MPa, *J. Chem. Thermodyn.*, 21, 561, 1989.
52. Pitzer, K. S., Thermodynamics of electrolytes. I. Theoretical basis and general equations, *J. Phys. Chem.*, 77, 268, 1973.
53. Marsh, A. R. W. and McElroy, W. J., The dissociation constant and Henry's law constant of HCl in aqueous solutions, *Atmos. Environ.*, 19, 1075, 1985.
54. Fritz, J. J. and Fuget, C. R., Vapor pressure of aqueous hydrogen chloride solutions, 0° to 50°C, *Ind. Eng. Chem.*, 1, 10, 1956.
55. Perry, J. H., Ed., *Chemical Engineers' Handbook*, 3rd ed., McGraw-Hill, New York, 1950.
56. Frantz, J. D. and Marshall, W. L., Electrical conductances and ionization constants of salts, acids, and bases in supercritical aqueous fluids. I. Hydrochloric acid from 100° to 700°C and at pressures to 4000 bars, *Am. J. Sci.*, 284, 651, 1984.
57. Ruaya, J. R. and Seward, T. M., The ion-pair constant and other thermodynamic properties of HCl up to 350°C, *Geochim. Cosmochim. Acta*, 51, 121, 1987.
58. Oscarson, J. L., Izatt, R. M., Brown, P. R., Pawlak, Z., Gillespie, S. E., and Christensen, J. J., Thermodynamic quantities for the interaction of SO<sub>4</sub><sup>2-</sup> with H<sup>+</sup> and Na<sup>+</sup> in aqueous solution from 150 to 320°C, *J. Solution Chem.*, 17, 841, 1988.
59. Oscarson, J. L., Gillespie, S. E., Christensen, J. J., Izatt, R. M., and Brown, P. R., Thermodynamic quantities for the interaction of H<sup>+</sup> and Na<sup>+</sup> with C<sub>2</sub>H<sub>3</sub>O<sub>2</sub><sup>-</sup> and Cl<sup>-</sup> in aqueous solution from 275 to 320°C, *J. Solution Chem.*, 17, 865, 1988.
60. Izatt, R. M., Redd, E. H., and Christensen, J. J., Applications of solution calorimetry to a wide range of chemical and physical problems, *Thermochim. Acta*, 64, 355, 1983.
61. Liu, C. and Lindsay, W. T., Thermodynamics of sodium chloride solutions at high temperatures, *J. Solution Chem.*, 1, 45, 1972.
62. Sillen, L. G. and Martell, A. E., Stability constants of metal-ion complexes, *Chem. Soc. (London) Spec. Publ.*, No. 17, 1964.
63. Perrin, D. D., Stability constants of metal-ion complexes. Part B. Organic ligands, in *IUPAC Chemical Data Series*, No. 22, Pergamon Press, Oxford, 1979.
64. Irish, D. E. and Brooker, M. H., Raman and infrared spectral studies of electrolytes, in *Advances in Infrared and Raman Spectroscopy*, Vol. 2, Clark, R. J. H. and Hester, R. E., Eds., Heyden, London, 1976, chap. 6.
65. Neilson, G. W. and Enderby, J. E., The coordination of metal aquaions, *Adv. Inorg. Chem.*, 34, 195, 1989.
66. Narten, A. H., Diffraction studies of liquids, *Acta Chim. Hung.*, 121, 173, 1986.
67. Akitt, J. W., Elders, J. M., Fontaine, L. R., and Kundu, A. K., Multinuclear magnetic resonance studies of the hydrolysis of aluminum(III). X. Proton, carbon-13, and aluminum-27 spectra of aluminum acetate at very high magnetic field, *J. Chem. Soc. Dalton Trans.*, p. 1897, 1989.
68. Jonas, J., Nuclear magnetic resonance and laser scattering techniques at high pressure, in *High Pressure Chemistry and Biochemistry*, Vol. 197, van Eldik, R. and Jonas, J., Eds., NATO ASI Series C, Reidel Publishing, New York, 1987, 193.
69. Seward, T. M., Metal complex formation in aqueous solutions at elevated temperatures and pressures, in *Chemistry and Geochemistry of Solutions at High Temperatures and Pressures*, Pergamon Press, Elmsford, NY, 1981, 113.
70. Ramette, R. W. and Palmer, D. A., Thallium(I) iodate solubility product and iodic acid dissociation constant from 2 to 75°C, *J. Solution Chem.*, 13, 637, 1984.
71. Bjerrum, J., Estimation of small stability constants in aqueous solution. The nickel(II)-chloride system, *Acta Chem. Scand. Ser. A*, 42, 714, 1988.

72. **Palmer, D. A. and Drummond, S. E.**, The molal dissociation quotients of water in sodium trifluoromethanesulfonate solutions to high temperatures, *J. Solution Chem.*, 17, 153, 1988.
73. **Fabes, L. and Swaddle, T. W.**, Reagents for high temperature aqueous chemistry: trifluoromethanesulfonic acid and its salts, *Can. J. Chem.*, 53, 3053, 1975.
74. **Dixon, N. E., Lawrance, G. A., Lay, P. A., and Sargeson, A. M.**, Synthetically versatile (trifluoromethanesulfonato)metal amine complexes, *Inorg. Chem.*, 23, 2940, 1984.
75. **Giordano, T. H. and Drummond, S. E.**, The potentiometric determination of stability constants for zinc acetate complexes in aqueous solutions to 295°C, *Geochim. Cosmochim. Acta*, in press.
76. **Senanayake, G. and Miur, D. M.**, Studies on liquid junction potentials in concentrated chloride solutions and determination of ionic activities and hydration numbers by the emf method, *Electrochim. Acta*, 33, 3, 1988.
77. **Palmer, D. A. and Hyde, K. E.**, A potentiometric determination of the stability constants of aqueous monochloroferrous(II) ion at high temperatures, *Geochim. Cosmochim. Acta*, submitted for publication.
78. **Palmer, D. A., Hyde, K. E., and Rosenberg, R. M.**, A study of the stability of cadmium chloride complexes in aqueous solution to high temperatures by a direct potentiometric method, *J. Phys. Chem.*, submitted for publication.
79. **Carmody, W. R.**, Studies in the measurement of electromotive force in dilute aqueous solutions. I. A study of the lead electrode, *J. Am. Chem. Soc.*, 51, 2905, 1929.
80. **Garrels, R. M. and Glucker, F. T.**, Activity coefficients and dissociation of lead chloride in aqueous solutions, *Chem. Rev.*, 44, 117, 1949.
81. **Greeley, R. S., Smith, W. T., Jr., Stroughton, R. W., and Leitzke, M. H.**, Electromotive force studies in aqueous solutions at elevated temperatures. I. The standard potential of the silver-silver chloride electrode, *J. Phys. Chem.*, 64, 652, 1960.
82. **Seward, T. M.**, The formation of lead(II) chloride complexes to 300°C: a spectrophotometric study, *Geochim. Cosmochim. Acta*, 48, 121, 1984.
83. **Heinrich, C. A. and Seward, T. M.**, A spectrophotometric study of aqueous iron(II) chloride complexing from 25 to 200°C, *Geochim. Cosmochim. Acta*, 54, 2207, 1990.
84. **Sweeton, F. H. and Baes, C. F., Jr.**, The solubility of magnetite and hydrolysis of ferrous ion in aqueous solutions at elevated temperatures, *J. Chem. Thermodyn.*, 2, 479, 1970.
85. **Seward, T. M.**, The stability of chloride complexes of silver in hydrothermal solutions up to 350°C, *Geochim. Cosmochim. Acta*, 40, 1329, 1976.
86. **Tremaine, P. R. and LeBlanc, J. C.**, The solubility of magnetite and the hydrolysis and oxidation of  $\text{Fe}^{2+}$  in water to 300°C, *J. Solution Chem.*, 9, 415, 1980.
87. **Gammons, C. H. and Barnes, H. L.**, The solubility of  $\text{Ag}_2\text{S}$  in near-neutral aqueous sulfide solutions at 25 to 300°C, *Geochim. Cosmochim. Acta*, 53, 279, 1989.
88. **Ruaya, J. R. and Seward, T. M.**, The stability of chlorozinc(II) complexes in hydrothermal solutions up to 350°C, *Geochim. Cosmochim. Acta*, 50, 651, 1986.
89. **Yang, M. N., Crerar, D. A., and Irish, D. E.**, A Raman spectroscopic study of lead and zinc acetate complexes in hydrothermal solutions, *Geochim. Cosmochim. Acta*, 53, 319, 1989.
90. **Marley, N. A. and Gaffney, J. S.**, Laser Raman spectral determination of zinc halide complexes in aqueous solutions as a function of temperature and pressure, *Appl. Spectrosc.*, 44, 469, 1990.
91. **Mesmer, R. E.**, Hydrolysis of iron(2+) in dilute chloride at 25°, *Inorg. Chem.*, 10, 857, 1971.
92. **Busey, R. H. and Mesmer, R. E.**, Thermodynamic quantities for the ionization of water in sodium chloride media to 300°C, *J. Chem. Eng. Data*, 23, 175, 1978.
93. **Basolo, F. and Pearson, R. G.**, *Mechanisms of Inorganic Reactions*, John Wiley & Sons, New York, 1967, chap. 5.
94. **Drummond, S. E.**, Magnesium hydrolysis to 250°C by EMF titration, in *Chemistry Division Annual Progress Report*, ORNL-6152, Oak Ridge National Laboratory, Oak Ridge, TN, 1985, 57.
95. **Mesmer, R. E.**, unpublished results.
96. **Tremaine, P. R. and LeBlanc, J. C.**, The solubility of nickel oxide and hydrolysis of  $\text{Ni}^{2+}$  in water to 573 K, *J. Chem. Thermodyn.*, 12, 521, 1980.
97. **Giasson, G. and Tewari, P. H.**, Hydrolysis of Co(II) at elevated temperatures, *Can. J. Chem.*, 56, 435, 1978.
98. **Perrin, D. D.**, The hydrolysis of metal ions. IV. Nickel(II), *J. Chem. Soc.*, p. 3644, 1964.
99. **Tugarlinov, I. A., Ganeyev, I. G., and Khodakovskiy, I. L.**, Experimental determination of hydrolysis constants of lead ions in aqueous solutions at temperatures up to 300°C, *Geochem. Int.*, 12, 47, 1975.
100. **Crerar, D. A., Susak, N. J., Borscik, M., and Schwartz, S.**, Solubility of the buffer assemblage pyrite + pyrrhotite + magnetite in NaCl solutions from 200 to 35°C, *Geochim. Cosmochim. Acta*, 42, 1427, 1978.
101. **Rafal'skiy, R. P. and Masalovich, A. P.**, Determination of the instability constants of lead chloride complexes at elevated temperatures, *Geochem. Int.*, 18, 158, 1981.

102. **Kaatz, U., Lönnecke, V., and Pottel, R.**, Dielectric spectroscopy on aqueous solutions of zinc(II) chloride. Evidence of ion complexes, *J. Phys. Chem.*, 91, 2206, 1987.
103. **Giordano, T. H.**, Angelsite (PbSO<sub>4</sub>) solubility in acetate solutions: the determination of stability constants for lead acetate complexes to 85°C, *Geochim. Cosmochim. Acta*, 53, 359, 1989.
104. **Angell, C. A. and Gruen, D. M.**, Octahedral-tetrahedral coordination equilibria of nickel(II) and copper(II) in concentrated aqueous electrolyte solutions, *J. Am. Chem. Soc.*, 88, 5192, 1966.
105. **Swaddle, T. W. and Fabes, L.**, Octahedral-tetrahedral equilibria in aqueous cobalt(II) solutions at high temperatures, *Can. J. Chem.*, 58, 1418, 1980.
106. **Frantz, J. D. and Marshall, W. L.**, Electrical conductances and ionization constants of calcium chloride and magnesium chloride in aqueous solutions at temperatures to 600°C and pressures to 4000 bars, *Am. J. Sci.*, 282, 1666, 1982.
107. **Pearson, R. G.**, Absolute electronegativity and hardness: applications to inorganic chemistry, *Inorg. Chem.*, 27, 734, 1988.
108. **Palmer, D. A. and Wesolowski, D. J.**, unpublished results.



## INDEX

## A

- Absolute activity, 35  
 Acetate, 492, 524—525  
 Acid-base equilibrium, 305, 308, 495—496  
 Activity change, 159  
 Activity coefficients, 7—12, 39, 66, 89, 279—419, 437  
   of aqueous species, 438  
   complexation and, 392—410  
     chloro, 399—402  
     constants and, 395  
     copper, 410  
     copper chloro, 399—400  
     ion pairing and, 406—410  
     lead chloro, 400—402  
     magnesium fluoride, 402—405  
     Pitzer model and, 395  
   concentration scales and, 348  
   control of, 493  
   defined, 290  
   determination of, 69  
   equilibrium thermodynamics and, 290—293  
   of hydrogen ions, 157  
   hydrological cycle and, 281—283  
   ion association models of, 293—294  
   ionic, 496  
   ion interaction models of, see Ion interaction approaches  
   mean, 11, 13—14, 88, 156, 298—299, 437  
   measurements of, 175—177, 181, 185  
   of mineral solubility, 442  
   modeling of, 65  
   Monte Carlo method for, 67  
   neutral solutes and, see Neutral solutes  
   for oxygen, 345  
   pH scales and, 352—359  
   Pitzer model and, 413—414, see also Pitzer model  
   in potentiometry, 165, 168—169, 175—177, 181, 185, 352—359  
   pressure and, 21—22, 299—300, 474  
   quotient of, 351  
   of sea salt, 315—317  
   in seawater, 300  
   seawater stoichiometry and, 283—290  
   single-ion, 91—92  
   of solute components, 210  
   of solutes, 239  
   strong electrolytes and, 313—329  
     mineral solubility and, 317—321  
     seawater and, 315—317  
     sulfuric acid and, 322—324  
     supersaturated solutions and, 327—328  
     thermodynamics and, 328—329  
     volatile type, 324—327  
     temperature and, 21—22, 298, 314  
     thermodynamic models of, 293  
     weak electrolytes and, see Weak electrolytes  
 Additivity, 6—7, 42, 60—61  
 Adenosine monophosphate (AMP), 186  
 Adiabatic compressibility, 3  
 Aerosols, 281, 295, 324—325, 327  
 Air solubility, 336  
 Alcohols, 186, see also specific types  
 Alkaline earth amalgams, 168  
 Alkalinity, 361  
 Amalgam electrodes, 166—169  
 Amines, 186, see also specific types  
 Amino acids, 186, see also specific types  
 Ammonia, 373—378  
 Ammonium, 179  
 AMP, see Adenosine monophosphate  
 Amygdalin, 186  
 Anhydrite solubility, 320  
 Anionic silver chloride, 158  
 Anion-reversible electrodes, 157  
 Anoxic systems, 281  
 Apparent molal enthalpy, 96, 298—299  
 Apparent molal heat capacity, 96  
 Apparent molal volume, 97, 474—476  
 Apparent molar quantities, 21—24  
 Approximation, see also specific types  
   Debye-Hückel, 57  
   generalized mean spherical (GMSA), 62  
   hypernetted-chain (HNC), 62, 64—67  
   linearization, 56  
   mean spherical (MSA), 62, 64, 67  
   Percus-Yevick (PYA), 62  
   reference hypernetted-chain (RHNC), 62, 65—66  
 Aprotic solvents, 183  
 Aqueous buffers, 162—163  
 Aragonite, 365—367  
 Association, see Ion association  
 Assymmetrical mixing, 114, 117, 122—125  
 Athermal solutions, 15—17  
 Atmospheric gases, 299, 302, see also specific types  
   properties of, 331  
   salting coefficients of, 416  
   Setchenow coefficients for, 336, 417  
   solubility of, 335—346  
     data on, 346—349  
     Pitzer model and, 337—346  
 Average force potentials, 40  
 Average potential, 46, 47

## B

- Barium, 179  
 Bilirubin, 179  
 Binary interactions, 84, 297, 458—459

Binary systems, 458—459, 470—477  
 Biologically based electrodes, 186—187  
 Bisulfate ions, 322  
 Bithermal equilibrium, 249  
 Bjerrum model, 501, 507  
 Boiling point elevation, 19, 211, 436  
 Boltzmann factor, 36  
 Borate, 162  
 Boric acid, 370—373  
 Born equation, 500  
 Boundary conditions, 52  
 Bromide interference, 184  
 Bronsted's postulate, 81  
 Buffer capacity, 352  
 Buffers, 162—163, 166, 354, 357, see also specific types  
 Bunsen coefficients, 333, 347

## C

Cadmium, 168  
 Calcite, 365—368  
 Calcium, 175, 179, 181, 521  
 Calcium carbonate minerals, 365—367  
 Calcium chloride, 175  
 Calcium didecyl phosphate, 175  
 Calcium electrodes, 176, 178—179  
 Calcium orthoborate, 372  
 Calcium sulfate, 321  
 Calorimetry, 455  
   ion association and, 506—515  
     dilution enthalpy and, 510—514  
     electrostatic considerations and, 507—510  
     mixing enthalpy and, 514—515  
 Canonical ensemble, 67  
 Canonical partition function, 32, 34, 36, 45  
 Carbohydrates, 186, see also specific types  
 Carbonate, 162  
   alkalinity of, 361  
   dissolved, see Carbon dioxide-dissolved carbonate system  
   equilibrium of, 365  
   Pitzer model and, 368—370  
   in seawater, 361—364  
 Carbon dioxide, 281, 308, 331—332, 360—361, 408  
 Carbon dioxide-dissolved carbonate system, 360—370  
   carbonic acid and, 360—361  
   Pitzer model and, 368  
 Carbonic acid, 360—361  
 Carboxylic acids, 186  
 Cation-reversible electrodes, 157  
 Cation-selective electrodes, 169—173, 186  
 Cell models, 44—47  
 Cell potential, 493  
 Ceramic membranes, 165  
 Cesium, 168  
 Charge-dipole interactions, 42  
 Charge-induced dipole, 41  
 Charging process, 55—56, 82  
 Chemical potentials, 5—12, 21, 62, 214  
   activity coefficients and, 301  
   in closed systems, 290—292  
   constant, 38  
   in electrolytes, 8—9  
   fixed, 67  
   gradient of, 240  
   Kirkwood-Buff equations and, 65  
   Kirkwood-Buff method and, 64  
   in marine chemistry, 291  
   in open systems, 292—293  
   potentiometry and, 156  
   pressure and, 438  
   of solid phases, 308  
   of solids, 437  
   solvent, 12  
   standard, 301  
   standard-state, 438—439, 450, 453, 455—456, 476  
   statistical mechanics and, 31, 33, 37—38  
   temperature and, 438  
 Chloranil electrodes, 184  
 Chloride, 179, 492  
 Chloride complexation, 517—518, 522—524  
 Chlorine, 175  
 Chlorinity, 284—285  
 Cholesterol, 179  
 Cholic acid, 179  
 Citrate, 179  
 Closed systems, 290—292  
 Closest distance of approach, 501  
 Closure assumption, 56  
 Cluster diagrams, 61  
 Cluster expansion, 57—59, 62  
 Cluster integrals, 40, 53, 58  
 Clusters, 64  
 Cluster summation method, 59  
 Cofactors, 186  
 Collective effects, 50, 53—54, 59  
 Colligative properties, 17—21, see also specific types  
 Combustion enthalpies, 210  
 Complexation, 392—410, see also specific types  
   acetate, 524—525  
   chloride, 517—518, 522—524  
   chloro, 399—402  
   constants for, 395  
   copper, 410  
   copper chloro, 399—400  
   hydroxide, 519—522  
   ion association and, 515—525  
   ion pairing and, 406—410  
   lead chloro, 400—402  
   magnesium fluoride, 402—405  
   Pitzer model and, 395  
 Component activities, 7—8  
 Composition fluctuations, 36—38  
 Composition scales, 7—12  
 Compressibility, 3, 60, 298, 300, 498  
 Computer codes, 132, 294  
   activity coefficients and, 305, 308

calcium sulfate solubility and, 321  
 mineral solubility calculations and, 440  
 Pitzer model and, 305, 308  
 Concentrated solutions, 82  
 Concentration scales, 287—288, 291, 295, 348, 411  
 Conductance, 493—495  
 Configuration integral, 32, 51—52  
 Conformality, 47, 49  
 Copper, 175  
 Copper chloro-complexes, 399—400  
 Copper salts, 399  
 Core repulsion, 41, 44  
 Correlation integral, 66  
 Correlations, 50, 62, 64—65  
   direct, 62  
   pair, 35, 49, 54, 61—62, 64, 69  
 Corresponding states, 47, 49  
 Cospheres, 44  
 Coulomb forces, 42—43, 50, 58, 63, 66  
 Coulomb interactions, 41, 50, 65  
 Coulomb potential, 53, 55  
 Coulomb's law, 65  
 Creatinine, 179, 186  
 Critical point, 68

## D

Debye charging process, 55—56, 82  
 Debye-Hückel approximation, 57  
 Debye-Hückel equations, 15, 64, 269, 270  
 Debye-Hückel expressions, 518  
 Debye-Hückel limiting law, 56, 59, 66—68  
   activity coefficients and, 313  
   ion interaction approaches and, 81, 83  
   isopiestic methods and, 270—271  
   strong electrolytes and, 313  
 Debye-Hückel limiting slope, 13, 297  
 Debye-Hückel parameters, 81, 87, 94, 98, 120  
   activity coefficients and, 296  
   dielectric constant of water and, 129—131  
   for enthalpy, 96  
   mineral solubility and, 443  
   temperature and, 297  
 Debye-Hückel relationship  
   ion association and, 495  
   Margules expansion model and, 470  
   potentiometry and, 158  
 Debye-Hückel term, 87, 120, 442, 470  
 Debye-Hückel theory, 54—58, 65. *see also* Potential energy  
   of Gibbs free energy, 509  
   ion association and, 509  
   ion pairing and, 62, 63  
   Margules expansion model and, 470  
 1-Decanol, 179  
 DHLL. *see* Debye-Hückel limiting law  
 Diagrams, 57—59, 61—62. *see also* specific types  
 Dibutylphthalate, 213  
 Dielectric constant, 43, 129—131  
 Differential relations, 2—5

Diffusion coefficients, 211  
 Dilution  
   enthalpy of, 510—515  
   heat of, 96, 104, 299  
   infinite, 40  
 3,5-Dinitrosalicylate (DNS), 178  
 Dioctylphenyl phosphonate, 175, 179  
 Dipole moments, 41  
 Direct correlation functions, 61—62  
 Dispersion forces, 42  
 Dispersion interaction, 41  
 Dissociation constants, 350, 387  
 Dissolved salts, 302—304  
 Distribution functions, 35, 45, 65  
 Divalent cation electrodes, 178  
 Divergences, 58  
 DNS. *see* 3,5-Dinitrosalicylate  
 Double-junction reference electrodes, 176, 181  
 Driving forces, 237, 240—241, 501—503  
 Dynamic methods, 212

## E

Effective potential, 47  
 Electrical conductance, 493—495  
 Electrochemical cells, 492—493, 516—518  
 Electrodes. *see also* specific types  
   amalgam, 166—169  
   anion-reversible, 157  
   biologically based, 186—187  
   calcium, 176—179  
   cation-reversible, 157  
   cation-selective, 169—173, 186  
   chloranil, 184  
   divalent cation, 178  
   double-junction reference, 176, 181  
   enzyme-based, 186—187  
   fluoride-selective, 184  
   gas-sensitive membrane, 187—188  
   glass  
     cation-selective, 169—173, 186  
     pH-type, 159—166, 185  
     sodium-selective, 176  
   hydrogen, 157—163  
   ion-exchange, 175—180  
   ion-reversible, 211  
   lead-selective, 182  
   liquid ion-exchange, 175—180  
   micro-, 181  
   neutral carrier-based, 181—182  
   palladium membrane, 157  
   pH, 159—166, 185  
   polymer-based ion-exchange, 175—180  
   of second kind, 182—184  
   silver chloride, 159  
   solid-state membrane, 184—185, 187  
 Electrolytes, 7—12  
   chemical potentials in, 8—9  
   electrophoretic effect for, 211  
   higher-valence, 211  
   ion interaction approaches and, 80, 86—91

- mineral solubility in. see Minerals, solubility of
  - mixtures of, 88—91, 169, 213, 436, 438—439
  - polyvalent, 156
  - pure. see Pure electrolytes
  - statistical mechanics for, 53—69
    - cluster expansion and, 57—59
    - Debye-Hückel theory and, 54—57
    - integral equations and, 59—62
    - ion pairing and, 62—64
    - Kirkwood-Buff method and, 64—65
    - numerical results and, 65—69
    - potential energy and, 54—57
  - strong. see Strong electrolytes
  - supporting, 492—493
  - thermodynamic quantity derivation for, 20—21
  - thermodynamics of, 210, 436
  - weak. see Weak electrolytes
- Electromotive forces of cells, 20—21
- Electrophoretic effect, 211
- Electrostatic forces, 81
- Electrostatic instability, 175
- Electrostatic potential, 54, 59
- e.m.f., 210, 213
- Energy, see also specific types
- calculation of, 64
  - conservation of (first law of thermodynamics), 3—4
  - free. see Free energy
  - Gibbs free. see Gibbs free energy
  - Helmholtz free, 2, 32—33, 54
  - internal, 60, 68
  - kinetic, 31, 63
  - potential. see Debye-Hückel theory: Potential energy
  - total, 3, 42
- Enthalpy, 2, 21—24
- apparent molal, 96, 298—299
  - apparent relative, 510—511
  - combustion, 210
  - Debye-Hückel parameter, 96
  - of dilution, 510—515
  - ion association and, 502, 508, 510—515
  - ion interaction approaches and, 95—97
  - isopiestic methods and, 238
  - mixing, 514—515
  - molal, 96—97, 298—299
  - molar, 22—24
  - partial molal, 97, 298
  - partial molar, 22—24
  - relative, 508, 510—511
  - relative apparent, 510—511
- Entropy, 2, 4, 32, 46, 456—457
- ion association and, 502
  - of mixing, 15—17
  - standard-state, 438
- Enzyme-based electrodes, 186—187
- Equations of state, 3
- Equilibrium constants, 291—292, 305
- defined, 520
  - extrapolated, 505—506
  - ion association and, 495, 505—506, 519—520
  - for mineral solubility, 437—439, 457
  - temperature and, 439
  - thermodynamic, 366
  - uncertainties in extrapolated, 505—506
- Equilibrium thermodynamics, 290—293
- Equilibrium vapor pressure, 237
- Evaporites, 318, 370
- Excess Gibbs energy, 85, 88, 95, 106
- isopiestic methods and, 272
  - Margules expansion model and, 471, 473—475, 477
  - mineral solubility and, 440
  - of nonelectrolytes, 470
  - pressure and, 474
  - from short-range forces, 139—143
- Expansivity coefficient, 498
- Extensive quantities, 2
- Extraction, 210—211

## F

- Faraday constant, 156
- Fluctuations, 36—38, 49, 55—57, 60, see also specific types
- Fluoride, 179
- Fluoride-selective electrodes, 184
- Formalisms. see also specific types
- in statistical mechanics, 31—37
- Formation constants, 393
- Fourth virial coefficient, 133
- Free energy, 34, 44, 54, 290
- diagrams of, 58
  - electrical contribution to, 50
  - equilibrium state of minimum, 290
  - Gibbs. see Gibbs free energy
  - Helmholtz, 2, 32—33, 54
  - local, 32
  - overall, 291
  - total, 64
  - unperturbed, 49
  - variational methods and, 50
- Free-ion activity coefficients, 407
- Freezing point depression, 17—19
- Freezing temperature depression, 211
- Fugacity, 39—40, 214—220
- Lewis rule of, 331
  - partial pressure and, 332
  - relative, 216

## G

- Gases, 156, 186, see also specific types
- atmospheric. see Atmospheric gases
  - imperfect, 77—80
  - nonideal solutions in imperfect, 77—80
  - solubility of, 303, 324—325, 346—349
  - in pure water, 415—416
- Gas-liquid equilibrium, 350
- Gas-sensitive membrane electrodes, 187—188
- Generalized mean spherical approximation (GMSA), 62



Geochemical models, 185, 294, 439  
 Gibbs-Bogoliubov principle, 50  
 Gibbs-Duhem relation, 12—14, 38, 144, 210, 438  
 Gibbs free energy, 2, 12, 97  
   cell reaction and change in, 20  
   as composition function, 210  
   Debye-Hückel theory of, 509  
   derivatives of, 95  
   excess, see Excess Gibbs energy  
   ion association and, 502, 509  
   isopiestic methods and, 214—220  
   isothermal, 210  
   measurements of, 210  
   minimization of, 319  
   partial molar, 210, 214  
   pressure and, 210, 474  
   temperature and, 210  
 Glass electrodes, see also specific types  
   cation-selective, 169—173, 186  
   pH-type, 159—166, 185  
   sodium-selective, 176  
 Gluconic acid, 186  
 Glucose, 186  
 $\beta$ -Glucose oxidase, 186  
 Glycerol, 213  
 GMSA, see Generalized mean spherical approximation  
 Grand canonical ensemble, 67  
 Grand canonical partition function, 32, 34, 36  
 Grand ensemble, 34  
 Grand partition function, 39  
 Guggenheim's equations, 81—82  
 Guntelberg charging process, 56  
 Gurney term, 44  
 Gypsum solubility, 318—321

## H

Hard core, 41, 43, 65  
 Harned cell, 158  
 Heat capacity, 2, 299, 455, 457  
   apparent, 96  
   ion interaction approaches and, 95—97  
   molal, 96  
   partial, 298  
   of solids, 456  
   standard-state, 438—439, 453, 457, 476, 480  
 Heat of dilution, 96, 104, 299  
 Heat of mixing, 127  
 Heat of solution, 104  
 Heat-transfer block, 237, 244, 266  
 Helmholtz free energy, 2, 32—33, 54  
 Helmholtz function, 32  
 Henderson equation, 352, 357, 518  
 Henry's law artifacts, 348  
 Henry's law constants, 302, 324—325, 329—330, 345, 351  
 Hexyl trifluoroacetylbenzoate, 179  
 Higher order terms, 131—132  
 HNC, see Hypernetted-chain  
 Hydration model, 503

Hydrobromic acid, 161  
 Hydrocarbons, 348—349, 417—418  
 Hydrochloric acid, 160—161, 183  
 Hydrochromic acid, 161  
 Hydrofluoric acid, 161—162, 378—380  
 Hydrogen, 181, 305  
   in aqueous solutions, 353—359  
   concentration scale for, 357—359  
 Hydrogen electrodes, 157—159, 160—163  
 Hydrogen peroxide, 186  
 Hydrogen sulfide, 385—388  
 Hydroiodic acid, 161—162  
 Hydrological cycle, 281—283  
 Hydrolysis, 516, 518—519, 521  
 Hydroxides, 166, 492, 519—522  
 Hypernetted-chain (HNC) approximation, 62, 64—67  
 Hypersaline waters, 281

## I

Ideal mixing, 47, 136—139  
 Ideal solutions, 348  
   defined, 15, 215, 272  
   statistical mechanics of, 33—34  
   thermodynamics of, 15—17  
 Impedance, 184  
 Imperfect gases, 77—80  
 Importance sampling, 51  
 Indium, 168  
 Induced moments, 42  
 Infinite dilution, 40  
 Inorganic ions, 186  
 Integral equations, 44, see also specific types  
   statistical mechanics and, 59—62, 64—65, 67  
 Intensive properties, 2  
 Intermolecular potentials, 42  
 Internal energy, 60, 68  
 Ion association, 491—525  
   acid-base equilibrium and, 495—496  
   association reactions and, 496—506  
   calorimetry and, 506—515  
   dilution enthalpy and, 510—514  
   electrostatic considerations and, 507—510  
   mixing enthalpy and, 514—515  
   complexation and, 515—525  
   constants for, 63, 351, 504  
   dilution enthalpy and, 510—514  
   driving forces for, 501—503  
   electrical conductance and, 493—495  
   electrochemical cells and, 492—493  
   electrostatic considerations and, 507—510  
   equilibrium of, 77—80, 93—95  
   equilibrium constants and, 495, 505—506  
   experimental methods for study of, 492—495  
   extrapolation of constants for, 504  
   hydration model and, 503  
   hydroxide complexes and, 519—522  
   ion interaction and, 304—306, 404, 510  
   mixing enthalpy and, 514—515

- models of, 293—294, 395, 404, 408—409, 496—498
- process of, 63
- solubility measurements and, 518—519
- thermodynamic constants for, 351
- thermodynamics of, 351, 498—501
- Ion-exchange electrodes, 175—180
- Ion-exchange equilibrium, 175
- Ion-exchange reactions, 184
- ionic activity coefficient, 496
- Ionic association, 64
- Ionic equilibrium in weak electrolytes, see under Weak electrolytes
- Ionic strength, 84, 129, 289—290, 316, 357, 406
- Ion interaction approaches, 75—146, 293—312, 436, see also specific types
  - additional-terms equations and, 133—136
  - application of, 439
  - asymmetrical mixing and, 114, 117, 122—125
  - Bronsted's postulate and, 81
  - computer codes and, 132, 294
  - Debye-Hückel effect and, 143—146
  - Debye-Hückel parameters and, 98
  - dielectric constant of water and, 129—131
  - dissolved salts and, 302—304
  - enthalpy and, 95—97
  - excess Gibbs energy and, see Excess Gibbs energy
  - general equations for, 82—86, 120—122
  - Guggenheim's equations and, 81—82
  - heat capacity and, 95—97
  - higher order terms and, 131—132
  - high temperatures and, 104—113
  - history of, 81—82
  - imperfect gases and, 77—80
  - ion association and, 93—95, 304—306, 404, 510
  - ionic strength and, 84, 129
  - ion-neutral interactions and, 129
  - ion pairing and, 304—306
  - to mineral solubility, 440—466
    - in binary systems, 458—459, 470—477
    - in quaternary systems, 465—466
    - in ternary systems, 460—465, 477—479
    - 25-degree temperature and, 441—452
    - variable temperature and, 453—466
  - mixed electrolytes and, 88—91
  - mixing terms and, 92
  - mixtures and, 113—120
  - molality-based, 436
  - mole fraction and, 136—139
  - multicomponent salt solutions and, 301—302
  - natural solutes and, 302
  - neutral solutes and, 92—93, 302—304
  - neutral species and, 131—132
  - nonideal solutions and, 77—80
  - parameters of, 296, 299—304, 306—312
  - Pitzer model and, see Pitzer model
  - pressure and, 95—97
  - pure electrolytes and, see Pure electrolytes
  - single-ion activity coefficients and, 91—92
  - single salt solutions and, 299—300
  - symmetrical mixing and, 114, 126—128
  - temperature and, 95—97
  - theory of, 82—86
- Ion-ion interactions, 371, 381, 388, 390
- Ionization, 493, 514
- Ion-neutral interactions, 129, 373
- Ion pairing, 62—64, 177—178
  - activity coefficients and, 304—306
  - applications of, 406—410
  - models of, 352, 395, 406—410
  - Pitzer model and, 304—306, 409
- Ion-reversible electrodes, 211
- Ion-selective microelectrodes, 181
- Iron, 179, 185
- Irreducible cluster integrals, 40
- Isocoulombic reactions, 495—496, 519—521
- Isopiestic activity coefficient, 181
- Isopiestic equilibrium, 221, 240
- Isopiestic measurements, 156
- Isopiestic methods, 209—272, see also specific types
  - accuracy of, 258—259
  - activities and, 214—220
  - chamber design for
    - errors and, 232—245
    - materials for, 264—266
  - data in
    - equations for representing, 268—272
    - sources of, 263—264
  - errors in, 251—262
    - chamber design and, 232—245
    - corrosion of sample cups and, 256
    - equilibration times and, 252—254
    - reagent purity and, 256—258
    - reference standard discrepancies and, 259
    - reuse of samples and, 252—254
    - sample cup corrosion and, 256
    - sample reuse and, 252—254
    - sample size and, 252—254
    - summary of, 262
    - weighing and, 259—262
  - experimental techniques related to, 249—251
  - fugacity and, 214—220
  - Gibbs energy and, 214—220
  - history of, 232—246
  - materials for construction of apparatus for, 264—268
  - Oak Ridge National Laboratory, 246—249
  - osmotic coefficients and, 214—220
  - publication of data in, 231—232
  - reference standards for, see Isopiestic reference standards
  - sample cups for, 256, 266—268
  - solubility determinations by, 262—263
  - sources of data in, 263—264
  - vapor pressure and, 214—220
  - weighing errors in, 259—262
- Isopiestic molality ratios, 229—230
- Isopiestic reference standards, 212—213, 220—232
  - for aqueous solutions
    - at 298.15K, 222—226

at other temperatures, 226—229  
 tertiary, 230—231  
 discrepancies in, 259  
 isopiestic molality ratios and, 229—230  
 for nonaqueous solutions, 231  
 publication of data on, 231—232  
 self-consistency among, 229—230  
 tertiary, 230—231  
 Isothermal compressibility, 3  
 Isothermal Gibbs energy, 210

## K

Kinetic energy, 31, 63  
 Kirkwood-Buff method, 64—65  
 Kirkwood-Buff theory, 37—38, 60

## L

Laar equation, 139  
 Lakes, 281, 369  
 Lanthanum, 169  
 Lattice models, 44—47  
 Lauric acid, 184  
 Lead, 175  
 Lead chloride, 522  
 Lead chloro-complexes, 400—402  
 Lead-selective electrodes, 182  
 Lecithin, 179  
 Lewis fugacity rule, 331  
 Ligands, 492  
 Limiting conductance, 493  
 Limiting slope, 13, 297, 508  
 Linearization approximation, 56  
 Liquid ion exchange electrodes, 175—180  
 Liquid junction, 157—158, 352, 359, 364, 493  
 Liquid-liquid extraction, 210—211  
 Lithium, 168—169, 179  
 Lithium aluminum silicate, 169  
 Local free energy, 32

## M

MacInnes convention, 359, 368  
 Magnesium, 168, 175, 178, 181, 521  
 Magnesium fluoride, 402—405  
 Magnesium orthoborate, 372  
 Malate, 179  
 Malonate, 179  
 Margules expansion model, 139, 436, 438, 466—479  
   in binary systems, 470—477  
   equations for, 470—477  
   in ternary systems, 477—479  
 McMillan-Mayer theory, 38—41, 61  
 Mean activity, 10—11, 158  
 Mean activity coefficients, 11, 13—14, 88, 156, 298—299  
 Mean electrostatic potential, 54, 59  
 Mean force potentials, see under Potentials  
 Mean modality, 11

Mean potential energy, 55  
 Mean potentials, 46, 54—55, 57, 59  
 Mean spherical approximation (MSA), 62, 64, 67  
 Metal complexation, see Complexation  
 Microelectrodes, 181  
 Minerals, see also specific types  
   calcium carbonate, 365—367  
   solubility of, 317—321, 435—484  
     activity coefficients of, 442  
     in binary systems, 458—459, 470—477  
     calculations of, 436—438, 440—441, 443  
       Margules model for, see Margules expansion model  
     computer codes for, 440  
     equilibrium constants for, 437—439, 457  
     ion interaction approaches to, see under Ion interaction approaches  
     modeling of, 438—440  
     osmotic coefficient of, 442  
     prediction of, 436, 439, 452, 465  
     pressure and, 438  
     in quaternary systems, 465—466  
     in ternary systems, 460—465, 477—479  
     theory of, 437—438  
     at variable temperatures, 453  
 Mixing, see also Mixtures; specific types  
   asymmetrical, 114, 117, 122—125  
   enthalpy of, 514—515  
   entropy of, 15—17  
   free energy of, 44  
   heat of, 127  
   ideal, 47, 136—139  
   parameters of, 440, 444, 449  
   random, 46—47  
   symmetrical, 114, 126—128  
   terms for, 92  
 Mixtures, see also Mixing; specific types  
   of electrolytes, 88—91, 169, 213, 436, 438—439  
   parameters for, 113—120  
   of solvents, 93, 160—161  
   of sugars, 213  
 Models, see also specific types  
   of activity coefficients, 65  
   Bjerrum, 501, 507  
   cell, 44—47  
   density-based, 496  
   geochemical, 185, 294, 439  
   hard-core, 41  
   hydration, 503  
   ion association, 293—294, 395, 404, 408—409, 496—498  
   ion-interaction, see Ion interaction approaches  
   of ion pairing, 352, 395, 406—410  
   lattice, 44—47  
   Margules expansion, see Margules expansion model  
   of mineral solubility, 438—440  
   Pitzer, see Pitzer model  
   primitive, 43, 62, 64—65, 67—68  
   restricted primitive, 43, 62, 67—68

thermodynamic, 293  
 of virial coefficients, 440  
 Modified Poisson-Boltzmann, 67  
 Molal compressibility, 300  
 Molal enthalpy, 96—97, 298—299  
 Molal heat capacity, 96  
 Molal ionic strength, 316  
 Molality, 77, 84, 437  
   ion interactions based on, 436  
   isopiestic, 229—230  
   scales of, 286  
   of sea salt, 289  
 Molal osmotic coefficient, 215  
 Molal volume, 95—97, 474—476  
 Molar enthalpy, 22—24  
 Molar fraction statistics, 272  
 Molar Gibbs free energy, 210, 214  
 Molar quantities, 5—7, 21—24  
 Molar volume, 104  
 Molecular correlation functions, 40  
 Molecular distribution functions, 34—36, 48  
 Molecular dynamics, 44, 50—53  
 Molecular interactions, 41—44, see also specific types  
 Molecular volume, 37  
 Mole fraction, 136—139, 288, 348  
 Mole fraction osmotic coefficient, 215  
 Mole fraction scales, 295, 348  
 Molinity, 286, 289  
 Monte Carlo method, 33, 43—44, 49, 62, 69  
   ion pairing and, 63  
   molecular dynamics and, 50—53  
   primitive model and, 65, 67—68  
 MSA, see Mean spherical approximation  
 Multicomponent salt solutions, 301—302  
 Multicomponent systems, 12—14, 26—28, 286—289, 348  
 Multipole moments, 42  
 Mutual fluctuations, 56

## N

Naphthalene, 334—335  
 National Bureau of Standards (NBS) scale, 353—354  
 NBS, see National Bureau of Standards  
 Nernst equation, 159  
 Nernstian behavior, 179  
 Nernst slopes, 176  
 Neutral carrier-based electrodes, 181—182  
 Neutral ion pairs, 408  
 Neutral solutes, 92—93, 302—304, 329—349  
   atmospheric gas solubility and, 335—346  
   empirical representations of solubility and, 332—334  
   gas solubility and, 346—349  
   Setchenow coefficients and, 334  
 Neutral species, 299  
 Nitrates, 179  
 Nitrites, 179  
 Nitrobenzene, 180

*o*-Nitrophenyl octyl ether, 179  
 Nonaqueous solvents, 160—161  
 Nonelectrolytes, 7—12, 470  
 Nonideal solutions, 77—80

## O

Oak Ridge National Laboratory isopiestic methods, 246—249  
 Onsager relationship, 494  
 Open phases, 5—6  
 Open systems, 292—293  
 Ornstein-Zernike equation, 61, 62  
 Osmolality, 221  
 Osmometry, 212  
 Osmotic coefficients, 12, 44, 64, 86, 89, 291  
   activity coefficient and, 13—14  
   excess, 272  
   isopiestic methods and, 214—220  
   mean activity coefficient and, 13—14  
   of mineral solubility, 442  
   Pitzer model for, 295—296, see also Pitzer model  
   pressure and, 474  
   of seawater, 314, 316, 413—414  
   water activity and, 438  
 Osmotic conditions, 39  
 Osmotic pressure, 19—20, 38—40, 220  
 Ostwald coefficient, 347  
 Oxalate, 179, 186  
 Oxalate oxidase, 186  
 Oxygen  
   activity coefficients for, 345  
   Henry's law constant and, 345  
   Pitzer model and, 344  
   solubility of, 332, 337, 343—344

## P

Pair correlations, 35, 49, 54, 61—62, 64, 69  
 Pairwise additivity, 42—43  
 Palladium membrane electrode, 157  
 Palladium oxide, 157  
 Partial heat capacity, 298  
 Partial molal compressibility, 300  
 Partial molal enthalpy, 97, 298  
 Partial molal volume, 97, 300, 474  
 Partial molar enthalpy, 22—24  
 Partial molar Gibbs free energy, 210, 214  
 Partial molar quantities, 5—7  
 Partial molar volume, 104  
 Partial molecular volume, 37  
 Partial pressure, 188, 332  
 Partition functions, 44—45, 47  
   cell models and, 46  
   formalism and, 31—34, 36  
   grand, 39  
   perturbation theory and, 48  
 PCBs, see Polychlorinated biphenyls  
 Penicillin, 186  
 Perchlorate, 179

- Percus-Yevick approximation (PYA), 62
- Periodate, 179
- Periodic boundary conditions, 52
- Perturbation, 48—50, 62
- pH, 91—92, 158, 358
- pH electrodes, 159—166, 185
- Phosphoric acid, 302, 380—385
- pH scales, 352—359, 364
- Pitzer model, 76, 185, 294—312, 332
  - activity coefficients and, 413—414
  - ammonia and, 374
  - ammonium and, 375
  - atmospheric gas solubility and, 337—346
  - boric acid and, 370
  - carbonate systems and, 368—370
  - carbon dioxide and, 368
  - complexation and, 395
  - consistency of, 359
  - copper chloro-complexes and, 399—400
  - copper salts and, 399
  - dissolved salts and, 302—304
  - ionic equilibrium and, 359
  - ion pairing and, 304—306, 409
  - lead chloro-complexes and, 400
  - limerick about, 229
  - multicomponent salt solutions and, 301—302
  - neutral solutes and, 302—304
  - parameters of, 296, 298—304, 306—312
  - pressure and, 412—413
  - single salt solutions and, 299—300
  - temperature and, 412—413
- Poisson-Boltzmann equation, 56—57, 65, 67
- Polychlorinated biphenyls (PCBs), 348, 350
- Polymer-based ion-exchange electrodes, 175—180
- Polyvalent electrolytes, 156
- Polyvinyl chloride membranes, 178—179
- Potassium, 168, 175, 179, 181
- Potential energy, 31, 42, see also Debye-Hückel theory
  - electrostatic, 59
  - ion pairing and, 63
  - mean, 55
  - statistical mechanics and, 54—57
  - total, 60
- Potentials, see also specific types
  - average, 40, 46—47
  - of average force, 40
  - cell, 493
  - chemical, see Chemical potentials
  - coulomb, 53, 55
  - drift in, 159
  - effective, 47
  - electrostatic, 54, 59
  - of Harned cell, 158
  - intermolecular, 42
  - liquid junction, 364, 493
  - mean, 46, 54—55, 57, 59
  - of mean force, 38, 42—44, 53—55
    - coulomb interactions for, 65
    - coulomb's law for, 65
    - formalism and, 35—36
    - integral equations and, 60
    - interionic, 82
    - ion interaction approaches and, 82—83
    - McMillan-Mayer formalism and, 61
    - pair correlation functions and, 61
    - solvent dipole and, 62
    - thermodynamic properties of ionic solutions and, 66
  - pairwise additive, 42
  - standard, 156, 158—159, 165, 167
  - zero-current, 176
- Potentiometry, 155—188, 517
  - accuracy of, 157, 164
  - amalgam electrodes in, 166—168, 169
  - biologically based electrodes in, 186—187
  - cation-selective electrodes in, 169—173
  - data in, 158—159
  - electrodes of second kind in, 182—184
  - enzyme-based electrodes in, 186—187
  - errors in, 165
  - gas-sensitive membrane electrodes in, 187—188
  - glass pH electrodes in, 159—166
  - hydrogen electrodes in, 157—159
  - ion-exchange electrodes in, 175—180
  - ion pairing and, 177—178
  - liquid ion-exchange electrodes in, 175—180
  - neutral carrier-based electrodes in, 181—182
  - pH scales and, 352—359
  - polymer-based ion-exchange electrodes in, 175—180
  - principles of, 156—157
  - results of, 165—168, 170—173, 183
  - selectivity of, 169—170, 181, 185
  - solid-state membrane electrodes in, 184—185
  - stability constants and, 185
  - transference and, 182—185
  - typical data in, 158—159
  - typical results in, 165—168, 170—173
- Practical osmotic coefficient, 215
- Pressure, 60, 475—476, see also specific types
  - activity coefficients and, 21—22, 299—300, 474
  - chemical potentials and, 438
  - equilibrium vapor, 237
  - excess Gibbs energy and, 474
  - fugacity and, 332
  - Gibbs energy and, 210, 474
  - ion interaction approaches and, 95—97
  - mineral solubility and, 438
  - osmotic, 19—20, 38—40, 220
  - osmotic coefficients and, 474
  - partial, 188, 332
  - Pitzer model and, 412—413
  - total, 210, 332
  - vapor, see Vapor pressure
- Pressure coefficient, 239
- Pressure derivative, 238
- Primary reference standards, 230
- Primitive model, 43, 62, 64—65, 67—68
- Probability density, 34—35
- Probability distribution, 52
- Pure electrolytes, 86—88, 299

parameters for, 98—104  
 for high temperatures, 104—113  
 variation for, 302  
 PVC, see Polyvinylchloride  
 PYA, see Percus-Yevick approximation  
 Pyrophosphate, 179

**Q**

Quaternary systems, 465—466  
 Quinhydrone, 184

**R**

Radial distribution functions, 35, 59, 121  
 Rainwater, 281—282  
 Raman spectroscopy, 293, 519  
 Random mixing, 46—47  
 Raoult's law, 214, 272  
 Rational osmotic coefficient, 215  
 Reactant concentrations, 166  
 Reagents, 256—258, see also specific types  
 Reference hypernetted-chain (RHNC) approximation, 62, 65—66  
 Reference standards, isopiestic, see Isopiestic reference standards  
 Reference state, 291  
 Regular solutions, 15—17  
 Relative fugacity, 216  
 Restricted primitive model, 43, 62, 67—68  
 RHNC, see Reference hypernetted-chain  
 Ring diagrams, 58  
 Rivers, 281  
 Rubidium, 168

**S**

Salinity, 283—286, 316, 410  
 Salting coefficients, 333, 416  
 Salting-in, 26—28, 333—334  
 Salting-out, 26—28, 333—334  
 Saturation index, 320  
 Scaled particle theory, 334—335  
 Sea salt, 300  
   activity coefficients of, 315—317  
   molality of, 289  
   molality of, 289  
   stoichiometry of, 289—290  
 Seawater, 281—282, 304  
   activity coefficients of, 300  
   artificial, 287—288, 355, 362  
   atmospheric gas solubility in, 335—346  
   carbonate system in, 361—364  
   conductivity of, 285  
   density of, 283—286, 410  
   hydrocarbons in, 348—349, 417—418  
   ion product of water in, 391—392  
   magnesium fluoride in, 402—405  
   major components of, 315—317  
   as multicomponent electrolyte solution, 286—289  
   osmotic coefficients of, 314, 316, 413—414

oxygen solubility in, 344  
 PCBs in, 348, 350  
 stoichiometry of, 283—290  
 Secondary reference standards, 230  
 Second virial coefficient, 84, 101  
 Selectivity coefficients, 185  
 Setchenow relationship, 294, 332, 334, 336, 347—348  
   for atmospheric gases, 417  
   for hydrocarbons, 349  
 Side reaction coefficient, 393  
 Silver chloride, 158—159, 519  
 Single-ion activity coefficients, 91—92  
 Single salt solutions, 299—300  
 Sodium, 179, 181  
 Sodium-selective glass electrodes, 176  
 Solid-state membrane electrodes, 184—185, 187  
 Solubility, 211  
   of air, 336  
   of anhydrite, 320  
   of atmospheric gases, see under Atmospheric gases  
   of calcium sulfate, 321  
   empirical representations of, 332—334  
   of gases, 303, 324—325, 346—349  
     in pure water, 415—416  
   of gypsum, 318—321  
   of hydrocarbons, 348, 417—418  
   isopiestic methods for determination of, 262—263  
   measurements of, 518—519  
   of minerals, see under Minerals  
   of naphthalene, 335  
   of oxygen, 332, 337, 343—344  
   of PCBs, 350  
   of salts, 308—309, 317—321  
   of silver chloride, 519  
 Solubility constants, 365  
 Solutes, see also specific types  
   activity coefficients of, 239  
   activity coefficients of components of, 210  
   activity of, 290  
   interactions among, 41  
   neutral, see Neutral solutes  
   reference state for, 291  
   solvent interactions with, 41—42  
 Solvent dipole, 62  
 Solvents, see also specific types  
   activity of, 12  
   aprotic, 183  
   chemical potentials of, 12  
   interactions between, 42  
   mixed, 93, 160—161  
   nonaqueous, 160—161  
   solute interactions with, 41—42  
 Spectroscopy, 293, 518—519, see also specific types  
 Stability constants, 185, 349, 396, 409  
   stoichiometric, 363  
   thermodynamic, 349, 351, 410  
 Standard potential, 156, 158—159, 165, 167

- Standard-state chemical potentials, 439, 445, 450, 453, 455—456, 476
- Standard-state entropy, 438
- Standard-state heat capacity, 438—439, 453, 457, 476, 480
- Standard states, 7—12, 290
- Standard-state volume, 475
- Starch, 179
- State equations, 3
- Static methods, 212, *see also* specific types
- Statistical mechanics, 29—70
- cell models of, 44—47
  - defined, 30
  - for electrolytes, 53—69
    - cluster expansion and, 57—59
    - Debye-Hückel theory and, 54—57
    - integral equations and, 59—62
    - ion pairing and, 62—64
    - Kirkwood-Buff method and, 64—65
    - numerical results and, 65—69
    - potential energy and, 54—57
  - exact theories of, 37—41
  - formalism in, 31—37
  - Kirkwood-Buff theory of, 37—38
  - lattice models of, 44—47
  - McMillan-Mayer theory of, 38—41
  - molecular dynamics and, 50—53
  - molecular interactions and, 41—44
  - partition functions and, 31—33
  - perturbation theory and, 48—50
  - theories of, 37—41, *see also* specific types
  - variational methods and, 48—50
- Stepwise formation constants, 520
- Stereochemistry, 524
- Stoichiometric dissociation constants, 350
- Stoichiometric equilibrium constants, 361—364
- Stoichiometric formation constants, 393
- Stoichiometric stability constants, 363
- Stoichiometry
- of sea salt, 289—290
  - of seawater, 283—290
- Streams, 281
- Strong electrolytes, 313—329
- mineral solubility and, 317—321
  - seawater and, 315—317
  - sulfuric acid and, 322—324
  - supersaturated solutions and, 327—328
  - thermodynamics and, 328—329
  - volatile, 324—327
- Sucrose, 179
- Sugars, 213, *see also* specific types
- Sulfur dioxide, 389—391
- Sulfuric acid, 322—324, 514
- Sulfurous acid, 166
- Supersaturated solutions, 262, 327—328
- Symmetrical mixing, 114, 126—128
- T**
- Tartaric acid, 179
- Temperature
- activity coefficients and, 21—22, 298, 314
  - boiling, 19, 211, 436
  - chemical potentials and, 438
  - Debye-Hückel parameters and, 297
  - derivatives of, 238
  - equilibrium constants and, 439
  - equilization of, 244
  - freezing, 211
  - Gibbs energy and, 210
  - gradients of, 233
  - heat capacity and, 456
  - ion interaction approaches and, 95—97
  - numerical expressions for dependence on, 480—484
  - Pitzer model and, 412—413
  - pure electrolytes and high, 104—113
  - seawater density and, 410
- Ternary systems, 460—465, 477—479
- Tertiary reference standards, 230—231
- Tetradecylammonium carbonate, 179
- Tetrahydrofuran, 179
- Thallium, 168
- Thermal expansion, 3, 210
- Thermal fluctuations, 55
- Thermodynamic equilibrium constants, 366
- Thermodynamic association constants, 351
- Thermodynamics, 1—28, 37
- activity coefficients and, 7—12, 328—329
  - apparent molar quantities and, 21—24
  - athermal solutions and, 15—17
  - basic functions in, 2—5
  - chemical potentials and, 5—12
  - of chloride species, 519
  - colligative properties and, 17—21
  - compressibility equation and, 60
  - database for, 439
  - derivation of quantities in, 20—21
  - differential relations between functions of, 5
  - of electrolytes, 210, 436
  - enthalpy and, 21—24
  - equilibrium, 290—293
  - excess in, 24—26
  - first law of, 3—4
  - Gibbs-Duhem relation and, 12—14
  - glass pH electrodes in studies of, 165
  - ideal solutions and, 15—17
  - of ion association, 351, 498—501
  - isopiestic methods and, 210
  - laws of, 3—5
  - modeling of, 293
  - molar quantities and, 5—7, 21—24
  - multicomponent systems and, 12—14, 26—28
  - partial molar quantities and, 5—7
  - physical meaning of quantities of, 3—4
  - potentials of mean force and, 66
  - regular solutions and, 15—17
  - second law of, 4
  - of strong electrolytes, 328—329
  - third law of, 4
  - two-component systems and, 12—14
  - volume and, 21—24

Thermodynamic solubility constants, 365  
 Thermodynamic stability constants, 349, 351, 410  
 Total energy, 3, 42  
 Total vapor pressure, 210  
 Transference, 182—185  
 Transport, 176, 183—184  
 Trichloroacetic acid, 166  
 Trifluoromethanesulfonate, 516  
 Trioctyl phosphate, 179  
 Tripentyl phosphate, 179  
 Triplet interactions, 297, 308  
 Tripolyphosphate, 179  
 Tris buffer, 166, 354, 357  
 Two-component systems, 12—14

**U**

Ultraviolet-visible spectrophotometry, 518  
 Unsymmetrical mixing, 114, 117, 122—125  
 Urea, 186  
 Urease, 186  
 Uric acid, 179, 186

**V**

Valinomycin, 176, 181  
 Vanadate-oxalate, 166  
 Van der Waals equation, 330  
 Van't Hoff equation, 336  
 Vapor pressure, 212, 214—220  
   depression of, 436  
   equilibrium, 237  
   total, 210  
 Variable coefficients, 82  
 Variance reduction methods, 51  
 Variational methods, 48—50  
 Vaterite, 365  
 Virial coefficients, 40, 84, 101, 133, 217  
   imperfect gases and, 77—80  
   mineral solubility and, 436, 440, 536  
   modeling of, 440  
 Virial equation of state, 331  
 Vitamin B, 179  
 Vitamin D, 179

Volatile strong electrolytes, 324—327  
 Volume, 21—24  
   apparent molal, 97, 474  
   ion interaction approaches and, 95—97  
   molal, 95—97, 474—476  
   molar, 104  
   partial molal, 97, 300, 474  
   partial molar, 104  
   partial molecular, 37  
   standard-state, 475  
 Volumetric data, 104  
 Volumetric properties, 97

**W**

Weak electrolytes, 349—392, 419  
   Henry's law constants for, 351  
   hydrogen ions and, 353—359  
   ion association constants for, 351  
   ionic equilibrium calculations for, 359—392  
     ammonia and, 373—378  
     boric acid and, 370—373  
     carbon dioxide-dissolved carbonate and, 360—370  
     hydrofluoric acid and, 378—380  
     hydrogen sulfide and, 385—388  
     ion product of water and, 391—392  
     phosphoric acid and, 380—385  
     sulfur dioxide and, 389—391  
   in natural waters, 350—352  
   pH scales and, 352—359  
   potentiometry and, 352—359  
   thermodynamic ion association constants for, 351  
   thermodynamic stability constants for, 351  
 Weighing errors, 259—262

**Y**

Young's rule, 294, 334—335

**Z**

Zero-current potential, 176  
 Zinc, 168  
 Zinc chloride, 522